MINUTES OF THE NINETEENTH EXPLOSIVES SAFETY SEMINAR

VOLUME I

BILTMORE HOTEL
LOS ANGELES, CA

9 - 10 - 11 SEPTEMBER 1980

SPONSORED BY
DEPARTMENT OF DEFENSE EXPLOSIVES SAFETY BOARD
ALEXANDRIA, VA

(2)

(6) MINUTES OF THE

NINETEENTH EXPLOSIVES SAFETY SEMINAR (19th)

[redacted]

[redacted]

Los Angeles, California

9-10-11 September 1980.

Volume I.

(12) 882

Sponsored by

Department of Defense Explosives Safety Board

Alexandria, Virginia 22331

(11) 1980

Approved for public release; distribution unlimited

PREFACE

This Seminar is held as a medium by which there may be a free exchange of information regarding explosives safety. With this idea in mind, these minutes are being provided for your information. The presentations made at this Seminar do not imply indorsement of the ideas, accuracy of facts presented, or any product, by either the Department of Defense Explosives Safety Board or the Department of Defense.

ALTON W. POWELL
Colonel, USAF
Chairman

These proceedings are published for information as an accommodation to the participants at the Seminar. The Department of Defense Explosives Safety Board cannot accept responsibility for the correctness of those papers which have been directly reproduced from copy furnished by the authors.

TABLE OF CONTENTS

VOLUME I

Volume II contains pages 875 thru 1813

WELCOME

Colonel Alton W. Powell, USAF
Chairman
Department of Defense Explosives Safety Board

Good morning, ladies and gentlemen. Welcome to the Nineteenth Department of Defense Explosives Safety Seminar.

It is my pleasure and privilege to welcome you to the Board's sponsorship and continuation of this highly respected traditional event. The Board members and the Secretariat want the next three days to be personally stimulating and professionally rewarding for you. As noted in your seminar program, we have scheduled a large number of what I believe to be interesting presentations by leading professionals from the United States and other nations. Your active participation in the scheduled events is absolutely necessary if we are to achieve the success experienced in the 18 preceding symposia. I encourage you to share my personal enthusiasm by exercising your personal initiative and ingenuity in the various sessions of this seminar.

Before proceeding with our program, let me introduce to you the current members of the Explosives Safety Board. From the Department of the Army, Colonel Bobby Robinson, represented by Mr. Larry Crawford, the Army Alternate, who is the Director of Safety for the Army Materiel Development and Readiness Command. From the Department of the Navy, Captain Dwight Agnew. Dwight is head of the Ordnance Materiel Management Branch in the Office of Chief of Naval Operations at the Pentagon; and from the Department of the Air Force, Colonel Jim McQueen. Jim is the Chief of Weapons Safety, Deputy Inspector General, Headquarters Air Force, at Norton Air Force Base, California.

Our impressive list of distinguished foreign participants includes:

·From the United Kingdom - Major General John Hamilton-Jones, President of the UK Ordnance Board.

·From the Republic of Korea - Major General Doo Jung Jin, Chief of Ordnance, Republic of Korea Army, and

·From France - Engineer General Jean Roure, Technical Inspector of Armament, Ministry of Defense, and

·From Australia - Commodore John N. Crosthwaite, President of the Australian Ordnance Council.

At this time, it is my pleasure to introduce our keynote speaker, Major General Len C. Russell, the Air Force Deputy Inspector General for Inspection and Safety and Commander, Air Force Inspection and Safety Center, Norton Air Force Base, California.

WELCOME

Colonel Alton W. Powell, USAF
Chairman
Department of Defense Explosives Safety Board

Good morning, ladies and gentlemen. Welcome to the Nineteenth Department of Defense Explosives Safety Seminar.

It is my pleasure and privilege to welcome you to the Board's sponsorship and continuation of this highly respected traditional event. The Board members and the Secretariat want the next three days to be personally stimulating and professionally rewarding for you. As noted in your seminar program, we have scheduled a large number of what I believe to be interesting presentations by leading professionals from the United States and other nations. Your active participation in the scheduled events is absolutely necessary if we are to achieve the success experienced in the 18 preceding symposia. I encourage you to share my personal enthusiasm by exercising your personal initiative and ingenuity in the various sessions of this seminar.

Before proceeding with our program, let me introduce to you the current members of the Explosives Safety Board. From the Department of the Army, Colonel Bobby Robinson, represented by Mr. Larry Crawford, the Army Alternate, who is the Director of Safety for the Army Materiel Development and Readiness Command. From the Department of the Navy, Captain Dwight Agnew. Dwight is head of the Ordnance Materiel Management Branch in the Office of Chief of Naval Operations at the Pentagon; and from the Department of the Air Force, Colonel Jim McQueen. Jim is the Chief of Weapons Safety, Deputy Inspector General, Headquarters Air Force, at Norton Air Force Base, California.

Our impressive list of distinguished foreign participants includes:

- From the United Kingdom - Major General John Hamilton-Jones, President of the UK Ordnance Board.

- From the Republic of Korea - Major General Doo Jung Jin, Chief of Ordnance, Republic of Korea Army, and

- From France - Engineer General Jean Roure, Technical Inspector of Armament, Ministry of Defense, and

- From Australia - Commodore John N. Crosthwaite, President of the Australian Ordnance Council.

At this time, it is my pleasure to introduce our keynote speaker, Major General Len C. Russell, the Air Force Deputy Inspector General for Inspection and Safety and Commander, Air Force Inspection and Safety Center, Norton Air Force Base, California.

KEYNOTE ADDRESS

By

Major General Len C. Russell

Air Force Deputy Inspector General
for Inspection and Safety
and
Commander, Air Force Inspection and Safety Center
Norton Air Force Base, California

At

Nineteenth Department of Defense Explosives Safety Seminar
Los Angeles, California
September 9, 1980

Good morning, ladies and gentlemen.

I am very pleased and honored to be able to address such a distinguished group of explosives safety experts. Collectively, you represent much of the free world's knowledge and expertise in the field, and I am not going to attempt to give you new insight into the technical aspects of your profession. What I will share with you is my view of explosives safety in today's Air Force; not only how we arrived at where we are today, but the direction we should go in the future. In explosives safety, as in all other areas of the profession of arms, we must understand the past to keep from repeating the mistakes of the previous generations, and we must carefully chart our path to ensure we can achieve operational goals with the limited resources available to us.

When I look at the professional explosives safety program that we have today, it is hard to believe that 15 years ago, on May 16, 1965, we had a disaster at Bien Hoa Air Base, Vietnam, that cost the lives of 26 men, destroyed 15 aircraft, and put a combat base out of operation for three days. Although we do not know exactly what initiated the disaster, we do know the cause. Commanders sanctioned serious violations of operational and storage procedures even after the potential for a serious mishap was identified. Our sister services can cite similar examples such as the loss of the Marine storage area at Da Nang and the explosives disaster aboard the USS Enterprise.

Why did this happen?

In the 1950s, our defense emphasis was based on nuclear superiority, and our conventional ammunition capability was seldom exercised. Most stockpiles were safely nestled in earth-covered, concrete bunkers at remote storage areas which posed little or no threat to lives and operational resources.

In 1961, President Kennedy established a national policy to develop a conventional war capability to counter aggression anywhere in the world. Our conventional munitions buy program soared. At most bases, war reserve munitions levels far exceeded their storage capability. Most of our munitions in the overseas theaters, such as USAFE and PACAF, were stored outside in open revetments. Although we have constructed many new storage facilities, limited real estate is still a major operational concern. But, during the 1960s, we paved the way for disaster.

By 1965, commanders in Vietnam were forced to accept greater risks due to the pressure of operational requirements. In February of that year, Air Force safety personnel conducted an explosives safety survey of air bases in Southeast Asia. They found serious safety deficiencies:

- Aircraft armed with forward firing ordnance had to be parked without concern for targets located in front of the aircraft. Aircraft were not sheltered or revetted.

- Large quantities of bombs were stored on the flightline, both between and behind the aircraft without adequate quantity-distance.

- Earthen revetments used for explosives storage were improperly constructed.

Although the team briefed commanders on the potential results of a mishap and the actions necessary to minimize the risks, commanders did not have dollar or physical resources with which to eliminate the hazards. Just three months later, Bien Hoa became a casualty of our own operational procedures. The conditions at the start of the mishap were virtually the same as the safety staff found in February. Cardinal principles of explosives safety were violated, and explosions propagated down a line of loaded aircraft like dominoes.

We re-learned our lessons the hard way at Bien Hoa. We had more to learn at the Marine storage area at Da Nang. The disaster started as a fire in an off-base trash dump. The fire spread to the Marine Corps storage area and then by way of flying fragments to the Air Force storage modules. The Air Force modules were designed for high-density storage of hard-cased high explosives; however, they were being used for cluster bombs packed in wooden crates. As the wooden crates burned, the CBUs detonated, throwing bomblets to other storage modules, causing other fires. The domino effect again.

Circumstances that can put a ground base out of commission for a few days wreak havoc on a Navy carrier. The hot exhaust from a starter unit on the deck of the Enterprise was only a few inches from a loaded rocket pod. The heat set off the rockets, and when the smoke finally settled, the Enterprise was out of action for months.

As a result of our experiences in Southeast Asia, we started to take a harder look at ways we could meet operational requirements yet maintain an acceptable degree of safety for our people and our operational assets. For example, we conducted a full-scale test, called "Big Momma," to determine the effect of steel bin revetments on preventing simultaneous or propagating explosions on explosives-loaded aircraft. "Concrete Sky" tested concrete-covered, steel-arch aircraft shelters which were designed to replace the steel bin revetments. On the storage side of the house, "Big Papa" tested the module concept for high-density storage of HE bombs. These tests showed that, under specific conditions, we could increase our storage capacity and aircraft parking capability without increasing the requirement for land, a vital concern then, as it is today. These tests were the start of a revolution in the application of explosives safety to operational requirements. This revolution is still underway, and it will affect the way you will be doing business in the years to come. The goal of the Air Force, the goal of the Department of Defense Explosives Safety Board, and your own personal goal must be to continue to provide the maximum degree of safety consistent with operational requirements.

How are we achieving this goal? The adoption of the UN classification system by the United States and other NATO nations in 1977 has done much to improve our cooperative efforts and mutual understanding of explosives safety requirements. Our current effort to standardize weapons design and test requirements is an encouraging step in the direction of improved operational capability and safety. Further, it should eliminate the needless expenditure of funds for additional weapons testing to meet the criteria of the different member nations. I look forward to General Hamilton-Jones' remarks on the NATO AC/310 Group's approach to this subject. A common ground of definitions, terminology, and requirements will enhance our capability to make valid decisions on programs like NATO cross-servicing.

I would like to pass on a few thoughts on that subject. NATO cross-servicing is an important concept because it increases the effectiveness of all our forces. Other NATO aircraft can land at a US operated base and be refueled and rearmed with US ordnance, and our aircraft can land at other NATO bases for similar servicing. We currently have certified the British BL755 and the French MATRA 250 bombs for use on our aircraft. We have a program, being coordinated by the weapons people at the Armament Division, Eglin AFB, to expand this capability to other NATO munitions, and we are planning to purchase some of these munitions for our own stockpile. We're not doing this to share the wealth of the munitions development contracts. We're doing it because it's good cooperative defense. It's going to save us a lot of money and improve our capabilities through greater interoperability.

The decisions which we make and the design and operational use of weapons, whether they are procured from US or allied sources, are based on a hazard classification system which, in the Air Force, uses a systems safety approach. The Nonnuclear Munitions Safety Board is the key organization in this sytem. The Board consists of voting members of each major command and has a responsibility for munitions in the design-to-target sequence. The Air Force Inspection and Safety Center representative acts as Safety Advisor to the Board. The primary function of the Board is to review and establish Air Force design safety criteria, standards, and requirements for nonnuclear munitions being developed by the Air Force, or being procured from other sources. The Board also evaluates, through analyses of engineering, development, and operational tests, how well new or modified munitions meet these criteria. Through this system we ensure that safety is designed into a weapon, not added on after it is operational.

An outgrowth of these munitions analyses was an identified need to evaluate the operational environment in which they are used. We had the challenge of producing a higher sortie rate, yet traditional safety philosophy dictated that refueling, maintenance, and ordnance loading be conducted separately. Our analysis of mishap data showed that the probability of mishap during any one of these activities was very low -- almost zero. What we weren't sure of was what would happen if we conducted the operations simultaneously. Would it create additional or more severe hazards or increase mishap probability? Could we load and refuel with engines running?

To answer these questions, the Air Force Logistics Command initiated a series of systems safety engineering analyses to study combat turnaround procedures for specific aircraft systems. They found that in some systems, specific safeguards were required for peacetime practice of the combat turnarounds, such as shutting down one engine or simulating fuel flow; and in some systems, simultaneous operations were prohibited. However, the majority of our combat turn procedures could be conducted simultaneously and in a safe manner -- a good initiative, both operational- and safety-oriented for increased combat capability.

These system safety concepts are applicable to other phases of the weapons business as well. Only when we combine mishap potential with mishap severity can we provide a meaningful risk assessment and logically determine how we can best allocate our limited resources.

We have also made progress in refining quantity-distance requirements for munitions storage locations. For example, we were able to reduce the distance required from igloos to military runways and taxiways by 40 percent. Once again, the key to this reduction is the probability of an aircraft actually being in the hazard zone when a mishap occurs. Through hazard analysis testing, we determined that most of our cluster munitions would not mass detonate. This enabled a classification change that significantly increased the quantity of these munitions we can safely store at our overseas bases and provides a greater combat capability where it is urgently needed. Similar tests of our air-launched missiles have shown that they too can be safely stored without the risk of mass detonation simply by maintaining a minimum separation between warheads. As an example, let's take a look at the AIM-7 Sparrow missile. If we maintain a warhead-to-warhead separation of only five inches, we can store an unlimited supply in a rocket storage, checkout, and assembly building or similar structure. They will not mass detonate, and the hazard distance for inhabited buildings is only 300 feet. That's an impressive reduction from the 1,200 feet required under our previous criteria -- and the key point is that safety is enhanced by meeting the new storage configuration requirements while at the same time we are increasing our combat capability. A similar test on the Maverick missile is in progress.

Actually, we have three tests underway which may further revolutionize our thinking. Distant Runner will be a test of hardened aircraft shelters to determine the attenuation of overpressure these hardened shelters offer against external explosions, as well as to the blast and fragment suppression capabilities of the shelter from internal detonations. As an added benefit, we will see what the ground shock effects are on nearby runways and taxiways. Our goal is to allow closer siting of facilities while still maintaining full protection of those facilities and our personnel. Construction of test facilities will begin shortly and the $5 million test will be complete by December 1981. Distant Runner plans will be discussed in one of the specialist sessions at this seminar.

Secondly, a related test of hardened support structures, such as squadron operations and maintenance facilities, is being conducted by the Army to determine the overpressure attenuation these facilities provide. The test results should be finalized in the next three months.

And thirdly, the Air Force has requested and the DDESB has funded scale model tests relative to the close-in suppressive effects afforded by standard igloos storing 100,000 pounds of explosives or less. These data should allow us to increase the storage capacity of igloos presently sited for less than 100,000 pounds. Some of the initial tests have been completed, and we are looking forward to preliminary reports on the results.

What does all of this mean in terms of our national priorities? First and foremost, explosives safety should support the mission, not impede it.

We believe that in a conventional war, air bases will be high priority targets of enemy forces since our aircraft represent an immediate and flexible threat to the enemy operation.

One way of protecting our fighter force is hardening of our facilities. This minimizes damage from enemy attacks and preserves our ability to launch airstrikes against his forces. Hardened facilities will also provide protection from the effects of an explosives mishap in peacetime and allow safe storage of larger quantities of munitions near their point of use. This will also enable us to readily support increased sortie rates required under combat conditions. While our storage and loading areas must not pose a greater threat to our survival than the enemy does, neither can we afford to wrap ourselves in an impregnable safety blanket by storing all munitions miles from the flightline, thereby reducing our sortie rates. I can't think of a more unsafe condition on an airfield than having enemy tanks drive through the front gate.

With the advent of insensitive high explosives, we are afforded the possibility of assuring safety without the need for vast quantity-distances because the probability of inadvertent initiation is low -- zero for all practical purposes. Using probability of inadvertent initiation as a criteria for explosives, hazard classification is a new concept. However, we have used probability in the past for some other phases of the stockpile to target sequence for explosives that are far more sensitive than IHE. For example, vehicles transporting explosives by road, rail, sea or air are not required to observe quantity-distance criteria, and this may well be the most hazardous and the most probable environment for an explosives accident. We accept the risks because we are confident that the safety features for these munitions ensure that the probability of initiation in this environment is very low. Without accepting these risks, shipping munitions by any means would be virtually impossible.

When you consider all of the safety features and characteristics which make detonation of class 1.1 explosives-filled weapons acceptably remote for everyday use, the characteristics of insensitive high explosives make acceptance of lesser distances a quite logical and prudent extension.

Our effort to establish a new classification for nuclear and conventional weapons using insensitive high explosives is a common sense step to rational hazard classification and risk assessment.

In the future, it will be vital that we have sufficient information concerning the nature and effects of specific weapons and the various suppression techniques used to protect adjacent operations. This information will allow us to make rational risk assessments, operational decisions, and choices between competing objectives. When our knowledge is shared, we can use our limited resources of time, people, and money effectively. That is your task this week.

This seminar can be a source of progress in our search for new knowledge and new applications. The extent to which you open your minds and share your thoughts with each other -- whether in formal or informal sessions -- will determine to a large extent our success in crossfeeding knowledge and developing the information necessary to make those hard decisions we will be forced to make and still ensure adequate safety is programmed into our plans and projects. Accidents like Bien Hoa, Da Nang, and the Enterprise must never happen again. We owe it to ourselves. We owe it to the people of the free world. I wish you luck and success in your conference.

Thank you.

PRECEDING PAGE BLANK-NOT FILMED

ADDRESS

By

Major General John Hamilton-Jones

Ministry of Defence
Ordnance Board
London, England

At

Nineteenth Department of Defense Explosives Safety Seminar
Los Angeles, California
September 9, 1980

PRESENTATION

Introduction.

My thanks to the Department of Defense Explosives Safety Board and Colonel Alton Powell for inviting me to speak here today. In selecting standardisation as a continuing theme, DDESB are right to recognise that only by continuous reminder and pressure can standardisation of defence hardware be improved in the western world. NATO as the single largest grouping of nations dedicated to peace and freedom have been responsible for deterring aggression by their combined military strength. Never has their position been more precarious and more under challenge than it is today. It is therefore appropriate to look at progress towards standardisation in the munitions and explosives field, the common currency of war. It is effort placed in this area that can make for the best use of our slender resources.

Defence within the NATO framework demands an equipment rationale of which standardisation forms an important part. Ideally, such a policy would imply acceptance by all NATO partners of a rationalised development and procurement plan, designed to provide a common range of defence equipment against agreed military requirements and product specifications. Production arrangements, quality assurance and testing would also be agreed and rationalised within a coordinated NATO industrial base, thereby ensuring the standardisation and mutual acceptability of all defence equipment and stores anywhere within the alliance.

As you may know, the Warsaw Pact has already met these requirements to a significant extent. Much of their battlefield equipment is already produced to common specifications, while standardised methods of testing, production and operation are widely accepted under Soviet direction. Although the Soviet system is far from perfect, it is evident that the substantial battlefield awareness enjoyed by the Pact conventional forces, which stem to a large extent from adoption of a strict standardisation policy, must not be under-estimated. The fact that within NATO, we are still unable to re-fuel each other's aircraft, indicates that NATO has failed where the Pact has succeeded.

We can also expect the West's ability to meet the Soviet bloc threat to become increasingly impaired if we cannot achieve a greater degree of equipment standardisation within a mutually acceptable range of weapon systems. Some of the reasons for our present inability to respond effectively may, I believe, be illustrated by reference to the difficulties which we still face within NATO, concerning the acceptance of a basic philosophy for rationalisation:

a. To meet operational performance requirements.

b. To production and other specifications.

c. To trial/test procedures and engineering practices.

Results So Far (Operational Requirements).

There is a mixed bag of results. On the bad side we see the tanks of the Alliance XMI/LEO 2/Chieftain/AMX 30 with no munitions interoperability. On the good side we see FH70/SP70/M198/GCT155 with good munitions interoperability. Yet, in both cases, the military requirement was boardly agreed. So, whilst there is a reasonably good record of agreeing operational requirements, we need to look more deeply into the problem for the answers to our failure to standardise.

Specifications.

In general, specifications continue to be written in accordance with national doctrine and practice. Here the slow process of coming together is being pursued through the concept of collaborative projects (e.g. MRCA, SP70/FH70), by which means it is hoped to encourage the adoption of more common codes of practice particularly within Europe and on both sides of the Atlantic. In this context, the collaborative concept is proving to be the most successful to date, probably because of the financial savings offered and the improved sales prospects which can follow from such arrangements.

Trials, Test, Engineering Practice/Quality.

Over the years, individual NATO partners have devised their own procurement systems and procedures, together with their associated (often single service) trials and testing arrangements. It is, therefore, inevitable in such circumstances that:

a. Weapon procurement programmes develop on the basis of national engineering practice.

b. Weapon systems and equipments develop in style and quality to a pattern which is based upon fundamental national experience, codes of practice, regulations, test and other procedures.

It is unfortunately still rare to find a genuine willingness by individual NATO partners to enbrace another country's practices at the expense of their own.

To illustrate this point, the UK has found that foreign equipment purchased by UK sometimes fails to meet a number of our own UK test requirements. Consequently equipment obtained in this way may have to be modified or is alternatively subject to the application of special to UK handling and storage restrictions. Foreign purchases of UK equipment have run into similar problems over here and in the FRG.

NATO Standardisation.

Within NATO we, therefore, have a situation where all countries agree that they require similar equipment, but we have yet to find an acceptable way of getting it.

Within NATO there are two organisations concerned primarily with standardisation. These are:

a. The Conference of National Armaments Directors (CNAD) - which deals essentially with standardisation matters during the design, development and production phases of the procurement cycle.

b. The Military Agency for Standardisation - which is responsible for the tactical and operational aspects of standardisation, as these relate to equipment which is entering or already in service and which ratifies Standardisation Agreements (STANAGS).

US and European R&D and production programmes are largely uncoordinated, except in a relatively small number of cases where some form of bi- or multilateral cooperative agreement may exist. In an endeavour to improve the situation, the NATO Executive Working Group set up Task Force 8 in 1977. This body was charged to make proposals for establishing closer links between the American and European Defence Procurement Systems and also between those operated by the European members of NATO - thereby creating a meaningful "two-way" flow of information across the Atlantic. Here I must stress that although NATO is endeavouring to move in this direction, we are still a long way from achieving a close degree of rationalisation. A number of common NATO weapon system requirements are, however, beginning to emerge.

AC/310.

To resolve the fundamental problems of common testing of munitions and explosives and to provide a rationale for a standard approach to design criteria and safety principles for munitions, Group AC/310 was formed in NATO in December 1979. Its TOR are shown and closely relate to those of my own organization, the UK Ordnance Board, since we in the UK have felt the need for a common tri-service independent assessment of weapons and explosives for many years. The tasks that AC/310 are expected to carry out for NATO are to develop from the existing national sources a common doctrine, tri-service where appropriate, for testing and test procedures, safety principles and associated design criteria.

The organisation to achieve the requirement is functional and is shown. The main committee has a chairman (currently from UK) who rotates among the nations and has representation from the chairmen of all the sub-groups. The sub-groups work to provide guidance to NATO on the lines I have described for their topics. The fundamental sub-group is that on the environment which staffs the NATO environmental STANAGs which, if adhered to, will promote many basic aspects of standardisation. The weapon system sub-groups are now forming and their TOR are in development.

As you will appreciate, it is to this group that those working within CNAD and MAS will be able to refer and for whose guidance AC/310 will be generating STANAGs concerning the philosophy and principles of design, safety and testing for explosive stores and the explosive elements of weapon systems. I must also stress here that AC/310 is the first attempt by NATO to establish a genuinely tri-service forum for the consideration of such matters. The importance of this group's function in relation to procurement standardisation within the alliance as a whole will, therefore, be evident.

PRECEDING PAGE BLANK-NOT FILMED

DISTANT RUNNER

A 5 Event High Explosive Test Series involving U. S. Air Force 3rd Generation Aircraft Shelters

by

ROBERT A. FLORY
Defense Nuclear Agency

DISTANT RUNNER is the nickname for a 5 event High Explosive Test series involving United States Air Force 3rd generation hardened aircraft shelters and taxiways/runways. This test series is an integral part of the overall Defense Nuclear Agency's Theater Nuclear Forces Survivability, Security and Safety (TNFS3) program and is scheduled for August through December 1981 at the White Sands Missile Range in New Mexico.

Stated objectives of the test are to:

1. Assess the capability of aircraft shelters to protect aircraft, munitions and personnel from external explosive effects (airblast and ground shock).

2. Assess the capability of aircraft shelters to contain or suppress internal detonation effects.

3. Assess collateral damage effects to and vulnerability of nearby runways/taxiways.

4. Accommodate Weapons Storage Vault testing if required and schedules permit.

Readiness of the United States Air Force Europe (USAFE) is being impeded by property constraints. A major problem the Air Force Theater Nuclear Forces are currently facing in Europe is the lack of available real estate for both construction of new aircraft shelters and location of additional, or increased capacity, explosive storage facilities. Operational needs dictate an increased sortie rate which translates into faster turn around time. This in turn, translates into storage of more munitions, both in the aircraft shelters and in close by uncovered sites. Overly conservative quantity distance (QD) factors are a major contributing cause to this limiting real estate problem and reduction of these quantity distance factors to the correct values will go a long way in alleviating the USAFE problem.

For aircraft shelters forty is the quantity distance criteria for the separation of aircraft munitions from populated areas. This criteria is currently applied whether or not the munitions are in hardened shelters. No credit is currently given for containment or suppression of accidental explosion effects by the shelter. Concrete Sky Phase IXB, a 1971 test, showed that a detonation in one shelter would not be likely to propagate to neighboring ones, however, other data obtained was not adequate to quantify the protection to populated areas provided by the shelter. Concrete Sky Phase IXB was a test in which an armed and fueled aircraft, equating to 4,63[illegible] lbs. Net Explosives Weight (NEW), was detonated in an open-ended, unreinforced concrete shelter of the type used in Southeast Asia. The aircraft shelters being tested in this program are 3rd generation shelters constructed of reinforced concrete with rear bulkheads and moveable front closure system. The new QD criteria derived from this test series should show a significant reduction. In the area of explosive storage facilities QD criteria, the current QD value from either an igloo or an open explosive storage site to parked aircraft is thirty. Currently this value is not reduced when the parked aircraft in question is located within an aircraft shelter even though all concede that its protection factor is greatly increased. This test should provide data that will allow a significant reduction of the current QD value. The third area of concern is the QD criteria for separation of explosive storage igloos or open storage sites from taxiways and/or runways. The current value of thirty (waived to 18) is considered overly conservative and should be greatly reduced by this test.

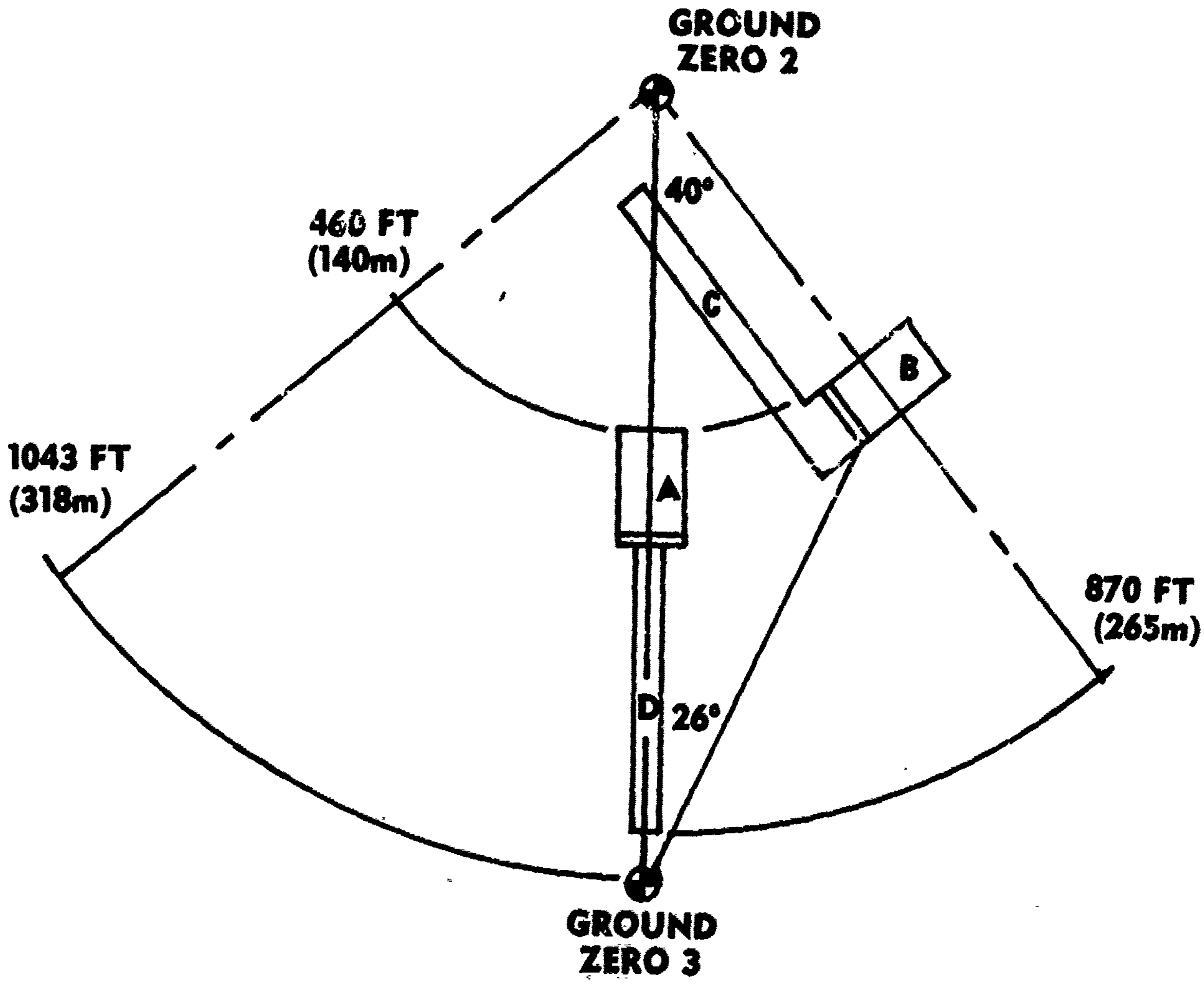

Figure 1. Test Bed Layout

The 1st event in this test series is a 100 lb NEW explosion inside shelter A. This will simulate the accidental detonation of a one sortie load of Air-to-Air missiles. In fact, 10 actual Air-to-Air AIM-9 warheads will be used. This event relates to the capability of the aircraft shelter to contain internal detonation effects. The detonation of 10 AIM-9 warheads will demonstrate the ability of the shelter to contain blast and fragments from this explosive quantity and weapon type. Events 2 and 3 are external detonations of 120 tons of high explosives each. These events will be used to assess the capability of the aircraft shelters to protect aircraft, munitions and personnel from external explosive events. Event 2 exposes Shelter A rear-on and Shelter B side-on. Event 3 exposes Shelter A front-on and Shelter B at an oblique angle. The high explosive used during these events will be Ammonium Nitrate with Fuel Oil. The explosives are situated so as to provide 15 psi incident overpressure and 490 psi-millisec free-field impulse at the shelter. Preliminary analysis indicated that this was the maximum loading allowable while retaining high confidence of avoiding significant damage to the shelters. It is anticipated that the average overpressure within the shelters will not rise above 1 psi. Assuming, as expected, that there will be no major structural damage and internal overpressures will be in the 1 psi range these tests will justify a quantity-distance factor of 5 for up to 275,000 lbs. of explosives in a standard storage igloo or a factor of 8 for up to 125,000 lbs of explosives in the open. By comparison, current QD values from either an igloo or an open storage site to parked aircraft is 30. These same two external shots will also be utilized in assessing the collateral damage effects to nearby runways. The arrangement of runways on this test will allow for a range of damage. Current QD values for distances between explosive storage igloos and open explosive storage areas to runways are 18 and 30 respectively. This test should allow these values to be reduced to 8 or less. Events 4 and 5 of this test series involve examining the suppression capability of the aircraft shelter to internal detonations. Event 4 will be the detonation of 2200 lbs. NEW of Mark 82 bombs hung on an excess RF101C aircraft. This is representative of a one sortie load of air-to-ground munitions. The aircraft will be in its normal position within Shelter B with the shelter doors closed. Event 5, utilizing Shelter A, will be identical to Event 4 except that there will be a total of 10,000 lbs. NEW of Mark 82 bombs, both hung on another excess aircraft and stored in the shelter. This is roughly representative of 4 sortie loads of air-to-ground munitions. In both events, catastrophic failure is expected. Debris patterns and overpressure readings in the surrounding area will be measured. The current QD from aircraft loaded with munitions to occupied areas is 40 with no consideration for suppression by the aircraft shelter. It is estimated that with shelter suppression the QD should be no higher than 20.

RELATIONSHIPS	Current QD Values	Post Test Estimated QD Values	Safety Distance (ft) Current/Estimated
Igloo to A/C Shelters	30	5	1950/325
Open Storage to A/C Shelters	30	8	1500/371
A/C Shelters to Occupied Bldgs	40	20	860/430
Igloo to Taxiway/Runway	18	8 or less	1170/520
Open Storage to Taxiway/Runway	30	8 or less	1500/371

Igloo contains 275,000 lbs. of explosive
Open Storage contains 125,000 lbs. of explosive
A/C Shelter contains 10,000 lbs. of explosive

Figure 2. Current vs. Post Test estimated QD Values

The last objective of DISTANT RUNNER is to accommodate the Weapons Storage Vault (WSV) testing if required and schedules permit. The WSV is a below grade vault designed to store one or more nuclear weapons within an aircraft shelter. The development of this vault is a separate effort and if a final design is completed in time it will be incorporated in Shelter B and appropriately instrumented.

Instrumentation for this test series consists of the following pressure gages, 44 free field, 33 on/in Shelter A, and 27 on/in Shelter B. There will be 79 accelerometers including 33 free field and pavement, 22 in each shelter and 2 below grade in Shelter A. For debris collection there will be a 5 degree prepared ground fan on three sides of each shelter out to 50 $(W)^{1/3}$. Additionally there will be impregnated fiberboard sheet bundles to act as targets for impacting debris. Debris energy and density will be measured by analysis of these targets. As a matter of further interest the concrete utilized in the two shelter arches will be color coded by location in the arch. This will aid in determining point of origin for debris. Up to 17 high speed cameras will also be utilized both inside and outside the shelters.

The current status of DISTANT RUNNER is as follows. The test group staff has been designated and is functioning. The contracts for instrumentation have been awarded. The construction contract for the two aircraft shelters was awarded to the John R. Davis General Contractors Inc. of El Paso, Texas on 5 August 1980. Mobilization of construction equipment is now taking place.

SPANGDAHLEM - AIR BASE

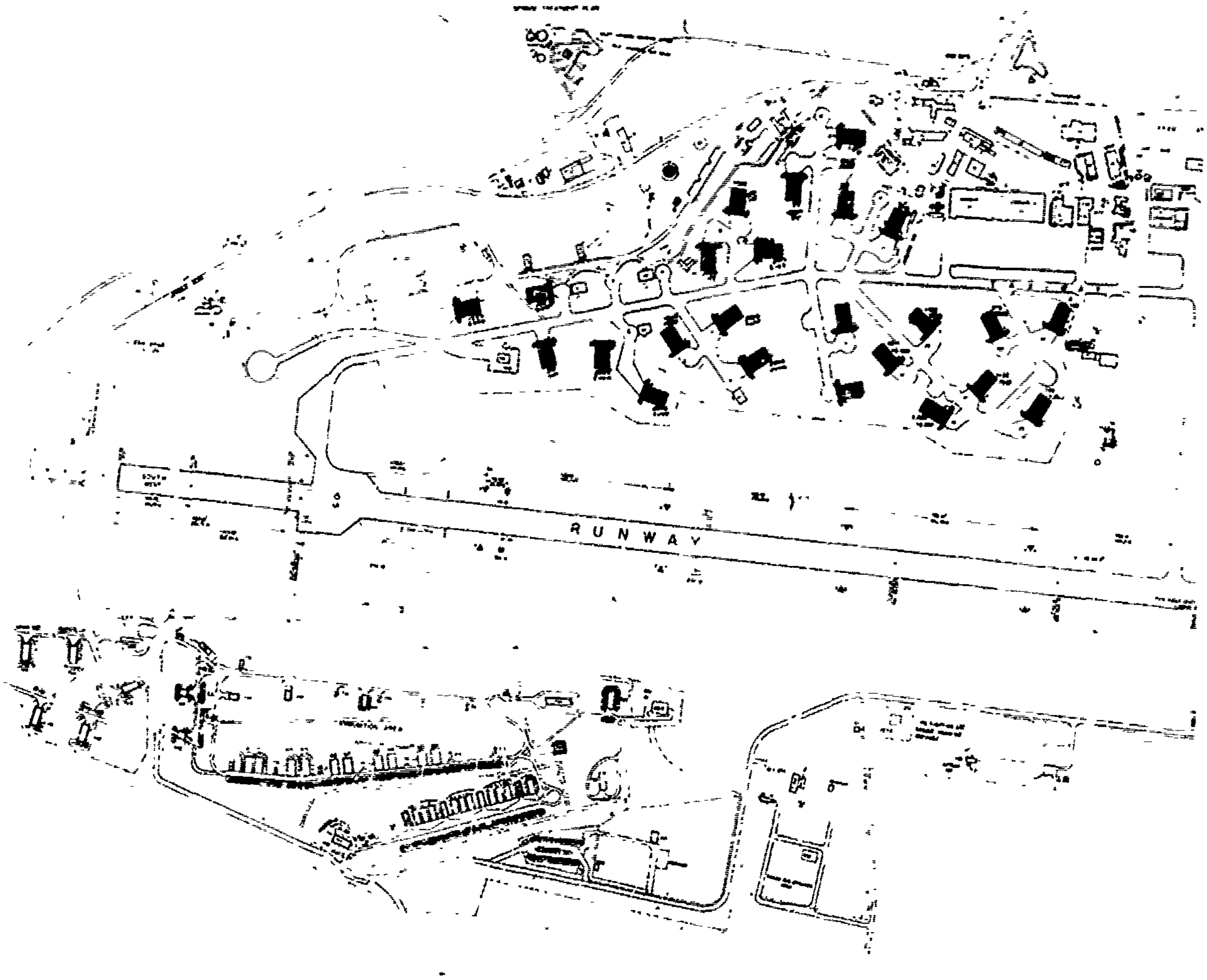

Figure 3-View of Spangdahlem Air Base showing relationship of explosive storage areas and aircraft shelters.

Figure 3 is a view of Spangdahlem Air Base showing the current relationship between the ammunition storage area and the aircraft shelters.

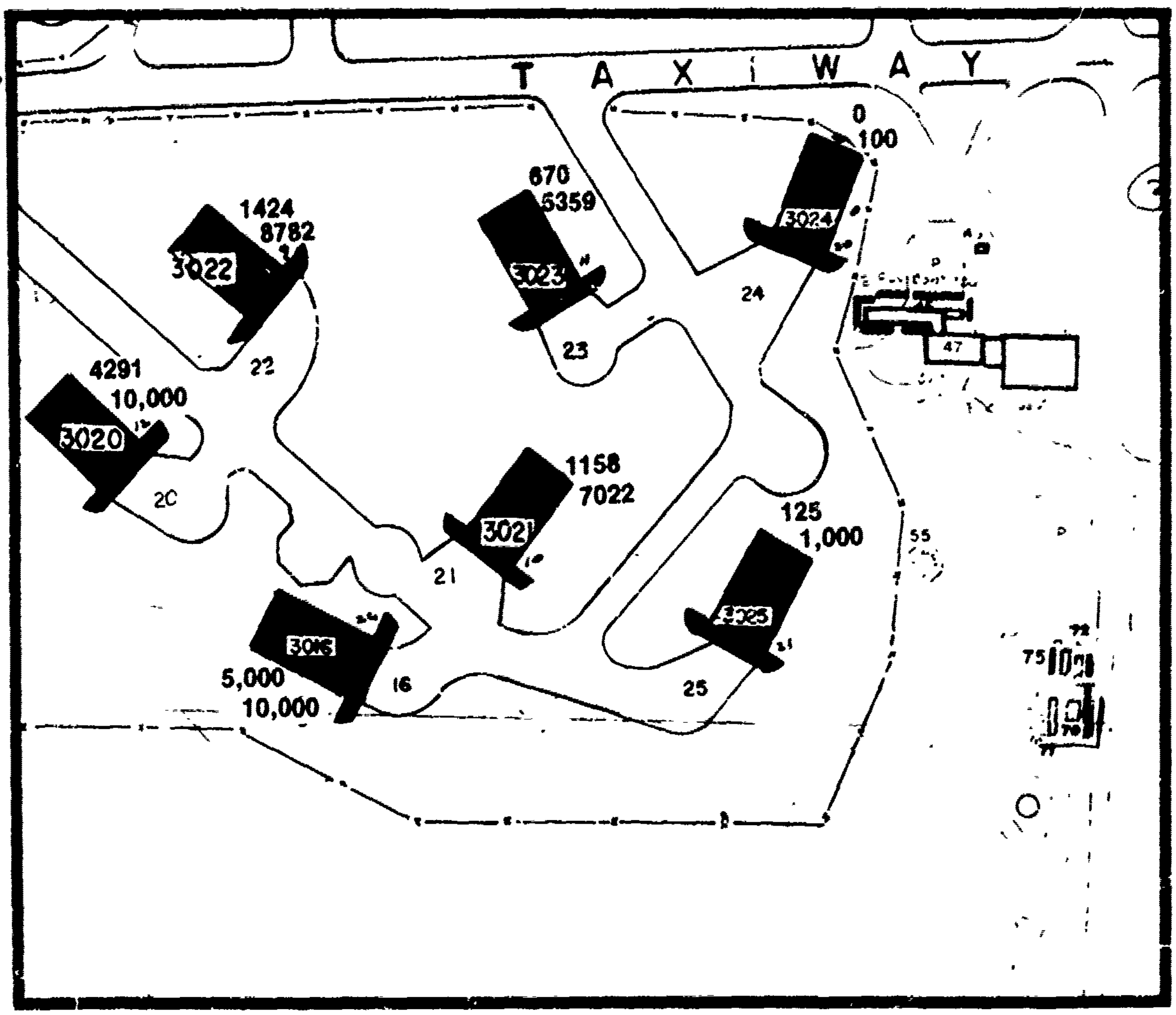

Figure 4 Portion of Spangdahlem Air Base showing A/C shelter current explosive weight limits and new explosive weight limits based on estimated new QD values.

Figure 4 is a blow up of a small portion of Spangdahlem's aircraft shelters. As an example of the direct benefits available from this test series the numbers beside each shelter indicate the current explosive weight limit and the new explosive weight limit based on the estimated new QD values. Additionally, based on estimated new QD values, there is now room for open munitions storage areas between the runway and the aircraft shelters.

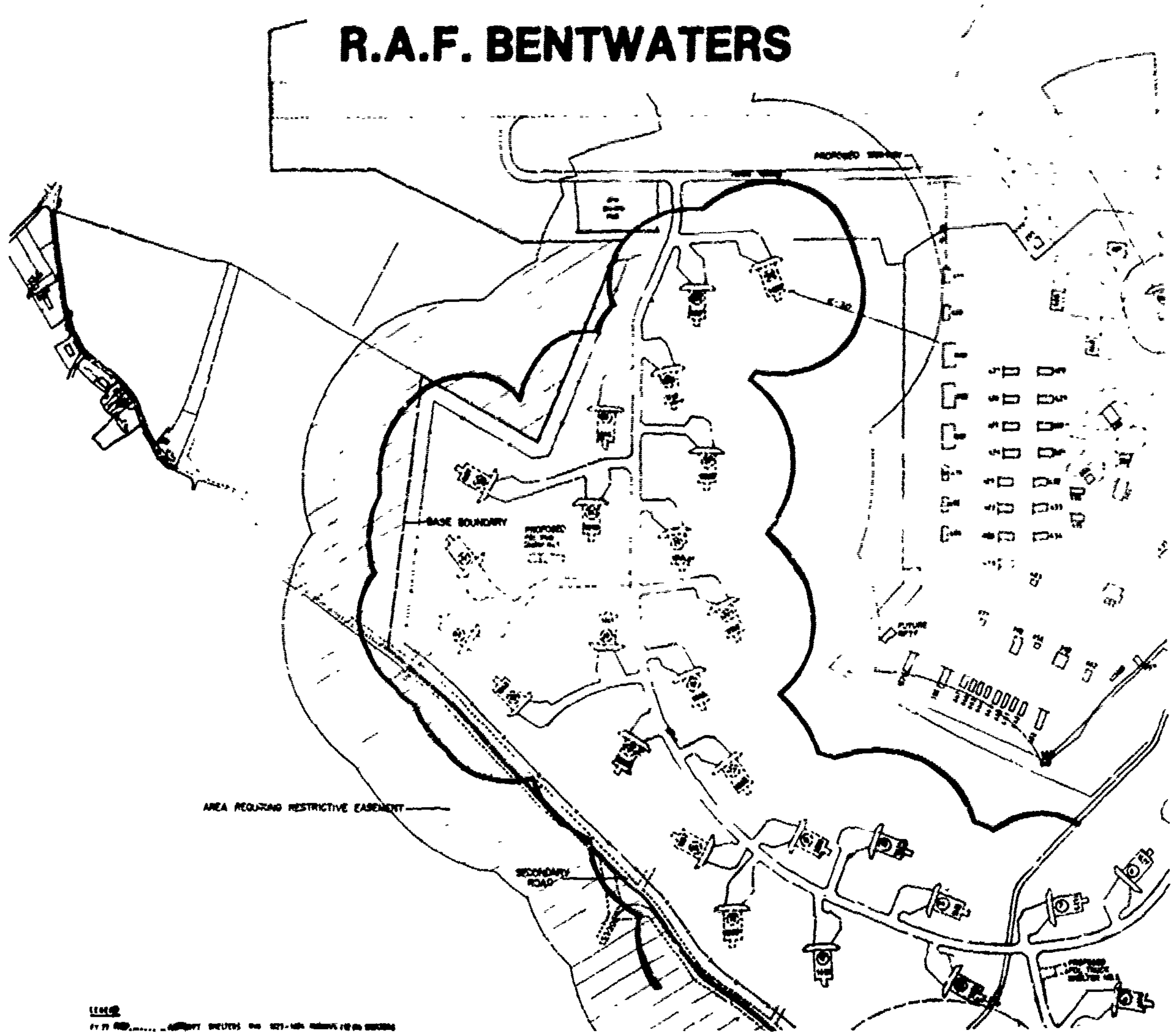

Figure 5
RAF Bentwaters Air Base with proposed A/C shelter sites and related safety areas.

Another example is the RAF base at Bentwaters. Figure 5 shows the proposed aircraft shelter layout. The safety restricted area goes well across the base boundaries. Ammunition storage in the first 8 explosive storage buildings is currently restricted to 59 tons. If the estimated test QD values are realized, explosives storage in these buildings could be raised to approximately 170 tons, or a 188% increase in capacity. Similarly the current shown restricted area around the aircraft shelters is for 5,000 lbs. of explosives storage in each shelter using a QD-value of 40. If this value is reduced to 20, as expected, then either (1) the safety area could be reduced to the smaller circled area or (2) explosive storage in the shelters could be increased to 40,000 lbs. per shelter keeping the original safety area.

PREDICTION OF THE BLAST AND DEBRIS HAZARD FROM AN ACCIDENTAL EXPLOSION IN A THIRD GENERATION NORWEGIAN AIRCRAFT SHELTER

by

P. K. Moseley
M. G. Whitney

ABSTRACT

The location of military aircraft shelters in Norway has created concern in recent years due to the blast and debris hazards which could result from an accidental internal explosion of ammunition stored in cubicles located in the floors of the shelters. A study was conducted to correlate an approximate engineering analysis with experimental results of model scale tests to determine a method to predict the blast field characteristics outside a third generation Norwegian aircraft shelter and the maximum expected debris distances from fragmentation of such a shelter following an explosion. Using shelter breakup patterns observed in the model tests, fragment velocities and maximum probable ranges are calculated based on internal loading of the shelter walls and roof by the resultant shock waves from the explosion. These fragment characteristics are compared to those which can be measured in the model tests. Also, external blast is both analytically and experimentally determined in several directions outward from the shelter. Based on the information obtained from the model tests and the engineering analysis, existing quantity distances for ammunition stored in an aircraft shelter may be more conservative than necessary. The prediction methods having the best correlation with the experimental results presented in this paper will provide necessary computational estimates for explosions in structures of analogous design for which model tests cannot be conducted for financial or other overriding factors.

I. INTRODUCTION

The location of military aircraft shelters in Norway has created some concern in recent years due to the blast and debris hazards which could result from an accidental internal explosion of ammunition stored in chambers located in the floors of the shelters. This study involves the correlation of an approximate engineering analysis with experimental results of model scale tests conducted in Norway to determine a method to predict the blast field characteristics outside a third generation Norwegian aircraft shelter and the maximum expected debris distance from fragmentation of such a shelter following an explosion. Due to the lack of information available regarding the blast and debris problem, a prediction method is needed for the particular problem of an accidental explosion in an ammunition chamber in the floor of a shelter. When an explosion occurs within such a structure, blast and fragments can cause serious damage to neighboring structures and can also affect personnel in the vicinity of the shelter. The walls of the shelter itself can fail and become sources of fragments which can be projected some distance and damage nearby structures or injure or kill base personnel. However, existing quantity distances for ammunition stored in the aircraft shelter may be more conservative than necessary. Initial indications from the analysis and the preliminary test results are that these quantity distances may be reduced. When the model tests are completed, the prediction methods having the best correlation with the experimental results will provide necessary computational estimates for explosions occurring in structures of analogous design for which model tests cannot be run for financial or other overriding factors. The preliminary results of the approximate engineering analysis and a brief overview of the model scale tests will be presented in this paper.

II. METHODS FOR PREDICTING EFFECTS OF INTERNAL BLAST LOADING

Internal blast loading was considered in order to determine velocities and, eventually, ranges of fragments from the shelter. Figure 1 shows a sketch of the typical Norwegian aircraft shelter studied in this analysis. The charges are stored in the underground storage room which can be seen in the left side of the shelter. Although not indicated in the figure, the shelter is covered by a layer of dirt.

The loading from an explosive charge detonated within a structure, whether vented or unvented, consists of two almost distinct phases. Reflected blast loading defines the first phase. It consists of the initial high pressure, short duration reflected wave, and perhaps several later reflected pulses arriving at times closely approximated by twice the average time of arrival, at the chamber walls. The later pulses are usually attenuated in amplitude because of irreversible thermodynamic processes. These pulses can be very complex in waveform because of the complexity of the reflection process within the structure. Maxima for the initial internal blast loads on the aircraft shelter can be estimated

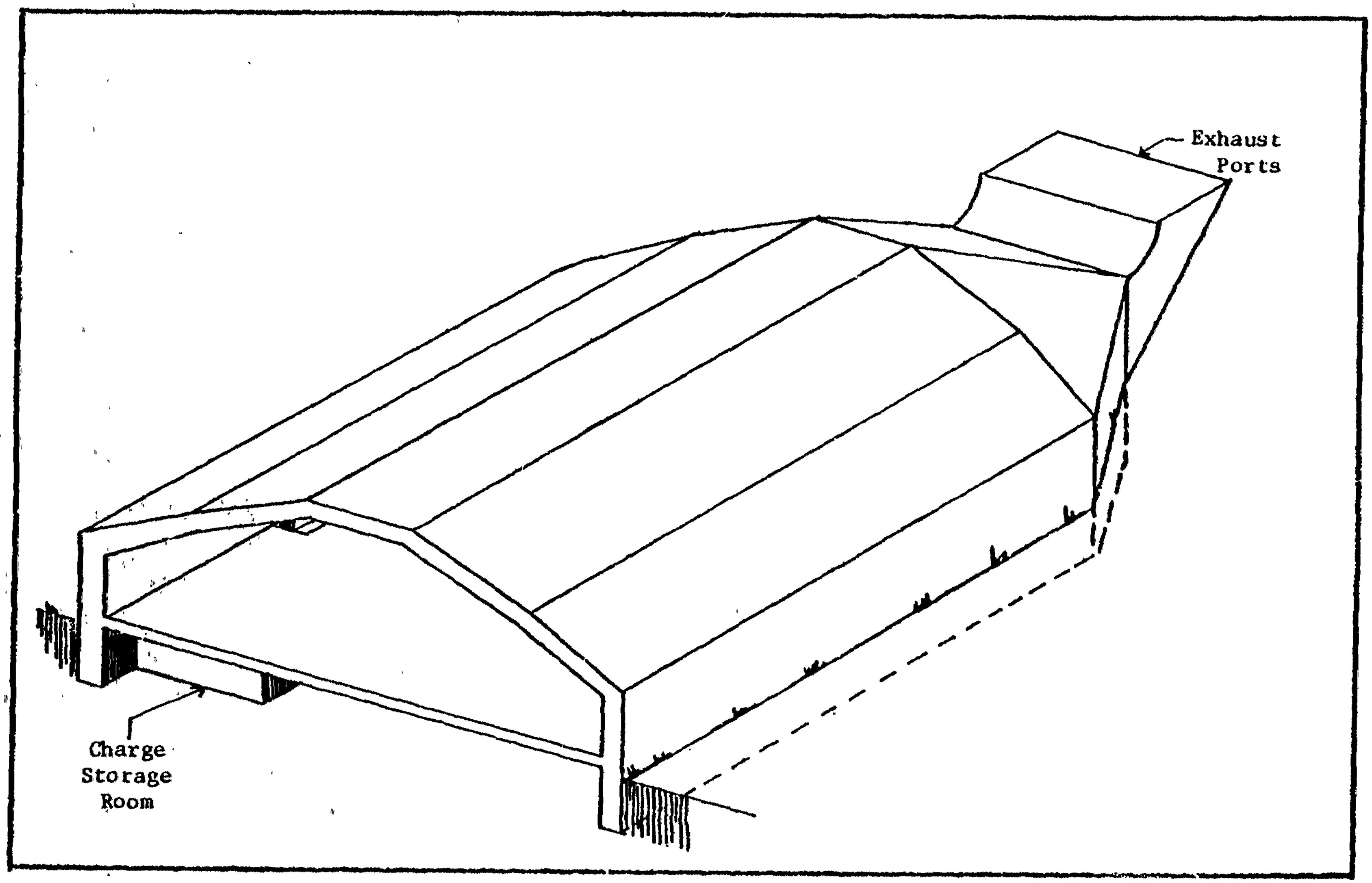

Figure 1. Typical Norwegian Aircraft Shelter

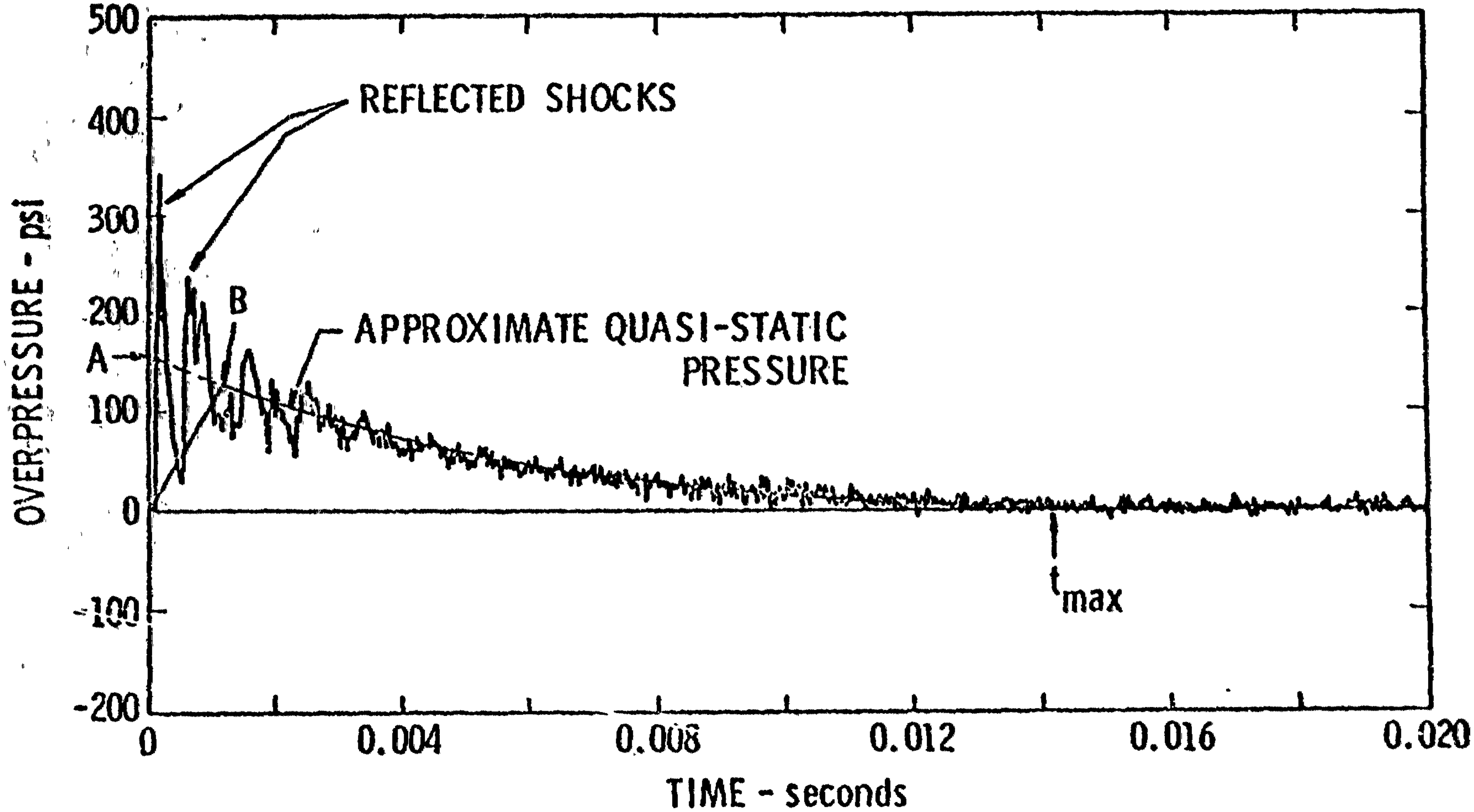

Figure 2. Typical Time History of Internal Pressure at Inner Surface of a Suppressive Structure (Reference 1)

from scaled blast data or theoretical analyses of normal blast wave reflection from a rigid wall. The shock waves reflected inward from the different surfaces of the shelter will coalesce and strengthen as they implode toward the center of the structure, then re-reflect to load the structure again. The second shocks will probably be somewhat attenuated, and after several such reflections, the shock wave phase of the loading will be complete.

The second distinct phase of the blast loading in an internal detonation occurs as the pressure of re-reflected shocks decays, and eventually settles to a slowly decaying level dependent upon chamber volume, structure vent area, and energy release of the explosion. This phase of the loading is known as the quasi-static pressure region. A typical pressure-time history at the inner surface of a chamber experiencing an internal detonation is shown in Figure 2 [1]. The blast history is characterized by the initial shock loading phase (which includes several reflected shocks) followed by the slowly decaying quasi-static pressure phase.

In order to characterize the blast loading on the inner surface of the shelter, two approaches were taken. One approach uses several simplifying assumptions and is relatively easy to calculate, while the second approach follows methods which more accurately define the real situation and, therefore, is more difficult to consider. The methods are as follows:

(1) The first method assumes that the charge is located at ground level the same distance from the door as to the center of the ammunition cubicle, but centered in the shelter (Figure 3). Also, the

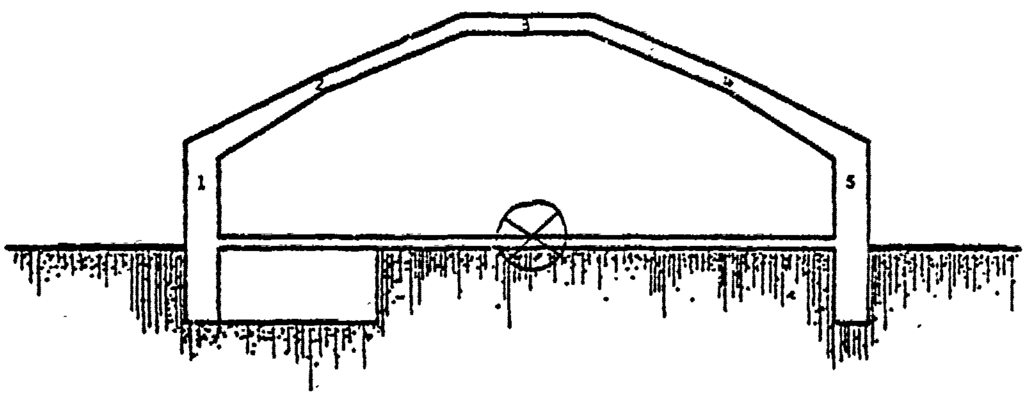

Figure 3. Identification of Surfaces (Cross-Sectional View)

charge is assumed to be spherical, i.e., it is treated as a point charge. As mentioned earlier, the blast loading can be separated into two phases, initial shocks and the quasi-static pressure realm. As suggested by reference 2, in a slowly responding structure, the initial reflected shocks can be combined and treated as a single shock of amplitude equal to 1.75 times the peak pressure and with impulse considered as 1.75 times the impulse at the position in question. Also, in order to simplify calculations, only reflected pressure and impulse from air blast curves are considered. This assumption ignores oblique loading of the surfaces. Because the charge is located on the ground surface, the ground is treated as an ideal reflecting surface and the charge weight considered in the analysis shall be twice the quantity to be stored in the shelter. Using these assumptions, blast pressure and impulse on a shelter surface can be characterized as a function of distance from the charge location. Hence, one can determine the closest and farthest distance from the charge to a shelter surface, choose several standoff distances (R) between these boundaries, and calculate pressure (P) and impulse (i) as discussed. The results can then be plotted as P or i versus R and a smooth curve can be drawn through the plotted points. The peak quasi-static pressure can be determined using Figure 4. As mentioned earlier, the quasi-static pressure (as well as initial shocks) is a factor in determining initial fragment velocity. Results of these calculations shall be discussed at the end of this section.

(2) The second method of determining blast loading involves procedures which are expected to describe blast characteristics more closely than that suggested above. This method assumes a charge location within the bounds of the ammunition storage area. It combines the use of a volume ratio method and results of an Eulerian computer code to be described later to determine the loading on the individual surfaces of the shelter.

Surfaces away from the charge encounter increased focusing due to the shape of the roof. It was felt that a ratio of the volume enclosed by a spherical shock front (of radius equal to slant range) to the volume of the chamber inside the blast wave front could be used to determine an equivalent charge weight for various distances from the charge center. In order to accomplish this, integration of a section of a sphere contained in the shelter shape was necessary. In order to simplify the integral, almost the exact cross-sectional shape of the chamber was used and assumed constant from the door to the rear of the chamber; i.e., the complex rear structure with the exhaust portal and sloping roof was ignored. Figure 5 depicts a floor and cross-sectional view of the regions in the shelter which were used to obtain integration limits for volume and, thus, equivalent charge weights. By selecting various slant ranges, R', which correspond to points on the walls and roof of the shelter, Figure 6 was created for obtaining charge weights for a wide range of values of R'.

If the surfaces in the simplified shelter shape are numbered as in Figure 3, the volume ratio method can be utilized in obtaining blast parameters for surfaces 3, 4, and 5. Because the charge is located near one side, the expected multiple reflections resulting from the geometry of the wall, roof and storage chamber should coalesce as a single shock front at some distance from the ammunition cubicle. Coalescence is assumed to occur before the blast wave reaches those surfaces farther away from the charge

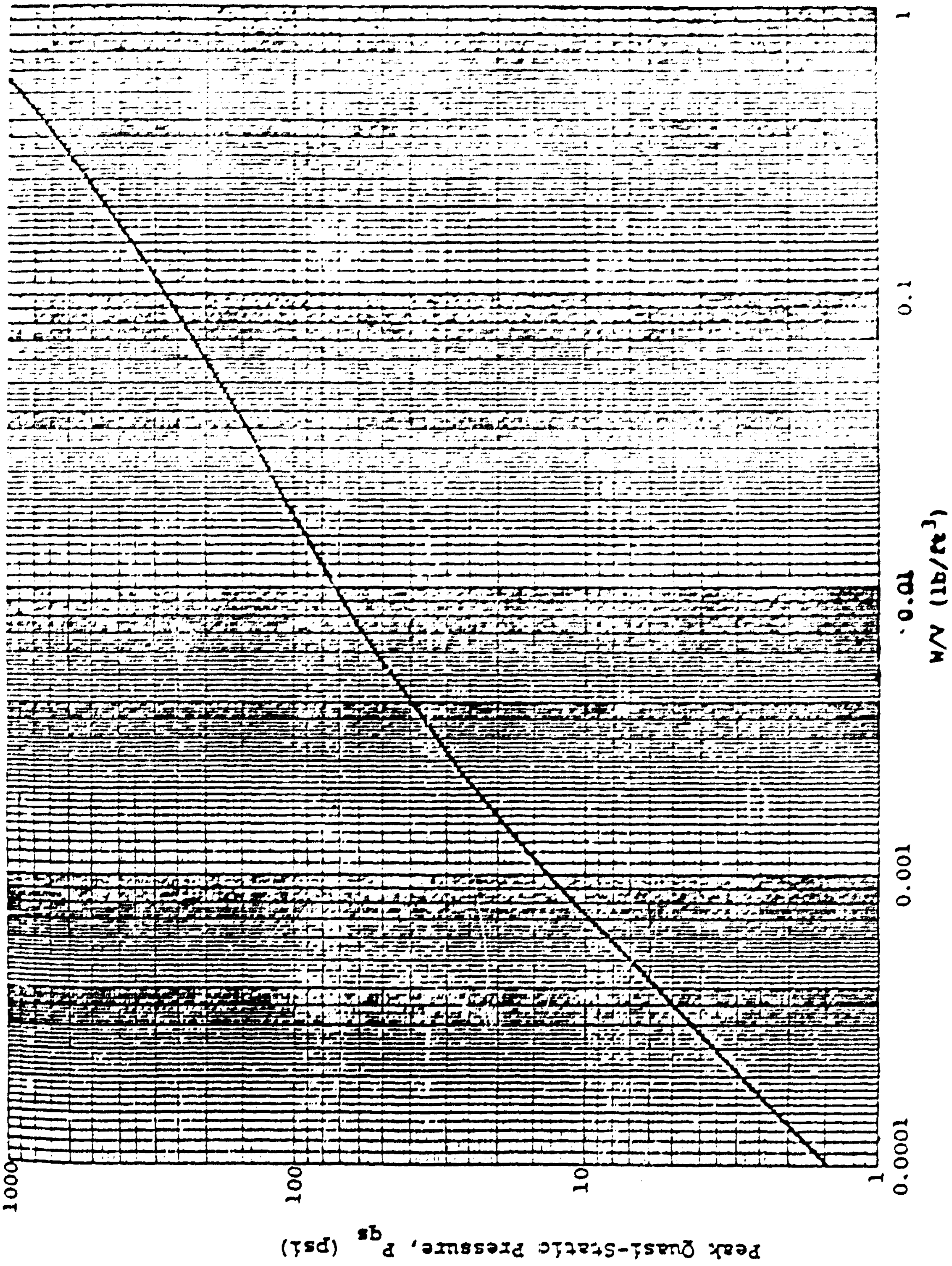
Peak Quasi-Static Pressure, P_{qs} (psi)
1000
100
10
1
W/V (lb/ft^3)
0.0001
0.001
0.01
0.1
1

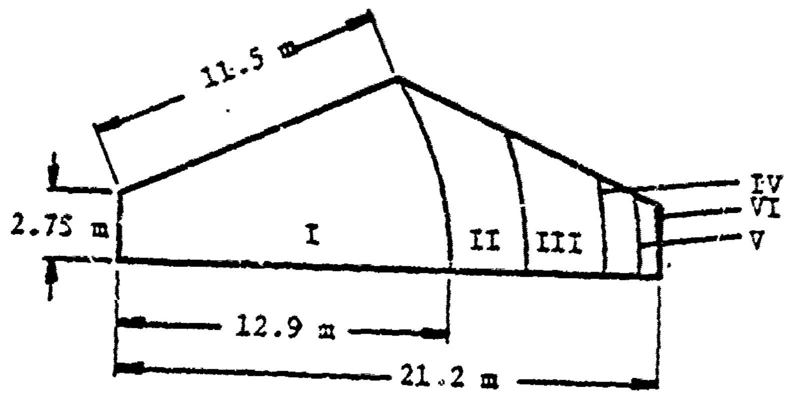

Cross-Sectional View

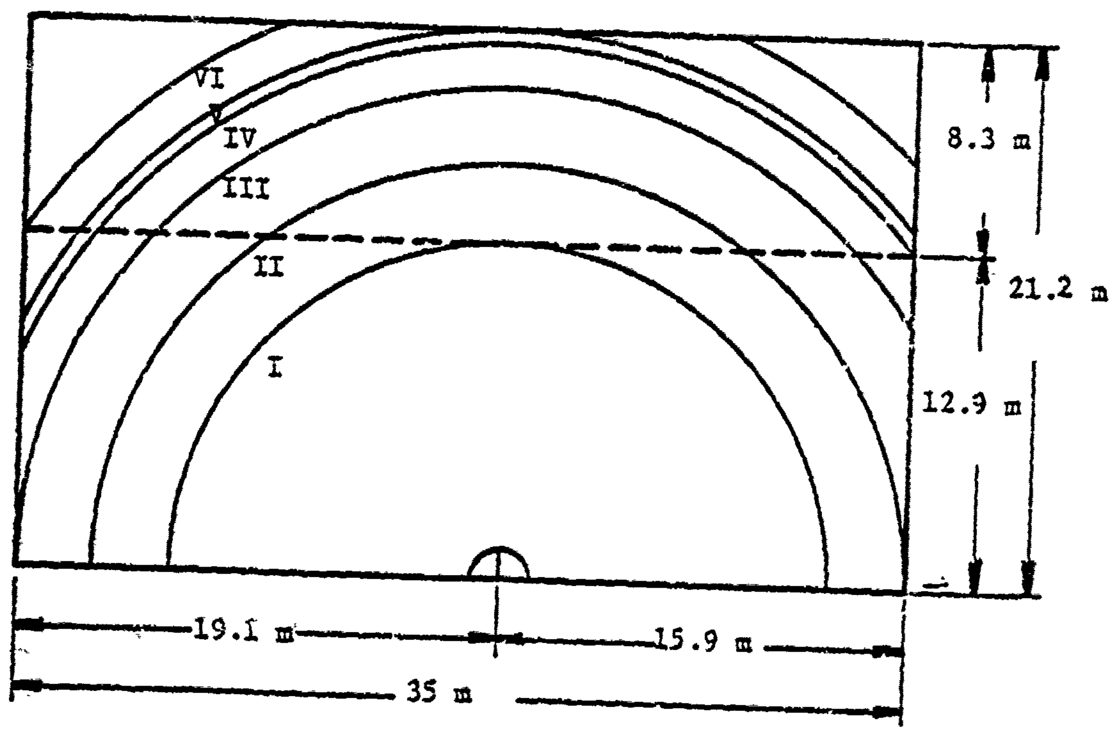

Floor View

Figure 5. Regional Representation for Establishment of Integration Limits

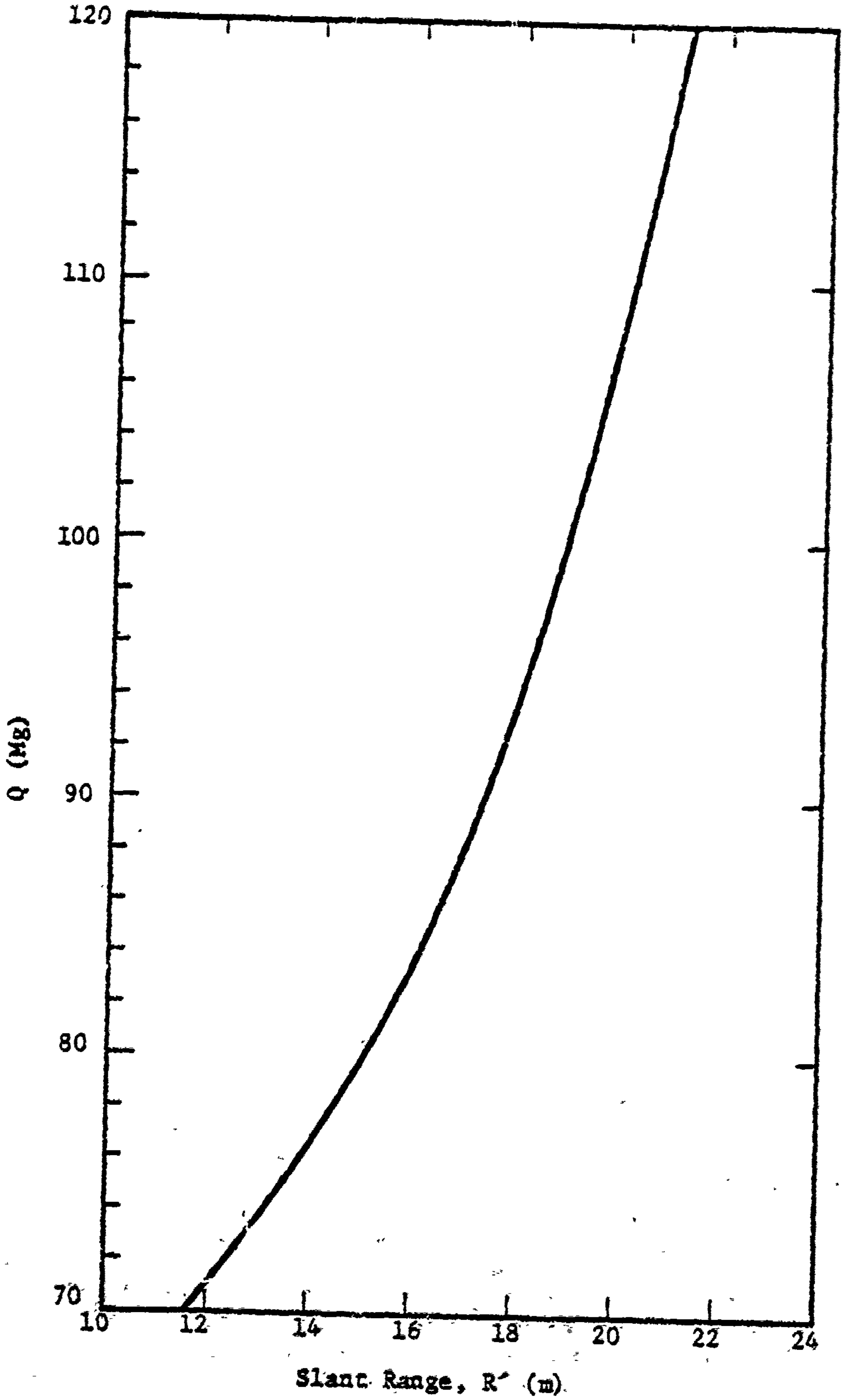

Figure 6. Equivalent Charge Weights for Various Slant Ranges

location; thus, the shock front could resemble a blast wave from a spherical charge located at ground surface near the sidewall next to the ammunition cubicle.

Surfaces 1 and 2 located very near the ammunition cubicle, however, should not be treated in this manner. These surfaces require a different method of determining pressure and impulse along their respective lengths. The location of the charge in the cubicle will be along the cubicle wall opposite the lift platform. Because the ammunition storage area runs almost the entire length of the shelter and ammunition is stored along the inside wall, this situation can be approximated by a line charge. It is believed that these two walls are loaded and reloaded several times and that they break into extremely small fragments under this load. However, there is an extreme lack of experimental data for close-in line charges. In order to obtain an estimate of how these surfaces are loaded, the two dimensional Eulerian computer code TUTTI was utilized.

The TUTTI program is a two-dimensional, Eulerian hydrodynamic code that is based on fluid-in-cell techniques. It has multiple material capability. In the present application, a LSZK detonation products equation of state is used for the explosive. Being two-dimensional, either a planar or axisymmetric analysis may be treated. The code is structured to allow for fluid motion around or through an arbitrary number of surfaces, thus permitting flow over solid obstacles or through perforated patterns of walls. The theory used to develop the code is presented by Gentry, et al. [3]. However, significant modifications have been made by U. S. Naval Surface Weapons Laboratory and by SwRI.

The flow field is divided into an arbitrary number of cells of various sizes. As used for the computational results presented herein, a planar geometry of fairly coarse grid description representing the confines of the shelter is provided in Figure 7. Explosive, located in the munition storage bay, is detonated to release high energy detonation product gases into the surrounding, confined air space. An ideal gas equation of state for air and the LSZK equation of state for TNT are used in the solution procedure. The solution procedure algorithms simultaneously solve the equations of conservation of mass, momentum and energy for hydrodynamic flow. Artificial viscosity terms are provided in the equations to assure that the numerical procedure is both stable and accurate. An internally generated time step similar to the current condition insures a time-stable solution.

Pressure gauges were placed at locations marked G in Figure 7. A line charge is placed in a corner of the ammunition cubicle. The program was allowed to run until the gauges along surfaces 1 and 2 had received maximum pressure from the reverberating shock waves. A pressure-time trace was output which was integrated to obtain impulse at each gauge location. The results indicate a much stronger loading on these two surfaces than on the other walls. Because surface 1 receives an especially strong load and gauge locations were very close together, an average impulse of 2.61×10^5 Pa. sec will be used for all points along that surface.

```
 NOR. A/C SHELTER
T= 0.          N=    0 *=MAXQ, .=CONTACT SURFACE, S=SOLID.
  0 + + + + + + + + + + + + + + + + + + + + + + + + + + + + + + + + + + + +
  1 + G               S S S S S S S S S S S S S S S S S S S S S S S S S S +
  2 +                 S S S S S S S S S S S S S S S S S S S S S S S S S S +
  3 +                 S S S S S S S S S S S S S S S S S S S S S S S S S S +
  4 +                 S S S S S S S S S S S S S S S S S S S S S S S S S S +
  5 + G                       G       G       G         G     G         G +
  6 +                                                                     +
  7 + G                                                                 G +
  8 +                                                                     +
  9 + G                                                               G S +
 10 + S S                                                           S S S +
 11 + S S S S G                                               G S S S S S +
 12 + S S S S S S   G                                   G   S S S S S S S +
 13 + S S S S S S S S S                               S S S S S S S S S S +
 14 + S S S S S S S S S S S S G       G       G S S S S S S S S S S S S S +
  0 + + + + + + + + + + + + + + + + + + + + + + + + + + + + + + + + + + + +
```

Figure 7. Coarse Description of Shelter Geometry
(Upside Down)

To obtain blast parameters along surfaces 3 through 5 and to account for oblique reflections, curves of pressure and impulse versus a scaled distance down a surface plotted from accumulated experimental data from single and multiple detonations for several Z values (or values of $R/Q^{1/3}$) in a previous SwRI project (Reference 4) were used. These curves are depicted in Figures 8 and 9. Loading on surfaces at the rear of the shelter shall be assumed to be reflected and the charge weight that was determined from the volume ratio at the distance to the respective surface will be used. As with the first procedure discussed earlier, peak quasi-static pressure can be determined from Figure 4.

As discussed previously, an average impulse of 2.16×10^5 Pa·sec is used for fragments from surface 1. Pressures and impulses for surfaces 2 and 5 are presented in Figures 10 and 11 as examples of blast parameters calculated using both the computer code and the volume ratio method.

III. ESTIMATION OF FRAGMENT BREAKUP

The analytical determination of a breakup pattern from an explosion inside an aircraft shelter presents a difficult problem. One possible method of estimating fragmentation would be to examine the spall stress and structural response of the shelter. Spall stresses were accumulated for various regions of the shelter. It is felt that spall can influence the structural integrity of the structure and its breakup pattern. Also, calculations were made to compare applied loads with structural response. "Beam strip" theory was used, and several "beams" were chosen which represent the various areas of the shelter. In other cases where less explosive is involved, one may be able to choose a fragmentation pattern by considering a combination of spall and bending results. However, from reviewing films of the initial model tests of the aircraft shelter, spall does not seem to be the determining factor in influencing the breakup of the shelter. Thus, some other method must be considered to predict a fragmentation pattern.

Due to the shape and structure of the shelter and the large amount of explosive involved, estimates of a breakup pattern based on spall stress and structural response is probably not valid. The results of the preliminary 1:20 scale tests were used to establish fragment sizes. Breakup is actually dependent on strain rate, which is not scaled in these tests. However, since the material properties in the full and model scale are identical, any dependence of these properties on strain rate would not be great. Thus, the prototype breakup will probably closely resemble the model breakup. This similarity of breakup, however, could most likely only be proven by comparing breakup patterns from small and large scale tests.

Of the preliminary tests, two involved the maximum scaled amount of explosive. The debris in these two tests were characterized by several large pieces of the shelter roof and walls and otherwise fairly small

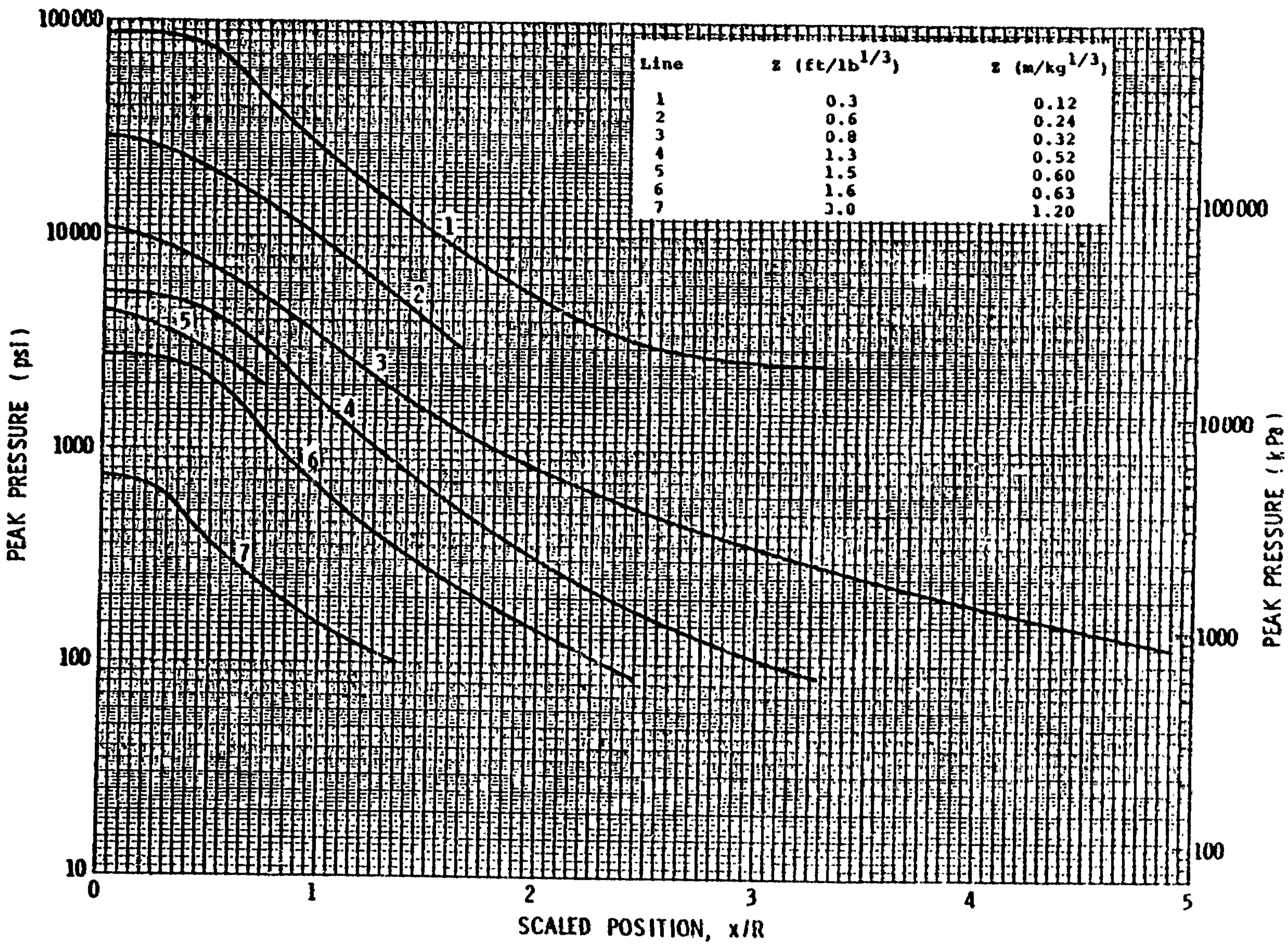

Figure 8. Peak Pressure versus Scaled Position for Different Scaled Distances (Reference 4)

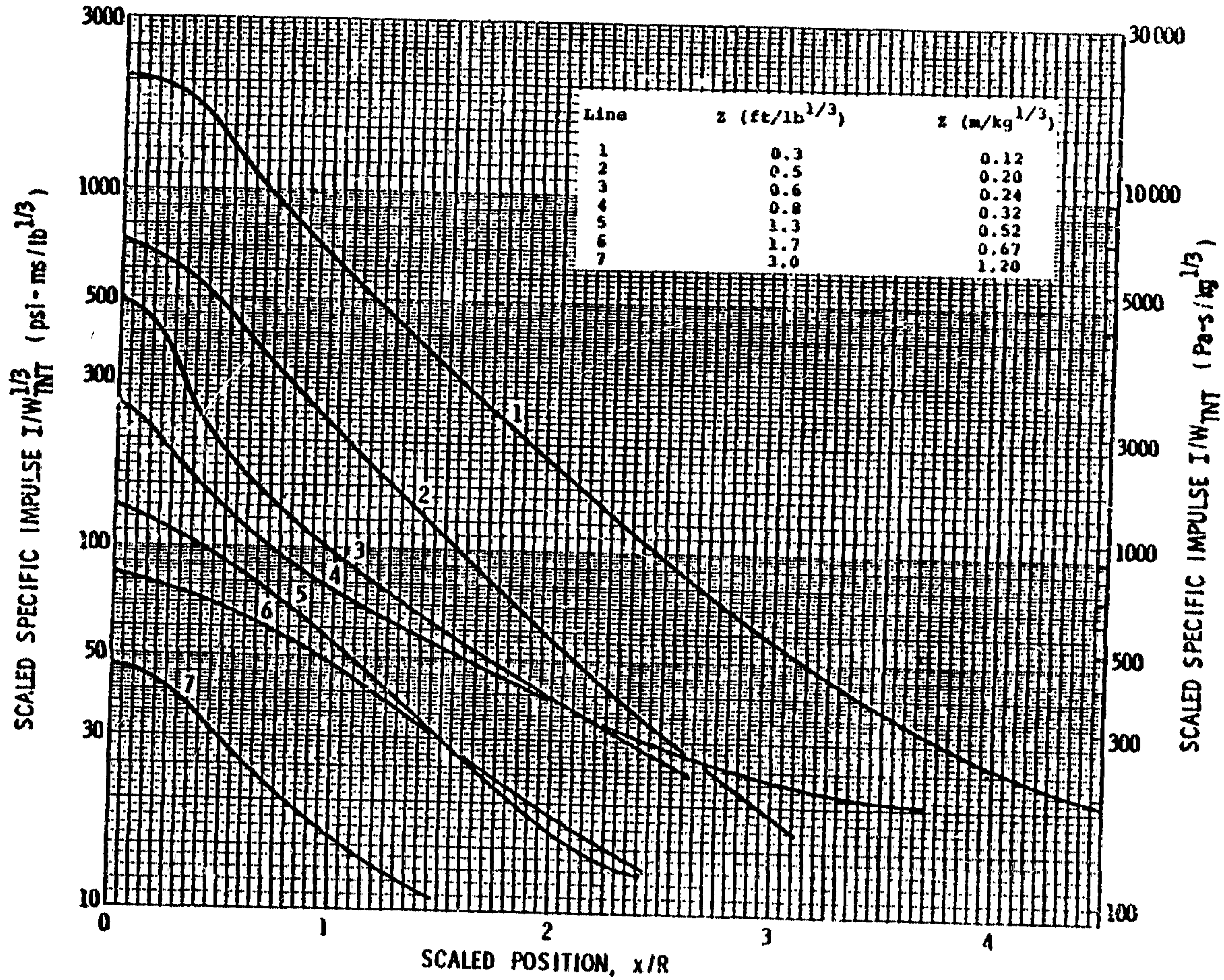

Figure 9. Scaled Specific Impulse versus Scaled Position for Different Scaled Distances (Reference 4)

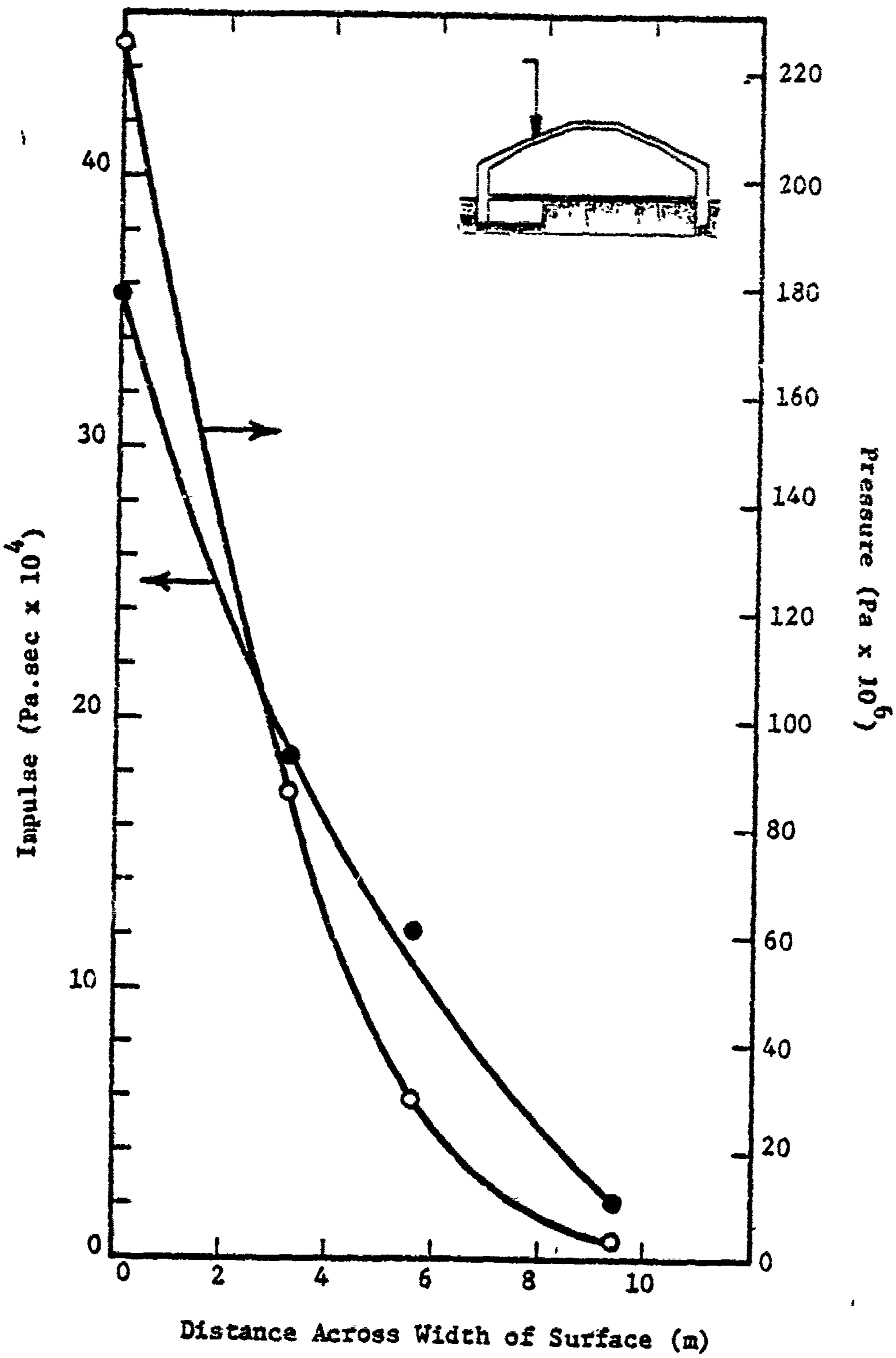

Figure 10. Pressure and Impulse Along Surface 2

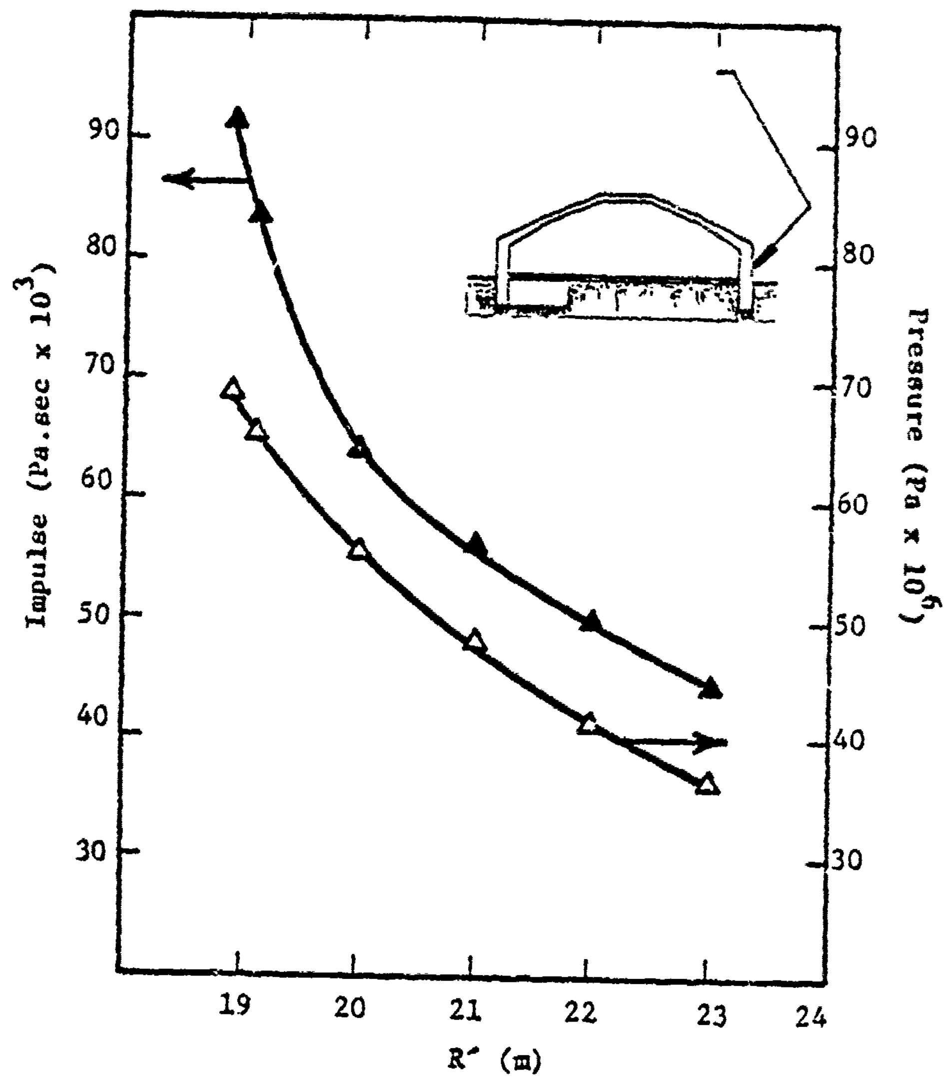

Figure 11. Pressure and Impulse Along Surface 5

fragments. The actual debris density was very low. If the assumption is made that the initial motion is independent of gravity, a fragment from the model will travel at the same initial speed and have the same trajectory angle as its counterpart from the prototype. Thus, the use of a breakup pattern similar to the breakup observed in the preliminary model tests should be a reasonable estimate of the actual breakup which will occur in an explosion in the prototype.

The results of the scaled tests are that fragment sizes range from very small chunks, particularly near the charge, up to complete panels such as from surface 5. Therefore, for surfaces 1 and 2 only small fragments were considered, and for surfaces 3 through 5 several fragment sizes were considered ranging from very small fragments up to the entire panel size. Surfaces at the rear of the shelter were considered as the size of the entire panel. Details on the assumed fragment sizes and locations are listed in Table 1.

The internal loading and structural patterns such as spacing between rebar in the concrete walls of the shelter can only suggest possible breakup following an explosion. A study of fragmentation using all the model test results will provide better insight to the actual breakup pattern which can occur in the full scale shelter.

IV. PREDICTION OF FRAGMENT VELOCITIES

The techniques used to determine the initial velocity of fragments from the shelter are described in this section. Basically, two different methods to predict initial velocities were considered. The first method consists of two phases. The first phase involves the initial impulsive loading from the blast wave. The second phase includes the expansion of the gases produced by the explosion products and the venting of these gases around the fragments as they leave the shelter. The second method is to determine initial velocity due to the buildup of quasi-static pressure alone in the shelter prior to fragmentation.

Assuming the surfaces receive an initial load followed by a force contribution of the expansion of the gaseous explosion products, the velocity of a particular fragment from a surface due to the shock load alone can be determined from

$$V = \frac{iA}{M}$$

where i is reflected specific impulse,
A is the area of the fragment, and
M is the mass of the fragment.

Table 1. Fragment Sizes and Locations

I.D. NO.	DESCRIPTION OR LOCATION OF ORIGIN	SURFACE AREA (m^2)	MASS (kg)
1	Surface 1: Size of rebar spacing	0.04	*1.13×10^2
2	Surface 2: Size of rebar spacing	0.04	7.87×10^1
3	Surface 2: Chunks toward the roof	42.21	6.75×10^4
4	Surface 3: Whole panel	108.0	1.86×10^5
5	Surface 3: 1/2 panel	54.0	9.30×10^4
6	Surface 3: 1/4 panel	27.0	4.65×10^4
7	Surface 3: 1/10 panel	10.8	1.86×10^4
8	Surface 3: 1 m^2 chunk	1.0	1.72×10^3
9	Surface 3: Size of rebar spacing	0.04	6.89×10^1
10	Surface 4: Whole panel	253.3	4.98×10^5
11	Surface 4: 1/2 panel	126.6	2.49×10^5
12	Surface 4: 1/4 panel	63.32	1.25×10^5
13	Surface 4: 1/10 panel	25.33	4.98×10^4
14	Surface 4: 1 m^2 chunk	1.0	1.97×10^3
15	Surface 4: Size of rebar spacing	0.04	7.87×10^1
16	Surface 5: Whole panel	74.25	*2.19×10^5
17	Surface 5: 1/2 panel	37.12	*1.09×10^5
18	Surface 5: 1/4 panel	18.56	*5.48×10^4
19	Slanted back panel	22.0	*6.50×10^4
20	Triangular back roof section	6.67	1.47×10^4
21	Rectangular back top roof section	32.0	5.51×10^4
22	Chunk with exhaust portals	50.0	3.98×10^5

* Mass of dirt is neglected so ranges obtained will be conservative.

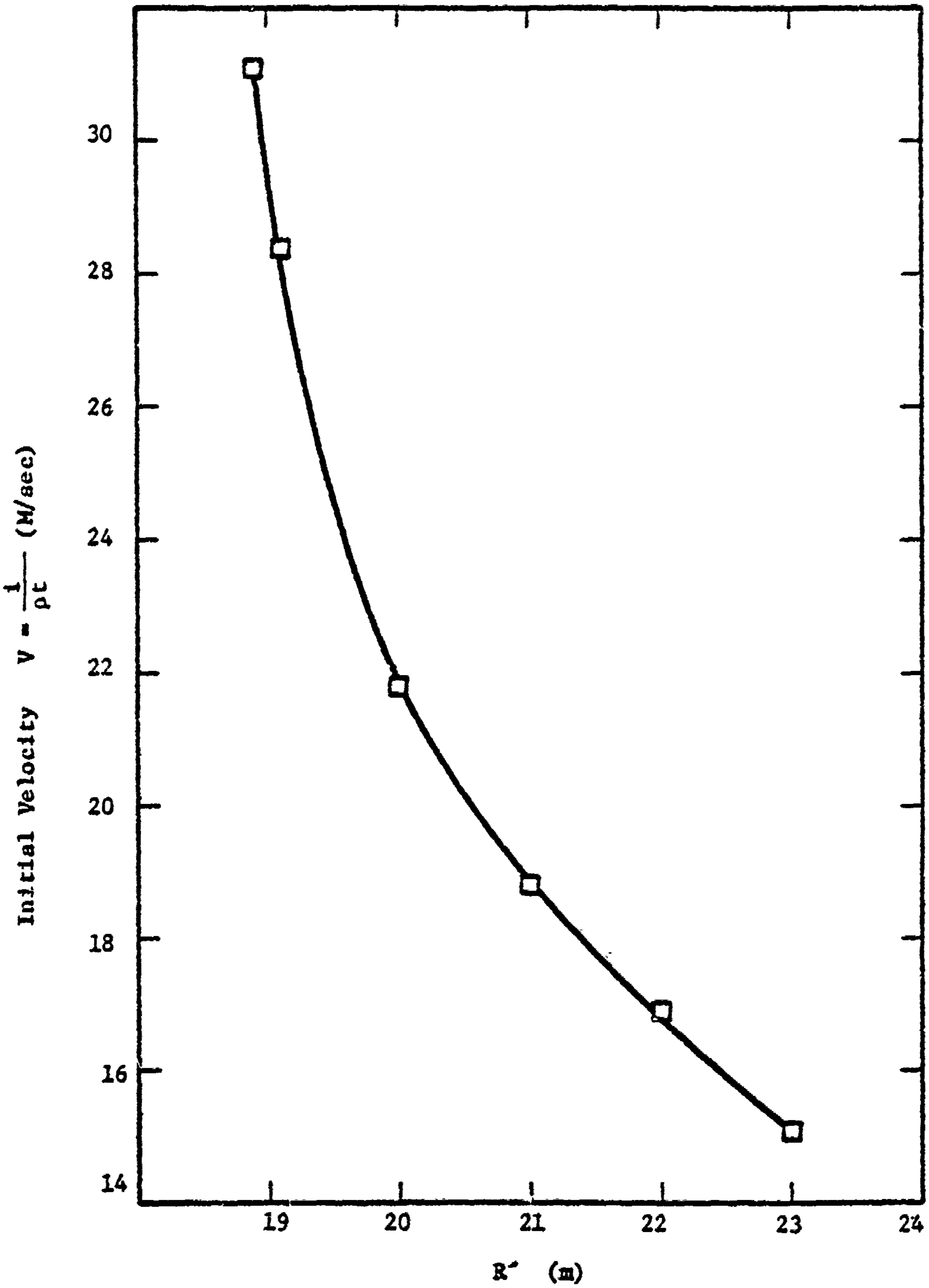

Figure 12. Estimated Velocity for Fragments From Surface 5

The impulse is extracted from the curve corresponding to the surface from which the fragment originated (see Figures 10 and 11). Slant range R′ is measured from the center of the assumed charge to the approximate geometric center of the fragment. To expedite prediction of velocity for any size fragment from a surface, figures, such as Figure 12, were created for surfaces 2 through 5 assuming an average thickness across each surface, i.e.,

$$V = \frac{iA}{\rho At} = \frac{i}{\rho t}$$

where ρ is the density of concrete, and
t is the average surface thickness.

These velocities are conservative in that the mass of the dirt cover is not included. The actual velocities of fragments originating from surfaces 1 and 5 will be reduced considerably because of the significant amount of dirt packed against these walls.

To obtain the velocity contribution caused by expansion and venting of the gaseous explosion products, the aircraft shelter was likened to a rupturing pressure vessel. A half cylindrical shape was assumed to simplify the burst. Utilizing the computer code CYLIN developed in a previous SwRI project (Reference 2), the assumed cylinder was allowed to fragment into ten panels (corresponding to twice the actual surfaces in the half cylindrical shelter), which already had obtained an initial velocity from the blast loading. Figure 13 shows the conceptualization of the cylinder separating into n fragments. The fragments are strips or panels which move

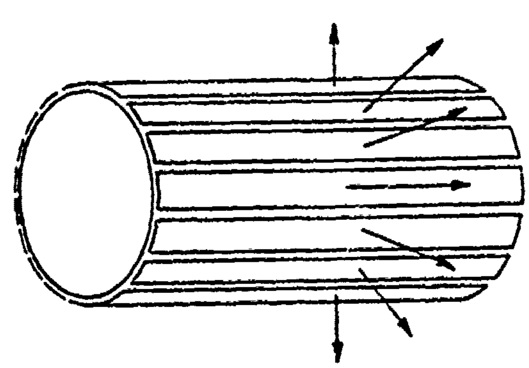

Figure 13. Conceptual Model of Bursting Confinement Vessel (Reference 2)

radially from the center of the cylinder. Motion of the door and heavy rear end of the shelter is not considered. A cylinder of length L and radius R is assumed to burst into n strip fragments of width d and thickness t. A cross section of each panel is a segment of the cross section of the cylinder having a segment height h and segment diameter d. In the analysis, the projected area of each strip is obtained from the surface area and the initial subtended angle of the strip at the center of the cylinder, or

$$A_p = 2LR \left[1 - \left(\cos \frac{2\pi}{n}\right)^2\right]^{0.5}$$

The area of a crack about any fragment at a given time is obtained by assuming the cracks only form lengthwise about the cylinder and by obtaining an equation for the crack width in terms of the initial radius of the cylinder and the radial distance r which the fragment has traveled at time t, or

$$W = \frac{2\pi}{n} [r(t) - R]$$

Thus, the crack area can be determined by

$$A_c = \frac{4\pi LR}{n} \left(\frac{r(t)}{R} - 1\right)$$

If an average initial velocity from the blast loading is calculated for fragments across each surface, this velocity can be input to the computer code as the initial velocity of equal strip fragments having mass equal to the mass of a given surface. The code is run once with a weighted average initial velocity to obtain the velocity contribution to a fragment from a particular surface due to the pressure buildup in the shelter. The result of this velocity contribution is approximately 17 m/sec. The addition of this velocity contribution to velocities from the initial blast loading provides initial velocities for input into the FRISB trajectory computer code for determining range of fragments from an explosion.

Another possibility which has been considered is that fragments from the walls and roof of the aircraft shelter receive an initial velocity solely from the buildup of quasi-static pressure following the explosion. To determine this velocity for a certain fragment, the computer code CYLIN is run, assuming no initial velocity before rupture of the cylindrical structure. If these assumptions are indeed valid, the fragments would start out at an initial velocity of approximately 35 m/sec. The distance a fragment will travel can again be determined using FRISB code results as described in the next section.

As a comparison to the velocities obtained using volume ratios to calculate equivalent charge weights (the main method described in this report), pressures, impulses and velocities were calculated for the simplified case where a spherical charge is centered in the shelter on floor level. Reflected pressures and impulses were assumed to be conservative. Velocities of fragments calculated in this manner compare quite favorably with the average weighted velocity of approximately 40 m/sec across all surfaces using the volume ratio method.

V. PREDICTION OF FRAGMENT RANGE

The range of a flying fragment from the exploding aircraft shelter is dependent on the lift and drag forces acting on the fragment. Two types of fragments are possible: (1) fragments whose geometry is such that both the lift and drag forces act on them during flight, i.e., long, relatively thin fragments and disc-shaped fragments; and (2) fragments whose geometry is such that only drag forces act with no contribution of lift forces. A method of predicting the distance traversed by a fragment was developed and computerized into a code entitled FRISB (Reference 2). In later work, a set of generalized curves was developed to estimate maximum fragment range by performing a model analysis to generate dimensionless parameters to describe the general problem, running the computer code FRISB to determine ranges for selected cases, and plotting the results as a series of curves (Reference 5).

Using the fragment sizes given in Table 1 at various locations on the shelter and trajectory angles obtained from studying the preliminary model test results, typical fragment ranges were calculated using the FRISB code. The distances traveled by fragments of the sizes studied in this analysis range from a few meters to a maximum of 140 meters.

These ranges are engineering estimates of probable maximum range of possible fragments. The ranges were determined using debris trajectories observed during the preliminary tests. If these same trajectory patterns appear in subsequent tests, the calculated ranges should be good predictors of distances traveled by full scale fragments from an actual explosion since the velocities are fairly low. However, it is possible for a fragment to "spin" and travel a much greater distance than reported here. Thus, to be positively conservative in predicting fragment ranges when quantity-distance standards are involved, one would have to use a maximum range obtained from the previously mentioned generalized curves for predicting maximum range (Reference 2). The probability that a fragment will spin like a disc and reach the maximum range obtained from these curves is very low. The calculated distances should provide good estimates of the actual trajectories of fragments from the aircraft shelter.

It should be stressed that the ranges reported here are based on trajectories of fragments in the preliminary model tests and velocities obtained using assumptions described in this report. The actual velocities should be lower mainly because (1) the mass of the dirt cover has been ignored in this analysis; and (2) the pressures and impulses were calculated assuming a charge location on floor level while the charge is actually in the ammunition cubicle beneath a concrete barrier, and its effects will be attenuated somewhat before reaching the inner walls of the shelter.

VI. EXTERNAL BLAST CHARACTERISTICS

Several methods of characterizing blast parameters as a function of distance from the shelter were considered for this study. Using the results of the external blast calculations, the effects of the blast wave were considered for structures and humans using methods discussed in Reference 2. Included are predicted distances at which minor structural damage, major structural damage, threshold of eardrum rupture, and threshold of lung damage occur for the various methods considered for determining the blast field.

The various methods of predicting the external blast are as follows:

(1) The simplest method for estimating external blast parameters is to consider a spherical charge that is not enclosed by the shelter, i.e., an open charge located on the ground surface. Also, one can assume that the ground surface acts as a perfect reflector; hence, twice the charge should be considered. Using standard scaled air blast curves for twice the charge weight, unscaled values of reflected and side-on overpressure, specific impulse and blast duration can be calculated. Results shall be given at the end of this section.

(2) Another method of estimating the blast field would be to subtract the predicted kinetic energy of shelter fragments from the "available charge energy" to solve for an effective charge weight. The "available charge energy" would be equal to twice the charge weight; once again, the ground is assumed to be a perfect reflecting surface. One could also subtract the strain energy imparted to the structure by the blast wave; however, review of preliminary model tests and consideration of some simple bending calculations reveal that the structure is grossly overloaded, and the strain energy should be negligible compared to the total energy available. Again, using the adjusted charge energy, standard scaled air blast curves can be used to predict unscaled air blast parameters as a function of distance from the charge. Results are given at the end of this section.

(3) The first two methods discussed consider a hemispherical blast wave with magnitude which is independent of direction (i.e., directionally from the front, back, or sides of the structure) and independent of whether the door is open or closed. Work done by Keenan and Tancreto (Reference 6) gives methods for predicting blast parameters in forward, back, and sideward directions about a vented chamber. However, differences exist between the dimensions of the aircraft shelter and the chambers considered in Reference 6. If the open door area is considered as a vent opening, the shelter resembles a rectangular box with a charge weight to volume ratio (Q/V) of 2.91 kg/m^3 and the charge located off center. Of the several types of chambers tested in Reference 6, the most similar to the aircraft shelter is a cubicle with one side open and the charge located in the geometric center. The charge to mass ratio is in the range of that tested by Keenan and Tancreto (1.01 - 4.01 kg/m^3). Also, the chambers tested by Keenan and Tancreto were designed to remain structurally intact which does not occur with the aircraft shelter. Despite these differences, Reference 6 was used to estimate blast parameters for comparison purposes.

Table 2 is a summary of damage predictions for the three external blast methods. Plots of pressure, duration (except method 3), and impulse versus distance are included in the report (Reference 8), however, they are not included here.

Table 2. Damage Predictions Using Different Blast Estimation Methods

Criteria	Distance (m)			
	Methods 1 and 2	Method 3		
		Front	Side	Back
Major Structural Damage	180	320	197	179
Minor Structural Damage	500	720	520	450
Threshold of Lung Damage	80	140	82	69
Threshold of Eardrum Rupture	120	218	131	117

VII. BRIEF SUMMARY OF MODEL TESTS

Based on the preliminary results of the approximate engineering analysis, recommendations were made for the remaining model tests currently being conducted in Norway. Tests are performed using scale 1:100 and 1:20 so that results can be compared to add credibility to the model scaling. Tests have already been conducted with the shelter door open and with the door closed. The blast and fragment characteristics with the door open or closed are not significantly different because the door is of relatively light construction compared to the rest of the structure, i.e., it will detach and vent much more quickly than the shelter roof and walls.

The different surfaces described in this paper are "color coded" on the models to enable a better determination of fragment origin when a test is completed. Also, numbers were placed at various distances down each colored surface to indicate origin. If the surface origin of the major fragments and fragment groups (areas where very small fragments cluster) can be determined, this information together with the terminal location of the fragments in relation to the shelter can be used to match trajectory angles to fragments using the test films and, thus, analytically develop plots of range versus polar ground angle which can be compared directly with similar plots of the experimental results. An example analytical plot is shown in Figure 14 using an estimated breakup pattern chosen from the fragment descriptions and trajectory angles assumed from the preliminary test films. (The door of the shelter points toward 270°, and angles are measured counter clockwise.)

Several 1:75 scale steel model tests were also conducted to try to determine the internal blast loads on the walls of the shelter experimentally. These results are being compared with the loads predicted in the engineering analysis. When all the model tests have been completed, all the experimental results will be compared to the analytical predictions to determine the most accurate prediction method. This analysis should give additional credibility to model tests conducted for other structures and should provide an accurate estimation method of blast and debris hazards in structures of analogous design in the future.

VIII. REFERENCES

1. Kingery, C. N., Schumacher, R. N., and Ewing, W. O., Jr., "Internal Pressures from Explosions in Suppressive Structures," BRL Interim Memorandum Report No. 403, Aberdeen Proving Ground, Maryland, June 1975.

2. Baker, W. E., Cox, P. A., Westine, P. S., Kulesz, J. J., and Strehlow, R. A., A Short Course on Explosion Hazards Evaluation, Southwest Research Institute, San Antonio, Texas, 1979.

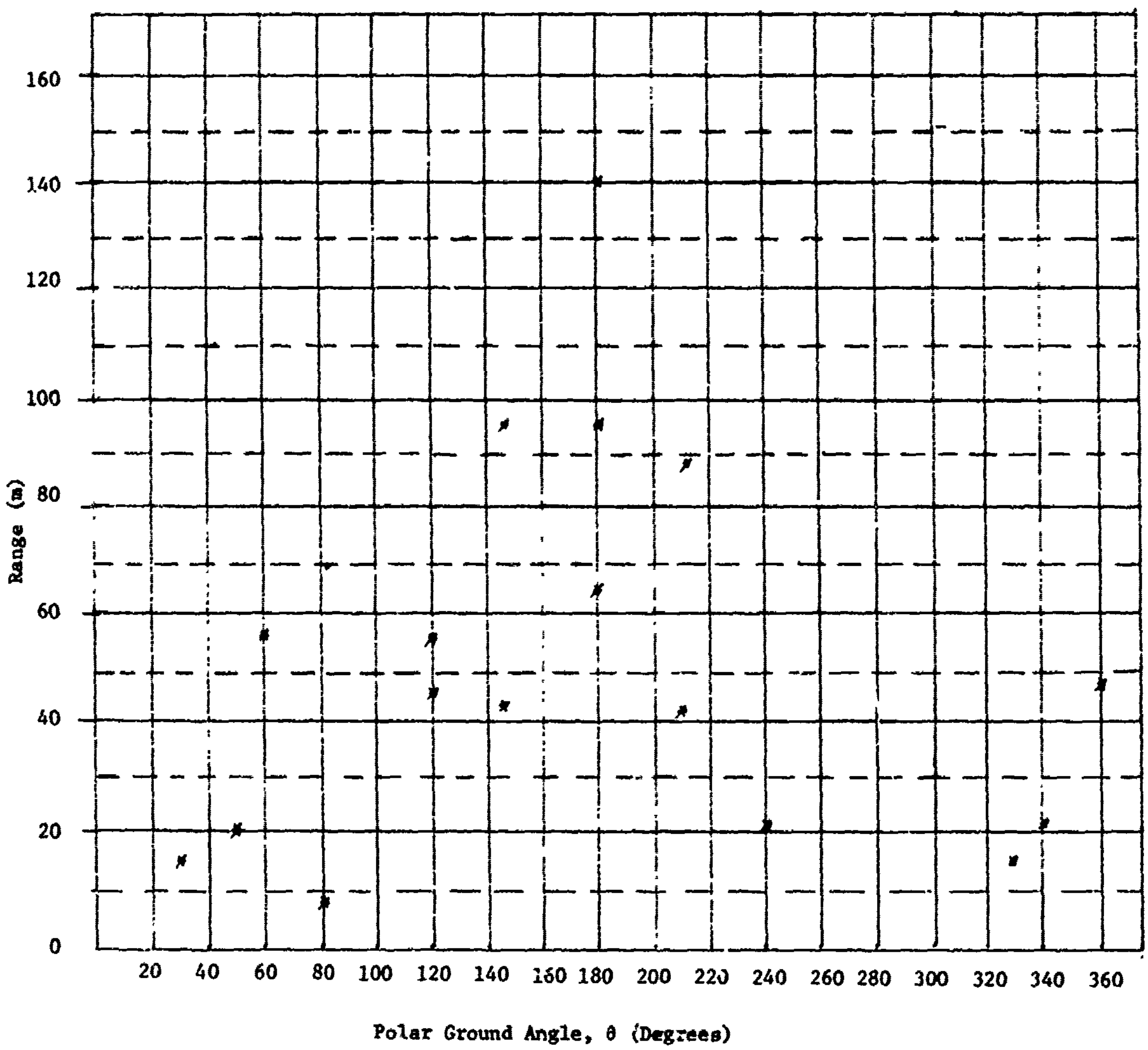

Figure 14. Debris Range versus Angle

3. Gentry, R. A., Martin, R. E., and Daly, B. J., "An Eulerian Differencing Method for Unsteady Compressible Flow Problems," Journal of Computational Physics, Vol. 1, 1966.

4. Hokanson, J. C., Esparza, E. D., and Wenzel, A. B., "Measurement of Blast Parameters on a Barricade Due to Simultaneous Detonations of Multiple Charges," Contract No. DAAA 21-76-C-0254, SwRI Project No. 02-4600, U.S. Army Research and Development Center, Dover, New Jersey, July 1977.

5. Baker, W. E., Kulesz, J. J., Ricker, R. E., Westine, P. S., Parr, V. B., Vargas, L. M., and Moseley, P. K., "Workbook for Estimating the Effects of Accidental Explosions in Propellant Handling Systems," NASA Contractor Report 3023, Contract NAS3-20497, NASA Lewis Research Center, August 1978.

6. Keenan, W. A. and Tancreto, J. E., Tech. Rept. 51-027, "Blast Environment from Fully and Partially Vented Explosions in Cubicles," Civil Engineering Laboratory, Naval Construction Battalion Center, Port Hueneme, California, February 1974.

7. Abrahamsson, E., "Operation Block," Royal Swedish Fortifications Administration, Report No. 119:5, May 1973.

8. Moseley, P. K. and Whitney, M. G., "Prediction of the Blast and Debris Hazard From an Accidental Explosion in a Third Generation Norwegian Aircraft Shelter," SwRI Project 02-5881, Norwegian Defense Construction Service, March 1980.

Development of Water Gels

as a

Safer Commercial Explosive

By A. B. Oppermann

If there is a common denominator among the hundreds of thousands of people (such as you and I) who are involved in the manufacture or use of explosives, it is safety.

Explosives are inherently dangerous and always have been recognized as such. In fact, when the Italian scientist, Ascanio Sobrero, discovered nitroglycerin in 1846, he found its behavior so unpredictable and frightening that he actually warned against its use. The history of the explosives industry since then has been one of looking for ways to do our jobs more safely.

Twenty years after Sobrero's warnings, Alfred Nobel discovered he could temper nitroglycerin's unstable behavior by mixing it with Kieselguhr, an absorbent diatomaceous earth. Nobel's discovery--dynamite--was the explosive of choice for the next hundred years, despite its two major shortcomings--it was relatively easy to detonate accidentally, and it could lead to severe headaches in workers who handled it or who inhaled postdetonation fumes.

Users of explosives lived with these shortcomings because there were no practical alternatives. Clearly, there was no simple solution to the perplexing problem of making safe a product that is useless if it is not powerfully destructive.

In the years following World War II, the massive growth in technology, information, and innovation led to a series of breakthroughs in explosives, coming at a rate of about one per decade.

In the 40's noncap-sensitive canned blasting agents replaced dynamite in large diameter blastholes, a significant breakthrough in safety in that it changed the direction of the quest for safety. While Du Pont and others still looked for ways to make dynamite safer, we also began to look for alternative explosives which would be inherently safer.

In the 50's ammonium nitrate/fuel oil mixtures in packaged and bulk form were developed and rapidly replaced the remaining uses of dynamite in large diameter holes. By the end of that decade, the major remaining large diameter uses of dynamite were in wet conditions, where ANFO formulations could not be used because of their lack of water resistance, and in tough shooting areas.

These last large diameter strongholds were eliminated in the 60's with the next breakthrough, the development of water gels or slurried explosives with solid sensitizers such as trinitrotoluene or TNT.

A major challenge remained: To find a way to adapt the inherent safety characteristics of water gels to small diameter applications. The solution was to develop a sensitizer which would be effective and safe in applications smaller than 100 mm. in diameter.

In the early 70's, Du Pont developed a system centered on monomethylamine nitrate, or MMAN, that has subsequently proven to be effective down to a diameter of 22 mm.

On January 24, 1974, a press conference was called to announce that Du Pont (the United States' largest producer of dynamite) would be out of the dynamite business by the end of 1976. The reason-- a water gel explosive had been developed that was as effective as dynamite but that was substantially, provably safer.

To date, we have manufactured well over a billion pounds of these gels, which we sell under the trademark Tovex®, without a single accidental detonation with the finished product.

The decision to drop a product line is not taken lightly, in any industry, for it requires substantial testing and proof that the replacement product is more effective, more economical, and safe--in this case, orders of magnitude safer.

I would like to share with you the information that led to the decision to drop dynamite and also some recent data based on our experience with, as I mentioned, more than a billion pounds of water gel explosives over the past 12 years.

Before doing that, please note that the data to be presented here are based on our experience with our proprietary MMAN-sensitized water gels. They may not be precisely applicable to all water gel explosives. However, with respect to product safety, while the specific data points may vary from one manufacturer's product to another's, the concept that water gels and slurries are orders of magnitude safer than dynamite is irrefutable.

I would first like to review some typical compositions of water gels and dynamites.

Tovex® vs. Dynamite
Composition

	Water Gels	Dynamites
Sensitizer	Explosive — • Smokeless Powder • TNT Non-Explosive — • Aluminum Pigment • Amine Nitrates	Explosive — • Nitroglycerine • Nitrostarch
Oxidizers	Ammonium, Calcium and/or Sodium Nitrates Perchlorates	Ammonium and Sodium Nitrates
Fuels	Coal, Aluminum, Oil, Sulfur, Sugar and/or Glycol	Carbonaceous Materials and Sulfur

To effectively replace dynamite, it was necessary to assess the critical properties which would be required. These next charts list those which we found to be most important and compares Tovex® Water Gel with dynamite.

Tovex® vs. Dynamite Properties

	TOVEX®	Dynamite
Density G/CC	.87-1.38	.80-1.60
Energy CAL/GM	750-1400	700-1100
Velocity M/S	3000-6000	1700-6000
Consistency	Fluid to Firm	Firm
Water Resistance	Good	Poor to Good

Tovex® vs. Dynamite Properties

	TOVEX®	Dynamite
• Initiation Sensitivity		
— Air Gap (32 MM Diameter) cm - 21°C (½ cartridge)	3 to 13	15-102
— Drop Test 5 KG Weight	121 CM (No Detonations)	25-76 (50% Point)
— Underwater Shock Initiation Pressure KG/CM²	1046	70-211
— 30-'06 Bullet Test	Fail	Detonation
— Low Temperature ... Initiation °C	-8	< -20

The development of Tovex® required an extensive testing program designed to assess the hazards of the proposed product. Since water gels were extremely insensitive, would not burn without a sustaining source of heat, and showed little or no reaction when subjected to standard safety screening tests, a new and more comprehensive system for evaluation of explosives hazards was required. Du Pont's initial program was intended to determine the appropriate procedures to be followed to avoid accidental detonation during the processing of water gels.

Objectives

- Identify Initiation Mechanisms of Water Based Explosives and Develop Tests to Determine Sensitivity to Each
- Identify Potential Initiation Points in the Process and Characterize and Quantify the Input
- Determine Quantitative Process Safety Margin

Although the objectives of these tests were evolved to measure manufacturing hazards, they are equally valid in assessing hazards in other situations in which the material could be subjected to unusual thermal or mechanical shock or abuse. Such situations occur in handling, in use and transportation, as well as in manufacturing. Of course, other hazards may occur in blasting, but up until the point at which the explosives are readied for blasting, the tests for manufacturing hazards are generally applicable.

Initiation Mechanisms

- Impact
- Minimum Energy
- Burning

Situations which might lead to accidental explosions were defined as impact, minimum energy input, and deflagration to detonation encouraged by confinement at elevated pressures. Each of these phenomona was examined for effect on various grades of Tovex® and a comparison was made with dynamite.

Impact Tests

- Flat Head 12 Gage Projectile
- 5 KG Drop Tests

Two types of impact testing were carried out. A flathead 12-gauge projectile weighing 35 g impacted water gels from a distance of 10 feet at varying velocities and a 5 kg weight was dropped from varying heights onto test samples.

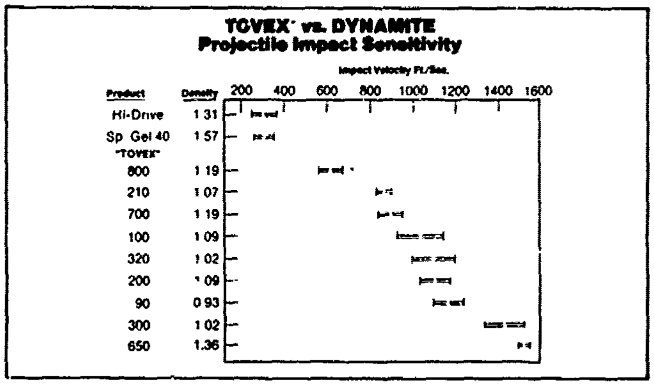

In projectile tests, the most sensitive type of Tovex® is only half as sensitive as dynamite with respect to projectile velocity.

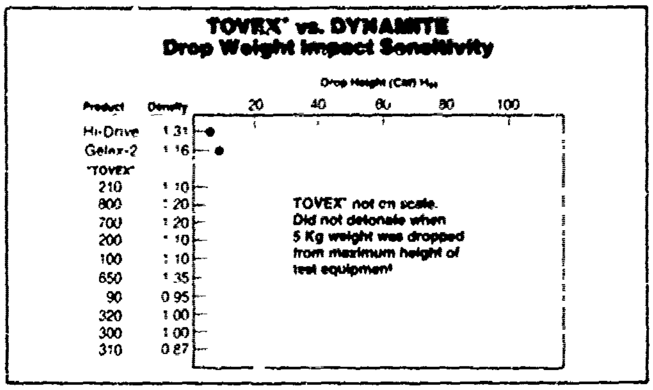

In drop tests, a 5 kg weight dropped 140 cm did not detonate the most sensitive Tovex® formulation. Therefore, there was no data for Tovex®. This compares with the 50 percent point for dynamite which is shown to be less than 10 cm.

After determining the maximum energies that Tovex® would be exposed to during the manufacturing process, we defined the minimum energies for detonation of Tovex® and dynamite.

Minimum-Energy Studies

- Graded Cap Series
- Detonating Cord

The minimum energy required to detonate Tovex® and dynamite were determined with blasting caps of various strengths and with detonating cord with varying core-loads.

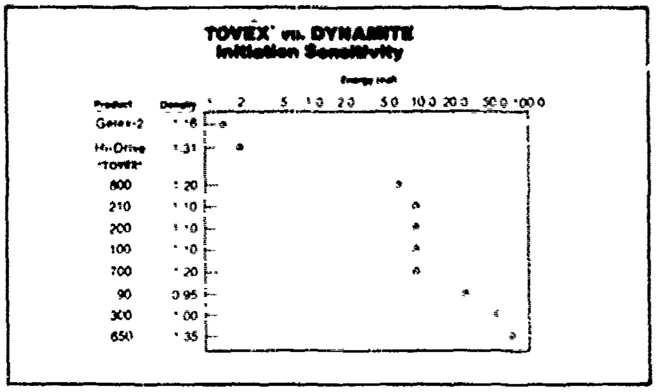

This chart compares the minimum energy required for initiation of Tovex® and dynamite. Even the most sensitive Tovex® required 30 times more energy than dynamite for detonation (6 cal. vs .2 cal).

Deflagration to Detonation

■ Closed Bomb Burning Tests

Another consideration in the program was the possibility of deflagration to detonation. Tests were conducted in closed pipe bombs to examine this phenomenon.

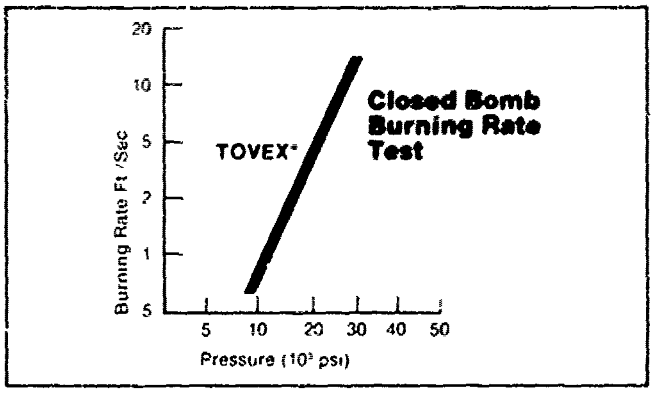

In these tests of Tovex® to encourage deflagration to detonation, conducted in closed containers, no detonations occurred even at elevated pressures. At the highest pressures, 30,000 to 40,000 psi, burning rates approached 20 ft. per sec. whereas deflagration to detonation is approximately 3,000 ft. per. sec.

These data you have seen certainly support the claim that water gels or slurries are many times safer than dynamite. Now, what is the track record? What has happened in the marketplace? It is quite dramatic.

Already water gel is used widely for mining, construction, and quarrying in the U.S. and throughout the rest of the world. In excess of 70% of the 650 million pounds of standard explosives (nonammonium nitrate types) consumed in the U.S. are water gels or slurries, with this figure growing rapidly at the expense of dynamite.

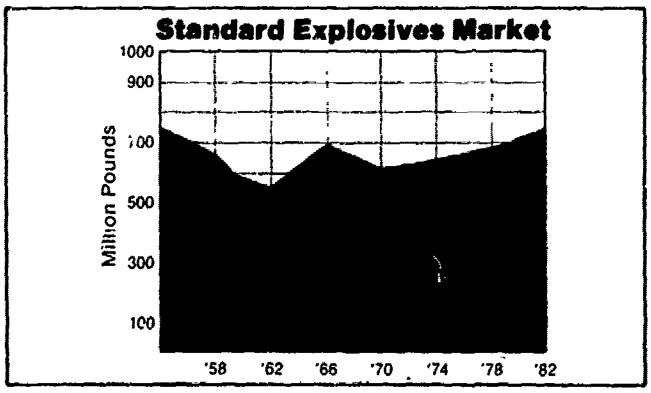

This chart graphically illustrates the trend to water gels in the U.S.

TOVEX® Countries

Ireland	Canada	Dominican Republic	Australia
France	Mexico	Trinidad	New Zealand
Portugal	Brazil	Jamaica	India
Italy	Chile	Panama	Japan
Norway	Peru	Venezuela	Philippines
Switzerland	Argentina	Costa Rica	Vietnam
Egypt	Uruguay	Honduras	Hong Kong
Saudi Arabia	Paraguay	Guyana	Malaysia
United Arab Emirates	Surinam	Nicaragua	Indonesia
Iran			China
Nigeria			
Swaziland			

Du Pont's Tovex® Water Gel is sold in over 50 countries, some of which are shown here.

With this wide exposure, it is obvious that water gel has proven to be a direct replacement for dynamite in virtually all uses and offers greater safety in transportation, handling, and use than nitroglycerin explosives.

The safety performance speaks for itself. As I pointed out earlier, Du Pont alone has manufactured their billionth pound of Tovex® within the last year, and, to date, no accidental detonations with the finished product have occurred. This is a 12-year record, unequalled in the explosives' industry. Accident data provided by the Institute of Makers of Explosives support this record and compare recent Tovex® experience with other explosives.

Explosives
Safety in Handling*

	Water Gels	All Others
Fatalities	0	79
Serious Injuries	0	109

*Accidents reported to the IME (1973-1978)

Explosives Fumes

Mine Measurements

U.S. BUREAU OF MINES — ANALYSIS OF NONCOAL MINE ATMOSPHERES: TOXIC FUMES FROM EXPLOSIVES

(Mine Safety Appliance Research Corp., 1977 Report No. BU MINES 10-77)

	Water Gels	Dynamite
Grades Tested	4	4
Number of Tests	10	16
Average Carbon Monoxide CC/200 GM	4 351	11 611
Average Oxides of Nitrogen CC/200 GM	706	2 209

Not only are water gels safer to manufacture, transport, and store, but when used, they generate less toxic gas.

The improved safety performance of water gels already is recognized by groups outside our industry.

- A major insurance compar is offering liability insurance to Du Pont explosives' distributors at substantially reduced premiums. The premium for Tovex® has been reduced to 40 percent of that for dynamite.
- New York City Fire Department has reduced the shielding requirements for trucks used to haul Tovex® Water Gels within the City of New York.
- The New York City water authority now uses specifications for explosives which preclude the use of dynamite in favor of water gels for construction work.
- Canada permits truckload quantities of 40 thousand pounds of water gels versus 10 thousand pounds of dynamite.

It is important to note that at least eight major manufacturers of explosives in the United States produce water gels or slurries.

Sources	
Apache	ES&C
Atlas	Gulf
Austin Powder	Hercules
Du Pont	Ireco

Conclusions

It would be wrong for me to suggest that water gels and in particular, Tovex® Water Gels, eliminate all the hazards associated with the transportation, storage, and use of explosives. Nevertheless, extensive testing results, plus the consumption of millions of pounds over a 12-year, accident-free period, do suggest that Tovex® Water Gel is very unlikely to detonate in accidents in which dynamite would detonate and that situations in which Tovex® would detonate will be highly infrequent.

Finally, I would urge that we all recognize the fact that water gels or slurries, are many times safer than dynamite, that they are readily available today in the U.S. and world wide, and that we encourage water gel use by implementation of regulations which will provide an incentive for the consumer to use these safer explosives.

PRECEDING PAGE BLANK-NOT FILMED

PBX's IN LARGE NAVY MUNITIONS

Fred L. Menz
Erwin W. Anderson
Naval Surface Weapons Center
White Oak, Silver Spring, Maryland 20910

INTRODUCTION

Major problems with large U.S. Navy munitions containing conventional TNT-based explosives, such as H-6, Tritonal, and Comp B, are violent fast cook-off reactions, sensitivity to fragment impact, explosive reaction during impact with hard (concrete) targets, and relatively poor underwater performance. Testing indicates that selected plastic-bonded explosives (PBX's) provide improvements in all areas. High-velocity fragment impact studies show that PBX's are less sensitive than Comp B, H-6, and HBX-1. Limited full-scale bomb and warhead fast cook-off tests have shown that these explosives give mild reactions during cook-off. A small number of full-scale bomb sled tests indicate that PBX's can survive a bomb target impact that causes violent reaction with Tritonal and H-6 loaded bombs. Torpedo and underwater mine weapon developments show that PBX's, appropriately formulated for underwater weapon application, have much greater explosive output than Tritonal or H-6.

This report will discuss the work on the PBX's in Large Navy Munitions Program, whose objective is to determine the feasibility of using plastic-bonded explosives in large munitions. The Mk 80 series bombs have been selected as convenient test warheads for containing the explosives. Initial evaluation of all explosives was conducted on either 250 pound class Mk 81 or 500 pound class Mk 82 bombs, with selected explosive compositions being tested in the 2000 pound class Mk 84 bomb. Seven Navy and Air Force candidate PBX's were being evaluated in this program. Included among these seven PBX's were aluminized, unaluminized, and underwater explosive formulations. The overall underwater and fragmentation/airblast performance has been assessed and compared to the current bomb fill, H-6. The response to cook-off, bullet impact, and sympathetic detonation will also be characterized. This program is providing the first large-scale, general assessment of the performance and safety characteristics of PBX's in a systematic and comparative test program.

U.S. NAVY PLASTIC-BONDED EXPLOSIVES

Research in plastic-bonded explosive technology has been proceeding during the past 20 years in the Navy. PBX's are heterogeneous explosive mixtures bonded together by a polymeric binder. PBX's can be loaded into weapons by one of four procedures, depending on their formulation. These loading procedures are pressing, casting, extruding, or injection molding. U.S. Navy nomenclature for designating PBX compositions is given in Table 1. At present, the U.S. Navy has five pressed, six cast, one extrudable, and one injection-loaded PBX compositions approved for service use (Table 2). Additional PBX's are under development; a list of currently interim qualified Navy main charge explosive PBX's is given in Table 3, along with potential applications.

BACKGROUND

In July 1967, the carrier USS Forrestal, on station in the Gulf of Tonkin, was conducting normal flight operations when a rocket inadvertently fired from an aircraft on the flight deck. The resulting fire and explosions cost the lives of 134 seamen, 74 million dollars in material damage to the carrier alone, and the operational loss of the carrier for an extended period.

In January 1969, a similar incident occurred aboard the USS Enterprise; numerous deaths and severe damage resulted. Both incidents were the result of what is termed "cook-off." When a confined explosive, such as exists in a weapon, is exposed to extreme heat such as a fuel fire, the violent reaction that occurs is known as "cook-off." In the above-mentioned accidents, ordnance was exposed to a fuel fire and as a result exploded violently, with considerable blast and fragment destruction. These incidents emphasized the need for explosives that react far less violently in fuel fires, thus eliminating such tragic events.[1]

Other incidents that have occurred as a result of violent reactions of the explosives in munitions include the 5-inch and 8-inch gun inbore prematures experienced during the Southeast Asian conflict and the railroad train explosions caused by fires in railway boxcars at Tobar, Nevada; Roseville, California; and Benson, Arizona in the late 1960's and early 1970's.

These, and other instances, emphasized the need to redirect some of the research and development within the United States Navy's explosives development program with specific goals to develop insensitive explosives with characteristics such as cook-off resistance and fragment impact insensitivity.

The utility of using insensitive explosives in Navy Munitions is addressed in formal Navy operational requirements. The operational problems that require insensitive explosives are:

(1) Unintentional initiations of munitions due to explosives' sensitivity to fire, fragment impact, and mechanical shock

(2) Aerodynamic heating of ordnance on high-performance aircraft

(3) Problems with munitions in hot gun barrels

(4) Potential vulnerability of munitions to point defense systems

(5) Reliability of munitions under extreme environmental conditions.

Standard melt-cast TNT-based explosives possess a number of well-known deficiencies (Table 4). Many PBX compositions have reduced or eliminated these deficiencies (Table 5). As can be seen from the list in Table 2, the typical application of PBX's in the past has been specialty, low production volume weapons, such as missile and torpedo warheads. With the greater emphasis placed on the use of insensitive explosives over the last ten years, more weapon systems are considering PBX's for use because of safety enhancement offered by these explosives at a given level of performance.

---

1 Fred L. Menz and David J. Edwards, New Navy Explosives Reduce Cook-Off Hazard, NAVSEA Journal, Oct 1975, Pg 59, Naval Sea Systems Command, Washington, D.C.

Very recently, this interest in insensitive explosive fills has been adopted by the Army, Air Force, and the Department of Energy, culminating in an in-depth study of insensitive high explosives and propellants (IHEP) and their effect on overall systems safety including manufacture, shipment, storage, and use.

PREVIOUS LARGE-SCALE SAFETY/SENSITIVITY STUDIES OF PBX'S

Plastic-bonded explosives represent a significant breakthrough in explosive composition development. In cook-off and bullet impact tests designed to evaluate resistance to initiation by fuel fires and high-velocity projectiles, respectively, PBX's have shown outstanding superiority over conventional explosives (such as Comp B, Tritonal, and H-6). This superiority is achieved by means of the elastomeric binder. In a cook-off situation, this binder decomposes by either endothermic or exothermic pyrolysis. The gases produced during the pyrolysis build up the internal pressure, which eventually ruptures the ordnance case. This allows the unconfined explosive to burn mildly, without producing destructive explosion and fragmentation. It has been conjectured that the rubbery nature of the elastomeric binder is the reason for the superior resistance to initiation by bullet impact. Such insensitivity greatly enhances the safety of ordnance items exposed to machine-gun fire and other high-temperature environments.

To determine the cook-off characteristics of these new explosives in actual explosive ordnance, a number of studies were performed by the U.S. Navy. Full-scale tests were conducted utilizing Mk 81 and Mk 82 bombs, 5"/54 projectiles, and both Mk 63 and Mk 24 Zuni warheads. As an example, a Mk 81 bomb loaded with a PBX was subjected to a standard fast cook-off test. The bomb was unlined and uncoated. This bomb, in normal use, is coated with a heat-resistance paint and has an asphalt-based liner on the inside for thermal protection. The test setup prior to ignition of the fuel is shown in Figure 1 (upper). After 2½ minutes in the fire, pressure buildup inside the bomb ruptured the ½-inch thick steel case, followed by non-violent burning of the explosive. There was not fragmentation of the case or detonation of the explosive. Post-test view is shown in Figure 1 (lower).

Under the same test conditions, bombs filled with Comp B, H-6, and Tritonal exploded violently, producing significant damage from airblast and fragments. For example, when an uninsulated and uncoated Mk 81 bomb loaded with Tritonal was subjected to this test, the bomb detonated after 2½ minutes. A Tritonal-loaded Mk 81 with normal coating and insulation survived for 10 minutes under the same test conditions, but then detonated.

In another experiment, four Mk 81 bombs loaded with the same type of PBX were simultaneously subjected to a slow cook-off environment. This experiment simulates the situation of a fire on the other side of a bulkhead from the bombs. The test setup is shown in Figure 2 (upper). The top two rows of bombs were filled with sand. No reaction occurred during the first 3 hours. Then, in the space of 3 minutes, three bombs split open and the explosive burned with no resultant fragmentation. The fourth bomb did not react. The test site after the cook-off is shown in Figure 2 (lower).

In a similar slow cook-off test, four Tritonal-loaded bombs survived for about 2½ hours. Then detonations and explosions occurred that completely cleared the test site, including a 3-ton steel shield, throwing some inert bombs as far as a quarter mile. A summary of these cook-off tests is shown in Table 6.

Limited bullet impact and qualitative fragment impact tests have been conducted within the Navy, using insensitive plastic-bonded explosives. It has been demonstrated that these materials are less sensitive to bullet/fragment impacts than other compositions, such as Comp B and A-3. Sled tests using Mk 80 series bombs have demonstrated that insensitive plastic-bonded explosives survive impacts into reinforced concrete targets.

TABLE 1. U.S. NAVY PBX NOMENCLATURE

P	Plastic
B	Bonded
X	Explosive
C	Experimental, China Lake
W	Experimental, White Oak
AF	Experimental, Air Force*
(I)	Interim Qualified
N	Final Qualified in Navy Weapon
1 through 99	Pressable
100 through 199	Castable
200 through 299	Extrudable
300 through 399	Injection Moldable

TABLE 2. U.S NAVY SERVICE-APPROVED PBX's

Explosive	Application
PBXN-1	Missile Warheads
PBXN-3	Missile Warheads
PBXN-4	Missile Warheads
PBXN-5	Boosters
PBXN-6	Boosters
PBXN-101	Missile Warheads
PBXN-102	Missile Warheads
PBXN-103	Torpedo Warheads, Mines
PBXN-104	Missile Warheads
PBXN-105	Torpedo Warheads, Mines
PBXN-106	Missile Warheads and Projectiles
PBXN-201	Burster Charges
PBXN-301	Multipoint Initiators

TABLE 3. INTERIM QUALIFIED PBX'S

Explosive	Potential Applications
PBXC-116(I)	Missile Warheads
PBXC-117(I)	Bombs
PBXW-107(I)	Bombs
PBXW-108(I)	Projectiles
PBXW-109(I)	Bombs
PBX(AF)-108(I)	Missile Warheads Projectiles

* The Air Force uses a different nomenclature for their PBX's: AFX, followed by a 3-digit number. Examples are AFX-108 and AFX-70B. Upon interim qualification by the U.S. Navy of an Air Force PBX, the nomenclature shown in Table 1 is used. For example, upon interim qualification of Air Force plastic-bonded explosive AFX-108, the Navy designation PBX(AF)-108 was given.

TABLE 4. DEFICIENCIES OF STANDARD MELT-CAST TNT EXPLOSIVES

1. Susceptible to sympathetic detonation in magazine and storage areas
2. Premature initiation upon impact with hard targets
3. Insufficient thermal stability
4. Increased performance results in increased sensitivity
5. Likely to produce violent explosive reactions in fuel fires
6. Subject to cracking and liquid exudation during extended storage
7. High shrinkage after casting with resulting large internal voids

TABLE 5. SOME ADVANTAGES OF TYPICAL PBX EXPLOSIVES

1. Thermal stability up to 150°C, as opposed to 80°C for TNT compositions
2. Elastomeric mechanical properties which decrease sensitivity to mechanical impact
3. Minimal or negligible shrinkage after casting
4. Less sensitive to shock than standard explosives with the same performance
5. Navy PBX's tend to burn rather than detonate when subjected to a fuel fire

TABLE 6. PBX COOK-OFF TEST RESULTS

Explosive	Warhead	Results
PBXW-107(I)	Mk 82 Bomb	Case ruptured. No frags. Only part of explosive burned.
PBXW-107(I)	Mk 82 Bomb	Tail plug ejected. Explosive burned. Case intact.
PBXW-106(I)	5"/54 Projectile	Nose plug ejected. Explosive burned. No damage to shell.
PBXC-116(I)	Mk 81 Bomb	Case split. Explosive burned. No frags.
PBXC-117(I)	Mk 24 Zuni	Mild rupture. No frags.

Figure 1

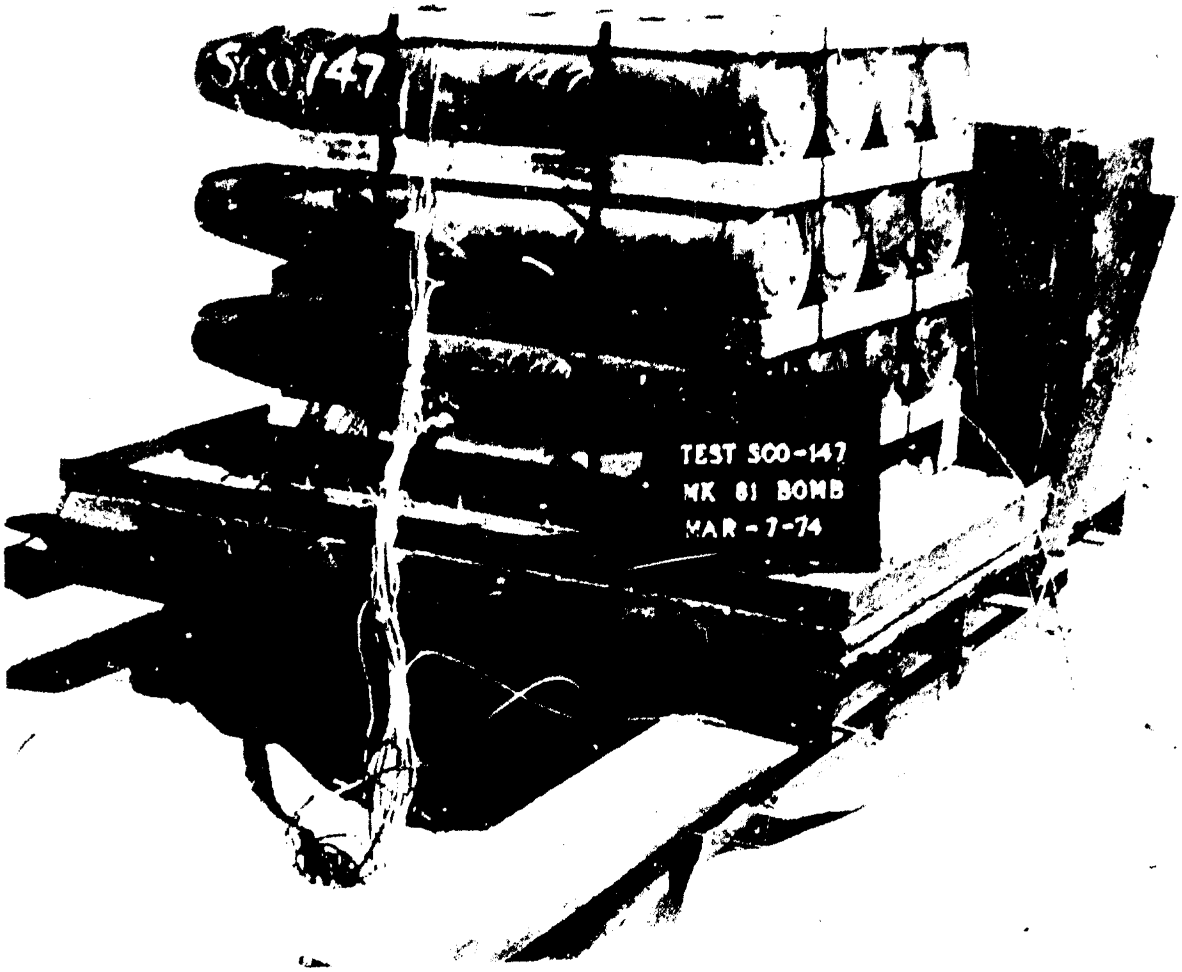

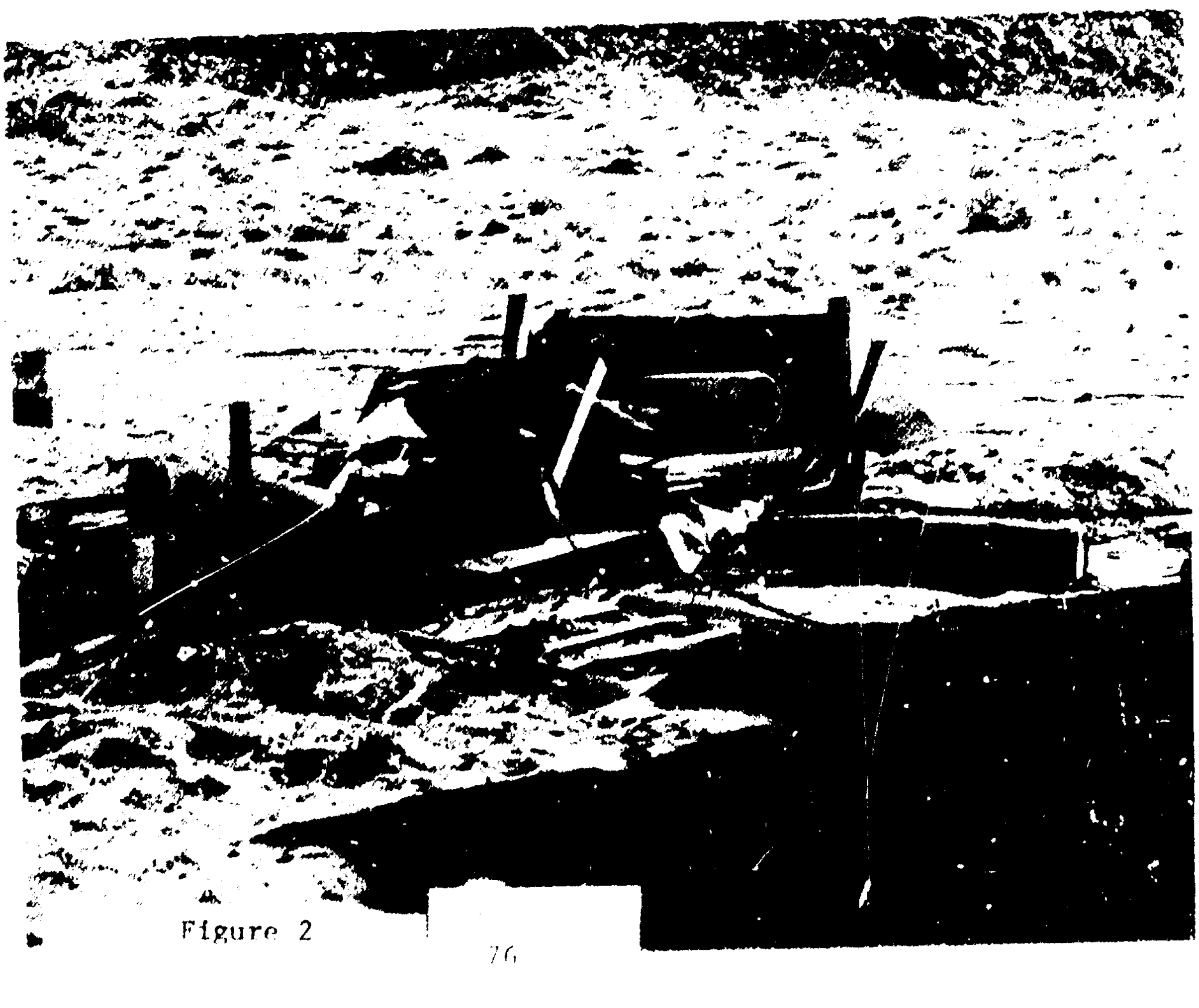

Figure 2

EXPLOSIVE POWER OF PYROTECHNIC COMPOSITIONS

J M JENKINS, R F NICHOLLS and M PEER
Royal Armament Research and Development Establishment, UK

1 INTRODUCTION

This paper describes the initial air-blast experiments being performed at RARDE to assess the explosive performance of pyrotechnic compositions. These experiments form part of a large programme which has two main objectives.

The first is to provide more accurate information on the hazard classification of pyrotechnics with respect to the current UN regulations for storage and transport.

The second, equally important, objective of the programme is to provide information pertinent to the design of effective operator protection and safer operating procedures. In order to support this latter objective a replica of one of our pyrotechnic manufacturing facilities is being constructed so that structural features, pyrotechnic screens and hazards, such as flying fragments, which arise outside the building can be assessed.

2 EXPERIMENTAL PROCEDURES AND RESULTS

Various pyrotechnic compositions were assessed in three experiments which were:

1 - To measure and assess the explosive power from various initiating stimuli.

2 - To measure the explosive power expressed in terms of the equivalent mass of TNT per unit mass.

3 - The likelihood and effects of sympathetic initiation in a practical storage situation.

The pyrotechnic compositions that were assessed are shown in Table 2. Only three compositions were assessed in Experiment 3.

2.1 Experiment 1

Three initiating stimuli were used; a fuzehead (match head), and electric detonator and a detonator boosted with a tetryl pellet (25 mm x 25 mm diameter). The composition was placed in a papier mache pot measuring 130 mm in diameter x 130 mm in height. The pot was placed on a short wooden post. The initiator was located at the geometric centre of the charge mass. As each charge was fired visual observation backed by foil gauge evidence was made to classify the response into one of the classes shown in Table 1. Figure 1 illustrates the experimental arrangement. The four foil gauges were installed at various distances from the charge to assist with the differentiation between a mild and severe explosion. An indication of the equivalent mass of the composition which exploded violently was obtained by means of an approximate calculation.

TABLE 1

Experiment 1:	Explosive Response Definitions
Burn	The pyrotechnic ignites and burns. The container lid opens but the container itself is not ruptured by the internal pressures developed.
Mild Explosion	The pyrotechnic ignites rapidly leading to rupture of the container and ejection of burning pyrotechnic.
Severe Explosion	The pyrotechnic ignites with considerable violence giving rise to air blast pressure which ruptures some of the installed foil gauges.

TABLE 2

Experiment 1: Explosibility - Summary of Results

No	Composition Ingredients	%	Function	Igniting Source	Burn	Mild Explosion	Severe Explosion	Equivalent mass approximation kg TNT per unit mass
1	Magnesium Barium Peroxide Binder	12 86 2	Primer	1 Match Head	X			0.01
				2 Detonator		X		
				3 Detonator and Booster			X	
2	Magnesium Sodium nitrate Calcium oxalate Binders	26 42 16 16	Flare	1	No response			0.03
				2		X		
				3			X	
3	Magnesium Strontium nitrate Chlorinated rubber Binders	38 43 5 14	Tracer	1	X			0.05
				2		X		
				3			X	
4	Magnesium Strontium nitrate Strontium peroxide Binder	30 53 5 12	Tracer	1	X			0.12
				2		X		
				3			X	
5	Potassium benzoate Potassium perchlorate	28 72	Whistler	1		X		0.13
				2		X		
				3		X		

TABLE 2 (Contd)

No	Composition Ingredients	%	Function	Igniting Source	Burn	Mild Explosion	Severe Explosion	Equivalent mass approximation kg TNT per unit mass
6	Magnesium	44	Yellow	1	X			
	Sodium nitrate	48	Signal	2		X		0.14
	Binder	8		3			X	
7	Magnesium	58	Flare	1	X			
	Sodium nitrate	38		2			X	0.15
	Binder	4		3			X	
8	Boron	30	Primer	1	X			
	Potassium nitrate	70		2		X		0.16
				3			X	
9	Magnesium	42	Green	1	X			
	Barium nitrate	17	Signal	2		X		0.21
	Potassium perchlorate	27		3			X	
	Binders	14						
10	Magnesium	55	Tracer	1		X		
	PTFE	40		2		X		0.23
	Viton	5		3			X	
11	Aluminium	40	Photo-	1	No response			
	Potassium perchlorate	60	flash	2		Not tested		0.42
				3			X	

NOTE: The possibility that the equivalent mass value less than 0.1 kg TNT per unit mass was produced by the initiating system alone was tested separately. A detonator and tetryl pellet were fired in a 130 mm papier mache pot without rupturing any foil gauges.

2.2 Experiment 2

Those compositions which displayed an approximate equivalent mass of 0.1 kg TNT per unit mass or greater in Experiment 1 were selected for a more rigorous assessment of the equivalent mass.

The equivalent mass of the selected pyrotechnic composition was found using the standard experimental apparatus shown in Figure 2. In this well established experiment the air blast parameters produced by a severe explosion are recorded in free air conditions, that is with freedom from interference to the primary shock wave by ground reflected shock waves. Free-air conditions were obtained by placing the explosive charge and twelve piezo-electric pressure transducers at a height of 4.5 m above ground. The twelve pressure transducers were connected to a multi-channel recording instrument.

The pyrotechnic composition was placed in a spherical container, 160 mm in diameter, giving a storage volume of 2.2×10^{-3} m^3. The containers were fabricated from high impact polystyrene and consisted of two hemispherical shells with an internal spider to retain a 25 mm x 25 mm (diameter) perforated tetryl pellet at the geometric centre and a filling cap (Figure 3). An L2A1 detonator was passed up a tube into the pellet after the spherical container was filled.

The recorded data were used to obtain an equivalent mass for each pyrotechnic composition. The results of Experiment 2 are shown in Table 3.

TABLE 3

Explosive Power Results

Composition No (from Table 2)	Explosive power/ kg TNT per unit mass
6	0.12
4	0.13
5	0.25
7	0.19
8	0.19
9	0.32
10	0.23
11	0.50

It can be seen that the results generally follow the order found using the foil gauges with the notable exception of Number 5, the potassium benzoate/potassium perchlorate composition. Further experiments along these lines are planned with larger masses of composition to determine the effect of mass on TNT equivalence particularly with those compositions with equivalence values of just under 0.1.

2.3 Experiment 3

While the results of Experiments 1 and 2 provide basic data on the explosive performance of pyrotechnic compositions additional data applicable to the storage situation was needed. Experiment 3 was devised to assess the explosive performance of pyrotechnics in a practical storage situation and in particular to examine the possibility of sympathetic initiation. Experiment 3 was divided into 3 parts.

2.3.1 Experiment 3A

This experiment is similar to Experiment 1 except that 3 kg of composition was placed in a storage canister (Figure 4). An indication of explosive power was obtained by means of foil gauges as before. A match head was used as the initiating stimuli. The fragmentation of the can was also studied. Three compositions were studied. They were the slow flare composition (No 2), the tracer composition (No 3) and the green signal composition (No 9). The explosive yield of the slow flare composition (No 2) and the tracer composition (No 3) was less than 0.01 kg of TNT, the cans remained substantially intact. The green signal composition destroyed the can and gave an average explosive yield of 0.23 kg of TNT for the can which contained approximately 3 kg of composition. There were large fragments which travelled many yards.

2.3.2 Experiment 3B

The experimental layout was as shown in Figure 5. The contents of the middle can being initiated by a match head. The same compositions were used as in 3A. The experiments with the slow flare and tracer compositions showed that flame propagation took place but the acceptor cans were not shattered; their contents burned smoothly. The experiment with the green signal composition resulted in a mild explosion with the three acceptor cans being initiated and disintegrating into large fragments.

2.3.3 Experiment 3C

In this experiment a stack of 12 cans was made, 3 layers, 4 cans to a level, the whole being supported by a wooden frame (Figure 6). One can in the centre layer being ignited by a match head. The stack with the slow flare composition burned steadily with no explosive events taking place, that for the tracer composition was similar but the whole event was over in a few minutes. With the green signal composition the stack exploded giving an average explosive yield of 0.6 kg of TNT which was quite small when one considers that the stack contained a total 36 kg of composition in the cans. The green flare composition caused many large fragments weighing ½ to 1 kg to be thrown tens of yards.

3 DISCUSSION

This work has shown that the explosive violence obtained from the ignition of pyrotechnic compositions varies with initiating stimulus and that it is difficult to correlate, other than in very general terms, the results of explosive power measurements on single charges with the effects in a storage situation.

With nearly all the compositions tested the explosive output was greater the more violent the initiating stimulus and compositions which burned relatively quietly with match head ignition could be made to produce a significant blast output with a detonator and tetryl pellet initiation.

The results of the stack trials showed that the more violent the response that was achieved in the explosive output tests then the more likely that the collection of cans would initiate and that the event would be more vigorous. However, they also showed that the events in the collected cans were much less violent than would be expected from the explosive output tests. With the tracer composition, the explosive output tests gave a TNT equivalence of 0.13 kg of TNT per unit mass but the trials with the storage cans gave rise to no observable blast pressure. Similarly, with the green signal composition the explosive output tests gave a TNT equivalence of 0.32 kg of TNT per unit mass but the storage can trials gave an average explosive yield of only 0.6 kg TNT for the whole stack containing 36 kg of composition. This does not mean that the explosive output result should be discarded as they will be more relevant in the manufacturing situation where large masses of composition are handled and in the magazine situation in which pyrotechnic compositions of varying explosive output are stored.

In the mixed magazine situation it will be very difficult to predict the violence of the overall event as explosive output derived from any particular composition can depend on the violence with which it is initiated by its neighbouring composition.

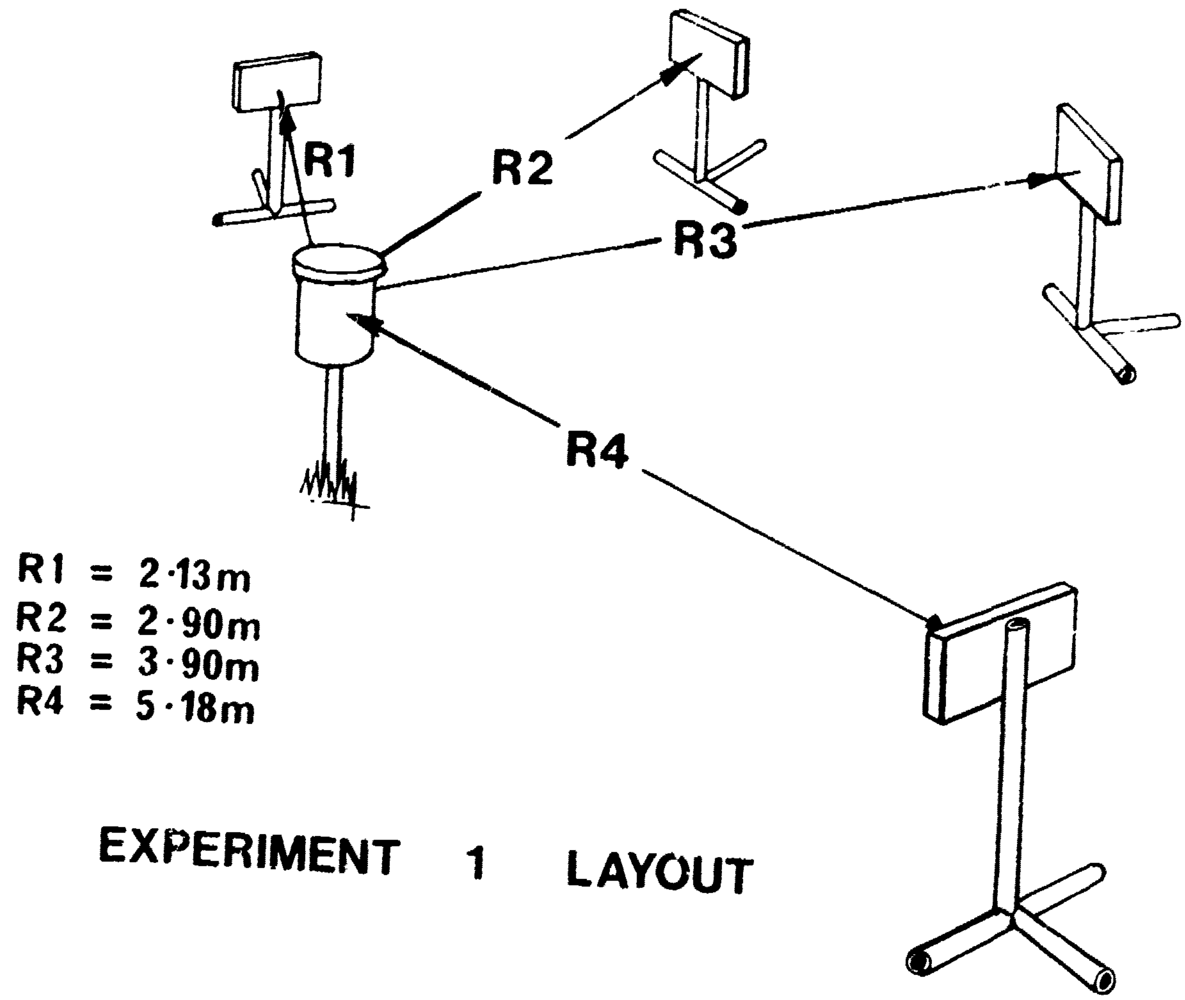

FIGURE 1

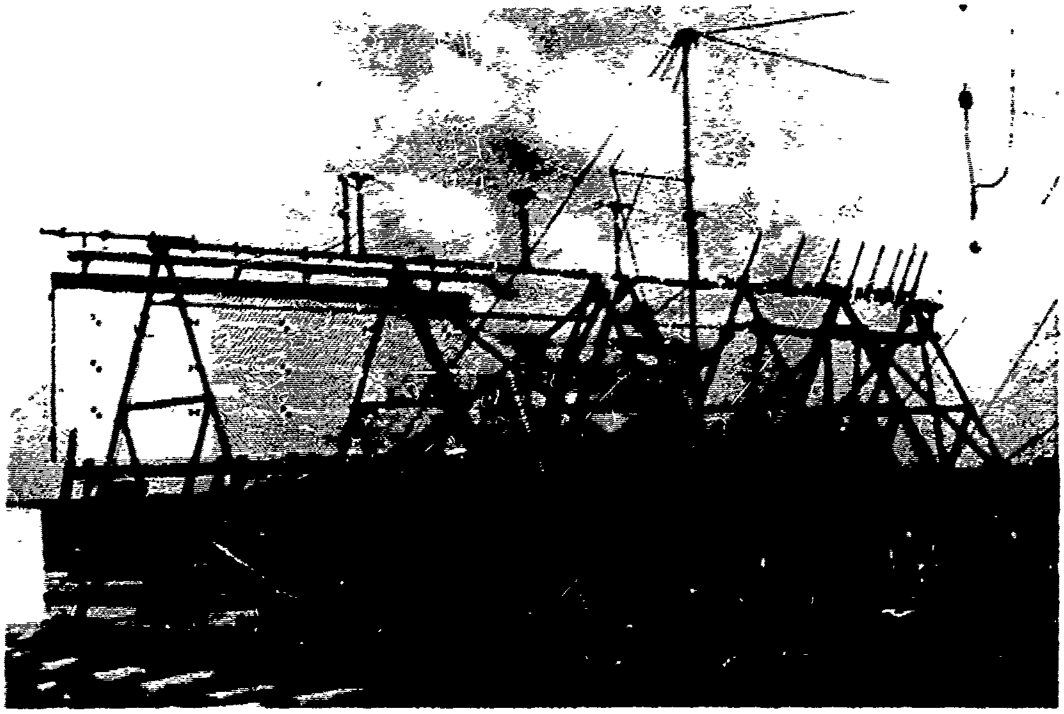

FIGURE 2

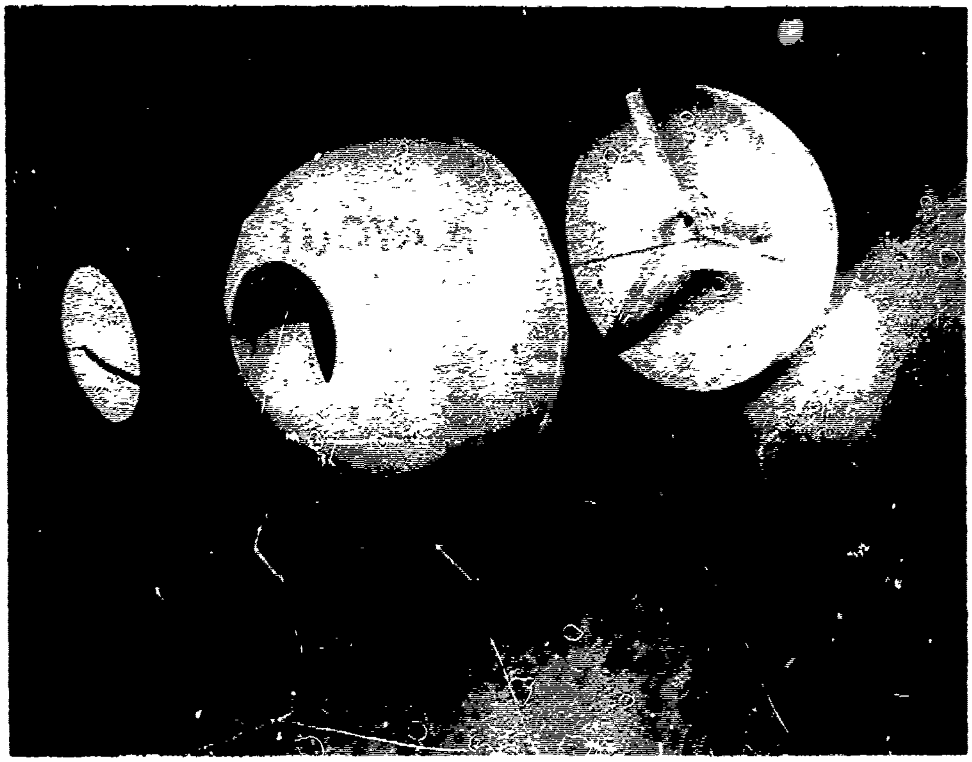

FIGURE 3

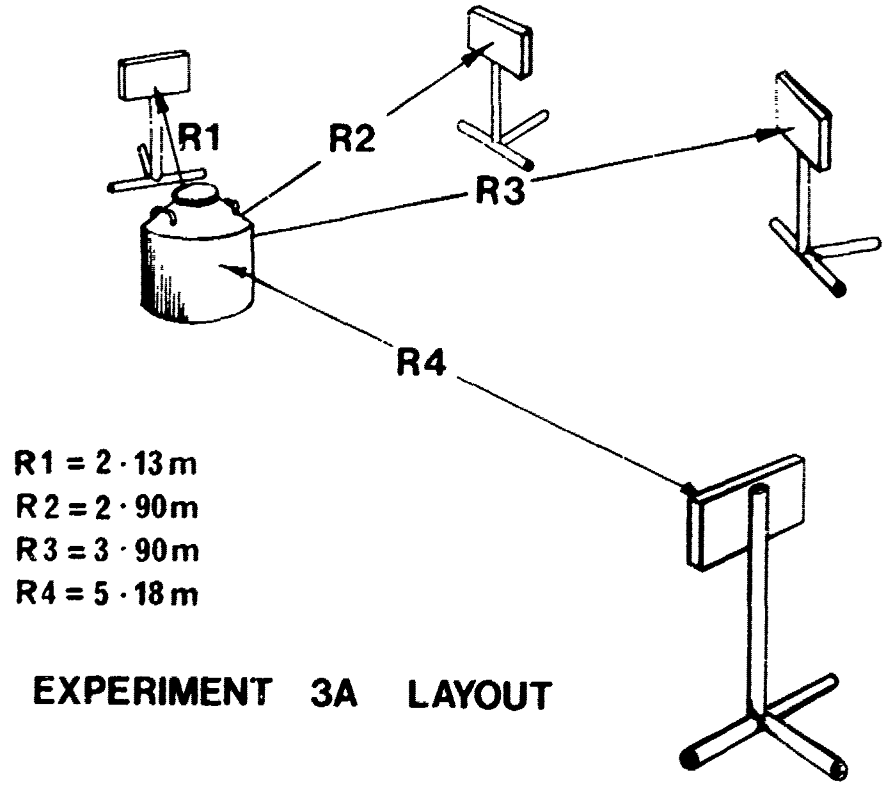

EXPERIMENT 3A LAYOUT

FIGURE 4

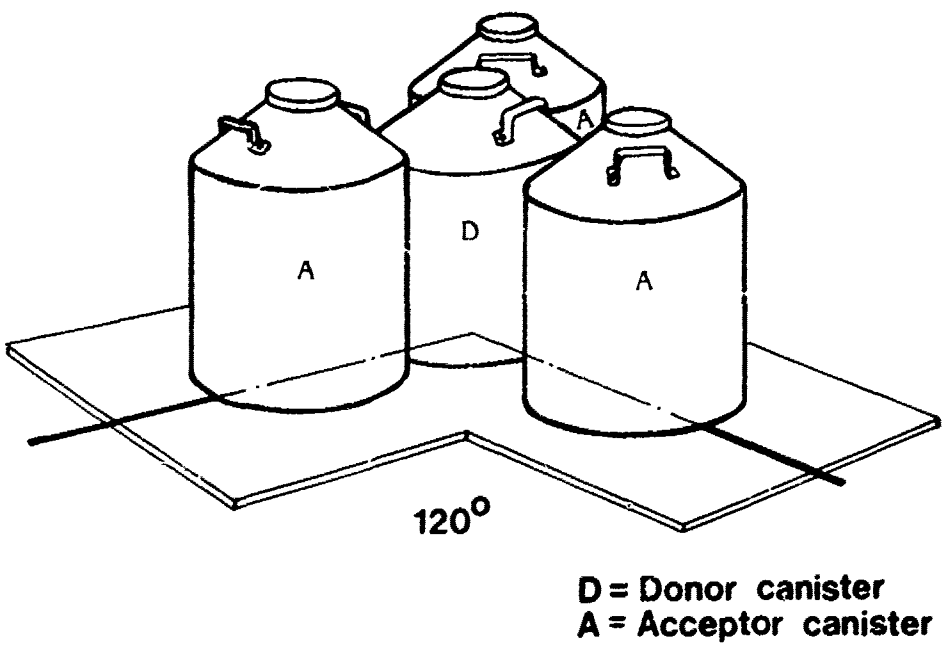

EXPERIMENT 3B LAYOUT

FIGURE 5

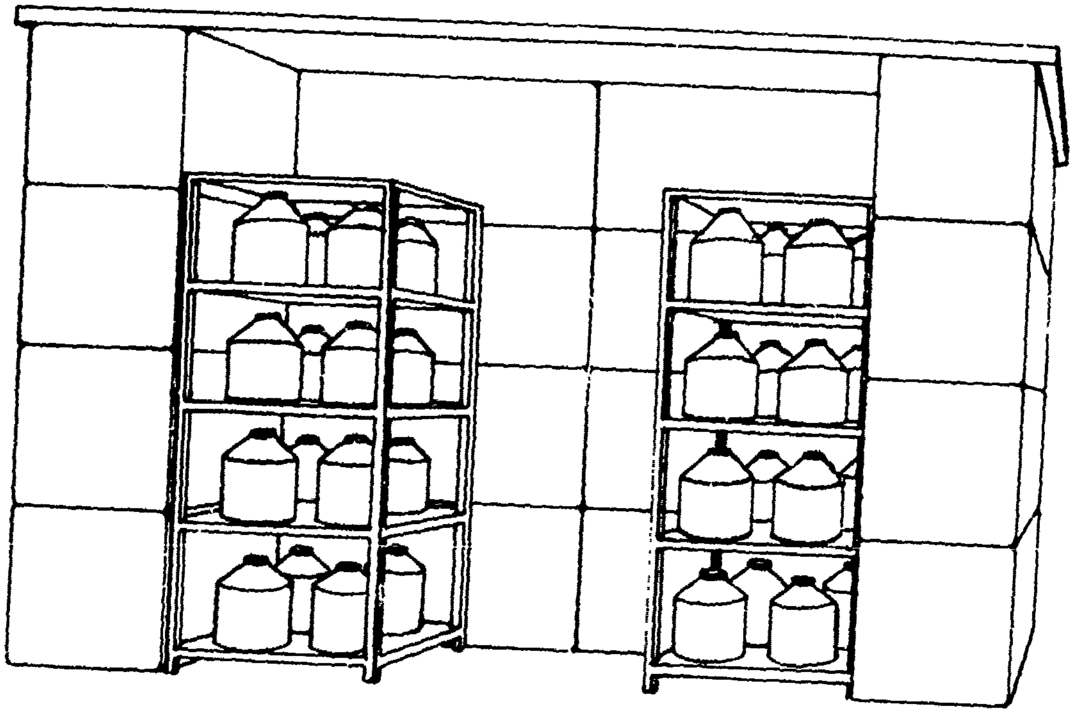

EXPERIMENT 3C LAYOUT

FIGURE .6

*No-Roll Process for Manufacture
of Double-Base and Composite-Modified
Double-Base Extrusion Compositions

CRAIG E. JOHNSON
PAUL F. DENDOR

Naval Ordnance Station, Indian Head, Maryland

ABSTRACT

The No-Roll Process is a recently developed method of manufacturing solventless double-base and composite-modified double-base propellants. This new process offers considerable advantages over processes currently in use; it is safer, more versatile and less costly.

Because it is a safer and more versatile process it is possible to incorporate energetic solids into the formulation. This makes it possible to manufacture gun propellants with higher impetus levels and extruded rocket propellants with higher specific impulse.

This paper describes the No-Roll Processing techniques and presents formulating data and test results of these gun propellants and rocket propellants.

BACKGROUND

Solventless double-base propellants are made in a lengthy series of processing steps. The methods are well established and accepted as being "the" way to make solventless double-base propellants. Some variations have been attempted in the U.S. and in Germany, but the time honored hot rolling techniques persists.

A water slurry of nitrocellulose (NC) is formed and the nitrate esters and other plasticizers are added to the mix. The mix is then dewatered using a Nutche filter or a centrifuge. The paste is aged to allow the plasticizers to start to enter the NC fiber. The damp material is then mixed with the water-affected ingredients in a horizontal mixer. This blends the "paste" into a more homogeneous material. This paste is first placed on hot differential rolls and then fed through hot, even-speed rolls a number of times. A well colloided smooth sheet of propellant is formed. The material is slit into strips, rolled up into "carpet rolls" and extruded in a vacuum extrusion press. The extruded strand is cut to length to complete the process.

*The opinions or assertions made in this paper are those of the author and are not to be construed as official or reflecting the views of the Department of the Navy or the naval service at large.

This process has the disadvantages of:

a. High cost, because of the many facilities required and many handling steps.

b. Being labor intensive because of the many hand operations necessary.

c. Being equipment intensive with specialized equipment and many facilities.

d. Being difficult to incorporate water-affected ingredients. For safety reasons the paste cannot be completely dried, and small amounts of water can hydrolyze or dissolve some ingredients.

e. Being impossible to add energetic solids to the mix because of safety considerations.

f. Occasional fires on the rolls cause equipment damage and concern.

This hot rolling method is used to make solventless double-base propellants such as N-5, HEN-12, NOSOL-318 and NOSOL-363. The products have the advantages of:

a. low volatile content of about 0.1%;

b. good dimensional stability with age; and,

c. reextrudable to other configurations after time.

A second way of manufacturing double-base propellants is the solvent method. This method has been developed to high levels of automation and instrumentation.

In the solvent method of manufacturing double-base propellants, a heavy duty horizontal mixer is used to mix nitrocellulose, plasticizers (energetic and/or inert), inert solids, energetic solids and volatile NC solvents into a dough like consistency. The NC is plasticized and partially disintegrated during this mixing to form a continuous binder phase to hold the solids together. The dough is blocked in a press and extruded through a screen into large diameter billets. These billets are then reextruded into the final, small diameter configuration. After cutting to length, the volatile solvents are removed by drying the propellant at elevated temperatures.

This solvent process, although widely used and less expensive than the hot rolling solventless process, has several disadvantages:

a. as the volatile solvents are removed from the grain it shrinks and changes dimension, thus producing lot-to-lot variability;

b. the web thickness is limited because of the time to remove the volatile solvents; and,

c. the volatile solvents cause an environmental problem because they are very difficult to remove from the hot drying air-stream in the drying ovens.

Because of the inherent dangers of solventless processing, little work has been done on increasing the energy of these propellants by the use of energetic solids loading. The British have used some nitroguanidine in their solventless propellant. ARRADCOM[1] has developed the so called solvent-solventless process, but this combines the cost of the two processes and is very labor intensive.

The inclusion of energetic solids in the double-base matrix can have very desirable ballistic benefits. Typically the impetus values of gun propellants can be raised from about 350,000 ft lb/lb to above 400,000 ft lb/lb. Rocket propellant specific impulse can be raised from about 200 lb-sec/lb to above 250 lb-sec/lb.

PROCESSING

The No-Roll Process was developed[2] to avoid the problem of the current art. The process is completed in fewer processing steps and with less manual handling during critical steps. For normal double-base propellants the following process is used.

1. A slurry of water-wet fibrous nitrocellulose and heptane is formed and the liquid plasticizers are added to the slurry. The materials are slurried together until the solids have dispersed and plasticizers have coated all of the nitrocellulose. The heptane is decanted.

2. The propellant is dried to remove the remaining heptane and complete the plasticization of the nitrocellulose.

3. The material is placed in a vacuum type solventless press and extruded to its final size. The strands are then cut to length.

The material from this process is similar to the conventionally manufactured propellant. We manufactured NOSOL gun propellants by the No-Roll Process and the extrusion properties, physical properties and ballistic properties were quite similar.

---

[1] J.S.Stack, Investigation of High Energy-High Density Smokeless Nitramine Extruded Double-Base Propellants, Picatinny Arsenal Technical Memorandum No. 4047 (Dover, New Jersey: May 1970).

[2] C.E.Johnson and P.F.Dendor, U.S. Patent 4,126,497, "Method of Preparing Solventless Double-Base Formulations Suitable for Extrusion."

We felt that the inherent safety of the process would allow us to include energetic solids in the formulations. With some processing modifications we developed the following process[3] which includes energetic solids.

1. A slurry of water-wet fibrous nitrocellulose and heptane is formed; the energetic solids are added to the slurry and the liquid plasticizers are added to the slurry. The materials are slurried together until the solids have dispersed and plasticizers have coated all of the solids. The heptane is decanted.

2. The propellant is dried to remove the remaining heptane and complete the plasticization of the nitrocellulose.

3. The material is placed in a vacuum type solventless press and extruded to its final size. The strands are then cut to length.

This process has been used to mix formulations containing up to 60% solids. Formulations have used nitrocellulose plasticized with metriol trinitrate, diethylene glycol dinitrate, nitroglycerine and various inert plasticizers. The energetic solids have consisted of RDX, HMX, nitroguanidine (NQ) or ammonium perchlorate (AP).

The No-Roll Process has several economic and safety advantages over the former methods:

a. it is a safe process that utilizes remote mixing in a dilute slurry;

b. efficient use of resources are obtained by recycling the process streams;

c. low labor costs are obtained because the process streams can be handled using process equipment instead of manual transfer;

d. low facilities cost because the process is simpler and more compact;

e. versatile formulations from conventional double-base to highly energetic HMX or RDX loaded formulations; and,

f. water soluble ingredients such as ammonium perchlorate can be added to the formulation.

EXPERIMENTAL

Our original intent was to find a method of manufacturing solventless double-base gun propellant using a lower cost method than was

---

[3] C.E.Johnson and P.F.Dendor, U.S. Patent 4,102,953, "Solids Loaded Solventless Propellant and Method for Making Same."

currently available. We started making NOSOL-318 and then began making NOSOL-363. The physical property results are shown in Table I, which compares two processing methods for NOSOL-318.

TABLE I
Tensile Properties NOSOL-318

Strain Rate 0.625 in/in/min

Temp °F	Process	Sm	Em	Sr	Er	Ym
-20	Conven.	5199	16.62	5199	16.62	58044
-20	No-Roll	5417	13.72	5417	13.72	64554
77	Conven.	699	38.95	688	40.0	2595
77	No-Roll	710	27.55	647	30.70	5885
120	Conven.	187	35.00	187	35.00	831
120	No-Roll	176	19.67	137	23.27	2164

Strain Rate 1.56 in/in/min

Temp °F	Process	Sm	Em	Sr	Er	Ym
-20	Conven.	5293	14.42	5293	14.42	68597
-20	No-Roll	5646	13.12	5646	13.12	68132
77	Conven.	918	38.66	918	38.66	4886
77	No-Roll	985	30.81	952	33.19	8007
120	Conven.	269	37.34	269	37.34	1086
120	No-Roll	244	20.19	214	24.69	2565

It is known that by adding energetic solids such as HMX or RDX or nitroguanidine to a double-base formulation it is possible to achieve greater impetus in gun propellants without increasing the flame temperature. These solids are commonly added to solvent-type formulations, but processing difficulties arise because of the shrinkage due to solvent evaporation after extrusion. Some limited success was obtained by ARRADCOM Dover, New Jersey with the solvent-solventless method, but this involved a multiplicity of handling steps. Standard solventless rolling techniques are unsuited for energetic solids loaded formulations because of the potential safety hazards involved.

The No-Roll Process can mix solventless double-base formulations containing large amounts of solids (up to 60%) in a dilute slurry.

The original formulation work using a solids loaded gun propellant composition was done using RDX, nitrocellulose, metriol trinitrate and triethylene glycol dinitrate. At this time the intent was to duplicate the flame temperature of the usual gun propellants but increase the impetus. As shown in Table II we achieved impetus of 396,000 ft-lb/lb at a flame temperature of 3052°K. Later we changed the approach in this program to decrease the flame temperature while keeping the impetus level of the usual gun propellant.

TABLE II

Several Nitramine Loaded Formulations, Chemical Theoretical Data and Extrusion Data

Ingredient	Formulation Number 74-43	76-20	77-23	78-10	78-11	78-19	78-22	78-29
Nitrocellulose	26.4	11.9	19.2	26.5	18.8	26.5	25.4	24.4
Plasticizers	33.5	33.0	33.0	33.4	26.1	33.4	34.5	35.5
Additives	0.1	0.1	0.1	0.1	0.1	0.1	0.1	0.1
RDX/HMX	40.0	55.0	47.7	40.0	55.0	40.0	40.0	40.0
Extrusion Results	GS	GS	RS	HPE	HPE	PS	HPE	GS
		FS	FS	PS	PS	---	GS	---
Impetus, ft-lb/lb	406K	396K	---	---	---	---	356K	---
Flame Temperature, °K	3310	3052	---	---	---	---	2652	---
NC/Plasticizer	.79	.36	.58	.79	.72	.79	.74	.69

GS = Good Strand: PS = Poor Strength: RS = Rough Strand: FS = Flexible Strand: HPE = High Pressure Extrusion

One of the more favorable aspects of the No-Roll Process is the ability of the process to disperse the ingredients and deagglomerate any particle clusters. We have always used the standard Class 5 (Class E) RDX in our formulations. We do not feel it is necessary to grind the RDX below this size of about 10 to 20 microns. As is shown in Figure 1 we feel that we have achieved a reasonable burning rate/pressure slope. The closed bomb data indicates a slope of 1.059 for a formulation using 40% RDX and 1.123 for a formulation using 55% HMX.

In addition to the solids loaded formulations using RDX, we developed some using nitroguanidine. We wanted to create a solventless variation of M-30, which has been used by the Army for many years. Its' composition and ballistic properties are shown in Table III. As it is conventionally manufactured, the M-30 must be processed with solvents, owing to its high viscosity. As was mentioned briefly in the background this means that solvents must be added to the formulation so the material will be extrudable. However, after extrusion, the solvent evaporates, and the propellant strands do not remain in the desired size or shape. An additional drawback is that residual solvents which remain in the propellant strands can affect its ballistic properties over a period of time, or in various physical surroundings. Hence, the desirability of a solventless formulation which could circumvent these problems.

In our tests using the No-Roll Process, we found that we could achieve a very close approximation of the M-30 impetus, and flame temperature. The compositions shown in Table III represent these nitroguanidine loaded solventless formulations.

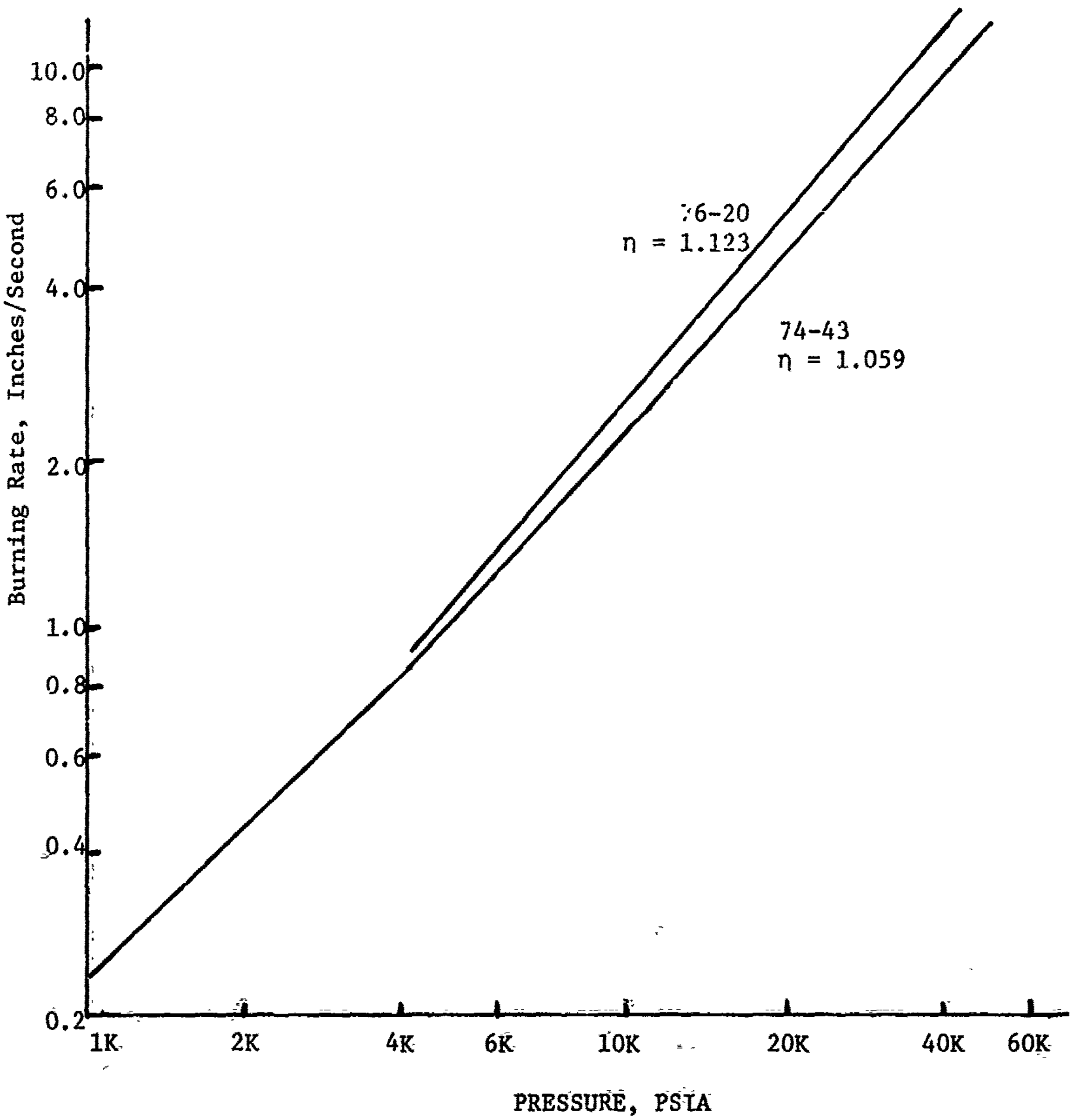

FIGURE 1

BURNING RATE DATA FOR NITRAMINE LOADED FORMULATIONS

TABLE III
M-30 and Solventless Variations, Chemical and Theoretical Data

Ingredient	M-30	Variation 1	Variation 2	Variation 3	Variation 4
	Formulation Type				
Nitrocellulose	28.0	27.0	23.0	26.4	30.0
Plasticizers	24.0	42.4	36.4	33.0	39.4
Additives	0.3	0.6	0.6	0.6	0.6
Nitroguanidine	47.7	30.0	40.0	40.0	30.0
Impetus, ft-lb/lb	364,000	363,826	368,195	365,672	368,480
Flame Temp, ^{o}K	3040	3028	3105	3087	3127
NC/Plasticizer	1.17	.64	.63	.80	.76

The compositions were processed normally and extruded through a 0.290 inch die with seven pins. Because of our die configuration, some of the compositions did not receive enough "working" in extrusion. These compositions did not show good consolidation and exhibited marginal strength. By re-extruding the grains, good strands were obtained. Moisture data, extrusion data, safety data, ballistic data and heat of explosion for the solventless variations are shown in Table IV and Figure 2.

TABLE IV
Experimental Data on No-Roll Solventless M-30 Variations and NOSOL

Analysis	Variation 1	Variation 2	Variation 3	Variation 4	NOSOL 363
	Formulation Type				
Moisture, %	---	0.10	0.10	0.20	0.25
Extrusion Pressure, psi	5400 to 9000	9000 to 10,000	9000 to 11,700	9000 to 10,350	4500 to 5400
Impact sensitivity, W/5Kg wt., mm	200	225	225	75	175
Friction sensitivity at 8 ft/sec, lb.	$\geq$980	$\geq$980	$\geq$980	$\geq$980	$\geq$980
Electrostatic sensitivity, joules	0.625	$\geq$12.5	$\geq$12.5	$\geq$12.5	$\geq$12.5
H.O.E., Cal/gm	---	972	949	1048	934
DDT Test 12" x 2" dia.	Negative (pressure burst)	---	---	---	---
Density gm/cc	---	1.510	1.553	1.620	1.516
Closed Bomb Burning Rate at 77^{o}F, $r = \beta P^{\alpha}$					
Coefficient, β	---	---	---	0.001097	0.000233
Exponent, α	---	---	---	0.858	0.987

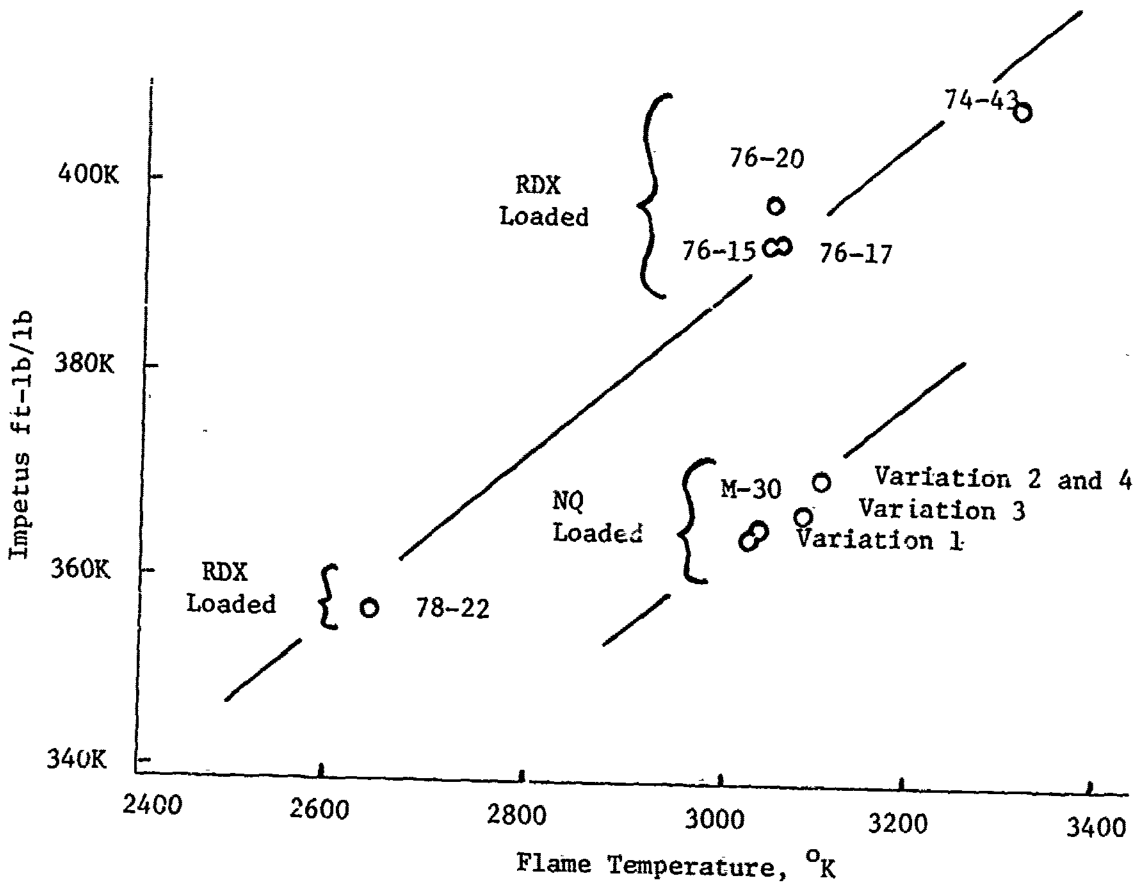

FIGURE 2
THEORETICAL BALLISTICS
PROPERTIES OF SEVERAL SOLID LOADED FORMULATIONS

A series of formulations was mixed using ammonium perchlorate (AP) as the energetic solid. The purpose of this program was to develop a low primary smoke rocket propellant. The use of AP in the formulation enhanced the specific impulse and density. We discovered that the card gap sensitivity put this material into a Class 1, Division 1 category. We began work to desensitize the formulations without unduly affecting the specific impulse or density.

A series of formulation variations was conducted to arrive at a composition that had a minimum card gap sensitivity. We found that by slight changes in the binder composition we could vary the card gap from 1.20 inches to zero. These changes were conducted on a 40% AP, 26.4% nitrocellulose, 31.5% plasticizer and 2.1% additives composition. The changes were primarily in the level and efficiency of the active plasticizers. The active plasticizers controlled the degree of gelatinization of the nitrocellulose and thus the solubility of the energetic plasticizer in the binder. The material extruded well and good strands were obtained. We extruded solid rods of 0.25 inch and 1.50 inch in diameter. Other similar formulations were manufactured using 50% and 60% ammonium perchlorate. Physical property data are shown for these formulations in Table V. The refractive index of ammonium perchlorate is close to that of the binder so a transluent material is obtained. The nitramine loaded material is opaque. Either the AP or the nitramine loaded formulations could be used as smokeless rocket propellants.

TABLE V
Physical Property Data on Several AP Compositions

	Sm	Em	Sr	Er	Ym
+77°F					
40% AP	407	23.4	415	27.4	5764
50% AP	393	9.0	334	14.8	10685
60% AP	300	9.0	246	13.9	6702
+165°F					
50% AP	81	6.96	81	6.96	1786
60% AP	59	5.54	59	5.54	1389
-65°F					
50% AP	3315	5.92	3315	5.92	70619
60% AP	2595	5.19	2595	5.19	60961

The safety of this processing procedure is still being investigated, but based on the safety analysis of similar processing we believe the No-Roll Process is significantly better than conventional processing.

For some of the safety considerations we used data that had been obtained on previous processes. Compositions consisting of 30% energetic material and 70% heptane were initiated with a C-4 booster material.[4] These mixtures did not propagate, indicating that the slurries are non-detonable. This is not to say that the ingredients as they are added could not be detonated, but the mixing slurry is only a deflagration hazard.

After decanting and drying, the No-Roll processed material looks like a dried crumb. This material has been subjected to a deflagration to detonation transition (DDT) test. A heavy wall 2 inch pipe was loaded with the dried crumb. Pipe caps were used to seal both ends and the formulation was ignited using a hot nichrome wire at the base end of the pipe. In all tests to date, the material has ignited and burned causing a simple pressure rupture of the pipe or a shearing of the pipe threads. In no case was there a detonation. Thus if the material were initiated in the extrusion press, a fire would be the only detrimental result.

SUMMARY

The No-Roll Process is a new method of processing solventless double-base and composite solids loaded double-base formulations. The product can be directly extruded. The process offers significant safety and cost benefits over conventional methods of manufacture. The results with RDX, AP and NQ loaded formulations have been favorable.

[4] D.H.Carstater etal Development of the Inert-Diluent Concept for the Manufacture of Double-Base and Composite-Modified Double-Base Propellants, U.S. Naval Propellant Plant Technical Memorandum Report 210 (Indian Head, Maryland: September 1963).

Paper Presented At The:

Department of Defense Explosives Safety Board

GUN PROPELLANT PROPAGATION IN AIRCONVEYING SYSTEMS

by

C. James Dahn
Safety Consulting Engineers, Inc.
Rosemont, Illinois 60018

ABSTRACT

A test program was conducted to determine the propagation parameters of fire and explosions in airconveying systems of 4 inch and 6 inch diameter up to 160 ft. long, airconveying systems for transport of gun propellants. Pressure pulse and flame propagation was monitored during testing. Low bulk density gun propellants propagation properties were established. Propagation rate tests were also conducted utilizing various venting configurations and pulse feed propagation in up to 160 ft. pipe. Very high propagations were found in some airconveying configurations.

INTRODUCTION

Pneumatic conveying systems have been utilized for transporting of gun propellants from one building or location to another since the early 1950's. Radford Arsenal and Naval Ordinance Station both have utilized airconveying systems extensively for transporting gun propellants. Both continuous airconveying and pulse feed airconveying systems have been utilized. Trationally, vacuum conveying systems are utilized for airconveying of propellants. A typical configuration is shown in Figure 1. Here, for the continuous propellant flow, a pickup wand draws the powder from a hopper under vacuum and transports it to a cyclone separator. Here, the propellant drops out of the air stream into a drop leg. From here, as the propellant builds up in the leg, a Dustex Boot Valve permits the powder to drop out into a hopper. The air is normally taken from the cyclone into a wet scrubber and from there into an airconveying fan.

As a result of plant modernization efforts, Olin Corporation had contracted Safety Consulting Engineers, Inc. to study the explosion propagation characteristics of airconveying of low density powders when changing from air piping of 4 inch to 6 inch diameter. The pipe diameter increase was prompted by increasing output of the airconveying transport systems between blending and glazing operations and packout. The transport distance on the plant improvement was extended up to 160 ft. As a result, concern was expressed regarding the time a propagation could transfer from one building to another. If this time interval was shorter than the response time of a fire suppression system, a serious hazard could exist in the receiving operation.

As a result of this concern, a series of airconveying propagation tests were conducted to characterize this phenomenon.

SHORT RUN AIRCONVEYING PROPAGATION TESTS

A low density rolled ball propellant was selected for evaluation of propagation tests. This propellant, WC 452, has characteristics as shown in Table 1. Here, we see that the propellant has a very small web size and has a modest nitroglycerin content.

Four inch and Six inch diameter airconveying systems were configured at the Safety Consulting Engineers, Inc. test site as illustrated in Figures 2 and 3. Approximately 30 pounds of propellant was placed in a transfer bucket in which the airconveying wand was located. Propellant was then airconveyed under vacuum over to a cyclone which dropped the propellant out into a receiving bucket. In the test setup, the piping went directly from the cyclone into the blower. The powder transfer distances range from 35 to 58 ft. in this series of tests. In all cases, the propellant was transferred with an air velocity of 5500 ft. per minute. A bypass valve on the blower was utilized to balance the air in the system. The blower utilized for this test was a 7 1/2 Hp. New York type of blower which had approximately 1200 cfm airflow capacity.

In this series of tests, the propellant powder-to-air ratio was varied and methods to relieve the propagating reaction in the pipes was tested. The propagation rates were monitored by SCE design infrared sensors detecting flame front propagation. These sensors were located in various positions in the piping.

A typical test setup for the 6 inch airconveying system is illustrated in Figure 4. The ensuing explosion yielded pipe fragmentation and destruction of the test setup and is illustrated in Figure 5. A 6 inch diameter schedule 10 pipe was utilized in this test.

The variation of powder-to-air ratio made a significant difference in the propagation velocity and times. This effect is shown in Figure 6. The 6 inch diameter airconveying system's propagation for equal powder-to-air ratios are nearly double.

Propagation velocity measurements at various increments down the pipe was conducted on the 4 inch airconveying system. The same system was tested incorporating blowout flaps at stations 20 ft. apart from each other. The resultant times and velocities versus distance from trigger are illustrated in Figure 7. Here, we see that for the 4 inch airvey system, the propagation velocities are still accelerating after a 40 ft. length of pipe travel.

PROPAGATION PRESSURE PULSE MEASUREMENTS

In this series of tests, two piezoelectric pressure gauges were mounted in the airconveying piping at a distance of 21 ft. from each other. The infrared fire propagation sensors were placed at a distance of 20 ft. apart. At each station, the infrared sensor was approximately within 1 ft. of the pressure transducer. The airconveying setup showing locations of the infrared sensor and pressure transducer are illustrated in Figures 8 and 9. The pressure transducer output cable was placed in a plastic pipe to prevent fire damage during the tests. The first test conducted employing the pressure transducers utilized a 6 inch diameter airveying system with a powder-to-air ratio of 0.15. The propagations were initiated by a blasting cap within 6 ft. of the transfer wand. The resultant explosion fragmented the 6 inch pipe and totally destroyed the pressure transducers.

The next series of tests was conducted at 4 inch diameter airconveying piping. In this series of tests, pressure output at various stations was greater than 300 psi as illustrated in Figure 10. The test was conducted at the powder-to-air ratio of 0.18 pounds per ft.

A typical infrared propagation sensor output for a 6 inch airconveying system is shown in Figure 11.

INITIATOR EFFECT ON PROPAGATION

Airconveying propagation tests were conducted utilizing squibs as initiators to determine if the blasting cap output could have caused excessively high propagation rates. The results as shown in Table 2 reveal that the propagation rate does not change appreciably due to initiator type.

160 FT. PROPAGATION TESTS

A new airconveying system was laid out so that a 160 ft. of straight pipe for 6 inch schedule size could be utilized. Continuous flow airconveying propagation tests were conducted in this configuration as shown in Figure 12. In these tests, the propagation rates were exceedingly high even with low powder-to-air ratios. The shortest time interval between trigger at station 4 and fire in the hopper at the cyclone was 40 milliseconds. These tests were compared to tests conducted at shorter pipe lengths. A significant increase in final velocities were noted on the 6 inch airconveying system as the piping length increased up to 160 ft. as illustrated in Figure 13. In contrast, the 4 inch diameter airconveying pipe distance from 20 to 40 ft. in length yielded very little difference in propagation rates.

PULSE FEED PROPAGATION TESTS WITH 160 FT. LENGTH PIPE

The 160 ft., 6 inch diameter airconveying system was modified to permit pulse feeding into the system. This was done by placing the first pulse into a hopper and dumping the second pulse by a swinging bucket as illustrated in Figures 14 and 15. The quantity of powder in each pulse was varied to determine the characteristics of the powder pulse as it transfers down the line and also at propagation rate in case of explosion. A removable plug was located at the bottom of the hopper to permit the powder in the hopper to be drawn into the airconveying line at the correct time. A time sequence was then initiated to drop the second powder pulse.

In the first series of tests, the powder pulse length and velocities were monitored by using infrared sensors with light backgrounds. Thus, as the powder went by, the output of the sensor changed according to the concentration of the powder. The four stations used to monitor both the propagation and the pulse shaping is shown in Figure 16. Numerous tests were conducted to characterize the two powder pulses prior to propagation testing. Pulse velocity and pulse width for powder pulses ranging from 2 to 5 pounds yielded results as illustrated in Figure 17. Here, we see that for a 5 pound pulse, the pulse width in the piping was 120 ft. for the first pulse. The powder pulse velocities increased for small quantities of propellant, but as propellant quantities reached 4 and 5 pound sizes, the velocity did not change appreciably in the airconveying line. In this series of tests, it was discovered that the two powder pulses merged into one prior to the end of the 160 ft. run as illustrated in Figure 18. In this figure, we see that the powder concentrations smooth out and reduce as the powder goes down the piping.

Pulse propagation tests were conducted by firing caps and squibs at various timings of the second pulse in the airconveying system. A typical example of the explosion propagation output and the initial test setups are shown in Figures 19 and 20. The damage shown in Figure 20 was typical of a mild explosion. Severe explosions fragment the 6 inch diameter shedule 10 piping into sizes ranging from 2 inch square to 1 ft. square. Typical 160 ft. pulse feed airconveying propagation test results are shown in Figure 21. Here, we see that a propagation did not occur when the second pulse was only 40 ft. down the line from the hopper. The locations of the pulse were monitored by using backlighting on the infrared sensors to determine the powder concentration. The propagations were monitored when the light output from the flame exceeded that of the light source. In all the pulse feed testing, the powder-to-air ratio ranged from 0.25 to 0.28 pounds per cubic foot. When the leading edge of the powder pulse was located near the center point of the 160 ft. pipe, propagation occurred. In one test on a squib ignition, propagation did not occur into the drop leg, however, propagation did occur up to the cyclone. In summary, the pulse feed propagation tests yielded results varying in times from 40 milliseconds to 250 ft. milliseconds from initiator firing.

CONCLUSIONS AND RECOMMENDATIONS

Based on the testing program conducted, low density propellant propagates at very high rates in the airconveying systems even at low powder-to-air ratios (0.15 lb per cu. ft.). These propagations are significantly faster in 6 inch airconveying lines as compared to 4 inch. With a powder-to-air ratio of 0.15, the propagation accelerates in a 6 inch airconveying system, whereas, in a 4 inch system the rate approaches constant. The pressure of the explosion propagation in a 4 inch pipe exceeds 300 psi. There is a noticeable reduction in response time of the pressure transducers as compared to infrared sensors (i.e. pressure wave preceeds the flame in the piping).

Squibs, as compared to blasting caps as initiators, did not alter the propagation rates in the airconveying system.

In the 160 ft.-6 inch diameter airconveying system, under continued air flow, propagations between initiation at the transfer station to receiver bin was less than 40 milliseconds in several cases. This is faster than the high speed fire suppression system's capability. Utilization of vent flaps and weak elbows did not reduce the propagation rates in airconveying systems appreciably.

Pulse feed airconveying does not appreciably lower the propagation times from receiver to transfer stations. Actually, the damage to the piping is excessively greater by using pulse feed as compared to continuous flow, because the powder-to-air ratio is doubled.

It is recommended that propagation characterization tests be conducted on any low density gun propellant that has moderately high NG contents to properly delineate its propagation characteristics. It is also recommended that further study be conducted in the area of explosion vent relief at the cyclone end. It was noted in the tests, that propagations would go right through the Dustex boot, with very little damage to the Dustex boot itself. When drop legs of significantly longer lengths than those tested are used, significant explosion output can occur. Critical thickness of the powder can be exceeded quickly.

TABLE 1 CHARACTERISTICS OF LOW DENSITY WC 452 PROPELLANT FOR AIRVEY PROPAGATION TESTS

1.	Average Grain Diameter (Inches)	0.0145 (0.037 cm)
2.	Web (Inches)	0.0100 (0.025 cm)
3.	Gravimetric Density	0.540 gm/cc
4.	Nitrogen Content of NC	13.15%
5.	NG Content	13.5%
6.	Impetus (ft/lb/lb)	359,000
7.	Relative Quickness	237
8.	Heat of Explosion (cal/gm)	1025

TABLE 2 DIFFERENCE IN PROPAGATION RATES DUE TO CAP VERSUS SQUIB INITIATION IN 4 INCH AND 6 INCH AIRVEY SYSTEMS WITH POWDER RATIO OF 0.13 AND V = 55 fpm

SIZE AIRVEY	ITEM	DISTANCE	SQUIB AT WAND	BLASTING CAP AT WAND
6 Inch	Propagation Time (IR)	20 ft.	18 ms (1200 fps) 22 ms (910 fps)	12 ms (1700 fps) 20 ms (1000 fps)
		160 ft.	40 ms (4000 Fps) 80 ms (1928 Fps)	- -
4 Inch	Propagation Time (IR)	20 ft.	-	35 ms (571 fps) 40 ms (500 fps)
	Propagation Time (IR) (Pressure Pulse)	21 ft.	-	25 ms (840 fps)
	(IR)	20 ft.	-	30 ms (667 fps)
	Peak Pressure	20'ft	-	300 psi > powder ratio = 0.180 50 psi with powder ratio = 0.12

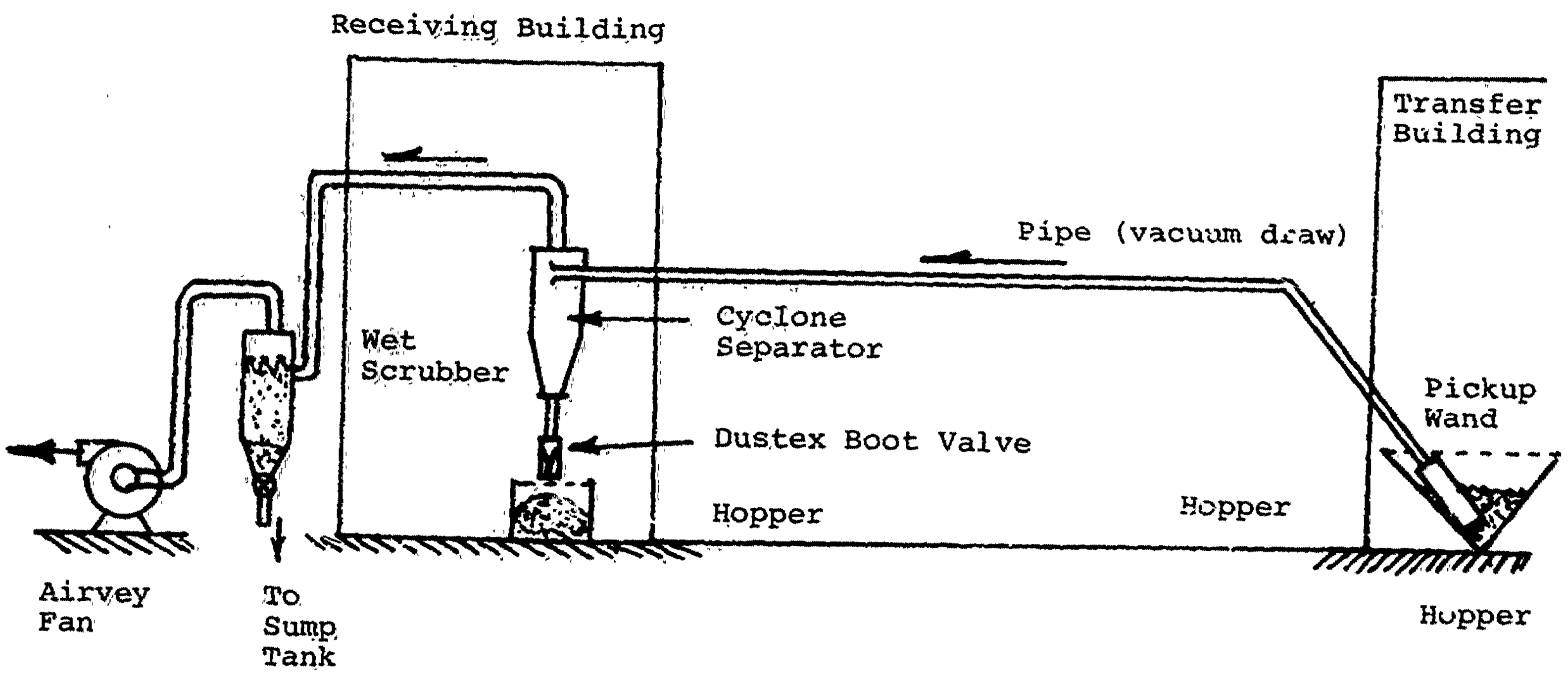

Figure 1. Typical Vacuum Air Conveying System for Properllant Transfer

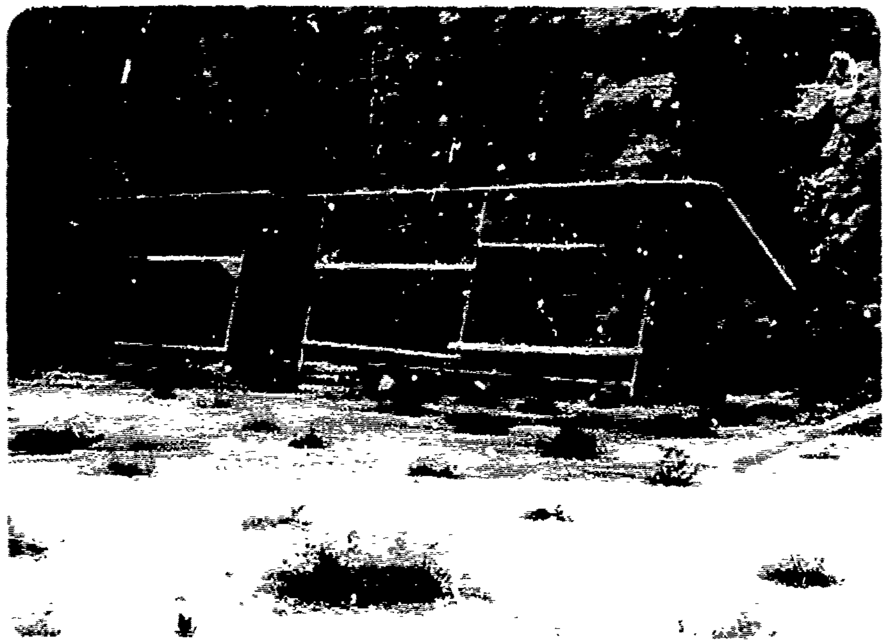

Figure 2. Air Conveying System Test Setup Vacuum Draw Fan System

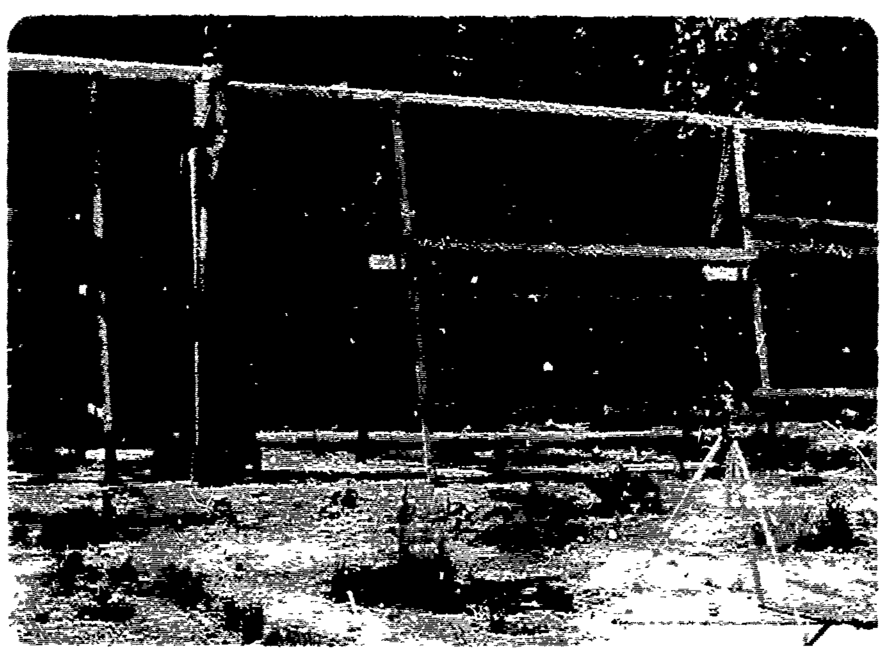

Figure 3. View Showing Cyclone and Drop Leg with Dustex Valve at Powder Exit

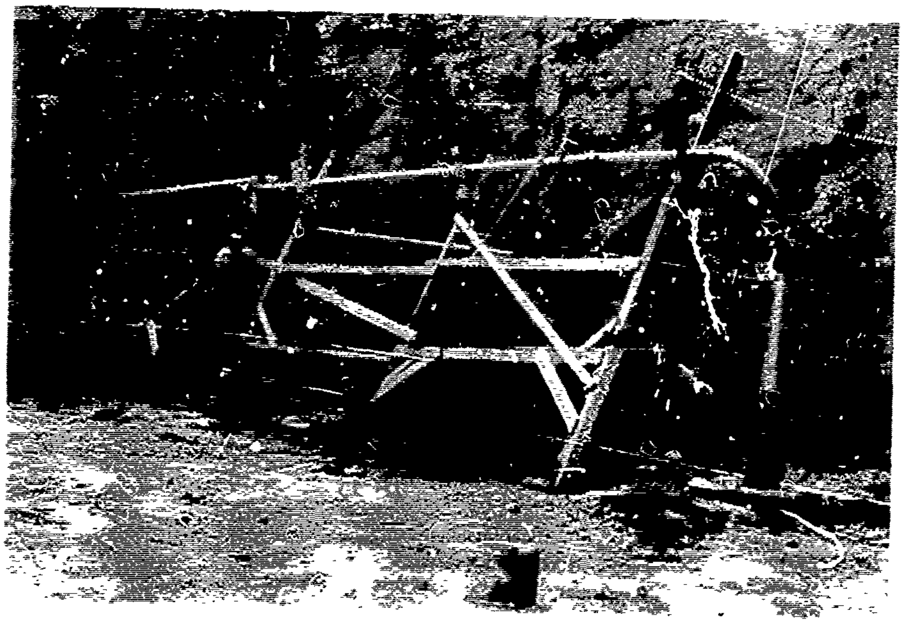

Figure 4. Setup of 6 Inch Airvey System

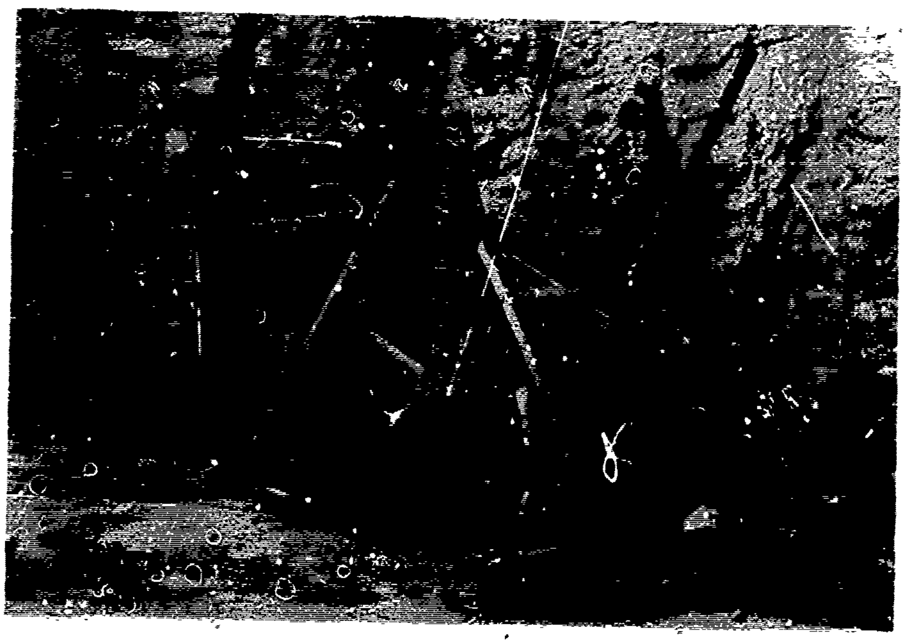

Figure 5. Setup After Major Explosion Propagation and Output of 6 Inch Airvey System

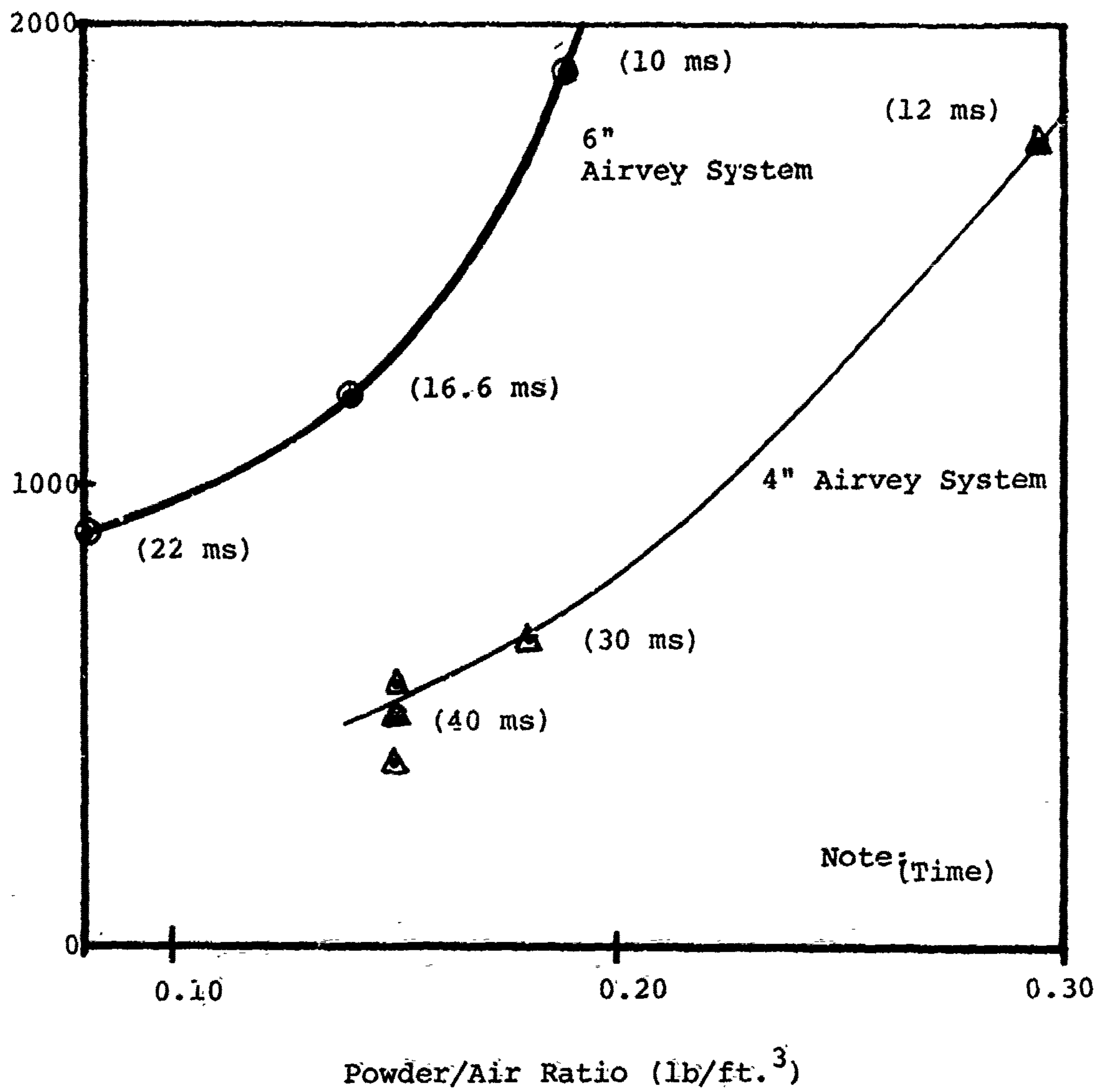

Figure 6. Propagation Velocity Variation with Powder to Air Ratio for 4 Inch and 5 Inch Airvey Systems. Measured in 20 Ft. Length Starting 10 Ft. From Wand.

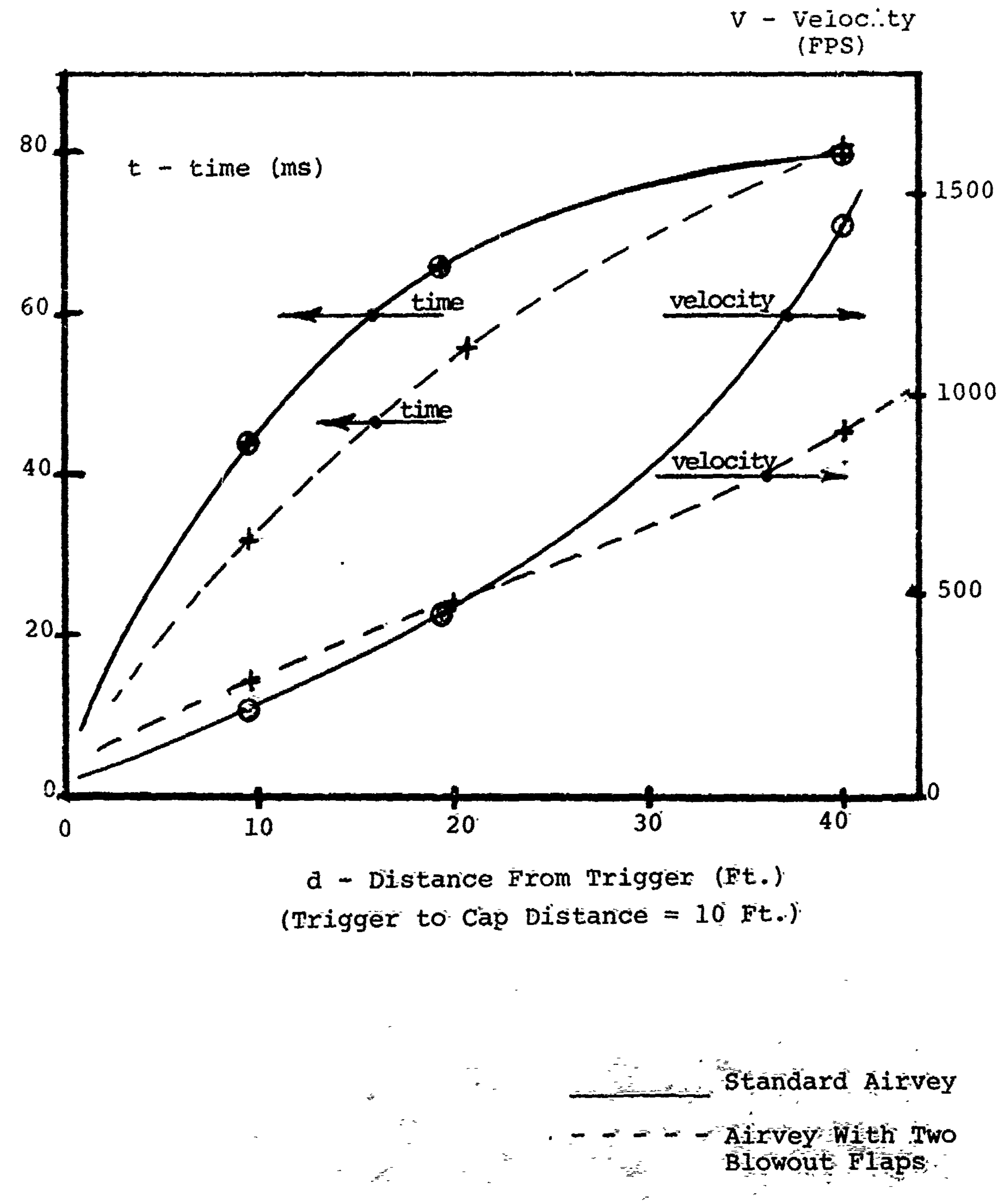

Figure 7. 4 Inch Airvey System Propagation Test Results - Powder to Air Ratio = 0.16 at 5500 FPM Air Velocity

Figure 8. Pressure Transducer Measurement Setup For 4 Inch Airvey System

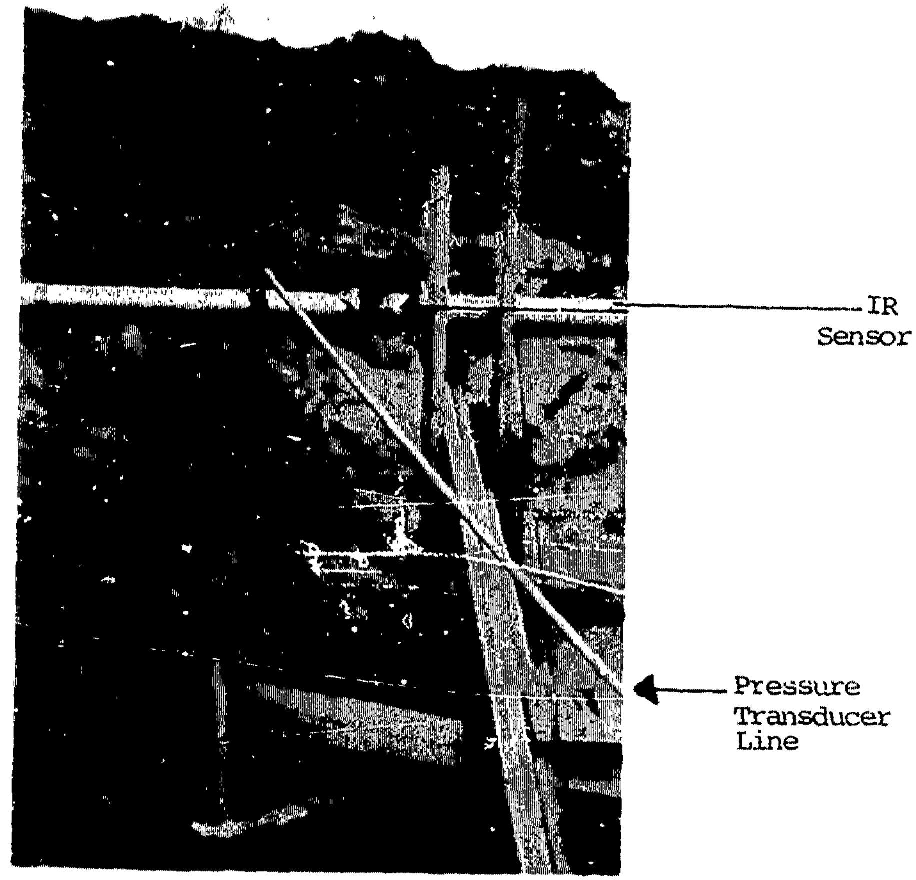

Figure 9. Locations of Pressure Transducer and IR Sensors at One Station - 4 Inch Airvey System

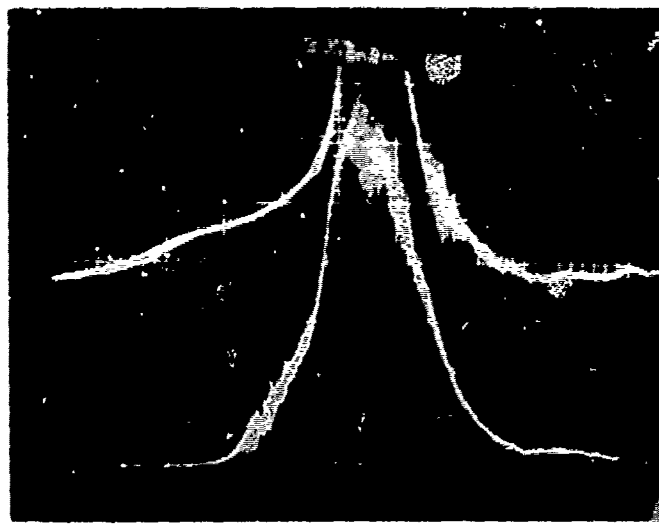

Figure 10. Typical 4 Inch Airvey System Propagation Test Pressure Transducer Output Powder Ratio of 0.18 lb/ft^3

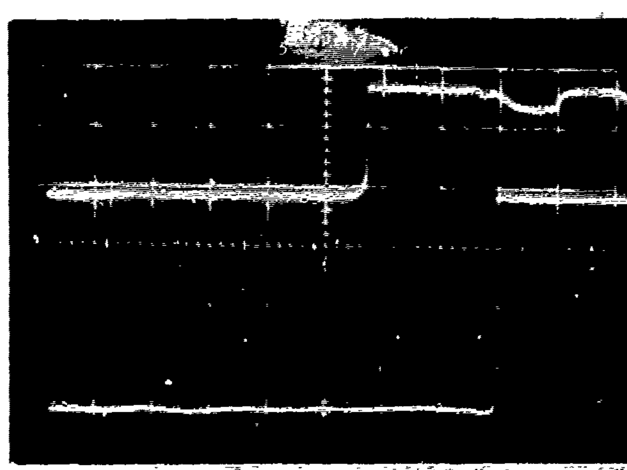

Figure 11. Typical Infrared Propagation Sensor Output of 6 Inch Airvey System

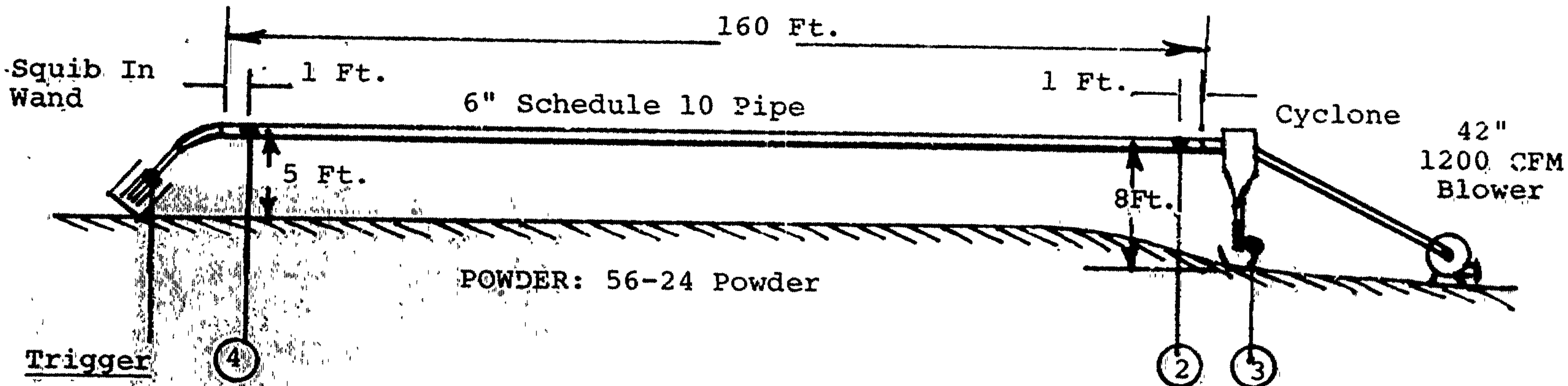

TEST NO.	DATE	TEMP.	REL. HUMIDITY	POWDER TO AIR RATIO	AIR VELOCITY UNDER LOAD	TIME TO FIRE FROM BLOWER START	TIME FROM TRIGGER TO #3 DUSTEX EXIT	TIME FROM #4 TO #2
1	9 Sept. 1978	80	85	0.16	5000 fpm	5 sec.	158 ms	83 ms
2	17 Sept. 1978	86	85	0.13	5000 fpm	7 sec.	#4 to #3 = 40 ms	

Figure 12. Several Continuous Airvey (160 ft. long) Propagation Test Results

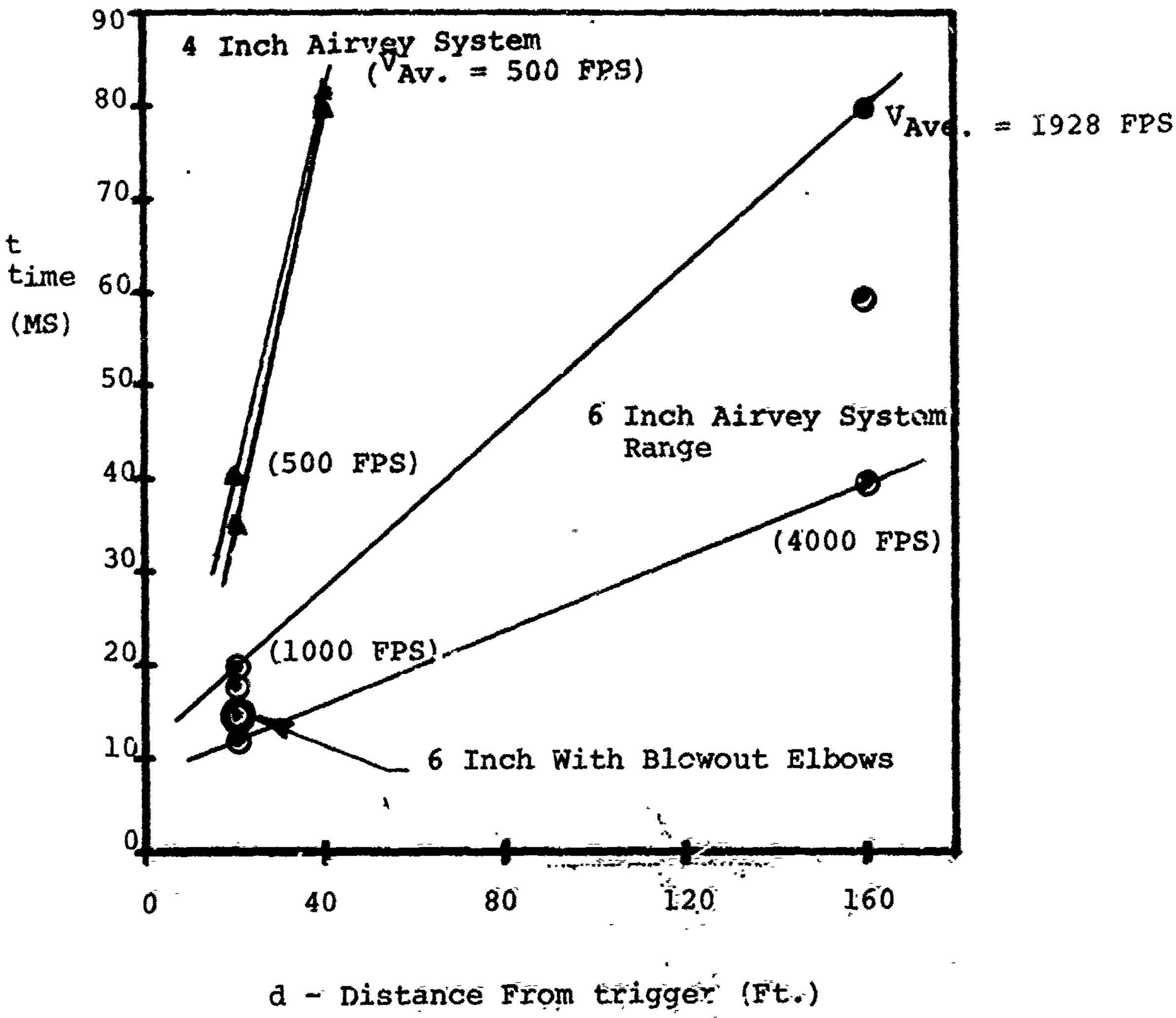

Figure 13. Propagation Time in 4 Inch and 6 Inch Airvey Systems at Powder Ratio of 0.150 lb/ft^3 and 5500 FPM Air Velocity

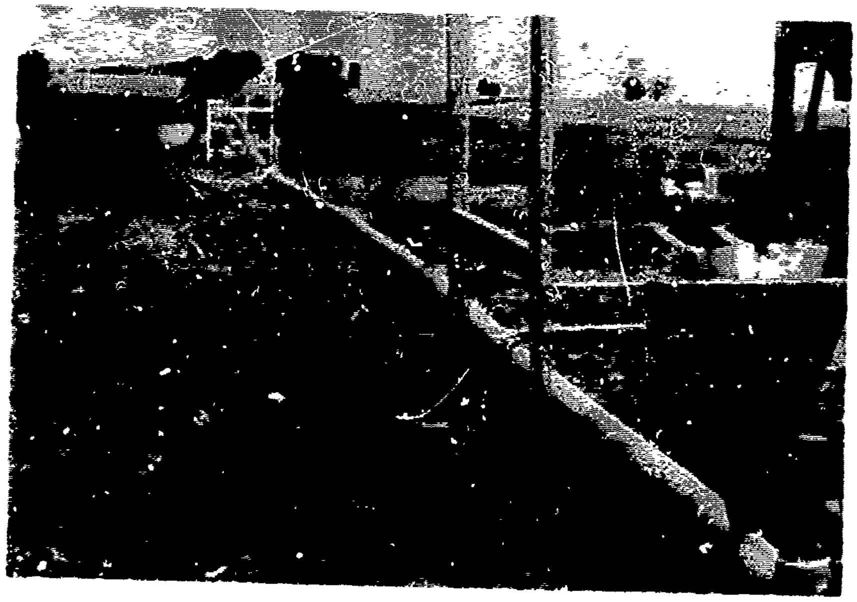

Figure 14. Test Setup for 160 Ft. Long - 6 Inch Diameter Airvey System Propagation Tests - Drop Bucket in Armed Position

Figure 15. Same as Above, Except Drop Bucket Dumped into Hopper

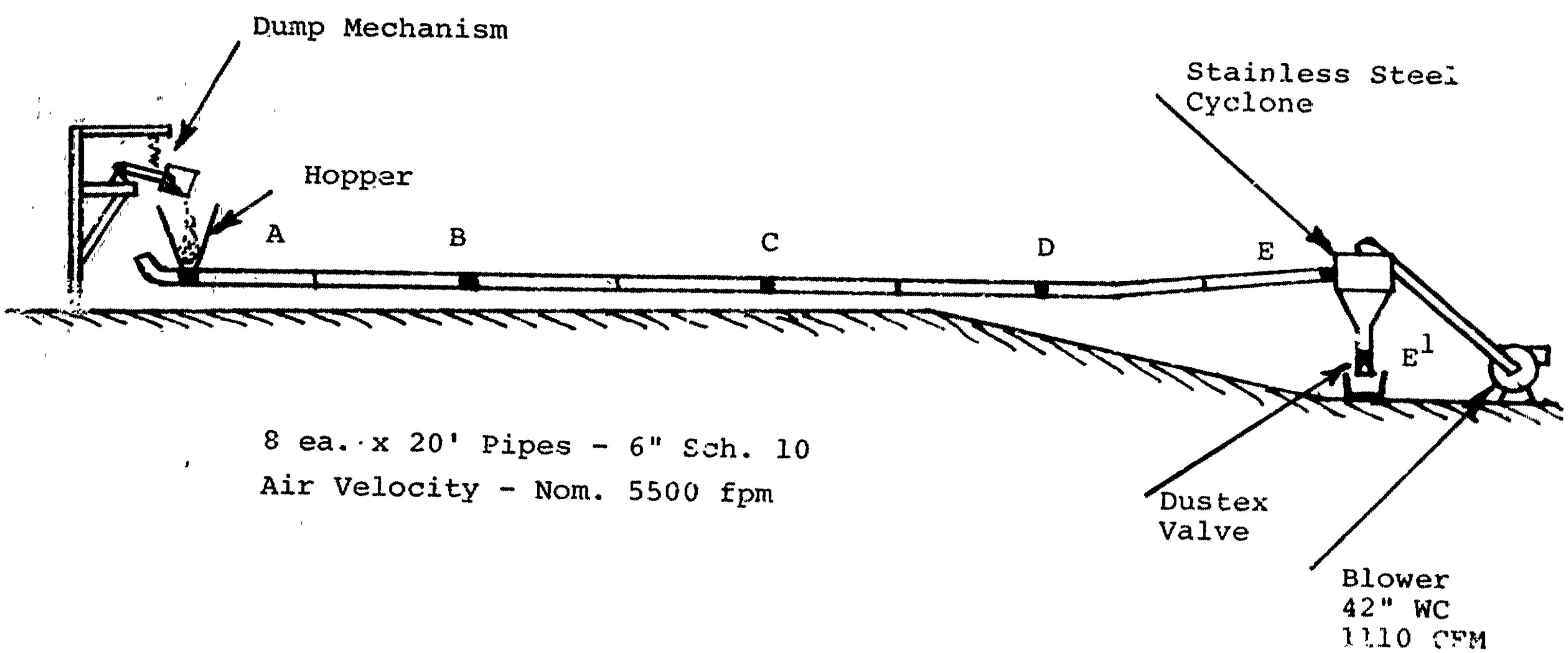

Figure 16. 160 Ft. Pulse Airvey Test Setup - 6 Inch Schedule 10 Pipe

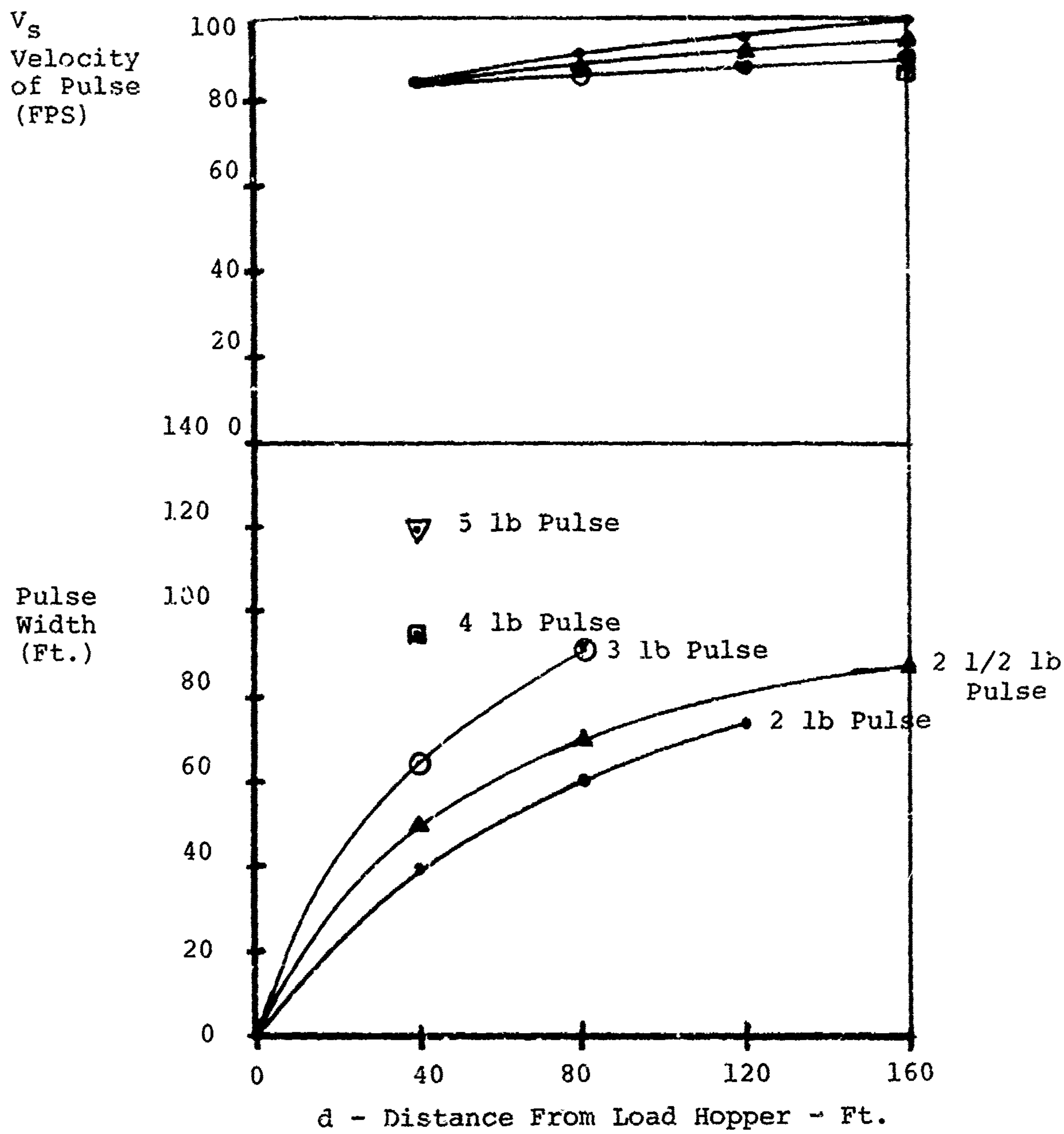

Figure 17 Powder Distribution and Velocity for Slug Feed Flow in 6 Inch Airvey Powder Ratio = 0.28 lb/ft.[3]

*Run 14 c
W_{p_1} = 2.5 lb W_{p_2} = 2.5 lb

STATION

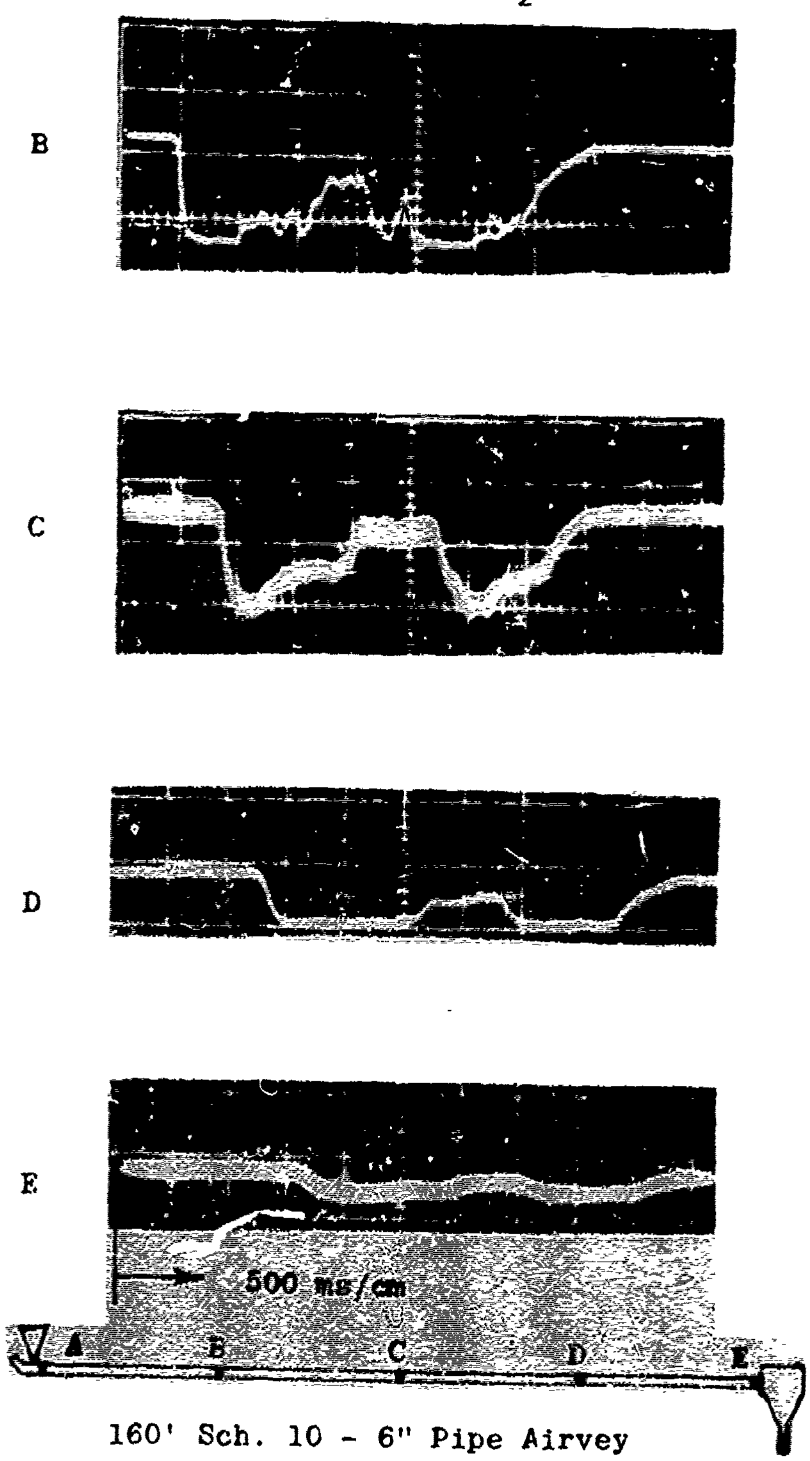

160' Sch. 10 - 6" Pipe Airvey

*Hopper Diam. = 2.55 inch.

Figure 18. Powder Distribution & Pulse Velocity Measurements - Two Pulses 1 Second Apart Hand Poured 2.5 lb. Pulses Into Hopper

Figure 19. Aerial View of 160' Ft. Long 6 Inch Diameter Airvey System Prior to Test

Figure 20. Setup After Propagation Test

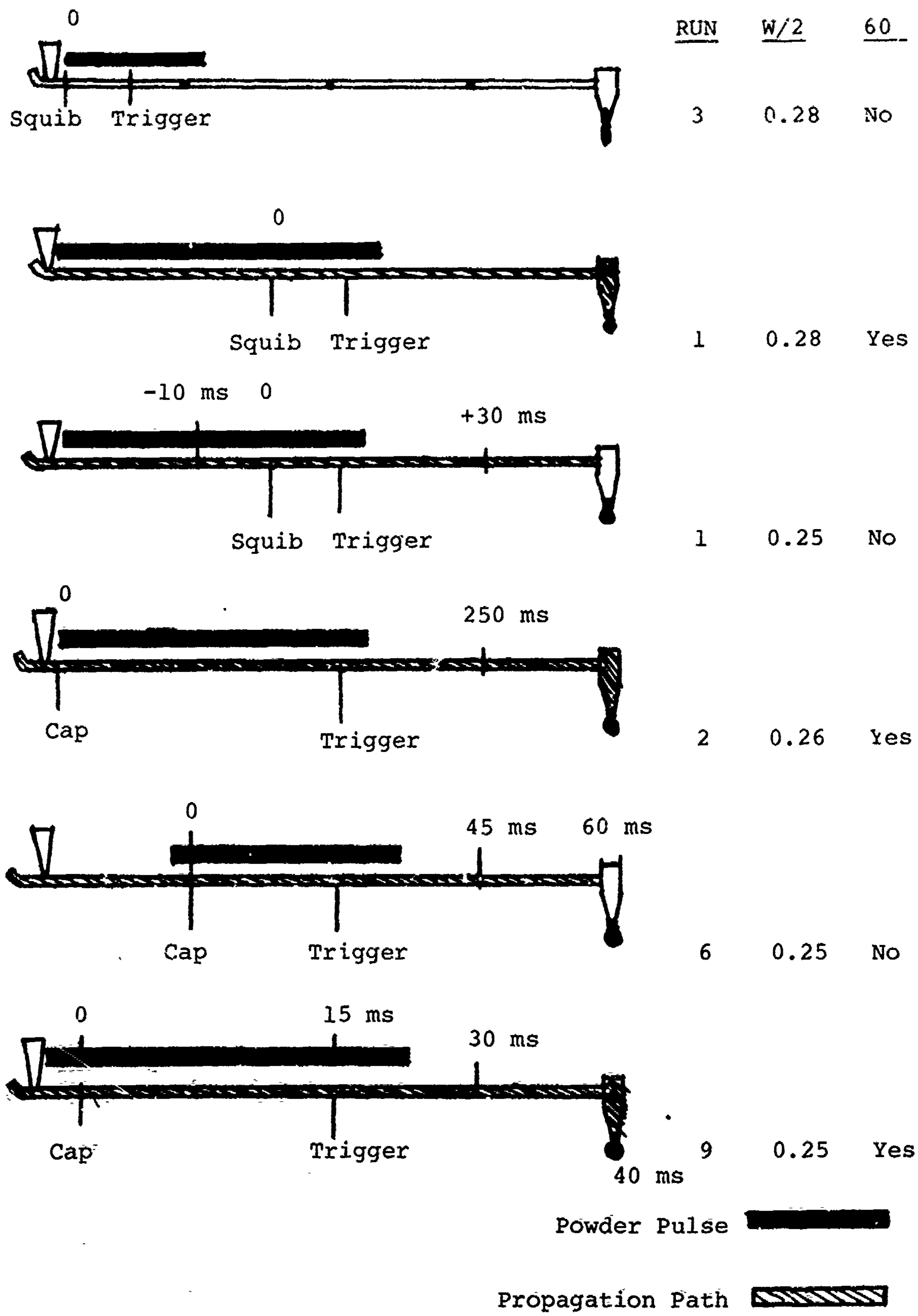

Figure 21. Typical 160 Ft. Pulse Fed Airvey Propagation Test Results

PRECEDING PAGE BLANK-NOT FILMED

UCID- 18251

Lawrence Livermore Laboratory

INTERIM REPORT ON USE OF STEEL FIBERS IN CONCRETE SLAB CONSTRUCTION
TO RESIST SPALL CAUSED BY HIGH-EXPLOSIVE BLAST EFFECTS

R. K. Mullins and C. F. Baker

September 7, 1979

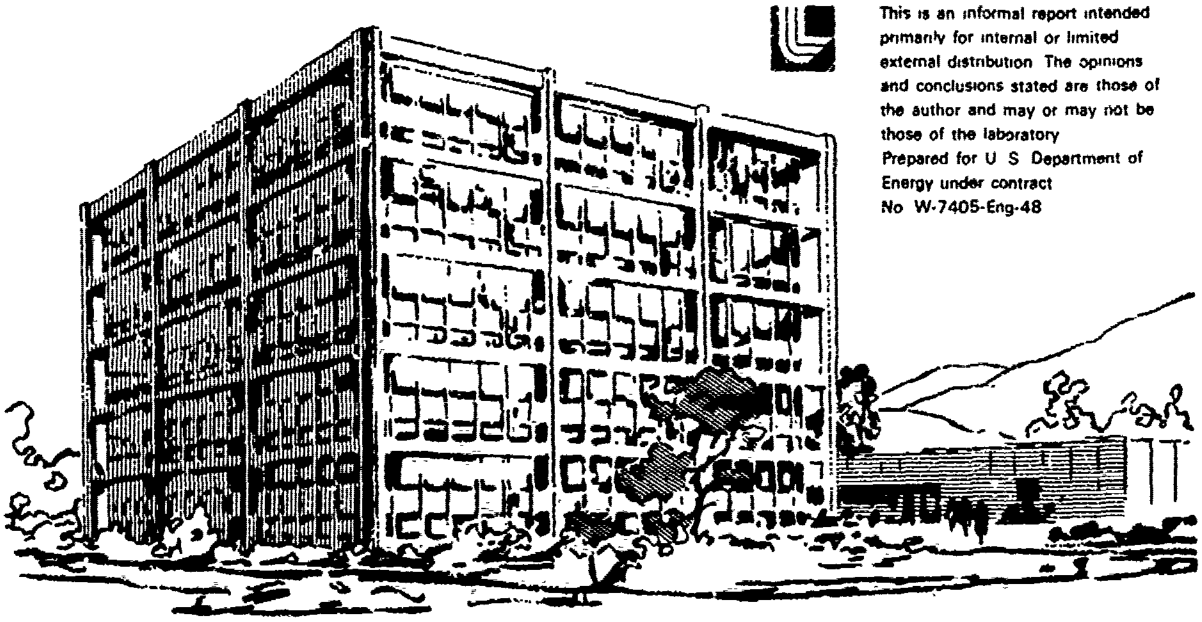

This is an informal report intended primarily for internal or limited external distribution The opinions and conclusions stated are those of the author and may or may not be those of the laboratory

Prepared for U S Department of Energy under contract No W-7405-Eng-48

INTERIM REPORT ON USE OF STEEL FIBERS IN CONCRETE SLAB CONSTRUCTION TO RESIST SPALL CAUSED BY HIGH-EXPLOSIVE BLAST EFFECTS

ABSTRACT

In this report we discuss the use of steel fibers in reinforced concrete slab construction. These fibers help to reduce the spallation of concrete from the reverse side of slabs subjected to close-in, high-explosive detonations. The effects of detonations of 20- and 49-lb charges of Composition 4 on seven 5-ft × 5-ft × 18-in.-thick reinforced concrete slabs are presented. Slabs were conventionally reinforced in both faces, with three slabs being additionally fiber-reinforced. Distances from the charge center to face-of-slab ranged from 10 in. to 36 in. Z factors ranged from 0.28 to 1.0. Concrete fragment velocities ranged from 17 ft/s to 70 ft/s. The slabs constructed with steel fibers showed significantly less damage and spall than similar slabs without fibers.

INTRODUCTION

A need existed for definitive information about concrete spall in blast-resistant structures. We present the detonation effects of 20- and 49-lb charges of Composition 4 on seven 5-ft × 5-ft × 18-in.-thick reinforced concrete slabs on shielding blocks (Figs. 1 and 2). Work has been done by the U.S. Corps of Engineers,[1] the Amman & Whitney Co.,[2] and others with scale model structures. Testing at full scale conditions has been recommended as a result of most of these previous studies.

Structures that benefit from spall-resistant construction include safe dividing walls for high-explosive processing, machining, or inspection bays and bull noses, or protective walls for firing bunkers.

The objectives for this investigation are presented herein.

- Establish guidelines for existing construction. This allows high-explosive operations as close as possible to existing walls and maximizes use of floor space.
- Determine spall fragment velocities and sizes to be expected from accidental detonation.

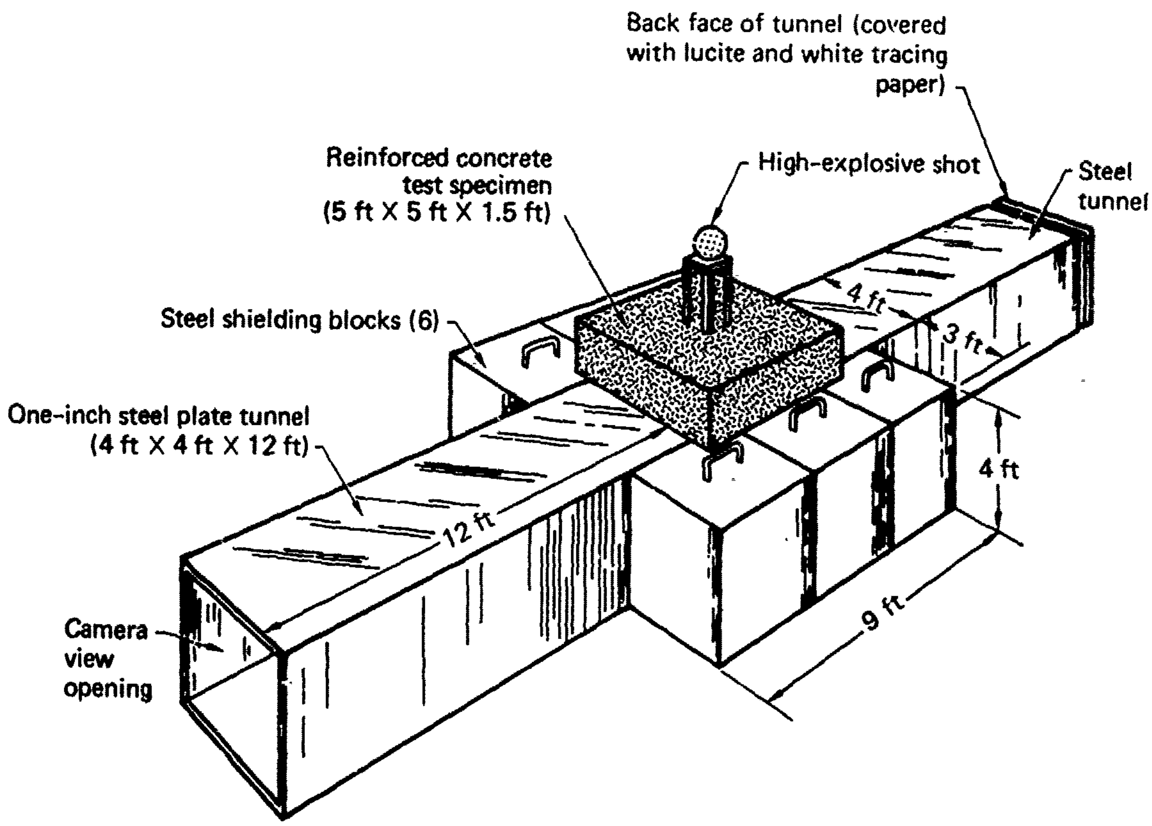

FIG. 1. Steel tunnel and slab support blocks.

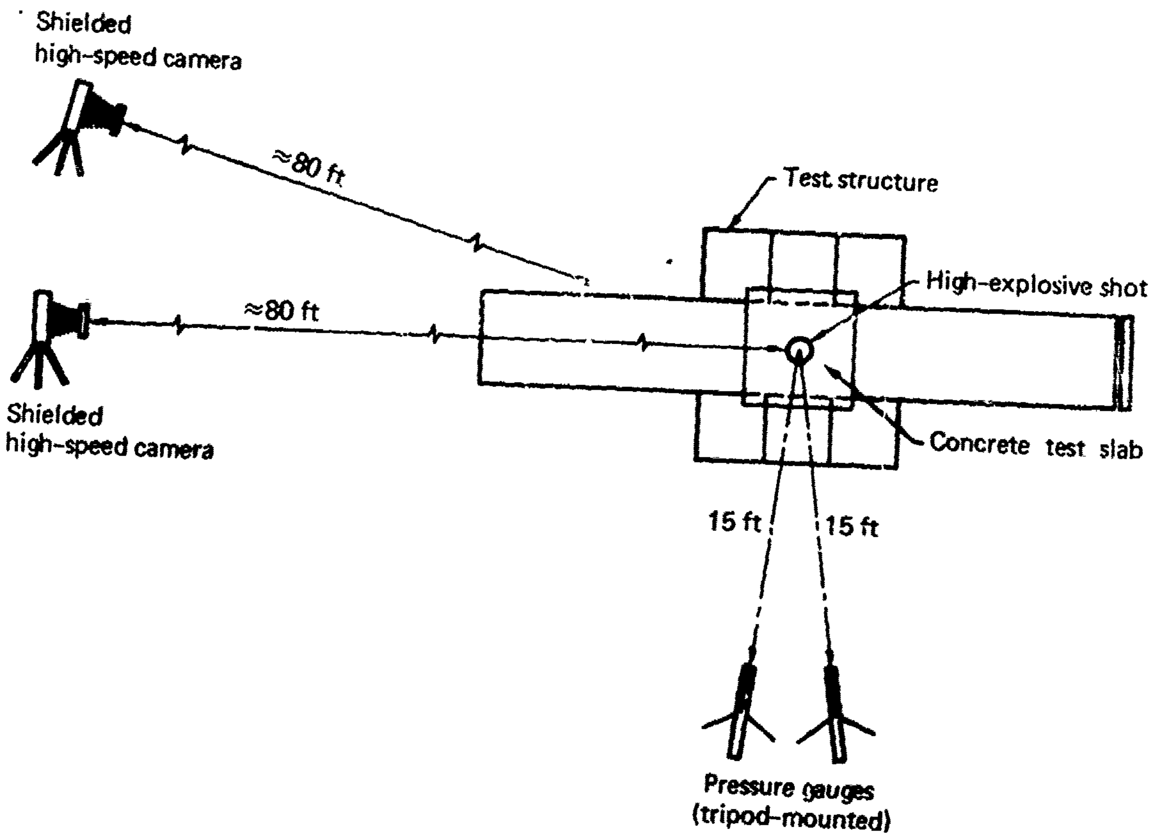

FIG. 2. Testing schematic--plan view.

- Advance Lawrence Livermore Laboratory (LLL) expertise in blast design, blast effects knowledge, and testing.
- Gain experience with design, cost, placement, and effectiveness of fibercrete mixes.

CONSTRUCTION MATERIALS

Conventional Concrete Mix Design

• Type II Portland Cement, 7 sacks/yd^3:		658 lb
• Concrete sand:		1240 lb
• 3/4-in. × No. 4 aggregate:		1860 lb
• Total water, 36 gal/yd^3:		300 lb
	Total	4058 lb

(Designed for 4000 psi minimum at 28 days.)

Fibercrete Mix Design

Gradation Letter--Primary Sizes

Sieve sizes:	100	50	30	16	8	4	3/8 in.	3/4 in.	1 in.
3/4 in. × No. 4:						2	21	93	100
Sand:	4	16	40	58	79	99	100	100	100

Combined

Sand (50%):	2	8	20	29	40	49	50	50	50
3/4 in. × No. 4 (50%):	0	0	0	0	0	1	10	46	50
Combined %:	2	8	20	29	40	50	60	96	100
Allow spec. limits:	1-5	5-15	12-25	20-35	27-45	35-60	45-75	55-100	90-100

	% Absorption	Specific gravity
3/4 in. × No. 4:	1.2	2.68
Sand:	1.5	2.68

Mix Design Procedures

a. Steel fibers:

- Use 1.25% by volume of steel (assumed)
- Volume = (0.0125)(27) = 0.3375 ft^3/yd^3
- 0.3375 ft^3 × 490 lb/ft^3 ≈ 165 lb/yd^3 0.010 in. × 0.022 in. × 1.00 in. long steel fibers

b. Air:

- Entrained air not used--no freeze thaw requirements
- Entrapped air = 1% = 0.27 ft^3/yd (assumed)

c. Aggregates:

- Fine aggregate (sand)
- Density = (62.4)(2.68) = 167.2 lb/ft^3
- Coarse aggregate 3/4 in. × No. 4
- Density = 62.4(2.68) = 167.2 lb/ft^3
- Calculate k factor after volume of other ingrediants are determined
- Volume of aggregates = k = 27 - vol. cement - vol. fly ash - vol. fibers - vol. air - vol. water - vol. admixture

d. Cement volume and fly ash:

- Use 7.5 sacks of cement for 4000 psi concrete at 28 days.
- $7.5 \text{ sacks} \times \frac{94 \text{ lb}}{\text{sack}} = \frac{705 \text{ lb}}{(62.4)(3.15)} = 3.59 \text{ ft}^3 \text{ cement/yd}^3$ before fly ash
- Substitute 12% by wt fly ash for cement:
  705 × (0.12) ≅ 84.6 lb cement replaced
  705 - 85 = 620 lb cement used 620/(94)(3.15) ≅ 6.6 sacks/yd
  84.6 × 1.2 lb fly ash/lb cement removed = 101.52
- Say $\frac{705 - 85}{(3.15)(6.24)} = 3.15 \text{ ft}^3 \text{ cement/yd}^3$ with fly ash

  Fly ash = 101.52, say $\frac{100 \text{ lb}}{(2.3)(62.4)} = 0.70 \text{ ft}^3$

e. Water volume:

- Assume $\frac{W}{C} = 0.40 \left[\frac{\text{lb water}}{\text{lb cement}}\right]$
- Volume of (cement + fly ash) = (3.15 + 0.70) = 3.85 ft^3
- Use original volume of cement for W/C ratio

  $\left[\text{Wt cement yd}\right] \times \left[\frac{W}{C}\frac{\text{wt water}}{\text{wt cement}}\right] = \text{wt water/yd}$

  $(3.59)(62.4)(3.15)(0.40) = 282 \text{ lb wt water/yd}^3$

  $\frac{282 \text{ lb}}{8.33 \text{ lb/gal}} = 33.85 \text{ gal water/yd}^3$

  $$\frac{33.85 \text{ gal}}{7.48 \text{ gal/yd}^3} = 4.53 \text{ ft}^3 \text{ water/yd}^3$$

f. Admixtures:

- Daratard HC or Pozzolith 300R--water reducing agent with set retarder.
- Use Daratard HC at the rate of 3 fluid oz/sack of cement.
- Daratard HC specific gravity = 1.18 or 9.83 lb/gal.
- 6.6 sacks/yd × 3 oz/sack = 0.155 gal/yd^3 (say 20 oz/yd^3)

  $\frac{0.155 \text{ gal}}{7.48 \text{ gal/ft}^3} = 0.02 \text{ ft}^3/\text{yd}^3$

g. Aggregate weights:

- k = 27 - 3.15 vol. cement - 0.70 vol. fly ash - 0.3375 vol. fibers
  - 0.27 vol. air - 4.53 vol. water - 0.02 vol. admixture = 17.99 ft^3
- Sand: 17.99 ft^3 × 0.50 × 167.2 lb/ft^3 = 1504 lb/yd^3
- 3/4 in. × No. 4: 17.99 ft^3 × 0.50 × 167.2 lb/ft^3 = 1504 lb/yd^3
- Water adjustment: Assume 3% water in sand; 0% water in 3/4 in. × No. 4 material.
- 1504 lb × 0.03 = 45 lb
- 282 lb total water - 45 lb sand = 237 lb batch water
  = 28.45 gal batch water

Fibercrete Mix Design Summary

Batch weights for the particulars included in the fibercrete mix design are listed in Table 1.

TABLE 1. Batch weight summary (1 yd^3).

Item	Volume, ft^3	Batch weight
Fiber (U.S. Steel)		
(0.010 in. × 0.022 in. × 1.00 in.)	0.338	165 lb
Air entrapped	0.27	--
Aggregates (SSD):	17.99	3010 lb
• Sand--3% free moisture	9.72	1550 lb
• 3/4 in. × No. 4--0% free moisture	9.0	1500 lb
Cement (Type II)	3.15	620 lb (6.6 sacks)
Fly ash	0.70	100 lb
Water	3.80	2.85 gal (+2 gal/yd^3 added at site)
Admixtures (Daratard HC)	0.02	20 fluid oz
Total:	27.0 ft^3	≈4175 lb

Handling and Batching

We accomplished the 6-yd fibercrete batching with a 7-yd ready-mix truck at a standard ready-mix concrete batching plant. The sequence and timing of operations follow:

- A total of 1800 lb of aggregate was added to 7-yd ready-mix truck at 0940 hr.
- Thirteen, 40-lb boxes of fibers were manually added from a loading platform to the revolving drum (approximately one-half of the fibers for this batch). (See Fig. 3.)
- Remainder of aggregate was added to revolving drum.
- Remainder of fibers was added to revolving drum (twelve, 40-lb boxes).
- Water, cement, and admixtures were added to revolving drum. Batching was complete at 1025 hr; 35 min batch time (complete batching).

FIG. 3. Adding steel fibers to mixer (40-lb boxes of U.S. Steel Fibercon). Fibers were added manually from platform to revolving drum of ready mix in truck.

- Arrived on job at 1045 hr.
- Started pouring at 1050 hr.
- Finished pouring at 1140 hr. Time from batch to pour: 1.25 hr (acceptable with retardant).

Because of the fibermix consistency, we had to vibrate the concrete down the concrete truck chute. The pour required a relatively flat angle chute. The measured slump cone averaged 4 in. for three tests. The 5-ft × 5-ft × 18-in.-high forms were placed on the ground; although the concrete had a 4-in. slump, thorough vibration was required to place and consolidate. We added 2 gal/yd^2 of additional water to the fibermix at the job site. (Refer to Figs. 4-7.)

Costs

- Fiber reinforced concrete:
  \$44.36/yd^3 + 165 lb fibers at 0.21/lb = \$79.01/yd^3
- Nonfiber reinforced concrete = \$44.20/yd^3

Fibers

We used United States Steel Fibercon steel fibers in the testing (0.010-in. × 0.022-in. × 1.000-in. rectangular cross section steel fibers).

Reinforcing Steel

We used ASTM A615 Grade 60 deformed bars for reinforcing steel during testing. Bars were No. 8 reinforcing steel on 6-in. centers each way in each face. The steel was 1-in. clear from the face of the concrete. We did not use lacing steel for these tests.

Sampling and Testing

We cast seven concrete cylinders for both normal and fiber reinforced concrete. The results are tabulated in Table 2.

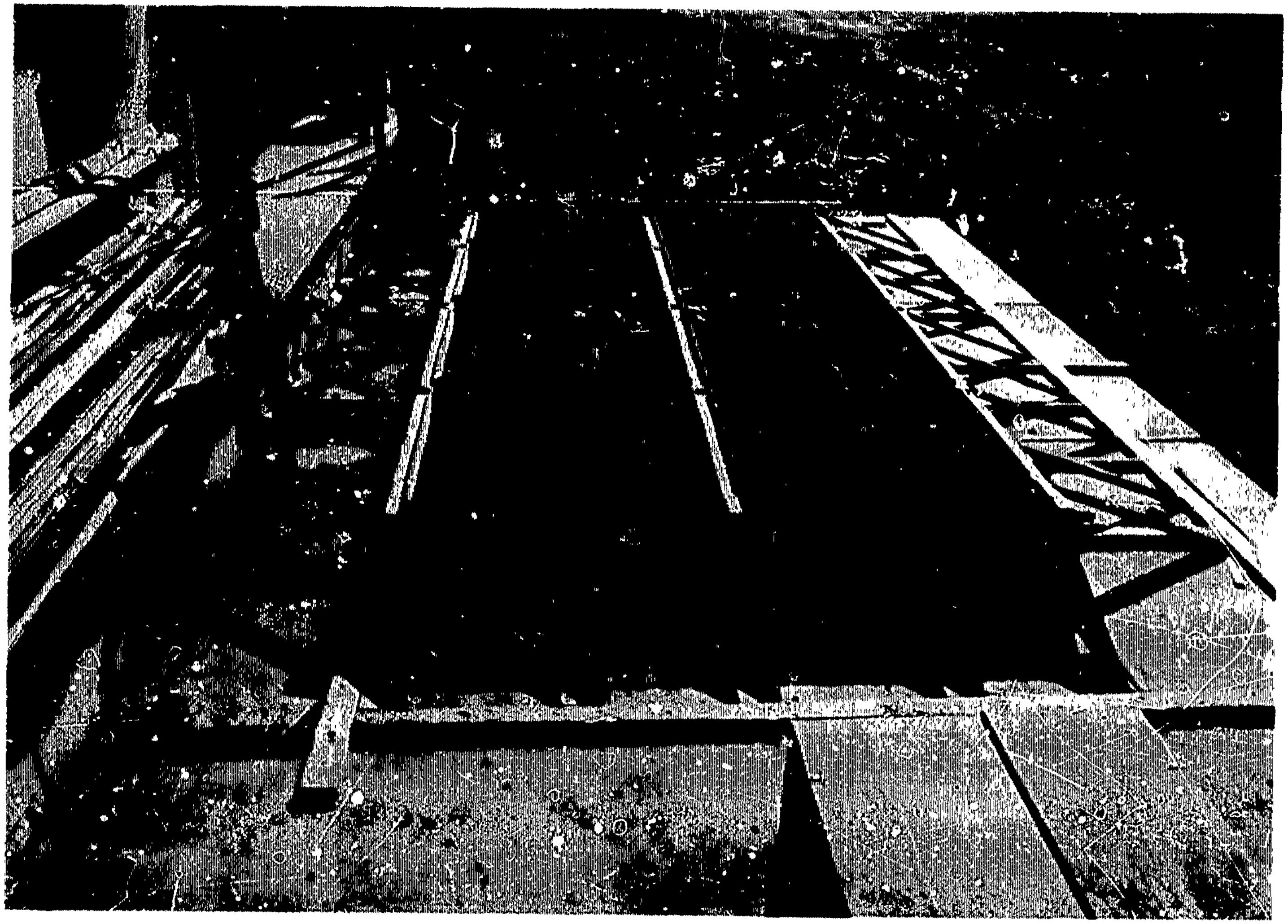

FIG. 4. Forms with rebars in place. Forms ready for pour with mixture of fiber and nonfiber reinforced concrete (5-ft × 5-ft × 18-in. slabs--8 each).

FIG. 5. Finishing four fibercrete slabs.

FIG. 6. Placing fibercrete. This mix of approximately 4-in. slump was very stiff and hard to move and required vibration and manual assistance to move it down the placement chute. The fibercrete did not flow well in the forms with vibration. Exact placement and extra vibration are required.

FIG. 7. Fiber balls (2-3 in. diam) were found in the fibercrete. These balls are all fibers coated with mortar from the mix and caused by less than perfect methods used in adding the fibers to the mix.

TABLE 2. Compressive strength failure of reinforced concrete cylinders.

Concrete: F = Fiber N = Nonfiber	N	F	N	F	N	F
Age, days	10	10	14	14	28	28
Compressive	3620	3170	4020	3700	4430	4060
Strength	3530	3260	3820	3900	4460	4410
Failure, psi					4650	4430
				Average:	4513	4300

The 28-day compressive strength failure averages are close for both fiber and nonfiber reinforced mixes. The mixes are considered equivalent for comparison purposes.

TEST DESCRIPTIONS

Slab Construction

We constructed eight slabs (5-ft × 5-ft × 18-in.-thick); seven were tested. We built four slabs with conventional reinforced concrete and four with fiber reinforced concrete. We used No. 8 reinforcing steel on 6-in. centers each way in each face. We also cast the slabs with lifting eyes.

Test Layout

We mounted the test slabs on shielding blocks, as shown in Figs. 1 and 2, and used 12-ft-long steel tunnels to prevent smoke and dust from prematurely obscuring the camera views. We also used a translucent lucite panel backed with white tracing paper as a background for the high-speed camera view. One high-speed camera viewed the test shot from a skewed angle. We aligned one camera's view with the longitudinal axis of the tunnel. Three "telltale" poles, with ends positioned 1, 2, and 3 in. from the underside of the slab, provided a reference for the camera. In addition, we drilled holes in the "telltale" poles with 1-in. centers. The spacing of the holes and the camera speed (frames/sec) were used to determine spall fragment velocities. We used two piezoelectric pressure gauges, 15 ft from shot center, to confirm high-explosive yield and repeatability of shots. The test slabs were supported on two sides with 6-in. bearing. (See Figs. 8-12.)

Calculations

We performed calculations showing that the test slab provided a μ value (blast deflection/elastic deflection) of approximately 6 for 20 lb of high explosive (Composition 4) at 3 ft. The Z value (distance/weight•TNT 1/3) would be about 1 for this condition. From previous references and experience, moderate damage to the concrete and a possibility of spall were to be expected.

Diagnostics

High-Speed Cameras

We used two Hycam Model No. 4000 cameras to determine fragment velocity and fireball size. One camera viewed the slab surface in shadowgraph and ran at 2000 frames per second, which gave an interframe time of 0.5 ms. We measured slab surface and fragment velocities using the holes in the "telltale" poles to lay out a grid. The second Hycam, also running at 2000 frames per second, viewed the entire area in order to monitor fireball size, smoke leakage paths, etc.

We used two pressure gauges to monitor overpressure, time of arrival, and shock wave duration. These data were used for shot-to-shot comparison only and showed no significant differences or discrepancies. We used Kistler Model No. 201 gauges for this purpose, connected as follows:

Kistler transducer, Model No. 201	→	Kistler amplifier, Model No. 504-E	→	Tektronix oscilloscope, Model No. 647	←	Trigger

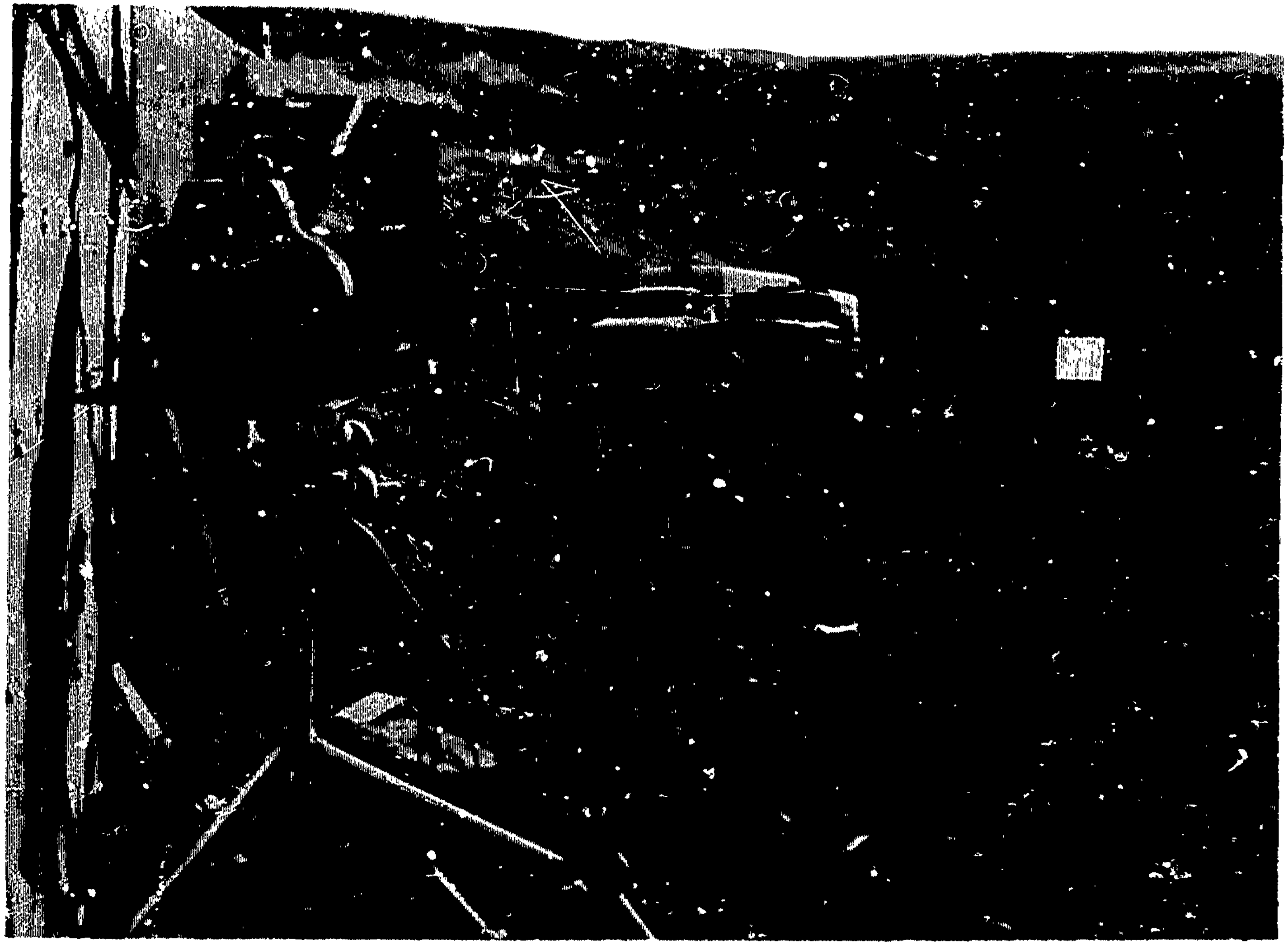

FIG. 8. High-speed (Hycam) camera used to photograph the high-explosive shots. This camera has a steel plate shield to minimize fragment damage.

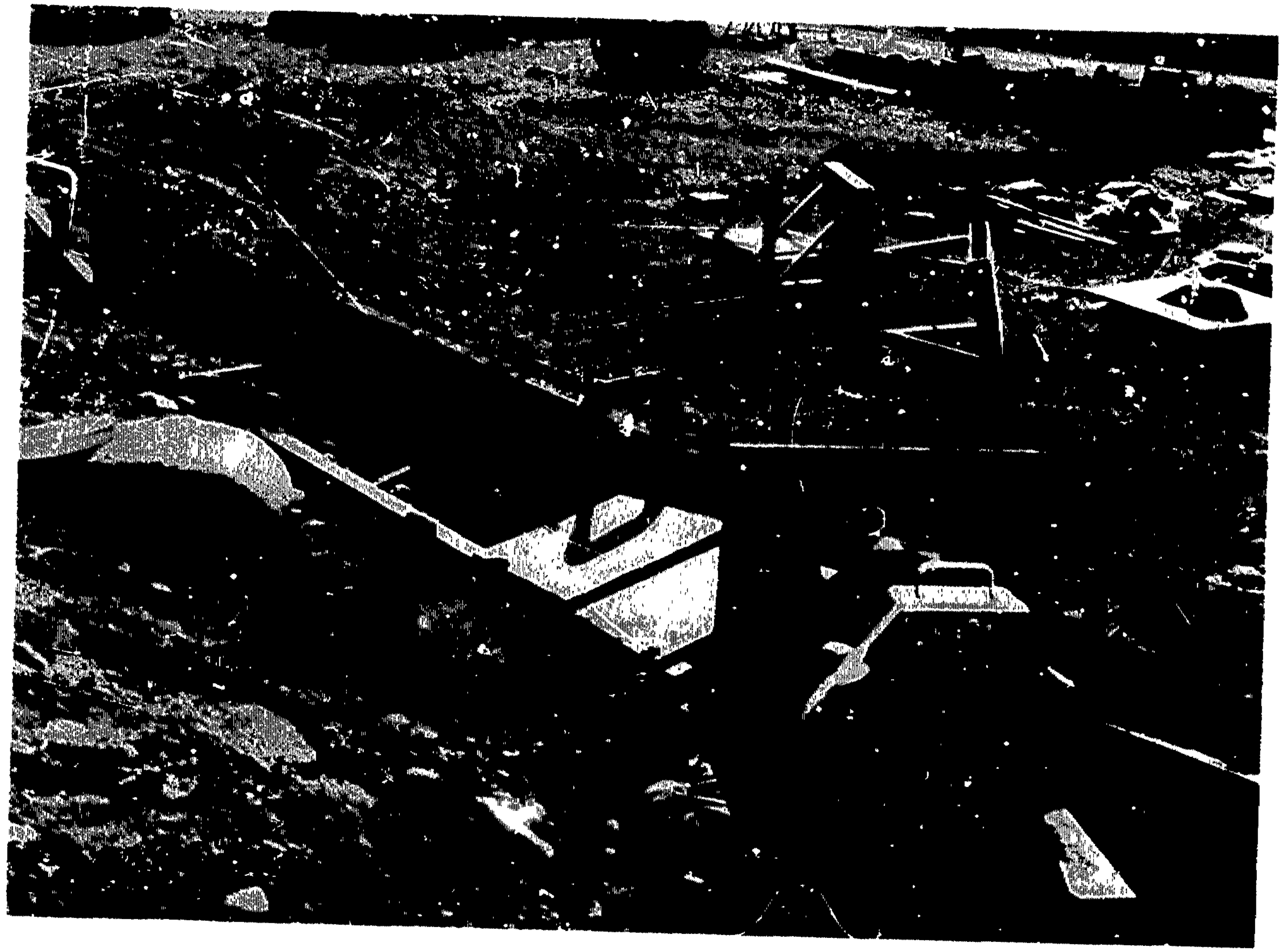

FIG. 9. High-speed camera (shielded) approximately 80 ft from test shot.

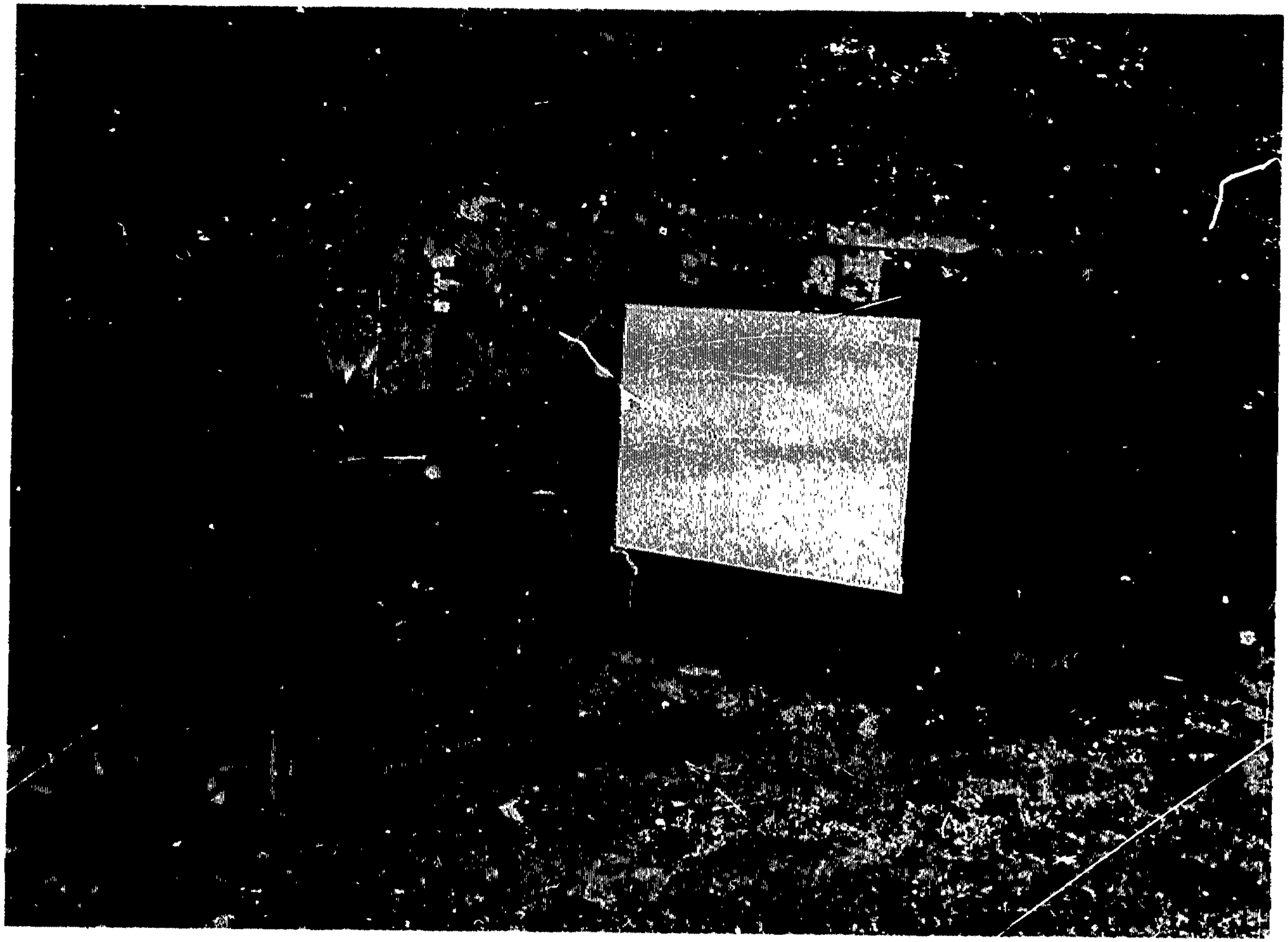

FIG. 10. Photo background using white tracing paper on a clear lucite panel. (Clamped on open end of steel tunnel.) Artificial lighting used on cloudy days.

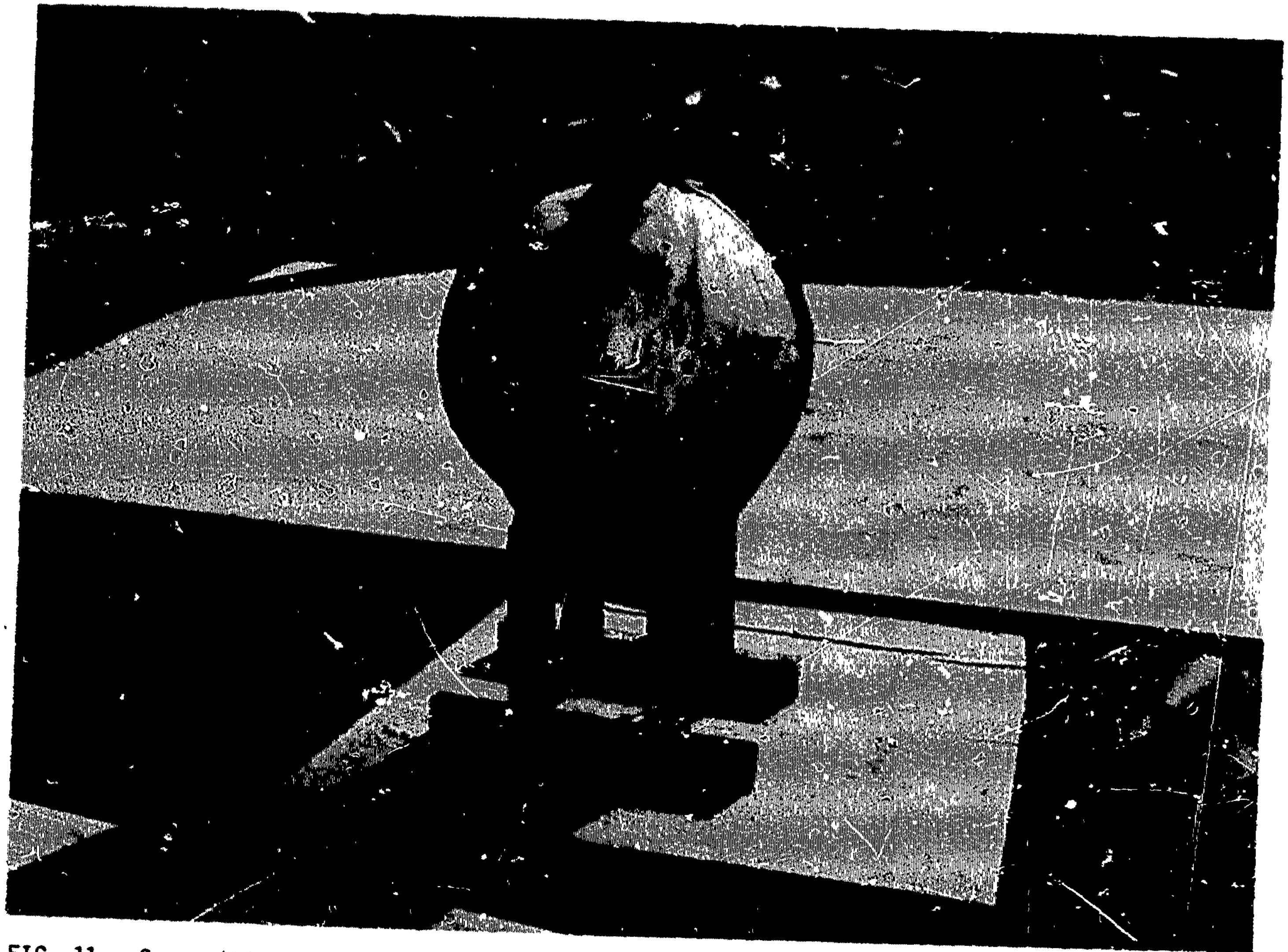

FIG. 11. Composition 4, high-explosive 49-lb, fiberglass-molded test shot that is mounted on concrete slab. (Two center detonators, spherical-shaped.)

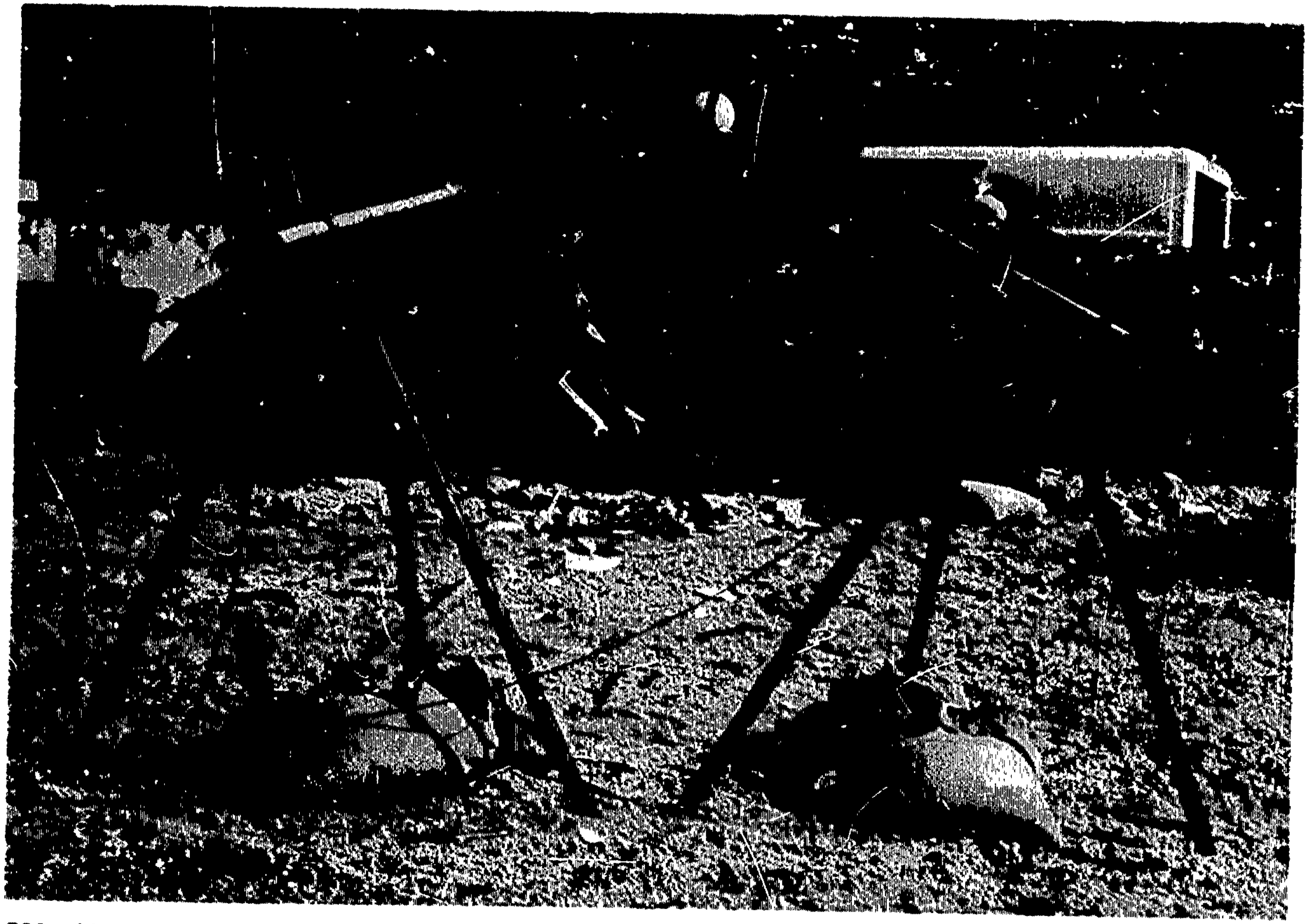

FIG. 12. Two piezoelectric gauges mounted 15 to 20 ft from the test shot, depending on shot size. The gauges measured the reflected pressure compared for each shot to ensure that the high-explosive yield was aoproximately equal.

TEST RESULTS

The characteristics, leading particulars, and results for the numerous test shots performed are contained in Table 3.

DISCUSSION

Test No. 400

This test at Z = 1.0 resulted in no spall. Hairline cracks were evident at centerline of bending. Scaled positive reflected impulse (Ir) psi-ms/lb•1/3 was 340. According to Ref. 3, 270 psi-ms/lb•1/3 should have been sufficient for spalling. (20 lb, C4 at 3 ft.)

Test No. 401

This test at Z = 0.5 used the same slab as Test No. 400 since we noticed so little damage. This test caused large cracks on unsupported edges. Some surface pitting resulted under the shot. No spall. Ir = 1050 psi-ms/lb•1/3. Reference 3 noted that 950 psi-ms/lb•1/3 would produce spall. (20 lb, C4, plain concrete.)

Test Nos. 402 and 403

These tests at Z = 0.28 resulted at 0.5 in. permanent deflection (bending failure) at midspan. Some pattern cracking and edge cracking. No spall. Ir = 2300 psi-ms/lb•1/3 vs 4000 psi-ms/lb•1/3 required for spall. (20 lb, C4 at 10 in., plain concrete slab.)

Test No. 404

This test at Z = 0.28, using fiber reinforced concrete, resulted in no damage. Ir = 6808. Ir = scaled positive reflected impulse = 2300 psi-ms/lb•1/3. (20 lb, C4 at 10 in., center of shot to face of concrete.)

TABLE 3. Results from test shots.

Shot No.	Date	Plain or fiber	Shot size, lb	Distance, in.	Impulse positive reflected, psi-ms	Z(ft/lb·1/3)	Fragment velocity, ft/s (avg. vel.: 3-10 in.)	Surface velocity, ft/s (avg. vel.: over first 3 in.)	Results
400	10/3/78	Plain	20	36	1000	1.0	--	--	Hairline cracks.
401	10/25/78	Plain	20	18	2975	0.5	--	--	Large cracks on unsupported edges. Surface pitting.
402	11/1/78	Plain	20	10	6808	0.28	--	45.8	Permanent deflection (0.5 in.) at midspan. Edge spall only.
403	11/7/78	Plain	20	10	6808	0.28	17.3	44	Edge cracking. Pattern cracking on spall side. No spall.
404	11/16/78	Fiber	20	19	6808	0.28	--	43	None.
405	2/2/79	Fiber	49	13.5	9177	0.28	68	100	Permanent deflection (2.25 in.) at midspan. ≈ 1/3 of surface spalled from bending.
[illegible]	2/8/79	Plain	49	13.5	9177	0.28	69.5	83	Complete spall. Bottom mat rebar displaced. Deflection (2.5 in.) at midspan.
407	2/16/79	Fiber	49	13.5	9177	0.28	58	72	Moderate spall. Large pattern cracks on underside of slab.

Test Nos. 405 and 407

These tests at Z = 0.28 on fiber reinforced concrete resulted in large permanent bending deflection (2.25 in.). Some minor spall. Ir = 9177 psi-ms•1/3. (49 lb, C4 at 13.5 in., center of shot to face of concrete.) (Refer to Figs. 13-27 for reference to Test Nos. 405-407.)

Test No. 406

This test at Z = 0.28 plain concrete resulted in complete spall of concrete and loss of bottom face rebar. Ir = 9177 psi-ms.

CONCLUSIONS AND RECOMMENDATIONS

- The fiber reinforced concrete reduced impact spall and prevented bending spall in the range of tests performed.
- Spall is impulse-related rather than scaled distance-related. We observed a wide variety of results for Z = 0.28 with varying high-explosive amounts.
- Fiber reinforced concrete showed no spall for Z = 0.28 and Ir $\leqslant$ 9177 psi-ms.
- Plain concrete demonstrated impact spall between Ir = 6808 psi-ms (none) and Ir = 9177 psi-ms (total face).
- Concrete spall does not appear to be nearly as great a problem as predicted from earlier literature. The limiting design value should be Ir $\leqslant$ 6800 psi-ms, rather than Z = 2.5 for plain concrete slabs. Wall thickness will have to be factored into this judgment, since this applies to 18-in. slabs.

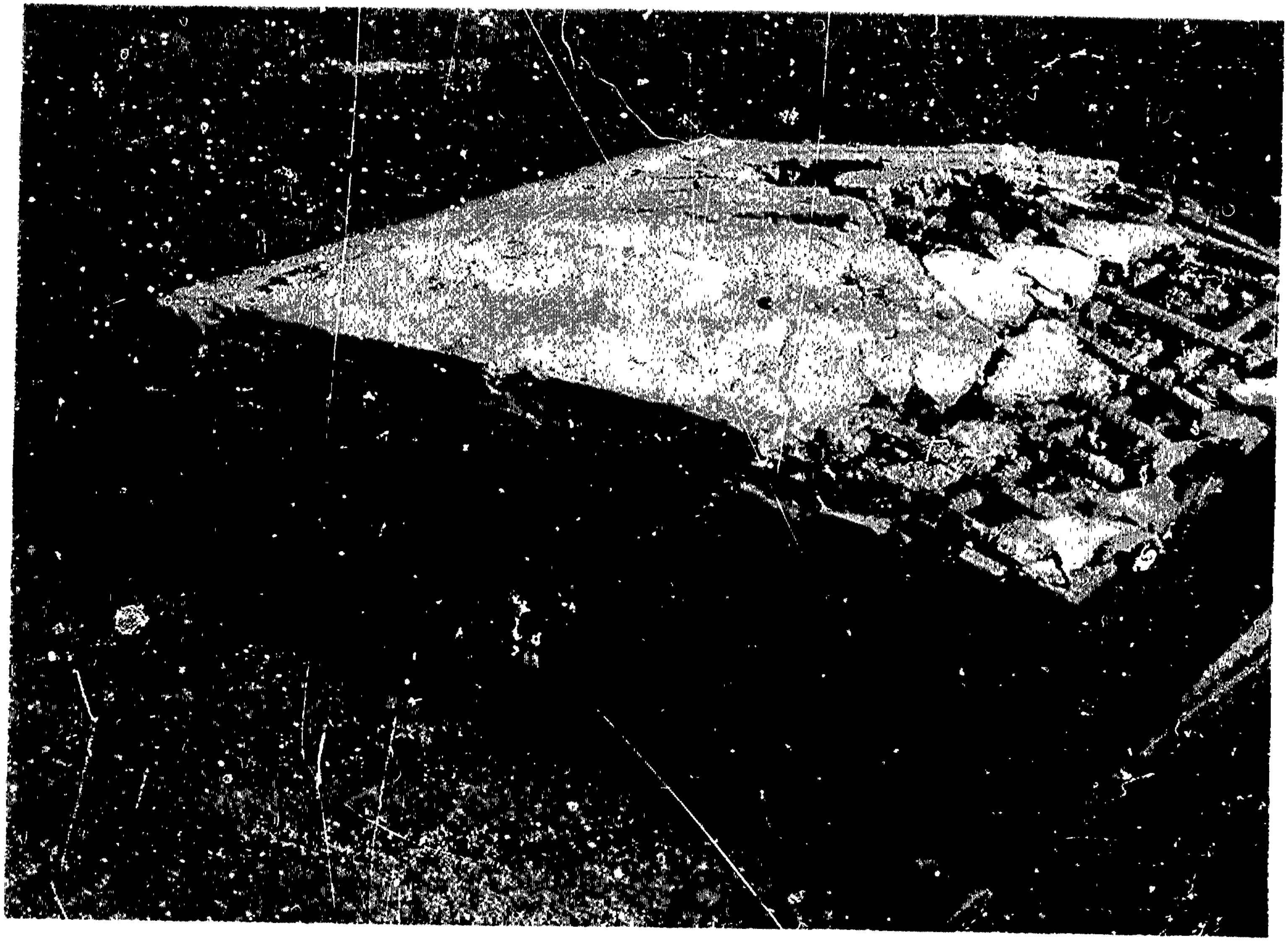

FIG. 13. Test sho. No. 405. Similar to No. 407 bending failure. Notice shear cracks on edges.

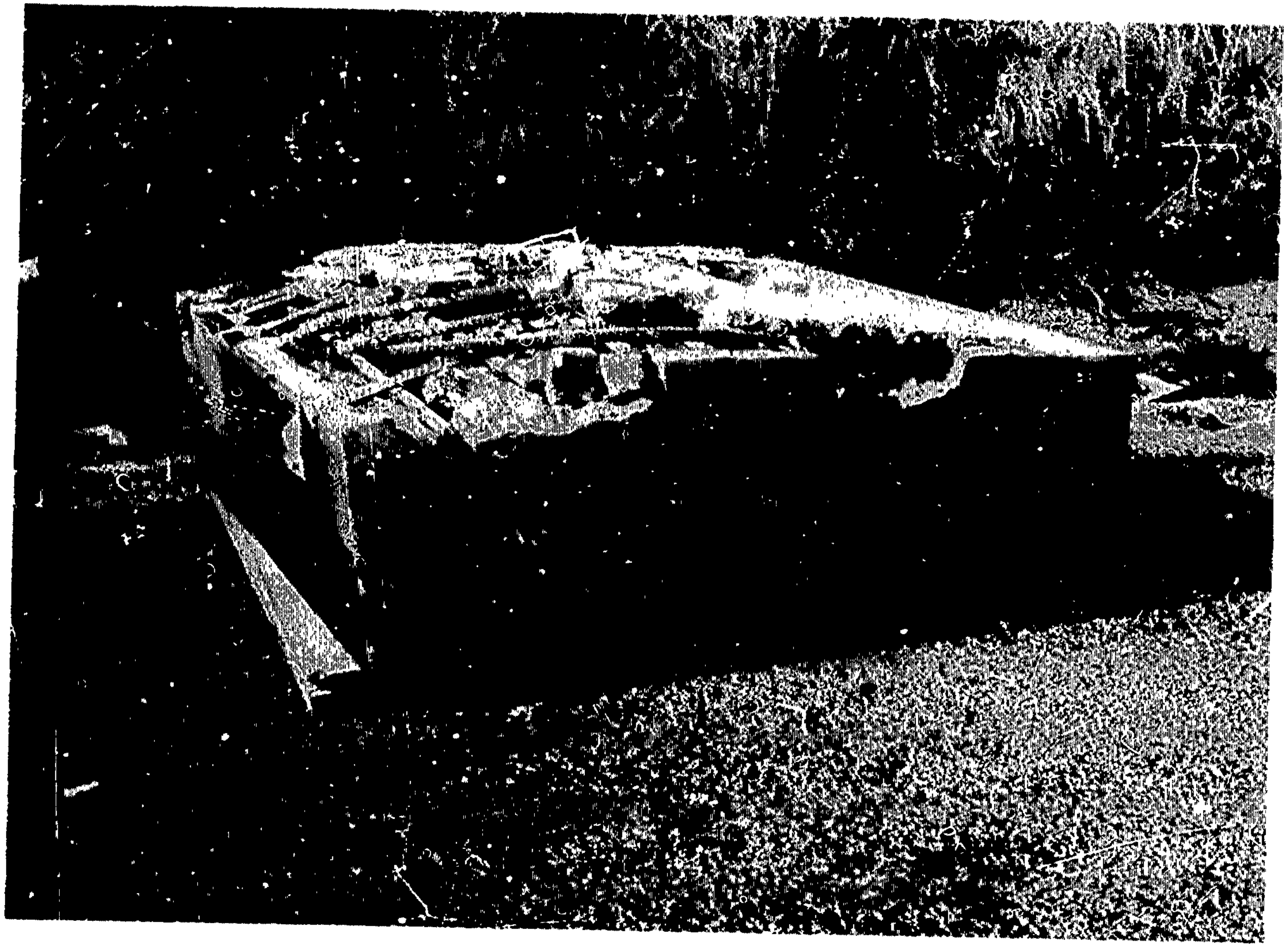

FIG. 14. Test shot No. 405. Similar to No. 407. Fiber reinforced. Demonstrates bending failure.

FIG. 15. Test shot No. 406--before.

FIG. 16. Test shot No. 406, showing underside (spall side). Note three "telltale" poles 1, 2, and 3 in. clear of concrete. One-inch spacing of holes in poles provided reference for fragment velocity measurements.

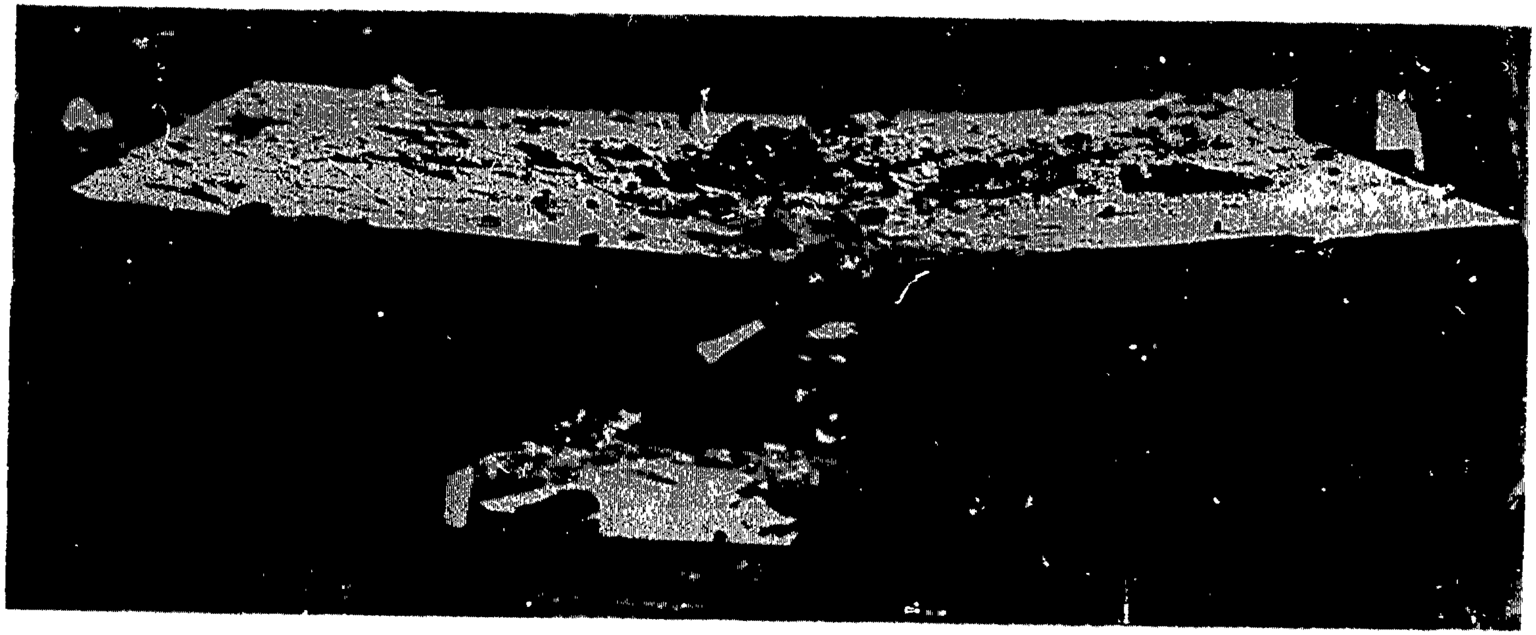

FIG. 17. Test shot No. 406--after (nonfiber reinforced).

FIG. 18. Test shot No. 406--after.

FIG. 19. Test shot No. 406--after (from top).

FIG. 20. Test shot No. 406. Permanent deflection of 2.25 in. (6 cm).

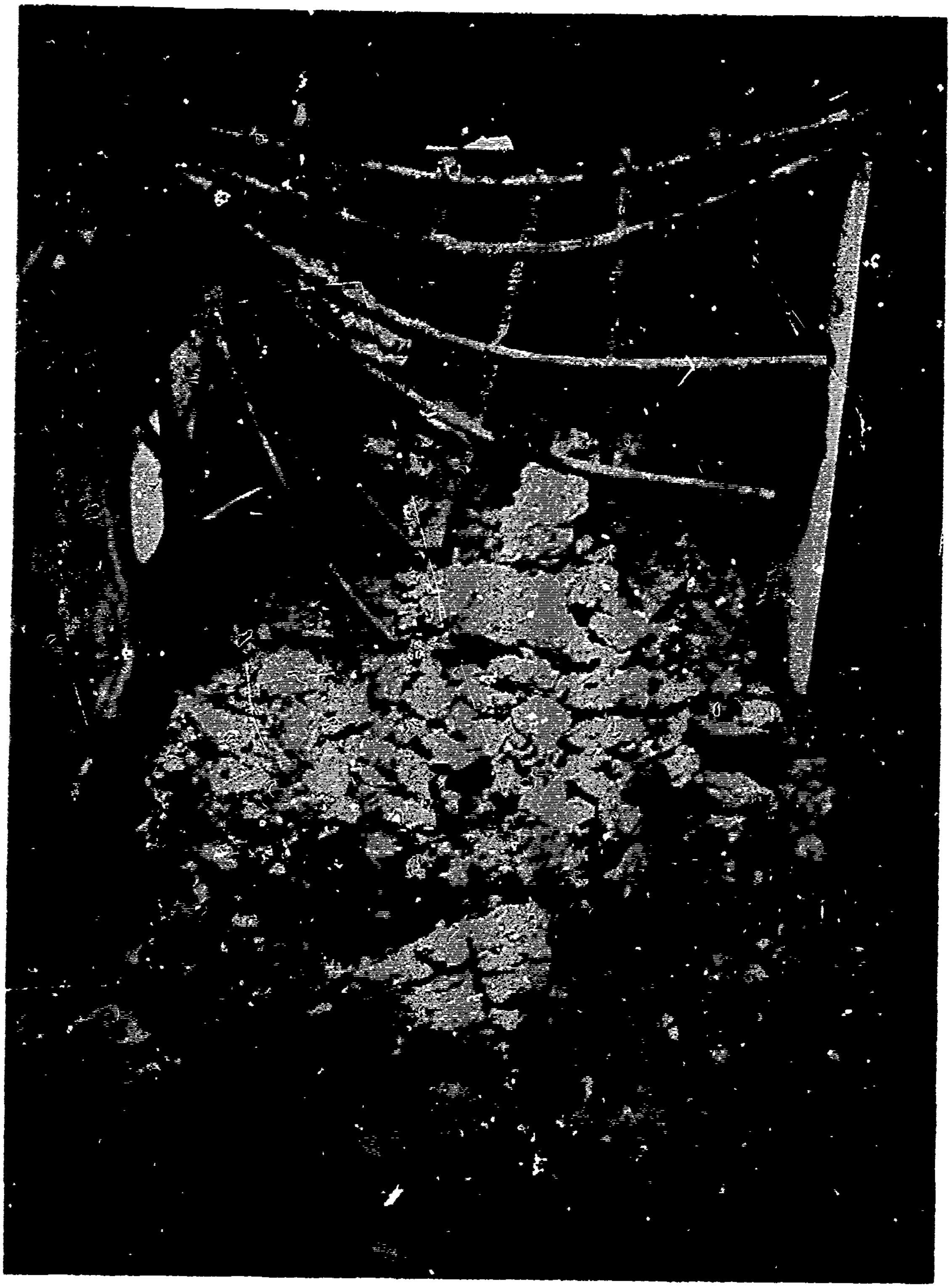

FIG. 21. Test shot No. 406--underside.

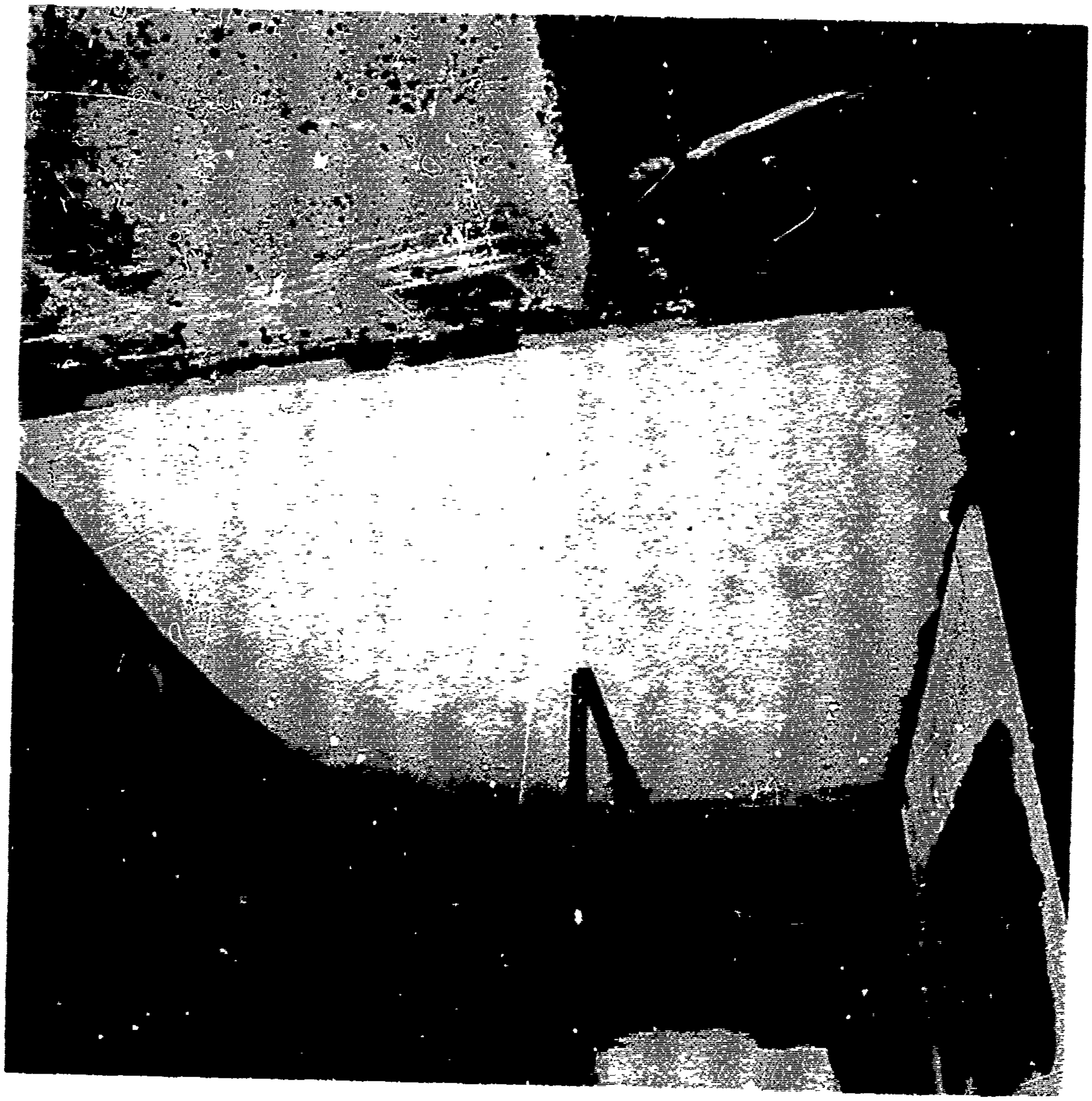

FIG. 22. Test shot No. 407--underside (spall side). Only one "telltale" pole with 1-in. hole spacing shown. Note grout at edges to minimize smoke and dust intrusion, which would obscure photographs.

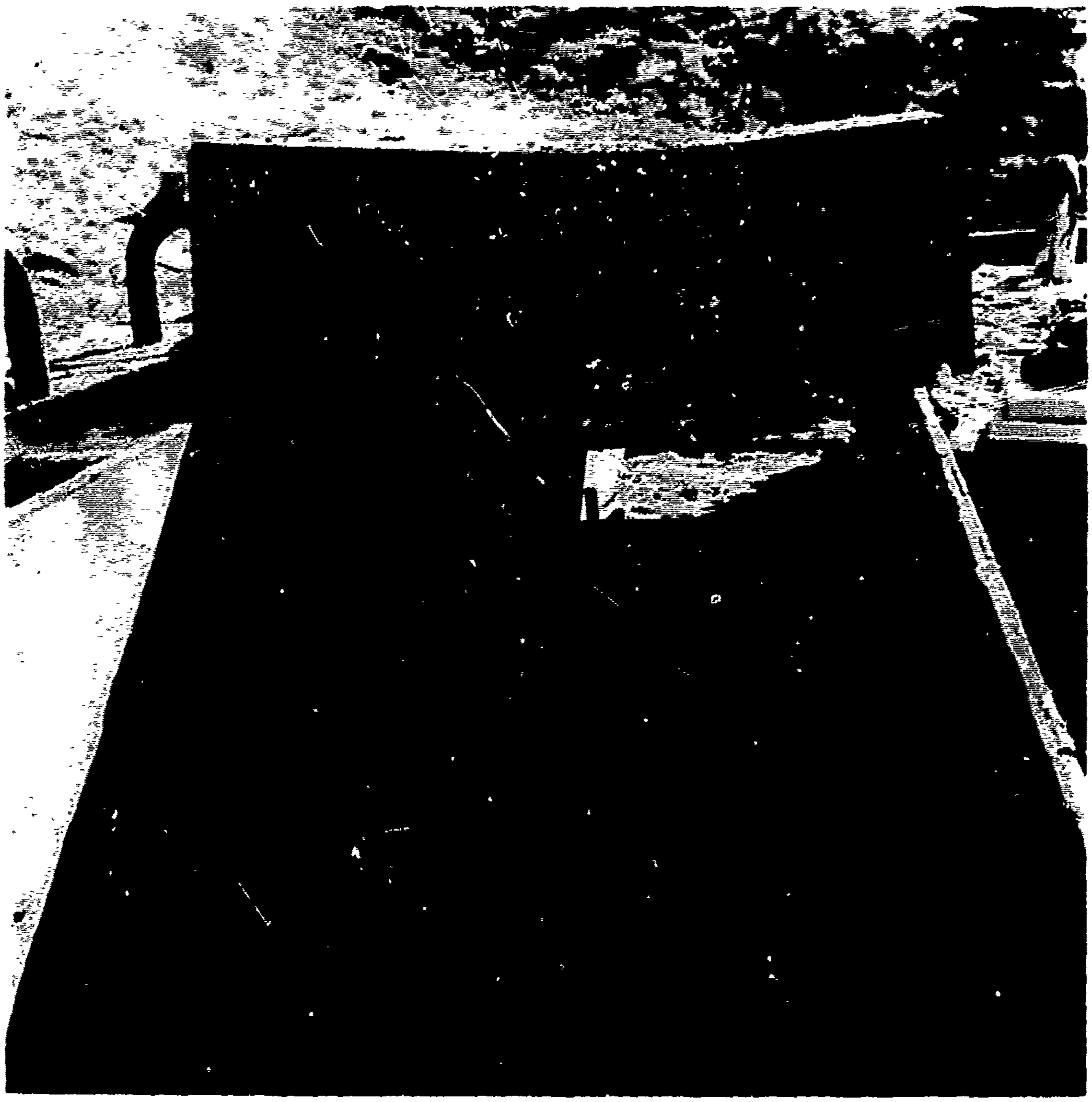

FIG. 23. Test shot No. 407--after detonation. Note shear failure--large diagonal cracks on side. Bending failure has caused permanent slab deflection.

FIG. 24. Test shot No. 407--underside. Some concrete chunks displaced. Note bent "telltale" pole, which was originally 1-in. clear of bottom surface.

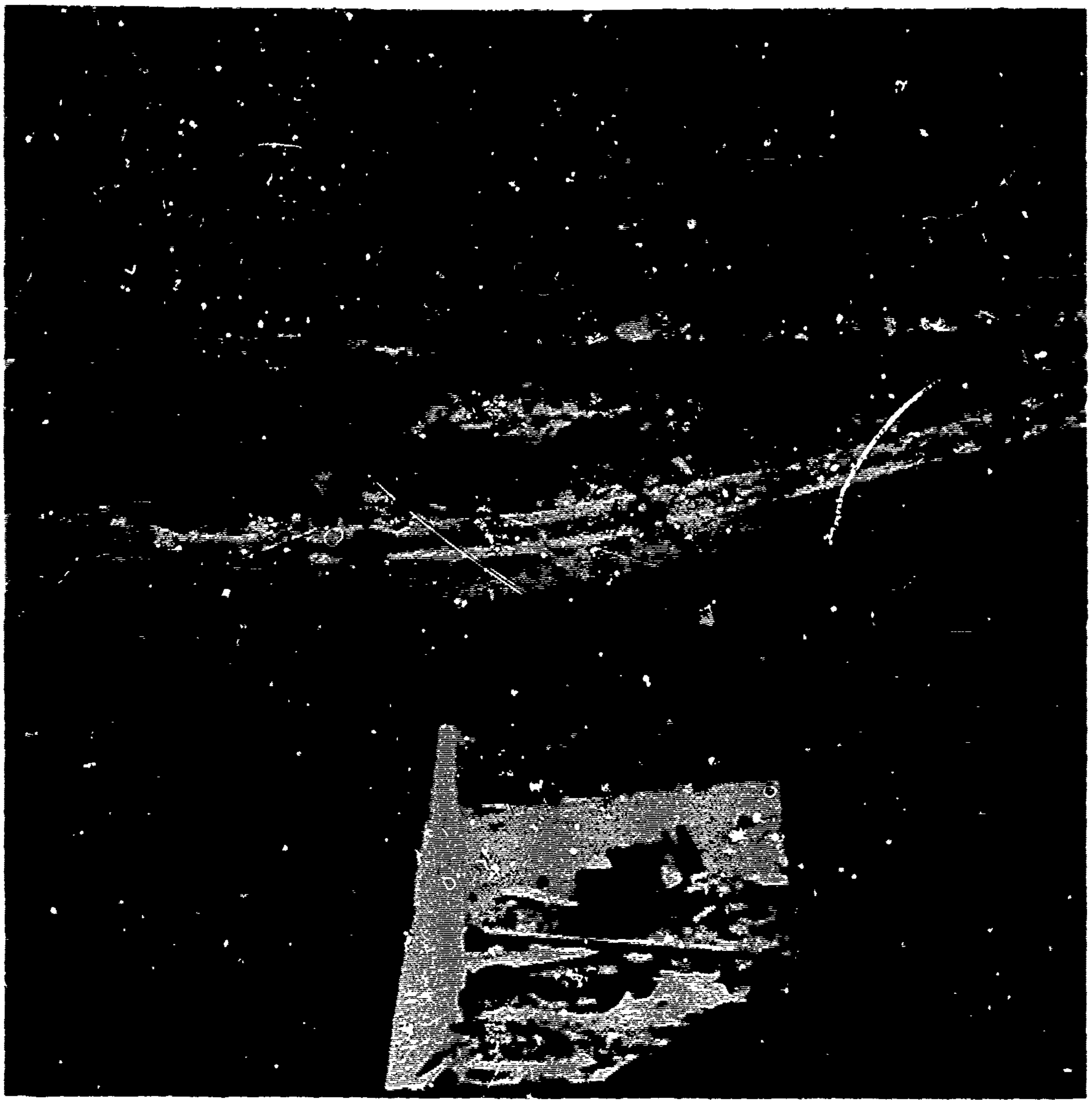

FIG. 25. Test shot No. 407. Large concrete chunks on bottom did not spall because of fiber reinforcing.

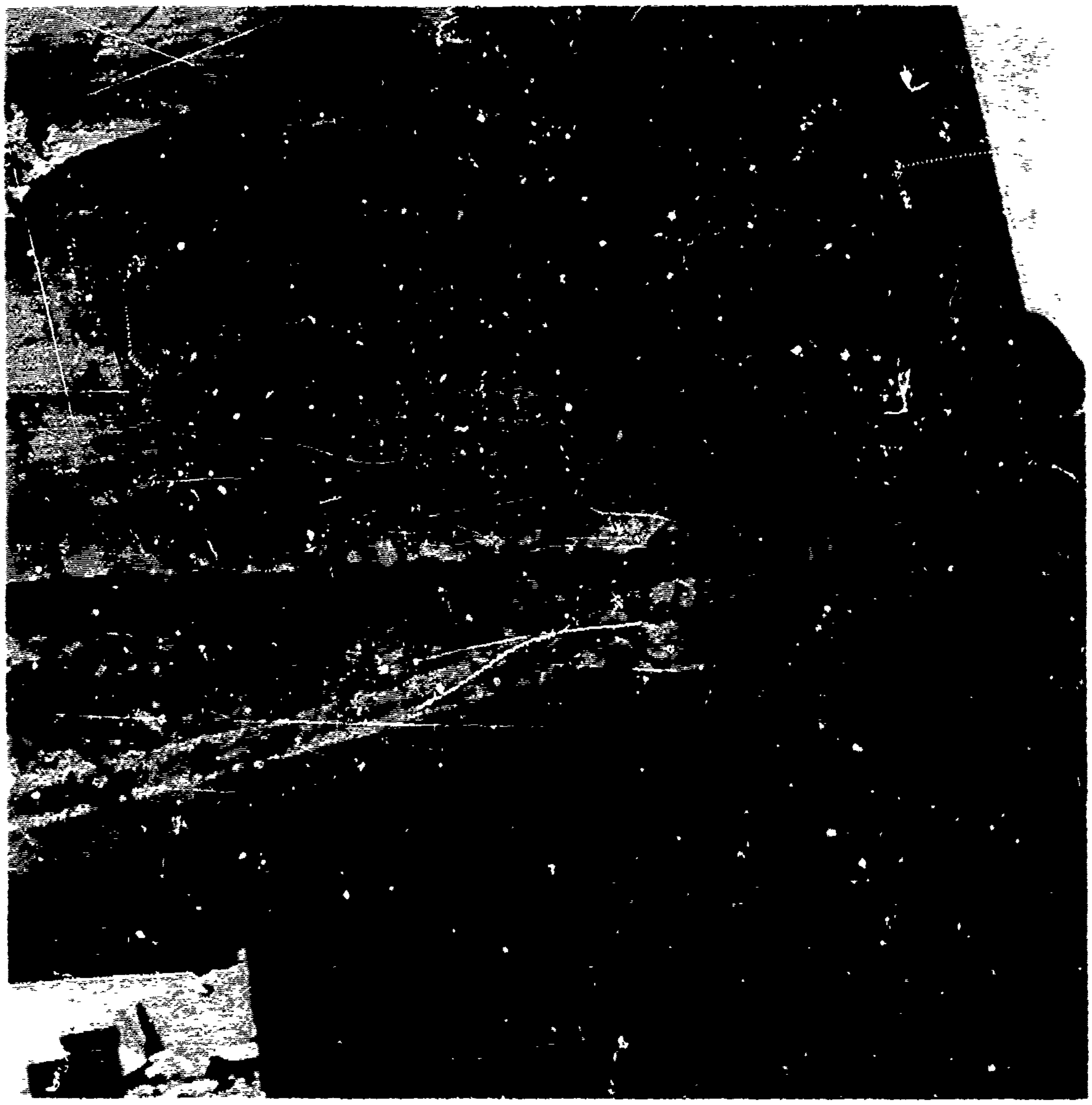

FIG. 26. Test shot No. 407--detail.

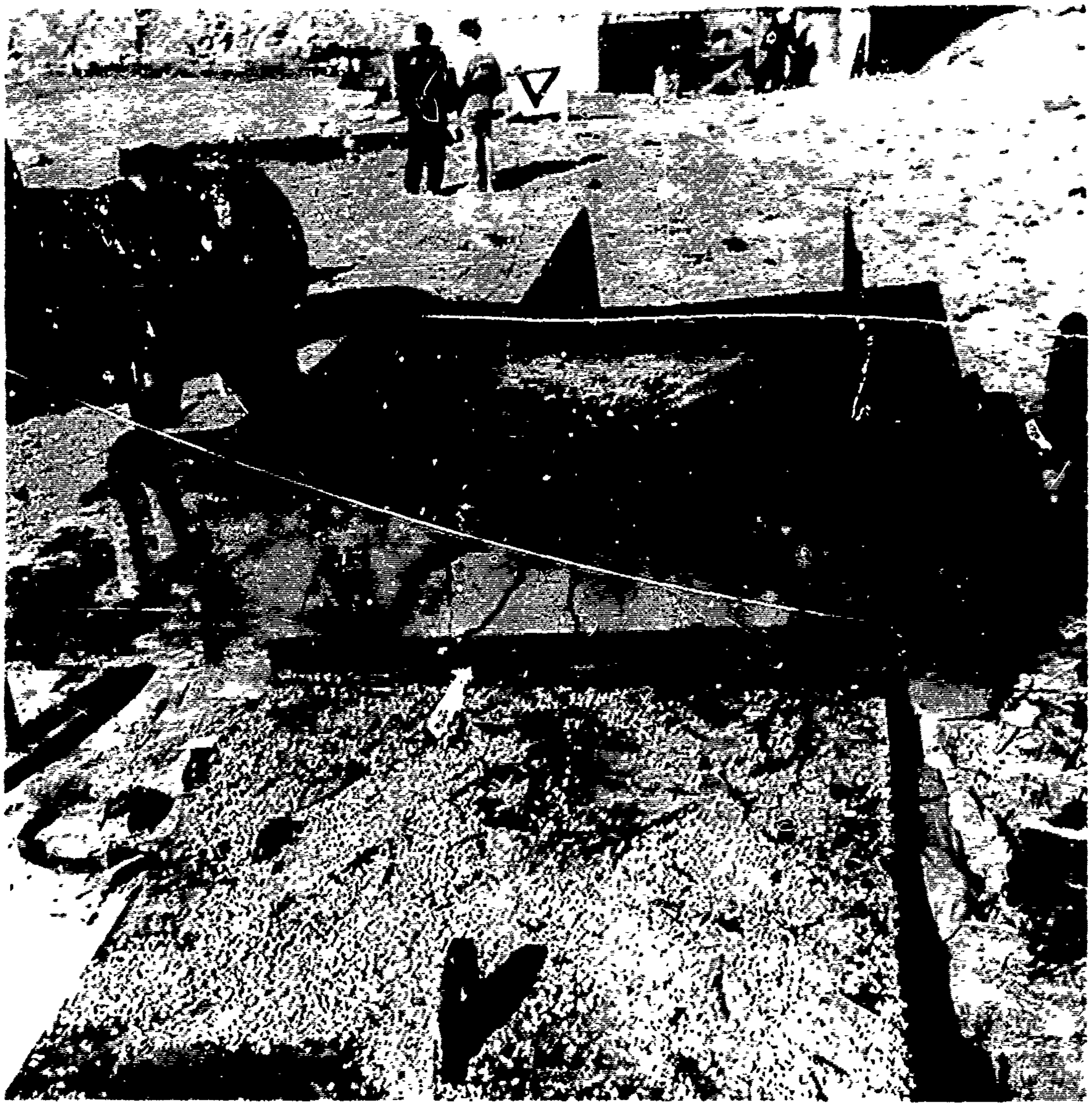

FIG 2[illegible]. Test shot No. 407. Note surface pitting on shot side. Note large shear cracks and permanent deflection (bending).

REFERENCES

1. G. R. Williamson, *Response of Fibrous-Reinforced Concrete to Explosive Loadings*, Department of the Army, U.S. Corps of Engineers, Technical Report No. 2-48 (1966).
2. *Supporting Studies to Establish Safety Design Criteria for Storage and Processing of Explosive Materials. Interim Report No. 1 of One-Third-Scale Reinforced Slab Tests*, Amman and Whitney Co., for Picatinny Arsenal, N.J. (Cohen and Dubbs, N.Y., 1965), Technical Memorandum C-1.
3. *Industrial Engineering Study to Establish Safety Design Criteria for Use in Engineering of Explosive Facilities and Operations--Wall Response*, Amman and Whitney, for Picatinny Arsenal, N.J. (1963).

JAD/rls

RESULTS AND ANALYSIS

OF

STRENGTHENED STEEL BUILDING BLAST TESTS

By

Frederic E. Sock, Ammann & Whitney
Norval Dobbs, Ammann & Whitney
Paul Price, ARRADCOM
Joseph Caltagirone, ARRADCOM

ABSTRACT

This paper summarizes recent ARRADCOM tests for the development of design criteria and procedures for steel structures located in pressure ranges of 7.0 psi or less. Test procedures and results on a strengthened steel building are presented in this paper. The data presented here, together with those in PTA Report 4837 and ARRADCOM Report ARLCD-CR-77008, should be implemented in the blast-resistant design of steel structures within facilities for manufacture and storage of explosive materials.

INTRODUCTION

The U.S. Army, under the direction of the Project Manager for Production Base Modernization and Expansion, is engaged in a program to modernize and expand its ammunition production capability. In support of this program, the Energetic Systems Process Division of the Large Caliber Weapons Systems Laboratory, ARRADCOM, with the assistance of Ammann & Whitney, Consulting Engineers, has for the past several years, been engaged in a broad-based program to improve explosive safety at these facilities. One segment of this program deals with the development of design criteria for explosion-resistant protective structures.

Steel buildings used for protective structures range from pre-engineered buildings for low overpressures (about 1 psi) to strengthened steel buildings for high overpressures. In the design of these strengthened steel buildings to withstand High Explosive (HE) and other types of explosions, standard structural members can be utilized. However, because of the transient nature and the relatively high intensity of the blast loads, certain procedures and criteria have to be met in designing these structural members.

In order to furnish data for establishing reliable safety design procedures for buildings exposed to blast overpressures, a specially designed strengthened steel building was subjected to challenges provided by detonation charges at various locations around the building. This paper describes the series of tests that were performed on the strengthened steel building at Dugway Proving Ground (DPG), Utah, in June 1979. The recorded damage levels are evaluated and compared with those predicted by methods and criteria given in References 1 and 2. Recommendations pertaining to the design of strengthened steel buildings for resisting blast overpressures are provided.

Test Description

A specially designed strengthened steel building was subjected to blast tests at the U.S. Army Dugway Proving Ground during the month of June 1979. A total of seven tests were conducted, subjecting the structure to the detonation of 2,000 pounds of high explosives at various distances from it (see Figure 1) and recording the resultant dynamic pressure, deflection and status deflection of the structure. Instrumentation to record the structural response consisted of electronic self-recording deflection and pressure gages. Figures

2 and 3 show typical deflection and pressure gage set-up, respectively.

The overall dimensions of the stengthened steel building were 80 feet long by 20 feet wide by 12 feet high. The building was divided into four bays in the longitudinal direction, each of which was approximately 20 feet wide. The primary structural framework in the transverse direction consisted of three interior rigid frames and an exterior rigid frame at both ends.

The columns, girts, beams, girders and purlins were wide-flanged members with a minimum static yield stress of 36,000 psi. The walls and roof consisted of 18- and 20-gage cold-formed steel panels having a minimum static yield stress of 33,000 psi.

The test structure was provided with 15 deflection gages which were located as shown in Figure 1. These gages measured the deflection time histories (vertical and horizontal) of one end frame, the center frame, one longitudinal frame, two girts, one purlin, and a roof and wall panel. Pressure gages were also used to record the blast loads acting on the structure. A total of 20 pressure gages were located around the structure such that enough data was collected to quantitatively analyze the structure's response.

Test Results

Table 1 summarizes the strengthened steel building test results, including the free-field pressures; center, end, longitudinal frames, girt and panel displacements; and a brief description of typical damage for each test.

Tests Nos. 1 and 2 were left out of Table 1 because of failure of the measuring instruments during both tests. However, the only damage observed during Test 2 was a crack that appeared at the concrete base around Column A3.

A minimal amount of damage was incurred in Test 3 (3.2 psi). The overlapping panel joints were opened approximately 3/8 inch half-way between Frames 2 and 3. In some places, the panel was slightly disengaged where it was fastened to the foundation and girts. Gage D13 recorded a displacement of 1.78 inches which corresponded to a rotation of the supports of approximately 4 degrees. This value is greater than the reusable criteria of 0.9 degree for a cold-formed member. The damage is attributed to the connection detail at the foundation and its effect is to relieve the loading on the panel, thereby reducing its deflection.

Slight web crippling was also observed at the center girt near the column.

More extensive damage was apparent in Test 4 (3.5 psi). The blastward panels were torn loose from points where they were supported at the foundation and girts (see fig. 4). The roof panels buckled under the increased loading at points between purlins near the blastward wall (Wall A). Most of the damage to the panels occurred at those places damaged in a previous test.

The resulting damage in Test 5 (5.31 psi) was similar to that in the previous test. However, damage was not incurred in one of the sidewalls (Wall 5). The damage to Wall A was slight and limited to reopening the panel seam and Column 3. Some web crippling was also apparent in the wall panels in Wall 5 near the lower girt and the buckling in the roof panels between the first two purlins (observed in Test 4) increased.

Repairs, as in other tests, were done to the structure before Test 6 (6.79 psi). Damage to Wall 5 was more severe than the previous test; this included web crippling at the foundation joint, and the lower and middle girt for the full width. Some web crippling was also observed in the upper girt in Wall A. The panel seam between Frames 2 and 3 was reopened and several foundation-connecting screws pulled out. In addition, buckling was observed on some of the roof purlins and several roof panel seams opened between Frames 3 and 7.

The major structural damage which occurred in Test 6 consisted of failure of some of the foundation bolts as shown in Figure 5. Examination of the connections showed that two bolts were properly installed, but two others on the easterly side were improperly installed (cut-off was essentially at the floor wall) and one of these failed.

The foundation bolts that failed during the previous test were repaired before Test 7 (4.21 psi). Almost all the panels in Wall B between Frames 2 and 5 were ripped loose from the lower girt and foundation, and some of the panel seams opened (Wall B was the blastward wall in this test). Web crippling was apparent on all girts and some of the purlins buckled under the blast load. Slight damage was observed in the wall and roof panels; this included missing foundation screws at the panel joints in Walls 1, 5 and A.

Evaluation of Test Results

An attempt is made in this section to understand fully the behavior of the structure as demonstrated by the test results. Evaluation of the displacements of the center, end and longitudinal frames, blastward wall girts and panels, and the roof deck will also be presented in this section.

The behavior of the center frame did not vary significantly from one test to another. It was observed that a significant positive sidesway displacement occurred during the negative phase of the loading on the blastward wall. This also corresponded to the positive phase of the loading on the backwall. The positive displacement was then followed by a significant (almost the same value as the positive sidesway displacement) negative displacement as the loading left the structure. However, the peak sidesway displacement occurred after almost all of the loading was off the structure.

The behavior of the structure can be explained by the phasing of the blast loading as follows: the first positive peak displacement is a result of the net positive loading on the blastward walls and backwalls. During rebounding of the frame, the negative pressure on the blastward wall and the positive pressure on the backwall are both acting in the same direction and in phase with each other, thus producing another significant negative sidesway displacement. Finally, as the structure rebounds from the positive loading on the rear walls and negative loading on the blastward wall, a peak positive displacement of the structure is obtained. The sequence of events is best illustrated by Figures 6 through 9.

The behavior of the rigid frame was somewhat similar to that of the center frame. The displacement curves in Figures 10 and 11 show that the first peak positive sidesway displacement occurs during the positive and negative phases of the blast loading on the leeward and blastward walls, respectively. However, unlike the center frame, the peak positive displacement is followed by a significant negative displacement occurring while some loading is still on the structure. Although the center and end frames both have a period of vibration of approximately 200 milliseconds, the faster response of the end frame (vibrations damp out faster) can be attributed to the smaller mass (smaller tributary area) carried by it.

The longitudinal frame, subdivided into four bays, had three deflection gages (D8, D9 and D10) positioned to monitor its behavior during the tests. Some of the gages were overwhelmed during most of the tests and, as a result, insufficient data was collected to adequately evaluate the frame's behavior. Figures 12 and 13 show the sidesway displacement of the frame for Tests 5 and 6. It is interesting to note the high frequencies of vibration exhibited by the frame (fundamental period of frame is 400 msecs).

Pressure gages were positioned in the interior of the structure to record the pressure levels during the tests. Previous tests done on a similar structure - a pre-engineered building - indicated that the effects of the internal pressure (which were approximately 40 percent of the incident pressures) on the frame responses were significant. However, from inspection of the test results on the strengthened steel building, it was concluded that the buildup of internal pressure would not affect the responses of the frame since it was approximately 16 percent of the incident pressures for all tests.

The ductility ratios and rotations associated with the displacements of the girts have been compared to the design criteria presented in Reference 1 as follows: the 2.5-inch displacement of the upper girt in Test 4 (3.5 psi) corresponds to a rotation of 1.19 degrees, which is between the reusable criteria of 1 degree and non-reusable criteria of 3 degrees. The corresponding ductility ratio is 1.25 based on an elastic deflection of 2 inches.

The panel displacements recorded by Gage D13 already account for the displacements of the girts. Based upon past experience with a pre-engineered building, the deflection gages were mounted to frames which were attached to the members (purlins and girts) supporting the panel. Thus, a direct measurement of panel displacements were obtained. For Trial 6, the 4-foot long panel (distance between girts) showed a 7.6-inch displacement during rebound. This corresponds to a rotation of 18 degrees, which is far greater than the reusable criteria of 0.9 degree. The opening of the panel seams and the pull-out of several screws connecting the panels to the foundation are consistent with the criteria. The effect of this was to relieve the load of the panels. Test results also showed the inadequacy of the roof panels. Buckling of the panels was evident after all the tests. A displacement of 1.87 inches during Test 7 (which corresponds to a rotation of 3.6 degrees) and the raising of the panels at their seams are consistent with the reusable criteria of 0.9-degree rotation.

To further evaluate the test results, a series of dynamic analyses were performed for several pressure levels using single- and multi-degree-of-freedom models to represent the structural systems. The multi-degree-of-freedom models were analyzed with the DYNFA Computer Program (ref. 2), while numerical integration techniques were used in analyzing the single-degree-of-freedom system. The models utilized in the program for the different frames are shown in Figures [illegible] and 15. The results of these analyses compared to the test data for the center, rigid and longitudinal frames as shown in Figures 12 and 13, and 16 through 21. The actual blast pressures recorded during the tests were used in the computer analyses. For the center frame, a very good correlation of the first positive and negative peak displacements were made for Tests 3 and 4. However, no correlation existed for Tests 5 ands 6, as the first positive peak displacements were almost 2.5 times greater than the corresponding DYNFA values. Further analyses are underway to determine the reasons for the differences.

An excellent correlation of the first cycle of the sidesway displacement was made for Test 5 of the rigid end frame. Dynamic analyses for Test 7 did not provide the same correlation obtained in Test 5. Similarly, the analyses for the longitudinal frame for Tests 5 and 6 yielded peak positive displacements that far exceeded the test results. Again, further investigations are underway to determine the causes.

To enhance the evaluation of the test structure, additional analyses were performed to determine the behavior of the secondary members (girts and purlins), and their effect on the responses of the frames. The peak girt displacements listed in Table 2 are the absolute values as recorded by the gages (D11 and D12). The true or relative displacements - the column displacements accounted for - were obtained by subtracting the gage (D1 or D2) readings from the corresponding displacements by D11 or D12.

Figure 17 shows that the responses of the secondary members did not significantly alter the first half cycle of the sidesway displacement of the center frame. However, the rebound was altered considerably because less energy was absorbed by the girts and the remaining energy was transferred to the frame, thereby creating a greater elastic response in the rebound phase. The model used in the computer analysis is shown in Figure 22.

CONCLUSIONS AND RECOMMENDATIONS

Conclusions

On the basis of the test results and analytical evaluations, it was seen that the strengthened steel building survived blast overpressures as high as 7.0 psi. However, the wall and roof panels failed at a pressure range of 3.2 psi to 4.21 psi. Furthermore, it is concluded that the methods and procedures of References 2 and 3, when used in the design of a strengthened steel building, yield fairly accurate estimates of the response of the structure and the sizes of the members.

Recommendations

It is recommended that the methods and procedures of References 2 and 3 be extended for the design of strengthened steel buildings to include the following:

1. The negative phase of blast loading.

2. Increase in the yield strength of the cold-formed panels due to the effects of cold-working.

3. The interaction between the secondary member (girts and purlins) responses and the frame responses.

4. The interactions between the panel responses and the secondary member responses.

It is also recommended that other revisions be made so as to fully develop the full capacity of the structure. These include:

1. Providing bigger washers or other means to prevent the heads of panel screws from pulling through the metal.

2. Strengthening the connection of wall panels at the foundation.

3. Using high-strength bolts and increasing the capacity of anchor bolts to be consistent with the blast capacities of the structure.

REFERENCES

1. HEALEY, J.J., et al., "Design of Steel Structures to Resist the Effects of HE Explosions", Technical Report 4837, prepared by Ammann & Whitney, Consulting Engineers, New York, N.Y., for Picatinny Arsenal, Dover, N.J., 1975.

2. STEA, W., et al., "Non-Linear Analysis of Frame Structures Subjected to Blast Overpressures", Report ARLCD-CR-77008, U.S. Army Armament Research and Development Command, Dover, N.J., May 1977.

3. Department of the Army, "Structures to Resist the Effects of Accidental Explosions (with Addenda)", Technical Manual TM 5-1300, Washington, D.C., June 1969.

4. DOBBS, N., et al., "Blast Capacity Evaluation of Cold-Formed Steel Panels", Report under preparation by Ammann & Whitney, Consulting Engineers, New York, N.Y., for U.S. Army Armament Research and Development Command, Dover, N.J.

Table 1. Summary of strenghened steel building test results

Test No.	Free field pressure (kPa)	Peak horizontal displacement: Ctr frame (mm)	End frame (mm)	Long. frame (mm)	Girt (mm)*	Panel (mm)	Description of damage
3	22.06	32.77	-	-	51.05 41.91	45.21	Wall A a. Corrugation fillers were dislodged from the floor connections between Frames 2 and 3, and 3 and 4. b. The overlapping panel joints were opened approximately 0.95 cm (3/8 in) half-way between Frames 2 and 3. c. Three foundation mounting screws at the panel joints at Frames 3 and 4, and half-way between Frames 2 and 3 pulled out and the overstrip bent out. d. Slight web crippling was apparent at the center girt near Frame 3. e. A panel-to-girt screw and panel joint screw had come out between Frames 2 and 3 at the center girt.
4	24.13	33.53	-	20.07	75.18 64.77	-	In Wall A, three panels (one at A3, one at A4, and one between Frames 2 and 3) were torn loose from the foundation, and lower and middle girts. Web crippling increased in the wall panels at the lower and center girts. The wall-to-roof flashing was detached at the center section. The roof panels buckled between the two purlins on the A wall side from Frames 1 through 4. The concrete at the 4-inch angle iron foundation connection showed movement at the angle between Columns A3 and A4. Shock effects during Trial 3 caused the blast door to fly open. Therefore, prior to Trials 4 and 5, the blast door was propped shut with a 4 x 4.

* Absolute displacements of girts are listed here. Relative displacements are obtained by subtracting displacement of girt at column from displacement.

Table 1. Summary of strengthened steel building test results (continued)

Test No.	Free field pressure (kPa)	Peak horizontal displacement: Ctr frame (mm)	End frame (mm)	Long. frame (mm)	Girt (mm)*	Panel (mm)	Description of damage
5	36.61	37.34	13.21	-	59.44 58.93	167.64	Wall 5 showed web crippling in the wall panels only at the lower girt. Wall A damage was slight and limited to reopening of the panel seam at Column 3, reloosening of the roof flashing at Column 3, and the center of the instrument replacement panel was bulged outward at the base connection. The office sheetrock wall studs separated from the upper plate and the upper portion of the wall shifted toward the open bay area. The office door was open and jammed against the floor. Sheetrock panels were loosened. The buckling in the roof panels between the first two purlins increased between Frames 3, 4 and 5. The grout cracking increased.

* See Note on previous page.

Table 1. Summary of strengthened steel building test results (continued)

Test No.	Free field pressure (kPa)	Peak horizontal displacement: Ctr frame (mm)	End frame (mm)	Long. frame (mm)	Girt (mm)*	Panel (mm)	Description of damage
6	46.82	35.31	18.29	-	64.77 61.21	192.53	Damage to Wall 5 included web crippling at the foundation joint and the lower and middle girts for the full wall width. Web crippling occurred at the upper girt from Wall A to above the door, but not to the right of the door. The panic hardware on the blast door was broken and the door could not be opened. Flashing on the right side of the door was loosened. Wall A showed very little damage. The panel seam between Frames 2 and 3 next to Gage D13 was reopened and several foundation connecting screws pulled out. Wall 1 showed minor web crippling at the girt connecting hat sections. In the roof, buckling was increased between the two northernmost purlins, between Frames 2 and 3. Four roof panel seams opened between Frames 4 and 5. Three panel seams opened between Frames 3 and 4. Column 24A showed three broken foundation bolts. Examination proved that two were properly installed. Of these, the inside bolt ruptured and the other two stretched approximately 0.635 cm (1/4 in). The two bolts on the easterly side were improperly installed (cut off essentially at the floor level) and extended only through the grout.

* See Note on previous page.

Table 1. Summary of strengthened steel building test results (concluded)

Test No.	Free field pressure (kPa)	Peak horizontal displacement: Ctr frame (mm)	End frame (mm)	Long. frame (mm)	Girt (mm)*	Panel (mm)	Description of damage
7	29.03	53.1	20.32	-	52.07 93.73	45.97	Wall B was ripped loose from the foundation from Frame 2 through 5. All these panels, except the two closest to Frame 5, were ripped loose from the lower girt. Most of the panel seams were intact. The seam two panels east of Column 4 opened and the seam two panels east of Column 3 opened from the foundation to the middle girt. Web crippling was apparent at all girts.
							The wall panels in Wall B between Frames 1 and 2 showed web crippling but little other damage.
							Roof flashing was removed between Frames 2 and 4, and loosened between Frames 1 and 2 (Wall B).
							The only apparent damage to Wall 1 were missing foundation screws at Panel Joints 1, 2 and 7 from Wall B.
							Wall 5 showed only one mounting screw missing from the blast door flashing.
							On Wall A, the roof flashing was loosened from Frames 2 through 4.
							The 13 central panels in the roof were torn loose from the purlins at the Wall B edge and the second purlin. Five of these were loosened from the third purlin and bent back to the center purlin.
							The six panels west of Column B3 were lifted 30.5 cm (12 in) and the next five panels were raised 50.9 cm (20 in). The panel over B3 was broken loose on the west side, but still attached on the east side. The next five panels east were torn loose and folded back to the center purlin. The first was up 43.25 cm (17 in); the second 71 cm (28 in); the third 81 cm (32 in); the fourth 66 cm (26 in); and the fifth, bowed in center but touching the wall purlin. The next panel was loose from the wall purlin, but not peeled back. The next two panels were still attached. The next panel was over Frame 2 and was broken loose, but not peeled back. The remaining panels over the office were still attached, but showed buckling downward between the first two purlins and upward over the second purlin from Wall B.

* See Note on previous page.

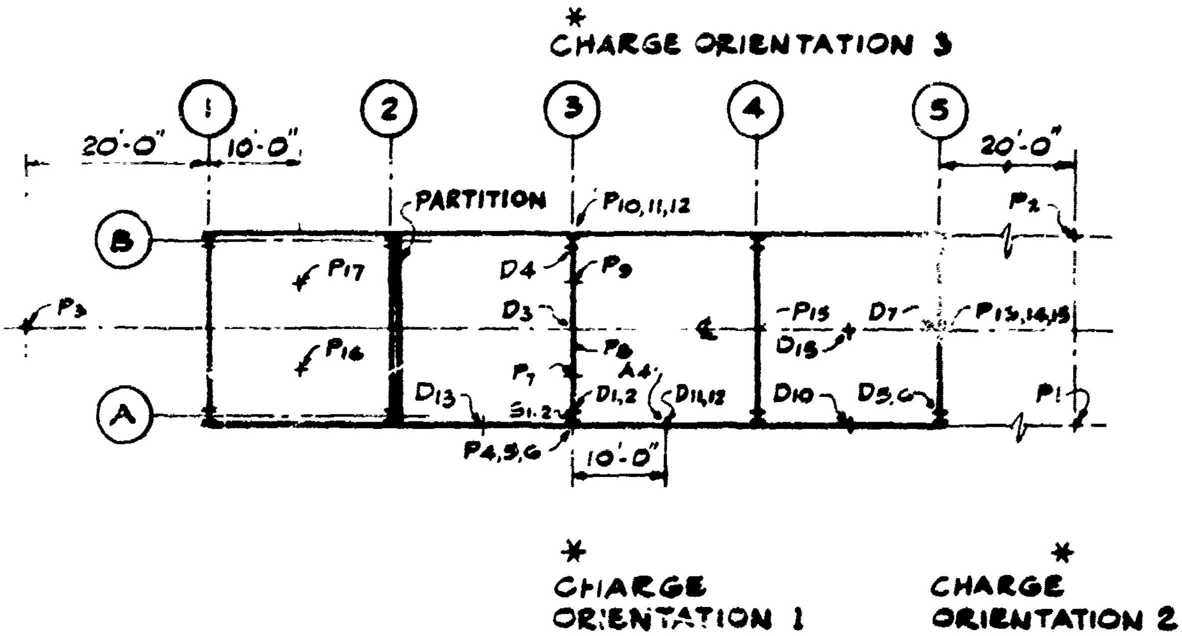

TEST SCHEDULE				
TEST NO.	CHARGE SIZE (lbs)	PRESSURE (PSI)	CHARGE ORIENTATION (REFER TO SITE PLAN)	DISTANCE FROM FRONT WALL (FT)
1	3000	0.50	ORIENTATION 1	931
2	"	1.20	"	417
3	"	3.0	"	206
4	"	TBD	"	162
5	"	3.0	ORIENTATION 2	155
6	"	TBD	"	141
7	"	3.0	ORIENTATION 3	141

Figure 1

SITE AND GAGE LOCATION PLAN FOR STRENGTHENED STEEL BUILDINGS

Figure 2. Typical deflection gage set up

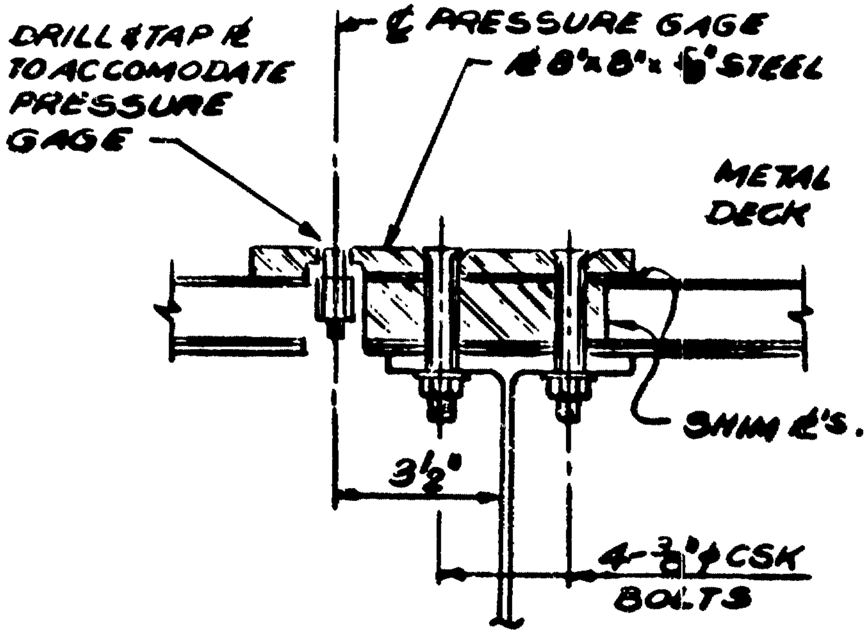

Figure 3. Typical pressure gage attachment detail

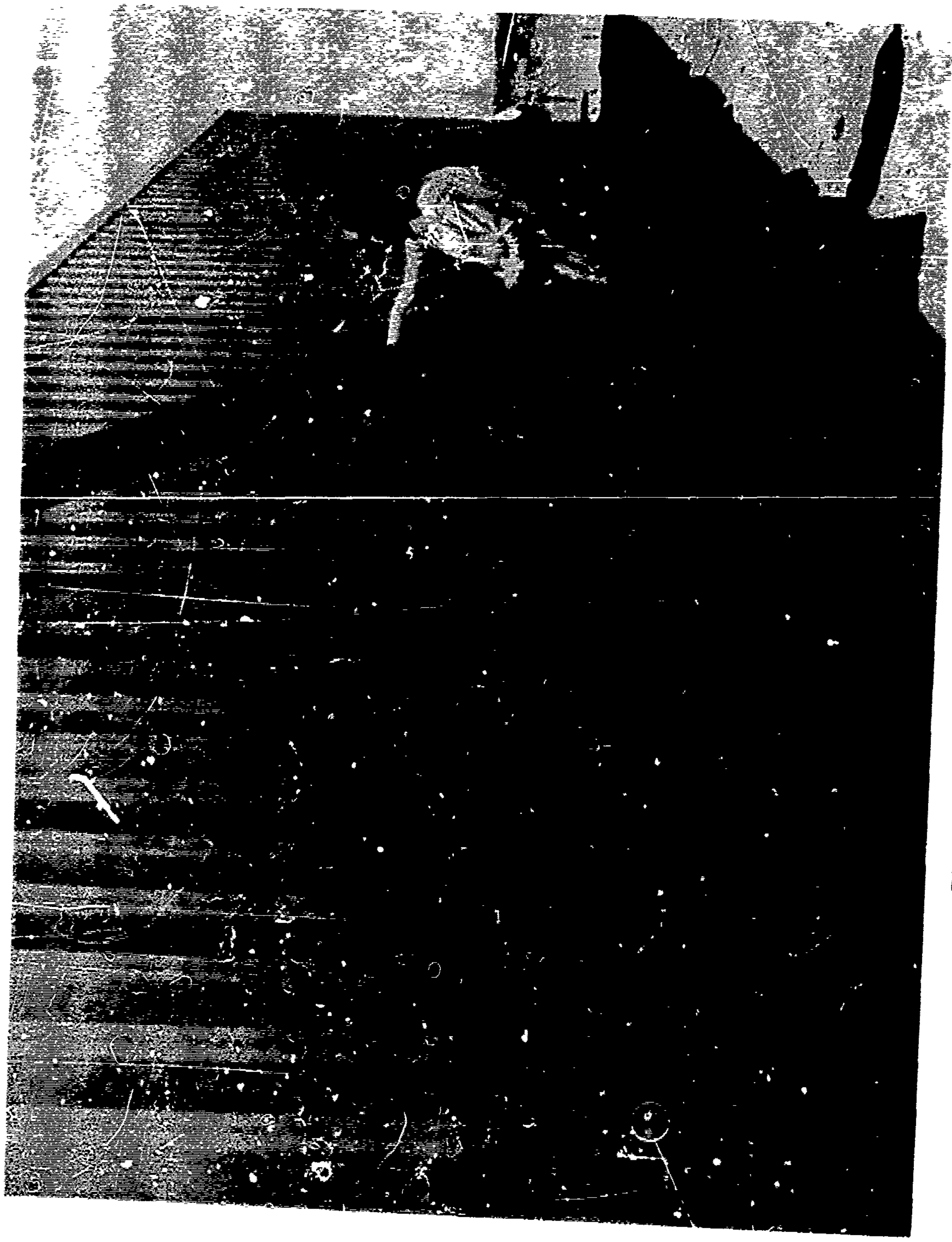

Figure 4. Damaged panels in Test 4

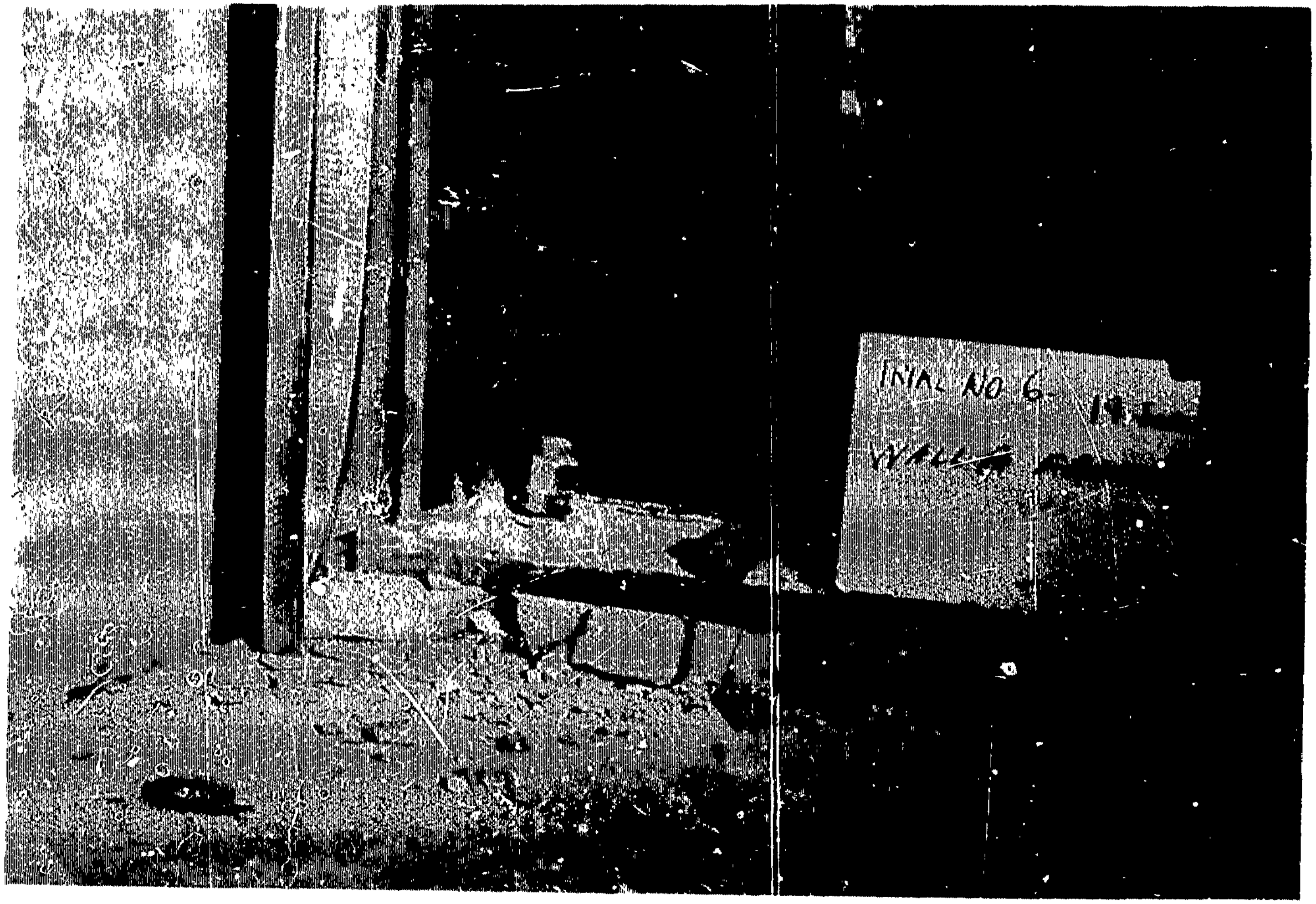

Figure 5. Failure of foundation bolts at column base

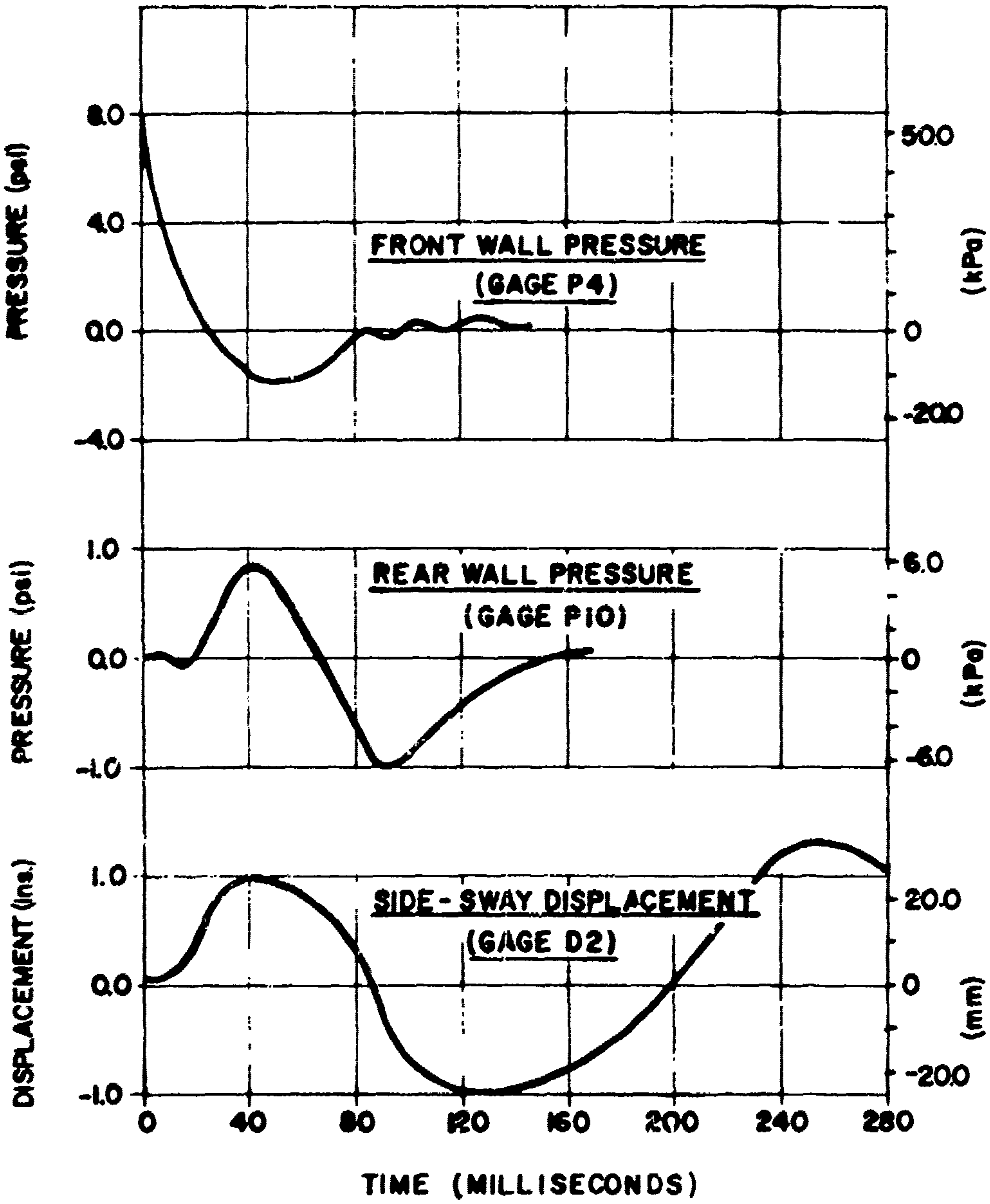

Figure 6. Measured building pressures and side-sway displacement for Test 3

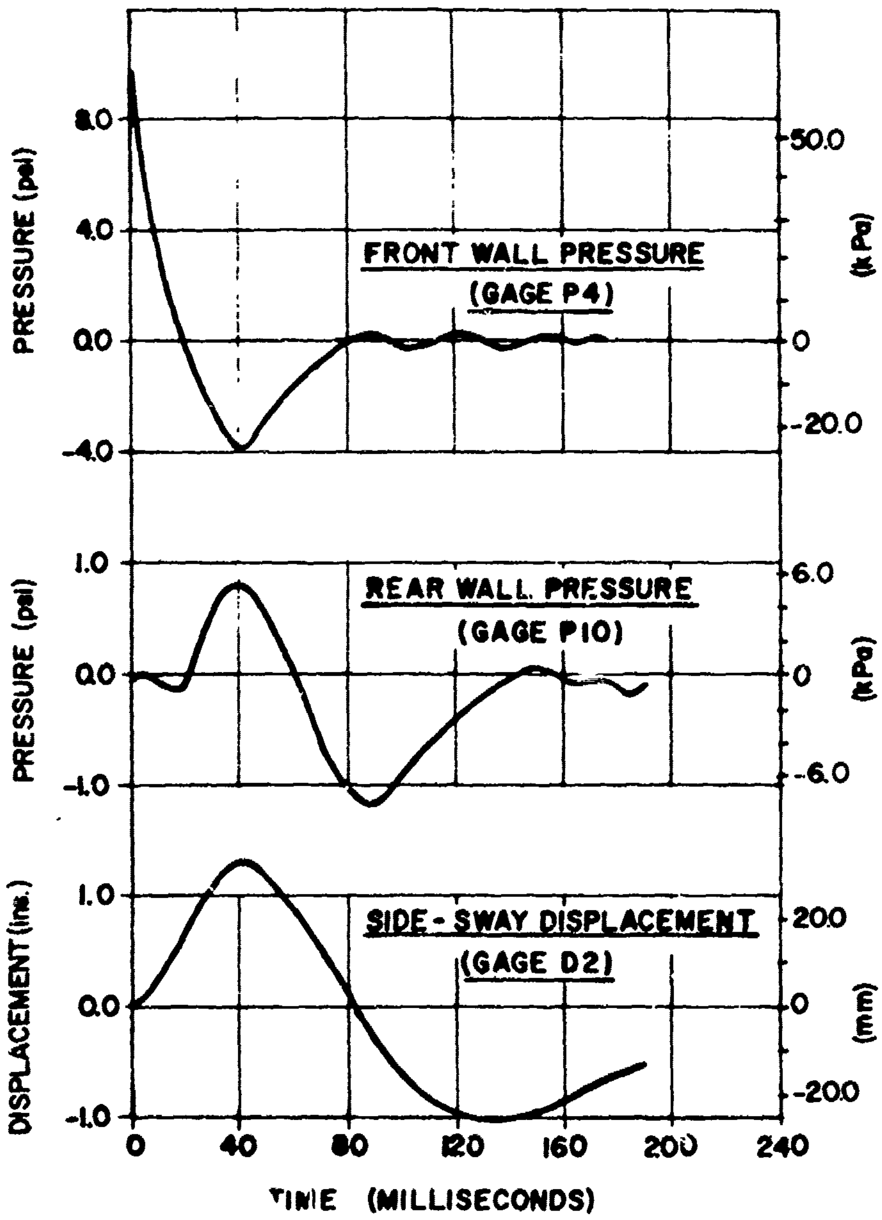

Figure 7. Measured building pressures and side-sway displacement for Test 4.

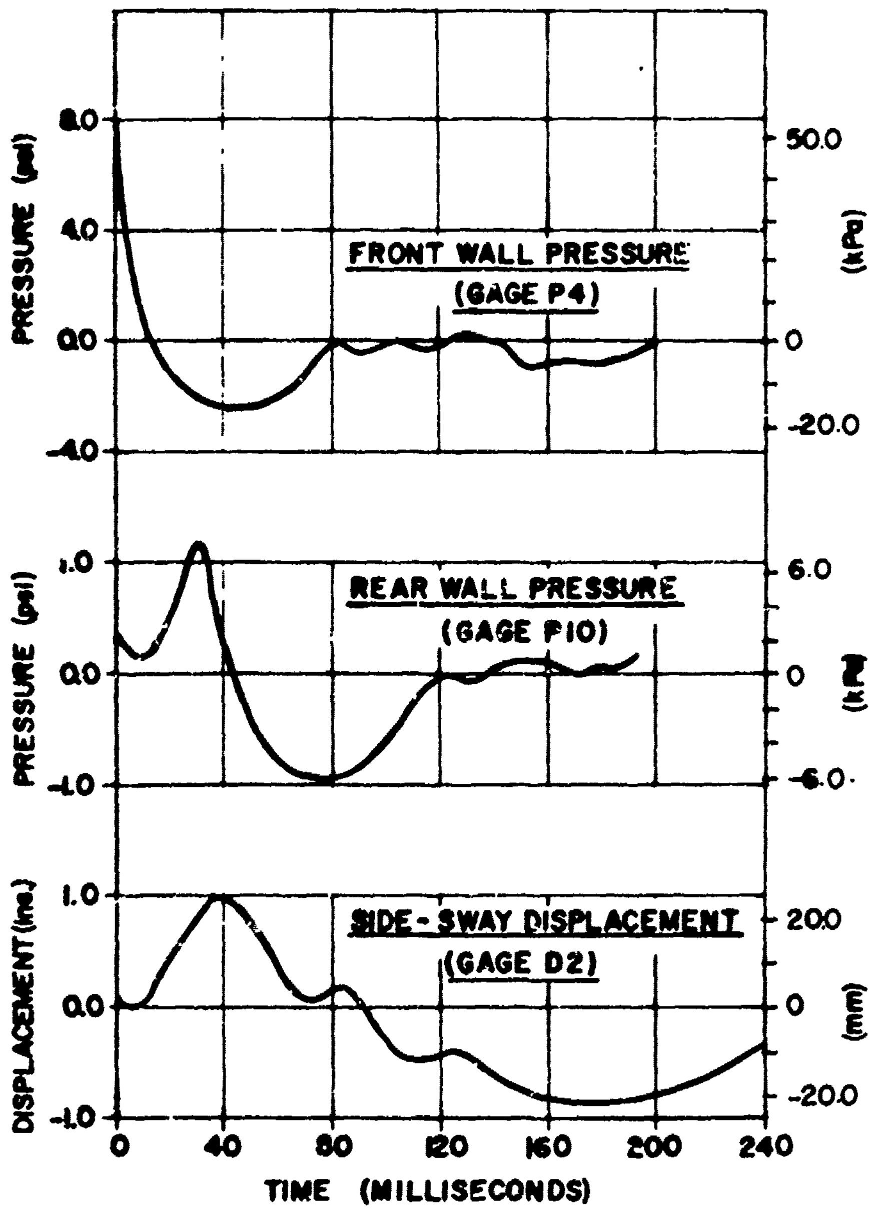

Figure 8. Measured building pressures and side-sway displacement for Test 5

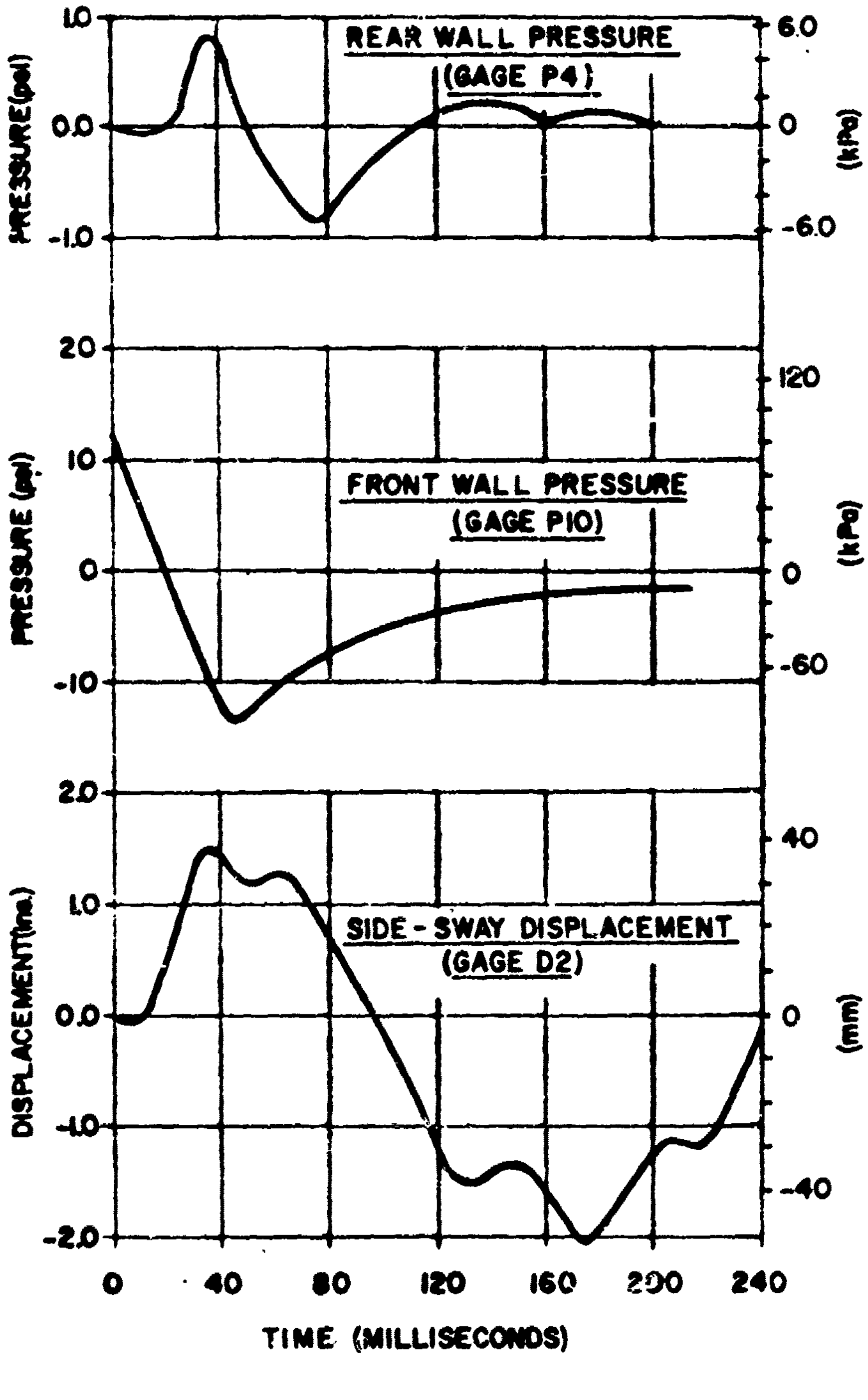

Figure 9. Measured building pressures and side-sway displacement for Test 7

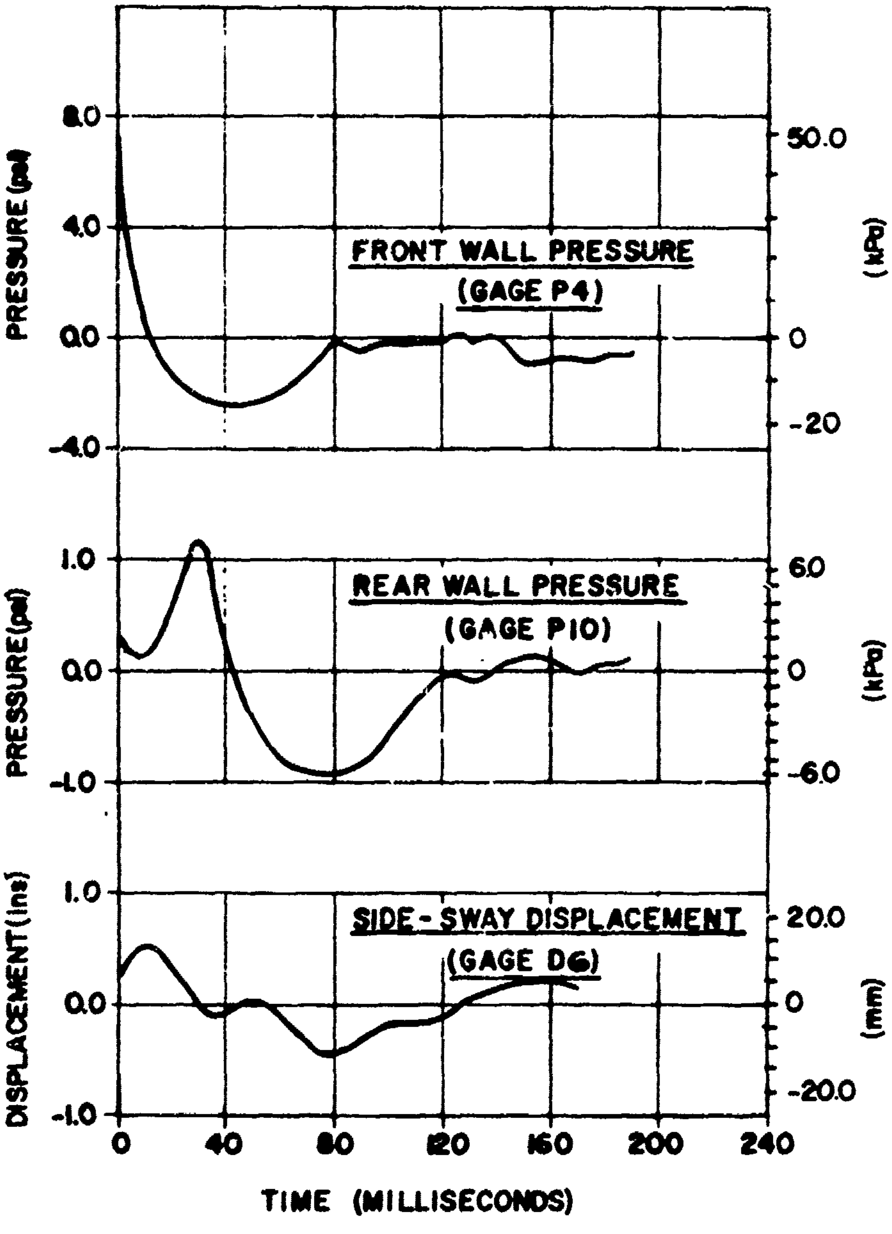

Figure 10. Measured building pressures and side-sway displacement of rigid end frame for Test 5

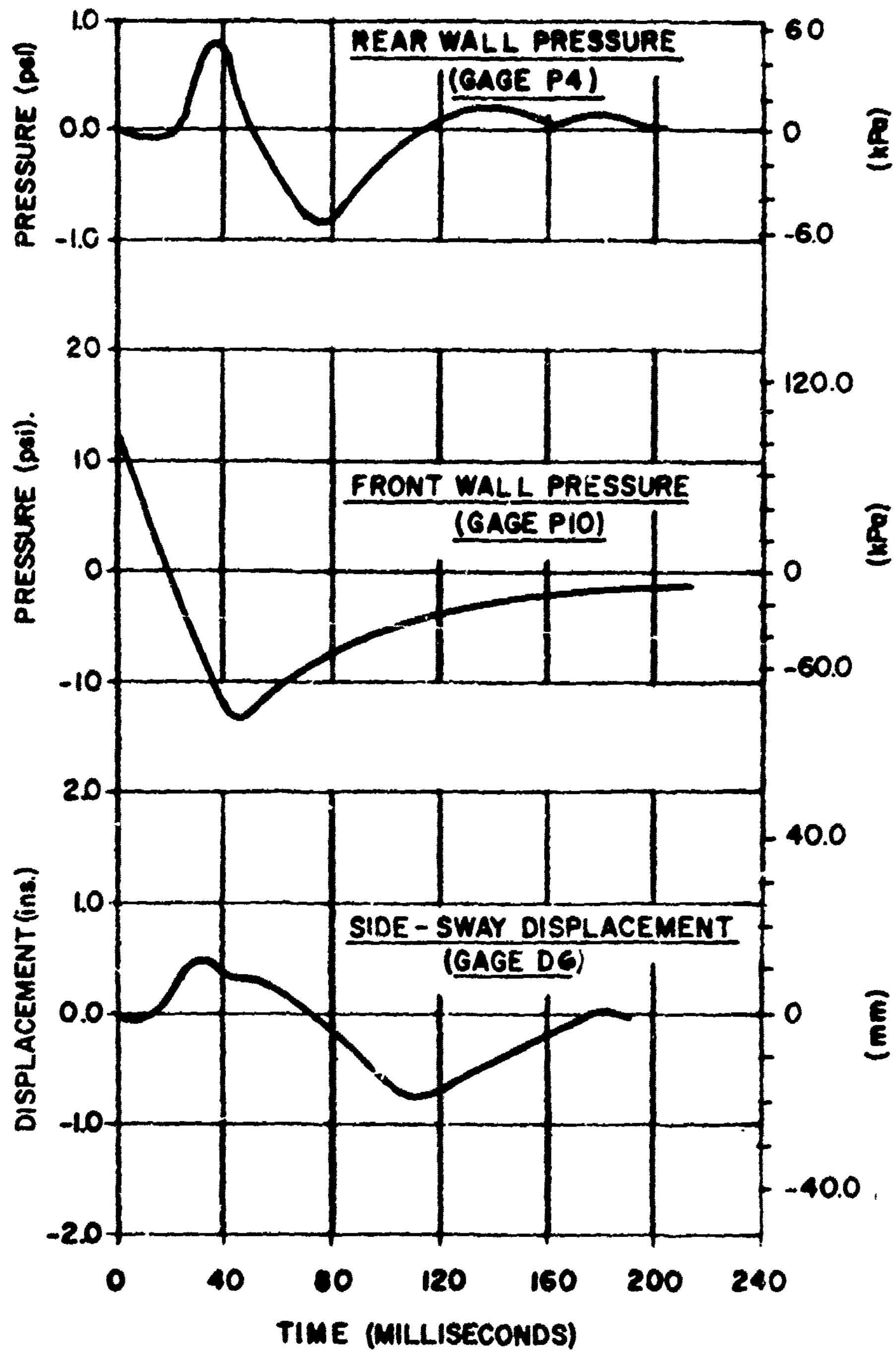

Figure 11. Measured building pressures and side-sway displacement of rigid end frame for Test 7

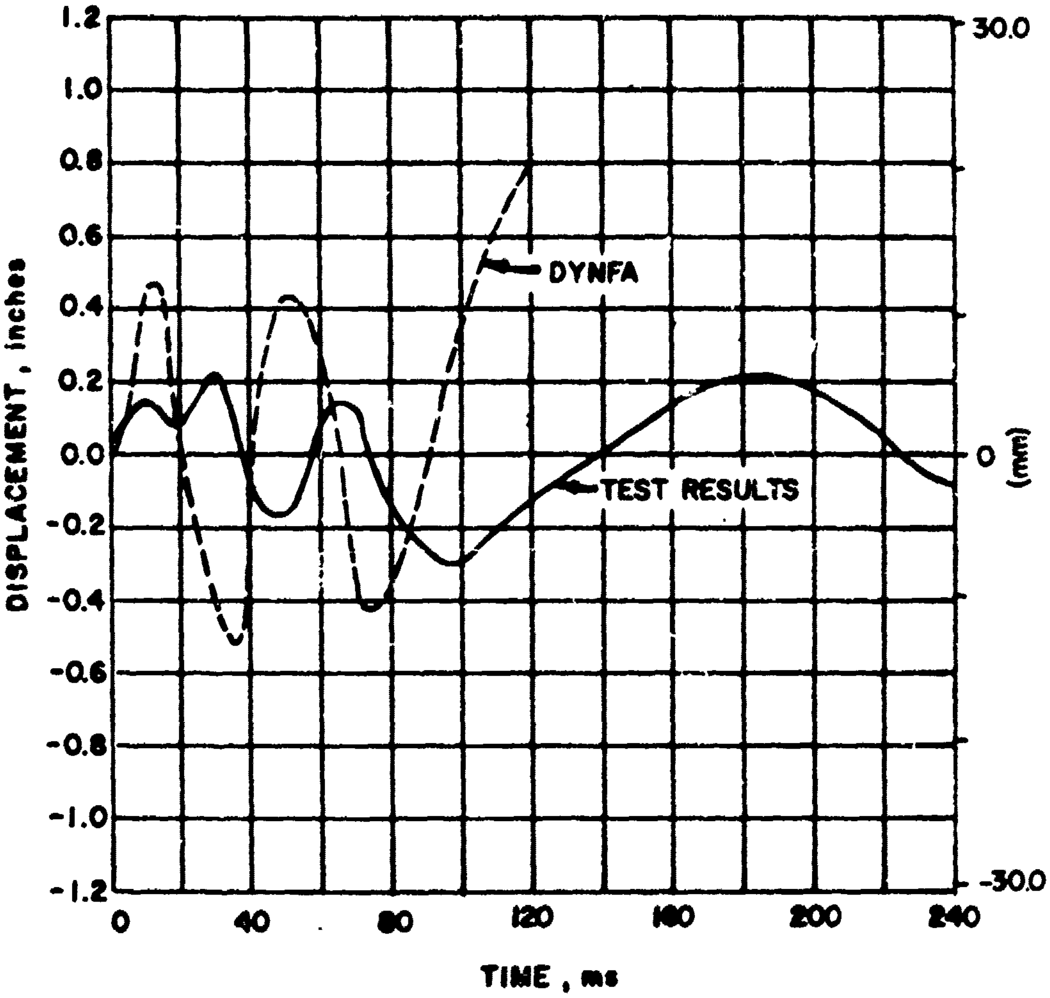

Figure 12. Longitudinal frame side-sway displacement, test and analytical results for Test 5

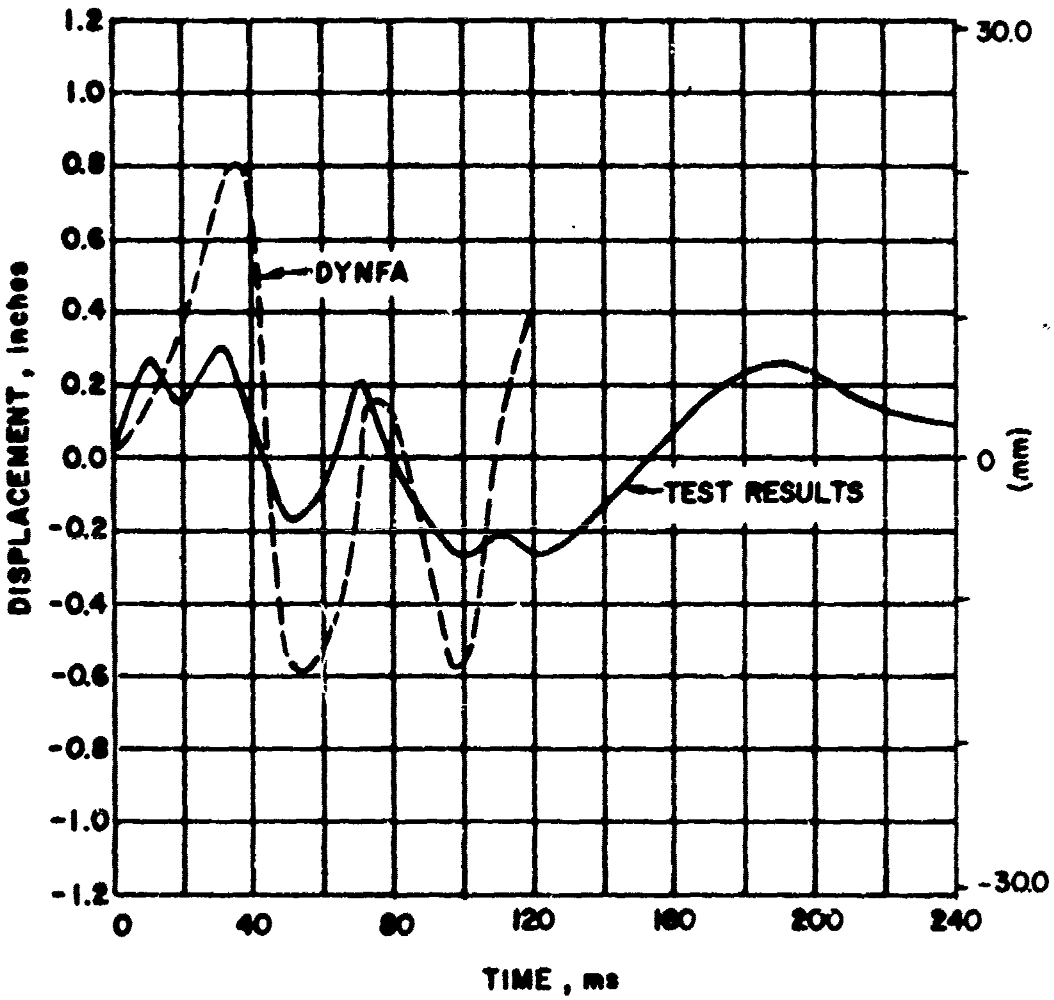

Figure 13. Longitudinal frame side-sway displacement, test and analytical results for Test 6

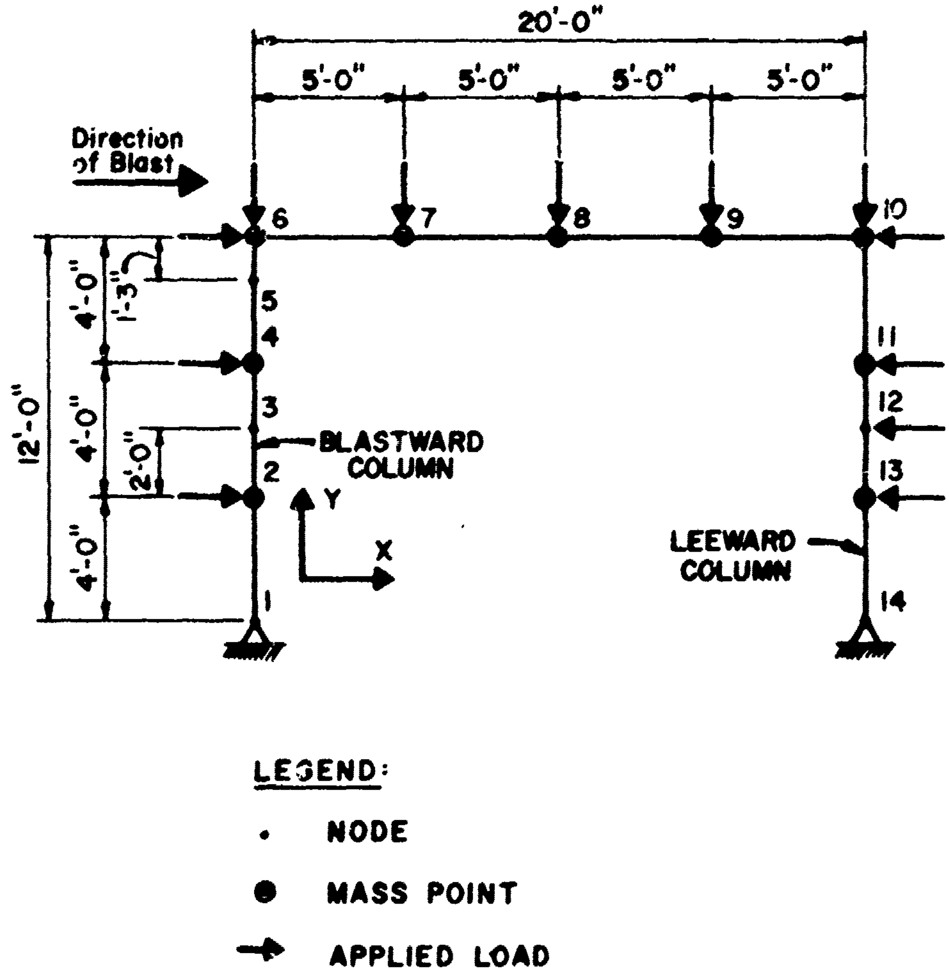

Figure 14. Basic transverse frame model

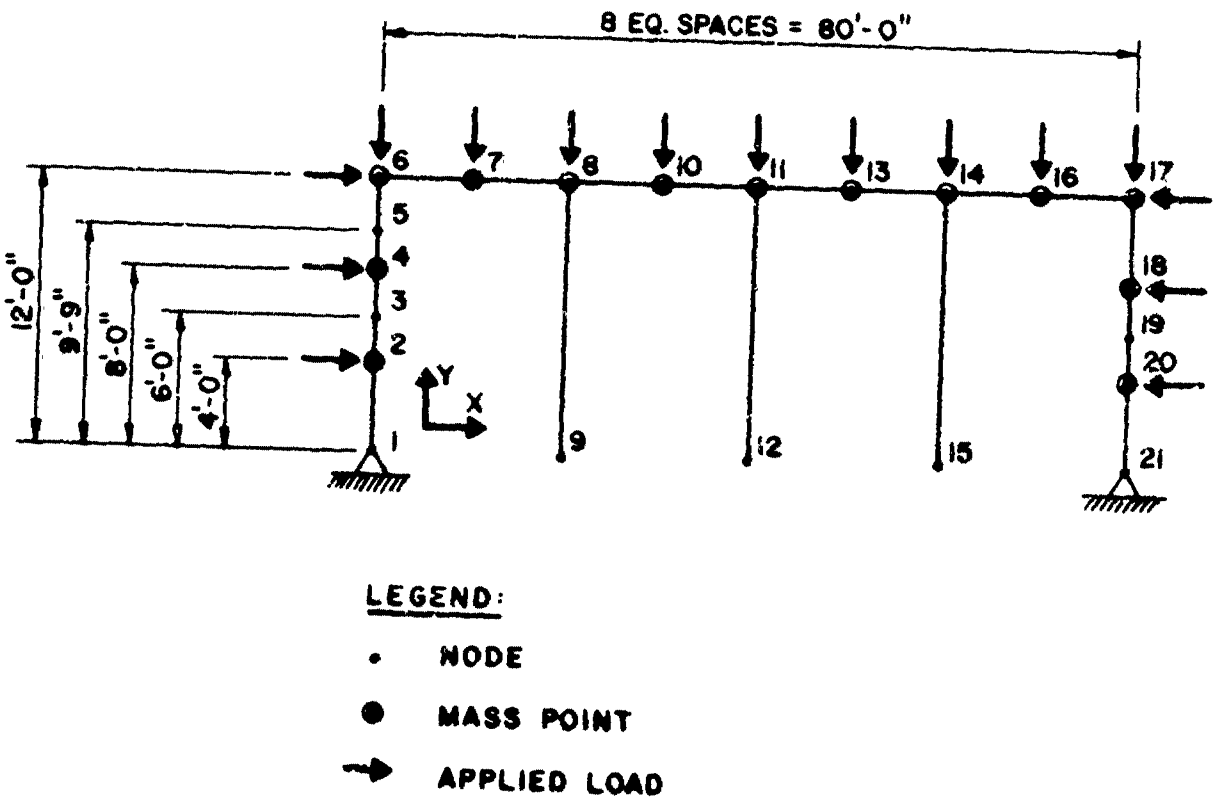

Figure 15. Longitudinal frame model

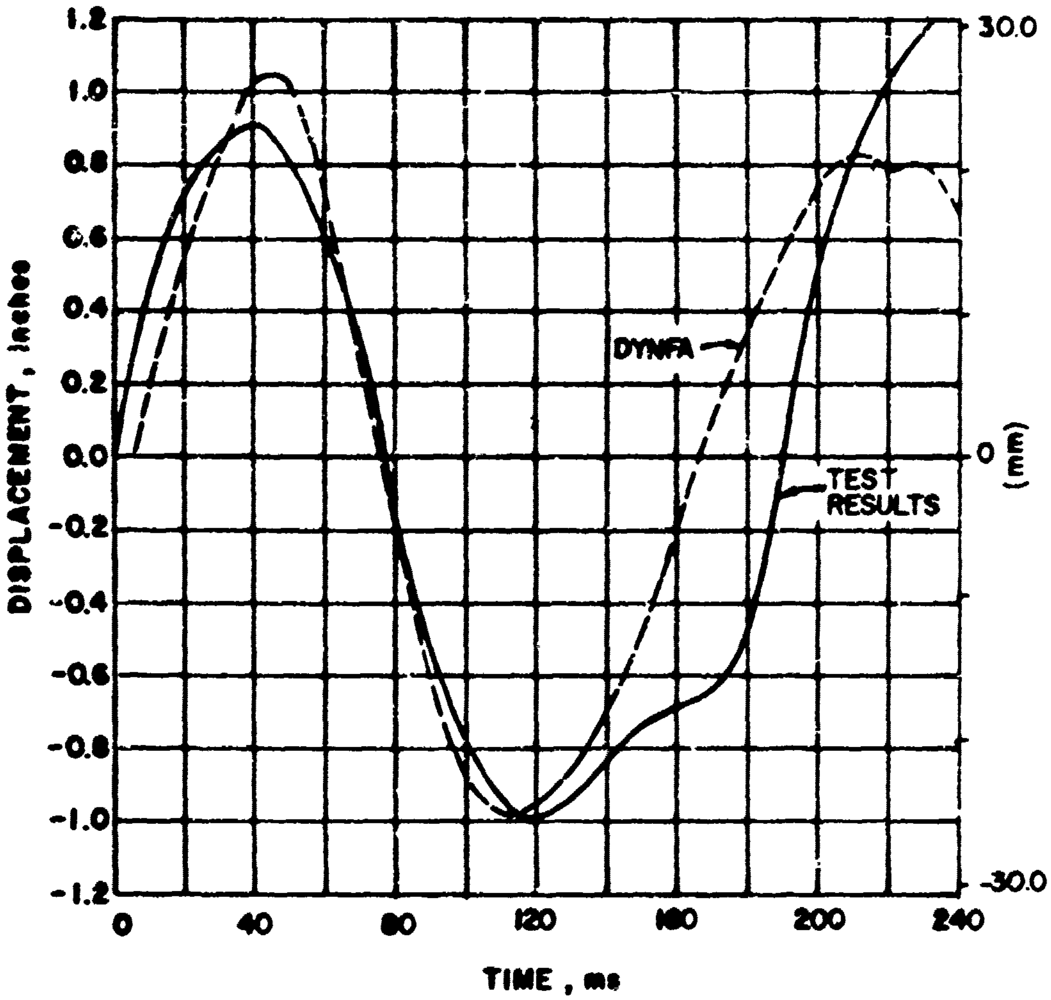

Figure 16. Center frame side-sway displacement, test and analytical results for Test 3

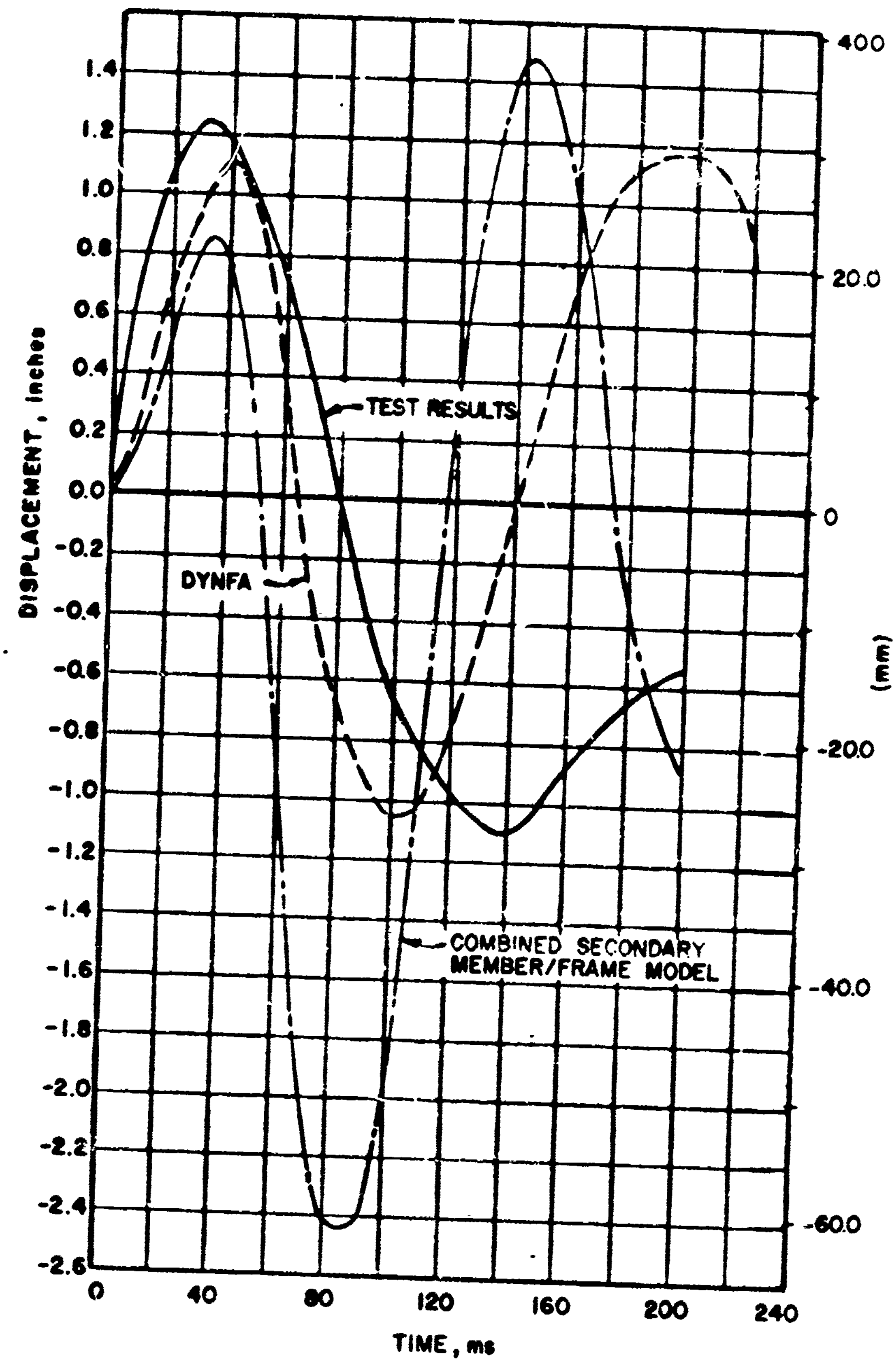

Figure 17. Center frame side-sway displacement, test and analytical results for Test 4

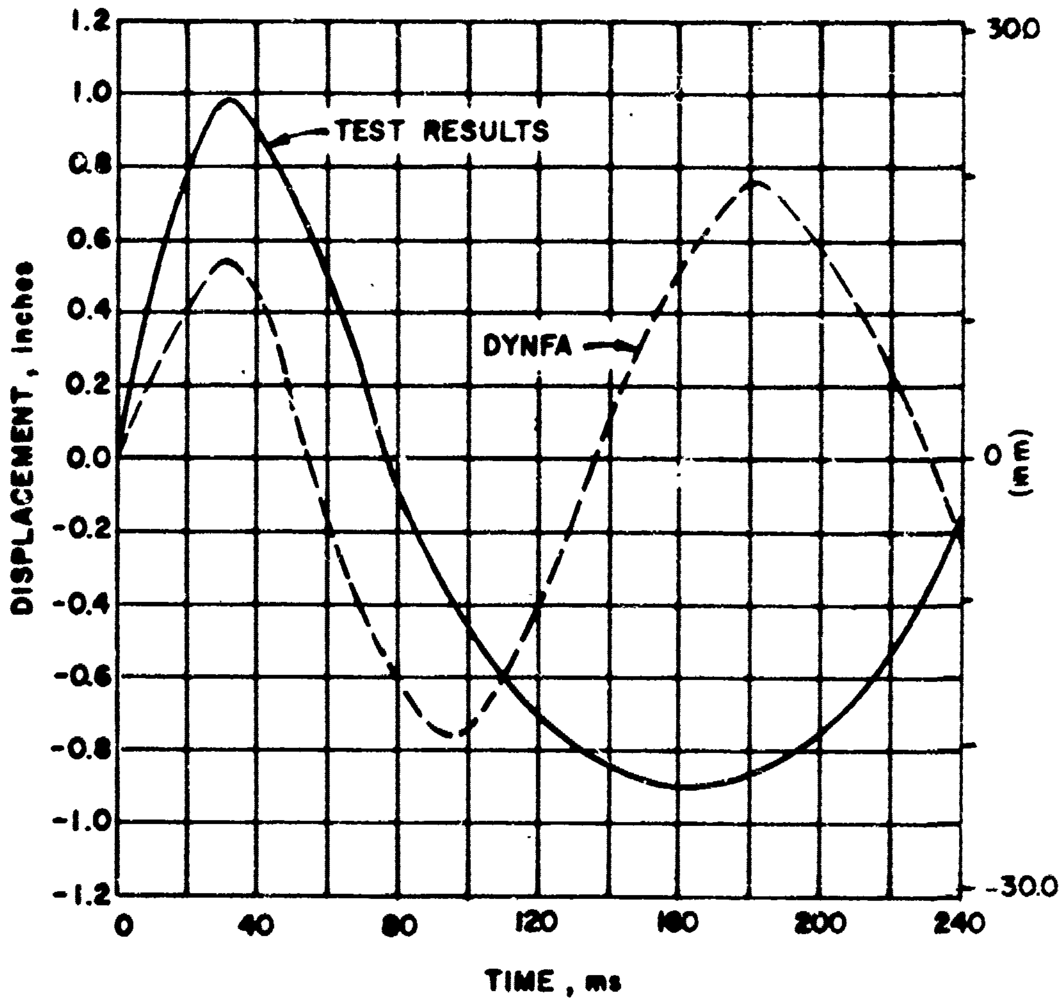

Figure 18. Center frame side-sway displacement, test and analytical results for Test 5

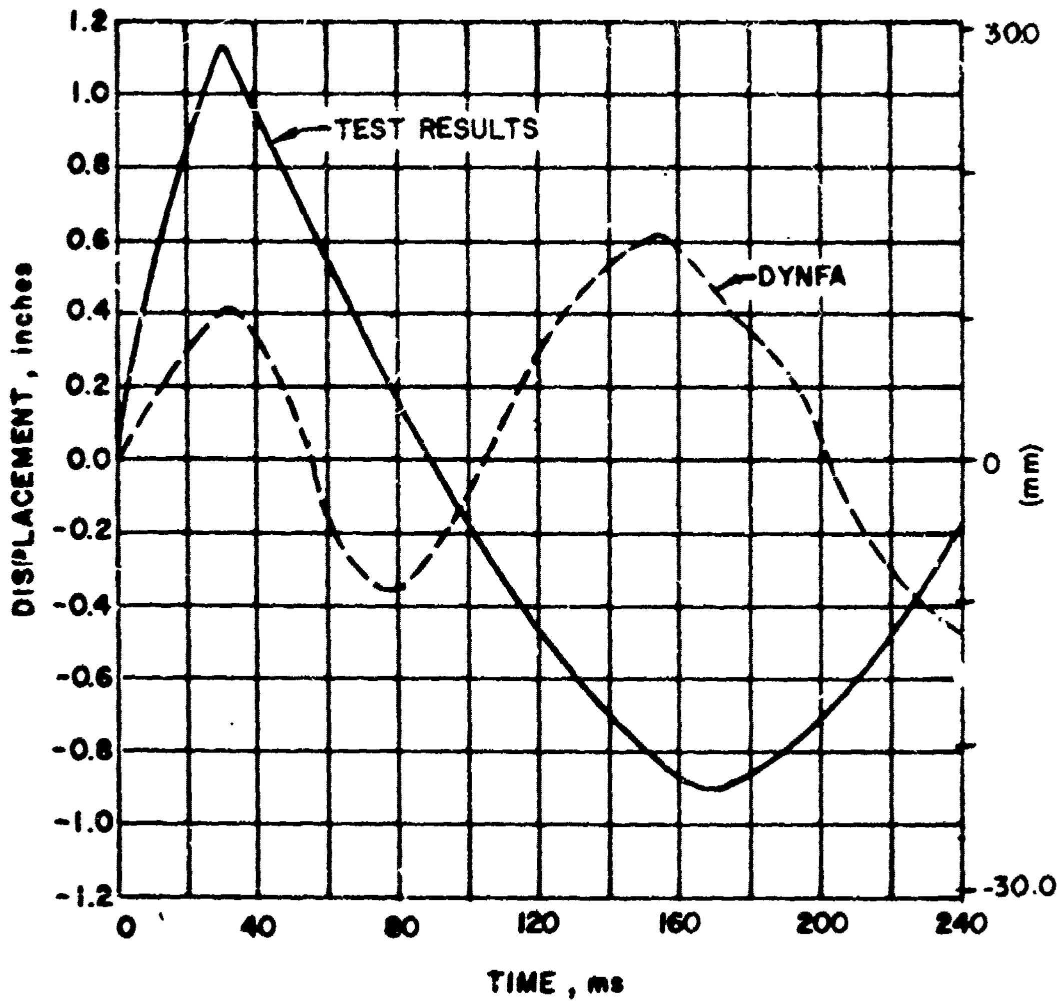

Figure 19. Center frame side-sway displacement, test and analytical results for Test 6

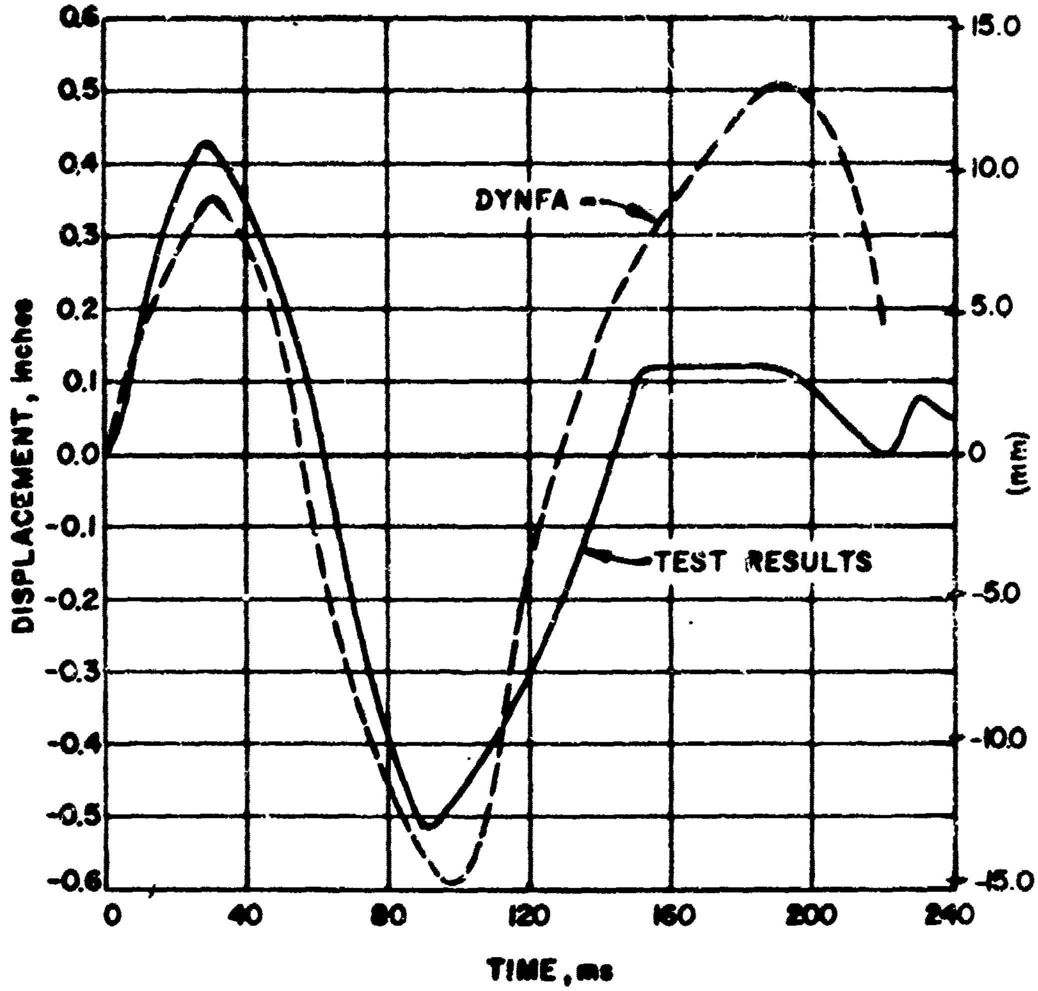

Figure 20. Rigid-end frame side-sway displacement, test and analytical results for Test 5

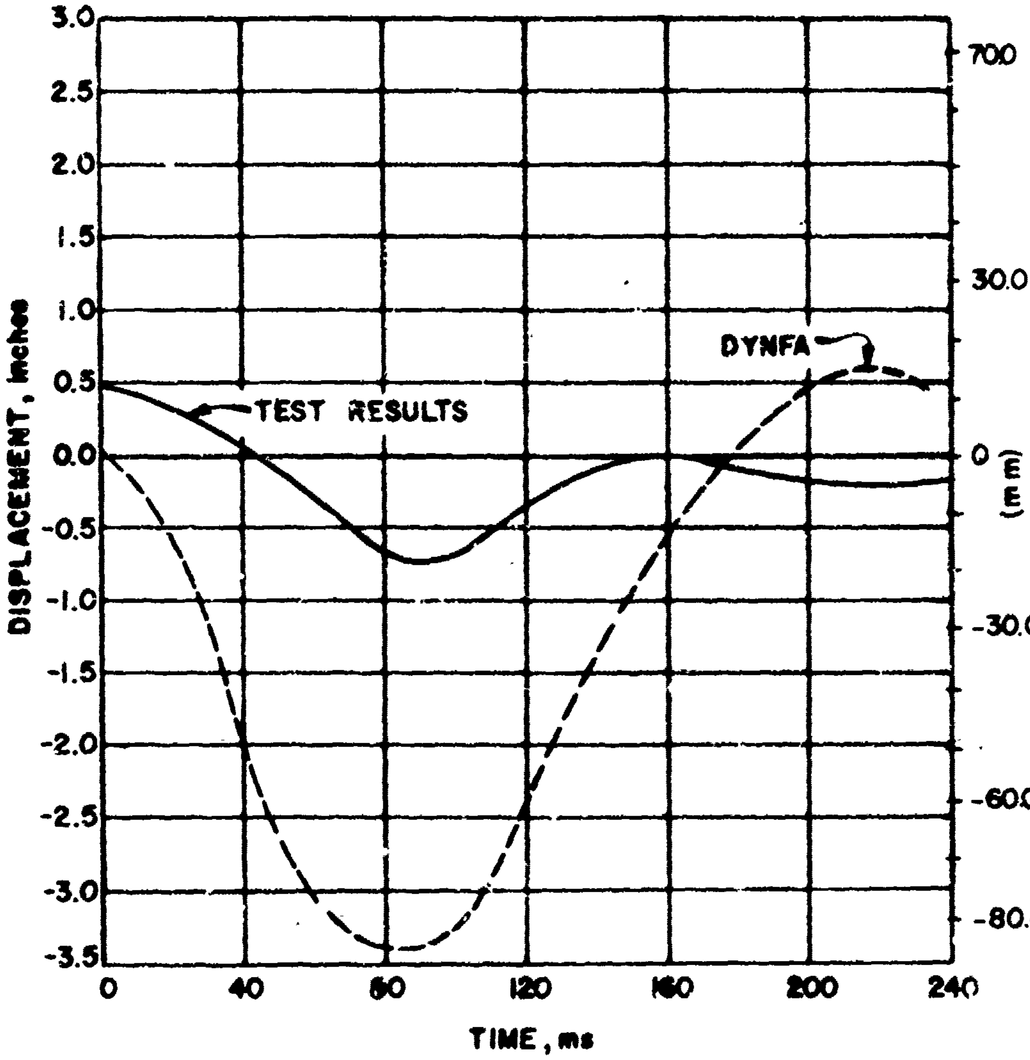

Figure 21. Rigid-end frame side-sway displacement, test and analytical results for Test 7

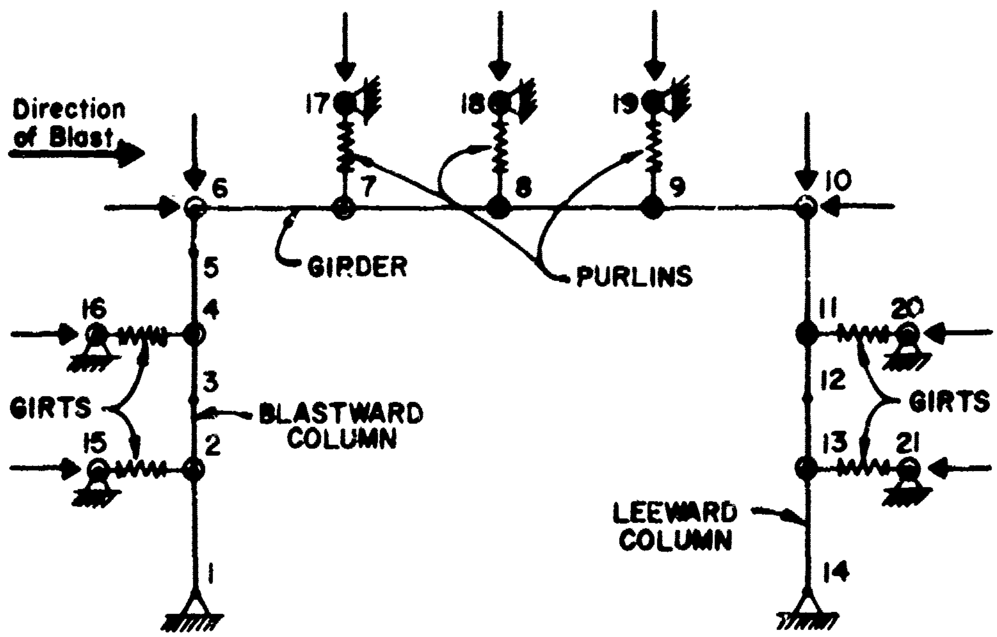

NOTE:

FOR NODE DIMENSIONS & LEGEND, SEE FIGURE 19.

Figure 22. Basic transverse frame model including purlins and girts

DRAG-TYPE FRAGMENT MOTION IN TWO-DIMENSIONS

by

John P. Riegel III

ABSTRACT

An important problem in the history of ballistics and explosives is that of determining the motion of a projectile or fragment. Most researchers currently utilize numerical approximations on digital computers to estimate impact or transient trajectory conditions. This procedure requires a relatively large number of calculations in "stepping" to the point of interest. In this paper, a solution describing the two-dimensional motion of a drag-type fragment with velocity squared dependence is presented. Approximate analytical solutions for the equations of motion are presented, as well as a simpler solution for the special case where the striking elevation equals the initial elevation and the initial vertical component of the velocity is positive. For trajectory calculations which do not require accounting for the effect of wind or decreasing air resistance as a function of altitude, these solutions should provide a valuable tool to researchers.

I. INTRODUCTION

In general, the trajectory of a projectile can be determined by balancing the forces and moments acting on the projectile. If the projectile characteristics and the launch conditions are well defined, a solution might include (Reference 1):

- Normal force,
- Drag,
- Lift,
- Magnus force,
- Static moment,
- Damping moment,
- Magnus moment,
- Roll damping moment.

Unfortunately, when a scientist or engineer is required to estimate transient or terminal flight characteristics for fragments, it is often impractical or impossible to assess the distribution of forces over the fragment accurately. As an example, consider the detonation of a fragmenting tubular bomb. In this case, it is highly probable that both the projectile characteristics and the launch conditions will be assumed based on an engineer's evaluation of the break-up pattern. As a result, very few of the launch conditions can be accurately defined for a given fragment.

In this paper, it is assumed that the initial velocity components of the fragment, the fragment mass, and the presented area can be determined. It is further assumed that the fragment's trajectory will not be affected by lift, magnus force, static moment, damping moment, magnus moment, or roll damping moment. However, the solutions presented will account for the effects of gravity and drag, the two most significant parameters governing the motion of a "chunky" fragment.

When a fragment is ejected vertically upward, its motion is opposed by both gravity and air resistance as indicated in Equation 1.

$$\ddot{Y}_1 = -g - \frac{A_y C_{Dy} \rho}{2m} \dot{Y}_1^2 \tag{1}$$

where $\ddot{Y}_1$ = vertical acceleration upward (positive)

A_y = presented area

C_{Dy} = drag coefficient for vertical components

ρ = mass density of air

$\dot{Y}_1$ = fragment velocity

m = fragment mass

g = gravity

However, when a fragment is travelling towards earth, the equation becomes:

$$\ddot{Y}_2 = -g + \frac{A_y C_{Dy} \rho}{2m} \dot{Y}_2^2 \qquad (2)$$

where $\ddot{Y}_2$ = acceleration downward

$\dot{Y}_2$ = fragment velocity downward (negative)

If the fragment has a horizontal velocity component, it is opposed only by air resistance as in Equation 3.

$$\ddot{X} = -\frac{A_x C_{Dx} \rho}{2m} \dot{X}^2 \qquad (3)$$

where $\ddot{X}$ = horizontal acceleration

$\dot{X}$ = fragment velocity in horizontal direction

A_x = presented area

C_{Dx} = drag coefficient for horizontal component

ρ = mass density of air

m = fragment mass

In this paper, the motion of a fragment possessing both vertical and horizontal velocity components is described. Previously, researchers have described this motion by considering the balanced forces over the projectile as it moves along its trajectory (References 1,2). This procedure generally requires the simultaneous numerical approximation of equations similar to Equations 4 and 5.

$$\ddot{Y} = -g - \frac{A C_D \rho \, (\dot{X}^2 + \dot{Y}^2)}{2m} \sin \alpha \qquad (4)$$

$$\ddot{X} = -\frac{A C_D \rho \, (\dot{X}^2 + \dot{Y}^2)}{2m} \cos \alpha \qquad (5)$$

where $\ddot{Y}$ = vertical acceleration

$\dot{Y}$ = vertical velocity

$\ddot{X}$ = horizontal acceleration

$\dot{X}$ = horizontal velocity

g = gravity

A = area presented in the direction of the resultant motion

C_D = drag coefficient

ρ = mass density of air

m = fragment mass

g = gravity

α = trajectory angle

The numerical approximation is attained by solving the equations repeatedly, incrementing by some time interval after each solution. In this manner, one can "step" through the trajectory until the point of interest is reached. However, this type of solution is generally unnecessary for fragments because the initial conditions cannot be defined well enough to warrant this degree of accuracy. By comparison, the solutions presented here can be used with most hand calculators to obtain a relatively accurate, slightly conservative answer.

The velocity and translation solutions are given in the following two sections. The final two sections include procedures for utilizing the solutions and conclusions.

II. VELOCITY SOLUTIONS

In this section, the velocity solutions to Equations 1, 2, and 3 will be developed. For convenience and clarity, these equations are rewritten as first-order equations. Equation 1 becomes:

$$\frac{dV_1}{dt} = -g - \frac{K_y}{m} V_1^2 \tag{6}$$

Equation 2 becomes:

$$\frac{dV_2}{dt} = -g + \frac{K_y}{m} V_2^2 \tag{7}$$

and Equation 3 becomes:

$$\frac{dV_x}{dt} = -\frac{K_x}{m} V_x^2 \tag{8}$$

where V_1 = upward velocity

V_2 = downward velocity

V_x = horizontal velocity

g = gravity

m = mass

$K_y = \dfrac{A_y C_{Dy} \rho}{2}$

$K_x = \dfrac{A_x C_{Dx} \rho}{2}$

A_y = area presented along vertical axis

A_x = area presented along horizontal axis

C_{Dy} = drag coefficient for vertical component

C_{Dx} = drag coefficient for horizontal component

ρ = mass density of air

Equation 6 can then be rearranged and solved as follows.

$$m \frac{dV_1}{dt_1} = -mg - K_y V_1^2 \tag{9}$$

$$\int_{V_{10}}^{V_1} \frac{m}{\left(\frac{mg}{K_y} + V_1^2\right)} dV_1 = -K_y \int_{t_{10}}^{t_1} dt_1 \tag{10}$$

where t_{10} = initial time

V_{10} = initial upward velocity

Equation 10 is in a standard form which yields (Reference 3):

$$\frac{1}{\sqrt{\frac{mg}{K_y}}} \tan^{-1}\left(\frac{V_1}{\sqrt{\frac{mg}{K_y}}}\right)\Bigg|_{V_{10}}^{V_1} = -\frac{K_y}{m} t_1 \Bigg|_{t_{10}}^{t_1} \tag{11}$$

From Equation 11, the solution for V_1 is obtained:

$$V_1 = \sqrt{\frac{mg}{K_y}} \tan\left[-\sqrt{\frac{K_y g}{m}} (t_1 - t_{10}) + \tan^{-1}\left(\frac{V_{10}}{\sqrt{\frac{mg}{K_y}}}\right)\right] \tag{12}$$

In addition, the rise time (t_1) required for the fragment to slow down to a specified velocity ($V_1 \leq V_{10}$) is given by:

$$t_1 = -\sqrt{\frac{m}{K_y g}} \left[\tan^{-1}\left(\frac{V_1}{\sqrt{\frac{mg}{K_y}}}\right) - \tan^{-1}\left(\frac{V_{10}}{\sqrt{\frac{mg}{K_y}}}\right)\right] + t_{10} \tag{13}$$

The time required for the fragment to attain its maximum height occurs when $V_1 = 0$. Substituting into Equation 13 yields:

$$t_{1(max)} = \sqrt{\frac{m}{K_y g}} \tan^{-1}\left(\frac{V_{10}}{\sqrt{\frac{mg}{K_y}}}\right) + t_{10} \tag{14}$$

Equation 7 is solved as follows:

$$m \frac{dV_2}{dt_2} = -mg + K_y V_2^2 \tag{15}$$

$$\int_{V_{20}}^{V_2} \frac{dV_2}{\left(-\frac{mg}{K_y} + V_2^2\right)} = \frac{K_y}{m} \int_{t_{20}}^{t_2} dt_2 \tag{16}$$

where t_{20} = time where fragment starts to fall, generally equal to $t_{1(max)}$

V_{20} = initial downward velocity

Equation 16 is a standard form (Reference 3) which results in the following solution for the velocity of the falling fragment.

$$V_2 = -\sqrt{\frac{mg}{K_y}} \tanh\left[\tanh^{-1}\left(\frac{-V_{20}}{\sqrt{\frac{mg}{K_y}}}\right) + \sqrt{\frac{K_y g}{m}}\,(t_2 - t_{20})\right] \tag{17}$$

Equation 17 can be arranged to determine the fall time, t_2, required for the fragment to attain a particular velocity.

$$t_2 = +\sqrt{\frac{m}{K_y g}}\left[\tanh^{-1}\left(\frac{-V_2}{\sqrt{\frac{mg}{K_y}}}\right) - \tanh^{-1}\left(\frac{-V_{20}}{\sqrt{\frac{mg}{K_y}}}\right)\right] + t_{20} \tag{18}$$

Finally, Equation 8 can be solved

$$m\frac{dV_x}{dt_x} = -K_x V_x^2 \tag{19}$$

$$\int_{V_{x0}}^{V_x} \frac{dV_x}{V_x^2} = \frac{-K_x}{m} \int_{t_{x0}}^{t_x} dt_x \tag{20}$$

Solving Equation 20 for V_x gives:

$$V_x = \frac{1}{\frac{1}{V_{x0}} + \frac{K_x}{m}\left(t_x - t_{x0}\right)} \tag{21}$$

where V_{x0} = initial horizontal velocity.

Alternatively, solving for time yields:

$$t_x = +\frac{m}{K_x}\left(\frac{1}{V_x} - \frac{1}{V_{x0}}\right) + t_{x0} \tag{22}$$

where t_x is less than or equal to the total time of flight.

III. TRANSLATION SOLUTIONS

Integration of the velocity solutions presented in Equations 12, 17, and 21 with respect to time yields the displacement solutions. Solving Equation 12 provides the solution to the vertical displacement during the time the fragment is rising.

$$\frac{dy_1}{dt_1} = \sqrt{\frac{mg}{K_y}} \tan\left[-\sqrt{\frac{K_y g}{m}}(t_1 - t_{10}) + \tan^{-1}\left(\frac{V_{10}}{\sqrt{\frac{mg}{K_y}}}\right)\right] \tag{23}$$

$$\int_{y_{10}}^{y_1} dy_1 = \sqrt{\frac{mg}{K_y}} \int_{t_{10}}^{t_1} \tan\left[-\sqrt{\frac{K_y g}{m}}(t_1 - t_{10}) + \tan^{-1}\left(\frac{V_{10}}{\sqrt{\frac{mg}{K_y}}}\right)\right] dt_1 \tag{24}$$

Equation 24 then leads to

$$y_1 = \frac{m}{K_y}\left[\log\left\{\frac{\cos\left[\tan^{-1}\left(\frac{V_{10}}{\sqrt{\frac{mg}{K_y}}}\right) - \sqrt{\frac{K_y g}{m}}(t_1 - t_{10})\right]}{\cos\left[\tan^{-1}\left(\frac{V_{10}}{\sqrt{\frac{mg}{K_y}}}\right)\right]}\right\}\right] + Y_{10} \tag{25}$$

The solution of Equation 26, which was developed from Equation 17, describes the vertical position of the fragment as it travels towards the ground.

$$\frac{dy_2}{dt_2} = -\sqrt{\frac{mg}{K_y}} \tanh\left[\tanh^{-1}\left(\frac{-V_{20}}{\sqrt{\frac{mg}{K_y}}}\right) + \sqrt{\frac{K_y g}{m}}(t_2 - t_{20})\right] \tag{26}$$

Equation 26 is solved as follows (Reference 3):

$$y_2 = -\frac{m}{K_y}\left\{\log\cosh\left[\tanh^{-1}\left(\frac{-V_{20}}{\sqrt{\frac{mg}{K_y}}}\right) + \sqrt{\frac{K_y g}{m}}(t_2 - t_{20})\right] - \log\cosh\left[\tanh^{-1}\left(\frac{-V_{20}}{\sqrt{\frac{mg}{K_y}}}\right)\right]\right\} + y_{20} \tag{27}$$

Likewise, Equation 21 can be solved to obtain the horizontal displacement, as shown in Equations 28 and 29.

$$\frac{dx}{dt} = \frac{1}{\frac{1}{V_{x_0}} + \frac{K_x}{m}\left(t_x - t_{x_0}\right)} \tag{28}$$

$$x = \frac{m}{K_x}\left\{\log\left[1 + V_{x_0}\frac{K_x}{m}\left(t_x - t_{x_0}\right)\right]\right\} + x_0 \tag{29}$$

Equations 25, 27, and 29 can be rearranged to solve for time for a fragment to reach a certain position. Equation 25 then becomes:

$$t_1 = -\sqrt{\frac{m}{K_y g}}\left(\cos^{-1}\left\{\left[\cos\tan^{-1}\left(\frac{V_{10}}{\sqrt{\frac{mg}{K_y}}}\right)\right] e^{(y_1 - y_{10})\frac{K_y}{m}}\right\} - \tan^{-1}\left(\frac{V_{10}}{\sqrt{\frac{mg}{K_y}}}\right)\right) + t_{10} \tag{30}$$

Equation 27 becomes:

$$t_2 = +\sqrt{\frac{m}{K_y g}}\left(\cosh^{-1}\left\{e^{\left[-\frac{K_y}{m}\left(y_2 - y_{20}\right) + \log\cosh\tanh^{-1}\left(\frac{-V_{20}}{\sqrt{\frac{mg}{K_y}}}\right)\right]}\right\} - \tanh^{-1}\left(\frac{-V_{20}}{\sqrt{\frac{mg}{K_y}}}\right)\right) + t_{20} \tag{31}$$

Equation 29 becomes:

$$t_x = +\frac{m}{V_{x_0} K_x}\left\{e^{\left[\frac{K_x}{m}\left(x - x_0\right)\right]} - 1\right\} + t_{x_0} \tag{32}$$

IV. PROCEDURES

Although the solutions which have been presented may seem unwieldy at first, they can be utilized quite readily by programming them into a computer, or by developing nondimensional plots from the equations. In this section, several scaled terms will be defined and plotted.

The equations presented in this paper yield three scaled velocities. The scaled rise velocity $\bar{V}_R$ is defined as:

$$\bar{V}_R = \frac{\cos\left[\tan^{-1}\left(v_1\sqrt{\frac{K_x}{mg}}\right)\right]}{\cos\left[\tan^{-1}\left(v_{10}\sqrt{\frac{K_x}{mg}}\right)\right]} \tag{33}$$

The scaled fall velocity $\bar{V}_F$ is defined as:

$$\bar{V}_F = \frac{\cosh\left[\tanh^{-1}\left(-v_2\sqrt{\frac{K_y}{mg}}\right)\right]}{\cosh\left[\tanh^{-1}\left(-v_{20}\sqrt{\frac{K_y}{mg}}\right)\right]} \tag{34}$$

The scaled horizontal velocity $\bar{V}_H$ is given by:

$$\bar{V}_H = \frac{v_{x_0}}{v_x} \tag{35}$$

The solutions presented also provide three scaled displacements. The nondimensional upward displacement $\bar{D}_R$ is defined as:

$$\bar{D}_R = (y_1 - y_{10})\frac{K_y}{m} \tag{36}$$

Downward displacement $\bar{D}_F$ is given by:

$$\bar{D}_F = (y_{20} - y_2)\frac{K_y}{m} \tag{37}$$

Finally, the horizontal displacement $\bar{D}_H$ is given by:

$$\bar{D}_H = (x - x_0)\frac{K_x}{m} \tag{38}$$

A single plot can be used to describe the relationships between the three scaled velocities and the corresponding displacements. All three relationships are of the form:

$$\bar{V} = e^{\bar{D}} \tag{39}$$

where $\bar{V} = \bar{V}_R$, $\bar{V}_F$, or $\bar{V}_H$

$\bar{D} = \bar{D}_R$, $\bar{D}_F$, or $\bar{D}_H$

These relationships are presented in Figure 1.

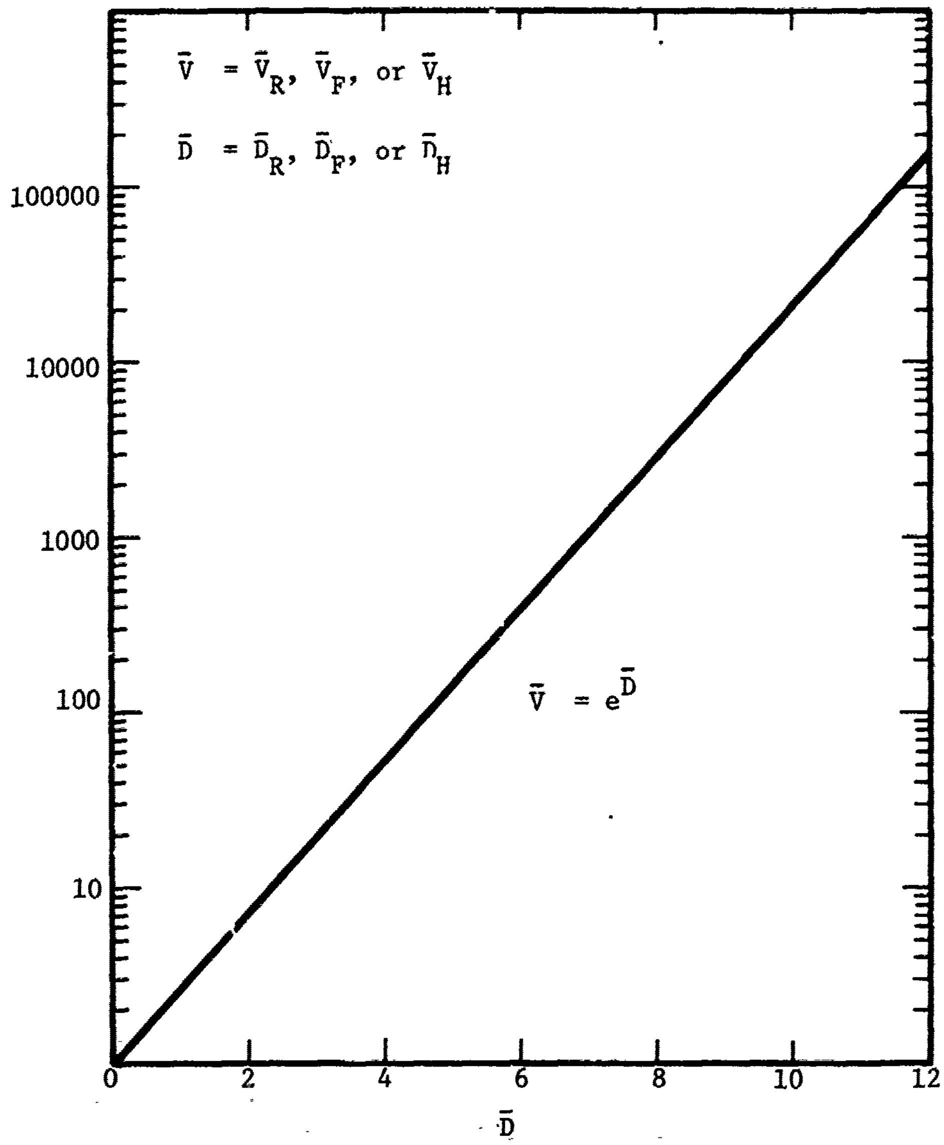

Figure 1. Scaled Velocity vs Scaled Displacement

By defining three scaled times, the motion of a fragment can be determined. The scaled rise time $\bar{t}_R$ is:

$$\bar{t}_R = (t_1 - t_{10})\sqrt{\frac{K_y g}{m}} \quad (40)$$

where $\bar{t}_R \leq \tan^{-1}\left(\frac{V_{10}}{\sqrt{\frac{mg}{K_y}}}\right)$

The scaled fall time $\bar{t}_F$ is given by:

$$\bar{t}_F = (t_2 - t_{20})\sqrt{\frac{K_y g}{m}} \quad (41)$$

The scaled horizontal time $\bar{t}_H$ is given by:

$$\bar{t}_H = (t_x - t_{x_0})\,\frac{V_{x_0} K_x}{m} \quad (42)$$

These scaled times can be determined by utilizing the information in Figure 1 and the following relationships:

$$\bar{t}_R = \tan^{-1}\left(V_{10}\sqrt{\frac{K_y}{mg}}\right) - \tan^{-1}\left(V_1\sqrt{\frac{K_y}{mg}}\right) \quad (43)$$

$$\bar{t}_F = \tanh^{-1}\left(-V_{20}\sqrt{\frac{K_y}{mg}}\right) - \tanh^{-1}\left(-V_2\sqrt{\frac{K_y}{mg}}\right) \quad (44)$$

$$\bar{t}_H = \frac{V_{x_0}}{V_x} - 1 \quad (45)$$

Figure 2 is presented as an example of the type of specialized graphical solution which can be obtained from the relationships presented. Figure 2 is a plot of the scaled vertical component of the striking velocity V_2 versus the same component of the initial velocity V_{10} for the special case where the launch elevation equals the impact elevation. The need for this particular solution developed from a requirement to estimate the impact kinetic energy of fragments emanating from a bomb. In this problem, the vertical component of the striking velocity was the only parameter needed, resulting in the simple relationship:

$$\bar{V}_2 = \sin\left(\tan^{-1}\bar{V}_{10}\right) \quad (46)$$

where $\bar{V}_{10} = V_{10}\sqrt{\frac{K_y}{mg}}$

$\bar{V}_2 = -V_2\sqrt{\frac{K_y}{mg}}$

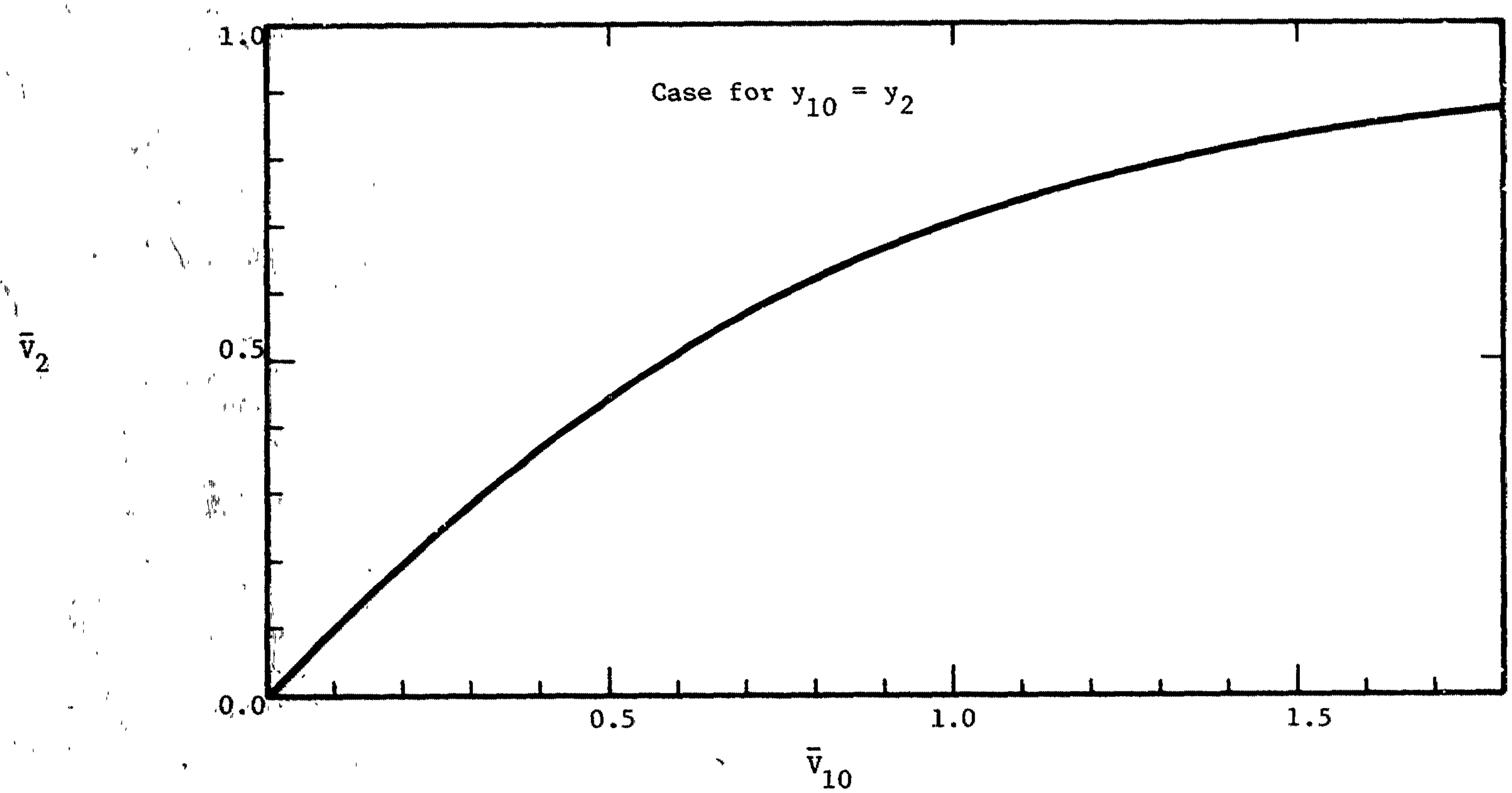

Figure 2. Scaled Initial Vertical Velocity vs Scaled Final Vertical Velocity

EXAMPLE

GIVEN: A spherical fragment with the following characteristics

$A_y = 2.182 \times 10^{-2}\ ft^2$

$A_x = 2.182 \times 10^{-2}\ ft^2$

$C_{Dy} = 0.47$

$C_{Dx} = 0.47$

$m = 3.683 \times 10^{-2}\ lb \cdot s^2/ft$

$\rho_a = 2.378 \times 10^{-3}\ lb \cdot s^2/ft^4$

$g = 32.174\ ft/s^2$

$t_{10} = 0$

$t_{x_0} = 0$

$y_{10} = 0$

$x_0 = 0$

$V_{10} = 600\ ft/s$

$V_{x_0} = 200\ ft/s$

FIND: Maximum height, range, time of flight, impact velocities.

SOLUTION:

1. Define K_x, K_y

$$K_x = \frac{A_x C_{Dx} \rho_a}{2} = 1.219 \times 10^{-5}\ lb \cdot s^2/ft^2$$

$$K_y = \frac{A_y C_{Dy} \rho_a}{2} = 1.219 \times 10^{-5}\ lb \cdot s^2/ft^2$$

2. Determine the maximum height.

a. The maximum height for an object initially moving upward occurs when the rise velocity V equals zero. Equation 33 can be used to determine $\bar{V}_R$ at the maximum height.

$$\bar{V}_R = \frac{1}{\cos\left[\tan^{-1}\left(V_{10}\sqrt{\frac{K_y}{mg}}\right)\right]} = 2.169$$

b. Use the value obtained in "a" and Figure 1 to determine the scaled displacement $\bar{D}_R$.

$\bar{D}_R = 0.8$

c. Solve for the height using Equation 36.

$$\bar{D}_R = (y_1 - y_{10}) \frac{K_y}{m}$$

$$y_1 = \bar{D}_R \frac{m}{K_y} + y_{10} = 2.417 \times 10^3 \text{ ft}$$

d. Solve for the rise time using Equations 43 and 40.

$$\bar{t}_R = \tan^{-1}\left(V_{10}\sqrt{\frac{K_y}{mg}}\right) = 1.092$$

$$\bar{t}_R = (t_1 - t_{10})\sqrt{\frac{K_y g}{m}}$$

$$t_1 = t_{10} + \bar{t}_R\sqrt{\frac{m}{K_y g}} = 10.58 \text{ sec}$$

3. Determine vertical impact velocity.

a. Solve Equation 37 to find $\bar{D}_F$.

$$\bar{D}_F = (y_{20} - y_2)\frac{K_y}{m} = 0.8$$

b. Use this value to determine $\bar{V}_F$ from Figure 1.

$\bar{V}_F = 2.169$

c. Use Equation 34 to find the vertical impact velocity V_2.

$$\bar{V}_F = \frac{\cosh\left[\tanh^{-1}\left(-V_2\sqrt{\frac{K_y}{mg}}\right)\right]}{\cosh\left[\tanh^{-1}\left(-V_{20}\sqrt{\frac{K_y}{mg}}\right)\right]}$$

$$V_2 = -\sqrt{\frac{mg}{K_y}}\tanh\left[\cosh^{-1}\left(2.169\left\{\cosh\left[\tanh^{-1}\left(-V_{20}\sqrt{\frac{K_y}{mg}}\right)\right]\right\}\right)\right]$$

Note that if $V_{20} = 0$ this reduces to:

$$V_2 = -\sqrt{\frac{mg}{K_y}}(0.8875) = -2.77 \times 10^2 \text{ ft/sec}$$

d. Determine fall time using Equations 44 and 41.

$$\bar{t}_F = \tanh^{-1}\left(-V_{20}\sqrt{\frac{K_y}{mg}}\right) + \tanh^{-1}\left(-V_2\sqrt{\frac{K_y}{mg}}\right) = 1.415$$

$$\bar{t}_F = (t_2 - t_{20})\sqrt{\frac{K_y g}{m}}$$

$$t_2 = t_{20} + \bar{t}_F\sqrt{\frac{m}{K_y g}} = 13.71 \text{ sec}$$

4. Determine total time t_T of flight.

a. Sum rise and fall times.

$$t_T = t_1 + t_2 = 24.29 \text{ sec}$$

b. Total time of flight equals t_x at impact.

$$t_x = 24.29 \text{ sec}$$

5. Determine horizontal impact velocity.

a. Determine scaled horizontal time.

$$\bar{t}_H = (t_x - t_{x_0})\frac{V_{x_0} K_x}{m} = 1.608$$

b. Determine the impact velocity using Equation 45.

$$\bar{t}_H = \frac{V_{x_0}}{V_x} - 1$$

$$V_x = \frac{V_{x_0}}{\bar{t}_H + 1} = 76.69 \text{ ft/s}$$

6. Solve for the maximum range.

a. Find $\bar{V}_H$ using Equation 35.

$$\bar{V}_H = \frac{V_{x_0}}{V_x} = 2.608$$

b. Use Figure 1 to determine $\bar{D}_H$.

$$\bar{D}_H = 1$$

c. Find the total horizontal displacement using Equation 38.

$$x = \bar{D}_H \frac{m}{K_x} + x_0 = 3.02 \times 10^3 \text{ ft}$$

V. CONCLUSIONS

The solutions presented in this paper are suitable for solving a special class of problems. The procedures can be used to estimate the trajectory of any projectile or fragment whose motion is dependent solely on drag and gravity. In general, this means that the solutions should provide accurate results for "chunky" fragments. On the other hand, the trajectories of fragments which are heavily influenced by lift should not be estimated using the procedures presented here.

Further limitations exist due to some assumptions which were made in order to simplify the equations. The presented areas, drag coefficients, air density, and acceleration due to gravity are considered constant throughout the trajectory of the fragment. As a result of these assumptions, certain limitations are implied. First, the fragment should not be rotating about any axis which will cause fluctuations in the presented areas or drag coefficients. Second, the fragment's velocity should not exceed the speed of sound or else the assumption of a constant drag coefficient becomes invalid. Finally, the vertical displacement should not be so great as to cause major fluctuations in the air density and gravity terms.

It is important to recognize that the separate vertical and horizontal solutions presented here provide approximate solutions for "chunky" fragments. Unfortunately, the author did not have time to fully evaluate the accuracy of the solutions prior to this conference. However, an assessment of the error for the range predicted by this method was made by A. E. Sherwood (Reference 4). Sherwood concluded that the "uncoupled" approximation resulted in a longer predicted range due to "understating the correct total drag force at each point along the trajectory by the factor $(\sin^4\Theta + \cos^4\Theta)^{1/2}$," where Θ is the trajectory angle. He also compared the results to Cranz' ballistic tables (Reference 5), varying the ballistic coefficient* from 0.1 to 100 and the initial trajectory angle from 15° to 75°. He concluded that the estimated range is always high, but is usually within 20% except for very high initial trajectory angles. Although the limits of the error which occurs in the predicted velocity and time-of-flight have not been investigated by the author, they should also be conservative.

Currently, the solutions presented should provide a quick, simple method of predicting trajectory conditions for drag-type fragments. In future work, the author feels that it should be possible to develop a correction factor as a function of initials conditions (i.e., trajectory angle and ballistic coefficient) which would reduce the error associated with these solutions.

---

*Ballistic coefficient is the squared ratio of a fragment's initial velocity to its freefall terminal velocity.

REFERENCES

1. AMCP 706-242, "Engineering Design Handbook: Design for Control of Projectile Flight Characteristics," Headquarters, U. S. Army Materiel Command, Sept. 1966.

2. Baker, W. E., Kulesz, J. J., Ricker, R. E., Westine. P. S., Parr, V. B., Vargas, L. M., and Moseley, P. K., "Workbook for Estimating the Effects of Accidental Explosions in Propellant Handling Systems," NASA CR 3023, Contract NAS3-20497, Lewis Research Center, Aug. 197 .

3. Samuel M. Selby (Editor-in-Chief), Standard Mathematical Tables, The Chemical Rubber Co., 21st Edition, 1973.

4. Sherwood, A. E., "Effect of Air Drag on Particles Ejected During Explosive Cratering," Journal of Geophysical Research, Volume 72, No. 6, March 15, 1967.

5. Cranz, C., "Lehrbuch der Ballistik I," Äussere Ballistik, Berlin, 1925.

DEBRIS HAZARDS FROM EXPLOSIONS IN ABOVE-GROUND MAGAZINES

by

Hans A. Merz M.ASCE/SIA
Basler & Hofmann
Consulting Engineers
Zurich, Switzerland

ABSTRACT

This paper presents the results of research for a better understanding of debris hazards from explosions in above-ground magazines and for the quantitative prediction of debris hazards in risk analyses. Two kinds of debris hazards are distinguished:

- Debris dispersal of the crater material
- Debris dispersal of the building material

In the case of debris dispersal of the crater material, the results of an extensive review and evaluation of the existing literature are presented. A statistical analysis of the major properties such as crater dimensions, crater volume and mass, and debris density is shown.

In the case of debris from buildings, the results of model tests in the scale of 1 : 10 are presented, and a quantitative model for the prediction of these hazards is outlined.

Paper presented to

Nineteenth Explosives Safety Seminar, 9-11 September 1980
The Biltmore Hotel, Los Angeles, California, USA

INTRODUCTION

In order to predict and, if possible, mitigate the hazardous effects on persons and goods in the case of accidental explosions in explosives magazines, the method of risk analyses has been introduced in Switzerland (see the corresponding papers held at the 17th and 18th DDESB-Seminar). When evaluating the risk or the expected damage to the environment of an explosives magazine, the various types of explosion effects have to be taken into account, and for each of them a quantitative model for describing their effects on persons and goods is necessary. One of these effects is the debris dispersal which in many cases is a predominant hazard and also the most spectacular part of such destructive events.

This paper deals exclusively with the debris hazards from explosions in above-ground magazines. It is the purpose to present some of the results of research conducted within the last years in Switzerland and to promote future research for a better understanding of these important effects of accidental explosions.

GENERAL DESCRIPTION OF DEBRIS HAZARDS

When talking about debris hazards from explosions in above-ground magazines, two effects have to be distinguished:

1. The *debris hazards from the crater material:* In intermediate and farther distances of an explosion, these debris have a *"rain-type"* characteristic (see figure 1). Due to the relatively large initial flight angles, persons are usually only endangered, when the debris fall back to earth, but not during their flight. How much a person is endangered, depends primarily on the amount of material or the horizontal debris density (in kg/m^2) and the debris characteristics such as debris size and velocity.

2. Phenomenologically quite different are the *debris hazards associated with the destruction of a building.* Usually these hazards have to be considered even in the case of small explosions not yet forming an ef-

fective crater. These debris have a *"bullet-type"* characteristic (see figure 1). Due to the mostly flat trajectories, often more or less parallel to the ground, these debris are capable of endangering persons along their entire flight trajectory, and not only when they fall back to earth. The horizontal debris density observed after the explosion is therefore no longer the decisive factor to describe the dangerous effects on persons. In this case, the vertical debris flow (in kg/m^2) or, in connection with the velocity and size of the debris, the vertical energy flow is the important parameter to describe the hazard to persons.

In the following, each of these two debris effects will be shortly described in more detail.

DEBRIS HAZARDS FROM THE CRATER MATERIAL

Quite a number or papers can be found in the literature which deal with the crater formation and the debris dispersal from surface explosions. They range from investigations of test or accidental explosions to theoretical models. However, these papers often deal with rather specific questions and situations and cannot readily be used for the purpose of risk analyses. It therefore was necessary to combine this information in a single crater ejecta model.

Based on the available literature, all elements of crater formation and debris dispersal were investigated separately and then combined in a simple and physically consistant model. In order to obtain a generally valid model, which is simple to apply in reality, the explicit treatment of parameters such as the soil types, charge shapes and so on was omitted. The important factors of the model were only correlated with the charge size. However, the corresponding uncertainty in the prediction which accounts for the influence of all other factors, was statistically evaluated.

The approach of this crater ejecta model is outlined in figure 2; and consists of four steps:

1. Investigation of *crater dimensions* from surface explosions:
   Using data from test and accidental explosions, a regression analysis was performed which led to the prediction of average crater dimensions and a statistically determined probability distribution around the mean value owing to the uncertainty of all the parameters not accounted for in the regression analysis (figures 3 and 4). The comparison with existing crater formulae shows which formulae represent mean values and in which "safety factors" were included (figure 5).

2. Investigation of *crater volume* and *ejecta mass:*
   Based on the previous investigations of crater dimensions and additional data on volume and ejecta mass from test or accidental explosions, a similar regression analysis was performed. The corresponding mean relationship between crater volume, ejecta mass and charge size are shown in figures 6 and 7. Again, a statistically evaluated probability distribution was defined, which accounts for the uncertainty in the prediction due to the various parameters not explicitly treated in the regression analysis.

3. The information on crater volume and ejecta mass was the starting point for the investigation of the *debris dispersal:*
   As mentioned earlier, the hazards of crater debris with "rain-type" characteristics can be described in a first step by the horizontal debris density. Therefore, all relationships for the prediction of debris density found in the open literature were used as "data base" for the determination of a "generally valid" formula. After extensive mathematical treatment in order to make these relationships comparable as well as possible, they were plotted in one diagram. As it can be seen from figure 8, the difference between the extreme relationships amounts to a factor of more than 1000. This would mean that the debris density can vary in reality between 1 kg/m^2 or 1 t/m^2, for instance! Without trying to find the reason for these almost unbelievable differences, a mean relationship and a corresponding probability destribution was computed (see figure 8).

In order to check the consistancy of this relationship with previous investigations of the crater formation, the debris density was integrated and compared with the crater mass relationship in figure 7. Without going into details of the assumptions concerning the validity of the debris density function in the near field of a crater, it was found that the mean debris density relationship satisfies the condition of *mass conservation*, i.e. it corresponds to the previously determined crater mass relationship (see figure 9). However, the uncertainty in the crater mass prediction when using the integrated debris density function is considerably larger than the one obtained previously. The possible reasons for these descrepancies shall not be discussed here. For the moment, it can be stated that the mean debris density function in figure 8 is physically consistant by satisfying the condition of mass conservation. However, additional research is necessary to improve the prediction of hazards from crater debris dispersal.

DEBRIS DISPERSAL FROM THE BUILDING MATERIAL

The dispersal of building material in the case of accidental explosions is so far not extensively treated in the literature. Therefore, model tests in the scale of 1 : 10 with concrete model magazines shown in figure 10 were performed. The results of these tests are presented in the following. As it will be shown later, they are but a first step on the right track to the understanding of this phenomenon, and further research will be necessary.

During these tests, two imporant things could be observed:

1. There are a few distinct directions in which most of the wall debris are projected, corresponding to the four directions perpendicular to the wall surface.

2. The trajectories of wall debris are flat and often more or less parallel to the ground. Together with the larger velocities of the debris as compared with the ejected crater material, large debris ranges can be observed.

The observed directed projection of wall debris can be explained as follows: Due to the fact that the reinforced concrete model magazines represented a ductile construction of considerable strength, the actual destruction of the magazines was primarily produced by something like a chamber pressure acting perpendicularly on the four walls and pushing them into the four predetermined directions. The initial peak blast waves did not contain enough energy to completely desintegrate this ductile and rather strong construction. However, had a brittle construction of our model magazines been used, the directional effect would not be that pronounced.

It can therefore be concluded that the dispersal of wall debris is heavily influenced by:

1. The type and strength of the construction of a magazine (ductile or brittle): The more strength and ductility, the more has a directional dispersal in specific directions to be expected (see figure 11).

2. The shape of the building itself more or less determines the direction of the debris dispersal in the case of a ductile construction (see figure 12).

After these more phenomenological observations, the problem of quantifying these debris hazards will be addressed.

As mentioned earlier, the predominantly flat trajectories of wall debris led to the conclusion that these hazards cannot be described by the horizontal debris density after the explosion only. Structural debris can endanger persons more or less along the entire trajectory. Therefore, the vertical debris flow, indicated in figure 13 which can be correlated with the energy flow, is a more appropriate measure of the hazard.

Based on the model tests, in which data on the debris trajectories were recorded photographically and the location, size and density of the debris after the explosion were measured, a theoretical model for the prediction of this debris flow was set up. There is no need to go into the details of this model here, because, given information on the distribution of debris size, initial angles and velocities - it is a mathematically straight forward problem as indicated in figure 13.

With the debris flow model it is easily possible to deduce information on the debris density to be observed after the explosion. It therefore was possible to compare the actual measurements of horizontal debris density with the prediction from the debris flow model as shown in figure 14. Though the comparison is far from being perfect, it shows that the general characteristics are reproduced by the debris flow model. The considerable scatter of the data points around the predicted curve does certainly not surprise those who have once made debris density measurements. On the other hand, it demonstrates that the present model can be improved in the future. It is believed, however, that an important first step in the right direction has been made.

As an example, the predicted debris flow in function of the distance in the directions perpendicular to the walls of a rectangular concrete magazine with a wall thickness of 50 cm and a charge size of 30 t of TNT is shown in figure 15. Together with corresponding lethality criteria, this type of information will be used in the future in risk analyses for above-ground magazines in Switzerland. That the special dispersal of building material in the case of accidental exposions has to be taken into account with such a model, is demonstrated in figure 16, where measured horizontal debris density contours from the model tests are shown. The crosslike picture of debris density clearly shows that building debris have a considerably larger range than those from the crater. Together with the fact that building debris can have a velocity as much as ten times larger than crater debris and fly almost parallel to the ground, the importance of this explosion effect is even larger than it appears in this figure.

The findings outlined in this paper can be summarized as follows:

1. It has to be distinguished between the debris dispersal of the *crater material* and the *building*.

2. The dispersal of the crater material has a *"rain-type" characteristic*. It therefore can be measured in terms of *horizontal debris density*.

3. The model for prediction of debris density from the ejected crater material should be *physically consistent* and satisfy the condition of mass conservation. The observed discrepancies have to be investigated.

4. The dispersal of building material has a "bullet type" characteristic. It therefore should be measured in terms of *vertical debris flow.*

5. The directions of the projected building debris is *predetermined* by the *type of the construction* (ductile-brittle), *the strength* and by the *form of a building.*

6. A *first step* for a *model to predict debris flow* has been presented. Improvements and additional tests are necessary to account for the observed discrepancies.

7. Due to the flat trajectories of building debris, the higher velocities and the larger ranges, these explosion effects often represent the *predominant hazard.*

REFERENCES

(1) Basler & Hofmann AG:
"Splitter & Trümmerwirkung bei Explosionen: Literaturübersicht"
TM 555.2-44, August 1978
(Literature on Fragment and Debris Effects from Explosions)

(2) Basler & Hofmann AG:
"Grösse und Auswurfmasse von Kratern in Lockergestein bei Oberflächen-explosionen"
B 555.2-50, April 1979
(Dimensions and Ejecta Mass of Craters in Soil from Surface Explosions)

(3) Basler & Hofmann AG:
"Trümmermassendichte und maximale Trümmerflugweite beim Krater-auswurf"
B 555.2-56, Januar 1980
(Debris Density and Maximum Debris Range of Crater Ejecta)

(4) Basler & Hofmann AG:
"Modellversuche für oberirdische Explosivstoffmagazine"
Teil 1: "Konzeption und Durchführung"
Teil 2: "Versuchsdaten und Fotodokumentation
Teil 3: "Auswertung und Resultate"
B 952-4, März 1980
(Model Tests for above-ground Explosives Magazines)

(5) Eidg. Militärdepartement:
"Technische Vorschriften für die Lagerung von Munition (TLM 75)"
Teil 2: "Grundlagen für die Sicherheitsbeurteilung von Munitions-anlagen"
(Swiss Regulations on the Safety Assessment of Ammunition Storage Magazines)

(6) E.B. Ahlers:
"Debris Hazards - A Fundamental Study"
Report DASA - 1362 for US Defense Atomic Support Agency,
IIT Research Institute, Chicago, USA, 1963

(7) A.D. Rooke, Jr., B.L. Carnes, L.K. Davis:
"Cratering by Explosions: A Compendium and an Analysis"
Report N-74-1, US Army Engineer Waterways Experiment Station
Vicksburg, Miss. USA, Jan 1974

(8) M.M. Swisdak:
"Explosion Effects and Properties, Part I: Explosions in Air"
White Oak Laboratory, Silver Spring, Maryland, USA, Oct. 1975

(9) "Manual on NATO Safety Principles for the Storage of Ammunition and Explosives"
Appendix 4, Working Draft, April 1978

(19) "Hazards of Chemical Rockets and Propellants Handbook"
Volume I, AD-889763
Chemical Propulsion Information Agency
The John Hopkins University, Silver Spring
Maryland, USA, May 1972

Additional references are listed in the report (1) - (4)

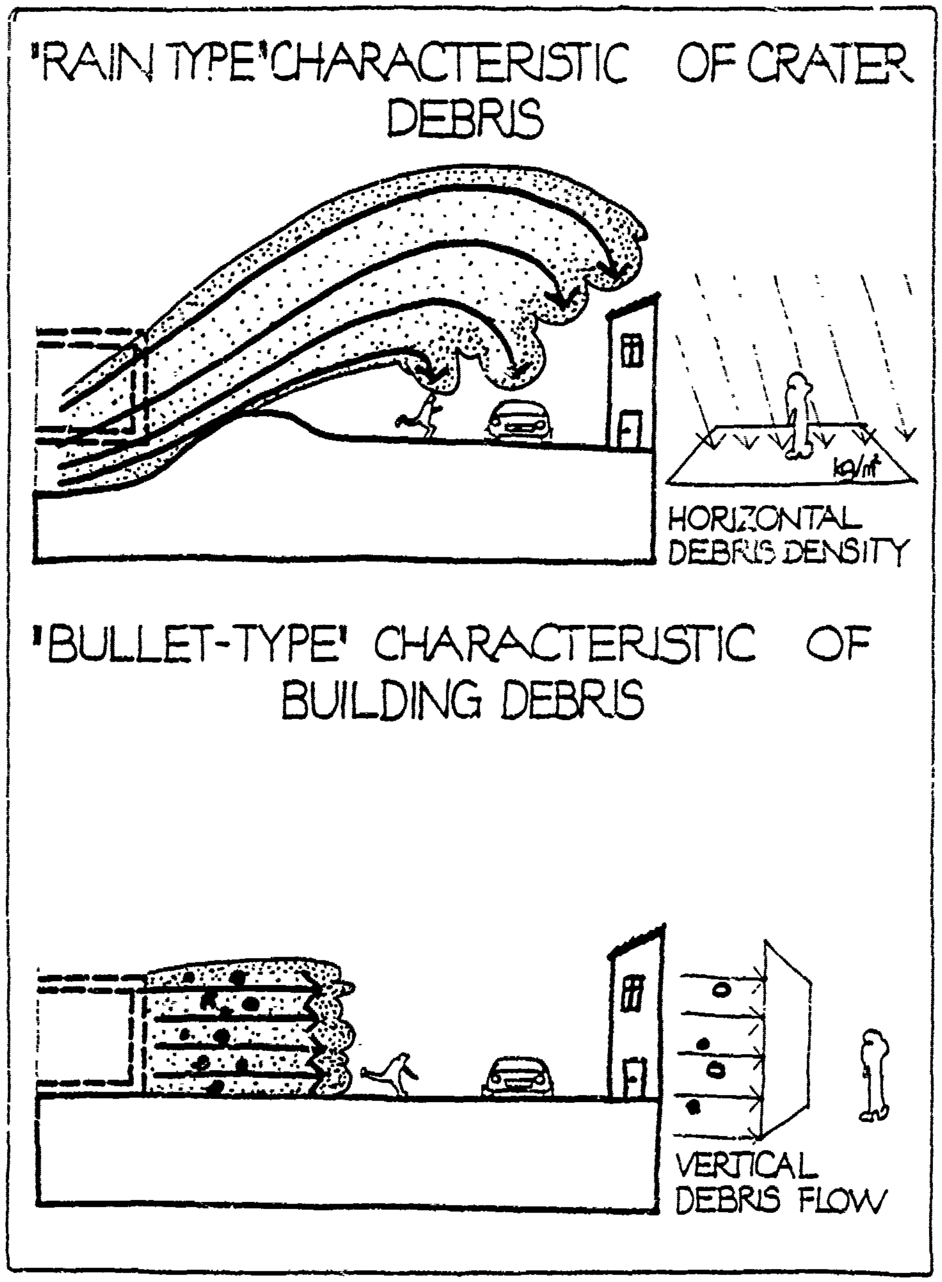

Figure 1: The two types of debris hazards from explosions in above-ground magazines

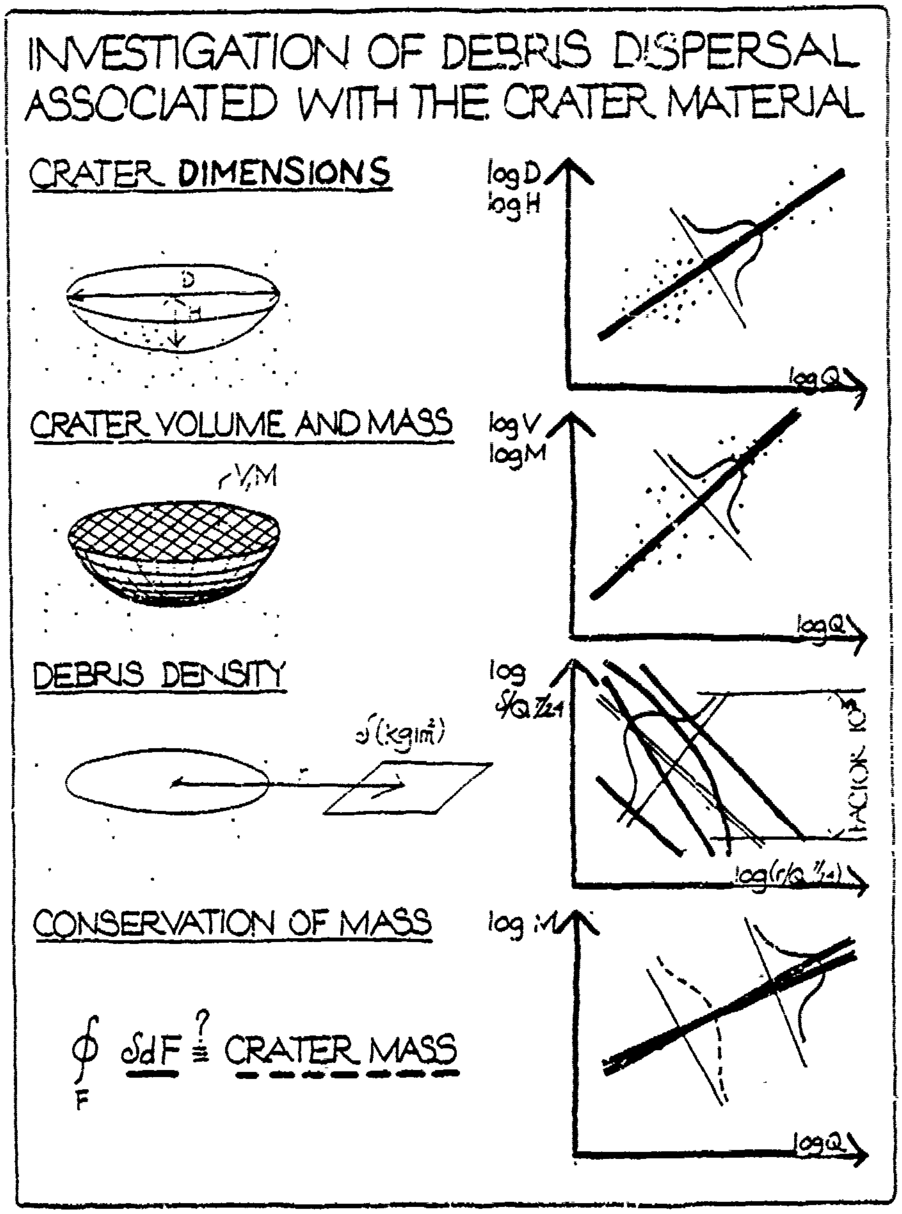

Figure 2: General approach for the investigation of debris dispersal of crater material

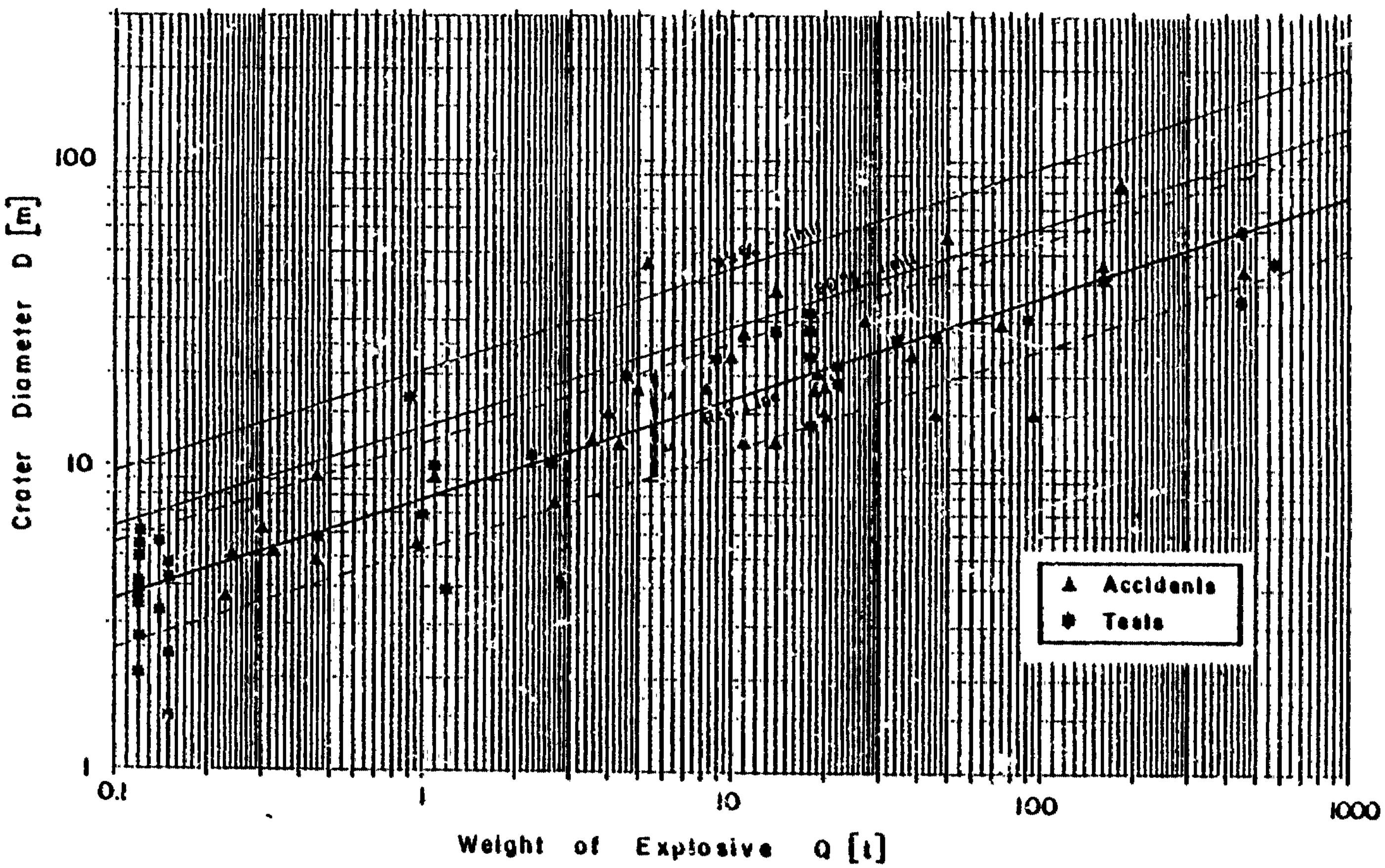

Figure 3: Crater Diameter versus weight of Explosive: Data points and regression line

$D(m) = 7.8 \cdot Q(t)^{0.33}$

Standard deviation of Gaussian distribution $\sigma = 0.18$

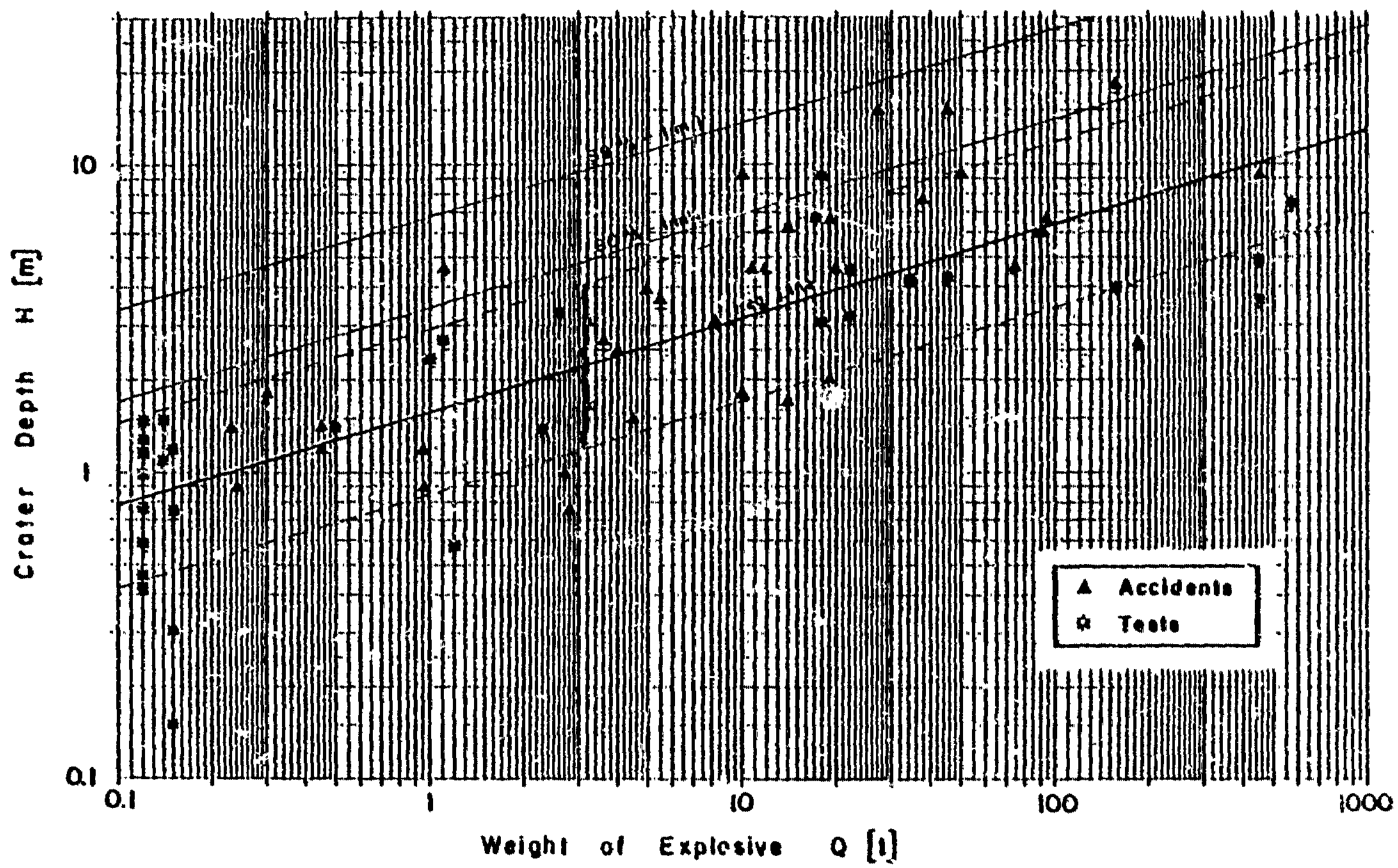

Figure 4: Apparent crater depth versus weight of Explosive: Data points and regression line

$H(m) = 1.6 \cdot Q(t)^{0.30}$

Standard deviation of Gaussian distribution σ = 0.27

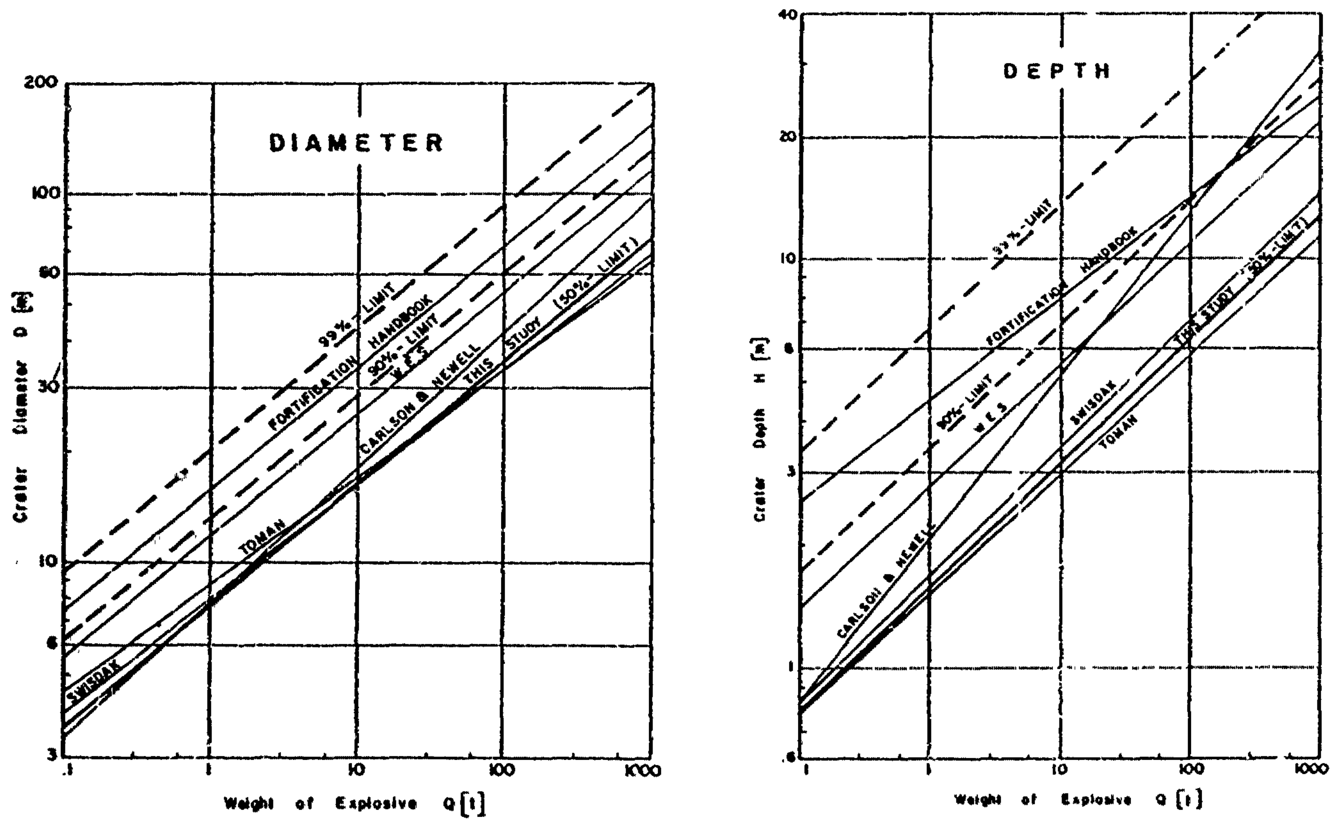

Figure 5: Comparison of crater dimension relationships with existing formulae from the literature

(Sources see next page)

No.	Reference	Crater Diameter *)	Crater Depth *)	Remarks
1	"Cratering from H.E. Charges, Analysis of Crater Data" Techn. Report No. 2-547 US Army Waterways Experiment Station, Vicksburg, Miss., USA (1961)	$D = 3.0 \cdot Q^{1/3}$ (ft, lb) equivalent to $D = 12 \cdot Q^{0.33}$ (m, t)	$H = 0.9 \cdot Q^{0.3}$ (ft, lb) $H = 2.8 \cdot Q^{0.3}$ (m, t)	Factors 3.0 and 0.9 are mean values of four soil type categories (No. 1 - 4)
2	"Handbook i Fortifikasjon, Vapenwirkninger" (Fortification Handbook), Oslo (1964)	$D = 1.6 \cdot Q^{1/3}$ (m, kg) equivalent to $D = 16 \cdot Q^{0.33}$ (m, t)	$H = 0.8 \cdot Q^{1/4}$ (m, kg) $H = 4.5 \cdot Q^{0.25}$ (m, t)	Factors 1.6 and 0.8 are mean values for dry and saturated soil. Relationships also used in "Manual on NATO Safety Principles for Storage of Ammunition and explosives", Part II (1976)
3	J. Toman: "Summary of Results of Cratering Experiments" Lawrence Radiation Laboratory, Livermore, Cal., USA (1969)	$D = 67 \cdot Q^{1/3.4}$ (m, kt) equivalent to $D = 8.3 \cdot Q^{0.295}$ (m, t)	$H = 11.5 \cdot Q^{1/3.4}$ (m, kt) $H = 1.5 \cdot Q^{0.295}$ (m, t)	Alluvium soil conditions
4	R. Carlson, R. Newell: "Ejecta from Single-Charge Cratering Explosions", Vol. I Sandia Laboratories, Albuquerque, New Mexico, USA (1970)	$D = 1.5 \cdot Q^{0.37}$ (ft, lb) equivalent to $D = 7.9 \cdot Q^{0.37}$ (m, t)	$H = 0.31 \cdot Q^{0.40}$ (ft, lb) $H = 2.1 \cdot Q^{0.40}$ (m, t)	Playa soil conditions
5	M.M. Swisdak: "Explosion Effects and Properties", Part I, White Oak Laboratory, Silver Spring, Maryland, USA (1975)	$D = 2.4 \cdot Q^{5/16}$ (ft, lb) equivalent to $D = 8.0 \cdot Q^{0.31}$ (m, t)	$H = 0.50 \cdot Q^{5/16}$ (ft, lb) $H = 1.7 \cdot Q^{0.31}$ (m, t)	Factors 2.4 and 0.50 are mean values for alluvium, sand and playa soil conditions

*) First relationship: quoted from reference
Second relationship: converted to metric system

Figure 5 continued: Selected crater dimension relationships from the literature

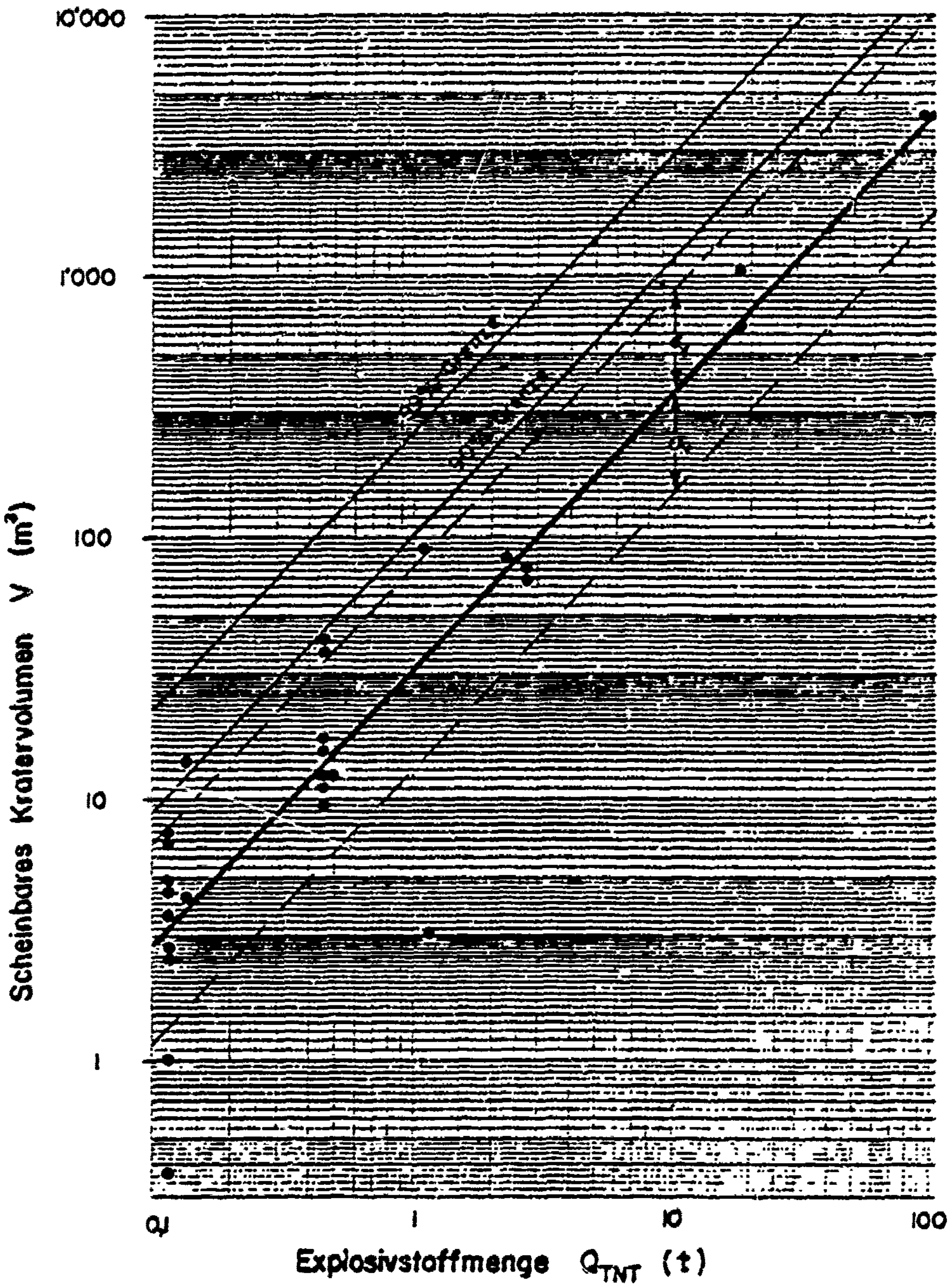

Figure 6: Apparent crater volume versus weight of explosive
$V(m^3) = 32 \cdot Q(t)^{1.06}$
Standard deviation of Gaussian distribution $\sigma = 2.4$

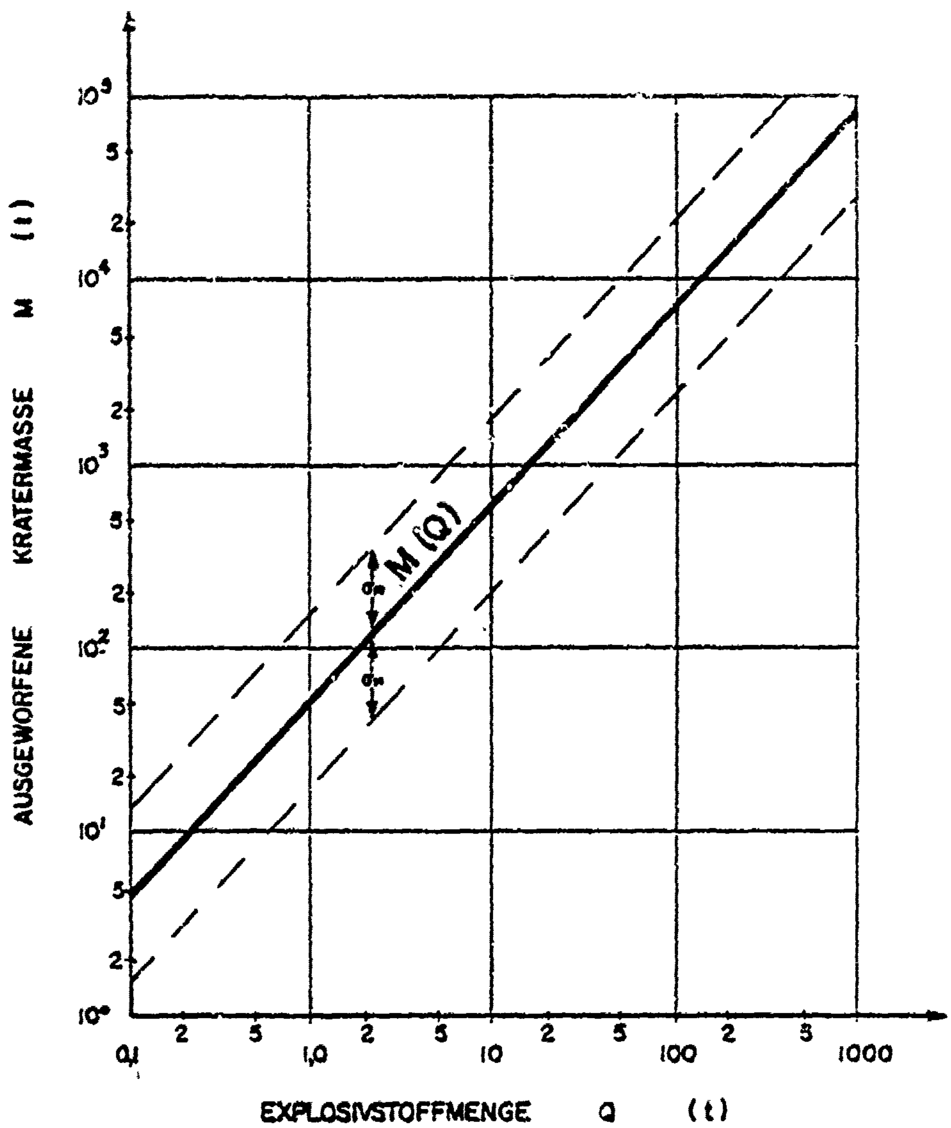

Figure 7: Total ejected mass versus weight of explosive

$M(t) = 51 \cdot Q(t)^{1.06}$

Standard deviation of Gaussian distribution $\sigma = 2.4$

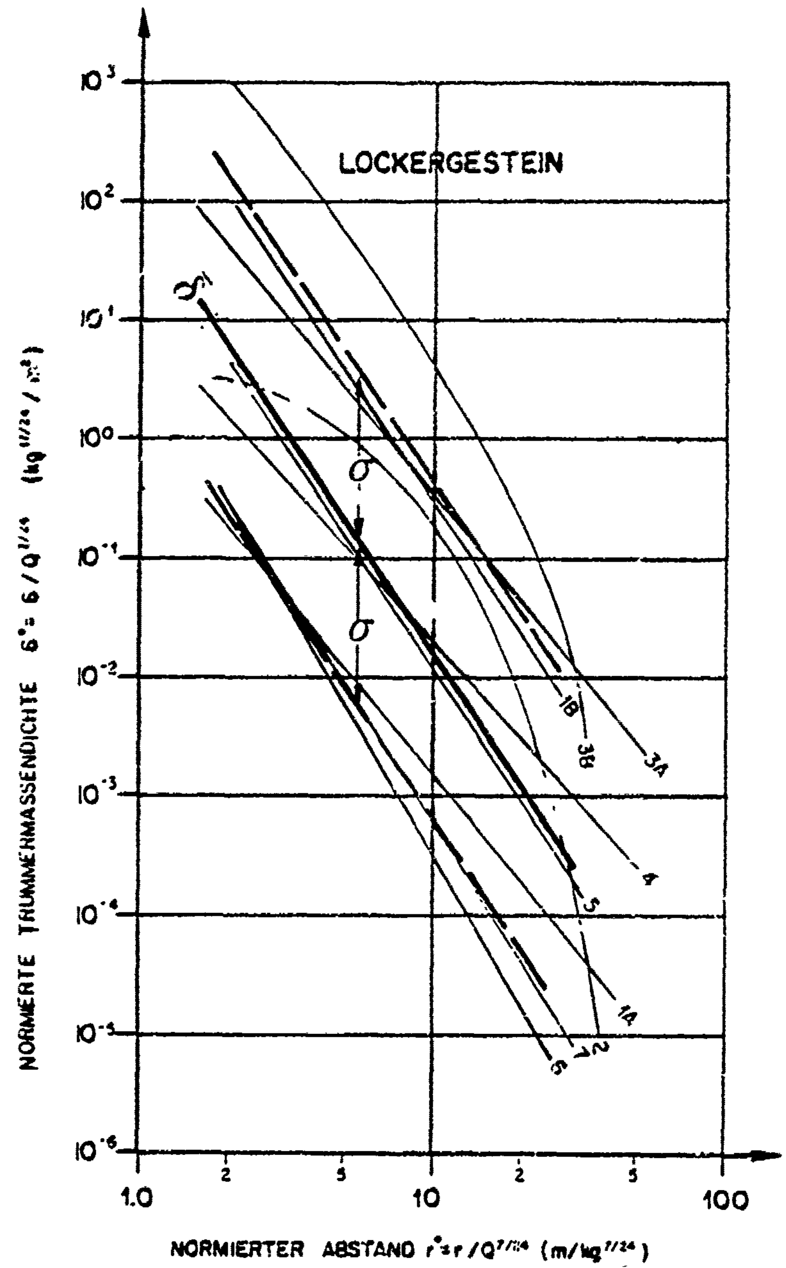

Figure 8: Relationships for crater material dispersal taken from the literature (see following page for sources) for surface explosions on soil

Mean relationship $\overline{\delta}_L$:

$$\overline{\delta}_L(\mathrm{kg/m^2}) = 27 \cdot Q(\mathrm{kg})^{1.4} \cdot r(\mathrm{m})^{-3.6}$$

Standard deviation $\sigma_L = 26$

Nr.	Analytische Beziehung: Originalform	Analytische Beziehung: in SI-Einheiten: kg/m², kg, m	Gültigkeitsbereich	Literaturquelle
1A 1B	$\delta(Q,r) = k \cdot r^{-n} \cdot Q^{n-1}$ mit $k = 1,3 \cdot 10^{4}$ (Mittelwert), $n = 2,93$ $k = 1,4 \cdot 10^{5}$ (Mittelwert), $n = 3,65$ in lb/ft², ft, tons	$\delta(Q,r) = 0,0038 \cdot Q^{1,93} \cdot r^{-2,93}$ $\delta(Q,r) = 0,00013 \cdot Q^{2,65} \cdot r^{-3,65}$	$Q < 45$ t $Q > 45$ t	Hazards of Chemical Rockets Handbook [19]
2	$\delta(Q,r) = 2,8 \cdot Q^{0,42} \cdot e^{-0,35} \cdot r \cdot Q^{-0,29}$		$Q > 1$ t	TLM 75/Teil 2 [17]
3A 3B	$\delta(Q,r) = 40 \cdot Q^{1,6} \cdot r^{-3,0}$ $\delta(Q,r) = 7,4 \cdot Q^{1,75} \cdot r^{-2,65} \cdot e^{-0,0073 \cdot r}$		30 kg < Q < 450 kg 4,5 t < Q < 450 t	NATO [18]
4	$\delta(Q = 1000\ \text{lb}, r) = 3,34 \cdot 10^{4} \cdot r^{-2,70}$ in lb/ft², ft	$\delta(r) = 6,6 \cdot 10^{3} \cdot r^{-2,70}$	$Q = 450$ kg	Carlson & Newell [15]
5	$\delta(r) = 2,58 \cdot 10^{8} \cdot r^{-3,65}$ für $Q = 9,1 \cdot 10^{4}$ kg		$Q = 91$ t	Carlson & Jones [16]
6	$\delta(Q = 10^{6}\ \text{lb}, r) = 2,5 \cdot 10^{10} \cdot r^{-4,1}$ in lb/ft², ft	$\delta(r) = 9,6 \cdot 10^{8} \cdot r^{-4,1}$	$Q = 454$ t	Norwegen-Bericht [7]
7	$\delta/\varsigma \cdot V_{a_2}^{-1/3} = 0,047\,(r/r_a)^{-3,88}$ in lb/ft², ft³	$\delta(Q,r) = 0,72 \cdot Q^{1,6} \cdot r^{-3,9}$ (vgl. Annahmen im Text)	$3 < r/r_a < 50$	Portrayal of Ejecta [9]

Figure 8 continued: Selected relationships on debris dispersal

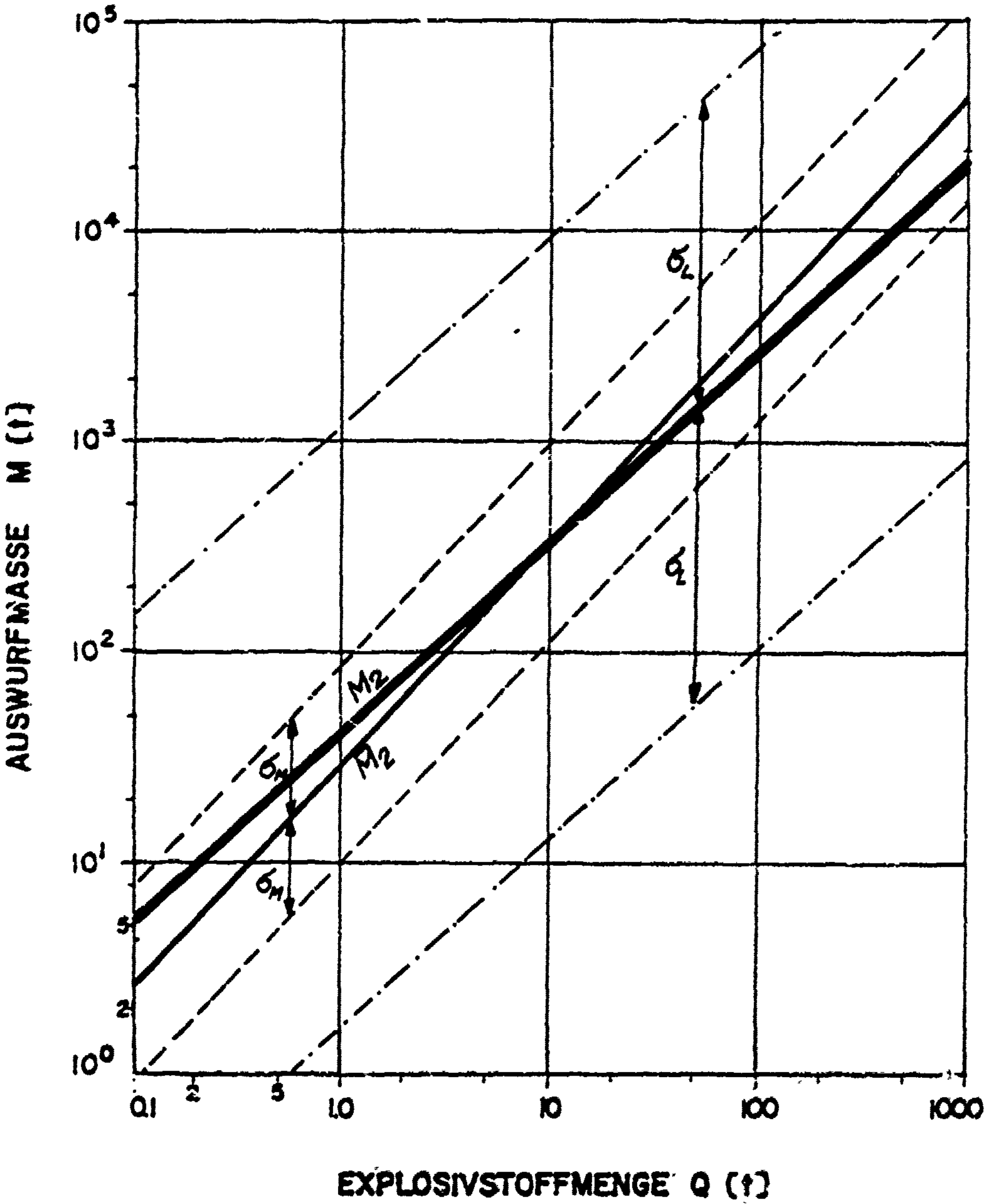

Figure 9: Condition of mass conservation:
Comparison of integrated mean debris density function of figure 8 with crater ejecta function of figure 7:
Integrated debris density function:

$$M_2 = 2\pi \int_{r_0}^{R} \delta_L \cdot r \cdot dr$$

r_0 = 3 · crater radius R = maximum debris range

Ejected mass between r_0 and R $\bar{M}_2 = 0.5 \cdot M_{\text{total ejected mass}}$ (see figure 7)

Note difference in uncertainty!

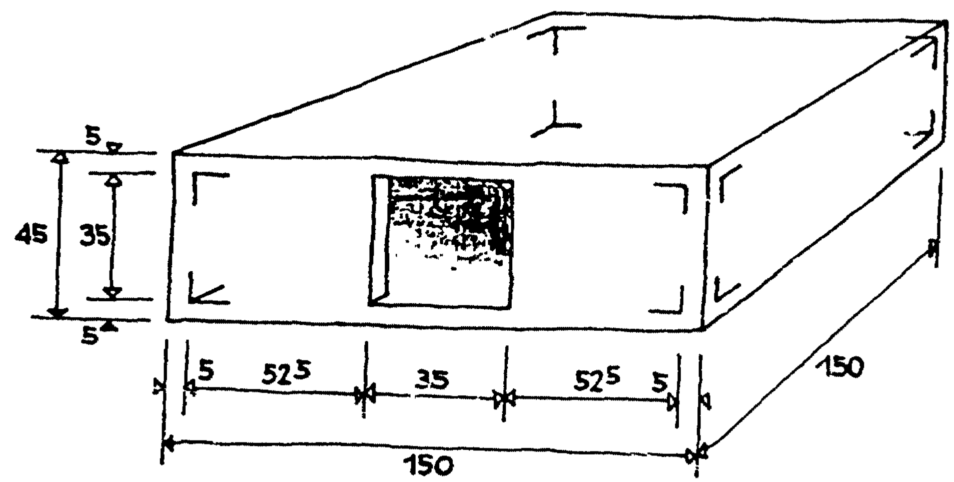

Figure 10: Model test for above ound magazine
Model structure in the scale 1: 10

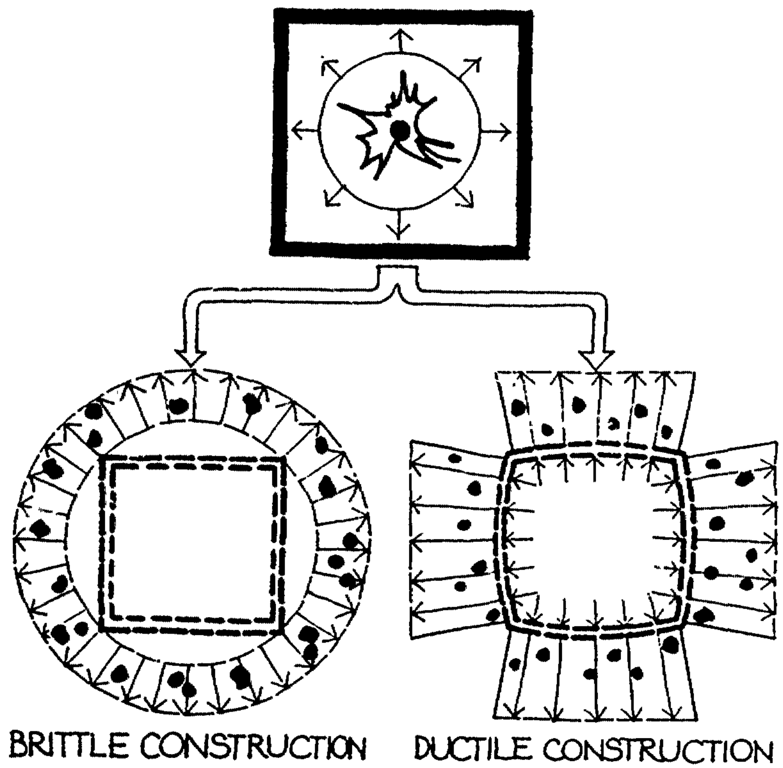

Figure 11: Influence of strength and ductility on direction of building debris

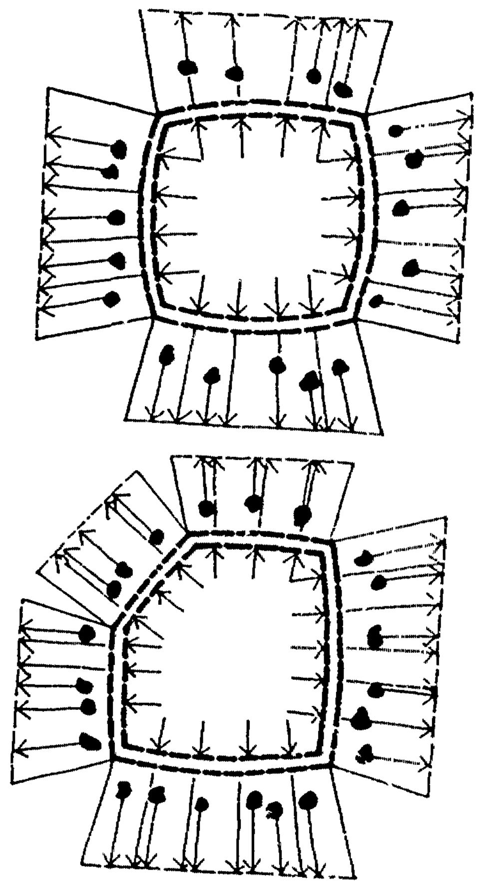

Figure 12: Influence of shape of building with ductile construction on direction of building debris

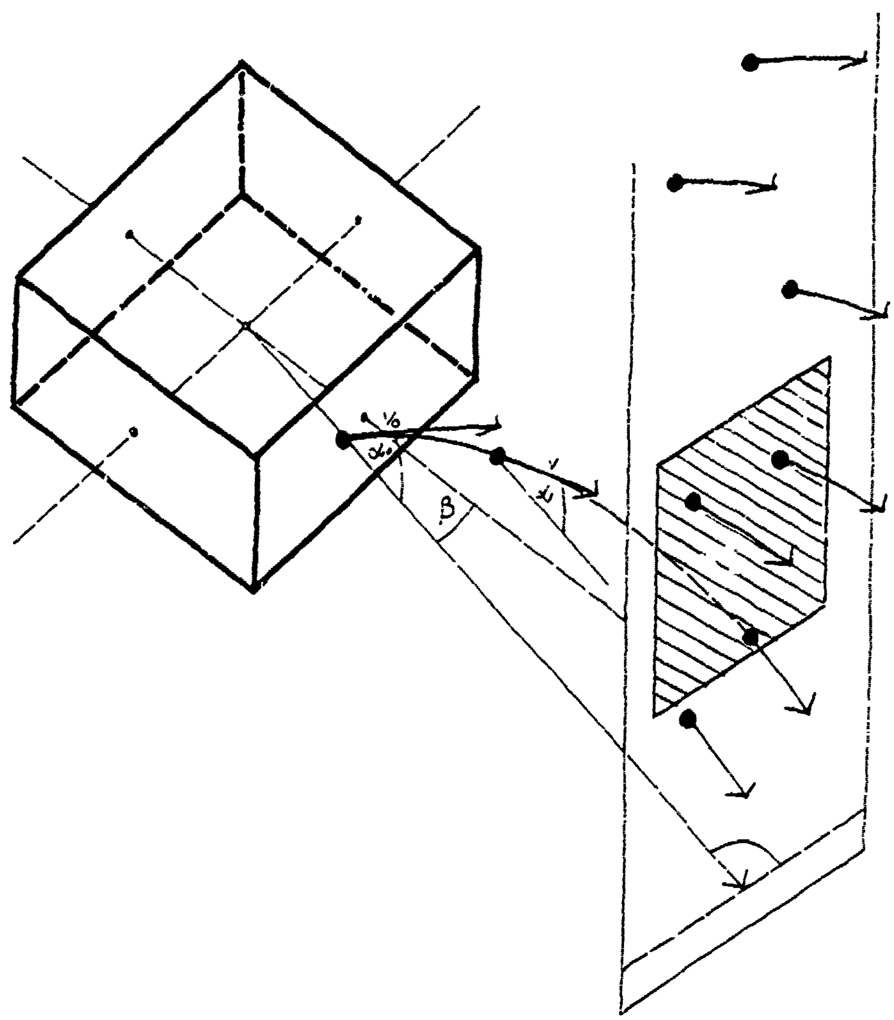

Figure 13: Definition of vertical debris flow and general description of the mathematical model

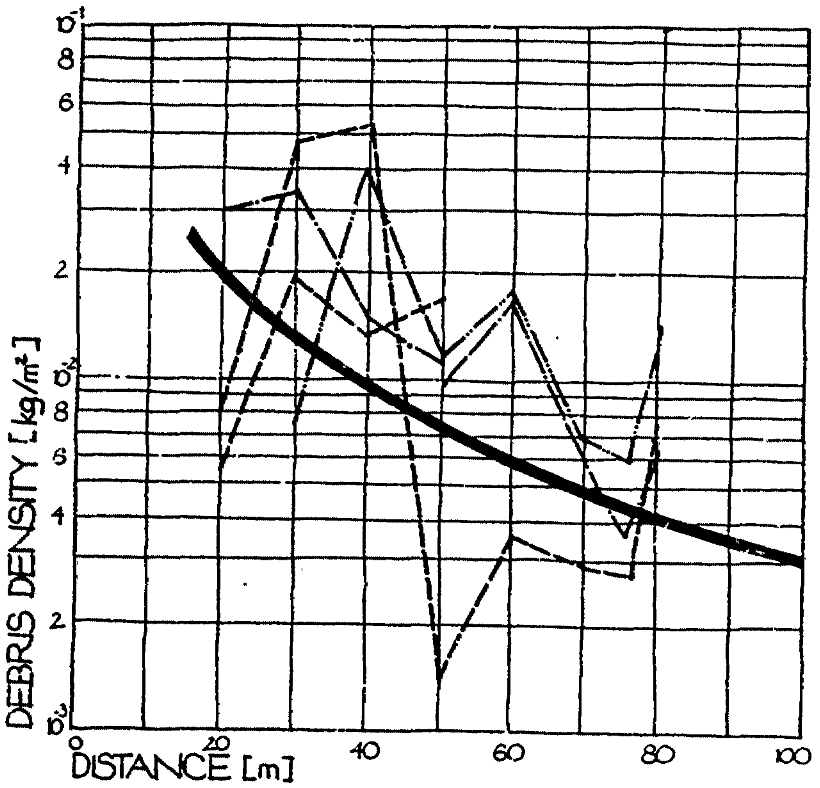

Figure 14: Comparison of measured and computed debris densities for building material (Test data from model tests)

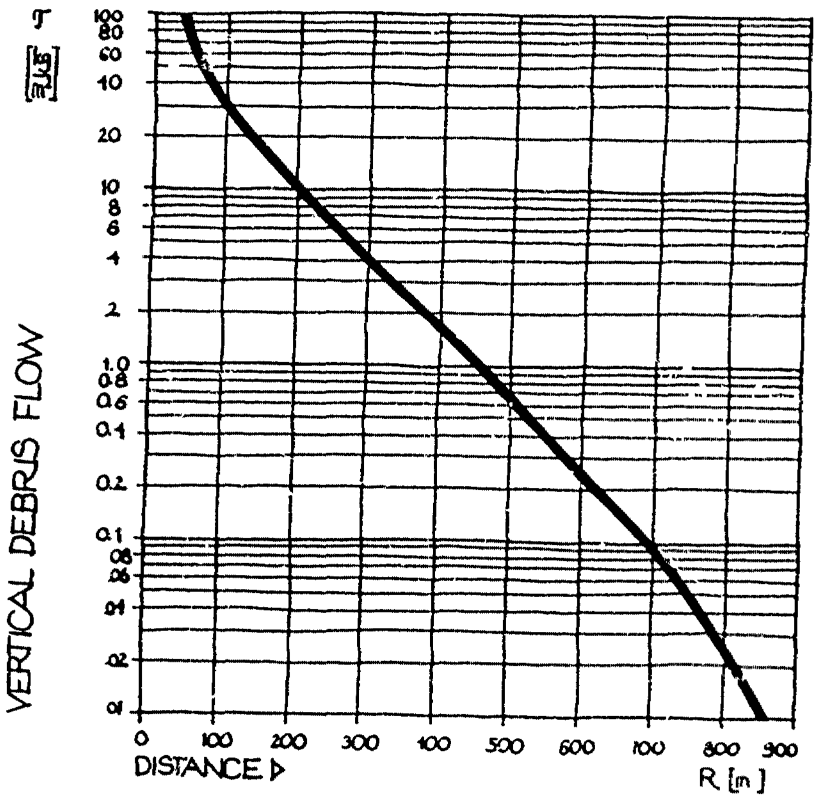

Figure 15: Example of predicted debris flow as a function of distances for an explosion of 30 t of TNT in the directions perpendicular to the side walls of a concrete magazine

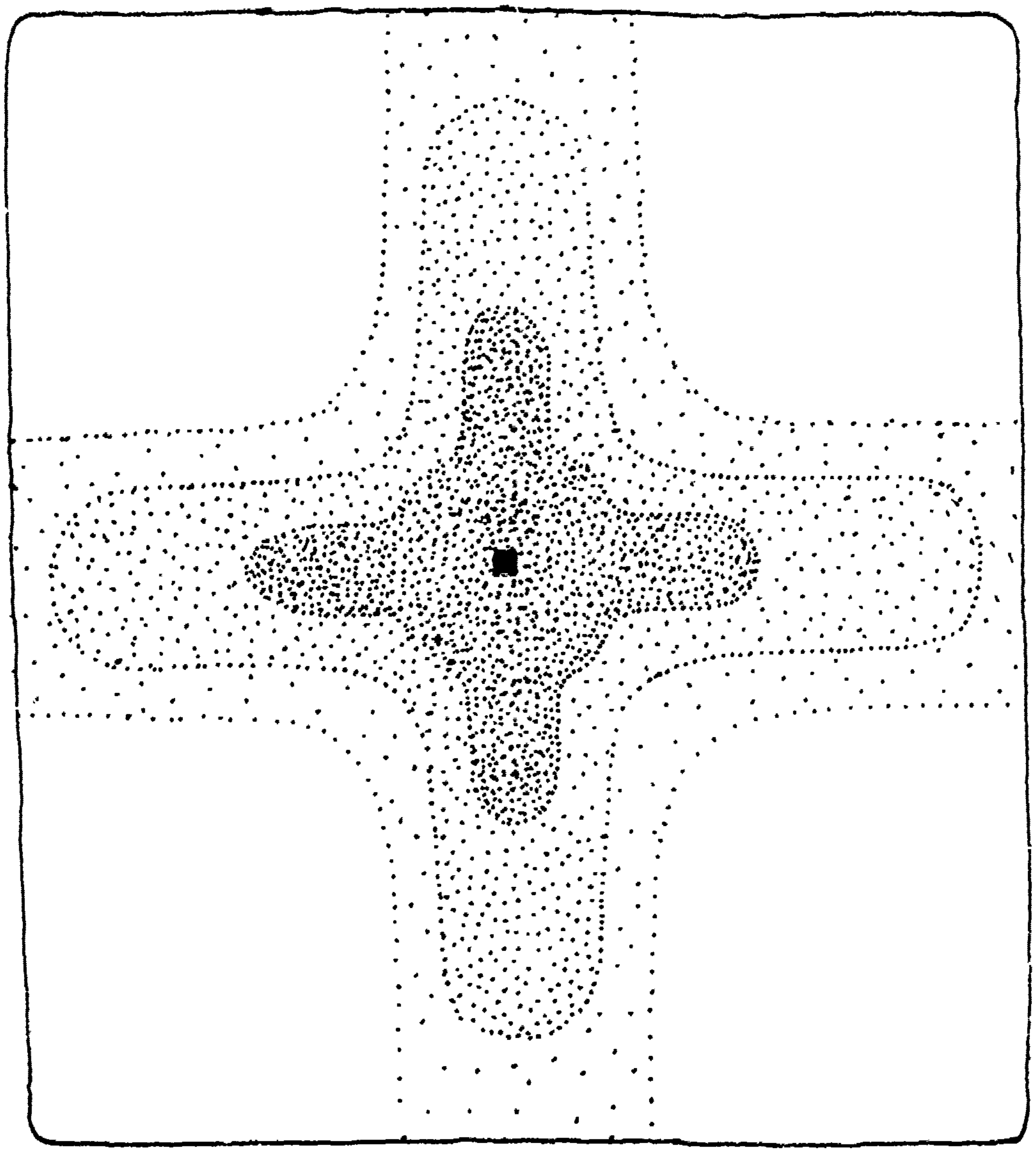

Figure 16: Schematic picture of measured debris density of building and crater material during model tests

Note: Larger range of building debris in predetermined directions

PREDICTION OF DEBRIS WEIGHT AND RANGE DISTRIBUTIONS
FROM ACCIDENTAL EXPLOSIONS INSIDE BUILDINGS

by

James J. Kulesz
Patricia K. Moseley
Van B. Parr

ABSTRACT

This paper describes a method for predicting fragment impact weight and range distributions resulting from accidental explosions inside buildings. A thorough fragment data base was created from a literature search through the available files at the DDESB for accident reports containing fragmentation data from accidental explosions in buildings. Similitude theory was used to group and plot the data in a meaningful fashion and a statistical analysis was performed on fragment weight, range, nondimensional range (by area) and distributions. Based on this statistical measure, there were adequate grounds for not rejecting any of the hypotheses that the data sets belong to the appropriate chosen distributions. Once one knows the energy of the explosive involved and calculates the total weight of the building destroyed, one can use the graphs to estimate a fragment missile map in terms of fragment weight and range. This information can then be used to estimate fragment safety requirements without conducting expensive experiments.

I. INTRODUCTION

The analysis described in this paper was funded by the Department of the Army on Contract No. DACA87-79-C-0091 entitled "Preparation of a Manual for Prediction of Blast and Fragment Loadings on Structures."[1] This paper describes a portion of this manual which contains a set of predictive curves in which an architect-engineer can analytically generate a post-accident missile map resulting from an explosion inside a building. The sections which follow contain a similitude analysis for developing a suitable means of ordering the data, a description of the accident data used in the analysis, the fragment weight and range prediction model, and the conclusions.

II. SIMILITUDE ANALYSIS

When performing a model analysis, one generally lists all of the parameters which in some way could affect the problem and develops a complete set of nondimensional pi terms[2]. After a complete set of pi terms is formed, one eliminates terms which are invariant or can be derived by other pi terms through known physical interrelationships. In this study described by this paper, data were acquired from reports describing debris which was accumulated after accidental explosions. Thus, the amount of data gathered in the form of a detailed missile map is very limited. Because of this, we elected to make the model analysis as simple as possible and confine it to parameters for which information from the accident reports was available.

Table 1 contains a list of parameters which could be acquired from some of the accident reports and which is germane to the problem. Notice that the initial velocity and trajectory angle of the fragment have not been included since these parameters could not be determined for individual fragments from the accident data. The information which could be acquired from the accident reports was the type of building; an estimate of the energy E of the explosion; weight W of the fragments collected; in some cases, an estimate of the average area A of the fragments; range R traveled by the fragments; and, for nondimensionalizing the analysis, the gravity constant g which is assumed to be invariant.

Table 2 contains two nondimensional terms which were formed from the parameters listed in Table 1. The first pi term states that, for two scaled explosions in buildings, the ratio of the range divided by the square root of the area for fragments from the one explosion should be similar for the other scaled explosion. The second pi term states that the product of the range and weight of a fragment divided by the energy of the explosion should be similar for different scaled explosions.

Table 1. Parameters for Debris Mass and Range Analysis

Symbol	Parameter	Dimension
E	Energy of Explosion	FL
M	Mass of Fragment*	FT^2L^{-1}
A	Average Presented Area of Fragment	L^2
R	Range of Fragment	L
g	Gravity Constant	LT^{-2}

*Note that weight is the product of the mass and gravity constant. That is, $W = Mg$

Table 2. Nondimensional Relationships for Debris Mass and Range Analysis

$\pi_1 = \frac{R}{\sqrt{A}}$	nondimensional range
$\pi_2 = \frac{RMg}{E}$	nondimensional energy

III. ACCIDENT DATA

A thorough fragment data base was created from a literature search through the available files at the Department of Defense Explosive Safety Board for accident reports containing fragmentation data from accidental explosions in structures such as those at the Pantex Plant in Amarillo, Texas. Extracted data include characteristics of the explosion source, building descriptions and characteristics of fragments, such as weight, size and range. Those references which had the most useful information were selected as a data base and were separated into three groups by estimated energy of the explosion or explosive yield. Tables 3, 4 and 5 summarize the explosion source and building characteristics for seven references in the data base. These were the only references out of several hundred references examined which contained all of the information which we feel was absolutely necessary. The one reference in Table 3 consisted of an explosion with an estimated energy of approximately 1.6×10^7 ft lb. The explosions depicted in Table 4 had explosive energies on the order of 5×10^8 ft lb. Table 5 contains data from three sources with energies of approximately 1×10^{10} ft lb. Fragment characteristics for each group were extracted from associate missile maps or calculated from descriptions given in the references. The reader should note that all buildings, except one, were made primarily of concrete.

IV. PREDICTION MODEL

Statistical analyses were performed on fragment weight, range, nondimensionalized range (by area) and nondimensionalized energy. These useful relationships allow one to predict fragment distributions in weight and range following an accidental explosion of a given energy in a building similar to those buildings described in this data base. A discussion of the statistical analyses performed to determine impact weight, range, and size distributions is given below. This is followed by a procedure for using the graphs presented to estimate fragment mass and range for similar explosions.

The fragment weight and range data for each of the energy levels were sorted in ascending order. The total numbers of fragments for all of the accidental explosions in each energy level were counted. The ordered data (by weight and range) for explosions from each energy level were then divided into groups containing five percent of the total number of fragments. Thus, the data were subdivided into groups from the 5th to the 95th percentile by number of fragments as shown in Table 6. For example (see Table 6), for those explosions having an energy of 1.6×10^7 ft-lb, five percent of the fragments had a weight below 0.22 lb, 10 percent below 0.58 lb, 15 percent below 0.87 lb, etc. Also, five percent of the fragments were in the 0.22-0.58 lb range, five percent in the 0.58-0.87 lb range, etc.

Table 3. Accident Data Base for Explosion Energy of 1.6×10^7 ft-lb_f

	EXPLOSION SOURCE					BUILDING CHARACTERISTICS			
Reference	Material	Quantity (lb)	Shape	Orientation to Bldg	Estimated Energy (ft·lb)	Shape	Dimensions	Volume (ft^3)	Construction/Material
Explosion in Nitration Bldg 3045 Radford Army Ammution Plant, VA 11-02-78	Nitrocellulose (Nc)	$\geq$ 10 lb for resultant damages to have occurred analysis concluded 10.81 lb	slurry	On second floor of Bldg 3045 in feeder to centrifuge	1.6×10^7	4 story rectangular	36 ft x 72 ft x 33 ft high (11 ft between floors)	$\approx$ 28,512 ft^3 per floor; however, an opening was provided in third floor above centrifuges up to fourth so volume of third floor is increased to include fourth; volume of system involved = 995ft^3.	Steel frame with reinforced concrete slab floors, separated by steel I-section columns; brick masonry end-walls; acrylic plastic glazed side walls (unbarricaded); dimensions of bricks in end walls: inner course-2 1/2 in. x 3 7/16 in. x 7 3/4 in. outer - 2 1/2 in. x 3 5/8 in. x 8 in.

Table 4. Accident Data Base for Explosion Energies Around 5 x 10^8 ft-lb_f

	Explosion Source					Building Characteristics			
Reference	Material	Quantity (lb)	Shape	Orientation to Bldg	Estimated Energy (ft·lb)	Shape	Dimensions	Volume (ft^3)	Construction/Material
Bacchus Plant Accident Report WA No. 112, Contract AF 04(647)-243, Hercules Powder Company Magna, Utah. 10-05-61	Rocket propellant slurry mix (VCA)	350.0	Slurry		5.2 x 10^8	Rectangular			3 Sides-12 in. Reinforced Concrete 1 Side - Wood Frame; Wood Floors; Asbestos Shingle Roof; no Fire Walls or Doors; 3 Concrete Sides Backed up With Earth Mound. Front Protected by a 12 in. Sand Filled, Wood Constructed Bullet Shield.
Hercules Powder Company, Virginia Explosion in Bldg 3560, Block Breaker C-line Area. 02-11-63	Nitrocellulose for M-5 Formulation	130.0 in equipment; 440.0 in buggy	Blocks of nitrocellulose to be mechanically broken down	Inside, (fairly centered)	8.4 x 10^8	Box-Like	15.6 ft x 15.6 ft; Height not Given; Long Porch on Front.		Wood Frame on Concrete Foundation; Asbestos Shingle Roof
Explosion at Pantex Plant, Amarillo, Texas 03-30-77 (Two Detonations of Two Different H.E. Explosives)	LX-09 LX-14	76.0 75.0 151.0 Total	Rough Billets to be Machined	Within Bay 8 Along South Wall of Bldg 11-14A	3.4 x 10^8	One-Story Rectangular	151 ft x 63 ft x 18 ft High	171,234	Concrete Cavity-Wall Type Block; Interior Steel Frame Consisted of 4 H.E. Machining Bays, an H.E. Remote Operation Bay, a Remote Control Room, a Metrology Lab Work Area, a Staging and Material Storage Area, and an Office

Table 5. Accident Data Base for Explosive Energies Around 1×10^{10} ft-lb$_f$

	EXPLOSIVE SOURCE					BUILDING CHARACTERISTICS			
Reference	Material	Quantity (lb)	Shape	Orientation to Bldg	Estimated Energy (ft-lb)	Shape	Dimensions	Volume (ft^3)	Construction/Material
Incident at Alleghany Ballistics Lab 04-27-63 (Hercules Powder Company)	(1) Four Polaris A3 Second Stage Fiberglass cased Motors; (2) 90% Nitroglycerin Casting Solvent; (3) High Energy Casting Powder; (4) Scrap Casting Solvent (above); (5) Residual Casting Solvent	(1) 33,500 lb (propellant) (2) 4,800 lb (3) 855 lb (4) 250 lb (5) 30 lb	(1) Four Motors Were in Various Stages of Processing; (2) In two Stainless Steel Desiccators Suspended From Overhead Monorail Beam; (3) In Metal Powder Boxes	(1) Throughout Casting Bay Area in Bldg (one awaiting transfer to pit). (2) In a Room adjacent to Casting Bay and Nearest to Pit Containing One Motor; (3) In room Adjoining Solvent Mentioned in Aspirator Catch Tank	(2) 1.0×10^{10}	Rectangular high bay with smaller rectangular building attached.	High bay: 71 ft x 42 ft x 48 ft high. Smaller building: 32 ft x 42 ft x 20.67 ft high.	170,912	Concrete Block and Wood Frame
Explosion in NG Area No. 2 Radford Army Ammunition Plant, Virginia 01-06-78 (Mainly Bldg 9463 -nitrating house	Nitroglycerin	4,200 lb		Within Bldg 9463	9.3×10^{9}	Rectangular	62.5 ft x 37.5 ft approximated from drawing; height is approximately 15 ft from first floor to ceiling; basement in bldg.		Reinforced Concrete Walls Backed by Earth in Nitration House; Steel Floors; Storage Houses are Light Wood Frame, Brilast Board (Collapsible)
Motor Detonated High Order During Static Testing; Redstone Arsenal, Alabama. 08-19-59 Bldg 7857	One Nike Zebls Sustainer Motor	6891 lb of Petrin Arylate in Battleship Hardware (loaded weight of motor and nozzle = 10,654 lb)		Within North Bay in Test Stand	1.2×10^{10}	Retangular			18 in. Reinforced Concrete Walls. Barricaded on North and South Walls by 12 in. Reinforced Concrete Further Reinforced by Earth Cover with Minimum Width of 23 ft and Minimum Depth of 3 ft; Roof was 18 in. Reinforced Concrete Slab Over Test Bays

Table 6.

Cumulative Percentiles for Plotting Fragment Weights and Ranges

	$E = 1.6 \times 10^{7}$ ft-lb		$E = 5.0 \times 10^{8}$ ft-lb		$E = 1.0 \times 10^{10}$ ft-lb	
Percentile	Weight (lb)	Range (ft)	Weight (lb)	Range (ft)	Weight (lb)	Range (ft)
5	0.22	6	0.20	44	0.054	218
10	0.58	7	0.40	58	0.082	270
15	0.87	9	0.65	70	0.120	325
20	1.02	11	0.88	89	0.160	375
25	2.18	11	1.20	103	0.220	410
30	2.61	11	1.68	113	0.300	460
35	3.92	11	2.26	118	0.410	496
40	4.35	11	2.72	125	0.490	532
45	5.22	12	3.65	132	0.650	566
50	7.61	14	4.90	141	0.870	616
55	8.70	16	6.72	147	1.260	672
60	10.44	19	9.08	159	1.520	710
65	11.55	24	10.50	170	2.000	780
70	15.37	28	13.08	180	2.670	832
75	24.36	32	21.90	193	4.200	920
80	31.32	46	29.58	207	5.440	1000
85	50.20	52	45.48	233	10.000	1080
90	104.40	77	84.00	266	16.320	1218
95	187.90	146	172.10	324	50.000	1485

Figures 1 and 2 are plots of the percentile points along with an "eyeball" line fit to the points. The mean was estimated as the logarithm (to the base e) of the 50th percentile. The standard deviation was estimated [3] as two-fifths of the difference between the logarithms of the 90th and 10th percentiles.

Table 7 is a listing of the estimated means and standard deviations for the log normal (to the base e) distributions. A "W" statistic [3] for goodness of fit was calculated for each of the distributions. The approximate probability of obtaining the calculated test statistic, given that the chosen distribution is correct, was then determined. These results are also shown in Table 7. Figure 3 is a graph of the probability percentage points of the "W" statistic. As it is customary to consider values of probability for the "W" statistic exceeding 2 to 10 percent as adequate grounds for not rejecting the hypothesis that the data belong to the chosen distribution, the fits for all data except the range data for an energy of 1.6×10^7 ft-lb are much more than adequate. The "W" statistic for ranges in that energy level is slightly less than 10 percent and thus, is still adequate.

Figure 1 can be used to estimate the percentage of fragments (for a given energy level) which will have a weight W_i, equal to or less than a particular W_i. For example, if we wished to estimate the percentage of fragments which would have a weight equal to or less than 10 lb for an energy level of 1.0×10^{10} ft-lb, we would refer to Figure 1 and on the weight axis (abcissa) at 10 lb go upward to the intersection of the line for 1.0×10^{10} ft-lb. Then, at the intersection point read the value from the ordinate, which is 86 percent. Conversely, if we wanted to estimate what weight 90 percent of the fragments would not exceed, we would enter the chart on the 90 percent line, go over to the intersection with the curve and read downward to the weight axis the value 16 lb. Estimates for percentage of fragments between two weights can be made by determining the difference between corresponding percentage points. Figure 2 can be used in the same manner for the range.

Table 8 contains a listing for the percentiles for nondimensional range ($\overline{R}$) and nondimensional energy ($\overline{E}$), respectively. Table 9 contains the estimated means, standard deviations, "W" statistics and "W" statistic probabilities for the data presented in Figures 4 and 5. One can readily observe that the "W" statistic probabilities in all of the cases shown in Table 9 greatly exceed the 2 to 10 percent criterion (see above) for not rejecting the hypothesis that the data belong to the chosen distribution. Thus, the log normal distributions shown in Figures 4 and 5 adequately describe the functional format of the data. One would expect this to be the case since one can readily observe that the data points plotted on the figure fall near the plotted lines for all of the data.

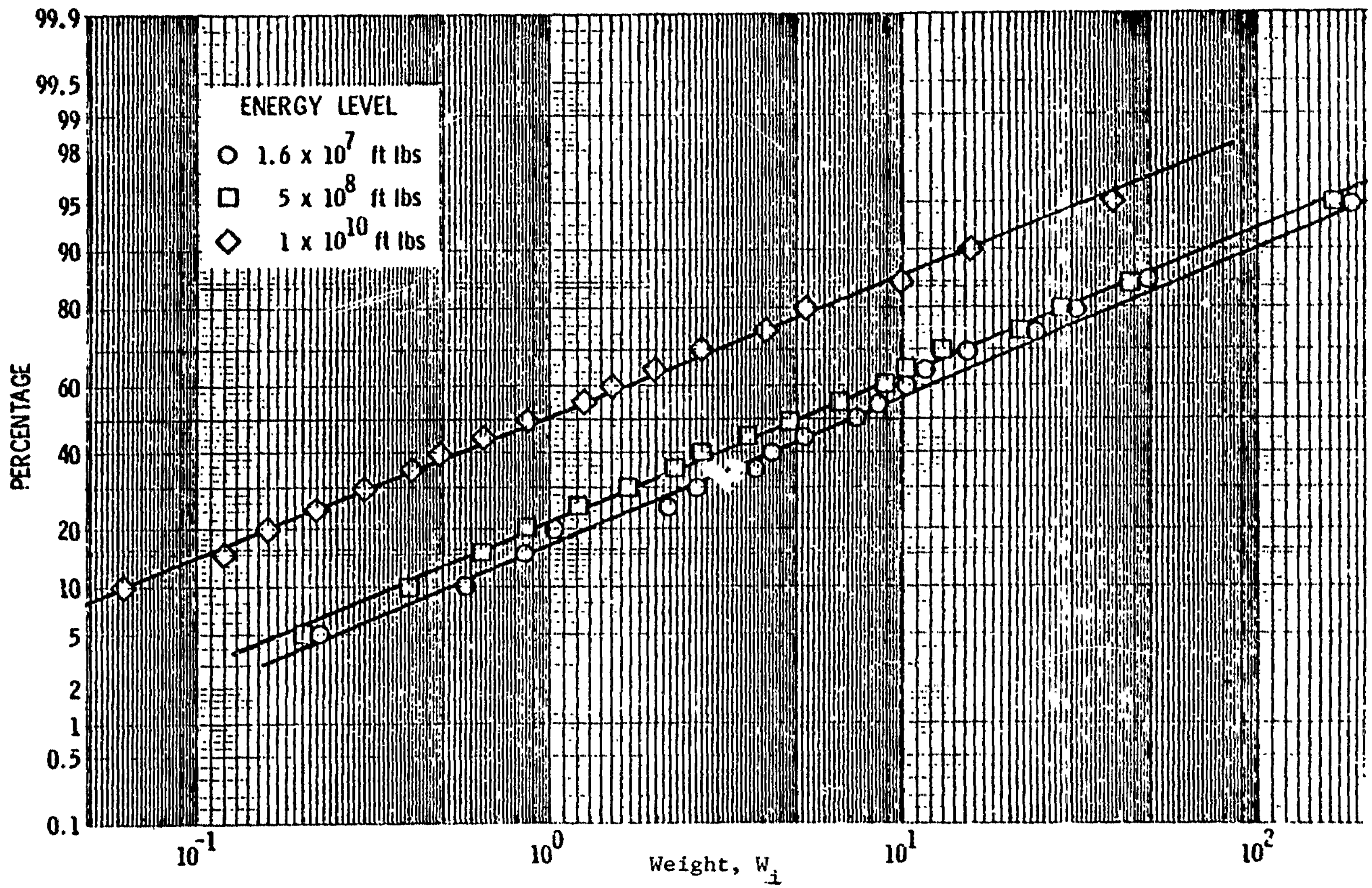

Figure 1. Cumulative Probability Distribution, Fragment Weight (lb)

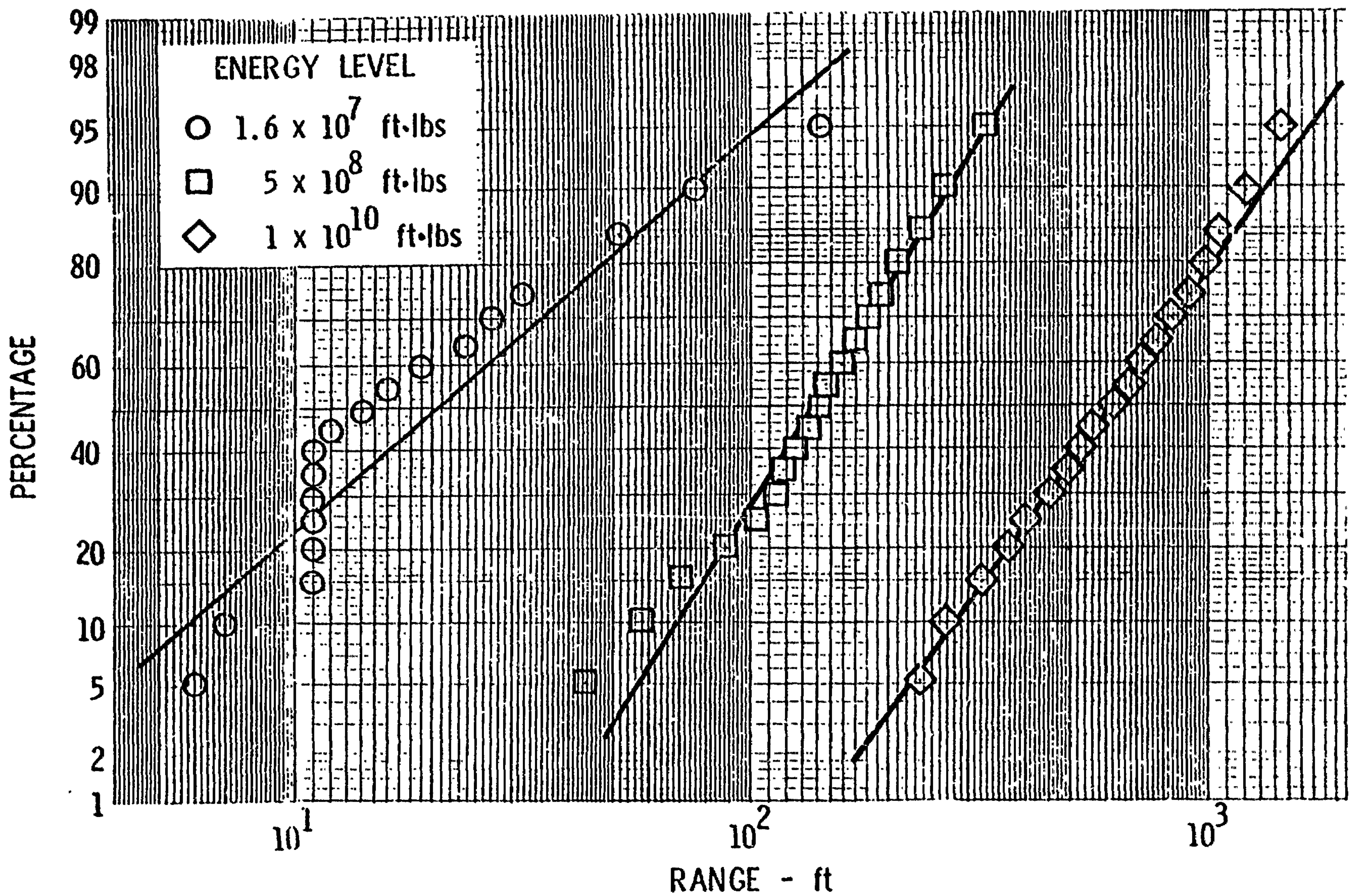

Figure 2. Cumulative Probability Distribution, Fragment Range (ft)

Table 7.

Listing of Estimated Means, Standard Deviations, and "W" Statistics for Log-Normal Distributions for Weights and Ranges of Fragments

Weight*

Energy Level (ft-lb)	Estimated Mean	Estimated Standard Deviation	"W" Statistic	Probability
1.6×10^{7}	1.94	2.11	0.992	0.999
5.0×10^{8}	1.64	2.12	0.990	0.996
1.0×10^{10}	0	2.22	0.981	0.935

Range

Energy Level (ft-lb)	Estimated Mean	Estimated Standard Deviation	"W" Statistic	Probability
1.6×10^{7}	3.02	0.961	0.915	0.095
5.0×10^{8}	4.99	0.549	0.980	0.922
1.0×10^{10}	6.41	0.631	0.989	0.994

* Weight equals the product of the mass and gravity constant, i.e. W = Mg.

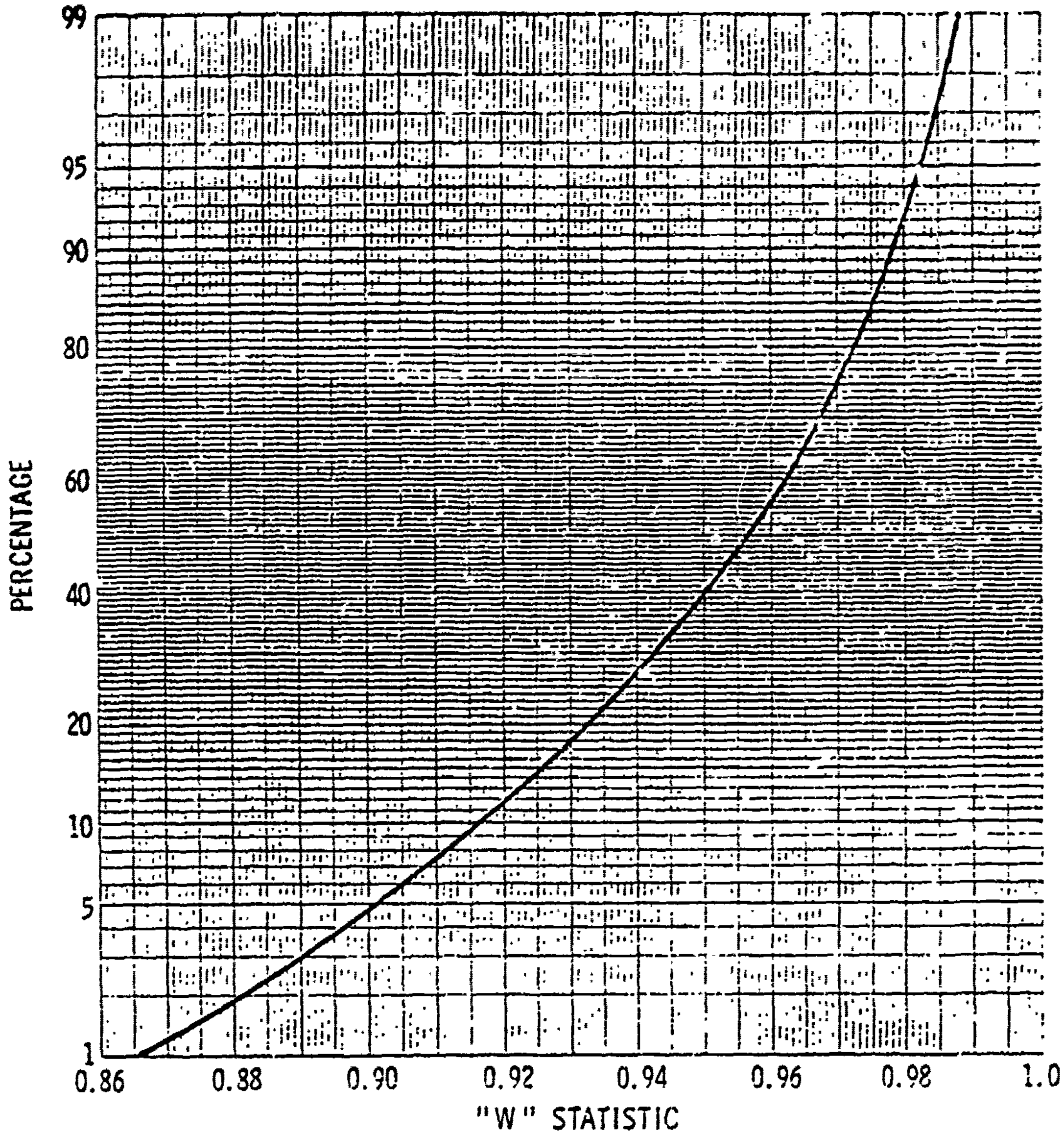

Figure 3. Approximate Probability Percentage Points (n - 19)

Table 8.

Percentiles for Plotting Fragment Nondimensional Ranges ($\overline{R}$)* and Nondimensional Energy ($\overline{E}$)+

	$E = 1.6 \times 10^{7}$ ft·lb		$E = 5.0 \times 10^{8}$ ft·lb		$E = 1.0 \times 10^{10}$ ft·lb	
Percentile	$\overline{R}$	$\overline{E}$	$\overline{R}$	$\overline{E}$	$\overline{R}$	$\overline{E}$
5	2.65	2.78×10^{-7}	21.4	4.94×10^{-8}	374	2.10×10^{-9}
10	5.06	5.29×10^{-7}	46.5	9.72×10^{-8}	525	3.67×10^{-9}
15	7.79	7.61×10^{-7}	62.6	1.91×10^{-7}	646	5.30×10^{-9}
20	11.0	1.14×10^{-6}	76.4	2.41×10^{-7}	755	8.06×10^{-9}
25	13.5	1.79×10^{-6}	89.2	3.47×10^{-7}	915	1.14×10^{-8}
30	17.0	2.69×10^{-6}	131	4.38×10^{-7}	1030	1.55×10^{-8}
35	22.0	3.59×10^{-6}	177	5.54×10^{-7}	1140	2.28×10^{-8}
40	24.1	5.23×10^{-6}	200	7.32×10^{-7}	1330	2.92×10^{-8}
45	28.9	8.07×10^{-6}	226	8.80×10^{-7}	1490	3.94×10^{-8}
50	31.5	9.54×10^{-6}	273	1.04×10^{-6}	1640	5.46×10^{-8}
55	38.2	1.06×10^{-5}	298	1.44×10^{-6}	1820	7.15×10^{-8}
60	41.5	1.30×10^{-5}	321	2.10×10^{-6}	2090	9.83×10^{-8}
65	49.4	1.60×10^{-5}	377	2.64×10^{-6}	2280	1.37×10^{-7}
70	64.4	2.02×10^{-5}	429	3.26×10^{-6}	2550	1.86×10^{-7}
75	76.3	2.77×10^{-5}	478	4.40×10^{-6}	2840	2.68×10^{-7}
80	90.3	4.29×10^{-5}	582	6.57×10^{-6}	3240	4.29×10^{-7}
85	108	8.22×10^{-5}	806	1.18×10^{-5}	3840	7.22×10^{-7}
90	147	1.23×10^{-4}	1080	1.66×10^{-5}	4720	1.35×10^{-6}
95	323	2.59×10^{-4}	1350	5.24×10^{-5}	5880	3.11×10^{-6}

* $\overline{R} = R/\sqrt{A}$

\+ $\overline{E} = (RMg)/E$

Table 9.

Listing of Estimated Means, Standard Deviations and "W" Statistics for Log-Normal Distributions for Nondimensional Range ($\overline{R}$) and Nondimensional Energy ($\overline{E}$) of Fragments

Nondimensional Range ($\overline{R}$)

Energy Level	Estimated Means	Estimated Standard Deviation	"W" Statistics	Probability
1.6×10^{7}	3.384	1.467	0.996	0.999
5.0×10^{8}	5.371	1.297	0.980	0.922
1.0×10^{10}	7.378	0.889	0.989	0.994

Nondimensional Energy ($\overline{E}$)

Energy Level	Estimated Means	Estimated Standard Deviation	"W" Statistics	Probability
1.6×10^{7}	-11.80	2.12	0.986	0.981
5.0×10^{8}	-13.58	2.09	0.993	0.999
1.0×10^{10}	-16.61	2.44	0.984	0.966

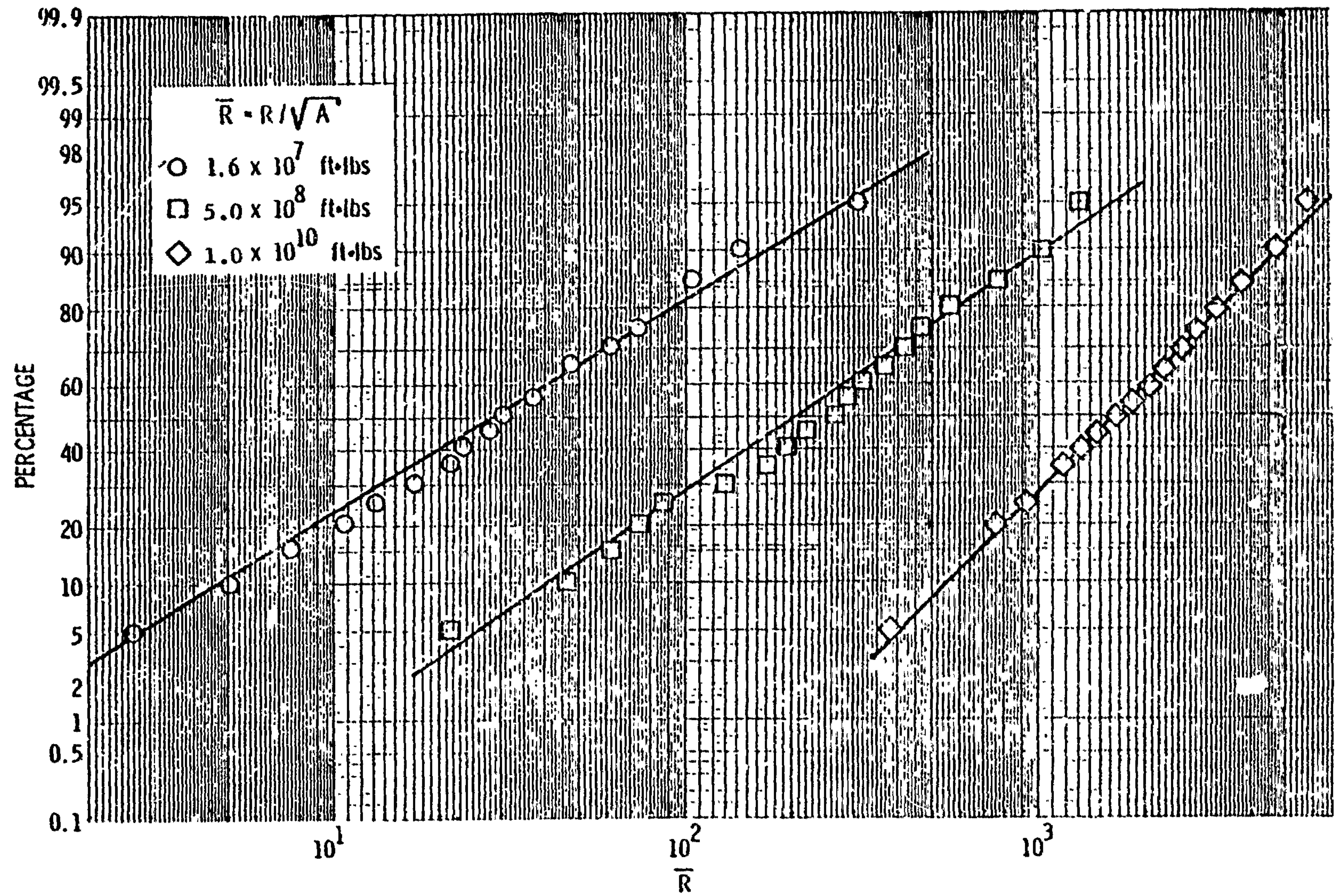

Figure 4. Cumulative Probability Distribution, Nondimensional Range, $\overline{R}$

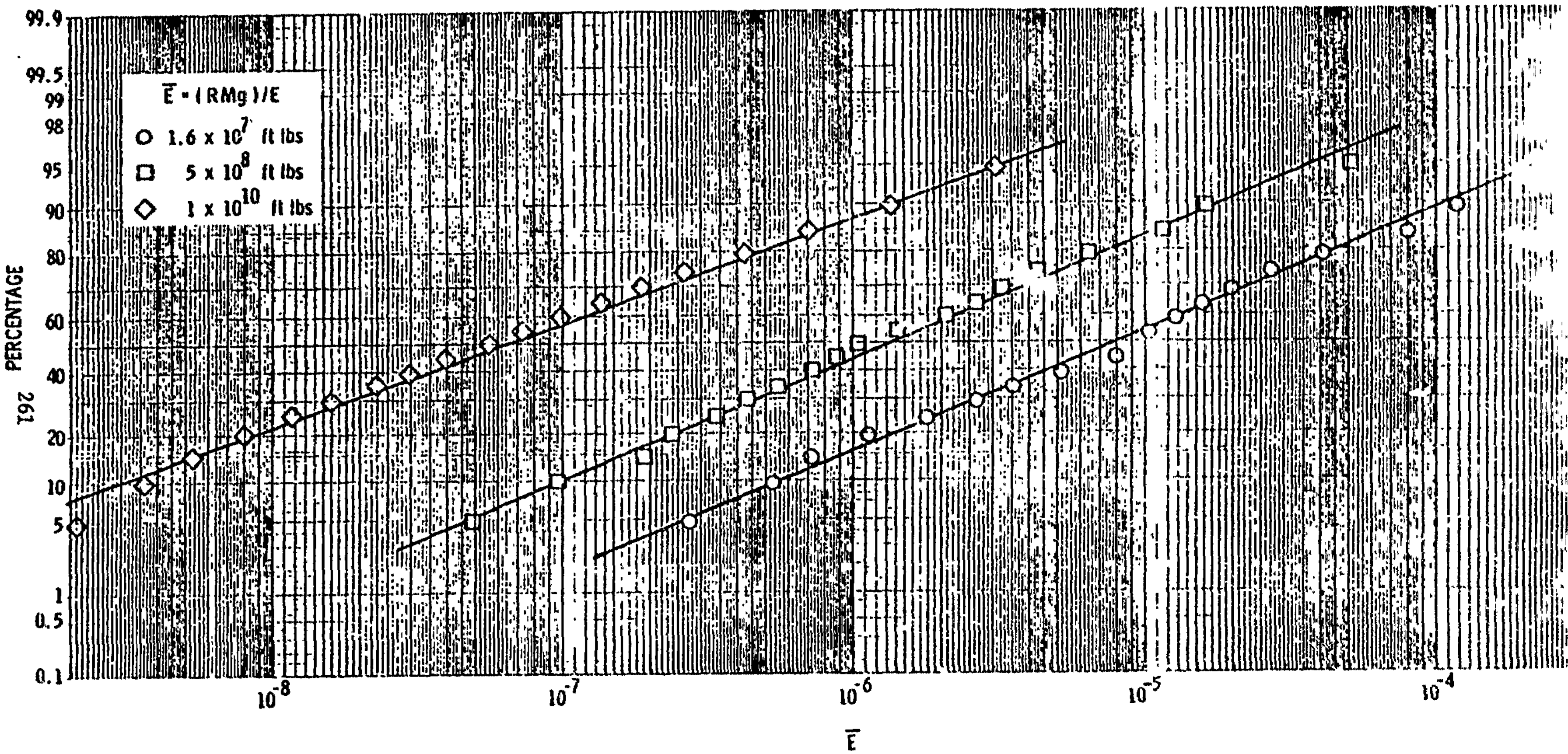

Figure 5. Cumulative Distribution, Nondimensional Energy, $\overline{E}$

Although the curve fits are good for distributions of nondimensional range and nondimensional energy, neither curve can easily be used to create a hypothetical missile map at the present time. Future work is needed to establish a functional relationship between fragment range and area before Figure 4 can be used. Also, one must establish a functional relationship between fragment weight and range to be able to use Figure 5.

It is interesting to note that the lines on Figures 1, 4 and 5 are almost parallel. That is, that the standard deviations are almost equal for all the log normal distributions. This leads to the speculation that if more experimental data are acquired in the future at various energy levels, it may be possible to derive a scale factor from the energy ratios and magnitude which is related to the mean of a particular distribution of interest (either weight, nondimensional range or nondimensional energy). Figure 2, the plot for the range percentiles, is an exception to this speculation due to the large number of fragments collected at one close-in distance (11 ft) from the explosion with an energy of 1.6×10^7 ft-lb (see Table 6). It should be noted that data from only one accident were included at this energy level. A larger data base may have caused the distribution to shift to a position more nearly parallel with the distributions of range for the other two energy levels.

A procedure for estimating the number of fragments of a given mass interval which will fall within a given distance from an explosion source in a building is as follows:

1) Estimate W_B = total destroyed weight of the building (portion of the building which has fragmented). This estimate will depend mainly upon the amount of explosive stored or machined in the building at any given time and the building structure and shape.

2) Using the weight distribution in Figure 1, obtain the average weight of a fragment from the explosion, W_a, by reading it off the appropriate curve at the 50th percentile. The total number of fragments from the explosion is then

$$N_f = \frac{W_B}{W_a} \tag{1}$$

3) Using the range distribution in Figure 2, take equal percentage increments (0-10%, 10-20%, etc.) or equal range increments (0-10 ft, 10-20 ft, etc.) and find the number of fragments, N_{f_1}, in each increment. (If equal percentage increments were taken, the number of fragments in each increment is, of course, the same.)

4) Again using the weight distribution in Figure 1, determine the percentage of fragments in a particular weight interval. The total numbers of fragments in each range interval have already been calculated (Step 3). Thus, the number of fragments of a particular weight in a particular range interval (distance out from the source) can be determined.*

V. CONCLUSION

This paper demonstrates that it is possible to estimate fragment weight and range distributions for building types similar to those described in the data base which are subjected to internal high explosive detonation. To do this, one needs to determine the total energy of the explosion (heat of detonation of the high explosive involved) and the total weight of the building which fragments. Using the methods described in this paper, one can generate a hypothetical missile map giving fragment mass and range. This missile map can then be used to establish safe standoff distances around work or storage areas.

As is true in any analysis, there is always the need for more data. The data base for this study consisted of seven well-documented accidents out of several hundred accident reports. To refine the analysis presented in this paper and extend it to other building types, it is necessary for future high explosive accidents to be better documented and for careful researchers to conduct model experiments.

VI. REFERENCES

1. Baker, W. E., Westine, P. S., Kulesz, J. J., Wilbeck, J. S., Cox, P. A., "A Manual for the Prediction of Blast and Fragment Loading on Structures," U. S. Army Corps of Engineers, Huntsville Division, (in publication).

2. Baker, W. E., Westine, P. S., and Dodge, F. T., Similarity Methods in Engineering Dynamics, Hayden Book Company, Inc., Rochelle Park, New Jersey, 1973.

3. Hahn, G. J. and Shapiro, S. S., Statistical Methods in Engineering, John Wiley and Sons, Inc., New York, New York, 1967.

*The major assumption made in this procedure is that all weights are distributed log normally in a given interval of range. Since we could find no correlation between weight and range, for a given energy level and since weight is log-normally distributed over each energy level (which covers the entire range), there is no reason to assume that weight is not log normally distributed within a given range increment.

PRECEDING PAGE BLANK-NOT FILMED

"DEPENDENCE OF FLYROCK RANGE ON SHOT CONDITIONS"*

Julius Roth
Management Science Associates
Mountain View, California

Most blasting accidents in open pit or strip mining operations are caused by flyrock. Similarly, flying debris is expected to be a major hazard in many deliberate or accidental blasts involving military explosives, or in blasting operations performed by DOD. A model has been developed to relate maximum flyrock range to shot conditions encountered in surface mining and "calibrated" with measured flyrock velocities and/or flyrock ranges found in mining and explosives literature. The model adapts the Gurney formula for the velocity of explosively-propelled plates or fragments to blasting practices in surface mines, and these flyrock velocities are then used to compute maximum flyrock range from ballistic trajectories. It is believed that this model can also be adapted to estimating the maximum range of headwall and door fragments propelled by the accidental explosion of a storage igloo.

*Work sponsored by U.S. Department of the Interior, Bureau of Mines, "Dependence of Flyrock Range on Shot Conditions," Contract J0387242.

INTRODUCTION AND QUANTITATIVE FORMULATION OF THE FLYROCK PROBLEM

By far the greatest single hazard in surface mine blasting operations is flyrock. Flyrock accounts for approximately half of all blasting-related accidents in surface mines (or somewhat more than one-third if fall of ground accidents are also included in blasting-related accidents).[1] Clearly, improved blasting practices and more definitive blasting regulations are still needed to minimize the flyrock hazard. The current study was aimed primarily at developing a flyrock model that would assist in the development of such regulations.

The approach used in the present study is to relate initial flyrock velocity to shot conditions and then use ballistic trajectories to compute maximum flyrock range. This approach is entirely justified because the effects of air friction are quite small for typical flyrock sizes and velocities. Furthermore, since safety is the prime consideration, it is the maximum flyrock range that defines a safe blast area, and in a ballistic trajectory the maximum range is obtained with flyrock propelled at an initial angle of 45°. Thus, determination of initial flyrock velocity completely determines maximum flyrock range. Most of the discussion will be limited to consideration of flyrock from "vertical" faces of open pit benches.

For flyrock at an initial velocity υ_0 and an initial angle θ, the horizontal range L (i.e., return of the projectile to its original elevation) is given by

$$L = \frac{\upsilon_0^{\,2} \sin 2\theta}{g} \tag{1}$$

where g is acceleration of gravity. Maximum flyrock range L_m is obtained when $\theta = 45°$, or

$$L_m = \upsilon_0^{\,2}/g. \tag{2}$$

If the flyrock originates at an elevation of h above ground level, then (as shown in Appendix A) the maximum range L'_m for return of the projectile to ground level is given by

$$L'_m = \frac{L_m}{2}(\sqrt{1 + 4h/L_m} + 1). \tag{3}$$

Other equations which will be useful in the interpretation of some of the data are:

$$t_m = \frac{\upsilon_o \sin^2\theta}{g} \tag{4}$$

where t_m is the time for the projectile to reach its maximum elevation h_m, and

$$h_m = \frac{\upsilon_o^2 \sin^2\theta}{2g}. \tag{5}$$

The Gurney formula[2] successfully predicts initial velocities of metal plates and metal fragments propelled by explosives.[3] Consequently, it is logical to attempt to adapt the Gurney approach to the determination of initial velocities of rocks propelled by explosives, or more specifically, to flyrock velocities obtained in bench blasting.

The general form of the Gurney equation is

$$\upsilon_o = \sqrt{2E}\, f(c/m) \tag{6}$$

where $\sqrt{2E}$, the so-called Gurney constant, is characteristic of the explosive used; c and m respectively are the masses (total, or per unit length, or per unit area) of explosive and material that is propelled; the form of the function f depends on the geometry of the system. It can be shown that initial flyrock velocity correlates much better with c/m than with more familiar terms such as powder factors.

Figure 1a is a schematic representation of the rock breakout produced by the detonation of one borehole of a typical bench blast, with explosive column length ℓ, stemming length s, and burden to the free face b. Shot conditions are assumed to be such that breakout occurs only at the "vertical" free face in the region of length ℓ. We idealize the situation by considering that the homogeneous rock surrounding the borehole acts as a "rigid wall" in all directions except that of breakout to the free face. This breakout per borehole has the shape of a prism. Also shown is the total volume of the rock broken (parallelopiped) that is conventionally used in computing powder factors. In Figure 1a it was assumed that the breakout angle is 90°, thus the breakout width at the free face is 2b. If this angle is α rather than 90°, the breakout width at the free face is $2b\tan(\alpha/2)$. Then, per unit length of loaded borehole:

$$c/m = \frac{W/\ell}{\rho_m b^2 \tan(\alpha/2)} \tag{7}$$

where W/ℓ is the explosive weight per unit length of borehole and ρ_m is the density of the rock. That α is indeed close to 90° is shown in Table 1. The α's in this table are based on measurements of the amount of rock broken, but are certainly overestimated as explained in footnote a/ of this table.

For flyrock from the vertical face (see Figure 1b) and for the geometry of the system considered (as shown in Appendix B)

$$\upsilon_o \approx \sqrt{2E'}\ \sqrt{c/m} \tag{8}$$

where $\sqrt{2E'}$ is slightly less than $\sqrt{2E}$ because the direction of detonation is tangential to the rock and not head-on as in the derivation in Appendix B. The relation between $\sqrt{2E}$ and $\sqrt{2E'}$ was examined by the writer[3] who also showed that for most explosives

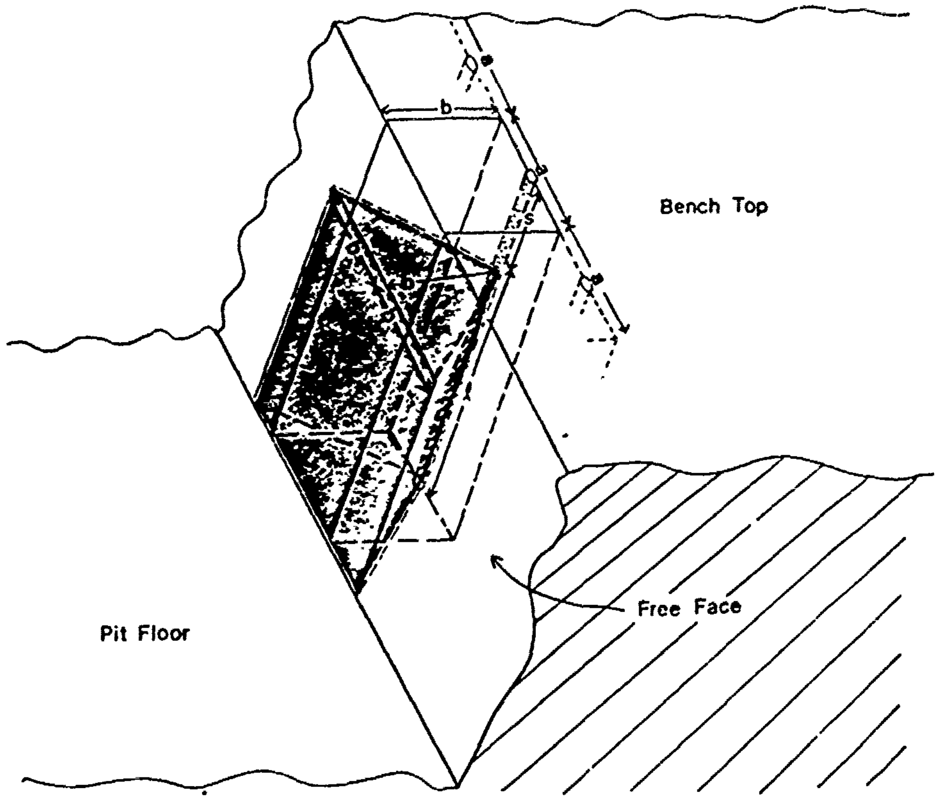

Figure 1a: THREE-DIMENSIONAL VIEW OF A BENCH BLAST

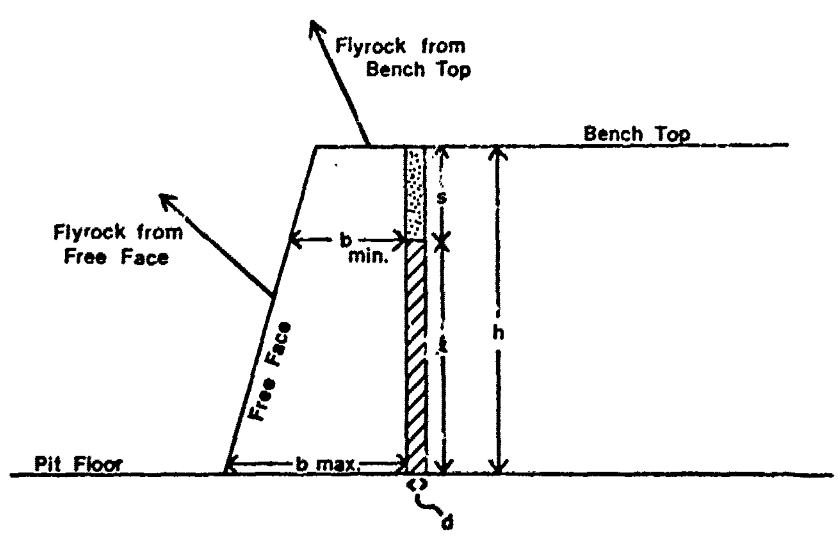

Figure 1b: PLAN VIEW OF A BENCH BLAST

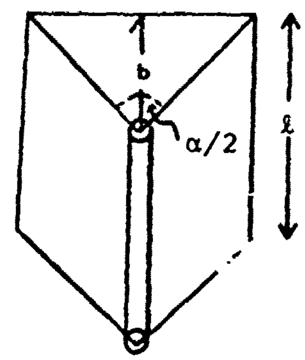

Source	b (cm)	d* (mm)	α (°)	W (g)	Rock
Noren (Ref. 4)	17.8	38.1	100 a/	9.2 b/	Granite
"	22.9	"	110 a/	"	"
"	27.9	"	100 a/	"	"
"	33.0	"	90 a/	"	"
"	40.6	"	90 a/	"	"
"	53.3	"	95 a/	"	"
"	91.4	"	120 a/	"	"
Ladegaard-Pedersen (Persson (Ref. 5)	45.0	27.0	108 a/	15.0	Granite
"	"	"	" a/	20.0	"
"	"	"	" a/	30.0	"
"	"	"	" a/	35.0	"
"	"	"	" a/	40.0	"
"	"	"	" a/	50.0	"
"	45.0	"	" a/	85.0	"
"	40.0	"	106 a/	"	"
"	35.0	"	104.5 a/	"	"

* d = borehole diameter.

a/ Assumed rock broke out at uniform angle over entire hole depth. If, as expected, break is beyond hole depth, above α's are too large.

b/ g/cm

Table 1: BREAKOUT ANGLES IN BENCH BLASTING

$\sqrt{2E'} \approx D/3$ where D is the detonation velocity of the explosive. However, for ANFO, which is the explosive used in most surface mine blasts, $\sqrt{2E'} \approx 0.44D$ (see Appendix C). In what follows we will use

$$\upsilon_o \approx 0.44D\sqrt{c/m} \tag{9}$$

for ANFO shots and

$$\upsilon_o \approx \frac{D}{3}\sqrt{c/m} \tag{10}$$

for most of the other shots.

All of the above refers to shots in a single borehole. Interactions between boreholes will be examined later.

Effect of Rock Properties

In the derivation of equation (8) (see Appendix B) we ignored any energy-consuming effects other than those required to impart kinetic energy to the flyrock and the detonation product gases. Obviously, this is an oversimplification since rock fracture consumes some of the available chemical energy of the explosives. Similarly, generation of seismic waves in the rock, and the formation of the crushed rock zone immediately around the borehole, also consume energy. Rock breakage (at least most of the breakage), seismic wave generation and crushed zone formation are substantially complete before the breakout rock mass attains the velocity υ_o (see Appendix E and Refs. 8 and 9). Thus, correction terms for these energy losses must be introduced into equations (8) (9) or (10).

For a given homogeneous rock blasted with a given explosive, one might expect that the:

1. energy consumed in rock fracture is proportional to m;
2. seismic energy is proportional to c;
3. energy to form the crushed zone is proportional to c.

Assumptions 2 and 3 are fully justified by the data in references 10 and 11 and reference 9, respectively. Assumption 1 is more difficult to justify. The energy to fracture homogeneous rock should really be proportional to the number of fragments into which the mass of rock breaks, or more properly to the new surfaces created by fracture. However, inter-fragment friction during break-up and possibly plastic deformation of the fragmented material will also absorb energy. If fracture produces approximately equidimensional fragments, assumption 1 is valid. If the number and size of fragments varies greatly with shot dimensions (even though a given explosive is used to blast a given rock mass), assumption 1 is invalid. In the limit of large burdens and small charges it is known that shots break rock into large chunks or slabs, whereas under normal production blasting, rock is fragmented into many roughly equidimensional pieces.[12] Clearly, assumption 1 can be valid only over a limited range of m/c. Hopefully, it is valid over the "normal" range of m/c in production blasting.

Taking into account the above energy losses, equation (B-4) of Appendix B has to be modified as follows:

$$cE' - c(K_1 W_s + K_2 W_c) - m(K_3 W_r) \approx \frac{1}{2} m \upsilon_o^2 \tag{11}$$

where W_s = seismic energy generated by a unit weight of explosive

W_c = energy to crush a unit weight of rock

W_r = energy absorbed in breaking out a unit weight of rock

K_1, K_2, K_3 are proportionality constants.

According to equation (11)

$$\upsilon_o^2 \approx 2E'(c/m) - 2K_3 W_r - 2(K_1 W_s + K_2 W_c)c/m$$

or

$$\upsilon_o^2 \approx 2E'\left(\frac{c}{m}\right)\left[1 - \frac{K_1 W_s + K_2 W_c}{E'}\right] - 2K_3 W_r \,. \tag{12}$$

According to equation (12), a plot of υ_0^2 vs. c/m should give a straight line of slope $2E'(1 - \frac{K_1W_s + K_2W_c}{E'})$ and intercept of $-2K_3W_r$. In what follows $\sqrt{2E'}$ will be replaced by 0.44D or D/3 depending on whether the main explosive charge is ANFO or any other explosive.

Effects of Multiple Boreholes

Consider a series of shots in which spacing between vertical boreholes, all of diameter d, is 2/3b, b, and 4/3b as shown in a top-view sketch in Figure 2. In every case assume that hole (1) fires 1/2 second before hole (2) and also assume that the breakout angle is 90°. For a "typical" round, the rock broken by hole (1) will have moved some 10 - 20 feet from its original position, thus creating a new free face for hole (2). The new minimum burdens for hole (2) are respectively 0.471b, 0.707b, and 0.943b for conditions (a), (b), and (c) in Figure 2. Obviously, condition (a) has the potential of throwing rock four times further than condition (c) since (from equations 2, 7, and 8) it can be shown that the maximum flyrock range, L_m, is proportional to $(d/b)^2$.

Normally, the delay between adjacent holes in the front row of a shot is much less than 1/2 second. Thus. displacement of the rock broken by hole (1) (still assumed to fire before hole (2)) is much less than in the above examples. Also hole (2) fires (in part) into a "curtain" of broken and expanding rock. Nevertheless, because commercial delay devices can occasionally be erratic, it is desirable from the point of view of minimizing flyrock to maintain borehole spacing $\geq 4/3b$, so that even gross mistiming does not create very small burdens between adjacent boreholes. Unfortunately, this can result in poor fragmentation. Thus, some compromise is necessary.

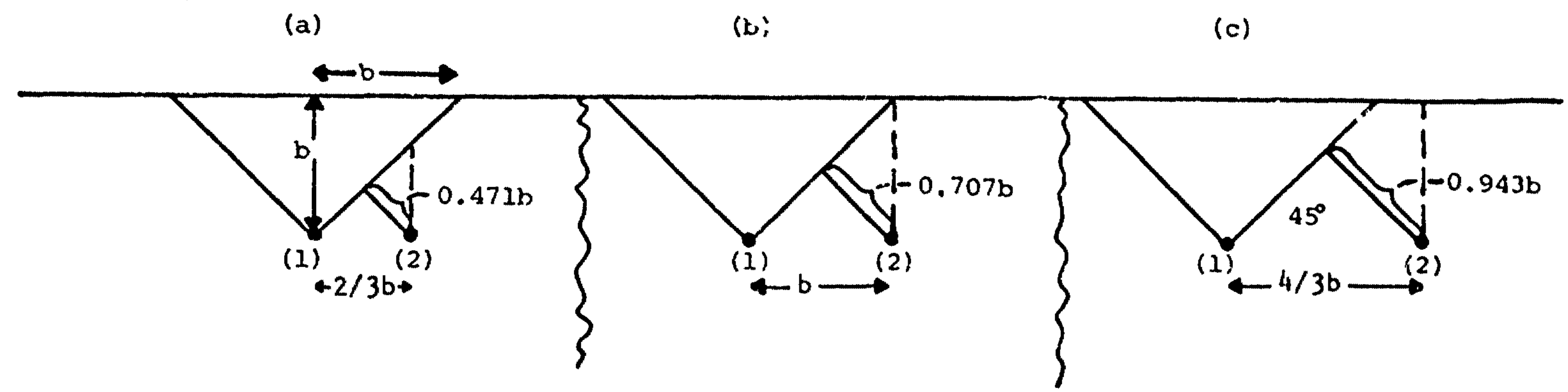

Figure 2: SCHEMATIC TOP-VIEW OF BENCH BLASTS WITH VARYING BOREHOLE SPACINGS

Above, we examined the potentially dangerous effects of multiple-hole bench blasting. However, under proper conditions multiple-hole shooting may actually reduce flyrock range. This is so because properly delayed multiple-hole shots will produce more fragmentation than the same shots fired "instantaneously". In these delayed shots it is likely that more of the chemical energy of the explosive is used in fragmentation processes than in the instantaneous shots and less energy is thus available to propel the broken rock. Quantitative formulation of this effect will be very difficult, but experimental corraboration is available from the studies of Forsberg and Gustavsson[13], who found that instantaneous rounds throw rock further than short-period delay rounds.

These compensating effects suggest that, in the absence of unduly long delays between neighboring holes, highwall flyrock ranges from single holes or multiple holes can be substantially equivalent.

There is fairly wide-spread belief that improper delay sequencing can result in excessive flyrock from unrelieved back row holes. Under favorable conditions, this may indeed happen and produce "wild" flyrock and certainly flyrock in unexpected directions. The rationale for this belief is as follows. If a back row hole shoots before the holes in front of it have detonated and moved some of the rock between it and the free face, the effective burden on the back row hole is so large that it cannot be broken by the detonation of the back row hole. Consequently, this detonation is "relieved" by producing excessive "cratering" (and flyrock) at the top of the bench. However, such a sequence of events is limited to conditions for which the explosive load is less than a "critical" depth below the bench top. With sufficient stemming, both actual blasting experience* and experiments[14].

* The writer witnessed a production shot in an open pit coal mine in which 9 holes were fired within a few seconds of each other without <u>any</u> apparent "relief" at the vertical face or bench top. Each hole contained about 1,500 lb. of ANFO but had 40 feet of stemming and an average burden of 38 feet.

indicate that there will be no such cratering even in the absence of any nearby free face other than the bench top.

Estimation of Maximum Flyrock Range

We shall use equation (12) to compare measured and computed flyrock velocities. According to equation (12) a plot of the measured velocity squared (υ^2_{obs}) vs. c/m should be linear with a slope of $2E'(1 - \frac{K_1 W_s + K_2 W_c}{E'})$ and an intercept of $-2K_3W_r$, provided that all velocity measurements are made with the same explosive. If measurements made with several different explosives are to be compared with theory, some method of normalizing the measured velocity data must be developed. It will be shown in Appendix E that the observed velocities can be normalized to a common 2E' or to a common D^2 since 2E' is directly proportional to D^2. To illustrate this normalization scheme, suppose that most of the velocity data for a given rock type is for a dynamite whose Gurney constant ($\sqrt{2E'}$) $\approx D_1/3$ where D_1 is the detonation velocity of this dynamite for the conditions of the measurement. No correction factor will be applied to the observed flyrock velocities generated with this explosive. Now suppose that ANFO at a detonation velocity of D_2 was used to obtain some of the velocity measurements in the above rock type. The normalization factor applied to these latter measurements (i.e., the factor by which υ^2_{ANFO} is multiplied) is:

$$\frac{2E'_{ANFO}}{2E'_{dynam}} = \frac{(0.44D_2)^2}{(D_1/3)^2} .$$

We will illustrate the method of "proving-in" our computed flyrock velocities with flyrock data for granite. For each measured flyrock velocity datum we computed c/m via equation (7), or from the total amount of rock broken and the total explosive charge weight, whenever such data were available. If no information on the breakout angle α was available, it was assumed that $\alpha/2 = 45^0$ (see Table 1). A least-squares linear regression fit was then used to obtain the most probable values of the slope and intercept of a linear plot of measured flyrock velocity squared versus computed c/m. For each set of data points we also computed a correlation coefficient $r = S\sigma_x/\sigma_y$ where S is the linear regression slope and σ_x and σ_y are the standard deviations of the x and y values. A correlation coefficient approaching unity shows that the y and x values can indeed be represented by a linear relation.

Measured flyrock velocities and computed c/m's for granite are shown in Table 2. The linear regression slopes and intercepts for these data are as follows:

Granite: $\upsilon_o^2 = 3.487 \times 10^6 (c/m) - 584$ $(m/sec)^2$ (13)
(17 data points; r = 0.999; normalized to D/3 = 2300 m/sec)
When all the data in Table 2 are used, except those from References 17 and 18 and the two data points at the bottom of the group of data taken from Reference 15, r = 0.971 and

$$\upsilon_o^2 = 3.66 \times 10^6 (c/m) - 518 \quad (m/sec)^2 \quad (13a)$$

All the data of Table 2 are plotted in Figure 3 to provide a visual confirmation of the validity of the proposed linear relation between υ_o and c/m. Note that the slope and intercept of the line based on all the data (Equation 13a) is quite similar to the slope and intercept of the line based on data from which three datum points have been omitted (Eq. 13).

The datum point labelled L&K (and the bottom entry in Table 2) is derived from Langefors[18] claim that the maximum burden-to-diameter ratio to just barely break rock is 46. This ratio gives a $c/m \approx 1.9 \times 10^{-4}$ (from Eq. 7) and since it is claimed that rock is just barely broken $\upsilon_o^2 \approx 0$.

The scanty data for dolomite and limestone vary too much to permit determination of an accurate relationship such as the one in equation (13). Consequently, the following equation is at best an approximation:

Dolomite and Limestone: $\upsilon_o^2 \approx 3 \times 10^6 (c/m) - 200$ $(m/sec)^2$ (14)
(7 data points; normalized to 0.44D = 1880 m/sec. References 16, 19, 20, and 21)

Data Source	Explosive	D/3 (km/sec)	Normalized* v^2_{obs} (m/sec)^2	c/m x 10^4	Computed† v_o^2 (m/sec)^2
Ref. 15	EL-506C	2.30	1050	4.68 a/	1109
"	"	"	234	2.25 a/	252
"	40%PETN/NaCl	1.08	254	≈2.18 a/	≈237
"	60% "	1.50	174	≈1.95 a/	≈157
"	EL-506C	2.30	104 b/	1.96 a/	160
"	"	"	94 b/	1.80 a/	105
"	"	"	90.3	2.10 a/	209
"	"	"	24 c/	1.20 a/	-105
"	"	"	12.3 c/	0.72 a/	-272
Ref. 4	Dynamite	1.28	490	2.54	363
"	"	"	3730	11.70	3557
"	"	"	5695	18.32	5865
"	"	"	14500 c/	30.52	10119
"	"	"	8730 c/	36.54	12253
"	"	"	19150 c/	39.83	13366
"	"	"	28500	83.27	28513
Ref. 16	Gelamite D	1.995 d/	249	2.53	359
"	"	"	753	3.17	582
"	"	"	1202	4.93	1196
Ref. 5	Dynamex	1.00	3885	12.86	3961
"	"	"	2304	9.92	2936
"	"	"	4826	17.32	5576
Ref. 17	ANFO	2.07 f/	278 e/c/	2.10	209
Ref. 18	---	---	≈0 g/c/	≈1.9 f/	≈140

* Normalized to D/3 = 2.30 km/sec   † $v_o^2 = 3.487 \times 10^6 (c/m) - 584.$

a/ Ref. 12 gives explosive weight W and the total weight of rock broken m_t; $c/m = (\frac{W}{m_t})(\frac{\ell_1}{h})$ where ℓ_1=length of borehole and h=height of rock.

b/ Charge diameter less than borehole diameter.

c/ Not used in computing slope and intercept.

d/ 0.38D

e/ Shots in hematite ore.

f/ 0.44D

g/ It is claimed that maximum burden to borehole diameter ratio to break rock is 46. In computing c/m for this ratio we assumed $\rho_c/\rho_m = 1/2$

Table 2: COMPARISON OF OBSERVED AND COMPUTED FLYROCK VELOCITIES IN GRANITE BENCH SHOTS

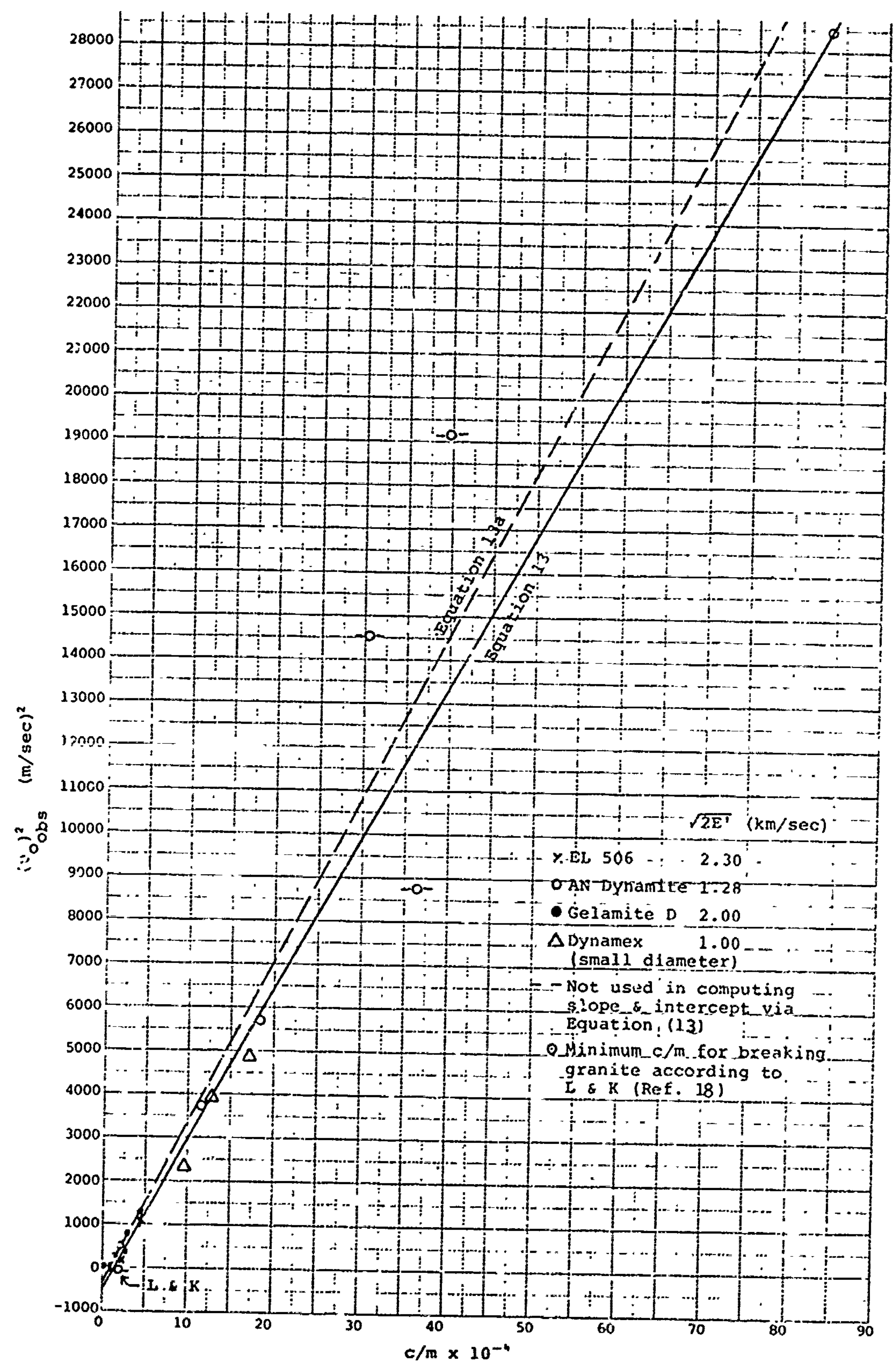

Figure 3: PLOT OF OBSERVED FLYROCK VELOCITY VS. c/m FOR BENCH SHOTS IN GRANITE

Examination of Table 2 reveals that for $c/m \leq 1.5 \times 10^{-4}$ equation (13) does not hold. Indeed the data of reference 15 show some half-dozen points in this region with finite flyrock velocities, whereas equation (13) predicts zero flyrock velocity. These low flyrock velocities in the region of $c/m \lesssim 1.5 \times 10^{-4}$ may be due to spalling. Spall velocities v_{fs} (i.e., free surface velocities) in the elastic range are given by

$$v_{fs} = 2c_o\varepsilon \tag{15}$$

where c_o is the longitudinal sound velocity in the rock and ε is the strain in the rock at its free surface boundary. Table 3 shows that there is reasonable accord between spall velocities calculated by equation (15) and the observed fly velocities in the low c/m range. Note that all these velocities are quite low.

Observed* and computed flyrock ranges are compared in Table 4. In general, computed ranges should be equal to or greater than observed ranges, since in the computation it is assumed that the initial flyrock angle Θ is 45°, but in reality this angle is usually either greater or less than 45°. Most "vertical" faces are not truly vertical. Consequently, the burden to the free face varies along the explosive column (see Figure 1b). The computed flyrock ranges in Table 4 are based on minimum burden whenever there was sufficient information to determine a minumum burden. In most reports of blasting accident investigations the "burden" usually quoted is the separation between rows of holes. This "burden" can be different from the minimum, average, or maximum burden to the free face which are the burdens required for the computation. The accident reports do not give the maximum flyrock range but only the distance from the shot to where the victim was located. Moreover, there is usually no indication how this distance was measured or estimated. Most of the observed flyrock ranges extracted from Reference 1 were obtained by scaling

* Our own observations or data gleaned from blasting accident reports.

Rock	Sound Velocity $c_o \times 10^{-3}$ (m/sec)	Stress $\sigma \times 10^{-7}$ (dynes/cm^2)	Strain $\varepsilon \times 10^4$ (μ inch/inch)	Free* Surface Velocity v_{fs} (m/sec)	Observed Velocity (m/sec)
Granite	5.20	5.86	2.93 a/	3.0	1.8
"	"	8.45	4.23 a/	4.4	3.5
"	"	8.97	4.48 a/	4.7	4.9
"	"	14.5	7.25 a/	7.5	6.8
"	"	19.3	9.66 a/	10.0	9.5
Sandstone b/	1.52	-	25	7.5	5.8
"	"	-	25	7.5	4.0
"	"	-	20	6.0	2.7
"	"	-	13	4.0	≈0

* $v_{fs} = 2c_o\varepsilon$

a/ $\varepsilon = \frac{\sigma}{Y}$ where Y is Young's modulus = 2×10^{11} dynes/cm^2 according to Ref. 14. σ from Ref. 15.

b/ Crater shots; ε from curves in Ref. 14.

Table 3: SPALL VELOCITIES IN GRANITE AND SANDSTONE

Mine†	Rock	Borehole Diameter d (inches)	Burden b (feet)	Height of Explosive Column ℓ (feet)	Weight of Explosive/Ft. W/ℓ (lbs./ft.)	$c/m \times 10^4$	$\sqrt{2E}$ (ft/sec)	ψ^2 (ft/sec)^2	L_m* (feet)	L'_m** (feet)	L_{obs} (feet)
Annapolis Quarry	Granite	3	10	≤ 52 a/	~4.6	~2.9	~6350 b/	3720	~115	~150	300-350
Mine J	Porphyry	9	27	30	27.8	2.18	6710	2019 c/	63	85	~100
Mine P	Porphyry	7-7/8	25	15	16.7	1.53	6640	88 c/	3	8	< 50
Mine K	Diorite	9-7/8	27	25	32.6	2.71	6710	3592 c/	112	133	~100
Mine X	Diabase	6-1/2	21	69	19.8	2.24	6550	2093 c/	65	107	< 200
Mine [illegible]	Taconite	9-23	44	26	~210 d/	~5.2	6200 b/	9377 c/	291	315	200-400
Mine D	Sandstone	6-1/4	18	12.5	11	2.42	6480	1738	54	64	~50
Mine [illegible]	Shale	9	12	20	22.5	11.17	6700	30115 e/	935	955	~400
Mine C	Shale	15	36	~70	~50	~2.5	6700	~1340 e/	~40	~75	~20
Mine B	Shale	15	≤ 38	46	~70	≥ 3.5	7020	≥ 5115 e/	≥ 160	≥ 200	~300
Kolin Coal	Shale	5	≤ 12	5	7.0	≥ 3.5	6300	≥ 4125 e/	≥ 128	≥ 130	210
Roberson Coal	Shale	6-1/4	≈ 13 f/	9	11.3	≈ 4.8	5480	≈ 8465 e/	≈ 260	≈ 270	400
Mine W	Limestone	6-3/4	13	38	13	4.52	6580	~14193	~441	~476	~300
Mine [illegible]	Limestone	6-1/2	~13	117	12	~4.2	6550	~13015	~405	~500	~350
Mine U	Limestone	6-3/4	~9	60	13	~9.4	6580	~32170	~1000	~1060	~900
Carbon Limestone	Limestone	6-1/4	~15	~45	8.3	~2.2	5480	~5480	~170	~205	600 g/
Fernsteat Quarry	Limestone	3-1/2	7	39	3.5	4.46	5750	~10665	~335	~370	450 g/
Quarry	Limestone	3	8	~56	4.23	3.78	4670 h/	5751	179	230	120
Mine R	Dolomite	6	12	50	11	4.24	6450	~12650	~390	~435	~250

† Same designations as in Appendix B of Reference 1. Data for named mines from MESA Reports.
* From Equation 2.
** From Equation 3 but with ℓ substituted for h.
a/ Value shown is height of quarry face.
b/ Slurry explosives with $\sqrt{2E'} \approx D/3$; all others are ANFO with $\sqrt{2E'} = 0.4$ D
c/ Used Equation 13.
d/ Average loading in a tapered borehole.
e/ Used Equation 16.
f/ Burden not given in report; estimated from bench width and number of rows.
g/ Flyrock from bench top.
h/ Semi-gel; D/3

Table 4: COMPARISON OF OBSERVED AND COMPUTED FLYROCK RANGES FOR FLYROCK FROM VERTICAL FACES

still-camera records of the various shots witnessed, but several ranges are "eye-ball" estimates made immediately after a shot. Incidentally, all the data in Table 4 are based on production shots in actual surface mines. None of these data are derived from experimental studies or exploration shots.

Taking into account the several uncertainties listed above, agreement between the observed and computed flyrock ranges shown in Table 4 is quite satisfactory. However, all computed values for flyrock ranges in limestone and dolomite shots should be considered to be provisionary because of uncertainty in the values of the constants of Equation (14).

Note that only five of the 19 shots listed in Table 4 threw rock 400 feet or more. In at least one, and probably two, of these five shots the flyrock originated from the top of the bench and not from the vertical face. This may suggest that most "wild" (far-ranging) flyrock does not originate from vertical faces - an implication that will be examined in Section 7.0. A similar conclusion can be reached on the basis of Swedish studies.[19]

Generalized curves for estimating flyrock range on the basis of the model presented above are shown in Figures 4 and 5.

Flyrock from Bench Tops

Under certain conditions; e.g., when the explosive load comes close to the borehole collar, most of the flyrock originates from the top of the bench. In effect, such shots produce a "crater" in the bench top. There are two main problem areas in applying a Gurney-type treatment to estimating bench top flyrock velocities. First, the assumption of a rigid wall for all the rock that is not ejected is much less defensible than in the case of vertical face rock breakout. Second, c/m for bench top flyrock is difficult to estimate since it will depend on crater dimensions which vary with depth of charge burial, rock type, etc. Although a preliminary treatment of the range of flyrock from bench tops was presented in Reference 20, in the present paper we will give only the

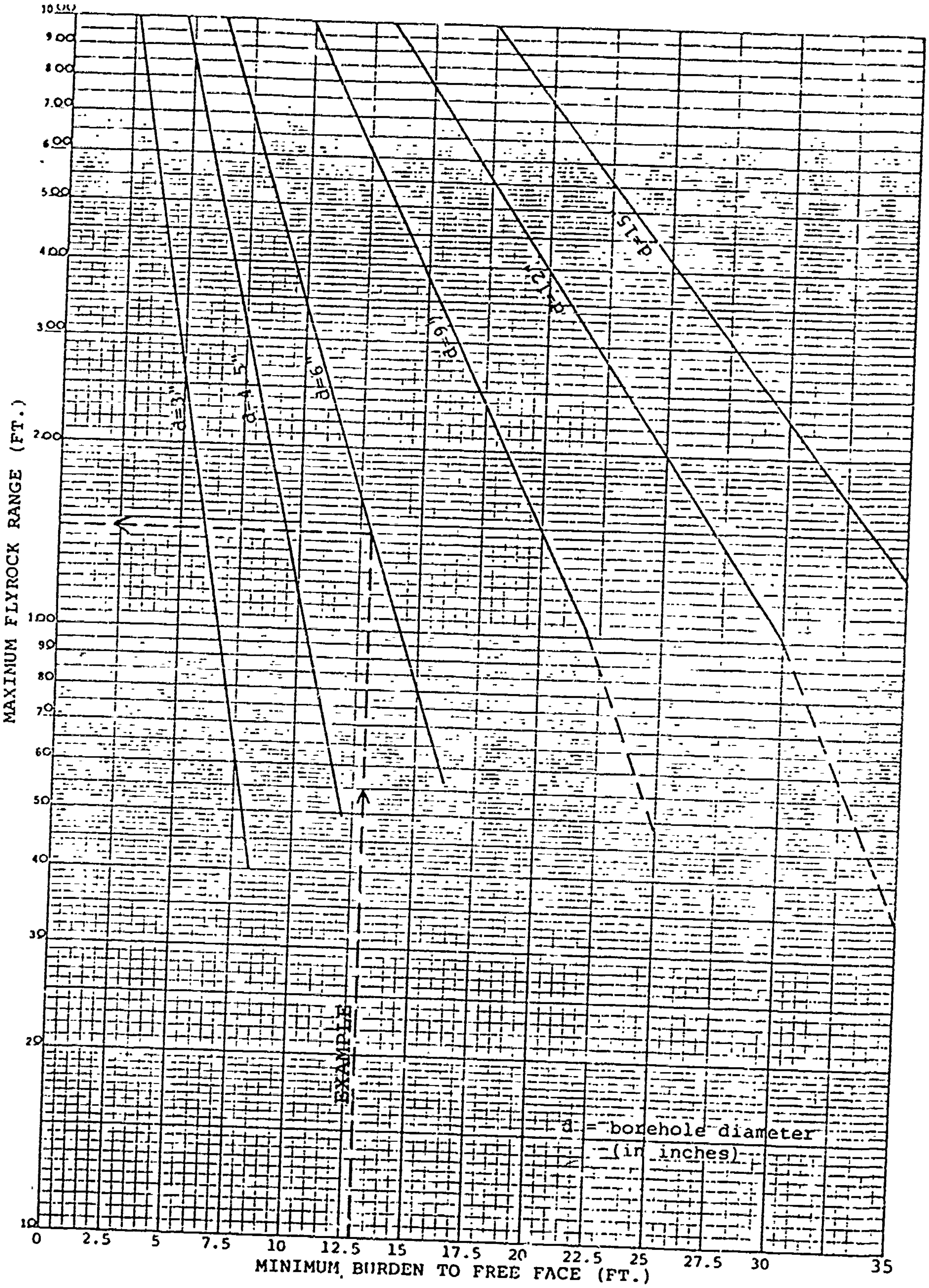

Figure 4: MAXIMUM RANGE OF VERTICAL FACE FLYROCK FROM ANFO-LOADED SHOTS IN GRANITE (FIXED BOREHOLE DIAMETERS)

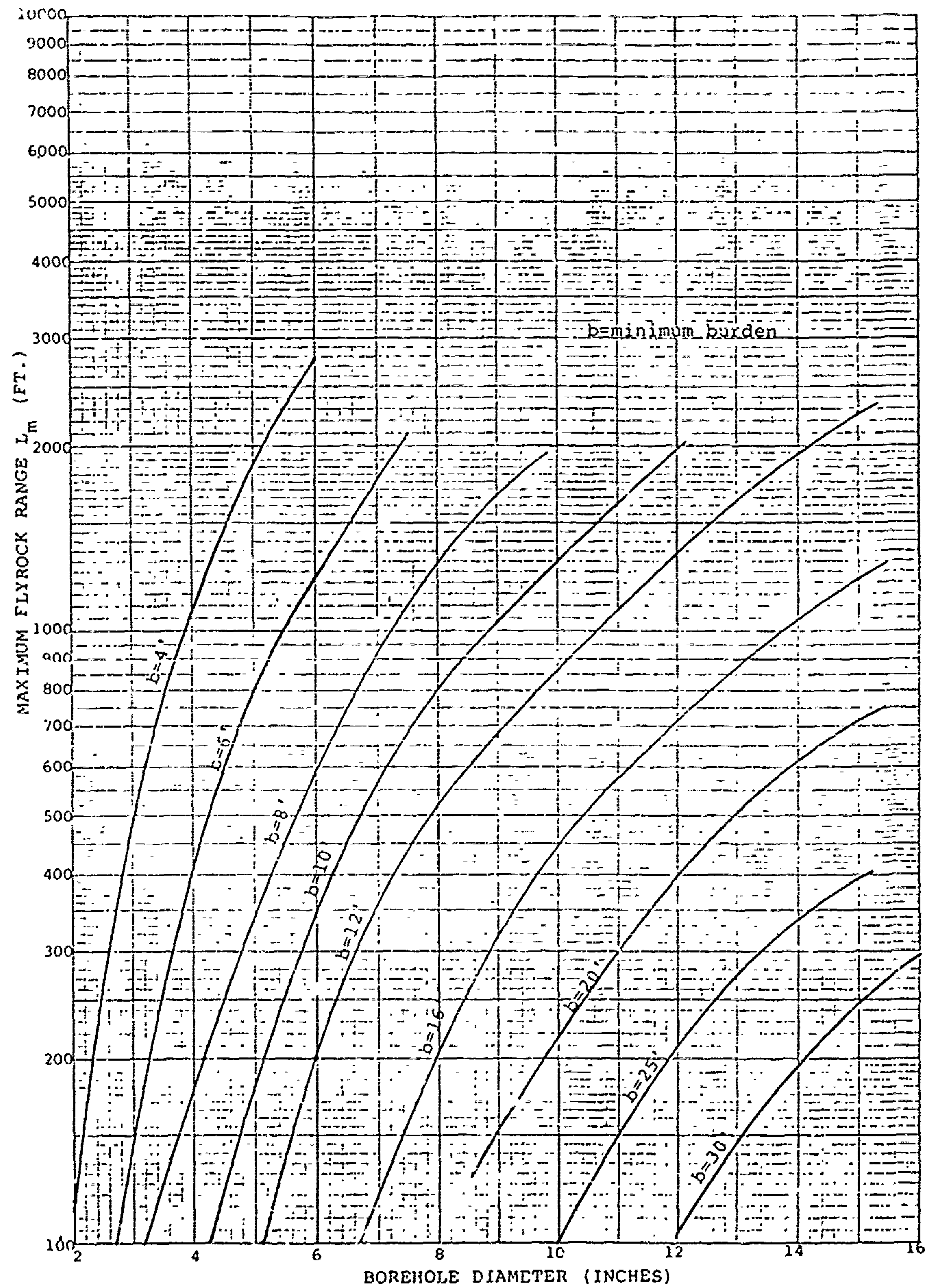

Figure 5: MAXIMUM RANGE OF VERTICAL FACE FLYROCK FROM ANFO-LOADED SHOTS IN GRANITE (FIXED BURDEN)

condition for minimum flyrock range. The condition for essentially no flyrock from bench tops for stemmed shots is:

$$s/W^{1/3} \geq 2$$

where s is the distance in feet from the borehole collar to the top of the explosive column, and W is the explosive weight in pounds.

Application of Flyrock Model to Accidental Explosions

Rough estimates of debris range of accidental explosions of munition bunkers can be made on the basis of the model presented. For example, consider a bunker that is built into the side of a hill and is fully loaded with high explosive munitions all of which are assumed to detonate within a very short time interval. Far-ranging debris is assumed to originate solely from the head-frame of the bunker. The range is estimated via Equations (8) and (2) taking c as the total explosive load in the bunker and m as the weight of the head frame.

References

1. Roth, J., et. al., "Evaluation of Surface Mine Blasting Procedures," Management Science Associates, Bureau of Mines Contract No. J0366017 (1977).

2. Gurney, R. N., Ballistics Research Laboratory Report No. 405 (1943).

3. Roth, J., SRI Laboratory Technical Report No. 001.71 (1971).

4. Noren, C. H., "Colorado School of Mines Quarterly," 51, 222 (1956).

5. Ladegaard-Pederson, A., and Persson, A., "Svedefo Report," DS 1973:13 (1973).

6. Anonymous, DuPont Blaster's Handbook, 175th Anniversary Edition, p. 242 (1978).

7. Ibid, p. 308.

8. Cook, M. A., The Science of Industrial Explosives, Chapter 10 (1974).

9. Nicholls, H. R., and Hooker, V. E., "RI 6693", p. 43 (1965).

10. Nicholls, H. R. and Duvall, W. I., "RI 6806", pp. 12-14, (1966).

11. Nicholls, op. cit., p. 43 (1965).

12. Noren, C. H., and Porter, D. D., Proceedings 3rd Congress of Int. Soc. Rock Mech., Vol. 2B, 1371 (1974).

13. Langefors, U., and Kihlstrom, B., Rock Blasting, pp. 46-49, Almquist and Wiksell, Stockholm (1963) (Quotation).

14. Duvall, W. I., and Atchison, T. C., "RI 5356", pp. 34-35 (1957).

15. Bergmann, O. R., et. al., "Int. J. Rock Mech. Min. and Geomech.," Abstract, Vol. 10, 585 (1973).

16. Petkof, B., et. al., "RI 5849," p. 9 (1961).

17. Chung, S., et. al., "Preprint 10th Canadian Symposium on Rock Mechanics," (1975), and Chung, S., "Report from CIL Explosives Research Lab, September 16, 1975.

18. Langefors, U., op. cit., p. 70 (1963).

19. Lundborg, N., et. al., Engineering and Mining Journal, 95, (May 1975).

20. Roth, J., "A Model for the Determination of Flyrock Range as a Function of Shot Conditions," U.S. Bureau of Mines, Contract No. J0387242, (April 1979).

APPENDIX A

ELEVATION CORRECTION FOR BALLISTIC TRAJECTORIES

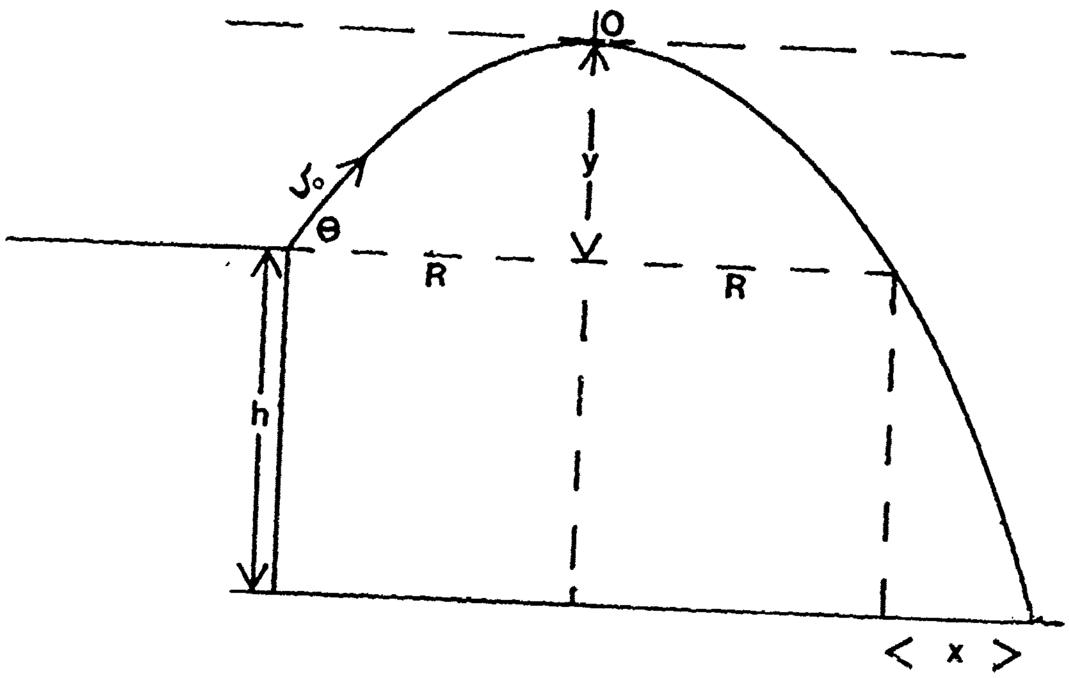

Parabolic trajectory starts at velocity υ_o, angle θ and elevation h_o. Place coordinate origin at 0, then:

$$y = cR^2 \quad \text{and} \quad y + h = c(R + x)^2$$

or dividing:

$$1 + \frac{h}{y} = 1 + \frac{2x}{R} + \left(\frac{x}{R}\right)^2 \quad \text{and} \quad (x/R)^2 + \frac{2x}{R} - \frac{h}{y} = 0$$

or

$$x^2 + 2xR - \frac{h}{y}R^2 = 0$$

and

$$x = \frac{-2R + \sqrt{4R^2 + 4hR^2/y}}{2} = -R + R\sqrt{1 + h/y} = R(\sqrt{1 + h/y} - 1)$$

but from Eqs. (1) and (5), $y = R/2$ (y is called h_m in Eq. 5), therefore

$$x = R(\sqrt{1 + 2h/R} - 1) = (L_m/2)(\sqrt{1 + 4h/L_m} - 1)$$

since $R = L_m/2$.

Finally,

$$L_m' = L_m + x = (L_m/2)(\sqrt{1 + 4h/L_m} + 1).$$

APPENDIX B

DERIVATION OF THE GURNEY EQUATION FOR A PLATE DRIVEN BY A HEAD-ON DETONATION ORIGINATING AT A RIGID WALL

The sketch below represents a cross-sectional view of the system at some time after initiation.

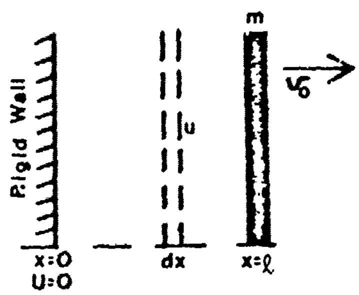

m = mass/unit area of propelled material

c = mass/unit area of explosive

U = expansion velocity of product gases at $x = 0$

The Gurney assumptions are:

a. Product gas density, ρ, is uniform at any given time.

b. Velocity distribution u of the expanding product gases is linear; thus an element of gas, dx, has a mass/unit area of ρdx and the entire product gas mass is $\rho\int_0^{\ell} dx = \rho\ell$

1. Conservation of mass (and assumption a):

$$c = \rho\ell \tag{B-1}$$

2. Kinetic energy of plate $= \frac{1}{2}m\upsilon_o^2$ (B-2)

3. Kinetic energy of gas $= \frac{1}{2}\int_0^{\ell}\rho u^2(x)dx$, but from assumption b $u(x) = \upsilon_o(\frac{x}{\ell})$, therefore

$$\frac{1}{2}\int_0^{\ell}\rho\ \frac{\upsilon_o^2\ x^2}{\ell^2}\ dx = \frac{\rho\upsilon_o^2}{2\ell^2}\int_0^{\ell}x^2dx = \frac{\rho\ell\upsilon_o^2}{6}$$

Substitution from Equation (B-1) gives

$$\text{K.E. gas} = \frac{c}{6} \upsilon_o^2 \tag{B-3}$$

4. If all the explosive energy E goes into K.E. of gas and plate, then from conservation of energy:

$$cE = \frac{1}{2} m \upsilon_o^2 + \frac{c}{6} \upsilon_o^2 \tag{B-4}$$

or

$$2E = \left(\frac{m}{c} + \frac{1}{3}\right) \upsilon_o^2 \tag{B-5}$$

and

$$\upsilon_o = \sqrt{2E} \left(\frac{m}{c} + \frac{1}{3}\right)^{-1/2} \tag{B-6}$$

If $m/c >> 1/3$ $\quad \upsilon_o \simeq \sqrt{2E} \sqrt{c/m}$ (B-7)

APPENDIX C

CORRELATION OF THE GURNEY CONSTANT WITH DETONATION VELOCITY

The writer showed[3] for head-on detonations the Gurney constant $\sqrt{2E}$ can be expressed as

$$\sqrt{2E} \approx \frac{0.605}{\Gamma-1}D \qquad \text{(C-1)}$$

where detonation product gases are assumed to obey a polytropic equation of state with a coefficient Γ such that

$$P_j = \frac{\rho_o D^2}{\Gamma+1}$$

where P_j is the detonation pressure, ρ_o is the initial density of the explosive and D is the detonation velocity. For tangential detonations the Gurney constant $\sqrt{2E'}$ is given by

$$\sqrt{2E'} \approx 0.95\sqrt{2E}\ . \qquad \text{(C-2)}$$

For many explosives $\Gamma \approx 2.8$. Then, according to Equations (C-1) and (C-2)

$$\sqrt{2E'} \approx D/3\ . \qquad \text{(C-3)}$$

However, for ANFO, P_j and D data obtained at Lawrence Livermore Laboratories* give $\Gamma \approx 2.3$. Consequently, for ANFO

$$\sqrt{2E'} \approx 0.44D\ . \qquad \text{(C-5).}$$

* Finger, M., et. al., "Proc. 6th Detonation Symposium," 729, (1976).

LEW-II - A Minicomputer Controlled Lightning Early Warning System

William W. Shurtleff
Division 1521
Sandia National Laboratories
Albuquerque, NM 87185

ABSTRACT

One of the problems with open-air testing using explosives is that a high static charge or nearby lightning strike has the possibility of prematurely igniting the explosives. Sandia National Laboratories has developed a system (LEW-II) which takes data from a matrix of potential gradient sensors and rebroadcasts this information to test operators using explosives. By this method, the system gives early warning of possible hazards and allows safe storage of explosive materials. This paper describes the LEW-II system and its use as a hazard warning and weather data collection system.

INTRODUCTION

One of the dangers of handling explosives is that a static spark or nearly lightning strike can cause their premature detonation. This is especially true in the Southwestern part of the United States where the low humidity allows large static buildups at all times of the year. Sandia National Laboratories in Albuquerque, New Mexico, a prime contractor to the Department of Energy, maintains a large number of testing sites which use explosives for shock tests, rocket sled test, etc. These sites need to be warned when there are large static (potential gradient) buildups in the area so that explosives can be safely stored. This paper describes such a warning system called the Lightning Early Warning II System (LEW-II).

The present system is actually the third version of a lightning warning system. The initial system, first put a line in 1969, was based around a relay scanner which collected potential gradient information from a small number of sensors and retransmitted it to simple displays. If the operators did not have the locations of the sensors memorized, the information did not mean much. Also the relays were not very reliable in a 24 hour, 7 day a week environment. In 1974, the relay system was replaced by a minicomputer controlled system with a more complete pg sensor matrix, weather stations, and displays using LED accentuated maps (1). The limitations to this system were: 1. Most pg information came in over telephone lines, thus limiting the movement of sensors and creating maintenance problems because telephone lines are notoriously error prone, 2. The displays could show at the most the state of 16 sensors with a LED "on" for sensors with readings over 2000 volts/meter (V/M) and "off" for lesser readings, . Any physical change in sensor location required a complete re-drawing of the silkscreened display map, and 4. The display could only be viewed by a small number of people due to its faceplate design. These disadvantages promoted a redesign of the computer system to the new system called LEW-II which should be completely operational in October, 1980 (2).

LEW-II OVERVIEW

A conceptual block diagram of the LEW-II system is shown in Figure 1. The entire system is controlled by a minicomputer system located at a central area. The minicomputer system contacts the pg sensor matrix using a radio frequency (RF) link. The RF link eliminates the need for the telephone lines and allows easy movement of pg sensors. There is also a single remote weather station which sends data to the computer on command. All the information input to the computer is formatted for local computer display, recorded for archiving purposes, and then rebroadcast to user displays over RF link and a single multidropped telephone line. New displays use CRT and microprocessor technology to enhance information understanding. All the major system components are described in the next section.

SYSTEM COMPONENTS

Sensors

The potential gradient sensors are based around a Sweeney P.G. Probe (B. K. Sweeney Manufacturing Company, Denver, Colorado) and a Sandia built RF control monitor (RFPG-II).

The probe is shown in Figure 2 and the RF monitor in Figure 3. The probe is based on the use of a radioactive source to create an ion cloud around it. As the pg increases, the ion flow to a plate is modified which creates a current proportional to potential gradient. This current is amplified and converted to a frequency for long distance transmission. The RF monitor system inputs this frequency proportional to potential gradient, and transmits the data back to the central computer when the monitor receives a correctly coded digital RF input (system code). The code is seven bits long allowing up to 128 possible RF stations. Both parts of RFPG-II (probe and monitor) are powered by batteries which are recharged using photovoltaic solar cells. Expected replacement time for the battery is six months, the same time span as the probe calibration cycle. A block diagram of the RFPG-II system is shown in Appendix A.

Central Computer System

The central computer system controls all the data acquisition, reformatting, storage, and rebroadcasting. It consists of an HP21MX series minicomputer with floppy disc, CRT terminal paper tape reader, and printing terminal as support peripherals. (See Figure 4) The floppy disc is used for program and data storage. The CRT terminal is used for initial program setup and central operator information display. The system is controlled using the RTE-M operating system and the application programs are written in BASIC language.

Data acquisition and output is controlled through two interfaces, the RFPG interface and the Weather Station interface. The computer, through the RFPG interface, sends out station codes and receives back potential gradient information. The RFPG interface is also used to transmit display data both by multi-drop telephone line and radio frequency link. The Weather Station interface is used to gather wind speed, wind direction, and temperature data from up to four weather stations; there is only one weather station in the system now.

The computer has access to all pg data about once a minute and to weather data about once every 15 minutes. This constant pg access rate could change to one based on maximum rate-of-change of pg if the battery drain on the RFPG-II inputs is too high.

Displays

There are two types of displays which the test operators use to look at the potential gradient data. The older type display is a carryover from the previous LEW system and uses a fixed map and LED matrix to represent pg stations (Figure 5). The newer display is somewhat similiar, but uses a CRT screen for the map and a microprocessor for display control (Figure 6). With both displays, the operator can continuously display the reading from one station of his choice as large LED characters plus the highest reading in the system. He can set caution and alarm limits which trigger audible and visual alarms, and contact closures when the limits for his displayed station are exceeded. On the older display map, LED lamps are lit when a station exceeds 2000 V/M. On the newer display CRT, the map is drawn by the microprocessor using information sent from the computer. All the stations pg readings are displayed and stations which exceed the preset "alarm" limit are blinking while the ones between "caution" and "alarm" set points are in reverse video. This CRT display information is also brought out to a rear connector as composite video. This allows a number of remote CRT displays to be generated from one central LEW-II display.

TYPICAL SYSTEM USAGE

Central Operator

Whenever the system is "rebooted" or brought up from a cold start, the central system operator must enter such information as the date, time-of-day, non-operational stations, and data storage information. From then on, the system operates automatically providing him with a pg map display and current system information. At any time, he can activate programs which can do such tasks as print historical information (archived on the floppy disc), run diagnostic maintenance programs, and print system status. These programs do not affect the normal data input, reformatting, and transmission of display information.

Remote Test Operator

The remote test operator uses the LEW-II Display as an integral part of his Standard Operating Procedures for explosives handling. The display can either be tied directly into a safety interlock network using the caution and alarm contact closure, or the map can be used to gauge the direction of movement of any lightning storms in the vicinity. In any case, the combination of map display, local pg reading, and caution/ alarm capabilities makes the LEW-II Display a very versatile safety warning device.

CONCLUSIONS

Historically, the earlier LEW systems have proven to be reliable, useful aids to safe explosive handling. It is hoped that the greater versatility and better human oriented output of the LEW-II system will make it an even more useful system.

References

1. A Minicomputer-Controlled Lightning Early Warning/Meteorological System, W. W. Shurtleff, SLA-74-0134, 1974.

2. "LEW-II": The New Lightning Early Warning System at Sandia National Laboratories, J. P. Boettger, Explosive Engineering and Safety Conference, June 3, 1980, Las Vegas, Nevada.

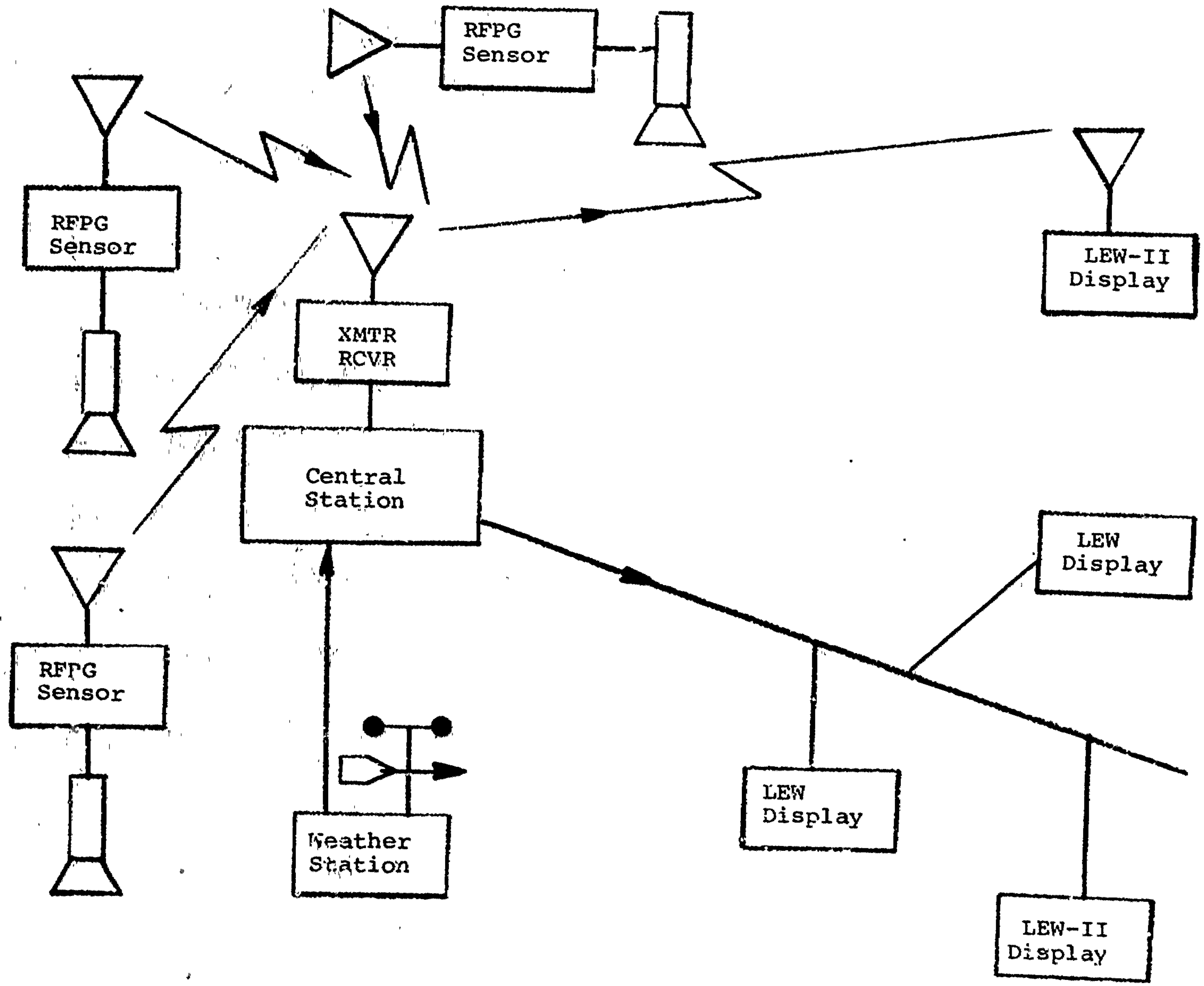

Figure 1. LEW-II Functional Block Diagram

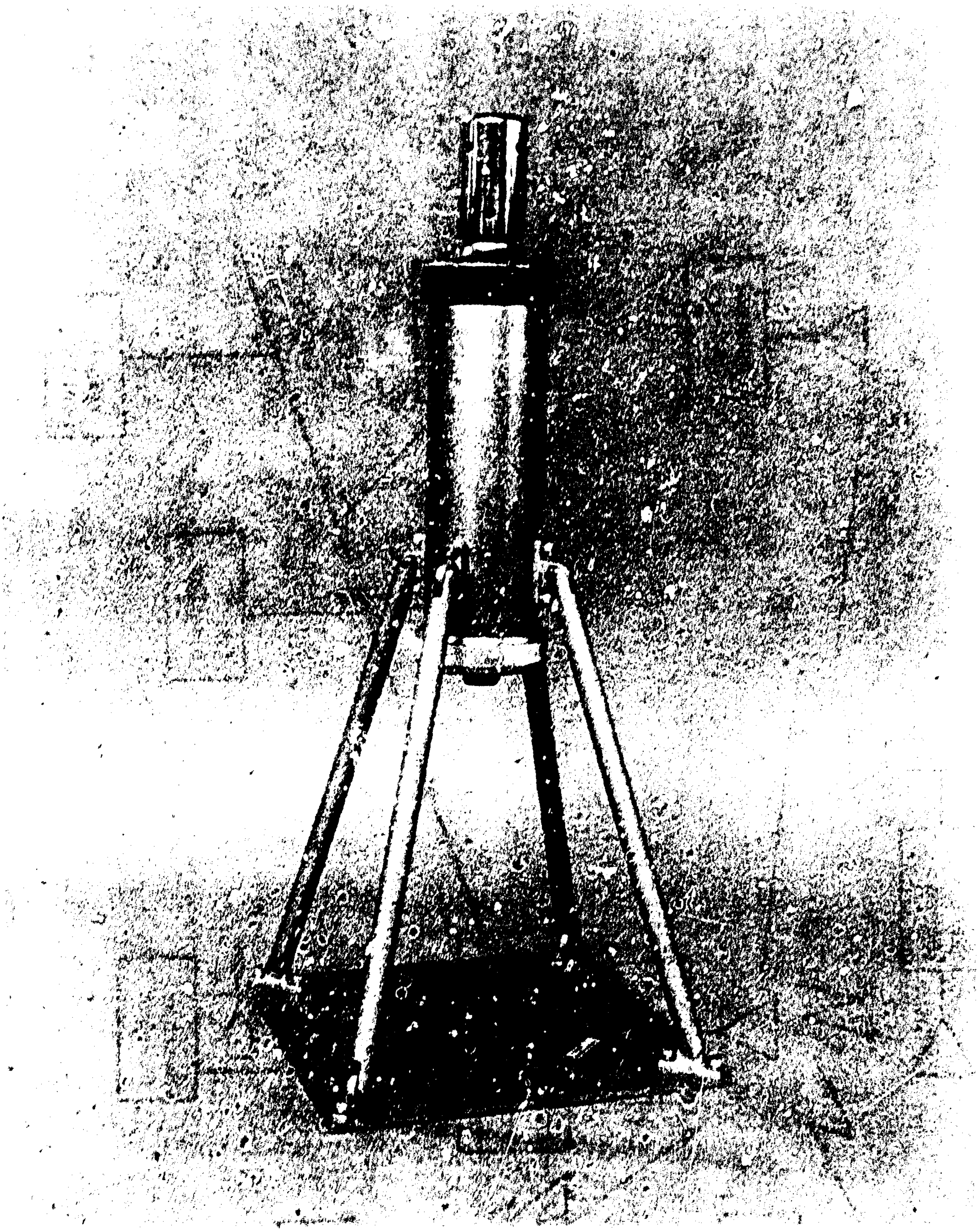

Figure 2. Sweeny Potential Gradient Probe

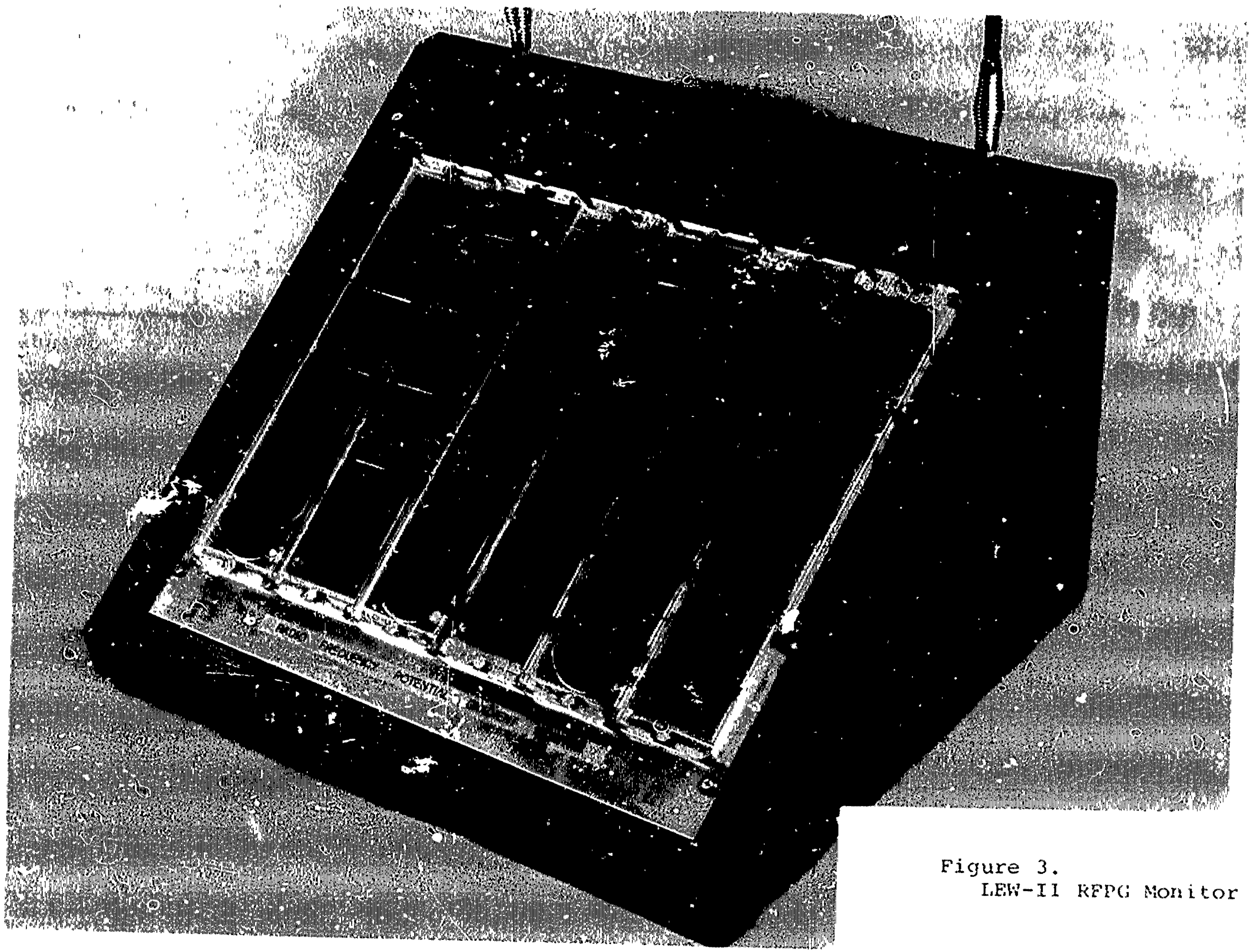

Figure 3.
LEW-II RFPG Monitor

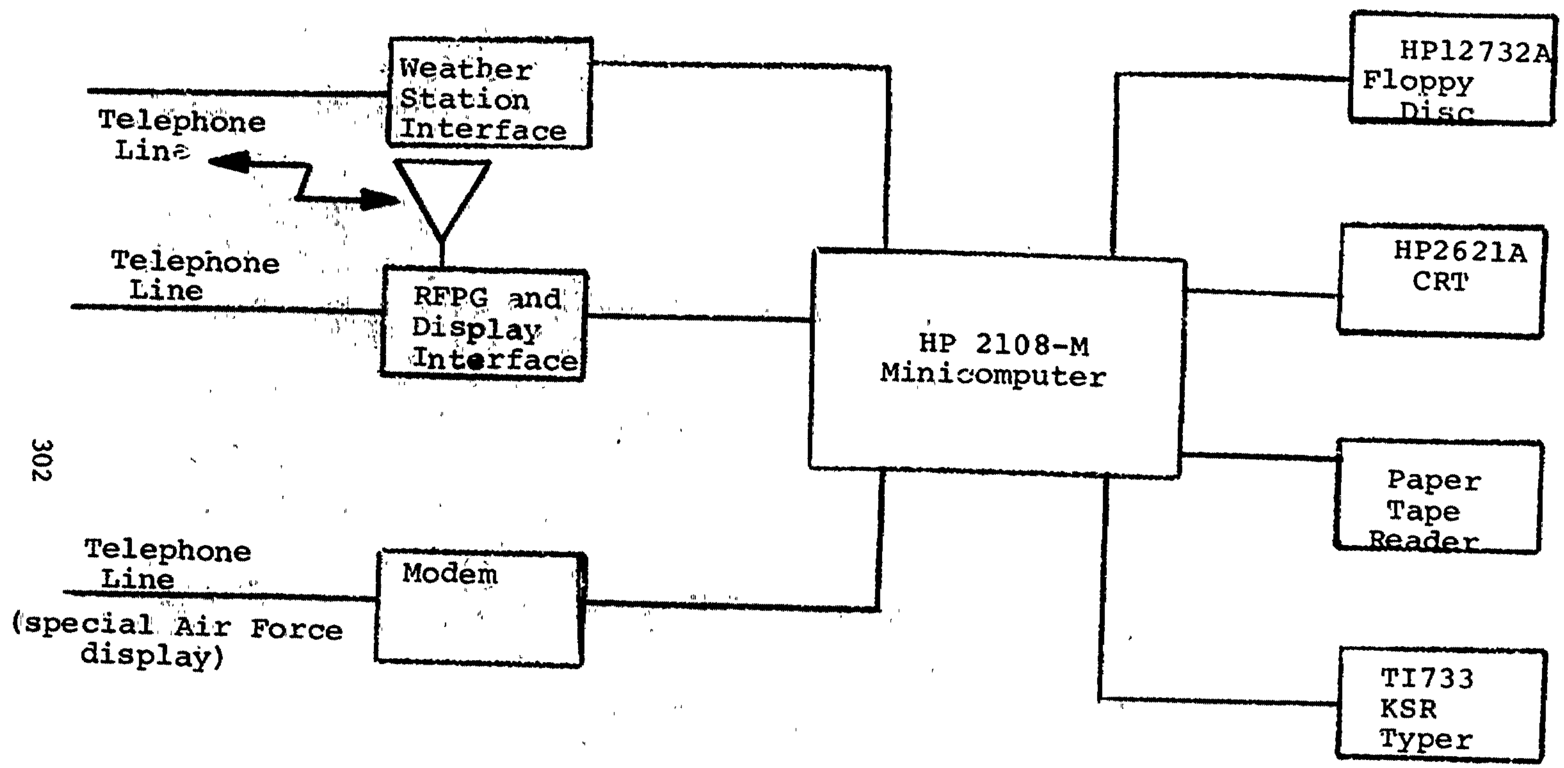

Figure 4. LEW-II Central Station

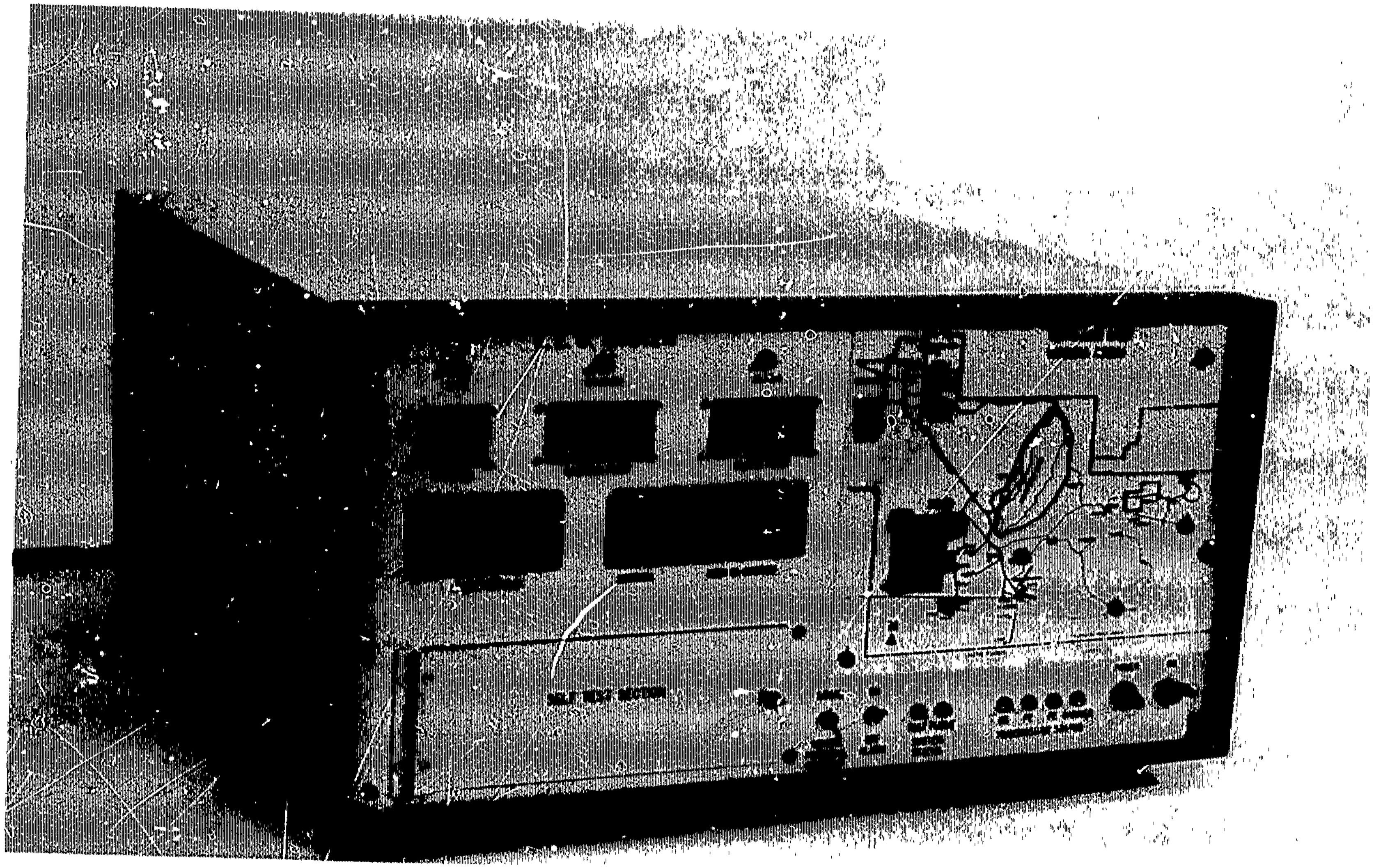

Figure 5.
Previous User Display

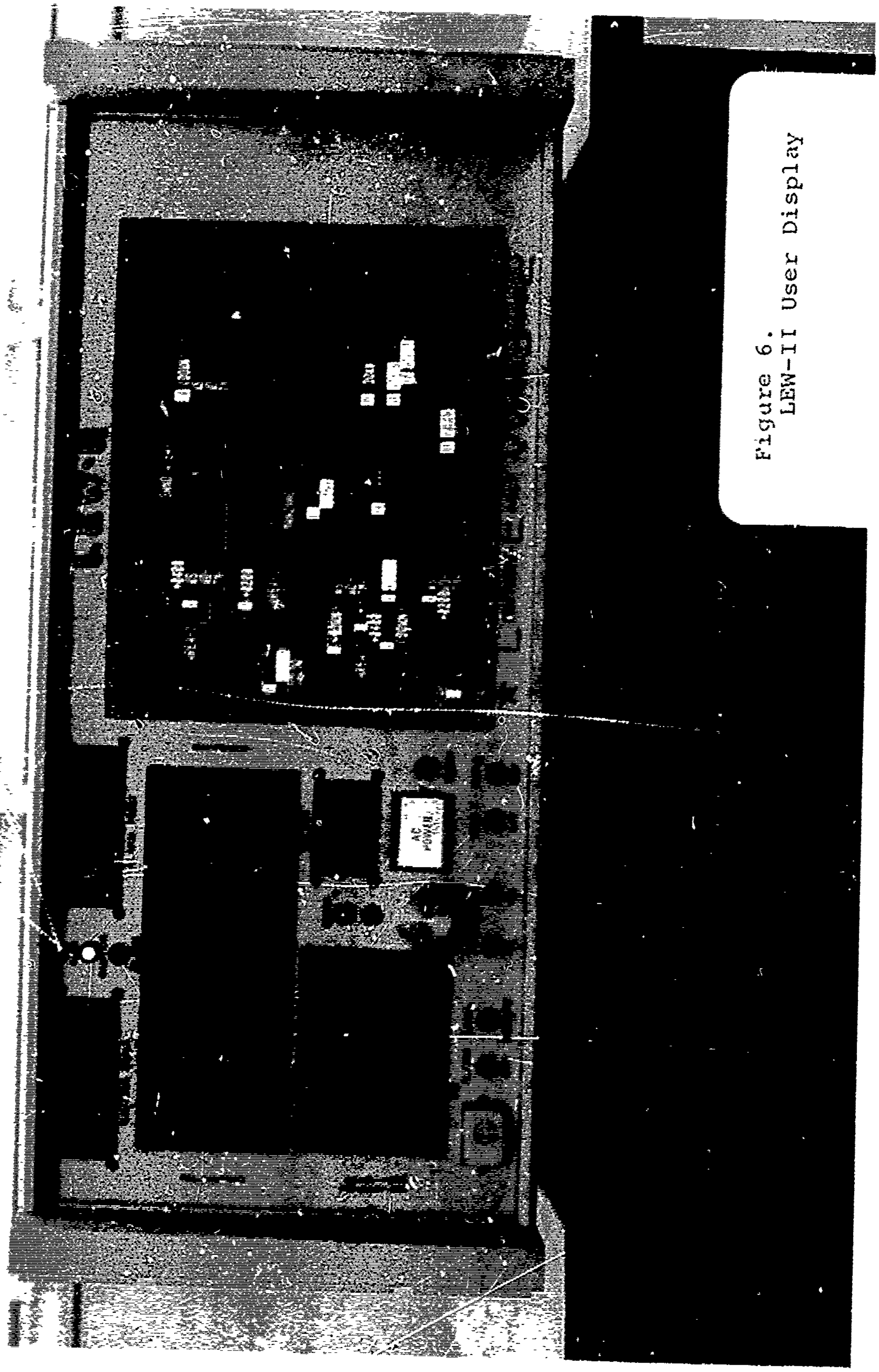

Figure 6.
LEW-II User Display

LIGHTNING PROTECTION AT INDIANA ARMY AMMUNITION PLANT

by

Charles C. Huang

US Army Engineer Division, Huntsville

I. INTRODUCTION

During July and August 1978 several thunderstorms occurred in the area where the Indiana Army Ammunition Plant (INAAP) is located. While there was no structural damage, the electrical systems at the Black Powder Manufacturing facility were damaged at several places by lightning. The damage was investigated and evaluated by INAAP personnel who concluded that the existing grounding and lightning arresters appeared deficient and recommended that a study be conducted to identify the deficiencies in the design or installation of the lightning protection system and to recommend corrective action. Also, it was planned that lessons learned from this facility's experience, when properly documented, would benefit the design and installation of other plant facilities with regard to lightning protection.

In February 1979, the Munitions Production Base Modernization and Expansion Agency, Dover, New Jersey, requested that the US Army Engineer Division, Huntsville, conduct the study. The study was completed and documented in the report entitled "Lightning Protection Study US Army Ammunition Plants," [52]* from which this paper is adapted.

II. BACKGROUND

The Black Powder Manufacturing Facility at INAAP was designed in 1973-1974; its construction was completed in 1977 and process equipment was installed and checked out in 1979. Lightning damage to lightning

*Bracketed numbers appearing throughout the text indicate cited references listed at the end of this paper.

arresters, electronic equipment and underground electrical cables occurred several times during the equipment installation and checkout period. The more severe damage occurred in July and August 1978. Lightning strokes were seen at the 140-foot lighting towers, and subsequent inspection revealed that four out of six lighting towers had sustained damage.

The design of the facility was required to comply with the following safety codes: AMCR-385-100, Safety Manual; NFPA 78, Lightning Protection Code; National Electrical Code (NEC); and OCE Guide Specification, Lightning Protection System.

During the intervening years, the revisions to these codes caused some of the requirements to differ from those of 1973 when the facility was designed. It follows that some design features that satisfied the 1973 requirements no longer comply with today's code requirements. In addition to the investigation into the current compliance with the codes, a literature search was conducted to obtain the latest information on lightning phenomena and lightning protection technology that could be used as guidance for design improvements, or as a basis for future revisions to the current safety codes.

Following completion of the study, a follow-up visit was made to INAAP in May, 1980; it was found that satisfactory progress had been made on implementing recommended corrective actions.

III. DESIGN REVIEW AND ONSITE INVESTIGATION

Based on our design review and onsite investigation conducted in April 1979, the findings on the lightning damage are summarized below.

A. Equipment Damage

The equipment damaged by the lightning in July and August 1978 is listed below in Table 1.

TABLE 1

1. Fox 2/30 Computer	2 - Memory Units
2. Modicon	1 - Power Supply P421
3. Process Control Console	1 - Pushbutton SW 51-R
	7 - Line Receiver Printed Circuit Boards

TABLE 1 (Continued)

4. Lighting Towers	4 Sets - Circuit Breakers, Connectors, Cables, Contactors and Control Transformers
5. Emergency Power System	Automatic Transfer Switch and Controls
6. Honeywell Fire Alarm System	Tens of Thousands of Dollars Worth of Lightning Protectors and Electronics
7. Power System	Lightning Arresters Blew Up, Fuses Blew Up, Transformer Burned

B. Primary Power System

The 12-kV primary distribution system was frequently struck by lightning. It is protected by an overhead shield wire and by lightning arresters along the pole line. The original design called for distribution class explusion-type (7-kV) lightning arresters, but these arresters were changed to valve-type lightning arresters of the same class and rating for installation. Later it was found that the 7-kV valve-type (distribution class) lightning arresters were inadequate and they were replaced by ones rated at 12 kV. During the thunderstorms in July and August 1978, several lightning arresters blew up and a transformer burned. The current AMCR 385-100 requires intermediate class valve-type arresters for the protection of the primary system.

C. Secondary Power System

No lightning arresters were provided in the design and none were originally installed on the 480-V distribution system. As a result the more sensitive equipment was damaged (see Table 1).

Recently, properly sized solid state Transtectors were installed. They appear to be providing adequate protection. The current AMCR 385-100 requires the installation of valve-type secondary arresters for the secondary power system.

D. Street Lighting System

The 480-V street lighting system, which has no lightning arresters, is installed below the 12-kV lines and generally shielded from direct strokes of lightning. The equipment in this system experienced some damage due to moisture in the enclosures, but this problem was eliminated when heaters were installed to maintain dry enclosures.

E. Lighting Towers

Lightning had struck these towers on several occasions, but apparently did not damage the light assembly and circuits at the top of the towers, but did damage components at the base and the power leads. The resistance from the ground rods to earth was measured and found in the range of 5 to 12 ohms. No lightning arresters were installed at the base of the towers. Another possibility of arcing which damaged cables and components at the base of the tower is due to water accumulated in the cavity of the tower base. Improvement in grounding, installation of lightning arresters and proper drainage at the tower base are needed. Further, the electrodes should have been connected to the nearest counterpoise as required by AMCR 385-100. The pole grounds were not tied into the system ground counterpoise.

The intent of the original design was to use the 140-foot lighting towers to serve as grounded masts each of which would provide a cone of protection. Each tower served as an air terminal and had two ground electrodes. The height and base of the cone of protection were established according to the AMCR 385-100 (i.e., the height of the cone is the height of the mast and the circular base of the cone has a radius equal to twice the height of the mast). During the construction, however, these lighting towers were relocated further away from buildings for fear that if the towers collapsed they might fall on nearby buildings. This action jeopardized the originally planned shielding effect on the buildings.

F. Uninterruptable Power System (UPS)

The computer (Fox 2/30) and the Modicon module power supply, which are connected to the UPS, were damaged. Other sensitive equipment items damaged in the process control console include one pushbutton switch, seven line receiver printed circuit boards, and two line driver printed circuit boards (see Table 1).

G. Honeywell Fire Alarm System

Field sensor and data link lines of the system were protected by Honeywell lightning protectors. These lightning protectors were found inadequate as evidenced by the fact that a significant quantity of lightning protectors and electronics was destroyed during thunderstorms in the past.

H. Underground Cable

Unshielded cables enclosed in plastic conduits are used for power and control circuits. The only shielded cables in plastic conduits are those used for computer, analog and television circuits. Lighting tower supply cables were considerably damaged. The insulation of the control cables may have been degraded by high voltage transients. The Honeywell fire alarm sensor circuit and data links may also have suffered damage, even though these low-voltage circuits still appear to be functioning.

I. Buildings

The installation of integrally-mounted lightning protection systems on buildings was found to be incomplete and required a detailed survey to determine safety compliance.

A survey of INAAP subsequent to the April 1978 onsite investigation indicates that all air terminals are correctly installed with the exception of those on the roof of the Raw Material Building where the steel ladders extend above the top of the nearby air terminals [53]. It was also found by INAAP personnel that: [53]

1. Separate grounding paths had been provided for each system and all metal piping and other conductors had been grounded at the service entrance to buildings.

2. All metal bodies had been properly bonded; all equipment had used separate ground wires.

3. All lightning arresters, overhead ground wire and pole-mounted equipment had been separately grounded.

4. Door frames had not been grounded.

5. All conductive floors had been properly connected to grounding plates.

J. Ground Resistance

During the April 1979 onsite investigation, several measurements were made of typical ground resistances. The data obtained are listed below in Table 2.

TABLE 2

FROM	TO	RESISTANCE (OHMS)
Plant Entrance Pole - 12-kV Line Lightning Arrester (LA)	Earth	5.40
Reservoir Pole		
12-kV Line LA	Earth	2.5
Aerial Wire	Earth	2.5
Reservoir Building Ground Pipe	Earth	0.15
Plant Counterpoise	Earth	0.15
Process Building	Counterpoise	0.14
Lighting Tower Ground Rod (with 2 ground rods; not connected to counterpoise)	Earth	6 to 12
*Lighting Tower Ground Rod (with 4 ground rods; connected to counter-poise)	Counterpoise	2.3 to 6.2

*Measurements made by INAAP personnel subsequent to the April 1978 onsite investigation. [53]

K. Soil Resistivity

Subsequent to the April 1978 onsite investigation, INAAP personnel made additional ground measurements to determine typical soil resistivity at INAAP. The four-terminal method used for the measurements was in accordance with the manual for the Megger Earth Tester. The soil at the time of testing was wet from recent rains. [53] The results are tabulated below in Table 3.

TABLE 3

Location No.	Probe Spacing	Probe Depth	Indicated Resistance	Calculated Resistivity
1	240"	12"	2.66 ohms	10,188 ohm-cm
2	240"	12"	1.99 ohms	7,621 ohm-cm
3	120"	6"	5.20 ohms	9,959 ohm-cm
4	120"	6"	4.33 ohms	8,291 ohm-cm

L. Safety Criteria Review

The principal regulatory documents which provided safety criteria for lightning protection design in 1973 either have been updated or are under revision. Table 4 summarizes their current status.

TABLE 4

Design Criteria Principal Documents	Available for Original Design-1973	Available Since 1973
AMCR-385-100, SAFETY MANUAL	1970 1971 Change	Change 2 - 1974 Change 3 - 1977
NFPA 78, Lightning Protection Code	1971	1977
NEC	1971	1977
OCE Guide Specifications	Similar to AMCR-385-100	(Under Revision)

IV. MANDATORY CORRECTIONS

Based on the findings of the design review and the onsite investigation, the following corrective actions are necessary in order to comply with the current safety code requirements.

CORRECTIONS	REFERENCE
1. Replace all existing expulsion-type lightning arresters (LA) with intermediate valve-type LA on the primary side of the main disconnect switches or circuit breakers.	AMCR 385-100-6-11
2. Provide secondary valve-type LA on each secondary service entrance.	AMCR 385-100-6-11
3. A surge-protective capacitor shall be connected to each ungrounded service conductor.	NEC 1978-502-3
4. Earth resistance of each ground connection shall not exceed the limits required.	AMCR 385-100-8
5. All ground rods should be connected to a common counterpoise where possible.	NFPA 78 LPC 1977 3-22
6. Ground the air terminals and 140-foot lighting towers properly.	AMCR 385-100-8-3
7. Install missing air terminals and bond all door frames.	AMCR 385-100

V. DISCUSSION

During the past several years there has been considerable concentration on the development of lightning protection technology. Some of the principal subjects reviewed during the study include: Shielding, Surge Arresters, Systems Protection Philosophy, and Equipment Vulnerability. A slow process is involved in incorporating the advanced technological data into the regulatory documents, which, as a result, inevitably trail the state-of-the-art by several years. As an example, if the Black Powder Facility at INAAP had been designed in 1973 to comply with today's safety criteria, many of the difficulties experienced at the plant could have been avoided. It is deplorable that the safety of a plant becomes inadequate even before the plant begins production. It follows that a conscientious designer, while he must comply with the current safety codes, should be knowledgable about the state-of-the-art in lightning protection, and capable of identifying potential problems peculiar to the design project on hand and judiciously applying up-to-date data to seek solutions to problems.

The information on lightning protection that was gleaned during the study is grouped under various topics and presented below. This is an attempt to provide a glimpse of copious information available and useful for the planning of lightning protection systems for future projects. For those who wish to read the original papers, the bibliography at the end of the paper will be found useful.

A. Lighting Towers

The six 140-foot lighting towers are the highest structures at the facility and their attraction of direct strokes is highly probable. For instance, for an Isokeraunic Level (IKL) of 45 at INAAP, the likelihood of direct strokes can be roughly expressed as follows:

Direct Stroke Probability [54]
(Strokes per Year, 45 IKL)

Flat earth	23 per square mile
Roof, 25 ft high	0.15 per 40,000 sq ft
Overhead ground wire, 60 ft high	1.5 per mile
Mast height, ft	
70	0.23 each mast
250	1.5 each mast
500	3.0 each mast

A rough estimate based on the above data indicates that any one of the towers could be struck by lightning within less than two years. After the initial stroke, the atmosphere may still be inonized providing for the formation of a dart leader (see Figure 1) which provides a path for subsequent strokes without the process of steps. A lightning flash

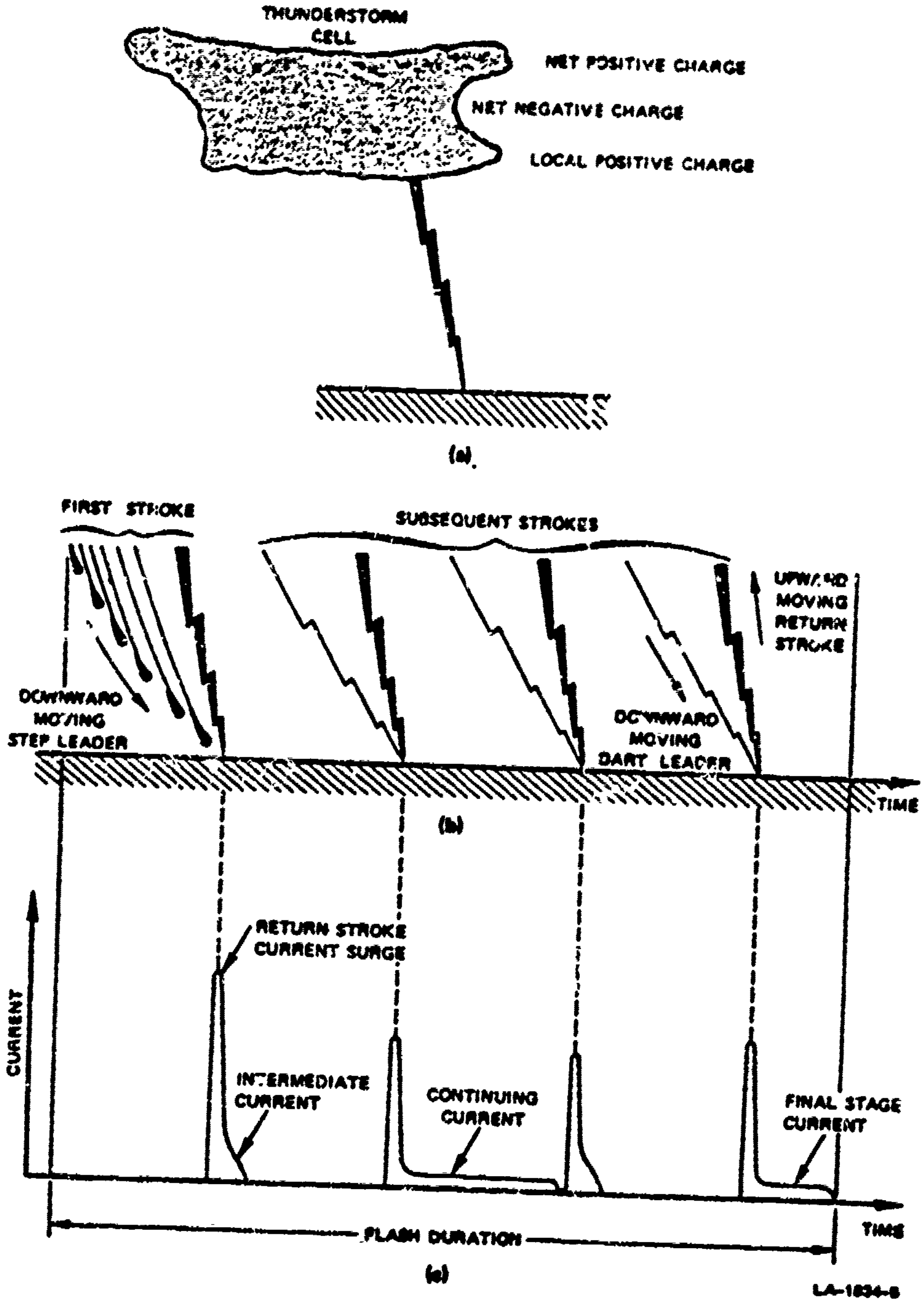

Figure 1. Schematic Illustration of Processes and Currents Occurring During a Flash to Ground*

* Extracted from Reference [9]

may include several strokes. According to '. C. Dodge (NASA Hdq., 13 Feb 79, NASA Workshop on Lightning Thunder Days (ISOKERAUNIC MAP), "The flashing rate of a given thunderstorm varies with storm lifetime, latitude, season and specific meteorology, but variability is so great that the flash rate per the conventionally used thunderstorm day relationship is virtually undefined." [23, 24, 25, 27. 28, 29, 30, 31, 32, 33, 34, 39, 40]

A typical current waveform of the predominant type of lightning stroke, illustrated in Figure 2, rises to its crest value in 1.5 μsec (t_1) and decays to half the crest value in 40 μsec (t_2). For example, if the

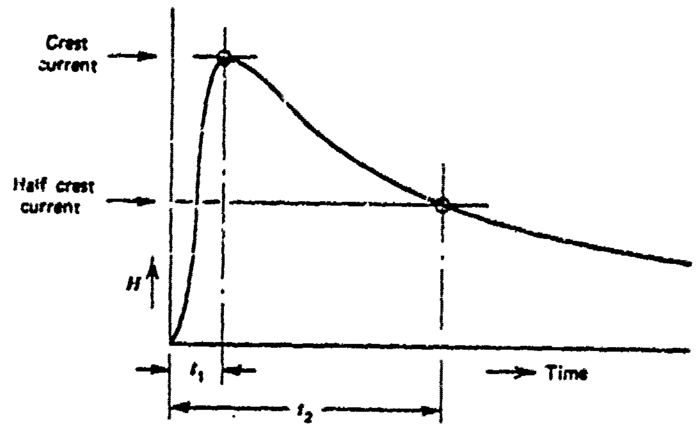

Figure 2. Typical Lightning-current Wave Shape.

crest (peak) current is 100 kA, the waveform is then described as 100 kA, 1.5 X 40. For a 140-foot high tower, the lightning stroke current according to Golde [50] (as illustrated in Figure 3) would be on the order of 35 kA.

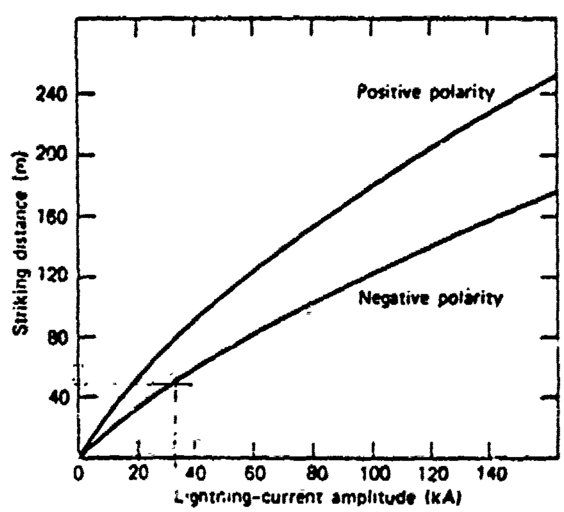

Figure 3. Striking Distances of Negative and Positive Lightning Strokes.

This is the magnitude of a lightning stroke of average severity. The most severe lightning environment found in the general area of INAAP could have a crest current of 200 kA for the first stroke and 100 kA for the second stroke. The current rate of rise of the first stroke could be 90 $kA10^{-6}s$ and that of the second stroke 180 $kA10^{-6}s$. [4, 10, 11, 12, 9]

The importance of lowering the ground resistance in conducting lightning stroke current to the earth can be illustrated by a numerical example as follows. The top of the lightning protection system is raised to a potential with respect to earth as given by the basic formula:

$$u = iR + L\,di/dt$$

For the purpose of illustration, let us assume an intense lightning crest current i = 100 kA injected to the 140-foot lighting tower and a ground resistance of R = 12 ohms. The ground resistance is a measured value from two ground electrodes of the lighting tower to the earth (see Table 2). Since there is no horizontal ground wire provided beyond the ground electrodes, the second term $L\left(\frac{di}{dt}\right)$ is ignored for a rough estimate of the potential difference at the base of the tower with respect to earth. Thus, u = 1.2 MV with a voltage of such magnitude, damage of equipment at the base and damage of buried cables around the tower should be expected.

B. Zone of Protection

Based on the work of Whitehead and Lee [37], the latest design data have been adopted by NFPA78-1977 for the zone of protection provided by a single aerial mast or an overhead ground wire exceeding 50 feet high. For a 150-foot high mast the zone of protection lies under the arc which is tangent to the earth and the mast, with a radius equal to the striking distance of the lightning (the height of the lighting tower in this case) as shown in Figure 4. The 300-foot diameter rolling sphere principle is based on the assumption that an adequate clearance exists between the mast and protected buildings to provide a BIL of 1400 kV. (A clearance of 7.6 feet would be required based on 185 kV for one foot of air insulation.)

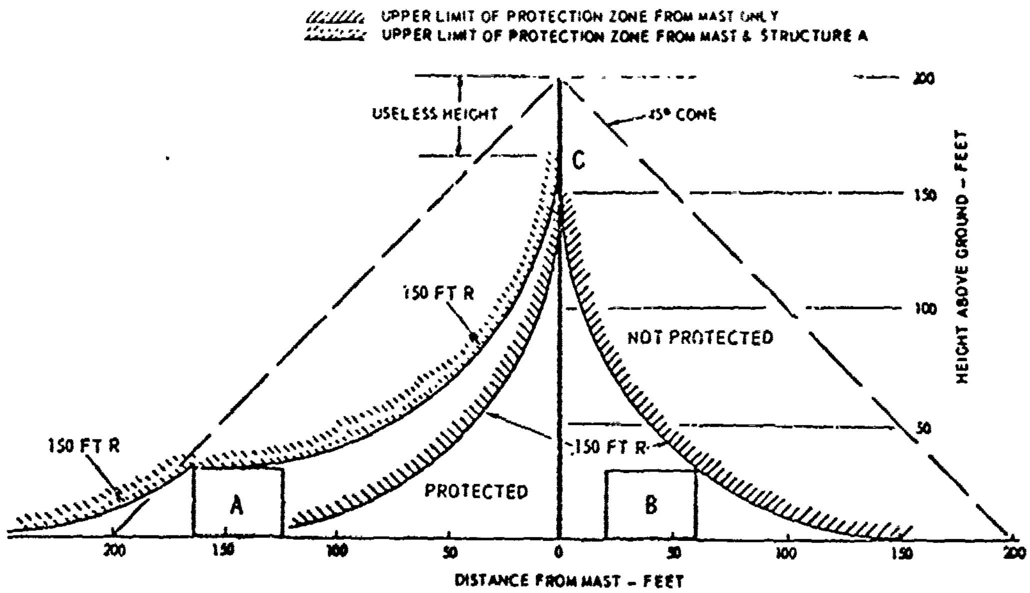

Figure 4. 300-ft Diameter Rolling Sphere Principle*

* Extracted from Reference [37]

NFPA78-1977 considers that a 100-foot high mast should provide adequate protection, and its associated zone of protection is defined by a 200-foot diameter rolling sphere. This regulatory document also specifies that the minimum clearance between the mast and a building is 6 feet.

The zone of protection provided by masts and overhead ground wires as defined in the current AMCR 385-100, Chapter 8, may need to be reviewed and updated as appropriate to reflect the current design guidance available.

C. Shield Wire

The 12-kV primary distribution system at INAAP is shielded by an overhead ground wire (shield wire). When lightning strikes occur, the shield wire is struck and conducts some energy to ground. The shield wire also reduces the induced over-voltage on the line by 25 to 40 percent and reduces the steepness and duration of the over-voltage transients. When the lightning stroke energy level exceeds the basic insulation level (BIL) of the shield wire, a lightning flashover from the shield wire to the system phase wire occurs and injects part of the lightning energy onto the line. (The air spacing around a shield wire is generally considered to have a BIL of 185 kV per foot. A wood pole is about 35 kV per foot, and a 10 inch diameter by 5-3/4 inch high disc insulator is normally rated at 95 kV.)

It has been found, however, that overhead lines below 69 kV may not be readily protected by the shield wire because the separation between the shield wire and the lines is usually too small to provide adequate insulation [54]. It has been the practice of using lightning arresters to protect the equipment in the system. In areas of IKL 30, the number of arresters required for each mile of line is indicated below in Table 5. These numbers are based on the probability of four outages per year for 100 miles of overhead distribution line. [54] If this practice is followed, lightning arresters for 12-kV lines would be required on every wood pole at a spacing of approximately 132 feet.

TABLE 5

	Line Voltage, kV	No. of LA Per Mile on Each Phase
Wood Pole and Cross Arms	13	40
	35	15
	45	7
Steel Poles and Cross Arms	13	47
	35	27
	45	15

D. Lightning Arrester

AMCR 385-100 requires intermediate, valve-type lightning arresters on the primary side of the transformer and secondary, valve-type lightning arresters as close as possible to the electrical service entrance to the building.

Our recommendation on locations of lightning arresters on the primary distribution system is shown in Figure 5.

In order to select a cost-effective lightning arrester, the following factors must be taken into consideration:

1. The impulsive withstand strength of the protected equipment.

2. The arresters' capacity for lightning surge current.

3. The arresters' voltage rating at the power frequency (i.e., 60 cycle voltage) and their capacity for clearing the crest of follow current.*

*The follow current is defined as the power or system current that flows in an arrester after it has been sparked.

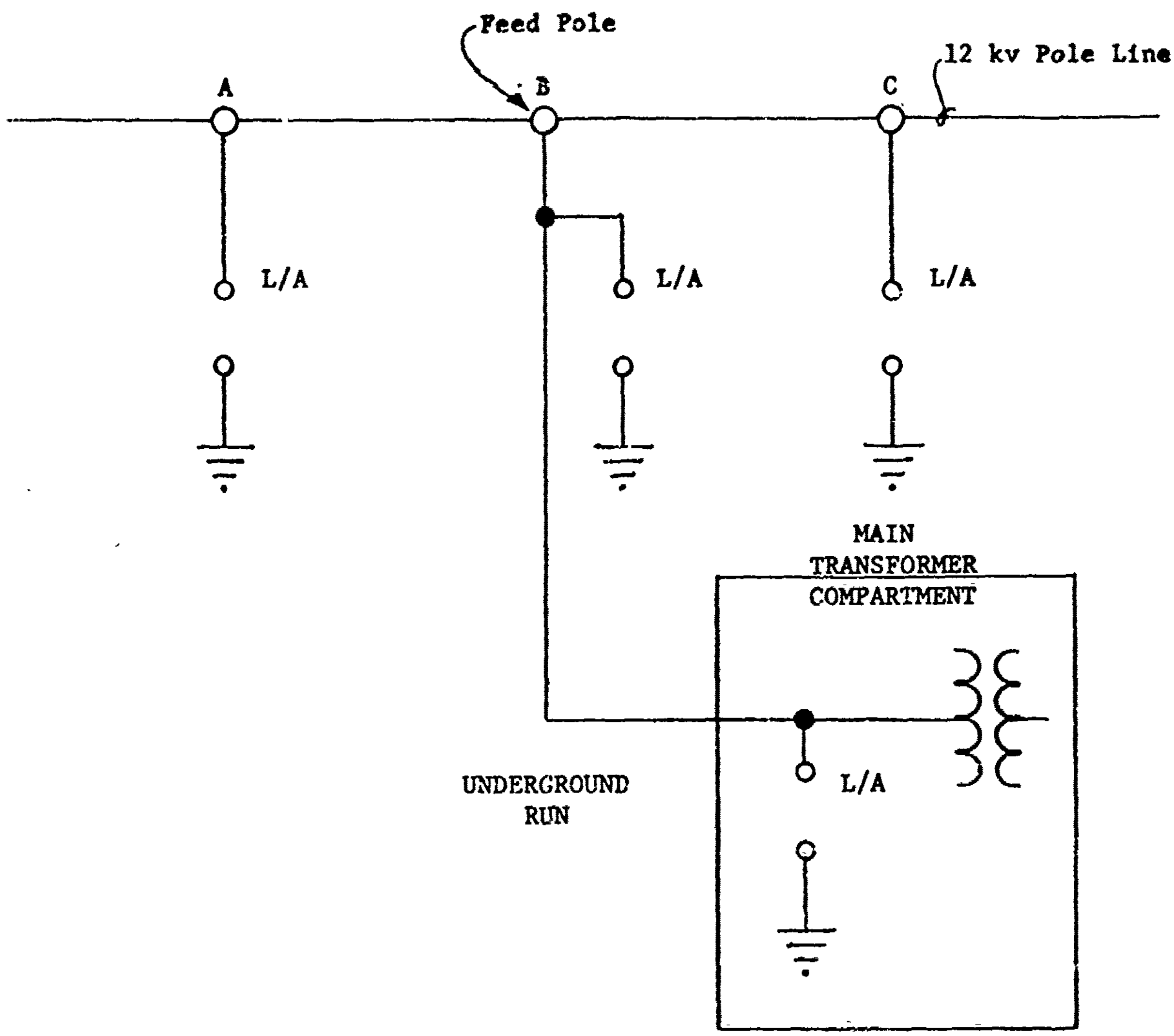

NOTE: At dead end poles feeding critical loads, either (A) or (C) LA

Figure 5. Schematic - Location of Lightning Arresters

The voltage rating of an arrester must not be exceeded. This rating is the maximum voltage of power frequency applied to the arrester's terminal against which the arrester can interrupt and restore itself to an insulator. The rating is maximum and has no plus tolerance [51]. If a lightning arrester is improperly selected, it will fail to function as required. If the lightning arresters are under capacity they will blow up and if they are over capacity they will render no protection to equipment in the system. The repeated failure of the lightning arresters in the past at INAAP manifested the deficiency of selecting lightning arresters which were inadequate with regard to rated capacity.

E. Sensitive Equipment

It has been determined that many electronic components cannot tolerate any significant transient energy without malfunctioning or experiencing damage. Tables 6 and 7 show the minimum energy levels which will cause a malfunction or a burnout of typical electronic components.

In view of the failure of the control equipment and the Honeywell fire alarm system at INAAP, it may be inferred that the original design did not provide adequate protection for this sensitive equipment. For a proper design, interfaces between various types of circuits must be arranged to protect against unwanted coupling, and more effective surge protectors must be provided.

The underground wiring for process control systems and other low-voltage and sensitive circuits should be enclosed in steel conduits without mixing power and signal or control wiring. Separate grounding must be used for each type of system and should be connected to earth at one point in each complex [14].

Protective devices are available to achieve any desired degree of protection. Principal types of protective devices for sensitive equipment are listed in Tables 8 and 9. To apply these devices to attain the level of protection needed, a sound engineering evaluation must be performed to match surge protectors of proper type and adequate capacity with the types of equipment to be protected. The ground resistance from the electrode to earth should be low, and the surge protectors must be located as close as possible to the protected equipment. It has been suggested that the ground resistance for grounding such sensitive equipment should be at a level of about 3Ω or less. [54]

Table 6. Examples of Energy to Cause Permanent Damage*

TYPE	ENERGY, JOULES	MALFUNCTION
Relay (1 amp)	1×10^{-1}	Welded contact
Relay (low current)	2×10^{-3}	Welded contact
Microammeter	3×10^{-3}	"Slammed meter"
Fuel Vapor	3×10^{-3}	Ignition
Explosive Bolt	6×10^{-4}	Ignition
Squib	2×10^{-5}	Ignition
Squib	6	Ignition
Filter Pin Connector	4×10^{-2}	Leakage
Solid Tantalum Capacitor	1×10^{-3}	Not stated
Metal Oxide Resistor	8.7×10^{-2}	10% Resistance Change Predicted
Metal Film Resistor	1.2×10^{-2}	" " " " "
Carbon Film Resistor	1.1×10^{-1}	" " " " "
Wire Wound Resistor	3.8×10^{-1}	" " " " "

*Extracted from Reference [49]

Table 7. Minimum Energy Level To Cause Burnout or Upset*

Function	Device	Minimum energy (J)
To cause burnout	Microwave diode	1×10^{-7}
	Analog integrated circuit	8×10^{-6}
	Field-effect transistor	1×10^{-5}
	High-speed switching diode	2×10^{-5}
	Switching transistor	5×10^{-5}
	Digital integrated circuit	8×10^{-5}
	Tunnel diode	5×10^{-4}
	Rectifier diode	6×10^{-4}
	Relay	2×10^{-3}
	Silicon controlled rectifier	3×10^{-3}
	Microammeter	3×10^{-3}
	Audio transistor	5×10^{-3}
	Vacuum tube	1.0
To cause circuit upset	Integrated digital circuit (flip-flop)	4×10^{-10}
	Discrete component digital circuit (flip-flop)	1×10^{-9}
	Memory core	3×10^{-9}

* Based on Reference [49]

Table 8. Characteristics of Some Protective Devices*

SECONDARY ARRESTERS	VOLTAGE CLAMPING RATIO	ENERGY MAX	TIME OF RESPONSE	MODE
Carbon Blocks	High	High	Slow	Crowbar
Spark Gaps	High	High	Slow	Crowbar
Thyristors with Resistors		High	Slow	Crowbar
Gas-Discharge Tube	High	High	Slow	Crowbar
Metal-Oxide Varistors (MOV)	Medium	High	Fast	Crowbar (Short Life)
Silicon, Solid-State Multiple Stage	Low	High	Fastest	Transient Clipping

*Based on Reference [1]

F Rotating Machinery

The impulse withstand level of the insulation in rotating machines is usually lower than the level of insulation in stationary electric apparatus. It has been suggested that a special surge arrester together with an LC circuit (see Figure 6) be used to provide protection for isolated rotating machines, especially for those located in remote areas where little shielding is available.

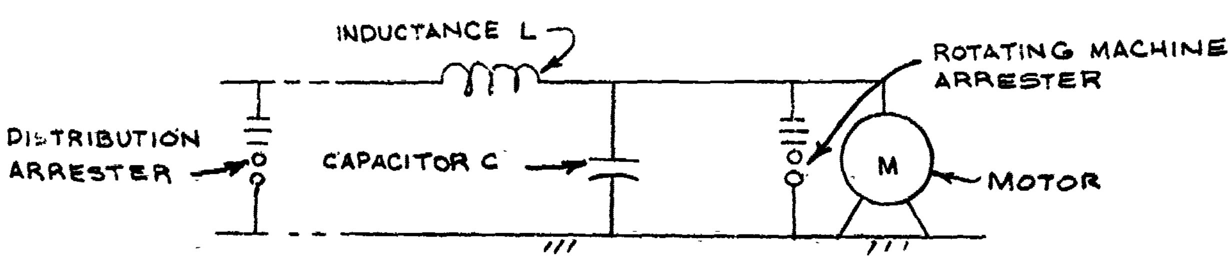

Figure 6. Protection for Rotating Machines

If there is a step-down transformer between the line and the motor, the transformer supplies all the required inductance. Capacitors are still required for each motor terminal (about 1 μfd for 480 V).. If the motor is operated off the voltage of the line, air inductance is needed for each incoming line (about 200 μ henry). [54]

Where there are four or more motors at a location operated in parallel from a line, the transient voltage resulting from lightning branches into four or more paths and is thus reduced. The reduction in voltage by branching has been found to be a suitable protection in itself, and there is no need for additional protection. It has been suggested, however, that wherever three or fewer motors are installed in a location from an exposed line, the protection of special surge arresters and LC circuits should be provided. [54]

G Underground Cables

AMCR 380-100, Chapter 6, requires that the last 50 feet of light and power service to explosive buildings must be underground. Service to inert buildings may be overhead. In practice, central process control rooms (or buildings) and other low-voltage circuits involving critical and sensitive equipment are usually fed by underground cables. Because of economic considerations, the use of plastic conduits is a common practice. Plastic conduits are non-conductive (except for a certain semi-conducting polyethylene type) and provide no shielding for the cables inside. From a lightning protection viewpoint, metal conduit is an ideal application for underground cables. Metal conduit, however, is expensive and is normally justified only for cables to equipment whose failure may result in significant loss of production time or jeopardy of safety.

Apart from the use of metal conduits, the lightning protection for underground cables using plastic conduits can be greatly improved at low cost by providing separate underground shield wires. These wires protect the cables from direct strikes by conducting some of the energy to earth. (Aerial masts or overhead ground wires also provide shielding within their zones of protection.) The zone of protection of underground shield wires and the clearance required between conduits and the shield wire must be established with consideration for the severity of lightning incidence and the earth resistivity at the site.

With the protection of shield wires, induced transient disturbances at a lesser magnitude still exist on the cables. For protecting critical and sensitive equipment, the use of appropriate surge protectors is the solution. As stated earlier to minimize induced transients, wiring for process control systems should be enclosed in conduits and not mixed with wiring for power systems or low-voltage signals.

Table 9. Comparison of Transient Protectors*

TYPE	FAILURE MODE/ OPERATED CONDITION	SELF-EXTINGUISH AFTER SURGE	RESPONSE TIME - ESTIMATE (SEC)	PEAK PULSE CURRENT FOR 1ms (AMP)	PEAK ENERGY - 1 ms PULSE (JOULES)	VOLTAGE RANGE (VOLTS)
Gas Discharge devices - (Bipolar) (Spark Gap)	Open almost shorted	Yes (Possible)	10^{-6}	10^3 or more	10^2 to 10^3	75 to 10,000
Semi-Conductor Breakdown Diodes (unipolar)	Short clamped	Yes	10^{-9}	1 to 10	10^{-2} to 10^1	4 to 200
$ZnO-Bi_2O_3$ varistors (Bipolar) MOV varistors	Degraded then shorted clamped	Yes	10^{-9}	50 to 100	1 to 10^2	33 to 1400

* Based on Reference [19]

VI. CONCLUSIONS

It is well stated in NFPA 78-1977: "The best time to design a lightning protection system for a structure is during the planning phase and the best time to install the system may be during construction." It is found in this study that retrofitting costs both time and money. Based on what has been learned from this study, the following suggestions are submitted to the engineering and safety communities for their consideration and actions.

A. The design agency should follow a systematic approach to obtain a safe and cost-effective system for lightning protection for a given facility. This approach should be no different from any other engineering task requiring sound engineering practice and observance of code requirements in order to attain prescribed objectives. Figure 7 illustrates a flow chart showing the steps that may lead to a sound and economic design. (1) The site information, particularly the data on ground resistivity, should be obtained in the early stages of planning so that appropriate schemes can be developed to use the earth as an effective discharge terminal. (2) The susceptibility of various protected equipment must be recognized so that proper type and adequate rating of surge diverters can be selected for particular applications. (3) While observance of code requirements is mandatory, judicious use of up-to-date information on lightning protection technology for solving certain less common design problems should be encouraged. (4) Safety and economics are the ultimate goals of any engineering endeavor. Developing alternatives during planning for cost evaluation is one way to obtain the most cost-efficient and safe design.

B. The safety community should maintain the codes in such a way that they are as close as possible to the current state-of-the-art in lightning protection technology. More frequent updating is a solution. It is recommended that AMCR 380-100, Chapters 6 and 8 be reviewed and updated as appropriate.

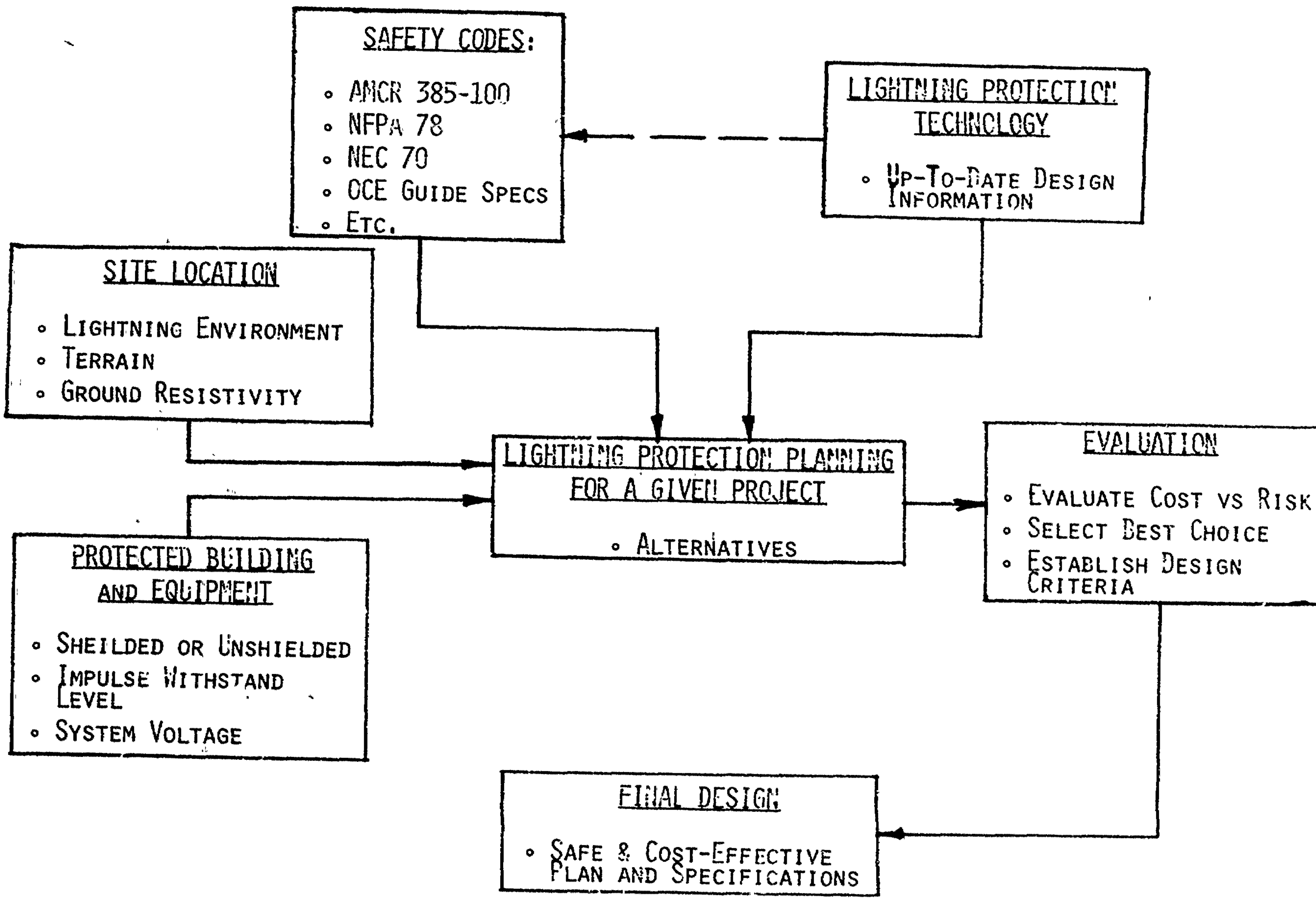

Figure 7. Design Flow Chart

LIGHTNING TECHNOLOGY

BIBLIOGRAPHY

1. *FAA/Florida Institute of Technology Workshop on Grounding and Lightning Technology*, March 1979, Report No. FAA-RD-79-6 (AD-A065410)

2. *FAA/Georgia Institute of Technology Workshop on Grounding and Lightning Protection*, May 1978, Report No. FAA-RD-78-83 (AD-A058797).

3. *FAA/Florida Institute of Technology Workshop on Grounding and Lightning Protection*, May 1977, Report No. FAA-RD-77-84 (AD-A043908).

4. *FAA/Georgia Institute of Technology Workshop on Grounding, Bonding and Shielding*, May 1976, Report No. FAA-RD-76-104 (AD-A027362).

5. *FAA/Georgia Institute of Technology Workshop on Grounding and Lightning Protection Seminar*, May 1975, Report No. FAA-RD-75-106 (AD-A013618).

6. *FAA/Georgia Institute of Technology Workshop on the Grounding of Electronic Systems*, March 1974, Report No. FAA-RD-74-147 (AD-785858).

7. *FAA/Georgia Institute of Technology Grounding, Bonding and Shielding Practices and Procedures for Electronic Equipments and Facilities* - Vol 1, "Fundamental Considerations," December 1975, Report No. FAA-RD-75-215/1 (AD-022332).

8. *FAA/Georgia Institute of Technology Grounding, Bonding and Shielding Practices and Procedures for Electronic Equipments and Facilities* - Vol 2, "Procedures for Facilities and Equipment," December 1975, Report No. FAA-RD-75-215/2 (AD-A022608).

9. N. Cianos and E. T. Pierce (McDonald-Douglas Astronautics Company, California), "A Ground-Lightning Environment for Engineering Usage," August 1972, (Bibliography-180 listings), (AD-907891).

10. M. A. Uman (Westinghouse Research Labs, Pittsburg, Pa), *Lightning*, (McGraw-Hill Book Company, 1969).

11. R. H. Golde, *Lightning*, Vol 1, "Physics of Lightning," (Comprehensive Bibliographies), (Academic Press, 1977).

12. R. H. Golde, *Lightning*, Vol 2, "Lightning Protection," (Comprehensive Bibliographies), (Academic Press, 1977).

13. R. H. Golde, *Lightning Protection*, (Edward Arnold Publishers, 1973).

14. W. G. Williams (Picatinny Arsenal, New Jersey), "Control System Grounding for Munitions Production Base Modernization and Expansion," October 1977, Report No. TR-ARTSD-77-004 (AD-B023780L).

15. R. M. Cosel (USAF/RADC), "FAA Lightning Protection Study: Handbook of Installation Procedures for Selected Solid State Equipments," October 1977, Report No. FAA-RD-77-170 (AD-A047730).

16. E. Muller, H. Steinbigler, and J. Wiesinger, "On the Numerical Calculation of Induced Voltages on Surfaces Neighboring Lightning Conductors," Translated: September 1977, Original: 1972, Foreign Technology Division Report No. FTD-ID(RS)-T-1288-77 [Proprietary (Copyright)], (AD-B024557L).

17. J. Wiesinger, "Determination of Induced Voltages in the Vicinity of Lightning Conductors and Dimensioning Rules Derived Therefrom," Translated: September 1977, Original: 1970, Foreign Technology Division Report No. FTD-ID(RS)T-1496-77 (AD-B025344L).

18. R. Vaselich and J. Dixon, (Naval Weapons Lab), "Lightning Protection Documentation," Report No. NWL-AR-124 (AD-763667).

19. FAA/RADC, "FAALightning Protection Study-Lightning Protection Devices," April 1974, Report No. FAA-RD-74-104 (AD-781319).

20. University of Queensland, Australia, "Principles of Protection of Ground Based Radio Stations and Other Installations from Damage by Lightning," June 1977, Report No. T/N-2/77 (AD-A048178).

21. R. A. Fisher, "Analysis of Lightning Effects on Launch Vehicle Ground Support Electrical Cables," *General Electric Company, April 1975 Conference on Lightning and Static Electricity*, Culham Lab., England.

22. G. K. Huddleston and G. G. Bush (USAF/RADC), "FAA Lightning Protection Study: Lightning Protection Requirements for Mark III Instrument Landing System (Category III)," February 1975 Report No. FAA-RD-75-73 (AD-A011489).

23. W. Frost and D. Cam, *Proceedings: Second Workshop on Meteorological and Environmental Inputs to Aviation Systems UTSI*, March 1978, Report No. FAA-RD-78-99.

24. J. W. Kaufman, "Terrestrial Environment (Climatic) Criteria Guidelines for Use in Aerospace Vehicle Development - 1977 Revision," November 1977, Section XIII: Atmospheric Electricity, *NASA* TM 78118.

25. "Surface Atmospheric Extremes (Launch and Transportation Areas)," Revised: June 1974, Report No. NASA SP-8084.

26. F. A. Fisher (General Electric Co.) "Lightning Protection of Launch Facilities at Kennedy Space Center," *Technology Today and Tomorrow: Proceedings of the Tenth Space Congress, Cocoa Beach, Florida*, 1973, pp. 8-25 to 8-30.

27. M. A. Uman, et. al., "An Unusual Lightning Flash at Kennedy Space Center," *Science*, Vol 201, July 7, 1978, pp. 9-16.

28. M. A. Uman, et. al, "Effects of 200 km Propagation on Florida Lightning Return Stroke Electric Fields," *Radio Science*, Vol II, December 1976, pp. 985-990.

29. L. H. Ruhnke, "Atmospheric Electricity Problems at Kennedy Space Center - Rockets and Launch Operations Protection From Atmospheric Electricity at Kennedy Space Center, Discussing Current and Future Lightning Suppression," *Technology Today and Tomorrow Canaveral Council of Technical Societies, Proceedings of Eighth Space Congress, Cocoa Beach, Florida (A71-36442)*, Vol 1, pp. 3-11, 3-12, 18-31.

30. M. A. Uman, et. al., "Electric Field Intensity of the Lightning Return Stroke," *Journal of Geophysical Research*, Vol 78, June 20, 1973, pp. 3523-2529.

31. M. A. Uman, et. al., "Currents in Florida Lightning Return Strokes," *Journal of Geophysical Research*, Vol 78, No 18, June 1973.

32. E. T. Pierce (SRI, Menlo Park, California), "Lightning Discharges to Tall Structures," 1967, (AD-815943).

33. E. A. Jacobson, et. al., "Electrostatic Field Changes and Recovery Curves Produced by Florida Lightning," *Conference on Cloud Physics, Tucson, Arizona, October 21-24, 1974 Proceedings (A75-44379 22-47) Boston, AMS*, 1975 p. 399.

34. J. M. Livingston, et. al., "Electric Fields Produced by Florida Thunderstorms," *Journal of Geophysical Research*, Vol 83, January 20, 1978, pp. 385-401.

35. "Lightning Protection for Saturn Launch Complex 39," September 1963, Report No. NASW-410-20-13-22.

36. General Electric Company High Voltage Laboratory, "Analysis of Lightning Effects on Launch Complexes 34 and 37," (Contract NASW-410 for NASA), July 1964, Report Nos. NASA X72-76615 and NASA CR-126811 (AD 26510591).

37. R. H. Lee, "Protection Zone for Buildings Against Lightning Strokes Using Transmission Line Practice," *1977 Industrial and Commercial Power Systems Conference*, IEEE 0093-9994/78/1100-046550.75.

38. *Electrical Protection Fundamentals Rural Electrification Administration Telephone Engineering and Construction Manual*, Section 801, Issue No. 3, July 1974.

39. M. Brook (New Mexico Institute of Mining and Technology, Socorro, New Mexico 87801), "Lightning Properties and Associated Emissions," February 1979.

40. "Lightning," *Mosaic*, November 1978.

41. *Safety Manual AMCR-385-100*, Sections 6 and 8.

42. *National Electric Code*, 1978.

43. *Lightning Protection Code NFPA 78*, 1978.

44. Indiana AAP Project 5732084 Black Powder Manufacturing Facility ECP-F8G 035, Revise Power System Grounding, October 6, 1977.

45. "American National Standard Guide for Application of Valve-Type Lightning Arresters for Alternating - Current Systems," ANSI C62.2, 1969.

46. "IEEE Standard for Surge Arresters for Alternating - Current Power Circuits," ANSI C62.1, 1975 and IEEE STD 28, 1974.

47. "Radford Army Ammunition Plant Specific Requirements for Control System," (Project 5792875), 30 April 1976.

48. E. J. Fagan and R. H. Lee (E. I. DuPont de Nemours and Company, Wilmington, Delaware), "The Use of Concrete Enclosed Reinforcing Rods as Grounding Electrodes," 1969.

49. B. D. Faraudo and L. C. Martin (Lawrence Livermore Laboratory PEM Note 52), "Review of Factors for Application in Component Damage Analysis," September 1976.

50. J. L. Marshall, "Lightning Protection," (John Wiley & Sons 1973).

51. E. Beck, "Lightning Protection for Electric Systems" (McGraw-Hill, 1954).

52. F. R. Smith (Huntsville Division, Corps of Engineers) "Lightning Protection Study, US Army Ammunition Plants, Indiana Black Powder Manufacturing Facility," 1 January 1980, Report No. HNDTR-80-41-ED-FD.

53. N. A. Forbes (Indiana Army Ammunition Plant), "Grounding and Lightning Protection at the Black Powder Plant," 10 June 1980.

54. R. H. Lee, "Presentation Notes and Reference - Grounding and Lightning Protection," 25-26 March 1980 (The University of Alabama in Birmingham, Continuing Education Program).

ORDNANCE GROUNDING

as Specified and as Practiced

R. C. Carson

HARPOON ORDNANCE SAFETY MANAGER
McDonnell Douglas Astronautics Company
St. Louis, Mo. 63166

Abstract

Ordnance Grounding practices are frequently inconsistent because of vague and sometimes misleading grounding requirements. DOD documents attempt to cover a broad spectrum of grounding needs with a single philosophy or set of requirements. Proper grounding techniques are essential to ordnance safety and should not be left to the possibility of erroneous interpretation. This paper addresses some of the pitfalls in following DOD documents. This paper describes the grounding techniques employed at the MDAC Harpoon production facility at St. Charles, MO and the problems encountered while installing the grounding system. Additionally, this paper offers guidelines for improving the DOD ordnance grounding requirements consistent with the need to maintain explosive safety.

Introduction

Ordnance grounding seems to be the subject of more conversations, discussions, and arguments than any other subject related to explosives. It is usually discussed in generaltities or philosophical terms. The various documents specifying ordnance grounding include statements such as "ordnance shall be grounded at all times." This is not always practical, and in some cases may be more hazardous than no ground at all. This may be particularly true with many of today's sophisticated weapons and built-in safety features. It is common in today's weapon for electro-explosive devices (EED's) to incorporate 25K volt static discharge protection, and to have switching devices (e.g, relays) that maintain a short and ground on EED bridgewires until they are activated. Grounding requirements do not need to be relaxed, however, they should specify in terms applicable to today's weapons and with adequate examples to reduce the possibility of incorrect grounding.

Grounding Practices

The Harpoon Production Facility (Figure 1) at St. Charles, Missouri has a lightning protection and grounding system that utilizes the standards promulgated by DOD 4145.26M, OP-5, and DM-4; that is: No. 2/0 AWG stranded bare copper wire, cad-welded joints, and bronze U-bolt connections. Its buried copper cable is the proper distance from the building with ground rods at specified distances along the periphery of the ground cable. There is a Primary grounding system (lightning protection) and a Secondary grounding system. The primary system consists of five (5) lightning poles 110 feet tall which provide the cone of protection for the entire building. These lightning poles are connected to the primary ground girdle. The secondary ground system consists of a secondary ground girdle which is utilized for building ground, electrical ground, and Ordnance (static) ground.

One of the problems encountered during construction of the Harpoon Production Facility at St. Charles was associated with maintaining a separate isolated ordnance ground system within the building per OP-5 requirements. An ordnance ground system that is isolated from building structure and the electrical system is necessary to avoid ground loops which would cause current flow through the ordnance in the event of an electrical system short or

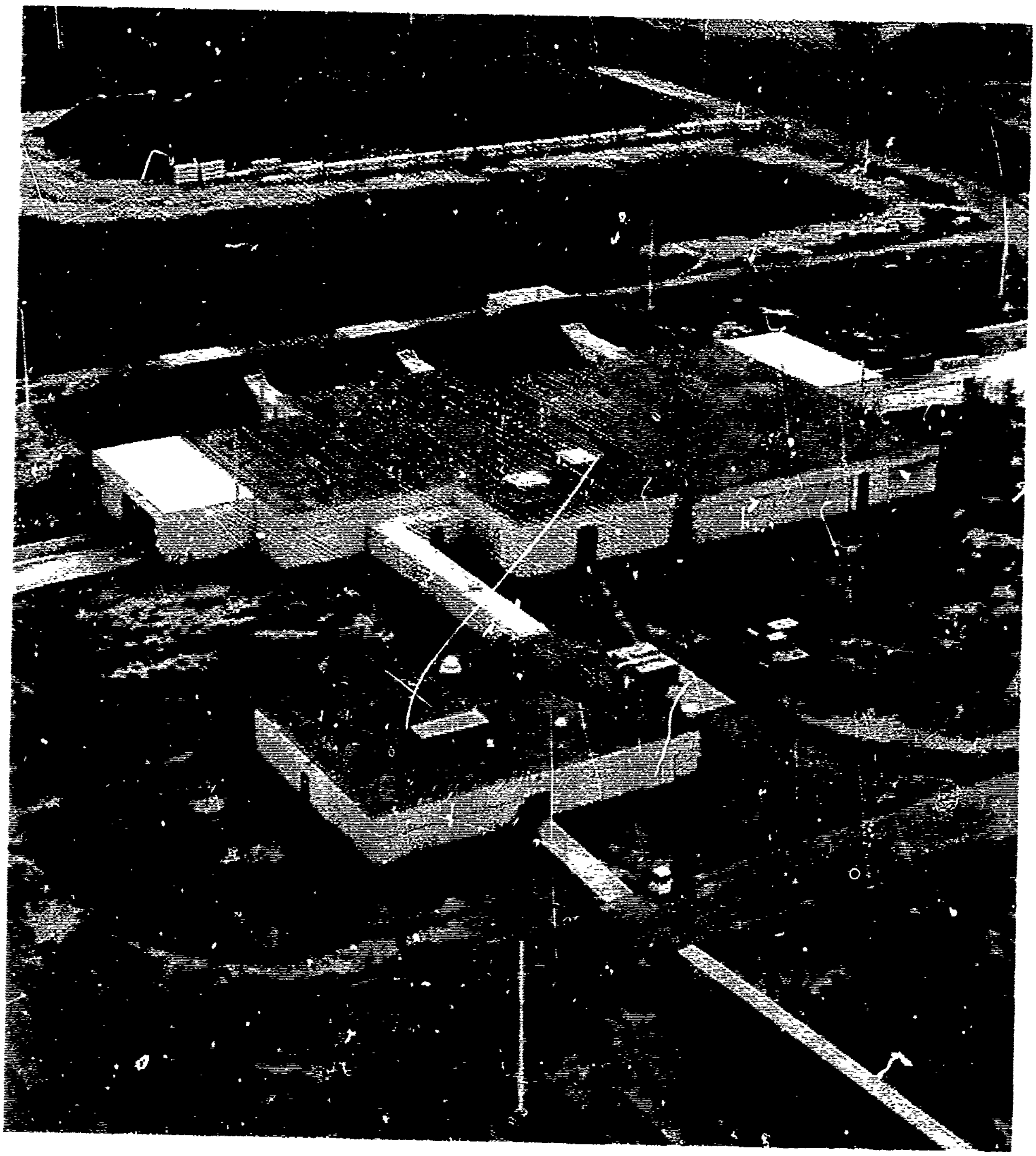

FIGURE 1

building structure developing a current from the electro-magnetic flux of a lightning strike.

In accordance with DM-4, "Electrical Engineering Design Manual," bare stranded cable was used throughout the ground girdle and ground system installation, including the conductors to the interior of the building and througnout the interior of the building. As a result of using bare wire, the various ground systems were inadvertently connected to each other within the building. That is; the Ordnance Ground was connected to the building ground: 1) where the bare wire was laid across the reinforcement rods in the concrete, and 2) where the overhead crane system is attached to the building structure. The Harpoon production building is poured concrete, including the roof. Supporting the overhead crane system from the roof resulted in connecting the ground systems together. To correct this situation, a separate isolated ground system was added to the building. To accomplish this, insulated stranded wire leads were brought from the girdle surrounding the building to the inside of the building and connected to an insulated, isolated stranded wire, which is used as the ordnance ground. This ordnance ground system is kept insulated and isolated from the building and electrical system. It is utilized for ordnance grounding only.

The facility contains an overhead bridge crane and monorail system which is supported by steel reinforcing rods in the concrete. Since we use this crane and monorail system continuously to move missiles and missile sections around the building, this overhead system had to be isolated from ordnance. In some cases rubber pads were already provided on the handling of equipment to protect the missile from handling damage. The rubber pads provide some electrical isolation as well. Where a handling tool provided direct contact with the missile and wire rope was used to lift the handling tool, nylon strapping was used to replace the wire rope. This nylon webbing provides the required insulation. In yet other cases isolation links were obtained for the cranes. The isolation links provide the electrical isolation, however, are undesirable because they reduce the hook clearance height.

The most important aspect of the ground system installation and daily use is the avoidance of ground loops that could provide current paths through the missile or missile sections. The manufacturing flow was analyzed to assure that multiple grounds are not connected at any one time. The possibility of current paths being created to the ground system is greatly reduced by the elimination of electrical power and electrical tools in the missile operations building. The Harpoon Production facility has all pneumatic cranes and hand tools and has eliminated electric tools and equipment in the ordnance assembly area. Figure 2 shows the special pneumatic fixture for missile handling. The procedure employed is to disconnect any grounds prior to mating a missile or section with the overhead crane/monorail system.

Another problem encountered during the ground system installation is related to the testing of missiles by a computer controlled Missile Subsystem Test Set (MSTS). The operation of missile systems are tested and verified by the MSTS. During this testing it is important to maintain a single ground reference. The ground connections for the various cabinets comprising the MSTS are brought to a single point and from there are connected to the secondary ground girdle. While the missile is connected to the MSTS. the test equipment and the missile necessarily have a common ground. This is technically a violation of the rule on separate grounds, however, it is the safe way to test the missile. Two grounds could create a greater hazard by causing ground loops or providing an undesired pat for energizing the ordnance ground; that is, a short in the electrical system energizing the ordnance ground via the electrical ground.

Required Updating

The documents providing the guidance for designers of ordnance facility, describe ordnance grounding requirements in vague terms. The list of documents in the reference section is not an all inclusive list, however, there are eleven (11) documents listed which contain ordnance grounding descriptions in various terms and to varying degrees of detail.

The governing specifications, such as DOD 4145.26M, NAVSEA OP-5, and AFM 127-100 should differentiate between the safety requirements for the various types of ordnance facilities, e.g, a facility which pours or machines explosives and one which bolts warheads to missiles. They should differentiate

FIGURE 2

between the manufacturing of initiators and a facility that installs them. There is a great deal of difference which can result in the savings of many thousands of dollars between a facility that has to deal with explosive dust and one in which the explosives are previously encased in metal (a warhead). The design of a facility wherein explosive dust is present needs to differ greatly from one where the final assembly of missiles takes place.

Additional descriptive information should be published in these documents in regards to ordnance grounding principles and requirements. This additional information should include some of the following. A description of the theory behind ordnance grounding describing the various levels of requirements which are applicable to the various types of facilities. For example, a facility at which explosive material is handled or machined in the raw form would require an extreme degree of safety including grounding because of the potential for explosion from a dust/air mixture and static discharge. These facilities may have no electrical equipment in the explosive areas but are very concerned with static discharges. On the other hand, a missile assembly plant where the explosives are contained within metal housings and with no explosive vapors or dust, the primary concern may be from electrical shorts or lightning strikes. Various illustrations are required which describe acceptable grounding schemes for the various types of facilities and various configurations of facilities. e.g., a test cell adjacent to an operations building may have the same secondary grounding girdle or an independent girdle. Figure 3 illustrates schematically the ground system for the building shown in Figure 1. This figure includes the primary system showing the cone of protection and the secondary system. Separate secondary girdles could have been laid around the test cells without sacrificing safety or the reliability of the ground system.

Examples for Specifications

Figure 4 shows a typical ordnance test cell operation. In one case, the missile is being tested from the control room by a special battery operated tester. It is relatively easy, in this case to run a ground wire from the ordnance ground bus in the test cell to the tester located in the control room and thereby maintain a common ground.

LIGHTNING PROTECTION AND GROUNDING SYSTEM

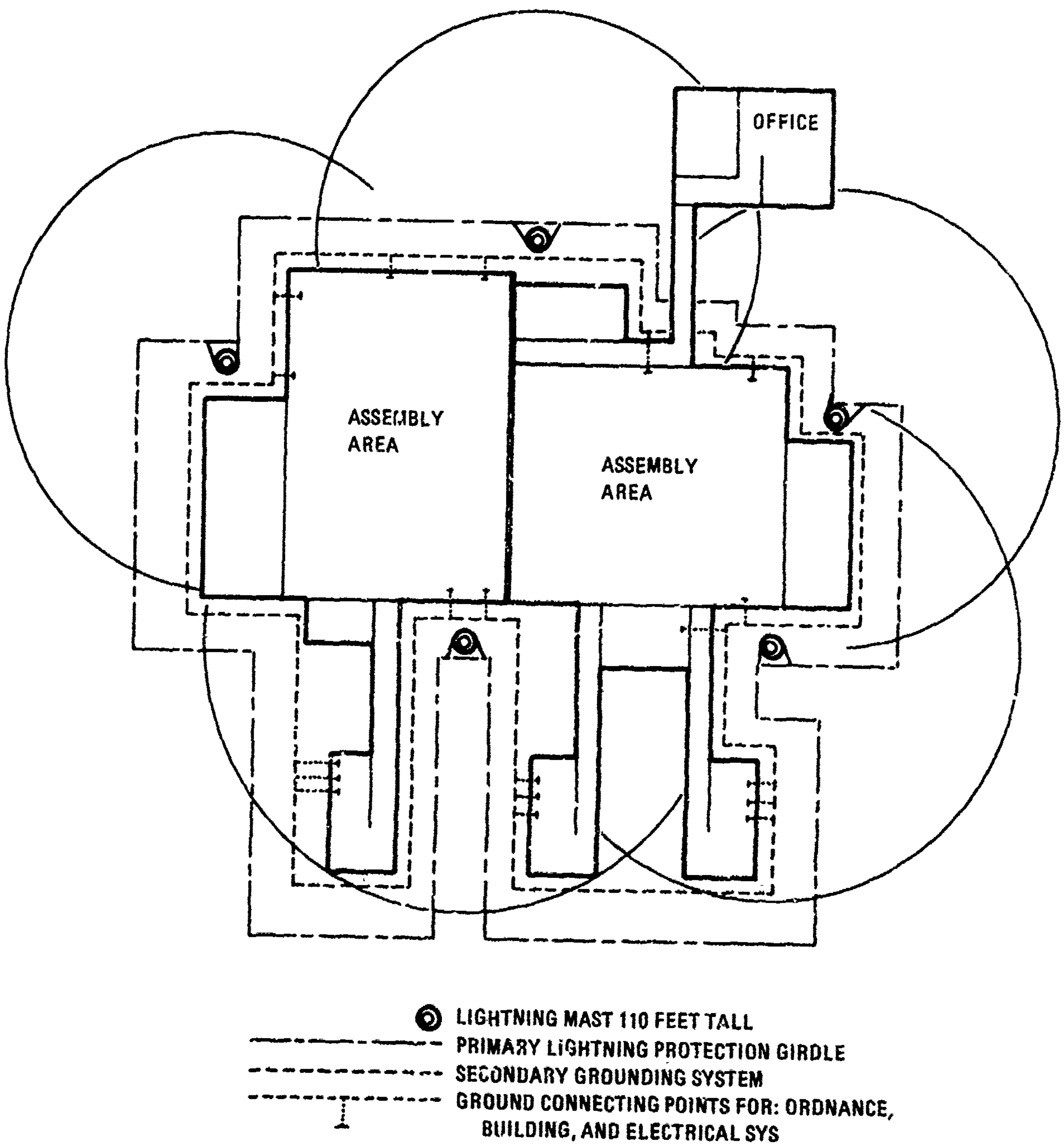

FIGURE 3

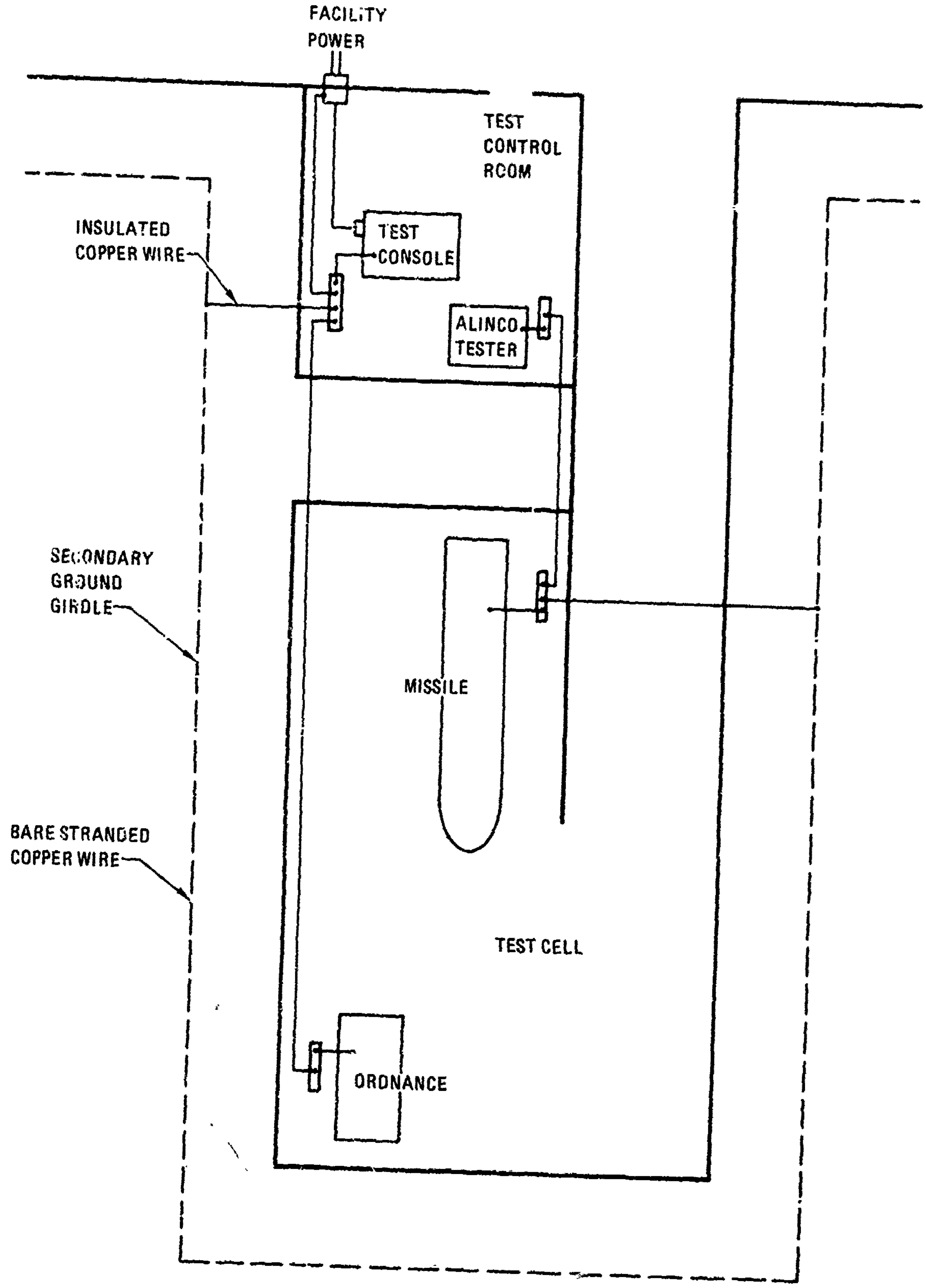
FACILITY
POWER
TEST
CONTROL
ROOM
INSULATED
COPPER WIRE
TEST
CONSOLE
ALINCO
TESTER
SECONDARY
GROUND
GIRDLE
MISSILE
BARE STRANDED
COPPER WIRE
TEST CELL
ORDNANCE

FIGURE 4

In the other example shown in Figure 4, the ordnance item is being tested by an electrical powered test console. For this situation, the ground in the electrical receptacle should not be utilized as it is wired back to the transformer ground. Instead, a special ground bus should be wired between the ordnance station, the test console, the receptacle, and then by insulated wire to the secondary ground girdle. This method assures one ground path during testing and avoids possible ground loops. This type of installation is required to comply with the intent of the specifications, specifically OP-5, however, additional examples and descriptive information should be included in the specification for the user to apply to any type of installation.

The same approach as is mentioned above is used on more complex test equipment as is shown in Figure 5 In this installation, the electrical power receptacle grounds, the test consoles, and the test stand with the missile are connected to a common point, which in turn is connected by insulated wire to the ground girdle. Again, it is important to disconnect the facility electrical ground from the test equipment to avoid ground loops. Figure 6 schematically illustrates this type of grounding system and may be useful in the governing specifications.

Summary

In summary: DOD 5154.4S, DOD 4145.26M, NAVSEA OP-5, and other ordnance facility controlling documents require updating to illustrate the various grounding needs and requirements that are broached herein. These documents need to include illustrations and examples of the various types of grounding installations that are acceptable. The one example in OP-5 leads the user to believe that there is only one acceptable grounding scheme. DOD 4145.26M which is the governing document and should have an entire section on acceptable ordnance ground schemes has nothing on ordnance grounding, except personnel grounding. At this time, there are ordnance facilities being constructed in the U.S. and many foreign countries to handle U.S. Navy Weapons. If the proper guidance is not available in the documents mentioned previously, incorrect criteria may be utilized and thereby create unnecessary hazards in our industry.

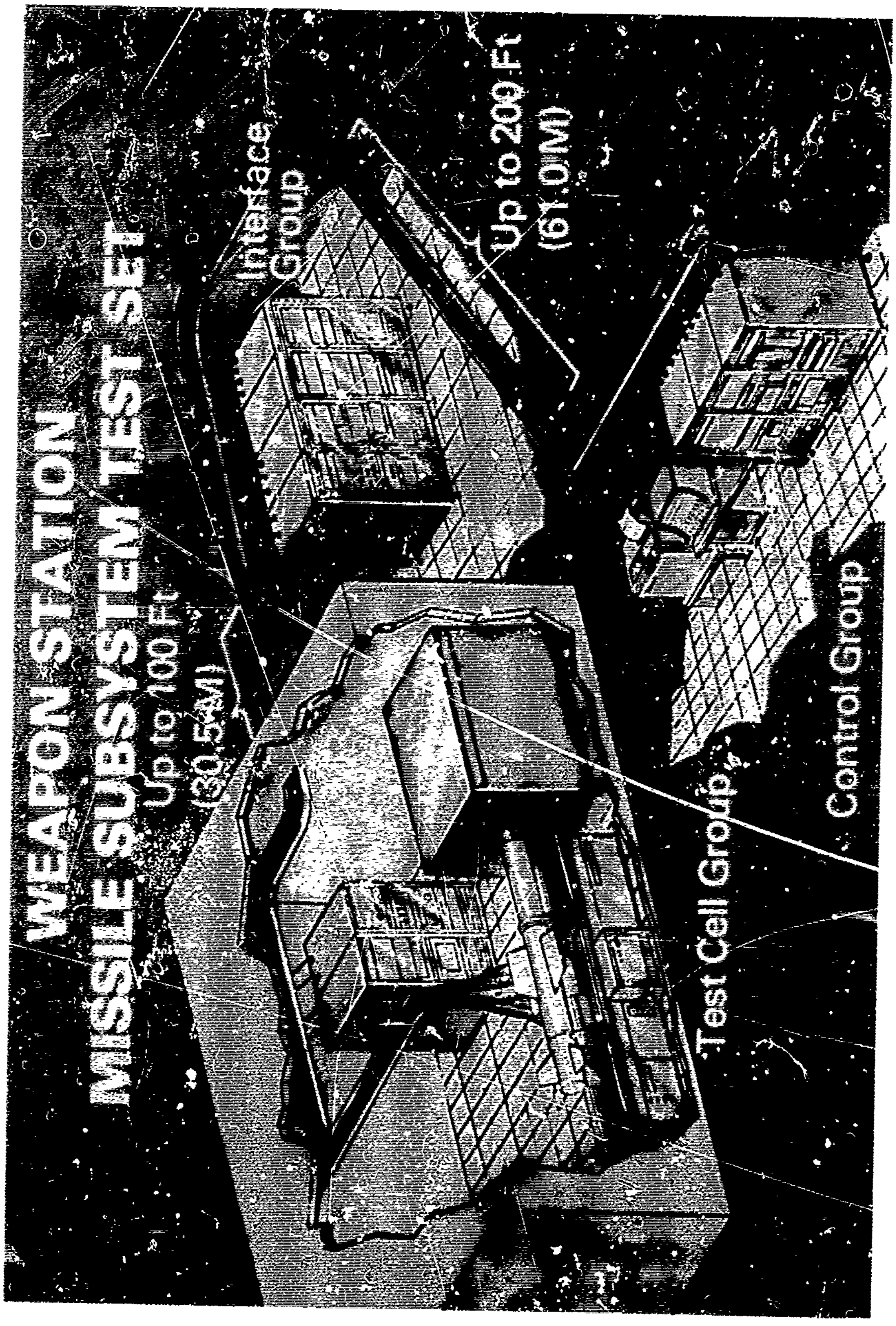
WEAPON STATION
MISSILE SUBSYSTEM TEST SET
Up to 100 Ft
(30.5 M)
Interface
Group
Up to 200 Ft
(61.0 M)
Test Cell Group
Control Group

FIGURE 5

MSTS/MISSILE GROUNDING

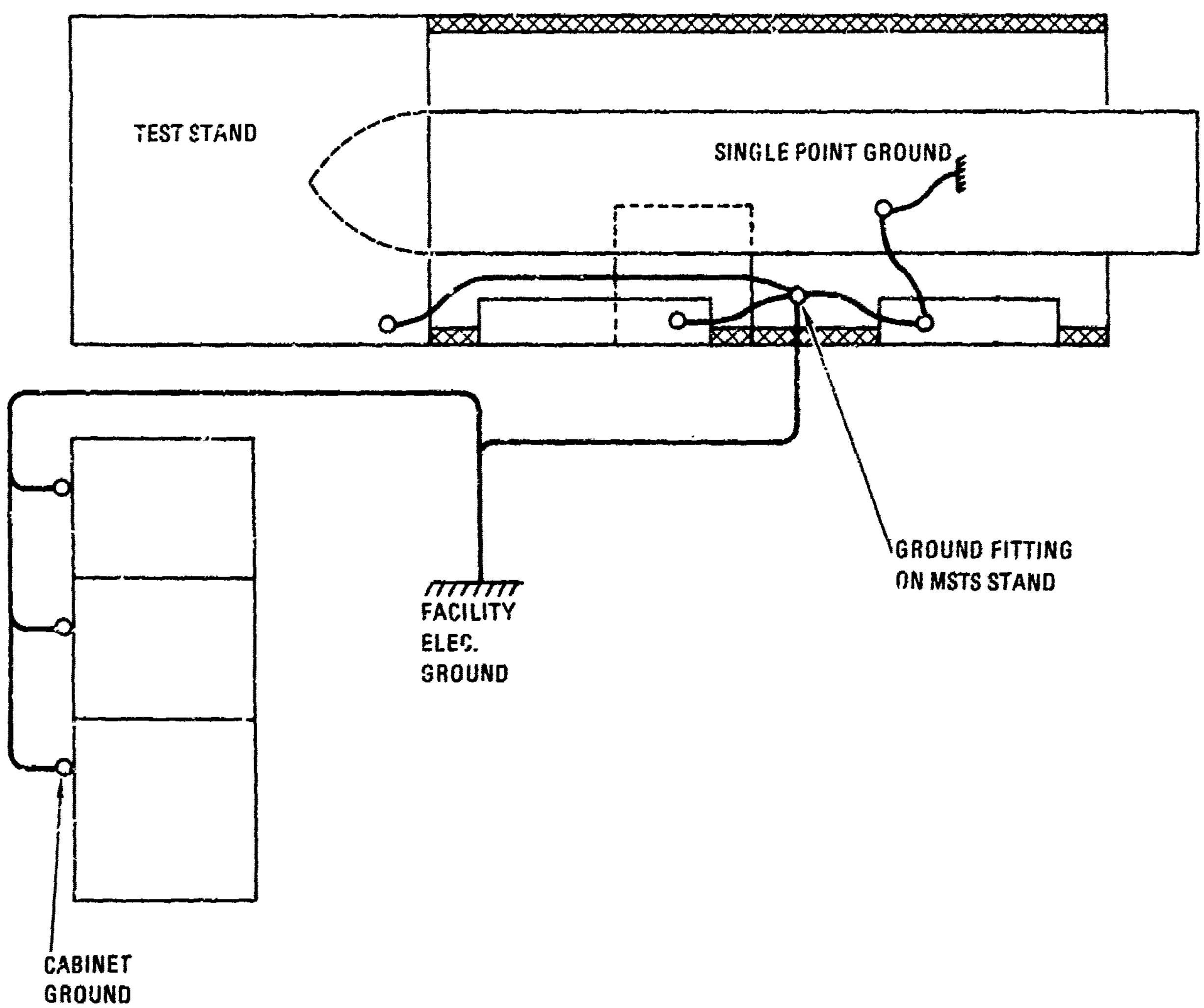

FIGURE 6

REFERENCE DOCUMENTS

1. DOD 5154.4S DOD Ammunition and Explosive Safety Standards.

2. DOD 4145.26M, DOD Contractors Safety Manual for Ammunition, Explosives and Related Dangerous Material.

3. NAVSEA OP-5, Ammunition and Explosives Ashore - Safety Regulations for Handling, Storing, Protection, Renovation, and Shipping.

4. AFR 127-100, Explosive Safety Standards.

5. NAVFAC DM-4, Design Manual - Electrical Engineering.

6. AFM-88-9, Electrical Design - Lightning Protection System.

7. NAVFAC P-80, Facility Planning Factor Criteria.

8. NAVORD OD 10773, Safety Principles for Operations Involving Electro-Explosive Devices.

9. UL 467, Grounding and Bonding Equipment.

10. NFPA 77-1972, Static Electricity 1972.

11. NFPA No. 78-1975, National Electric Code.

PRECEDING PAGE BLANK-NOT FILMED

DISSIPATION OF ELECTRO STATIC CHARGES AND PREVENTION OF STATIC GENERATION THROUGH CONDUCTIVE COATINGS AND GROUNDING DEVICES

Mr. J. Paul Glenn
Walter G. Legge Company, Inc.
122 East 42nd Street
New York, NY 10168

Effective elimination of explosion and fire hazards where flammable and explosive materials are made, stored, or handled requires the prevention of electrostatic charges from any source. First - What is static electricity? For all practical purposes, static electricity may be defined as an electrostatic charge caused by friction between two dielectrics. Materials such as wool, silk, synthetic fiber, rubber and glass are excellent insulators or dielectrics and consequently build static charges very rapidly. Motion creates static by contact or friction. All that remains to cause a static spark is an accumulator and a discharge path. Secondly - How to prevent static accumulation? Grounding or direct electrical passage to earth is the only completely effective means of preventing an accumulation of static charges. The first step in the prevention of build up in a given area is the provision of a common ground. In other words, an equalizer of electrical potential between all persons and objects in the area.

Flooring is the obvious choice as the object to which most things are in contact. The provision of a conductive floor with all bodies in electrical contact with the floor and consequently with each other and the floor in contact with ground is the simplest method of grounding. The conductive floor acts as a huge intercoupler between all floor borne equipment, personnel and ground for the elimination of any differences of electrical potential.

The second step is to insure electrical contact of all bodies to the floor. This is accomplished by the use of conductive footwear or suitable personnel grounding devices.

Bench tops, tote boxes and containers should all be either metal or coated with a conductive coating. If metal surfaces must be painted for rust prevention, conductive seals should be used as a sealant. All surfaces and equipment should be tested periodically with a 500 volt generator type ohmeter and personnel tested on a qualified shoetester before each entry into the hazardous area. The question of proper resistance of a conductive floor is a highly controversial subject. Ordnance specifications run from a low of zero ohms resistance to a high of 250,000 ohms, and NFPA Bulletin 56A calls for a lower limit of 25,000 ohms, and an upper limit of 1 megohm. Thus, it is important that the resistance be in accordance with the local specification. Ordnance specifications are much lower than NFPA, thus there is less disagreement on stated resistance. This, of course, is because ordnance is concerned only with electrostatic dissipation and not with electric shock. Where there may be a shock hazard, and the floor is below 25,000 ohms, the personnel shoes or grounding devices must have adequate resistance to insure a minimum of 25,000 ohms between person and ground. These precautions insure that all possible electrostatic charges are safely dissipated and cannot cause a fatal spark. As the threshold value of electrostatic sparking is approximately 1100 volts or less, these simple precautions are a must.

Conductive floors are available in many types. However, they must be spark proof as well as conductive and this narrows the field. Many of the chemical type floors such as epoxy, polyester, polyurethane, as well as the resilient vinyl floorings, are attractive and well suited to hospital operating rooms. This type of material is unsuited to the needs of industry, ordnance plants, ammunition depots, etc. Heavy traffic and spillage of solvents requires a heavy duty coating which will stand up to the traffic and accept patching readily so down time is kept to a minimum. These coatings are available in a heavy duty material which is troweled or brushed on to a thickness of 1/16". As a complementary material, a paint-like coating is also available for lighter duty. This material may be brushed or rolled on, dries in an hour, and will accept normal traffic, and can be supplied in black, grey, maroon, or green, where colors other than black may be desired.

The term conductive floor by definition means that the flooring shall provide a path of moderate electrical conductivity. By its very nature and character this flooring is sensitive and must be treated as an electrical connector and not like other floors in the building. Many factors affect the resistance of a conductive floor--from dust to humidity. Dirt, grime, soap, wax and most spillage are dielectrics and will insulate a floor very rapidly. To be sure this does not happen, resistance readings must be taken at intervals of not longer than one month and in extra sensitive areas, much more often. Records of these readings should be logged and compared from reading to reading. Thus, any decided change in resistance will be noted, and the problem alleviated before it becomes serious. Humidity is also an important factor in the care and maintenance of conductive floors. Humidity control is helpful in the prevention of static build-up as at 50% a fine film of indiscernible moisture is deposited on all surfaces, forming a conductive path most helpful in bleeding off static charges as they are generated. Various humidity measuring devices are available. The most popular and trustworthy of these is the sling psychrometer, a simple device which, when swung in the air as required, measures humidity by absorption in a measuring wick.

The greatest care must be exercised in the choice of maintenance materials for conductive floors or coatings as improper maintenance is the most common cause of malfunctioning floors. There are seals, cleaners and polishes made specifically for conductive floors which will not alter the resistance of the floor and these materials should be used exclusively. In the case of malfunctioning floors, there are materials which raise the resistance and materials to lower the resistance. Although these materials are available, the most positive approach is to use the proper materials and the proper program.

EXPLOSION CONTAINMENT VESSELS AND MATERIALS EVALUATION FOR LOW SERVICE TEMPERATURE APPLICATIONS*

by

B. Dale Trott and John J. White, III
Battelle, Columbus Laboratories
Columbus, Ohio

and

Barber S. W. Poe
U. S. Naval Explosive Ordnance Disposal Facility
Indian Head, Maryland

ABSTRACT

Previous papers presented at this seminar demonstrated the technology for portable, spherical vessels for explosion containment applications based on the elastic-plastic response of ductile steels, such as A537. This paper summarizes the extension of this technology to low service temperatures (-30 F, -34.4 C) by means of proper materials evaluation. It is argued that the Navy explosion bulge test is a viable method for judging the required fracture resistance properties needed for the intended application. Materials considered and explosion bulge test results are given. The nil-ductility transition temperature of steel is emphasized. Experiments on full scale prototypes of the latest vessel design show the superiority of HY80 steel for low service temperature applications.

* Sponsored by the U. S. Naval Explosive Ordnance Disposal Facility, Indian Head, Maryland, under Contract Nos. N00174-76-C-0103, N00174-76-C-0187, and N00174-77-C-0372.

INTRODUCTION AND SUMMARY

The design criteria for lightweight, portable (or transportable), completely-enclosed blast containment vessels for explosive ordnance disposal (EOD) applications has been investigated at Battelie's Columbus Laboratories since 1971.[1-9] In 1976, the FBI provided a vessel description[10-12] that could be adopted as a prototype by individual elements of the civil EOD community. Additional knowledge has been acquired since then, and the U. S. Navy has recently type-classified the Mk 634 Mod 0 Explosive Devices Container[13] for use by the military EOD community. Battelle provided the design and development[6-8] for the Mk 634 Mod 0. This paper gives a description of a very significant aspect of the underlying research, namely the evaluation and selection of materials for use in vessel fabrication.

Previous Battelle research efforts[1,3,4,5] on explosion containment chambers concentrated on designs of doors, fixtures, and cradles; elastic and elastic-plastic responses; effects of charge size, shape, and casing; and fragment suppression. The evaluations were carried out primarily at 70 F (21 C). Material selection was important in that A537 steel was recommended as a cost-effective choice with good strength, ductility, fracture toughness, formability (hot pressing), weldability, and availability. After the concept of portable (or transportable) containment devices was demonstrated, it was possible to attack the problem of a practical design effective at a low service temperature.[8] A low service temperature requirement of -30 F (-34.4 C) was selected for tri-service application. This paper describes the impact of this requirement on material selection and gives some of the data obtained in our evaluations.

Interest in explosion containment devices is extensive for a number of reasons, however, in most cases the weight limit and service temperature problems common to EOD applications are less severe. We have benefited from most of the explosion containment literature and have referenced much of it previously. Some additional efforts by the Frascati[14] and Los Alamos[15,16] groups should be identified. To our knowledge, little research has been directed specifically at material evaluation for explosion containment vessels. We are, however, indebted to the vast effort to understand the phenomena of fracture, especially the contributions of the Naval Research Laboratory.[17-23]

A preliminary study[6] of various materials properties was made to determine what the primary issues of materials selection for explosion containment vessels are. The following items are definitely important and have been considered in our work, although the rank ordering can be debated:

- Satisfactory fracture resistance at the lowest service temperature during a standard (explosive) loading cycle
- Weldability including fracture resistance of the weld metals and heat affected zones
- Formability, e.g., by hot pressing
- Availability in the quantity required
- Cost of materials and fabrication
- Containment performance as measured by density, modulus, strength, and ductility
- Satisfactory fatigue resistance if frequent small explosive loadings are anticipated

Previous efforts to evaluate explosion containment vessel materials, if any, apparently relied on typical laboratory fracture test results, such as the Charpy V-notch impact energy, the advice of materials scientists, and the accumulated experience of previous explosion containment experiments. Experimental demonstration of a material's capabilities prior to vessel construction usually was not attempted. Explosively induced fatigue failure of materials remains an unknown entity at this point.

It was concluded that the greatest need of the current NAVEODFAC program was the development of an affordable data base on material fracture resistance under meaningful test circumstances. Sample temperature and high strain rate during plastic deformation in the presence of a suitable flaw became the key circumstances of interest. The Navy explosion bulge test[22,23] was selected as capable of providing the most direct evidence of material suitability from the standpoint of fracture resistance. Dynamic tear tests appear to have a good scientific basis for addressing this question, but correlations with directly related applications were not available.

Approximately 50 explosion bulge tests were completed on eight selected materials. It was confirmed that 1020 carbon steel and A537, Class 1 steel are brittle at the low service temperature, whereas HY80 steel and AISI 304 stainless steel offer excellent fracture control. The toughness of the weld zone material is problematical in all cases, including the HY80 weldment. Results on HY80 and AISI 4340 heat treated to 120 ksi (828 MPa) were inconclusive. The low strength of aluminum alloy, such as 6061-T6, is a limiting factor, even on an equal weight basis. Most surprisingly, Frostline steel proved to be inadequate during both bulge and full scale experiments at the required low service temperature. Additional investigation of the heat treatment procedure for Frostline appears to be merited.

The basic conclusion of this paper is that HY80 steel is the most practical choice available to the military EOD community when building an explosion containment vessel with a low service temperature requirement. The civilian community may have no other choice than to use a stainless steel, such as AISI 304, due to the availability problems with HY80. Some time in the foreseeable future, we expect that one or two of the HSLA steels will be proven acceptable for this application. In the meantime, the EOD community is advised not to risk the use of unproven materials, especially if low service temperature explosive applications are anticipated. The results given in this paper indicate that explosion bulge testing is a viable method for judging the fracture performance properties of a candidate material.

The remainder of this paper consists of a brief summary of the fracture control evaluation method, a survey of key results of explosion bulge testing, documentation of material limitations in full scale vessels, and our conclusions. The Appendix gives a brief review of scaling law calculations that may be used for elastic design purposes. As this is only a partial presentation of our more recent work on explosion containment vessels, the reader may wish to consult References 6-8 for engineering details and additional data. Additional publications are planned.

FRACTURE CONTROL EVALUATION METHOD

The subject of fracture control is a broad area of active research at present and no attempt is intended here to provide more than a brief discussion of the aspects most pertinent to the blast containment problem. When a structural plate or blast containment chamber fractures or ruptures, the mode of failure may range between two extremes. Here we choose to call these extremes, plain strain fracture and plain stress fracture.

Plain strain fracture is characterized by fracture surfaces that generally run normal to the direction of the applied maximum stress. In steels the fracture surfaces usually have a rough granular appearance. Very little, if any, plastic strain is associated with this fracture mode. It is the characteristic fracture mode of brittle materials. Very little energy is required for the propagation of plain strain fractures.

Plain stress fracture is characterized by smooth fracture surfaces that run through the plate thickness at an angle near 45 degrees to the direction of applied maximum stress. Failure occurs by shear-type plastic slipping. Considerable local plastic deformation of the material adjacent to the fracture surfaces is observed. The generation of this extensive zone of plastic deformation absorbs considerable energy for the propagation of this fracture mode. If failure is unavoidable, this is the desired fracture mode.

Various mixtures of both limiting modes of fracture often are observed on fractured metal surfaces. When this occurs, the material nearest the free surfaces fails by plain stress fracture with the formation of characteristic shear lips at near 45 degrees. The central portion fails in plain strain with the characteristic 90 degree orientation and rough, granular appearance of the surfaces.

The fracture mode that may occur in any particular instance is influenced by several factors. These include the material properties (at the temperature of interest), the plate or structure thickness, and the geometric constraints associated with the structural design. The latter two factors are related to the degree of restraint to plastic deformation offered by the structure. This in itself is a very extensive subject, but it suffices to say here that increasing the restraint by, for example, increasing the plate thickness can shift the fracture mode from largely plane stress to mostly plain strain. In the range of temperature, where the material properties affect the fracture mode, increasing the plate thickness of a given material can shift the fracture transition toward higher temperatures.

The principal concern in this paper is the influence of material properties on the fracture mode that occurs. The material property of primary interest is fracture toughness. It is a measure of resistance to crack propagation. Classically it has been measured by the K_{Ic} fracture toughness parameter, by the DT (dynamic tear test) energy, and by the C_v (Charpy-V impact test) energy. All three of these tests provide meaningful numerical values, and in the range of temperatures above the brittle transition range in steel they show a definite correlation to one another.[17,18,21] To make useful application of these laboratory-generated numerical values, however, it is necessary to correlate them with expected in-service performance of real structures. For many structural steels and applications involving working stresses at or below the static yield strength, these correlations exist and are proving of considerable value in fracture-safe design.[22]

To achieve the desired low weights for portable blast containment chambers, the vessels are designed to absorb the blast energy by overall plastic deformation of the structure.[1-4] In the range of stresses above the yield stress there is a paucity of laboratory data for correlation on real structures. Another test, which measures the resistance to fracture propagation under conditions closely similar to the intended explosive containment applications, is the explosion bulge test.[22,23] This test has the significant advantage of being nearly self-correlating to the intended full scale structural application, and hence it was the test selected as an evaluation tool in this work.

For a crack to propagate, it must start from some initiation site. Generally the initiation site takes the form of a flaw in the structure, which serves as a local stress concentration point to drive the stresses at the ends of the flaw high enough to produce propagation of the fracture. In the present application, the remaining flaws as a result of the fabrication process can be kept quite small by non-destructive test and good quality control methods. However, larger flaws may be generated in use by the impact of fragments from a metal-cased contained explosive blast. Thus very good flaw tolerance for the material chosen for the blast containment application is necessary.

It is important to ask the question of how materials may be evaluated to determine when the maximum resistance to fracture propagation has been achieved Figure 1 shows an example of the generalized fracture analysis diagram (FAD) taken from Reference 17. In this diagram, the ordinate is the nominal stress level applied to the structure in question, plotted in terms of the material strength properties of yield stress and ultimate tensile stress. The abscissa is, in effect, a sliding linear temperature scale, which may be indexed to a specific steel by identification of the steel nil ductility transition temperature (NDT on Figure 1). As indicated on the figure, in the stress-temperature regions of the plot below and to the right of the CAT curve, fractures will not propagate. This generalized diagram has been developed as the result of very extensive testing and documented field failure experience over a period of many years, and may be regarded as highly reliable, for steels having fracture transition effects with temperature, in the range of stresses up to the material yield strength. Deviations from the curve are typically not more than ± 10 F (5.5 C), although in some steels the NDT to FTE transition may occur in a 40 F (22.2 C) temperature span.

In Figure 1, the initial, sharp-ended flaw sizes necessary for the initiation of a fracture which will propagate continuously in a stressed structure are indicated by dashed lines. These are the critical flaw sizes. Note that the critical flaw size decreases for increasing stress level in the structure at all temperatures below the FTP. At temperatures below the NDT, the critical flaw size may fall below the limit detectable by non-destructive means as the operating stress reaches the yield strength of the material. A design which will not be prone to catastrophic failure is clearly impossible under these circumstances.

For blast containment structures loaded well above the yield stress and which may contain appreciable flaws created by fragment impact, it becomes clear from Figure 1 that an operating temperature above the FTP for the selected material will provide the maximum protection from premature catastrophic fracture.

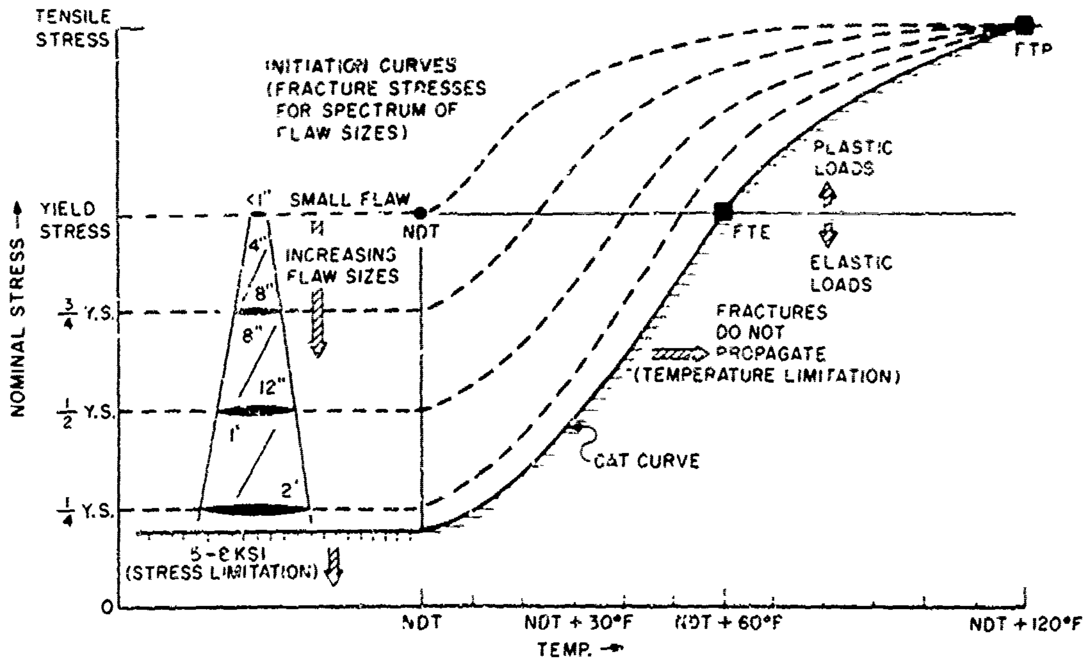

FIGURE 1. GENERALIZED FRACTURE ANALYSIS DIAGRAM, AS REFERENCED BY THE NDT TEMPERATURE

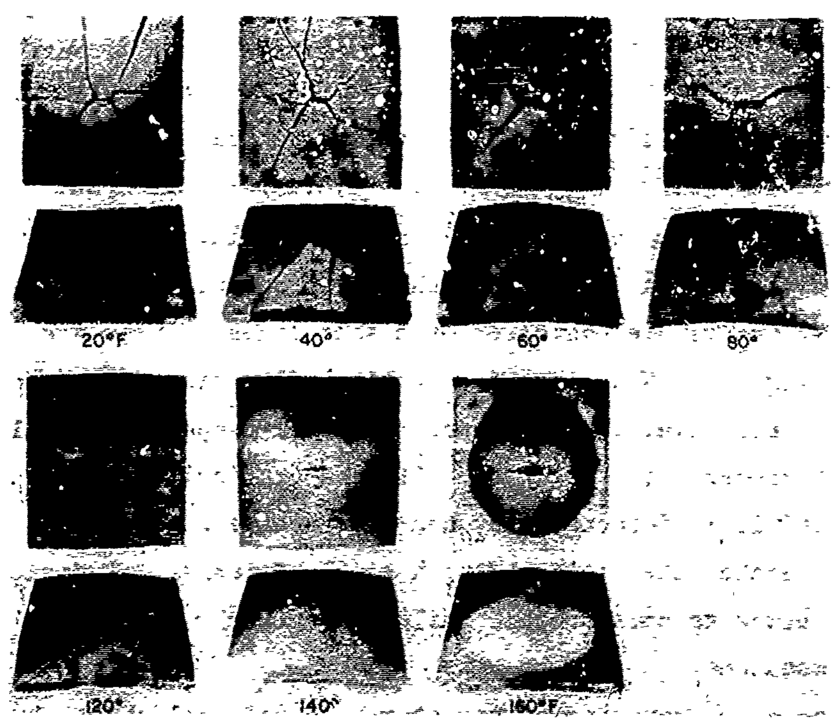

FIGURE 2. EXPLOSION CRACK-STARTER TEST SERIES IN 20° F STEPS ILLUSTRATING THE DRAMATIC INCREASE IN FRACTURE TOUGHNESS OF STEELS ABOVE THE NDT TEMPERATURE (FOR THE STEEL SHOWN, NDT=20° F FTE=70° F, AND FTP=140° F)

The explosion bulge test has been standardized as a means for the evaluation of weldments.[23] In its standard form, a 20-inch (50.8-cm) square plate of nominal 1-inch (2.54-cm)-thickness is placed over a heavy plate containing a 12-inch (30.5-cm)-diameter hole with a specified fairing of the edges of the hole. This heavy plate serves as a die to guide the formation of the bulge. As the name implies, a bulge is formed in the test plate by the action of the blast wave from the detonation of an explosive charge that is placed at some standoff from the plate. The charge size and standoff are adjusted to provide the desired degree of plate bulge per shot. A hard, brittle metal weld bead is placed across the center of the plate on the tensile (downward) side, and it is notched to provide a source for a small, naturally running crack into the test plate.

Figure 2 shows a typical variation in the results obtained[17] with the explosion bulge test as a function of temperature. In general, the occurrence of a flat break as shown for 20 F (-6.7 C) signals a test at or below the NDT. In the temperature range between NDT and FTE, plastic deformation bulging of the plate occurs accompanying fracture. Fractures propagate off the plastically deformed bulge through the elastically deformed edges showing that the test temperature is below the FTE. In the temperature range between the FTE and FTP, fractures do not propagate off the plate edge and becomes less severe as the FTP is approached. At and above the FTP, increased explosive loading may be employed to produce a full hemispherical bulge, as shown for the plate tested at 160 F (71.1 C), without appreciable propagation of the fracture.

This latter performance was the property sought in the materials selection process of this program[6] at a temperature of -30 F (-34.4 C). This is the best performance that can be monitored by a test of the explosion bulge type, and, aside from overall toughness improvements, it is the best performance a material is capable of. However, this performance still may not guarantee the absence of a non-propagating fracture in the blast containment application in the presence of a (large) flaw, because geometric bulging effects at the flaw can serve to intensify the stress at the crack tips to exceed the material ultimate strength at general stress levels in the vessel wall below the ultimate strength. Nevertheless, materials which show little or no crack propagation in a bulge test extended to large deformations should be optimum materials for the purpose of the control of fracture to the highest possible applied stress levels.

Explosion Bulge Experiments

This section presents a brief survey of approximately 50 explosion bulge experiments conducted[6,8] during this program.

Experimental Method

Figures 3 and 4 show the die used and a typical explosive setup. A spherical charge of composition C-4 high explosive was used for convenience. For most of the shots, a 10-lb (4.54-kg) charge was centered 11-inches (27.9-cm) above the die face. The design shot for the current explosion containment vessels[7,8,13] is a 10-lb (4.54-kg) charge at an equivalent standoff of 21-inches (53.4-cm). The 11-inch (27.9-cm) standoff not only produced a significant bulge in a mild steel plate but also corresponded to a reasonable vessel safety factor if a user underestimated a charge size or did not center the charge properly. This engineering approach to the explosion bulge test differs in several respects from the Navy standard.[23]

Sample plate temperatures in the -60 F (-51.1 C) to +32 F (0 C) range were obtained by means of a cooling tank containing a mixture of methanol and dry ice. A simple alcohol thermometer was employed. The plate was lifted from the cooling tank, placed on the die, and bulge tested within 1-3 minutes.

Materials Selected

Table 1 gives a list of eight materials selected for experimental evaluation by means of the bulge test. The steel series of 1020, A537, Frostline, and HY80 represent the principal progression of available, formable materials with a trend from lower cost, lower fracture quality to higher cost, higher fracture quality. These materials all possess the ductile-to-brittle transition. Most stainless steels do not have this property. AISI 304 was evaluated as an available backup material with higher cost, higher fracture quality, medium containment performance capabilities. Titanium alloys have excellent properties, but the cost was judged to be prohibitive. Aluminum alloy could be a realistic choice in some circumstances, and the 6061-T6 was

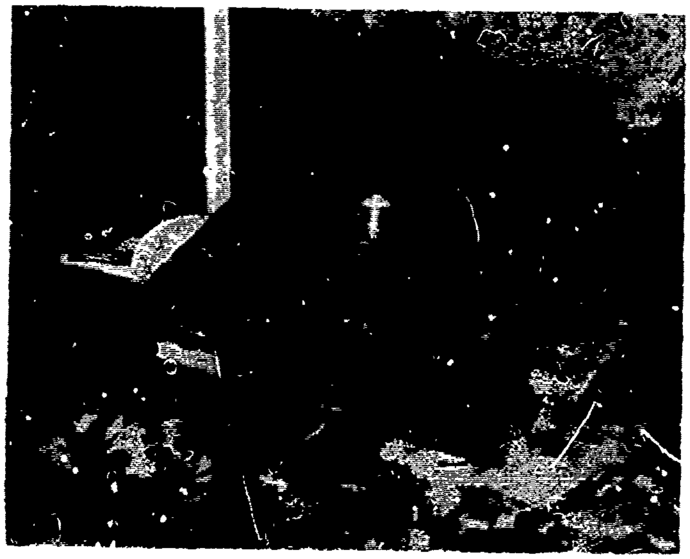

FIGURE 3. VIEW OF THE HY100 MEDIUM ALLOY STEEL DIE USED FOR THE EXPLOSION BULGE EXPERIMENTS

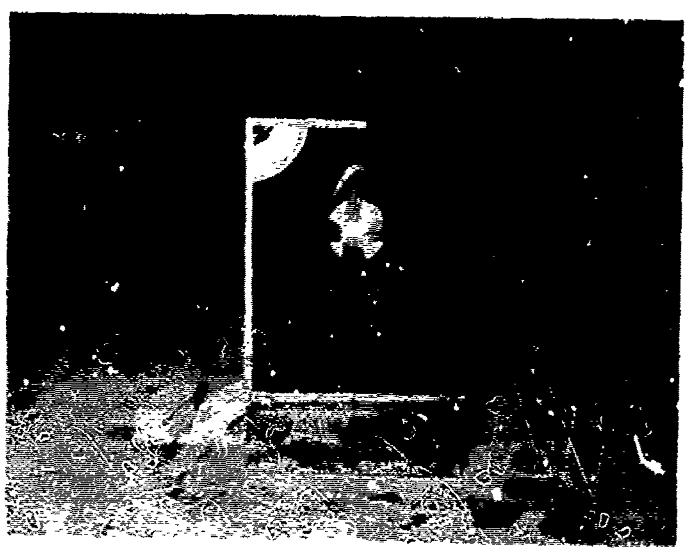

FIGURE 4. TYPICAL EXPERIMENTAL ARRANGEMENT FOR AN EXPLOSION BULGE EXPERIMENT, SHOWING A 7-LB (3.18 KG) C-4 CHARGE SUSPENDED WITH A 15-INCH (38.1-CM) STANDOFF ABOVE THE CENTER OF A 20" X 20" X 1" (50.8-CM X 50.8-CM X 2.54-CM) TEST PLATE MOUNTED ON THE TEST DIE.

TABLE 1. FINAL SELECTION OF MATERIALS FOR EVALUATION OF BLAST CONTAINMENT CAPABILITY

Material No.	Material Type	Description	Number of Explosion Bulge Experiments
1	Commercial Carbon Steel	1020	7
2	High Strength Steel	HY80	7
3	Medium Strength Steel	A537, Class 1	6
4	Medium Strength Steel[a]	Frostline, Grade 60	4
5	Stainless Steel	AISI 304	2
6	Aluminum Alloy[b]	6061-T6	4
7	High Strength Steel[c]	AISI 4340, Grade 110-120	5
8	High Strength Steel[d]	HY110-120	4

(a) Two plates of locally heat-treated Frostline were available for crack starter explosion bulge tests at -30 F (-34.4 C).

(b) A commercially available aluminum alloy 6061-T6 was substituted because AA7004 was not readily available.

(c) Material heat treated for a tensile strength of 110-120 ksi (759-828 MPa) were obtained by local heat treatment.

(d) Two plates of the HY80 previously purchased were heat treated locally to a material with properties in the HY110-120 range of specification.

NOTE: In order to minimize confusion, a test code was introduced.[6] For example, Shot 6-3-1 refers to material number 6 (aluminum alloy 6061-T6), plate number 3, and shot number 1 on that plate. Unless stated otherwise, the crack starter employed was notched Murex Hardex N as specified in NAVSHIPS 250-637-6.

chosen for availability reasons over the first choice AA7004. If greater strength became an explosion containment issue, which is not the case at present, then steel systems such as AISI 4340 and HY80 can be heat treated to the 120 ksi (827 MPa) static yield strength region. Reasonable fracture quality is possible, however, the weldability related properties are problematical. Further details are given in Reference 6. Table 1 explains the test code referenced below.

1020 Carbon Steel Results

Commercial carbon steel 1020 plates were used to gain familiarity with the explosion bulge test. Shot 1-2-1 at 60 F (15.6 C) gave a maximum strain of 3.6 percent on the back surface as determined from a 1/2-inch (1.27-cm)-grid. This led to the adoption of the standard shot described above.

Figures 5 and 6 dramatize the brittle nature of 1020 carbon steel at -30 F (-34.4 C). Shot 1-1-3 did not employ a crack starter and resulted after two milder shots at 60 F (15.6 C) that gave a cumulative bulge of 1-1/16-inches (2.70-cm). Shot 1-3-1 at -30 F (-34.4 C) did not employ a crack starter either, and the plate (not shown) simply bulged 1-1/8-inches (2.86-cm). The reduced ductility available or a small flaw in Plate 1 would account for the apparent discrepancy.

Figure 6 illustrates the brittle fracture that occurs in 1020 carbon steel when a crack starter is introduced on the back surface. Shot 1-5-1 (not shown) was identical to Shot 1-4-1 except that a standard notched Murex Hardex N crack starter was used.

These results serve to warn local-government EOD groups not to adopt locally fabricated vessels made with potentially unsafe materials. The danger is related to cold temperature use, not explosive overloading!

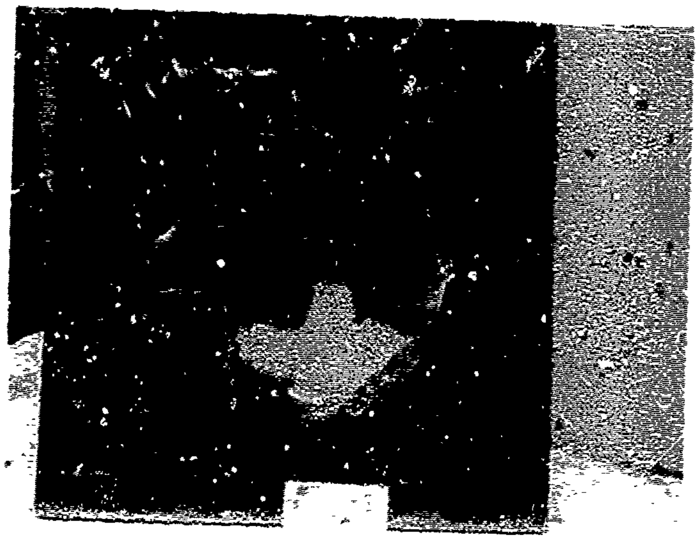

FIGURE 5. BOTTOM VIEW OF THE 1020 CARBON STEEL PLATE AFTER SHOT 1-1-3 AT -30 F (-34.4 C)

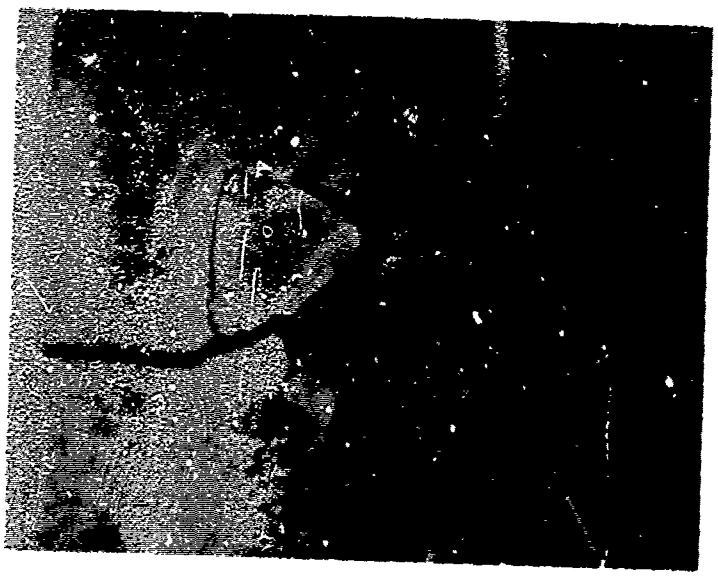

FIGURE 6. BOTTOM VIEW OF THE REASSEMBLED 1020 HOT ROLLED CARBON STEEL PLATE WHICH EXPERIENCED BRITTLE FRACTURE DURING SHOT 1-4-1 at -30 F (-34.4 C). THE CRACK STARTER WAS CUT ON THE HORIZONTAL EDGE BETWEEN THE TWO CENTRAL PIECES.

A537 Steel Results

A537, Class 1 steel is thought to be the most cost effective material available in the U. S. for room temperature explosion containment applications.[1-4,10-12] Unfortunately, the nil-ductility transition temperature (NDT) is too high. Figures 7 and 8 illustrate that a ductile fracture occurs at -30 F (-34.4 C) and at 32 F (0 C) when a crack starter is present. Observe that the cracks initiated and propagated in material loaded above the yield point and did not propagate in the elastically loaded material near the edges. Such cracks in spherical vessels would not be arrested but would run around the surface due to the uniform loading of the vessel above the yield strength.

Frostline Steel Results

When the low service temperature requirement of -30 F (-34.4 C) was first introduced, it was anticipated that Frostline steel would be a cost effective choice to replace A537 steel for portable explosion containment vessels. Frostline material[6,7] is a fine grained, columbium bearing alloy carbon steel with 1.37 percent manganese, 0.16 percent carbon, 0.16 percent silicon, and 0.028 percent columbium (niobium). The physical properties of the plates were a yield strength of 61.2 ksi (425 MPa), a tensile strength of 81.6 ksi (567 MPa), and a Charpy V-notch impact energy of 117 ft-lb (159 J) at -75 F (-59.4 C). The Frostline Steel product discussed in this paper is marketed by Lukens Steel Company.

Identical results were obtained for the explosion bulge tests on two plates at -30 F (-34.4 C). Figure 9 shows that a small, nearly through thickness crack developed on the first shot. This result suggests that Frostline has a high crack initiation energy. Figure 10 indicates that the critical flaw size had been achieved. In Shot 4-1-2 the plate fractured in a nearly plain strain (low energy) manner. The findings are superior to those on A537 steel but inadequate for application at -30 F (-34.4 C).

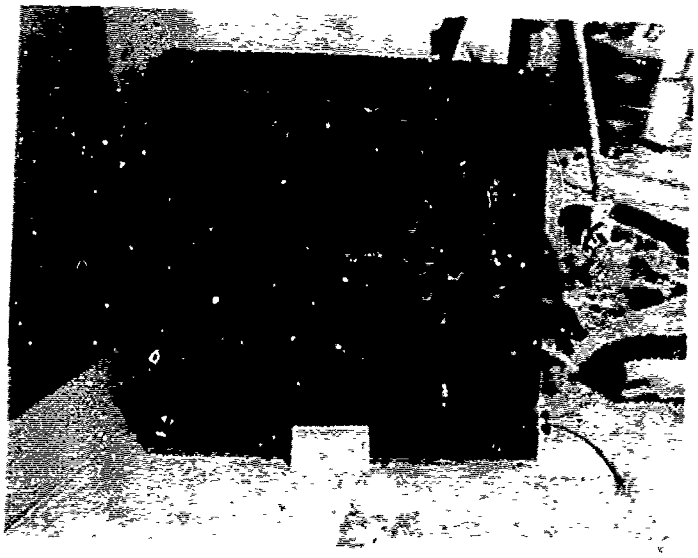

FIGURE 7. BOTTOM VIEW OF THE A537 STEEL PLATE AFTER SHOT 3-2-1 AT -30 F (-34.4 C)

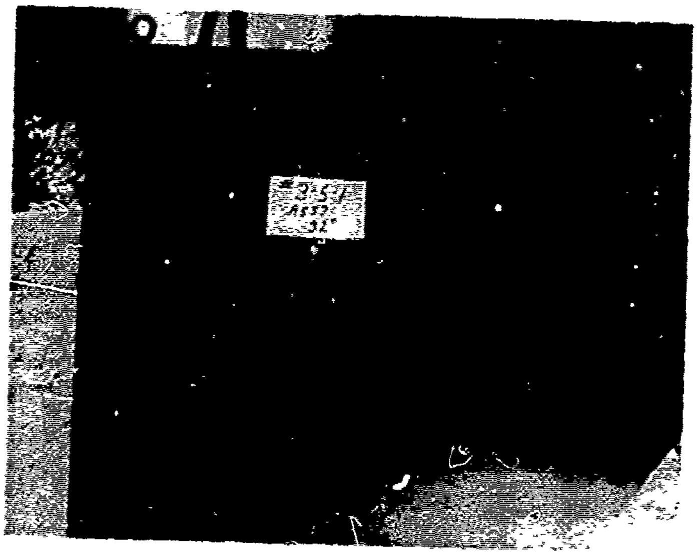

FIGURE 8. BOTTOM VIEW OF THE A537 STEEL PLATE AFTER SHOT 3-5-1 AT 32 F (0 C)

FIGURE 9. BOTTOM VIEW OF THE FROSTLINE STEEL PLATE AFTER SHOT 4-1-1 AT -30 F (-34.4 C)

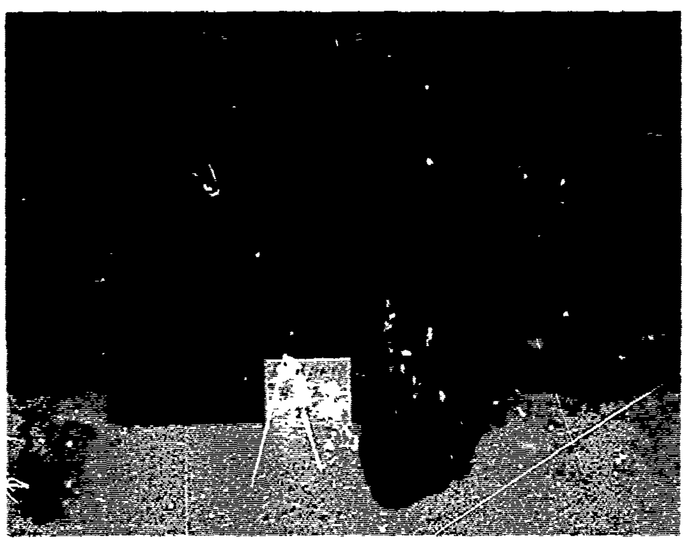

FIGURE 10. BOTTOM VIEW OF THE FROSTLINE STEEL PLATE AFTER SHOT 4-1-2 AT -30 F (-34.4 C)

HY80 Steel Results

HY80 is a well known, highly successful, medium alloy steel developed for low service temperature applications, such as submarine hulls.[22] As expected from a wealth of accumulated experience, the material stood up perfectly to the explosion bulge tests. Figure 11 is a close-up view of the crack starter region of Plate 1 after four shots at -30 F (-34.4 C). A cumulative bulge of 1-13/16-inches (4.60-cm) was recorded. Figure 12 indicates that the material has excellent properties at -60 F (-51.1 C). In this case, no cracks appeared after three shots.

Prior to the construction of HY80 the vessels,[8] crack starter explosion bulge tests were made on welded HY80 plates. Figure 13 shows that a crack developed on the second shot at -30 F (-34.4 C). The crack terminated in the plastically deformed zone, which qualifies it to pass the Navy acceptance standard[23] for plates tested at 0 F (-17.8 C). For the present application, however, this performance is indicative of less toughness than is regarded as desirable, since the entire vessel may be plastically deformed. The results suggest that in the presence of a sharp crack flaw approximately 1/2-inch (1.3-cm) long (the width of the brittle weld bead) that a catastrophic failure could occur at -30 F (-34.4 C).

The above experience illustrates the need for careful work when manufacturing explosion containment vessels. Exhaustive testing is not usually possible. In this case, Navy authorities on HY80 welding provided useful advice on weld preparation, such as grinding weld surfaces smooth. Subsequent bulge testing[8] indicated that the weld material could provide excellent performance in the absence of a large sharp flaw. Figure 14 shows the post test appearance of a welded plate after four shots at -30 F (-34.4 C).

FIGURE 11. CLOSE-UP VIEW OF THE CRACK STARTER ON THE HY80 STEEL PLATE AFTER SHOT 2-1-4 AT -30 F (-34.4 C)

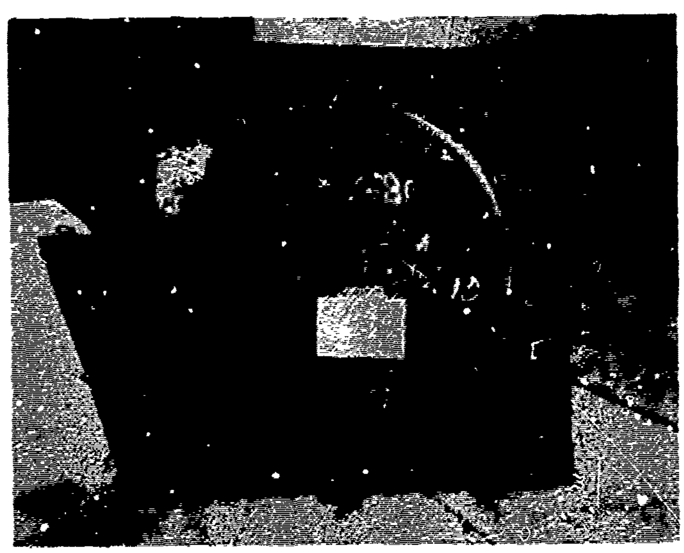

FIGURE 12. BOTTOM VIEW OF THE HY80 STEEL PLATE AFTER SHOT 2-2-3 AT -60 F (-51.1 C)

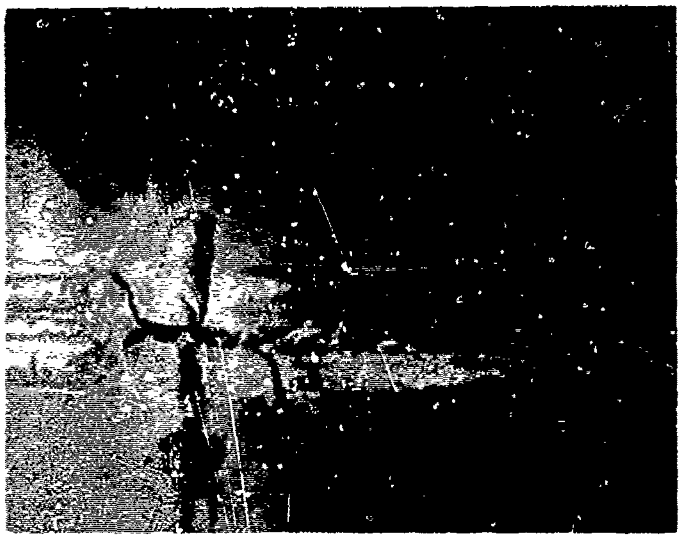

FIGURE 13. CLOSE-UP VIEW OF THE CRACK STARTER ON THE FIRST WELDED HY80 STEEL PLATE AFTER SHOT 2 AT -30 F (-34.4 C)

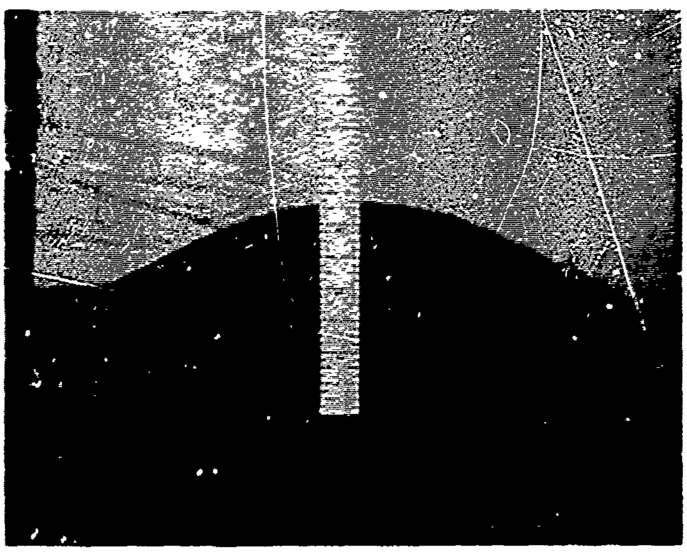

FIGURE 14. SIDE VIEW OF THE SECOND WELDED HY80 STEEL PLATE AFTER SHOT 4 AT -30 F (-34.4 C)

Other Steel Results

Due to its cost and strength characteristics, stainless steel was not regarded to be a cost effective material for a potentially widespread EOD application. Its good fracture toughness and corrosion resistance properties have led, however, to a few explosion containment applications. Stainless steels with good weldability are thus reliable backup materials for the present application. To demonstrate this fact, a single plate of AISI 304 was tested twice at -30 F (-34.4 C). The findings were quite similar to the HY80 results, except that the bulge height per shot was greater due to the lower yield strength.

Availability is an attractive feature of AISI 4340 steel. Grade 200 is a common structural material with low fracture toughness. Weldability is also a potential problem area. By heat treating the material to the 120 ksi (827 MPa) yield strength level, we found that good fracture toughness obtains. A crack on the third shot on the first plate (not shown) did run out three-inches (7.6-cm) before arresting. At this time, we regard the evaluation as inconclusive.

Based on Figure 12, it is easy to see that some of the fracture toughness of HY80 could be traded off for additional strength. A single plate of HY80 was thus heat treated to a yield strength of 120 ksi (827 MPa). The results of two bulge tests on this material were similar to the HY80 findings shown in Figures 11 and 12. In light of our experiences with the HY80 welding, we expect that a research effort may be needed to obtain sufficient properties at -30 F (-34.4 C) in the weld material.

6061-T6 Aluminum Alloy Results

After the various constraints of explosion containment vessel design are applied, some aluminum alloys are found to have potential for application.[6] Unlike static structures where strength is a dominant property, explosion containment capability depends on density, modulus, and strength. This statement is verified by Figure 15, which shows that the aluminum alloy plate bulged to a hemisphere and tore apart when exposed to the standard test adopted for steel.

A meaningful comparison of different metal plates having the same thickness is obtained by adjusting the charge standoff distance to obtain cases of equal energy absorption at the plate centers. The impulse approximation was used for this calculation.[6] As a result, the standoff distance for aluminum alloy plates was increased to 18-1/2-inches (47.0-cm).

Shot 6-2-1 at -30 F (-34.4 C) with no crack starter was quite successful, that is, the plate bulged 1-3/4-inches (4.45-cm) without a crack. A sharp crack was cut into the third aluminum plate. Shot 6-3-1 bulged 1-7/16-inches (3.65-cm) and surface cracks developed.

Figure 16 gives the result of Shot 6-3-2. The crack starter was the only flaw of significance. The results point to the inferior strength and ductility of aluminum alloy compared to steel.

MATERIAL LIMITATIONS IN FULL SCALE VESSELS

The purpose of this section is to show the relationship between the explosion bulge test data[6] and the limited amount of in-service data[7,8,13] available at the low service temperature of -30 F (-34.4 C). The NAVEODFAC development testing and TECHEVAL philosophy for explosion containment vessels calls for a statistically sufficient number of explosive tests under the circumstances of normal use plus a modest program to investigate the limitations of the designs and materials.[1-4]

Chamber Design

The data discussed in this section are for development models of the type-classified Mk 634 Mod 0 Explosive Devices Container.[13]

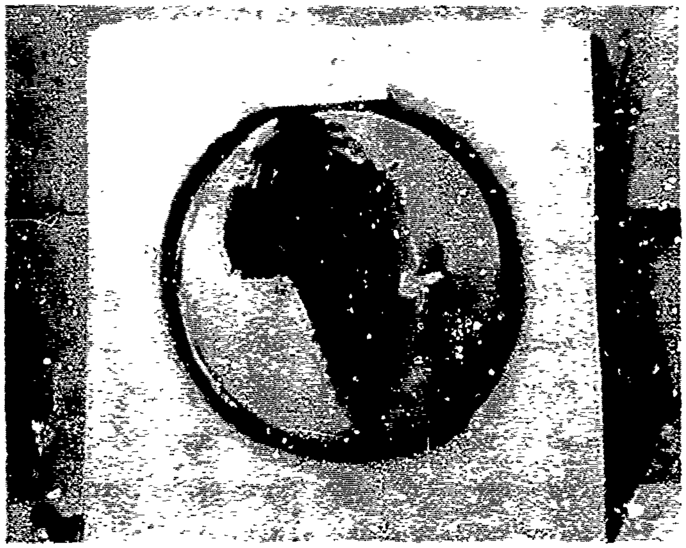

FIGURE 15. CLOSE-UP BOTTOM VIEW OF THE 6061 ALUMINUM ALLOY PLATE AFTER SHOT 6-1-1 AT -30 F (-34.4 C)

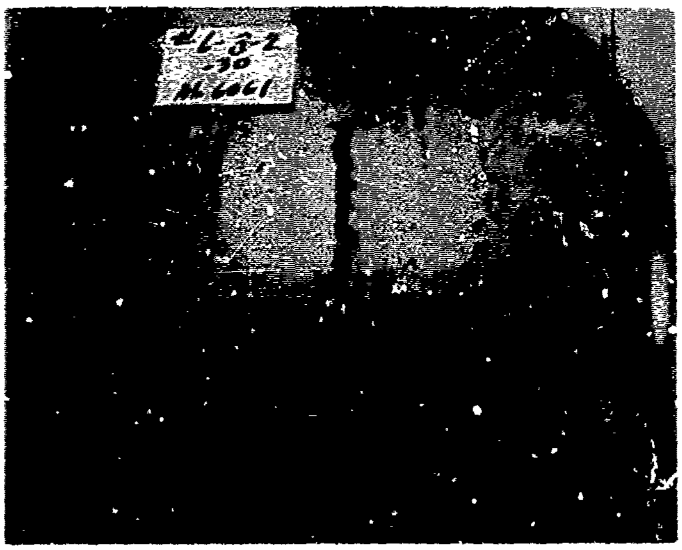

FIGURE 16. CLOSE-UP BOTTOM VIEW OF THE ALUMINUM ALLOY 6061 PLATE AFTER SHOT 6-3-2 AT -30 F (-34.4 C)

Figures 17 and 18 give front and side views of a vessel fabricated from Frostline steel. The spherical vessel is 3.5 ft (107 cm) in diameter, 0.90 inches (2.29 cm) in thickness, weighs 2,200 pounds (998 kg), and has a 21.75-inch (55.3-cm)-diameter access port with a circular door. The hemispherical heads were hot pressed by Lukens Steel Company. The machining, welding, inspecting, and development evaluations were completed at Battelle.

The 3.5-inch (8.9-cm)-thick door has a hingeless design that makes an internal overlapping seal on the inside of the access port reinforcing ring. The door is raised and lowered by means of a 12-volt dc electric/manual winch mounted at the top of the reinforcing ring. A five-legged spider assembly with a captive 1-inch (2.54 cm) -diameter bolt is used to provide positive support for the chamber door in the fully closed position during road travel or explosive testing. A discussion of further design considerations and details will be published elsewhere.

Frostline Steel Vessel Explosive Evaluation

The vessel shown in Figures 17 and 18 experienced 22 10-lb (4.54 kg)-shots and one 20-lb (9.08 kg)-shot at room temperature for a cumulative strain of 1.674 percent average strain.(7) Following the evaluation of the second vessel, this vessel survived three more 10-lb (4.54 kg)-shots at temperatures of 34 F (1 C), 22 F (-5.5 C), and 20 F (-6.5 C), respectively. The success of this series illustrates the role of the NDT and critical flaw sizes as indicated in Figure 1.

Figures 19 and 20 describe(1) the catastrophic failure on the first 10-lb (4.54 kg)-shot of the second Frostline vessel at -30 F (-34.4 C). The failure initiated at a single point in the heat-affected zone adjacent to the reinforcing ring and then spread through numerous branches. There was no visible defect in the region of initiation. The occurrence of nearly brittle fracture shows that Frostline steel has low resistance to the propagation of fracture at this temperature, despite the vendor's claim of unusually high Charpy V-notch impact energy. The

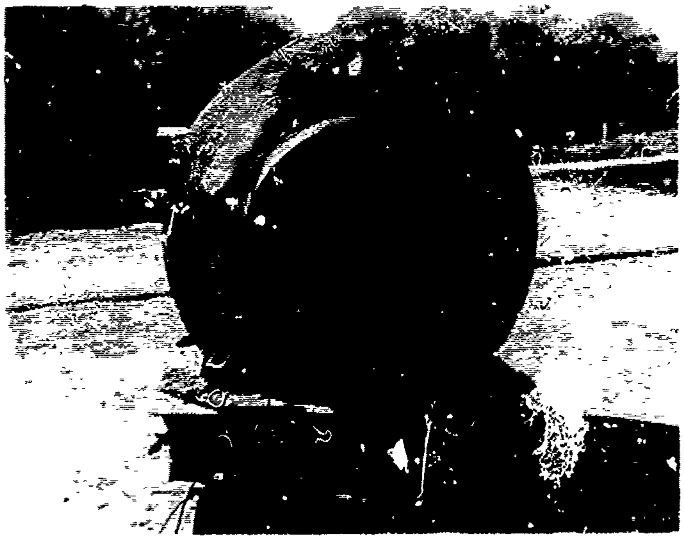

FIGURE 17. FRONT VIEW OF THE FIRST 3-1/2-FT (107-CM) EXPLOSION CONTAINMENT VESSEL FABRICATED FROM FP.TLINE STEEL AFTER SHOT NO. 23

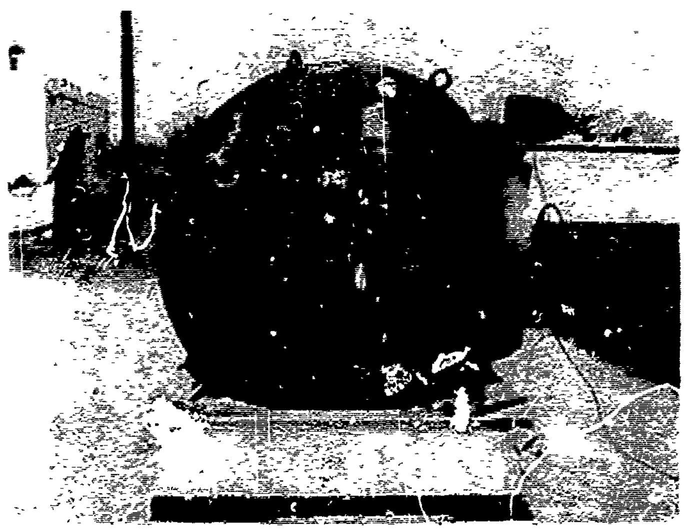

FIGURE 18. SIDE VIEW OF THE FIRST 3-1/2-FT (107-CM) EXPLOSION CONTAINMENT VESSEL FABRICATED FROM FROSTLINE STEEL AFTER SHOT NO. 23

FIGURE 19. VIEW OF THE PIECES OF VESSEL 2 FABRICATED WITH FROSTLINE STEEL AFTER FAILURE ON THE FIRST SHOT AT -30 F (-34.4 C)

FIGURE 20. CLOSE-UP VIEW OF SOME FRACTURE PATHS OF VESSEL 2 FABRICATED WITH FROSTLINE STEEL AFTER FAILURE ON THE FIRST SHOT AT -30 F (-34.4 C)

failure of this vessel actually confirmed earlier dynamic tear test results[7] by Battelle.

This Frostline vessel was capable of containing a 30-lb (13.6 kg)-shot at room temperature. Once again, the reader is cautioned to understand that this vessel failure was not due to explosive overloading or to any known problems with fabrication but with the fracture control properties of the Frostline material at the low service temperature. In this particular case, we believe that progress with the Frostline steel application could be made by seeking an improved heat treatment procedure for the 0.90-inch (2.29-cm)-thick, 3.5-ft (107 cm) -diameter hemispherical heads following hot pressing. As dramatized fully by Figures 19 and 20, Frostline steel is regretfully (for cost reasons) not a near-term solution to the material selection problem for the -30 F (-34.4 C) low service temperature requirement.

HY80 Steel Vessel Explosive Evaluation

Three chambers similar to the one shown in Figures 17 and 18 were fabricated from HY80 steel.[8] It is this version that has been type-classified as the Mk 634 Mod 0 Explosive Devices Container. The only problem encountered concerned the low temperature explosion bulge testing experience related to Figure 13. This led to greater care in finishing the welding work.

The first 3-1/2-ft (107-cm)-diameter vessel contained 20 individual 10-lb (4.54-kg) spherical composition C-4 charge detonations located at the chamber center. The average accumulated strain was only 0.178 percent. Seven of these detonations were conducted with the chamber near -30 F (-34.4 C).

Figures 21 and 22 give front and rear views of the second vessel fabricated from HY80 steel. The vessel is seen to have local bulges due to the containment of 12 individual 10-lb (4.54-kg) C-4 charges of spherical, cylindrical, and flat rectangular shape, located various distances offcenter. The average accumulated strain was 2.4 percent, and the maximum accumulated strain was 7.2 percent.

FIGURE 21. FRONT VIEW OF THE SECOND 3-1/2-FT (107-CM) VESSEL FABRICATED WITH HY80 STEEL AFTER 12 OFF-CENTER 10-LB (4.54-KG) SHOTS. A CENTERED 20-LB. (9.08-KG) CHARGE AND THE EDGE OF THE INSIDE SEALING, HINGELESS DOOR MAY BE SEEN.

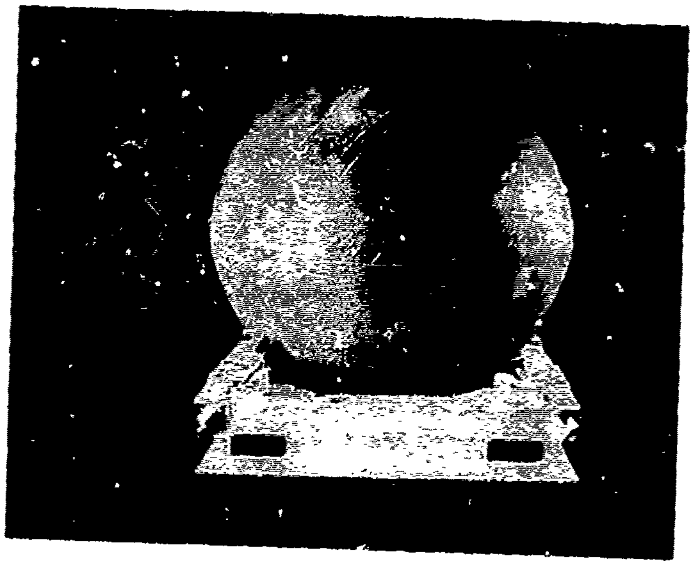

FIGURE 22. REAR VIEW OF THE SECOND 3-1/2-FT (107-CM) VESSEL FABRICATED WITH HY80 STEEL AFTER 12 OFF-CENTER 10-LB (4.54-KG) SHOTS

Three additional centered spherical shots of C-4 were then fired in the second vessel to determine the limitations of the HY80 material at room temperature. The first of these was the 20-lb (9.1-kg) charge positioned in the horizontally sliding basket assembly observable in Figure 21. The average and maximum accumulated residual strains increased to 2.67 and 7.4 percent, respectively. A 30-lb (13.6-kg) charge then increased the average and maximum accumulated strains to 3.81 and 7.9 percent, respectively.

Figures 23 and 24 give the results of Shot 15 on the second HY80 vessel. The vessel failed by high energy ductile fracture and separated into two pieces. A single origin was in the heat-affected zone near the location of a weld repair made following Shot 12. Based on measurements of the rear portion of the failed vessel, the average and maximum accumulated residual strains had increased to 7.1 and 9.3 percent, respectively. This series of explosive experiments demonstrates the truly remarkable containment capability of properly designed HY80 steel chambers.

CONCLUSIONS

Based on its development and application history and on its excellent performance during the Battelle explosion bulge experiments,[6] it was anticipated and confirmed experimentally[8] that HY80 steel is a superior vessel material for the low temperature service requirement. Unfortunately, the cost and the availability (military demand and control) of HY80 steel poses some problems for civilian and local government application. Also, the welding and inspection requirements are demanding, although these problems occur with all explosion containment vessel fabrication. A joint program between Federal and local governments could solve much of the cost, availability, and indemnity problems. In the long term, it would appear imperative that the fracture control properties of Frostline or some HSLA steel be improved to meet the low service temperature requirement.

The following list of observations, conclusions, and implied recommendations summarizes the Battelle viewpoint of the progress with

FIGURE 23. VIEW OF FRONT PIECE OF THE SECOND 3-1/2 FT (107-CM) VESSEL FABRICATED WITH HY80 STEEL AFTER FAILURE AT 70 F (21 C) FROM A 40-LB (18.2-KG) CHARGE

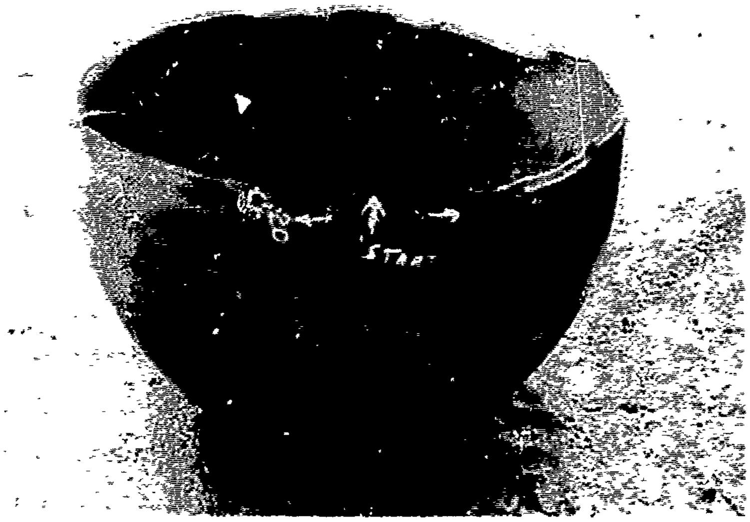

FIGURE 24. VIEW OF THE REAR PIECE OF THE SECOND 3-1/2-FT (107-CM) VESSEL FABRICATED WITH HY80 STEEL AFTER FAILURE AT 70 F (21 C) FROM A 40-LB (18.2-KG) CHARGE. LOCAL STRAINS AS HIGH AS 7.9 PERCENT EXISTED PRIOR TO THE FATAL SHOT 15

materials evaluation for explosion containment application, particularly for the -30 F (-34.4 C) low service temperature requirement:

- Steel alloys are cost effective relative to other materials, such as titanium and aluminum alloys
- Cost effective steels have the ductile to brittle transition temperature property
- Vessels normally fail due to low temperature use, not explosive overloading
- Steel materials are thus fracture control property limited, not strength/ductility property limited
- The Navy crack starter explosion bulge test is a viable method for judging the fracture control properties of a candidate material
- HY80 steel is the most practical near-term material for use by the military EOD community
- Stainless steels, such as AISI 304, may be applied successfully at some sacrifice of cost and maximum contained explosive weight capability
- Welding problems represent a major concern for <u>all</u> related applications and should be researched, inspected, and tested for quality
- Local-government officials should be careful to avoid the use of vessels fabricated from materials with unproven properties
- Existing vessels fabricated from materials with unproven materials should be evaluated for restrictive use or remotely tested for capabilities under appropriately extreme conditions
- A joint program between the Federal and local governments could increase the use of high quality vessels
- Further efforts to evaluate HSLA steels could lead to the identification of a more cost effective containment material

- The choice of a higher low service temperature standard, for example, 0 F (-17.8 C), for civilian EOD applications could lead to the selection of an adequately evaluated, more cost effective material for near-term application
- Officials interested in fabricating a vessel according to the FBI description should consider both the design[13] and materials selection[6-8] progress that has been made in the interim before finalizing their plans

ACKNOWLEDGEMENTS

Several persons on the Battelle staff contributed to the success of this project. Particularly worthy of mention are Dr. Joe H. Brown, Jr. for managerial support, Joseph G. Dunleavy for advice on material properties, Dr. Joseph W. Spretnak (OSU faculty) for advice on material evaluations, Herbert W. Mishler for welding expertise, William H. Stefanov and others for welding, and W. F. Schola and S. C. Green for explosive experimentation. Regretfully, Mr. Dunleavy and Dr. Spretnak are now deceased. The continued interest of Lennard J. Wolfson and John Butler of NAVEODFAC and Joseph E. Backofen, Jr. and Guy C. Throner of Battelle is greatly appreciated.

APPENDIX

The purpose of this brief appendix is to review some recent progress with the development of a simple scaling law for the sizing of spherical explosion containment vessels having an elastic response.[9] The advantage of this scaling law is the ease of making preliminary design calculations.

The scaling law project used computer calculations to establish the formula

$$\varepsilon_m = e^{P_1} \left(\frac{\rho}{\rho_0}\right)^{P_2} \left(\frac{E_1}{E_0}\right)^{P_3} \left(\frac{d}{d_0}\right)^{P_4} \left(\frac{h}{h_0}\right)^{P_5} \left(\frac{W}{W_0}\right)^{P_6}, \qquad (1)$$

where ε_m is the maximum first-cycle strain, e is Euler's constant, ρ is the material density, E_1 is the effective material modulus $E/(1-\nu)$, d is the vessel diameter, h is the vessel wall thickness, and W is the weight of explosive detonated. To obtain the dimensionless independent variables indicated in Equation (1), take ρ_0 = 1-lb/in.^{3} (1 gm/cm^3), $E_0 = 10^6$ psi (10^9 Pa), d_0 = 1 ft (1 m), h_0 = 1 in. (1 cm), and W_0 = 1 lb (1 kg), as the English and SI reference units, respectively.

Table 2 gives values[9] of the six parameters, $P_1 \ldots P_6$, based on calculations for four selected materials and four selected vessel designs (diameter and wall thickness specifications). The difference between the two types of least squares fitting results is not significant for engineering purposes. The scaling law is estimated to have 5% agreement with calculations that agree within 10% with experimental measurements.[2,3]

Figure 25 indicates the predicted maximum first-cycle elastic response of vessel design B if any of four selected nominal material types are assumed.[9] Vessel design B corresponds to the shell dimensions of the Mk 634 Mod 0 pictured in Figures 17-24. The plot labeled for material 3 is for a steel alloy vessel. Note that the elastic limit for the steel alloy version of design B is approximately 10 lb (4.54-kg) of explosive. Thus the observed accumulated residual plastic strain per 10-lb (4.54-kg)-shot[7,8] is relatively small.

TABLE 2. ELASTIC SCALING-LAW PARAMETERS

Four Materials and Four Vessel Designs		
Parameter	Nonlinear Fit	Log Linear Fit
1 -Eng. Units	-4.522 ± 0.162	-4.436 ± 0.155
-SI Units	(-1.945 ± 0.070)	(-1.903 ± 0.065)
2	-0.424 ± 0.029	-0.410 ± 0.028
3	-0.577 ± 0.033	-0.591 ± 0.032
4	-1.283 ± 0.028	-1.293 ± 0.027
5	-1.034 ± 0.032	-1.026 ± 0.030
6	0.771 ± 0.002	0.772 ± 0.002
χ_{rms}	0.0446	0.0425

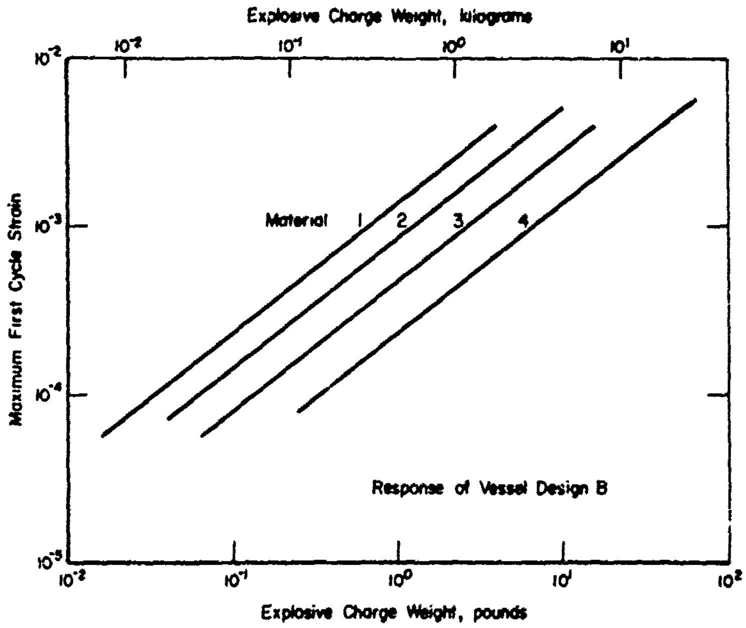

FIGURE 25. MAXIMUM FIRST-CYCLE STRAIN VERSUS EXPLOSIVE CHARGE WEIGHT FOR VESSEL DESIGN B. A PLOT BASED ON THE NONLINEAR FIT PARAMETERS IN TABLE 2 IS GIVEN FOR EACH OF FOUR MATERIALS, (1) ALUMINUM, (2) TITANIUM, (3) STEEL, AND (4) TUNGSTEN ALLOYS.

REFERENCES

(1) Trott, B. D., Backofen, J. E., White, J. J., and Wolfson, L. J., "Trailer-Mounted Chamber for Containment of 40 Pounds of TNT", Minutes of the Seventeenth Explosives Safety Seminar, Volume I, 687-708 (1978), AD A066 568.

(2) White, J. J., Trott, B. D., and Backofen, J. E., "The Physics of Explosion Containment", Physics in Technology, 8, 94-100 (1977).

(3) Trott, B. D., Backofen, J. E., White, J. J., and Petty, J., "Design of Explosive Blast Containment Vessels for Explosive Ordnance Disposal Units", AMMRC MS 78-3, Proc. of the Army Symposium on Solid Mechanics, 1978 - Case Studies on Structural Integrity and Reliability, 215-288 (1978), AD A059 834.

(4) Trott, B. D., Backofen, J. E., White, J. J., and Wolfson, L. J., "Blast and Fragment Containment Capability of Portable Chambers", Minutes of the Eighteenth Explosives Safety Seminar, Volume I, 687-708 (1978), AD A066 568.

(5) Backofen, J. E., Wolfson, L. J., and Shock, J. D., "Suppression of Fragment Damage by Means of Frangible Surrounds", Minutes of the Eighteenth Safety Seminar, Volume II, 1751-1766 (1978), AD A066 568.

(6) White, J. J., Trott, B. D., and Schola, W. F., "Development of Comparative Data on the Blast Containment Capability of Several Materials", NAVEODFAC TR-189, Final Report to Naval Explosive Ordnance Disposal Facility, Contract No. N00174-76-C-0187, Battelle, Columbus Laboratories (May 1978), AD B028 042L.

(7) Trott, B. D., and White, J. J., "Design and Evaluation of an Experimental Multipurpose Blast Containment Chamber", NAVEODFAC TR-196, Final Report to Naval Explosive Ordnance Disposal Facility, Contract No. N00174-76-C-0103, Battelle, Columbus Laboratories (October 1978), AD B033 126L.

(8) Trott, B. D., "The Construction and Evaluation of Prototype Blast-Containment Chambers", NAVEODFAC TR-210, Final Report to Naval Explosive Ordnance Disposal Facility, Contract No. N00174-77-C-0372, Battelle, Columbus Laboratories (May 1979), AD B040 696L.

(9) White, J. J., and Trott, B. D., "Scaling Law for the Elastic Response of Spherical Explosion-Containment Vessels, Experimental Mechanics, 20, 174-177 (1980).

(10) "Explosive Confinement Vessel", General Information Bulletin 76-9, FBI Bomb Data Program (1976).

(11) "Total Containment Bomb Trailer", Int. Def. Rev., 10, 1183 (1977).

(12) McDanolds, R. T., "Explosive Containment Chamber for FBI Bomb Data Program", Tech. Memo. 2218, Picatinny Arsenal, Dover, N.J. (January 1977), AD B016 780.

(13) Florschutz, G. B., "Development and Testing of the Mk 634 Mod 0 Explosive Devices Container", NAVEODFAC TR-229, Naval Explosive Ordnance Disposal Facility, (March 1980), AD B047 693L.

(14) Herlach, F., and Knoepfel, H., "On the Containment of Explosions", L.G.I. 63/23, EURATOM-C.N.E.N., Frascati, Rome, (November, 1963).

(15) Rogers, B. T., "Containment Vessel Cookbook", M-2 TM-249, Los Alamos Scientific Laboratory, Los Alamos, New Mexico (March 1975).

(16) Karpp, R. R., Duffey, T. A., and Neal, T. R., "Response of Containment Vessels to Explosive Blast Loading", LA-8082, Los Alamos Scientific Laboratory, Los Alamos, New Mexico (June 1980).

(17) Pellini, W. S., and Puzak, P. P., "Fracture Analysis Diagram Procedures for the Fracture-Safe Engineering Design of Steel Structures", NRL Report 5920, U. S. Naval Research Laboratory, Washington, D. C. (March 15, 1963), AD 402 116.

(18) Pellini, W. S., "Advances in Fracture Toughness Characterization Procedures and in Quantitative Interpretations to Fracture-Safe Design for Structural Steels", NRL Report 6713, U. S. Naval Research Lab., Wash., D. C. (April 3, 1968), AD 669 690.

(19) Goode, R. J., Judy, R. W. Jr., and Huber, R. W., "Procedures for Fracture Toughness Characterization and Interpretations to Failure-Safe Design for Structural Titanium Alloys", NRL Report 6679, U. S. Naval Research Laboratory, Washington, D. C. (December 5, 1968), AD 681 043.

(20) Judy, R. W. Jr., Goode, R. J., and Freed, C. N., "Fracture Toughness Characterization Procedures and Interpretations to Fracture-Safe Design for Structural Aluminum Alloys", NRL Report 6871, U. S. Naval Research Lab, Wash., D. C. (March 31, 1969), AD 687 396.

(21) Pellini, W. S., and Loss, F. J., "Integration of Metallurgical and Fracture Mechanics Concepts of Transition Temperature Factors Relating to Fracture-Safe Design for Structural Steels", NRL Report 6900, U. S. Naval Research Laboratory, Washington, D. C., (April 22, 1969), AD 688 417.

(22) Pellini, W. S., "Principles of Structural Integrity Technology", Office of Naval Research, Arlington, Virginia (1967), AD A039 391.

(23) "Standard Evaluation Procedures for Explosion Bulge Testing (Weldments) Including Preproduction Tests of HY-80 Steel", NAVSHIPS 250-637-6, Bureau of Ships, Navy Department, Washington, D. C.

BASIS FOR DESIGN OF REINFORCED CONCRETE STRUCTURES FOR COMPLETE CONTAINMENT

By

Norval Dobbs
Samuel Weissman
Frederick Sock

AMMANN & WHITNEY, CONSULTING ENGINEERS

and

Paul Price

U.S. ARMY RESEARCH AND DEVELOPMENT CENTER

ABSTRACT

Modern-day explosive manufacturing and loading facilities require increased protection to achieve a safe operating system. They are required to be designed to provide full containment of an explosion. This paper discusses the basis for full containment design of explosives and presents conclusions and recommendations based on some tests that were performed at various U.S. Army Research Centers.

BASIS FOR FULL CONTAINMENT DESIGN

Introduction

Modern-day explosive manufacturing and loading facilities require increased protection to achieve a safe operating system. However, present methods of manufacture and storage allow lesser space than that required for a given quantity of explosive materials. Such concentrations of explosives increase the possibility of the propagation of explosions.

Consistent with present safety regulations, those facilities that prevent explosion propagation, damage to materials or injury to personnel, are being designed to provide full containment of an explosion.

Two main sources are available to establish a basis for the design criteria for full containment of explosives. These include:

1. Regulatory design manuals and reports, and

2. Results of full-containment cell tests performed recently at Tooele Army Depot, Utah, and at the U.S. Army Armament Research and Development Center (ARRADCOM) in Dover, New Jersey.

Design Manuals

In June 1969, the tri-service design manual, "Structures to Resist the Effects of Accidental Explosions" (hereafter referred to as TM 5-1300 or ref. 1) was approved as the regulatory manual for the design of reinforced concrete structures to resist the effects of HE-type explosions. Reference 1 contains methods and criteria to determine the output from an explosion, its effects on a structure and subsequently the structural response.

Blast Loads

The interior surface of a structure which fully or nearly fully contains an explosion is initially subjected to high intensity blast pressures and their reflections that are similar to the pressures produced in cubicle structures. These high intensity pressures are immediately followed by lower pressures which are produced by the accumulation, within the structure, of the gaseous products of the explosion. Figure 1 shows a typical pressure-time record at a point on a wall surface of a full containment cell. The high peaks are due to the multiple reflections of the initial shock and are relatively short in duration (several milliseconds), while the lower pressures which are denoted as "P_m" have a long duration as compared to shock wave pressures. The maximum mean pressure (P_m) is used as the basis for design (for full containment cells) and is a function of the charge weight, contained volume of the chamber, and venting area.

Reference 1 (TM 5-1300) provides data relating both to high intensity, short duration loads as well as long duration pressures. Figure 2 (corresponding to Figures 4-54 through 4-62 of Reference 1) indicate the impulse loads associated with blast loads on surfaces each of which has four adjoining surfaces (as shown in Figure 3) which are typical of full containment cells. These loads used in combination with the long duration loads given in Figure 4 will provide the data necessary to establish the blast environment in full containment cells. It should be realized that the data given in Figures 1 through 3 are blast loads produced by the detonation of TNT in confined chambers. More recently, data developed for Composition B and other types of explosives are given in References 2 and 3.

To illustrate the use of the above data, let us assume a structure configuration as shown in Figure 5. The main cell of this structure has a volume equal to 41,000 cubic feet and is subjected to the blast effects of 660 pounds of TNT detonated at a location indicated in Figure 4 and approximately 3 feet above the cell floor. For this case, the average blast loads acting on the closest wall will have peak average shock and gas pressures which are equal to 544 psi and 120 psi, respectively. The duration of the shock pressures will be equal to approximately 8 msec. Since the gas pressure will expand from the main cell into the staging area, it will reduce in intensity until stabilized at a peak pressure of 78 psi. This latter pressure will remain within the structure unless it is reduced either by:

1. The uncontrolled venting through openings to the atmosphere.

2. The controlled venting to the atmosphere, or

3. Permitted to decay by heat dissipation through the building surfaces.

In the case of the first method, contaminates will be released, the magnitude of which will be determined by the size of the openings. With the second method, the contaminates can be passed through filters at a controlled velocity which will not destroy the filters. The third method will require a considerable amount of time and will require the structure to sustain the pressures over a very long period of time. Of the three, the second method appears to be the safest. However, if the size of the openings can be limited and filters designed to sustain the blast pressures, then the first method may have merit.

Structural Response

Procedures for determining the response of reinforced concrete structures to blast loads are contained in Sections 5 and 6 of TM 5-1300. Section 5 presents the structural behavior of reinforced concrete whereas Section 6 presents the method of analyses to be used. Although these procedures have been developed for structures subjected to either fully vented internal explosions or structures subjected to external blast loads (acceptor structures), they are equally applicable to the design of structures used as full containment cells.

Figure 6 of this report presents a diagramatical representation of a typical "Explosive/Protective System". At the lower part of this system is the so-called "Protection Category" where either personnel, equipment and/or sensitive explosives are to be protected. This may be achieved by enclosing the acceptors to be protected and preventing the blast pressures from entering the enclosure, or by enclosing the donor and preventing the effects of an explosion from escaping to the atmosphere. The first method is usually used since it is generally the more cost effective system. However, where contaminates are involved, the second method is now being utilized.

The magnitude of structure response and deformations which can be permitted is dependent upon the building use and the number of detonations involved. When design of the structure specifies one incident only, then plastic deformations may be permitted. However, these deformations should be limited to "Limited Deflections" as specified in Figure 7 and specifically limited to 3-degree rotations or less for smaller structures and 2 degrees or less for structures similar in size to the proposed Damage Weapons Facility structure. Structures subjected to multiple detonations usually will have to be designed elastically.

Verification Tests

The design data presented in TM 5-1300 has been verified by more than 250 structural response tests. These tests included both full structures and building components. The cost for performing these tests entirely on a full-scale basis would have been prohibitive. Therefore, a series of tests were initiated whereby the scaled model testing of "laced" reinforced concrete (ref. 1) could be verified. This test series was referred to as "The Bay Structure Test Series" (ref. 4).

The bay structure (fig. 8) consisted of a 3-wall cubicle type structure with one wall and roof open to the atmosphere. Each wall utilized composite construction; i.e., two laced reinforced concrete panels separated by sand fill. Each panel of the full-scale structure was 2 feet thick, while the sand separating the donor and acceptor panels was 4 feet thick. Each wall of the full-scale structures was 10 feet high. The backwall was 40 feet long, while the length of each side wall was 20 feet. The floor slab varied in thickness from 2 feet adjacent to the walls to 1 foot thick in the central portion of the bay. The model structures consisted of a one-third, one-fifth, one-eighth and one-tenth scale version of the full-scale structure. All structural properties, including dimensions and the reinforcement, were modeled in comformance to the structural properties of the full-scale structure.

Each model of the bay structure was tested four times. The explosive weights used in each of the full-scale tests were 2,000, 3,000, 5,000 and 7,000 pounds, for a total cumulative charge weight equal to 17,500 pounds of HE. The charges of the smaller model tests were scaled accordingly.

Figure 9 illustrated the results of the first round of tests performed on the five models. There was essentially no difference in the wall responses of the five structures. Damage to the floor slabs of the two small models was slightly greater than that of the three larger structures. This difference was attributed to the fact that the small structures were built in a laboratory and placed upon a subbase of unconsolidated soil. The three large models were poured in-place and, therefore, were poured against the subsoil which had been compacted. The structural damage sustained in the other three rounds of tests was comparable to the first round. The results of this test series have verified that scaling of a laced reinforced concrete structure can be achieved.

Other Design Reports

More recently, other design reports have been published which supplement TM 5-1300. These include Reference 5 which provides data relating to the design of "Steel Structures to Resist the Effects of HE Explosions" and Reference 6 which deals with "Primary Fragment Characteristics and Impact Effects on Protective Barriers". Both of these reports are presently used as design manuals and their contents will be included in the revised edition of TM 5-1300.

Full Containment Structure Tests

Portable Explosive Containment Cell

This cell was designed for Tooele Army Depot and consists of a structural steel structure used for the demilitarization of "8-inch Chemical Projectiles". The structure is comprised of three main sections (fig. 10). The center section, which is cylindrical in shape, has a diameter and length equal to 10 feet and 24 feet, respectively. The two end sections are built-up flat plates which are bolted to the ends of the cylinder. Entrance to the structure for either personnel or the projectiles is through blast doors which are located in the end panels. Since the structure will contain toxic material, it must be fully sealed (fig. 11) against leakage in the event of an explosion. Hydraulic operators are required to compress these seals.

The cell was tested for an explosive quantity equal to approximately 10 pounds of Composition B. This quantity is approximately 20 percent greater than the explosive quantity in the projectile. The structure satisfactorily sustained the test and has received "Safety" approval to be used as part of the "demil" operation equipment.

ARRADCOM Test Structure

This test structure is a reinforced concrete structure, cylindrical in shape, whose interior dimensions are 11 feet 3 inches in diameter and 10 feet 0 inches high. This structure is a one-fourth scale model of a proposed melt/pour building.

The cylindrical wall of the structure is 9 inches thick. This thickness was predetermined by the wall thickness required to prevent a steel fragment, whose weight is one pound and is travelling at a velocity of 7,000 fps, from penetrating the wall (36 inches) of the full-scale building. The roof and floor slabs of the model are circular in shape, each having a thickness of 1 foot 6 inches. Both the roof and floor are cast monolithically with the wall. The wall and slabs are reinforced with "laced" reinforcement per TM 5-1300.

Entrance to the model is through a 2-foot 6-inch by 2-foot 6-inch opening in the cell wall. The opening is protected by a structural steel double leaf blast door which is a one-quarter scale model of the full-scale 10-foot by 10-foot door. Gas seals similar to those used in the portable containment cell were not provided around the door periphery.

The exterior surface of the cylindrical wall and the top of the roof slab are provided with spall shields. These shields retain any spalling due to the internal blast loads of the concrete over the exterior reinforcement. The spall shields consist of "Sturdy-Rib" cold-formed metal siding that is supported by structural steel "Tee" sections. The tees, in turn, are anchored to the concrete wall and slab by anchor bolts. The bolts are anchored by being hooked around the interior surface of the exterior reinforcement. If the bolts were past fully through the concrete, a shock load applied to the bolts at the cell interior would be transmitted through the bolts to the exterior and could rupture the exterior bolt heads.

Figure 12 is a photograph of the structure which was tested, while Figure 13 illustrates many of the construction details of the test structure.

The ARRADCOM test structure was designed to withstand the internal blast effects of 50 pounds of Composition B which is a one-quarter model of the 3,200 pounds of Composition B to be housed in the full-scale building. The structure was designed to undergo plastic deformations as a result of the 50-pound test. The circumferential reinforcement in the cylindrical wall was designed to sustain maximum strains of approximately 1.5 percent. The roof and floor slab reinforcement was designed to permit support rotations of approximately 1.5 degrees.

Since TM 5-1300 was developed for rectangular structures, a method had to be developed to establish the shock pressures in cylindrical structures. Some information was obtained from the Ballistic Research Laboratory relating blast loads in cylindrical structures. This data was compared to blast loads calculated from TM 5-1300 for a rectangular structure which had the same volume as for a cylindrical one. The pre-shot calculations were performed in this manner and, as shown later, were found to be slightly conservative.

Two 1.5-inch diameter structural steel pipes were positioned in the cylindrical wall, one each adjacent to each side of the entrance. These pipes are used to vent gas pressures to the atmosphere.

In order to quantitavely evaluate the results of the tests, a series of pezioelectric gages were installed within the cells to record the high intensity shock and gas pressures associated with the internal explosion. These gages were mounted at various locations on the wall and roof slab surfaces in order to obtain a record of the variation of blast loads within the structure. Electrical leads for the gages were passed through 0.5-inch diameter conduits which were embedded in the walls. The pressure records provided a pressure/time variation of the blast loads. In addition, a series of still and motion picture records of each test were obtained. The still photos recorded the pre- and post-shot condition of the structure, whereas the motion pictures were used to record the exterior of the structure during testing. Three cameras were used, one having a speed of 24 fps and two with a speed of 4,000 fps. The three cameras were positioned facing the entrance of the structure. Also, each test was viewed on video tape.

To date, nine tests were performed (Table 1). The first six tests were used to calibrate the instrumentation or determine methods of initiating the explosives. The purpose of the last three tests was to evaluate the structure response. Results of these reponse tests are best seen from the motion picture records as described below.

In Test No. 7, where 43 pounds of Composition B were detonated at the center of the cells, flames were seen to be forced out through both vent pipes and around the door. The flames escaped from around the door since, as explained earlier, no blast seals were provided. As described for a Portable Containment Cell, methods are now available where this blast leakage around the edges of doors can be prevented. Smoke was also observed to have escaped through the instrumentation electrical conduits. This leakage could have been eliminated with the use of electrical glands.

An investigation of the interior surfaces of the structure indicated that slight concrete spalling over the interior reinforcement of the wall had occurred. This was attributed to the fact that small sections of the wall had to be patched due to the occurrence of surface voids during construction. In addition, the interior surfaces of the structure were glazed as a result of the high termal energy produced by the explosion. This glazing was caused by the breakdown of the sand in the concrete. No loss in strength was caused by the glazing. Slight cracks were visable at the intersection of the roof slab, and the wall on the interior surface and at the mid-height of the exterior surface of the door pilaster. No other cracks were visable at the interior of the structure. Since the spall shields covered the exterior of the surfaces of the wall and roof, these surfaces could not be investigated for cracking. It is intended that at the conclusion of the tests, the shield will be removed and the exterior surfaces fully inspected. The blast doors were fully operable after the tests.

A misfire occurred in Test No. 8, with the explosive charge being damaged beyond repair.

The results of Test No. 9 were similar to those described above for Test No. 7. The slight cracking observed in the previous test was slightly larger after this test. No additional cracking was observed. Glazing effects of Test No. 7 were not increased in this test. The door was also operable after this test series.

A post-shot analysis of the blast pressures within the structure indicated that a better representation of the blast loads by using TM 5-1300 could be achieved by assuming a rectangular structure which has the same surface area as the cylindrical structure. Since the loads used in the design were conservative, it follows that the structure can withstand a large detonation. Therefore, it is planned that this structure be tested one more time using a 70-pound charge of Composition C-4.

CONCLUSIONS AND RECOMMENDATIONS

Based on the discussions presented in the preceding sections, the following conclusions and recommendations are made:

1. Design procedures are presently available for the design of laced reinforced concrete full containment cells.

2. The procedures of Item 1 are applicable to cylindrical as well as rectangular structures.

3. Similitude of structural response of full-scale laced reinforced concrete structure can be achieved using a small-scale model.

4. It is generally more cost effective to enclose the acceptors to be protected and prevent the blast pressures from entering the enclosure.

REFERENCES

1. "Structures to Resist the Effects of Accidental Explosions", U.S. Army Technical Manual TM 5-1300, U.S. Navy Publication NAVFAC P-397 and U.S. Air Force Manual AFM 88-22, Washington, D.C., June 1969.

2. "Blast Environment for Fully and Partially Vented Explosions in Cubicles", Civil Engineering Laboratory, Naval Construction Battalion Center, Port Hueneme, California.

3. PROCTOR, J.F. and FILLER, W.S., "A Computerized Technique for Blast Loads from Confined Explosions", from Minutes of the 14th Annual Explosive Safety Seminar, New Orleans, Louisiana, November 1972.

4. COHEN, E., DEDE, M. and DOBBS, N., Ammann & Whitney, Consulting Engineers, "Full and Model Scale Tests of Bay Structures", Technical Report 4168, Picatinny Arsenal, Dover, New Jersey, December 1971.

5. HEALEY, J., DOBBS, N., WEISSMAN, S., PECONE, G., VELLOZZI, J. and AMMAR, A., Ammann & Whitney, Consulting Engineers, "Design of Steel Structures to Resist the Effects of HE Explosions", Technical Report 4837, Picatinny Arsenal, Dover, New Jersey, August 1975.

6. HEALEY, J., WEISSMAN, S., DOBBS, N. and WERNER, H., Ammann & Whitney, Consulting Engineers, "Primary Fragment Characteristics and Impact Effects on Protective Barriers", Technical Report 4903, Picatinny Arsenal, Dover, New Jersey, December 1975.

Table 1. ARRADCOM Structure Tests

Test	Charge weight (lb)	Charge type	Date performed	Purpose
1	1	Comp B	9 Aug 78	Instrument Check
2	1*	Comp C-4	9 Aug 78	Instrument Check
3	2	Comp B	9 Aug 78	Instrument Check
4	4	Comp B	9 Aug 78	Instrument Check
5	2	Comp B	18 Aug 78	Instrument Check
6	4	Comp C-4	28 Aug 78	Instrument Check
7	43	Comp B	6 Sep 78	Structural Response
8	54*	Comp B	2 Nov 78	Structural Response
9	50	Comp C-4	2 Nov 78	Structural Response

*Misfire - Explosive split in pieces.

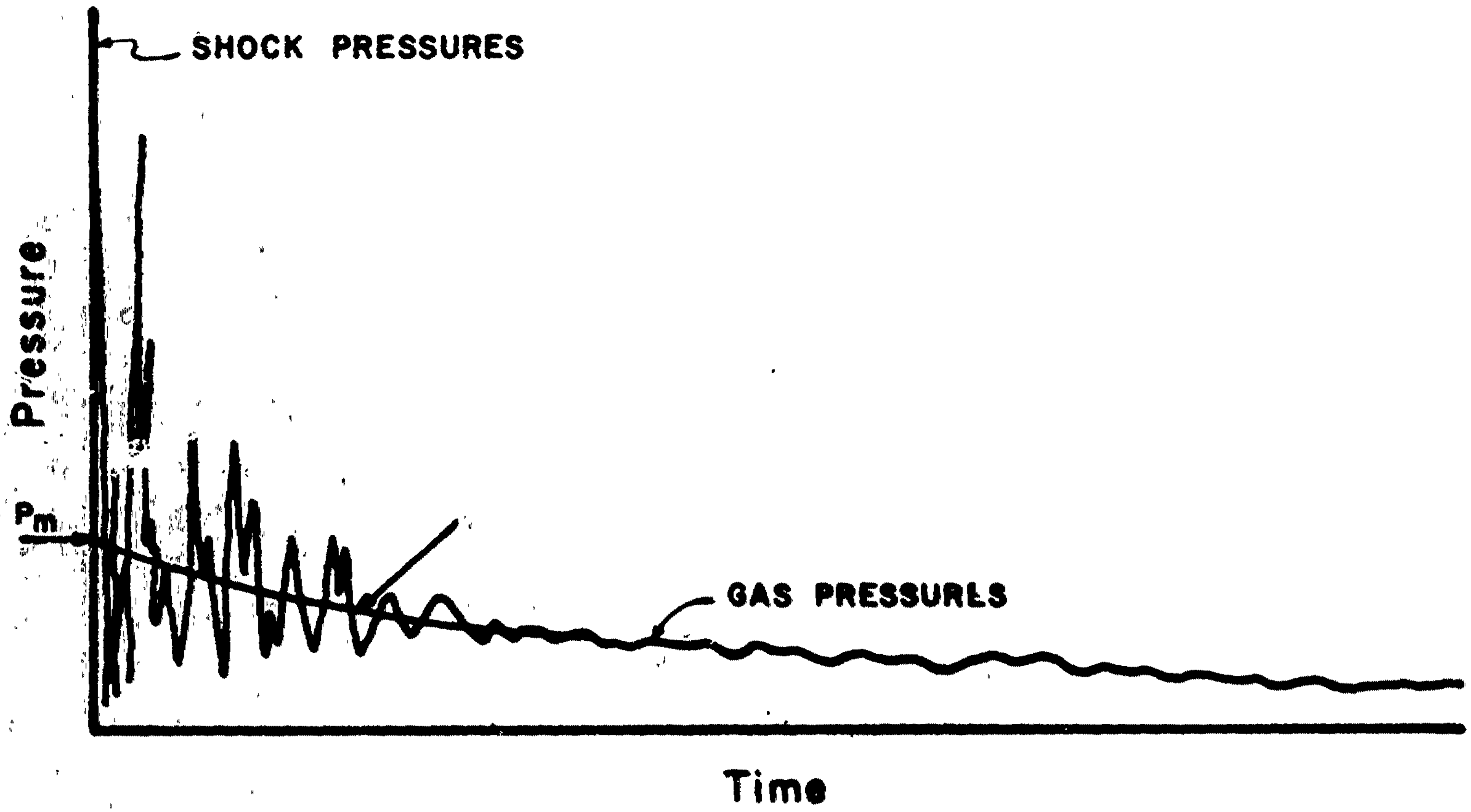

Figure 1. Typical pressure time record.

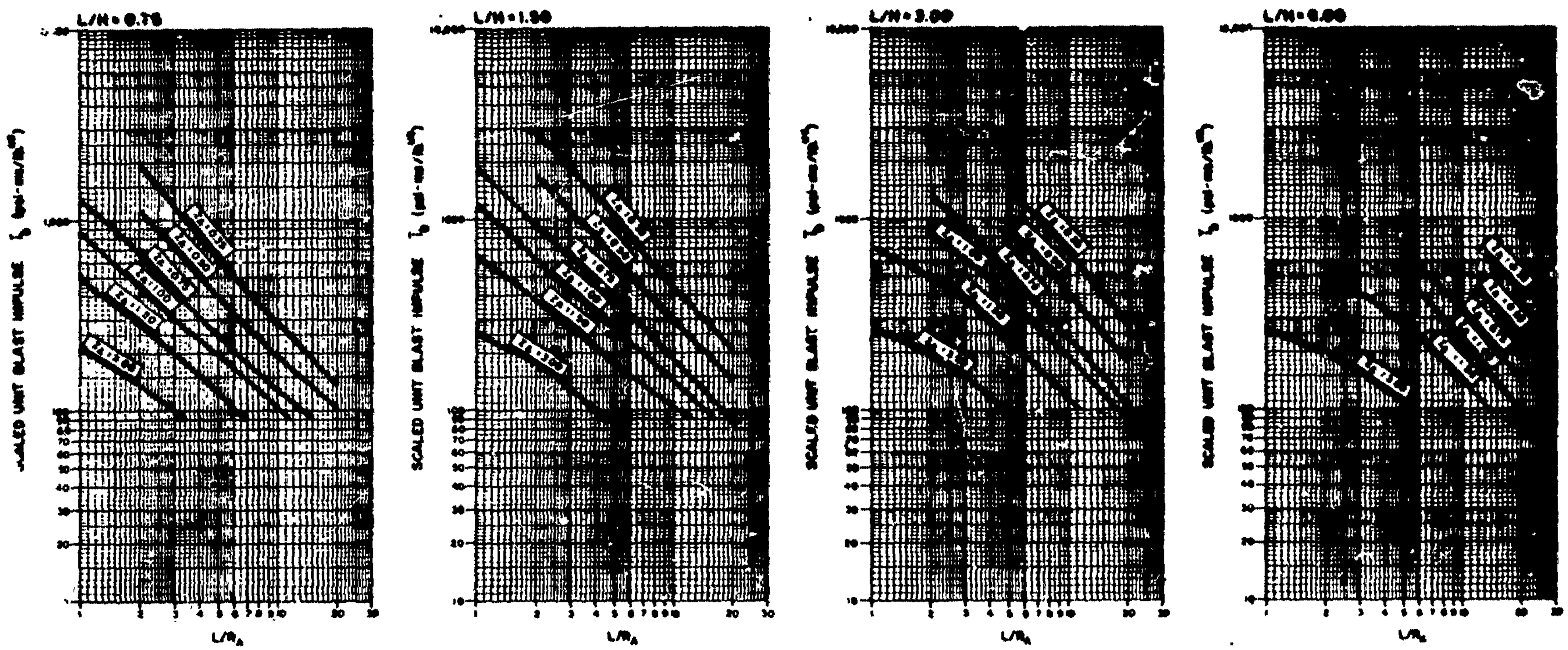

Figure 2. Scaled average unit blast impulse.

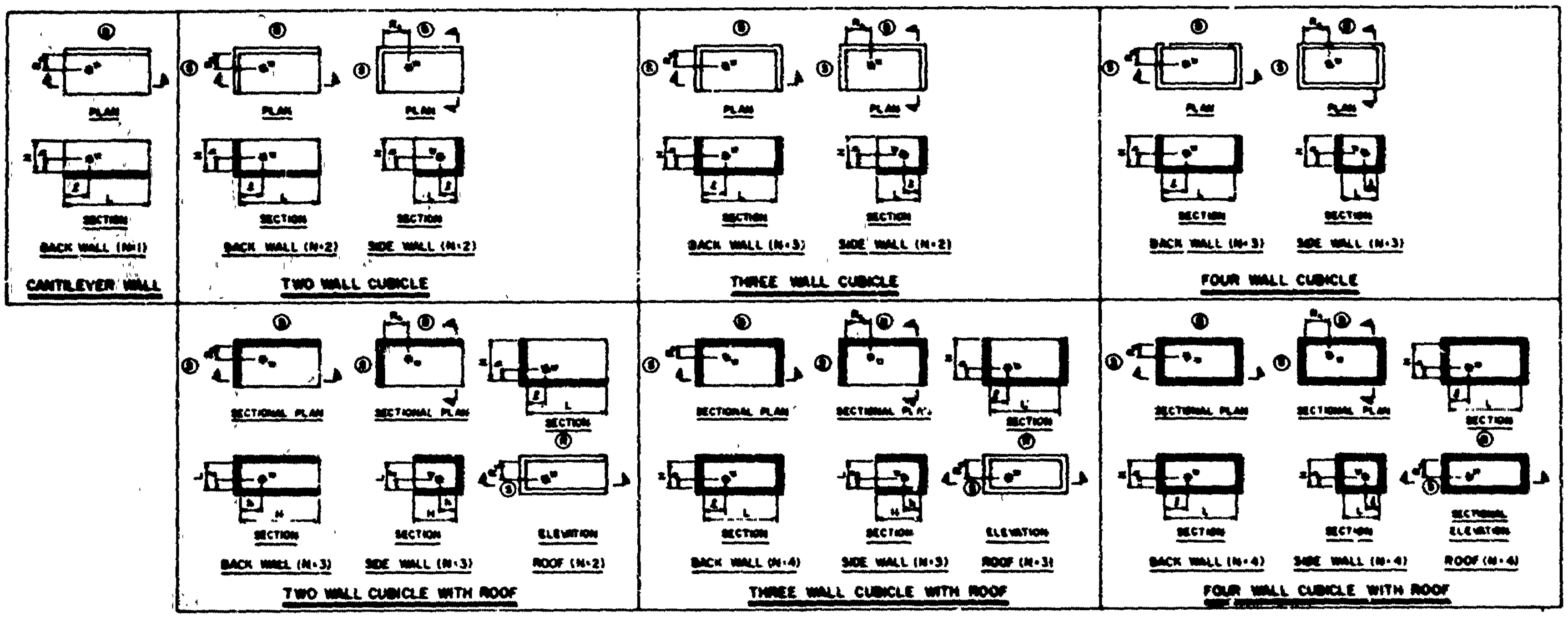

Figure 3. Barrier and cubicle configuration and parameters.

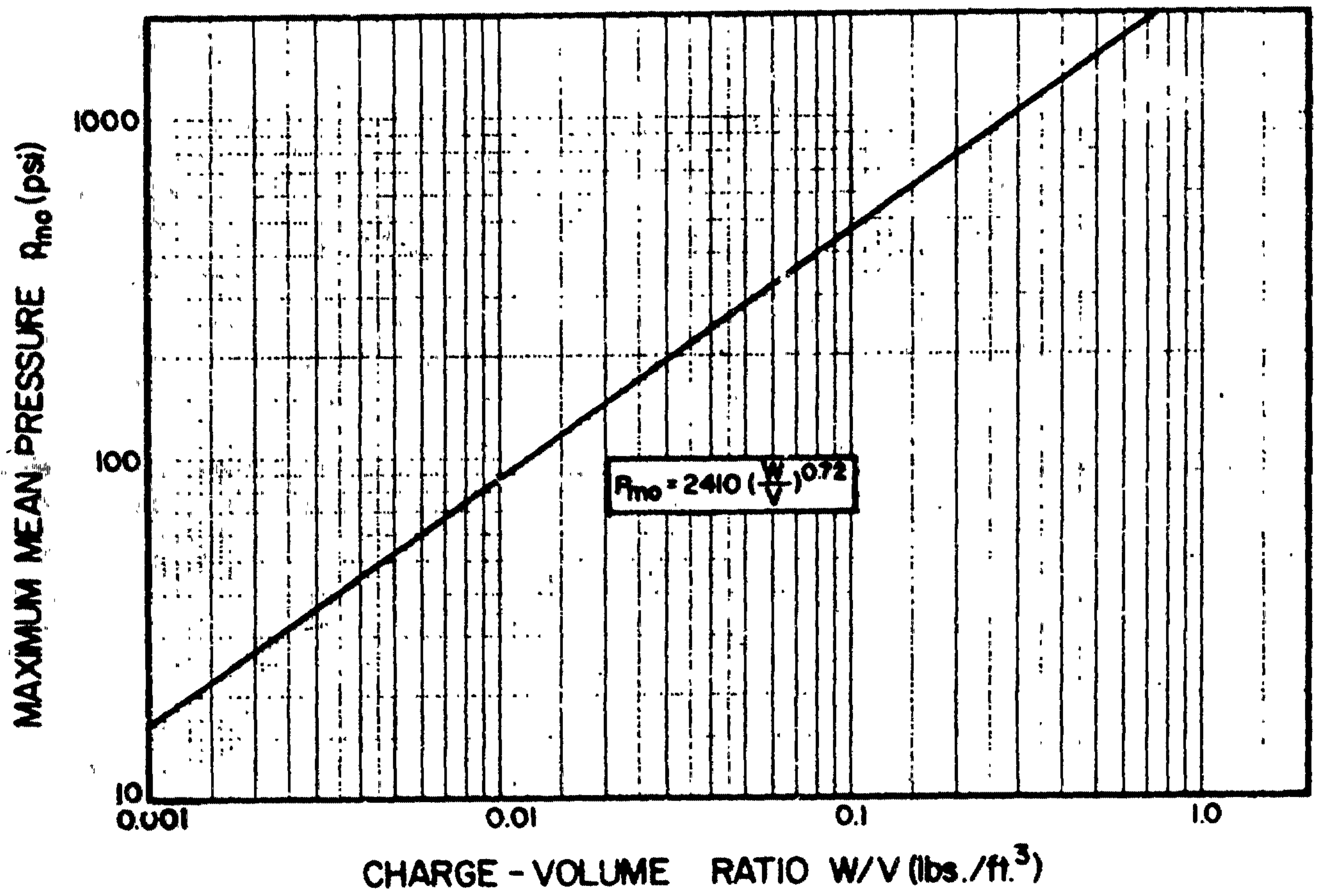

Figure 4. Maximum mean pressure in partially vented chamber.

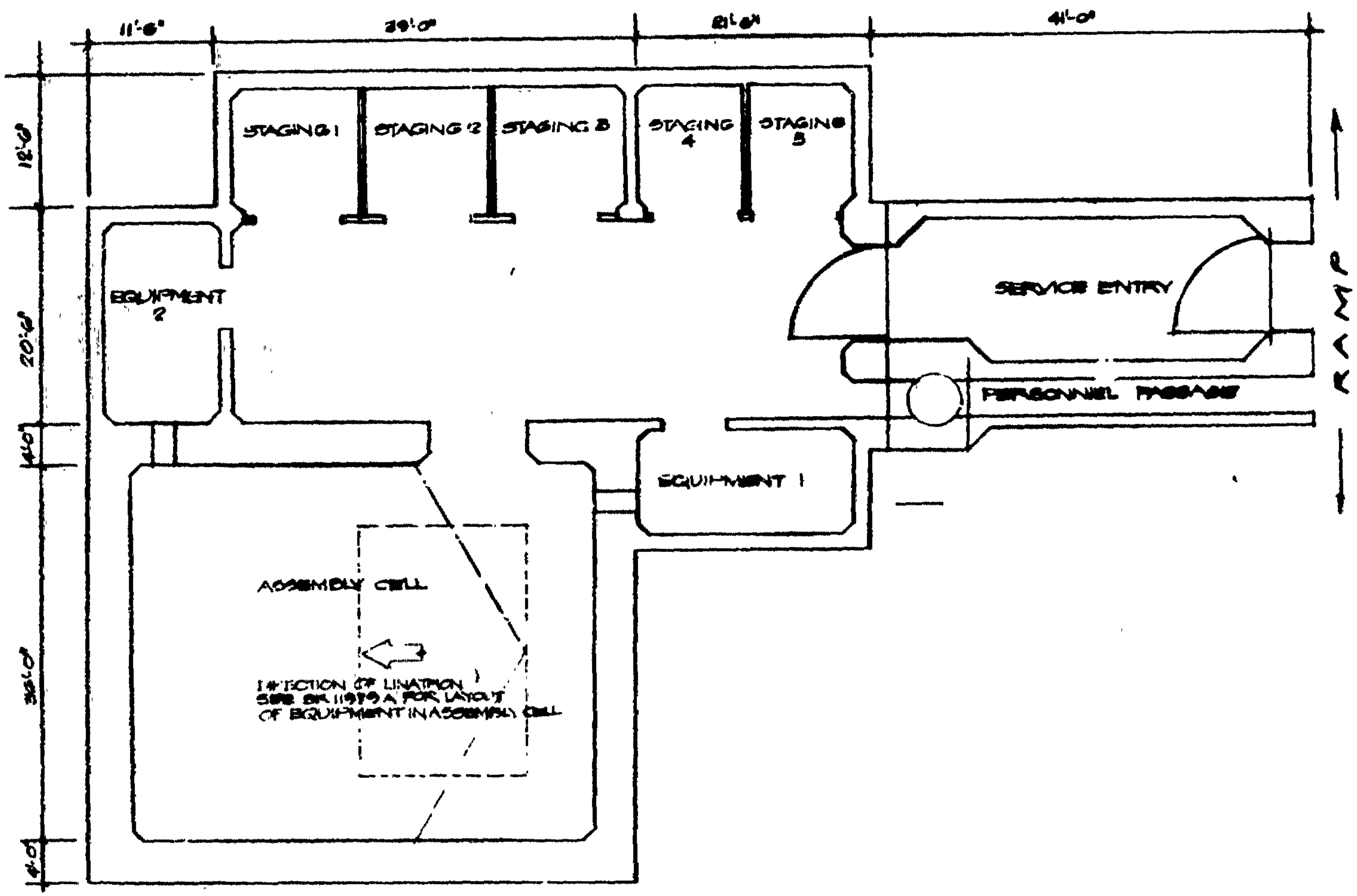

Figure 5. Structure configuration.

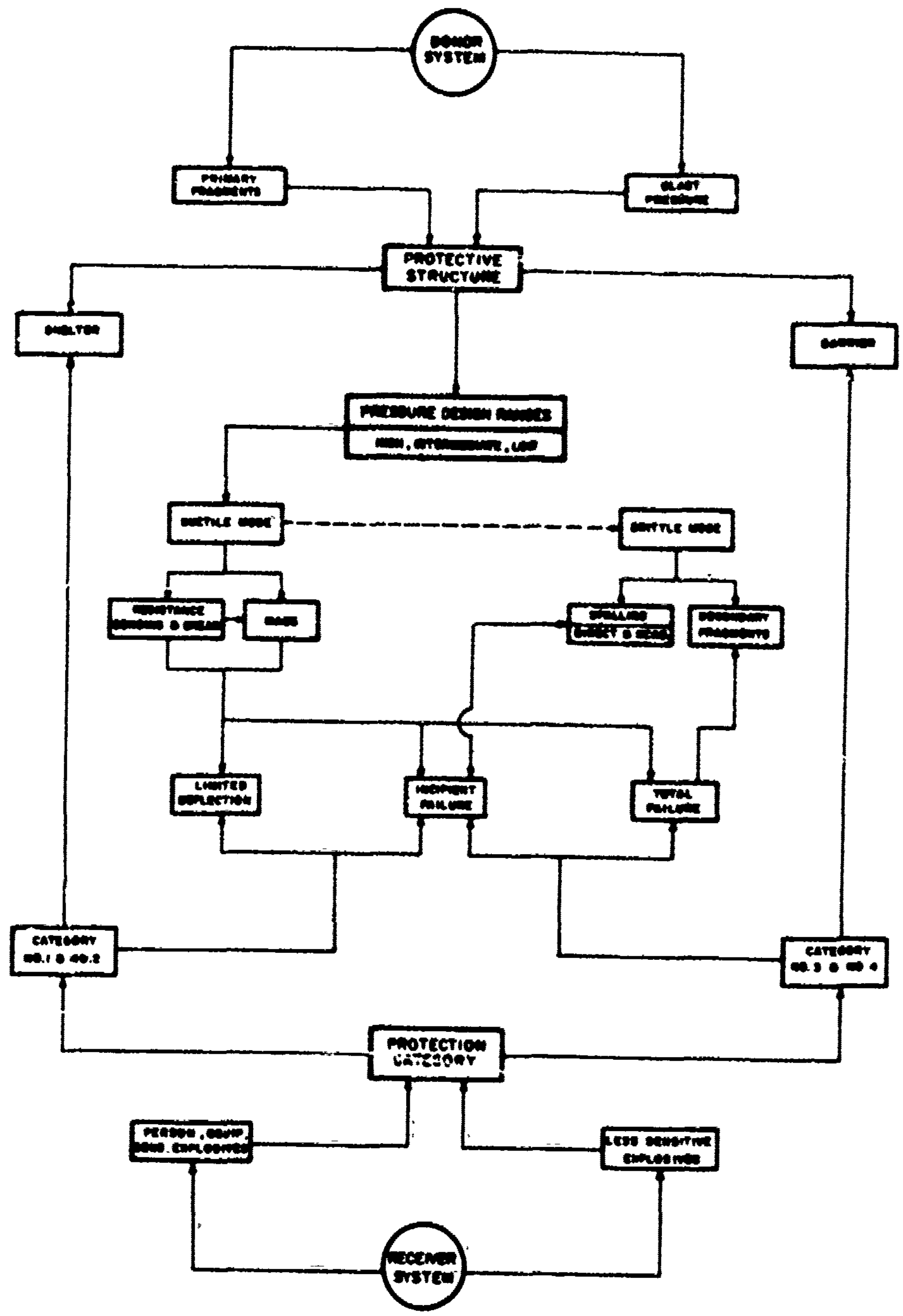

Figure 6. Explosion protective system.

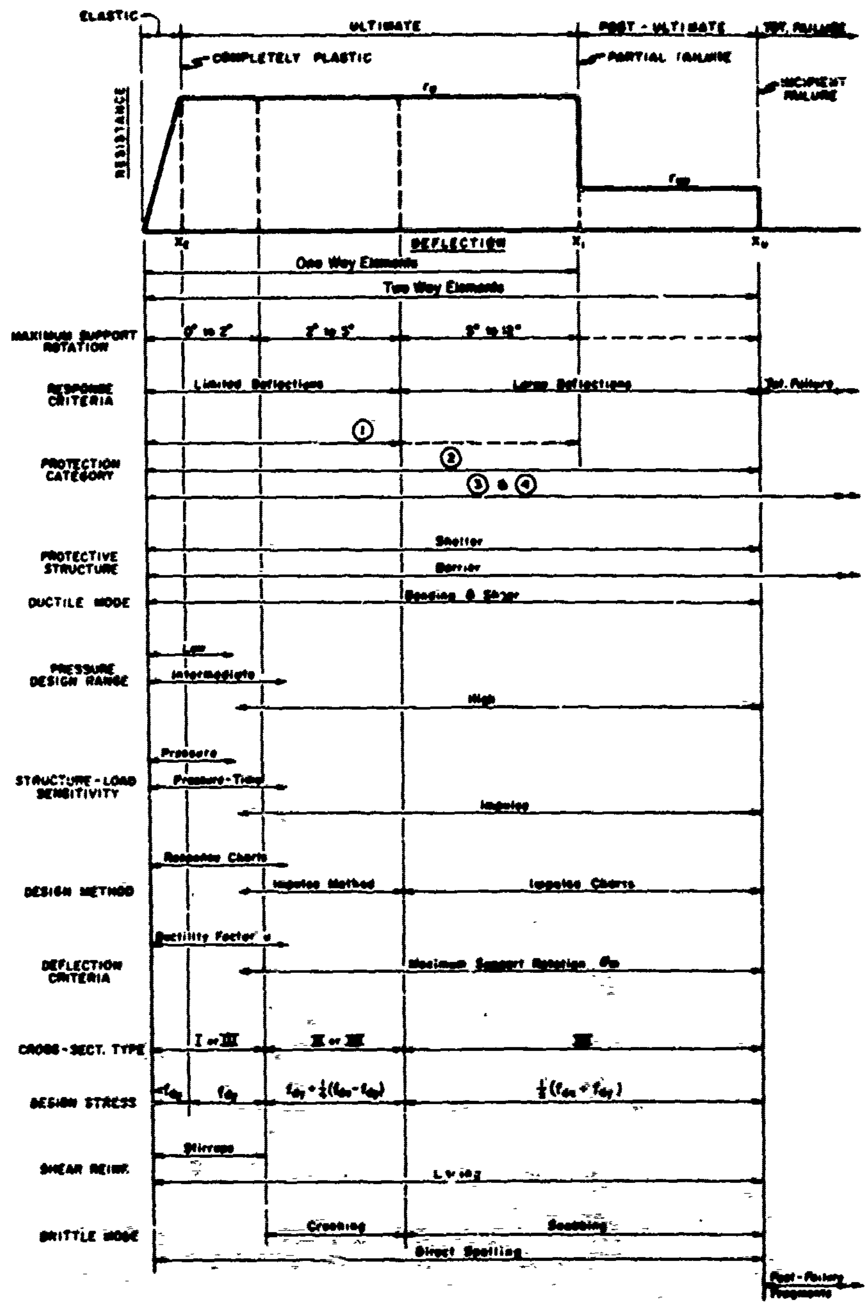

Figure 7. Relationships between design parameters.

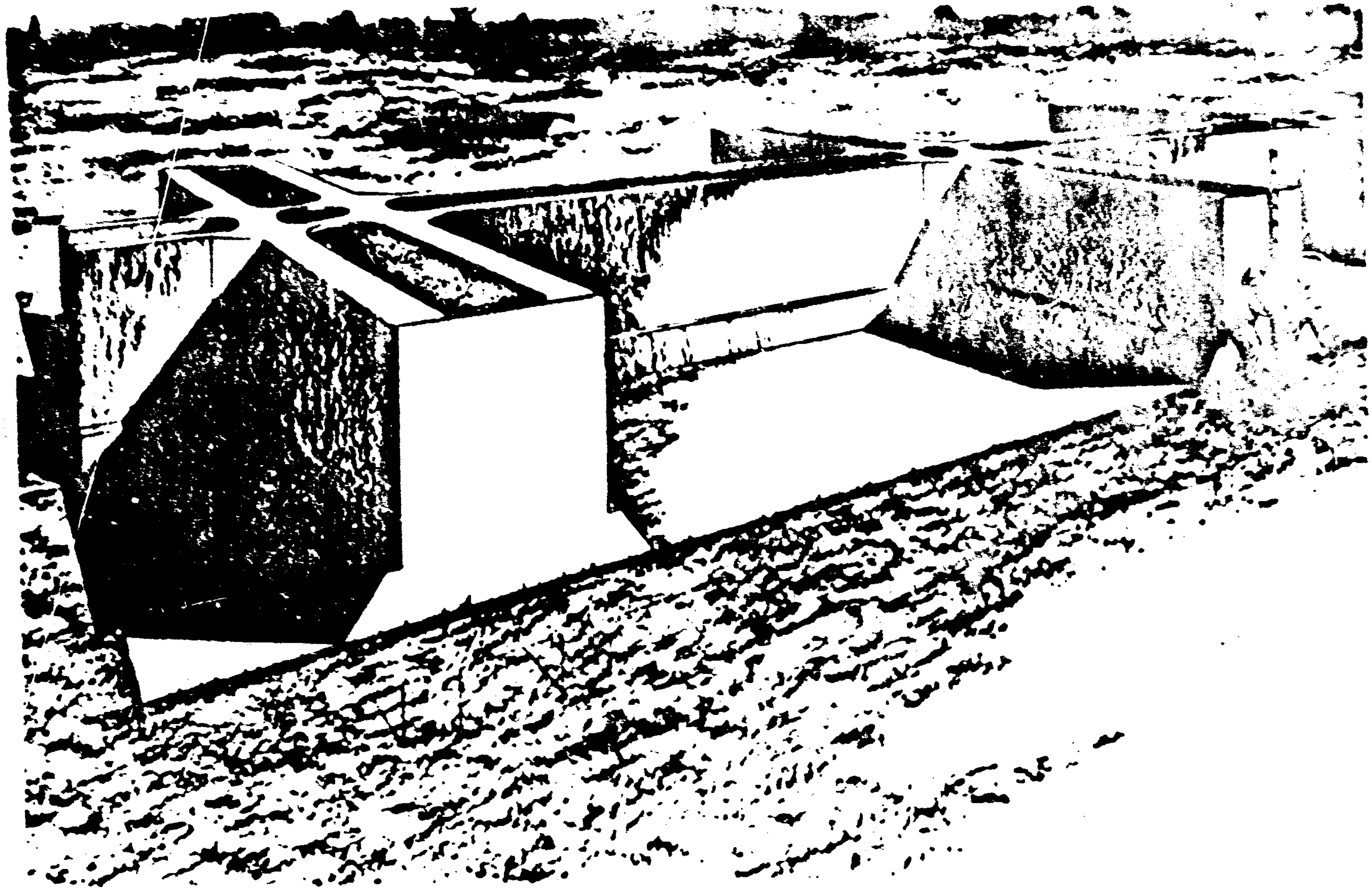

Figure 8. Cubicle structure

FULL SCALE, 2000 POUNDS

ONE-THIRD SCALE, 75 POUNDS

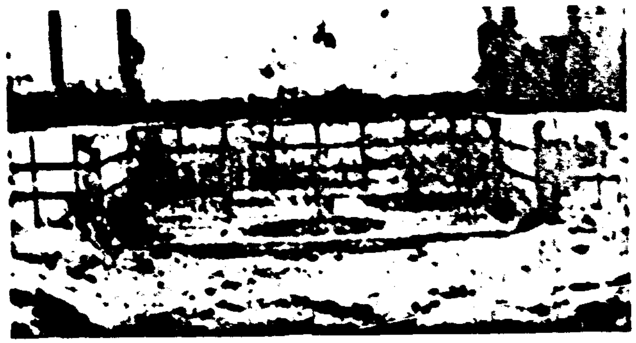

ONE-EIGHTH SCALE, 4 POUNDS

ONE-FIFTH SCALE, 16 POUNDS

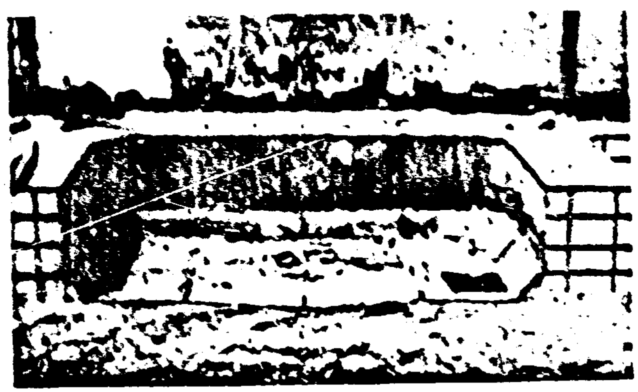

ONE-TENTH SCALE, 8 POUNDS

Figure 9. Cubicle test results.

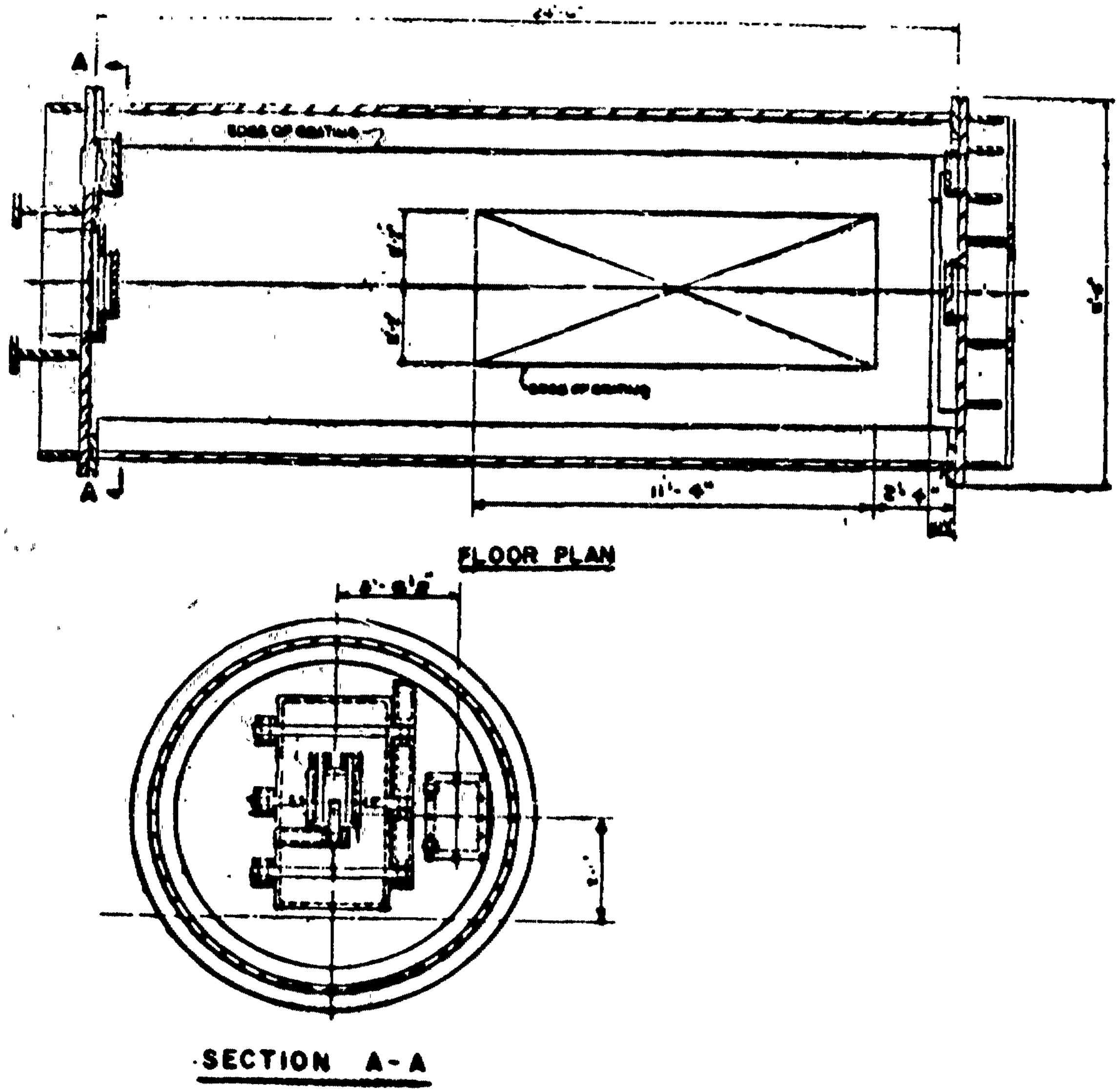

Figure 10. Structural steel test struc'ural.

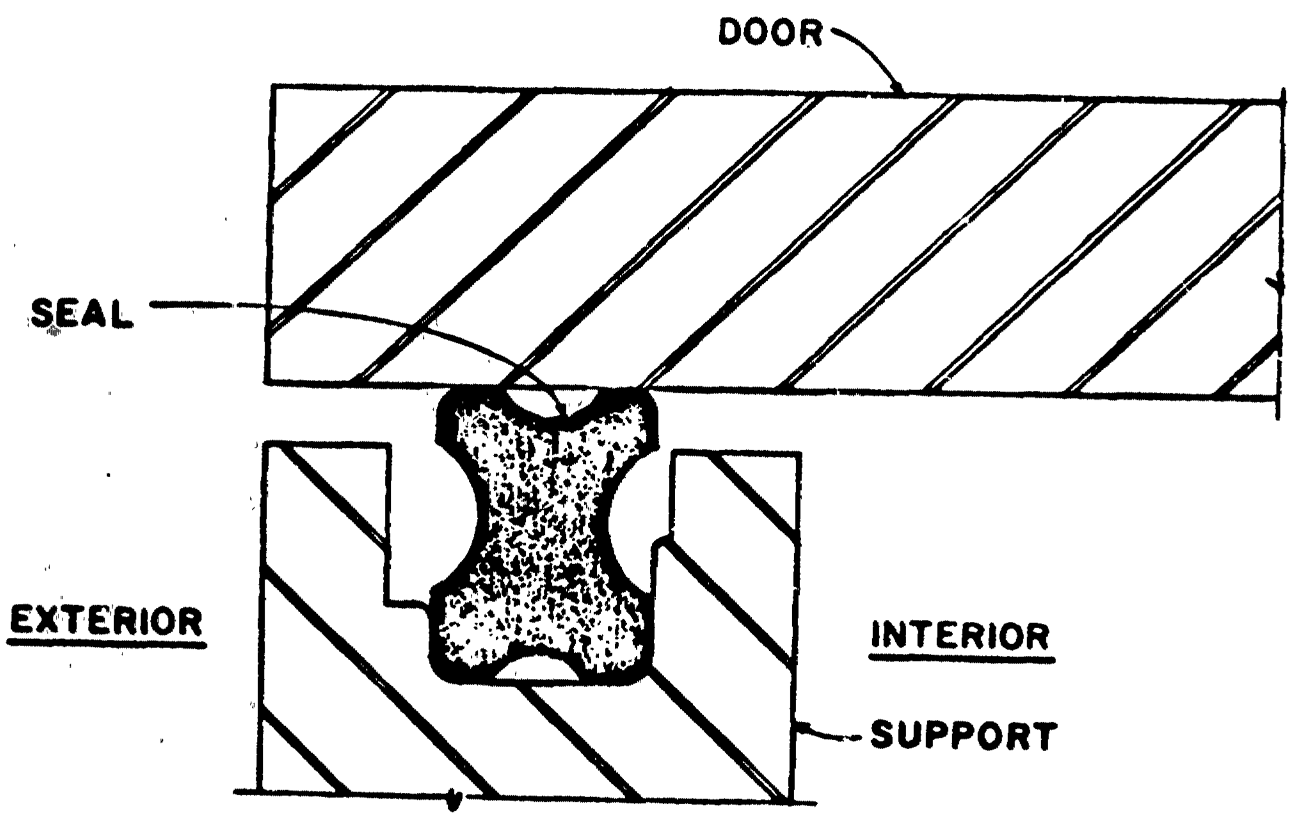

Figure II. Typical seal detail.

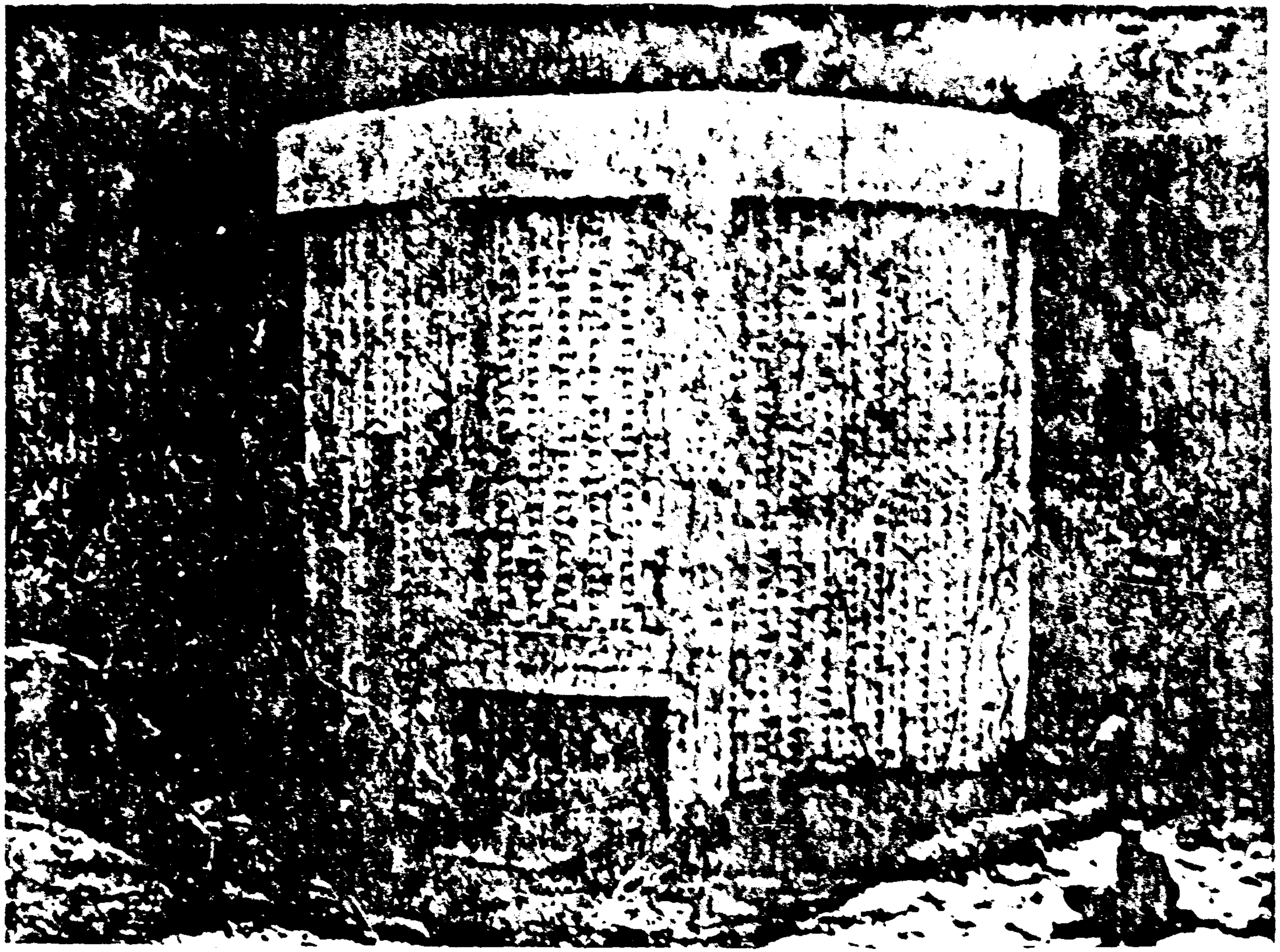

Figure 12. Cell structure.

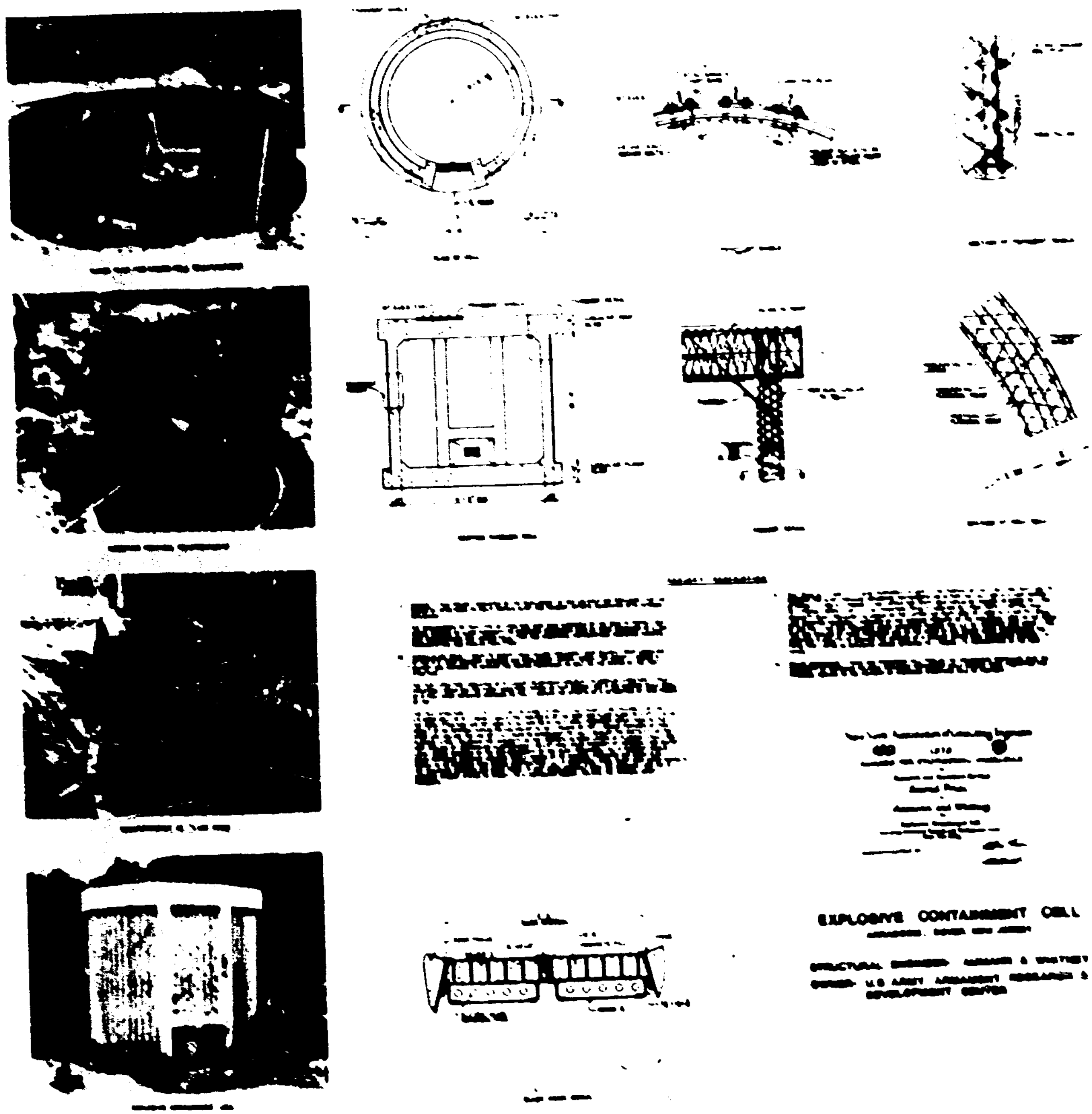

Figure 13. Cell structure details.

EXPLOSION VENTING IN BUILDINGS

BY

James J. Kulesz
Gerard J. Friesenhahn

ABSTRACT

Many vented, explosion-resistant structures must have vents covered by closures to maintain proper internal atmospheric conditions, or for other reasons. These closures are usually intended to be frangible and rapidly displace or fragment from the effects of internal explosions. This paper discusses the probable effects of closures on the venting process, and gives some prediction curves for the gas venting phase of the internal explosions, based on exercise of a relatively simple gas dynamic computer code.

The computer code incorporates three distinct phases of venting for the building. The first phase represents the case where a vent cover travels a finite distance, such as through a tunnel or the thickness of a thick wall, before any venting takes place. For this analysis, an equation of motion is developed which describes the effect of the quasi-static pressure on the velocity of the vent panel, and pressure decreases due to simple adiabatic expansion as the volume of the room changes. During the second phase of venting, the vent panel has cleared the tunnel or wall and the room begins to vent into the atmosphere. The energy of the gas is divided among energy expended during gas expansion, the kinetic energy of the vent panel and energy losses due to the gas flowing around the vent panel. The third phase of venting occurs after the vent panel is sufficiently far from the vent opening that it no longer interrupts the flow of the exiting gas. During this phase of venting, the gas vents through an orifice based on the ideal gas law and sonic or subsonic gas flow, depending upon the relative pressures between the room and the atmosphere.

I. INTRODUCTION

The analysis described in this paper was funded by the Department of the Army on Contract No. DACA87-79-C-0091 entitled "Preparation of a Manual for Prediction of Blast and Fragment Loadings on Structures [1]." This paper deals with a portion of this manual which describes venting of structures subjected to internal high explosive detonations and subsequent quasi-static pressure rise. The sections which follow contain a description of the major elements of the computer code which was developed to make the predictions, a model analysis detailing appropriate ways in which to present the numerically generated results for maximum usage, the results of the computations, and the conclusions.

II. COMPUTER CODE

Prior to this study, work has been performed describing the pressure-time profile for venting blast-resistant structures subjected to internal explosions. In these studies, however, the vents were always open holes [2,3] and the effects of vent covers were ignored. Not accounting for the inertial effects of the vent panels could result in underestimating the time for venting and nonconservative blast loading. The computer program which we developed allows for the effect of the vent panel in constricting the gas flow. In addition to determining the pressure history inside the chamber, it also calculates the velocity of the vent panel, if it remains intact.

Figure 1 is a schematic representation of the vented chamber. The blast-resistant room has thick walls with thickness L. The vent panel is either adjacent to the ground or, as shown in the figure, high

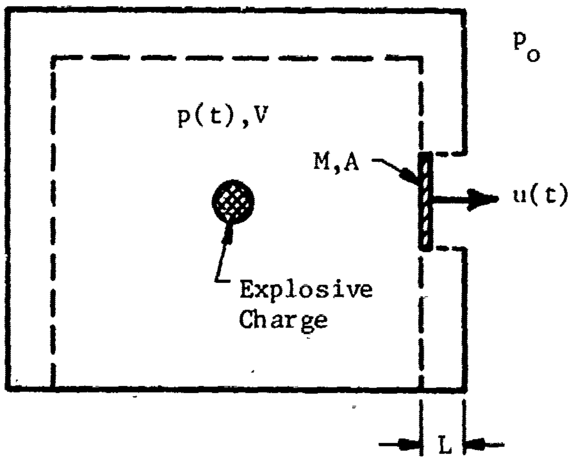

Figure 1. Schematic of Vented Chamber (First Phase)

enough above the ground that gas flow is not affected by the ground surface. The room has a volume V and pressure as a function of time p(t). Pressure outside the room is ambient pressure p_o. The vent panel has mass M, presented area A and velocity as a function of time u(t). The impulsive shock loading, from the first shock wave and immediately following reflections, imparts an initial velocity u_o to the vent panel. The velocity of the vent panel then increases as it travels through the wall due to adiabatic expansion of the gases. After the panel begins to clear the wall, it acquires additional velocity from gas expansion but some of the energy of the gas is lost through venting. Finally, after the vent panel moves away from the wall, it is no longer affected by, not does it affect, the flow of gases out of the opening.

The computer code VENT which we developed is composed of three distinct phases of venting. The first phase represents the case where a vent cover travels a finite distance, such as through a tunnel or the thickness of a thick wall, before any venting takes place. During this phase of venting, we used the technique demonstrated by Kulesz, et al. [4] for accidental explosions onboard a Navy submarine tender. The equation of motion for the vent panel is

$$M\ddot{x} = [p(t) - p_o]\ A \tag{1}$$

where $\ddot{x}$ is the acceleration of the panel (second derivative with respect to time t). At start of time, p_o is the peak quasi-static pressure and it is assumed the pressure does not change appreciably during a small increment of time Δt. The velocity of the panel at time $t + \Delta t$ is then

$$u\ (t + \Delta t) = [p(t) - p_o]\ \frac{A\ \Delta t}{M} + u(t) \tag{2}$$

The portion of the vent panel at time $t + \Delta t$ can be obtained from

$$X\ (t + \Delta t) = [p(t) - p_o]\ \frac{A\ (\Delta t)^2}{2M} + u(t)\ \Delta t + X\ (t) \tag{3}$$

Internal pressure p(t) from one time t to another $(t + \Delta t)$ can then be determined by assuming adiabatic expansion as given by

$$p(t + \Delta t)\ V(t + \Delta t)^{\gamma} = p(t)\ V(t)^{\gamma} \tag{4}$$

where γ is the ratio of specific heats of the gas and is approximately 1.4.

During the <u>second phase</u> of venting, the vent panel has cleared the tunnel or wall and the room begins to vent into the atmosphere. The energy of the gas is divided among energy expended during gas expansion, the kinetic energy of the vent panel and energy losses due to the gas flowing around the vent panel. To perform this phase of the analysis, our computer program uses a modified version of the technique developed by Taylor and Price [5], Baker, et al. [6] and Kulesz, et al. [4]. Reference 4 calculates the velocity of fragments and gas state variables for bursting rectangular cylinders, Reference 5 for bursting spheres, and Reference 6 for bursting cylinders. To use the bursting pressure container solutions for a vented chamber, one has to convert the problem into one of equivalent geometry. Figure 2a shows the chamber with exiting vent panel. The initial energy of the gas is partitioned among the kinetic energy of the panel, the increase in effective volume (the volume of the initial chamber, area times the wall thickness, plus the area times the exterior travelled distance X), and the loss of energy as the gas expands into the outside atmosphere. Baker, et al. [6] modified the bursting spherical pressure vessel technique of Taylor and Price [5] so that it could be used for bursting cylindrical pressure vessels as shown in Figure 2b. The symmetry of the problem allowed them to use an iterative technique to solve for the relative position X of the two halves of the cylinder and the gas state variables. Also because of symmetry, one can easily determine the parameters associated with one half of the vessel. For our problem involving a gas chamber which is accelerating a vent panel and releasing gas to the atmosphere, it was also necessary to introduce symmetry into the problem. As far as velocity is concerned, it makes no difference if one is in the reference frame of the vent chamber (vent chamber stationary or vent chamber moving). By allowing the vent panel to remain stationary at the position of the vertical dotted line in Figure 2c, one can introduce a mirror image of the chamber as shown in the figure. The shape of the chamber has been adjusted to assure that the gas exit area around the perimeter E for each chamber (gas exit area + EX_1 = EX_2 = $EX/2$) is the same as that shown in Figure 2a. Also, the initial pressure $p(0)$, volume $V(0)$ and temperature $\Theta(0)$ in each one of the two chambers shown in Figure 2c must be the same as that of the original chamber (Figure 2a). Finally, since we have switched to the frame of reference of the vent panel, one can establish an equation of motion for the chamber, or equivalently the vent panel, by allowing each of the equivalent vent chambers of Figure 2c to have a mass M equal to that of the vent panel (i.e. $M_1 = M_2 = M$). The equations of motion are then

$$M_1 \frac{d^2 X_1}{dt^2} = A\, p(t), \text{ with } X_1(0) = 0, \frac{dX_1(0)}{dt} = V_1 \qquad (5)$$

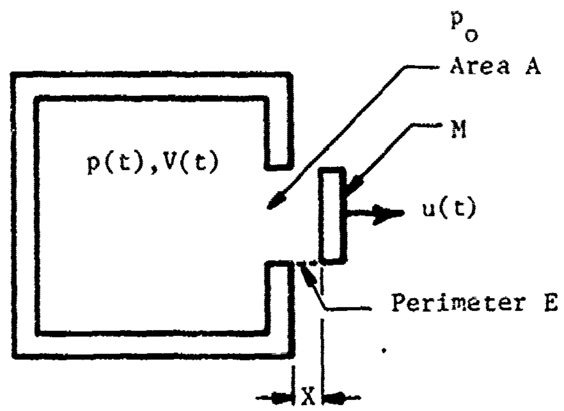

(a) Vented Chamber

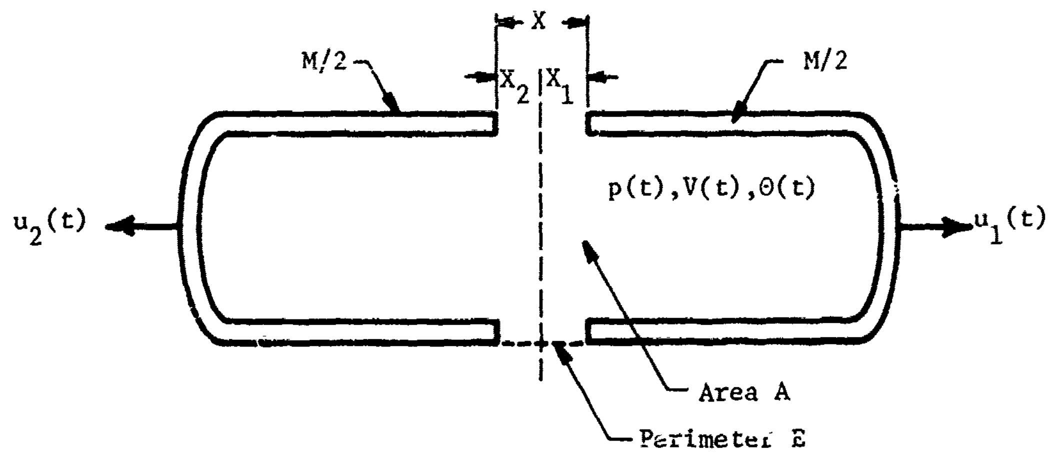

(b) Bursting Cylindrical Pressure Vessel (Ref. 5)

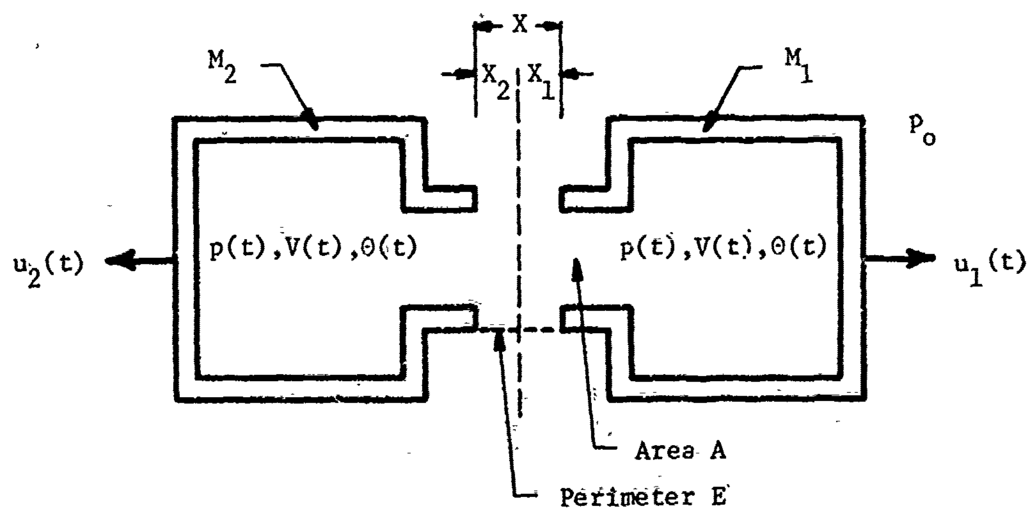

(c) Equivalent Vented Chamber

Figure 2. Vented Chamber (Second Phase)

$$M_2 \frac{d^2 X_2}{dt^2} = A\ p(t), \text{ with } X_2(0) = 0, \frac{dX_2(0)}{dt} = V_2 \qquad (6)$$

where $V_1 = V_2$ = velocity of vent panels after the first phase of venting. Using the ideal gas law and nondimensional forms of the equations to generalize the solution as suggested by Baker, et al. [6], one obtains the following two equations which must be solved simultaneously using an iterative solution:

$$g'' = 4\ P_* \left[1 - \frac{g'^2}{4(P_*)^{\frac{\gamma - 1}{\gamma}}} \right]^{\frac{\gamma}{\gamma - 1}} \qquad (7)$$

$$P_*' = \frac{\frac{-\beta\gamma}{\alpha}\ g\ P_*^{\frac{3\gamma - 1}{2\gamma}} - \gamma g' P_*}{\left(\frac{\gamma - 1}{2}\right)\alpha + g} \qquad (8)$$

where g is a nondimensional distance,
P_* is a nondimensional pressure,
γ is the ratio of specific heats,
α is a nondimensional gas equation of state term,
β is a nondimensional gas discharge term, and
primed terms denote first and second derivatives with respect to nondimensional time.

To establish symmetry for the case where the vent panel is near the ground surface, one must first create a mirror image similar to going from Figure 2a to 2c, and then create a second mirror image by reflecting the initial chamber and first mirror image about the ground plane. The resulting symmetrical second mirror image original chamber combination will be similar to that shown in Figure 2c except that the mass, volume and throat area of each half will be twice as large as those of the original chamber.

The third phase of venting occurs after the vent panel is sufficiently far from the vent opening that it no longer interrupts the flow of the exiting gas. We assumed that this occurred when the gas exit area around the perimeter of the nozzle equaled the throat area. Using Figure 2c, this occurs when $EX_1 = EX_2 = A$. During this last phase of venting, we use a gas venting computer code which considers gas venting through an orifice based on the ideal gas law and sonic or subsonic gas flow, depending upon the relative pressures between the room and the atmosphere. This portion of the venting process uses the methods described by Owczarek [3], Baker and Oldham [2] and Esparza, et al. [7].

The gas venting computer program called VENT which was developed for this analysis allows one to vary the quasi-static pressure, volume, vent area, vent height, vent width, vent mass, initial vent velocity acquired from blast wave loading, the vent tunnel length, ambient pressure, ambient temperature, discharge coefficients, and time increments during the calculations. The computer code also considers cases where the vent panel is adjacent to the ground or high enough above the ground that gas flow is not affected by the ground surface.

III. MODEL ANALYSIS

A model analysis [8] was performed to determine the functional format of the parameters involved in the gas venting process. The list of physical parameters is presented in Table 1. With V, p_o and a_o used as "repeating" parameters, the dimensionless terms are as shown in Table 2. Observe that all response terms, $\overline{p}(t)$, $\overline{u}_f$, $\overline{i}_g$ and $\overline{T}$ can be obtained if $\overline{p}(t)$, the scaled pressure history, is known. Also, some of the dimensionless terms can be eliminated to simplify the analysis. The ratio of specific heats, γ, can be excluded, as its value is constant. The scaled quasi-static pressure, $\overline{P}_1$, is a function of scaled charge energy, $\overline{E}$. Hence, knowledge of the value of one of these dimensionless terms implies knowledge of the value of the other. Thus, $\overline{E}$ was eliminated. By a similar process, initial scaled panel velocity $\overline{u}_o$ can be eliminated. The initial panel velocity, for a panel of given mass, will be determined by the initial shock loading (reflected impulse) imparted to the panel. The magnitude of the impulse was determined by the charge energy (weight) and the geometry (charge shape, orientation, and location inside the cubicle). The charge energy is implicitly expressed in $\overline{P}_1$, and the scaled wall panel mass is $\overline{M}$. The same geometry was used in all calculations, with the following simplifying assumptions:

1) A bare spherical charge was located in the geometric center of a cubicle.

2) No reflection factor was added for interaction of blast waves with the cubicle floor.

3) The standoff from the charge was assumed to be constant over the entire vent panel (instead of calculating a slant range); hence, producing a specific impulse dependent of location on vent panel.

Table 1. Physical Parameters Affecting Venting

Symbol	Description	Units
E	Energy	FL
V	Volume	L^3
A	Vent area	L^2
P_1	Quasi-Static pressure (absolute)	F/L^2
γ	Ratio of specific heats	-
H	Wall thickness	L
P_o	Ambient pressure	F/L^2
a_o	Speed of sound in air	L/T
M	Mass of vent	FT^2/L
u_o	Initial panel velocity	L/T
t	Time	T
$p(t)$	Pressure history (Pressure as a function of time)	F/L^2
i_g	Gas impulse (Integral of pressure history)	FT/L^2
T_d	Duration of vent stage of internal explosion	T
u_f	Final panel velocity	L/T

Table 2. Dimensionless Terms for Vented Chamber

$$\bar{E} = \left(\frac{E}{p_o V}\right)$$

$$\bar{A} = \left(\frac{A}{V^{2/3}}\right)$$

$$\bar{P}_1 = \left(\frac{P_1}{p_o}\right)$$

$$\gamma = (\gamma)$$

$$\bar{H} = \left(\frac{H}{V^{1/3}}\right)$$

$$\bar{M} = \left(\frac{M a_o^2}{p_o V}\right)$$

$$\bar{u}_o = \left(\frac{u_o}{a_o}\right)$$

$$\bar{t} = \left(\frac{t a_o}{V^{1/3}}\right)$$

$$\bar{p}(t) = \left(\frac{p(t)}{p_o}\right)$$

$$\bar{u}_f = \left(\frac{u_f}{a_o}\right)$$

$$\bar{i}_g = \left(\frac{i_g a_o}{p_o V^{1/3}}\right)$$

$$\bar{T} = \left(\frac{T a_o}{V^{1/3}}\right)$$

These simplifications were made because the gas venting problem is already complicated without addition of several more dimensionless terms to specify geometry effects.

The functional format for the pressure history becomes, after the above simplifications,

$$\bar{p}(t) = \frac{p(t)}{p_o} = f\left(\frac{A}{V^{2/3}}, \frac{P_1}{p_o}, \frac{H}{V^{1/3}}, \frac{Ma_o^2}{p_o V}, \frac{ta_o}{V^{1/3}}\right) \qquad (9)$$

$$= f\ (\bar{A}, \bar{P}, \bar{H}, \bar{M}, \bar{t})$$

The scaled gas impulse $\bar{i}_g$ is the time integral of $\bar{p}(t)$ over the duration $\bar{T}_d$ of the gas venting:

$$\bar{i}_g = \int_o^{\bar{T}_d} \bar{p}(t)\ d\bar{t} \qquad (10)$$

or

$$\bar{i}_g = \frac{i_g a_o}{p_o V^{1/3}} = f_1\ (\bar{A}, \bar{P}_1, \bar{H}, \bar{M}) \qquad (11)$$

Similarly, $\bar{T}_d$, the scaled duration of gas venting, is

$$\bar{T}_d = \frac{T_d a_o}{p_o V^{1/3}} = f_2\ (\bar{A}, \bar{P}_1, \bar{H}, \bar{M}) \qquad (12)$$

IV. RESULTS

The computer code was run separately for cases where the vent panel was located on the ground and for cases where the panel was off the ground (i.e., where the gas flow was not disturbed by the ground). It was found that for cases where the vent panel is the whole wall, there is no difference in the results. In the limit of small vent panel areas, however, ~20% of the wall area, the results are unclear at this time due to an insufficient number of computational runs. The parameter values used in the computations scanned several orders of magnitude, as follows:

Charge energy	1 - 1000 lb TNT
Cubicle volume	1000 - 30,000 ft^3
Vent area	20% to 100% of the area of one wall
Wall thickness	0 - 6 ft
Ambient pressure	14.7 psi
Specific weight of vent panel	0 - 300 lb/ft^2
Speed of sound	1116 ft/sec
Discharge coefficient	0.6

Observe that the results can be used at altitudes other than sea level simply by using the proper values for ambient atmospheric pressure and sonic velocity in calculating the scaled values.

The results of the calculations are presented in Figures 3 through 6. The curves for $\overline{M} = 0$ are similar to those obtained by Esparza, et al. [7]. Figures 3 and 4 incorporate the effect of a real vent panel with mass, but are for scaled wall thickness of zero. Figures 5 and 6 incorporate the effect of having a wall thickness or several wall thicknesses for the vent panel to traverse before actual venting can begin. No attempts were made to depict the final vent panel velocities graphically, as the parameter is not essential for structural design, although it may be desirable to know for fragment hazard determinations. Additional work is needed to develop the curves presented in Figures 3 through 6 to determine final velocities of the vent panel, and to determine errors induced by ignoring or simplifying the geometry of the explosion. When using these figures, one must use a consistent set of units so that the dimensionless terms are truly dimensionless.

V. CONCLUSION

This paper describes a method for predicting gas impulse and blowdown time for venting of a structure after an internal HE explosion. The technique allows for constriction of gas flow due to the inertia of the vent panels. The computer code VENT was developed to perform the calculations. A model analysis was then used to determine the most beneficial manner in which to present the numerically generated data so

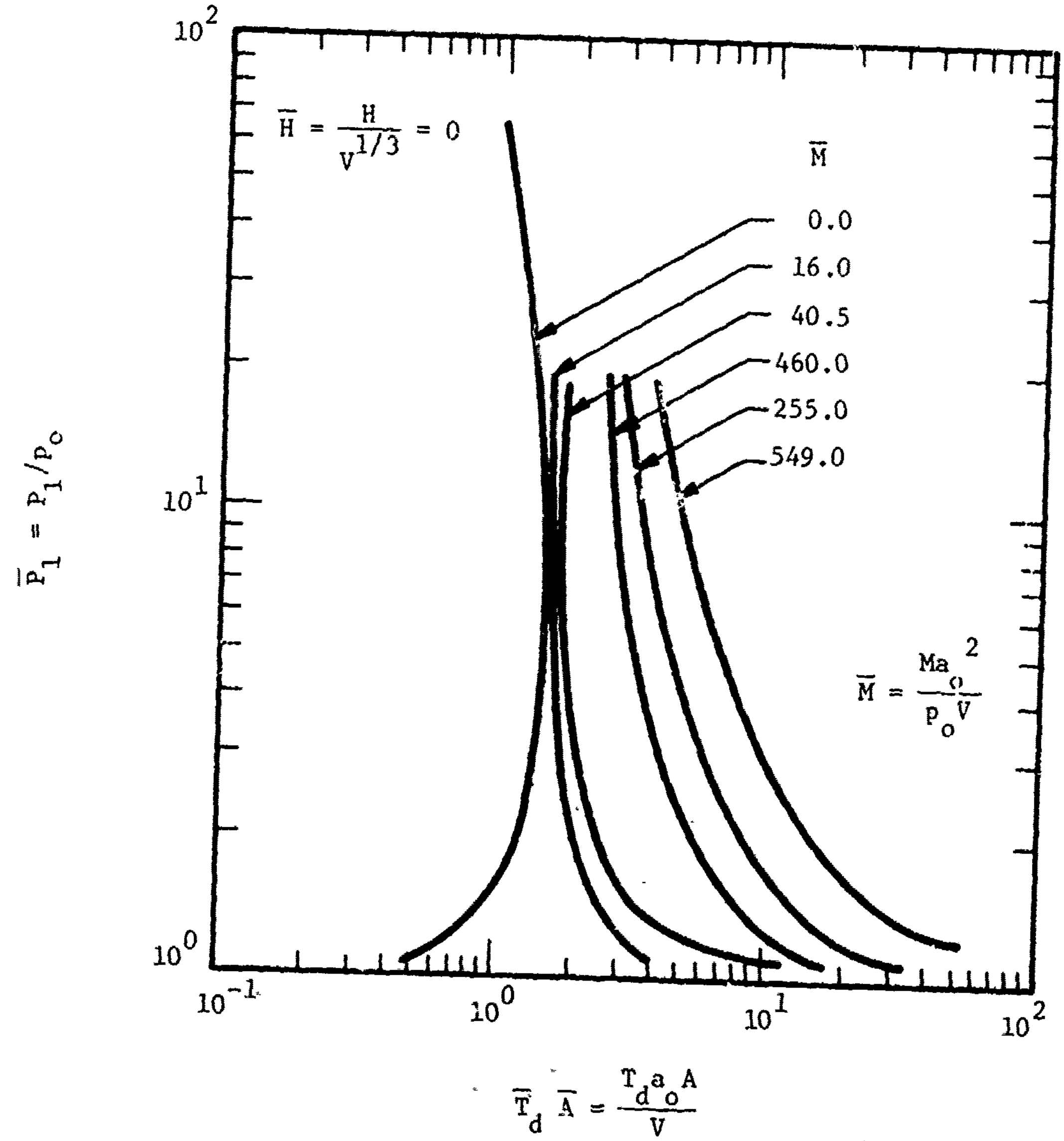

Figure 3. Plot of Scaled Pressure versus Scaled Duration (Various $\bar{M}$, $\bar{H} = 0$)

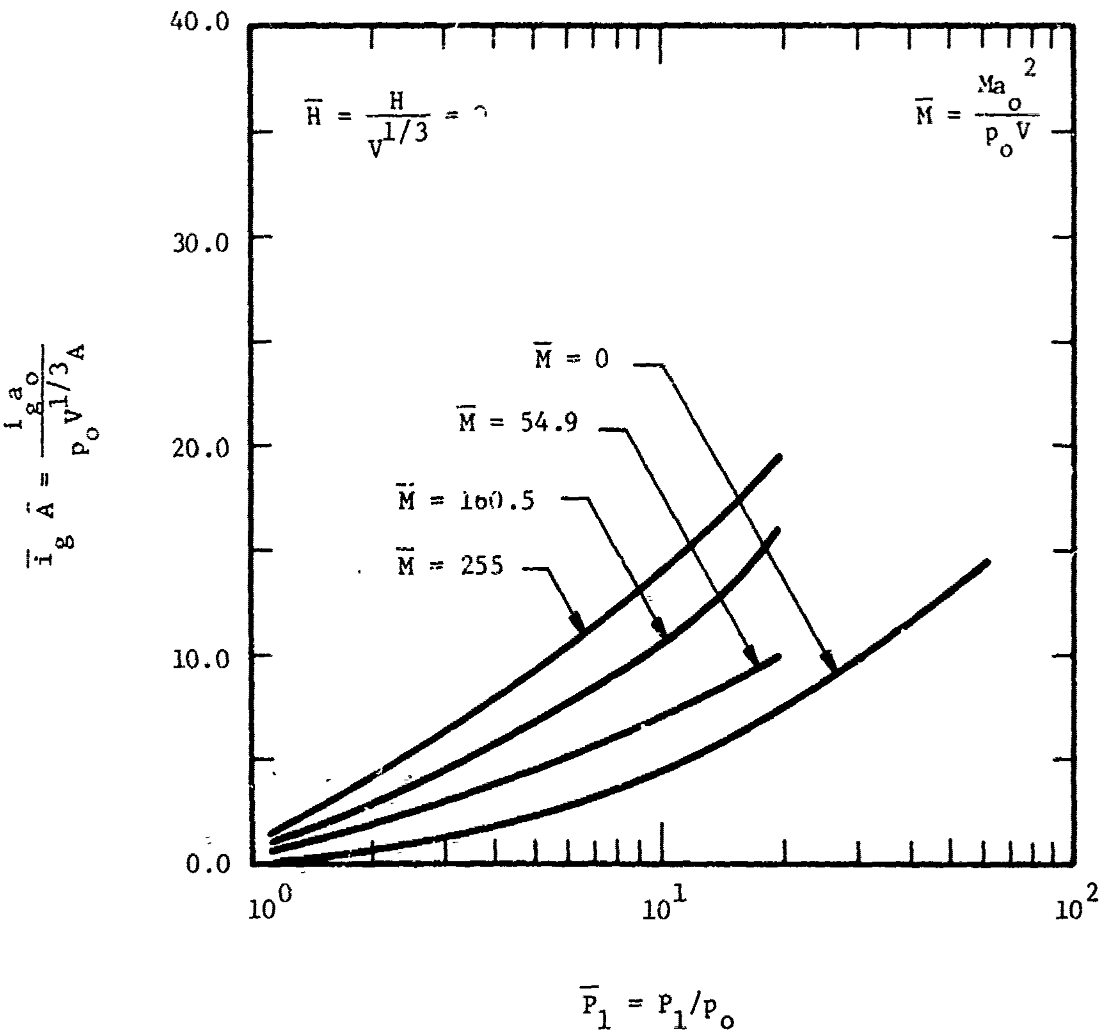

Figure 4. Plot of Scaled Gas Impulse versus Scaled Pressure (Various $\bar{M}$, $\bar{H}$ = 0)

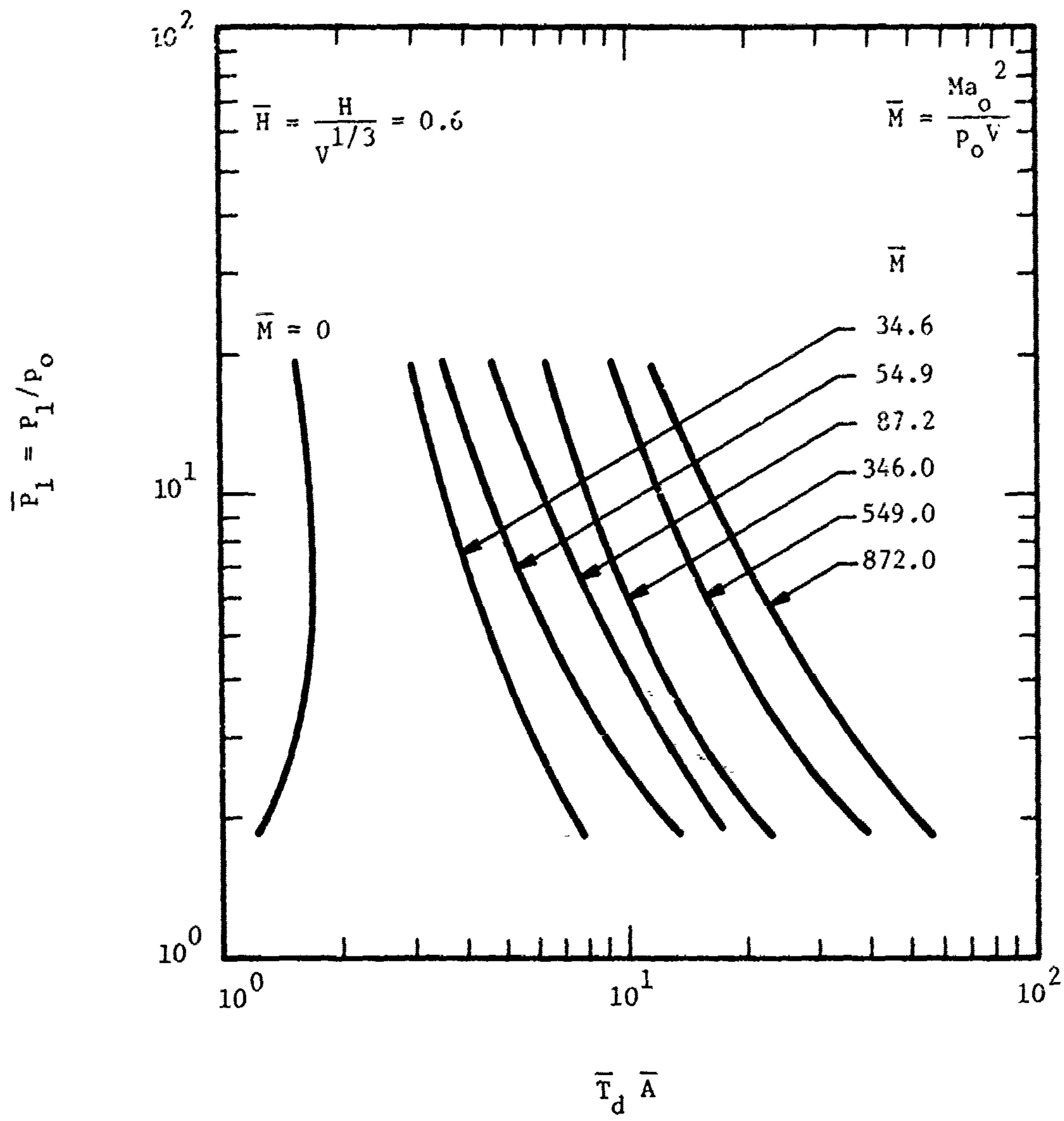

Figure 5. Plot of Scaled Pressure versus Scaled Distance (Various $\overline{M}$, $\overline{H} = 0.6$)

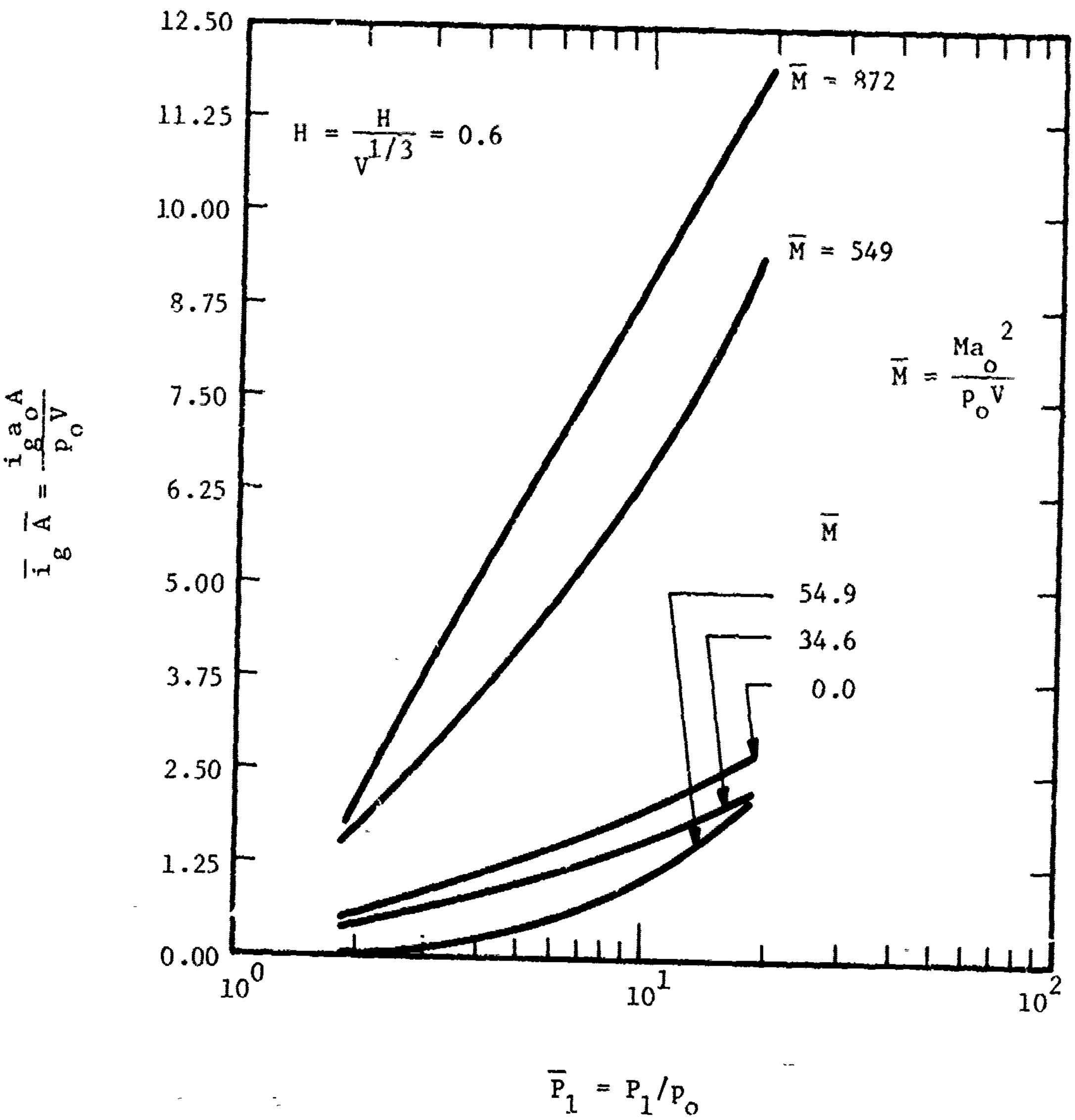

Figure 6. Plot of Scaled Gas Impulse versus Scaled Pressure (Various $\overline{M}$, $\overline{H}$ = 0.6)

that it would have broad application. The paper also contains plots of scaled quasi-static pressure versus scaled duration and scaled gas impulse versus scaled quasi-static pressure for various scaled vent panel masses and two scaled wall thicknesses or tunnel lengths through which the panel must travel before venting begins. The technique can be used as an aid in the design of pressure relief systems and, as is true for most analytical solutions, could benefit from experimental verification.

VI. REFERENCES

1. Baker, W. E., Westine, P. S., Kulesz, J. J., Wilbeck, J. S. and Cox, P. A., "A Manual For The Prediction of Blast and Fragment Loading on Structures," SwRI Draft Final Report for U. S. Army Corps of Engineers, Huntsville Division, (in publication).

2. Baker, W. E. and Oldham, G. A., "Estimates of Blowdown of Quasi-static Pressures in Vented Chambers," Edgewood Arsenal Contractor Report EM-CR-76029, Report No. 2, November 1975.

3. Owczarek, J. A., Fundamentals of Gas Dynamics, Int. Textbook Co., Scranton, PA.

4. Kulesz, J. J., Moseley, P. K., and Baker, W. E., "Fragment and Blast Hazards from Explosions in a Tender Torpedo Workshop," Vol. 1, Final Report Prepared for the David Taylor Naval Ship Research and Development Center, Contract No. N00014-77-C-0658, November 1978.

5. Taylor, D. B. and Price, C. F., "Velocities of Fragments from Bursting Gas Reservoirs," ASME Transactions, Journal of Engineering for Industry, November 1971.

6. Baker, W. E., Kulesz, J. J., Ricker, R. E., Bessey, R. L., Westine, P. S., Parr, V. B. and Oldham, G. A., "Workbook for Predicting Pressure Wave and Fragment Effects of Exploding Propellant Tanks and Gas Storage Vessels," NASA CR-134906, November 1975.

7. Esparza, E. D., Baker, W. E. and Oldham, G. A., "Blast Pressures Inside and Outside Suppressive Structures," Edgewood Arsenal Contractor Report EM-CR-76042, Report No. 8, December 1975.

8. Baker, W. E., Westine, P. S., and Dodge, F. T., Similarity Methods in Engineering Dynamics, Hayden Book Company, Inc., Rochelle Park, New Jersey, 1973.

Testing of Missiles to Determine Hazards From Fragments and Overpressure

Mr Arlie E. Adams

U.S. Air Force Logistics Command

Wright-Patterson Air Force Base Ohio

ABSTRACT

Changes in Quantity-Distance criteria, introduction of new aircraft that carry larger missiles, increased emphasis on readiness, and the inability to acquire more land for the parking of aircraft loaded with munitions have dictated the need for a better understanding of the blast and fragmentation hazards associated with certain missiles. Personnel of the Ogden Air Logistics Center have used an inexpensive method of determining these hazards. It was determined that the AIM-7 and AIM-9 missiles would not mass detonate as configured on the alert trailer and aircraft. Also, the distance required for protection from hazardous fragments was determined to be less than the 1250 foot criteria required for untested munitions. As a result, the USAF was able to avoid several expensive land purchases and to increase the number of these missiles allowed in one location. Similar testing of the AGM-65 "Maverick" missile is underway.

1. At the seventeenth Explosives Safety Seminar, Mr Perry J. Flikas, Deputy Assistant Secretary of Defense (Installations and Housing) in his discussion on "Explosives Safety Management-50 Years After Lake Denmark" highlighted the presently accepted practice of protecting the public from our munitions and explosive facilities by providing a large land area or clear zone around the explosives facilities. He also discussed the need for valid information to support a decision on whether to spend our limited dollars to buy more real estate to adequately protect the public from our facilities, or, to buy more military hardware. Mr Flikas stressed that to make a decision between buying more real estate or more hardware we must have the specific information needed to calculate the risks involved. The need for these decisions stems in part from the minimum inhabited building distance of 1,250 ft applicable for one to thirty thousand lbs of explosives unless specific information, i.e., test data, shows that at a lesser distance, the density of fragments having an impact energy of 58 ft pounds or more, decreases to one or less in a six hundred square foot area.

The need to determine the true fragment hazards associated with our USAF alert aircraft and munitions storage facilities was driven by this 1,250 foot distance and by an evolutionary change in aircraft and armament. Many of our air defense sites were origanlly constructed to support an F-102 aircraft and its armament (Figure 1). We now have F-4 aircraft at these same or similar locations with the same support facility, a rocket storage and checkout building (Figure 2). The F4 aircraft with its increased armament has caused an increase in the number and size of missiles stored at each location and caused enough concern within the Air Force to have the Ogden Air Logistics Center conduct a series of tests on these missiles as they are stored in their all up round configuration, and as they are located on the aircraft. The concern was caused by the exposure of several other facilities located less than the desired twelve hundred fifty foot distance from the explosives. Before we could justify buying more real estate or relocating our alert facilities, we had to determine what the true hazard was.

The AIM-7 and AIM-9 missiles are carried on a munitions trailer with a rack which separates the all up round missiles as shown in Figure 3. The approximate location of the missiles on the F-4 aircraft is shown in Figure 4. If the missiles, when loaded on the trailer were to mass detonate, they would project a large number of fragments further than the fragments from just one missile would be projected.

There are several different versions of the AIM-9 missile; however, the Mark 8 warhead with a net explosive weight of 10.5 lbs of HBX and the Mark 17 motor with a net explosive weight of 43 lbs of double base propellant were selected for this test as they were surplus to USAF needs, and presented a fair representation of the AIM-9 family. The Mark 38 warhead with a net explosive weight of 20 lbs of PBX-1 and the Mark 6 motor with a net explosive weight of 70 lbs polybutadine/ammonium perchlorate propellant were selected to represent the AIM-7 missile. These decisions were driven by what was available in the inventory.

TEST OBJECTIVES:

The test goals were to determine if the AIM-9 missiles would mass detonate, or, would propagate as they are carried on the aircraft and on the trailer; to determine if the AIM-7 missile would mass detonate, or, propagate as they are carried on the trailer; and to determine if the detonation of either the AIM-7 or AIM-9 missile when carried on the trailer would cause a detonation of the other type of missile.

TEST EQUIPMENT

The test area was set up as shown in Figure 5. Pressure measurements were made with Bikini static blast pressure gauges located fifteen and twenty-five feet from the warhead; and with Kistler 50psi, 20khz blast pressure transducers, also located fifteen and twenty-five feet from the warhead.

Fragments were collected in three ways. A fragment trap consisting of ninety-six sheets of one-half inch insulating fiberboards (Celotex) was placed three hundred feet from the warheads. A second trap was placed 500 feet from the warhead. (The trap at five hundred feet was repositioned to one hundred feet after the test started because an insufficient number of hits were recorded). Four sections of plastic film, each with an area of 1,200 square feet, were laid out to collect fragments impacting at 900 feet and 1,250 feet from the warhead. Two 600 square foot areas of plywood were erected to see if any high speed fragments were projected beyond the test area. (These "fences" were erected 1,250 feet south of the warhead and 1,500 feet north of the warhead.

TEST RESULTS

The actual testing conducted is summarized in Figure 6. Detailed test results, shown in Figures 7-11, were determined by examination of the pressure records and by examination of the residue. The test results are published in "Ogden ALC Airmunitions Test Report, Hazard/Quantity Distance Test of Mixed Trailer Loading and Storage of AIM-7 and AIM-9 Missiles, MMWRME-TE-76-S63191, November 1976." The AIM-9 warheads would propagate but would not mass detonate when separated by up to twenty-two inches of free air space; and, the AIM-7 warheads would not propagate with as little as five inches separation. It was also determined that detonation of one AIM-9 warhead would propagate to other AIM-9's but not to the AIM-7 missiles loaded on the same trailer. Detonation of one of the AIM-7 missile warheads would not propagate to the other AIM-7's nor to the AIM-9 missiles.

ANALYSIS OF DATA

The analysis of fragmentation data was not as easy as was the analysis of the pressure data. The number of AIM-7 warhead fragments collected by the fragment traps and the fragment density computations-without consideration of energy level-are shown in Figure 8. Similar data for the AIM-9 warhead fragments data are shown in Figure 10. The Ogden Air Logistics Center was unable to establish a satisfactory correlation between the penetration into the witness bundles and the energy level of the fragments because of the differing fragment shapes.

Several attempts were made to correlate the depth of penetration with kinetic energy using the penetration and energy level of a round of 5.56mm ammunition as a comparison standard. Figures 12-14 show the unresolved difficulties encountered in trying to extrapolate the penetration curves down to the 58 foot-pound kinetic energy level. This correlation was deemed to be inappropriate because the fragment traps had to be located close to the warheads to allow the collection of enough fragments to form a satisfactory data base. However, the energy level of fragments at this close distance was too high on the scale and made extrapolation down to 58 foot-pounds an unreliable comparison. At the recommendation of the DDESB the available data was sent to the Naval Surface Weapons Center, White Oak Laboratory. Personnel at White Oak Laboratory used a computer analysis to determine the theorotical range and terminal velocity of the fragments for several launch angles. The velocity and kinetic energy of the fragments were then plotted against the range of the fragments. The range at which the average fragment from the AIM-7 warhead would fall below 58-foot pounds was then determined to be about 650-feet. A corresponding range for the average fragment from the AIM-9 warhead was determined to be about 350-feet. These energy levels - range plots were compared with the fragment densities recorded during the test. The recommendations of the Navy and USAF were submitted to the DDSB along with the data. The DDESB subsequently approved an inhabited building distance of 300 feet for both the AIM-7 and the AIM-9 missile.

TESTING OF AGM-65 "MAVERICK" MISSILE

Arena testing of the Maverick Missile during D T & E furnished enough information to justify an inhabited building distance of 450 feet for a single missile. However, the present launcher for the Maverick missile, the LAU-88, can carry three missiles and the fighter aircraft can carry two launchers, and six missiles. The DDESB has approved, pending completion of tests, an inhabited building distance of 600 feet for three missiles.

The Maverick missile warhead is a shape charge warhead loaded with 85 pounds of Comp B. Based upon the composition of the rocket motor propellant and by analogy to previously tested missiles, the USAF has been using an HE Equivalency of 131.5 pounds for the missile.

When loaded on the LAU-88 launcher the center missile is locateo 22½ inches from the two missiles on the shoulder stations. When both pylons on the F-4 aircraft are loaded with three missiles the distance between the inboard missiles is nine feet ten inches.

The testing now underway has shown that initiation of one of the three missile warheads on a LAU-88 launcher will cause the mass detonation of all three warheads. Preliminary results also indicate that the motors (the present inventory motor and the new reduced smoke rocket motor) do not contribute to the detonation; and, the HE equivalency of 131.5 pounds can be reduced to the 85 pounds NEW of the warhead.

Several ways to determine fragment energy are being tried. High speed photo coverage of a 22 gage steel "flash panels" will show the light of the detonation around the panel, and will show light through the panel as the fragments pass through. The time interval from detonation to light showing through the panel will be used to calculate the average velocity of the fragments. A representative sample of fragments will be recovered from a bundle of fibreboard panels located next to the flash panel. These recovered fragments will be used to determine the weight of the average fragment. The kinetic energy will be calculated using the average velocity and average weight.

Another method of determining fragment velocity is being tested. Electrically conductive tape has been placed on the front of a bundle of fibreboard panels. The change in resistance of the tape will indicate the time of arrival of a specific fragment. Those particular fragments can then be recovered and weighed.

This test program is still underway. However it will not be completed soon because of higher priority tests being conducted in the same area or requiring the limited support equipment.

F102 AIRCRAFT

ARMAMENT

MISSILE	WEIGHTS
AIM 4	WARHEAD 4.84 LBS
	ROCKET MOTOR 26.5 LBS
AIM-26/B	WARHEAD 14.5 LBS
	ROCKET MOTOR 60.0 LBS
	HE EQUIVALENCE 37.5 LBS

fig. 1

F-4 AIRCRAFT

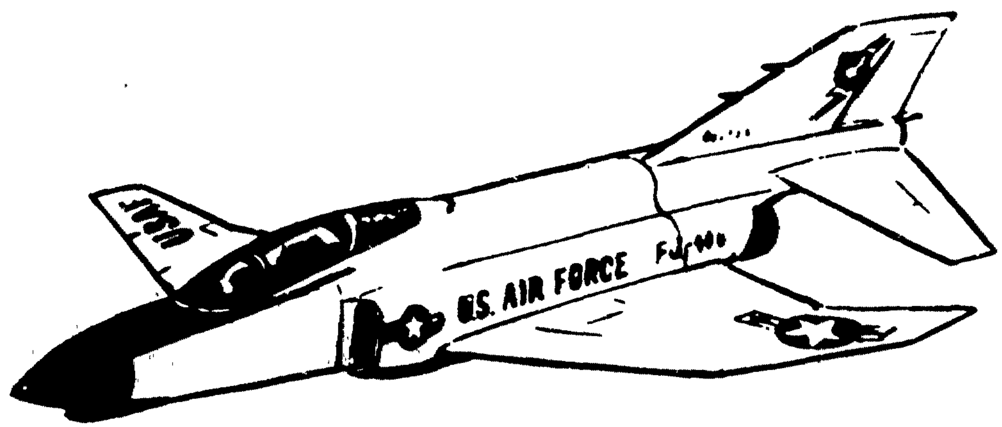

ARMAMENT

MISSILE	WEIGHTS	
AIM-7	WARHEAD	20
	ROCKET MOTOR	70/92
AIM-9	WARHEAD	10.5
	ROCKET MOTOR	43

fig. 2

TRAILER LOAD CONFIGURATION & SPACING

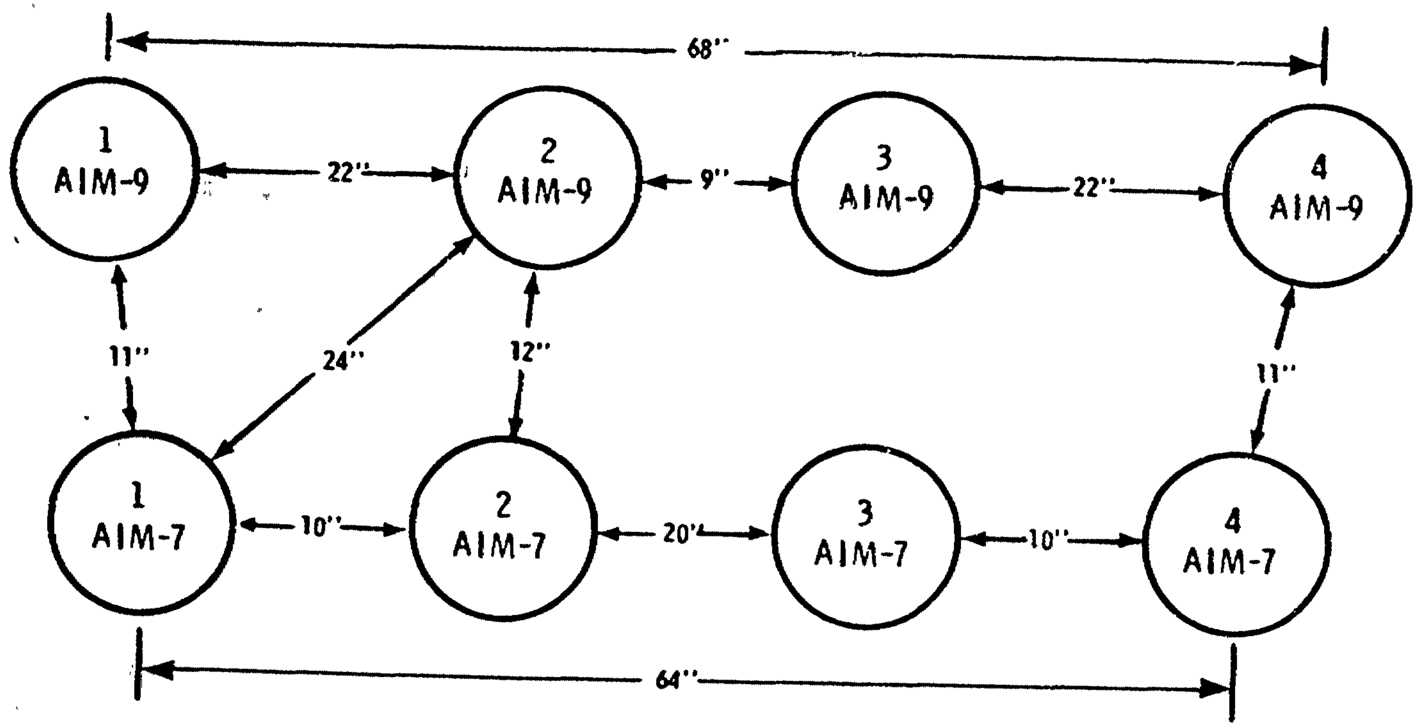

fig. 3

F-4 AIRCRAFT MISSILE STATIONS

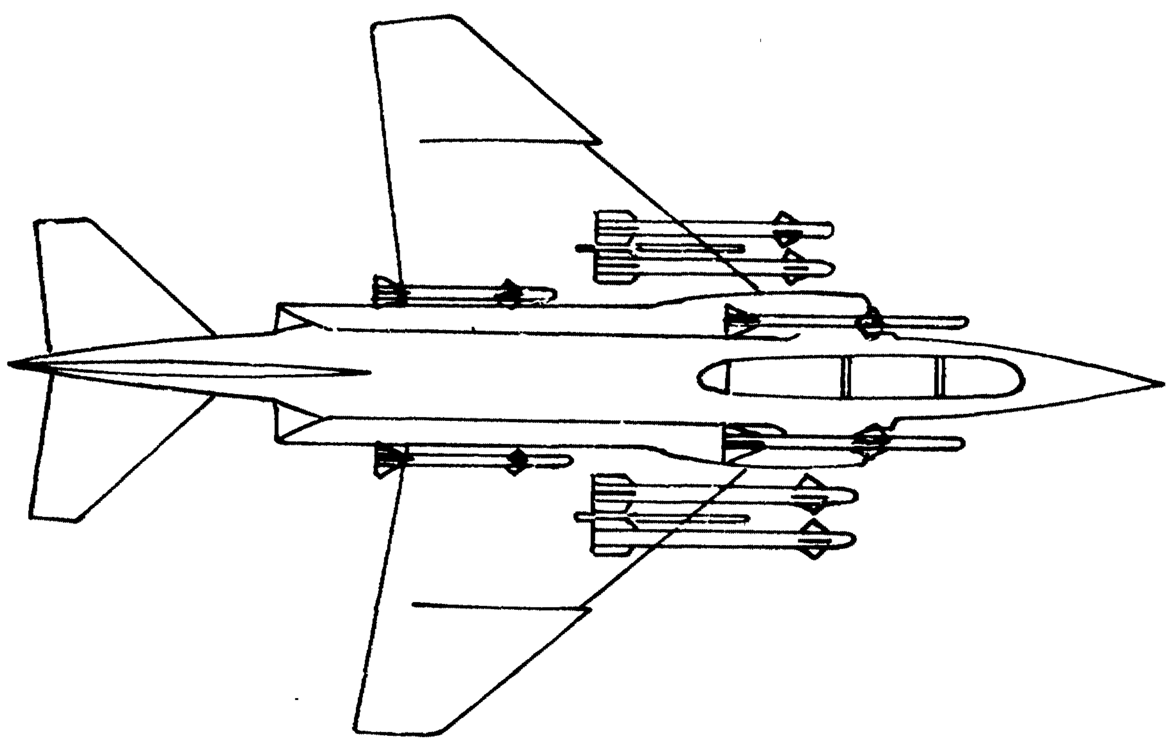

fig. 4

TEST LAYOUT

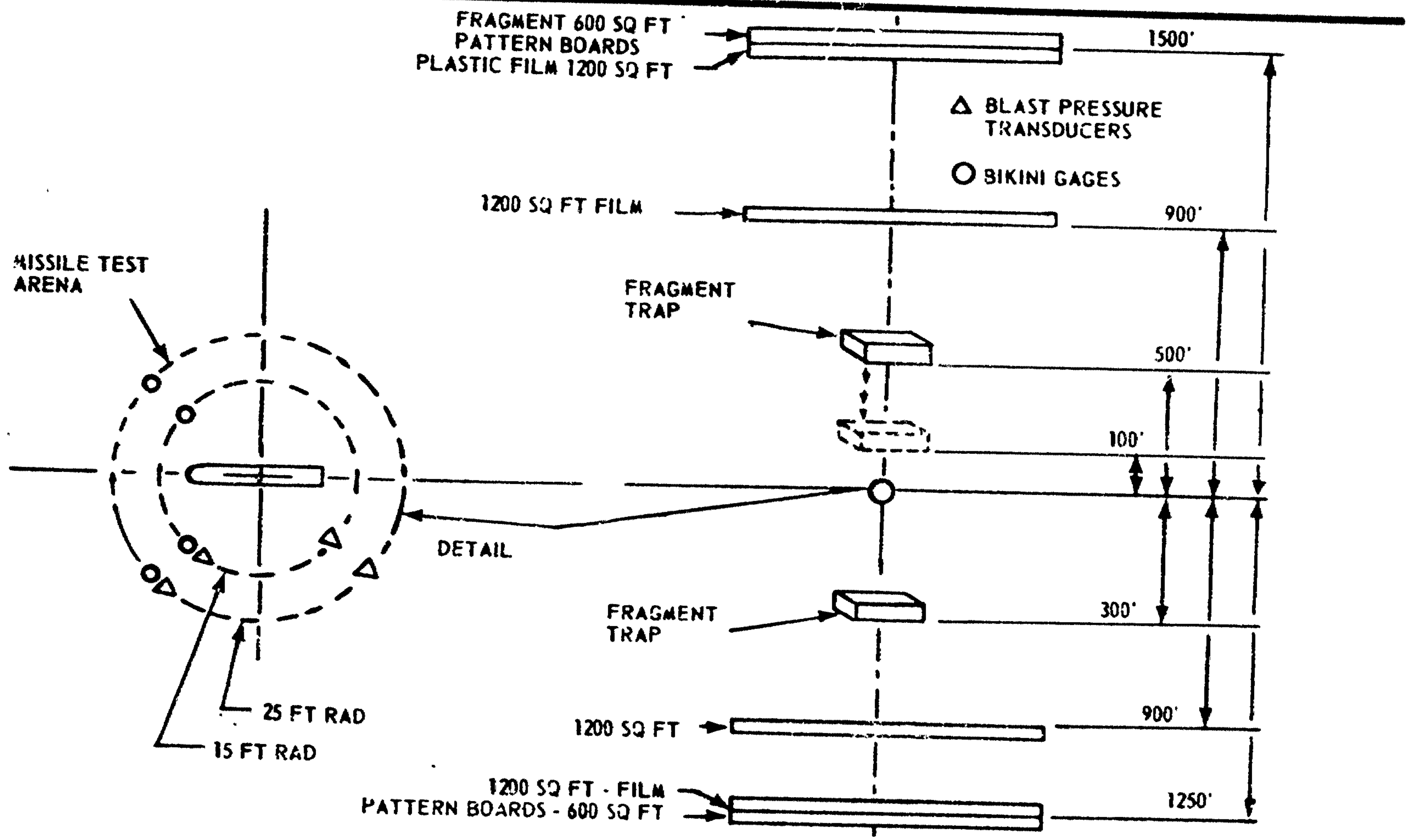

fig. 5

TEST CONDUCTED

CONTROL TESTS	NO. OF TESTS	PURPOSE
AIM-9 WHD	3	PRESS/FRAG
AIM-7 WHD	3	PRESS/FRAG
AIM-7 MISŠILE	1	PRESS/FRAG (MTR CONTRIBUTION)

WARHEAD TESTS	NO. OF TESTS	PURPOSE	CONFIGURATION
AIM-7	3	PRESS/FRAG	0 Ø 0
AIM-9	4	PRESS/FRAG	0 Ø 0
AIM-7/AIM-9	1	PRESSURE	Ø 0
AIM-9/AIM-7	1	PRESSURE	Ø 0

TRAILER TESTS			
4 AIM-7 AND	2	PRESSURE	0 Ø 0 0
4 AIM-9			0 0 0 0
			0 0 0 0
			0 Ø 0 0

fig. 6

AIM-7 TESTS - PRESSURE DATA

TEST NUMBER	ITEMS/ SEPARATION	PEAK PRESSURE PSI (25 FEET)	POSITIVE IMPULSE (PSI-SEC) (25 FEET)	REACTION
4	1 WARHEAD	11.64	.0267	CALIBRATION SHOT
5	1 WARHEAD	13.86	.0243	CALIBRATION SHOT
6	1 WARHEAD	13.52	.0282	CALIBRATION SHOT
7	1 WARHEAD AND MOTOR	12.69	.0267	NO CONTRIBUTION FROM MOTOR
8	3 WARHEADS; 10" AND 20" SEPARATION	13.71	.0314	NO PROPAGATION
9	3 WARHEADS 10" AND 10" SEPARATION	14.28	.0319	NO PROPAGATION
16	3 WARHEADS 5" AND 5" SEPARATION	12.81	.0345	NO PROPAGATION

fig. 7

AIM-7 TESTS FRAGMENT DATA

FRAGMENT TRAPS

DISTANCE IN FEET	NO OF FRAGS	PENETRATION IN INCHES MINIMUM	MAXIMUM	AVERAGE	AVERAGE WEIGHT (GRAMS)
100	21	0.5	14.5	9.12	21.9
300	5	2.5	6.5	3.7	25.7

FRAGMENT DENSITY OF 1 / 600 FT^2 AREA:

696 FEET - STATISTICAL DISTRIBUTION

661 FEET - SPHERICAL RADIAN RATIO DENSITY (100 FT TRAP)

886 FEET - SPHERICAL RADIAN RATIO DENSITY (300 FT TRAP)

fig. 8

AIM-9 TESTS PRESSURE DATA

TEST NUMBER	ITEMS/ SEPARATION	PEAK PRESSURE (PSI) AT 25 FEET	POSITIVE IMPULSE AT 25 FEET (PSI-SEC)	REACTION
1	ONE WARHEAD	10.44	.0204	CALIBRATION SHOT
2	ONE WARHEAD	9.71	-	CALIBRATION SHOT
3	ONE WARHEAD	10.10	.0204	CALIBRATION SHOT
10	3 WARHEADS 9" AND 22" SEPARATION	15.52	.0259	ACCEPTOR AT 9" DETONATED
11	3 WARHEADS 9" AND 9" SEPARATION	18.34	.0361	BOTH ACCEPTORS DETONATED
15	3 WARHEADS 12" AND 18" SEPARATION	17.20	.0432**	BOTH ACCEPTORS DETONATED
18	3 WARHEADS 22" AND 22" SEPARATION	12.82	.0267	DETONATION APPARENTLY PROPAGATED TO ONE ACCEPTOR AT 22" SEPARATION

**DATA AT 15 FEET

fig. 9

AIM-9 FRAGMENT DATA

FRAGMENT TRAPS

DISTANCE IN FEET	NO OF FRAGS	PENETRATION IN INCHES MINIMUM	MAXIMUM	AVERAGE	AVERAGE WEIGHT (GRAMS)
50	43	3	20.5	10.4	2.8
100	20	6	14.5	9.8	2.8

COLLECTED FRAGMENTS

1 @ 500 FT.

2 @ 900 FT.

3 @ 1250 FT

FRAGMENT DENSITY OF 1 / 600 FT^2 AREA

884 FEET - COLLECTED FRAGMENT DENSITY

518 FEET - SPHERICAL RADIAN RATIO DENSITY (100 FOOT TRAP)

381 FEET - SPHERICAL RADIAN RATIO DENSITY (50 FOOT TRAP)

fig. 10

CROSS PROPAGATION TESTS

TEST NUMBER	CONFIGURATION	PEAK PRESSURE AT 25′ (PSI)	TOTAL POSITIVE IMPULSE AT 25′ (PSI-SEC)	REACTION
12	AIM 7 DONOR W / AIM 9 ACCEPTOR 11 INCHES SEPARATION	18.48	.0475	DETONATION PROPAGATED TO AIM-9
13	AIM 9 DONOR W / AIM 7 ACCEPTOR 11 INCHES SEPARATION	12.34	.0235	DETONATION DID NOT PROPAGATE TO AIM 7
14	TRAILER TEST	13.53	.0267	DETONATION OF AIM-7 DID NOT PROPAGATE
17	TRAILER TEST	15.37	.0314	DETONATION OF AN AIM 9 PROPAGATED TO NEXT AIM 9 (9 INCHES SEPARATION) BUT NOT TO ANY OTHERS.

fig. 11

AIM 7/9 FRAGMENT ENERGY

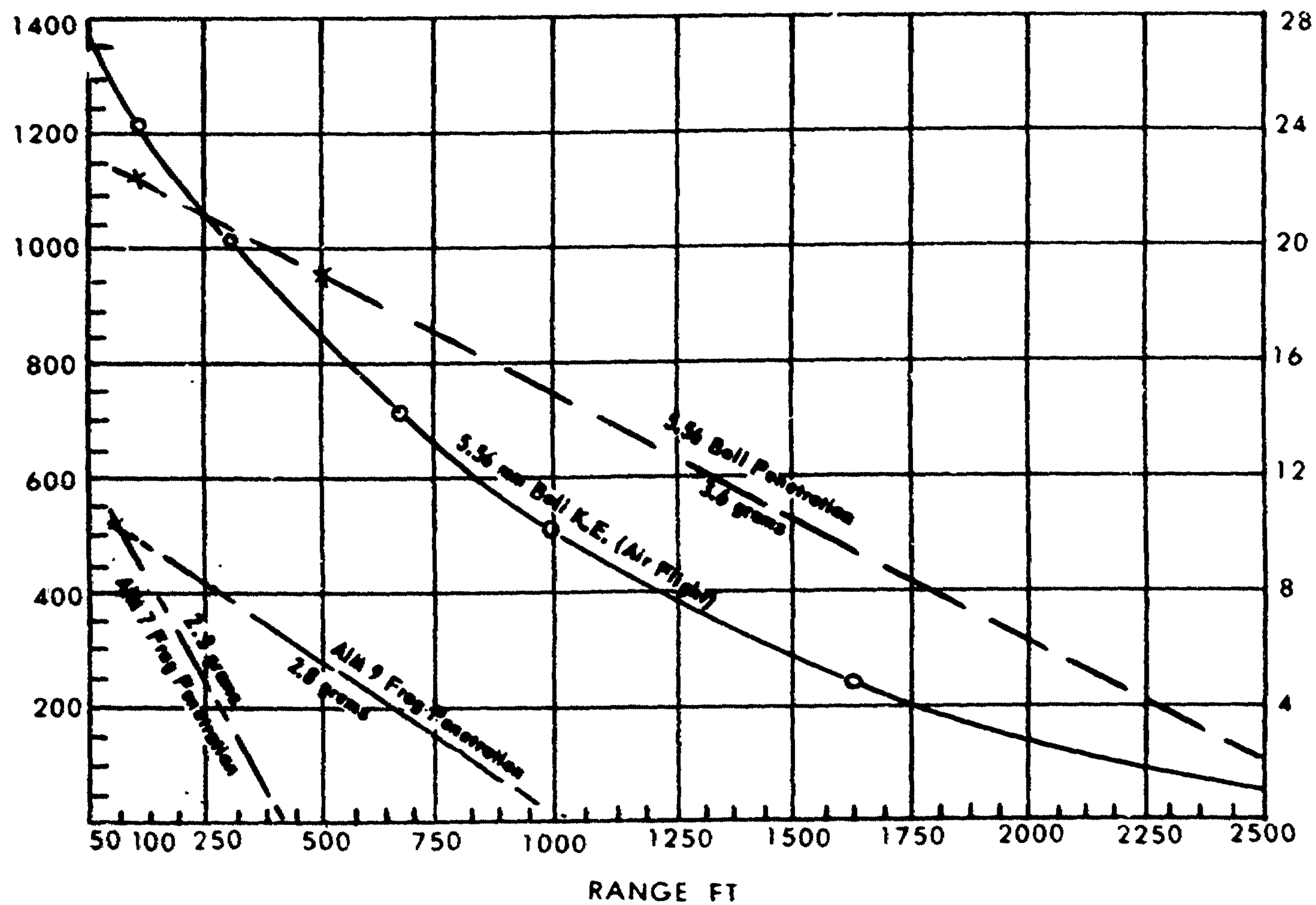

fig. 12

AIM-7 PENETRATION/ KINETIC ENERGY

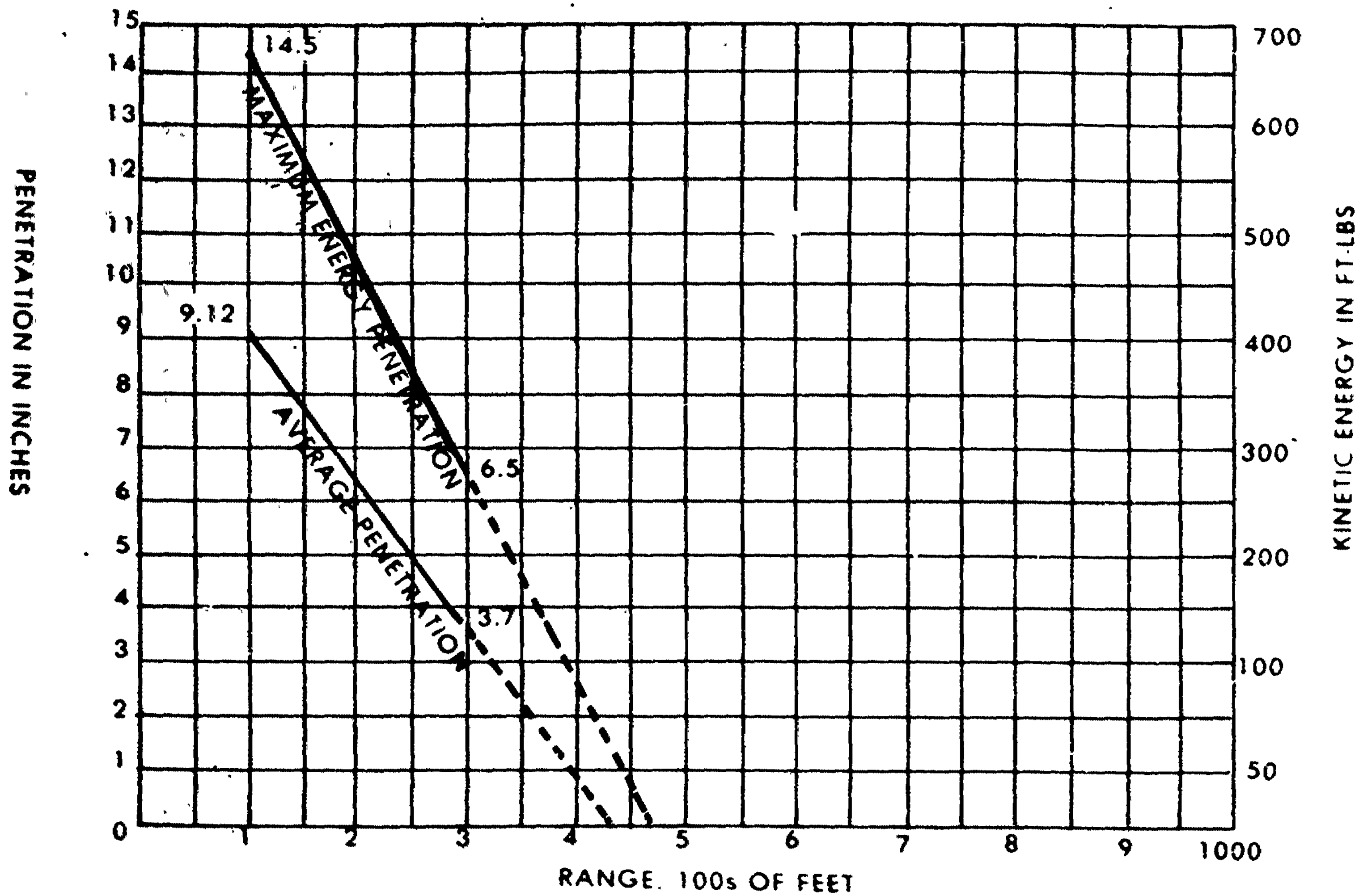

fig. 13

AIM-9 PENETRATION/KINETIC ENERGY

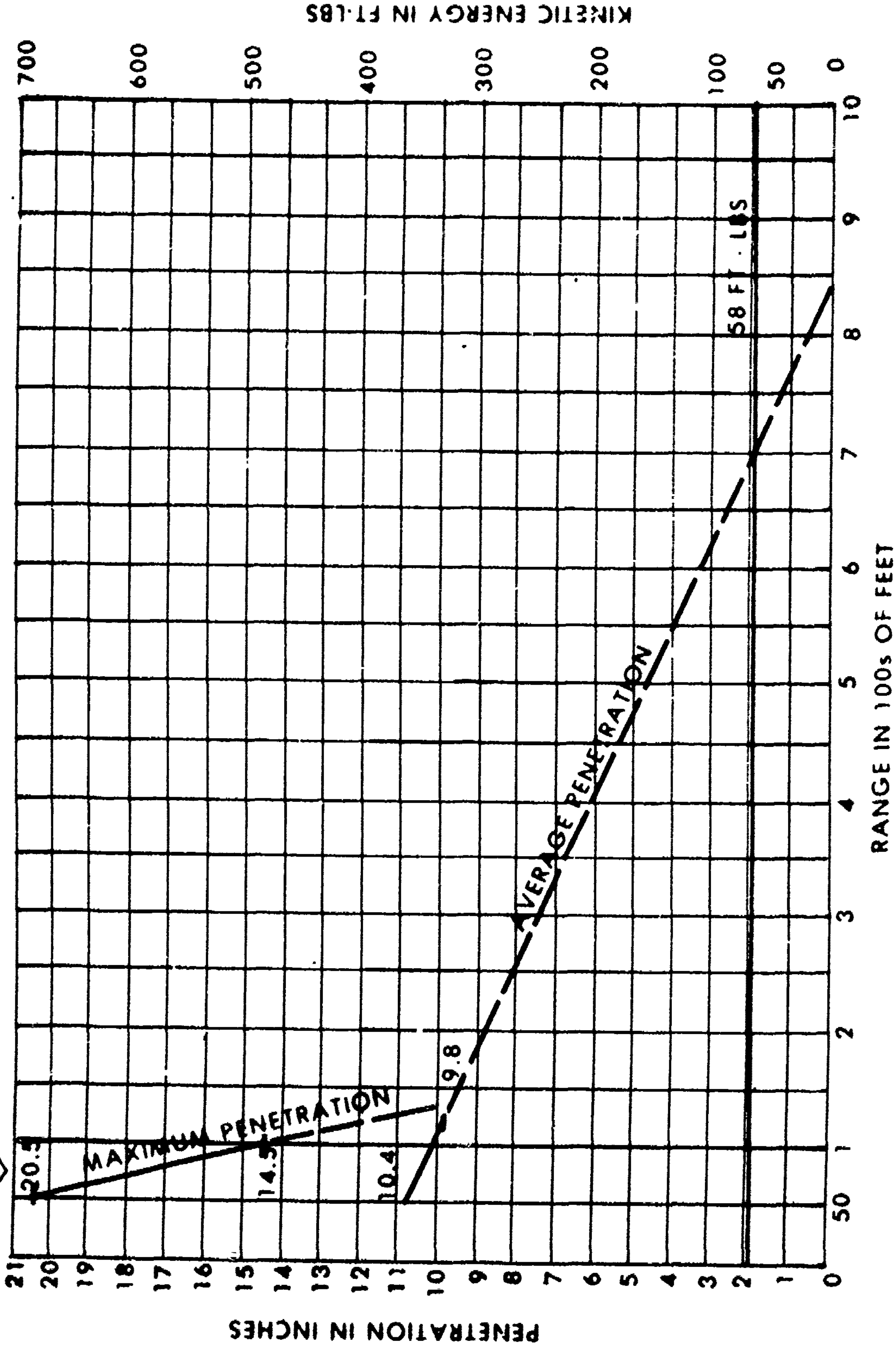

fig. 14

PRECEDING PAGE BLANK-NOT FILMED

FRAGMENT HAZARD INVESTIGATION PROGRAM (LARGE-SCALE DETONATION TESTS)

by

J. G. Powell
W. D. Smith, III

NAVAL SURFACE WEAPONS CENTER
DAHLGREN, VIRGINIA 22448

1. INTRODUCTION

The Department of Defense Explosives Safety Board (DDESB) is conducting a continuing program to evaluate the fragment hazards produced by the accidental detonation of stored munitions. In support of this effort, the Naval Surface Weapons Center was funded in July 1975 to conduct the Fragment Hazard Investigation Program. The purpose of the program is to provide the DDESB with the necessary fragmentation data to improve or to substantiate the quantity-distance (QD) standards for the safe and efficient storage of stacked munitions according to specific hazard classifications. Previous programs attempted to use far-field fragment recovery in limited predetermined areas to quantify the hazards. The current program will use near-field fragment characterization data in conjunction with far-field collection data to predict far-field fragment density. The ultimate goal is to provide a methodology for the determination of QD standards for all hazard classifications. The hazard classification under investigation in this report is the Mass-Detonating Hazard Materials (Class 1, Division 1).

The major effort of this program to date has been focused on the mass-detonating Army M107 155mm (TNT loaded) projectile. Close-in arena and far-field collection tests of various projectile and pallet stacking configurations have been conducted concurrent with supporting analytical studies. Fragmentation data were generated on projectile clusters which simultaneously detonate and on those which detonate by means of natural communication. The effort addressing the simultaneously detonated projectiles was documented in NAVSWC Technical Report TR-3664, reference (a). This effort, combined with experimental findings from the projectiles that detonated by means of natural communication, was documented and presented at the 18th Department of Defense Explosives Safety Board seminar (reference (b)). The largest projectile configuration detonated for the combined effort (designated small-scale arena tests) consisted of one pallet (eight projectiles) of M107 155mm projectiles.

This paper presents the experimental findings from the large-scale static detonations of 8, 16 and 36 pallets of 155mm projectiles stacked in various storage configurations. These data will be combined with the experimental findings from the small-scale tests of reference (a) and (b) to validate equations previously developed for the prediction of far-field fragment density. A description of the large-scale tests and an analysis of the far-field collection data will be presented. The implications of the test results upon existing quantity distance criteria will be discussed.

2. TEST PROGRAM

2.1 BACKGROUND

The large-scale pallet detonation tests were designed based upon the results of small-scale fragmentation arenas of single pallets detonated by means of natural communication. The single pallet detonations showed that high velocity (6200 ft/sec), high density fragment concentrations were forming at the positions shown in Figure 1. Consequently, the large-scale detonation tests were

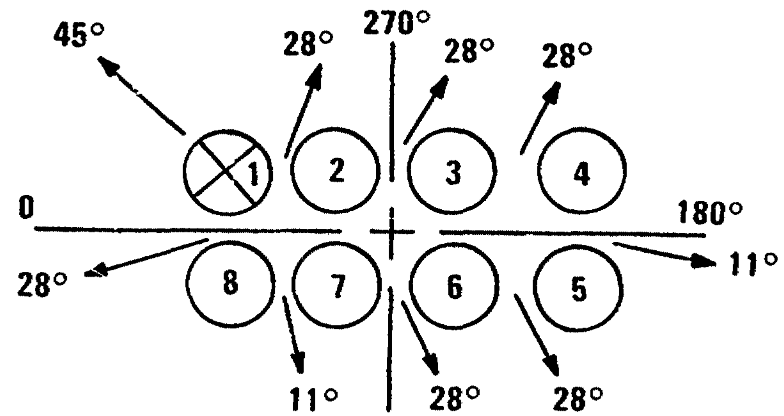

PROJECTILE NOS.	AZIMUTH FRAGMENT CONCENTRATION LOCATION PREDICTED	ACTUAL*
1 & 2	242°	240°
2 & 3	242°	240°
3 & 4	242°	240°
4 & 5	170°	173°
5 & 6	118°	127°
7 & 8	118°	127°
8 & 1	101°	107°
8 & 2	28°	23°
	315°	322°

*DATA FROM TEST NO. QS-155-S8

FIGURE 1

FRAGMENT CONCENTRATION LOCATIONS FOR DETONATION OF PROJECTILE NO. 1

set up to collect fragments between ranges of 500 to 2700 feet as a function of azimuthal angle relative to the stack. The small-scale single pallet detonations also indicated that the number of fragments in the concentrations was related to the number of pallet interaction areas (space between two adjacent projectiles where fragment collisions occur). The number of pallets detonated (eight, sixteen and thirty-six) was therefore selected to evaluate the relationship between the far-field (range greater than 1100 feet) fragment density and number of interaction areas.

2.2 TEST PROCEDURE AND CONFIGURATION

The large-scale test series was conducted at the White Sands Missile Range on the Dice Throw Test Site during the period 2 August 1979 to March 1980. Approximately 255 acres of high elevation desert were bladed clear of foliage, and surveyed according to range and azimuthal location for fragment collection data. The collected fragments were sorted, weighed and documented according to spatial zones. The presented area of the fragments was measured with a planimeter or an Electro-optic Icosahedron gage depending upon fragment size. Blast overpressure data were also measured for each test. The blast gage locations were chosen in accordance with the procedures of the revised TB-700.2 (Chapter 6) to record forty, ten, four and one psi. Figures 2-4 show the far-field fragment collection area, the blast gage locations, the stack configuration and the donor projectile(s) location for the detonation of 8, 16 and 36 pallets of 155mm projectiles, respectively.

2.2.1 OBSERVATIONS

The fragment recovery data for the large-scale pallet detonations presented in Figures 5 thru 7 showed that the fragment concentrations were forming at the same relative angular positions (60°-100°) as was predicted based upon the small-scale single pallet arena data. Furthermore, the number of fragments recovered was found to be directly proportional to the number of interaction areas (N_{IA}) in the stack.

The blast overpressure data is presented in Table 1. The data show that the measured overpressure is consistently higher for the 95° ray than for the 5° ray. This indicates that the blast overpressure is also affected by the number of interaction areas.

3. ANALYTICAL EFFORT

The analysis of the large-scale pallet detonation test data was divided into the three sections listed below:

a. Fragmentation characterization

b. Prediction of far-field fragment density

c. Implications upon existing QD criteria

A detailed discussion of each topic is presented in the following sections.

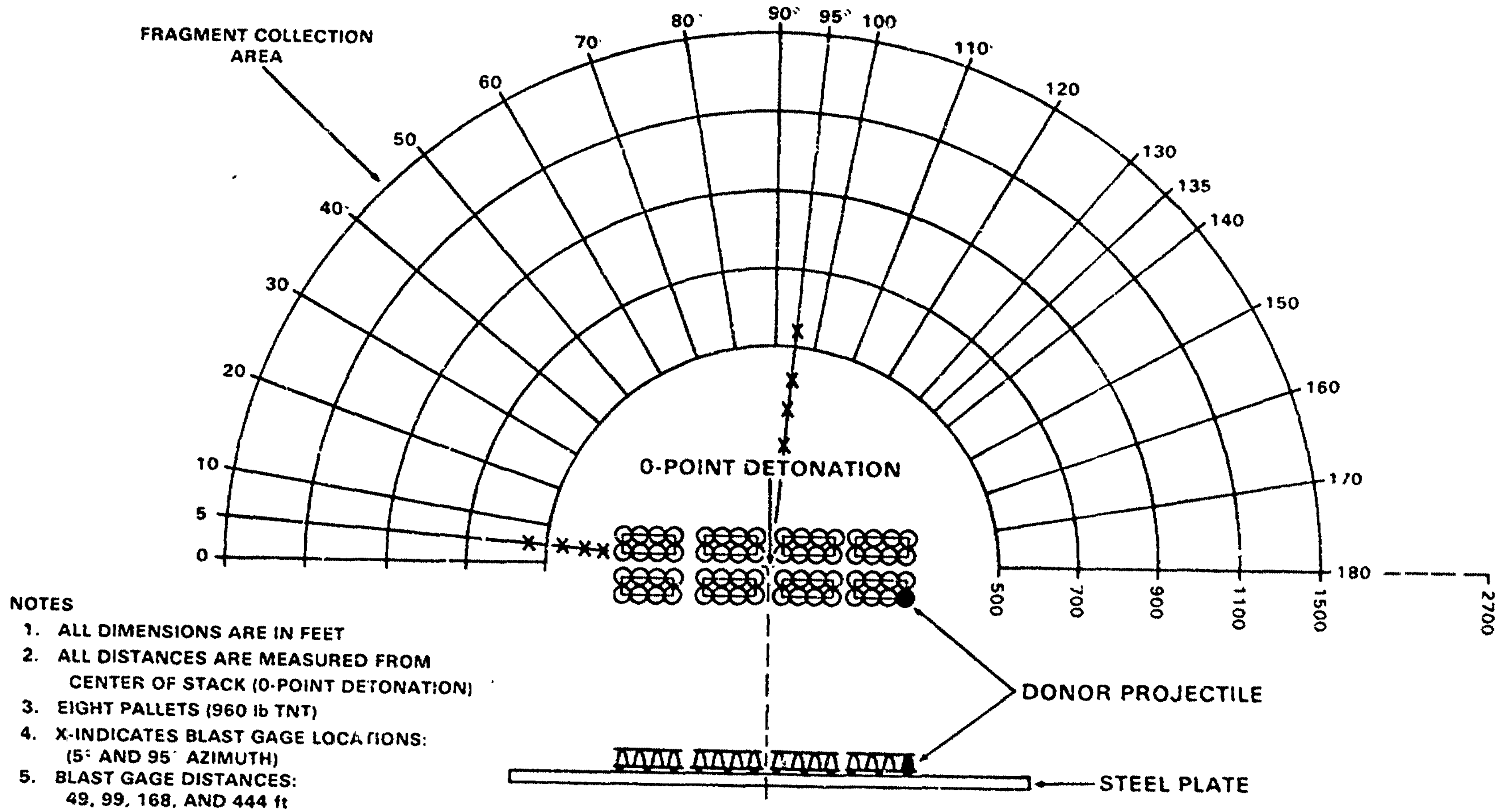

FIGURE 2

FRAGMENT COLLECTION AREA FOR THE DETONATION OF EIGHT PALLET OF 155MM PROJECTILES

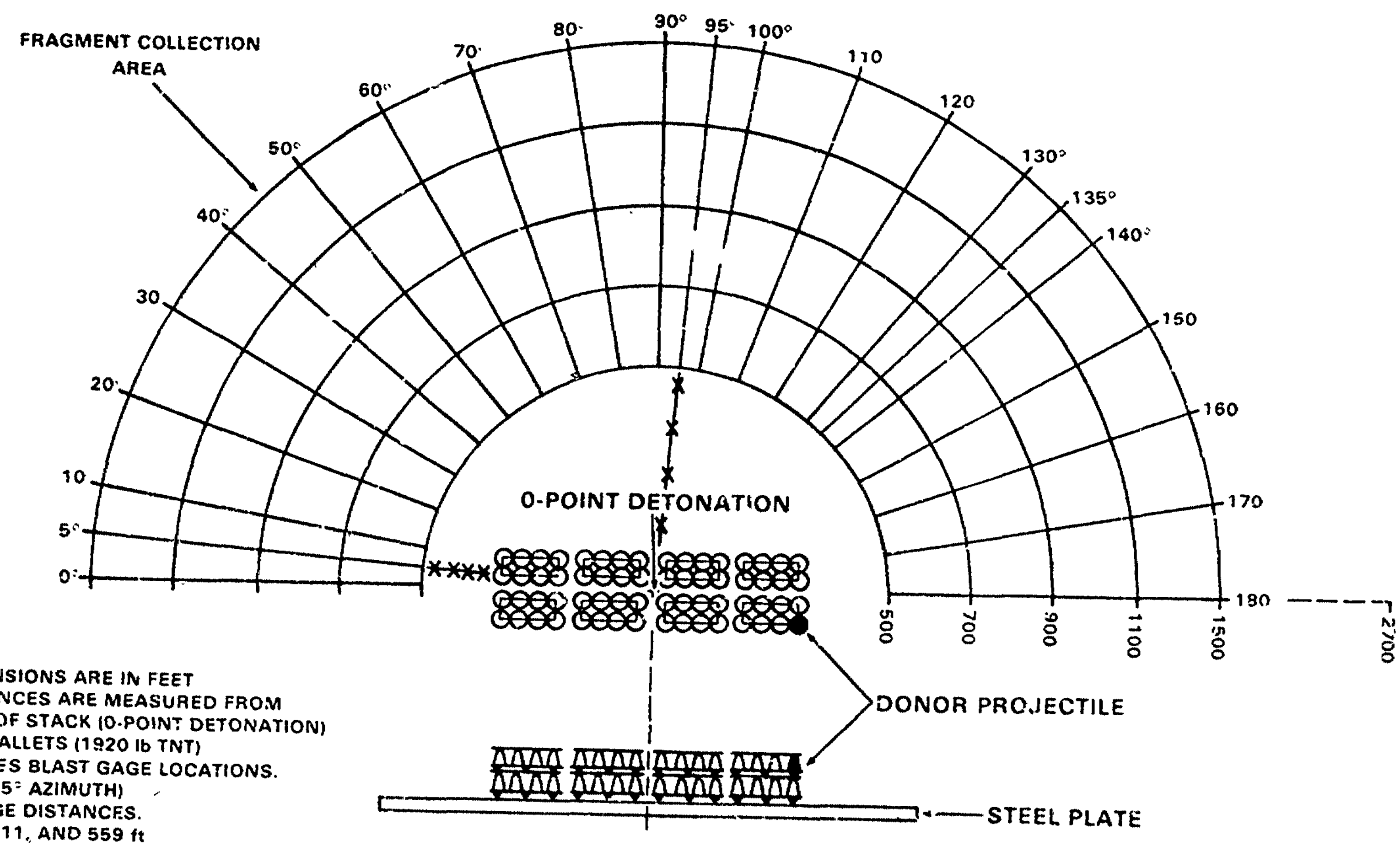

FIGURE 3

FRAGMENT COLLECTION AREA FOR THE DETONATION OF SIXTEEN PALLETS OF 155MM PROJECTILES

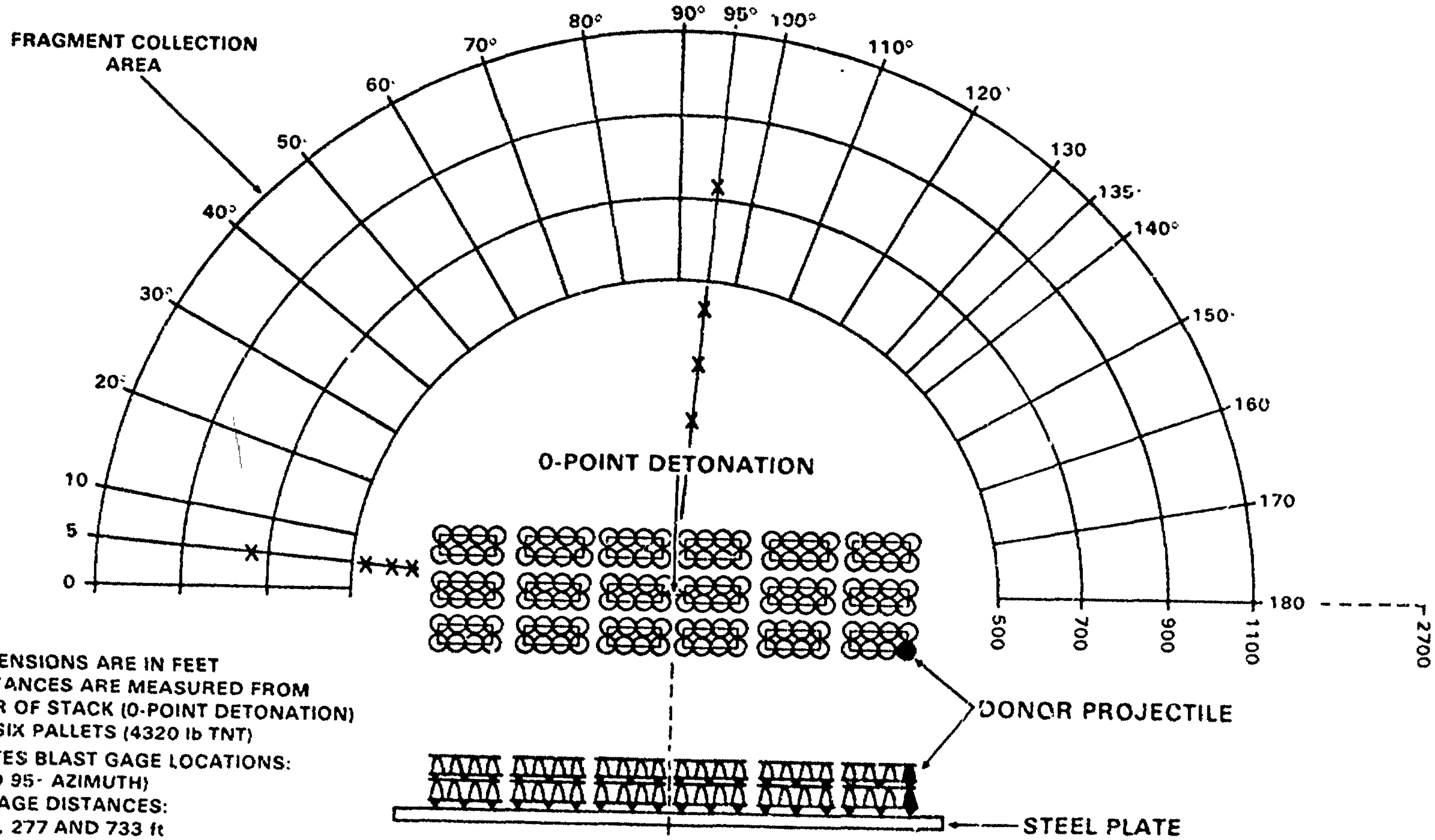

NOTES:
1. ALL DIMENSIONS ARE IN FEET
2. ALL DISTANCES ARE MEASURED FROM CENTER OF STACK (0-POINT DETONATION)
3. THIRTY-SIX PALLETS (4320 lb TNT)
4. X-INDICTES BLAST GAGE LOCATIONS: (5° AND 95° AZIMUTH)
5. BLAST GAGE DISTANCES: 81, 163, 277 AND 733 ft

FIGURE 4

FRAGMENT COLLECTION AREA FOR THE DETONATION OF THIRTY-SIX PALLETS OF 155MM PROJECTILES

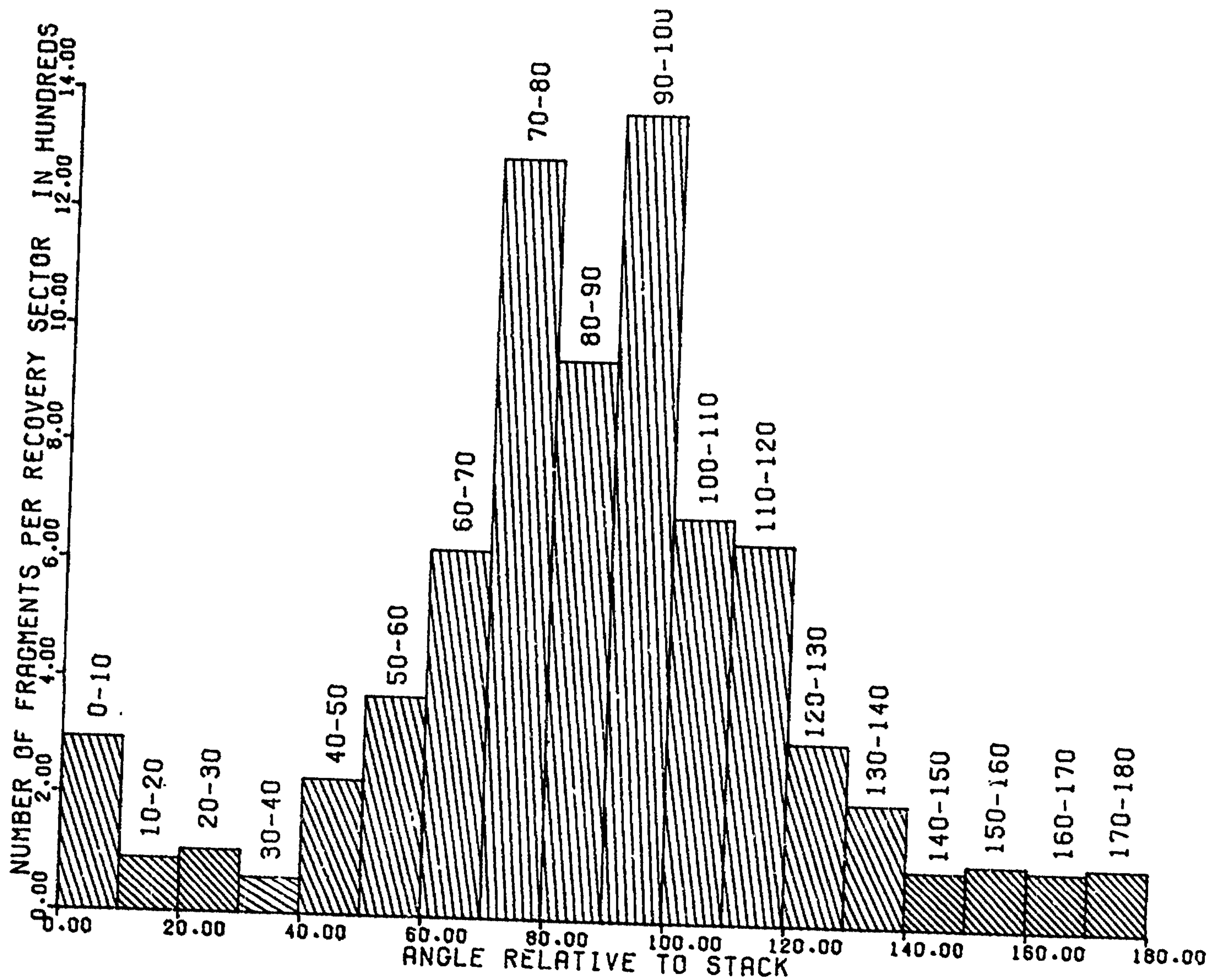

FIGURE 5
TOTAL NUMBER OF FRAGMENTS RECOVERED PER RECOVERY SECTOR FOR EIGHT PALLET DETONATION TEST

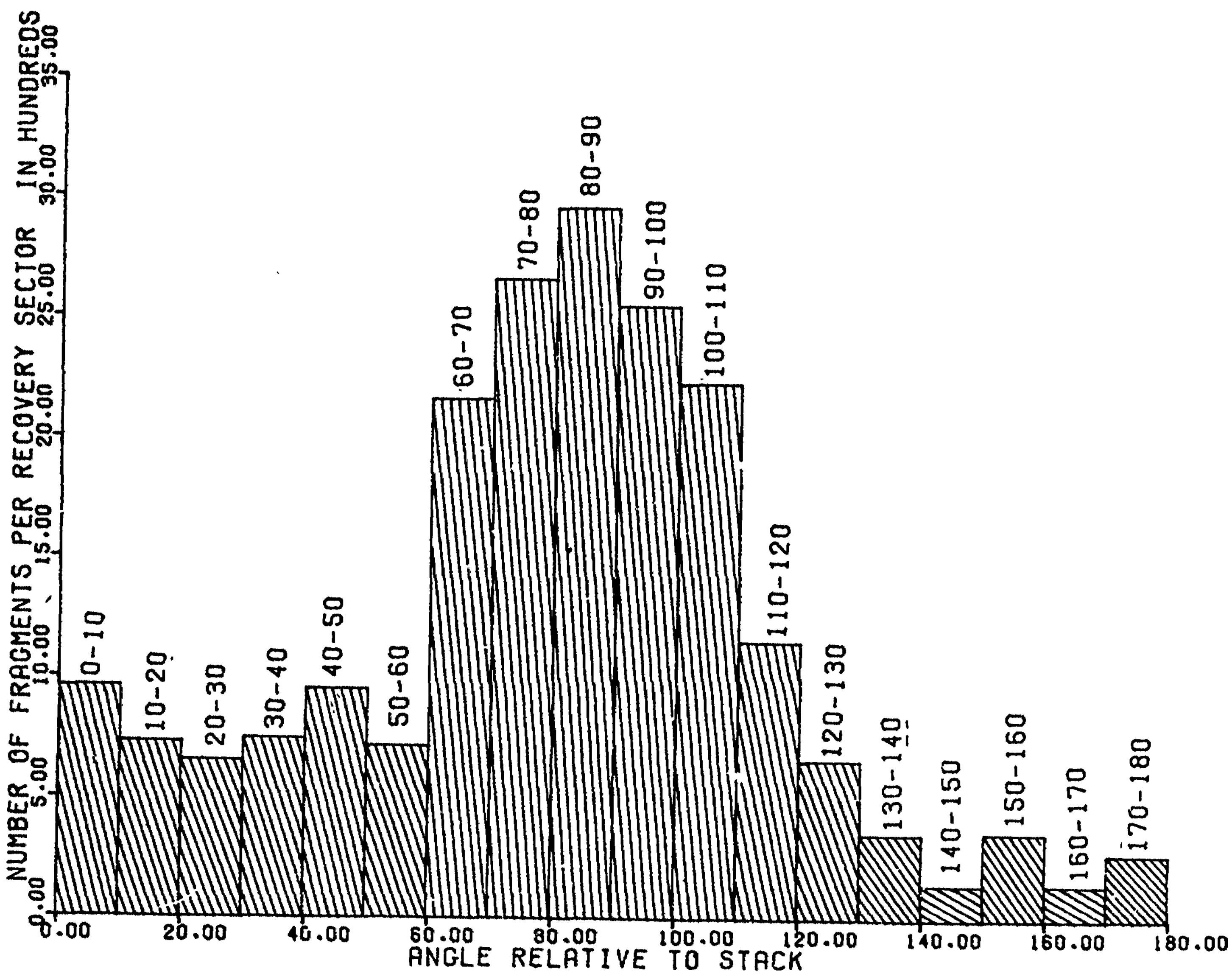

FIGURE 6
TOTAL NUMBER OF FRAGMENTS RECOVERED PER RECOVERY SECTOR
FOR SIXTEEN PALLET DETONATION TEST

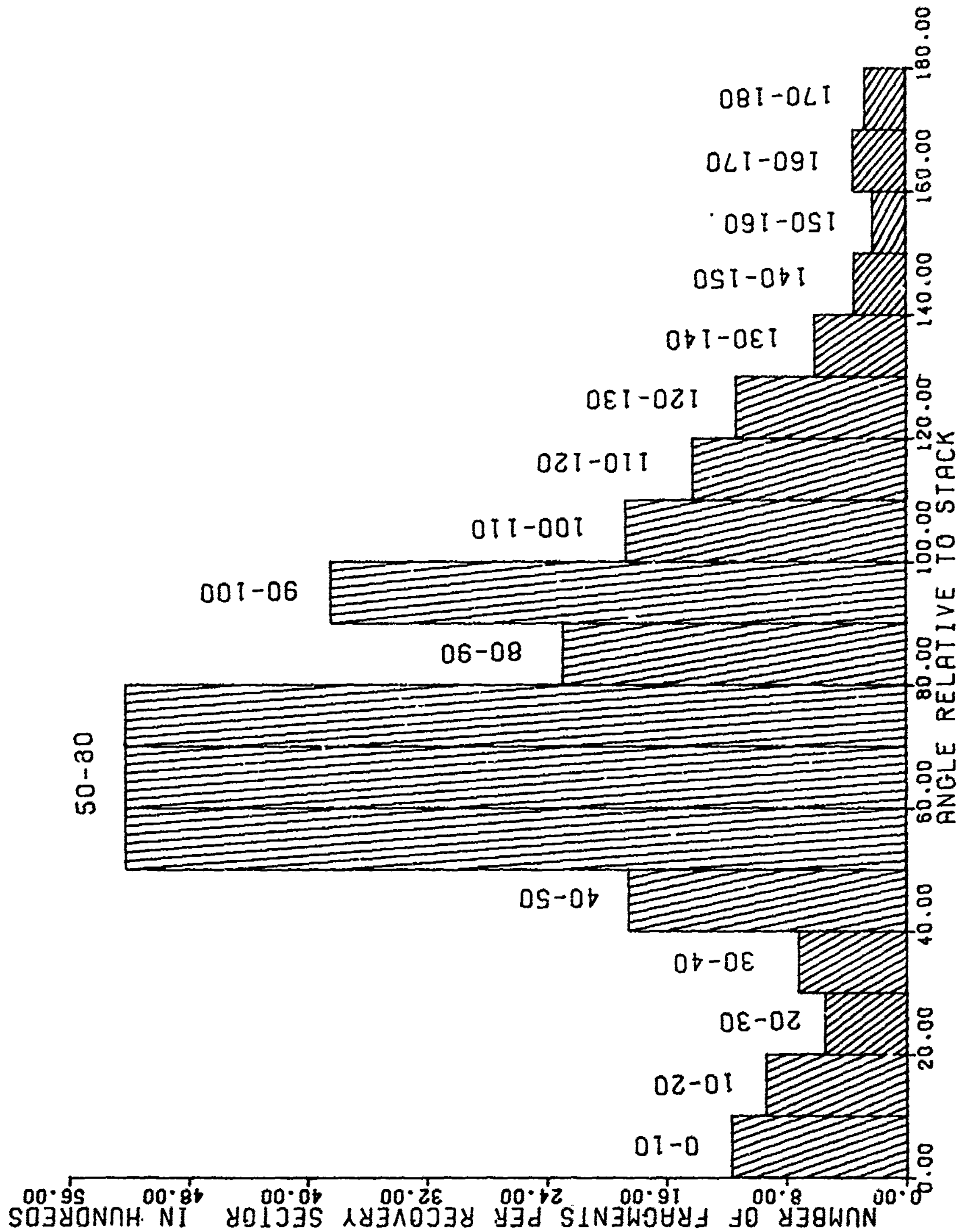

FIGURE 7
TOTAL NUMBER OF FRAGMENTS RECOVERED PER RECOVERY SECTOR
FOR THIRTY-SIX PALLET DETONATION TEST

TABLE 1

Test	Measured Overpressure (PSI)		Number of Interaction Areas	
	5°	95°	5°	95°
8 - pallets (960 lbs. TNT)	22.9	*36.8	2	15
	6.8	8.4		
	2.8	2.3		
	0.8	0.7		
36 - pallets (4320 lbs. TNT)	25.2	96.5	4	46
	8.4	11.2		
	3.5	3.4		
	0.9	0.5		

*Exceeded gage calibration level of 36.8 psi.

3.1 FRAGMENTATION CHARACTERIZATION

Characterization of the fragments recovered from the large-scale pallet detonations was accomplished by analyzing the fragment weight-number distribution (Mott Plot) and the fragment shape distribution (number-gamma). The fragments analyzed for each test were chosen from the interaction areas only.

3.1.1 MOTT PLOT

Figure 8 presents the weight-number distribution data for the eight, sixteen and thirty-six pallet detonations. Also plotted are the data from the small-scale single pallet arena test. The similarity of the slopes of a first-order least squares fit to each test is quite evident. The calculated mean fragment weight (μ) is also similar for each test.

3.1.2 NUMBER-GAMMA DISTRIBUTION

Figure 9 presents the number-gamma distribution for the eight, sixteen and thirty-six pallet detonations and the small-scale single pallet arena test. The similarity of the slopes of a least squares first-order fit to each test is clearly apparent.

3.2 FAR-FIELD FRAGMENT DENSITY PREDICTION

The fragmentation characterization data and recovery data clearly show that the large-scale pallet detonations are directly related to the small-scale single pallet arena test. Therefore, the use of the empirical fragment density relations presented in references (a) and (b) should be possible. The relation is

$$N(R>R_1) = N_{OA} N_{IA} e^{-K_1 R^{0.37}} \qquad (1)$$

where $N(R>R_1)$ = number of fragments per degree of azimuth with range greater than R_1

N_{OA}, K_1 = constants developed from small-scale single pallet number-gamma distribution

N_{IA} = number of interaction areas in stack of interest

3.2.1 VALIDATION OF PREDICTION

The accuracy of eq. (1) can be evaluated by converting it to

$$N_{R_{12}} = 10. \left[N(R>R_1) - N(R>R_2)\right] \qquad (2)$$

where $N_{R_{12}}$ = number of fragments per ten degree recovery zone between ranges

R_1 and R_2 and comparing the calculated number of fragments to the large-scale

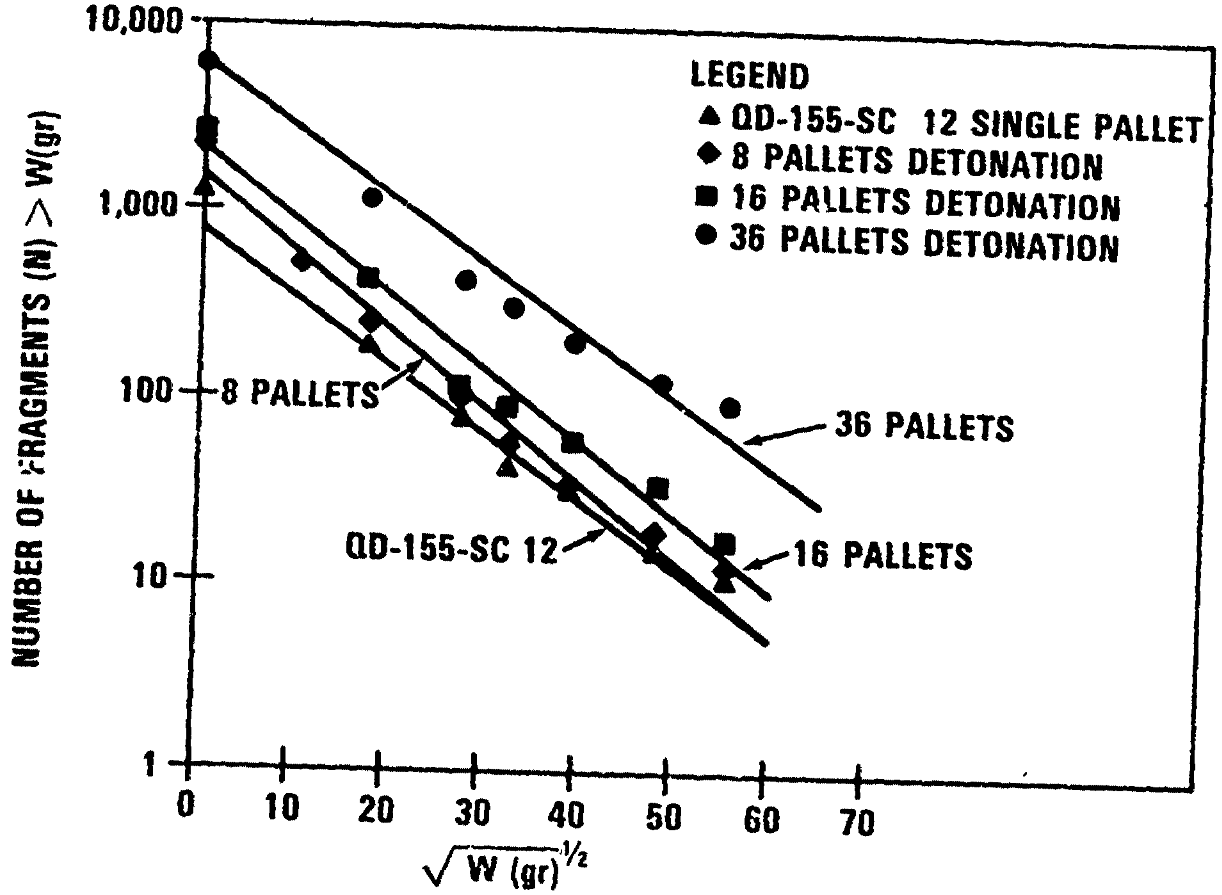

FIGURE 8

MOTT PLOT COMPARISON FOR INTERACTION AREA FRAGMENTS

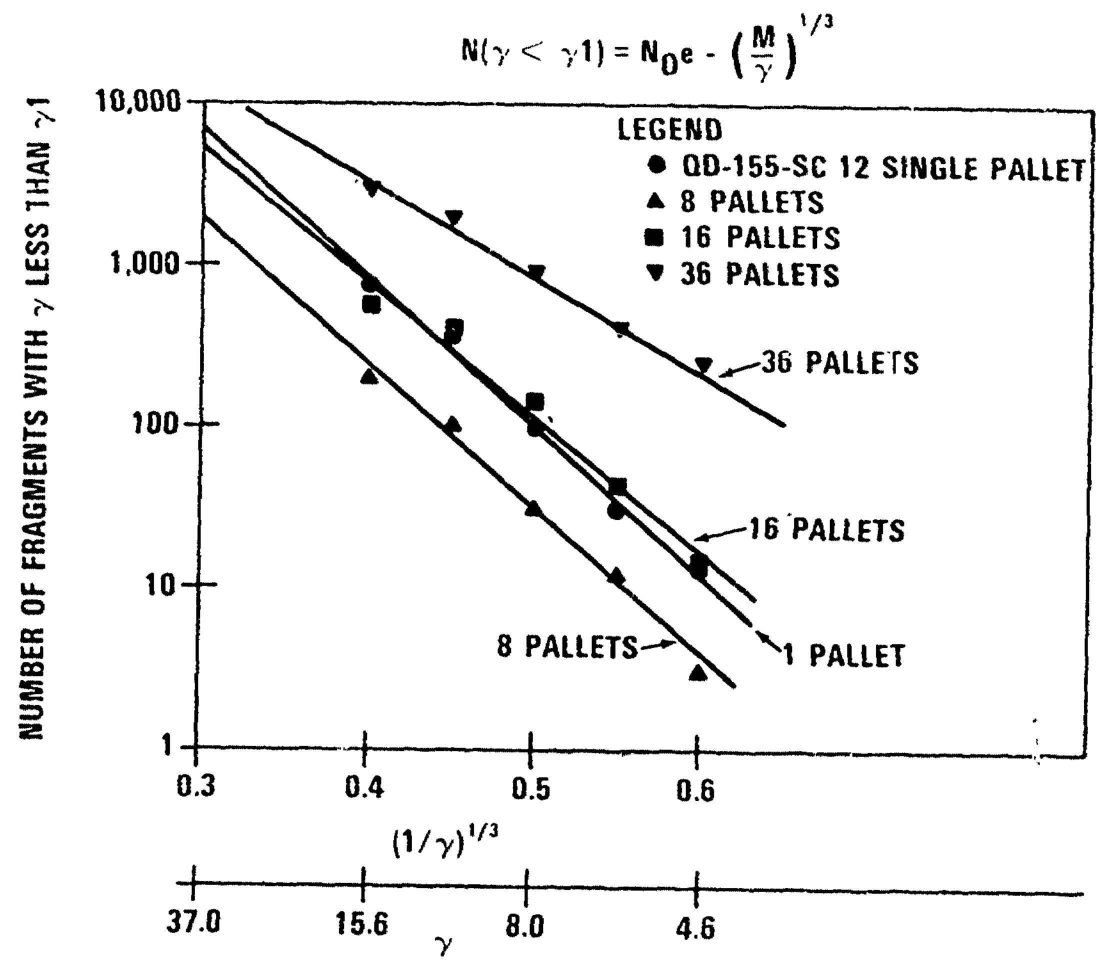

FIGURE 9

COMPARISON OF GAMMA DISTRIBUTION FOR INTERACTION AREA FRAGMENTS

pallet detonation recovery data. Table 2 presents the results of these calculations for the eight (N_{IA} = 15), sixteen (N_{IA} = 30) and thirty-six (N_{IA} = 46) pallet configurations. Also shown are the number of fragments actually recovered for each test. Comparison of the predicted and recovered number of fragments shows that eq. (2) (and, therefore, eq. (1)) is extremely accurate for the thirty-six pallet configuration and somewhat less accurate for the eight and sixteen pallet configurations.

3.3 IMPLICATIONS OF RESULTS UPON EXISTING QD CRITERIA

Figures 10 and 11 compare the actual hazardous fragment (kinetic energy 58 ft-lbf or greater) densities for each test to the existing QD criteria ($KW_{EX}^{1/3}$) for inhabited buildings and permissible hazardous fragment density (one fragment/600 sq. ft.). The data show that the existing QD criteria underestimates the fragment hazards for the configurations tested. Table 3 presents the QD criteria required to meet the current hazardous fragment criteria for these configurations.

3.4 CONCLUSIONS

The analysis of the large-scale pallet detonation test data proves that small-scale tests can be used to predict the far-field fragment hazards for large stack detonations. The existing QD criteria is inadequate to handle the fragment hazards produced by the detonation of 155mm TNT loaded projectiles in an open (non-magazine) storage configuration. Furthermore, guidelines for stacking of 155mm pallets need to be developed to minimize the contribution of the pallet interaction areas to the far-field fragment hazards.

4. CONTINUING EFFORT

It is planned to continue the test and analysis effort to determine if the theoretical framework developed for the M107 155mm ammunition can be applied to other mass-detonating ammunition.

Large-scale tests of Non-Mass Detonation Ammunition (Class 1, Division 2) are presently underway at the WSMR to gather far-field fragment data. Pallets of 40mm AA ammunition and 105mm cartridges are being subjected to bonfire tests. Fragments from these tests are being collected and analyzed to determine the potential fragment hazards.

5. REFERENCES

(a) NSWC Technical Report TR-3664, Oct 1978; Subj: Fragment Hazard Investigation Program

(b) Minutes of the Eighteenth DOD Explosives Safety Board Seminar; Subj: Fragment Hazard Investigation Program

TABLE 2

PREDICTED AND RECOVERED NUMBER OF FRAGMENTS
PER RECOVERY ZONE FOR LARGE-SCALE PALLET DETONATIONS

$$N_{R_{12}} = 10 \left[N(R > R_1) - N(R > R_2) \right]$$

	Number of Fragments Per Ten Degree Zone					
	Predicted			Recovered		
Range (ft.)	8	16	36	8	16	36
1100-1500	231	462	709	156	311	680
1500-1900	74	148	229	22	93	287
1900-2300	28	56	88	3	10	82
2300-2700	12	24	38	0	2	14

*The following parameters were used:

$N_{0A} = 10329.1$

$K_1 = 0.616$

$N_{IA} = 15$ (8 pallet), 30 (16 pallet), 46 (36 pallet)

$V = 6200$ ft/sec

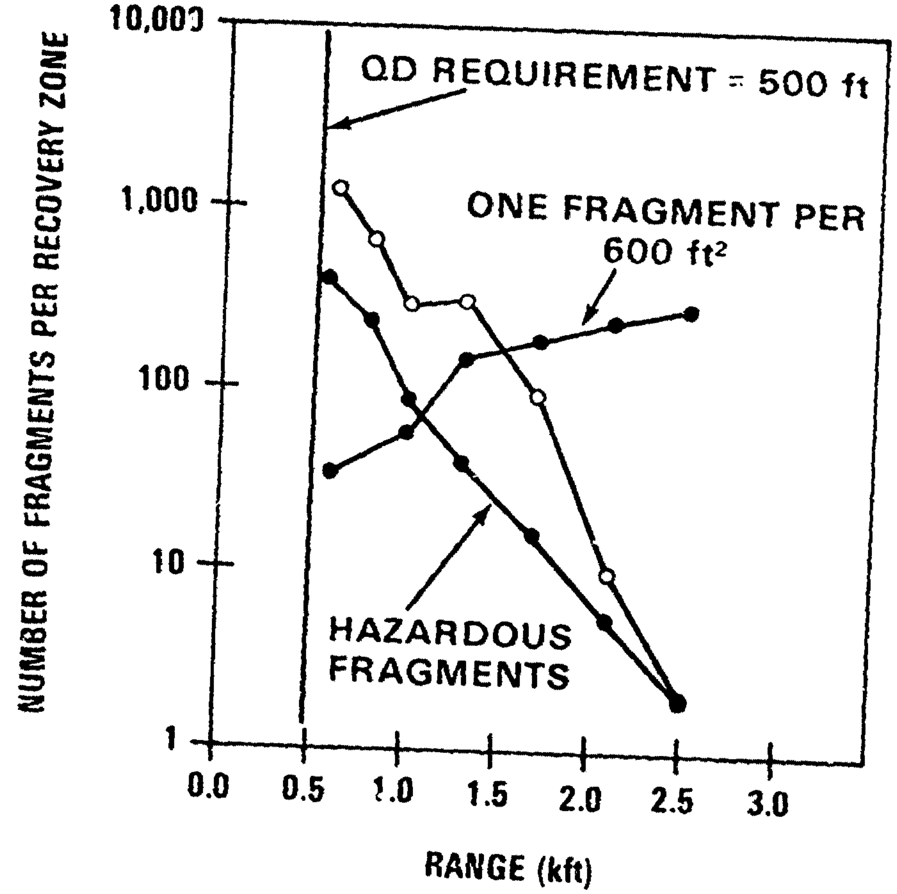

FIGURE 10

NUMBER OF FRAGMENTS PER RECOVERY ZONE FOR 16 PALLET INTERACTION AREA

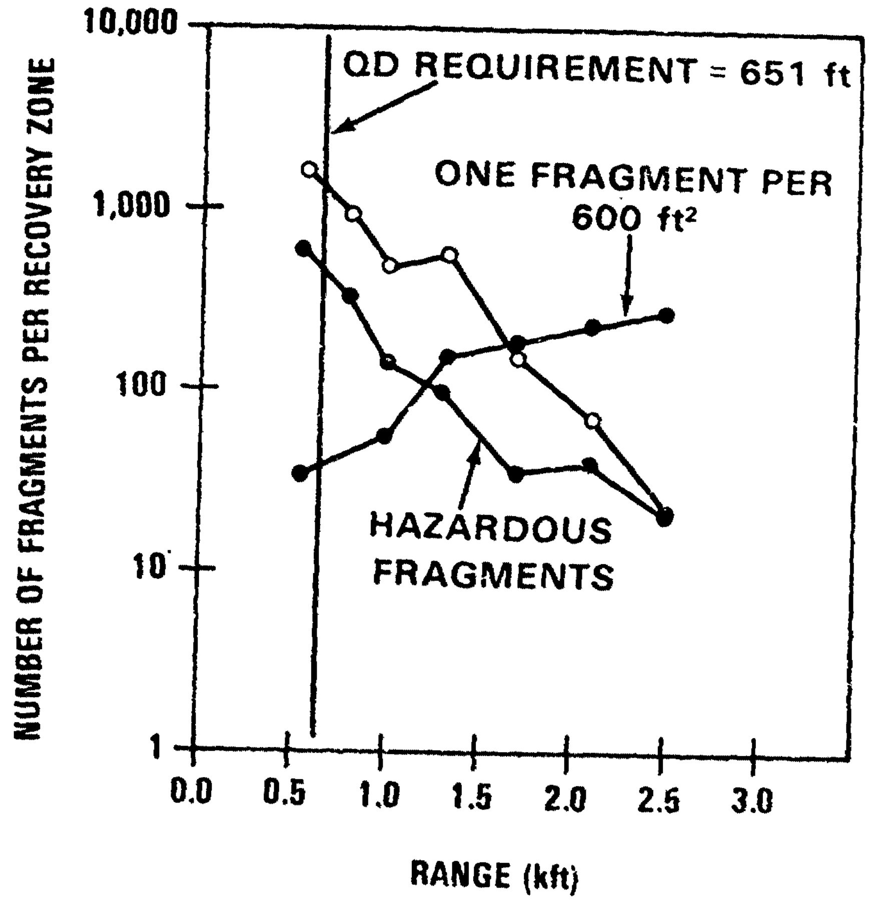

FIGURE 11

NUMBER OF FRAGMENTS PER RECOVERY ZONE FOR 36 PALLET INTERACTION AREA

TABLE 3

REQUIRED QD CRITERIA FOR LARGE-SCALE 155MM PALLET DETONATION TESTS

	QD Criteria (ft.)	
Stack Size	Existing ($KW_{EX}^{1/3}$)	Required for Fragment Hazard
Eight Pallets	400	950
Sixteen Pallets	500	1050
Thirty-Six Pallets	651	1200

NOHARM, NO FOUL

Paper Presented at

Nineteenth DOD Explosives Safety Seminar
Biltmore Hotel
Los Angeles, California
9-11 September 1980

by

William A. Keenan
Civil Engineering Laboratory
Port Hueneme, California 93043

PURPOSE

This paper presents an overview of the need, concept, and benefits for the Navy Ordnance Hazards Analysis and Risk Management (NOHARM) system (Ref 1). NOHARM is a software system designed to generate information necessary for the assessment and management of risks to personnel and property exposed to hazards from the Navy ordnance logistics system. NOHARM is expected to improve substantial' · the chance of identifying ordnance operations, safety waivers, mas :· plans, and military construction (MCON) projects which constitute "NO: · .M, no foul." The NOHARM system is a long-range product of the NAV· .C Explosives Safety Facilities (NESF) Project directed by the Civil Engineering Laboratory (CEL) and sponsored by the Naval Facilities Engineering Command (NAVFAC) (Ref 2).

BACKGROUND

In accordance with DOD Directive 5154.4, the Department of Defense Explosives Safety Board (DDESB) establishes, recommends, and enforces safety standards to guide DOD components in preventing hazardous conditions and limiting human and economic risks. One DDESB standard involves Explosives Safety Quantity Distance (ESQD) tables which specify the minimum "safe" distance from unhardened facilities to potenti..l sources of explosions and fires (Ref 3). The ESQD tables, rigorously enforced by DDESB, are the basis for developing master plans and assessing the safety of proposed MCON projects and existing facilities.

The ESQD tables evolved from the American Table of Distances, prepared in 1910 by the Institute of Makers of Explosives from available records of catastrophic fires and explosions. For the past 70 years, the ESQD tables have provided a simple approach to explosives safety during a period when the technology base was simply not available to predict and assess human and economic risks.

The fundamental philosophy behind the safety standards is not predicated on the probability of an explosion occurring. Instead, the approach is to m.-imize safety under assumed minimally favorable conditions. Every act. · possible is taken to minimize the probability of an explosion, but the location and design of facilities are based on the assumption that the Maximum Credible Explosion (MCE) will occur somehow, sometime, during the life of the facility. This approach to safety decisions is often referred to as the pessimism or maximin criterion in which the objective is to maximize safety under minimally favorable conditions. The maximin approach is often criticized on the grounds that to expect the most pessimistic estimate of the hazard to always occur is not a rational approach for either planning facilities and ordnance operations or judging the safety of people and property. This position was exp .sed by the keynote speaker at the 17th DOD Explosives Safety Seminar. In view of historical records of accidental explosions and the high cost of construction and real estate in today's market, he expressed the opinion that "perhaps the probability of occurrence should be included in the computations of safety standards and we should adopt that most misused of military concepts -- the calculated risk. Misused because it frequently refers to a guess, not to a calculation - and the means of calculating the risk are often not known. This is a subject that needs consideration in the years ahead" (Ref 4).

Better management of explosives safety must start from the present practice of applying ESQD arcs and move deliberately toward calculated improvement. The mechanism for improvement is the NOHARM system which builds without discontinuity on the strength of current safety criteria while compensating for its many weaknesses. Development of a NOHARM system that considers all factors influencing risk and risk decisions is a challenging technology goal. The effort requires an extraordinary degree of cooperative effort on the part of specialists from many diverse fields. But the present and future problems at the waterfront are so critical to in-port fleet readiness that the challenge must be met.

Problem

Ordnance activities in today's Navy are located primarily at the waterfront, especially since 1975 when the Army was designated single service manager for conventional ammunition. At the waterfront, in-port fleet readiness is threatened by continuing conflicts between fleet operational requirements, explosives safety criteria, and economic considerations (Ref 5). The conflicts stem from constraints imposed by the number and size of ESQD arcs, the shrinking supply of unencumbered, buildable land area, the high economic value of coastal real estate, the rising cost of construction, and encroachment by the private community.

The severity of the problem is evident from the following conditions at the waterfront.

(a) The ordnance logistics system is operating at less than optimum to prevent ESQD arcs from encumbering existing facilities and adjacent private communities.

(b) The estimated cost to eliminate approximately 250 existing safety waivers exceeds $400 million using current technology, just to maintain current fleet readiness posture. If all these safety waivers were summarily canceled, a large percentage of all ordnance operations would be stopped, with catastrophic effects on fleet contingency readiness everywhere.

(c) It is increasingly difficult for NAVFAC to develop base master plans and MCON projects which are affordable and meet safety, budget, and operational constraints.

(d) There is a growing interest in government to require risk assessments of dangers to public health and safety, and to rationalize government regulations in light of these assessments (Ref 6).

Risk

The concept of risk must be understood to grasp the significance of the NOHARM system. The concept of risk is illustrated in Figure 1. The area common to all circles represents risk. Risk is the probability of occurrence of a specific consequence. Risk is often used to mean either the probability of a given dollar loss from injuries, fatalities, and damage (economic risk), the probability of a particular person being a fatality (individual risk), or the probability of exceeding a given number of fatalities (group or societal risk). The magnitude of risk depends on the vulnerability of the target (fragility of people and buildings to explosions effects), target exposure (location of building or person relative to the explosive hazard, and length of time person is exposed to the hazard), and the severity of the hazard (probability of a given yield of explosion or fire). Individual, group, or economic risk usually includes the risks resulting from all possible locations and yields of explosions and fires.

Safety

Safety is the condition of freedom from unacceptable risks. What constitutes acceptable risk is a political question which must be determined in the political arena by the decision makers. Definition of risk acceptance criteria has received considerable attention in recent years and is under study by CEL (Ref 7). In the opinion of the author, he usefulness of NOHARM is marginal unless the political community, with input from the scientific community, can agree on risk acceptance criteria. The criteria are needed to interpret risk estimates generated by NOHARM and identify "unsafe" conditions.

Some investigators believe that risk acceptance criteria are not needed. Instead, NOHARM should measure and rank the effectiveness of alternative risk mitigative strategies based on their cost effectiveness, defined as the reduction in risk (benefit) relative to the cost to implement the strategy. The strategy offering the greatest cost effectiveness, within allowable funds, should be implemented by the decision makers. This approach will not necessarily result in a uniform level of risk for all Navy bases and MCON projects. Further, it is difficult to implement in the "real" world because of the way MCON funds are allocated, funds must be designated for safety, the demands it places on high level authorities to participate in all safety decisions, the opportunities it presents to bias safety decisions, and the problem of assessing the benefits of using the MCON funds for purposes other than reducing risk. However, cost effectiveness is an ideal measure for ranking the order in which existing safety waivers should be eliminated. In the opinion of the author, the cost effectiveness approach should be applied in the development of master plans and MCON projects but only after excluding those risk mitigative strategies which violate risk acceptance criteria.

Risk Mitigation

A change in the vulnerability, exposure, or hazard results in a change in the magnitude of risk. Possible risk mitigative strategies include procedural, structural, and locational changes. The traditional approach to mitigate risk is to increase the separation distance between the hazard source and target (i.e., reduce the exposure). This approach requires real estate and often increases the logistics burden. Often, the cheapest strategy is to reduce the severity of the hazard by reducing the probability of a mishap; the probability of an explosion, given a mishap; or the probability of sympathetic detonation, given an explosion. This strategy involves safety training of personnel, changing ordnance handling procedures, increasing the reliability of equipment, reducing the sensitivity of explosives, reducing the amount of stored explosives, etc. Another strategy is to reduce the target vulnerability by hardening the building to resist explosion effects. This strategy requires additional MCON funds.

Constraints imposed by economic, safety, and fleet operational requirements often cloud the best strategy for mitigating risk. These constraints are illustrated in Figure 2. All points inside a circle represent risk mitigative strategies that satisfy the constraint associated with the circle. The area common to all circles represents strategies that satisfy all constraints. Among these acceptable strategies is a unique strategy that satisfies all constraints and, in addition, offers the greatest cost effectiveness. This particular strategy is the one decision makers should implement at the Navy base; it is acceptable to all parties in the decision making process and offers the greatest benefit to the Navy.

CONCEPT

NOHARM will be a software system that operates on existing NAVFAC computer hardware. The development goal for NOHARM is to incorporate probabilistic methods into the assessment and management of risks associated with the Navy ordnance logistics system. The primary objective is to identify "unsafe" conditions. The secondary objective is to measure the effectiveness of competing strategies for mitigating risks. To achieve these objectives, NOHARM must have the capability to estimate the explosives hazards resulting from ordnance operations, predict the resulting human and economic risks from all possible explosions and fires, assess these risks to identify "unsafe" conditions, and measure the effectiveness of competing strategies for mitigating unacceptable risks.

A data base acquisition and management system is needed to support NOHARM. The system must contain data base on ordnance logistics operations, primary and secondary mishaps, facilities and personnel, and risk mitigator costs. Portions of these data base already exist at various Navy activities.

Structure

The basic structure of NOHARM is illustrated in Figure 3. The software will consist of three distinct modules: explosives hazards model (EHM), risk prediction model (RPM), and risk mitigation model (RMM). Each module will be designed to facilitate the input of new technology as it becomes available.

Functions

NOHARM will require a complete description of all facilities, personnel, and ordnance operations at the Navy base. The following is a general description of the data base requirements and functions of each model.

Explosives Hazards Model. The EHM model will require a complete description of all types of ordnance operations, including transfer operations between piers and ships, storage operations in ammunition magazine areas, maintenance operations in buildings, and transport operations by truck and rail. For each operation the following types of data base are required: types of ordnance transactions comprising the operation; type and sequence of actions (mishap opportunities) in each transaction; number of transactions; location and net explosive weight of ordnance stores; probability of occurrence for all possible types of primary and secondary mishaps; conditional probability of detonation for each type of mishap and weapon; conditional probability of sympathetic detonation; and the location and physical characteristics of shielding between concentrations of explosives and possible mishaps. Given this data base, the EHM model will perform the following types of functions.

1. Determine for each ordnance operation the probability per year of all possible yields of explosions and fires, P(Y), associated with each concentration of explosives material, as illustrated in Figure 4b. P(Y) must account for all possible primary mishaps, such as dropping weapons; all possible secondary mishaps, such as ship collisions, earthquakes, and fires; and all possible causes of sympathetic detonation, such as blast, fire, fragments, and debris.

2. Determine for each concentration of explosives the probability per year of all possible yields of explosions and fires, P(Y), associated with each type of ordnance transaction comprising an ordnance operation, as illustrated in Figure 4a.

3. Determine for each concentration of explosives the maximum credible yield, defined as the detonation yield corresponding to a given probability, say 97%, of not being exceeded.

4. Identify the particular ordnance transactions and actions comprising the transaction which are major sources of explosions and fires.

5. Determine the blast, fragment, and debris environments at a particular target location, given the x and y coordinates of both the target and concentration of explosives material. This includes the probability distribution for the peak blast pressure and total impulse on each face of an equivalent rectangular-shaped structure, peak blast pressure inside the target structure, and the number of primary fragments (off weapon) and debris missiles per square foot of ground surface exceeding various energy levels upon impact.

Risk Prediction Model. Information from the explosives hazards model is input to the RPM model. The RPM model will estimate the magnitude and sources of human and economic risks for each building and its inhabitants, the entire base, and the private community.

The model will require a data base on exposures. The data base must describe the location, size, and construction of facilities, and the number, type, and exposure time of inhabitants. Construction data on conventional (unhardened) facilities will indicate the number and size of windows and doors, and the type of construction, such as masonry, timber, steel frame/corrugated metal cover, tilt-up reinforced concrete, etc. The description of windows will be an important component of the data base since historical records show that glass breakage is a major source of injuries from explosions. Given this data base and data input from the explosives hazards model, the RPM model will perform the following types of functions.

1. Determine for each target building the probability per year (or for a given detonation yield) of all possible levels of architectural plus structural damage, P(D), associated with a particular donor source, d, and with all possible donor sources, as illustrated in Figure 5a. Damage estimates will include effects from blast, primary fragments and debris, and secondary fires.

2. Determine the probability per year of all possible numbers of buildings, for each construction type, sustaining a given level of damage, P(M(D)), from a particular donor source and from all possible donor sources, as illustrated in Figure 5b.

3. Determine for each target building the probability per year of all possible numbers of individuals of each type in the building suffering various levels of injury severity, P(N(v)), from a particular donor source and from all possible donor sources, as illustrated in Figure 6a. Estimates of injury severity will include effects from internal blast, primary fragments and debris, and secondary debris and fires.

4. Determine for each target building and for all target buildings the probability per year of all possible numbers of fatalities, $P(N(v_1))$, and of a particular individual being a fatality, P(N=1), from a particular donor source and from all possible donor sources, as illustrated in Figure 6b.

5. Determine for each target building and for all target buildings the probability of all possible dollar losses from building damage, injuries, and fatalities, P(L($)), associated with each donor source and all possible donor sources, as illustrated in Figure 7. Express the loss in discounted dollars that considers the expected number of explosions during the useful life of the facility.

6. Plot a risk contour map for each type of building located on the Navy base, each contour line being the loci of points having a given probability of an individual being a fatality next year from all possible magnitudes and sources of explosions and fires on the Navy base, as illustrated in Figure 8.

<u>Risk Mitigation Model</u>. Information from both the explosives hazards and risk prediction models is input to the RMM model. The RMM model will measure and rank the effectiveness of alternative designs and locations for new and existing facilities, and alternative locations and operating procedures for ordnance operations. The RMM model will accept risk mitigative strategies, such as new ordnance handling procedures,

MCON designs, and master plans. NOHARM will rank their effectiveness and also identify other possible strategies, based on its knowledge of the magnitudes and sources of unacceptable risks. The model will require an extensive data base on mitigator costs. Details of the data base are not clear at this time. Given this cost data base and data inputs from the explosives hazards and risk prediction models, the RMM model will perform the following types of functions.

1. Determine for each MCON project the minimum design factor of safety (applied to deflections), maximum area of openings in the exterior shell, and minimum perforation resistance of the shell required to satisfy minimum risk acceptance criteria, given a description of its location, orientation, size, and type of construction.

2. Determine for each risk mitigator, α, the expected total economic loss (discounted), E(L($)), from damage and injuries, and the MCON plus O&MN cost of the mitigator, C($), as illustrated in Figure 9.

3. Determine for each risk mitigator, α, the expected total reduction in risk (benefit) divided by the total mitigator cost (MCON plus O&MN), as illustrated in Figure 10a. Also determine the expected total life cycle cost, ETC($), equal to the equivalent dollar benefit plus the total mitigator cost, and the expected net gain, ENG($), equal to the equivalent dollar benefit minus the total mitigator cost, as illustrated in Figure 4b.

4. Establish group risk acceptance criteria, P(N), for Navy bases, as illustrated in Figure 11, where P(N) is the probability per year of exceeding N fatalities.

5. Identify those risk mitigators where the risk to a particular individual, P(N=1), or to the group, P(N), exceeds risk acceptance criteria and, therefore, is considered "unsafe," as illustrated in Figure 12.

6. Identify each concentration of explosives material that results in an unacceptable level of individual or group risk and identify the buildings on the base where this condition exists.

7. Rank explosives safety waivers at the Navy base according to risk level and cost to eliminate. Identify how a fixed sum of MCON funds should be allocated to eliminate the safety waivers.

8. Determine if the human and economic risks, on and off base, from the Navy ammunition logistics system are greater or less than the risks from other types of man-made hazards and natural hazards.

9. Determine the level of individual and group risk acceptance implied by current DOD safety standards.

10. Determine the relative importance of blast pressures, primary debris and fragments, and secondary debris and fires on human and economic risks, as a function of type of construction, range, and type of ordnance operation.

DEVELOPMENT PLAN

The development plan for NOHARM is summarized in Table 1. There will be three evolutions of NOHARM, each evolution adding more capability to the software system. NOHARM-1 will have the capability to analyze the hazards in ordnance transfer operations between piers and ships, and economic risks from blast damage to conventional (unhardened) facilities and hardened structural members. The RMM model at this stage will be a noncommunicating software module that contains risk acceptance criteria and decision procedures for identifying "unsafe" conditions and measuring the effectiveness of risk mitigators but without the logic and controls for interfacing directly with the other two software modules.

NOHARM-2 will have refined capabilities of NOHARM-1 plus additional capability to analyze hazards from ordnance storage operations in magazine areas; estimate individual and group risks from effects of blast, primary fragments and debris, and secondary debris and fires; identify "unsafe" conditions on the Navy base; and measure the effectiveness of structural and locational type mitigators associated with target facilities and personnel. NOHARM-2 will have logic and controls to interface with the RPM model but not with the EHM model.

NOHARM-3 will have refined capabilities of NOHARM-2 plus additional capability to analyze hazards from weapon maintenance operations in buildings and ordnance transport operations (inside the Navy base) by truck and rail; estimate individual, group, and economic risks for hardened facilities; measure the effectiveness of procedural and locational type mitigators associated with ordnance operations; and establish the minimum design factor of safety required for hardened facilities to satisfy risk acceptance criteria.

The EHM, RPM, and RMM modules for each evolution of NOHARM will be developed in three phases. concept development phase, software development phase, and software validation/integration phase. The work flow chart for development of the EHM model of NOHARM is presented in Figure 13.

USERS

The users of NOHARM will be master planners, facility designers, operations and budget managers, safety regulators, and base commanders. They are the decision makers who participate in the development and selection of base master plans, MCON projects, and operational procedures which offer the best balance between cost, risk, and operational readiness. NOHARM will generate descriptive information required for each party to participate more effectively in the decision making process.

NOHARM will also be used by the research community. The system will be structured to examine the sensitivity of parameters, sources of uncertainty in output, and priority of new technology requirements.

BENEFITS

NOHARM is expected to provide the following benefits to NAVFAC in base master plan development and facility design; Naval Sea Systems Command (NAVSEA), as the technical agent for explosives safety, in monitoring and controlling explosives hazards and risks; and the Chief of Naval Operations (CNO) in establishing explosives safety policy and allocating MCON funds at the Naval Shore Establishment.

1. Serve as an effective communication medium for resolving conflicts between parties to the decision making process because of the broad range of relevant variables and the way the model parameters and output data correspond to descriptive information which has real life meaning to operational commanders, safety authorities, budget managers, master planners, and facility designers.

2. Provide a safety management tool for measuring and controlling effects of changes in ordnance mix, facilities, material handling equipment, operational procedures, population growth (public and private), and weapon characteristics as the fleet moves into new modes of operations, levels of fleet readiness, or berthing arrangements.

3. Bring into sharp focus potentially hazardous situations which might otherwise have gone undetected, the level of risk being accepted by current ESQD standards, and the increase in risk due to unavoidable deviations from established safety standards.

4. Facilitate master planning, budgeting, design, and safety review of facilities because the output data describe the benefits of many alternative risk mitigative strategies, and display what needs to be done and the level of risk being accepted.

5. Provide a permanent record of the severity and sources of risks at each building on a Navy base and the relative risk between Navy bases.

6. Display risk contour maps (Figure 8) for an entire Navy base to aid nontechnical analysts in planning MCON projects, visualizing the distribution of risk on the base, and assessing the risk to any facility or person. These maps have the potential of allowing a nontechnical person to estimate quickly the individual and group risk for a particular building or the entire base with "back-of-the-envelope" type calculations.

7. Identify parameters which either influence significantly or introduce large uncertainty in risk predictions.

8. Encourage partial solutions to safety problems.

9. Unscramble the present technology base on explosives hazards and explosion effects into an organized technology thrust which identifies the priority and benefits of new technology thrusts.

REFERENCES

1. Civil Engineering Laboratory. Contract Report: Initial conceptualization of an explosives risk-decision model, by L. L. Philipson. J. H. Wiggins Company, Sep 1979. (Technical Report No. 79-1364-1) (Contract N68305-79-C-0017).

2. __________. Unpublished Report: Project management plan for NESF project, by W. A. Keenan. Port Hueneme, Calif., Sep 1980.

3. Naval Sea Systems Command. NAVSEA OP-5: Ammunition and explosives ashore, vol 1, rev 5. Washington, D.C., Oct 1975.

4. P. J. Fliakas. "Keynote address," paper presented at 17th DOD Explosives Safety Seminar, Denver, Colo., Sep 1976.

5. Naval Facilities Engineering Command. Report: Naval Ammunition Logistics System (NALS) study, western portion. Washington, D.C., May 1978.

6. A. J. Large. "Risk-benefit debate," Wall Street Journal, Aug 1980.

7. Civil Engineering Laboratory. Contract Report: A review of acceptable risk criteria and approaches to their development, and comments on their potential application with the NOHARM system, by L. L. Philipson. J. H. Wiggins Company, Aug 1980. (Technical Report No. 80-1383) (Contract N68305-79-C-0017)

Table 1. Capabilities of Each Evolution of NOHARM System

NOHARM		Capability			
Evolution	Module Interfaces	Explosives Hazard Model (EHM)	Risk Prediction Model (RPM)	Risk Mitigation Model (RMM)	Data Base Acquisition and Management System
NOHARM-1	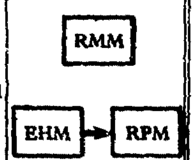	• Ordnance Transfer Operations (Ship-Pier) • Blast & Primary Fragments	• Damage to Conventional Facilities • Damage to Hardened Structural Members • Economic Risk • Effects of Blast Pressures	• Risk Acceptance Criteria • Decision Procedures • Identification of "Unsafe" Conditions	• Ordnance Logistics Operations (Transfer) • Primary & Secondary Mishaps • Facilities
NOHARM-2	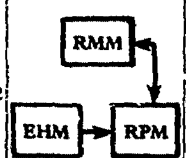	• Refined NOHARM-1 • Ordnance Storage Operations (Magazines) • Primary Debris & Fire	• Refined NOHARM-1 • Individual Risk • Group Risk • Effects of Primary Fragments & Debris • Effects of Secondary Debris & Fires	• Refined NOHARM-1 • Evaluation of Structural Type Mitigators • Evaluation of Locational Type Mitigators	• Refined NOHARM-1 • Ordnance Logistics Operations (Storage) • Mitigator Costs
NOHARM-3	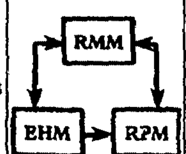	• Refined NOHARM-2 • Ordnance Maintenance Operations (Buildings) • Ordnance Transport Operations (Rail-Truck)	• Refined NOHARM-2 • Damage to Hardened Facilities	• Refined NOHARM-2 • Evaluation of Procedural Type Mitigators • Establishment of Design Factor of Safety	• Refined NOHARM-2 • Ordnance Logistics Operations (Maintenance) • Ordnance Logistics Operations (Transport)

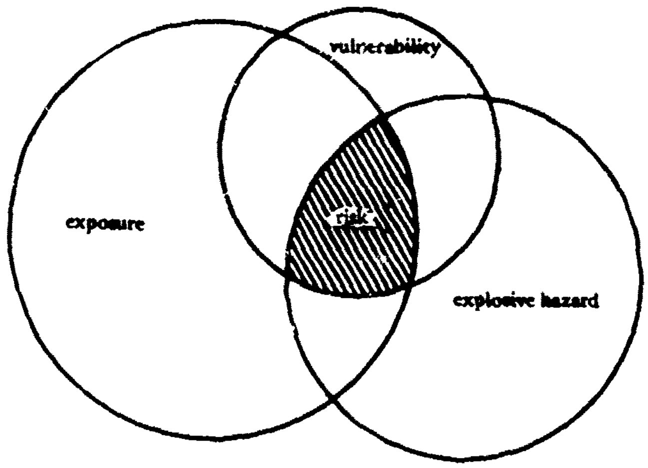

Figure 1. Concept of human and economic risk.

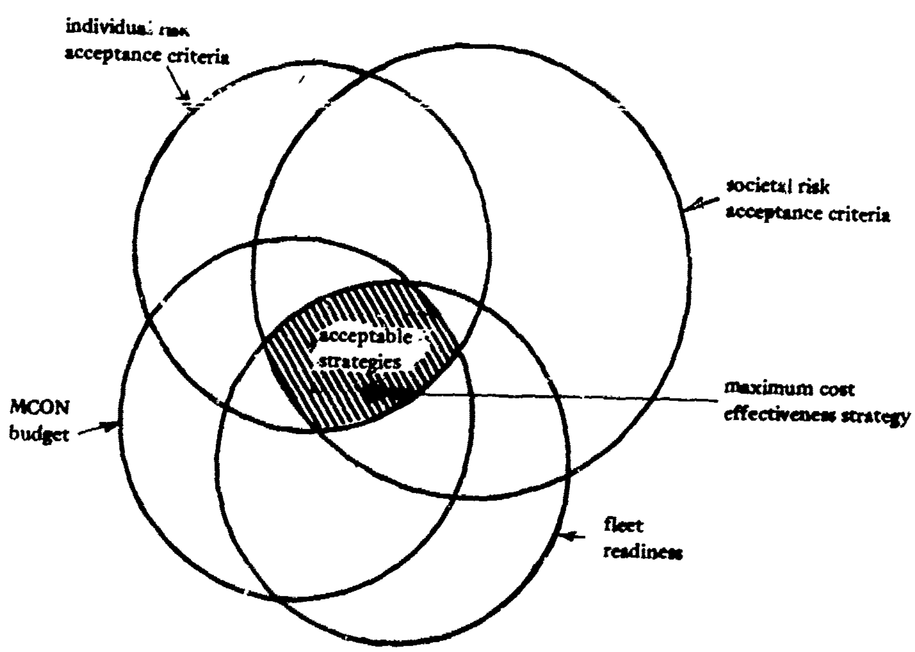

Figure 2. Constraints and risk mitigative strategies.

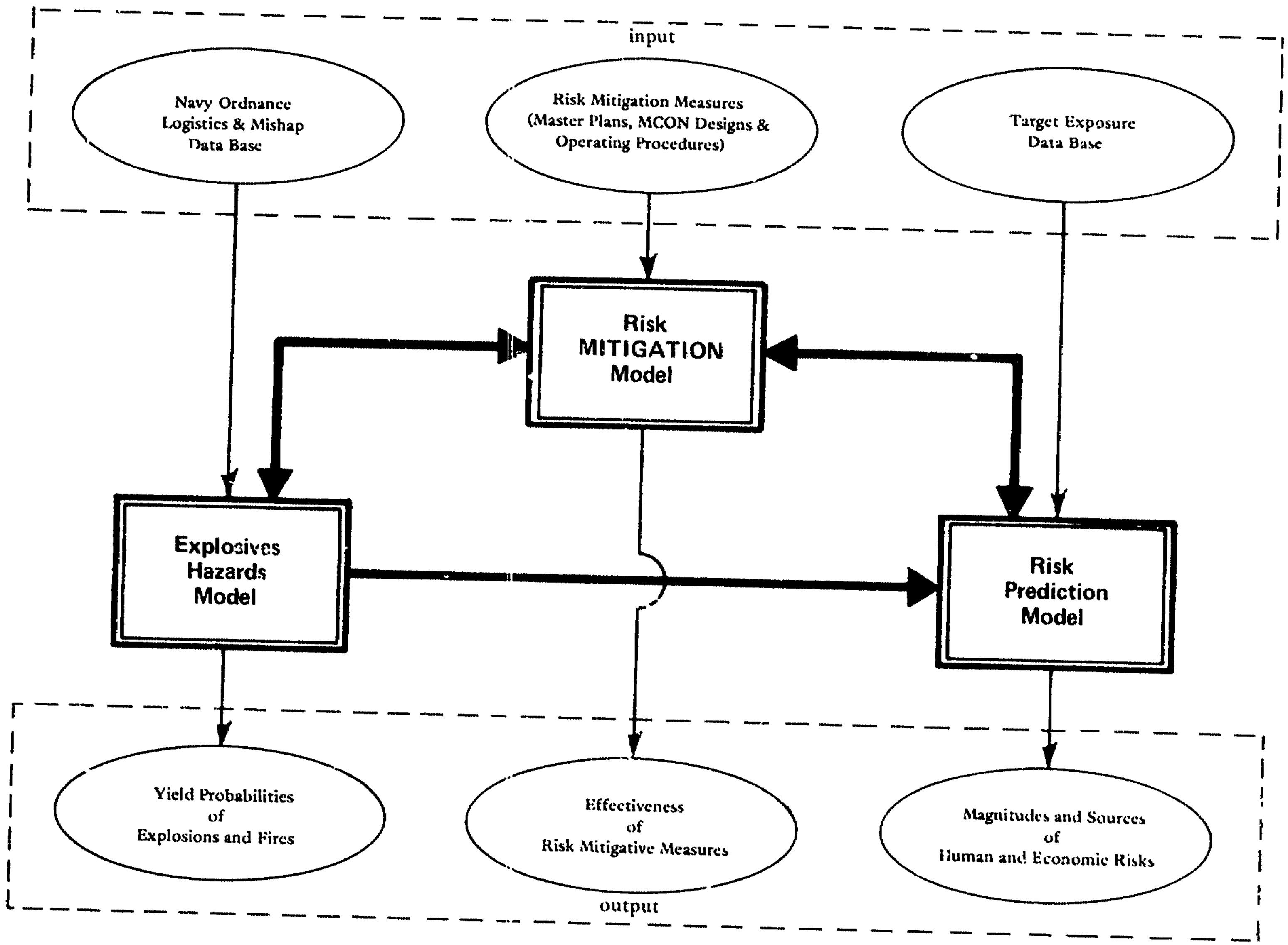

Figure 3. Conceptualization of NOHARM system.

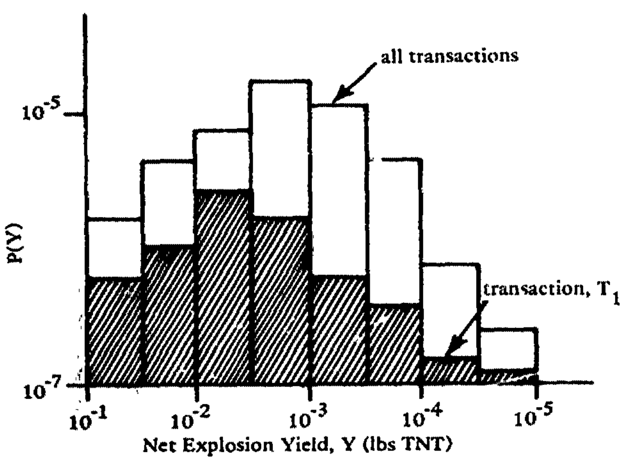

a. Probability per year of all possible yields of explosions for each type transaction involving Tender CANOPUS.

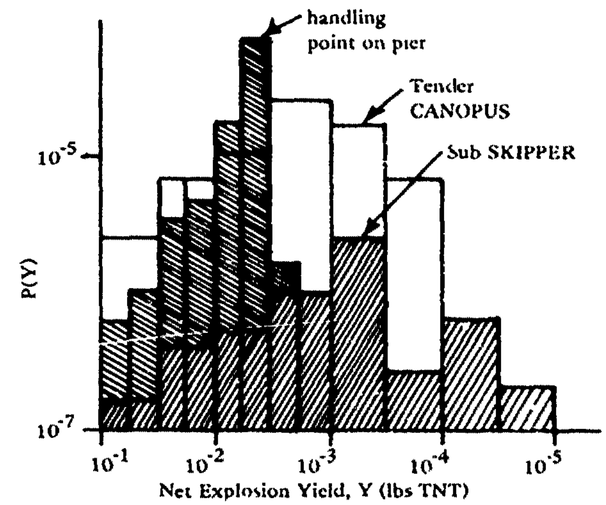

b. Probability per year of all possible yields of explosions for all stores of ordnance at tidewater area.

Figure 4. Typical descriptions of the explosives hazards.

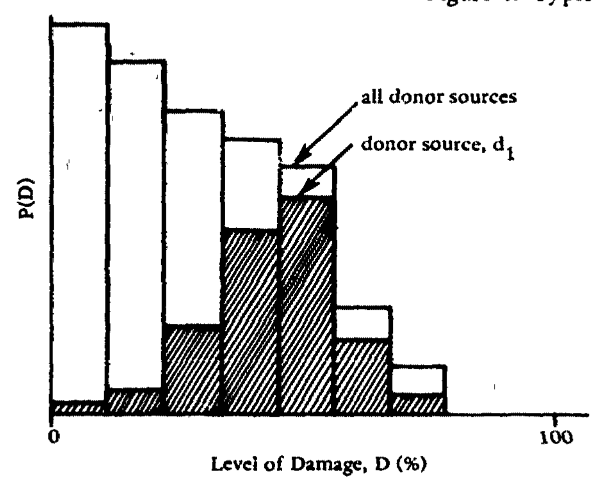

a. Probability of all possible levels of structural and architectural damage to building from given explosion sources.

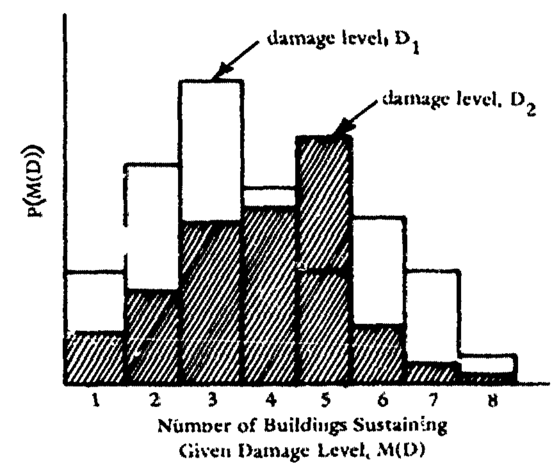

b. Probability of all possible numbers of buildings experiencing given damage level from all possible explosion sources.

Figure 5. Typical descriptions of the level and sources of facility damage.

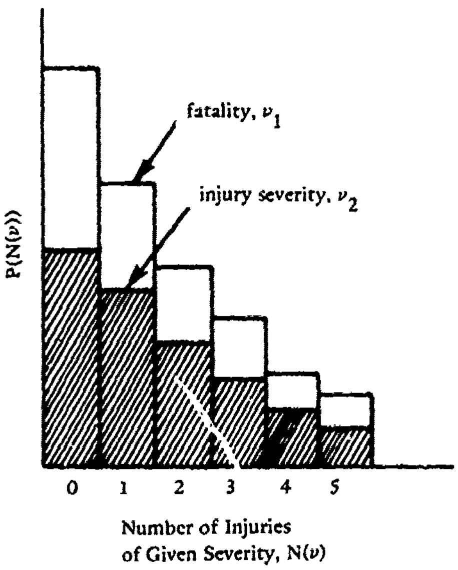

a. Probability per year of all possible numbers of injuries of given severity from all possible explosive sources.

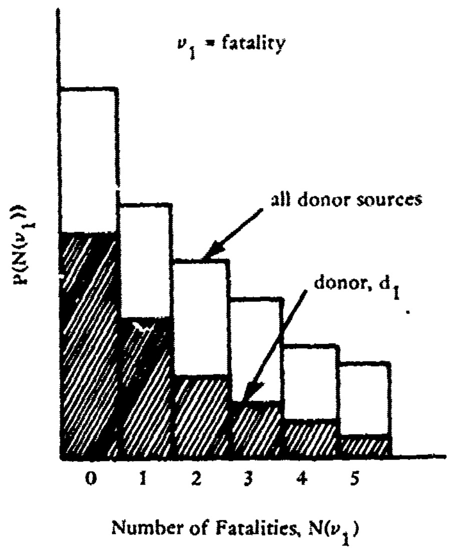

b. Probability per year of all possible numbers of fatalities in particular building from given explosion sources.

Figure 6. Typical descriptions of the severity and sources of injuries and fatalities.

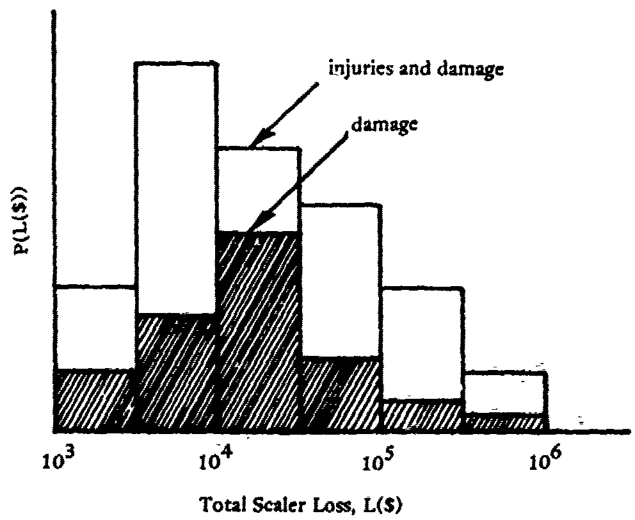

Figure 7. Probability of all possible economic losses from all possible sources of explosions.

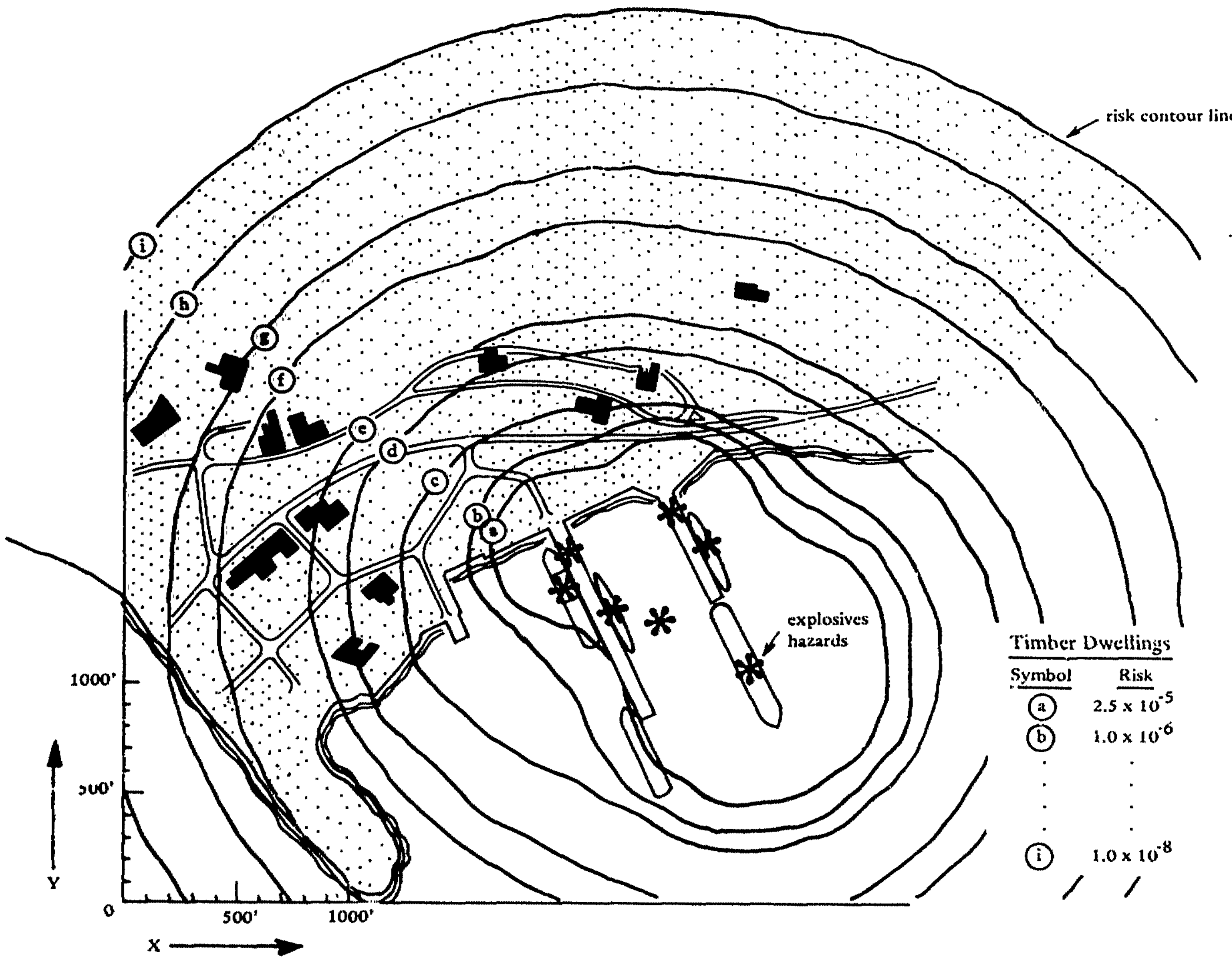

Figure 8. Illustration of risk contour map for timber dwellings at Port Atlantis.

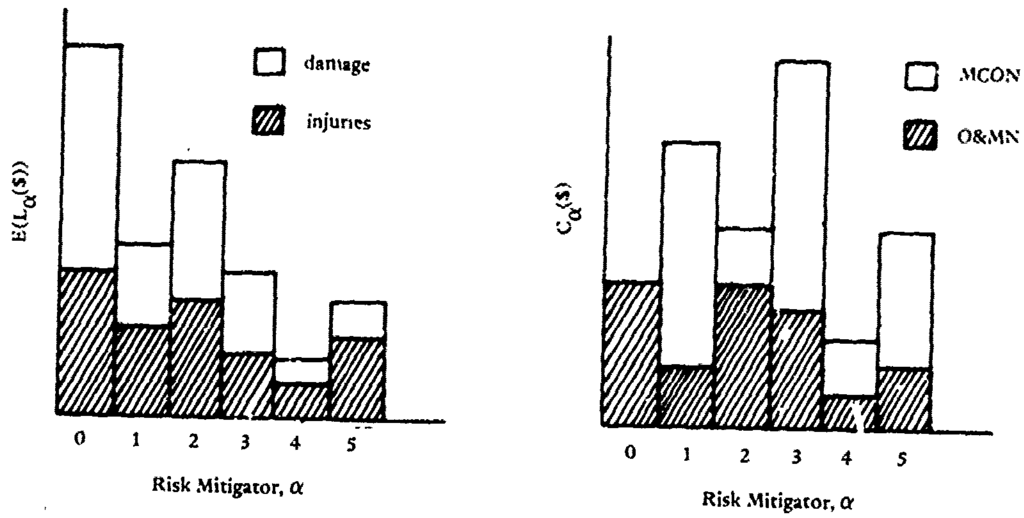

a. Expected total economic loss.

b. Estimated cost of mitigator.

Figure 9. Typical descriptions of costs associated with alternative risk mitigative strategies.

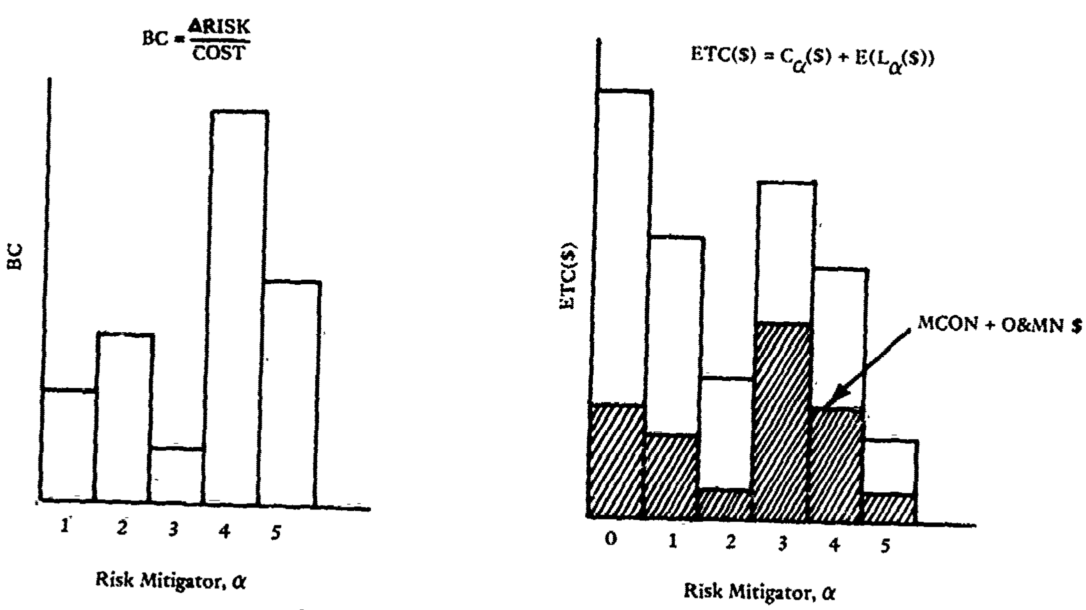

a. Expected reduction of risk (benefit) relative to mitigator cost.

b. Expected total cost of risk mitigator.

Figure 10. Typical measures of effectiveness for alternative risk mitigative strategies.

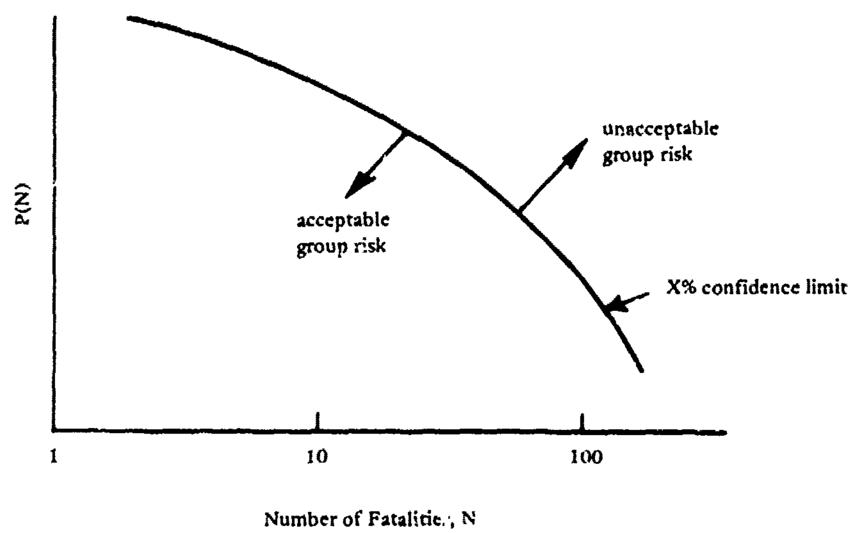

Figure 11. Concept of group-risk acceptance criteria.

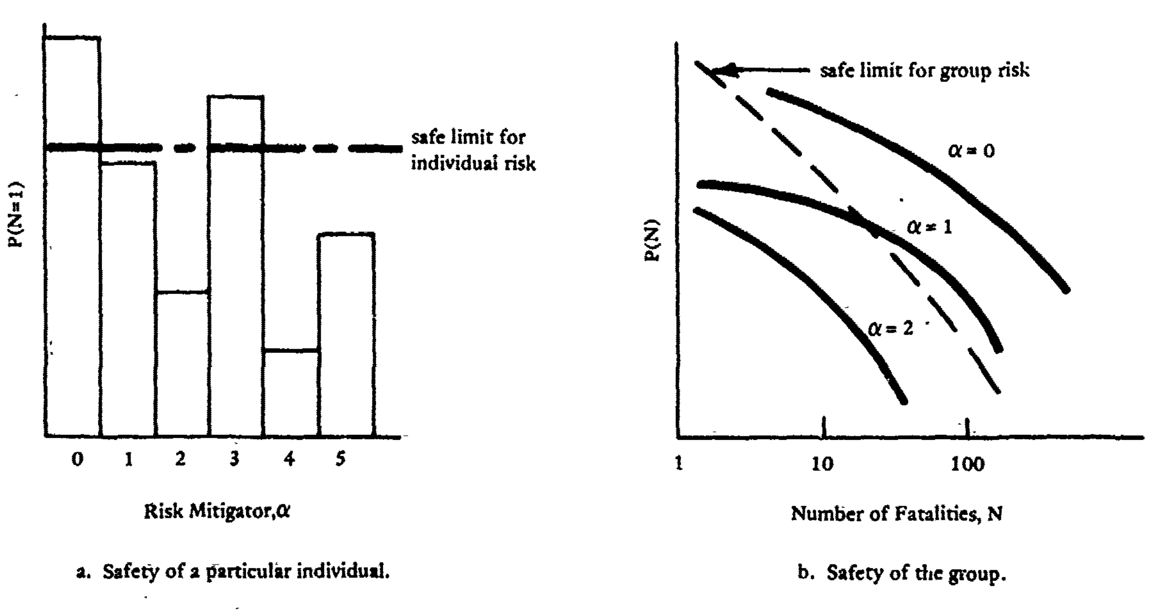

a. Safety of a particular individual.

b. Safety of the group.

Figure 12. Safety of risk mitigative strategies.

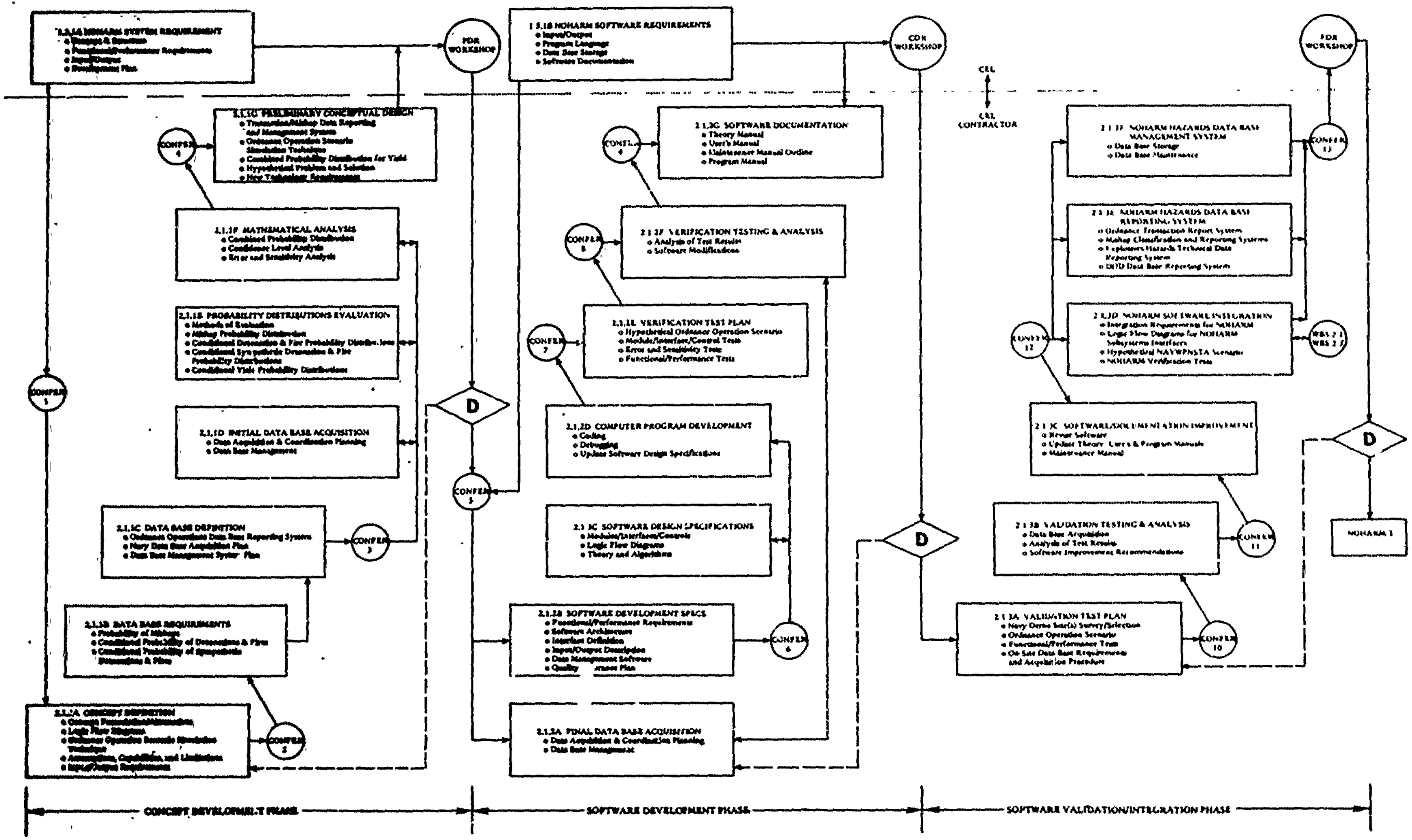

Figure 13. Work flow chart for development of Explosives Hazards Model for NOHARM.

INITIAL CONCEPTUALIZATION OF THE HAZARD MODEL OF THE NOHARM SYSTEM*

Presented to the

Nineteenth DoD Explosives Safety Seminar
Los Angeles, California

by

Lloyd L. Philipson

J. H. Wiggins Company
1650 South Pacific Coast Highway
Redondo Beach, California 90277

9 September 1980

*The material of this paper was developed under contract to the Civil Engineering Laboratory, sponsored by the NAVFAC Explosives Safety Facilities (NESF) Project of the Naval Facilities Engineering Command.

INTRODUCTION

An initial conceptualization is presented of the explosives hazard submodel of the Navy Ordnance Hazards Analysis and Risk Management (NOHARM) System, and the procedures so far considered for quantifying its elements.

NOHARM is to be developed to support safety decisions on facilities and ordnance logistics operations in tidewater areas of Navy bases [1,2,3]. Functional overviews are first given of its complete explosives risks estimation process, of which the hazard submodel is part, and then of the process by which NOHARM will assess the relative worth of, and support selecting from among alternative measures for mitigating risks deemed unacceptable.

The primary concern of this paper is the hazard submodel and its possible directions of development. First, potentially applicable procedures are defined for identifying and assessing the probabilities of occurrence of mishaps in ordnance logistics operations in Navy base tidewater areas that have some potential for leading to explosive reactions. Then an initial delineation is given of approaches to predicting the conditional probabilities of occurrence of an explosive reaction, given the occurrence of a mishap, and the probability distributions of the yields of the reaction that could then result.

The integration of these two sets of procedures provides the requisite inputs for the risk prediction submodel that follows in NOHARM, and that estimates the probabilities of possible levels of damage to structures and of injuries to personnel. In addition, the hazard submodel's outputs are directly usable for assessments of the probabilities of occurrence of explosions, and the probabilities, expected values and/or maximum credible values of the total possible yields of explosions as functions of time, for given operations, at given bases, and for specific locations at these bases where mishaps that initiate explosions might occur.

OVERVIEW OF CONCEPTUALIZED RISK ESTIMATION PROCESS

Figure 1 is a functional flow diagram for the overall process by which ordnance logistics risks will be estimated. For sake of simplicity, only the factors treated at each step in the process are shown. In fact, appropriate probability distributions will be developed for these factors [2]. The character of the distributions in the hazard submodel specifically will be discussed later in this paper. Figure 2 exhibits the process by which the output risk estimates are then incorporated in comparative cost-effectiveness or cost-benefit evaluations of potential risk mitigating measures.

In Figure 1, it is seen that, first, a specific mishap occurs in the handling or storage of explosives on a base. The mishap is described by such parameters as location, ordnance involved, type of logistics action in which it occurs, height of drop of the ordnance (if this occurs), magnitude of a fire from other sources that then involves the explosive material, etc.

An explosive reaction, ranging from a low-yield deflagration to a full-yield detonation, may then be initiated. The magnitude of a resulting fire, and/or

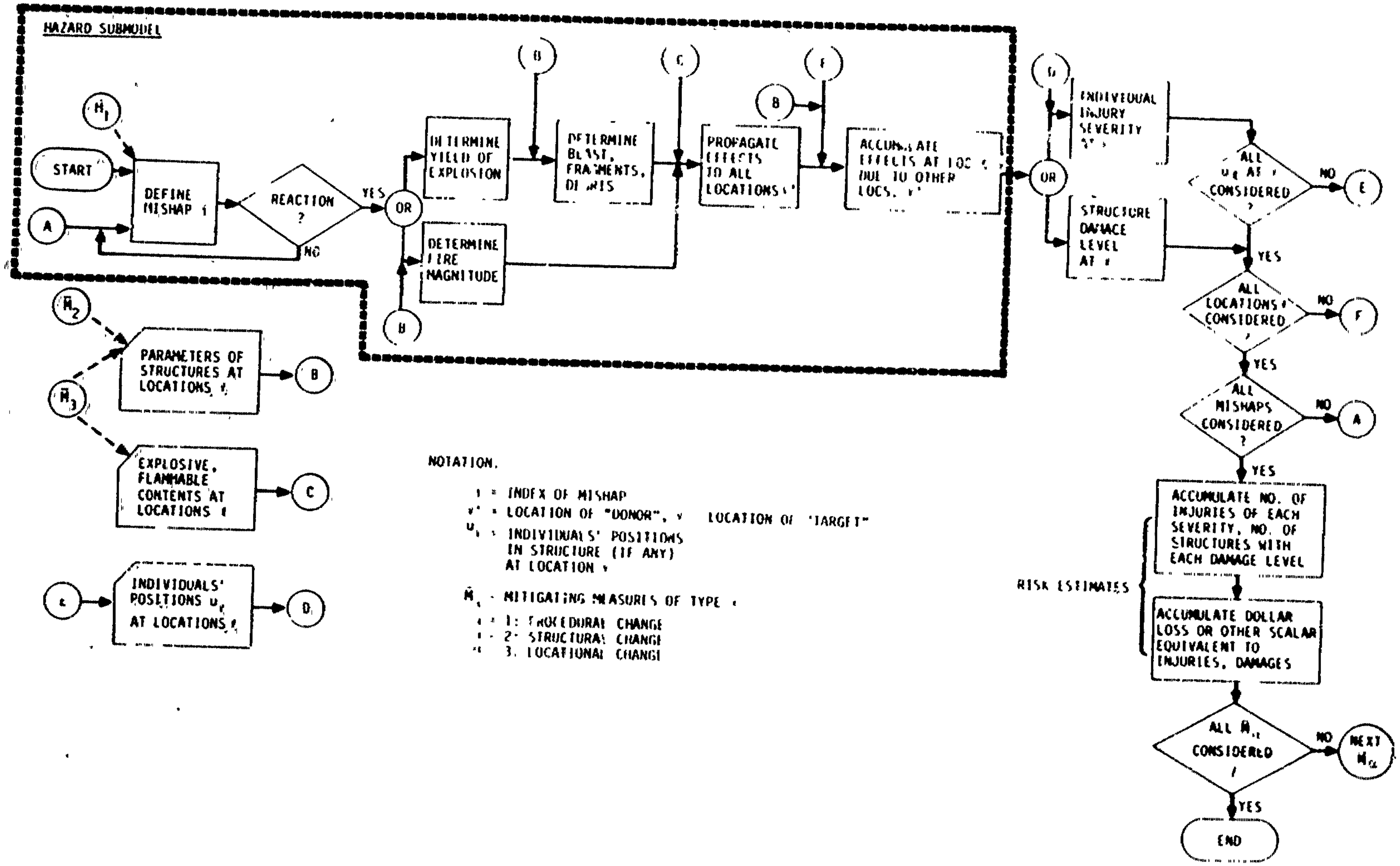

Figure 1. Explosives Risks Estimation Model: Conceptual Flow

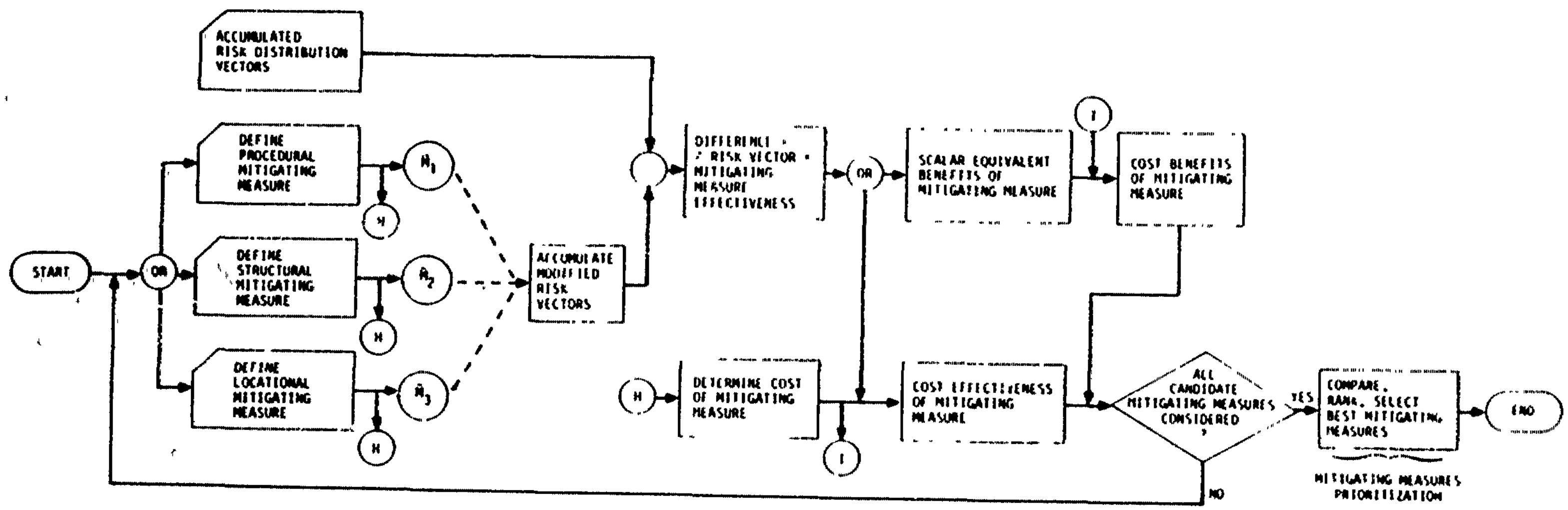

NOTES: (1) SEE FIGURE 3
(2) VIA FIGURE 3 OPERATIONS, AFFECTED BY M_n AS SHOWN IN FIGURE 1
(3) INCLUSIVE 'OR'

Figure 2. Conceptual Mitigating Measures Evaluation Flow

the yield of the explosion at the location of the mishap, are then determined. In the case of an explosion, the blast, fragments, and debris that result are also defined.

These effects are next propagated to all locations they can reach that are either points ℓ' where sympathetic explosions or induced fires may occur, or are points ℓ at which losses (fatalities, injuries, property damage) due to the mishap are calculated. These losses at ℓ may result not only from the initial mishap's primary effects, but also from accumulations of the secondary effects due to the sympathetic explosions and induced fires at the other locations, ℓ' .

At each location ℓ, structural damage and, for each individual at the location (individuals may, for instance, be at different places in a building at the loction) injury severity (ranging from none to fatal) are determined. After iterating over all individuals at ℓ, all such locations ℓ, and all mishaps of interest, the total number of injuries of each severity level, and all property damage at each damage level (ranging from none to fatal) are finally accumulated.

Throughout the risk estimation process, assessments of the effects of uncertainties in the probability estimates, and associated confidence statements for the model's outputs, are also developed.

Mitigating measures of three types: a procedural change to reduce explosives hazards or target exposures, a structural change to reduce target vulnerability, or a change in location of explosive materials or exposed targets, can be introduced into the foregoing process at appropriate data input points, as shown. The process of evaluation of these measures is next described.

OVERVIEW OF CONCEPTUALIZED MITIGATING MEASURES EVALUATION FLOW

Mitigation of the estimated risks from a given hazard or as accumulated over the various hazardous activities at a base will be decided upon if these risks are deemed unacceptable. Alternative means of providing this mitigation must then be evaluated, as described in Figure 2.

The accumulated loss risks developed in the risk estimation modeling are generally expressed as "vectors" of probability distributions for the occurrence, on a base and over a specified period of time, of each possible number of injuries of a given level of severity (including fatalities), and of each possible number of structures that suffer damage at a given level. Application of a given mitigating measure modifies these probabilities. The vector of the difference (Δ Risk) between the original and modified probability distributions then represents the <u>effectiveness</u> of the mitigating measure. Applying an appropriate set of dollar weights* to the components (probability distributions for the differences in injury severities and damage levels) of this effectiveness vector, can then lead to a "scalar" <u>benefits</u> representation

* A number of dollar equivalents for injury severity have been proposed by various agencies. Alternatively, non-dollar importance or <u>utility</u> weights may be employed.

in terms of the probability distribution of total equivalent dollar loss reduction.*

Relating the mitigating measure's cost to its vector effectiveness or scalar benefits then produces a cost-effectiveness or cost-benefits basis for ranking, and selecting the best from among a set of candidate mitigating measures.

THE HAZARD SUBMODEL: DEVELOPMENT OF MISHAP OCCURRENCE PROBABILITIES

The discussion of potential means for estimating the probabilities of occurrences of mishaps capable of causing explosive reactions in handled ordnance items begins with considerations of transactions in tidewater area ordnance logistics operations (OLO's), and their delineation in terms of sequences of individual actions, each of which provides an opportunity for one or more types of mishaps to occur**. The character of this "exposure" to a given type of mishap may vary from one action to another, and be time-or distance-dependent, or neither.

Procedures for identifying possible mishaps are next noted, based on both observational and predictive techniques. Then the major problem of inferring the probability of occurrence, and its associated uncertainty (confidence) distribution, for each possible mishap in each action is considered. (The probability of several types of mishaps (alternatively) able to occur in an action is recognized but is not treated in this paper.) Some alternate approaches potentially applicable to inferring the probabilities and associated confidence distributions for the occurrence of a mishap during a transaction, and then during an entire ordnance logistics operation, and on a base during a given period of time are briefly noted. Only the simplest case is considered of transactions with fixed packages of ordnance items, rather than variable packages due to breaking apart and combining actions.

The facilities, transaction and mishap data bases, and their associated reporting procedures, that are necessary to the development of these inferences are next introduced. The use of past logistics operations and mishap occurrence records for supplementing these data bases in the near future while they are being built up is also noted.

Transactions and Associated Data

An ordnance logistics operations (OLO) is considered to consist of a number of transactions each of which involves the taking of an ordnance package from its initial to its final location in the operation. Each transaction thereby

* Note that in principle other benefits factors could also be introduced here, such as averted incremental logistics costs due to the need to avoid a facility destroyed by an explosion, etc. Mitigating measure costs could also be accumulated taking into account the costs of many kinds of factors interfacing with the mitigating measure's implementation. Care will be required to treat such details adequately in decision analysis cases in which they are important; for comparisons and ranking of more or less similar candidate mitigating measures, however, these details should usually be able to be neglected.

**See the Glossary at end of the paper.

consists of a sequence of discrete actions, each of which provides an opportunity for the occurrence of a mishap. There may be several different types of mishaps that can occur in an action; however, it is assumed that only one of them can occur in any one execution of the action.

In discussing the development of a data base on the characteristics of mishap opportunities and mishap occurrences, it is presumed for now that all executions of a given discrete action in an OLO are essentially the same; i.e., the same handling procedures, equipment and personnel capabilities, mean time duration (actual times may vary randomly about this mean), mean distance of travel, etc., are involved in each execution. It is also presumed for the sake of simplicity here that possible variations in handled packages (due to their being combined or broken apart in the course of an OLO) can be neglected.

The Navy has previously established procedures, and also conducted special studies, that appear able to be extended to support the objective description of transactions. For instance, NAVSEA Instruction 5220.2 [4] includes a delineation of an action sequence diagramming and associated timing procedure that is required for certain ordnance handling activities not in tidewater areas. These procedures can be extended to tidewater area actions, making use of the same basic concepts, symbols and techniques. Each transaction is analyzed into its component actions such that each one can be described generically by one of the symbols shown in Figure 3. A time line connecting these symbols describes a given transaction, as illustrated in Figure 4. To support NOHARM's risk estimates, data are then acquired from observations of OLO's on the frequencies and other characteristics to be discussed below of the component actions, so as to enable predicting these characteristics for future OLO's and their transactions.

Initially, it is planned to characterize an Operation activity in Figure 3 as one of the following action types:

- Human handling
- Forklift handling
- Crane/boom handling

These action types are modeled as "instantaneous," discrete activities.

Transportation activities are designated as one of:

- Carrying by man
- Handtruck transport
- Rail transport
- Waterborne vehicle transport

with their time and/or distance characteristics generally also considered.

Delay and Storage activities are defined by the lengths of time and any special environmental conditions (e.g., open, sheltered, sheltered with controlled temperature) involved.

Inspection activities are aggregated with Human Handling Operations, unless some particular hazardous testing (not expected for tidewater operations) or

OPERATION. An operation occurs when an object is intentionally changed in any of its physical or chemical characteristics, is assembled or disassembled from another object, or is arranged or prepared for another operation, transportation, inspection, or storage. An operation also occurs when information is given or received or when planning or calculating takes place.

TRANSPORTATION. A transportation occurs when an object is moved from one place to another, except when such movements are part of the operation or are caused by the operator at the work station during an operation or an inspection.

INSPECTION. An inspection occurs when an object is examined for identification or is verified for quality or quantity in any of its characteristics.

DELAY. A delay occurs to an object when conditions except those which intentionally change the physical or chemical characteristics of the object, do not permit or require immediate performance of the next planned action.

STORAGE. A storage occurs when an object is kept and protected against unauthorized removal, shown by inverted triangle.

COMBINED ACTIVITY. When it is desired to show activities performed either concurrently or by the same work station, the symbols for those activities are combined as shown by the circle placed within the square to represent a combined operation and inspection.

Figure 3. Transaction Sequence Symbols* [4]

*Reprinted in NAVSEA Instruction 5220.2, by special permission from McGraw-Hill Book Company, from Industrial Engineering Handbook by H. B. Maynard, 2nd Ed., 1963. Page 2-21. c. 1963.

ACTION: MOBILE CRANE HANDLING

OPERATOR NO.	STEP NO.	DESCRIPTION
CHECKER	1	CHECK AND INSPECT MATERIAL
2	2	REMOVE/INSTALL RUNNERS/GROUND WIRE (WHEN REQUIRED)
2	3	PICK UP UNIT(S)
2	4	TRANSPORT TO 4 WHEEL WAGON
3 - 4	5	TRANSPORT WAGON TO DOCK
3 - 4	6	ATTACH SAFETY HOOKS
*	7	TRANSPORT TO RAIL/TRUCK WITH MOBILE CRANE
*	8	STOW UNITS, DETACH HOOKS
CHECKER	9	COMPLETE DOCUMENTATION

*Performed by Mobile Crane Crew

Figure 4. Illustrative Diagram of Portion of a Transaction Sequence (Ref. NWS, Concord, SOP1-100-3/77)

other manipulation of the ordnance item during inspection is involved. If it should turn out that the latter case is important, a separate Inspection action will have to be maintained, but this is neglected for the present.

Identification of Mishap Opportunities

The types of actions delineated in the previous section provide opportunities for various types of mishaps to occur. For NOHARM a set of such types has been defined so as to (1) establish a best fitting set of aggregated classifications of possible mishaps; (2) support predictions of the probabilities of occurrence of mishaps in specific actions, at least where adequate statistical records do not exist; and (3) be able to relate specific mitigating measures to identified mishap opportunities. Mishap types such as "drop package x feet due to human error," "puncture of package in crane/boom handling due to equipment failure," are called primary mishap types from which explosions can directly arise. External mishap types are also considered, such as earthquakes, aircraft crashes, ship collisions, externally-caused fires. These may lead directly to an explosion, but such mishaps may also indirectly contribute to the occurrence of an explosion by increasing the likelihood that some primary mishap will occur.

Four basic means are considered for identifying opportunities for such mishap types in ordnance logistics actions: subjective, records analysis, fault tree analysis and the conduct of experiments.

- Subjective Analyses

This procedure is akin to "Preliminary Hazard Analysis" in system safety programs. It consists of an organized, but qualitative, search for points in an action where something can go wrong, and if it does, some chance would exist for an explosion to take place. This procedure is, of course, the basic one already employed by Navy safety personnel in attempting to assure that all ordnance hazards are recognized and controlled to the extent possible.

- "Statistical" Analyses

Records searches, trend analyses and other quantitative summaries of mishap report data can lead to the recognition of the existence of certain hazards as common elements in sets of such data.

- Fault Tree Analyses

The detailed structuring via qualitative fault trees of the sequences of events leading to the occurrence of mishaps of concern can aid the discrimination of the most critical initiating events, e.g., human failures.

- Experimentation

Should some actions' complexities warrant it, an experimental program could be designed to distinguish mishap opportunities in them that normal operational observations might miss. In the process, time and other measurements can be made in support of the development of the mishap probability distributions next discussed.

Mishap Probability Estimates

The estimation of the probability of occurrence of any specific type of mishap in the course of a given action depends both on the nature of the action and of the mishap. Three specific categories of mishaps are defined.

- Mishaps with Constant Probabilities of Occurrence per Execution of a Given Action - the Binomial Case

If (1) the occurrence of a mishap in a given execution of an action is known to neither affect nor be affected by the mishap's occurrence in any other execution of the action, and (2) if the probability of the action is known to be constant over all executions of the action (i.e., does not change from action to action because the action itself has essentially constant characteristics, or because the mishap's cause is essentially independent of any possible variations in the action's characteristics), then the number of occurrences of the mishap in a given number of executions of the action is distributed binomially. The probability of occurrence per action of the mishap, p, is estimated by the ratio of the number of observed occurrences in a given sample of actions to the number of actions in the sample.

- Mishaps with Constant Rates of Occurrence per Unit Time or per Unit Distance During an Action - the Exponential Case

The simplest functional dependence of mishap occurrence probability on the characteristics of an action is that of a constant mean rate of occurrence per unit time of duration of the action, α; or for actions where it is more relevant than time, per unit distance traveled in the action, β .

In this case, the probability of occurrence of the mishap during an action of any given time duration t or distance d is the exponential

$$p(t) = 1 - e^{-\alpha t},$$

or

$$p(d) = 1 - e^{-\beta d},$$

respectively.

- General Cases

Especially since actions involving humans are predominant in a transaction, it may be anticipated that significant variability will, in fact, be present in the rates and/or probabilities of occurrence of some mishaps. The establishment of appropriate formulations for mishap probabilities and their estimation procedures for these general cases must be left for future data acquisitions, analyses and experimentation. For example, <u>decreasing</u> the time duration of some given action may well <u>increase</u> the rate per unit time (and so perhaps the probability) of occurrence of a mishap if involved personnel tend to err more often under more hurried conditions. On the other hand, human boredom or exhaustion may become important over relatively long duration actions, or over the duration of an unusually large number of transactions.

Confidence Distributions

Standard formulations exist for the "confidence distribution" (that is, the probability distribution for the "true" probability given its estimate from a random sample of observations) for both the binomial and exponential, as well as many other cases. From these distributions, upper limits for any level of confidence can, in particular, be established.

Transaction, OLO and Base Mishap Probability Inferences

NOHARM's risk estimation process that has been outlined combines the estimate and associated confidence limits for the probability of occurrence of each type of mishap in each type of action to develop inferences on the probabilities of occurrence of each type of mishap (1) per each type of transaction, (2) per OLO, and/or (3) over a period of time at a given Navy base or set of bases. Various analytical and computational procedures are available for this. They are initially considered in Reference 3; however, their discussion would be too lengthy to give here.

Data Reporting Systems

Thus, given the requisite data, the mishap probability inferences necessary for NOHARM's risk estimates can be carried out. As with all other risk management efforts, however, the data acquisition problem is a difficult one. Its resolution is planned to begin with a thoroughgoing assessment of the Navy's present ordnance-related logistics activities and mishap data reporting systems and data bases. Then directions such as the following will be taken in each data area of concern.

- Logistics Operations Reporting

A procedure now exists in the Navy for the development of ordnance logistics diagrams and associated time information, and submittal of this information to a central organization, the Naval Ammunition Production Engineering Center (NAPEC). This procedure and its underlying requirements and authorities are described in NAVSEA Instruction 5220.2 [4]. Adaptation of this procedures to the NOHARM System's requirements appears to be entirely feasible.

- Facilities Reporting

Associated with the reporting of logistics operations would be a data base on the facilities involved in, or near to the ordnance logistics operations. This would support NOHARM's recording of the locations and characteristic of munitions storage and handling facilities, and of the explosion and fire vulnerability characteristics of nearby structures. The data base would be updated whenever changes are made in any of the facilities.

- Mishaps Reporting

A mishaps reporting system to support the NOHARM System would be developed as a straightforward extension of existing procedures for Navy accident/incident reports; i.e., those associated with the Material (Property) Damage (OPNAV 5102/2), Explosive Mishap Supplement (OPNAV 5102/2E), Accidental Injury/Death (OPNAV 5102/1), and perhaps, Motor Vehicle Accident (OPNAV 5102/3) Reports.

Note that for accurate accounting of losses deriving from mishaps, procedures will need to be established to follow-up significant mishap occurrences over some time, to determine ultimate injury/fatality consequences and final dollar losses.

Initial Mishap Probability Inferences

While the above reporting systems are developed and begin to provide data, NOHARM must operate as effectively as possible with the far less well-tailored data available from existing records. It can only be noted here that this will entail the development of procedures for synthesizing past OLO's and transactions in terms of sequences of specific actions from relatively gross information on volumes of ordnance items handled. Mishap records are also inadequate except in the rare cases when damage or injuries have resulted, due almost always, however, to causes other than explosions. Thus, the mishap identification procedures noted earlier that do not depend on records will be used to define the opportunities for mishaps in the actions of the synthesized OLO's and transactions.

Various statistical procedures will then enable usable inferences of mishap occurrence probabilities (e.g., upper confidence limits, Bayesian estimates employing judgemental inputs). Due to their great rarity, the probabilities of occurrence of mishaps with explosions cannot practically be inferred in this direct way. Instead, as was outlined in Figure 1, explosive reaction probabilities will be determined conditional on the occurrence of specific mishaps. Then their total probabilities of occurrence will be the products of the mishap occurrence probabilities times the conditional probabilities of the reactions given the occurrence of the mishaps. The estimation of these conditional reaction probabilities is next discussed.

DEVELOPMENT OF CONDITIONAL EXPLOSIVE REACTION, YIELD AND SYMPATHETIC EFFECTS PROBABILITIES

Various mechanisms for initiating explosive reactions, given the occurrence of a mishap, are first noted. Then an overview is given of the various types of explosive reactions that occur. Three primary types of initiating mechanisms are next discussed in terms of the methodology (or data) available for estimating reaction probabilities. The three mechanisms are fire, impacts from drops, and fragment impacts. A brief discussion is then given of exemplary methods for estimating the probability of a sympathetic detonation of an ordnance package due to fragments from an initial explosion nearby.

Types of Reactions

Given the ignition of explosive material, the primary effects blast (shock wave) effects, thermal effects (heat), and high velocity fragments of the container of the explosive. A high-order detonation is not always obtained from the ordnance, however, particularly in the case of an accidental initiation of a reaction.

A useful, if somewhat simplistic categorization of possible reactions is given in Table 1.

Table 1. Categories of Explosive Reactions

DETONATION: MUNITION PERFORMS ESSENTIALLY IN DESIGN MODE. MAXIMUM POSSIBLE AIR SHOCK FORMED. ESEENTIALLY ALL OF CASE BROKEN INTO SMALL FRAGMENTS. BLAST AND FRAGMENT DAMAGE AT MAXIMUM.

THERMAL EXPLOSION: VIOLENT PRESSURE RUPTURE AND FRAGMENTATION OF MUNITION CASE WITH RESULTING AIR SHOCK. MOST OF METAL CASE BREAKS INTO LARGE PIECES WHICH ARE THROWN ABOUT WITH UNREACTED OR BURNING EXPLOSIVE. SOME BLAST AND FRAGMENTATION DAMAGE TO ENVIRONMENT.

DEFLAGRATION: EXPLOVIVE IN MUNITION BURNS. CASE MAY RUPTURE OR END PLATES BLOW OUT; HOWEVER, THERE IS LITTLE FRAGMENTATION OF THE CASE WITH NO FRAGMENTS THROWN OVER ABOUT 50 FEET. NO DISCERNABLE DAMAGE DUE TO BLAST OR FRAGMENTATION, BUT ONLY TO HEAT AND SMOKE OF FIRE.

BURNING REACTION: THE ORDNANCE ENERGETIC MATERIAL UNDERGOES COMBUSTION. DURING THIS REACTION, THE ENERGETIC MATERIAL ENCLOSURE MAY OPEN AND VENT; THE BURNING REACTION PRESENTS A MINIMAL HAZARD TO FIRE FIGHTING PERSONNEL.

However, gradations in these reactions can occur. For instance, a partial detonation might result when a deflagration has been accidentally initiated and a Deflagration-to-Detonation Transition (DDT) occurs. The probability of a DDT depends upon factors such as the confinement of the explosive and its porosity.

One way of treating the range of reactions this implies is shown in Figure 5. The four types of reaction defined above are assumed as distinct outcomes representative of all possible ones given that a reaction occurs. Figure 5a illustrates the conditional probabilities of a reaction of each type, given a reaction occurs. Figure 5b illustrates the equivalent yield, in terms of the blast effects produced, for each category of reaction, for some set of initiating conditions. In combination, the probabilities of alternative possible yields can be calculated in particular.

Reactions Initiated by Fire

Given exposure to fire, existing explosive materials will generally react in some manner after a few seconds of exposure to a temperature of about 200 degrees Celsius. For new ordnance being developed, tests are conducted to determine the reaction of the ordnance to an enveloping flame environment and a slow heating environment. These are known as the Fast Cook Off and Slow Cook Off tests. Results of these tests are available for many ordnance items

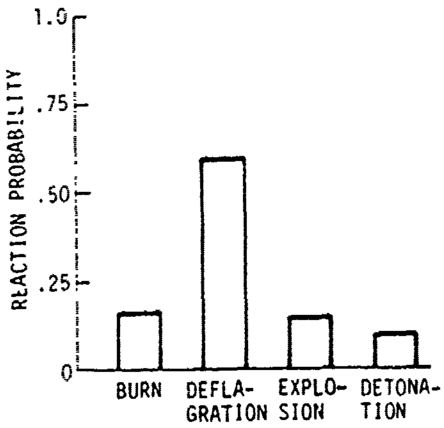

Figure 5a. Reaction Probabilities

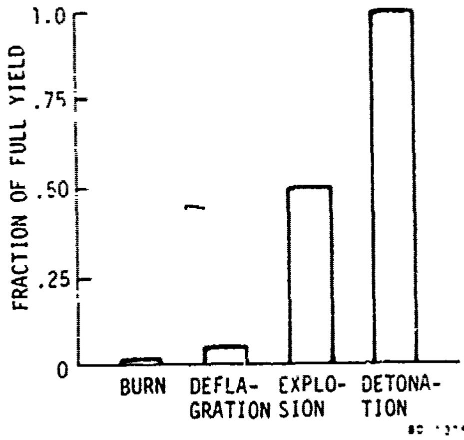

Figure 5b. Yields

currently in the inventory and are of use in estimating the time required for existing ordnance to react in the presence of fire.

For example, Fast Cook Off data are presented in [5] for 11 different types of ordnance. Results are given for the average and minimum cook off times for the ordnance; e.g., for the MK 82 bomb the average time was 180 seconds and the minimum time was 144 seconds. The number of tests needs also to be known, to enable determination of confidence limits on such values.

Reactions Initiated by Impact

A relatively more likely type of mishap is the accidental drop of ordnance items through human error or equipment failure. For realistic drop heights and most ordnance types, however, the probability of an explosive reaction is generally small.

An analysis of available drop data is presented in [5] for a total of 280 drops from heights up to 40 feet (the standard WR-50 test height). Only one reaction occurred, a deflagration for a MK 56 mine dropped 40 feet onto a studded steel plate.

If, in fact, the reaction probabilities are as low as appear to be commonly accepted by the explosives community, then testing to prove this would be prohibitively expensive. This is illustrated by a concise analysis presented in [5]. However, analytical procedures for extrapolating from limited test data are possible. As a simple example, suppose that tests have established that the average velocity required for a reaction for a bomb with transverse impact against a steel target is 350 ft/sec. Secondly, suppose that the probability of reaction follows a cumulative log-normal distribution, with velocity as the independent variable, with a standard deviation of 200 ft/second. The following table gives the reaction probabilities that then can be calculated.

Table 2. Calculated Reaction Probabilities for Impacts

IMPACT VELOCITY (FT/SEC)	REACTION PROBABILITY
20	$<10^{-6}$
50	.0003
100	.02
200	.22
300	.49
400	.70
550	.83
600	.90

The calculated number of reactions at a 50 ft/sec velocity is thus only about three reactions per ten thousand impacts (for a transverse impact against a steel target).

If a value of 900 ft/sec is used as the average velocity required for a reaction for normal impact against concrete targets, reaction probabilities would be considerably smaller and would be, in essence, vanishingly small at a 50 ft/sec impact velocity.

Reactions Initiated by Fragments

Reactions might be either accidentally or deliberately caused by bullets or accidentally caused by fragments from other exploding ordnance. Generally, fragment velocities in excess of 2000 ft/sec appear to be required to initiate detonations.

Because fragments from one item of ordnance can cause another item of ordnance to detonate sympathetically, there has been considerable research into case fragmentation and detonation of adjacent ordnance.

The estimation of the probability of occurrence of a sympathetic reaction of a receptor ordnance package due to fragments from an exploding donor package depends on the number and initial mass and velocity distribution of the donor fragments, their decelleration in flight to a final velocity distribution at the receptor (which depends on their ballistic coefficients), and the probability that one or more of them will hit the receptor. The probability distribution of the sufficiently great impacting fragments' velocities then translate into system reaction probabilities. The kinds of estimates required for these factors are next briefly noted.

Impact Velocities Required for Reactions

Empirical equations have been developed for estimation of velocities required to initiate a detonation. Factors such as geometric orientations and shaped warhead effects can be important as well as the effects of multiple fragments and combined effects such as those of fragments and hot gasses. However, detonation by a simple fragment is much better understood than detonation by multiple fragments or combined effects. The ignition of lower-order reactions has so far received little attention.

For example, the Jacobs (or Jacobs-Roslund) equations have been developed by Naval Surface Weapons Center researchers at White Oak, Maryland, to give estimates of the minimum velocities at which fragments will cause detonations of cased explosives of various thicknesses. In this equation, the case thickness and the diameter (but not the mass) of the fragment are the primary independent variables, with appropriate constants to account for the type of explosive material, fragment material, and casing material.

Initial Velocities

Estimates for the average initial velocity of fragments from the casing of detonating explosives can be obtained from the well-known Gurney formula [6,7]. This formula gives, however, only an estimate for the average velocity. A distribution of velocities about the average value can be estimated, employing test data. For example, an initial fragment velocity distribution has been inferred from the resulting pattern of debris remaining on the ground after a destruction test on a Minuteman missile [8].

Decelleration

After a fragment is propelled away from the source of the initial detonation or explosion, it is decellerated by air drag. The following figure illustrates the fragment velocity as a function of distance for an assumed value of 5 pounds per square foot for the ballistic coefficient.

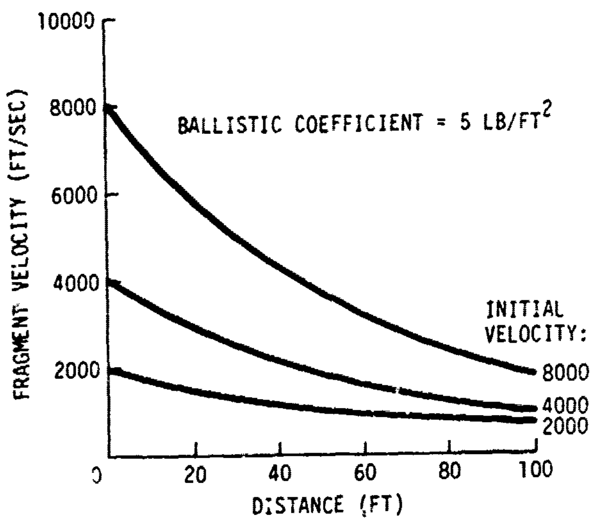

Figure 6. Variation of Initial Fragment Velocity

There can be large variations in the ballistic coefficients of different fragments [8]. Figure 7 illustrates the effects of changes in the ballistic coefficient.

Moreover, the value of the ballistic coefficient can also change in flight for a given fragment as it tumbles or burns, and its drag coefficient changes. The simplifying assumption used for calculating the curves shown above was that the specified value of ballistic coefficient applied to supersonic flight and that the subsonic drag coefficient would be one-half the supersonic value.

Hit Probability

By using appropriate probability distributions for initial fragment velocities, initial masses, and ballistic coefficient, then, the resultant distribu

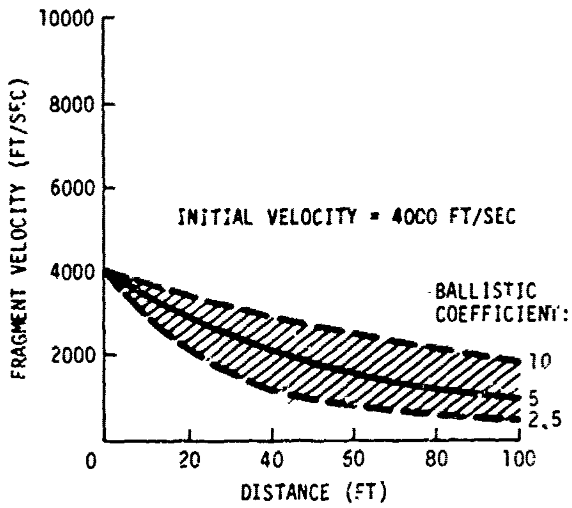

Figure 7. Variation of Ballistic Coefficient

tion of fragment velocities at any distance can be calculated. The probability of detonation (or other reaction) of an ordnance package, given that it is hit by a fragment can then be estimated. The probability that a hit occurs can be derived on the basis of simple geometric principles. For instance, at a distance R, the surface area of the sphere centered on the original detonation is $4\pi R^2$. If an ordnance package at that distance has a presented area of A, and there are N fragments uniformly spread over the sphere, then

$$N_{Hit} = \frac{N\ A}{4\pi R^2}$$

gives the expected number of hits on the ordnance package. Assuming independent effects for the fragments, then the equation

$$P_{Survive} = \left(P_{Sur/Hit}\right)^{N_{Hit}}$$

gives the overall survival probability for the ordnance package if $P_{Sur/Hit}$ is used for the single-hit survival probability.

Overall Sympathetic Reaction Probability

The final estimate for the probability of a sympathetic detonation (or, generally, other reaction) as a function of distance between the donor and receptor of the fragments is obtained by appropriately combining the probabilities of the factors that have been discussed. The character of the result is illustrated by Figure 8.

CONCLUSIONS

The NOHARM System is in concept capable of supporting the Navy's ordnance logistics safety assessments and decision making. Success in its evolutionary implementation depends critically on two areas of development: (1) mishap opportunity and occurrence data acquisition and/or synthesis by analytical

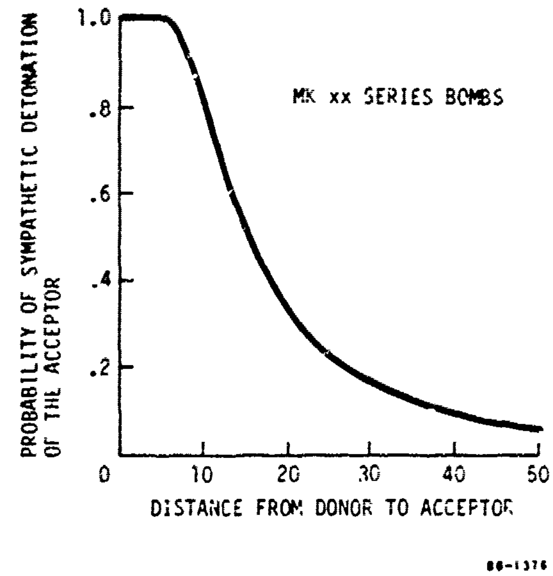

Figure 8. Example of Effect of Distance on Probability of Sympathetic Detonation

means such as have been described in this paper, in order to derive mishap occurrence probability estimates; and (2) conditional explosive reaction and yield probability estimates, primarily by analytical means but supported by well-designed test activities in areas that this paper has also attempted to illustrate.

Early actions in the first area should include:

- Establish facilities, logistics transactions and mishap reporting systems
    - Establish initial report forms/procedures
    - Critique and revise as necessary
    - Conduct tests of their application; revise as necessary
    - Establish coding and analysis techniques for developing modeling inputs from data files

- Develop procedures for deriving modeling inputs from existing OLO and mishap records (to support NOHARM processes while above reporting systems mature)
    - Synthesize number of nominal transactions from past logistics operations
    - Synthesize nominal action sequences composing transactions
        - Types
        - Time/distance durations

- Select statistical inference techniques based on assessments of initial data acquisitions, reviews and analyses

In the second area, the factors briefly noted in this paper require a significant increase in the intensity of their investigation. Three primary initiating mechanisms have been considered. One is impact such as might result from accidentally dropping ordnance. The second is fire. The third is the impact of high velocity fragments on ordnance casings.

For impacts from drops, it appears that bombs and projectiles, typically designed to safely absorb high shock levels, may have very low probabilities of reaction if dropped from heights associated with normal tidewater logistics operations. Energy levels sufficient to crack the ordnance casing appear to be required. Thinner-skinned torpedos and mines doubtlessly present more of a hazard. Estimation of reaction probabilities and yields by statistical testing alone would be extremely expensive. Substantial reliance on judgement and analysis, <u>supported</u> by test data, therefore is required.

For fires, the Fast Cook Off test data that are available, although they are not abundant, nevertheless are useful as a starting point for developing a probabilistic model of ordnance reactions due to fires.

A good deal has been done on estimating the velocities required by fragments to initiate detonations. The work has emphasized detonations rather than low-order reactions, and has emphasized deterministic rather than probabilistic methods. Nevertheless, it provides a reasonable starting place for the development of a probabilistic model.

The modeling of sympathetic explosive communication has been discussed here only in relation to detonations due to impacts from high velocity fragments. The possibilities of sympathetic communication by a spreading fire or by burning fragments also need to be addressed. For the high velocity fragments, probabilistic methods for estimating fragment masses exist. The Gurney equation can be used for a deterministic estimate of fragment velocities from detonating ordnance. Available velocity and mass data must be reviewed in order to construct statistical distributions for these variables. Similarly, variations in fragments' ballistic coefficients can significantly affect their impact velocities at longer distances and statistical distributions need to be developed for the values of these coefficients.

ACKNOWLEDGEMENTS

The author wishes to express his gratitude for the support and encouragement of W.S. Keenan of the Navy Civil Engineering Laboratory in the preparation of this paper, and for the major contributions to the explosive reactions discussion by his associate at the J.H. Wiggins Company, E. Ostermann.

GLOSSARY

<u>Ordnance Logistics Operation (OLO)</u>

The movement of a specific set of ordnance items among two or more specific locations during a specific period of time. For example, a tidewater OLO could be the offloading of a designated number of each of several kinds of ordnance items from a ship at a pier, the handling (including breaking apart and/or combining of packages of these items) and transport to rail cars of these items, and the loading of the items into the rail cars.

Transaction

The movement of one package (unit, pallet, etc.) of ordnance items from its initial to its terminal location in an OLO. A transaction is described as a definite sequence of discrete actions.

Action

The event consisting of the performance of one given function in the course of a transaction. For example, an action can be the carrying of a package with a forklift vehicle from one point on a pier to another (requiring some small amount of time), or it can be the storage (for several days) of a package, together with a quantity of other packages, in a rail car on a siding adjacent to the pier. Each action provides an opportunity for the occurrence of a mishap.

Mishap

A mishandling of an ordnance package in an action that has some possibility of leading to, or contributing to, the occurrence of an explosive reaction by an ordnance item in the package. Several different kinds of mishaps may be possible during a given action (e.g., drops of the package from different heights, the occurrence of an external fire).

REFERENCES

1. Keenan, W. A., "Analysis of Risk and Risk Mitigative Policies." Paper presented to the 18th Explosives Safety Seminar, San Antonio, Texas, September 1978.

2. Philipson, L.L., "Initial Conceptualization of an Explosives Risk-Decision Model." Prepared for the Navy Civil Engineering Laboratory. J. H. Wiggins Company, Technical Report No. 79-1364-1, 30 September 1979.

3. Philipson, L.L. and E. Ostermann, "Further Development of Ordnance Hazards Modeling Logic for NOHARM System." Prepared for the Navy Civil Engineering Laboratory. J.H. Wiggins Company, Technical Report No. 79-1375/1376, March 1980.

4. Naval Sea Systems Command, "Preparation and Use of Standard Operating Procedure (SOPS) and Guidelines Concerning Use of Standard Operating Procedure Requirements (SOPRS) for Production and Processing of Ammunition." NAVSEA Instruction 5220.2, 18 February 1976.

5. Naval Surface Weapons Center, Dahlgren Laboratory, "A Methodology for Estimating the Probability of an Explosive Accident During Navy Tidewater Logistic Sequences." Prepared for the Navy Civil Engineering Laboratory, Draft Report No. NAVSWC/DL TR-_______, October 1979.

6. Rindner, R. M., "Response of Explosives to Fragment Impact." Picatinny Arsenal. Annals of the New York Academy of Sciences, Vol. 152, October 1968.

7. Petes, J., "Blast Characteristics." Naval Surface Weapons Center. Annals of the New York Academy of Sciences, Vol. 152, October 1968.

8. Collins, J. D., et al., "Development of an Explosion Velocity Model Using Debris Impact Scatter." J.H. Wiggins Company, Technical Report No. 74-3029-1, November 1974.

PRECEDING PAGE BLANK-NOT FILMED

PRACTICAL APPLICATION OF QUANTITATIVE RISK-COST-CRITERIA TO EXPLOSIVES SAFETY

Th. Schneider
Basler & Hofmann
Consulting Engineers
Zurich, Switzerland

Abstract

In former DDESB Seminars the general ideas of a new safety concept introduced in the Swiss Military Department have been presented. This concept is based on a quantitative assessment of risks by means of a so-called risk analysis. The decisions about the necessary effort for safety are based on the marginal cost for risk reduction.

In this paper, three examples are briefly presented in which this new concept of safety assessment has been applied in practice. One example concerns an amelioration program for all large ammunition storage facilities, the second example deals with the choice of the magazine type for a specific storage facility and the third example concerns the necessary safety measures for the transportation of ammunition between a factory and its storage facilities.

The experiences and advantages of the applied methodology are briefly summarized.

Paper presented to

Nineteenth Explosives Safety Seminar, 9-11 September 1980
The Biltmore Hotel, Los Angeles, California, USA

Since we have had the opportunity to take part in the DDESB Seminar, we have tried to inform you about the concept we have introduced in the field of explosives safety within the Swiss Military Department during the last ten years.

In a paper presented at the 17th Seminar in Denver we summarized the very basic ideas of this concept. The main characteristics are the following (figure 1):

- Introduction of a quantitative risk value which is basically defined as the expected loss or damage caused by a dangerous activity. Thus, this risk value is a function of the probability and the consequences of the possible dangerous events. This expected damage or loss is regarded as a realistic measure for safety.

- Introduction of a safety assessment procedure which is subdivided into two basically different parts called risk analysis and risk appraisal. This separation is made because we think that the predominantly technical analysis of the risks should be clearly distinguished from the indispensable value judgements involved in every safety decision.

The big question which is raised by such an explicit and quantitative treatment of risks is the unavoidable question of what risks are acceptable or, in other words, "How safe is safe enough?"

In a paper presented at the 18th Seminar in San Antonio we tried to give you an idea of our approach to this decisive question. The main points of our philosophy can be summarized as follows (figure 2):

- We start from the fact that risk mitigation is basically a question of the economic effort we make for safety measures. The more money we invest, the more we can reduce a risk; in this figure you see the typical curve representing the relation between risk and expenditures for safety. In the real world, risks will never become zero and above this our limited funds will always force us to accept a certain residual risk.

- Starting from this fact and postulating what we want to attain a maximum of safety for our available resources, we have come to the conclusion that the marginal costs for risk reduction are the most reasonable criterion to decide how far we should go with our safety efforts. This means that in every system about which we decide - e.g. ammunition storage, ammunition fabrication, ammunition transportation, but also for any other hazardous activity - the tangent to the risk-cost-curve should have the same slope at the point of the chosen solution. If we speak about fatal risks to persons, these marginal safety costs have the meaning of the cost per life saved. How we have fixed the values for these marginal costs quantitatively is discussed in the above cited paper.

. Finally, a third point has to be mentioned. Society does obviously not judge all risks in the same way. In the paper an approach how to distinguish different risk categories by specific psycho-social factors is presented. For the different risk categories, different values of the safety criterion are being applied.

It has to be mentioned that this marginal cost criterion does not cover the problem of safety criteria entirely. The expected damage or loss is only one aspect of a hazardous event. Quite another aspect is the individual risk of each single person involved. This individual risk has to be controlled independently from the expected loss. For several, mainly practical reasons this aspect shall not be covered in this paper. I may mention that for rare events it is usually of secondary importance.

The two papers mentioned so far could be regarded as rather theoretical. Therefore, I would like to show you now in this paper how we have applied this safety concept in real problems and what has been our experience with it so far.

In the following, three examples are briefly presented. All three examples concern explosion hazards but are, nevertheless, quite different. As the time for this presentation is very limited, I would like to show you just roughly what the problem was and how the above mentioned methodology has been applied.

Example number one concerns the system of our large underground ammunition storage facilities. These facilities differ significantly from each other concerning age, layout, site conditions, environment, etc. With the existing regulations, it became more and more difficult to manage this system in a reasonable and somehow consistant way. In the last years a study has been performed which should assess the actual risk this system represents, define the necessary improvements, give priorities for these improvements and show which level of safety should reasonably be provided. The first step of this study consisted therefore in a risk analysis of all existing facilities. This resulted in a diagram as shown in figure 3, in which the risk values for each single storage facility are plotted in decreasing order. Of course, the actual number is much bigger than shown in this figure. It may be specially interesting to know that the largest and smallest risk value differed by several orders of magnitude.

The sum of all these risk values represented the total risk R_E of this system to the public in our country at that time. Thus, this risk R_E was the starting point for our amelioration program. In the next step, all possible safety measures which could reduce the risk have been studied for each specific facility and their risk reduction and costs have been evaluated. In this context, all reasonable structural or other technical measures, but also organizational measures have been considered. The applicacable measures have been plotted in decreasing order of their risk reduction/cost-ratio in a risk-cost-diagram starting at the point of the existing risk R_E. The curve we get by doing this is an objective basis showing us what degree of safety is attainable in dependance of the money we are willing to invest in our program. Here comes now the question how far we should go with our effort! This question is easy to answer if we apply the marginal cost criterion I have mentioned above. Where the line with the respective slope touches this curve, we have our solution.

I cannot go into details in this brief presentation, although it is quite clear that there are many interesting questions when we look at the details. I may mention that this amelioration program is now being successfully implemented. Especially where civilian administrations have to be involved in this program, its clear concept shows to be helpful in any discussion about the expediency of this program.

Example number two concerns the decision which type of structure should be chosen for a specific storage facility which had to be built in our country.

In Switzerland, we basically use four types of storages magazines: aboveground box type concrete magazines, earth covered magazines, buried magazines and underground magazines in rock. For the latter we have the possibility to make use of different special safety measures which reduce and even almost eliminate the dangerous effects of an accidental explosion on the surroundings. I would like to mention specially the so-called selfclosing block-system which is actually a huge explosion valve which has been developped in an international European cooperation.

As the risk for the surroundings is decreasing and the costs are increasing for these different solutions, we are confronted with a decision amongst competing objectives. In the specific case we are discussing here, aboveground magazines were not accepted because they would impair the scenery of the very special landscape of this site in an untolerable way. The decision concerning the remaining magazine types was again based on a systematic comparison of risks and costs. The application of the same marginal cost criterion showed quite clearly which solution for this specific problem is consistant with our general safety philosophy.

The last example is maybe the most interesting because, in this case, it would have been especially difficult to make an assessment based on the usual type of regulation. It concerns the regular transport between an ammunition factory and its storage facilities for explosive materials. In this specific case a main road had to be crossed. This crossing was regarded as a specially risky point of the system and an underpass had been proposed to avoid this risk. As this solution would have produced costs of approximately 5 Mio $, doubts rose whether this project was really reasonable. The main question was: How can you show in a rational way whether this underpass is necessary or not or what alternative measures are more reasonable? At least in Switzerland, no regulation would really help you to answer this question. Up to now, this kind of decision is made in a quite arbitrary way.

The analysis performed in this case revealed several interesting facts:

- It could be shown that the crossing represents only 50 % of the risk of the entire transport system. Thus, by eliminating it, the risk could at maximum be reduced by a factor 2.

- In contrast to this, much simpler measures which are effective throughout the whole transport system and not only at one of its points are much more efficient for the risk reduction.
- By analysing all the different critical events (more than 100 different events have been investigated quantitatively step by step) the risk showed to be concentrated on a few very specific situations. The detailed analysis and specification of these situations, including the critical explosives involved, allowed to propose very tailor-made measures, whose effectiveness is extremely high.

The result of this analysis could again be presented in a risk-cost-diagram. For reasons of simplification, I have not put all investigated measures in this diagram. Important measures have been: the efficient marking of the vehicles, more effective fire-fighting equipment and, especially, more effective safety training for the personnel involved.

Taking again the same marginal cost criterion, it could be shown that these cheap measures would reduce the risk to an extent that further measures are not justified any more. That the underpass was out of discussion is not necessary to point out.

It might be mentioned that in this specific case representatives of the concerned community and state, thus persons not belonging to the defence administration, have been involved in the decision making. It has been a very positive experience, how this kind of methodology brought a good discipline in the discussion and gave everybody a chance to understand the background of the decision.

This leads me already to the conclusions of this presentation which should summarize the most important experiences we have made so far:

The first conclusion is, of course, that these ideas and procedures are actually applicable in reality. The three cases mentioned here are by the way not the only examples. Actually, we are trying to look at all decisions of this type in exactly the same way. Of course, the degree of sophistication of the analysis can vary considerably from case to case.

Our experience has further shown that this methodology brings us a big step forward in the direction of rationality and transparency and gives us a much better view over the actually decisive facts of a problem than we usually had so far. Furthermore, we see clearly what the technical experts' task should be and where their competence ends - that is at the point at which we have to decide which effort we are willing to make for safety.

Another experience is that a generally accepted, clearly defined and uniform methodology simplifies the communication between the different parties involved. Especially if such a methodology is orientated to real facts rather than to formal rules and regulations everybody is able to contribute to the problem solving and, therefore, is much more motivated to give a positive contribution.

Finally, this approach has brought the possibility of comparing quite different situations because it is not tailor-made for any specific problem. Furthermore, the marginal cost criterion brings by itself a consistancy for safety decisions which lies on a quite high level and, therefore, leads away from isolated problem solving. I may mention that we have applied this same approach and the same criteria also in quite other fields of safety as e.g. road accidents.

Many other advantages could be discussed, especially if we would go into more details. However, the only way to get a real feeling about whether these ideas are helpful or not is by trying to apply them oneself.

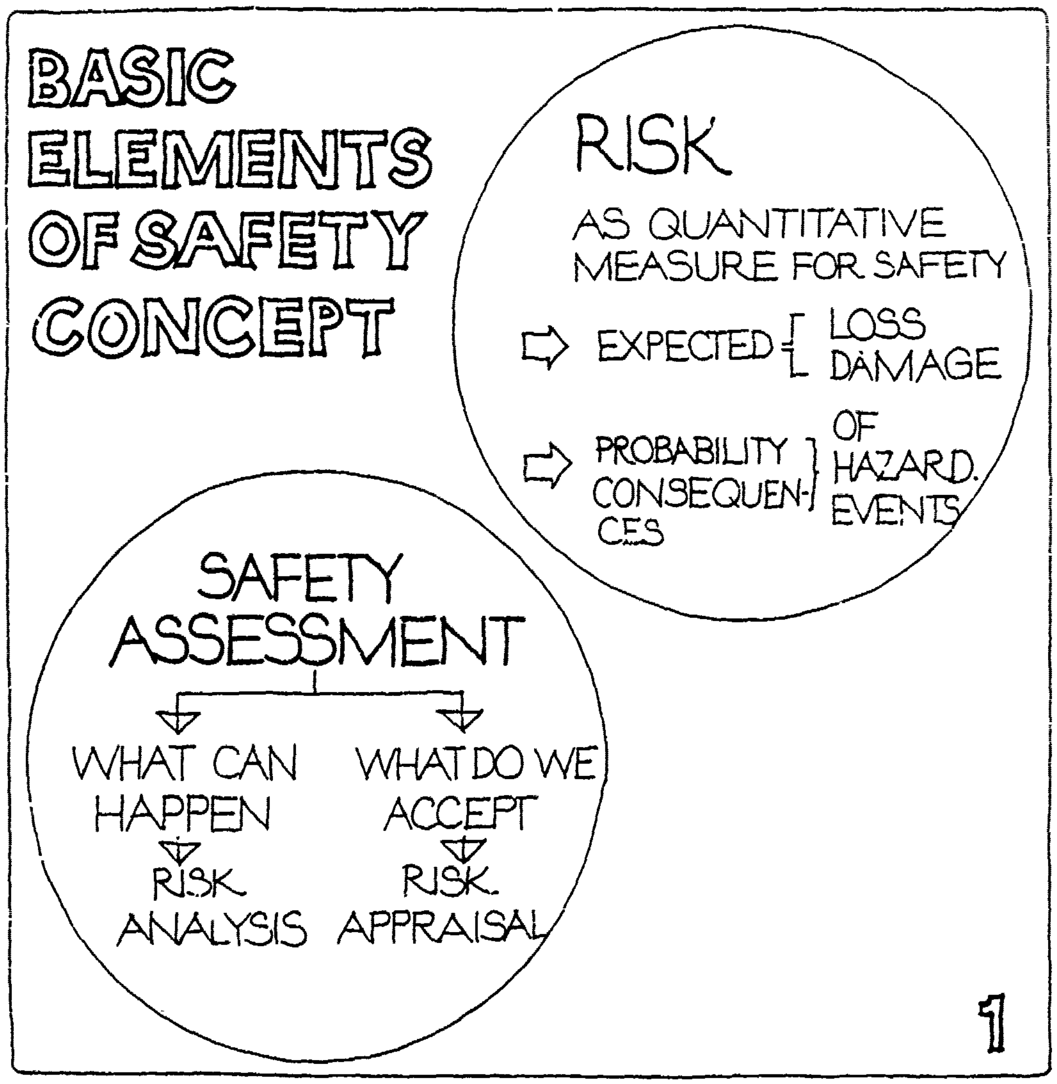
BASIC ELEMENTS OF SAFETY CONCEPT
RISK
AS QUANTITATIVE MEASURE FOR SAFETY
EXPECTED LOSS DAMAGE
PROBABILITY CONSEQUENCES OF HAZARD. EVENTS
SAFETY ASSESSMENT
WHAT CAN HAPPEN
RISK ANALYSIS
WHAT DO WE ACCEPT
RISK APPRAISAL
1

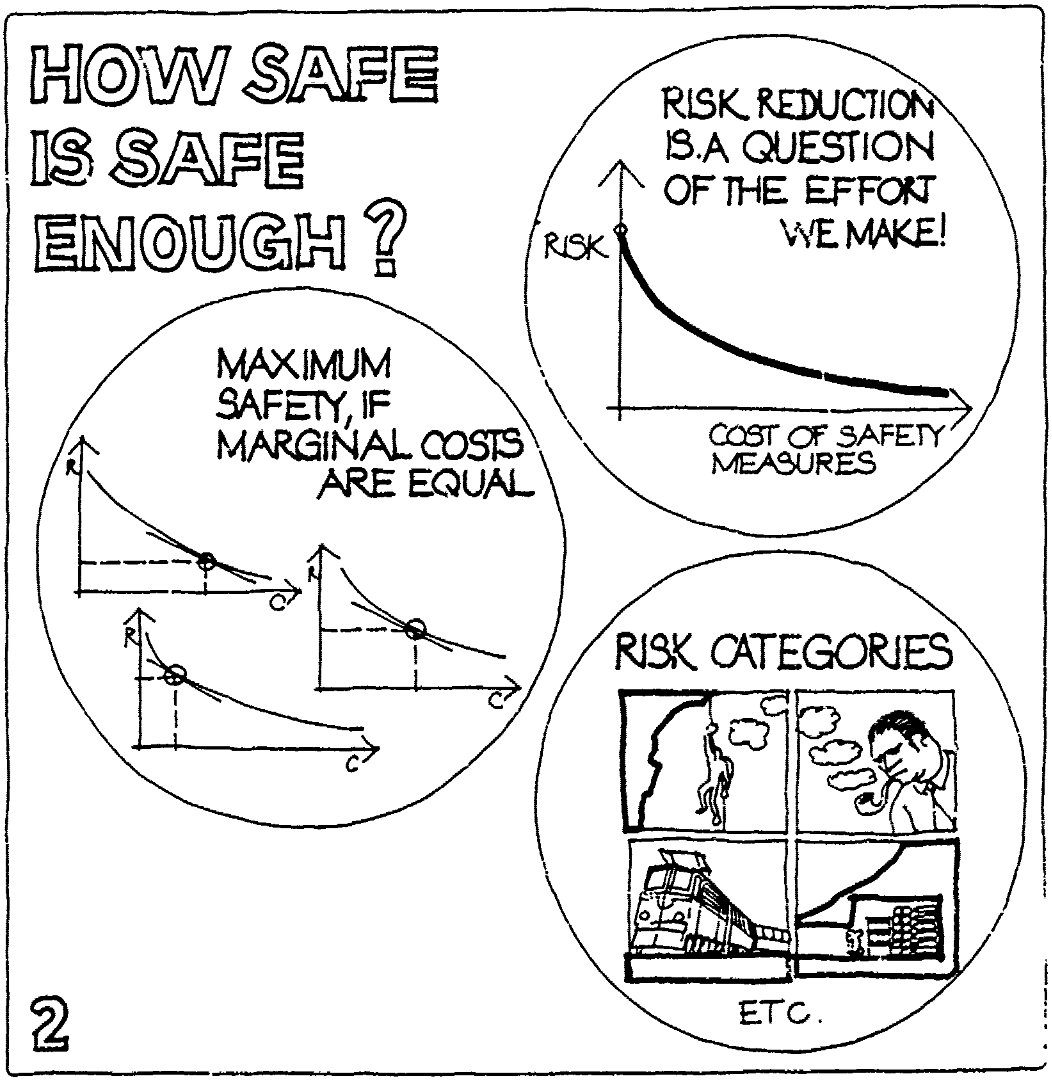
HOW SAFE
IS SAFE
ENOUGH ?
RISK REDUCTION
IS A QUESTION
OF THE EFFORT
WE MAKE!
RISK
COST OF SAFETY
MEASURES
MAXIMUM
SAFETY, IF
MARGINAL COSTS
ARE EQUAL
R
C
RISK CATEGORIES
ETC.
2

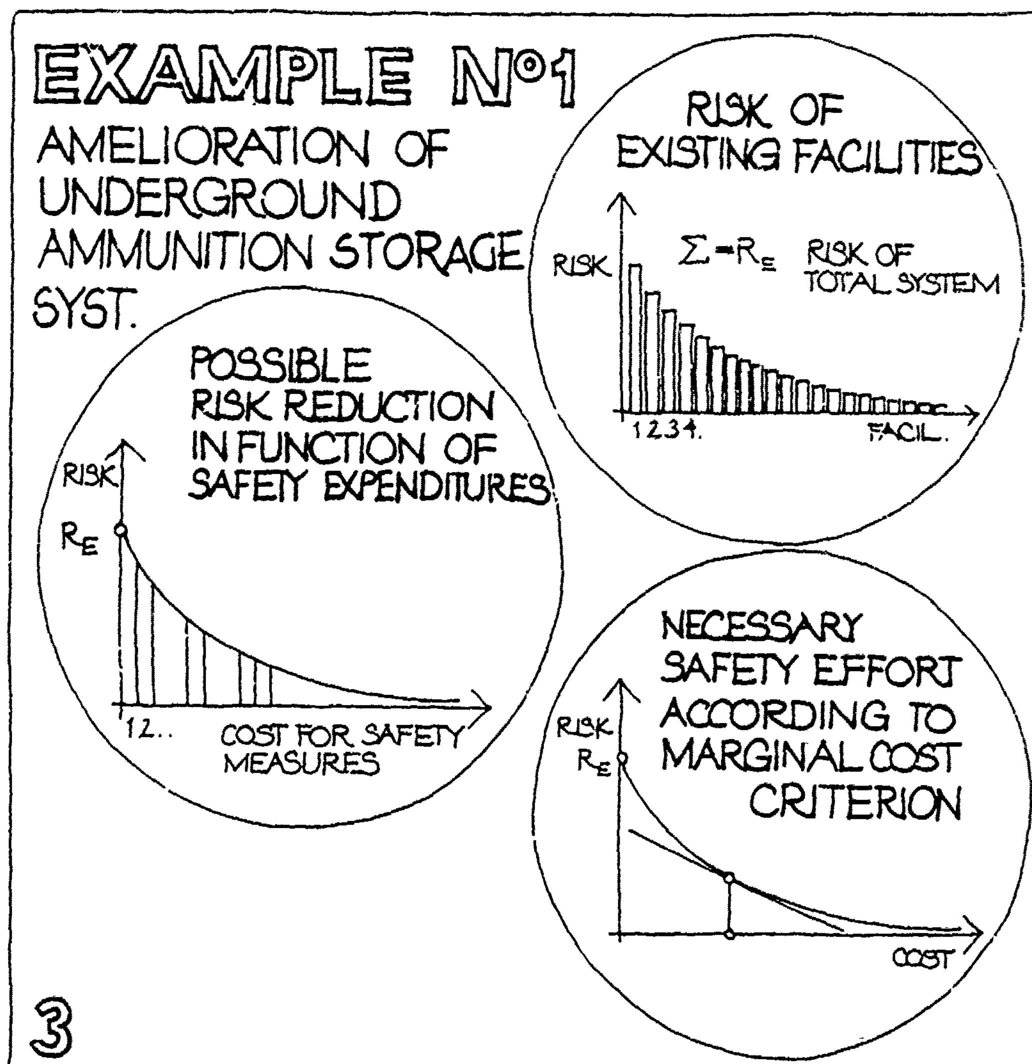
EXAMPLE N°1
AMELIORATION OF UNDERGROUND AMMUNITION STORAGE SYST.
RISK OF EXISTING FACILITIES
RISK
Σ = R_E RISK OF TOTAL SYSTEM
1 2 3 4.
FACIL.
POSSIBLE RISK REDUCTION IN FUNCTION OF SAFETY EXPENDITURES
RISK
R_E
1 2 . .
COST FOR SAFETY MEASURES
NECESSARY SAFETY EFFORT ACCORDING TO MARGINAL COST CRITERION
RISK
R_E
COST
3

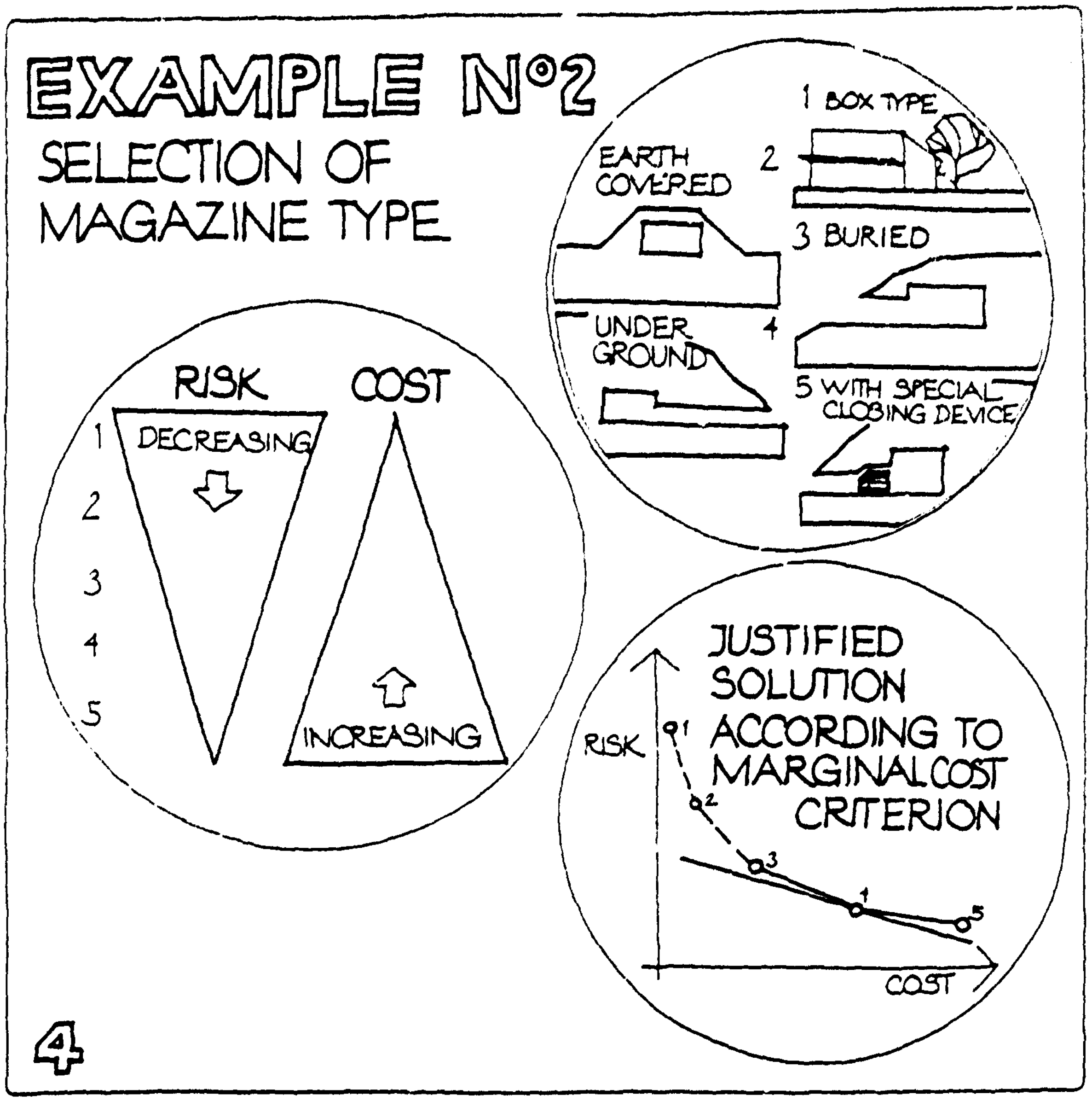
EXAMPLE N°2
SELECTION OF MAGAZINE TYPE
1 BOX TYPE
2 EARTH COVERED
3 BURIED
4 UNDER GROUND
5 WITH SPECIAL CLOSING DEVICE
RISK
COST
DECREASING
INCREASING
1
2
3
4
5
JUSTIFIED SOLUTION ACCORDING TO MARGINAL COST CRITERION
RISK
COST
4

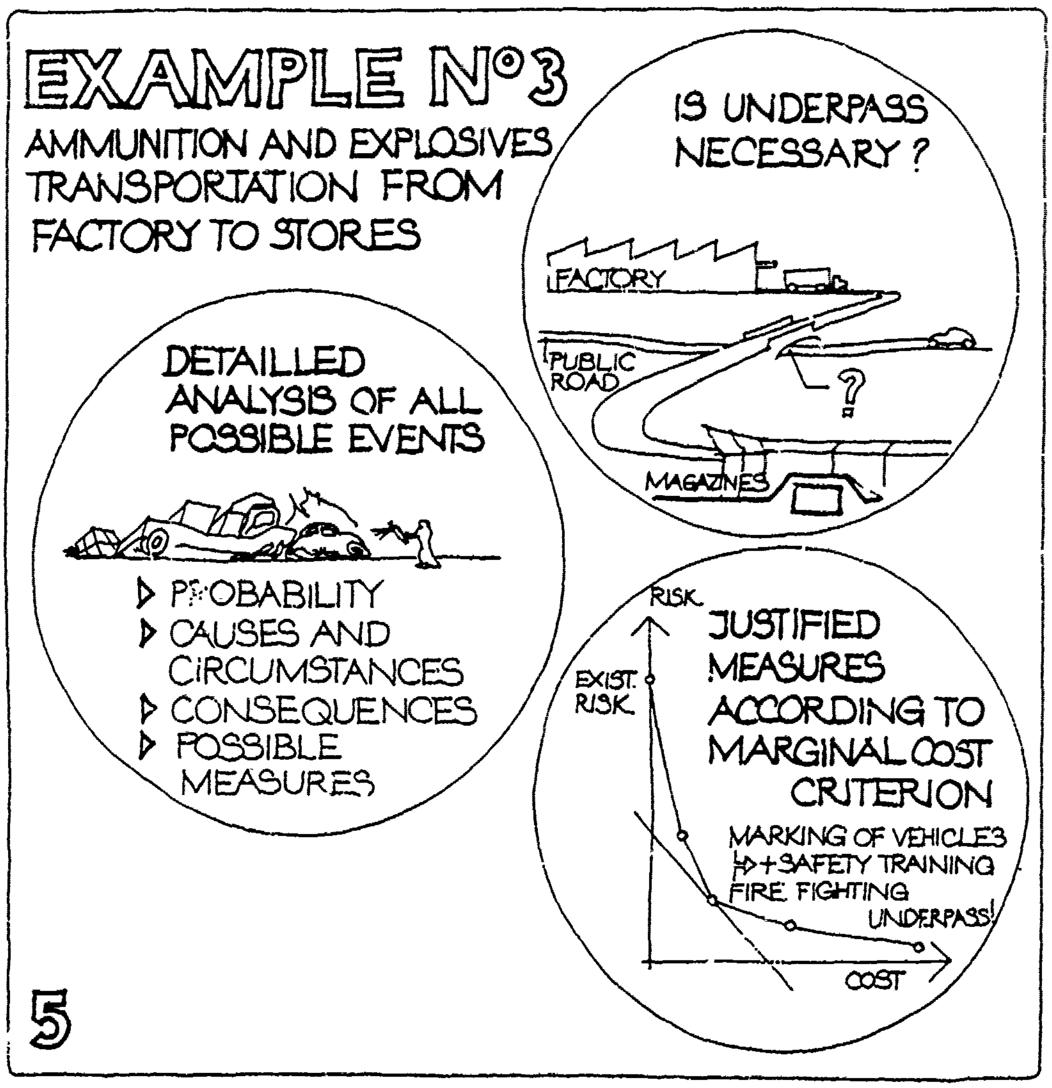
EXAMPLE N°3
AMMUNITION AND EXPLOSIVES TRANSPORTATION FROM FACTORY TO STORES
IS UNDERPASS NECESSARY ?
FACTORY
PUBLIC ROAD
?
MAGAZINES
DETAILLED ANALYSIS OF ALL POSSIBLE EVENTS
PROBABILITY
CAUSES AND CIRCUMSTANCES
CONSEQUENCES
POSSIBLE MEASURES
RISK
JUSTIFIED MEASURES ACCORDING TO MARGINAL COST CRITERION
EXIST. RISK
MARKING OF VEHICLES
+SAFETY TRAINING
FIRE FIGHTING
UNDERPASS!
COST
5

CONCLUSIONS

- APPLICABLE IN REAL PROBLEMS
- IMPROVEMENT OF RATIONALITY AND TRANSPARENCY
- IMPROVEMENT OF COMMUNI-CATION AND PARTICIPATION
- CONSISTENCY ON HIGHER LEVEL

6

PRECEDING PAGE BLANK-NOT FILMED

ESKIMO VI MODEL TESTS

Charles N. Kingery

Ballistic Research Laboratory
Aberdeen Proving Ground
Maryland, 21005

ABSTRACT

This paper will be a summary of the results obtained from a series of high explosive tests using 1/50th scaled donor and acceptor models of a three-bay storage magazine. The work is reported in "Eskimo VI Model Tests", C. Kingery, ARBRL-TR-02215, January 1980.

A 1.27 kg charge was used to simulate 158760 kg stored in a full-size magazine. In this paper emphasis will be placed on effect of headwall materials and charge configuration on the blast propagation from the 1/50th scaled donor model.

I. OBJECTIVE

The objective of this project was to determine through the use of 1/50th scaled donor and acceptor models the blast loading to be expected on the Smokeless Powder/Projectile, Type II-B Munition Storage Magazine.

II. TEST PROCEDURE

The test procedures required to meet the stated objective were first, to design and construct the models; second, design the explosive source; and third, select the instrumentation system.

A. Model Magazine Design

The design and construction of the donor and acceptor models are described in the following sections.

1. The Donor Model. The donor model was a 1/50th scale of the full size magazine. A sketch is shown in Figure 1. The dimensions associated with the letters in Figure 1 are presented in Table I.

Table I. Dimensions of Full-Size Structure and Donor Model

	Full-Size Feet	Full-Size Metres	1/50 Scale Metres
a*	95.0	28.96	0.579
b*	50.0	15.24	0.305
c*	13.0	3.96	0.079
d*	15.2	4.63	0.093
e	25.0	7.62	0.152
f	97.0	29.57	0.591
g	3.8	1.16	0.023
h	44.0	13.41	0.268
i	77.0	23.47	0.469
j	19.4	5.91	0.118
k	1.5	0.46	0.009
l	1.0	0.30	0.006
m	121.0	36.88	0.737
n	52.0	15.85	0.317

*Interior Dimensions

The model material was 0.006 m (1/4 inch) masonite. A portion of the headwall was cut and hinged to allow insertion of the charge after the earth cover was installed. The material for the hinged portion was varied to determine the sensitivity of the blast propagation to headwall material.

A scaled reinforced concrete slab was constructed and used for the roof of the donor magazine.

2. The Acceptor Models. There were three 1/50th scale, non-responding acceptor models constructed of cast concrete. The gage mounts and cable conduits were mounted in a wooden mould. The scaled size of the full scale structure included the earth cover. A photograph of the acceptor model R and the donor model in-place is shown in Figure 2.

B. The Test Charge

A 158760 kg (350000 lbm) explosive source was designated as the full size charge mass to be considered as stored in a type II-B magazine. When scaled by 1/50 the charge should be 1.27 kg (2.80 lbm). To represent munition stored in a large floor area magazine the charge was configured in the shape of an H with the detonator hole at the center of the crossbar. The charge dimensions and shape are shown in Figure 3.

C. Test Instrumentation

The test instrumentation consisted, (1) PCB Electronics, Inc. Models 113A22, 24, and 28 with quartz sensing elements and built-in source followers, and (2) a Honeywell 7600 tape recorder having a frequency response of 80 kHz.

D. Test Layout

The locations of the acceptor models with respect to the donor model are shown in Figure 4. The safe separation distance for structures to the front and rear of the donor is $0.8Q^{1/3}$ while the side to side distance is $0.5Q^{1/3}$, where Q is the mass of the explosive in kilograms. The locations of the gages on the structures are also shown in Figure 4.

E. Test Matrix

Three test firings were planned for this project but it became obvious after three shots there was a requirement for further testing because of the sensitivity of the blast propagating from the front of the donor to the confinement of the headwall. A description of the tests are described below.

Shot 1 - The headwall of the donor was hinged and lightly taped. The roof of donor model was a scaled reinforced concrete slab. Model R was inadvertently placed at a separation distance of 0.666 m, instead of 0.866 m.

Shot 2 - The headwall of the donor was heavely taped because of the excessive overpressures recorded on Model F. The donor roof was again a concrete slab and Model R separation distance was corrected to 0.866 m.

Shot 3 - The headwall consisted of two layers of 1/4 inch masonite. Other donor parameters were held constant.

Shot 4 - Two changes were made on this shot. A plaster board material was used for the roof of the donor and a 1/4 inch glass headwall was inserted in place of the masonite.

Shot 5 - This shot had a concrete roof and headwall with a slight modification of the charge configuration. The uprights of the "H" were 20.62 cm and the crossbar was 12.61 cm. The charge weight remained the same.

Shot 6 - The roof and headwall were the same as Shot 5 and the charge configuration was the same as Shots 1, 2, 3, and 4, as shown in Figure 3.

III. RESULTS

The results will be presented in the form of tables listing the peak overpressure and impulse recorded at each gage station for each shot. Graphs showing the variation of these two parameters versus headwall material will also be presented.

A. Peak Overpressure at Gage Stations on Models F, S, and R

The values of peak overpressure recorded at gage stations on the three acceptor models are listed in Table II. When a gage recorded two significant shocks both values are listed in the table with a "/" to separate them.

1. Peak Overpressure on Model F. The values of peak overpressure listed in Table II for gage stations F-1, F-2, F-4, and F-6, (along the centerline of the model), for shots 2, 3, 4, and 6 are plotted in Figure 5. It can be seen in this figure that the blast loading on the slope as recorded at gage station F-1 is quite high and is very sensitive to the headwall conditions. In Figure 5 through Figure 10 the symbol SM means single masonite, DM means double masonite, G means glass, and C stands for concrete. The values range from 4598 kPa for the single masonite headwall down to 2551 kPa for the glass headwall. The glass

Table II. Peak Overpressure at Gauge Station Locations on Models F, S, and R

Gauge Station Location	Distance From GZ m	Shot Number 1	2	3	4	5	6	SHOT $\frac{1+2+6}{3}$
		Peak Overpressure P_s						
		kPa	kPa	kPa	kPa	kPa	kPa	kPa
F - 1	0.890	---	4598	3123	2551	2977	4257	4428
F - 2	1.103	2385	1893	1411	880	1164	1795	2024
F - 3	1.116	1579	2061	1439	591	1209	1356	1665
F - 4	1.182	1758	1645	1055	912	1120	1432	1611
F - 5	1.194	1897	1729	1298	682	1249	1746	1791
F - 6	1.261	1694	1563	895	1001	670	1307	1521
F - 7	1.272	1351	1469	1129	727	1047	1189	1336
S - 1	0.698	1945	1522	1102	1404	1008	1374	1613
S - 2	0.931	790	647	521	677	570	455	630
S - 3	0.949	453	484	508	400	593	408	448
S - 4	1.128	557	427	421	473	491	308	431
S - 6	1.143	471	391	328	347	391	362	408
S - 7	1.325	364	309	285	313	353	234	302
								$\frac{2+6}{2}$
FF - 1	1.180	---	475	388	374	405	414	444
R - 1	0.964	421/691	277/499	290/544	388/784	408/730	247/478	262/488
R - 2	1.024	1175/961	867/791	607/944	1334/1201	1330	672	774/732
R - 3	1.024	593/819	378/776	338/872	470/1281	1192	331/608	354/692
R - 4	1.024	830/807	440/743	410/677	516/1230	767/1063	400/633	420/688
R - 5	1.043	1248/1000	1090/813	952/807	1222/1087	971	595/777	842/795
R - 6	1.182	288	201	238	366	299	213	207

Notes: Shot 1. Front Headwall Free Hinge - Concrete Roof - Structure R Separation Distance 0.666 m.

was approximately the same density as concrete but was much stronger and caused greater blast suppression to the front.

Along the centerline of the roof of Model F the peak overpressure decays as the shock front moves away from the explosive source on shots 2, 3, and 6, while the glass headwall shot 4 shows a slight increase in peak overpressure.

2. Peak Overpressures on Model S. The peak overpressures along the centerline of Model S are presented in Figure 6. Here the trend is mixed and the type of headwall appears to have only a small effect on the blast attenuation to the side of the structure. The double masonite headwall used on Shot 3 has the greatest attenuating effect at gage station S-1 on the slope.

3. Peak Overpressure on Model R. The peak overpressure recorded at three selected stations on Model R, as presented in Figure 7, show a logical trend. The stronger the headwall, the higher the pressure propagated to the rear. With the strong glass headwall the peak overpressure is higher at R-1, R-2, and R-6. Only the first peak is listed at gage position R-1.

B. Overpressure Impulse at Gage Stations on Models F, S, and R

The values of overpressure impulse obtained from the gage stations on Models F, S, and R are listed in Table III.

1. Overpressure Impulse on Model F. The overpressure impulse does not follow the same trend in blast attenuation as established from the peak overpressure. At gage station F-1, as shown in Figure 7, the single masonite headwall recorded the highest impulse while the double masonite headwall was the lowest. Along the centerline of Model F the overpressure impulse on all shots is higher at station F-6 than at station F-2. The glass headwall has the lowest values at stations F-2, F-4, and F-6.

2. Overpressure Impulse on Model S. The values of overpressure impulse listed in Table III for gage stations S-1, S-2, S-4, and S-7 are plotted in Figure 9. Here again the impulse does not show the same trend as the peak overpressure attenuations although the concrete headwall gave lower values of both peak overpressure and overpressure impulse on the roof of Model S. It is interesting to note that the impulse for all shots is higher at gage station S-4 than at S-2 or S-7.

3. Overpressure Impulse on Model R. The values from only three gage stations R-1, R-2, and R-6 were plotted in Figure 10. Here the peak overpressure and overpressure show the same trend. That is, the glass headwall produces higher values on Model R and the concrete headwall produces the lower values.

Table III. Overpressure Impulse at Gauge Station Location on Models F, S, and R

Gauge Station Location	Distance From GZ m	Shot Number 1	2	3	4	5	6	SHOT $\frac{1+2+6}{3}$
		Overpressure Impulse, I						
		kPa-ms	kPa-ms	kPa-ms	kPa-ms	kPa-ms	kPa-ms	kPa-ms
F - 1	0.890	---	510	399	421	---	---	---
F - 2	1.105	233	183	190	121	162	164	193
F - 3	1.116	191	184	182	84	---	104	160
F - 4	1.182	261	220	223	108	147	174	218
F - 5	1.194	293	278	249	94	156	162	244
F - 6	1.261	305	230	222	159	141	183	239
F - 7	1.272	294	195	189	90	115	145	211
S - 1	0.698	208	169	153	179	152	142	173
S - 2	0.931	118	104	99	96	76	60	94
S - 3	0.949	129	114	114	83	77	56	100
S - 4	1.128	127	136	113	117	94	77	113
S - 6	1.143	138	130	117	124	79	70	113
S - 7	1.325	102	89	80	91	90	77	89
								$\frac{2+6}{2}$
FF - 1	1.180	---	110	106	109	98	105	108
R - 1	0.964	184	177	184	220	208	169	173
R - 2	0.024	266	245	239	310	291	185	215
R - 3	1.024	235	223	223	282	267	174	198
R - 4	1.024	282	203	196	258	263	161	182
R - 5	1.043	255	230	229	280	249	197	214
R - 6	1.182	107	91	92	108	91	90	91

C. Effect of Charge Configuration

The donor model roof and headwall were the same on shots 5 and 6. The difference in the two shots was in the configuration of the charge. The dimensions and configuration of the charge for all shots except shot 5 are shown in Figure 3. On shot 5 the uprights of the H were 20.62 cm and the crossbar was 12.61 cm. The two charge configurations are shown in Figure 11. The charge weights remained the same (1.27 kg). The small difference in the charge configuration produced large differences in the blast propagation to the front, side, and rear of the Models.

1. Peak Overpressure and Impulse on Model F. The same gage positions will be compared as in the proceding figures where the effect of headwall material was presented. The values of peak overpressure and impulse measured on Model F from shots 5 and 6 and listed in Tables I and II are plotted versus distance in Figure 12. Both peak overpressure and overpressure impulse were lower on shot 5 than shot 6 at all gage stations.

2. Peak Overpressure and Impulse on Model S. The peak overpressure and impulse listed in Tables I and II for shots 5 and 6 on Model S are plotted in Figure 13. The peak overpressure and impulse recorded from shot 5 are higher than shot 6 at all gage locations with the exception of S-1. Here the peak overpressure is higher on shot 6 than on shot 5.

3. Peak Overpressure and Impulse on Model R. There were four gage locations in the headwall of Model R located to the rear of the donor. Only one gage station (R-5) has been used in the headwall comparisons and therefore the same location will be used in this comparison. In Figure 14 it can be seen that both the peak overpressure and impulse recorded on shot 5 are greater than recorded on hot 6. From Tables I and II it should be noted that both peak overpressure and impulse are also greater at gage stations R-2, R-3, and R-4 on shot 5 than shot 6.

IV. PREDICTIONS FOR ESKIMO VI

The blast loading predictions for ESKIMO VI structure will be treated separately because it is planned to be a one-half scale of the full size structure. All linear dimensions of the full size structure must be divided by 2 and the charge weight must be divided by 2^3 or 8. Therefore the charge weight should be 19844 kg. In order to scale the model results to the ESKIMO VI condition, all linear distances and time must follow the following scaling technique.

$$\frac{R_{1/2S}}{(Q_{1/2S})^{1/3}} = \frac{R_m}{(Q_m)^{1/3}} \quad \text{then} \quad R_{1/2S} = R_m \left(\frac{W_{1/2S}}{Q_m}\right)^{1/3}$$

and $R_{1/2S} = R_m \left(\frac{19844}{1.27}\right)^{1/3}$, $R_{1/2S} = R_m\ (25)$

where $R_{1/2S}$ = distances for 1/2 scale structure

R_m = distance for model

$Q_{1/2S}$ = charge weight for 1/2 scale test

Q_m = charge weight for model test

Assuming standard sea level conditions, model distances, arrival time, impulse and duration must be multiplied by 25 to predict the ESKIMO VI blast parameters. The volume of the ESKIMO VI structure should be the full-scale volume $1895.6m^3$ divided by 8 or $237m^3$.

Predictions of the blast parameters for the ESKIMO VI test are given in Table IV for pentolite at standard sea level conditions. These values should be corrected for temperature and altitude of the test site as well as any differences in the explosive charge effectiveness.

IV. CONCLUSIONS

Two factors that may effect the blast parameters propagating from a scaled model donor magazine are the headwall material and the charge configuration.

From the results of the test firings it appears that a strong or heavy headwall will (1) cause some attenuation of peak overpressure to the front of the donor, (2) cause some enhancement of peak overpressures to the side of the structure and to the rear of the structure when compared with the weaker headwalls.

For most of the gage positions these same conclusions can be drawn for the overpressure impulse.

On shot 6 where the uprights of the H were longer than shot 5 it appears that (1) the peak overpressure to the front is greater but (2) the peak overpressures to the side and to the rear are lower than recorded on shot 5.

The overpressure impulse follows the same trend as noted for the overpressure.

Table IV. Predictions for ESKIMO VI

Station Number	Distance From GZ	Arrival Time	Peak Overpressure		Overpressure Duration	Overpressure Impulse	
	m	ms	kPa	psi	ms	kPa-ms	psi-ms
F - 1	22.25	8.62	4428	642	---	---	---
F - 2	27.56	11.50	2024	294	17.75	4825	700
F - 3	27.90	12.25	1665	242	11.75	4000	580
F - 4	29.55	13.00	1611	234	22.00	5450	790
F - 5	29.85	14.10	1791	260	30.25	6100	885
F - 6	31.52	14.45	1521	221	27.25	5975	867
F - 7	31.80	15.30	1336	194	27.50	5275	765
S - 1	17.45	14.90	1613	234	15.50	4325	627
S - 2	23.28	20.52	630	91	26.50	2350	341
S - 3	23.72	20.50	448	65	19.50	2500	362
S - 4	28.20	27.12	431	62	31.50	2825	410
S - 6	28.58	28.22	408	59	21.50	2825	410
S - 7	33.13	34.35	302	44	25.25	2225	323
FF - 1	29.50	32 08	444	64	30.50	2700	392
R - 1	24.10	31.88	262/488	38/71	22.75	4325	627
R - 2	25.60	33.12	774/732	112/106	17.25	5375	780
R - 3	25.60	32.80	354/692	56/100	18.00	4950	718
R - 4	25.60	31.98	420/688	61/100	17.00	4550	660
R - 5	26.08	35.52	842/795	122/115	18.50	5350	776
R - 6	29.55	38.88	207	30	26.25	2275	330

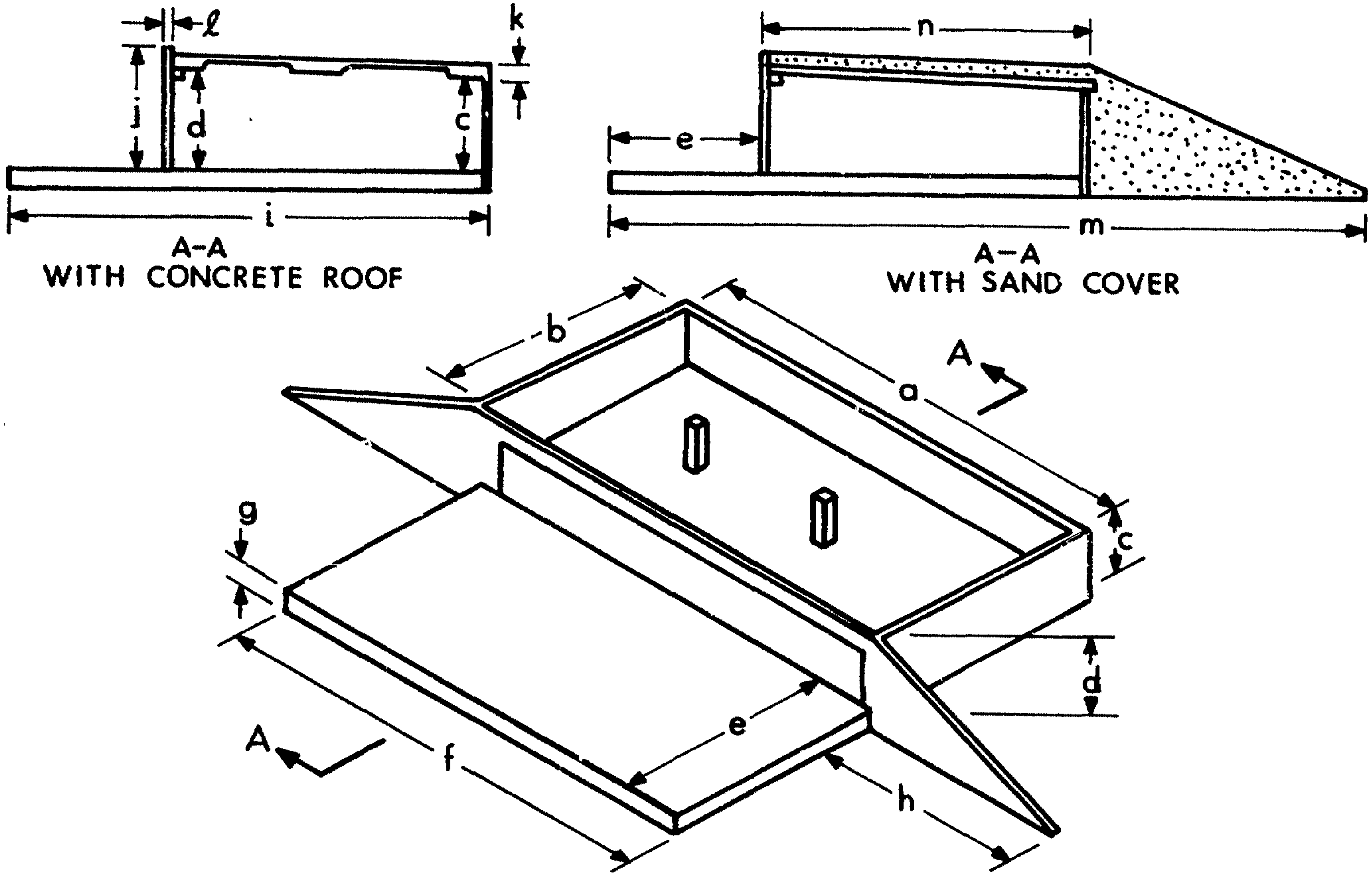

Figure 1. Sketch of the 1/50th scale donor model.

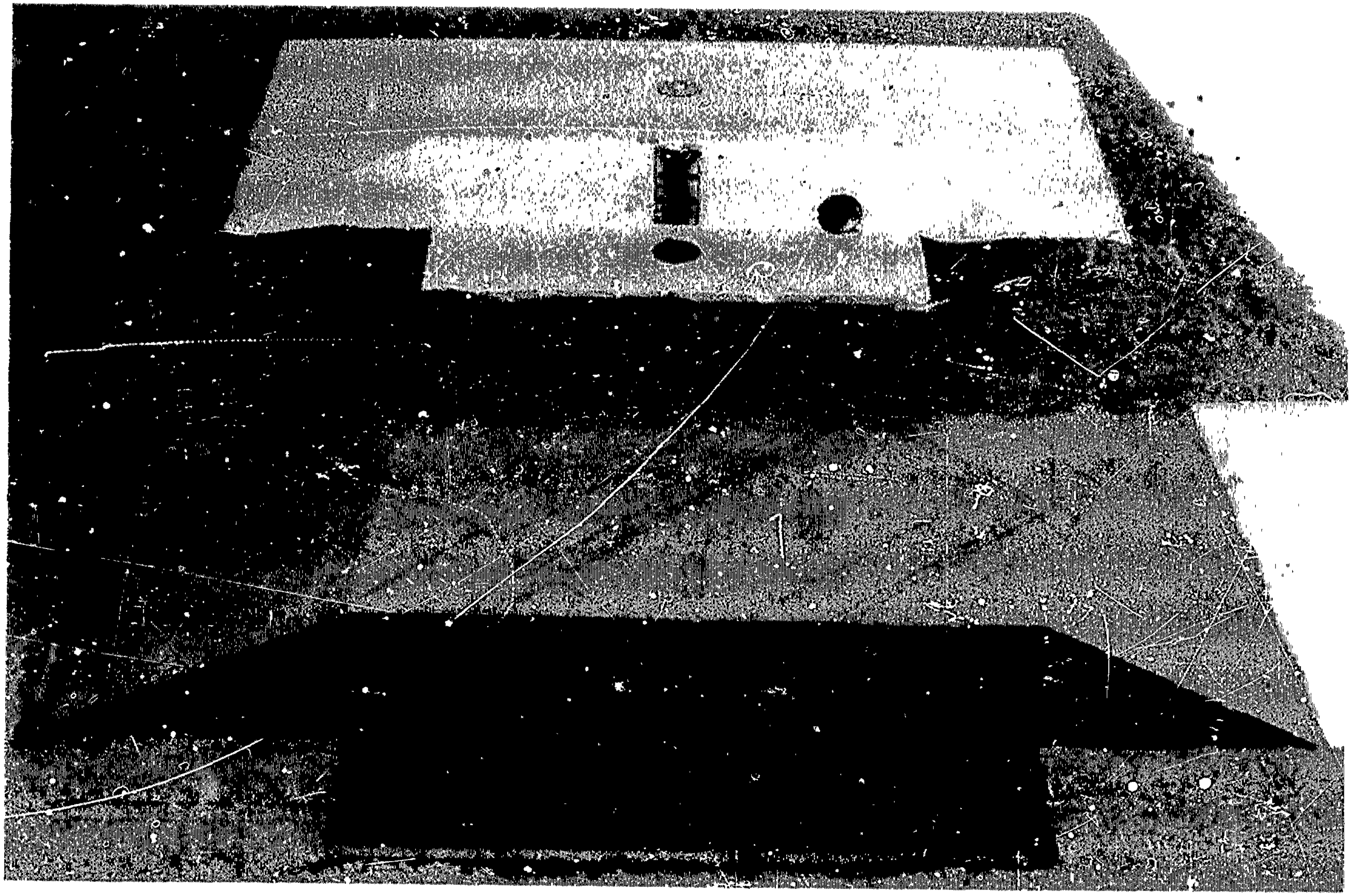

Figure 2. Photograph of donor model and acceptor model R implace.

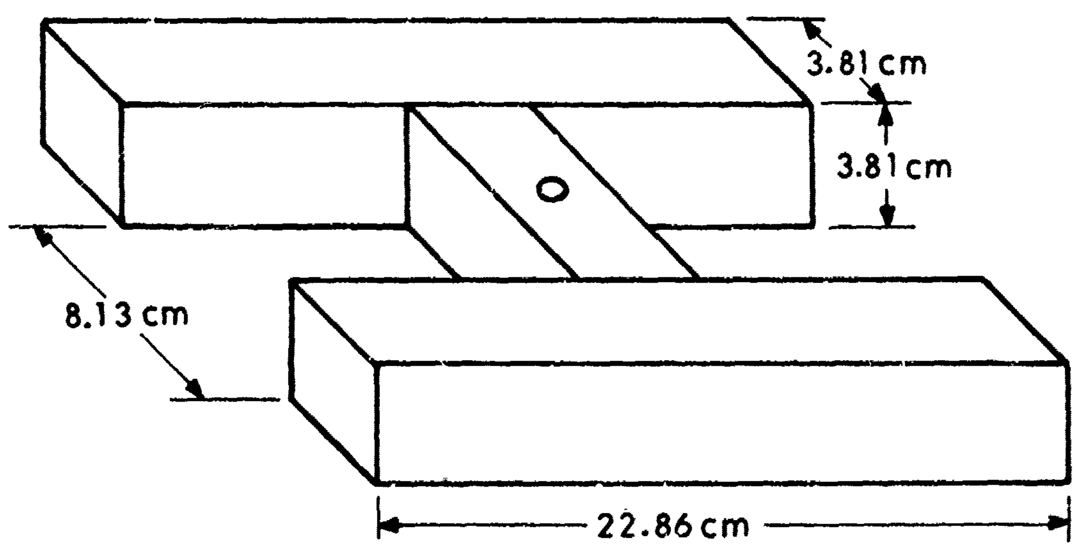

Figure 3. Charge configuration and dimensions.

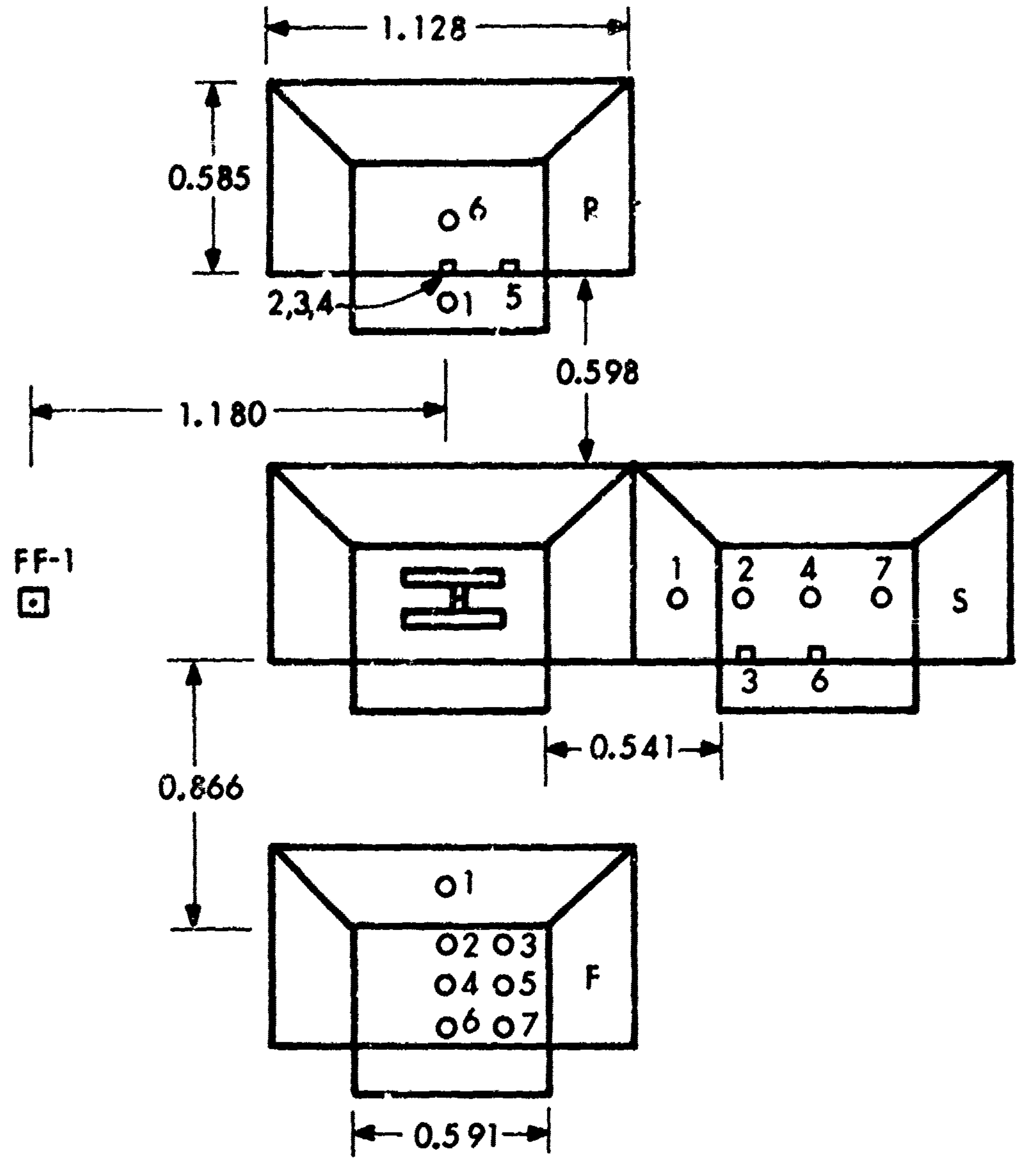

Figure 4. Test layout.

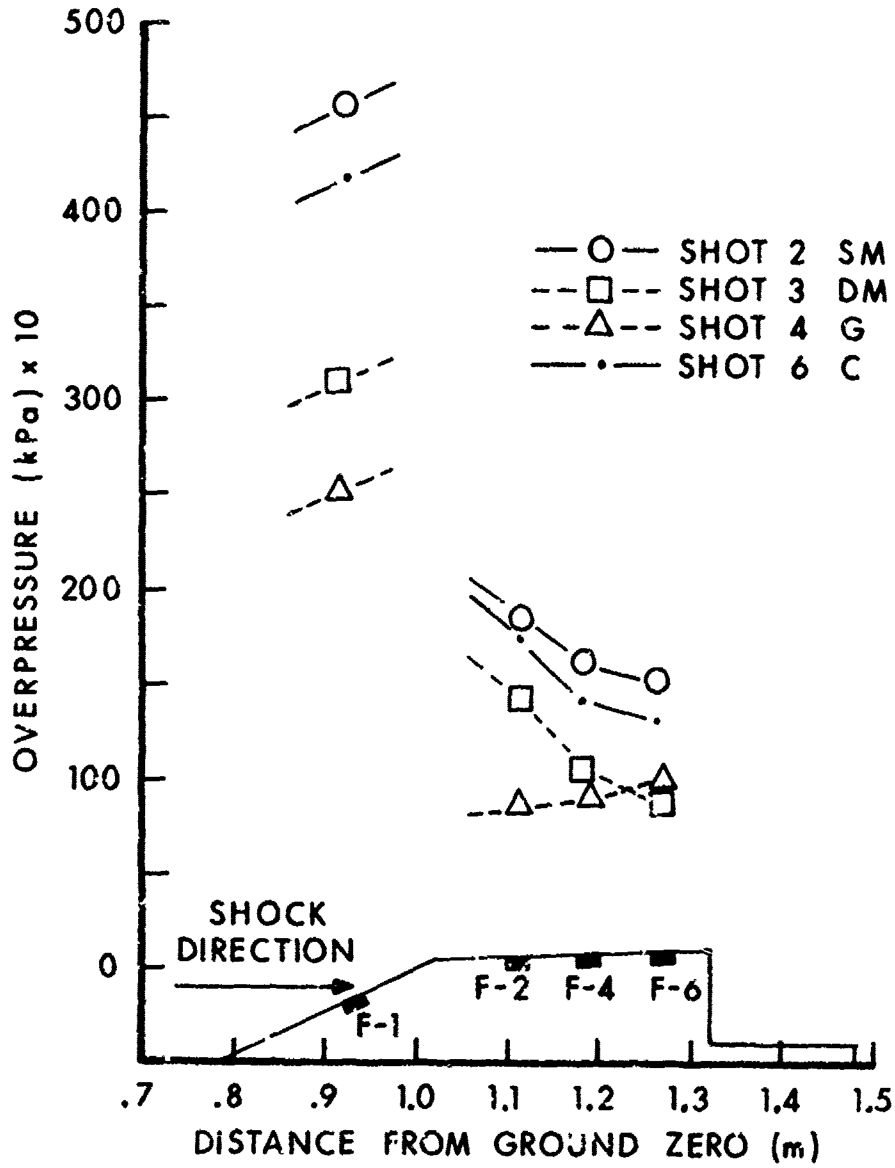

Figure 5. Peak overpressure versus distance on Model F.

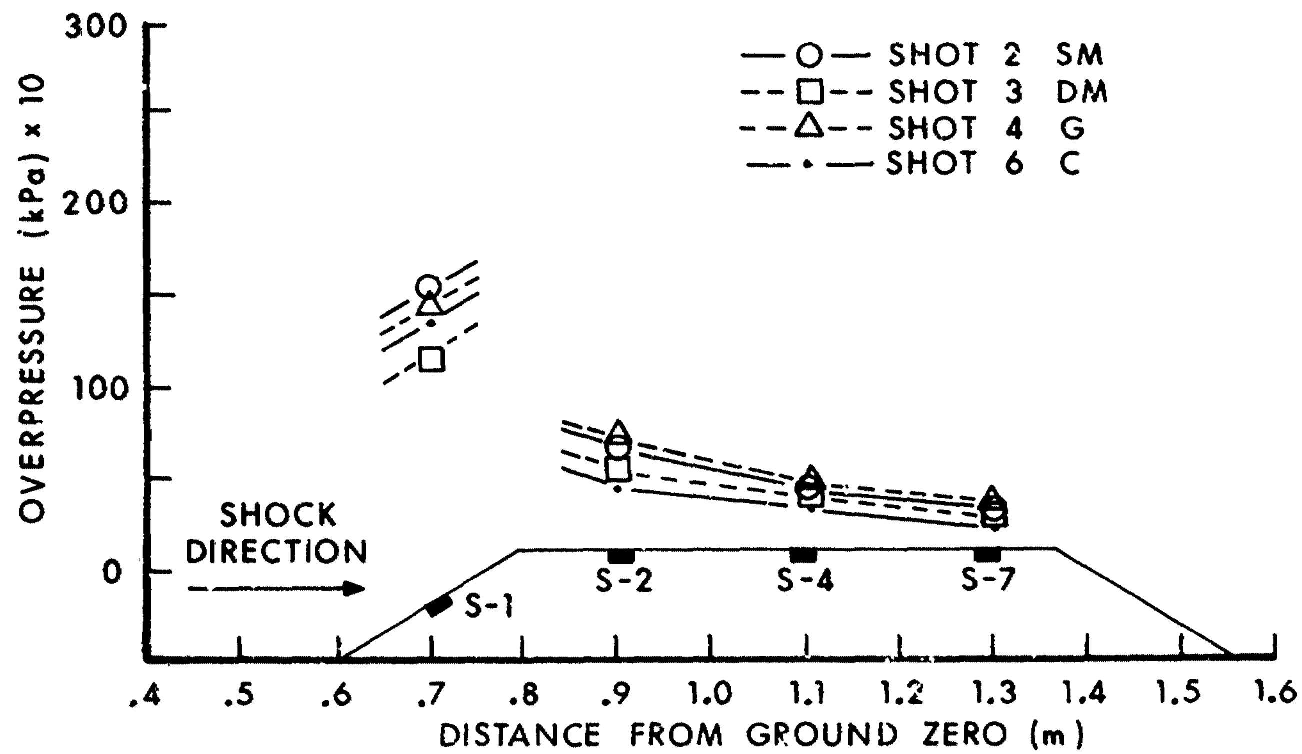

Figure 6. Peak overpressure versus distance on Model S.

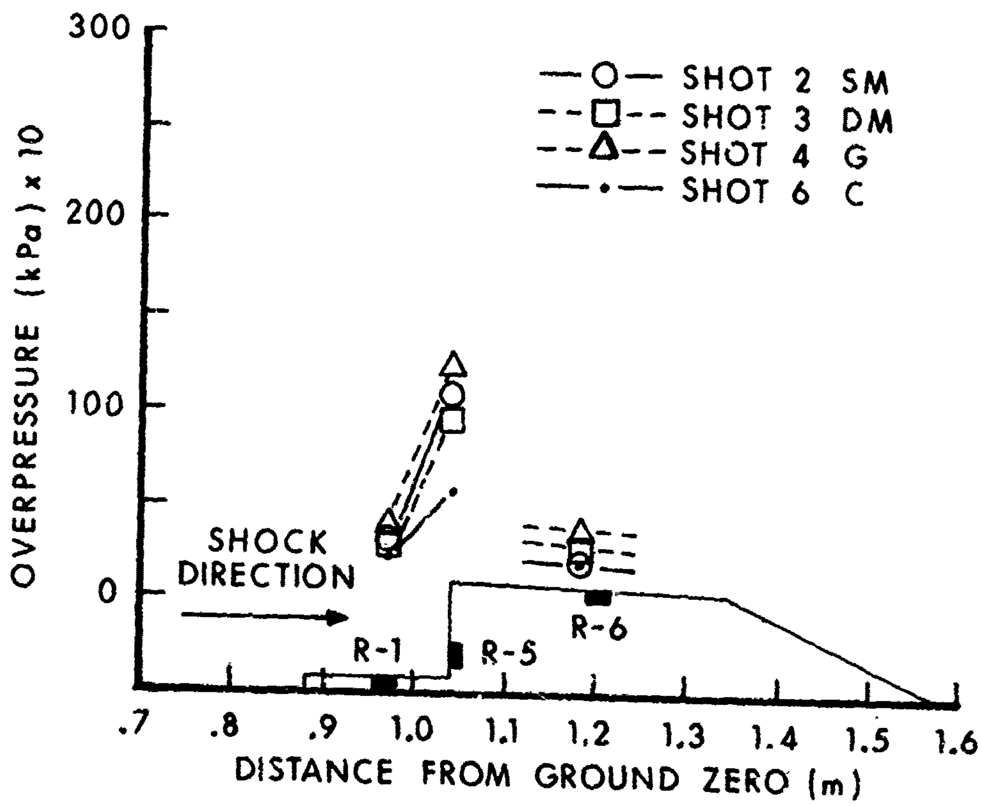

Figure 7. Peak overpressure versus distance on Model R.

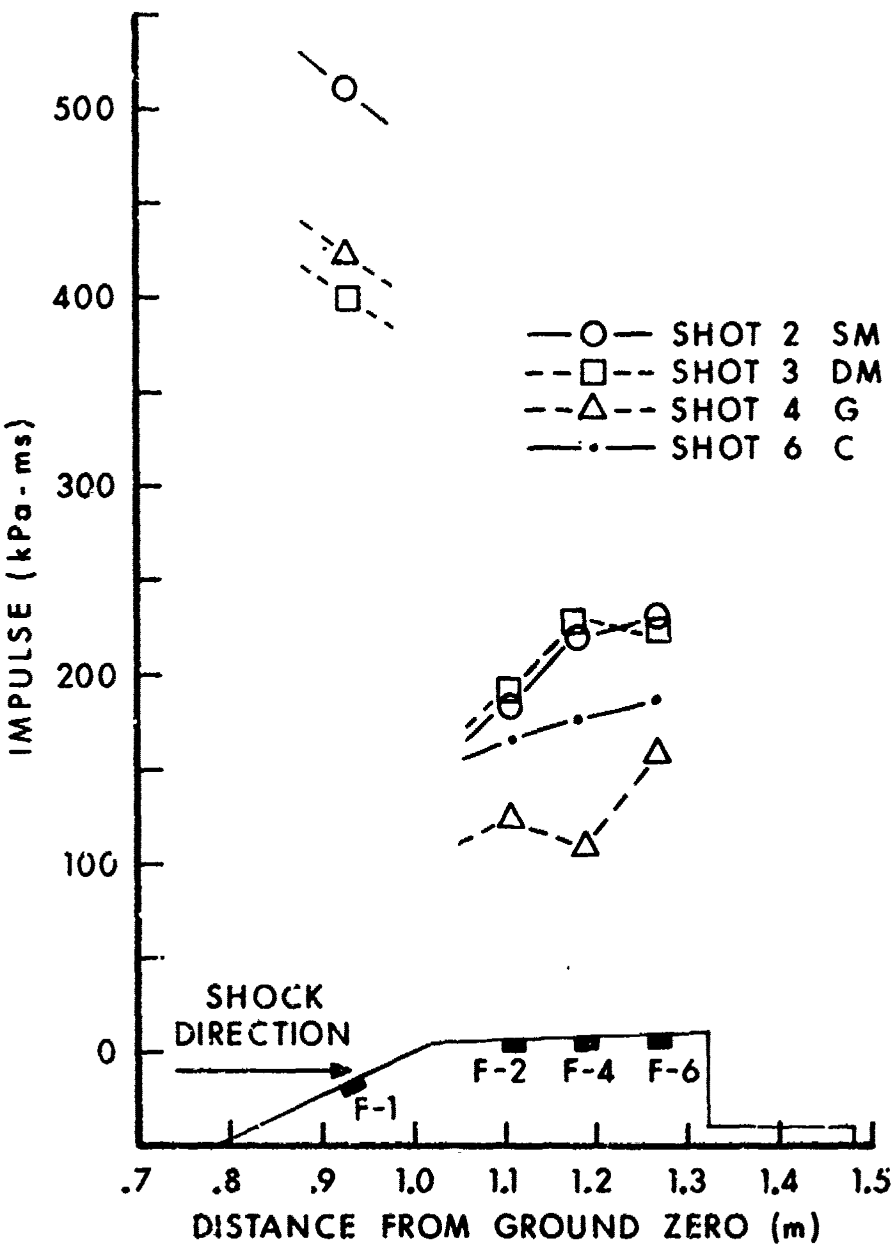

Figure 8. Overpressure impulse versus distance on Model F.

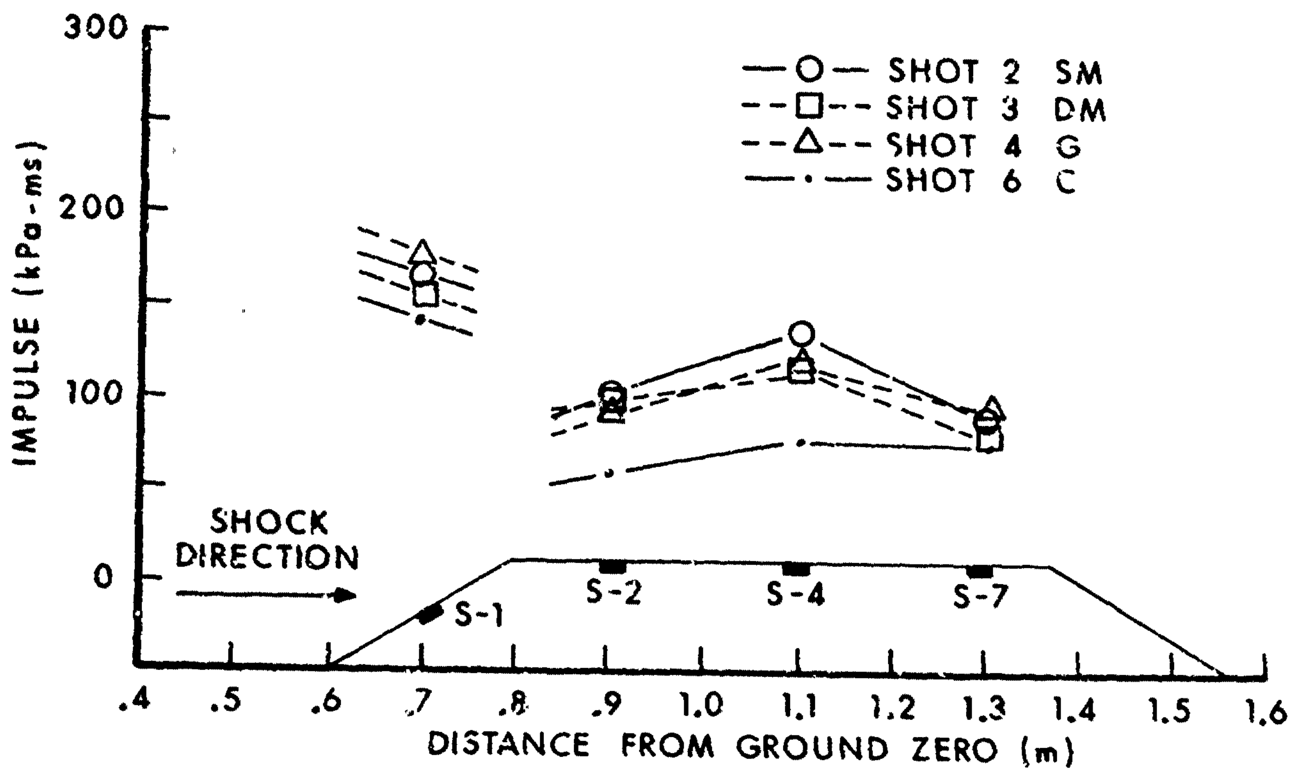

Figure 9. Overpressure impulse versus distance on Model S.

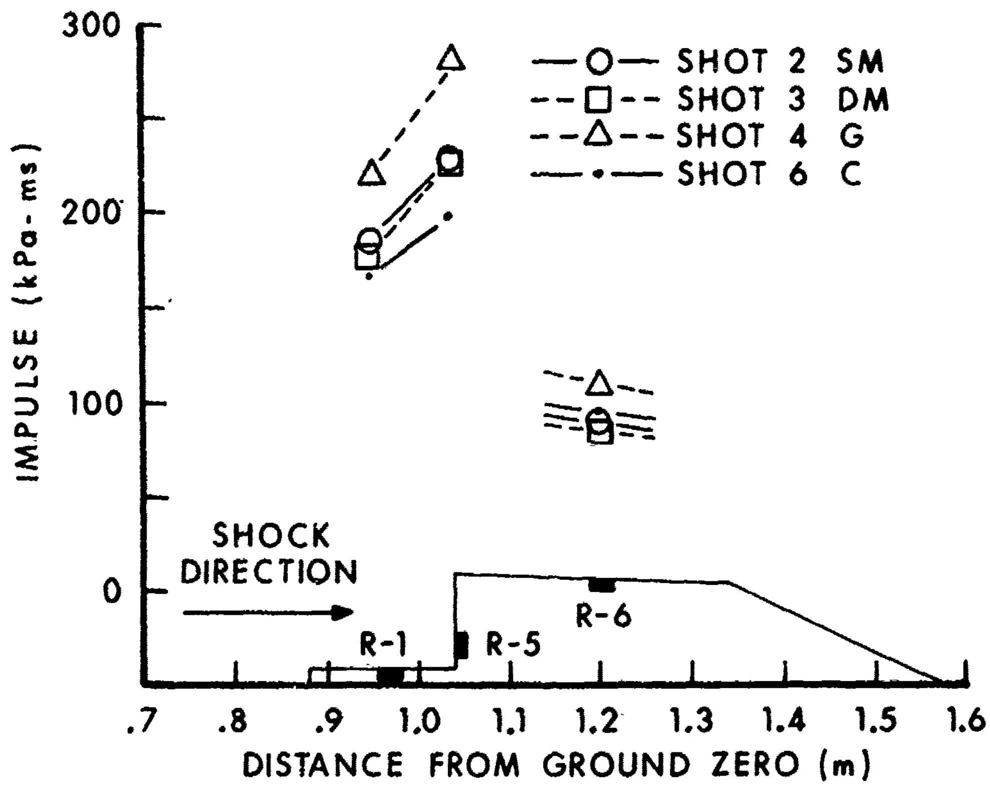

Figure 10. Overpressure impulse versus distance on Model R.

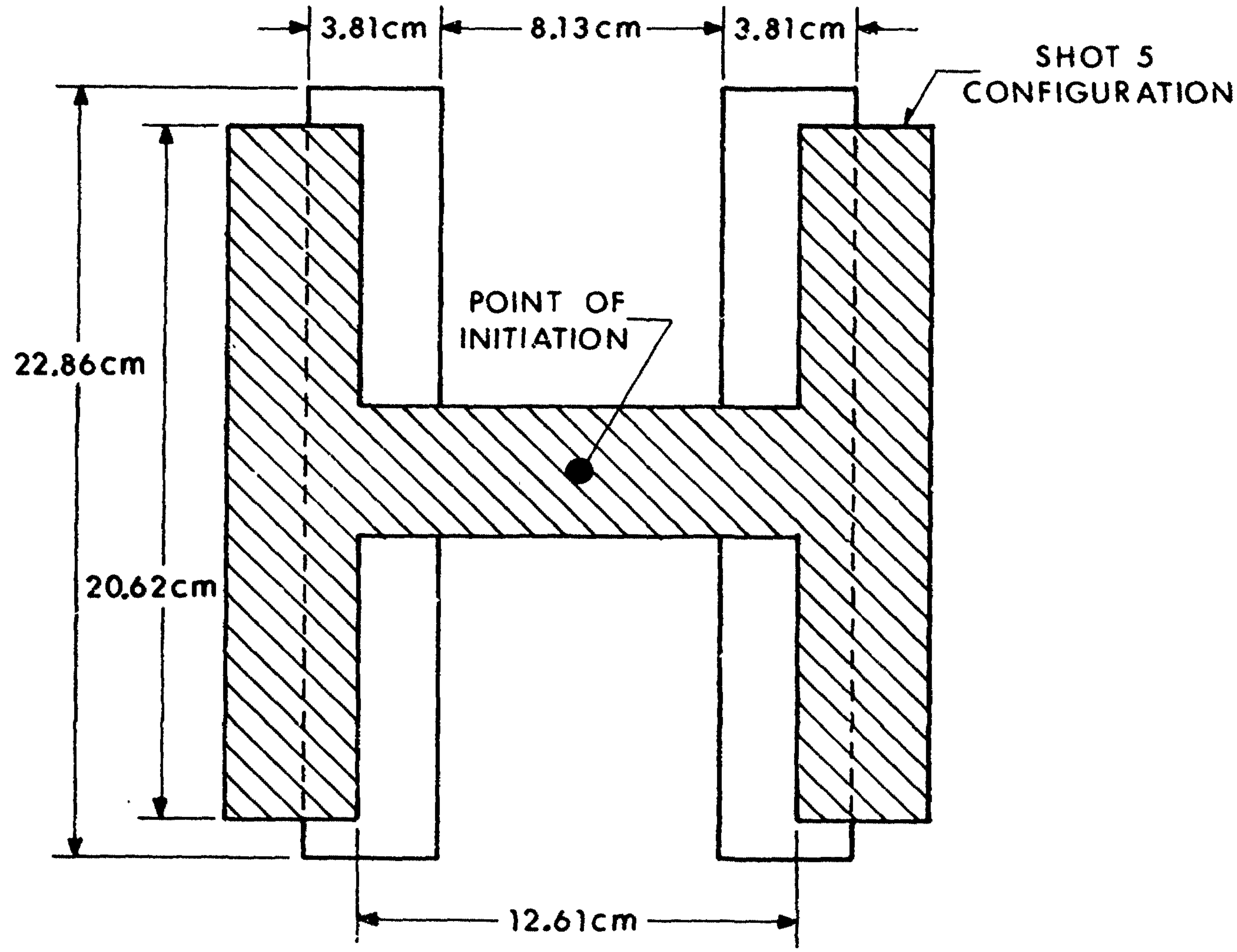

Figure 11. The two charge configurations.

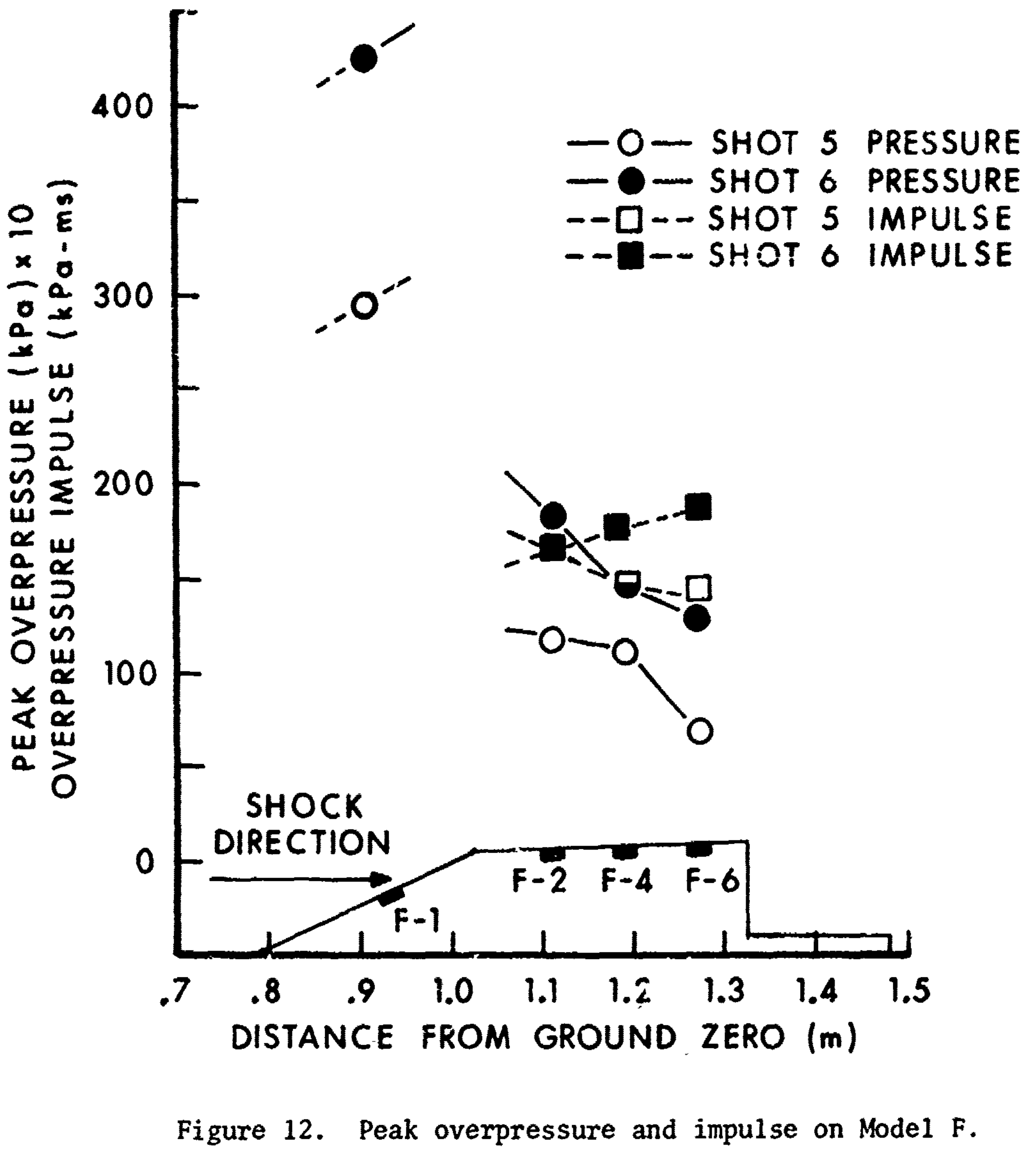

Figure 12. Peak overpressure and impulse on Model F.

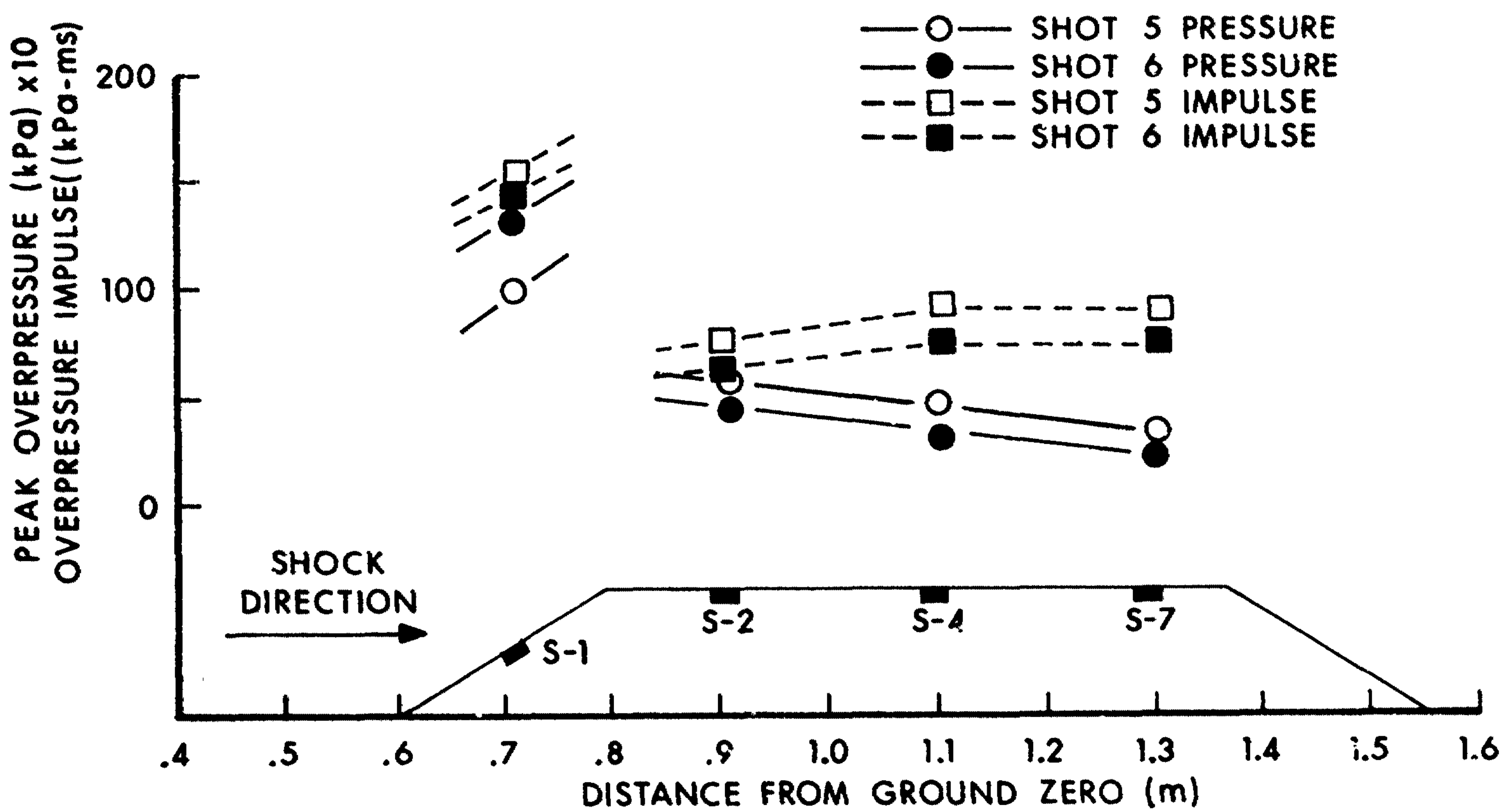

Figure 13. Peak overpressure and impulse on Model S.

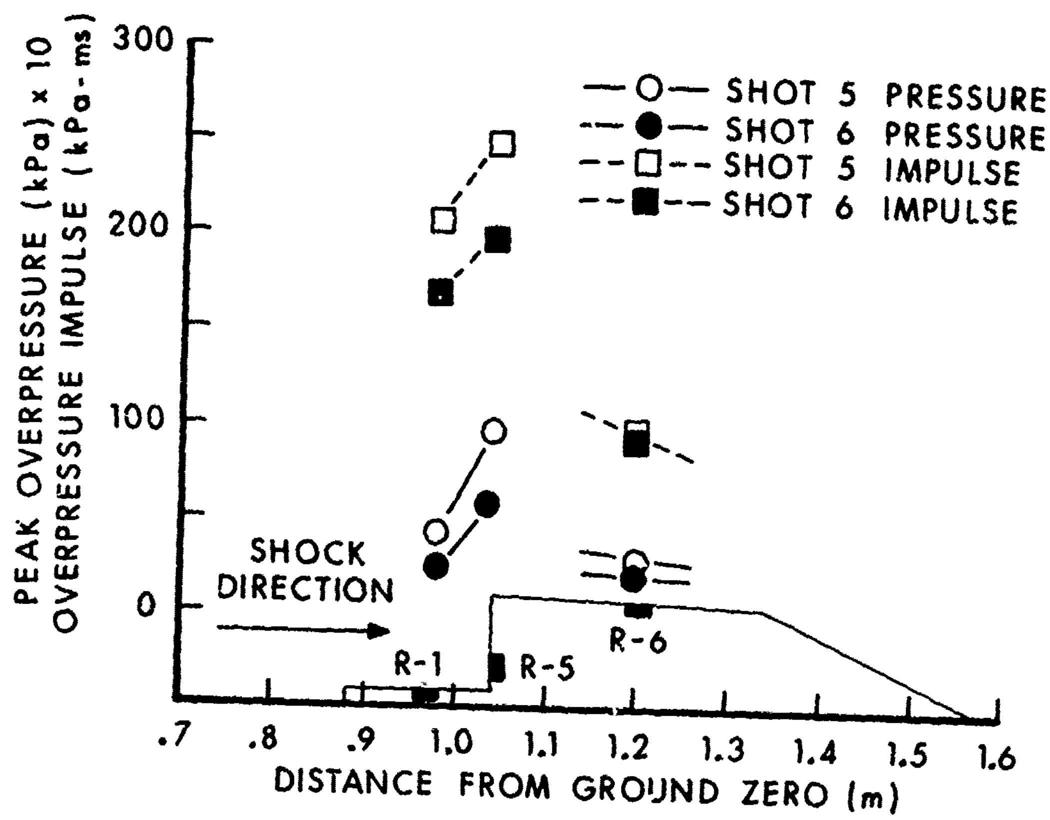

Figure 14. Peak overpressure and impulse on Model R.

ESKIMO VI - PRELIMINARY TEST RESULTS

Paper Presented to the

Nineteenth DOD Explosives Safety Seminar
Biltmore Hotel
Los Angeles, California
9-11 September 1980

By

PETE E. TAFOYA
Civil Engineering Laboratory
Port Hueneme, California 93043

ABSTRACT

ESKIMO VI, sixth in the series of Explosive Safety Knowledge IMprovement Operation Tests was conducted to test and evaluate the safety and performance under blast loading of earth-covered box-shaped (smokeless powder and projectile) storage magazines. Earlier ESKIMO tests have been performed to determine minimum separation distances necessary to prevent explosion communication between magazines and to test the performance of existing and proposed magazine designs at the minimum distances permitted by safety standards. ESKIMO VI evaluated the explosion resistance of flat-roofed, earth-covered, reinforced concrete construction magazines used by the U.S. Navy for storage of smokeless powder, projectiles, and missiles. The two magazines tested, the Type IIB (old design) and Type A (new design) magazines, were characterized by the box shape, similar geometric dimensions, interior three-bay design, and two entrance doors located in the headwall. Both designs were subjected to "worst case" intermagazine separation distance pressure loads. Both structures survived the test with limited damage. The Type IIB magazine sustained light to moderate structural damage while the Type A magazine sustained only light damage. The Type IIB doors failed during the blast and were blown into the structure, permanent roof deflections were limited (less than one inch) and minor cracking of the concrete roof and headwall was evident. The Type A magazine sustained primarily architectural damage to the roof parapet. Roof deflections (less than one-half inch) were noted accompanied with minor cracking of the concrete roof. Both magazines, if in the field, could be reusable after minor reworking.

Structurally speaking, the designs were also characterized by standard reinforced construction with a slab roof supported by two interior columns (either square tied or spirally reinforced) and covered with a uniform earth cover.

Prior to ESKIMO VI there was no adequate basis for allowing these magazines to be located at the minimum separation distances. Box magazines such as the Type IIB (currently in wide use in the field), had not been tested or specifically designed for overpressure loads, safety policy had required that they be sited at non-standard intermagazine separation distances and that their storage capacity be limited to one-half the weight of explosives allowed in a standard magazine. These requirements increased the amount of land needed for storage in box-shaped magazines without fully satisfying questions on their safety.

In view of the projected requirement for more box magazines, the Naval Facilities Engineering Command (NAVFAC) designed two new magazines for resisting blast loadings at standard intermagazine separation distances. The new designs, the Type A and the larger Type B, are intended to provide safe storage of explosives with a smaller land area than is currently required for existing box magazines of the IIB type.

The test was conducted using one-half scale structures. Both of the test magazines were complete structurally equivalent half-scale models of their respective prototypes. The donor structure was a mock-up of a Type IIB magazine and simulated the geometry and mass of the roof, earth-cover, and headwall of the prototype. The donor charge consisted of 60 Mark 16 torpedo warheads containing the equivalent to 44,000 pounds of TNT, corresponding to 350,000 pounds of of TNT at full scale.

Construction of the test structures began in October 1979 and was completed in June 1980; the test was conducted on July 23, 1980. All work was conducted under direct funding from NAVFAC and the Department of Defense Explosive Safety Board (DDESB). Naval Weapons Center (NWC) China Lake was the test site and test conductor with the Civil Engineering Laboratory (CEL) acting as project coordinator.

This report contains brief descriptions of: (1) construction of the test structures, (2) the explosive charge and donor structure, (3) test structure layout, (4) instrumentation, and (5) preliminary test results in the form of tabulated summaries, time series plots of instrumentation results accompanied with discussion, and photos of structural damage.

INTRODUCTION AND BACKGROUND

ESKIMO VI was the sixth in a series of explosions tests of earth covered magazine structures conducted at Naval Weapons Center, China Lake, CA. ESKIMO is an acronym for Explosive Safety Knowledge IMprovement Operation. The previous five ESKIMO tests (Ref 1-5) were conducted on full scale steel and concrete arch magazines. Previous ESKIMO test results were the basis for establishing intermagazine separation distances (Ref 6) required for "standard" arch-shaped magazines.

ESKIMO VI was designed to test and evaluate the safety and performance under blast loading of box-shaped (smokeless powder/projectile) storage magazines. Previous to ESKIMO VI, box magazines in the field had not been tested or specifically designed for overpressure loads. Safety policy therefore had required that they be sited at non-standard intermagazine separation distances and that their storage capacity be limited to one-half the weight of explosives allowed in a standard magazine. (See Table 1 for a listing of selected intermagazine spacings.) These requirements increased the amount of land needed for storage in box-shaped magazines without fully satisfying questions on their safety.

In view of the projected requirement for more box-shaped magazines, the Naval Facilities Engineering Command (NAVFAC) designed two new magazines for the blast loads at standard intermagazine distances. These new designs were intended to provide safe storage of explosives within a smaller land area than is currently required for existing box magazines.

The Department of Defense Explosives Safety Board (DDESB) and the Navy co-sponsored ESKIMO VI to investigate the structural response and safety of the existing (Type IIB magazine) and proposed (Type A magazine) box-magazine structures.

TEST OBJECTIVES

The objectives of the ESKIMO VI test were:

1. To evaluate the safety of existing box-shaped magazines at non-standard intermagazine spacings.

2. To demonstrate the safety of the new NAVFAC box-magazine designs for use at standard intermagazine spacings.

3. To develop improved load criteria, structural performance requirements, design methods and intermagazine spacings for box-shaped magazine roofs, walls, and doors.

GENERAL DESCRIPTION

Test Structures

ESKIMO VI tested two box-shaped magazines, the NAVFAC Smokeless Powder/Projectile Type IIB and the new NAVFAC Type A.

Due to the prohibitive expense of full scale structures, large scale model Type A and Type IIB test structures were tested with the appropriate scaled charge weight. The scale factor was one-half. A discussion of scaling and scaling laws is included in the ESKIMO VI test plan (Ref 7).

Type IIB Magazine

The Type IIB Smokeless Powder and Projectile Storage magazine (Ref 8) was selected for meeting the first objective for the following reasons: (1) there currently are large numbers of the Type IIB magazines in the field (an illustration of this magazine type is shown in Figure 1) and (2) the Type IIB dimensions are identical to that of the redesigned blast-resistant Type A magazine. The Type IIB magazine (full scale) is 52 ft deep and 97 ft wide with an inside height that varies from 13 ft at the rear wall to 15 ft-2 in. at the front wall. Dimensions of the scale model are one-half of those above (Fig 2). Construction drawings for the one-half scale Type IIB test structure are found in Reference 9. The Type IIB magazine has two interior columns and 10 pilasters with capitals. Three continuous drop panels are provided at the column lines between the side walls. Two doors are located at the loading platform. The Type IIB test structure duplicated the walls, roof, columns, pilasters, floor slab, footings, both doors, and earth fill. The nominal (full scale) depth of roof earth cover for these box designs is 2 feet. The model structures employed 1 foot of earth cover. The steel wingwalls, salvaged from ESKIMO V, were designed to retain the earth fill behind them. The ramp and platform in the model structures were replaced with compacted earth fill without concrete slabs, footings or steps and all other non-structural features were deleted.

Type A Magazine

The new NAVFAC Type A magazine (Ref 10) was tested to meet the second and third objectives. It was designed to provide the same interior dimensions as the Type IIB magazine. The Type A magazine roof is supported by two interior circular columns with drop panels. Aside from being much more massive and designed without pilasters, the major difference between the Type A and II B magazines is in the headwall design. The Type A magazine employs two sliding (built-up) doors which are supported on all four edges by large beam elements. The two doors are located at the loading platform. The Type A test structure duplicates the walls, roof, columns, footings, both doors (without hanging mechanisms) and earth fill. The nominal (full scale) depth of roof earth cover for these box designs is 2 ft. The model structure employed 1 ft of earth cover. Steel wingwalls, were used to retain the earth cover. The interior floor slab, ramp and loading platform in the model were replaced with compacted earth fill without concrete slabs, footings or steps and all other non-structural features were deleted. Construction bid package drawings of the one-half scale model Type A structure (Fig 3) are also included in Reference 9.

Magazine Test Doors

The double leaf, hinged doors located on the Type IIB (Fig 4) were approximately one-half scale models of the doors currently being used in the field. The model doors were designed to provide the same resistance as those on the full scale structure.

The single leaf sliding doors on the Type A magazine were chosen to meet Objective 3. Figure 4 illustrates this door type and drawings of the door's construction are included in References 9 and 10. In the interest of economy, the Type A doors did not include the hanging mechanisms and were fastened with no intention of preventing door rebound after loading.

TEST LAYOUT

Test Array

The test array is shown in Figure 5. The Type IIB magazine was located to the side of the donor, at a scaled distance of 1.25 $W^{1/3}$ (44 ft), and the Type A magazine to the front of the donor, at a scaled distance of 2 $W^{1/3}$ (70.5 ft).

Siting the Type IIB Magazine

Table 2 lists the predicted Type IIB structure loads at each of the intermagazine separation distances. These values indicated that the side-side orientation at a spacing of $1.25W^{1/3}$ would produce the critical Type IIB roof and headwall loadings.

Consideration was given to testing of the Type IIB magazine roof at the same standard front-back spacings as the Type A magazine roof. However, a preliminary structural response analysis based on previous ESKIMO tests and other pressure load data showed little chance that the IIB roof would safely resist the resulting loads. In comparison, the Type A roof, which was designed for these load magnitudes, uses twice the material and is considerably stronger than the Type IIB roof. Consequently, the Type IIB magazine was placed at the side-to-side orientation. Moreover, the predicted roof loads at the side-side spacing (which is the same for both the standard and non-standard spacings) was also predicted to exceed the strength of the IIB roof.

In response to the need for better pressure load data, DDESB tasked the Ballistics Research Laboratory (BRL) to run scale model tests of the proposed ESKIMO VI layout. Data from these model tests (Ref 11) indicated the loads, specifically the impulse, originally predicted were excessively conservative for the Type IIB magazine (37% high) and approximately the same for the Type A magazine (within 10% of previous values). Even with the decreased loading, a roof or headwall failure was not totally ruled out.

Siting the Type A Magazine

Table 2 presents the pretest predicted loads on a magazine at standard intermagazine separation distances (based on 1/50 scale model tests conducted by Kingery, Ref 11). The critical orientation for the roof (front-back) and headwall (back-front) are not the same. The Type A magazine headwall and door designs are based on methods proven by experience and test and are therefore designed with a high level of confidence. Less is known about flat slab design and analysis, especially for dynamic loads. Therefore, the Type A magazine was oriented to evaluate the safety of the roof system and the Type IIB oriented to evaluate the safety of the roof, headwall and doors.

The critical orientation, as shown in Table 2, is front-back at a $2W^{1/3}$ spacing. Since the Type A roof was designed for the expected test loads, test results will also provide valuable information on the adequacy of current design methods.

Donor and Explosive Charges

The test structures were located to the sides and to the front of the donor. In order to obtain the proper directional blast environment, the donor structure was constructed to simulate the mass properties and geometry of the earth-covered Type IIB magazine. The donor structure was designed by NWC, China Lake with structural steel roof and sidewalls and reinforced concrete headwall, and provided the most economical design within the mass and geometry requirements. The donor design details are included in Reference 9, sheets 10 and 11.

The donor charge weight was modeled to simulate a full scale explosive weight of 350,000 pounds of TNT, the design charge weight of the new NAVFAC Type A magazine. The donor charge consisted of surplus Mark 16 torpedos, requisitioned from the depot at Hawthorne, NV. A one-half scale test required the equivalent to 44,000 pounds of TNT (60 torpedos packaged in 15 groups, 4 torpedos per group). The charge distribution within the magazine was the same as that used by the Army Ballistic Research Laboratory (BRL) in the 1/50th scale model ESKIMO VI load determination tests (Ref 11). Figures 6 and 7 show details of the Mark 16 torpedo groups and their locations in the donor structure. Figure 8 is a photo of the torpedoes in-place prior to the test.

INSTRUMENTATION

General

Pressure-time gages recorded the directional blast environment from the box-magazine donor. Gages on the ground surface along gage lines at 0°, 90°, and 180° (see Table 3) recorded the free-field pressure-time environment while gages on the test structures recorded the blast environment at the magazines. The pressure gage measurements will be compared with results from the BRL scale model load tests and used to develop load criteria for box magazines. Soil pressure gages measured the load-time history at the soil structure interface and will be used to determine load attenuation through the soil medium.

Structural intrumentation recorded the time history response of the test structures. Standard resistive weld-on strain gages were located at selected rebar locations. Velocity and deflection gages were strategically located in the interior bays of the structure to measure the maximum vertical response of the roof and the maximum horizontal response of the wall.

Velocity gages were of the pendulum type, normally used in ground shock tests and were used as a backup to the standard displacement gages. Vertically-oriented velocity gages included a spring which compensated for gravitational effects on the pendulum. Deflection gages were linear motion potentiometers or linear variable differential transducers and were used to measure differential motion of the roof.

All air blast gages were installed in heavy gage mounts in order to read side-on pressure loads. Piezoresistive type gages were used on-structure and most free-field locations. BRL self-recording gages were used at a solid distances of fifty.

Locations of instrumentation used for structural response and blast environment measurements are summarized on Figures 9, 10 and 11.

ESKIMO VI DETONATION

At 10:27 a.m. on 23 July 1980, the donor charge was detonated. The explosive source in was designed to produce a maximum impulse of 410 psi-msec on the Type IIB magazine roof and a maximum of 885 psi-msec on the Type A magazine roof. Peak pressures (based on scale model tests) anticipated were 91 psi and 294 psi, respectively. Measurements of blast loading made during the test, however, that the actual loadings were significantly lower than the predicted level, and exhibited strong directional effects. The measured impulse loads ranged from 377 psi-msec with a reflected peak of about 105 psi on the Type IIB magazines, to 656 psi-msec with an initial peak of 360 psi on the Type A magazine.

It is believed the blast loads observed during the event are representative of an actual donor incident.

TEST RESULTS

Based on fragment size and data from recordings, it is concluded that complete, or essentially complete, detonation was achieved. Cratering was minimal (maximum depth of 5 ft) due to the containment afforded by the donor structure floor. Varying amounts of structural damage were incurred by the test magazines. Details of this damage are presented with illustrations in the following section. For comparison purposes, a photo of the structures prior to the test is included in Figure 12. Illustrations of the limited crater are shown in Figures 13 and 14.

Observed Structural Response

The Type IIB Magazine. On the Type IIB Magazine the headwall and roof received an impulse loading about 8% less than that predicted. The Type IIB structural response was as follows:

1. The doors were forced inward, bending past the door stops and were separated from their hinges, coming to rest in the corresponding rear corners of the magazine. The steel door stops at the top and bottom of the door opening remained intact. The door jams were partially separated from the concrete headwall in and around the hinge locations. This damage occurred when the hinges failed. Figures 15 through 17 illustrate this damage.

2. The concrete roof was cracked at and around the south column. Minor spalling did occur exposing portions of the reinforcing bar. Figures 18 and 19 indicated extent of damage in this area.

3. The concrete headwall and roof were lightly cracked. Minor pilaster damage was also reported. Figures 20 and 21 illustrates this damage. The north end of the Type IIB magazine sustained only light damage as illustrated by Figure 22.

The Type A Magazine. The Type A magazine was subjected to an impulse loading 25% less than anticipated. Minor structural damage was encountered. Damage was as follows:

1. The roof parapet (a low wall used to retain the soil on the roof) was severely damaged. Figures 23 and 24 illustrate this damage. The sliding doors, though not damaged, were torn loose from their attachments; this was expected since the doors were not attached to prevent rebound. Figure 23 illustrates this point.

2. Very little damage, if any, was sustained to the Type A interior. Figures 25 and 26 illustrate this point.

3. Cracking of the Type A magazine roof occurred but was not severe. Figure 27 illustrates this damage.

Data Derived from Instrumentation

Event Timing. All data, with the exception of the BRL self-recording gages, were recorded using: standard IRIG format B for the motion pictures, and binary coded one kilohertz timing for magnetic tape data from the piezoresistive pressure gages, displacement, velocity and strain gages.

Test event times derived from assessment of the piezoresistive pressure gage data and velocity data were based on a zero-time pulse indication derived from an ionization probe buried in the donor charge.

Motion Picture Photography. The main test event was recorded photographically by ground and air-based 16-mm, 35-mm, and 70-mm cameras using color film and video cameras. Film speeds were varied from 10 frames per second for some overall views to 8000 frames per second for cameras focused on headwalls, doors and the donor target. Figure 28 illustrates the six camera locations used for the test. All cameras except those trained on the donor target (camera #1) operated as planned. A full documentary film of test results should be available approximately January 1981.

Response Instrumentation.

Displacement Transducers. Displacement transducers were strategically positioned so as to measure the maximum displacements at the roof and headwalls. A summary of data derived from the displacement transducers is listed in Table 4. A representative plot of displacement data is shown in Figure 29. Time history records of all data are not included in this report due to its bulk, but are available from the author on request.

It should be noted that the displacement measured for the roof components (Table 4) was relative to the floor, (which moved due to ground shock). In order to acquire relative displacements to a non-moving frame of reference, velocity gages were attached at floor level and output integrated to acquire the floor movement during the event. Displacements relative to a non-moving frame of reference are listed in Table 5. Maximum roof displacements for the Type IIB magazine were 2.0 in. at location M1. Maximum roof displacements for the Type A magazine were 1.42 in. at location M4.

Velocity Gages. A summary of data derived from velocity gage output is shown in Table 6. Time history record plots are available from the author. A representative plot of this data is found in Figure 30. In general, the first motion after zero time is consistent with arrival of the blast wave.

Movement of the floor due to ground shock was also established by integration of velocity gage output. The purpose of these gages (gage number five for the Type IIB magazine and gages number four through seven on the Type A magazine) were used for determination of relative roof displacements (Table 5).

Pressure Gage Data. A summary of pressure gage output is listed in Tables 7 through 9. Time history record plots are available from the author. Figure 31 is a representative plot of this data. The purpose of measuring pressure data is to acquire the pressure loadings on the structure and surrounding areas for comparison with previous model data (Ref 11). Gages mounted on the roof indicated roof distributed loadings with respect to time are an important part of determining the response of the structure.

Soil Pressure Gages. A summary of data derived from soil gauge output is listed in Table 10. Time history record plots are available from the author. Figure 32 is a representative plot of this data. The purpose of these gages was to determine the load attenuation on the structure due to earth cover. Based on pressure loading a measure of attenuation through the soil can be established. For the Type IIB whose sidewalls nearest the donor was instrumented at heights 1/4h, 1/2h, and 3/4h, the attenuation was 65%, 70%, and 78%, respectively. Corresponding soil pressures on the Type IIB sidewall were 92 psi, 77 psi, and 58 psi with a reference surface pressure of 260 psi. The rear wall of the Type A magazine was also instrumented at 1/2h, 3/4h and measured pressures of 162 psi, 133 psi at the respective locations. Attenuation was 70% and 75% based on a reference surface pressure of 532 psi. The soil pressure gage located on the Type IIB magazine roof indicated an attenuation of 0% based on a soil pressure of 105 psi and reference surface pressure of 105 psi. The soil pressure gage located on the Type A magazine roof and at the 1/4h location on the rear wall were lost during the test.

Strain Gage Data. A summary of strain gage output is listed in Table 11. Time history record plots are available from the author. A representative plot of this data is included in Figure 33. Strain gages were installed on the reinforcing bars in the test structure in order to determine the structural. The purpose of this from the test data the internal load distribution and relate this information to a theoretical model.

CONCLUSIONS

In view of the minor structural damage sustained to the Type A magazine from the ESKIMO VI test the safety and performance of that structure under "worst case" standard intermagazine distance pressure loads has been confirmed. In addition, it was demonstrated that the Type IIB magazine would sustain only light to moderate structural damage when exposed to non-standard (side to side) intermagazine distance pressure loads. Moreover, as a result of data gathered from the test a data base suitable for use in a theoretical analysis of roof slabs has been generated.

Type IIB Magazine

It was shown by the performance of the Type IIB magazine that the current door design is inadequate for resisting loads generated by a 350 klb charge. Redesign of the headwall and door system would be necessary to resist such loads. A design similar to that of the Type A magazine is a viable alternative. Should a redesign be initiated, roof component stresses must be reviewed.

Consequently, a major redesign of the Type IIB magazine may be necessary for assuring structural performance and safety.

Type A Magazine

The minor damage sustained by the Type A magazine may imply the possibility of reducing steel and concrete construction requirements while still maintaining satisfactory performance under blast loading. Further theoretical studies can assess these reductions and the corresponding economic savings.

This theoretical work, scheduled for 1981, will add greatly to knowledge of analysis trying to determine the behavior of flat slabs and drop panel roofs. Data gathered from ESKIMO VI will play a major role in the determination of analytical models for this purpose.

RECOMMENDATIONS

Type IIB Magazine

Evaluation of post-shot data has indicated the door design in the Type IIB is inadequate for anticipated loadings. Consequently, it is recommended that; (1) A redesign of the Type IIB door system be initiated, and (2) ESKIMO VII test be initiated to test the redesigned door system.

In view of these stipulations non-standard spacing or download requirements currently imposed by OP-5 should be maintained until further investigation is carried out.

Type A Magazine

The safety and performance of the Type A magazine at standard intermagazine distances has been established by ESKIMO VI. In light of the minor damage incurred by the Type A, a structural overdesign may be evident. In order to assess this matter further, a theoretical analysis is recommended to evaluate the possible overdesign and possible economic savings which may be incurred in eliminating the over-conservatisms.

REFERENCES

1. Naval Weapons Center. "ESKIMO I Magazine Separation Test," by Frederick H. Weals, China Lake, CA, NWC, April 1973, 84 pp (NWC TP 5430, Publication Unclassified).

2. Naval Weapons Center. "ESKIMO II Magazine Separation Test," by Frederick H. Weals, China Lake, CA, NWC, September 1974, 90 pp (NWC TP 5557, Publication Unclassified).

3. Naval Weapons Center. "ESKIMO III Magazine Separation Test," by Frederick H. Weals, China Lake, CA, NWC, February 1976, 70 pp (NWC TP 5771, Publication Unclassified).

4. Naval Weapons Center. "ESKIMO IV Magazine Separation Test," by F. H. Weals and C. H. Wilson, China Lake, CA, NWC, March 1977, 52 pp (NWC TP 5873, Publication Unclassified).

5. Naval Weapons Center. "ESKIMO V Magazine Separation Test," by F. H. Weals, China Lake, CA, NWC.

6. Navy. NAVSEA OP 5 Vol I: Ammunition and Explosives Ashore, Change 5, 1 Oct 1976.

7. Civil Engineering Laboratory Technical Memorandum TM No. 51-80-06, "The ESKIMO VI Test Plan," by J. E. Tancreto and P. E. Tafoya, Naval Construction Battalion Center, Port Hueneme, CA, April 1980.

8. Dept. of the Navy's Bureau of Yards and Docks, "Standard Magazine Smokeless Powder/Projectile Type IIB, Yards and Docks Drawings #749771," Washington, D.C., 1956.

9. Naval Weapons Center China Lake, "Construct ESKIMO VI Magazines, NAVFAC Dwg. No. 6125900," China Lake, CA, July 1979.

10. Naval Facilities Engineering Command, "Box Magazine Type A Standard, NAVFAC Drawing #1404000," Alexandria, VA, 1978.

11. Ballastic Research Laboratory. Technical Report ARBRL-TR-02215: ESKIMO VI Model Tests, by C. N. Kingery, Aberdeen Proving Grounds, MD, Feb 1980.

12. Army Ballistic Research Laboratory. Memorandum Report No. 2680: Blast Parameters from Explosions in Model Earth Covered Magazines, by C. N. Kingery, G. A. Coulter, and G. T. Watson, Aberdeen Proving Ground, MD, Sep 1976.

Table 1.

REQUIRED INTERMAGAZINE SCALED SEPARATION DISTANCES* FOR STANDARD AND NON-STANDARD MAGAZINES

ORIENTATION	SCALED DISTANCE, ** $R/W^{1/3}$ STANDARD	NON-STANDARD
SIDE-SIDE	1.25	1.25
FRONT-BACK	2	6

* SELECTED WALL-TO-WALL DISTANCES FROM TABLE 5-12 OF NAVSEA OP-5

** R IS THE SEPARATION DISTANCE IN FT, W IS THE CHARGE WEIGHT IN POUNDS

Table 2.

PREDICTED MAGAZINE LOADS AT STANDARD INTERMAGAZINE SEPARATION DISTANCES (W=44,000 lb)

ORIENTATION (DONOR TO ACCEPTOR)	$R/W^{1/3}$ ($ft/lb^{1/3}$)	LOADED SURFACE	P * (psi)	i * (psi-ms)
FRONT-BACK	2	ROOF	294	885
SIDE-SIDE	1.25	ROOF	91	410
BACK-FRONT	2	ROOF	30	330
BACK-FRONT	2	HEADWALL	122	776
SIDE-SIDE	1.25	HEADWALL	65	410

* C.N. KINGERY, "ESKIMO VI MODEL TESTS," ARBRL-TR-02215, FEB 1980

Table 3.

FREE FIELD PRESSURE GAGE LOCATIONS ON LINES AT 0°, 90°, AND 180° FROM DONOR

RANGE* (ft)	$R/W^{1/3}$ ($ft/lb^{1/3}$)
70	2*
140	4
210	6
530	15
880	25
1760	50

* FOR W= 44,000 lbs.

$W^{1/3}$=35 $lbs.^{1/3}$

Table 4. Summary of Displacement Gage Data

Location of Transducer	Max.* Displacement (in.)	Mean Displacement From Initial Motion to Peak Excursion (in.)	Time From Det. Zero to Max. Displacement (msec)	Estimated Final Displacement at t = ∞*
Type IIB Magazine				
1. M1	2.0 (-2.0)**	.2	25	0.81
2. M2	1.6 (-1.92)	0.5	30	1.1
3. C2	+1.0 (-0.4)	0.4	31	.75
4. E1	1.25 (0)	0.25	28	1.1
Type A Magazine				
1. M1	+1.18(-1.16)	0.16	20	negligible
2. M4	1.42 (-.592)	0.30	20	negligible
3. C4	1.07 (-0.48)	0.21	22	negligible
4. E1	1.28 (-0.67)	0.133	22	negligible

*Positive values indicate downward motion.

**Maximum negative excursions are included for completness of data tabulation.

Table 5. Summary of Roof Displacements After Compensation for Floor Motion

Location of Measurement	Maximum Relative Displacement*
Type IIB Magazine	
1. M1	0.6
2. M2	0.2
3. C2	-.4
4. E2	-.15
Type A Magazine	
1. M1	.42
2. M4	1.01
3. C4	.75
4. E1	.96

*Positive values indicate downward motion.

**Maximum negative excursions are included for completness of data tabulation.

Table 6. Summary of Velocity Data

Location of Sensor	First Motion (msec)	Peak Velocity (ft/sec)*	Displacement (in.)*
Type IIB Magazine			
1. M2	30	+5 (-5)	1.25
2. M3	27	2.0 (-1.6)	1.0
3. E2	32	5.5 (-3.8)	1.875
4. C1	36	3.0 (-2.0)	-1.85
5. Floor	32	2.5 (-2.75)	-1.40
Type A Magazine			
1. M4	20	+8.6 (-6.0)	1.34
2. E4	21	9.88 (-5.57)	1.41
3. C1	20	+4.37 (-2.68)	.69
4. Floor @ M1	22	+1.0 (-1.0)	.76
5. Floor @ M4	23	+1.12 (-1.0)	-.41
6. Floor @ E1	22	+1.38 (-1.28)	.45
7. Floor @ C4	23	+1.2 (-1.35)	.325

*Positive values indicate downward motion.

Table 7. Summary of On-Structure Piezoresistive Pressure Gage Data

Gage Location	Gage Distance from Donor (ft)	Peak Overpressure (psi)	Impulse (psi-msec)	Time of Arrival Relative to Zero Time (msec)
Type IIB Magazine				
1. E1	80	80	320	27
2. M1	68	105	377	23
3. M2	68	*	*	*
4. W1	30	260	494	14
5. M3	68	50	382	27
6. J3	56	110	313	17
Type A Magazine				
1. E1	84	354	630	20
2. M4	90	232	650	20
3. E4	90	143	605	19
4. M7	98	50	609	27
5. M3	84	532	1,275	13
6. M1	84	360	656	18
7. M2	77	127	832	17

*Gage lost during test.

Table 8. Summary of Off-Structure Piezoresistive Pressure Gage Data

Gage Location	Gage Distance from Donor (ft)	Peak Overpressure (psi)	Impulse (psi-msec)	Time of Arrival Relative to Zero Time (msec)
1. 0-4*	140	112	650	47
2. 0-6	210	29	613	77
3. 0-15	530	9.3	185	270
4. 0-25	880	2.29	25.5	545
5. 90-2	70	49.2	330	19
6. 90-4	140	47.1	310	53
7. 90-6	210	26.2	300	85
8. 90-15	530	8.53	121	329
9. 90-25	880	**	**	**
10. 180-2	70	0.78	330	21
11. 180-4	140	29.1	290	54
12. 180-6	210	31.4	270	97
13. 180-15	530	6.4	115	331
14. 180-25	880	2.49	58.8	525

*First digit indicates angular orientation of gage line, second digit indicates scaled distance of gage.

**Channel failed during test.

Table 9. Summary of BRL Self Recording Pressure Gage Data

Gage Location	Gage Distance from Donor (ft)	Peak Overpressure (psi)	Impulse (psi-msec)	Positive Phase Duration (msec)
1. 0-50	1760	.346	23.59	149.2
2. 90-50	1760	.446	30.56	146.81
3. 180-50	1760	.2571	15.24	130.86

Table 10. Summary of Soil Pressure Gage Data

Location of Sensor	Peak Soil Pressure (psi)	Reference Surface Pressure	Soil Depth at Location (ft)	% Attenuation Based on Reference Surface Pressure
Type IIB Magazine				
1. M1	105	105	1	0
2. S4	91.9	260	3	65
3. S3	77.6	260	5	70
4. S5	58.0	260	7	78
Type A Magazine				
1. M6	*	532	3	*
2. M8	162	532	5	70
3. M7	133	532	7	75
4. M1	*	360	1	*

*Gage failed during test.

Table 11. Summary of Strain Gauge Data

Location of Sensor	Peak Strain (μ in./in.)	Average Strain (μ in./in.)
Type IIB Magazine		
1. S2	2115.0	900
2. M1	2823.0	564
3. M2	1472.5	394
4. M2	1235.5	311
5. M3	2912.0	434
6. C3	-1770.0 (+2200)	38
7. C3	-900 (1943)	600
8. E2	630	300
9. E2	1000.0	280
10. E1	2500.0	100
11. E1	500	100
Type A Magazine		
1. M5	2410.0	627
2. M1	1874.0	332
3. M4	430.0	32
4. M4	1046.0	364
5. M4	1359.0	504
6. M4	2554.0	102.0
7. M8	310.0	120
8. C1	-2350.0	110
9. C1	-5533.0	3843
10. C4	5613.0	4740
11. E1	2027.0	371
12. E4	2097.0	781
13. E4	1547.0	322

(+) Tension
(-) Compression

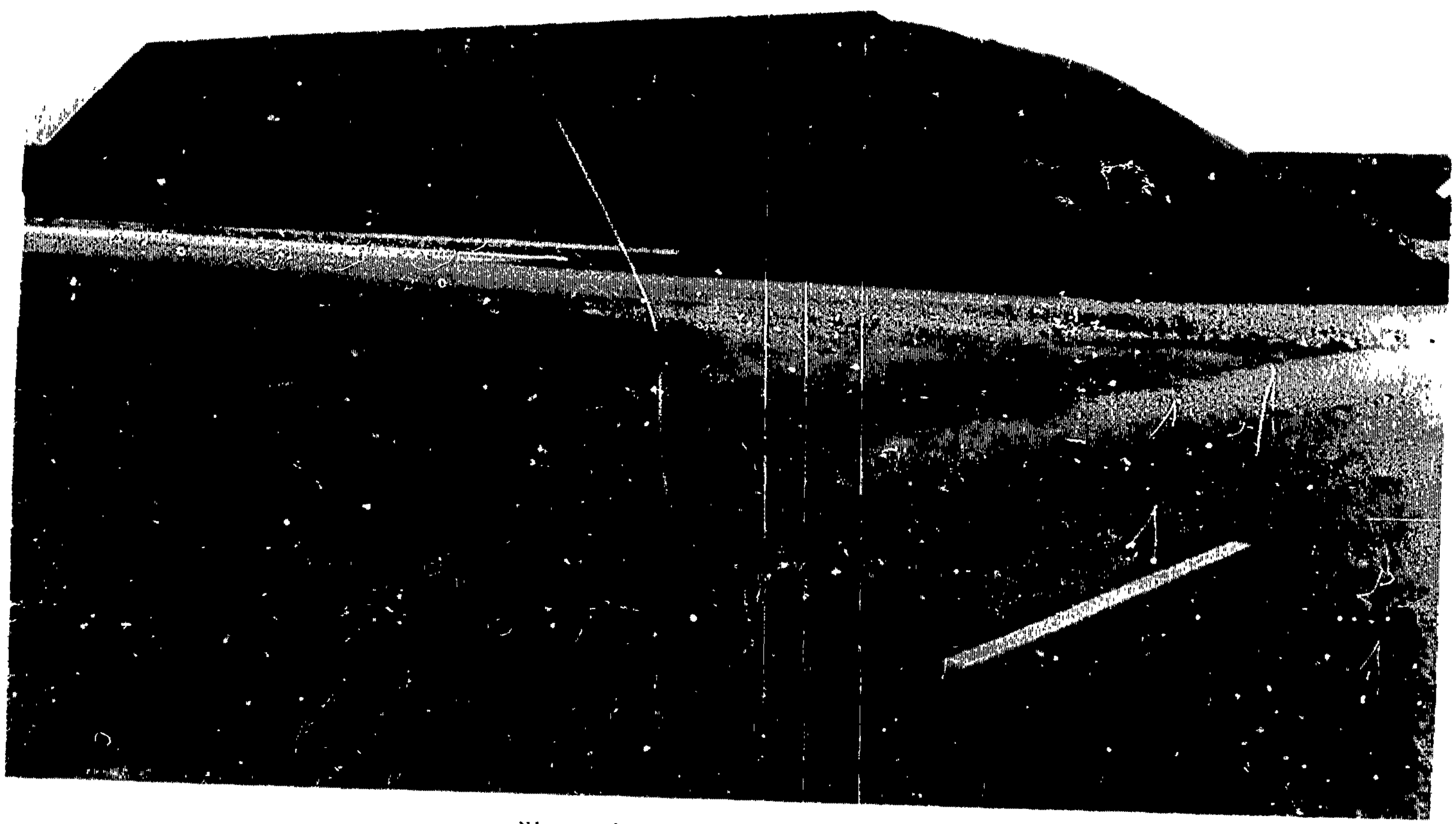

Figure 1. Typical Type IIB Magazine

Figure 2.

GENERAL DIMENSIONS FOR THE TYPE II B MAGAZINE (½ SCALE MODEL)

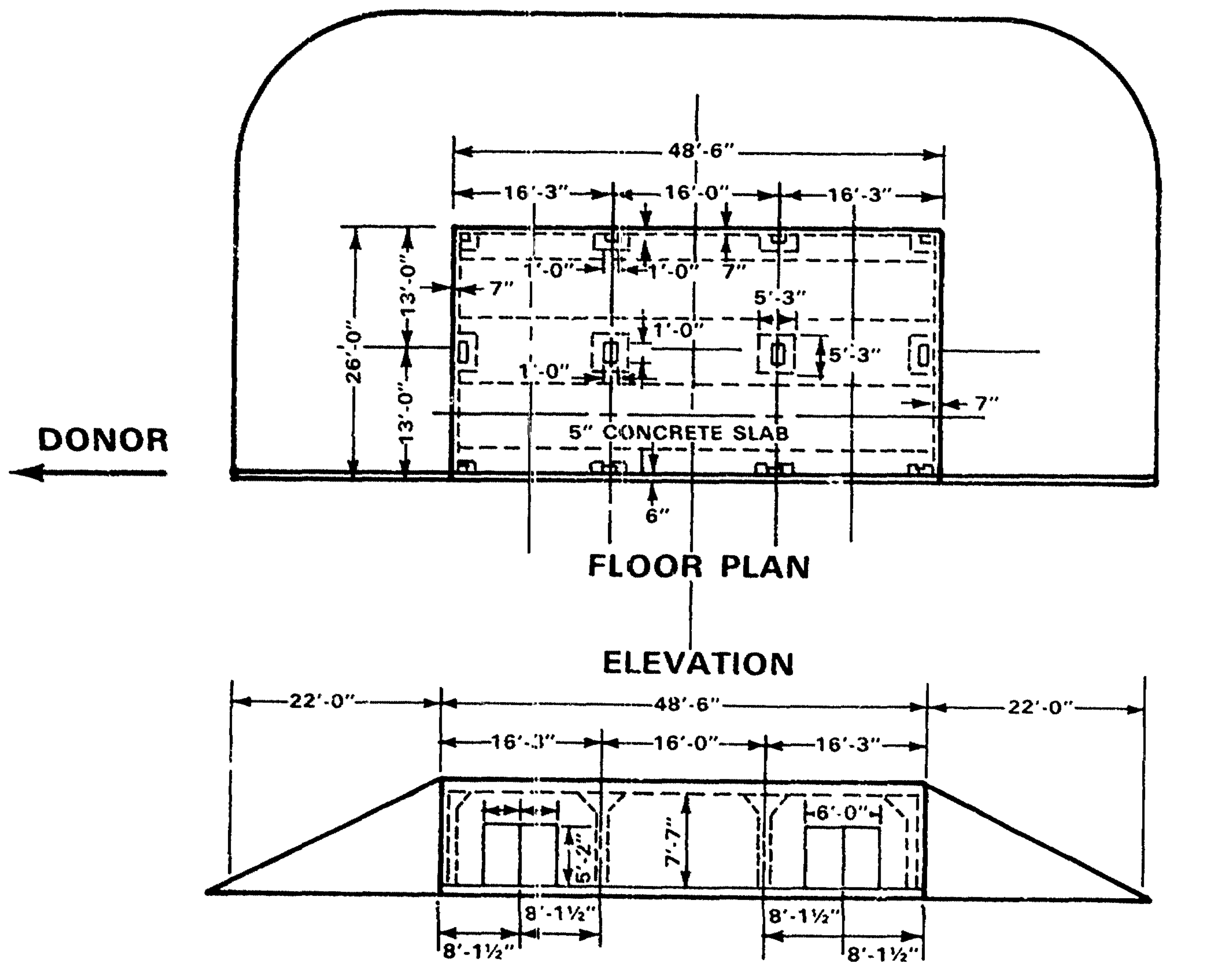

Figure 3.

GENERAL DIMENSIONS FOR THE TYPE A MAGAZINE (½ SCALE MODEL)

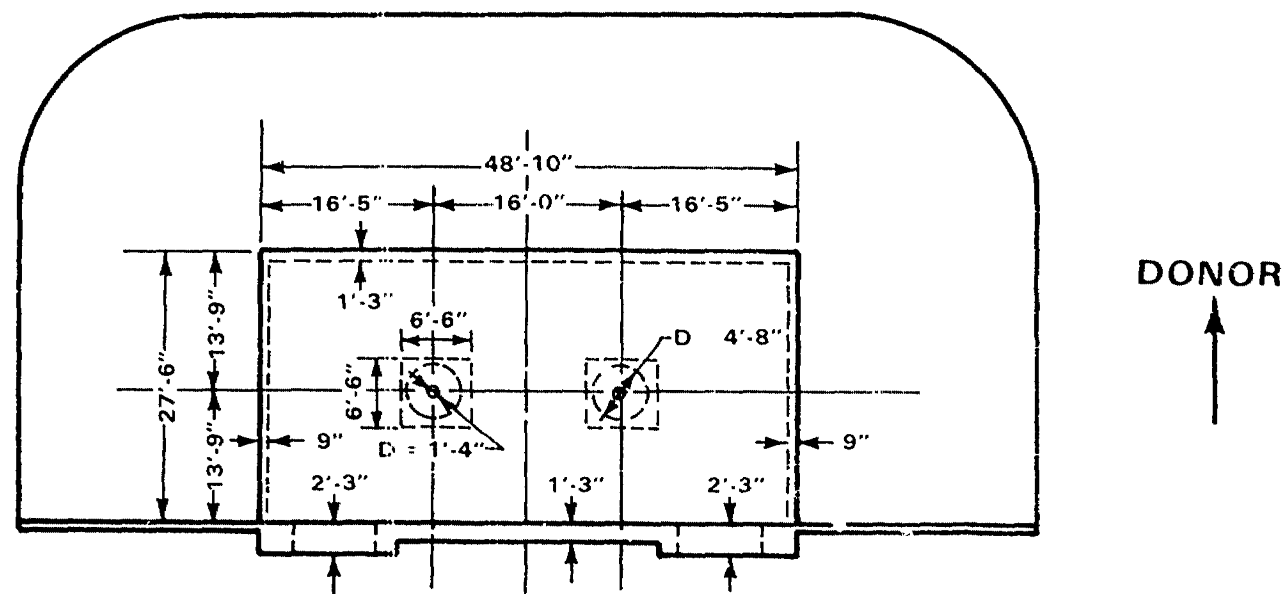

FLOOR PLAN

ELEVATION

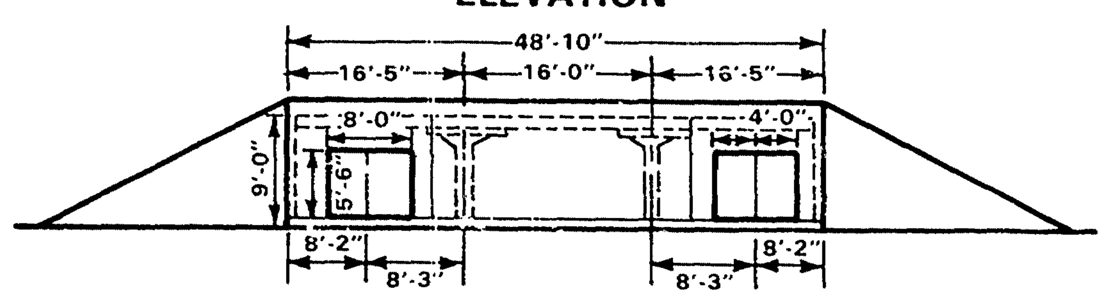

Figure 4.

DOOR TYPES USED ON ESKIMO VI TEST STRUCTURES

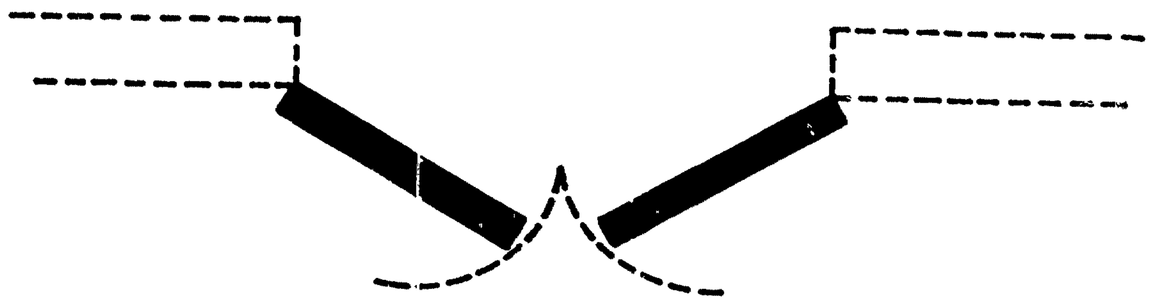

DOUBLE LEAF, HINGED
USED ON THE TYPE II B MAGAZINE

SINGLE LEAF, SLIDING
USED ON THE TYPE A MAGAZINE

Figure 5.

ESKIMO VI TEST LAYOUT

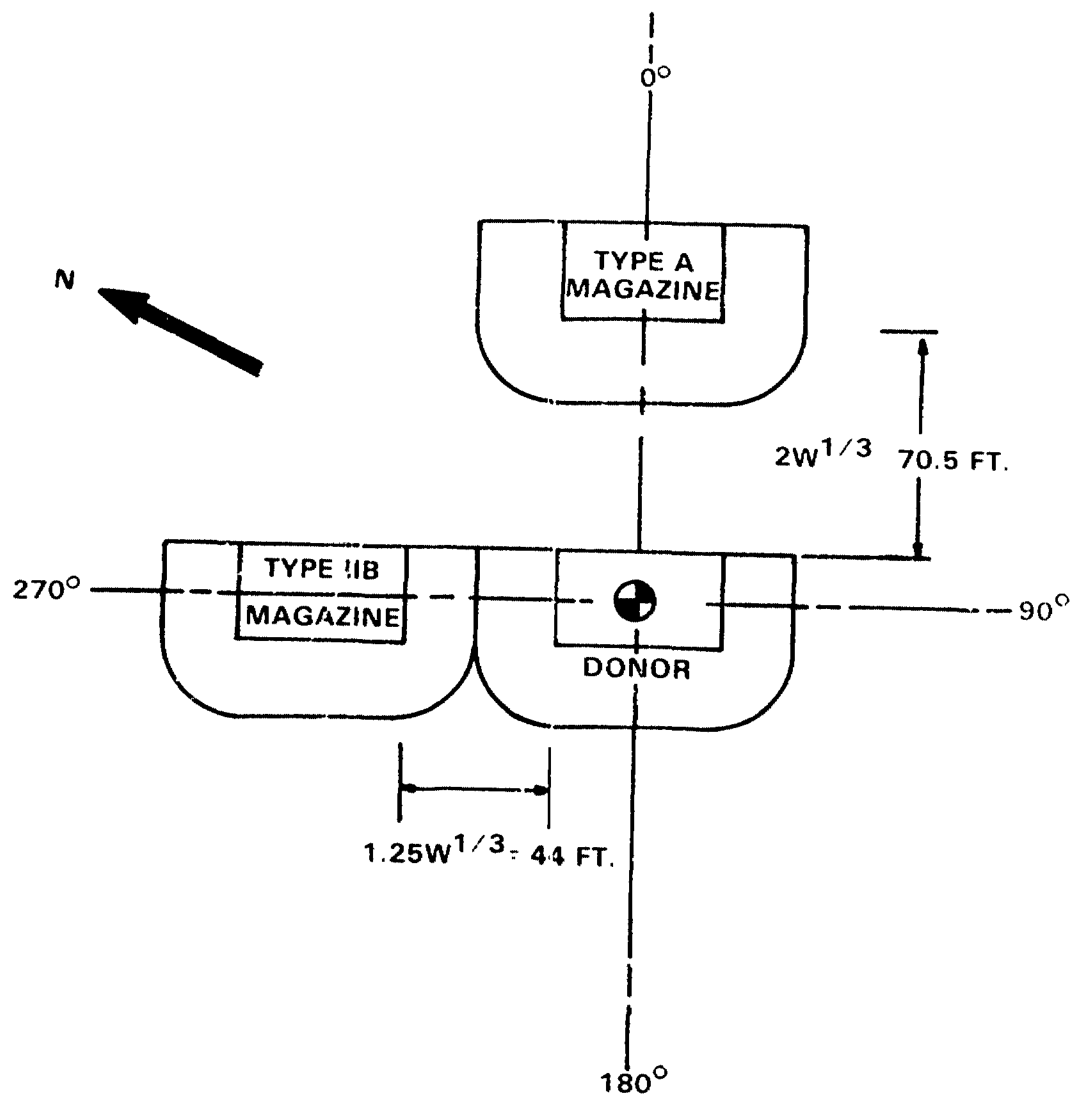

Figure 6.

ESKIMO VI EXPLOSIVE CHARGE LOCATIONS

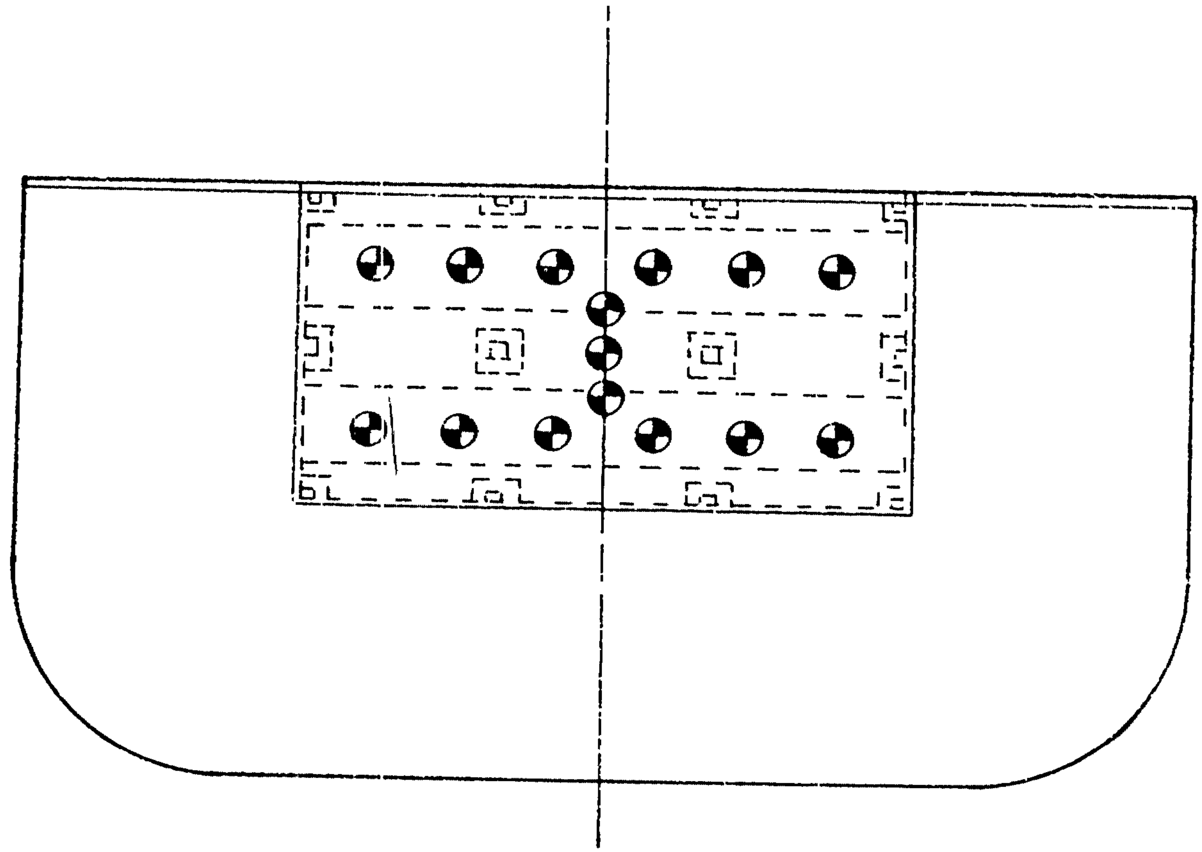

LOCATION OF MARK 16 TORPEDO GROUPS, 4 TORPEDOS PER GROUP

Figure 7.

WEAPONS REQUIREMENT, PALLETIZING
DOMESTIC UNIT LOAD
WARHEAD, TORPEDO, MK 16 MOD 6

UNIT LOAD DATA — DODIC/NALC NO.	FULL UNIT LOAD 1600	PARTIAL UNIT LOAD T600
WARHEADS PER UNIT LOAD	4	1
WEIGHT OF ONE WARHEAD (APPROX)	920 lbs	920 lbs
WEIGHT OF WOOD BASE (APPROX)	119 lbs	144 lbs
WEIGHT OF WOOD POSTS AND COVER (APPROX)	149 lbs	170 lbs
WEIGHT OF STEEL STRAPPING (APPROX)	20 lbs	20 lbs
GROSS WEIGHT OF UNIT LOAD (APPROX)	3968 lbs*	1254 lbs*
CUBE	69 cu ft	69 cu ft

* DO NOT USE FOR SHIPPING PURPOSES

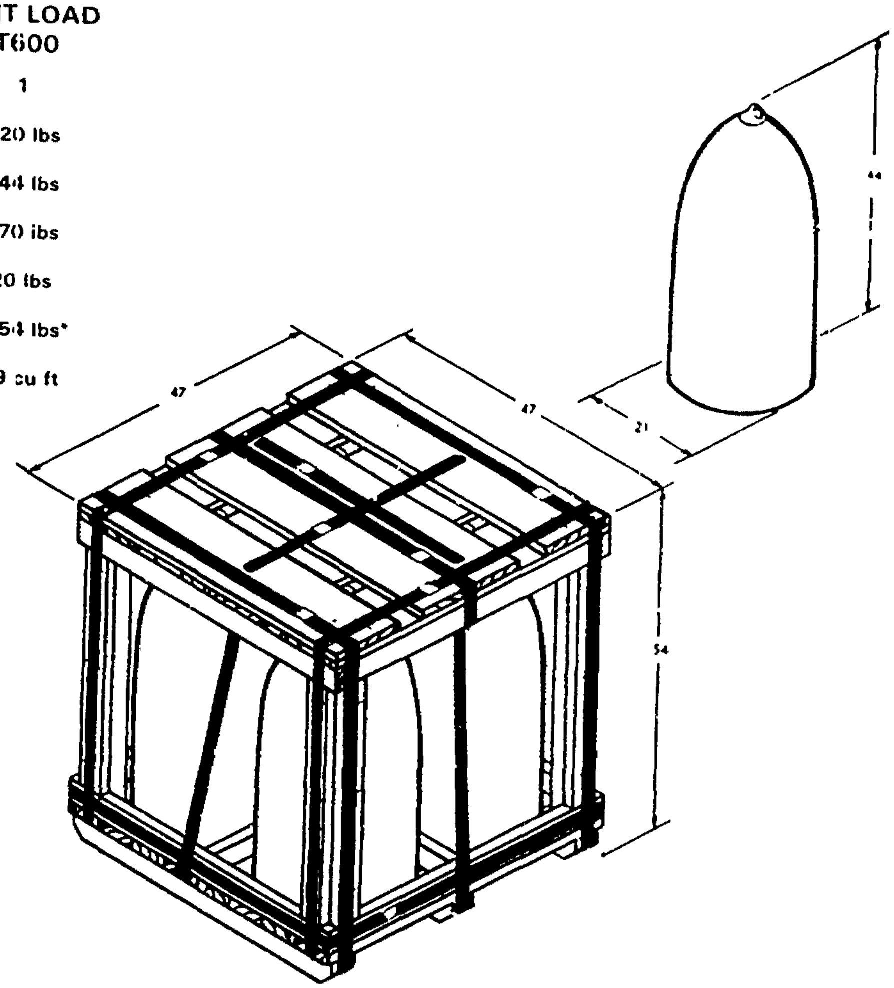

Figure 3. View Inside the ESKIMO VI Donor Illustrating Torpedo Placement.

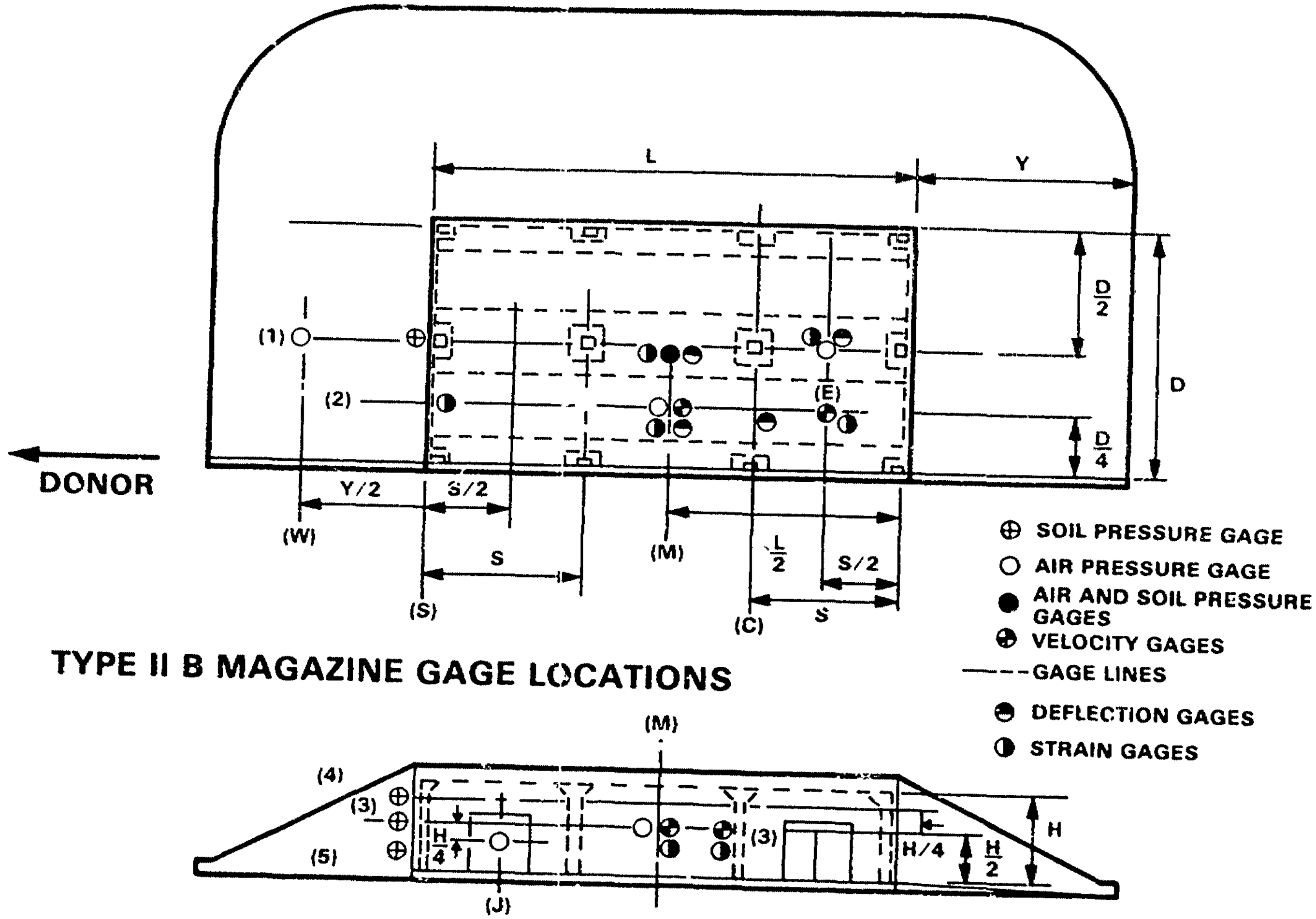

DONOR
L
Y
D
D/2
D/4
(1)
(2)
(E)
Y/2
S/2
S
(W)
(S)
(M)
L/2
(C)
TYPE II B MAGAZINE GAGE LOCATIONS
SOIL PRESSURE GAGE
AIR PRESSURE GAGE
AIR AND SOIL PRESSURE GAGES
VELOCITY GAGES
GAGE LINES
DEFLECTION GAGES
STRAIN GAGES
(4)
(3)
(5)
H/4
(J)
H
H/2

Figure 9.

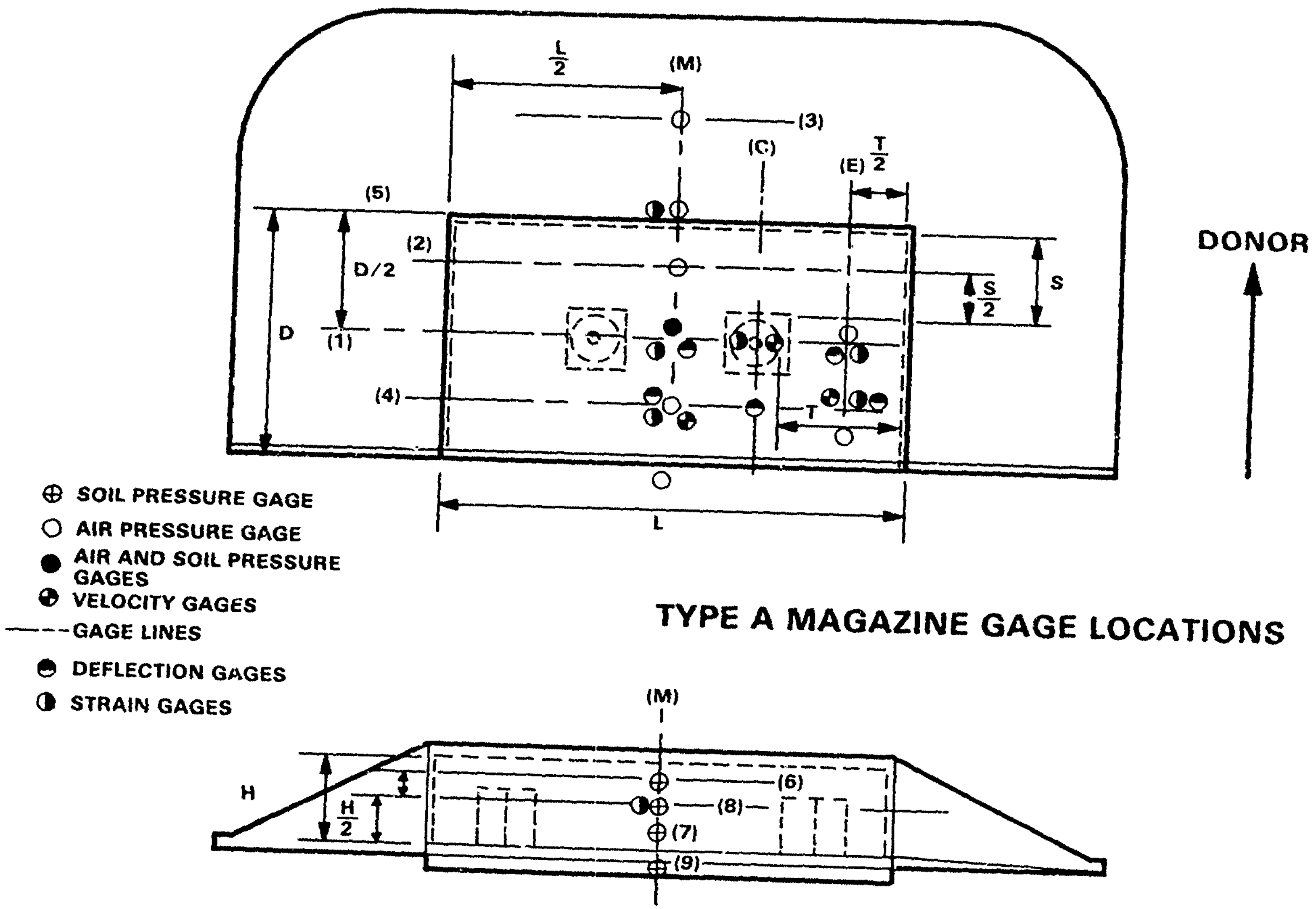
DONOR
L/2
(M)
(3)
(C)
(E)
T/2
(5)
(2)
D/2
D
(1)
(4)
S
S/2
T
L
⊕ SOIL PRESSURE GAGE
○ AIR PRESSURE GAGE
● AIR AND SOIL PRESSURE GAGES
VELOCITY GAGES
GAGE LINES
DEFLECTION GAGES
STRAIN GAGES
TYPE A MAGAZINE GAGE LOCATIONS
(M)
H
H/2
(6)
(8)
(7)
(9)

Figure 10.

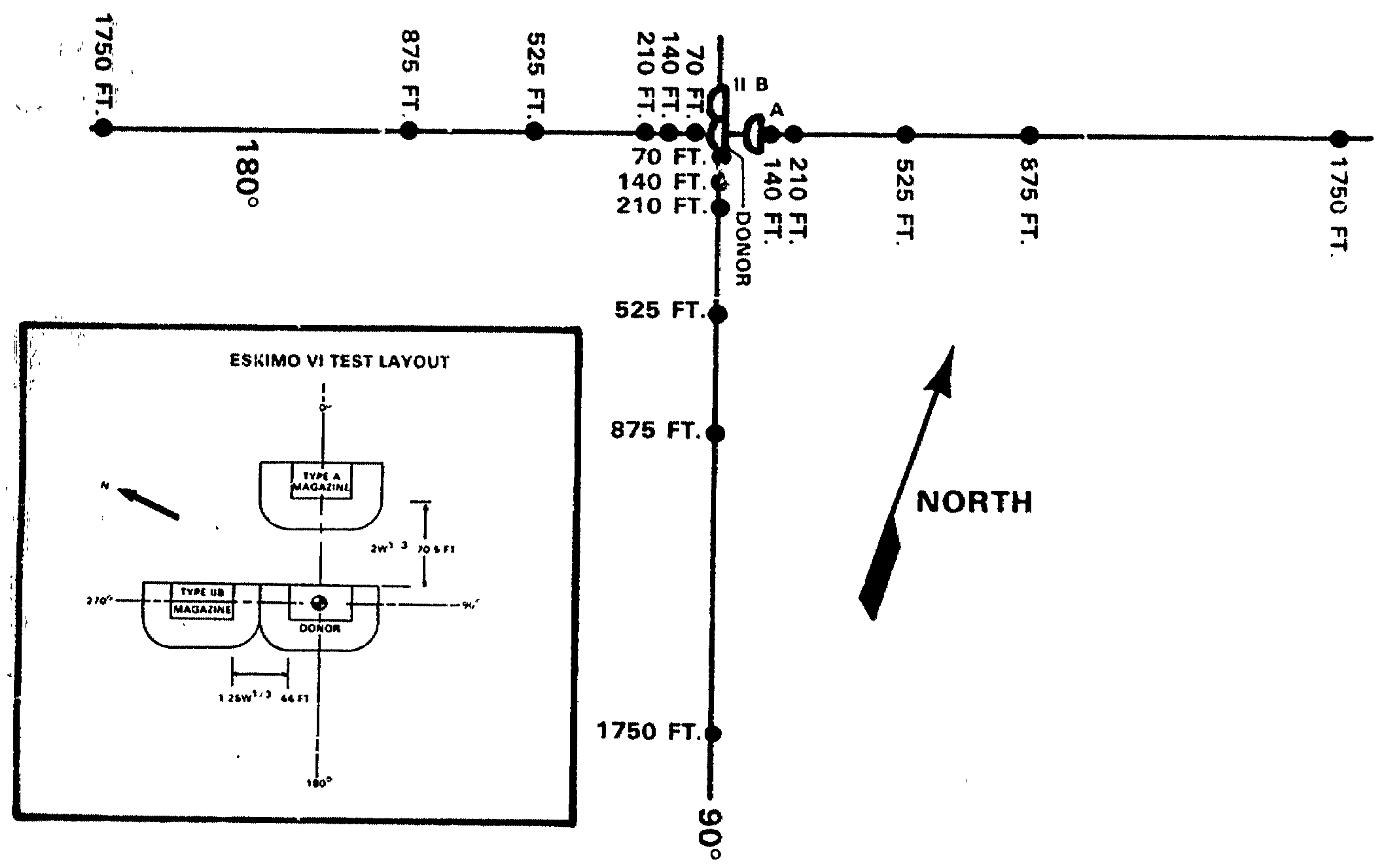

Figure 11. Free Field Pressure Gage Locations.

Figure 12. ESKIMO VI Test Structures Prior to Test Conduction.

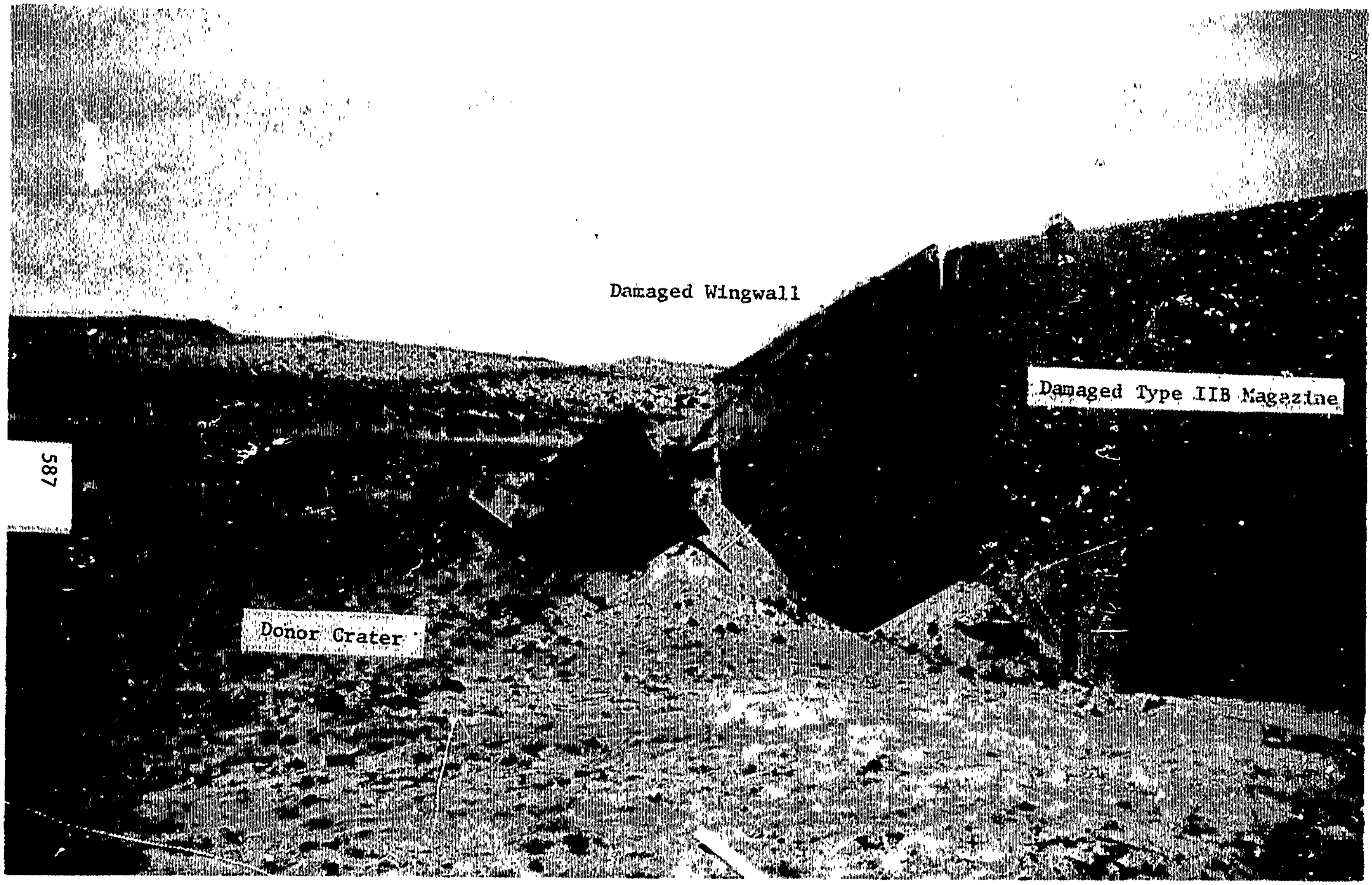

Figure 13. Donor Crater and Damage to Type IIB South Wingwall (View Looking South).

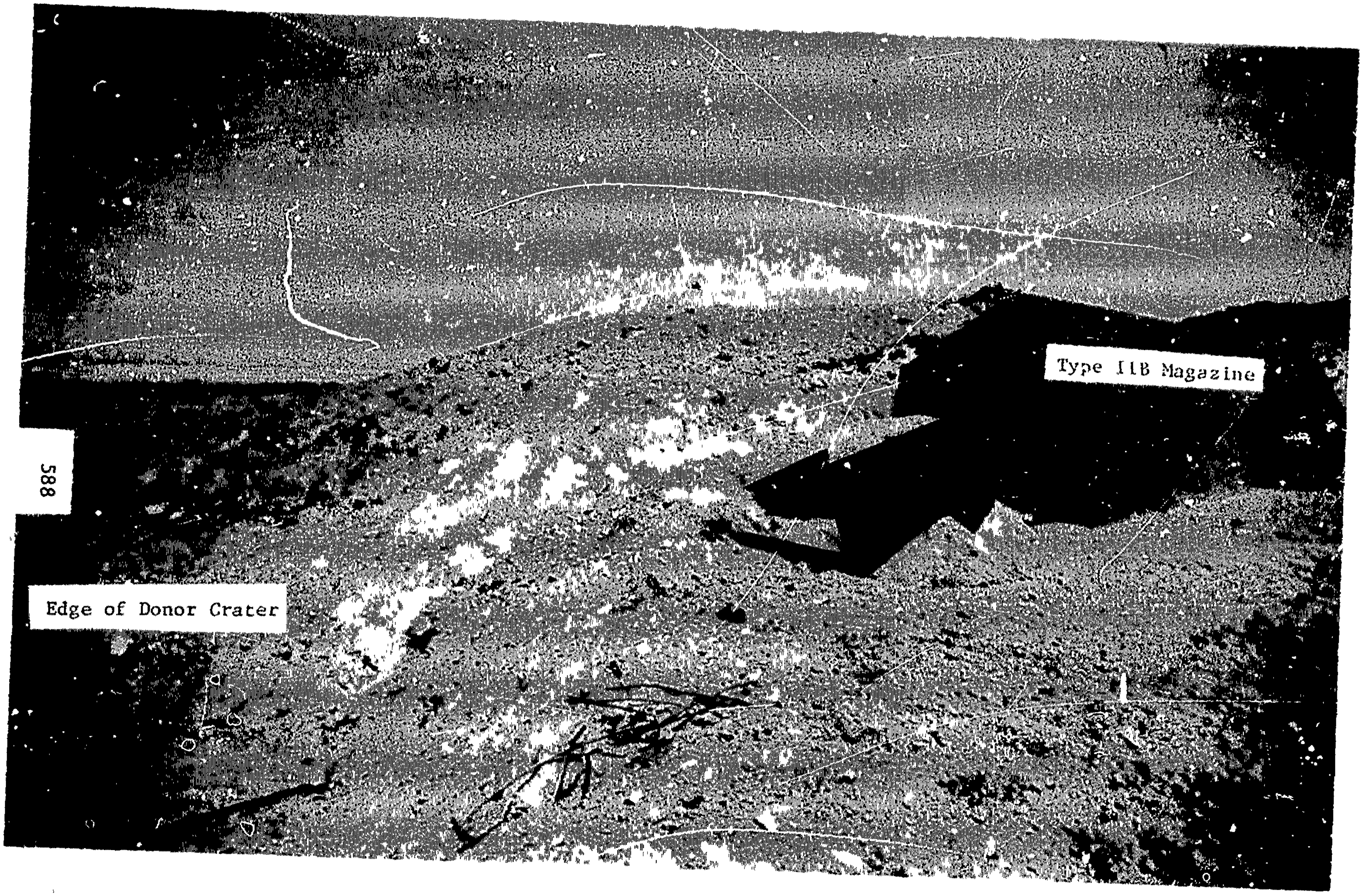

Figure 14. Donor Crater and Damage to the Type IIB's South Wingwall (View Looking North-West).

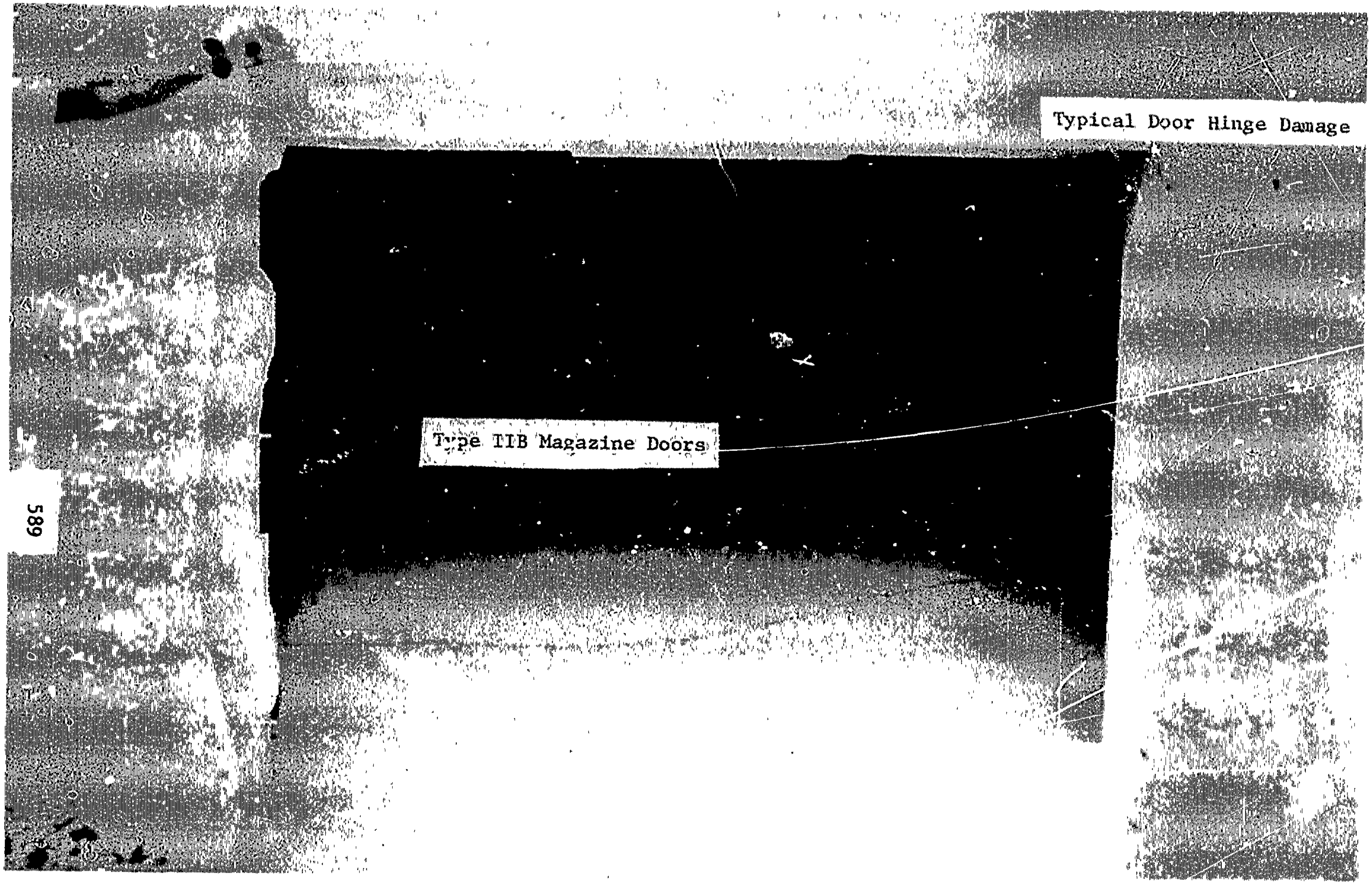

Figure 15. View Looking Into the Type IIB Magazine Illustrating Door Damage (View Into South Door Opening).

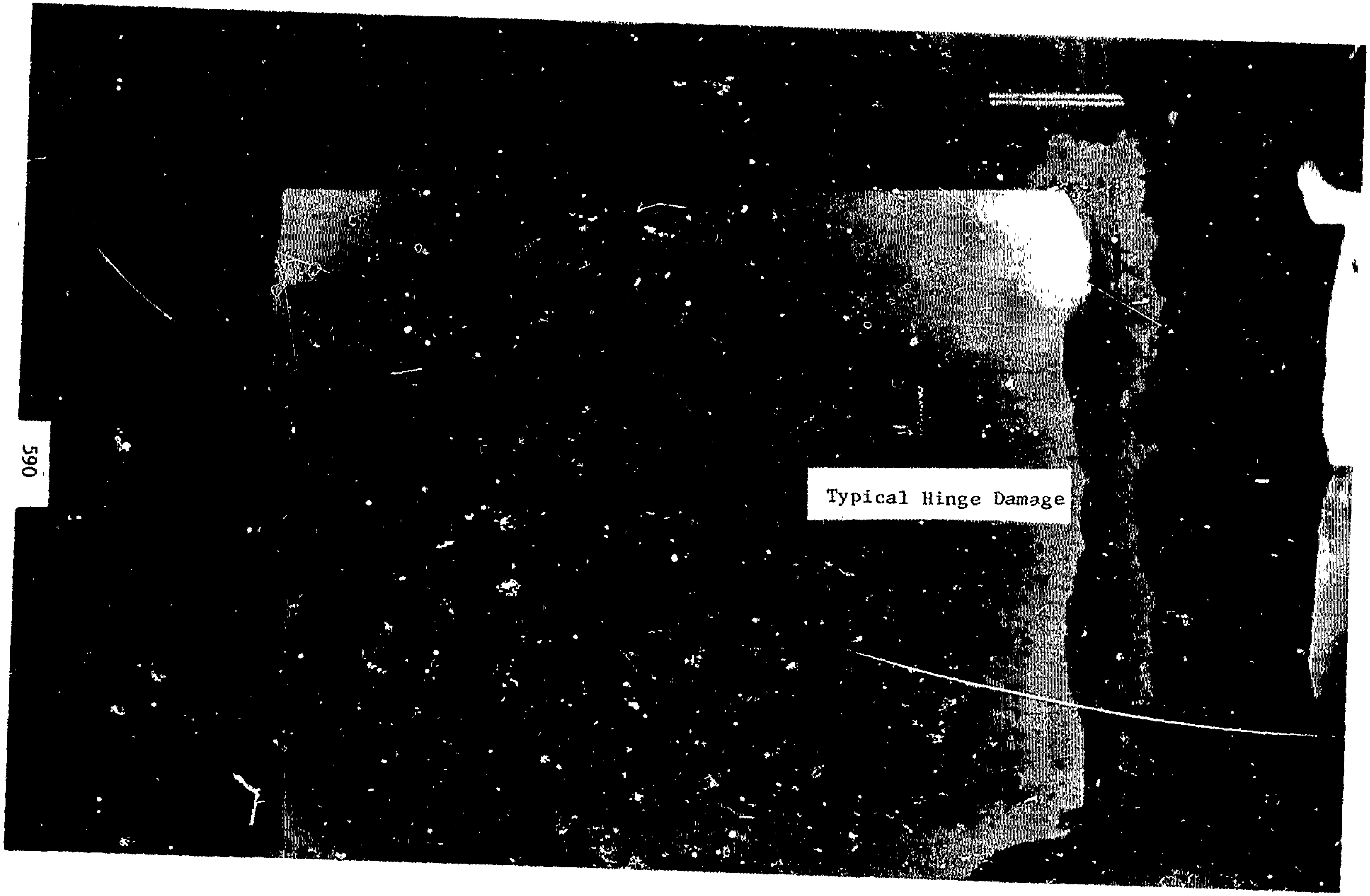

Figure 16. View Looking Out of the Type IIB Magazine Illustrating Door Hinge Damage (View Out South Door Opening).

Figure 17. Type IIB Magazine Doors Final Resting Place (View Looking into South Door Opening).

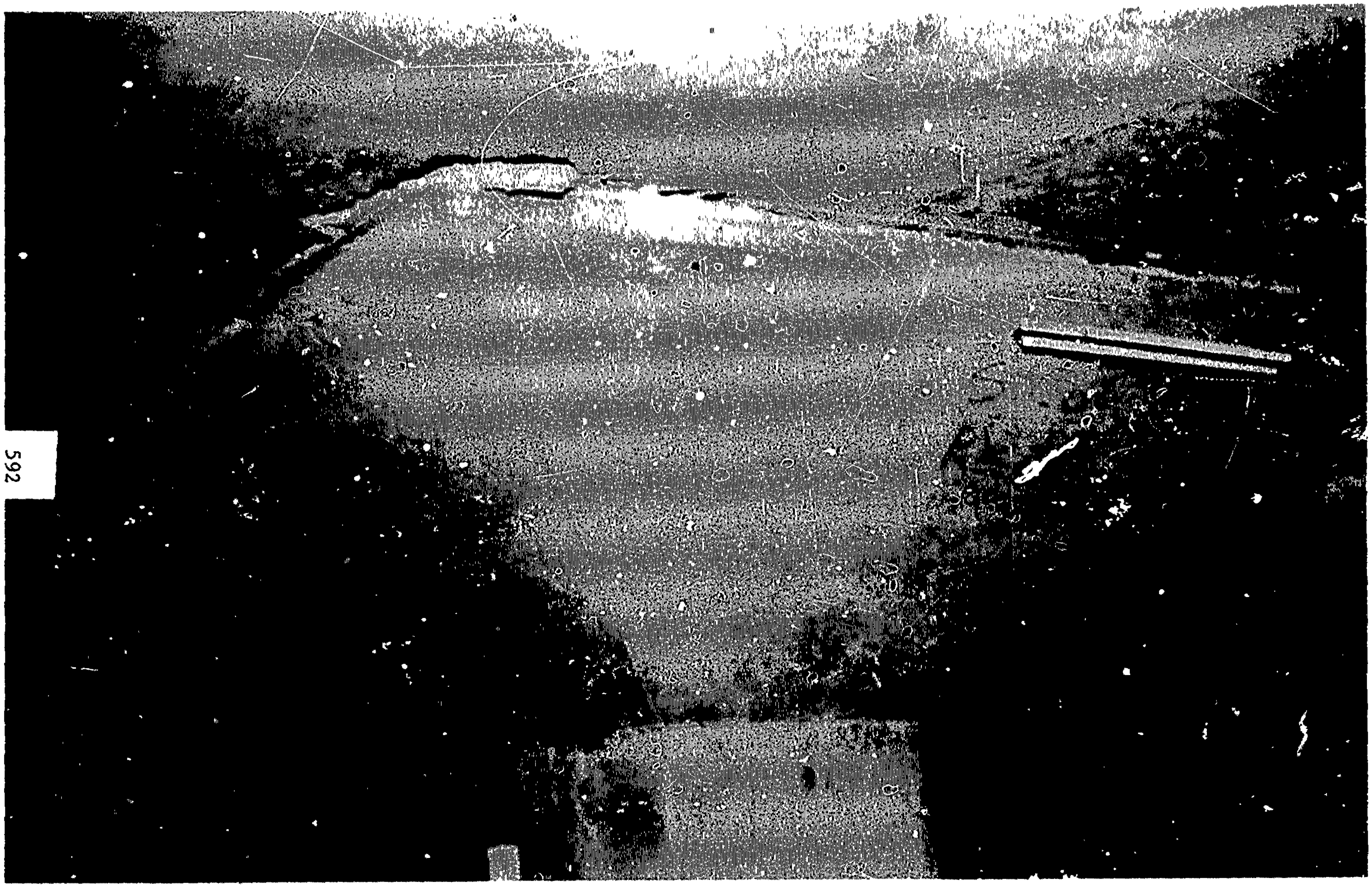

Figure 18. South Column Damage (View at Rear of South Column Capital).

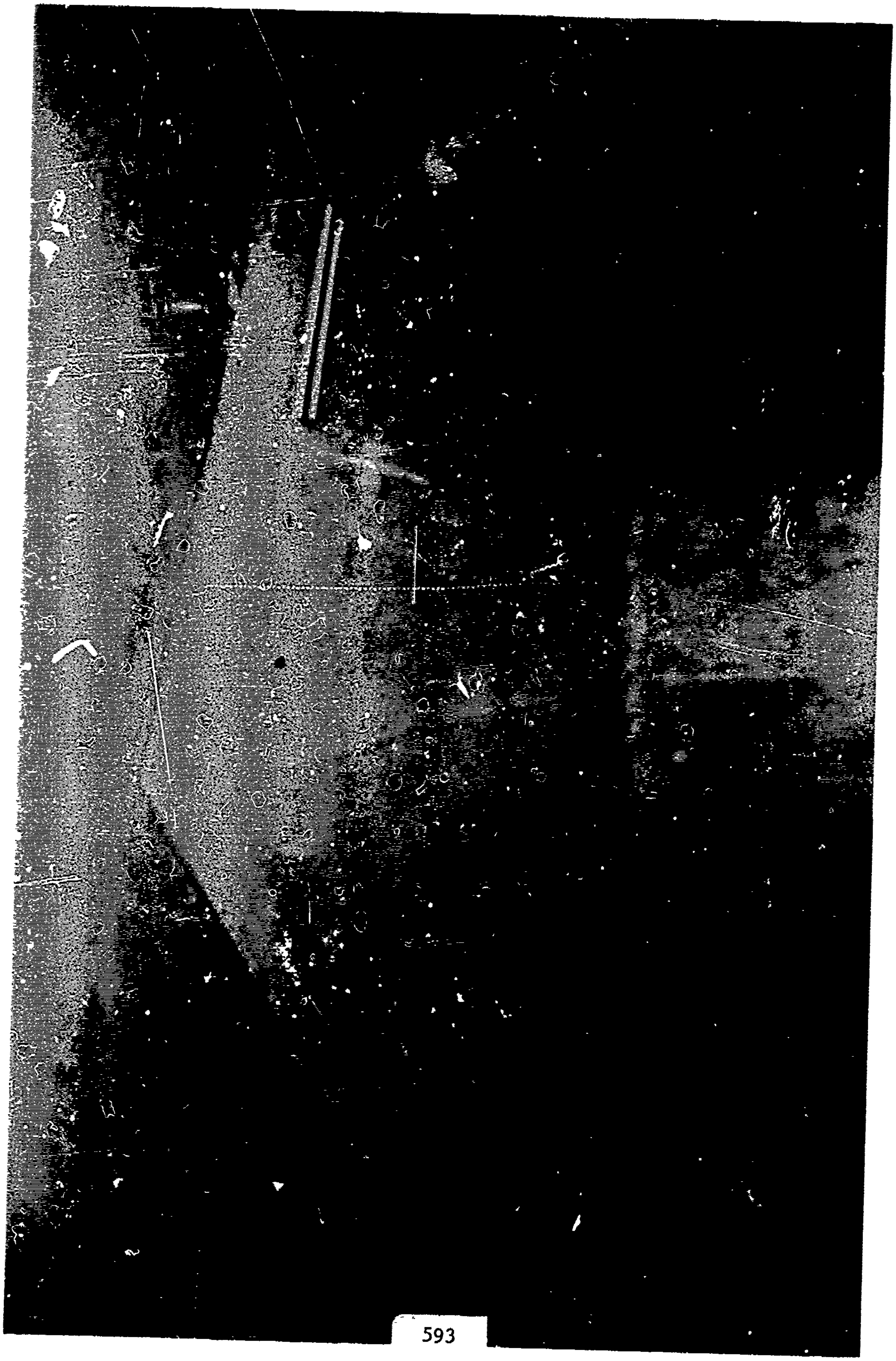

Figure 19. South Column Damage View at Front of South Column Capital.

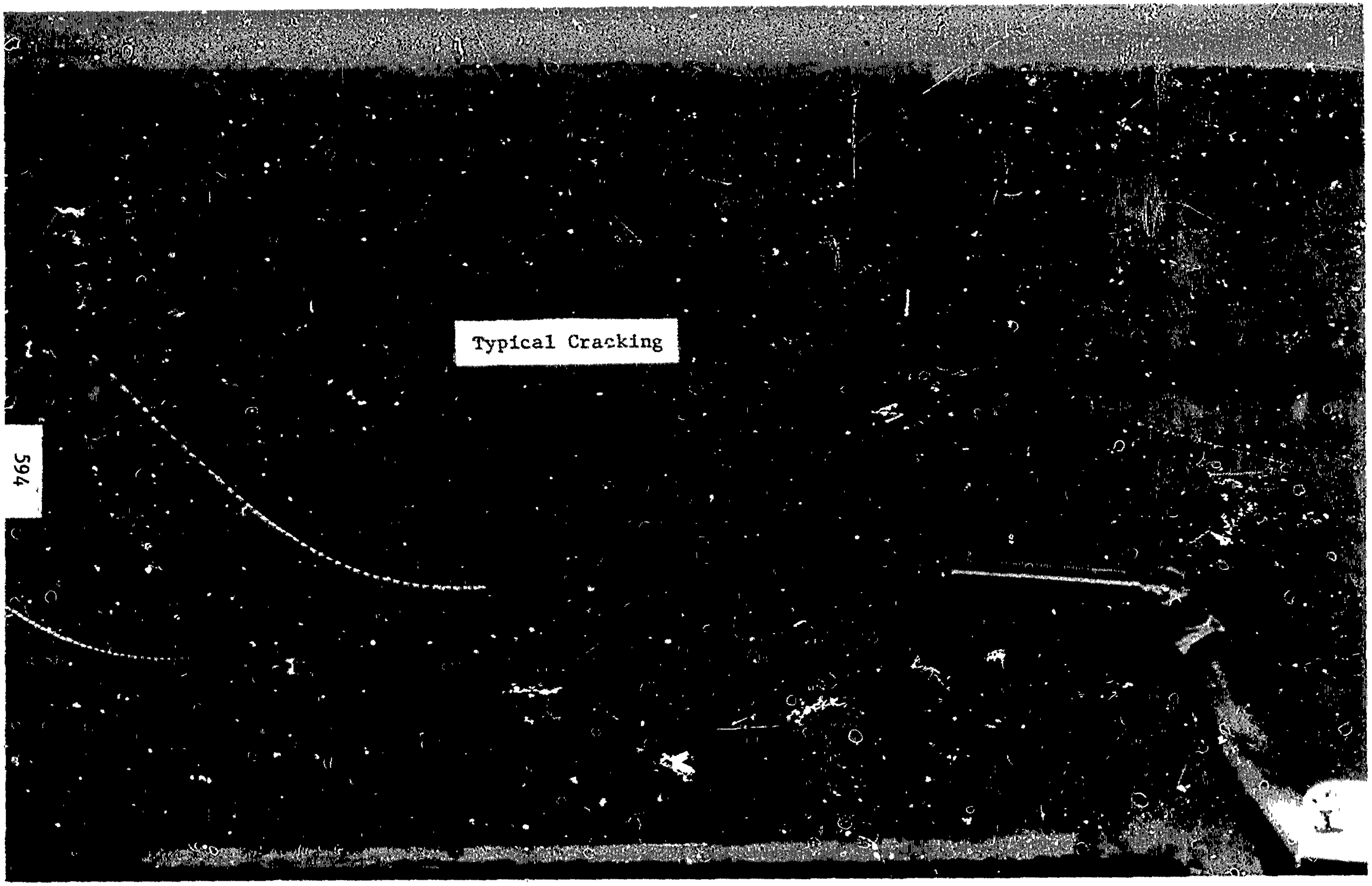

Figure 20. Typical Cracking Found Above the Type IIB South Door Opening.

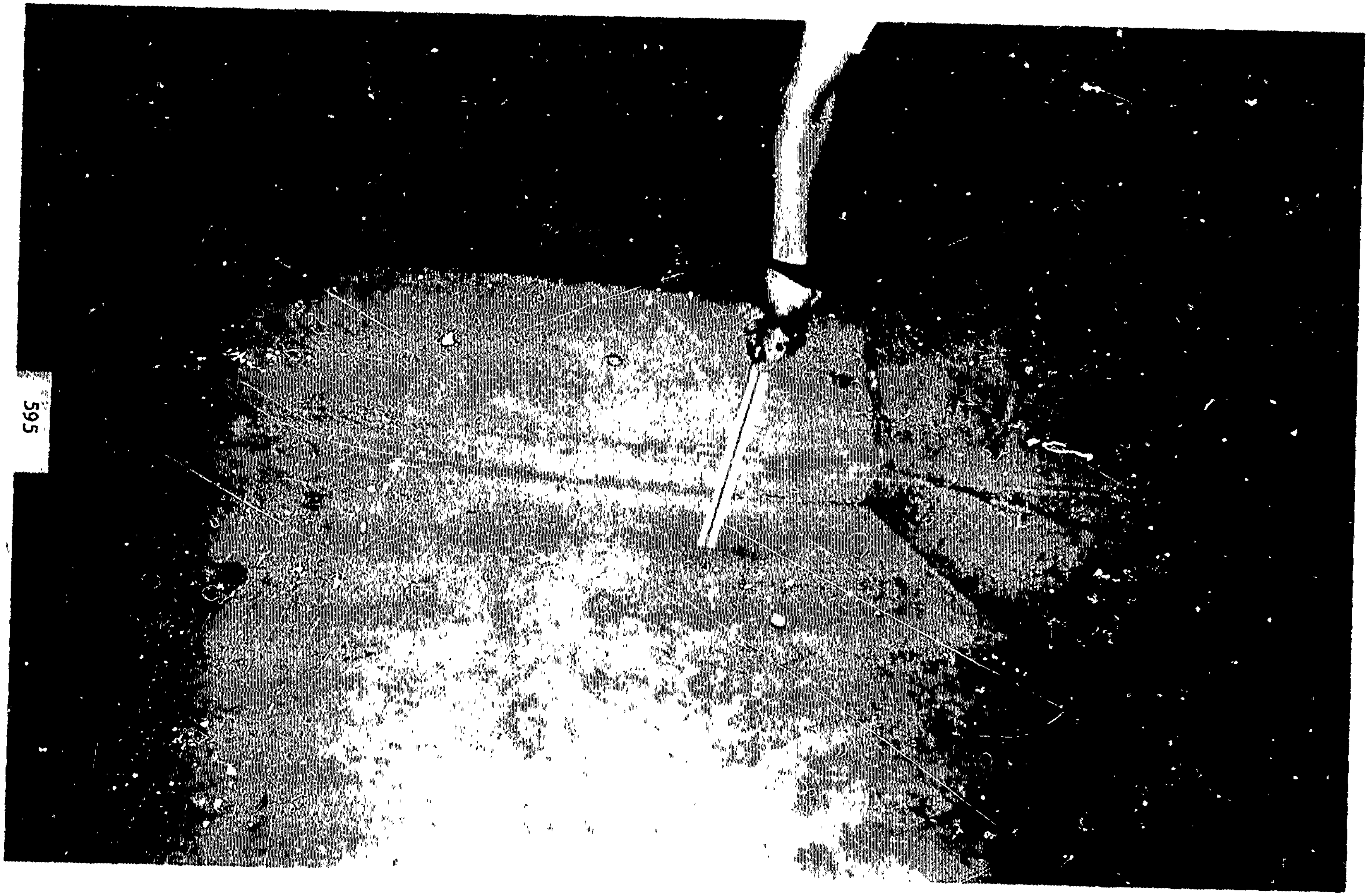

Figure 21. Type IIB Magazine Pilaster Damage (View of Center Pilaster-South Wall).

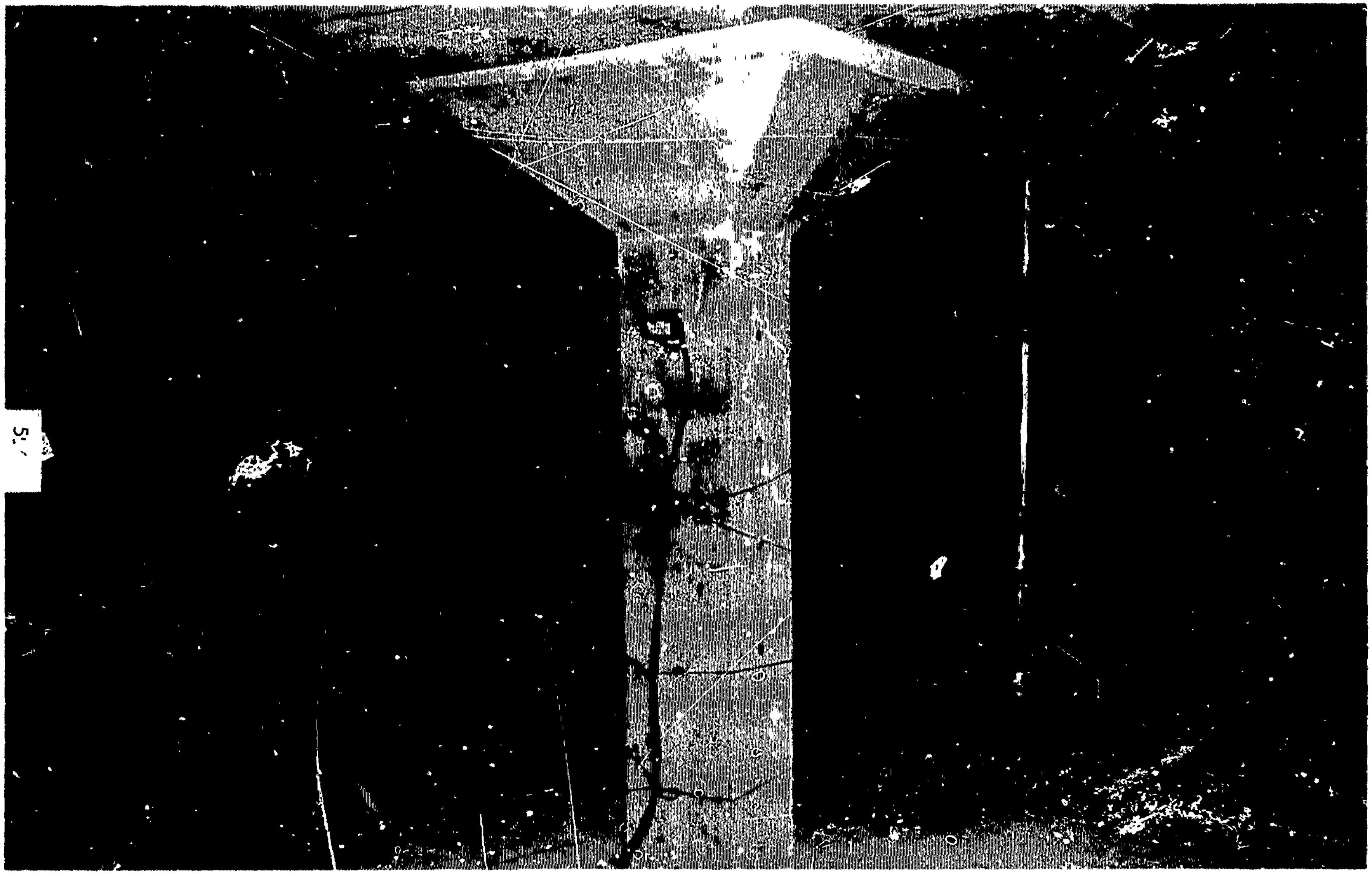

Figure 22. Type IIB Magazine North Column Illustration of Minor Damage (View Towards North-West Corner).

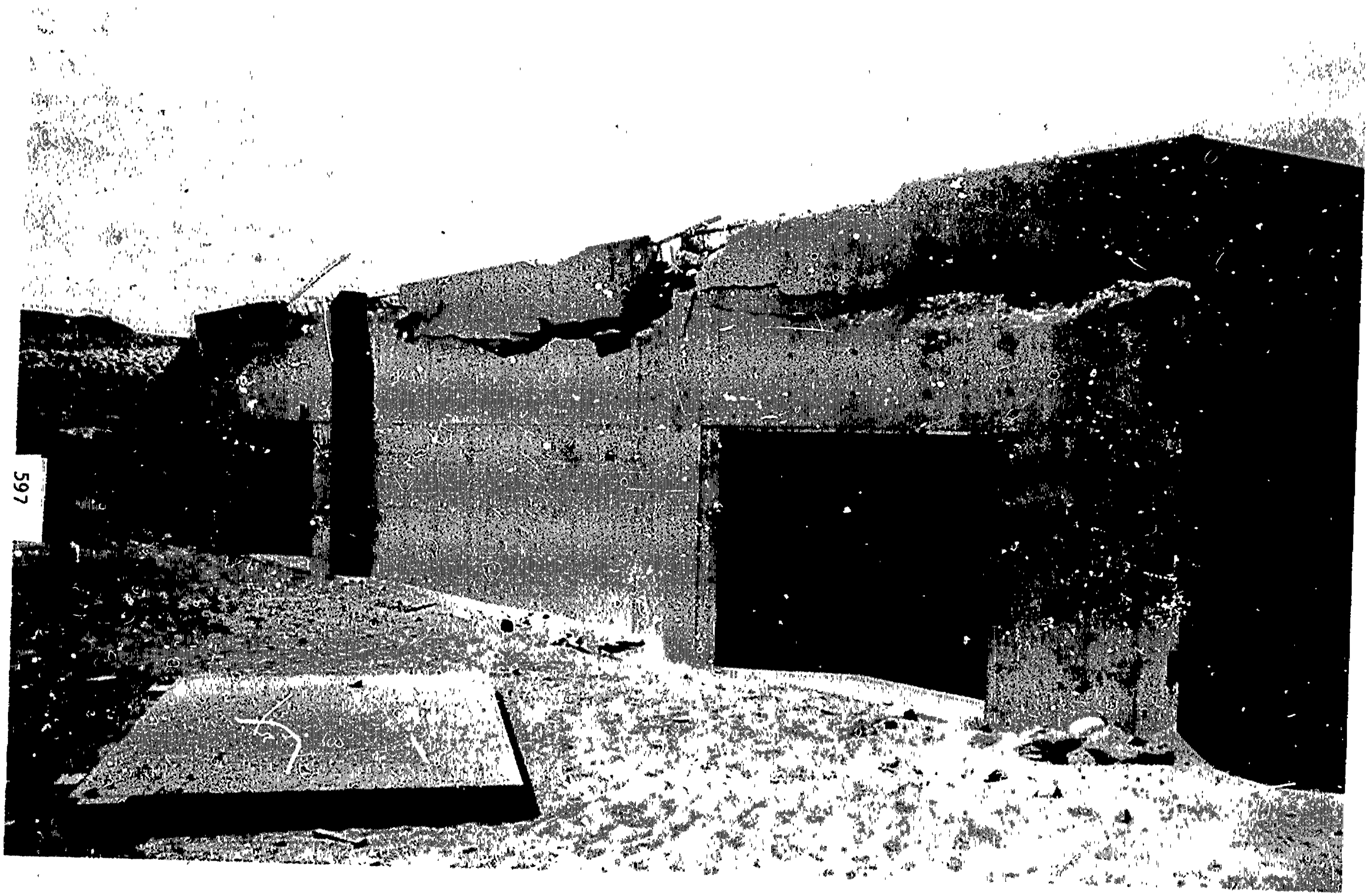

Figure 23. Type A Magazine Parapet Damage and Final Door Locations (View Towards South).

Figure 24. Type A Magazine Roof Parapet Damage (View From Roof Towards East).

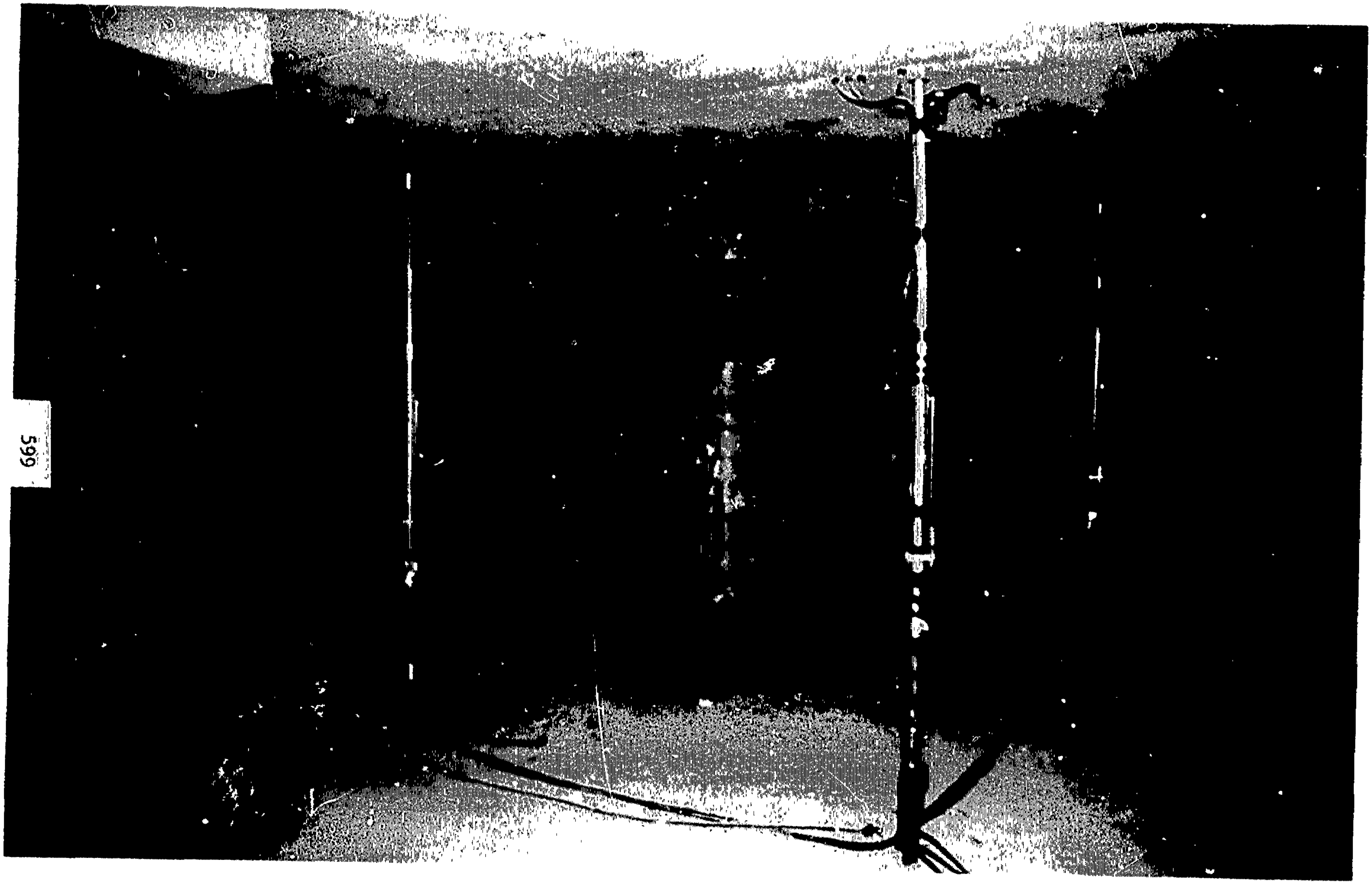

Figure 25. Type A Magazine Interior (View From North Door Opening).

OFFICIAL U. S. NAVY PHOTOGRAPH (LDH)
PORT HUENEME, CALIFORNIA

9607-80

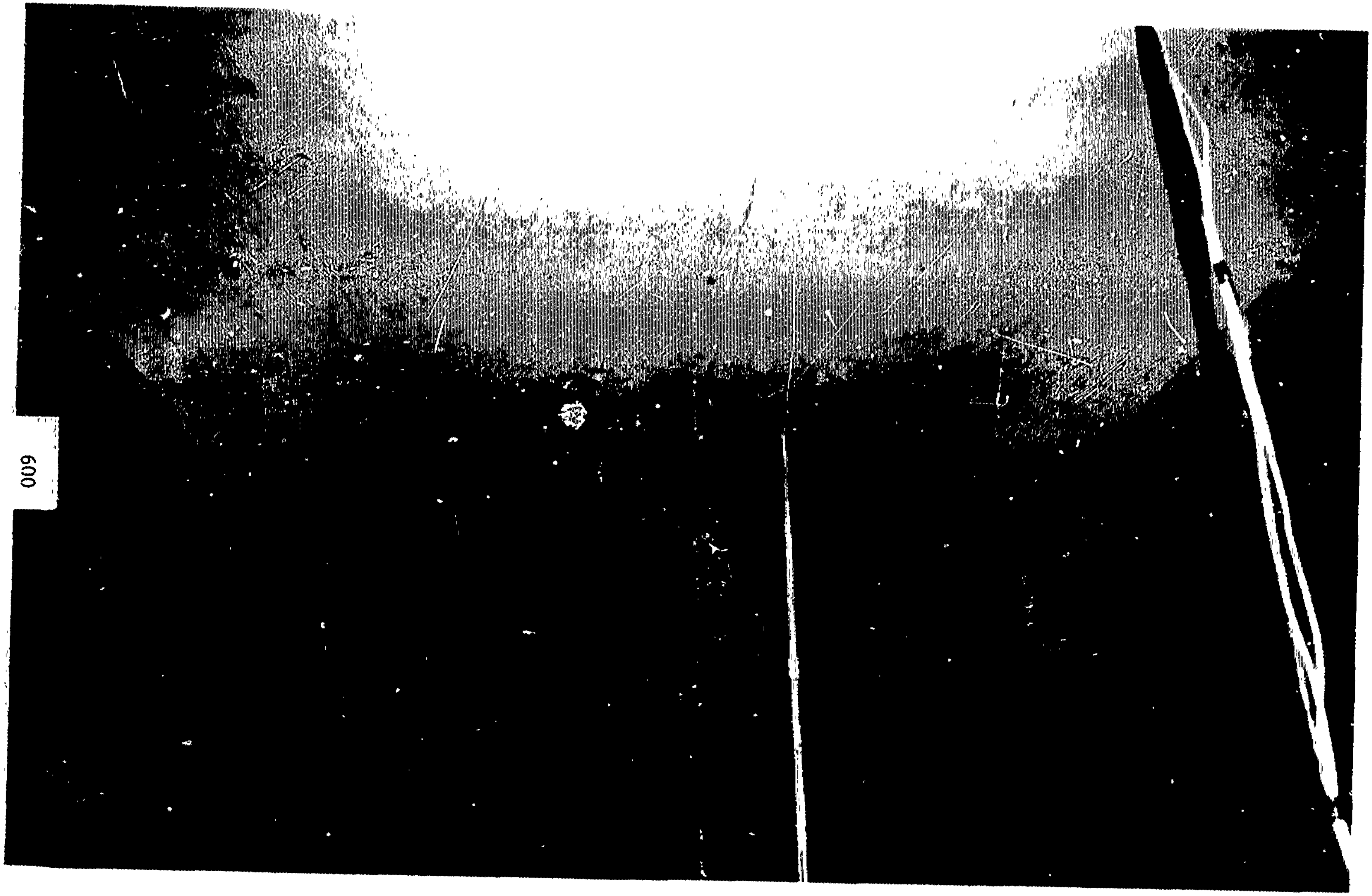

Figure 26. Type A Magazine Interior and Roof (View From North Door Opening).

OFFICIAL U. S. NAVY PHOTOGRAPH (LDH)
PORT HUENEME, CALIFORNIA

9611-80

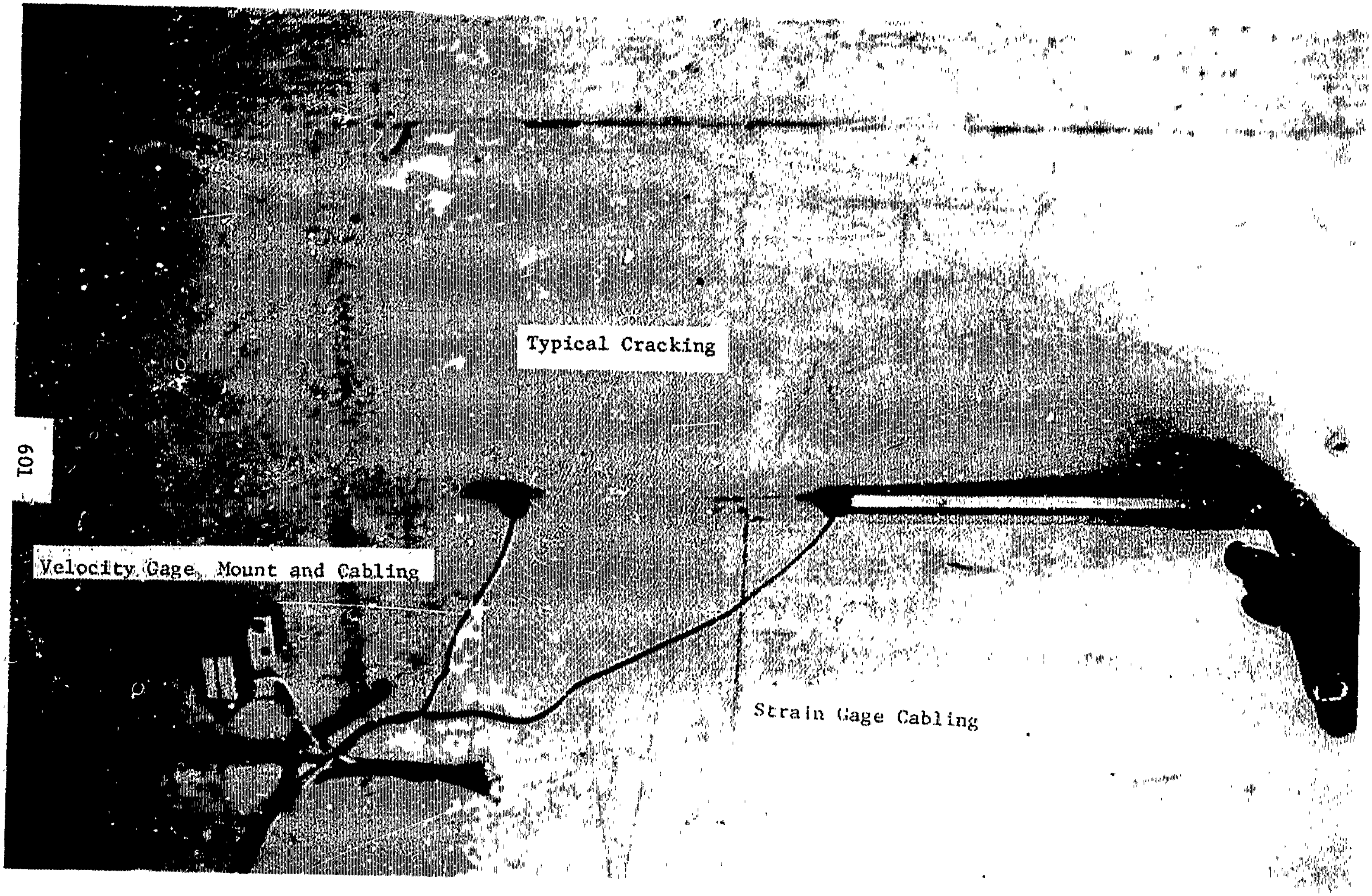

Figure 27. Typical Type A Magazine Roof Cracks.

OFFICIAL U. S. NAVY PHOTOGRAPH (LDH)
PORT HUENEME, CALIFORNIA

9602-80

ESKIMO VI CAMERA LOCATIONS AND FIELD OF VIEW DEFINITION

Figure 28.

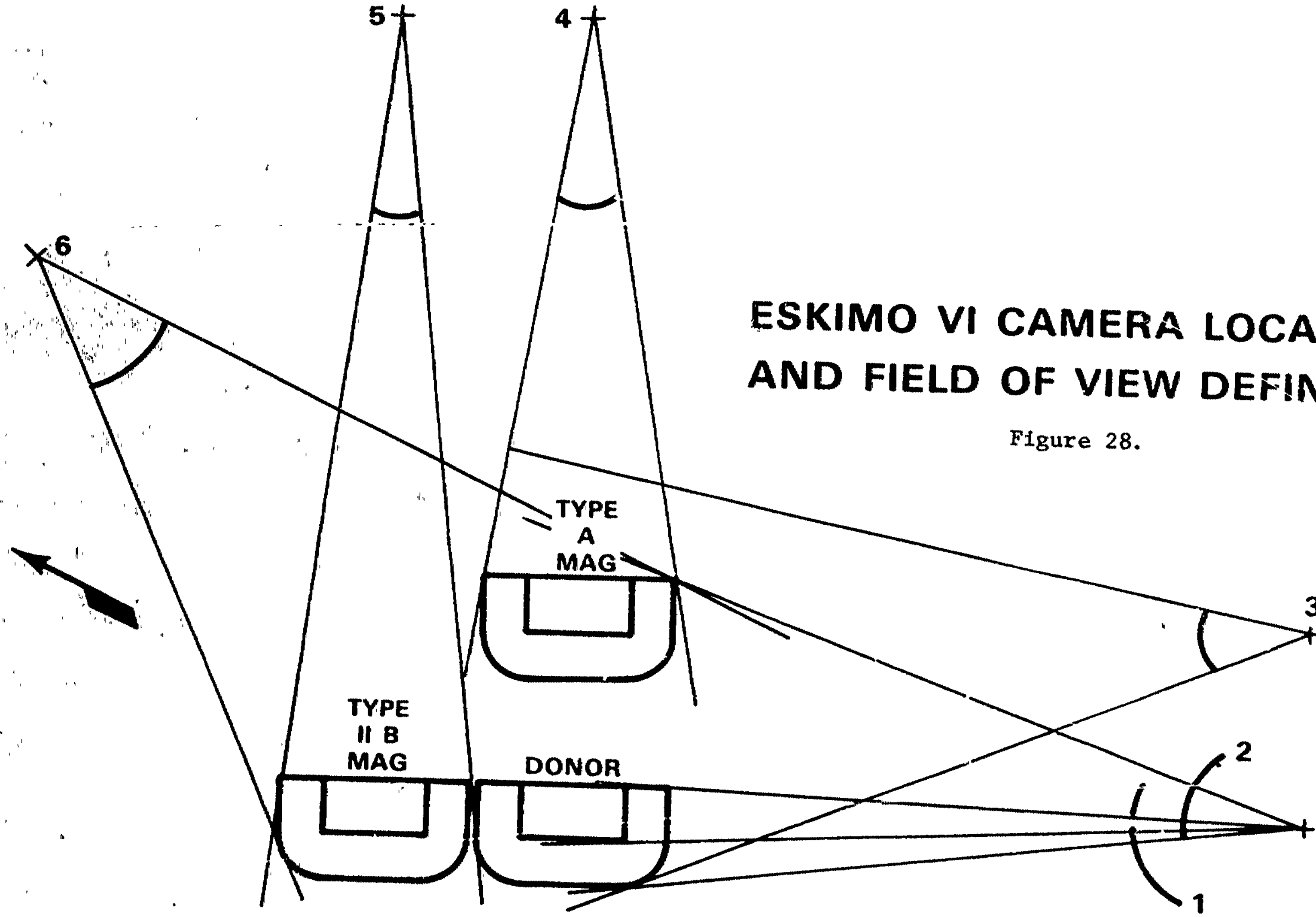

Figure 29. Typical Displacement Gage Output

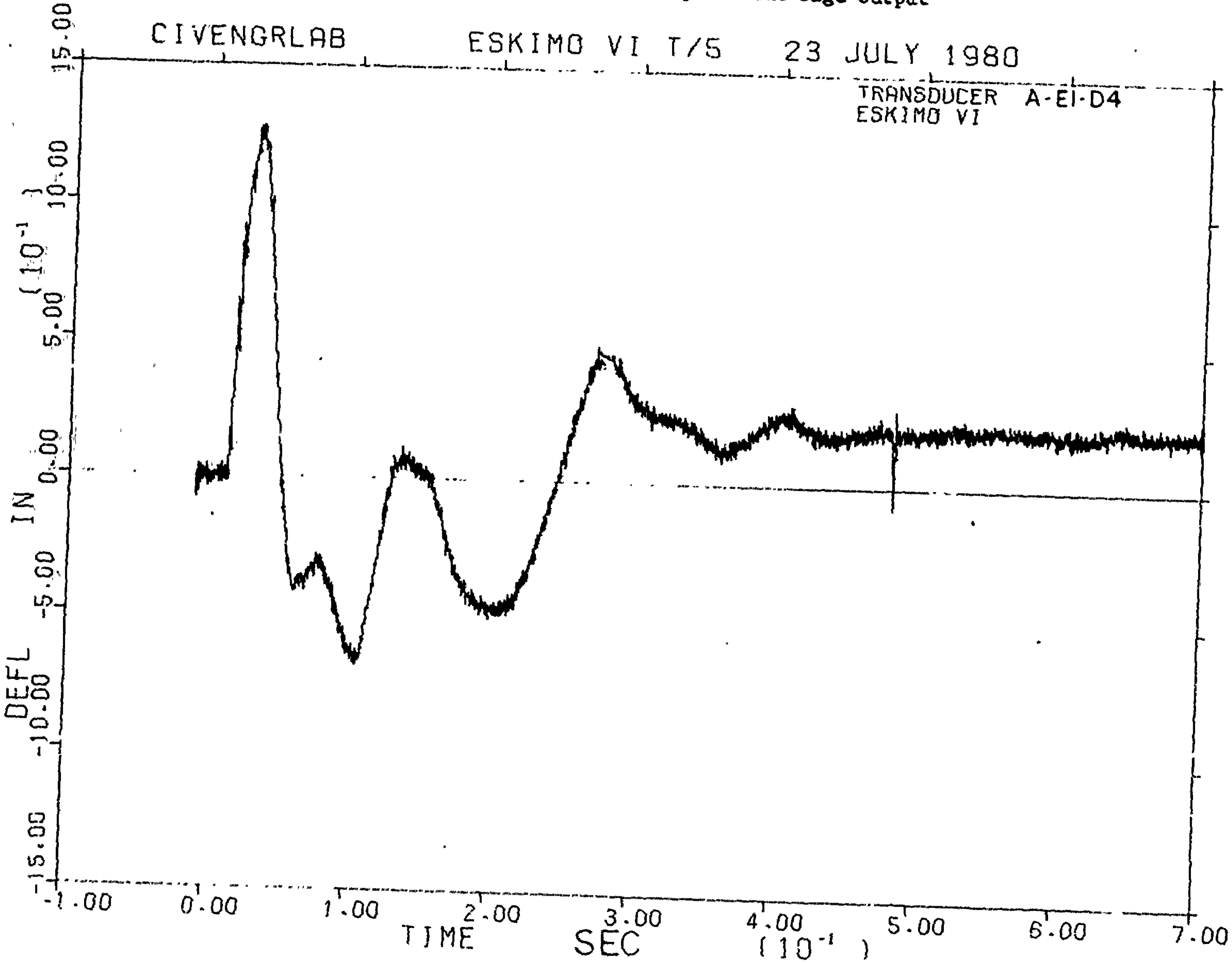

Figure 30. Typical Velocity Gage Output

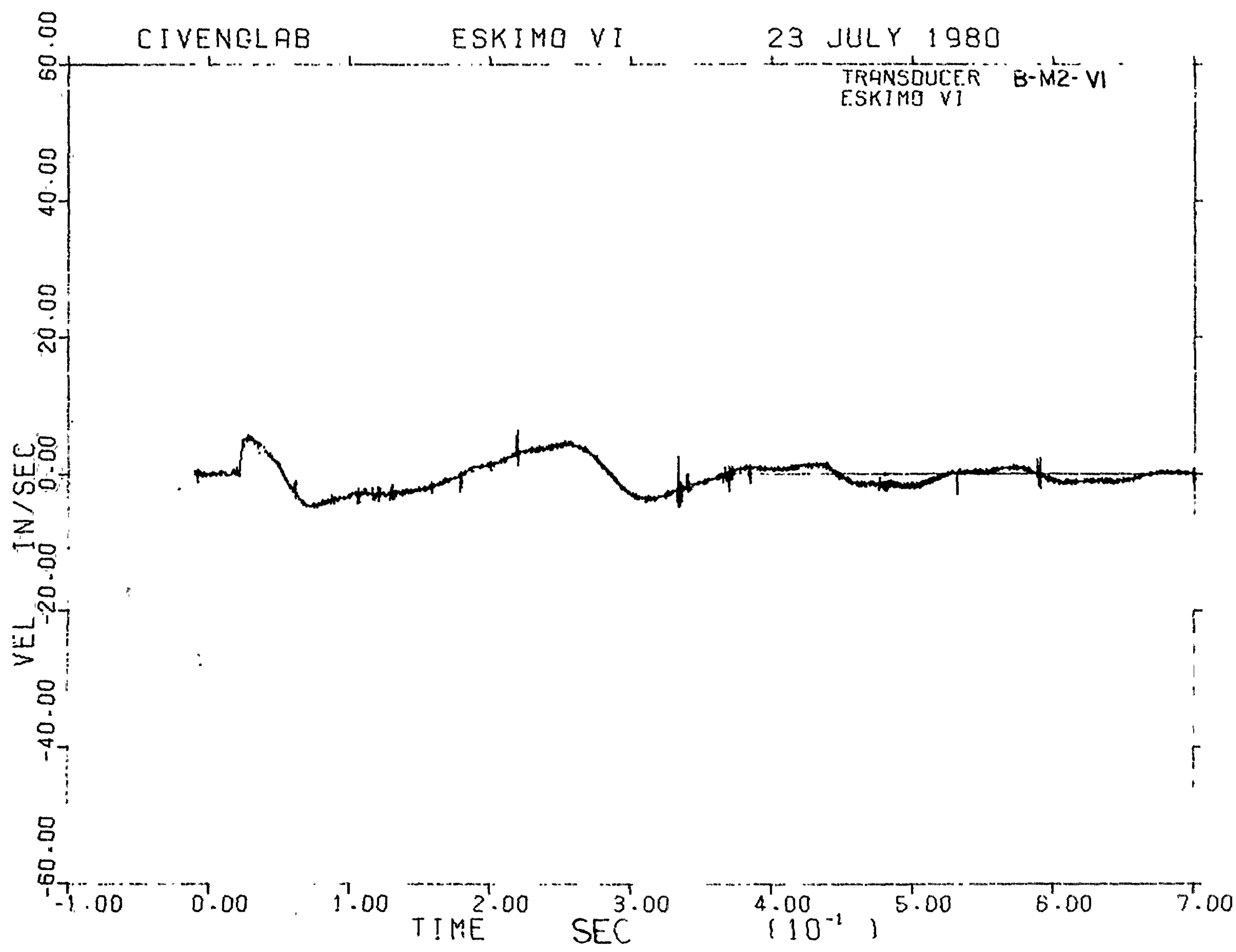

Figure 31. Typical Air Pressure Gage Output

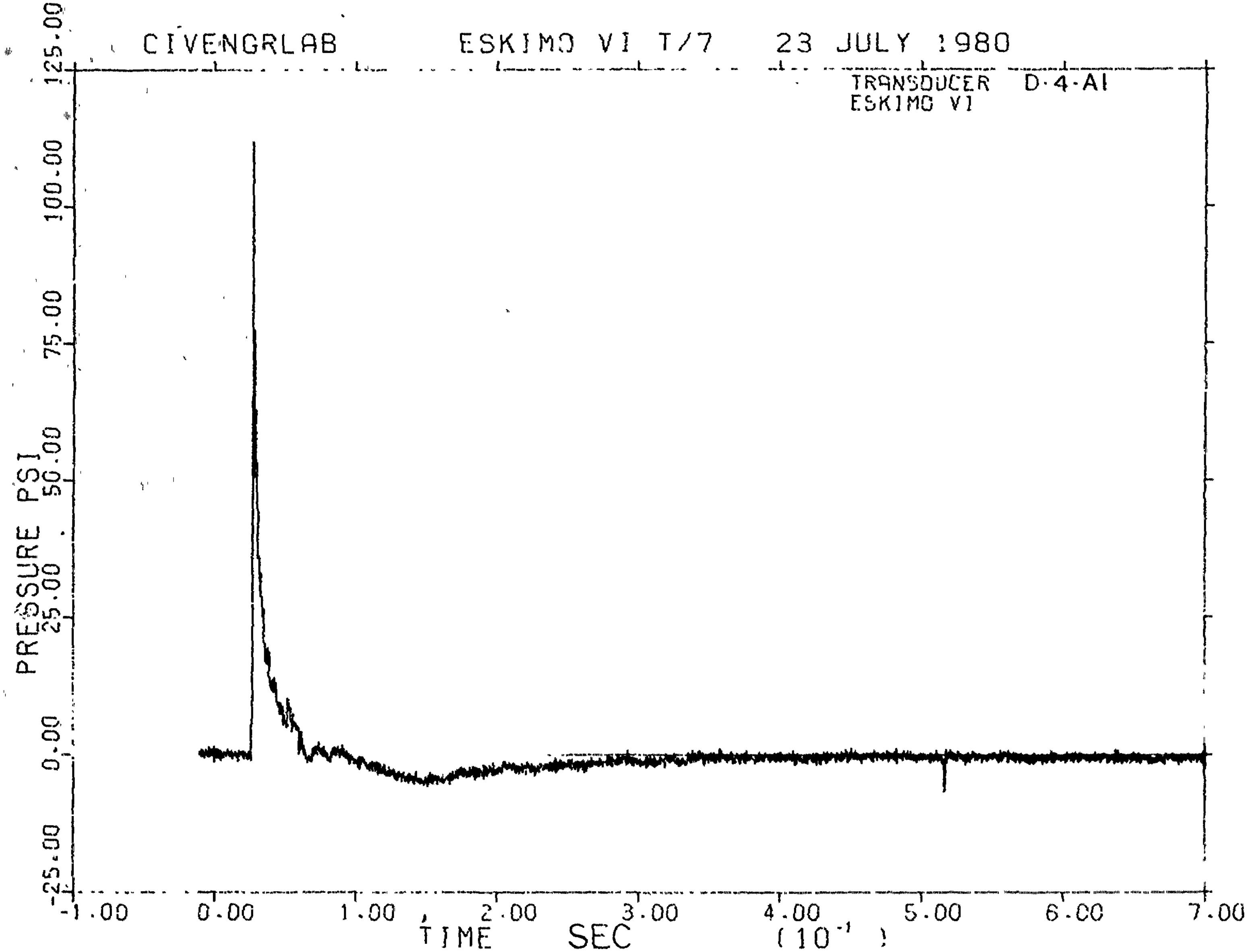

MAC/RAN PLOT OUTPUT

Figure 32. Typical Soil-Pressure Gage Output

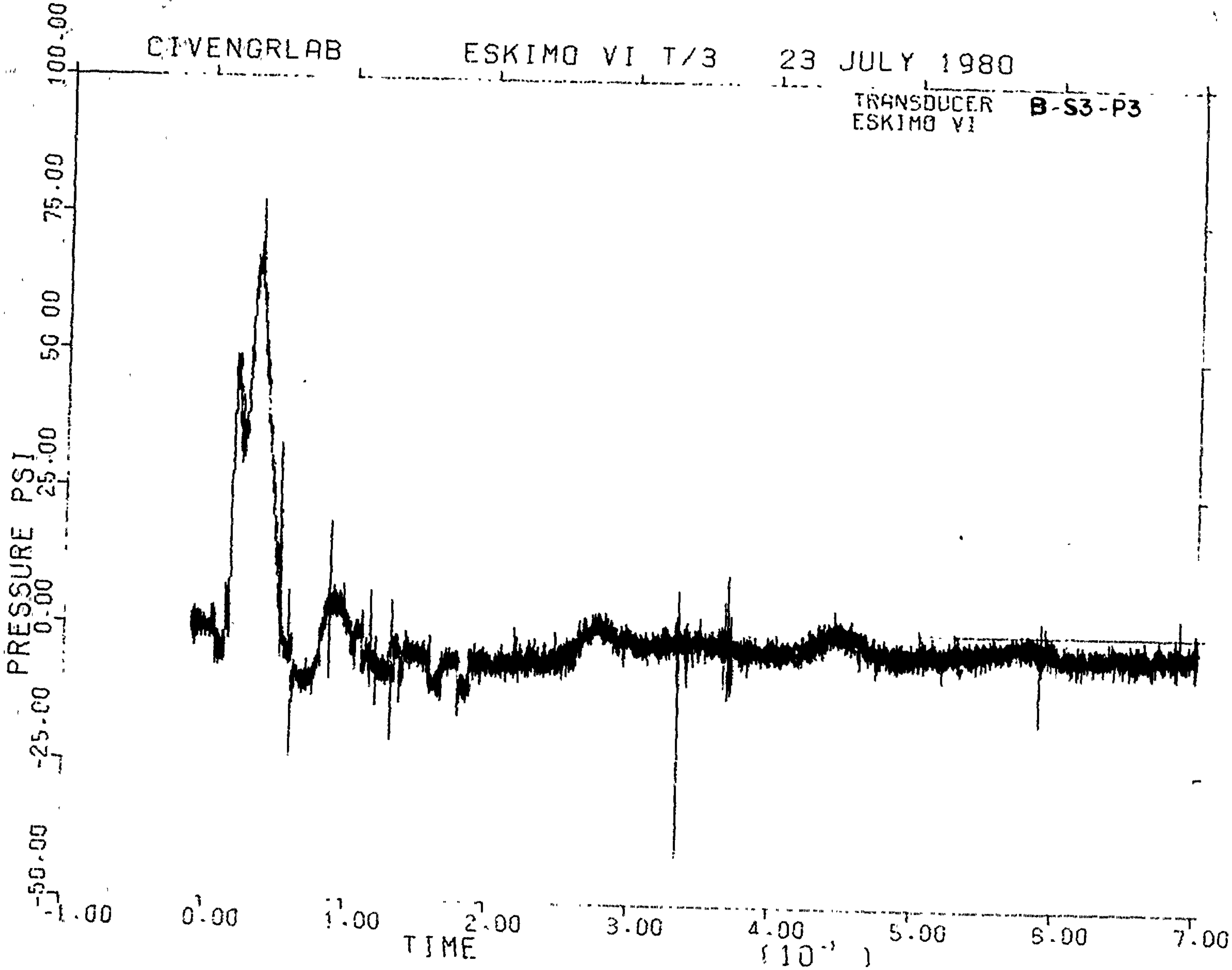

Figure 33. Typical Strain Gage Output

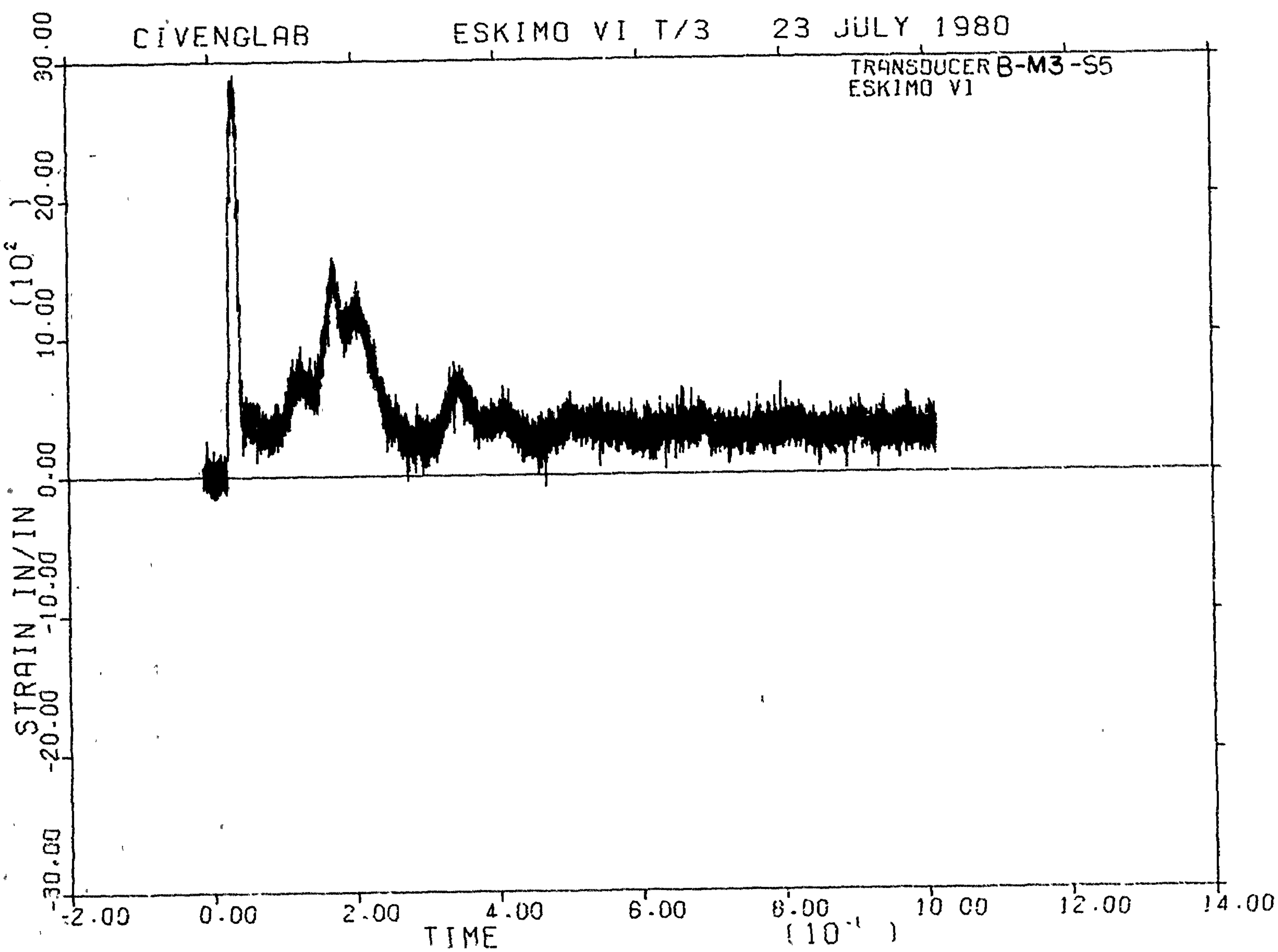

MAC/RAN PLOT OUTPUT

Revised Quantity-Distance Criteria for Earth-Covered Igloos

H. J. Reeves
US Army Ballistic Research Laboratory
Aberdeen Proving Ground, Maryland

INTRODUCTION

The storage of small quantities of Hazard Division 1.1 ammunition or explosives in igloo magazines can be prohibitive due to current Quantity-Distance restrictions. The "Manual on NATO Safety Principles for the Storage of Ammunition and Explosives" dated 1976, section 413.d , requires a minimum distance of 400 metres between inhabited buildings and igloos containing Hazard Division 1.1 ammunition or explosives. No minimum net explosive quantity is associated with this 400-metre restriction. These restrictions are based, in part, on the extrapolation of test data acquired during large scale field trials with net explosive quantities in the thousands of pounds.

Described in this paper are the results of limited full-scale field tests designed to characterize the hazards to an exposed site when limited quantities of bulk explosives, positioned inside an igloo, are statically detonated.

The objective of these tests was to collect debris (concrete fragments) and airblast data produced by the detonation of 68 kg (150 lb) and 206 kg (450 lb) TNT charges positioned inside earth-covered reinforced concrete igloos and analyze both airblast profiles and fragment distributions in terms of densities, weights, and their location relative to igloo orientation.

DESCRIPTION OF TESTS

All tests were conducted at the NAVAJO Depot Activity near Flagstaff, Arizona, where a total of four excess igloo magazines were made available for destructive tests in support of this effort. These igloos were declared as excess due to structural failures between the floor slab and the footings, in the floor slab, and in some cases in the arch crest. It is assumed that the influence of these defects on the test results can be ignored. All four igloos were constructed in 1942 according to government specifications and were earth covered to a depth of at least 2 feet, see Figure 1.

There was no pre-test site preparation involved in the first two tests. The igloos faced a large open field covered with desert-type vegetation to a height of 3 feet. However, the areas to the sides and rear of the igloos were relatively well maintained. Using the results of the first two tests for guidance, areas to the front, side, and rear of the remaining igloos, large enough to contain 5-degree recovery

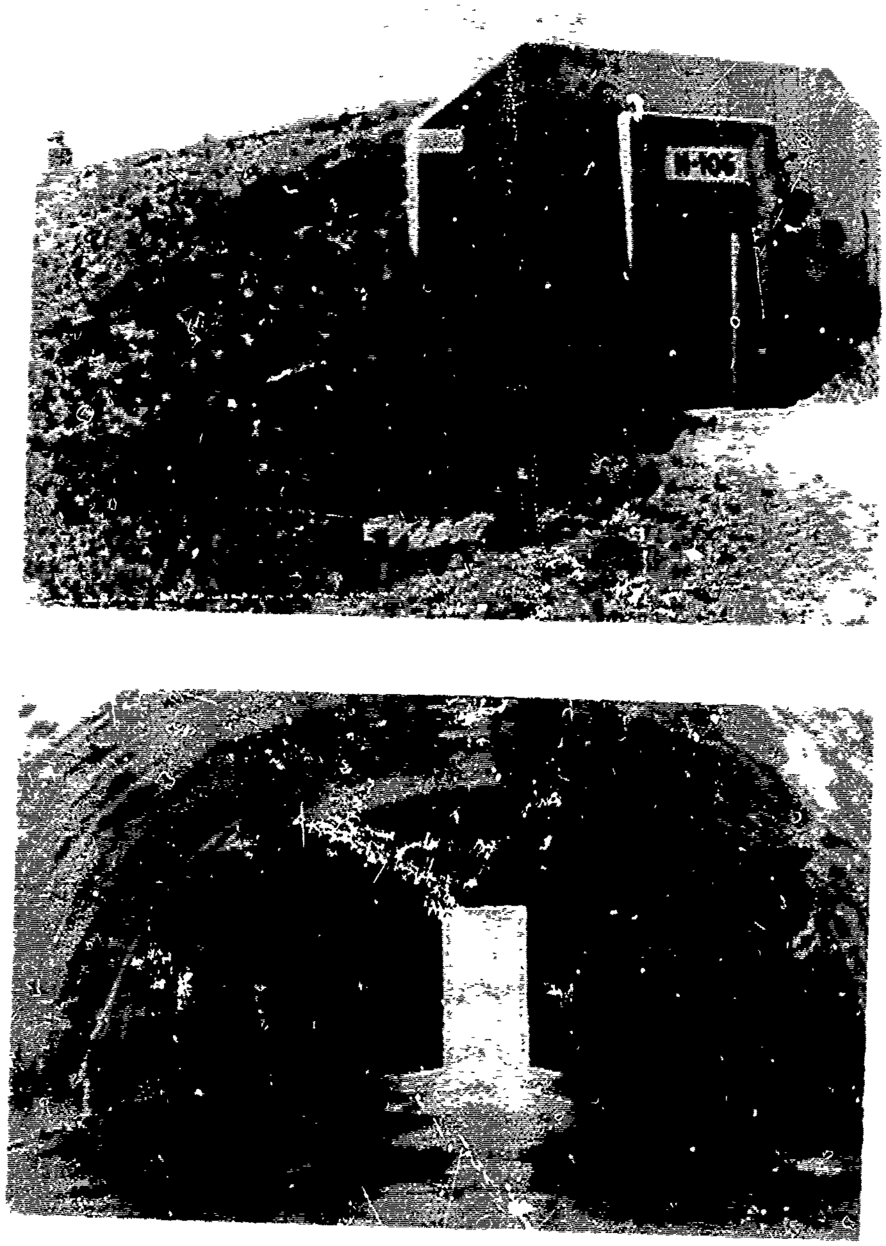

Figure 1. Standard Earth-Covered Igloo

sectors, were prepared using a grader. The recovery areas for each test are shown in Figures 2, 3, and 4. These recovery areas were searched after each test and the fragments catalogued in terms of numbers, weight intervals, and distance intervals. All distances were measured from the center of the igloo. A postage scale was used to establish fragment weights up to 2 pounds. The weight of fragments in excess of 2 pounds was estimated.

To provide a continuous record of the sequence of events, four 16mm cameras were positioned to photograph the front side and rear of the igloos. Air blast parameters were monitored by pressure transducers, flush mounted, via a teflon collar, to aluminum blocks positioned to the front and sides of the igloos in Tests 3 and 4.

In all four tests, 50-pound blocks of TNT, placed in the center of the igloos, were statically detonated using long lengths of Primacord connected to a remotely located mechanical-electrical safety block.

TEST RESULTS

All four igloos were completely destroyed in the test series. The doors were expelled from the test site --- remained airborne for 2 to 300 feet --- impacted the ground and started to roll --- coming to rest hundreds of feet from the impact point. The earth cover rose to a height of approximately 60 feet and settled with only minor scattering. All headwalls were fractured into several hundred pieces, many weighing in excess of 100 pounds. The rear walls were recovered intact and in place. The sidewalls fractured into large pieces and were recovered either in place, on the floor, or on the earth cover. Selected post test damage photographs are presented in Figures 5 through 10.

The results of the fragment collection effort are presented in Table I. It should be noted that the data for Tests 1 and 2 are suspect due to incomplete recovery, i.e., the recovery areas to the front of the igloos were not cleared of vegetation and some of the smaller fragments could have been overlooked. The condition of the prepared sites used in Tests 3 and 4 was such that all fragments were recovered. Because the prepared areas used in Tests 3 and 4 were larger than required for 5-degree search sectors, fragments are listed in Table I as being recovered either inside or outside the 5-degree sector.

The fragments recovered to the rear of the igloos were pieces of the vent stacks located outside and above the rear wall. This was verified by painting the vent stacks in Tests 3 and 4.

The highest pressures, 1.2 psi at 33 metres (109 ft) and 0.6 psi at 41 metres (136 ft), were measured in front of the headwall where the blast gages were offset from the centerline of the igloo to protect them from heavy concentration of debris. The expected pressures, at these

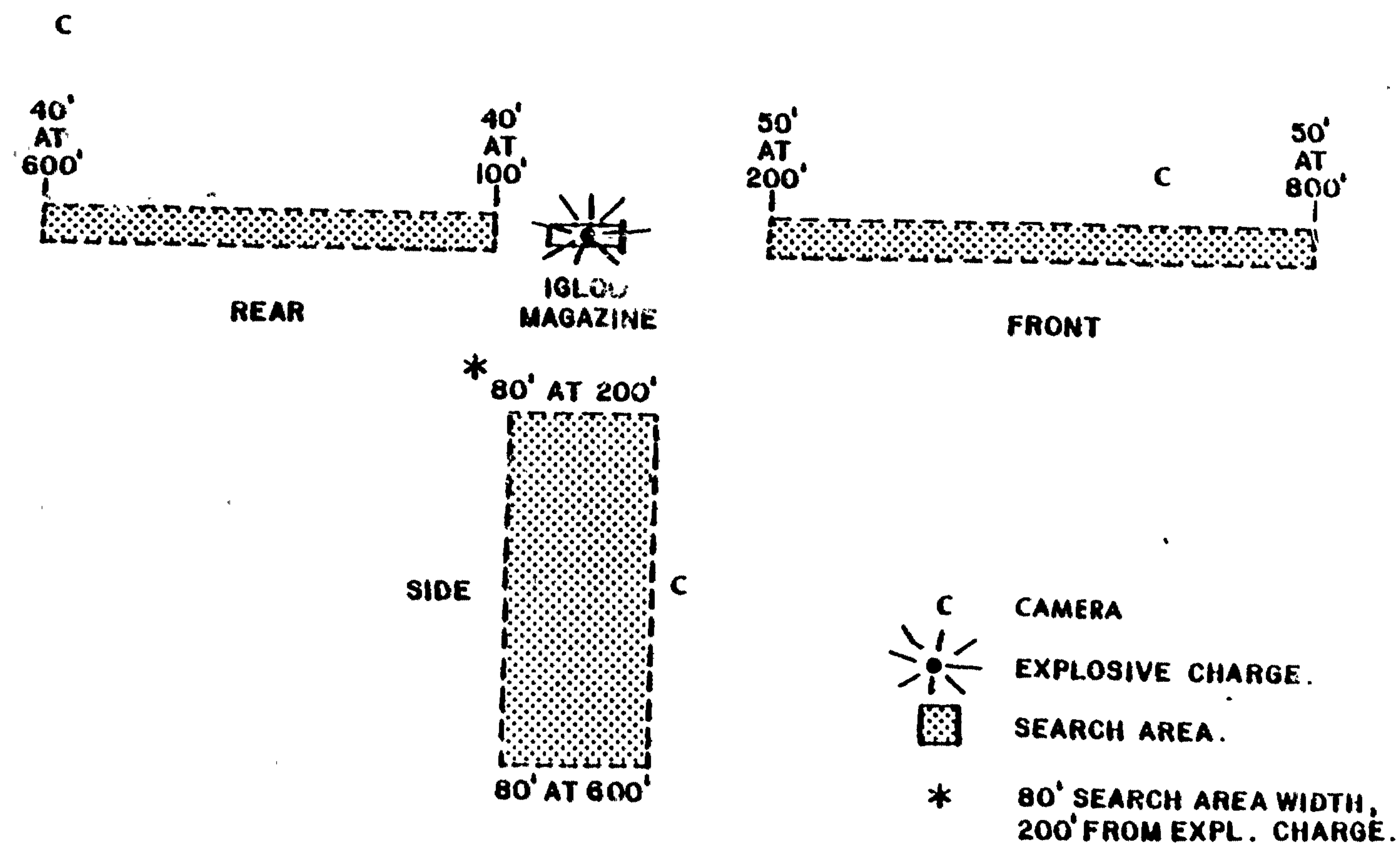

Figure 2. Field Test Setup No. 1 and 2

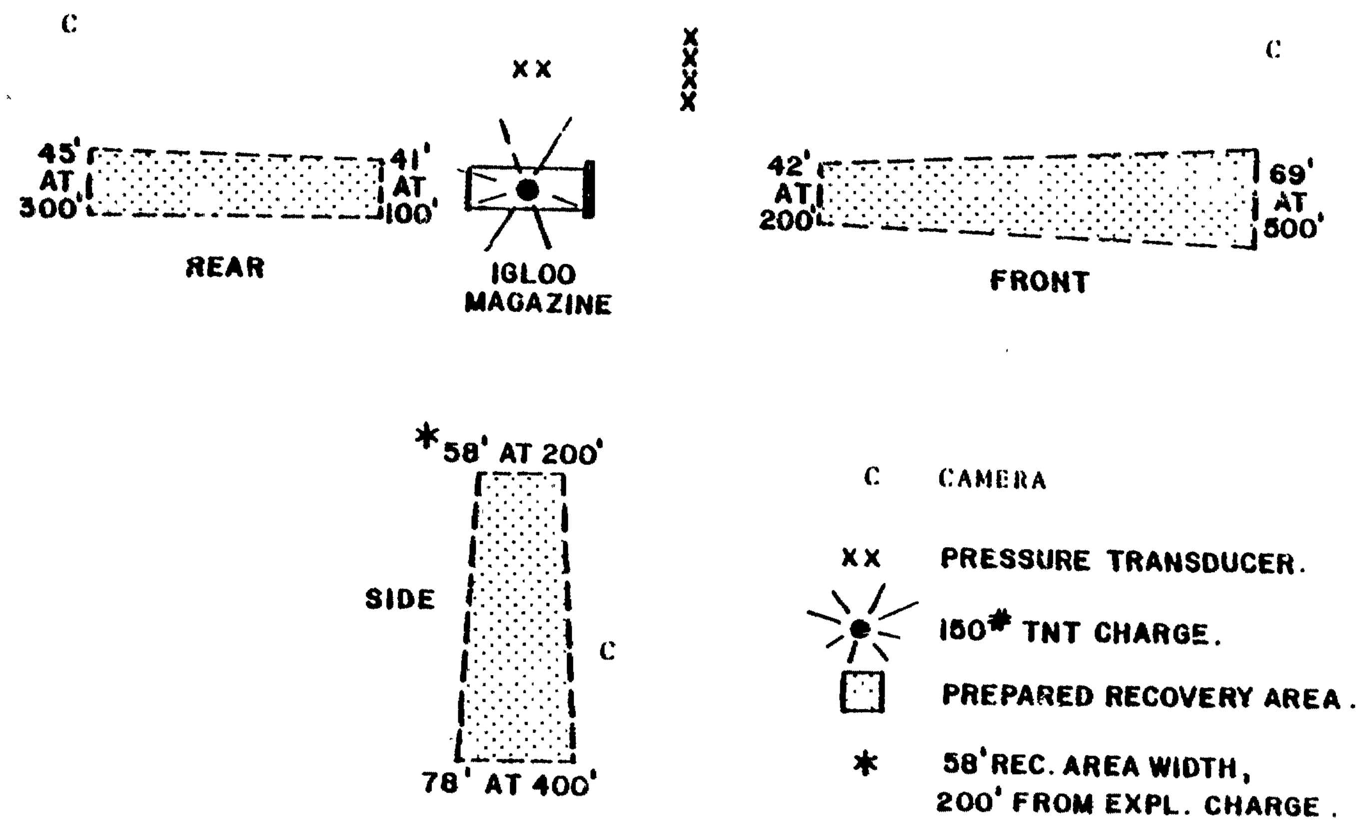

Figure 3. Field Test Setup No. 3

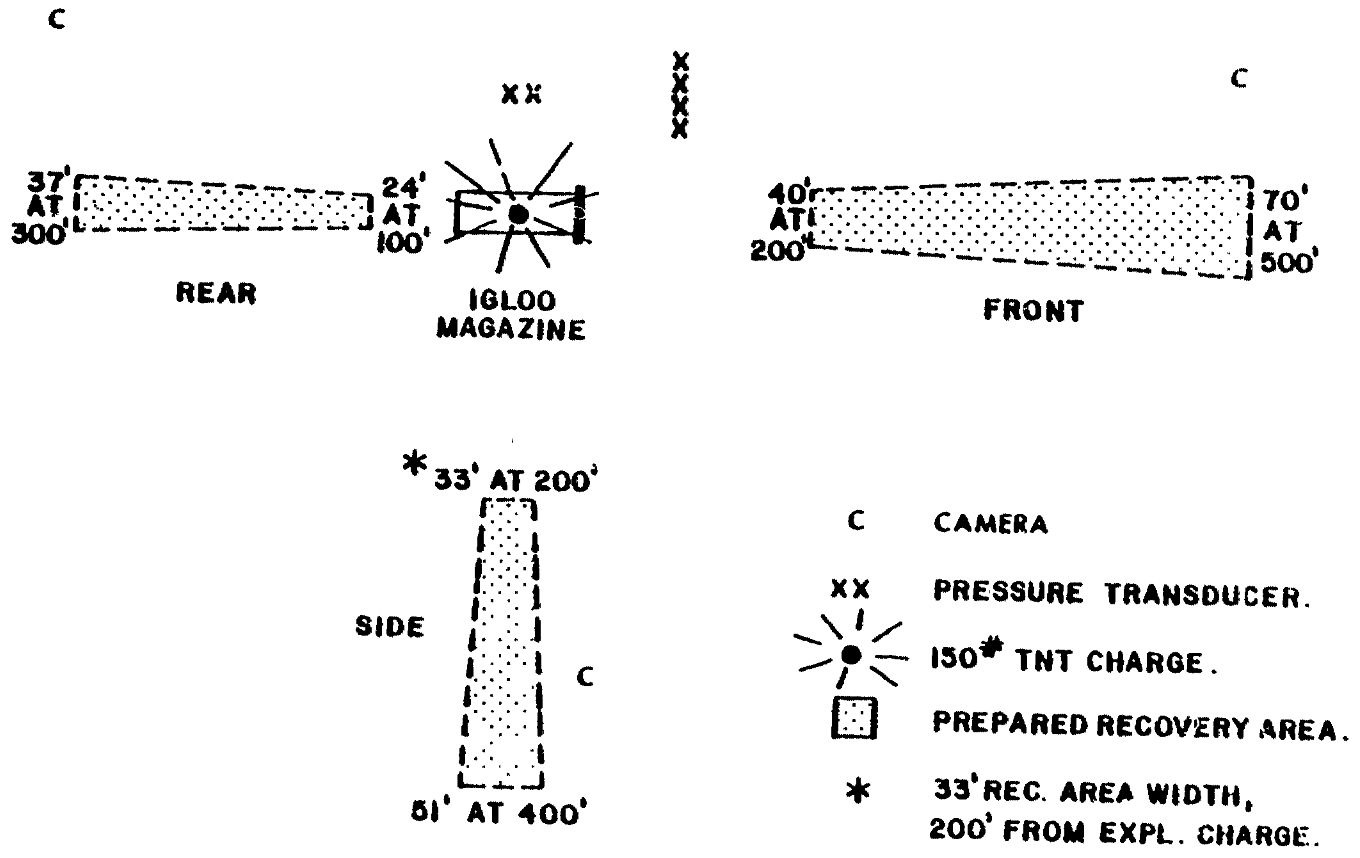

Figure 4. Field Test Setup No. 4

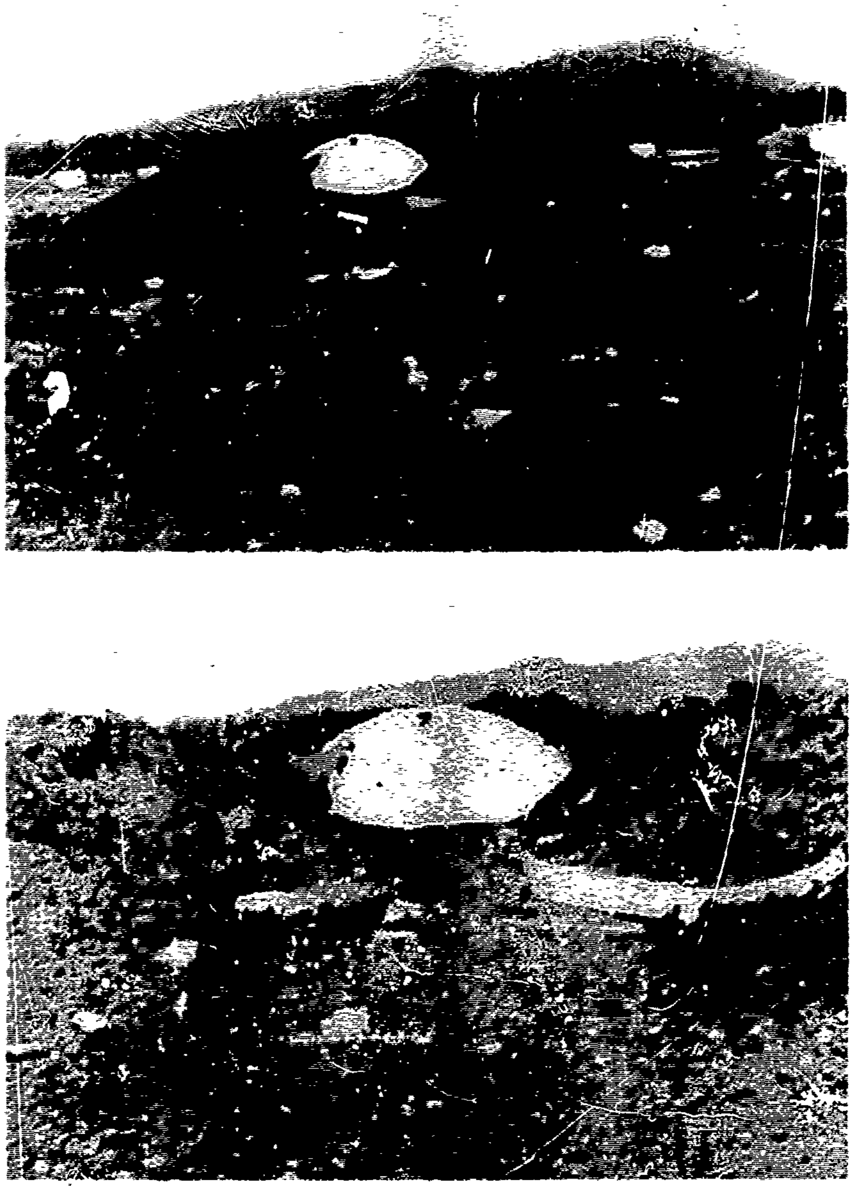

Figure 5. Test No. 1 - 450-lb Weight Charge

Figure 6. Test No. 1 - 450-lb Weight Charge

Figure 7. Test No. 3 - 150-lb Weight Charge

Figure 8. Test No. 3 - 150-lb Weight Charge

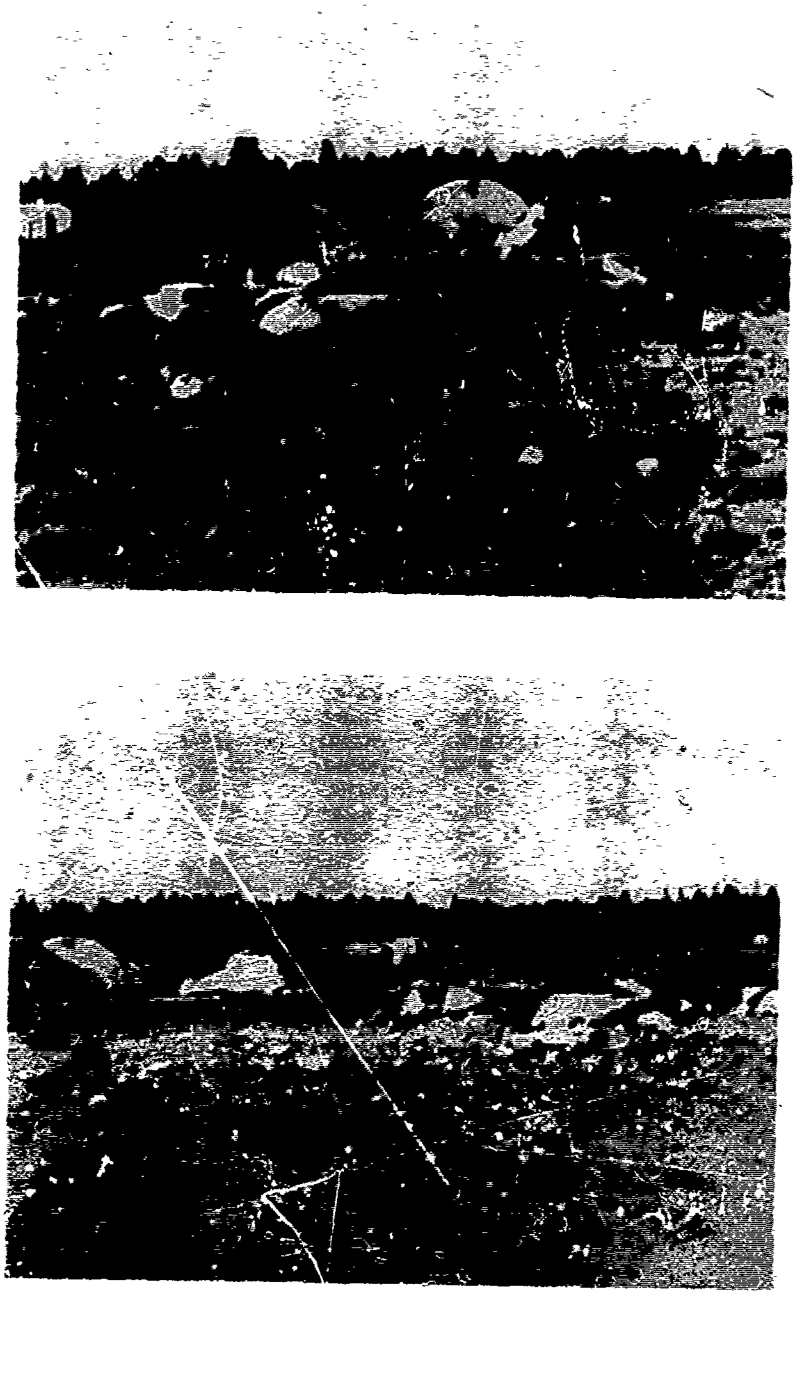

Figure 9. Test No. 4 - 150-lb Weight Charge

Figure 10. Test No. 4 - 150-lb Weight Charge

Table I. Test Results

Debris Distributions from Earth-Covered Igloo Tests

Test No.	Recovery Area	Distance (feet)	Weight (pounds) .4	.5	.6	.7	.8	.9	1-5	Greater than 5
1 No Site Preparation 450-Pound Charge Weight	FRONT OF HEADWALL	300-400	5	15	6	3	4		37	10
		400-500	14	8	2	2	5	4	17	5
		500-600	4		1		5		3	5
		600-700	1		1		3		4	4
		700-800							3	1
	SIDES OF IGLOO	200-300	2	3					4	
		300-400	1							
	REAR OF IGLOO	100-200	3			2	5	2	17	5
		200-300	1					1	3	2
		300-400			1			1		
		400-500		1	1					
2 No Site Preparation 150-Pound Charge Weight	FRONT OF HEADWALL	200-300	5	3			6	4	12	8
		300-400	2	1					4	
		400-500							1	
	SIDE OF IGLOO	100-200					1			
	REAR OF IGLOO	100-200								

Table I. Test Results (Continued)
Debris Distributions from Earth-Covered Igloo Tests

Test No.	Recovery Area	Distance (feet)	Weight (pounds) .4	.5	.6	.7	.8	.9	1.0	1-2	2-4	Greater than 4
3 Prepared Site 150-Pound Charge Weight	FRONT OF HEADWALL INSIDE 5° RECOVERY AREA	200-250	9	7	2	2	2		2	9	2	8
		250-300	2	2					1	4	2	3
		300-350	2	1								1
		350-400	2								1	1
		400-450	2	1				1				1
	FRONT OF HEADWALL OUTSIDE 5° RECOVERY AREA	200-300	16	15	4	4	3	2	5	16	10	9
		300-400	4	2	2				2	3	4	1
	SIDE OF IGLOO OUTSIDE 5° RECOVERY AREA	200-300			1							
		300-400								1		
			No debris recovered in 5° area on side of igloo at distances greater than 200 feet									
	REAR OF IGLOO INSIDE 5° RECOVERY AREA	100-150	1			1						
		150-200								1		
		200-250	2		1	1						
	REAR OF IGLOO OUTSIDE 5° RECOVERY AREA	100-200	4	1		1		1		1	2	2
		200-300	1								1	
		300-400								1	2	

Table I. Test Results (Continued)

Debris Distributions from Earth-Covered Igloo Tests

Test No.	Recovery Area	Distance (feet)	Weight (pounds) .4	.5	.6	.7	.8	.9	1.0	1-2	2-4	Greater than 4
4 Prepared Site 150-Pound Charge Weight	FRONT OF HEADWALL INSIDE 5° RECOVERY AREA	200-250	6	1	8	2	1		2	3	5	1
		250-300	2				1		2	1	1	3
		300-350	1		1			1	1	3	3	3
		350-400	1		1		1			1	2	
		400-450	2		2					1		1
		450-500	2									
	FRONT OF HEADWALL OUTSIDE 5° RECOVERY AREA	200-300	7	15	3	4	5	2	3	14	13	13
		300-400	4	1	4		1			2	4	2
		400-500	4	1						1	1	
	REAR OF IGLOO INSIDE 5° RECOVERY AREA	100-150	4	2	1	2			2	5	2	18
		150-200									1	1
	REAR OF IGLOO OUTSIDE 5° RECOVERY AREA	100-200	2	6	1	2	1	1		11	1	7
	SIDE OF IGLOO		No debris recovered in prepared area on side of igloo at distances greater than 200 feet.									

distances, for an unconfined charge of the same weight are 2.[illegible] psi and 2.1 psi. The highest pressure measure measured off the side of an igloo, 80 ft from the 150 lb charge, was 0.5 psi. The expected pressure at this distance is 4.7 psi, for unconfined charges.

DISCUSSION

The present safety criterion requires that the density of hazardous fragments not exceed one per 600 ft^2 when unprotected personnel are in the area. A hazardous fragment is defined as one having a kinetic energy of 58 ft-lb or greater. In this analysis it is assumed that any concrete fragment weighing 0.4 lb or greater satisfies the 58 ft-lb criterion. While this choice is conservative, it has only a minimal effect on the establishment of safe distance limits.

The fragment data for each test firing are presented in Figures 11 through 14, in terms of hazardous fragment densities/600 ft^2 versus distance for each of the three recovery areas. These distributions show that:

- The hazardous fragment densities were greater in front of the magazine than off to the sides and rear.
- The fragment density in front of the magazine decreased significantly when the charge weight was decreased from 450 lbs to 150 lbs.
- Varying the charge weight had only a minimal effect on fragment densities to the sides and rear of the igloos.

The pressures measured off the front and sides of the igloos in Tests 3 and 4 were significantly lower than those expected from an exposed charge of the same weight. This is consistent with the results of 1/50 scale model tests* conducted by the BRL to determine the effects of an accidental explosion occurring in standard munition magazines when filled with 100,000, 300,000, and 500,000 pounds of explosives.

Kingery, C., et al, "Blast Parameters from Explosions in Model Earth Covered Magazines," BRL-R-2680, Ballistic Research Laboratory (1976) AD032414.

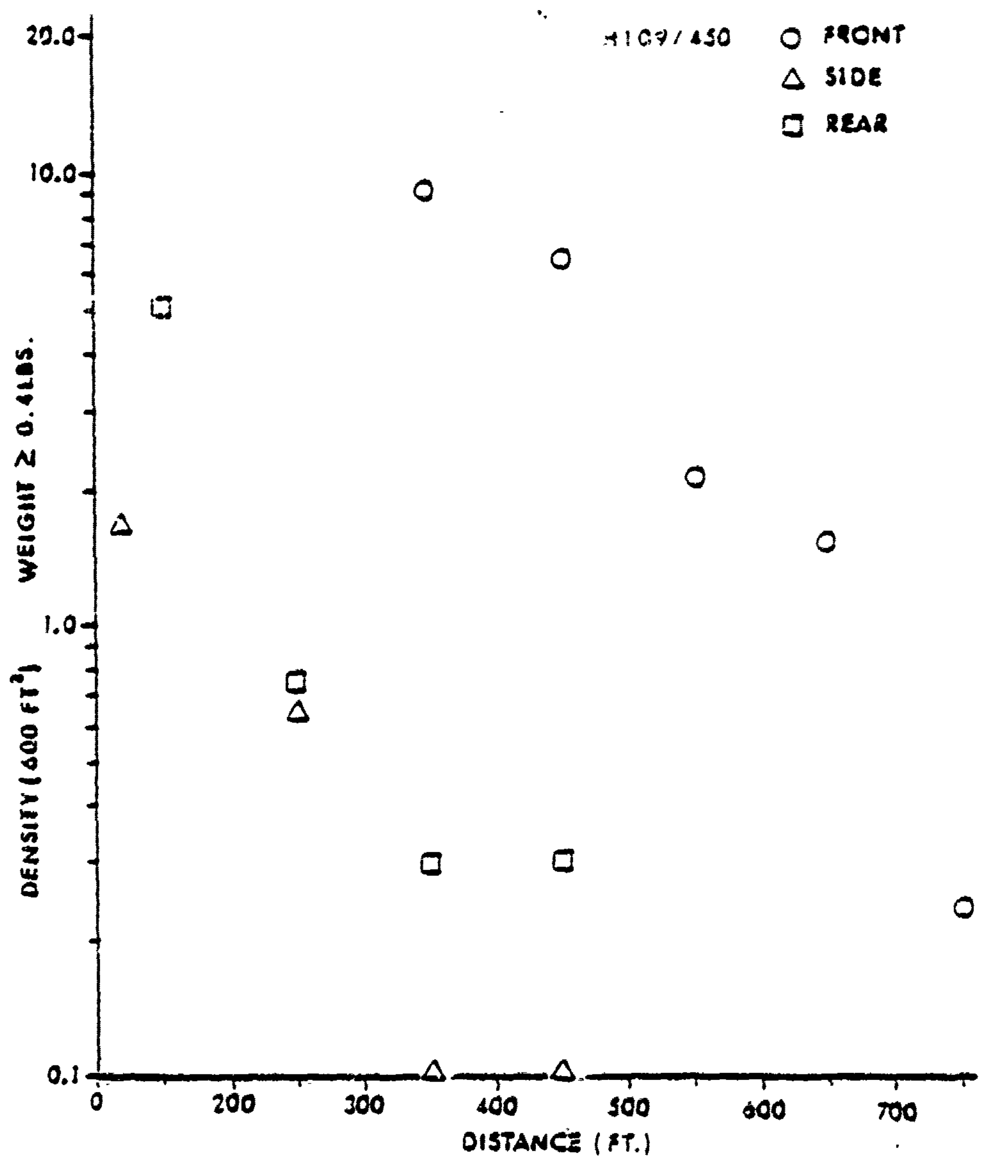

Figure 11. Hazardous Fragment Densities Versus Distance - 450-lb Charge Weight - No Site Preparation

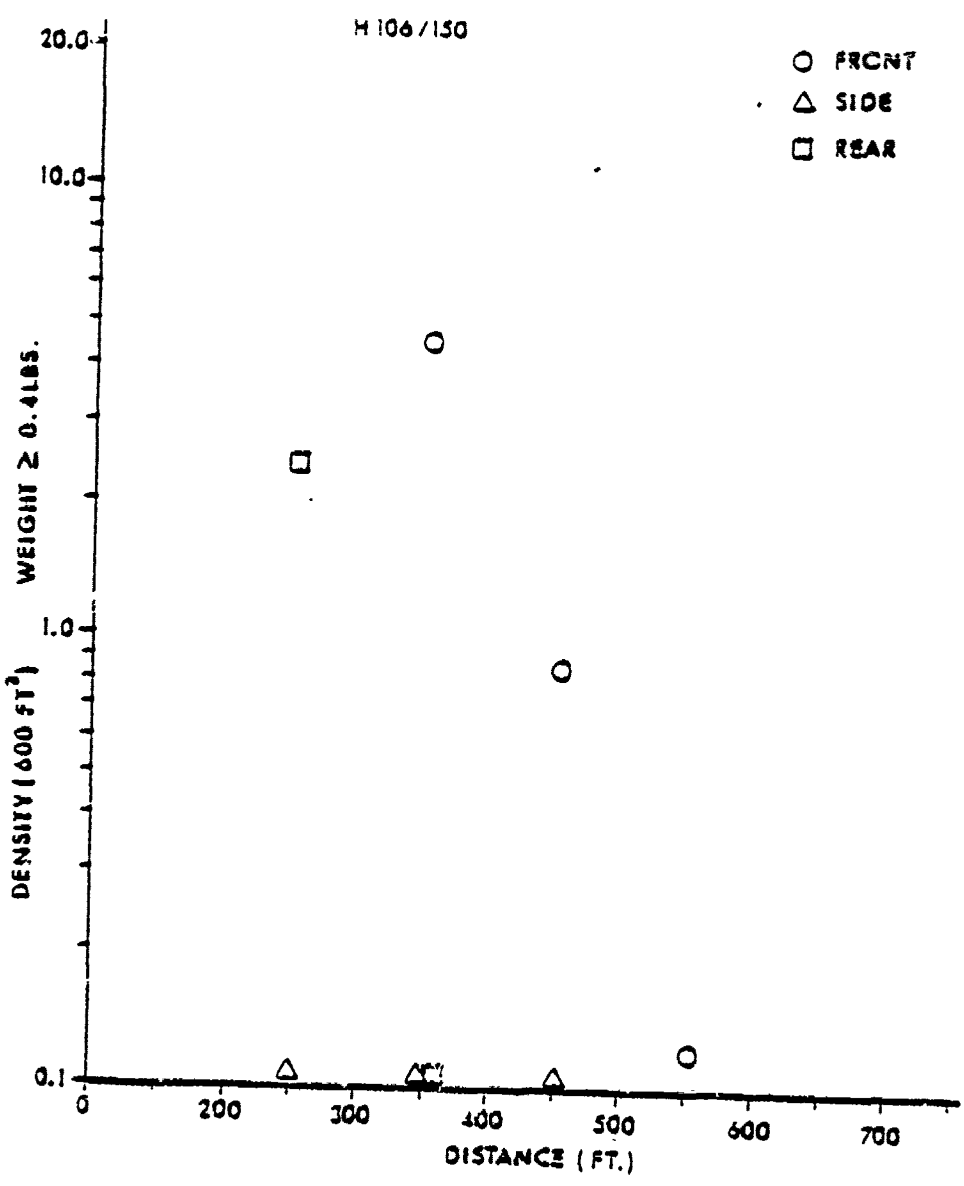

Figure 12. Hazardous Fragment Densities Versus Distance - 150-lb Charge Weight - No Site Preparation

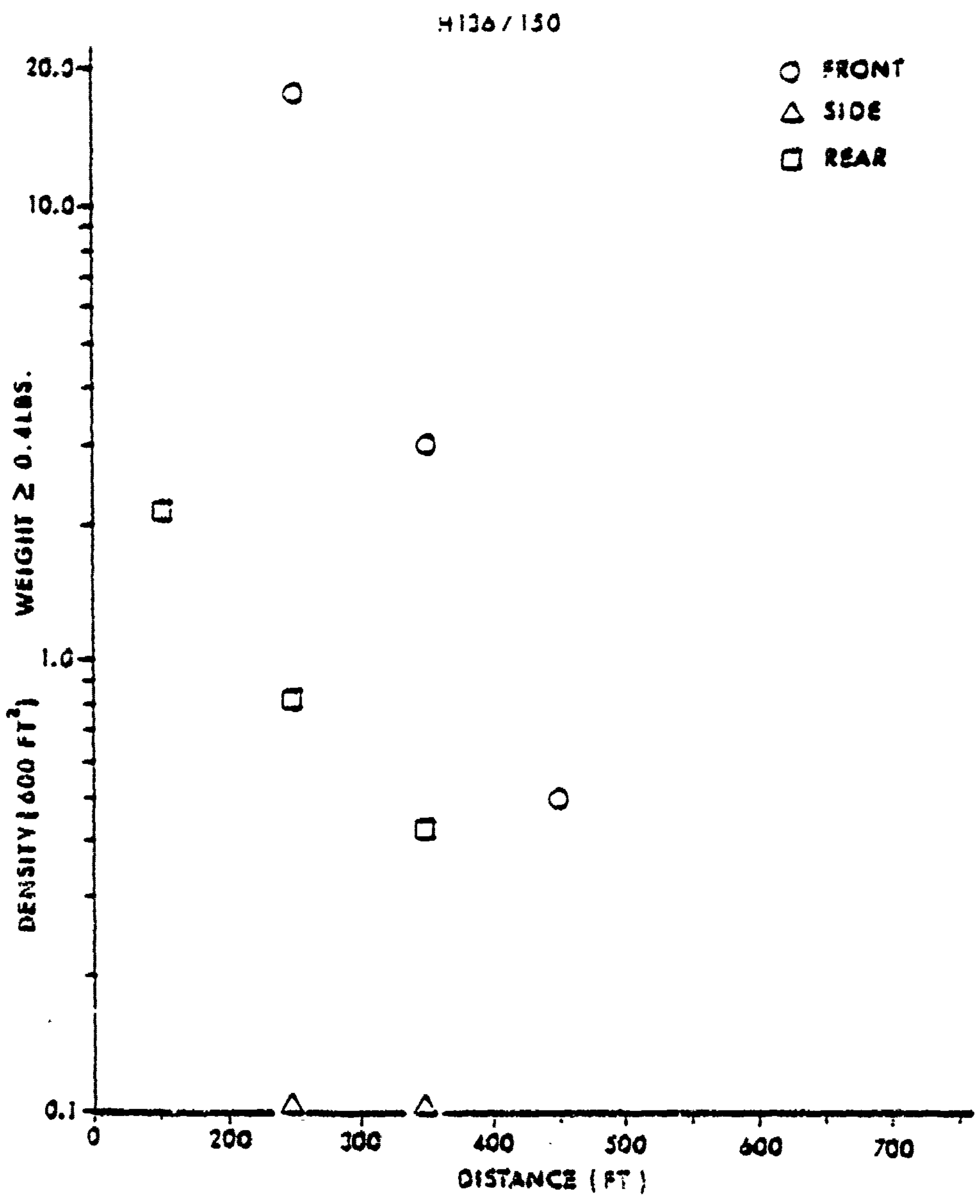

Figure 13. Hazardous Fragment Densities Versus Distance - 150-lb Charge Weight - Prepared Site

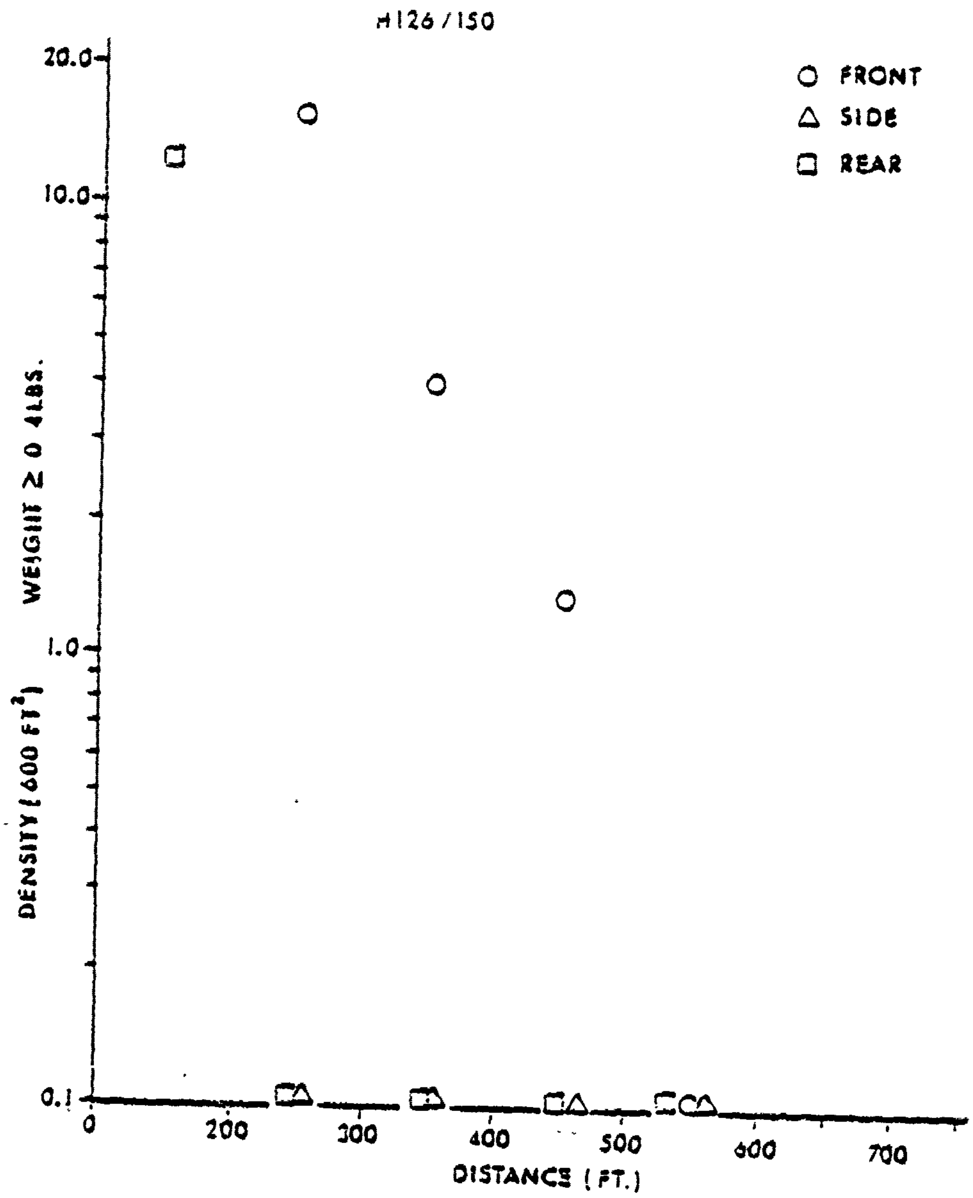

Figure 14. Hazardous Fragment Densities Versus Distance - 150-lb Charge Weight - Prepared Site

Data trends established in the model tests show that compared to the pressures recorded from an unconfined charge of the same weight:

- o There was a significant attenuation of peak overpressures to the sides and rear of the igloos, observed at close-in distances, becoming less as the distance from the charge increased.

- o Peak overpressures recorded along a blast line to the front of the structure were always greater than those recorded for the unconfined charge.

This was apparently due to focussing the blast energy from the three earth-covered sides to the front headwall.

The effects of focussing were observed in the Navajo tests where the pressures recorded to the front of the magazine were attenuated less than those off the sides. Even though pressures were not recorded along a blast line directly in front of the headwall because of the debris hazard, there is no reason to expect that the pressures in this area were higher than those expected from an unconfined charge. The effectiveness of the headwall in attenuating blast in the model tests can be ignored due to the very large, 1000,000-500,000 pound, charge weights. The presence of the headwall cannot be ignored in the Navajo tests with 150-pound charge weights.

While the decay rate of the peak overpressures from the Navajo tests are different than those from an unconfined charge of the same weight, they will continue to decay with distance.

The lowest overpressure causing building damage is usually that causing window glass failure. Penetration by glass fragments, accelerated by airblast, can produce serious wounds if they attain sufficient velocity. A criteria for estimating the probability of penetration of glass fragments to produce serious wounds, expressed as functions of fragment weight and impact velocity, has been established by the Lovelace Foundation.*

Bowen, I. G., et al, "Biological Effects of Blast from Bombs," AECU-3350. Prepared by Lovelace Foundation, June 1956.

An analysis* of glass fragments produced in large scale, 10,000- and 1,000,000-lbs TNT, tests show that:

- o Fragment size varies inversely with the peak pressure of the blast wave striking a window.
- o Fragment velocity is inversely proportional to fragment size and is directly affected by the duration of the pressure pulse.
- o Fragments produced by windows, both single and double strength glass, subjected to an incident pressure of about 1 psi, presented only a minimum hazard.

Only five fragments out of several hundred had incapacitation probabilities between 0.0 and 0.1 using the Lovelace criteria.

If we assume that the highest pressure in front of the headwalls in the Flagstaff tests was 1.5 psi at 100 feet, then an effective explosive charge weight of 36 lbs TNT can be estimated using cube root scaling techniques.** Pressure versus ground range curves for 36- and 150-lb TNT charges are presented in Figure 15. The 150-lb charge curve has been included to show the overpressure attenuation advantage provided by the igloo headwall.

Inspection of these pressure-range curves show that the hazards from window glass failure, resulting from the detonation of a 150-lb TNT charge, can be ignored because the range at which the pressure exceeds 1 psi is significantly less than the range at which the density of hazardous (concrete) fragments exceed one per 600 ft^2.

CONCLUSIONS

The current 400-metre minimum distance requirement between inhabited buildings and igloos containing Hazard Division 1.1 ammunition or explosives is excessive for small explosive weights. This is true for both fragment and peak overpressure hazards.

The use of a barricade in front of the headwall and a redesign of the vent stack would have reduced the density of hazardous fragments, in the Navajo tests, to an insignificant level.

The peak overpressure hazards to the sides and rear of earth-covered igloos are significantly lower than those directly to the front. These directional effects should be considered when establishing minimum distance requirements.

---

* *Custard, C. H., et al, "Evaluation of Explosive Storage Safety Criteria," Falcon Research and Development Company, May 1970.*

***Kingery, C. N., "Air Blast Parameters Versus Distance for Hemispherical TNT Surface Bursts," BRL R 1344, Ballistic Research Laboratory, Sep 66.*

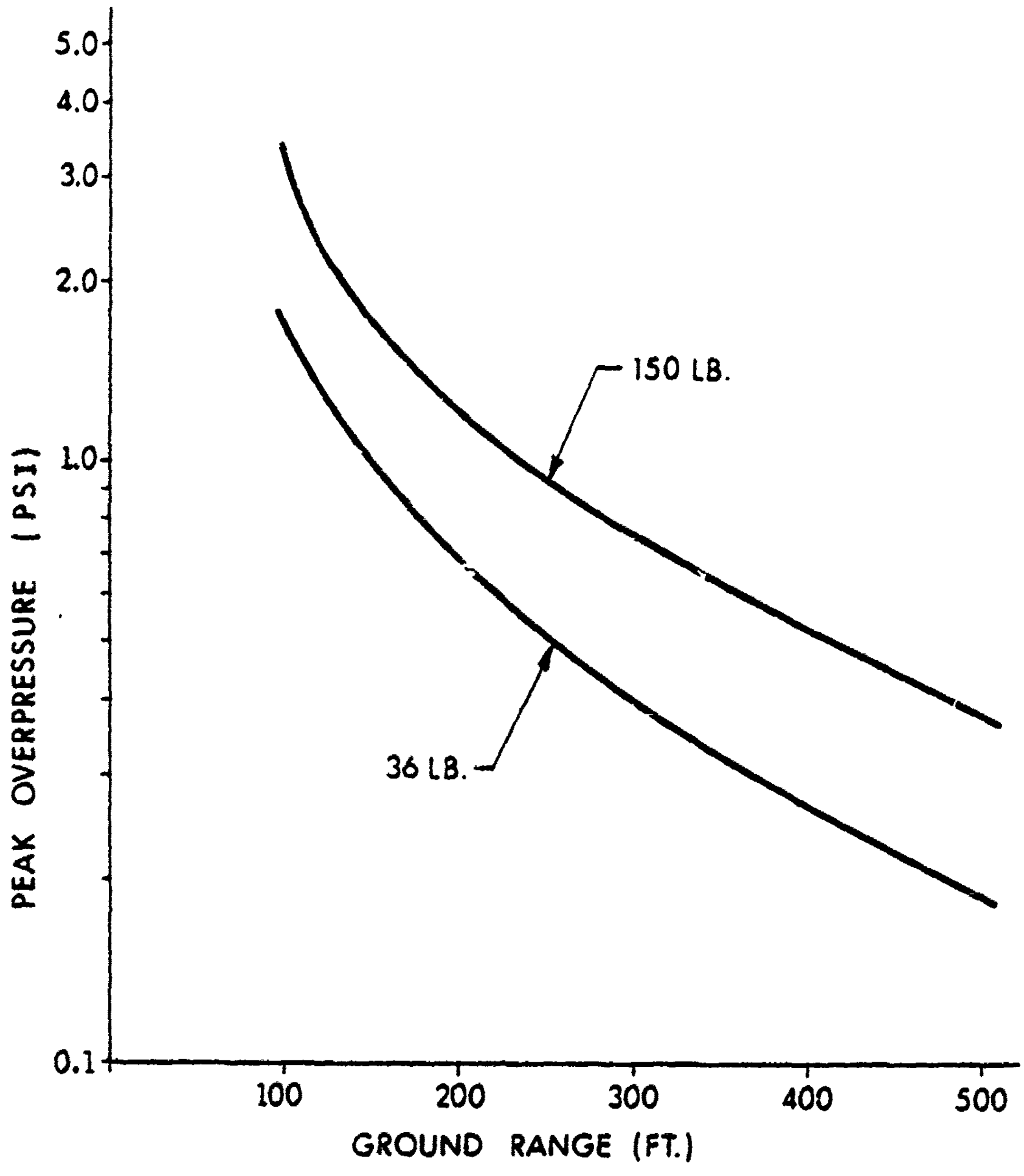

FIGURE 15. PRESSURE VS GROUND RANGE FOR 36 AND 150 LB. TNT CHARGES.

DESIGN CRITERIA FOR SOIL COVER OVER BOX MAGAZINES

Paper Presented to the

Nineteenth DOD Explosives Safety Seminar
Biltmore Hotel
Los Angeles, California
9-11 September 1980

By

William A. Keenan
Civil Engineering Laboratory
Port Hueneme, California 93043

DESIGN CRITERIA FOR SOIL COVER OVER BOX MAGAZINES

by

W. A. Keenan
Civil Engineering Laboratory
Port Hueneme, California 93043

PURPOSE

This paper presents design criteria for the minimum depth of soil cover required over the roof of a box-shaped ammunition storage magazine. The criteria apply to effects from an explosion inside the magazine. The criteria offer, for the first time, a deterministic design procedure for achieving either full containment of explosion effects or partial containment where debris is limited to some prescribed maximum distance from the magazine. The basis for the criteria is summarized and sample problem solutions are presented to illustrate its application and implications. The paper is condensed from Reference 1 which is a product of the NAVFAC Explosives Safety Facilities (NESF) Project directed by the Civil Engineering Laboratory (CEL) and sponsored by the Naval Facilities Engineering Command (NAVFAC).

BACKGROUND

The development of construction standards for ammunition magazines is empirical. The magazine is dimensioned to meet functional requirements, such as the number and size of doors, bulk storage capacity, floor area, and ceiling height. The box structure is usually designed to safely support a prescribed live load plus the dead weight of 2 feet of soil cover. The use of 2 feet of soil cover is almost a universal standard of unknown origin.

The design is then field tested to observe its behavior and safety performance. To avoid anomalies and uncertainty from scaling effects, the test structure is usually a full- or large-scale model. If the observed behavior and safety performance are acceptable, the design is then issued as a definitive standard for ammunition storage. Any requests for deviations from this standard, such as placing more than 2 feet of soil cover over the roof slab, are suspect and discouraged because of the empirical nature of the design process and the uncertainty in effects of any deviations on safety.

A deterministic design procedure that accounts for all parameters eliminates many of the problems resulting from the empirical design process. A deterministic procedure offers design flexibility to incorporate changes in functional, survivability, physical security, and safety requirements into construction standards without sacrificing the level of explosives safety. Further, a deterministic procedure offers a potential solution for altering existing magazines in the field to meet changes in performance requirements. For example, the design criteria presented in this paper clearly demonstrated that existing 1XT box-shaped magazines at WPNSTA Concord, although in violation of current safety standards, do not present a debris hazard to nearby inhabited buildings, and MCON Project 252, which provides for construction of six new magazines (estimated cost $492,000) at a more remote site, should be canceled.

The design criteria presented herein also brings into sharp focus the potential economic benefits of using soil mass, instead of the strain energy capacity of structural members, to control the performance of a magazine. Beginning in about the 1950s, there were significant advances in structures technology concerning the dynamic response and behavior of structural members under blast loads. Consequently, the prevalent design philosophy today is to meet performance requirements by designing strain energy capacity into structural members. This philosophy is often costly. Perhaps, we should revert backwards, at least in some cases, to the design philosophy prior to 1950 when the makers of explosives made liberal use of soil to meet performance requirements by converting blast energy to kinetic energy of the soil.

BASIS FOR CRITERIA

Typical box-shaped, earth-covered magazines are shown in Figures 1, 2, and 3. The box is reinforced concrete designed to safely support the dead weight of the soil cover. The roof slab is not reinforced to resist blast pressures from an internal explosion; the roof slab has essentially no capacity to resist uplift forces from an internal explosion by absorbing internal strain energy.

Possible failure modes for the soil-bermed roof are illustrated in Figure 4. Failure will occur either from shear and membrane forces which tear the slab free from its supports (Figure 4a) or from shock-pressure-induced tension and compression waves which pulverize the concrete and breech (break up) a local area of the slab (Figure 4b). In most cases, the internal strain energy absorbed in support and breeching failure is insignificant compared to the total energy imparted by the explosion, especially if the roof slab is not reinforced to resist internal pressures. Consequently, the upward motion of the roof slab must be resisted almost entirely by mass effects of the soil cover and concrete roof slab. Theories for the dynamic motions of the roof are formulated below.

Theory

Consider an explosion inside the box-shaped magazine shown in Figure 5. The magazine has a net explosive weight, W, internal volume, V, and door vent area, A. The soil cover has a depth, d_s, density, γ_s, and shear failure angle, α. The roof slab has a thickness, t_c, and density, γ_c.

<u>Blast Environment</u>. The explosion produces both blast and gas pressures inside the magazine. The time history of the pressure inside the box is shown in Figure 5a. According to Reference 2, the scaled total impulse is

$$\frac{i}{W^{1/3}} = 569 \left(\frac{A}{W^{2/3}}\right)^{-0.78} \left(\frac{W}{V}\right)^{-0.38} \tag{1}$$

and the scaled duration of the gas pressure is

$$\frac{T}{W^{1/3}} = 2.26 \left(\frac{A\ W^{1/3}}{V}\right)^{-0.86} \tag{2}$$

Equations 2 and 3 are empirical relationships derived from test data. The total impulse, i, includes effects of both blast and gas pressures.

Roof Response. The time history of the roof response from the pressures is shown in Figure 5a. If the time to maximum response of the roof, t_m, is much greater than the load duration (i.e., $t_m > 3T$), then t_m can be calculated, without introducing significant error, by considering only the total impulse, i, and neglecting the time variation in the pressure pulse. The impulse imparts an initial pseudovelocity to the roof equal to i/M where M is the total effective mass of the soil cover plus concrete slab per unit area of the roof. For $t_m/T \leqq 3$ and neglecting the strain energy absorbed during failure of the roof slab, the upward maximum displacement of the roof slab, x_m, is

$$\frac{d_s^{\,3}\ \gamma_s^{\,2}\ k^2 (x_m/d_s)}{W^{2/3}} = 108087 \left(\frac{A}{W^{2/3}}\right)^{-1.56} \left(\frac{W}{V}\right)^{-0.76} \tag{3}$$

and the time when the roof slab reaches its maximum displacement is

$$\frac{t_m}{T} = \frac{36255}{\gamma_s\ k\ d_s} \left(\frac{A}{W^{2/3}}\right)^{0.08} \left(\frac{W}{V}\right)^{0.48} \tag{4}$$

The factor k in Equations 3 and 4 depends on the failure mode of the roof slab and the characteristics of the earth-bermed roof. If the roof slab fractures along its perimeter (Figure 4a) and remains intact as it moves upward under the force of the explosion, the factor k, in Equations 3 and 4, is

$$k = \left(1 + \frac{\ell_3}{\ell_1}\right)\left(1 + \frac{2\ \ell_3}{\ell_2}\right)\left\{\frac{t_c\ \gamma_c}{d_s\ \gamma_s} + \frac{1}{2}\left[1 + \left(1 + \frac{d_s \cot \alpha}{\ell_1 + \ell_3}\right)\left(1 + \frac{2\ d_s \cot \alpha}{\ell_2 + 2\ \ell_3}\right)\right]\right\} \tag{5}$$

If instead the force of the explosion breeches the roof slab, concrete debris missiles of various sizes will be propelled upward along with a mass of soil cover. For a rectangular-shaped concrete debris missile of area $s_1 s_2$ and thickness t_c,

$$k = \frac{t_c \gamma_c}{d_s \gamma_s} + \frac{1}{2}\left[1 + \left(1 + \frac{2\, d_s}{s_1} \cot \alpha\right)\left(1 + \frac{2\, d_s}{s_2} \cot \alpha\right)\right] \qquad (6)$$

For a reinforced concrete roof slab, the most likely values for s_1 and s_2 are the spacing of the reinforcing bars in each span of the slab (Ref 3).

The depth of soil cover required to limit the roof response of a box-shaped magazine is determined from Equations 3, 4, and 5. Given the design parameters of a box-shaped magazine (namely, ℓ_1, ℓ_2, ℓ_3, α, A, V, W, t_c, γ_c, and γ_s), the factor k is calculated from Equation 4 and the minimum depth of soil cover, d_s, required to satisfy a prescribed failure criterion, x_m/d_s, from Equation 3. The computed value of d_s must be checked for accuracy using Equation 4 to determine if $t_m/T \geqq 3.0$. If $t_m/T < 3.0$, the computed value of d_s is overly conservative. The computation of d_s is direct for α = 90 degrees. For α < 90 degrees, the computation of d_s requires an iteration process. Given d_s, the computational process is direct for finding any other parameter, such as the maximum permissible charge weight, W, required to satisfy a prescribed failure criterion, x_m/d_s.

Roof Debris. If the internal explosion causes local breeching of the roof slab, as illustrated in Figure 4b, concrete debris missiles of various sizes will be propelled upward by the force of the explosion. These debris missiles are a potential hazard to inhabited areas outside the magazine.

The risk to people and property from debris missiles depends upon their number, mass, and striking velocity. According to NAVSEA OP-5, the safe range is beyond where no more than one debris missile per 600 ft^2 of land area strikes with an energy content exceeding 58 ft-lb (Ref 4).

A more conservative safety criterion is to define the safe range, R_s, as the range beyond where no debris missiles will strike the ground surface. If v_d is the missile launch velocity resulting from breakup of the roof slab, then this safety criterion is satisfied provided

$$v_d \leqq \sqrt{R_s\, g} \qquad (7)$$

Equation 7 is conservative; it neglects the energy dissipated from tumbling and air drag during missile flight. Further, it assumes that the debris missile is launched from the magazine at the critical launch angle producing the maximum throw range.

The minimum depth of soil cover necessary to satisfy Equation 7 is derived for the following assumptions: (a) no energy is lost in breaking the missile free from the slab, (b) the concrete debris missile enters free flight when $x = d_s$, (c) at $x = d_s$ the missile enters free flight at the launch angle which produces the maximum throw range, and (d) during free flight the missile experiences no loss of energy from effects of air drag and tumbling. For these assumptions, a conservative estimate of the maximum safe charge weight so that the strike range of concrete debris missiles will not exceed some prescribed R_s is

$$W = \left[4.63 \times 10^{-6}\, k^2\, d_s^{\,2}\, \gamma_s^{\,2} (2\, d_s + R_s) \left(\frac{A}{V^{0.487}}\right)^{1.56}\right]^{1.0564} \tag{8}$$

Rearranging terms, the safe range beyond which no concrete debris missiles will strike the ground surface is

$$R_s = \left[\frac{216{,}000\, W^{0.9466}}{k^2\, d_s^{\,2}\, \gamma_s^{\,2} \left(A/V^{0.487}\right)^{1.56}}\right] - 2\, d_s \tag{9}$$

The minimum depth of soil cover, d_s, required to limit debris missiles to some prescribed range R_s from an explosion of magnitude W is also found from Equation 9. The computation of d_s requires an iteration process because the value of k depends on d_s. In both Equations 8 and 9, the value of k should be calculated from Equation 6.

All preceding theory assumes that the blast energy, defined by Equation 1, is converted to kinetic energy of the soil and roof slab and the energy transfer is completed within time T given by Equation 2. This condition is not always the case. For certain ranges of the parameters, gas pressures are still present inside the magazine after the bermed roof has reached a stage of failure which provides a path for gas pressures to vent through the roof. For such cases, some of the blast energy defined by Equation 1 jets through the soil berm and vents to the atmosphere; i.e., all the blast energy is not converted to kinetic energy of the soil and roof slab. This phenomenon will occur if the duration of the gas pressure, T, exceeds the time when venting through the soil-bermed roof first begins. If venting through the roof first begins at time t_d, then all preceding theory is applicable if $t_d/T \geq 1.0$. For $t_d/T < 1.0$, Equation 3 overestimates x_m, Equation 8 underestimates the safe charge weight, and Equation 9 overestimates, by a wide margin for large charge weights, the maximum possible strike range of concrete debris missiles and the minimum depth of soil cover.

If venting through the bermed roof begins at time $t = t_d$ when $x = d_s$, then the critical time ratio is

$$\frac{t_d}{T} = \gamma - \sqrt{\gamma^2 - 2\,\gamma\,\bar{\gamma} - \frac{12161\, d_s}{W^{2/3}} \left(\frac{A}{W^{2/3}}\right)^{1.72} \left(\frac{W}{V}\right)^{1.72}} \tag{10}$$

provided $t_d/T \geq 1.0$

$$\text{where:} \quad \gamma = \frac{36255}{k\,\gamma_s\,d_s}\left(\frac{A}{W^{2/3}}\right)^{0.08}\left(\frac{W}{V}\right)^{0.48}$$

Soil Cloud. The explosion generates shock waves which strike the roof, walls, and floor. The waves reflect and bounce back and forth between these surfaces. Waves striking the roof slab result in a train of compression waves which travel upward through the concrete slab and soil berm at a velocity near the speed of sound. The compression waves compress the soil and lose energy as they travel upward. When each wave passes through the concrete-soil interface of the roof slab and the soil-air interface of the soil berm, a reflected wave forms and travels in the opposite direction. The reflected wave is a tension wave. The net stress in the soil berm at any time is equal to the difference between the stress in the compression and tension waves.

If the net stress is tension, it peels off successive layers from the outer skin of the soil berm. The peeling process continues, as the wave advances, until the energy in the wave is eventually dissipated by the nonlinear properties of the soil. The peeling process is most likely to occur within a relatively shallow outer layer of the soil berm. The peeling process may be repeated by trailing waves in the wave train. However, the trailing waves are less effective due to their lower energy content and interference with reflected waves. The peeling process, should it occur, throws soil particles into the air to form a soil cloud, as illustrated in Figure 4c.

The size and mass of the soil cloud is of academic interest but rarely presents a serious risk to people and property because of the low energy content of soil particles. Theory for predicting the size of the soil cloud and mass of soil pushed into the cloud is not available.

Experiment

An experiment was designed to validate the preceding theory for the dynamic response and behavior of the roof slab and soil berm of a box magazine. The experiment was designed by CEL and conducted by the WQEC Laboratory at WPNSTA Concord, Calif. (Ref 1).

The experiment involved detonating explosive charges inside small-scale box magazines and recording the response and behavior of the roof slab and soil berm.

Test Magazine. Design details of the test magazine are shown in Figure 6. The test magazine was approximately a 0.40 geometric scale model of the 1XT magazines (Figure 1) located at WPNSTA Concord. The floor, walls, entryway, and barricade of the test magazine were constructed from 3-inch-thick steel plate, joined together with full penetration welds. The test chamber was buried in the ground with the lip of the chamber flush with the ground surface (Figure 7).

The door on the magazine was 10 gauge steel sheet (0.14 inch) held in place at mid-height by two shear pins. The door was replaced after each test.

The test charge was Composition C-4 explosive shaped into a right cylinder with a length-diameter ratio equal to 1.0. The charge was positioned midway between the walls and 15 inches above the chamber floor.

The headwall and roof of the test magazine were constructed from 2- by 6-inch timbers (Figure 8). Strips of 14 gauge steel plate were nailed to the bottom face of the roof timbers. The steel strips overlapped adjoining timbers 3/4 inch to seal the roof from blast pressures and shield it from the products of combustion. Adjacent timbers (with metal strip attached) were not mechanically joined in any way; each timber was free to move upward independent of the others, except for the restraint provided by the overlapping metal strip. The timber roof rested on the top of the chamber walls (Figure 6). The roof timbers were not fastened to the chamber walls. This detail yielded a slightly conservative measure of the response and behavior for a typical bermed roof of a box-shaped magazine.

The roof timbers were covered with standard road base aggregate in a berm-like fashion. The maximum size of aggregate was 1/4 to 3/8 inch. The maximum weight of an aggregate was approximately 0.35 ounce. The berm was configured in such a manner that the soil depth, d_s, was extended for a distance d_s beyond the vertical extension of the chamber walls, except at the headwall. The area outside a projection of the roof slab onto the surface of the berm was spray painted white to improve photographic contrast in recording the failure mechanism of an earth-bermed roof. Beyond a distance d_s from the chamber walls, a slope of 1:2 was maintained to ground level. Figure 9 illustrates the configuration of the test magazine and the painted area of the berm prior to testing.

Instrumentation consisted of a Fastex Model WF-15 high speed motion picture camera and a Nikon F camera. The cameras recorded breakup of the earth berm and the motion of a target, marked in 6-inch increments, which was bolted directly to the midspan of the timber located over the center of the roof (Figure 8). A plywood backdrop with a 2-foot grid was placed behind the magazine to eliminate all background interference and enhance the contrast to better define the response and behavior of the bermed roof.

Test Results. The test results are summarized in Table 1. The vertical growth of the soil cloud and upward displacement of the timber roof as a function of time are plotted in Figures 10-14. Typical photographs of the earth-bermed roof at various stages of dynamic response and behavior are shown in Figures 15-22. A detailed discussion of results is presented in Reference 1. Test results demonstrated that air passages through the soil berm can occur when the maximum roof response exceeds the original depth of soil cover (i.e., $x_m/d_s > 1.0$). This particular test observation is critical to the formulation of design criteria for full containment of an ammunition magazine.

Theory Versus Experiment

The measured and predicted results for each test are compared in Table 2. The measured and predicted upward displacements of the roof slab as a function of time are plotted in Figures 10-14 for comparison.

Note that the entire history of the measured roof response is captured within the theoretical response curves for α = 85 and 90 degrees. Theory for α = 90 degrees provides the best correlation with measured roof response for three tests; α = 85 degrees provides the best correlation for two tests. This correlation strongly suggests that the theory (and equations derived therefrom) is reasonably accurate, at least within the range of parameters tested. Note that the correlation is excellent even in tests 7 and 8 where the roof slab was driven upward well in excess of the original depth of soil cover (i.e., $x_m/d_s > 1.0$). Most important, the excellent correlation implies that theory adequately describes the internal blast environment, and the acceleration, velocity, and displacement of an unrestrained roof slab at any instant of time. It is concluded that the theory yields slightly conservative estimates of the roof response and launch velocity of roof debris by assuming α = 90 degrees, at least for the road base aggregate used for the test magazines.

DESIGN CRITERIA

The following design criteria offer a basis for establishing a deterministic procedure for designing, analyzing, and site planning box-shaped ammunition storage magazines. Caution should be exercised in applying the criteria to very large W, large ratio of W/V, $A/V^{2/3} > 0.60$, arch-shaped magazines, a rectangular-shaped magazine with a large aspect ratio, and soils other than road base aggregate. Reasons for these limitations and others are presented in Reference 1. Further, the criteria are based on limited test data derived from small-scale tests. Additional theoretical studies and test data from large-scale magazines (currently underway) are needed to validate the criteria.

The criteria are no panacea for all ammunition storage problems. It appears that the economic benefits derived from the criteria are probably inversely proportional to the ratio W/V. The criteria offer a technique for eliminating certain safety waivers and introducing flexibility and economy into the design process and construction standards for ready service magazines, special weapons magazines, and missile test cells. In certain cases, the criteria may offer a means of increasing the survivability of parked aircraft without degrading safety.

Full Containment

Full containment is defined as the condition where the earth-bermed roof provides an <u>air-tight seal during the entire history of internal loading and berm response</u>. Full containment contains debris within the perimeter of the magazine. It also prevents products of combustion (i.e., chemical gases, fire, and blast pressures) from bleeding through the soil berm and into the atmosphere; all products of combustion are forced to vent through the doors/headwall.

Full containment requires $x_m/d_s \leq 1.0$. For design purposes let $x_m/d_s = 1.0$ and use Equation 3 to determine either the minimum depth of soil cover, d_s, maximum design charge weight, W, minimum magazine volume, V, or minimum vent area, A, required to achieve full containment. Assume α = 90 degrees and determine k from Equation 5 if breeching is precluded. Otherwise, assume α = 90 and determine k from Equation 6. Having satisfied the requirement that $x_m/d_s \leq 1.0$, check the accuracy of the solution by computing t_m/T using Equation 4. If $t_m/T \gtrsim 3$, the solution is a conservative but reasonable estimate. If $t_m/T < 3$, the solution is overly conservative and the degree of conservatism increases with decreasing t_m/T. The ranges of parameters for full containment relative to other modes of behavior are illustrated in Figure 23.

Partial Containment

Partial containment is defined as the condition where the earth-bermed roof provides an air-tight seal during the entire history of internal loading but not during the entire history of berm response. Partial containment prevents blast pressures from jetting through the soil berm; all blast pressures are forced to vent through the doors and headwall. Following escape of all blast pressures, the air-tight seal of the soil-bermed roof slab is broken, allowing products of combustion (i.e., chemical gases and fire) and roof slab debris to escape through the bermed roof.

Partial containment requires $t_d/T \geqq 1.0$. For design purposes let $t_d/T = 1.0$ and use Equation 10 to determine either the minimum depth of soil cover, d_s, maximum design charge weight, W, minimum magazine volume, V, or minimum vent area, A, required to achieve partial containment. Use Equation 6 to determine k and assume α = 90 degrees. There is no need to check the accuracy of the solution for partial containment. For the practical range of parameters, the requirements that $t_m/T > 3$ and $t_d/T \geqq 1$ are satisfied so the solution is a good estimate. The ranges of parameters for partial containment relative to other modes of behavior are illustrated in Figure 23.

Debris Hazard

Debris refers to concrete debris from the roof of the structural shell. The safe range from concrete debris is defined as the range beyond which no concrete debris missiles from the roof slab will strike the ground surface.

For design purposes, use Equations 8 and 9 to predict and control the debris hazard. Use Equation 8 to determine the maximum design charge weight, W, such that concrete debris missiles will not strike the ground surface beyond some prescribed range, R_s. Use Equation 9 to determine either the safe range, R_s, beyond where no concrete debris missiles will strike the ground surface, or the minimum depth of soil cover, d_s, required to limit concrete debris missiles to some safe range, R_s. In both Equations 8 and 9, use Equation 6 to determine k and assume α = 90 degrees. Check the accuracy of the solution by computing t_d/T using Equation 10. If $t_d/T > 1$, the solution is a conservative but reasonable estimate. If $t_d/T < 1$, the solution is overly conservative and the degree of conservatism increases with decreasing t_d/T. Note that the debris range is zero if the magazine provides full containment ($x_m/d_s \leqq 1$). The relationship between parameters affecting the debris hazard is shown in Figure 23.

Blast Hazard

A box magazine covered with soil to a depth sufficient to provide either full or partial containment is equivalent to a hardened three-wall box with a hardened roof. For such designs, the graphs in Figures 38 and 39 of Reference 2 are applicable for predicting approximately the external blast environment at any distance to the front, sides, and rear of the magazine. The predicted blast environment is approximate because the graphs in Reference 2 do not consider effects from the magazine headwall. According to these graphs, either full or partial containment will dramatically reduce the close-in blast environment (e.g., at NAVSEA OP-5 intramagazine and intraline distances) to the sides and rear. The benefits at NAVSEA OP-5 inhabited building distance are insignificant. For large box magazines, the reduction to the rear and sides should significantly reduce the vulnerability of adjacent magazines and slightly reduce the "safe" distance to direct-support facilities (facilities allowed at NAVSEA OP-5 intraline distance, $R/W^{1/3} = 18$ or approximately the 3.5-psi overpressure level).

The blast environment to the front will be greater than that from an ammunition magazine with say 2 feet of soil cover, but not by much according to Reference 2. If the increase is significant, this disadvantage might be overcome by orienting magazines in a herringbone pattern, as illustrated in Figure 24.

For designs with $t_d/T \leqq 1$, the external blast environment is somewhere between the blast environment from an unconfined surface burst and the environment predicted from Figures 38 and 39 of Reference 2. The exact environment depends upon effects of time-dependent venting on the external blast environment which is a subject for future research.

APPLICATION OF CRITERIA

The following explosives safety problems and their solutions demonstrate application of the design criteria presented in this paper. The first problem, concerning an operational safety waiver on 1XT magazines at WPNSTA Concord, is real. The solution given is the proposed solution for eliminating the safety waiver. All other problems are purely hypothetical. Further, the specified operational and performance requirements are not necessarily typical but were chosen to demonstrate several facets of the criteria.

Ready Service Magazine

Six fuze and primer magazines (1XT magazines) are located at WPNSTA Concord. The 1XT magazines are of the type shown in Figure 1. The depth of soil cover is 2 feet. The magazines store a total net explosive weight, W, equal to 8.0 pounds maximum of Class 1, Divisions 1 and 2, Category (04) material.

The 1XT magazines, located 80 feet from inhabited buildings, violate NAVSEA OP-5 safety standards which require a 400-foot minimum separation distance from any 1XT magazine to the inhabited buildings. This separation distance is intended to mitigate the debris hazard to the inhabited buildings.

Safety authorities indicate that the requirement for waivers could be removed if, given an inadvertent explosion involving 8 pounds TNT, it could be clearly demonstrated that explosion effects would be completely contained within the magazine or explosion effects would present no debris hazard to the inhabited buildings located 80 feet away.

Apply the theory in the paper to answer the following aspects of the problem and determine the safety of the 1XT magazines. The values of critical parameters for the 1XT magazine are given in Figure 25. For these values, Equations 3 and 10 (for $t_d/T = 1.0$) are plotted in Figure 25 where x_m/d_s is shown for any combination of W and d_s. Equations 9 and 10 (for $t_d/T = 1.0$) are plotted in Figure 26 where $\hat{W}$ is shown for any combination of d_s and R_s.

(a) Question: Will the soil-bermed roof of an existing 1XT magazine completely contain W = 8 pounds TNT?

Answer: Entering Figure 25 with $d_s = 2$ feet and W = 8 pounds for the 1XT magazines, find $x_m/d_s > 1.0$. Since full containment, as defined in this paper, requires $x_m/d_s < 1.0$, the 1XT magazines will not fully contain the explosion. By extrapolation, $x_m/d_s = 3.56$. Therefore, $x_m = (3.56)(2.0) = 7.12$ feet. Thus, the soil berm will not contain the explosion and the roof slab will rise 7.12 feet.

(b) Question: What is the maximum possible strike range of any concrete debris missile from the roof slab of the 1XT magazine?

Answer: Entering Figure 26 with $d_s = 2.0$ feet and W = 8 pounds for the 1XT magazine, find $R_s = 10$ feet. Thus, the maximum possible strike range of concrete debris missiles is 10 feet.

(c) Question: What soil cover depth is required to completely contain an explosion involving 8.0 pounds TNT?

Answer: For full containment, $x_m/d_s < 1.0$. Entering Figure 25 with $x_m/d_s = 1.0$ and W = 8.0 pounds, find $d_s = 3.2$ feet. Thus, 3.2 feet of soil cover are required to fully contain the explosion effects of 8 pounds TNT.

(d) Question: What is the maximum safe storage capacity of a 1XT magazine?

Answer: The minimum distance from a 1XT magazine to an inhabited building is 80 feet. Thus, $R_s = 80$ feet. Entering Figure 26 with $d_s = 2$ feet and $R_s = 80$ feet, find W = 52.3 pounds TNT. Thus, the maximum safe storage capacity is 52.3 pounds in order to limit concrete debris missiles to a range less than 80 feet. But to limit the blast pressures at the nearest inhabited building, current NAVSEA safety standards require $R_s \geq 40W^{1/3}$, inhabited building distance, or $W \leq (R_s/40)^3 = (80/40)^3 = 8$ pounds TNT. Thus, blast pressures, not debris, limit the safe storage capacity of a 1XT magazine to 8 pounds TNT.

(e) Question: Neglecting blast hazard, what is the safe storage capacity if the soil cover over the roof is increased from the present 2 feet to 3 feet?

Answer: Entering Figure 26 with $d_s = 3.0$ feet and $R_s = 80$ feet, find $W = 100$ pounds. Thus, neglecting blast hazard, an additional foot of soil on top of the existing 2 feet of soil cover increases the safe charge weight for debris hazard from 52 pounds to 100 pounds TNT.

(f) Question: For $W = 50$ pounds TNT, what is the critical depth of soil cover where any additional soil cover will not change the blast environment outside a 1XT magazine?

Answer: Entering Figure 25 with $W = 50$ pounds, $t_d/T = 1.0$ at $d_s = 0.43\,W^{0.341} = 0.43(50)^{0.341} = 1.63$ feet. Thus, adding soil to the roof slab will reduce the external blast environment (because $t_d/T < 1.0$) until $d_s = 1.63$ feet. For any $d_s > 1.63$ feet, blast and gas pressure will have escaped through the door opening before the roof slab has risen a sufficient distance ($x = d_s$) to allow them to vent through the soil berm; the blast environment outside the magazine will be identical for all $d_s > 1.63$ feet.

(g) Question: Based on the above analysis, recommend a solution to the safety waiver problem.

Answer: The safe charge weight for a 1XT magazine is 8 pounds TNT and is limited by blast pressure requirements. The maximum possible strike range of concrete debris missiles from the roof slab is 10 feet, much less than the range (80 feet) to the nearest inhabited building. The safety waivers on the 1XT magazine should be lifted and MCON Project P-252 (estimated cost $492,000) should be canceled.

Large Box Magazine

WPNSTA Atlantis Master Plan includes MCON Project P-51 which provides for construction of 40 large box-shaped ammunition magazines to store special weapons. The design charge weight, W, for each magazine is 8,000 pounds TNT equivalent.

Survivability, environmental control, and physical security are important factors in the design of the depot. The Special Projects Office requires a minimum soil cover of 8 feet over each magazine to defeat an assigned weapon threat. The base commander desires to have the minimum soil cover necessary to prevent nuclear material from being blown upward through the bermed roof into the atmosphere, should an HE explosion occur inside a magazine. The security office concurs; additional soil cover will increase the denial time of forced intrusion into a magazine. The safety office requests that the final construction standards for the depot be accompanied by documentation which clearly demonstrates that any deviations from established standards (e.g., a soil cover depth greater or less than 2 feet) will not degrade the level of explosives safety.

The master planners wish to examine the benefits of satisfying these requirements by arranging the magazines in a herringbone pattern, as illustrated in Figure 24. The design approach will be to provide at least 8 feet of soil cover but not less than the depth required to direct or vent <u>all</u> shock and gas pressures and debris through the headwall. This approach will reduce the blast and debris hazards to the sides and rear of any donor magazine but amplify and focus blast and debris effects to the front of the donor magazine. The herringbone pattern will suppress this effect by preventing the headwall and doors of any acceptor magazine from "seeing" the full face-on reflected pressures from any donor magazine.

Apply the criteria to answer the following aspects of the proposed design concept for the ammunition depot. Design parameters for the magazines are given in Figure 2. For these values, Equations 3 and 10 (for $t_d/T = 1$) are plotted in Figure 27 where x_m/d_s is shown for any combination of W and d_s. Equations 9 and 10 (for $t_d/T = 1$) are plotted in Figure 28 where W is shown for any combination of d_s and R_s. The solutions to the problem are derived from these figures.

(a) <u>Question</u>: What soil cover depth is required to completely contain an inadvertent explosion involving 8,000 pounds TNT equivalent? How high will the roof slab rise?

<u>Answer</u>: Full containment, an air-tight berm seal at all times, is defined as the condition where $x_m/d_s \leq 1.0$. Entering Figure 27 with $x_m/d_s = 1.0$ and W = 8,000 pounds, find $d_s = 23.8$ feet. Since $x_m/d_s = 1.0$, $d_m = (1.0)(23.8) = 23.8$ feet. Thus, 23.8 feet of soil cover over the magazine is required to fully contain the explosion effects of 8,000 pounds TNT. The roof slab will rise 23.8 feet.

(b) <u>Question</u>: What soil cover depth is required to provide an air-tight seal and prevent shock and gas pressures from jetting through the soil cover and instead force the pressure to escape through the headwall? How high will the roof slab rise?

<u>Answer</u>: To maintain an air-tight roof seal until all shock and gas pressures have escaped through the door openings requires $t_d/T \geq 1$. Entering Figure 27 with W = 8,000 and $t_d/T = 1$, find $d_s = 10.04$ feet. Thus, 10 feet of soil cover will provide an air-tight roof seal until all shock and gas pressures have escaped through the door openings.

Entering Figure 27 with W = 8,000 and $d_s = 10.0$, find by interpolation $x_m/d_s = 11.25$ or $x_m = (11.25)(10.04) = 113$ feet. Thus, with 10 feet of soil cover, an explosion involving 8,000 pounds TNT will drive concrete debris missiles 113 feet vertically into the air.

(c) <u>Question</u>: What is the maximum possible strike range of concrete debris missiles for 8 feet of soil cover? Is the strike range a good estimate?

Answer: Entering Figure 28 with $W = 8,000$ and $d_s = 8$, find $R_s = 316$. Thus, with 8 feet of soil cover, the maximum possible strike range of concrete debris missiles is 316 feet.

In Figure 28, the point corresponding to $W = 8,000$ and $d_s = 8$ feet lies barely in the shaded area. Thus, the predicted maximum possible strike range (316 feet) is conservative but not by a wide margin.

(d) Question: What minimum depth of soil cover is required so that the blast hazard instead of the debris hazard controls the safe distance from the ammunition depot to an unrelated inhabited area outside the depot?

Answer: To mitigate the risk to people and property from blast pressures, NAVSEA OP-5 requires a minimum separation distance from explosives stores to unrelated inhabited areas equivalent to $R_s = 40W^{1/3} = 40(8,000)^{1/3} = 800$ feet from the nearest large box magazine. Entering Figure 28 with $W = 8,000$ and $R_s = 800$, find $d_s = 4.55$. Thus, the "safe" separation distances from the rear and sides of a large box magazine to unrelated inhabited areas are identical for blast and debris if the soil cover is 4.55 feet. In other words, adding more than 4.55 feet of soil cover will not reduce the encumbered land area outside the perimeter of the ammunition storage depot.

(e) Question: What construction details should be incorporated into the design of the roof slab in order to achieve the most desirable failure mode?

Answer: Provide no compression steel near supports of the roof slab. Provide no bent-up rebars. Use small rebars, closely spaced, vice large rebars, widely spaced, in all areas of the roof slab. Provide no shear steel at slab supports; adjust the slab thickness so that the concrete resists the maximum applied shear stresses at supports from dead plus live loads. Provide a minimum separation distance between ordnance stores and the roof slab to reduce the chance of locally breeching the roof slab. The above factors need to be test validated but should improve the chance of achieving the most desirable failure mode, that illustrated in Figure 4a.

(f) Question: How does the total encumbered land area of the depot for $d_s \geqq 4.5$ feet compare with the land area for a traditional depot layout (parallel magazine rows and columns) and safety criteria ($R_s = 1,250$ feet for $W \leqq 30,000$ pounds TNT)?

Answer: Increasing the soil cover from 2 feet to $d_s \geqq 4.5$ feet reduces the band "width" of encumbered land outside the footprint of the magazine depot from 1,250 to 800 feet or 36%. The reduction is limited by safety requirements for blast pressures. Note that a depth of soil cover sufficient to force all blast pressures out the front of a magazine ($d_s \geqq 10.0$ feet) will not reduce significantly the blast pressures at inhabited building distance ($40W^{1/3}$) to the rear or sides or a donor magazine, although the reductions on acceptor magazines "closer-in" to the rear and sides of the donor are dramatic.

Missile Test Cell

WPNSTA Atlantis Master Plan includes MCON Project P-18 which provides for construction of missile test cells to support check-out of the CANOPUS Missile. The cells are adjacent to the weapons assembly area in Building 42. The net explosive weight (NEW) of the warhead plus 25% of the booster propellant is 300 pounds TNT equivalent. In accordance with NAVFAC P-397, the design charge weight, W, is 1.2(300) = 360 pounds TNT (Ref 5).

The design concept for the missile test cells is shown in Figure 3. Operational requirements call for a minimum ceiling height of 12 feet to accommodate a minimum hook height of 10 feet for an overhead crane and a floor area 15 feet wide and 30 feet long to accommodate the missile test stand plus test support equipment. The cells are sited remote from the support building (50 feet) to mitigate risks to people and property from blast effects. The plan is to mitigate the debris hazard by placing soil in a berm-like fashion over the roof of the test cell. The cell will be a conventional reinforced concrete design sufficient only to support the dead weight of the soil cover and a design live load (i.e., the concrete box structure is not blast hardened, except for the backwall). The backwall is designed to support the cell door from the explosion effects of W = 360 pounds TNT in the test cell. The pathway from each test cell to the weapons assembly area is covered with a frangible metal structure for weather protection.

Apply the theory in the report to answer the following aspects of the design concerning the soil cover. The values of critical design parameters for the CANOPUS Missile test cell are given in Figure 3. The solutions to this design problem will be derived from the equations in the paper.

(a) Question: What depth of soil cover, d_s, over the test cell will completely contain W = 360 pounds TNT?

Answer: Failure criteria for full containment (i.e., air-tight soil berm) require $x_m/d_s \leq 1.0$. For the design parameters given in Figure 3, $A/W^{2/3} = 180/(360)^{2/3} = 3.5569\ ft^2/lb^{2/3}$ and $W/V = 360/5{,}400 = 0.0667\ lb/ft^3$. From Equation 3,

$$\frac{d_s^{\,3}\,\gamma_s^{\,2}\,k^2(x_m/d_s)}{W^{2/3}} = 108087(3.5569)^{-1.56}(0.0667)^{-0.76}$$

$$= 1.1689 \times 10^5$$

Substituting known values and rearranging terms,

$$d_s = \frac{1.1689 \times 10^5\ (360)^{2/3}}{(145 \times 0.83 + 110\ d_s)^2} = \frac{5.9153 \times 10^6}{(120 + 110\ d_s)^2}$$

By trial and error, find $d_s = 7.22$ feet. Thus, 7.2 feet of soil cover is required over the missile test cell for the cover to fully contain the explosion effects from 360 pounds TNT.

(b) Question: What depth of soil cover, d_s, over the test cell will force all blast pressures to vent through the frangible wall and not to jet through the soil berm?

Answer: To prevent jetting of blast pressures through the soil berm requires $t_d/T \geqq 1.0$. From Equation 10 for $t_d/T = 1.0$,

$$1.0 = \gamma - \sqrt{\gamma^2 - 2(0.3)\,\gamma - \frac{12161 \times d_s}{(360)^{2/3}}(3.5569)^{1.72}(0.0667)^{1.72}}$$

and

$$\gamma = \frac{36255(3.559)^{0.08}(0.0667)^{0.48}}{(110\ d_s + 145 \times 0.83)} = \frac{1.094 \times 10^4}{110\ d_s + 120}$$

Therefore,

$$1.0 = \frac{1.094 \times 10^4}{110\ d_s + 120} - \sqrt{\left(\frac{1.094 \times 10^4}{110\ d_s + 120}\right)^2 - \left(\frac{0.6564}{110\ d_s + 120}\right) - 20.235\ d_s}$$

By trial and error, find $d_s = 2.1$ feet. Thus, a soil cover depth equal to 2.1 feet or greater will force all blast pressures to escape through the frangible wall and not to jet through the soil berm.

(c) Question: What depth of soil cover, d_s, over the test cell will prevent any concrete debris missiles from reaching the inhabited operating building located 50 feet away ($R_s \geqq 50$ feet)? Is the computed value of d_s a good estimate or instead overly conservative?.

Answer: From Equation 9 for $R_s = 50$ feet,

$$R_s = 50 = \left\{ \frac{216000\ (360)^{0.9466}}{k^2\ d_s^{\ 2}\ \gamma_s^{\ 2}\left[\dfrac{180}{(5400)^{0.487}}\right]^{1.56}} \right\} - 2\ d_s$$

$$50 = \frac{11.7923 \times 10^6}{(120 + 110\ d_s)^2} - 2\ d_s$$

By trial and error, find $d_s = 3.05$ feet. Thus, 3.05 feet of soil cover is required to prevent concrete debris missiles from possibly reaching the inhabited building located 50 feet away.

In (b) above we found $d_s \gtrless 2.1$ feet is required for $t_d/T \geqq 1.0$. Since $d_s = 3.05$ feet > 2.1 feet, the value $d_s = 2.1$ feet is a good estimate of the soil cover required to limit the maximum possible strike range of debris missiles to less than 50 feet.

(d) Question: Will the depth of soil cover found in (c) prevent blast pressures from jetting through the soil berm and in the process push concrete debris missiles helter-skelter into the air at velocities possibly exceeding those assumed in the theory? What is the blast pressure inside the test cell when this process begins?

Answer: Since $d_s = 3.05$ feet exceeds $d_s = 2.1$ feet which corresponds to $t_d/T = 1.0$, no shock or gas pressures will jet through the soil berm; all blast pressures will escape through the frangible wall.

(e) Question: What depth of soil cover is recommended? What is the maximum possible range of concrete debris missiles?

Answer: Use 3.05 feet of soil cover over the test cell to limit concrete debris missiles to strike ranges less than 50 feet where Building 42 is located.

(f) Question: What are the possible benefits of this design concept compared to the traditional blast resistant design using laced reinforced concrete?

Answer: Possible benefits are lower design and construction costs compared to the current safety standard which requires a laced reinforced concrete cell designed to resist the blast loading from 360 pounds TNT. The designer instead is instructed simply to design a conventionally reinforced concrete box culvert, 30 feet long, 15 feet wide, and 12 feet high. The culvert must safely support 3.05 feet of soil cover (plus any design live load requirements) which will extend at least 3 feet beyond the exterior face of each wall where the berm then slopes at 3:2 to the ground surface. The backwall must be blast hardened to support the blast hardened door to seal out blast pressures from escaping into the tunnel passageway.

The design concept also offers greater flexibility in meeting future operational requirements; more soil cover can be added to the soil berm if future operations require a larger rated charge capacity for the missile test cell.

IMPLICATIONS OF CRITERIA

1. The excellent correlation between theory and experiment is the basis for design criteria which offer, for the first time, a deterministic procedure for designing the earth cover over box-shaped ammunition storage magazines to control their structural performance and the debris hazard to prescribed levels.

2. The design criteria offer a technique for eliminating certain types of safety waivers and introducing flexibility and economy into the design process and construction standards for ammunition facilities without sacrificing the level of explosives safety. The criteria are especially applicable to facilities storing a small net explosives weight relative to the structure volume, such as ready service magazines, special weapons magazines, missile test cells, and aircraft shelters.

3. The design criteria offer an economical solution for altering certain existing magazines in the field to meet changes in operational and safety requirements. For example, required increases in the safe charge capacity of a missile test cell can be accommodated by simply adding more soil over the roof instead of constructing new test cells.

4. Given definitive construction standards for a magazine, containment and debris hazard diagrams of the type shown in Figures 25-28 could be made part of the standard drawings. The diagrams would provide the design flexibility to tailor the depth of soil cover to the particular operational, safety, and site plan requirements of each facility.

5. The prevalent design philosophy today is to meet performance requirements by designing strain energy capacity in the structural system. This philosophy is costly. Perhaps we should revert backwards, at least in some cases, to the design philosophy prior to about 1950 when the makers of explosives frequently made use of soil to meet requirements by converting blast energy in a donor to kinetic energy of the soil.

6. The potential benefits of the criteria justify closing technology gaps in the theory/criteria by pursuing the recommendations for future research outlined in Reference 1.

ACKNOWLEDGMENTS

Sincere appreciation is extended to the field personnel and staff at WPNSTA Concord for care in handling of the explosives. The quality of test data demonstrates a level of proficiency unsurpassed by any research organization.

Mr. Jerome Hopkins of CEL reviewed and computerized the theory. His thoroughness and timely response are appreciated.

REFERENCES

1. Civil Engineering Laboratory. Technical Report R-878: Design criteria for soil cover over box-shaped ammunition magazines, by W. A. Keenan (CEL) and L. C. Nichols (WPNSTA Concord). Port Hueneme, Calif., May 1980.

2. __________. Technical Report R-828: Blast environment from fully and partially vented explosions in cubicles, by W. A. Keenan and J. E. Tancreto. Port Hueneme, Calif., Nov 1975.

3. Naval Civil Engineering Laboratory. Technical Report R-621: Strength and behavior of restrained reinforced concrete slabs under static and dynamic loadings, by W. A. Keenan. Port Hueneme, Calif., Apr 1969.

4. Naval Sea Systems Command. NAVSEA OP-5: Ammunition and explosives ashore, vol 1, rev 5. Washington, D.C., Oct 1976.

5. Naval Facilities Engineering Command. NAVFAC P-397, Army TM-5-1300, and Air Force AFM 88-22: Structures to resist effects of accidental explosions. Washington, D.C., Jun 1969.

LIST OF SYMBOLS

A Vent area of magazine, ft^2

d_s Depth of soil cover over roof of magazine, ft

g Gravity, 32.2×10^{-6} $ft/msec^2$

h Vertical height of soil cloud, ft

h_m Maximum height of soil cloud, ft

i Total impulse of shock plus gas pressures, psi-msec

k Factor related to shear strength of soil berm and properties of roof slab

m Mass, $lb\text{-}msec^2/ft$

M Average unit mass of soil wedge plus roof slab, $psf\text{-}msec^2/ft$

$\bar{M}$ Total mass of soil wedge plus roof slab, $lb\text{-}msec^2/ft$

R Horizontal distance from magazine, ft

R_s Horizontal distance beyond which no debris missiles strike ground, ft

s_1 Length of concrete debris missile, ft

s_2 Width of concrete debris missile, ft

t Elapsed time from instant of explosion, msec

t_c Thickness of roof slab, ft

t_d Time when $x = d_s$, msec

t_m Time to maximum response of roof slab and soil cloud, msec

T Time duration of shock/gas pressure inside magazine, msec

v Velocity, ft/sec

v_d Velocity of roof slab when $x = d_s$, ft/sec

v_o Velocity at time $t = 0$, ft/sec

V Volume of magazine chamber, ft^3

W Net explosive weight, lb TNT

x Vertical displacement of roof slab, ft

x_d Vertical displacement of roof slab at $x = d_s$, ft

x_m Maximum vertical displacement of roof slab, ft

x_T Vertical displacement of roof at time $t = T$, ft

$\bar{y}$ Time constant related to centroid of pressure-time pulse

α Angle of shear plane failure for soil relative to horizontal, deg

ℓ_1 Length of magazine chamber, ft

ℓ_2 Width of magazine chamber, ft

ℓ_3 Thickness of magazine walls, ft

γ_c Density of roof slab, lb/ft^3

γ_s Density of soil berm, lb/ft^3

ϕ Angle of internal friction for soil

Table 1. Test Results[a]

NWSC Test No.	Test Parameters[b] — Charge Weight: C-4 (gm)	W	Soil Berm: γ_s	d_s (in)	Roof Slab: γ_c	t_c (in)	Scaled Parameters: $A/V^{2/3}$	v/V	$d_s/V^{1/3}$	Measured Results — Soil Cloud: h_m (in)	t_m	Roof Slab Response: x_m (in)	t_m	v_d	x_m/d_s	Remarks
3	169	0.51	124	27.2	32	2.64	4.81	0.0179	2.64	39.5	340	c	c	c	c	Headwall failed, door not in place
4	169	0.51	125	27.2	32	2.64	4.81	0.0179	2.84	33	350	12	220	d	0.44	#1 timber restrained
5	169	0.51	108	22.8	32	2.64	4.81	0.0179	2.38	51	430	20.5	320	d	0.90	Good test
6	398	1.20	108	30.0	32	2.64	2.72	0.0420	2.35	66	575	23.5	350	d	0.78	Good test
7	169	0.51	127	17.5	32	2.64	4.81	0.0179	1.83	65	550	22.5	340	5.4	1.29	Good test. Smoke vents at 590 msec
8	169	0.51	113	20.6	32	2.64	4.81	0.0179	2.15	77	560	24.0	320	4.8	1.17	Good test

[a] Unless otherwise noted, units are as indicated in List of Symbols.

[b] For all tests: $A = 3.07\ ft^2$, $V = 28.57\ ft^3$, $\ell_1 = \ell_2 = 3.00$ ft, $\ell_3 = 0.25$ ft

[c] Target obscured - no record

[d] $x_m < d_s$

Table 2. Theory Versus Experiment

Test No.	Test Parameters: W TNT (lbs)	d_s (in)	γ_s (lb/ft³)	Blast Load (Theory): $i/W^{1/3}$ (psi-msec/lb$^{1/3}$)	T (msec)	$T/W^{1/3}$ (msec/lb$^{1/3}$)	Effective Soil Mass Factor, k, Theory @ α= 90°	85°	80°	Soil Cloud: Height h_m (in.) Exper	Theory	Velocity v_0 (ft/sec) Exper[a]	Theory
3	0.51	27.2	124	771	14.9	18.6	1.30	1.41	1.54	39.5		14.6	
4	0.51	27.2	125	771	14.9	18.6	1.30	1.41	1.54	33		13.3	
5	0.51	22.8	108	771	14.9	18.6	1.31	1.40	1.51	51		16.5	
6	1.20	30.0	108	870	14.6	15.5	1.30	1.42	1.56	66		18.8	
7	0.51	17.5	127	771	14.9	18.6	1.31	1.38	1.46	65		18.7	
8	0.51	20.6	113	771	14.9	18.6	1.31	1.40	1.49	77		20.3	

Test No.	Roof Slab: Velocity @ X = d_s, v_d (ft/sec) Exper	Theory @ α= 90°	85°	80°	Maximum Displacement x_m (inch) Exper	Theory @ α= 90°	85°	80°	Time to Maximum t_m (msec) Exper	Theory @ α= 90°	85°	80°	Time Ratio t_m/T Theory @ α= 90°	85°	80°
3	b	b	b	b	c	11.5	9.7	8.2	c	244	224	206	16.4	15.0	13.8
4	b	b	b	b	12.0	11.3	9.5	8.1	220	242	222	[illegible]	16.2	14.9	13.7
5	b	b	b	b	20.5	21.2	18.4	16.0	320	331	308	[illegible]	22.2	20.7	17.3
6	b	b	b	b	23.5	27.9	23.2	19.2	350	380	346	315	24.5	22.3	20.3
7	5.4	6.7	5.5	4.2	22.5	25.8	23.2	20.8	340	365	346	328	24.3	23.2	22.0
8	4.8	4.1	1.0	b	24.0	23.6	20.8	18.3	320	349	329	308	23.4	22.0	20.7

[a] $v_0 = \sqrt{2gh_m}$

[b] $x_m < d_s$

[c] Target obscured — no record.

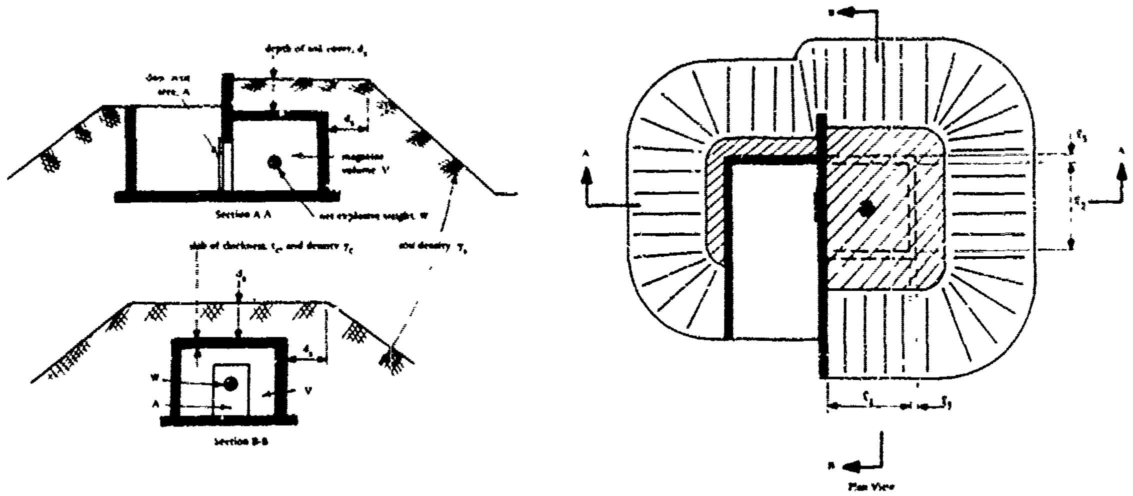

Figure 1. Typical earth-covered, box-shaped ammo storage magazine.

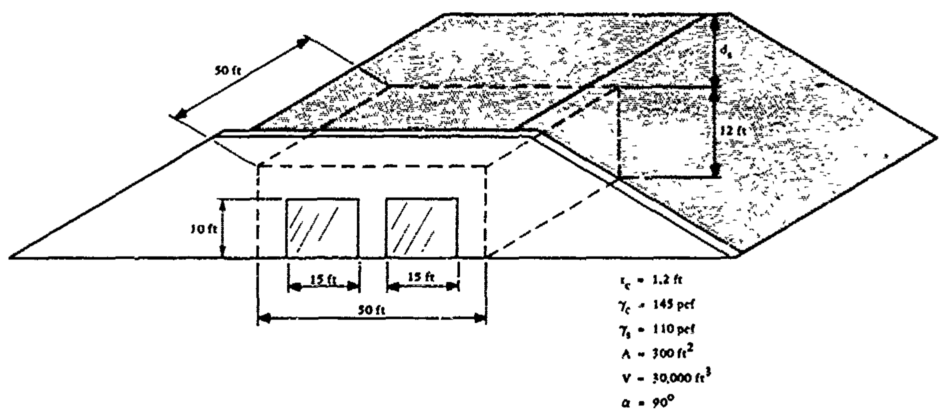

Figure 2. Details of large box-shaped magazine.

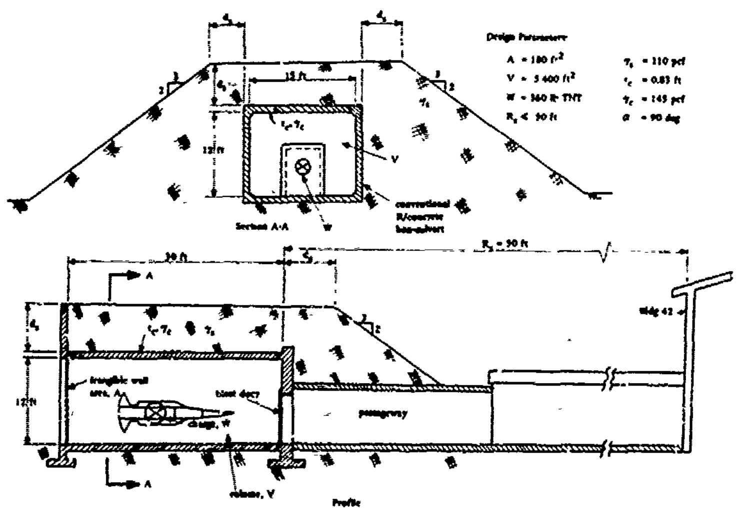

Figure 3. Design concept of test cell for CANOPUS Missile, WPNSTA Atlantis.

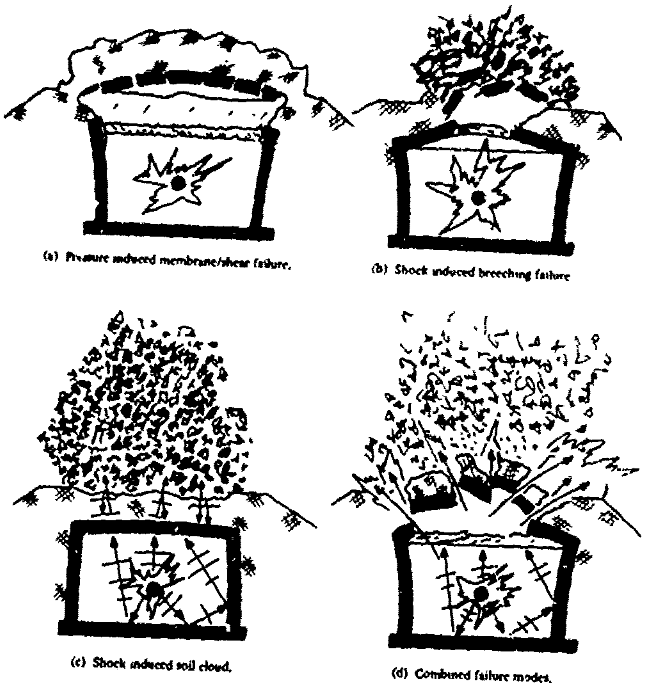

Figure 4. Failure modes of soil berm and roof slab.

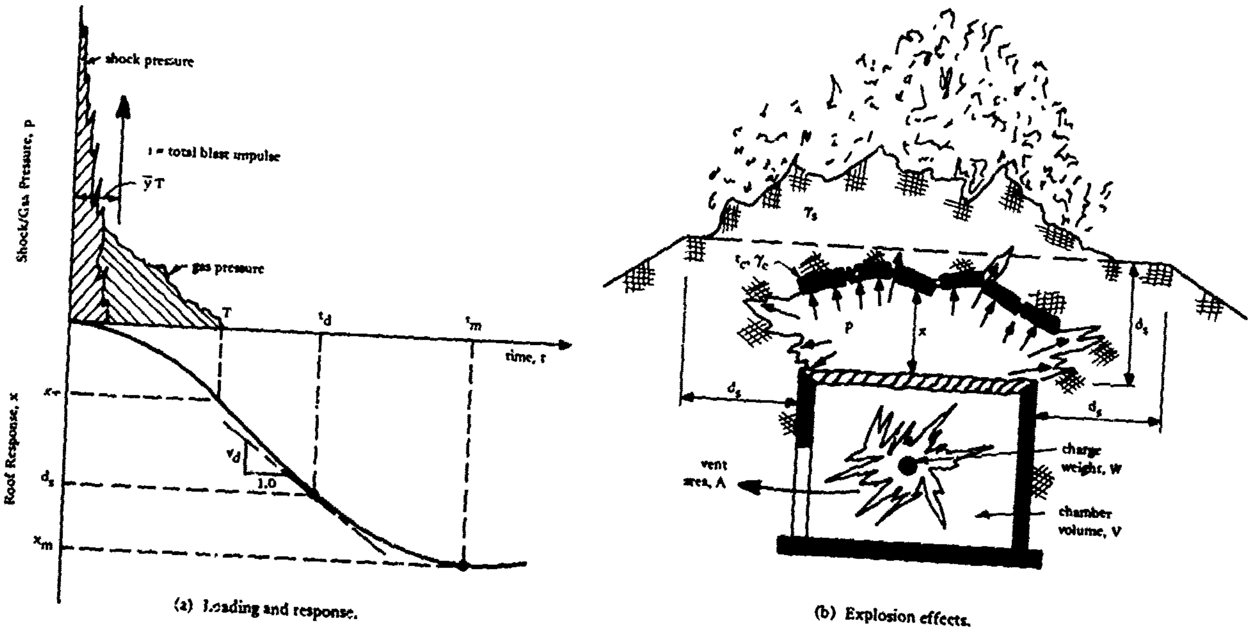

Figure 5. Time history of internal pressure and roof response for box magazine.

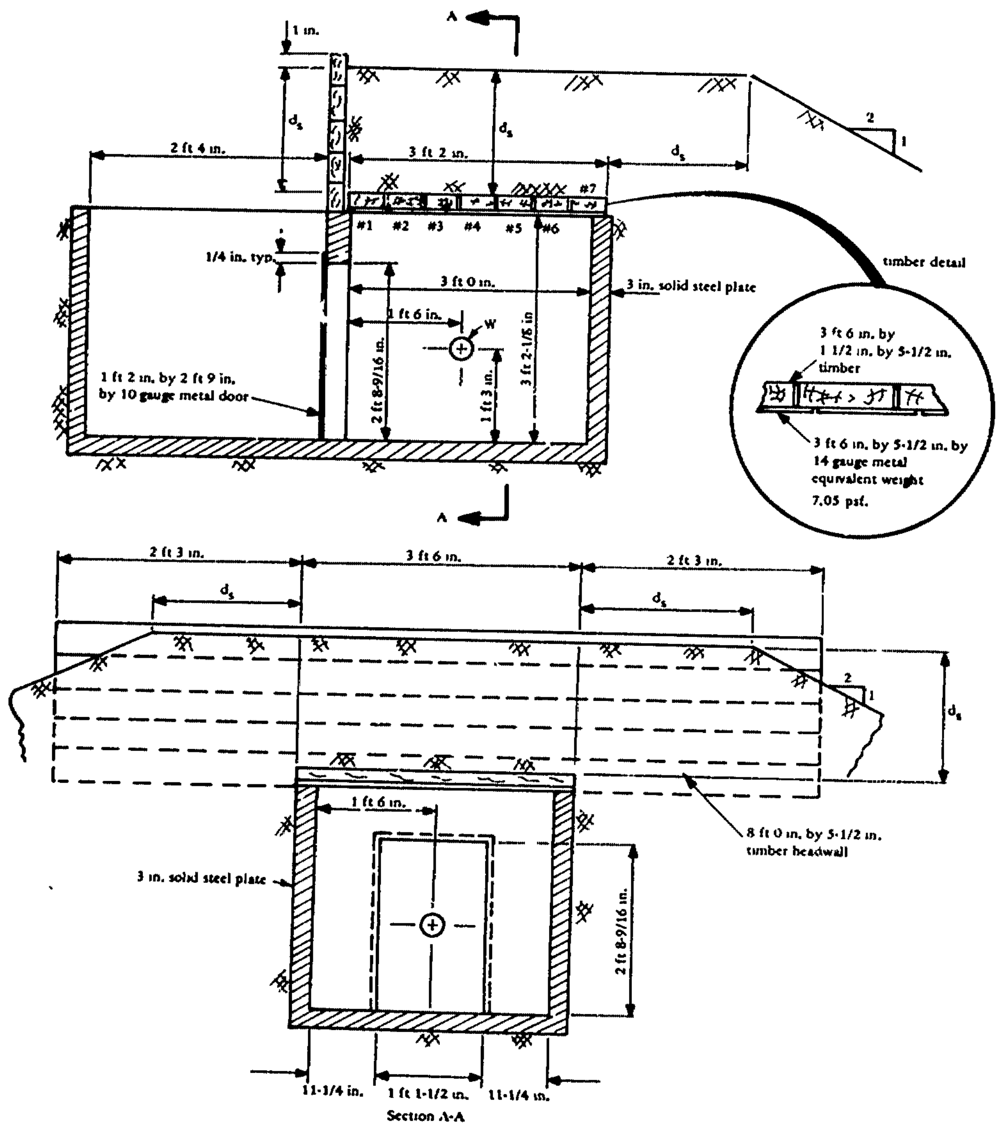

Figure 6. Design details of small-scale test magazine with timber/metal roof.

Figure 7. Steel test chamber for small scale test magazine.

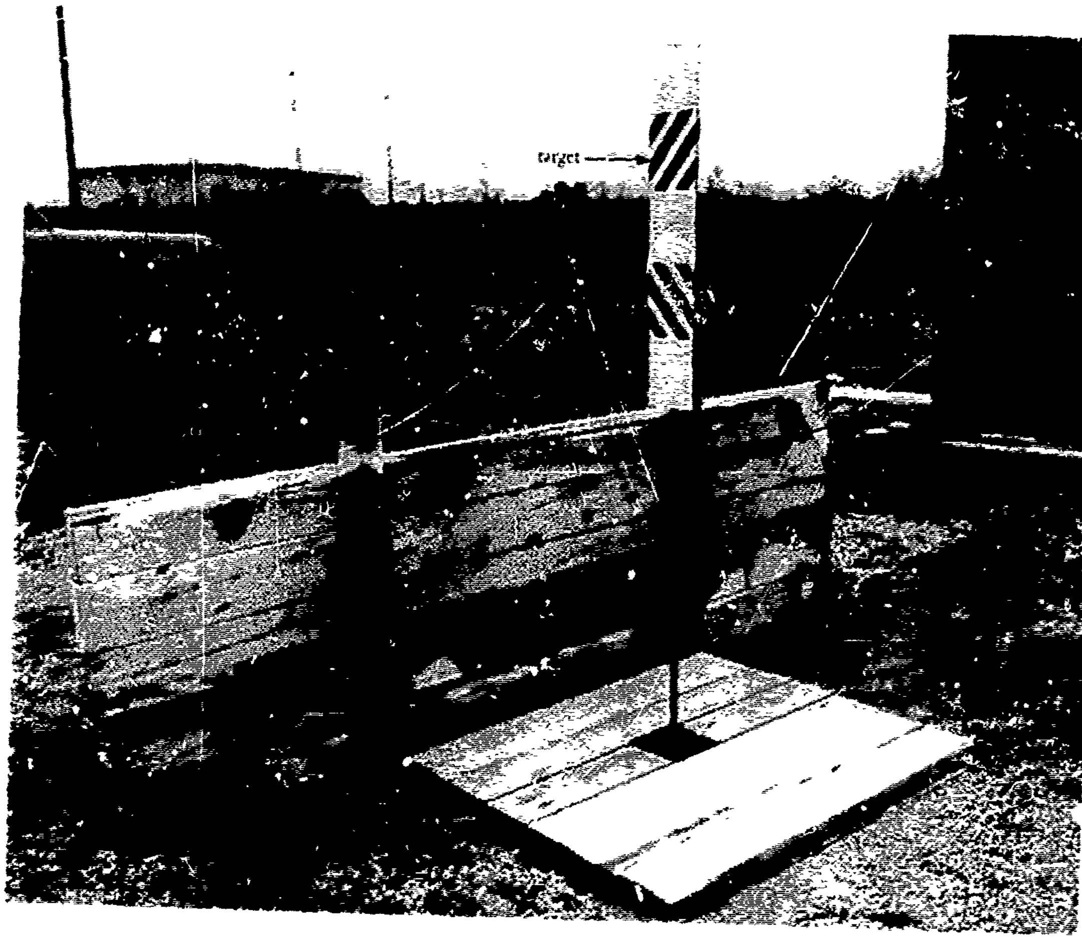

Figure 8. Timber headwall and roof without soil berm.

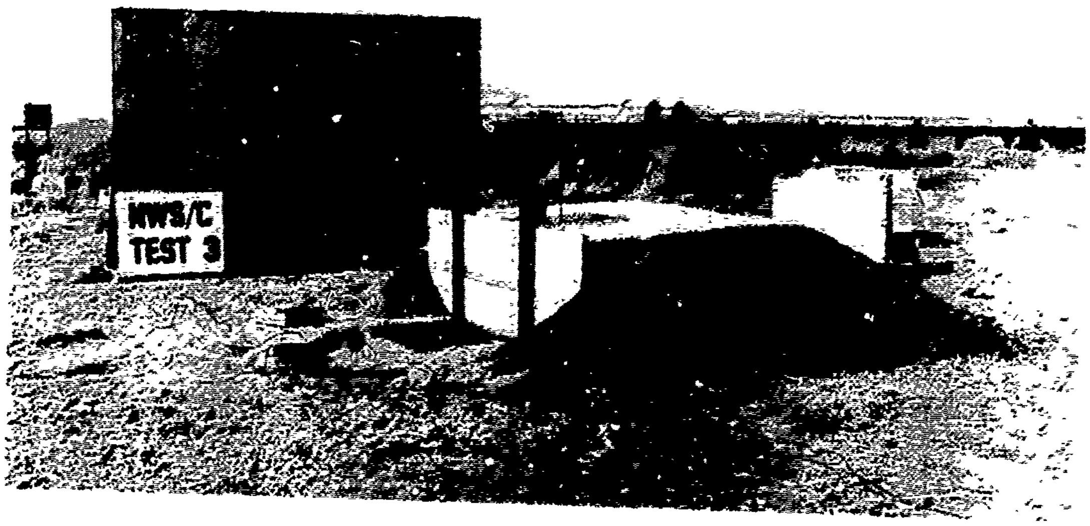

Figure 9. Test magazine with top of berm painted prior to test.

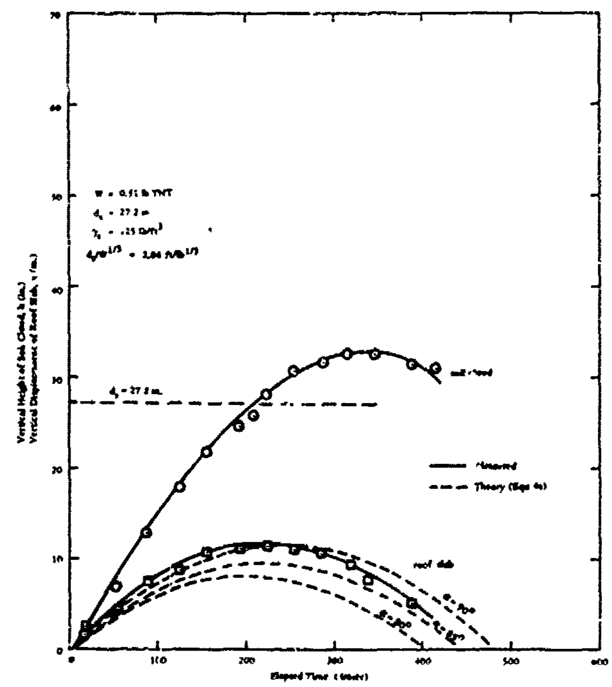

Figure 10. Growth of soil cloud and response of roof - Test 4.

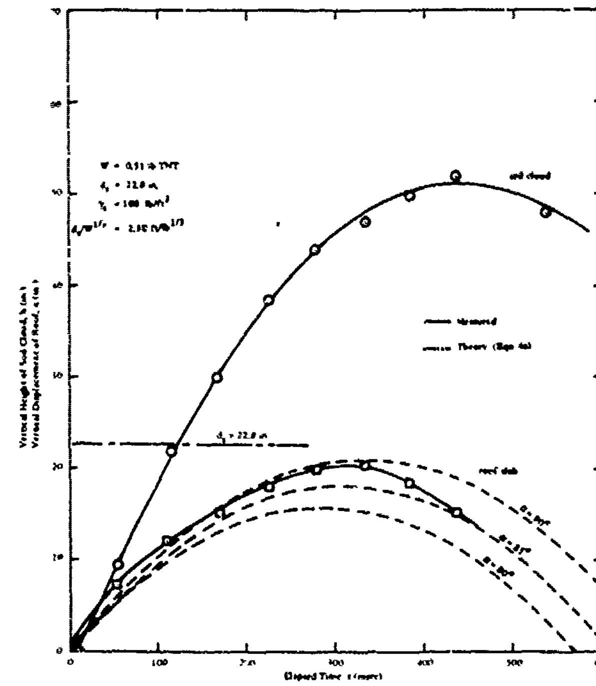

Figure 11. Growth of soil cloud and response of roof - Test 5.

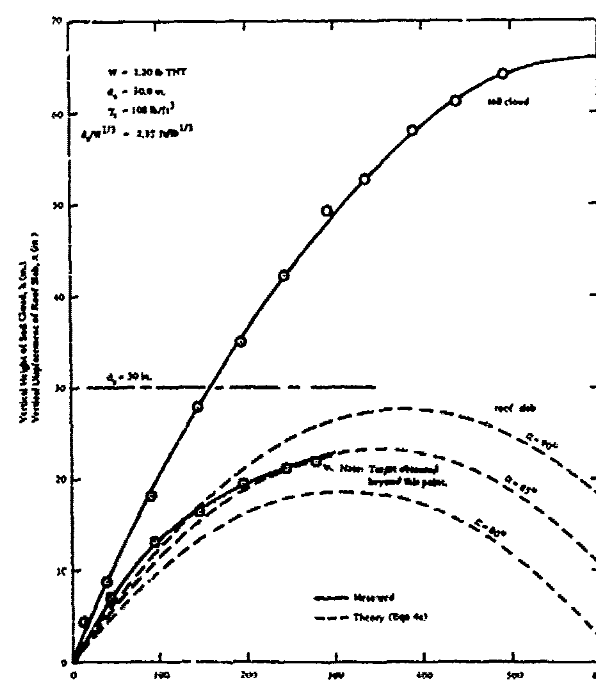

Figure 12. Growth of soil cloud and response of roof - Test 6.

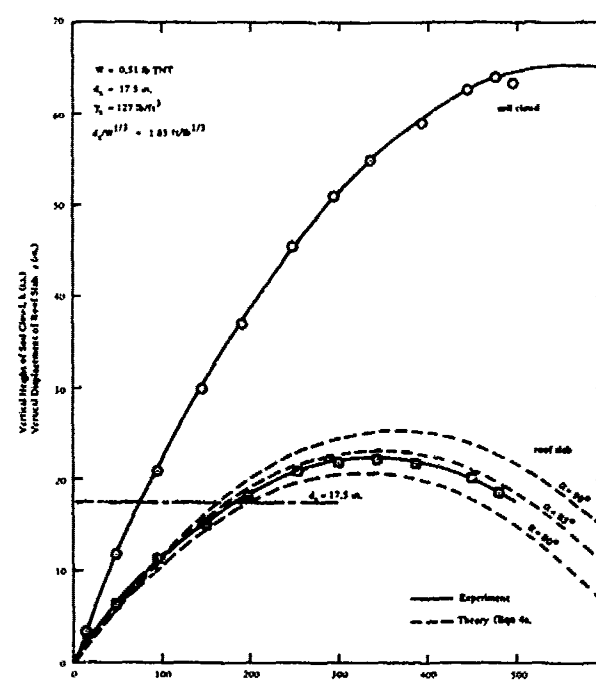

Figure 13. Growth of soil cloud and response of roof - Test 7.

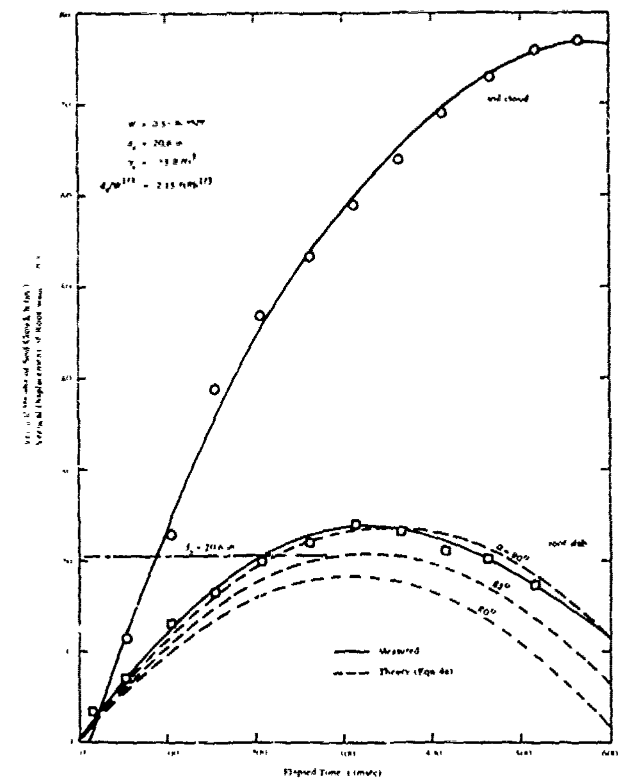

Figure 14. Growth of soil cloud and response of roof - Test 8.

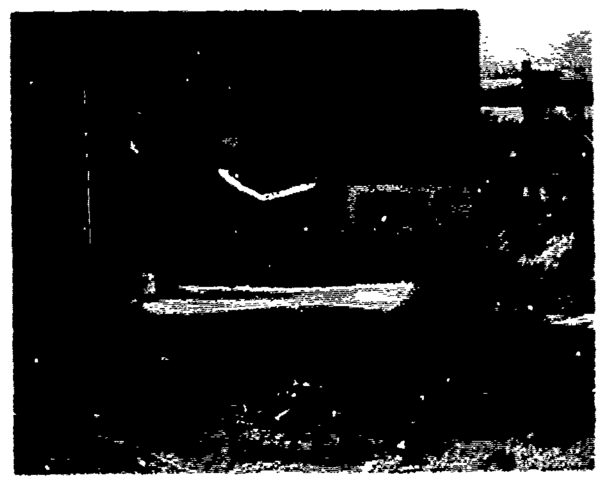

Figure 15. Pre-shot view of test magazine - Test 5.

Figure 16. View of test magazine shortly after time of detonation - Test 5.

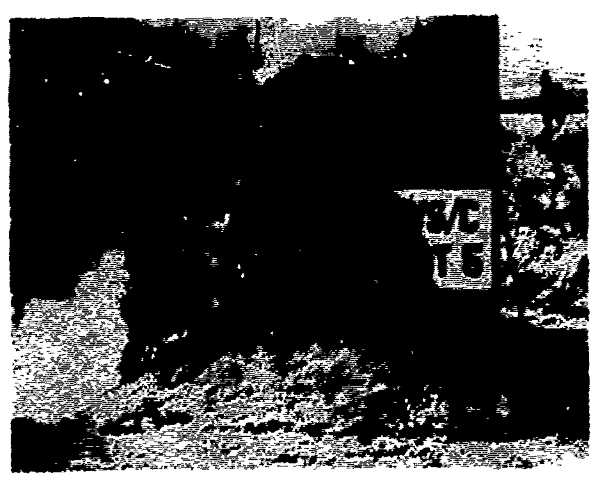

Figure 17. View of test magazine near time of maximum roof response - Test 5.

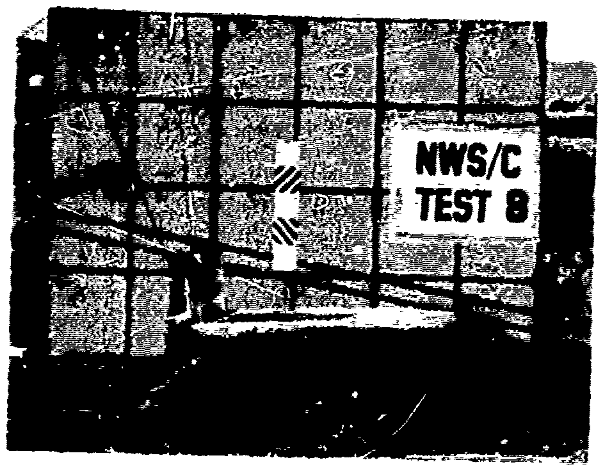

Figure 18. Pre-shot of test magazine - Test 8.

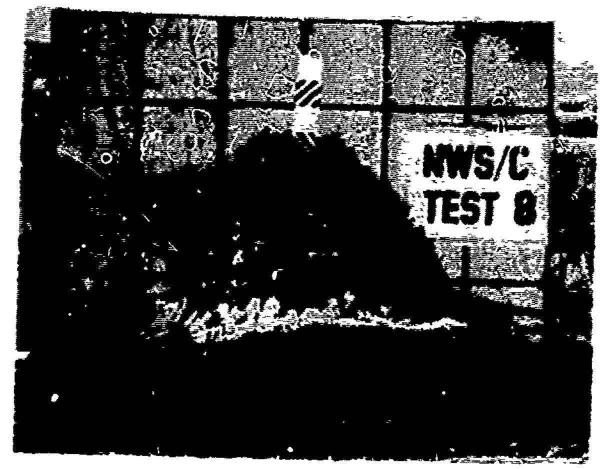

Figure 19. View of test magazine near time of maximum roof response - Test 8.

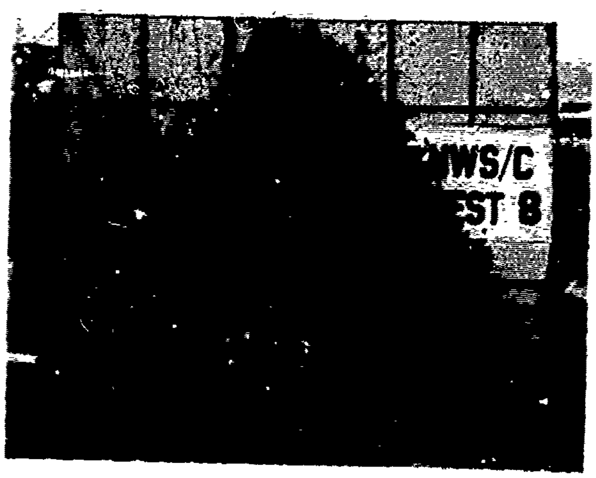

Figure 20. View of test magazine near time of maximum height of soil cloud - Test 8.

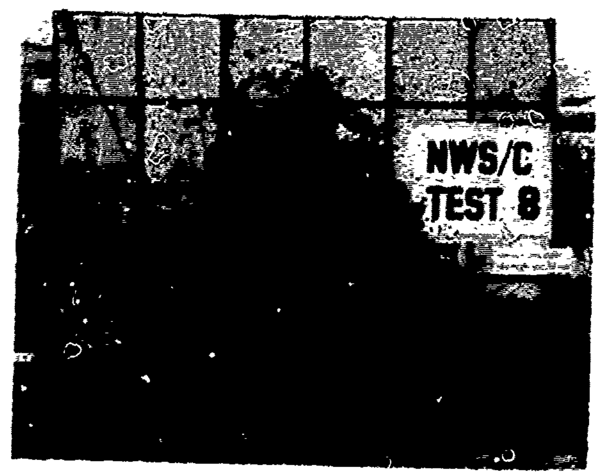

Figure 21. View of test magazine showing escape of gases through soil berm - Test 8.

Figure 22. Post-shot view of test magazine - Test 8.

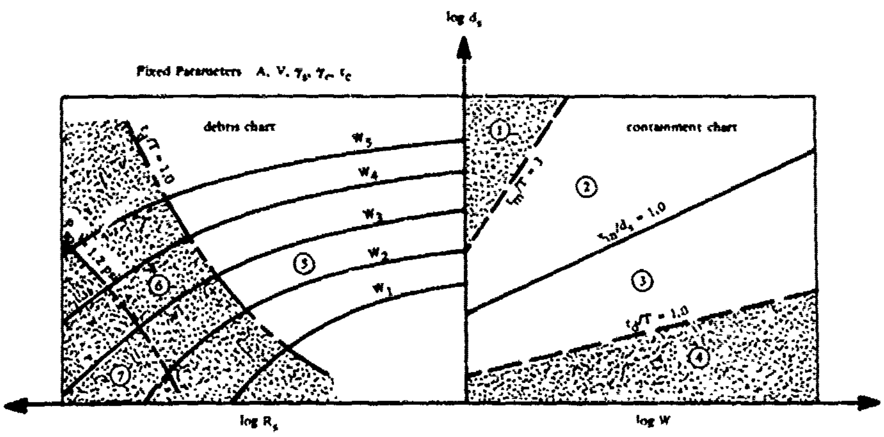

PERFORMANCE	REGION	COMMENT
Full containment	1,2	Air tight roof seal during entire history of blast loading and roof response. No concrete debris missiles.
	1	Prediction overly conservative.
	2	Prediction good but conservative.
Partial Containment	3	Air tight roof seal during entire history of blast loading.
Debris Hazard	3,4	Potential debris hazard outside magazine.
	4	Launch velocity of concrete debris missiles overly conservative. Some blast pressures jet/bleed through soil cover.
	5	Debris prediction good but conservative.
	6,7	Debris prediction overly conservative.
Blast Hazard	5,6	Leakage blast pressures exceed 1.2 psi.
	7	Leakage blast pressures less than 1.2 psi.

Figure 23. Debris and containment charts.

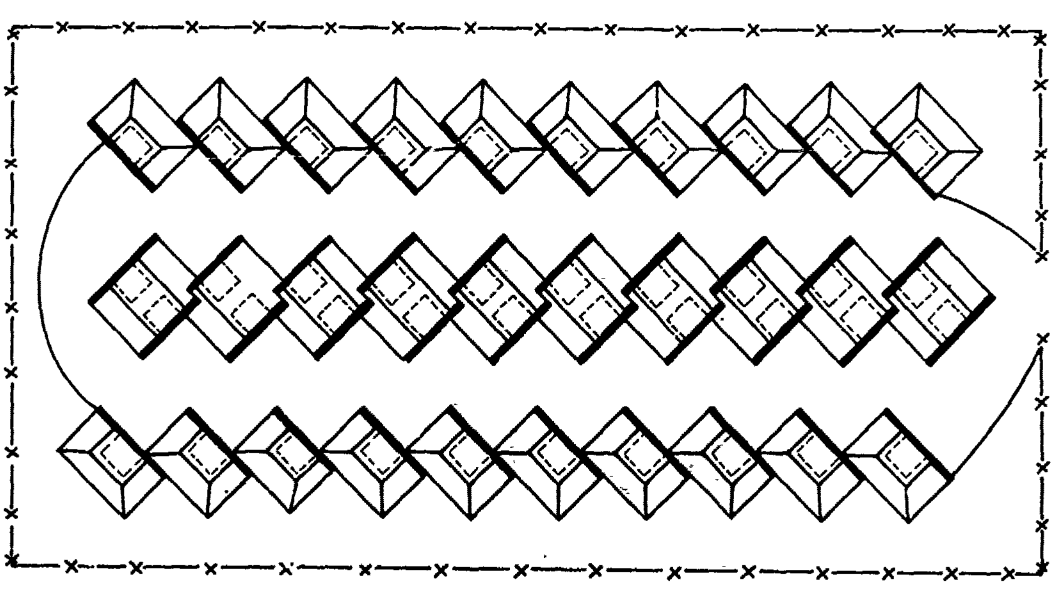

Figure 24. Herringbone-pattern for magazine depot, WPNSTA Atlantis.

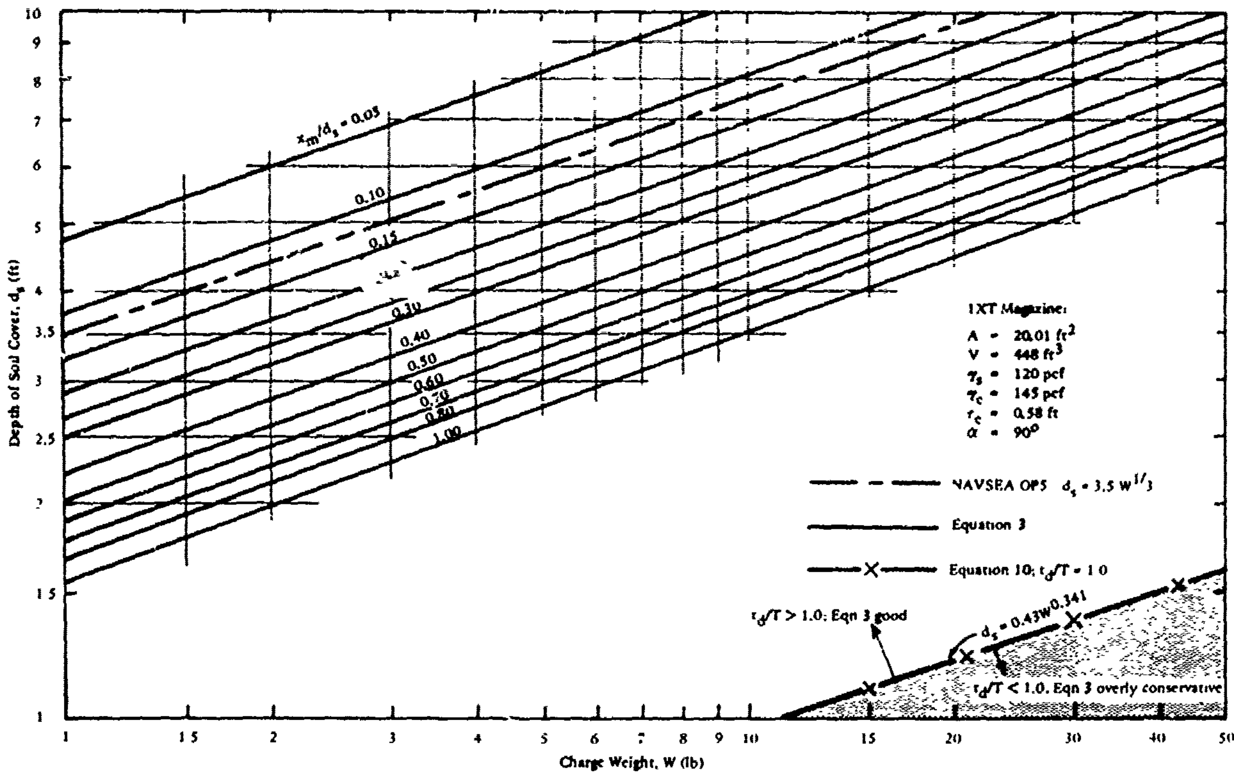

Figure 25. Containment of IXT magazine, WPNSTA Concord.

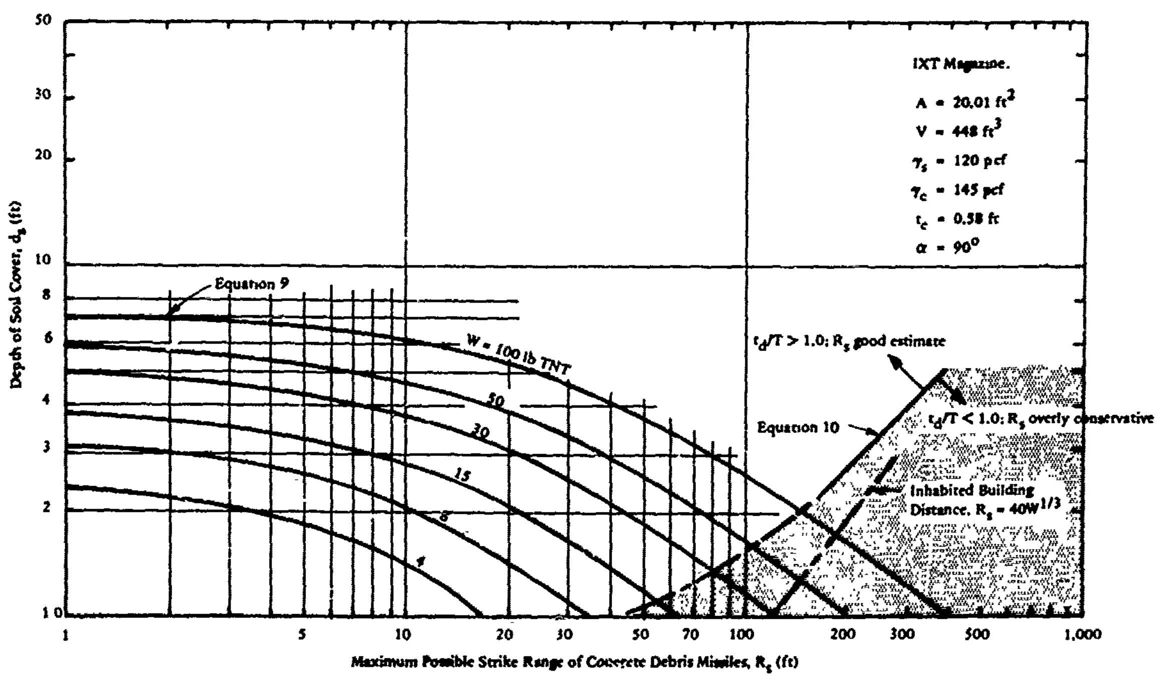

Figure 26. Debris hazard from breeching the roof slab of IXT magazine, WPNSTA Concord.

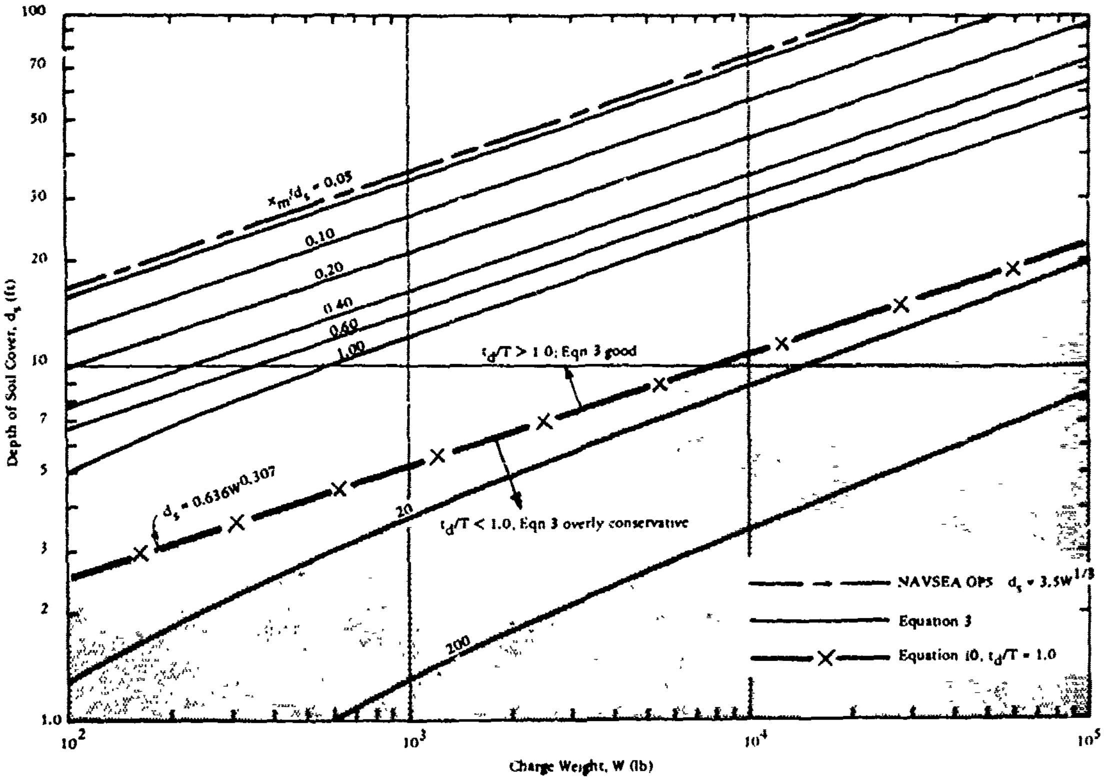

Figure 27. Containment of large box-shaped ammo magazine.

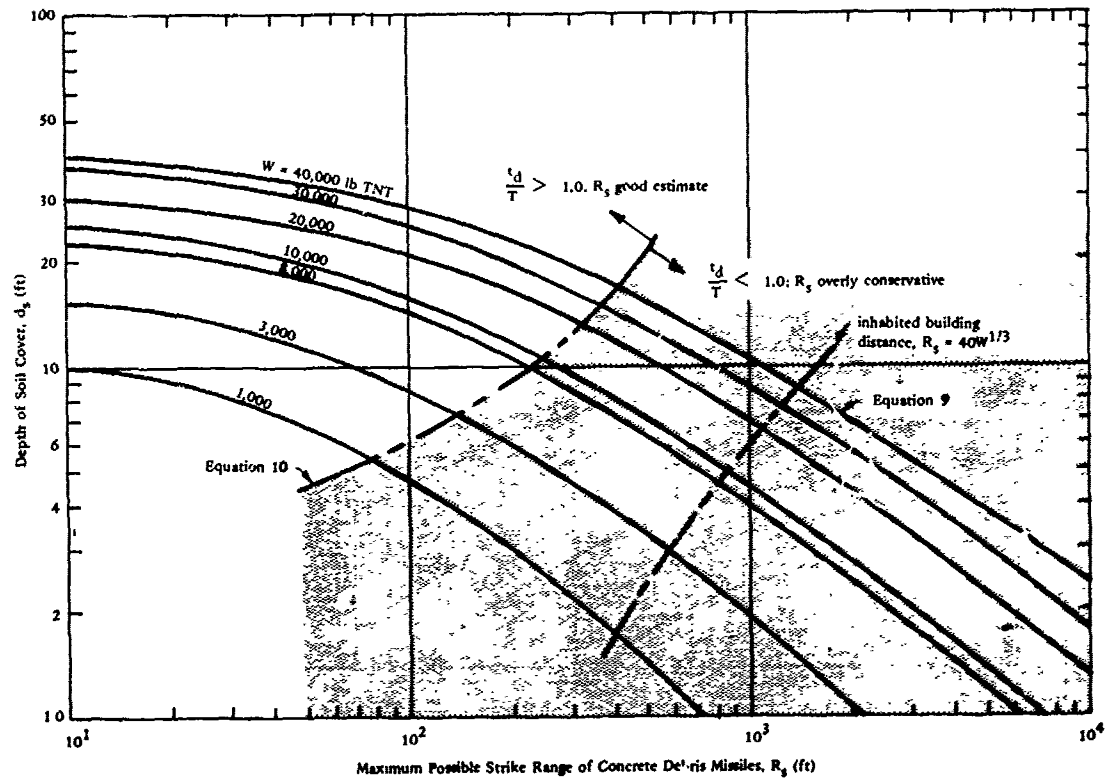

Figure 28. Debris hazard from breeching the roof slab of large box-shaped ammo magazine.

THE INTERIM QUALIFICATION OF A

DENSE BLASTING AGENT

FOR

MILITARY USE

Louis Avrami
Seymour Lopatin
Frank Vrabel

US Army Armament Research and Development Command
Dover, New Jersey 07801

ABSTRACT

The problems associated with a commercial blasting agent when considered for military use had a definite effect on the interim qualification program for that material. Besides being subjected to more stringent military specifications, the following criteria were addressed: safety, performance, initiation needs, vulnerability, toxicity, environmental impact, storability, availability of ingredients, producibility, loading, demilitarization and cost. The added characteristics of the blasting agent/explosive slurry mixture in its intended purpose required that a special laboratory test program be conducted in addition to the mandatory safety and performance tests stipulated in Army Bulletin TB-700-2 and the Triservice Qualification Manual. The impact of all the test results are discussed.

INTRODUCTION

For the past two decades the impact of blasting agents has completely revolutionzed blasting practices throughout the mining industry (Ref 1, 2). Industry was instrumental in the development of both the composition and delivery system for a large variety of these new "explosives" in commercial applications. The important advantage of the mixing and pumping system used in open pit mining operations is that the blasting agents are mixed on site from materials which are not considered explosive. A major factor in the acceptance of blasting agents is the safety properties of these mixtures (Ref 3).

However, the use of blasting agents by the military is still a relatively new innovation, but the unique characteristics to provide explosive power with low cost and increased safety make blasting agents potential candidates for military applications.

The paper describes the procedures required and fulfilled to accept a commerical blasting agent modified for military use in a specific application.

OBJECTIVE AND SPECIFICATIONS

The US Army has issued a requirement to develop a blasting agent for use by engineer troops to rapidly create large and effective anti-armor obstacles and to assist in tasks which require large quantities of explosives or munitions with significant savings in manpower, cost, time in target and logistic support when compared with conventional military explosives.

Listed below are some of the characteristics required for the blast agent:

a. A two component composition which when mixed properly form a detonable material over the temperature range from 241K (-32°C) to 325K (52°C).

b. One component will be liquid (a liquid oxidizer solution) and the other a dry powder (aluminum). Neither of the components will be detonable.

c. The components will be storable without degradation with temperature cycling from 241K (-32°C) to 336K (63°C) for a specified period.

d. The components will be capable of being mixed on-site by machine or by hand stirring over the temperature range of 241K to 325K without any special heating or cooling equipment.

e. The blasting agent can be poured directly into holes or trenches or placed in plastic bags for ease of handling or use against vertical targets.

f. The blasting agent will not detonate with a standard M-6 blasting cap in a 10 cm diameter by 61 cm long charge (unconfined) at 243K but with a detonable 227 g (1/2 pound) TNT or 50/50 pentolite booster charge.

g. The explosive output of the blasting agent as a cratering charge will be at least 1.5 times that of an equal weight of TNT.

h. The blasting agent must be capable of being neutralized after emplacement in the case of an aborted mission.

i. The blasting agent will be stable, pourable, pumpable and detonable for at least 5 days after mixing.

j. The blasting agent will not detonate when subjected to the 30 caliber rifle bullet test.

Another feature which was considered as an advantage logistically was storage. Military high explosives require secure storage in ammunition storage areas that are typically far from the majority of the target sites. This problem will be minimized in that the blasting agent components are non-explosive prior to being mixed together, the need for the rigid controls associated with handling, transporting and storing explosives is not required. This permits storage at or near the demolition target under minimal security.

DEFINITIONS

Prior to 1979 a blasting agent was defined as any material or mixture, consisting of a fuel and an oxidizer, intended for blasting, not otherwise classified as an explosive, and in which none of the ingredients is classified as an explosive, provided that the finished product, as mixed and packaged for use of shipment, cannot be detonated by means of a No. 8 blasting cap when unconfined. To classify a product as a blasting agent, both requirements, insensitivity to a blasting cap and lack of explosive ingredients, must be met.

However, in August 1979 (Ref 4) the Department of Transportation revised its definition of blasting agents for purposes of transportation. The new definition states that a blasting agent is a material designed for blasting which has passed the tests listed below and proved to be so insensitive that there is very little probability of accidental initiation to explosion or of transition from deflagration to detonation:

1. Blasting cap sensitivity test
2. Differential thermal analysis test
3. Thermal stability test
4. Electrostatic sensitivity test
5. Impact sensitivity test
6. Fire test

The latter definition complies with the United Nations 1.5 Hazard Classification (Ref 5).

The definitions above apply to dry blasting agents and slurry blasting agents.

COMPOSITION AND INGREDIENTS

The selection of the blasting agent for the bulk explosive system resulted from a contract awarded to IRECO Chemicals, Salt Lake City, Utah, which included the specifications noted above.

The composition of the slurry blasting agent, shown in Table 1, is designated Dense Blasting Agency DBA-105PM.

The proper mixing ratio for DBA-105PM is 64 ± 6% of the liquid component with 36 ± 3% of the powder component. The components are packaged in polyethylene containers so that two liquid containers mixed with one powder will provide 100 pounds of blasting agent. The average mixing times are 15 minutes at 20°C, 5 minutes at 63°C, and 30 minutes at -30°C.

Sodium perchlorate is the primary oxidizer ingredient. This is obtained at a nominal concentration of 60 percent in water. Ethylene glycol is added to the solution as a freezing point depressant and also as a fuel. Acetic acid is added to the liquid component to adjust the pH of the solution to 4.6 ± 0.1.

Powdered atomized aluminum powder coated wth 0.5% isostearic acid is the principal fuel. The coating is added to prevent the water-aluminum reaction. The guar gum is used as the thickening gelling agent to prevent the settling of the aluminum powder. It also provides an effective barrier against water intrusion. The potassium acid phthalate is the buffering agent which is used to maintain the acidity of the mixture.

Water is a most important ingredient of the dense blasting agent since it contributes materially to the explosive force when the slurry is properly initiated. Water serves as a source of the gaseous products which are required to do useful work. It also contributes to the total energy output by reacting with the aluminum. From the standpoint of safety water prevents high local pressures from developing when impacted by relatively slow moving objects. Water must be vaporized before ignition thus significantly delaying and limiting the temperature rise when the slurry is subjected to fire or other sources of heat.

To better understand some of the basic differences between blasting agents and explosives it would be helpful to compare the detonation process in each type of material. Blasting agents have relatively long reaction zones while explosives have much shorter reaction zones. In the detonation process the primary reaction occurs between the shock point and a rear boundary known as the Chapman-Jouget (C-J) plane. The length of the primary reaction zone is an inherent characteristic of each explosive substance or mixture. The critical diameter, or minimum diameter at which an explosive reaction will propagate dependably, is a function of the length of the reaction zone. Since military explosives such as PETN, RDX, and TNT have very short reaction zones, their critical diameters are quite small. Since blasting agents have longer reaction zones their critical diameters are therefore larger. In explosives with small critical diameters, most of the reaction is completed in the primary reaction zone, leading to high detonation pressures. In the dense blasting agents significant reactions occur behind the C-J plane. These include the reaction of larger ingredient particles and the oxidation of slowly reacting metallic fuels such as aluminum. As a result of these delayed reactions, detonation pressures for these products are generally lower than those for high explosives, because dense blasting agents have more of their energy released in the expanding gas phase of the explosion. Based on detonation pressure alone, high explosives will attain higher ratings, but in overall performance, blasting agents are quite competitive.

INTERIM QUALIFICATION PROGRAM

In order to obtain interim qualification for Army use each new explosive material, formulation, or mixture is subjected to the following criteria by an Interim Qualification Review Board: safety, performance, fuzing needs, vulnerability, toxicity, environmental impact, storability, availability of ingredients, producibility, loading, demilitarization and cost.

For the dense blasting agent DBA-105PM most of the criteria stipulated in the previous paragraph were addressed by data obtained from tests conducted in accordance with the following:

a. Army technical bulletin TB 700-2 (Ref 6).

b. Vol. IV, Joint Service Safety and Performance Manual for Qualification of Explosives for Military use (known as Tri-Service Qualification Manual) based on NAVORD Report OD-44811. (Ref 7)

c. Special laboratory tests (to be described).

(In a. and b. are listed all of the tests required by the DOT for a blasting agent.)

INTERIM QUALIFICATION TEST RESULTS

Tests According to Army Technical Bulletin TB-700-2)

1. Detonation (Blasting Cap) Test

Due to ambiguous results obtained with 2-inch paper cups, additional blasting cap tests were conducted. Cardboard cylinders, 3 1/4" D x 3 3/8" H, filled with DBA-105PM, and set on 2" x 4" x 6" lead witness block were tested by initiating a M-6 blasting cap completely submerged in the blasting agent. Four tests indicated that the DBA-105PM did not detonate or deflagrate.

2. Ignition and Unconfined Burning Test

a. In this test, a paper cup with blasting agent is placed in a cuspidor with fuel-oil-soaked sawdust. The sawdust is ignited with an electric match. Two tests were performed and the results were as follows:

(1) Test #1 - no explosion.
Ignition to burn - 116 seconds
Burn time of Blasting Agent - 64 seconds

(2) Test #2 - no explosion.
Ignition to burn - 92 seconds
Burn time of Blasting Agent - 76 seconds

b. In the second part of this test, four cups were put in a row in contact with each other and fuel-oil-soaked sawdust under the first cup. This also was lit by an electric match. No explosion occurrred. It took 320 seconds from ignition to start the blasting agent to burn and 105 seconds for the four cups to completely burn.

3. Thermal Stability Test

In this test, a 2-inch diameter, 4-inch high conductive rubber container filled with blasting agent was placed in an oven for 72 hours (over a weekend) at 76°C (total weight - 303 grams). The only change that occurred was a weight loss of 21.5 grams in the blasting agent.

4. Card Gap Test

The 50% probability point obtained in the large scale card gap test for DBA-105PM is 1.50 inches. For comparison purposes RDX (ρ = 1.64 gm/cc) has a 50% pt of 3.23 inches, Comp B (ρ = 1.66) 2.38 inches, and TNT (ρ = 1.60) 1.83 inches.

5. Impact Sensitivity Test

The Picatinny Arsenal and the NOL-Type 12 impact testers were used instead of the Bureau of Explosives impact tester. With the P.A. impact test no reactions occurred with 10 trials at 31 inches with a 2 kilogram weight. With the NOL-Type 12 tester no reactions occurred at 240 centimeters in 10 trials with a 2.5 kilogram weight. The Bureau of Explosives requires 10 trials at 3.75 inches with an 8 pound weight.

6. Additional Testing

The blasting cap, burn, thermal stability, electrostatic, friction, and impact tests were conducted on the liquid and powdered components separately for the Bureau of Explosives. That organization conducted its own tests on the separate components. The sodium perchlorate/ethylene glycol/water solution was judged to be Perchlorate, N.O.S. (not otherwise specified) and classed as Oxidizer according to DOT regulations. The isostearic acid coated/aluminum/guargum/potassium acid phthalate mixture was considered unnecessary to be classified.

Tests According to Triservice Qualification Manual

1. Mandatory

a. Impact Sensitiity

Reported in TB-700-2 test data.

b. Large Scale Gap Sensitivity

Reported in TB 700-2 test data.

c. Friction Sensitivity

The dense blasting agent DBA-105PM was tested on the ARRADCOM friction pendulum apparatus. In 10 separate tests no reactions of any type occurred with the steel shoe.

d. Electrostatic Sensitivity

Tests were conducted on the dense blasting agent with a voltage of 5000 VDC and a capacitance of .01 microfarad in an environment of 55% relative humidity and 20°C temperature. Twenty (20) consecutive tests conducted at the 0.25 joule level resulted in "no fires" occurring. Further tests indicated that initiation did not occur up to the 15 joule level. Tests conducted in dry samples of DBA-105PM produced the same results.

e. Thermal Stability

The explosion temperature test was conducted on the dense blasting agent. Due to the composition of the mixture, erratic timing results were obtained in the region of 267°C - 450°C. However, no ignitions or explosion occurred below 260°C.

f. Detonation Velocity

These results are included with the critical diameter results in the Performance Section.

2. Selected Background Information

a. Bullet Impact Sensitivity

The bullet impact test consisted of firing 30 caliber ball ammo into a 2" pipe nipple, 3" long, capped on one end filled with the

DBA-105PM. The distance between the rifle and sample was sixty (60 feet). Fifty (50) samples were tested and no actions or reactions occurred.

b. Vibration Test

A make-shift vibration test was conducted on a sample of DBA-105PM. Specifically, a regular 64/36 mixture was poured into a conductive container and installed into a paint vibrator. A sample was taken after 3 days of vibration and the test was stopped after 5 days. The 3-day sample density was 1.47 g/cc while the 5-day sample was 1.62 g/cc. Cap, burn, and impact tests did not show any increased sensitivity as compared to the regular dense blasting agent. The mixtures did not separate but were much thicker and harder to pour.

c. Compatibility with Standard Materials and 100°C Vacuum Stability Test

The 100°C Vacuum Stability Test was conducted with the blasting agent and various materials to determine the compatibility of the mixtures. The materials were aluminum, zinc, magnesium, copper, brass, steel, plastic polyethylene, cement, lime, lead, iron and stainless steel. Magnesium was the only material in this group that indicated excessive reactivity.

Additional tests were conducted with unleaded gas, low lead gas, isostearic acid, aviation gas, diesel fuel, lube grease, spindle oil and 30W oil. These tests were conducted at 65°C for 40 hours instead of 100°C due to the volatility of the samples. When tested with the dense blasting agent no excessive reactivity occurred with any of those samples.

Samples of the pigmented polyethylene container materials used to package the liquid and powder components also were tested with each of those components at 100°C for 40 hours. Negligible reactivity was obtained.

DTA/TGA thermograms were obtained on each of the blasting agent components and the mixture itself. With a 10°C min heating rate the blasting agent showed a well-defined weight loss of about 25% in the temperature range of 40° - 295°C. Another 13% was lost in the region 430° - 550°C. Slight thermal activity was evident between 495° - 560°C.

DTA/TGA thermograms were also obtained with blasting agent mixed with the same materials used in the compatibility/reactivity tests. Exothermal behavior was evident only with lube grease, 30W10 oil and magnesium. Only with magnesium did an ignitive oxidation exotherm occur at 567°C.

d. Bulk Density

Measurements of the density of the blasting agent were taken after the completion of the mixing period. Density measurements were taken as a function of time and temperature and these are noted with the detonation velocity data in Tables 2 and 3. Further details will be discussed in the Special Laboratory Test Phase.

e. Composition Analysis

The method to analyze the liquid and powder components of the DBA 105PM Blasting Agent has been developed. This covers the procedure to be used to evaluate the effects of storage of the separate components. For specification purposes the prepared synthetic mixtures report is being finalized.

The magnesium content was determined on eight aluminum samples furnished by ALCOA. The aluminum to be used in the blasting agent has an average magnesium content of 0.0024%. This value is well within the specification limit of 0.01% maximum set forth in the aluminum specification.

f. Viscosity

The viscosity measurements were obtained on DBA-105PM from a temperature range of -30°C to 63°C. The method followed by procedure outlined in ASTM D1823. At the colder temperatures the materials definitely became thicker but was still pourable. The viscosity ranged from 42,750 cps (centipoise) at -30°C to 21,500 at 63°C.

3. Performance

a. Detonation Velocity/Minimum Diameter

The critical diameter/detonation velocity measurements for the dense blasting agent were conducted in confined steel tubes since the manufacturer (IRECO) was conducting his tests in cardboard (unconfined) tubes.

At ambient conditions (20°C) detonation velocities were obtained with pipes of the following dimensions:

(1) 2.0" OD, 0.75" ID, 8" L.

(2) 2.675" OD, 1.2" ID, 12" L.

(3) 1.82" OD, 1.44" ID, 12" L.

Further testing with the 0.75" ID thick-walled pipe was restricted due to a lack of pipe. Testing with the 1.675" OD, 1.2" ID, 12" L pipe produced failures when tested at -30°C and +63°C.

The rest of the detonation velocity tests were conducted with the 1.82" OD, 1.44" ID, 12" L steel pipe. Detonation velocity test results as a function of mixing time and temperature are shown in Tables 2 and 3.

The five-minute mixture produced a detonation velocity at -30°C but failed at 20° and 63°C. The ten-minute mixture produced detonation velocities at all three temperatures. Fifteen minutes is the regular mixing time and detonation velocities were obtained at all three temperatures. Both the thirty-minute and one-hour mixtures produced detonation velocities at -30°C but not at +63°C. These tests were not conducted at ambient conditions.

Comparisons were made with the unconfined test data from IRECO. This will be discussed later in this report.

Special Laboratory Test Phase

1. Improper Mixtures

Impact, burn, cap and detonation velocity tests were conducted on improper mixtures (liquid/powder). In the detonation velocity tests the 3:1 and 1:1 ratios produced detonation velocities while the 1:2 and 1:3 failed. The results are tabulated in Table 3. Bulk density measurements were taken. In the P.A. impact test the 1:2 mixture did show a reaction at 19 inches while reactions above 30 inches were noted with the 1:1 and 1:3 mixtures.

2. Unsealed Heating of Open Containers

Unsealed samples of liquid and powder were heated at 63°C. The experiment had samples to be removed after 3 days, 5 days, 10 days, and 30 days. The 3-day sample did not show any significant weight loss. Also, the impact test and blasting cap test results of the mixture were essentially the same as the regular blasting agent. The 5-day sample lost 26% in the liquid and .78% in the powder. After 10 days the liquid had evaporated into crystalline form. The weight loss in the powder was essentially the same as the loss in the 3-day sample. An impact test on the crystalline sample did not produce any reaction on either the PA or NOL impact machine.

3. Mixing Characteristics at -30°C and 63°C

Liquid and powder samples were conditioned overnight at -30°C and 63°C and batches were mixed at 8, 10, 15, 30 min and 1 hour periods. The results on impact, burn, cap, and detonation velocity are shown in Table 3. The detonation velocity results are also listed in Table 2.

4. Long Term Sealed Storage at Elevated Temperature

Sealed liquid and powder samples have been stored in a heated atmosphere ranging from 63°C - 68°C (145°F - 155°F). At 1, 2, 6, and 12 months intervals, samples of each are to be taken and conditioned overnight at -30°C and 63°C. Picatinny Arsenal impact, blasting cap, and detonation velocity tests are to be performed. The one-month sample was not tested due to a shutdown in explosive operations. The 2-month sample was tested. The mixture obtained did not thicken properly. Both the detonation velocity tests at -30°C and 63°C failed and no reactions were obtained with the impact and blasting cap tests. A mixture of the 2-month liquid with standard powder produced an acceptable thickened blasting agent. However, the standard liquid mixed with the 2-month powder did not produce a proper mixture. This was very watery and the components did not stay mixed. The thickening characteristic was not present. A DTA/TGA thermogram of a guar gum sample dried for 18.5 days at 70° ± 5°C did not show any difference when compared to a sample (as is) from IRECO.

5. Maximum Separation Distance for Sympathetic Detonation

The maximum separation distance required to permit sympathetic detonation with the blasting agent was performed with the 1.4" ID pipes. The minimum "no-go" was 1 13/16" while the maximum "go" was 1 3/4".

6. Mixture of Blasting Agent/Fuel Oil and Blasting Agent/Water

Mixtures of blasting agent/fuel oil were mixed in ratios of 90/10, 80/20, 75/25, 60/40, and 50/50. Burning tests, blasting cap and detonation velocity tests were conducted. The results, listed in Table 3, indicate that no enhancement in explosive properties occurred with the tests conducted. With 10% and 50% fuel oil the mixtures did not detonate.

Mixtures of blasting agent/water were tested to determine the effect of dilution for safety and neutralization. In the detonation velocity test with 25% and 50% mixtures, a run-up time was noted but it quickly died out.

7. pH Measurements

Two series of tests were performed with pH measurements. In the first test blasting agent samples were prepared with pH's of 3.0, 4.6, and 9.0 and these were stored at ambient (31°C) and elevated temperatures (77°C).

The second test consisted of samples of each mixture prepared in the Special Laboratory Test Phase, i.e., regular, 5 min mix, 10 min mix, 3 day and 5 day vibration, improper mixtures and elevated temperature samples.

The first test series showed that the 3.0 pH ambient samples recorded 3.0 on the first day and 3.7 on the 67th day. The 3.0 pH samples stored at 77°C recorded 3.0 on the first day and 5.3 after 34 days. (The samples became dry after this date.)

The 4.6 pH ambient samples recorded 4.3 on the first day and 4.4 on the 67th day. Stored at 77°C these samples recorded 3.45 on the first day and 5.1 on the 34th day.

The 9.0 pH ambient samples recorded 9.7 on the first day and 6.4 on the 67th day. At 77°C these samples recorded 9.25 on the first day and 5.5 on the 34th day.

The pH's were adjusted with 10% acetic acid or 5% sodium hydroxide.

In the second series of tests the first pH readings were taken of the mixtures about 3 weeks to 6 weeks after the batches were made. Subsequently readings were taken 9 days and 40 days later. Slight increases in the pH value were noted in the regular mixtures, 15 minute and 10 minute mixing time. After 40 days the 15 minute regular batch went from 4.5 to 6.4 while a 10-minute mix went from 4.3 to 7.0. All the other samples did not show any significant difference.

8. Toxicity

The US Army Environmental Health Agency at Edgewood Arsenal, Aberdeen Proving Ground, MD., conducted tests on the liquid and powder components as well as on the DBA-105PM mixture. The findings indicate that goggles and rubber gloves should be worn when handling or mixing the dense blasting agent ingredients.

9. Cost

The total cost for DBA-105PM is approximately $1.00/lb, which represents a significant savings when compared to standard military explosives.

10. Comparison with IRECO Data

Table 4 lists the detonation properties tests conducted at IRECO Chemicals on the dense blasting agent DBA-105PM while Table 5 lists the results of the IRECO special tests (Ref 8). A comparison of the ARRADCOM and IRECO test data is shown in Table 6.

SUMMARY

All the data have been reviewed and analyzed by the Interim Qualification Review Board. A breakdown of the findings are as follows:

a. DBA-105PM has met the safety and mandatory requirements of TB 700-2 and the Tri-Service Manual. The conclusions for the water-based DBA-105PM are:

(1) It is not cap-sensitive.

(2) It is not impact-sensitive either with the PA or NOL tester.

(3) No reactions were obtained with the steel shoe on the large PA friction pendulum.

(4) It complied with the "no-fire' requirement at the 0.25 joule level for the electrostatic test.

(5) It did not detonate in the burn test.

(6) It met the requirements of the 100°C VST.

(7) The large scale gap test result of 1.50 inches indicates that it is less shock-sensitive than TNT.

(8) Growth and exudation data are not required for the application stated.

(9) The explosion temperature test indicated that no ignition or explosions occurred below 260°C.

(10) Detonation velocity values based on containment and density ranged from 2300 to 4000 m/sec.

b. The specific background, performance and special laboratory tests brought out the following findings:

(1) The DBA-105PM is not bullet-sensitive to a 30-caliber test firing.

(2) It is compatible to all standard metals except magnesium. It is also compatible to most materials associated with a motor vehicle.

(3) Detonation velocity tests conducted under the confined conditions noted produced some erratic results at extreme temperatures (-30°C and +63°C).

(4) Long term storage of sealed separate components (>2 month) conditioned at 63° - 65° indicates that the powder component will not thicken to produce a functioning blasting agent.

(5) pH measurements indicate that the mixed blasting agent values did not change under ambient storage for a period up to 67 days. At 77°C accetable pH's were obtained up to 34 days, after which the samples dried out.

(6) Comparison with IRECO data of similar tests indicate that the data was in agreement in all cases. In most instances the IRECO data were on a larger scale than that of ARRADCOM.

Taking cognisance of the problems which surfaced in b.(3) and b.(4), the Interim Qualification Review Board granted interim qualification for Army use for the dense blasting agent DBA-105PM. This was done since further results would be obtained from the field testing now being conducted by the Test and Evaluation Command at the Aberdeen Proving Ground, MD.

REFERENCES

1. M.A. Cook, Ind. Eng. Chem. 60, 44 (1968).

2. R.A. Dick, "The Impact of Blasting Agents and Slurries on Explosives Technology," US Bureau of Mines Information Circular 8560, 1972.

3. R.B. Clay, L.L. Udy, "Safety Aspects of Slurry Explosives," Minutes of the Eleventh Explosives Seminar, Memphis, TN, 9-10 September 1969, Armed Services Explosives Safety Board, Washington, DC, 1969.

4. Federal Register, Vol. 43, No. 238 - Monday December 11, 1978 - Blasting Agents, Final Rules.

5. "Transport of Dangerous Goods," United Nations Report ST/SG/AC.10/1/Rev. 1, United Nations Sales No. E.77.VIII. United Nations, New York, 1977.

6. Department of the Army Technical Bulletin TB 700-2, Explosives Hazard Classification Procedures, 19 May 1967.

7. Joint Services Evaluation Plan for Performed and Alternate Explosive Fills for Principal Munitions, Volume IX Joint Service Safety and Performance Manual for Qualification of Explosives for Military Use, published by Energetic Materials Division, ARRADCOM, Dover, NJ, 19 September 1972.

8. Unpublished Data, G.L. Hansen, IRECO Chemicals 1979.

TABLE 1
DENSE BLASTING AGENT
DBA-105PM
COMPOSITION

Ingredient	Percent (by weight)
LIQUID COMPONENT	
Sodium Perchlorate	51 ± 2.0
Water	39 ± 2.0
Ethylene Glycol	10 ± 2.0
Acetic Acid to adjust pH to 4.6 ± 0.1	
POWDER COMPONENT	
Aluminum (coated wtth .125% isostearic acid)	97.6 ± 2.0
Guar Gum	1.4 ± 0.2
Potassium Acid Phthalate	1.0 ± 0.2

TABLE 2

DETONATION VELOCITY DATA

Critical Diameter Steel Tube Dimensions	Density	Detonation Velocity (M/Sec) -30°C	20°C	63°C	Remarks
a. 1.82"OD, 1.44"ID, 12"L	1.51		3970		
	1.51		3750		
	1.39	3391			5 Min Mix
	1.47	2740			10 Min Mix
	1.52	3221			30 Min Mix
	1.57	2364			1 Hr Mix
	1.55			Failed	5 Min Mix
	1.66			3109	10 Min Mix
	1.67			2523	15 Min Mix
	1.79			Failed	30 Min Mix
	1.80			Failed	1 Hr Mix
	1.40		Failed		5 Min Mix
	1.45		3487		10 Min Mix
b. 2.0"OD, 0.75"ID, 8"L	1.51		3533		
	1.51		3717		
c. 1.675"OD, 1.2"ID, 12"L	1.51		3956		
	1.55	Failed			
	1.55			Failed	

TABLE 3
SPECIAL LABORATORY TESTS

	Density (g/cc)	P.A. Impact (Inches)	NOL Impact (CM)	Cap Test	Burn Test (Sec)	Detonation Velocity (m/sec)
A. Improper Mixtures (Liquid/Powder)						
1. 75/25 (3:1)	1.47	32	240 N.R.	No Go	538	3900
2. 50/50 (1:1)	1.71	30	240 N.R.	No Go	362	2222
3. 36/64 (1:2)	1.75	19	240 N.R.	No Go	348	Failed
4. 25/75 (1:3)	1.99	36 N.R.	240 N.R.	No Go	1127	Failed
B. Mixing Characteristics						
-30°C						
1. 5 min. Mix	1.39	29	240 N.R.	No Go	515	3391
2. 10 min. Mix	1.47	35	240 N.R.	No Go	392	2740
3. 30 min. Mix	1.52	29	240 N.R.	No Go	536	3221
4. 1 hour Mix	1.57	35	240 N.R.	No Go	195	2364
63°C						
1. 5 min. Mix	1.55	36 N.R.	240 N.R.	No Go	522	Failed
2. 10 min. Mix	1.66		240 N.R.	No Go	176	3109
3. 15 min. Mix	1.77		240 N.R.	No Go		2523
4. 30 min. Mix	1.79		240 N.R.	No Go		Failed
5. 1 hour Mix	1.80	25	240 N.R.	No Go		Failed
C. Mixtures with Fuel Oil and Water						
Blasting Agent/Fuel Oil						
1. 90/10				No Go	325	Failed
2. 80/20				No Go	340	-
3. 75/25				No Go	322	-
4. 60/40				No Go	450	-
5. 50/50				No Go	452	-
Blasting Agent/Water						
1. 75/25				No Go	700	1639 Died Out
2. 50/50				No Go	No Burn	1765 Died Out
3. 25/75				No Go	No Burn	

TABLE 4

DETONATION PROPERTY TESTS

AT IRECO CHEMICALS

Formulation: DBA 105 PM (1)

	Booster Charge Wgt (gms)	-30°C	20°C	50°C
Density (gm/cc)		1.47	1.47	1.52
1. Critical Diameter Tube Dimensions				
3" D x 18" L	160	Det (2790 M/sec	Det (3100 M/sec)	Det 3870 M/sec)
2½" D x 18" L	40	Det	Det	Det
2" D x 18" L	40	Det	Det	Det
1½" D x 18" L	40	Failed	Failed	Failed
2. Minimum Booster				
4" D x 12" L	8	Det	-	Det
3. Cap Sensitivity				
3" D x 18" L	-	Failed	Failed	Failed
4. Seismic Strength				
5000 gms			1.38 x TNT(4)	

NOTES:
(1) Hand mixed in 30 to 60 lb batches. Mixing Times: 1 Hr. @ -30°C, 15 Min @ 20°C, 5 Min @ 50°C
(2) Booster Charge: 50/50 pentolite
(3) Ensign - Bickford Primadet cap used at -30°C & 50°C. DuPont #8 cap used at 20°C.
(4) Average seismic strength for old mix DBA105P was 1.39 x TNT

Table 5. Special Tests on DBA-105PM Conducted at IRECO

		Reference
1. Tolerance Variation	66.3% Liquid, 33.7% Powder	64% Liquid, 36% Powder
4" Diam	Detonated, 3300 M/sec	Detonated, 3580 M/sec
3" Diam	Detonated, 2350 M/sec	Detonated, 2310 M/sec
2 1/2" Diam	Failed to detonate	Detonated, 2080 M/sec
2" Diam		Failed to detonate
Density	1.53	1.51
2. Mixing Errors (25°C)	3/1 Liquid/Powder	1/1 Liquid/Powder
4" Diam	Detonated, 2440 M/sec	Detonat
3" Diam	Detonated, 1500 M/sec	Detonated, 2700 M/sec
2 1/2" Diam	Failed to detonate	Failed to detonate
M6 Cap Test	Failed to detonate	Failed to detonate
Density	1.51	1.56
3. Water Dilution (25°C)	10% Water	15% Water
6" D Tube	Detonated, 3175 M/sec	Did not detonate

4. Gum Variations (25°C)	1.5%	1.2%	1.4%
4" Diam	Det, 3100 M/sec	Det, 4230 M/sec	Det, 3580 M/sec
3" Diam	Det, 1700 M/sec	Det, 2440 M/sec	Det, 2310 M/sec
2 1/2" Diam	Failed to detonate	Det, 2020 M/sec	Det, 2080 M/sec
2" Diam		Failed to detonate	Failed to detcnate
Density	1.54	1.52	1.51
5. M6 Cap Test	Failed to det.	Failed to Det.	Failed to Det.

Table 6. Comparison of ARRADCOM and IRECO test data on dense blasting agent DBA-105PM

1. Cap Sensitivity

ARRADCOM - Detonated No. 8 caps in blasting agent in tube 3 1/4" D x 3 3/8" L. - No reaction.

IRECO - Detonated M6 cap in blasting agent in tube 3" d x 18" L conditioned at -30°, 20° and 50°C - No reaction. Also conducted at 50°C with 4" D x 12" L with no reaction.

2. Bullet Impact

ARRADCOM - 50 samples loaded into 2" D steel pipe nipples, 3" L, capped on one end were subjected to 30 caliber ball ammo - No reactions.

IRECO - 2 samples loaded into 4" D x 12" L cardboard tubes and conditioned at 50°C were subjected to a 22 caliber rifle bullet - No reactions.

3. Gas Evolution

ARRADCOM - 5 g sample subjected to 100°C vacuum stability test for 40 hours produced 0.01 ml of gas.

IRECO - 25 lb sample subject to 72°C for 72 hours produced 10 ml of gas.

4. Critical Diameter

ARRADCOM - Blasting agent produced detonation velocity in heavy walled 0.75" ID x 8" L steel pipe (confined)

IRECO - Blasting agent detonated in 2" D x 18" L cardboard tube (unconfined).

Table 6. (contd)

5. Detonation Velocity

ARRADCOM - In confined steel pipe with densities ranging from 1.45 to 1.67 g/cc and conditioned at -30°, 20° and 63°C, detonation velocities ranging from 2364 to 3970 M/sec were obtained.

IRECO - In unconfined cardboard tubes 3" and 4" D x 18" L with densities ranging from 1.45 to 1.55 conditioned at -30°, 20°, and 50°C, detonation velocities were obtained ranging from 2540 to 3870 M/sec.

6. Improper Mixtures

ARRADCOM - Liquid/powder mixtures in ratios of 3:1, 1:1 1:2, and 1:3 were subjected to impact, cap, burn and detonation velocity tests. Only the 3:1 and 1:1 mixtures produced detonation velocities. The 1:2 mixture had a 10% PA impact value of 19 inches - the lowest of all the mixtures. None of the mixtures showed any response to the NOL impact and the cap test.

IRECO - The 3:1 and 1:1 mixtures produced detonation velocities in the 3" D tubes. These mixtures also showed no reaction to M6 cap test.

Additional tests by IRECO in changing the 2:1 mixture by + 5% did not show any significant effect. Also changes in the guar gum content to 1.2% and 1.5% from the 1.4% reference showed some slight differences in detonation velocity. Actually the data with the 64/36 mixture was the same as the 1.4$ guar gum.

7. Water Dilution

ADRADCOM - 75/25 and 50/50 mixtures of blasting agent and water initiated in steel pipes but died out quickly.

Table 6. (contd)

IRECO - A 10% dilution produced a detonation velocity of 3175 M/sec in a 6" D tube, but no detonation was achieved with a 15% mixture.

8. Reactivity/Contamination

ARRADCOM - Vacuum stability tests (reactivity tests) were performed with blasting agent and a various number of materials. Tests with aluminum, zinc, magnesium, copper, brass, steel, plastic, cement, lime, lead, iron, and stainless steel were conducted at 100°C for 40 hours. Additional tests with unleaded gas, low lead gas, isostearic acid, aviation gas, diesel fuel, lube grease, spindle oil and 30W10 oil were conducted at 65°C for 40 hours. Only with magnesium did an excessive reactivity occur.

IRECO - 15 g of sodium hydroxide pellets were added to 25 lbs of blasting agent mix in a 5" D bag. No exothermal or propagative reaction occurred after one week at ambient storage. Slight crusting occurred.

STANDARDIZATION OF MILITARY QUALIFICATION PROCEDURES FOR EXPLOSIVES, PROPELLANTS, AND PYROTECHNICS

L. AVRAMI AND R. F. WALKER
US ARMY ARMAMENT RESEARCH AND DEVELOPMENT COMMAND
DOVER, NJ 07801

ABSTRACT

The principles, criteria, and test methods by which energetic materials (explosives, propellants, and pyrotechnics) are developed and selected for military use are not well documented. This is more apparent in the propellant and pyrotechnic areas. The lack of a well-defined procedure frustrates both the inter-service acceptance of all types of formulations and the development of acceptable formulations by industry. More recently, the combined consequences of the RSI (Rationalization, Standardization and Interoperability) and the cooperative development and procurement programs among the NATO countries have further magnified the need for a well documented methodology to aid industrial planning and foster the inter-service, international acceptance of energetic material formulations.

This presentation will summarize the organizational and documentary approach which is now being adopted to develop the unified principles, tests and procedures which the NATO partners will use for the interim and final qualification of explosives, propellants, and pyrotechnics for military use. The approach calls for the services to establish the methodology and the acceptance criteria, but permits the continuing introduction of new or improved test technology, such as may come from industrial and university laboratories, in addition to government installations.

The principal features of the proposed NATO STANAG (Standardization Agreement) and the supporting manual of tests will be described.

I. INTRODUCTION

For several decades the procedures, principles and criteria to which explosives, propellants, and pyrotechnics (energetic materials) have been subjected in order to qualify for military use have been vague, confusing and not well documented. Efforts to standardize tests have been undertaken on-and-off for the past thirty years by different commands in one service, between services and agencies, and, in some instances, between countries, especially in Europe and the ABCA countries. Most of these efforts were small scale, local efforts to comply with the needs of a specific application or program. Beginning in the late 1960's, the high explosives community began to address this problem and develop a Joint Services Manual of Safety and Performance Tests and Criteria that was approved by the Joint Logistics Commanders. The lack of similar documentation for gun and missile propellants and pyrotechnics has more recently received attention. The overall problem has been further emphasized by the increased emphasis on the NATO-wide RSI program and the trend toward cooperative development and cross-procurement among NATO members.

Not only are principles and tests not adequately documented, but no repository or data bank of qualified materials and their properties is maintained so that information obtained in the past can be referenced to avoid the need for duplicate or repetitive testing by each new developer that is desirous of applying an established material in a new application.

The dearth of readily available information has frustrated and delayed the inter-service and international acceptance of new formulations and the development of acceptable formulations by industry. It has tended to foster the misconception that an energetic material that has been accepted for one application automatically becomes acceptable for all other applications, leading to problems late in the development cycle for new munitions that could have been avoided.

A general recognition of the deficiencies has led to the establishment within the US and NATO community of several committees and authorities. This paper summarized some of the initiatives that have been taken, and of the approach that is being followed in developing a more rational approach to the qualification of energetic materials for military use.

II. DEFINITION

In the context of NATO standardization and the usage adopted by DOD Explosives Safety Board the terms "energetic materials" and "explosives" are equivalent and virtually synonymous. The definition for explosives is that adopted by the United Nations, except that it is constrained only to those materials whose application requires that they shall explode reliably on demand. Thus defined, explosives include all solid, liquid and gaseous substances variously known as high explosives, boosters, primaries or initiators; gun and missile propellants; and pyrotechnic illuminants, delays, decoys, igniters and simulants, and flame and incendiary compositions.

III. RESPONSIBLE NATIONAL AND INTERNATIONAL BODIES

In order to understand the approach that is being adopted to develop improved documentation it is important to be aware of the relationship between the various organizations that are contributing to the effort.

There are international organizations, which in the military context include NATO and the ABCA (America, Britain, Canada, Australia or TTCP) members. There are also bi-lateral arrangements involving Data Exchange Agreements (DEA's), Memoranda of Understanding (MOU's) or Information Exchange Projects (IEP's) between NATO members and various DOD agencies or services. Lastly, there are organizations within the United States which have been assigned various responsibilities that relate to explosives safety and performance testing, and which serve to bring US positions to a focus before they are presented internationally. Each service also has internal mechanisms for developing single-service positions.

NATO Groups

Figure 1 illustrates the relationship between various elements of the NATO organization that contribute to the standardization of tests among NATO members. The AC/310 Groups of Experts was recently formed by the Conference of National Armament Directors as an independent cadre group that would lend emphasis to the need for agreed test and safety criteria for explosive materials and munitions. This group has provided a tri-service forum for the completion of several important tasks which will be described later in this paper, and which were initiated earlier by the Surface-Surface Artillery panel of the NAAG (NATO Army Armaments Group).

Joint Service Groups

The NATO initiatives combined with the RSI program also emphasized the need for the NATO members individually to improve the practices and procedures by which their representatives proposed, reviewed, and ratified the standardization agreements (STANAGS) that were generated by international consultation. In the USA the problem, as it relates to energetic materials, was discussed by the Joint Deputies for Laboratories Committee (JDLC), and the Joint Technical Coordinating Group for Munitions Development (JTCG/MD) under the Joint Logistics Commanders. As a consequence, the charter of the JTCG/MD Working Party for Explosives was revised with the specific purpose of assigning responsibilities for the development of improved documentation and international-interservice standardization of assessment procedures for energetic materials. The charter required that the Working Party coordinate and collaborate with other responsible technical bodies (Fig. 2) to round out the expertise that could be employed to fulfill its objectives. At the same time the JDLC wrote to the DOD Explosives Safety Board (DDESB) recommending collaboration with the R&D community in the development of refined tests and criteria for the qualification of explosives for military use.

Bilateral Agreements

The ratification of these initiatives provided an overall framework within which the very large task of sound documentation could be addressed. The framework was further strengthened by the establishment of an information exchange project (IEP) between the UK Ordnance Board and the DDESB on the topic of explosives test standardization, and by several other MOU's and DEA's with the UK, Germany, France, etc. that cover the same subject. These bi-lateral agreements have proved to be equally valuable to the NATO-sponsored and Joint Services bodies in easing the path to understanding and agreement in the complex, confusing and ill-disciplined technical area.

International Conferences

In parallel with the foregoing organizational initiatives, the JTCG/ML Working Party and the US Army's lead laboratory for energetic materials research and development at ARRADCOM, Dover, NJ have twice (in 1977 and 1979) sponsored an International Conference on the Standardization of Safety and Performance Tests for Energetic Materials (Ref. 1-3). These conferences brought together a much larger body of international experts than can attend the formal government committees and laid much of the foundation for what have become the principal documentation tasks.

IV. PRINCIPAL TASKS AND OBJECTIVES

The most immediate consequence of the foregoing planning and discussions was a general recognition that the principal tasks and objectives of NATO explosives standardization community should be:

1. To prepare a NATO standardization agreement on the principles and methodology for the acceptability of energetic materials (explosives) for military use.

2. To prepare a manual of tests and criteria that will permit the international and interservice acceptance of qualification data that has been obtained by individual service and industrial laboratories.

As discussed below these objectives have now been endorsed by the responsible NATO authorities and national custodian responsibilities have been assigned. The remainder of this paper describes the nature and present status of the work which has been undertaken to meet the objectives.

V. DRAFT AGREEMENT ON PRINCIPLES AND PROCEDURES

At the November 1979 meeting of the NATO Group of Experts on Explosive Materials agreement was reached on the development of STANAG 4170 "Principles and Procedures for the Assessment of Safety of Explosive Materials for Military Use. The UK will serve as the custodian and anticipates providing a draft for NATO consideration by the spring of 1980. It is expected that the title of the STANAG will be changed during the course of subsequent discussions to cover the broad topic of the interim qualification of high explosive, propellant, and pyrotechnic materials.

A preliminary draft of a STANAG has been submitted by the UK for review to DDESB and also the Chairman of AC/310, Group on Explosive Materials, who also is the Chairman of the JTCG/MD Working Party for Explosives and one of the authors of this paper. Several deficiencies were noted, and the US submitted a counterproposal which has received favorable consideration.

The principal features of the draft STANAG, as revised, are as follows:

1. The STANAG applies to all new explosives that are formulated for introduction into service.

2. The development and selection of propellants, explosives, and pyrotechnics for military use require the careful balancing of several, often opposing criteria, such as: performance on target, fuzing, vulnerability, toxicity, safety, storability, availability of ingredients, environmental impact, producibility, loading, demilitarization and cost.

3. Explosives are further defined as follows:

a. High Explosives. Chemical compounds or mixtures of substances which, in their application as primary, booster and main charges in warhead and demolition systems, are required to undergo exothermic chemical reaction with the evolution of gaseous products and to detonate.

b. Propellants. Chemical compounds or mixtures of substances used for propelling projectiles and rockets and to generate gases for powering auxiliary devices. When ignited, they burn or deflagrate to produce large amounts of gas capable of performing work, but in their application are required not to undergo a deflagration to detonation transition.

c. Pyrotechnics. Chemical compounds or mixtures of substances which, when ignited, undergo an energetic chemical reaction at a controlled rate intended to produce on demand and, in various combinations, specific time delays or copious amounts of heat, noise, smoke and light together with relatively small volumes of gas.

4. "New explosives" are defined to encompass:

a. Any modification to an existing composition or existing material specification.

b. An explosive of a type not hitherto in service.

c. The application of an existing explosive in a new munition/weapons system.

5. There are three principal stages in the development of explosives for military use:

a. The Research Phase: the discovery and assessment of new molecules in the laboratory. The principles governing safety and performance assessments at this stage are determined by local laboratories, and are not the subject of the agreement.

b. The Interim Qualification of the explosive material for use in a class of munitions or type of application. (This being the principal subject of the draft).

c. The Final or Type Qualification of an interim-qualified explosive for a specific munitions/weapons systems. (This is beyond the scope of the draft.)

6. The interim and final qualification (certification) of explosives is based on the results of tests and background information relevant to the criteria of paragraph 2 above. There are three types of test:

a. Mandatory tests: These are established tests, immediately recognizable as providing data essential for the assessment of the safety and performance characteristics of an explosive.

b. Prescribed tests: These are requested and/or designed by an approving authority to provide additional information relevant to a particular application of a material, or to provide additional information in instances where the data from the mandatory tests are inconclusive.

c. Optional tests: These may be introduced by the developer to supplement data from the foregoing tests or to substitute a new or advanced technique for an established test.

7. Because of the complexity of the phenomena that affect the sensitivity of an explosive to various stimuli, many tests are unable to provide clear, quantifiable measures of the hazard involved in the use of explosives. Judgments on overall safety and suitability for service are therefore necessary and are made by comparison of the test results obtained for new explosives, with those for explosives of known and proven safety and experience in similar applications. Further, since explosive hazards can be a function of even the smallest ingredients or impurities in a composition, every change in the composition or material specification necessitates consideration, and if necessary reassessment, to confirm the material's continued suitability for service. Any modification to an existing composition, or to the material specification of an explosive which has been interim qualified must be notified to the appropriate national authority. Where no requalification is considered necessary, a reasoned statement to that effect is to be provided to the receiving country.

8. A manual will be provided which will describe acceptable tests and pass/fail criteria.

9. The approving authority and specialist advisers of prospective service users who will agree on the minimum requirements for interim qualification of a new explosive. The assessment requires a knowledge of the intended application of the explosive material before the required information can be defined.

10. Each nation will identify approving authorities for the interim and final qualification (certification) of explosives. The authority will maintain an identification code to identify the qualified explosives and will maintain records and test data relating to each qualification (certification) or to the information base used to grant, deny, or restrict qualification (certification).

11. Upon request, each nation will provide copies of the qualification (certification) records to the recognized approving authorities of the other nations. One central repository will be selected for all the records and data.

VI. MANUAL OF SAFETY AND PERFORMANCE TESTS

The second task of the NATO community (Part IV), which is endorsed by the STANAG on Principles (Part V, para. 8), is to provide a manual of tests and criteria that will guide the materials developer. Therefore, it was also agreed by the NATO authorities in November 1979 that as a supporting document to STANAG 4170, an Allied Ordnance Publication No. 7 will be provided and entitled, "Tri-Service Manual of Safety and Performance Tests and Criteria for the Acceptance of Explosive Materials for Military Use." The United States will serve as the custodian and will aim to produce a first draft by June 1981.

The International Conferences held at ARRADCOM, Dover, NJ have played an important role in outlining the structure and initial content of a draft manual. Both structure and content have also been heavily influenced by the Joint Services Manual (Ref. 4) (in turn based on NAVORD OD 44811) developed and approved under the auspices of JTCG/MD as described in the Introduction.

The outline structure for the manual is as follows:

INTRODUCTION - will summarize content of STANAG and interpret to meet national interests, define the objective and scope of the manual.

INTERIM QUALIFICATION TESTS

Chemical tests - compatibility, storability, analyses, etc.
Safety Tests
Physical Property Tests
HE Performance Tests
Pyrotechnic Performance Tests
Gun and Propellant Performance Tests
Missile & Rocket Propellant Performance Tests

APPENDICES

Standardization Agreements (Listing)
Standard Reference Substances
Glossary of Terms
Approving Authorities
National Repositories

In developing the manual (Allied Ordnance Publication No. 7) the initial purpose is to accept all submissions without prejudice, providing sufficient information is provided that national experts can understand and reproduce the tests and that the ranking of common explosives with reference to the tests is clear. The manual is thus envisioned to be an evolving document and submissions for inclusion will be accepted for consideration at any time, and presented to national and NATO representatives.

This was one of the agreements reached at the Second International Conference on the Standardization of Safety and Performance Tests for Energetic Materials. At this Conference, which was a working meeting, discussion groups were established on methodology, propellant performance, pyrotechnic safety and performance, HE performance, chemistry and safety.

The task areas for the groups were defined as follows:

1. The Methodology Group was concerned with clarification of interim versus final qualification with the Introduction and Appendices for the manual, and would review existing formal requirements with respect to international agreements (STANAG's, etc.).

2. The Chemical Group was concerned with tests for compatibility, stability, storability, compositional information, reference materials, and so forth.

3. The groups on Physical Properties and Performance of explosives, pyrotechnics and gun propellants were concerned with the determination of dimensional stability, thermal and mechanical properties, detonation velocity, fragment velocity, blast, luminous intensity, spectral emission, force, flame temperature, erosivity and other measures of output and performance.

4. The Safety Group was concerned with safety tests such as sensitivity to various stimuli, initiation, vulnerability, and the like.

These study groups selected various laboratory tests for inclusion in a first rough draft of the manual. In making the selections, they were careful to consider the following guidelines:

a. Why is the test required?

b. When is it required?

c. What does it answer?

The only other condition for acceptance was that the submissions provided a sufficient description so that the nature of the tests, and the data provided by them, were understandable to other nations. The manual is conceived to be a "living" document, from which tests can be withdrawn or new tests inserted, as international agreement, usage and technology advances require. It was generally agreed that the availability of standard reference "explosive" materials will facilitate the international interpretation of data.

The status of the manual as of this report is as follows:

Prepare and circulate summary minutes	30 January 1980
Consolidate and distribute the lists of mandatory and prescribed tests, etc., prepared by five discussion groups	15 July 1980

Consolidate and distribute available test descriptions:

Manual Introduction and Chemical Tests	15 Sept 1980
Safety Tests	15 Oct 1980
HE Performance Tests	15 Nov 1980
Pyro Performance Tests	15 Dec 1980
Propellant Tests	15 Jan 1981
Estimated Date for Draft Document	June 1981

Assistance from the US technical community, whether in government, private industry, or universities, is earnestly solicited, particularly in providing the text and suggested acceptance criteria for performance tests for missile and gun propellants. Offers of assistance should be directed to the authors at ARRADCOM, Dover, NJ.

REFERENCES

1. L. Avrami, H.J. Matsuguma, R.F. Walker (Editors), "Proceedings of the Conference on the Standardization of the Safety and Performance Tests for Energetic Materials - Volume I." ARRADCOM Special Publication ARLCD-SP-77004, US Army Armament Research and Development Command, Dover, NJ, September 1977 (AD-E400 004).

2. L. Avrami, H.J. Matsuguma, R.F. Walker (Editors), "Proceedings of the Conference on the Standardization of the Safety and Performance Tests for Energetic Materials - Volume II", ARRADCOM Special Publication ARLCD-SP-77004, US Army Armament Research and Development Command, Dover, NJ, November 1978 (AD-E400 254).

3. R.F. Walker, H.J. Matsuguma, L. Avrami (Editors), Minutes of Second International Conference on the Standardization of Safety and Performance Tests for Energetic Materials, January 1980, held at ARRADCOM, Dover, NJ, 15-19 October 1979.

4. Volume IV, Joint Service Safety and Performance Manual for Qualification of Explosives for Military Use, Joint Technical Coordinating Group for Air Launched Non-Nuclear Ordnance Working Group for Explosives, 12 May 1972.

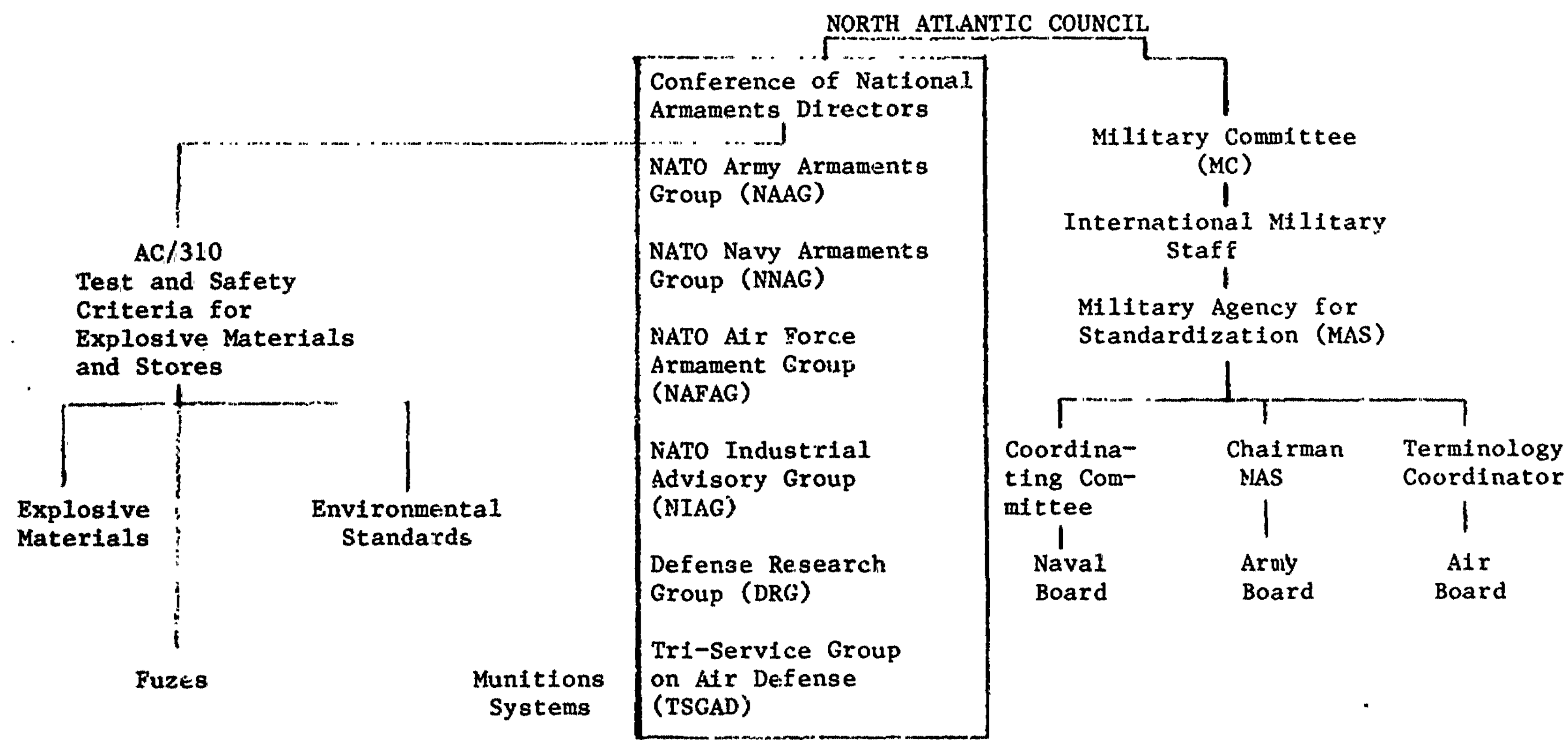

Figure 1. NATO Standardization Groups.

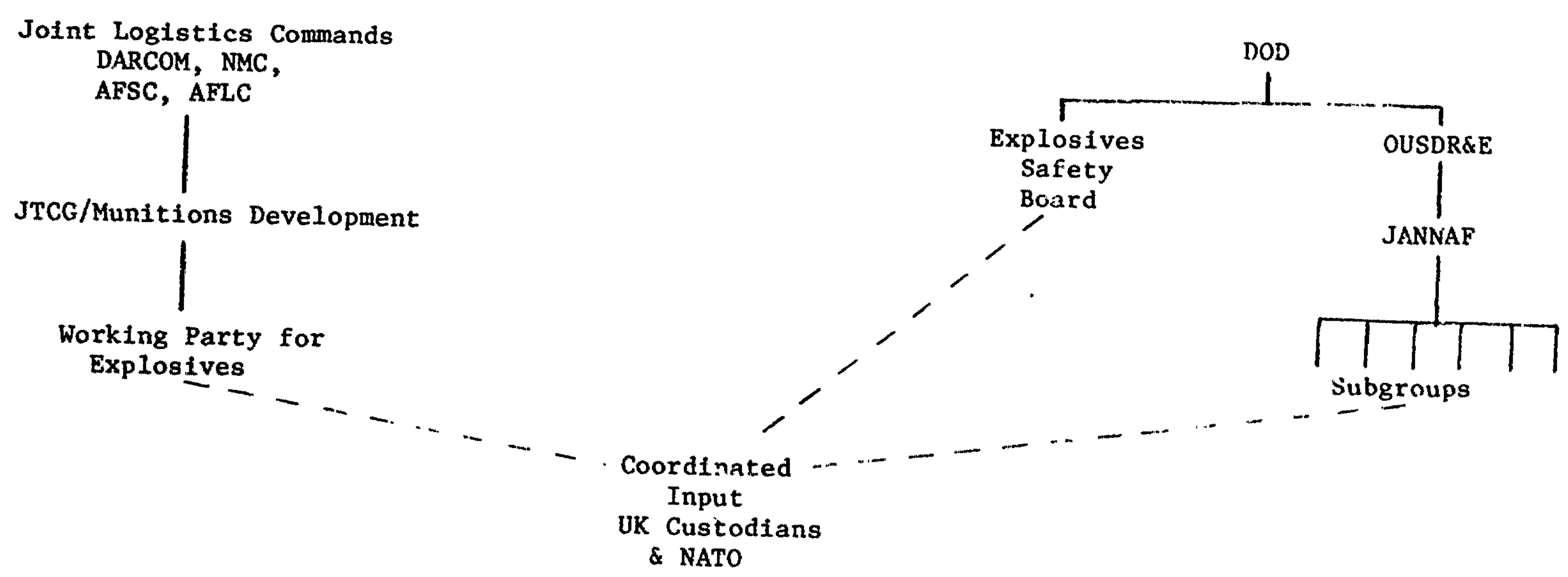

Figure 2. DOD & Joint Service Groups.

Paper Distributed At The:

Nineteenth DoD Explosives Safety Seminar
Los Angeles, California

LARGE CALIBER GUN PROPELLANT THERMAL STABILITY PREDICTION

by

C. James Dahn
Safety Consulting Engineers, Inc.
Rosemont, Illinois 60018

September 9, 1980

ABSTRACT

Methods were devised to evaluate the thermal stability of large caliber gun propellants in various size configurations and thermal environments. Subscale and large scale runaway reaction tests were performed on M1, M6, M30A1 and M31E1 gun propellants.

Correlations of test results with predictions were made yielding nearly identical results. By utilizing this method, ordnance personnel can determine safe handling and storage conditions for the gun propellants and associated ammunition.

INTRODUCTION

The storage of bulk propellant and ammunition for large caliber guns can generate significant hazards if the materials are allowed to self-decompose at elevated temperatures and enter into runaway reactions. In the past, unknown explosions have occurred in storage magazines for both explosives and propellants. This problem is aggravated for the large caliber gun system considerations since quantities of powder both in ammunition and in bulk form are larger than the small caliber. Thus, the likelihood of a spontaneous combustion (i.e. runaway reaction at elevated temperature) is much greater.

To evaluate these potential hazards, thermal stability analysis must be conducted on the large caliber gun propellants and their systems. Conventional gun propellants manufactured with nitroglycerin and nitrocellulose do have inherent storage problems due to loss of stabilizer in time. As a result, continued surveillance of gun propellants is required. Information must be gathered on the kinetics of decomposition in the propellants and their thermal characteristics. Thermal runaway reaction occurs when the heat generated due to slow decomposition of the material exceeds that which can be taken away in the mass of propellant. After a relatively long induction period, a sudden runaway reaction occurs and temperature reaches instantaneous ignition of the propellant.

The resultant explosions can be very devastating.

PROPELLANTS EVALUATED

Thermal decomposition characterization studies were conducted on the following Cannon propellants:

- M1 Propellant
- M6 Propellant
- M30A1 Propellant
- M31E1 Propellant

These propellants have basic properties as illustrated in Table 1. The M30 and M31 propellants have low nitrocellulose contents as compared to the other two. They also have approximately 20% nitroglycerin in their compositions. As a result, the force output is higher than for M1 and M6 propellants. Four grain configurations of M1 propellant were evaluated in this study. Their characteristics and web size are shown in Table 2. The physical characteristics of each of the propellant grain configurations are illustrated in Figure 1.

THEORETICAL

The first step in evaluating thermal stability of the propellants was that of conducting chemical kinetics tests to determine the Arrhenius kinetics constants (e.g. activation energy and frequency factor). Differential Scanning Calorimetry (DSC) techniques were utilized to determine these properties in accordance with ASTM Standard E 698-79[1,2]. With this information and other parameters, calculations can be made to determine the critical self-heating temperature of the materials as a function of configuration in quantities of material. The results of DSC tests at Safety Consulting Engineers, Inc. on the various propellants are shown in Table 3. Here we note that the M1 8-inch propellant has the lowest activation energy and frequency factors.

THERMAL DECOMPOSITION THEORY

When a propellant mass is stored at an elevated temperature, decomposition can occur at low rates. Heat loss in the materials governs whether the temperature can rise in the materials. Decomposition rates normally are extremely low at ambient and slightly higher temperatures. When temperatures increase, such as in storage, the decomposition rates increase. The stored propellant system enters a critical state when the heat generation rate exceeds the rate of heat dissipation. The rate of heat energy generated in decomposition and lost to the surroundings can be calculated in accordance with the following equations:

Decomposition Heat Energy Rate:

Heat Energy Rate Liberated by Internal Reaction:

$$E_h = \frac{dq}{dt} = Q\ V\ \rho\ Z\ e^{\frac{-E}{RT}} \text{ ....(Eqn. 1)}$$

Heat Loss Due to Newtonion Cooling:

$$E_L = \frac{dq_L}{dt} = \frac{\lambda}{d}\ S\ (\Delta T) \text{ ....(Eqn. 2)}$$

where

- Q - Heat of Decomposition (cal/gm)
- V - Volume of Material (cc)
- ρ - Density of Material (gm/cc)
- Z - Frequency Factor (1/sec.)
- E - Arrhenius Activation Energy (kcal/mol)
- T - Temperature of Material (^oK)
- λ - Thermal Conductivity (cal/gm-sec.-^oK)
- S - Surface Area (cm^2)
- d - Thickness of Material (cm)
- T - Temperature Difference from Surroundings

In approximately 1928, N. N. Semenov conducted nonsteady state thermal studies to determine runaway reaction and conditions. From his studies, the critical differential temperature for runaway reaction is found by the following equation:

$$\Delta T_{crit.} = k \; RT_a^2 / E \text{ .... (Eqn. 3)}$$

where

k - Constant Depending on Configuration

The critical temperature for runaway reaction as developed by Frank-Kamenetskii[3] as related to physical parameters is found by the following equation:

$$T_m = \frac{E}{R \ln (\rho \, r^2 \, Q \, Z \, E/\lambda \, R \, T_m^2 \, \delta)} \text{ .... (Eqn. 4)}$$

where

r - Slab Half Thickness or Radius for Cylinder on Sphere

δ - Frank Kamenetskii Shape Factor Derived From Equating Eqn. 1, 2 and 3

For Slab $\delta = 0.88$
Cylinder $\delta = 2.00$
Sphere $\delta = 3.32$

Calculations were made to determine the runaway reaction temperature for given sizes of slab configurations of cannon propellants. The results of these calculations are shown in Figures 2 and 3. Thus, giving enough time, at 100°C, M1 propellant/8-inch M1 will accelerate to decomposition in slab half thicknesses of 9 centimeters.

ADIABATIC EXPLOSION TIME

As worse case, the time to reach explosion at a given uniform temperature (adiabatic conditions) should be evaluated. This can be accomplished by using the following equation developed by Frank-Kamenetskii[3] and Mader/Zinn[5]:

$$t_{exp_{ad}} = \frac{C_p \, R \, T_1^2}{Q \, Z \, E} \, e^{E/RT_1} \text{ .... (Eqn. 5)}$$

where

C_p - Specific Heat (cal/gm°K)

Calculations were made for each of the cannon powders and are shown in Figures 4 and 5. A very dramatic difference occurs in runaway reaction times between each propellant at 100°C.

The time-to-explosion ranges from 200 hours to 28 hours for the Cannon propellant studied at 100°C uniform temperature.

NON-ADIABATIC EXPLOSION TIMES

An equation has been developed to determine the time-to-explosion when a given mass of hazardous material is instantaneously placed in contact with the hot surface. The equation developed by Mader & Zinn[5] is listed as follows:

$$t_{exp} = \left(\frac{C_p \rho r^2}{\lambda}\right) F \left[\frac{E}{T_m} - \frac{E}{T_1}\right] \text{........(Eqn. 5)}$$

where

T_m - Critical Temperature for Runaway Reaction Per Eqn. 3

T_1 - Instantaneous Contact Surface Temperature

F - Function Dependant on Geometry and the Initial Temperature

The function F is established from the graph shown in Figure 6. The calculations for each propellant for times ranging up through 100 seconds is shown in Figures 7 and 8. These calculations were based on a slab configuration with a thickness of 0.32 centimeters. This thickness was selected so that correlation with small scale experiments could be maintained as discussed later in this paper. Calculations were also conducted for slab thicknesses of 10 centimeters to simulate larger scale experimental verifications as reported later in this paper. The explosion times (listed in hours) at various initial surface temperatures for the Cannon propellants is shown in Figures 9 and 10. The 8" M1 propellant evaluated at Safety Consulting Engineers, Inc. shows consistently lower explosion times for given initial instantaneous temperatures. The runaway reaction characteristics for two Cannon propellants which have multiple perforations are shown in Figure 11. Two triple base propellants reaction time-temperature curves are shown in Figure 12. The M30A1 propellant tested appears to be more stable than M31E2 propellant in the temperature-time ranges evaluated. The 8 inch M1 and 8 inch M2 propellants runaway time temperature characteristics have been evaluated and are shown in Figure 13. On the same figure, adiabatic explosion temperature time relationship is listed. There is a marked difference between the two temperature time curves.

The effect of changing slab thicknesses for the 8 inch M1 propellant is shown in Figure 14. Here we see that in the upper temperatures ranging from 150 to 180°C, the reaction times are very similar to the three slab sizes. The knee of the slope for each of the curves as the slab thickness increases rises to higher length of time.

EXPERIMENTAL

To verify the theoretical calculations for runaway reaction time/temperature, various experimental configurations were utilized. The first configuration was that of time-to-explosion test devised by Henken and McGill[4], as described by R. Rogers[6]. In this test, a certain thickness of explosive sample was placed into a empty aluminum blasting cap shell and confined by an aluminum plug and appropriate seal mechanism. This cell was placed into a Woods Metal Bath at a constant temperature and time-to-explosion was monitored.

Since Cannon propellant configurations are very large as compared to this cell size, a propellant was ground and packed into a copper blasting cap case and sealed appropriately.

The runaway reaction times for Henken Woods Metal Bath temperatures near 200°C range from 10 to 50 seconds. The Henken test results are also shown in Figure 7 and 8. Each test was run approximately three times to verify the test result. An air cylinder was utilized to plunge the cell into the Henken Woods Metal Bath instantaneously.

In addition to these small scale tests, an intermdiate runaway test was configured at Safety Consulting Engineers, Inc. This test consisted of a slab of approximately 100 centimeters thick and 152 centimeters on a side. The propellant was placed into the aluminum chamber and packed snugly. The chamber was placed upon a laboratory heating plate held at a given temperature. This was accomplished by appropriate insulation. This setup is photographically illustrated in Figure 15. Temperature was monitored by temperature probes both on the hot plate and on the center surface of the propellant which contacted the hot plate. A typical time-temperature curve measured at the interface surface between the hot plate and the propellant is shown in Figure 16 for the 8 inch M1 propellant. Here, we see that the temperature rose to 150°C from an initial hot plate temperature of 150° in approximately 60 minutes. The time-to-explosion was recorded for the same propellant on Figure 13. The explosions occurred consistently within 1 hour after the surface of the propellant in contact with the hot plate reached 150°C. The total induction time was 2 hours from experimental data. This is shorter than the predicted 2½ hours from theory as shown in Figure 13. Thus, as size increases, there appears to be a deviation from the theory regarding runaway reaction times at a given instantaneous plate temperature.

SUMMARY AND RECOMMENDATIONS

Theoretical calculations can be made to determine the runaway reaction time-temperature characteristics of the various Cannon propellants. From this, safe storage time-temperature histories can be accurately monitored and compared to theory. Based on the experimental correlations, the larger scale propellant storage quantities temperature-time characteristics must be corrected to accommodate for variation in theoretical results (especially in large scale).

It is recommended that Cannon propellant shipping containers sizes temperature time experimental curves should be established to assure that adequate propellant storage can be maintained. Another compounding factor is that of loss of stabilizer in typical gun propellants. When this occurs, the kinetics data as described in this paper do not hold. As a result, their ability to spontaneously ignite or reach runaway reactions is accelerated. Thus, as done in the past, propellant monitoring is still required to assure adequate stabilizer contents.

REFERENCES

1. ASTM E 698-79, Standard Test Method for Arrhenius Kinetic Constants for Thermally Unstable Materials.

2. Dahn, C. James, "Chemical Compatibility and Safe Storage Considerations for Process Systems Hazards Analysis", Joint Symposium on Compatibility of Plastics and other Materials with Explosives, Propellants, and Pyrotechnics, May 1979.

3. Frank-Kamenetskii, D.A., "Diffusion and Heat Transfer in Chemical Kinetics", Plenum Press, 1969.

4. Henken, H. and McGill, R., Ind. Eng. Chem. 44 (1952) 1391.

5. Mader, C. L. and Zinn, J., "Thermal Initiation of Explosives" J. Appl. Physics, Vol. 31, No. 2, Feb., 1960.

6. Rogers, R. N., "Thermochemistry of Explosives", Thermo Chimica, ACTA II (1975).

7. Semenov, N. N., "Chemical Kinetics and Chain Reactions", Oxford, 1935.

TABLE 1

Basic Properties of Cannon Propellants

Property	M1	M6	M30	M31
Nitrocellulose	85.00	87.00	28.00	20.00
% N_2	13.15	13.15	12.60	12.60
Nitroglycerin	-	-	22.50	19.00
DNT	10.00	10.00	-	-
DBP	5.00	3.00	-	4.50
DPA	1.00	1.00	-	-
Nitrogranidine	-	-	47.70	54.70
2 Nitro DPA	-	-	-	1.50
Ethyl Centralite	-	-	1.50	-
Graphite	-	-	0.10	-
Specific Gravity	1.57	1.58	1.66	1.64
Force $\frac{\text{ft-lb} \times 10^{-3}}{\text{lb}}$	305	317	364	334
Heat of Explosion (cal/gm)	700	758	974	807
Gas Volume (mol/gm)	0.045	0.044	0.043	0.046

TABLE 2

Large Caliber Gun Propellant Configurations

PROPELLANT TYPE	APPLICATION	WEB SIZE (mm)	NUMBER OF PERFORATIONS
M1	8" - M1	0.429	Single
M1	8" - M2	1.092	Multi
M1	155mm M3A1	0.406	Single
M1	155mm M4A2	0.940	Multi
M6	M119A1	1.400	Multi
M30A1	Various Charges	2.160	Multi
M31E1	M188	1.478	Multi

TABLE 3

Chemical Kinetics Data
From DSC Tests At
Safety Consulting Engineers, Inc.

PROPELLANT TYPE	APPLICATION	ACTIVATION ENERGY (kcal/mol)	FREQUENCY FACTOR (1/sec.)
M1	8" - M1	45,020	9.65×10^{18}
M1	8" - M2	46,872	7.2×10^{19}
155mm	M3A1	52,174	1.7×10^{22}
155mm	M4A2	51,085	5.4×10^{21}
M6	M119A1	47,733	1.4×10^{20}
M30A1	Various	51,675	9.1×10^{21}
M31E1	M188	52,172	3.72×10^{22}

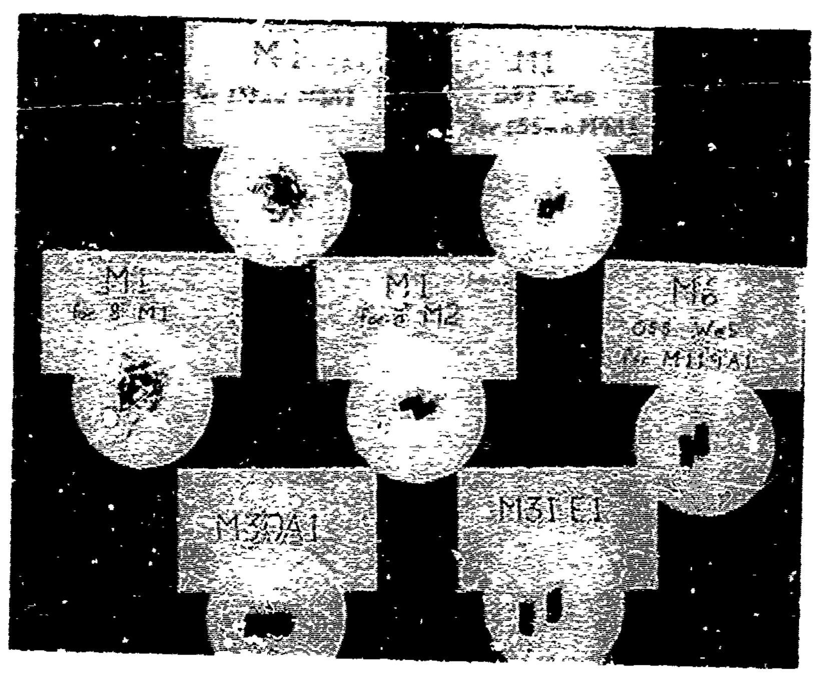

Figure 1. Propellant Grain Configurations

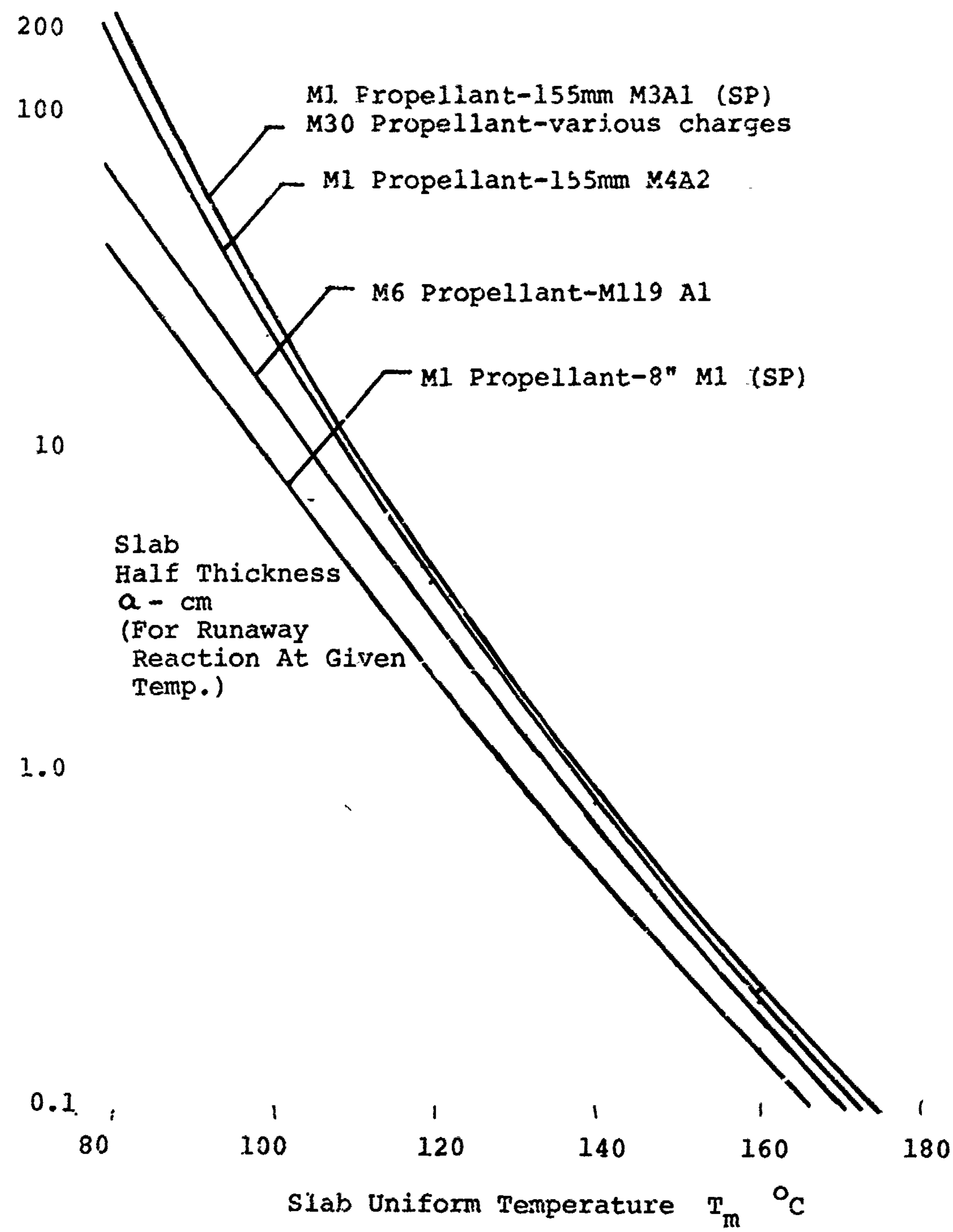

FIG. 2 - THERMAL SELF-HEATING REACTION CHARACTERISTICS OF M1, M6, AND M30A1 PROPELLANTS

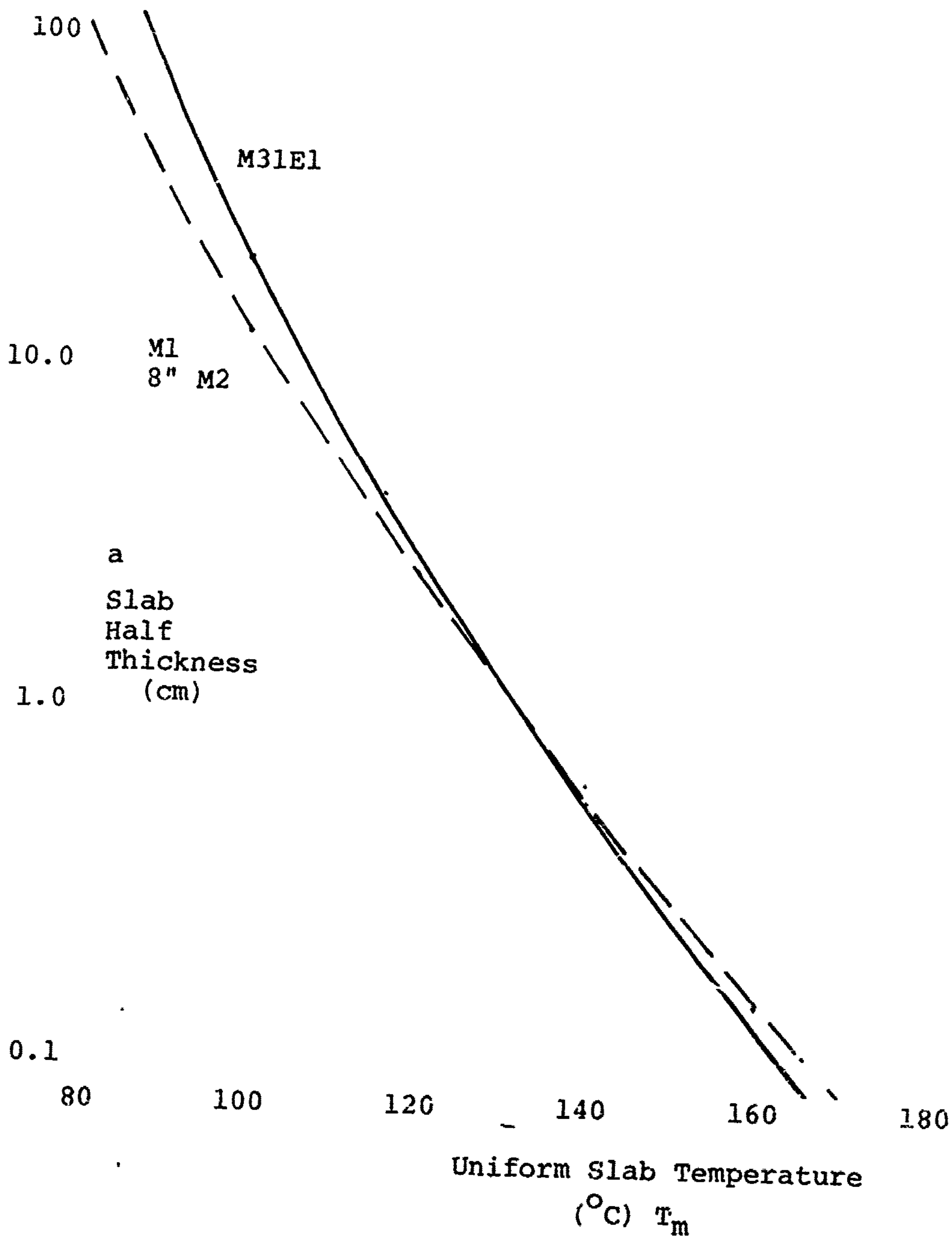

Figure 3. Thermal Self-Heating Characteristics of M1 (8" M2) and M31E1 Propellant

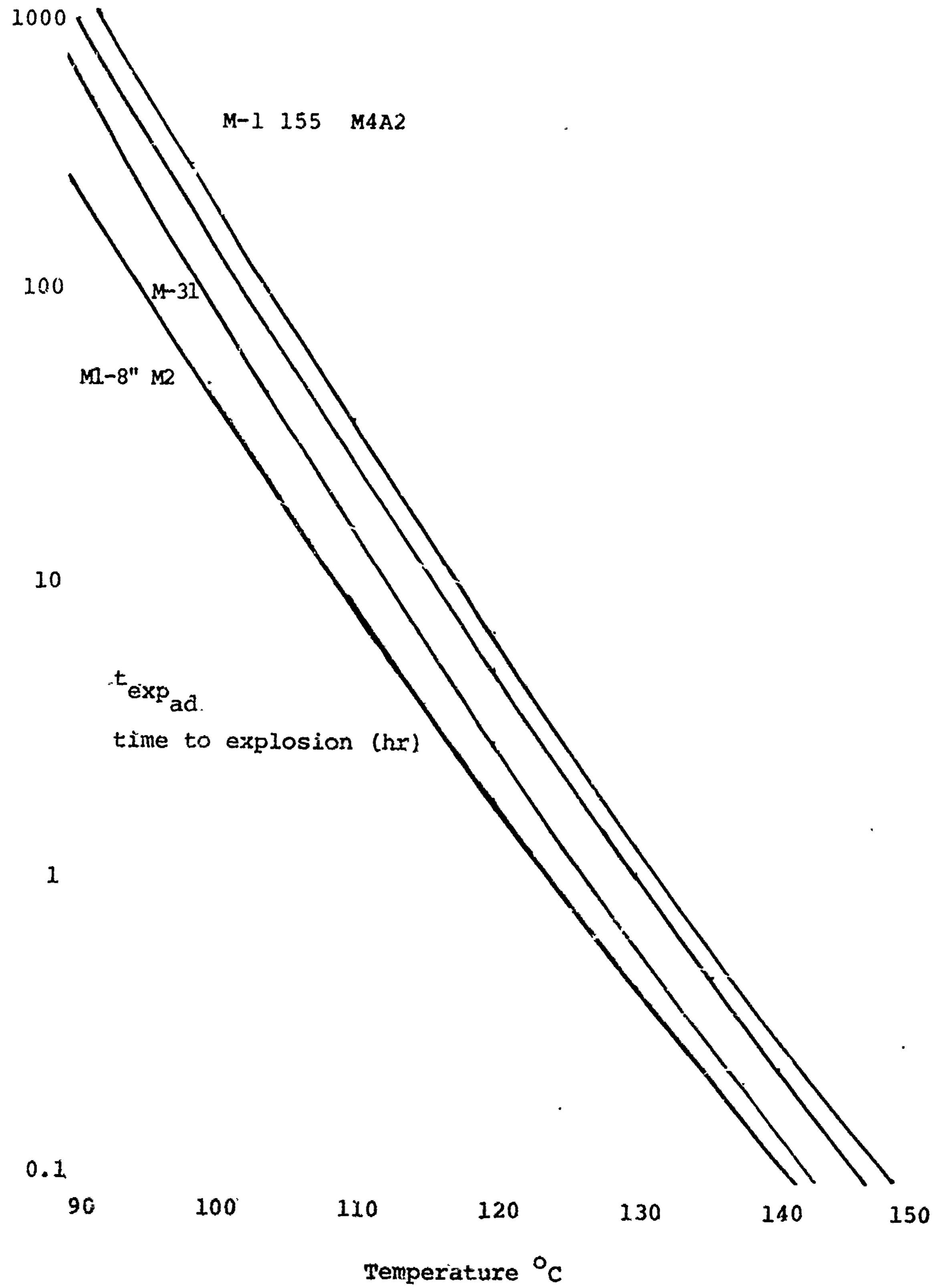

Figure 4. Adiabatic Runaway Reaction Temperatures for Various Cannon Powders - Part 1

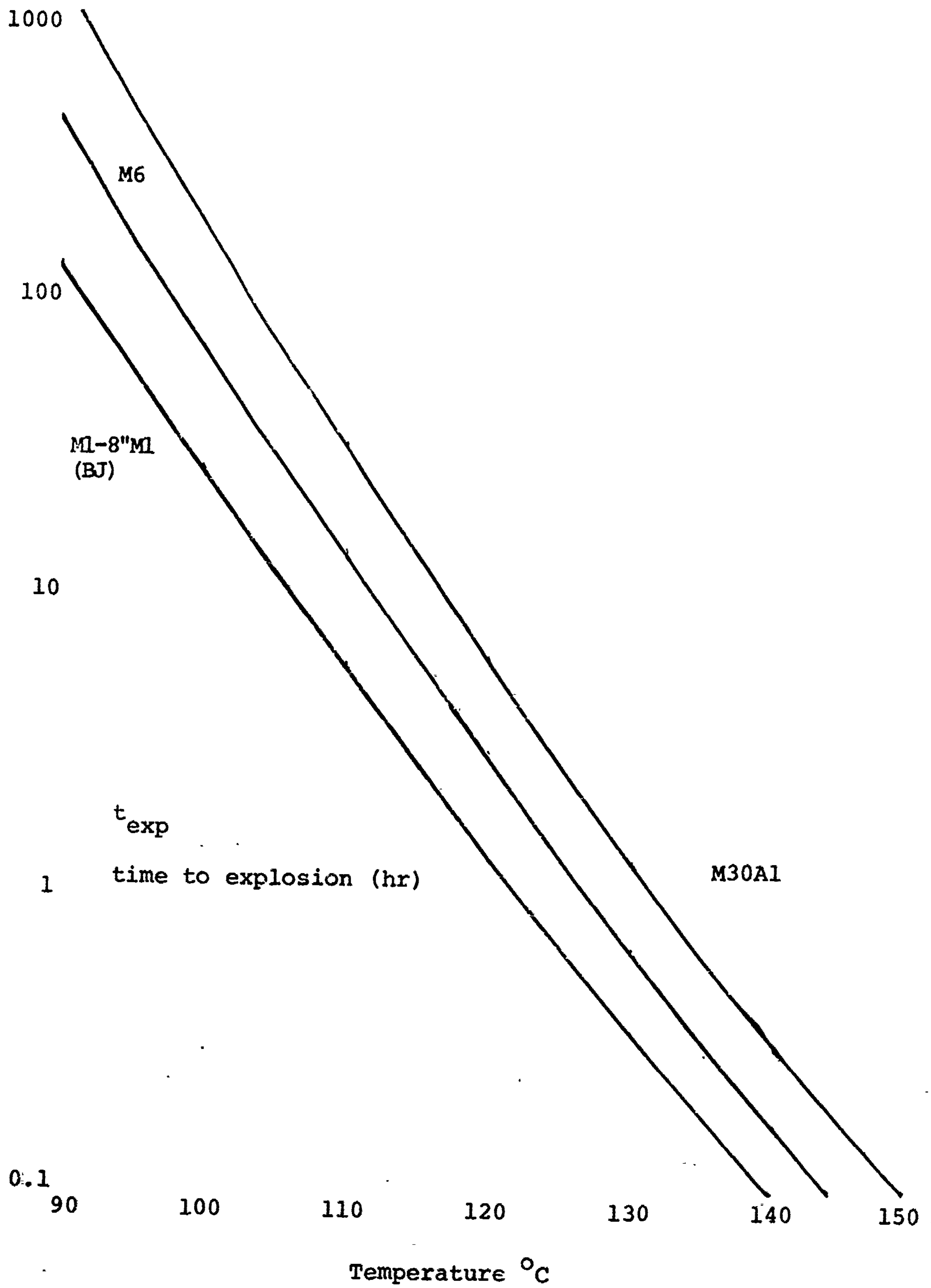

Figure 5. Adiabatic Runaway Reaction Temperatures for Various Cannon Powders - Part 2

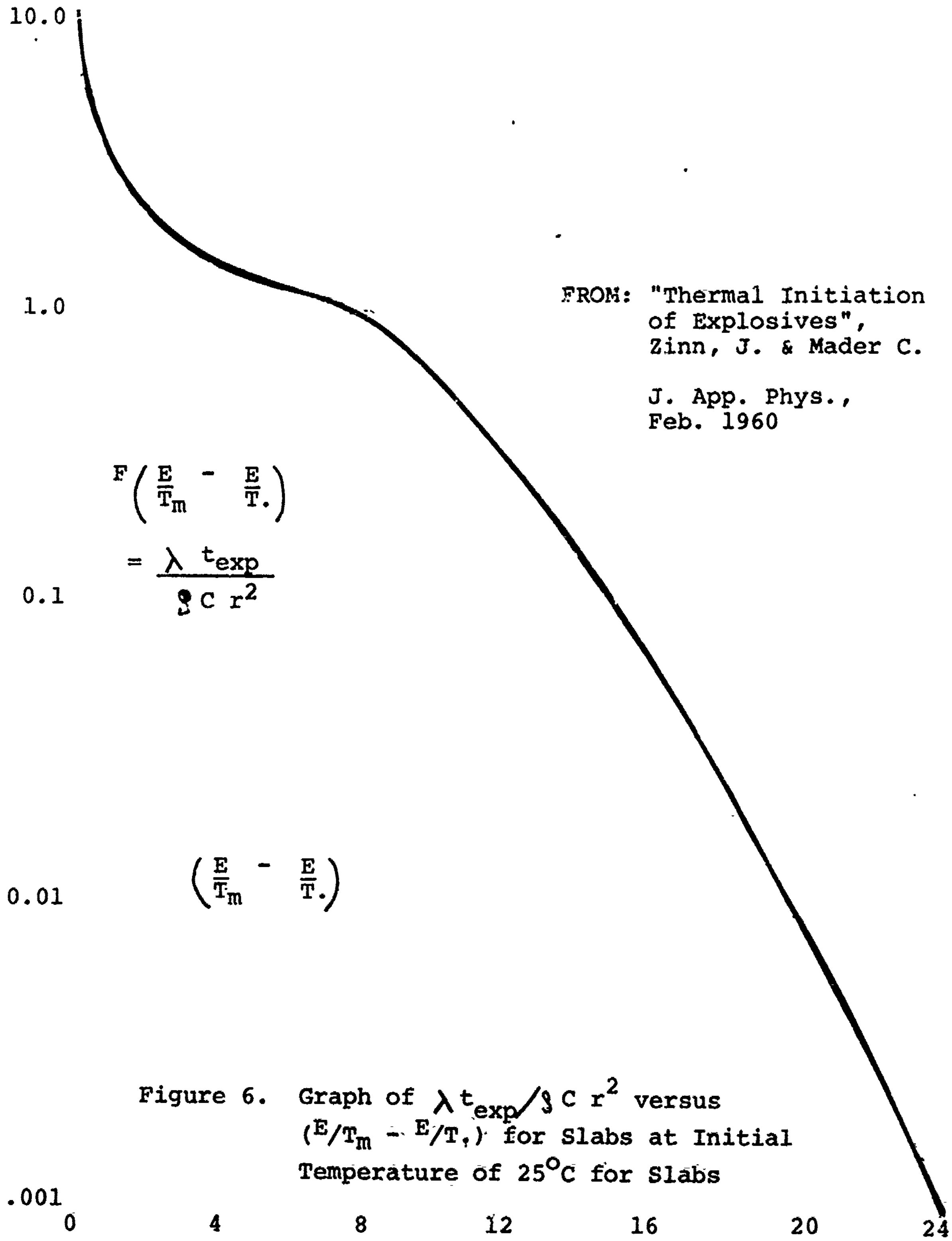

Figure 6. Graph of $\lambda t_{exp}/\rho C r^2$ versus $(E/T_m - E/T_\circ)$ for Slabs at Initial Temperature of 25°C for Slabs

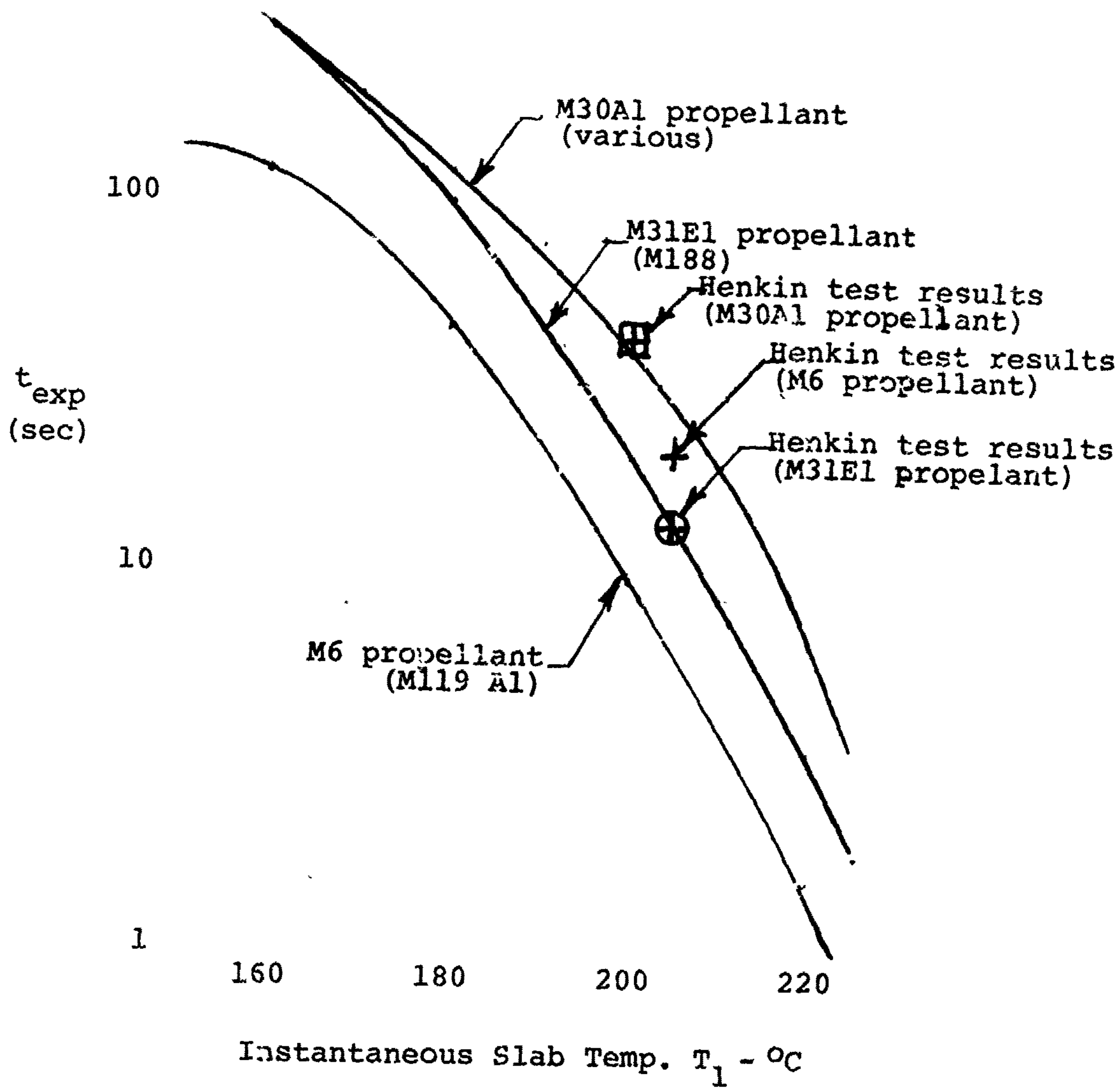

FIG 7 - PREDICTED TIME TO EXPLOSION OF M30A1 AND M31E1 PROPELLANT, FOR POWDER SLAB (INFINITE) THICKNESS OF 0.32 CM, AND HENKIN TEST RESULTS AT SAFETY CONSULTING ENGINEERS, INC.

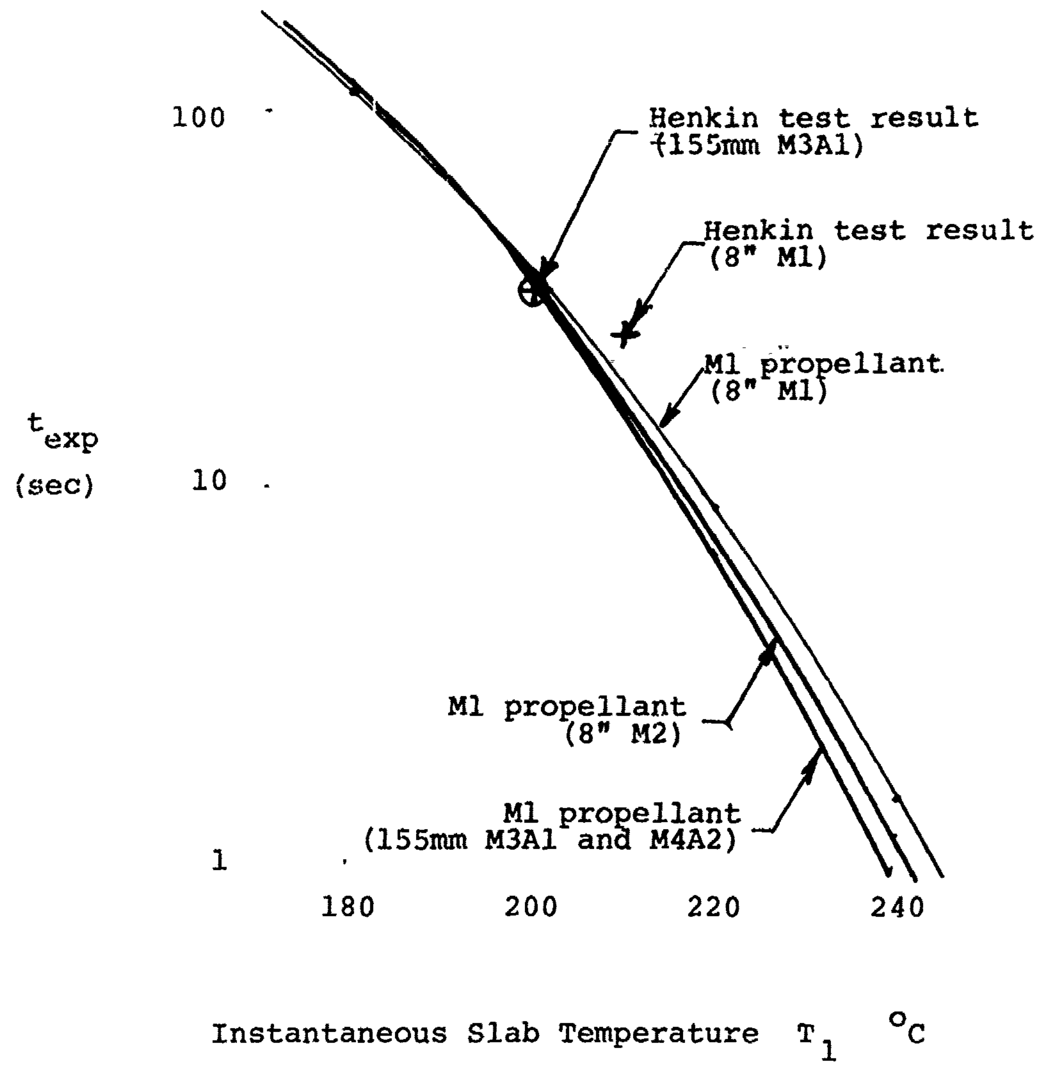

FIG 8 - PREDICTED TIME TO EXPLOSION OF M1 PROPELLANT FOR POWDER SLAB (INFINITE) THICKNESS OF 0.32 CM AND HENKIN TEST RESULTS AT SAFETY CONSULTING ENGINEERS, INC.

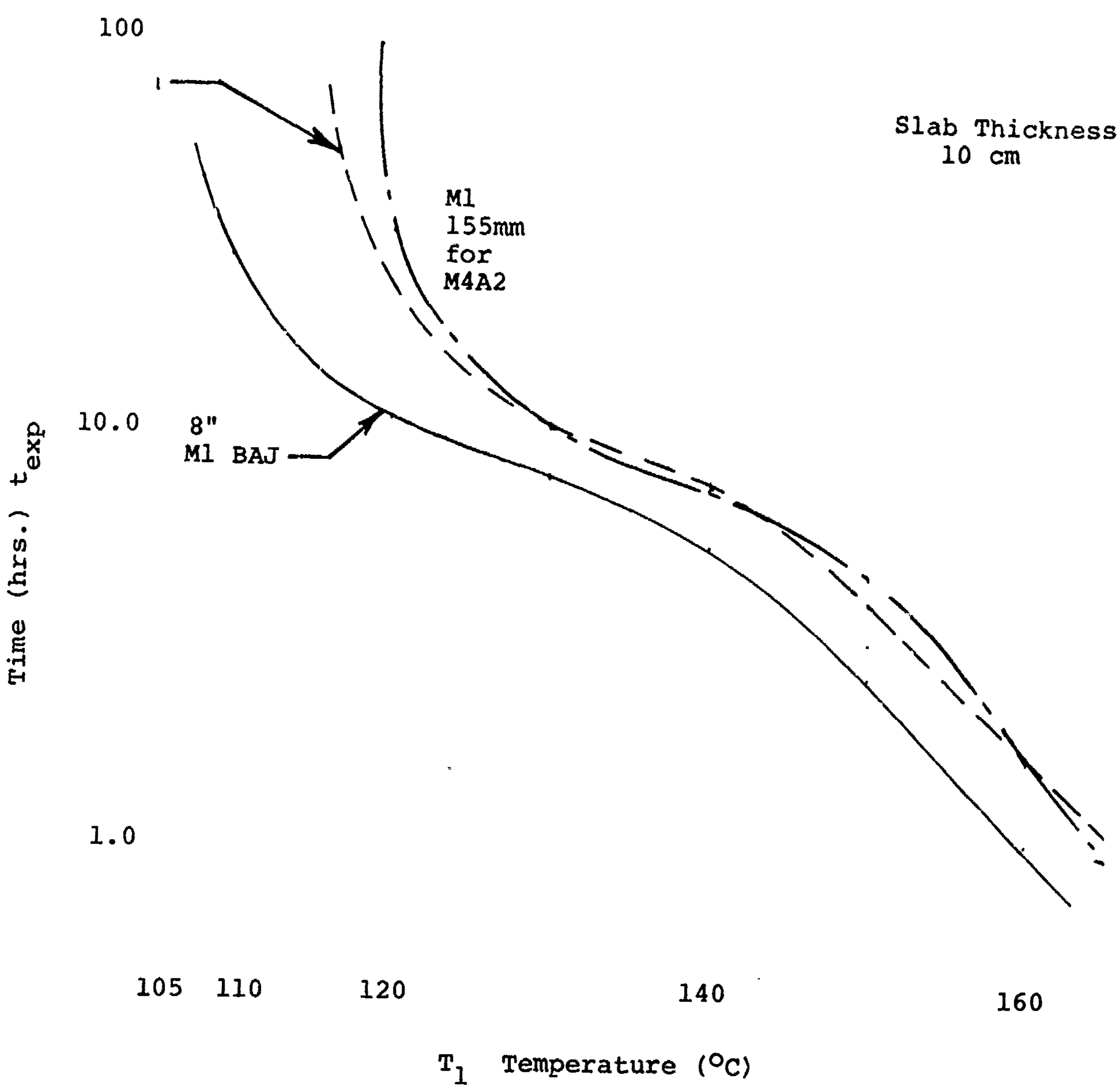

Figure 9. Runaway Reaction Time On a Slab Exposed to a Surface at Temperature (T_1) for Various Cannon Powders

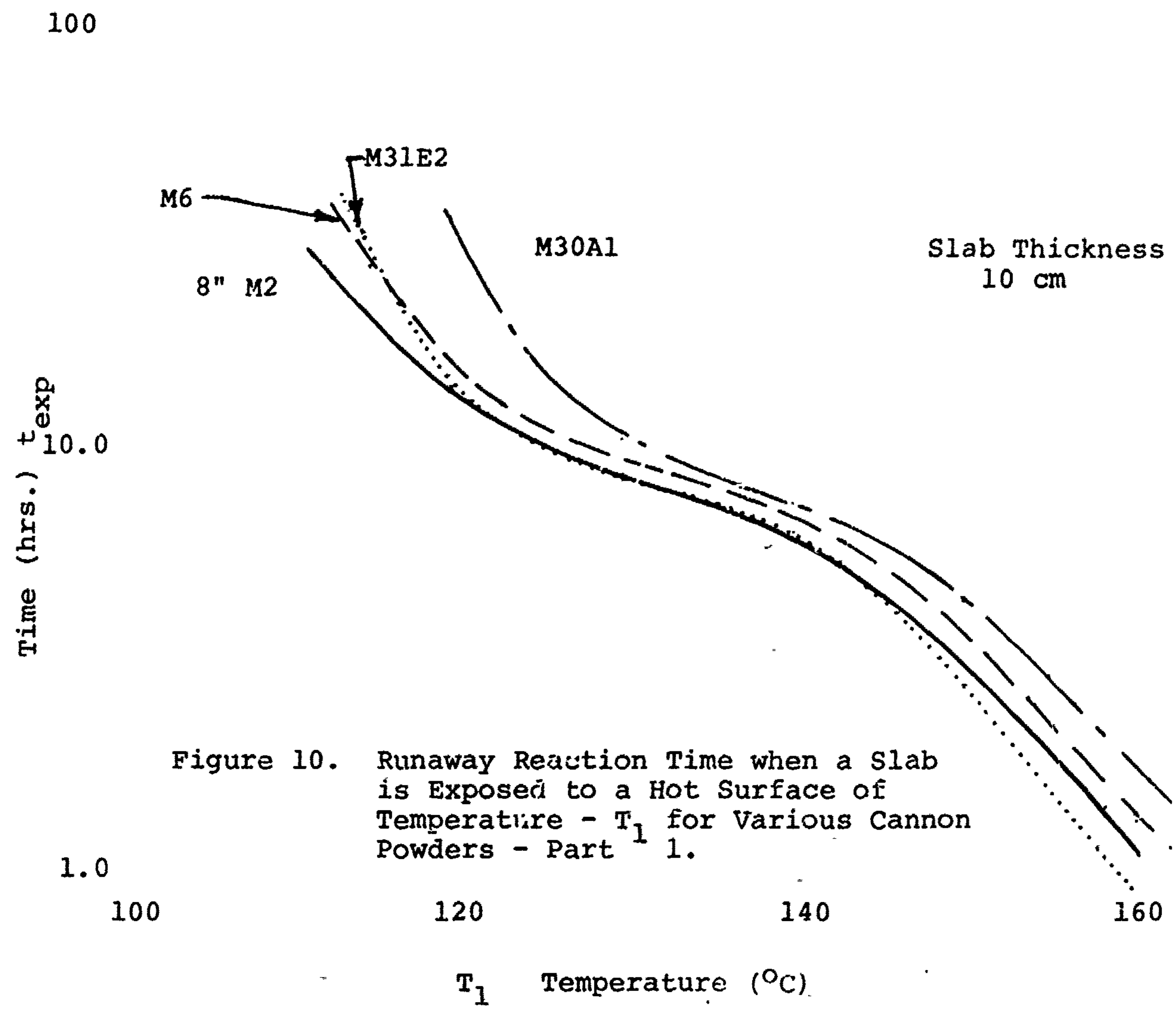

Figure 10. Runaway Reaction Time when a Slab is Exposed to a Hot Surface of Temperature - T_1 for Various Cannon Powders - Part 1.

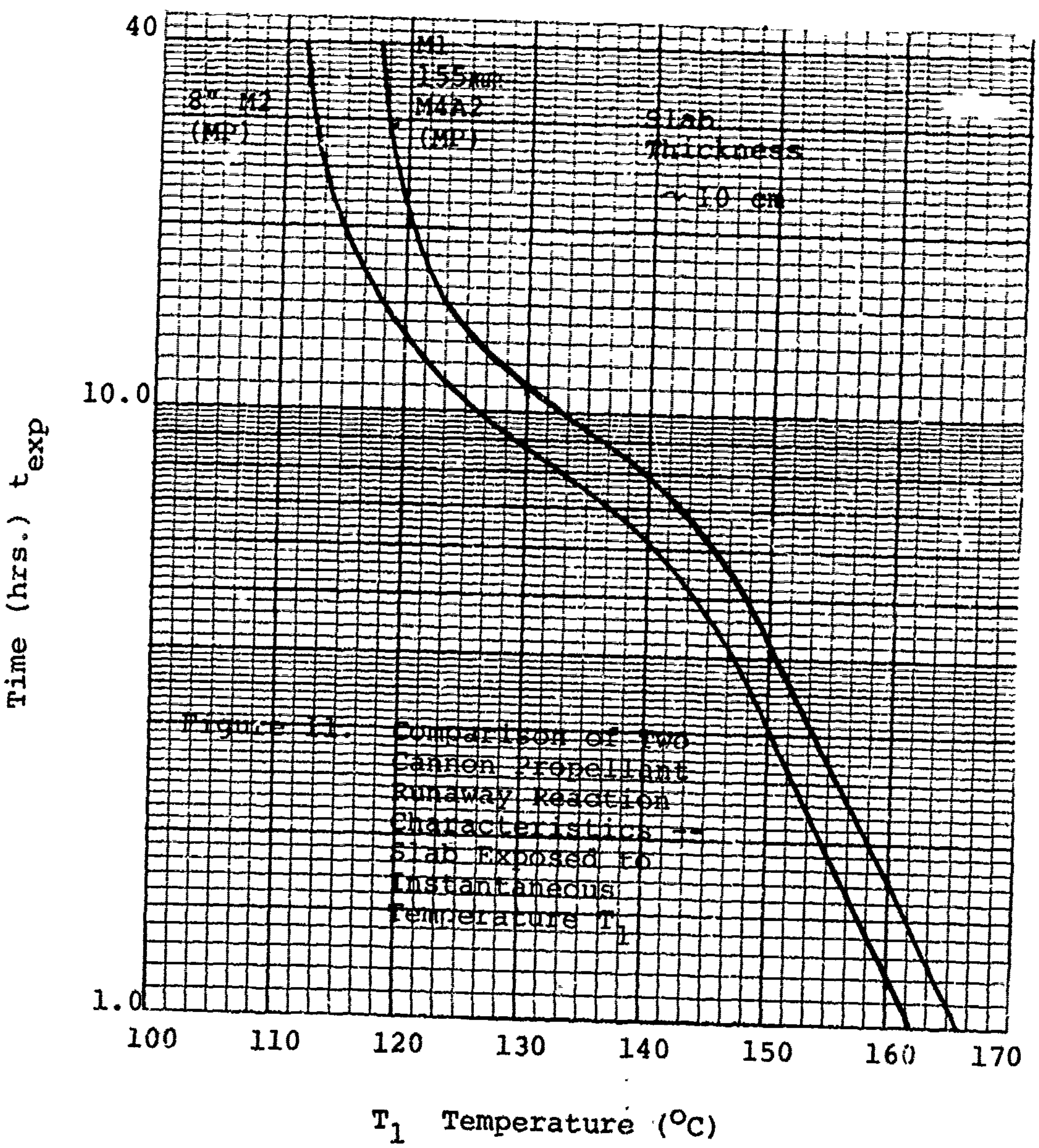

Figure 11. Comparison of Two Cannon Propellant Runaway Reaction Characteristics -- Slab Exposed to Instantaneous Temperature T_1

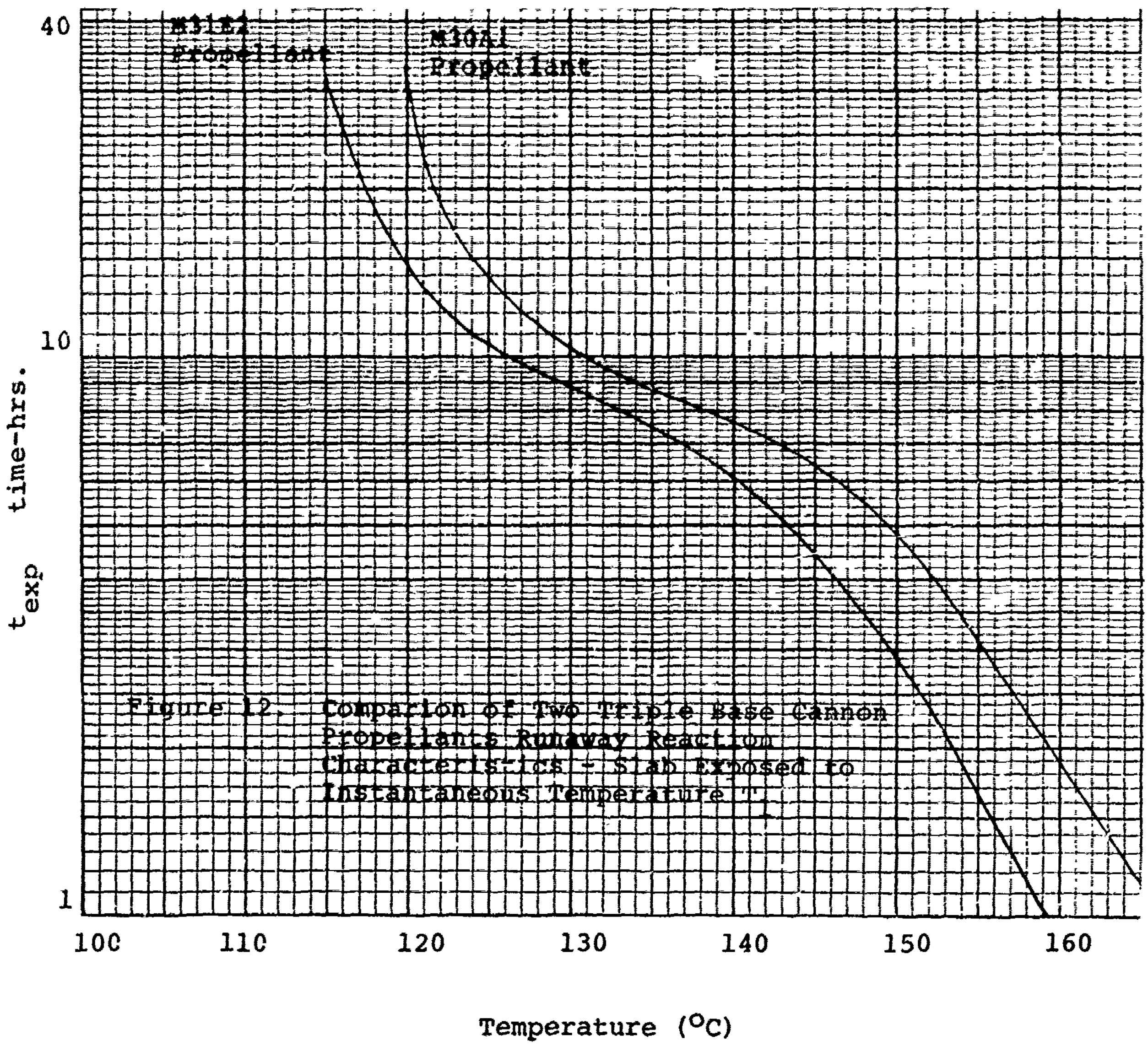

Figure 12. Comparion of Two Triple Base Cannon Propellants Runaway Reaction Characteristics - Slab Exposed to Instantaneous Temperature T_1

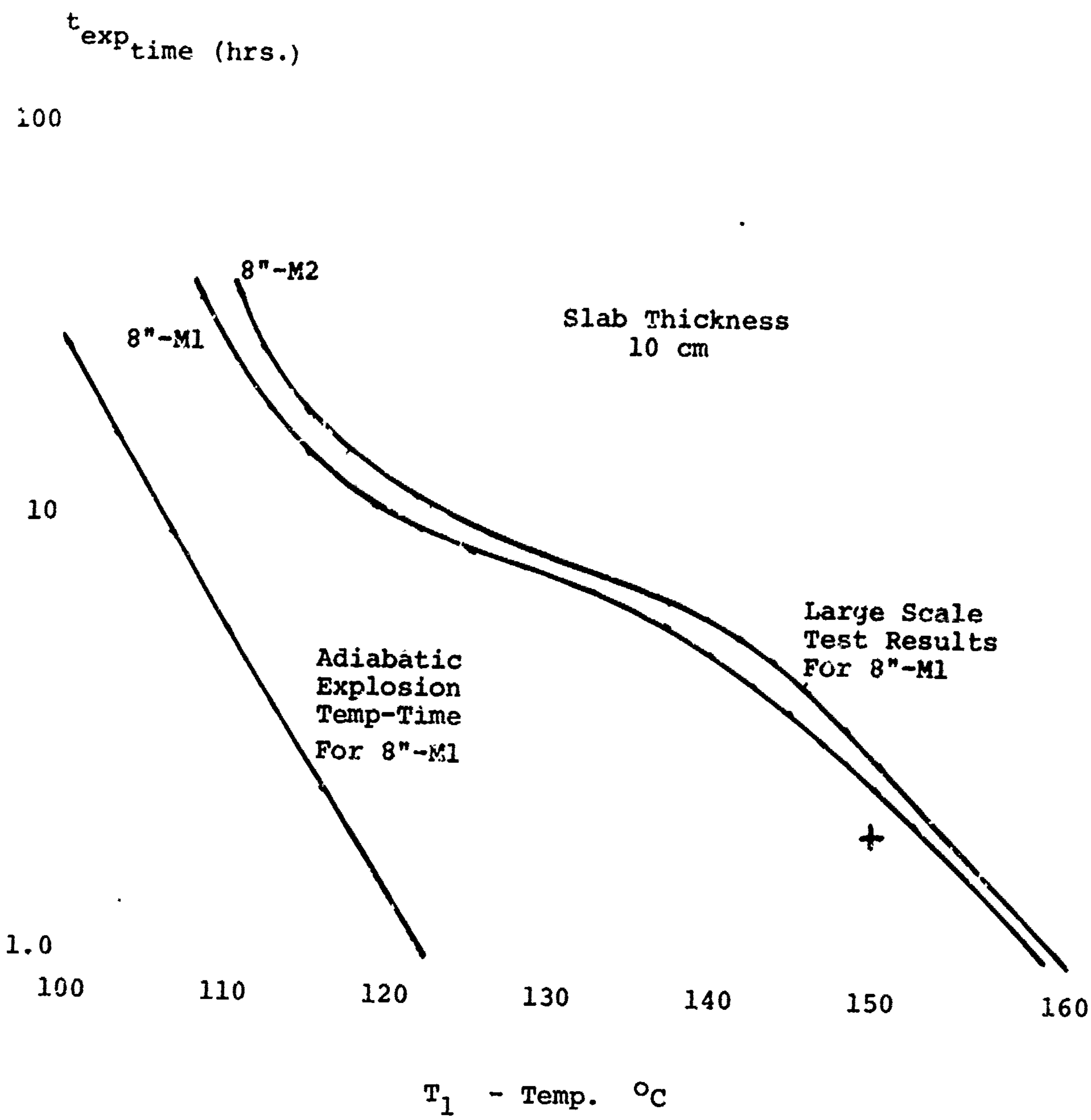

Figure 13. Comparison of Two Cannon Propellants for 8" Gun - Runaway Reaction Characteristics when Slab Exposed to Surface at Temperature - T.

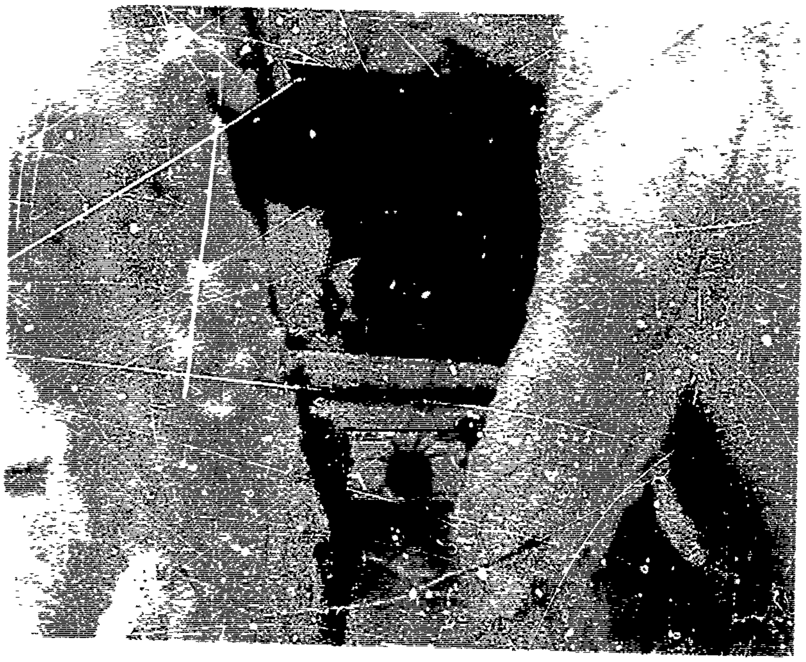

Figure 15. Aluminum test chamber

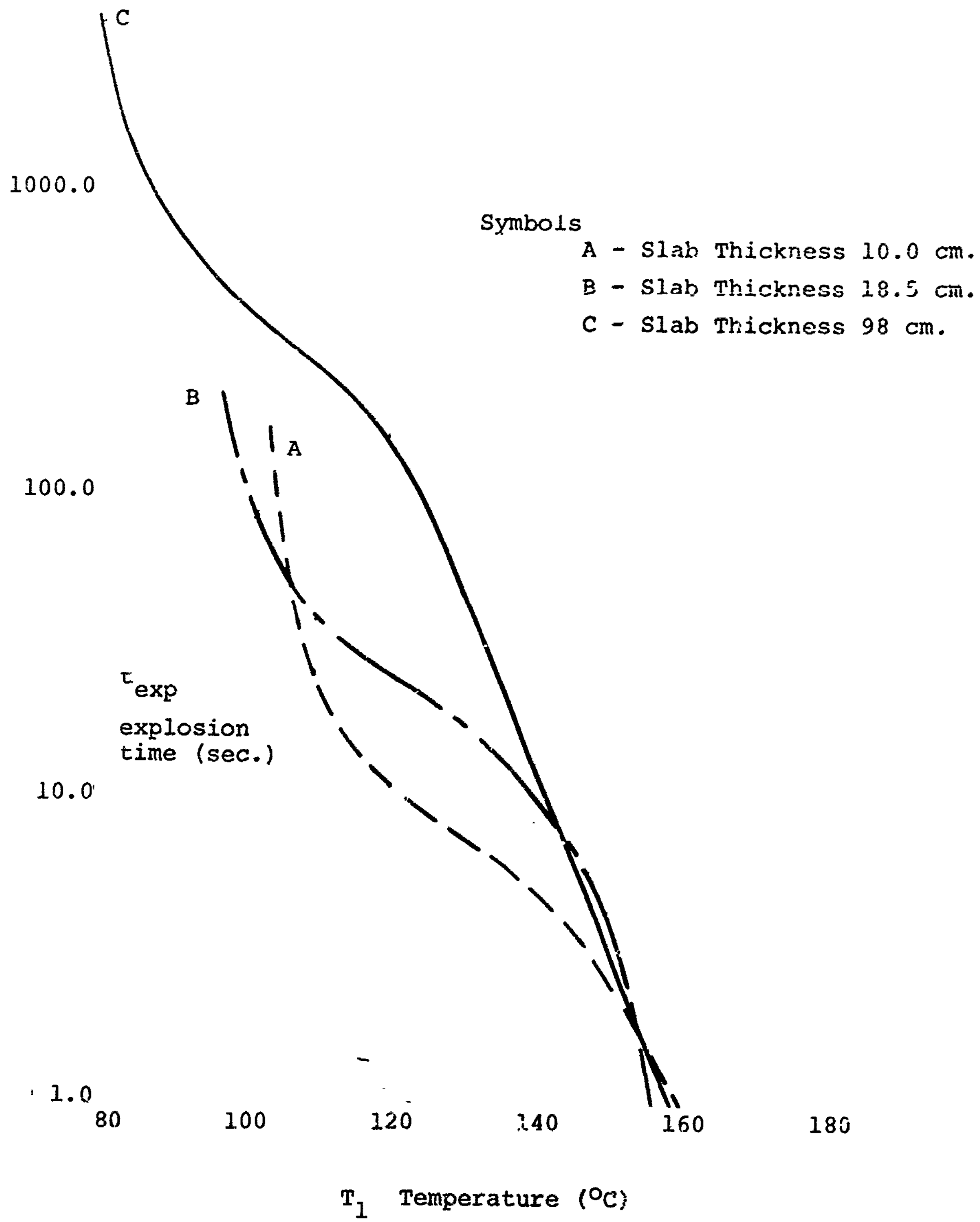

Figure 14. Effect of Slab Thickness on Time-to-Runaway Reaction when Subjected to Instantaneous Surface Temperatures for an 8"-M1 Propellant

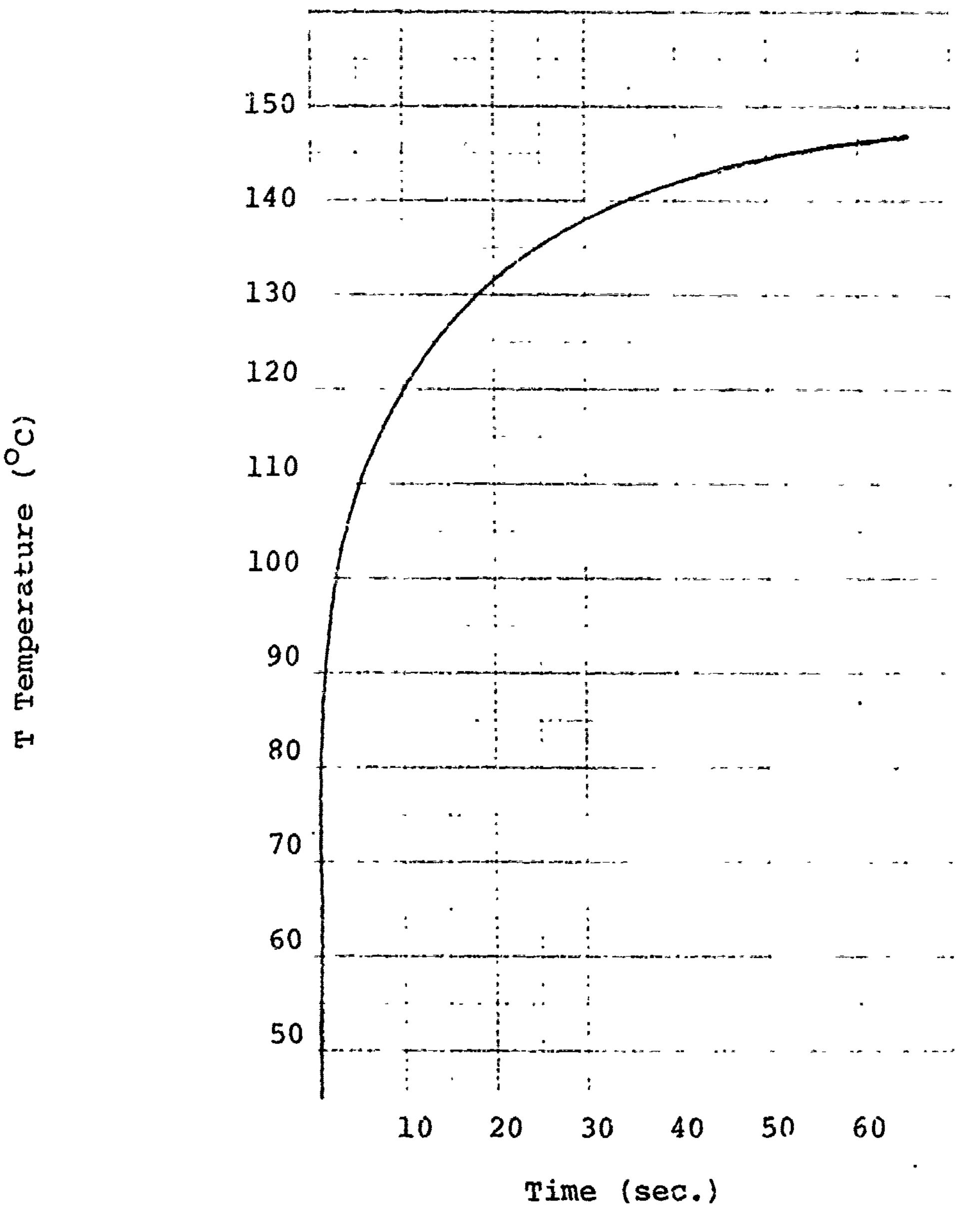

Figure 16. Temperature Profile for 4 Inch Thick Slab Exposed to a Surface at Temperature $T_1 = 150^{o}C$ - M1 Propellant for 8 Inch Gun

19th EXPLOSIVE SAFETY SEMINAR

PBXW-7, A New, Cook-off Resistant Booster Explosive

Ewrin W. Anderson
Vernon D. Ringbloom

Naval Surface Weapons Center
Silver Spring, Maryland 20910

Cook-off is the exothermic reaction observed when high energy materials, such as explosives or propellants, are subjected to a thermal environment in which their surface temperature exceeds the materials' critical temperature. Of particular interest to users of high energy materials is the severity of the exothermic reaction. Observed reaction levels for explosives range for relatively mild burning to detonation.

There is a requirement for cook-off resistant booster explosives for use in munitions handled aboard aircraft carriers and other Navy vessels. Considerable effort has been made to extend the time that munitions can survive in a fuel fire environment without detonating and to reduce the severity of the cook-off reaction.

No matter what approach is taken, such as ablative coatings, insulation, intumescent paint or a main charge explosive fill that burns quietly in a fuel fire, if the booster cooks off high order, it will often detonate any remaining main charge explosive. Thus, the effect of the efforts to increase the temperature resistance of given munitions is negated.

The approach taken in this effort has been to formulate various mixtures of TATB, RDX and a suitable binder, such as polytetrafluoroethylene (PTFE). TATB has been reported to decompose very mildly when exposed to high temperatures. However, it is also very insensitive to initiation and has a relatively low detonation pressure. The RDX is incorporated into the mix in order to increase sensitivity and detonation pressure to acceptable booster explosive levels. Pressed compositions have been formulated with TATB content ranging from 0 to 90% and RDX ranging from 5 to 95%. The binder level has been kept at 5%.

These compositions have been subjected to small scale fast cook-off tests. The results of this testing indicate that compositions with TATB content $\geq$ 55% react very mildly (a quiet burn) in a fast cook-off environment. Under similar test conditions, standard Navy booster explosives, such as CH-6 and tetryl, consistently detonate. Experimental techniques used in this project for simulating the fast cook-off environment are presented. Concurrent initiation sensitivity testing indicated that compositions with at least 20% RDX will initiate readily.

Based on the above cook-off and initiation studies, coupled with estimates of the detonation performance of these mixtures, an explosive composition, designated PBXW-7, consisting of 60% TATB, 35% RDX and 5% PTFE, was selected for further development.

PBXW-7 was subjected to Navy interim qualification safety testing, which includes, for example, such tests as the impact, electrostatic and friction sensitivity tests, transportation hazards tests, and the small scale gap test. The results of these tests will be presented and compared with those obtained on the standard booster explosives, CH-6 and tetryl. The results of the interim qualification testing indicates that PBXW-7 possesses safety characteristics which are a significant improvement over the safety characteristics of CH-6 and tetryl.

Additional, comparative cook-off testing of confined and unconfined charges of PBXW-7, CH-6 and tetryl confirmed the results of the initial studies conducted on the TATB/RDX mixtures, in that PBXW-7 cooks-off relatively mildly when both fast and slow heating rates are applied.

PBXW-7, A NEW, COOK-OFF RESISTANT BOOSTER EXPLOSIVE

ERWIN W. ANDERSON
VERNON D. RINGBLOOM

NAVAL SURFACE WEAPONS CENTER
WHITE OAK, SILVER SPRING, MARYLAND 20910

COMPONENT MATERIALS

RDX

TATB (1,3,5-TRIAMINO - 2,4,6-TRINITROBENZENE)

PTFE (POLYTETRAFLUOROETHYLENE)

PBXW-7 COMPOSITION

COMPONENT	% BY MASS
TATB	60
RDX, CLASS E	35
PTFE	5

NAVY BOOSTER EXPLOSIVES

TETRYL

CH-6

PBXN-5

FAST COOK-OFF TEST REACTION LEVELS

1. MILD BURN
2. MILD PRESSURE RUPTURE
3. VIOLENT PRESSURE RUPTURE
4. PARTIAL DETONATION
5. HIGH ORDER DETONATION

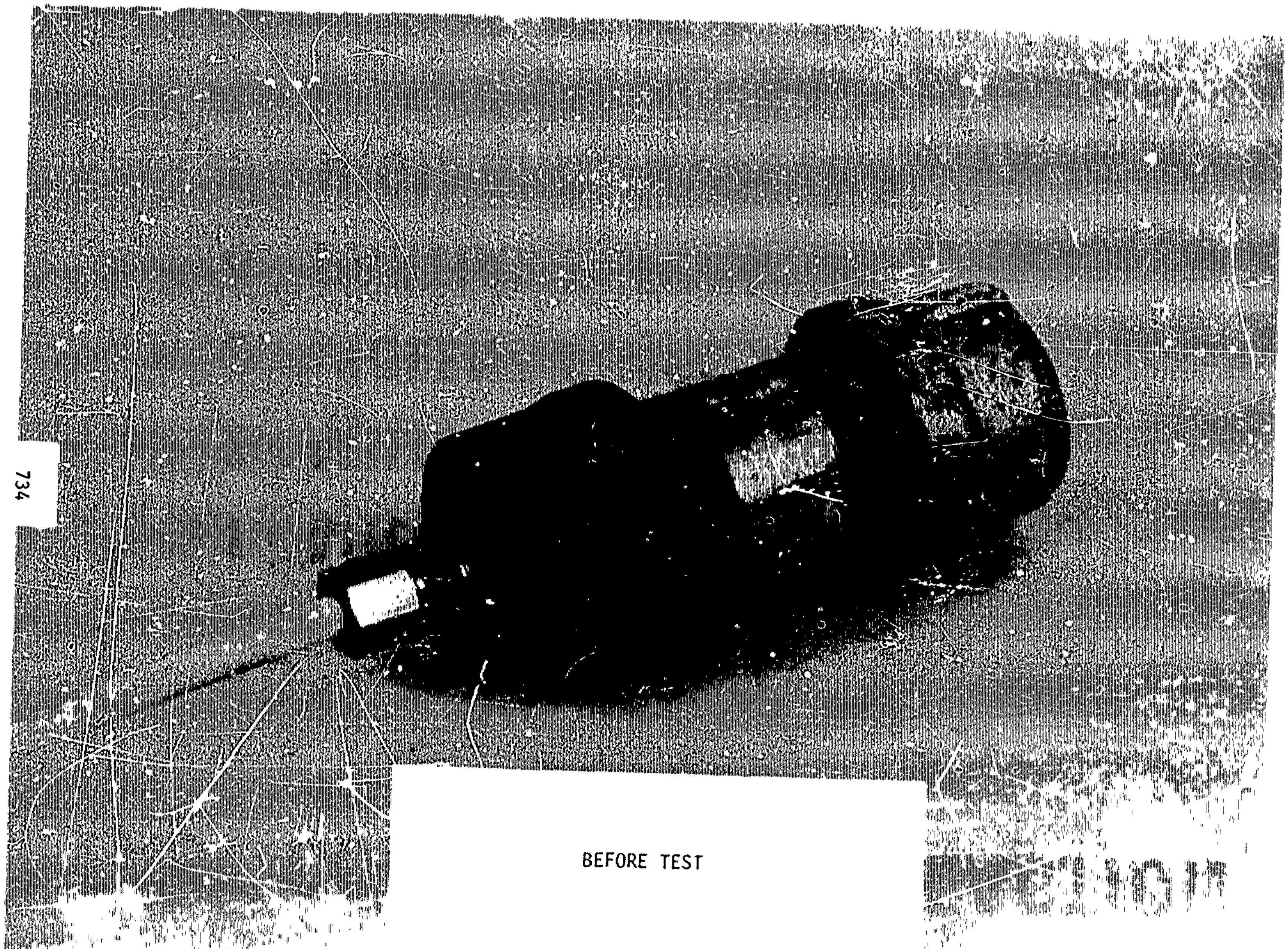

BEFORE TEST

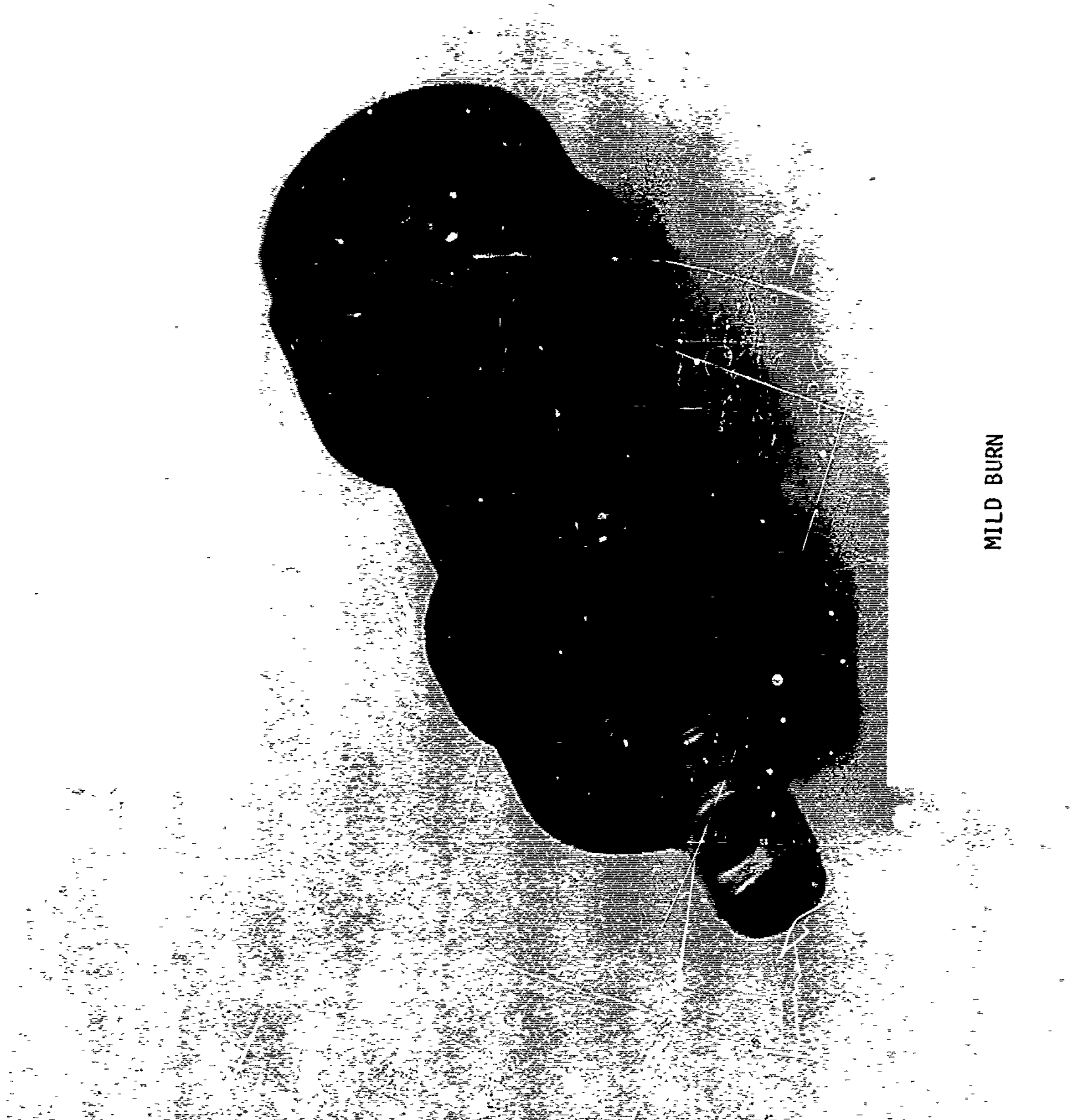

MILD BURN

MILD PRESSURE RUPTURE

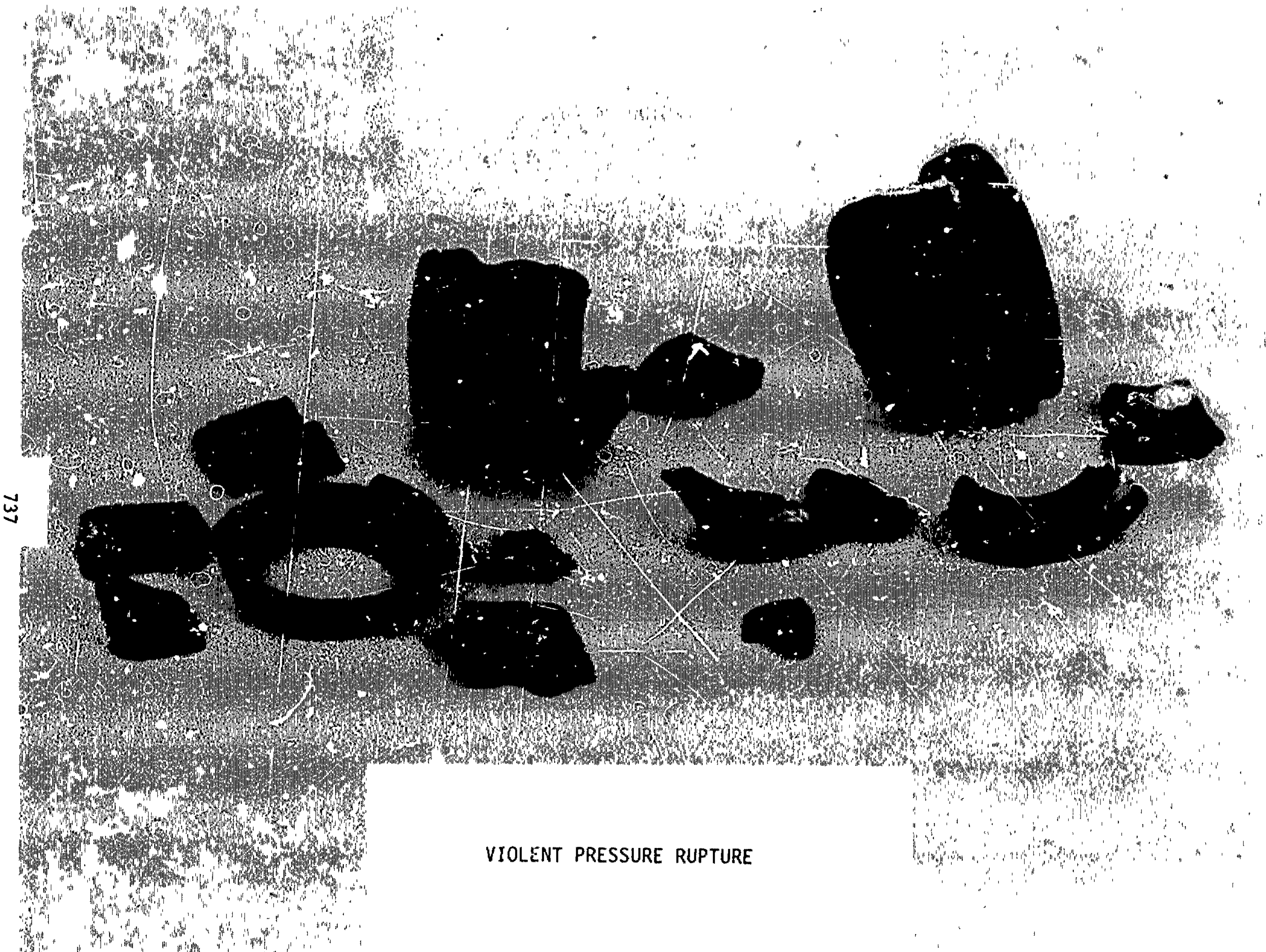

VIOLENT PRESSURE RUPTURE

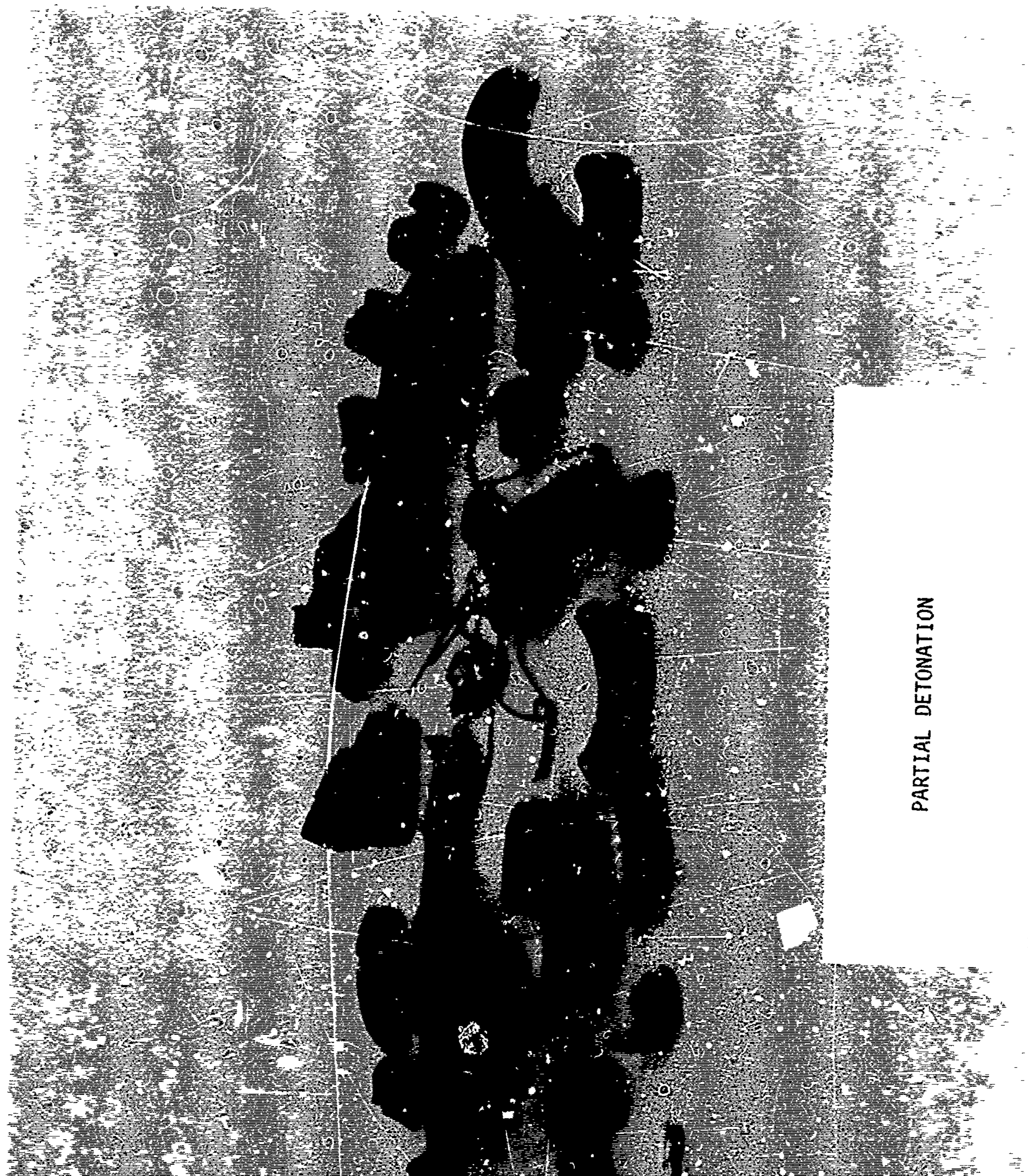

PARTIAL DETONATION

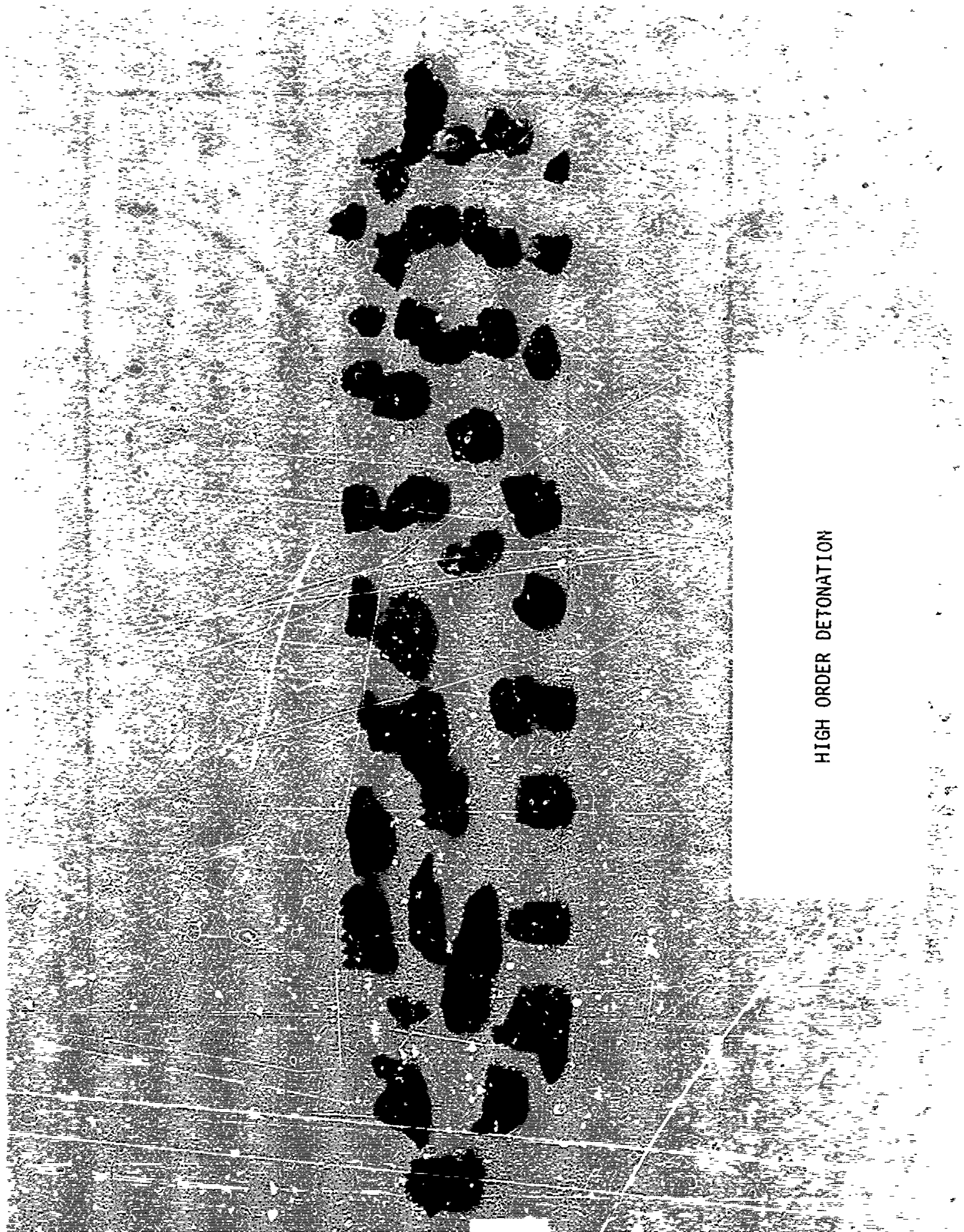

HIGH ORDER DETONATION

COOK-OFF TEMPERATURES
TATB/RDX/PTFE = X/95-X/5

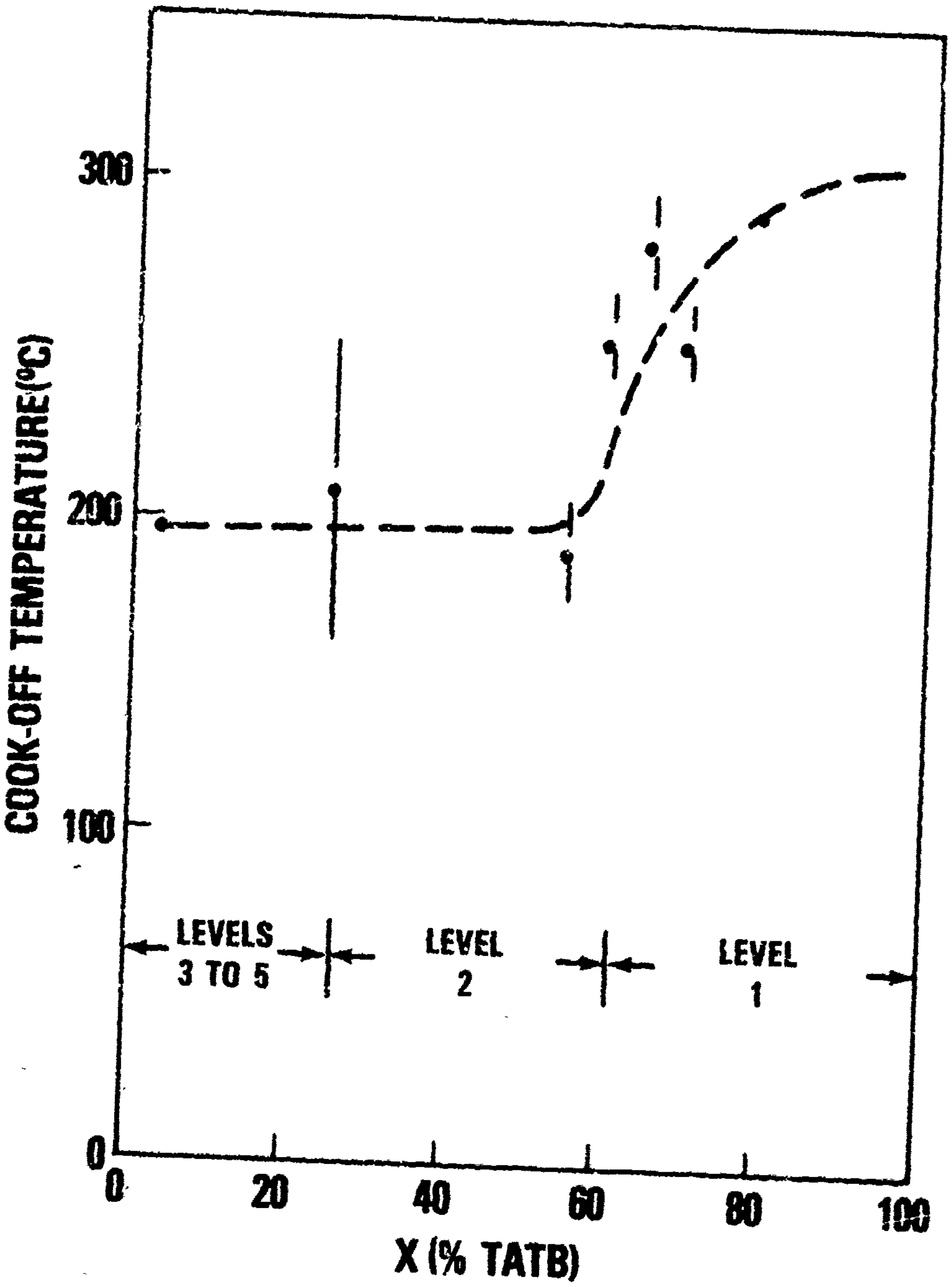

COOK-OFF TEMPERATURES AND REACTION LEVELS NAVY BOOSTER EXPLOSIVES

EXPLOSIVE	ρ (GM/CM^3)	COOK-OFF TEMPERATURE (°C)	REACTION LEVEL
CH-6	1.79	209	4
TETRYL	1.50 - 1.52	172	5

SUMMARY OF BOOSTER EXPLOSIVE COOK-OFF TESTS

TYPE OF COOK-OFF TEST/CONFINEMENT	PBXW-7	CH-6	TETRYL
FAST, HEAVY CONFINEMENT	MILD PRESSURE RUPTURE	PARTIAL DETONATION	HIGH ORDER DETONATION
FAST, TOTAL CONFINEMENT	MILD PRESSURE RUPTURE	-----	-----
SLOW, UNCONFINED	MILD BURN	-----	-----
SLOW, TOTAL CONFINEMENT	MILD AND VIOLENT PRESSURE RUPTURES	PARTIAL DETONATION	HIGH ORDER DETONATION

MANDATORY TEST RESULTS

TEST	PASS CRITERIA	PBXW-7
SMALL SCALE GAP	20 OUT OF 20 NO FIRES	20 OUT OF 20 NO FIRES
IMPACT SENSITIVITY	20 OUT OF 20 NO FIRES AT 12 CM	20 OUT OF 20 NO FIRES AT 12 CM
VACUUM THERMAL STABILITY (ml/gm/48 HRS)	<2.00	0.25
HOT WIRE IGNITION	20 OUT OF 20 NO FIRES AT BOTH 4,000 AND 15,000 PSI LOADING PRESSURE	20 OUT OF 20 NO FIRES AT EACH PRESSURE
ELECTROSTATIC SENSITIVITY	20 OUT OF 20 NO FIRES AT 10,000 VOLTS	20 OUT OF 20 NO FIRES
FRICTION SENSITIVITY	50% > 250 LBS FORCE	50% POINT >> 980 LBS FORCE 20 OUT OF 20 NO FIRES AT 980 LBS FORCE
DETONATIONVELOCITY (m/sec)	BE DETERMINED	7,600 at ρ 1.747

NSWC

IMPACT SENSITIVITY TEST RESULTS

SAMPLE	50% HEIGHT (cm)	σ	COMMENTS
TETRYL	30.2	0.14	COVERED 5 LEVELS 20-50.5 cm
TETRYL (X768)	23.1	0.25	COVERED 4 LEVELS 12.5-40.5 cm
PBXW-7 (I.D. 2573)	53.7	0.12	COVERED 4 LEVELS 40.5-80.5
PBXW-7 (I.D. 2617)	39.5	0.15	COVERED 5 LEVELS 25.5-64.0
PBXW-7 (I.D. 2619)	46.1	0.15	COVERED 5 LEVELS 25.5-64.0
CH-6 (X850)	26.9	0.09	COVERED 4 LEVELS 20.0-40.5
RDX (X691) STANDARD	22.2	0.12	COVERED 5 LEVELS 16.0-40.5

SMALL SCALE GAP TEST (SSGT) DATA FOR PBXW-7, CH-6 AND TETRYL

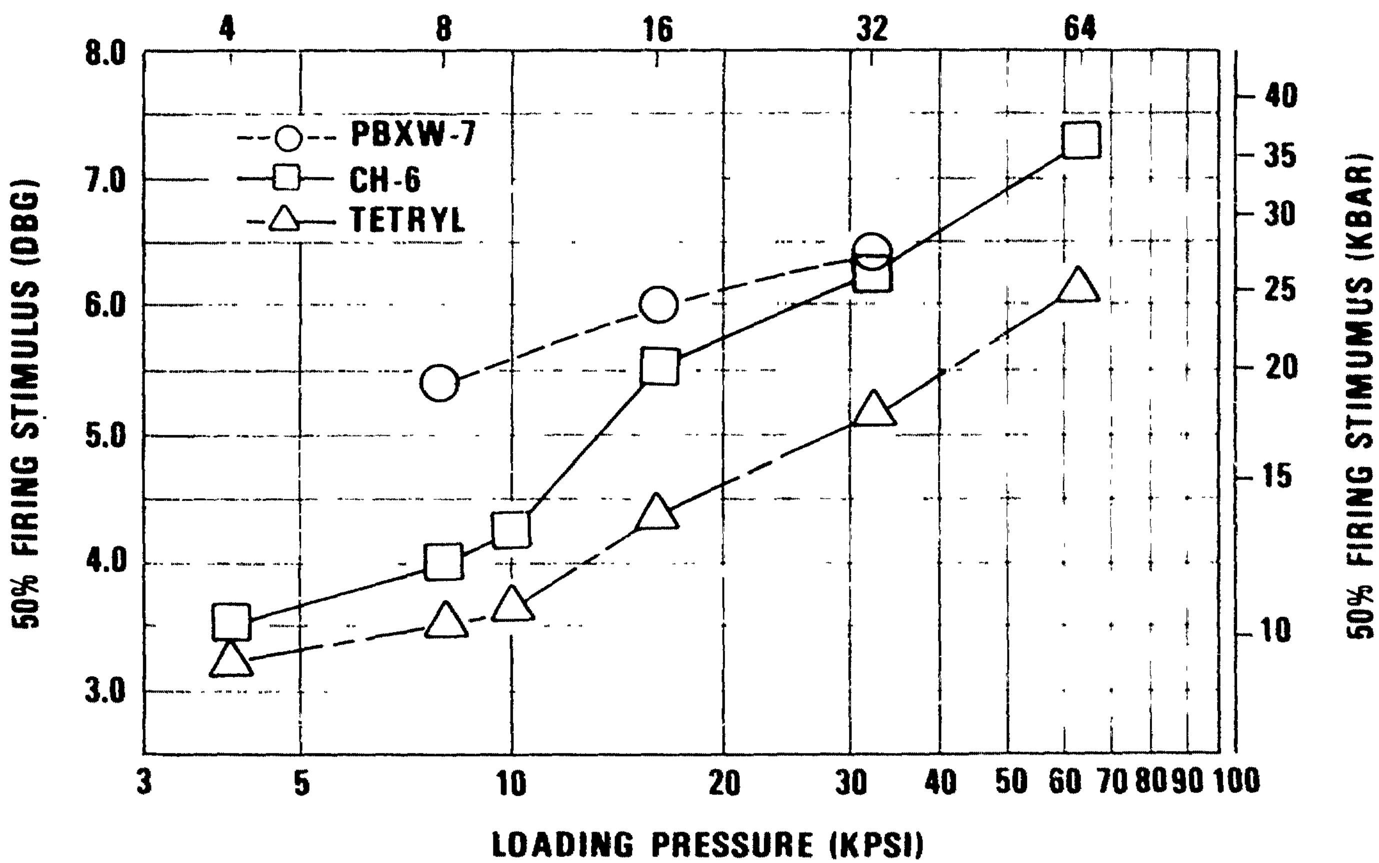

CALCULATED DETONATION PRESSURE AND VELOCITY OF PBXW-7 AS % TMD

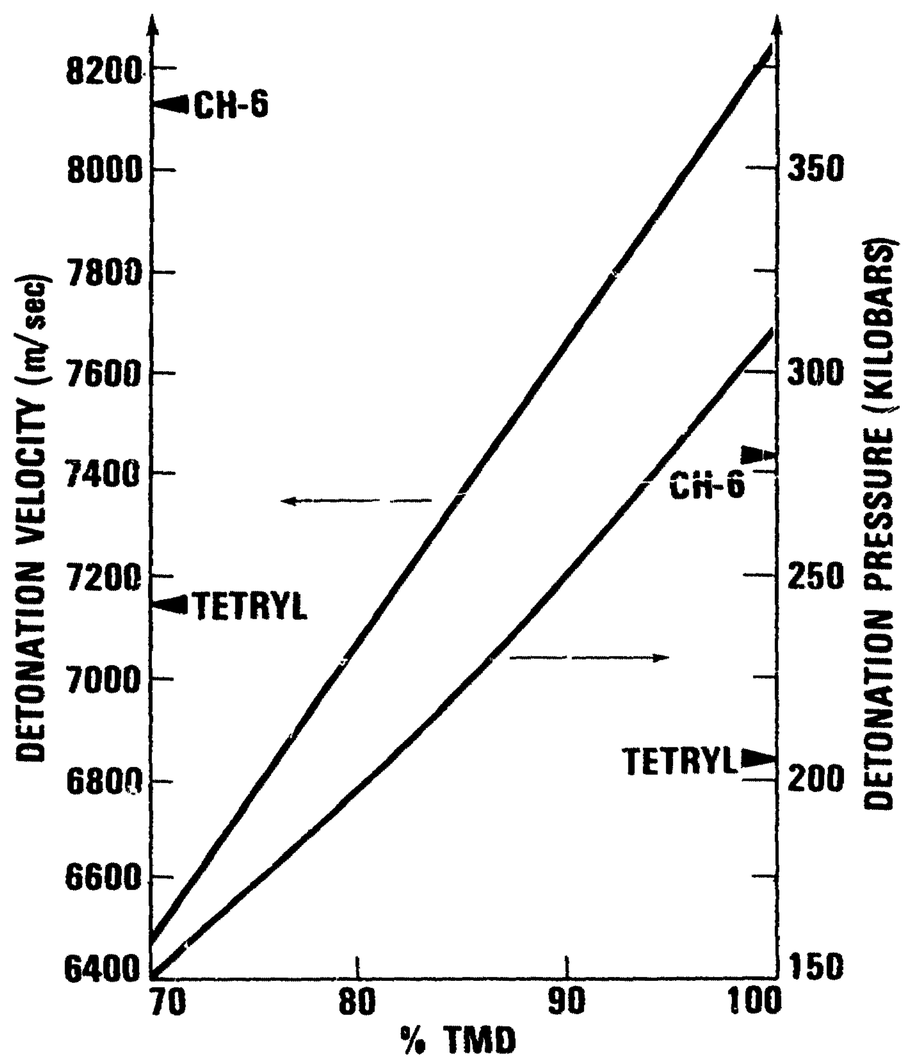

BOOSTER LOADING PRESSURE VERSUS DETONATION VELOCITY CH-6, PBXW-7 AND TETRYL

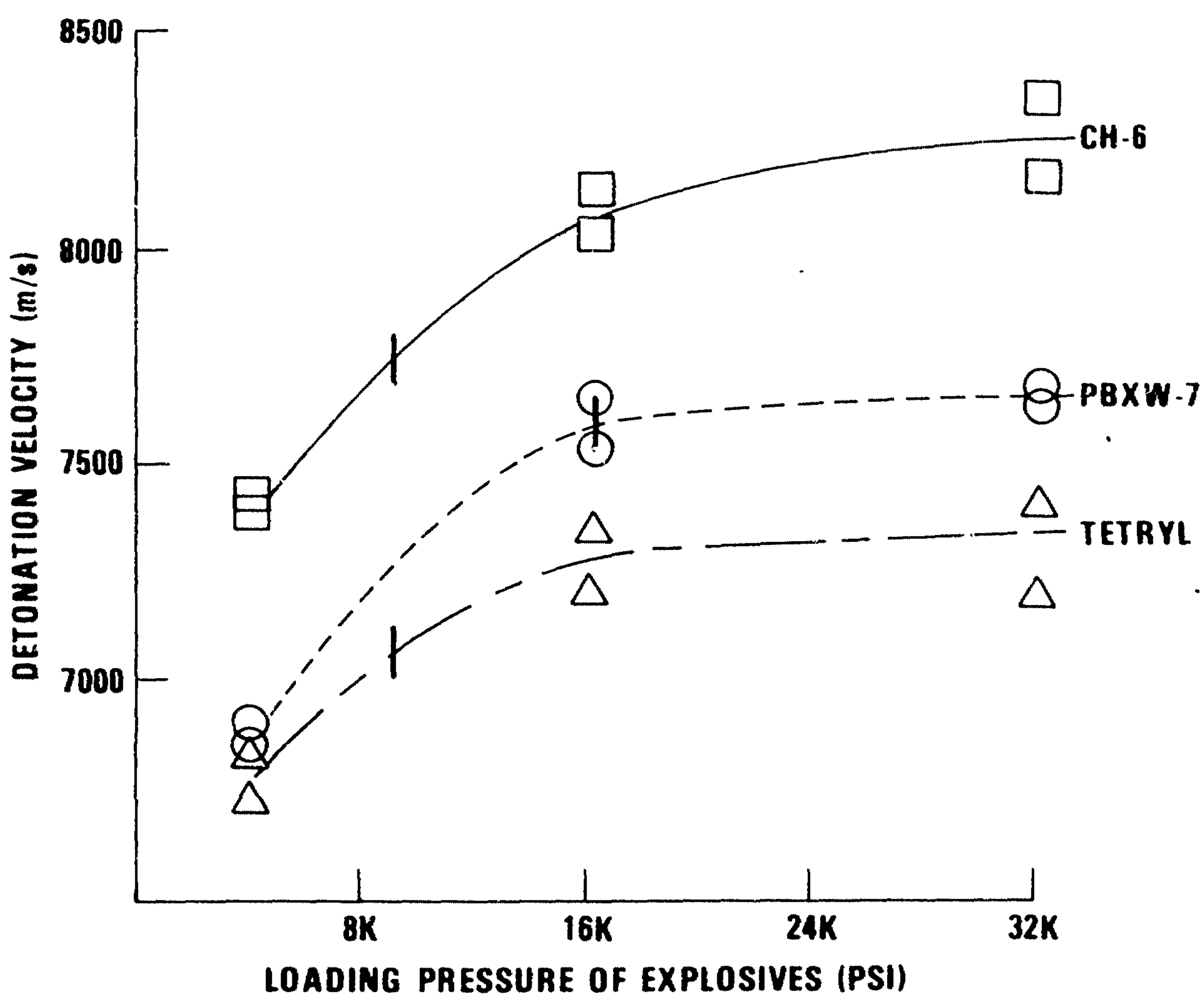

BOOSTER PELLET DENSITY VERSUS DETONATION VELOCITY OF CH-6, PBXW-7 AND TETRYL

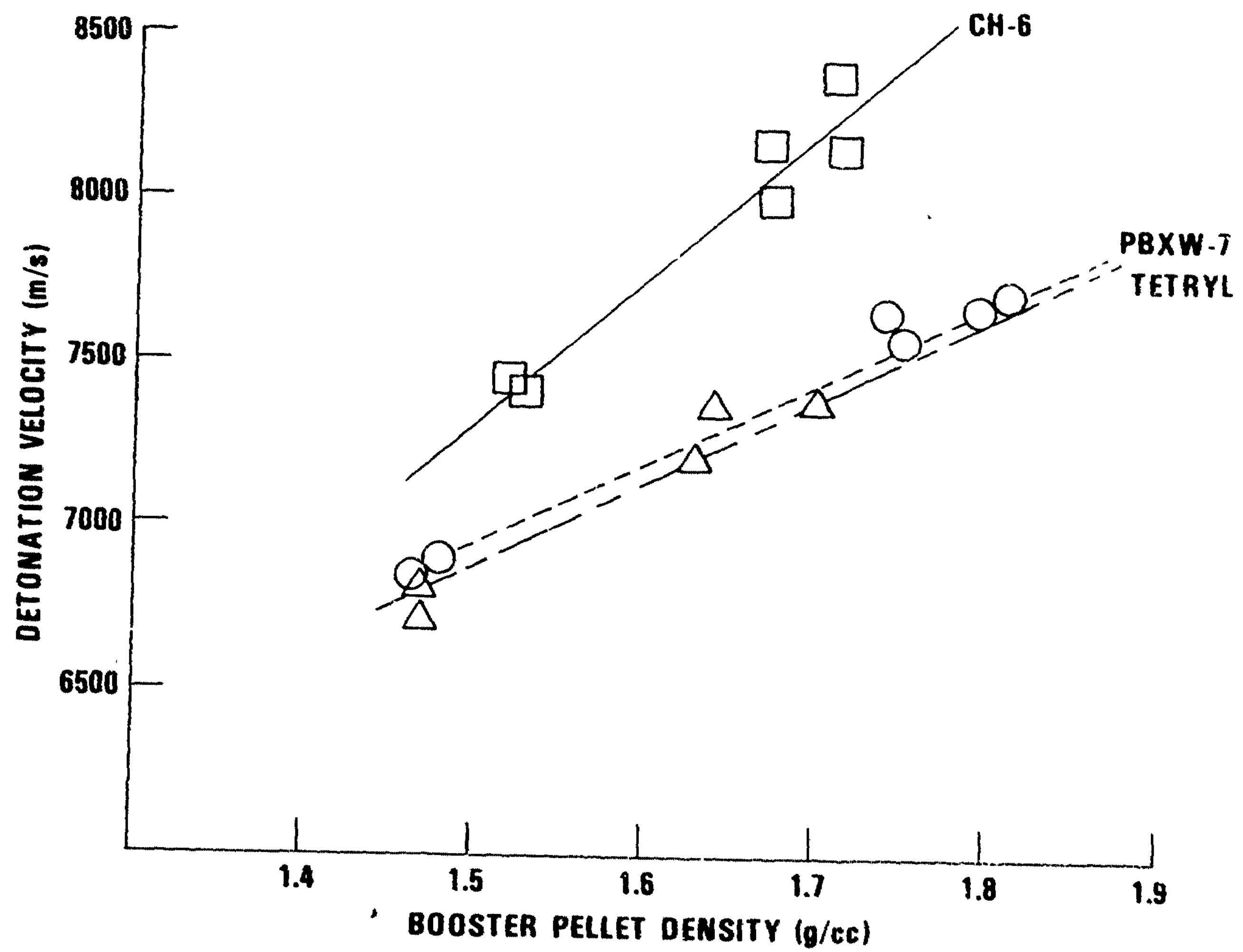

NSWC

FEASIBILITY OF INCORPORATING THE COOK OFF RESISTANT BOOSTER EXPLOSIVE, PBXW-7, INTO THE FM-117 BOMB FUZE

- ITS ABILITY TO BE INITIATED BY THE PRESENT FMU-117 BOMB FUZE LEAD
- ITS OUTPUT, AS COMPARED TO CH-6 AND TETRYL

TESTS CONDUCTED IN THE SIMULATED FMU-117 FUZE HARDWARE

A. BOOSTER OUTPUT OF PBXW-7 WHEN INITIATED BY A DUPONT NUMBER 8 BLASTING CAP. (STANDARD)

B. BOOSTER OUTPUT OF THE SAME PELLETS WHEN INITIATED BY THE DESIGNED FMU-117 FUZE LEAD. (10K PSI)

C. SAME AS "B" ABOVE EXCEPT TETRYL WITHIN THE LEAD WAS CONSOLIDATED AT 4K PSI.

D. BOOSTER OUTPUT OF THE SAME PELLET WITH THE LEAD/BOOSTER INTERFACE PENALIZED BY INSERTION OF EITHER 20 MILS OR 50 MILS PLASTIC BARRIERS BETWEEN THE LEAD AND BOOSTER.

SUMMARY

1. PBXW-7 AT CONSOLIDATION PRESSURE OF BETWEEN 8K AND 32K PSI WERE READILY INITIATED BY THE STANDARD "AS DESIGN" FMU-117 FUZE LEAD.

2. THE SAME PELLETS WERE ALSO READILY INITIATED BY A "PENALIZED" FMU-117 FUZE LEAD.

3. GOOD TRANSFER WAS OBSERVED WHEN THE LEAD/BOOSTER INTERFACE WAS PENALIZED BY INSERTION OF 20 AND 50 MIL PLASTIC BARRIER BETWEEN THE LEAD AND BOOSTER.

4. SINCE THE OUTPUT OF PBXW-7 IS EQUAL TO THAT OF TETRYL, PBXW-7 SHOULD BE ADEQUATE TO INITIATE THOSE EXPLOSIVE INITIATED BY TETRYL.

DEMOLITION/SALVAGE PROJECT FOR DISPOSAL
OF NITROCELLULOSE PRODUCTION FACILITIES AT
SUNFLOWER ARMY AMMUNITION PLANT, DESOTO, KANSAS

BY

THOMAS M. LOUSHINE
SAFETY AND HEALTH MANAGER
SUNFLOWER ARMY AMMUNITION PLANT
DESOTO, KANSAS 66018

DEPARTMENT OF DEFENSE
EXPLOSIVE SAFETY SEMINAR
SEPTEMBER 1980

ABSTRACT

An 18 month project to dispose of 143 buildings was initiated in Oct 1978 at Sunflower Army Ammunition Plant. Most of the buildings had been used during the 1940's to manufacture and press nitrocellulose for the production of single base propellant. Complete decontamination of the facilities was not performed at the time of shutdown, allowing residual nitrocellulose to completely dry over the following several years. Due to the extreme heat and shock sensitivity of dry nitrocellulose, this disposal project required considerations beyond the normal hazards associated with building disposal. The purpose of this paper is to point out these considerations and accompany a visually presented account of this disposal project.

DEMOLITION/SALVAGE PROJECT FOR DISPOSAL OF NITROCELLULOSE PRODUCTION FACILITIES AT SUNFLOWER ARMY AMMUNITION PLANT, DESOTO, KANSAS

INTRODUCTION

Sunflower Army Ammunition Plant (SFAAP) is a propellant production installation under the US Army Armament Materiel Readiness Command, ARRCOM, a subcommand of the US Army Development and Readiness Command, DARCOM. Located 20 miles west of Kansas City, Kansas, construction of SFAAP was initiated in the early 1940's. Materials produced included nitrocellulose (NC) and nitroglycerin (NG) for the purpose of producing single and double base cannon and rocket propellants.

Production was halted later in the 1940's and the various production lines were placed in a layaway status. Many of the buildings were later used during the early 1950's, 1960's and early 1970's; however, certain NC facilities were not required after the 1940's production time. Those particular facilities, referred to as "B" and "C" lines, were placed in a layaway condition, but without having been decontaminated in a normal manner. Normal decontamination would have included thorough flushing of all process lines and equipment and some disassembly to assure that a 3X decontamination level had been attained. (The 3X level of decontamination means that no contamination can be visually noted on accessible surfaces.) Due to funding shortages and some explosive incidents, decontamination was halted and the facilities were laidaway in a worse than 3X condition.

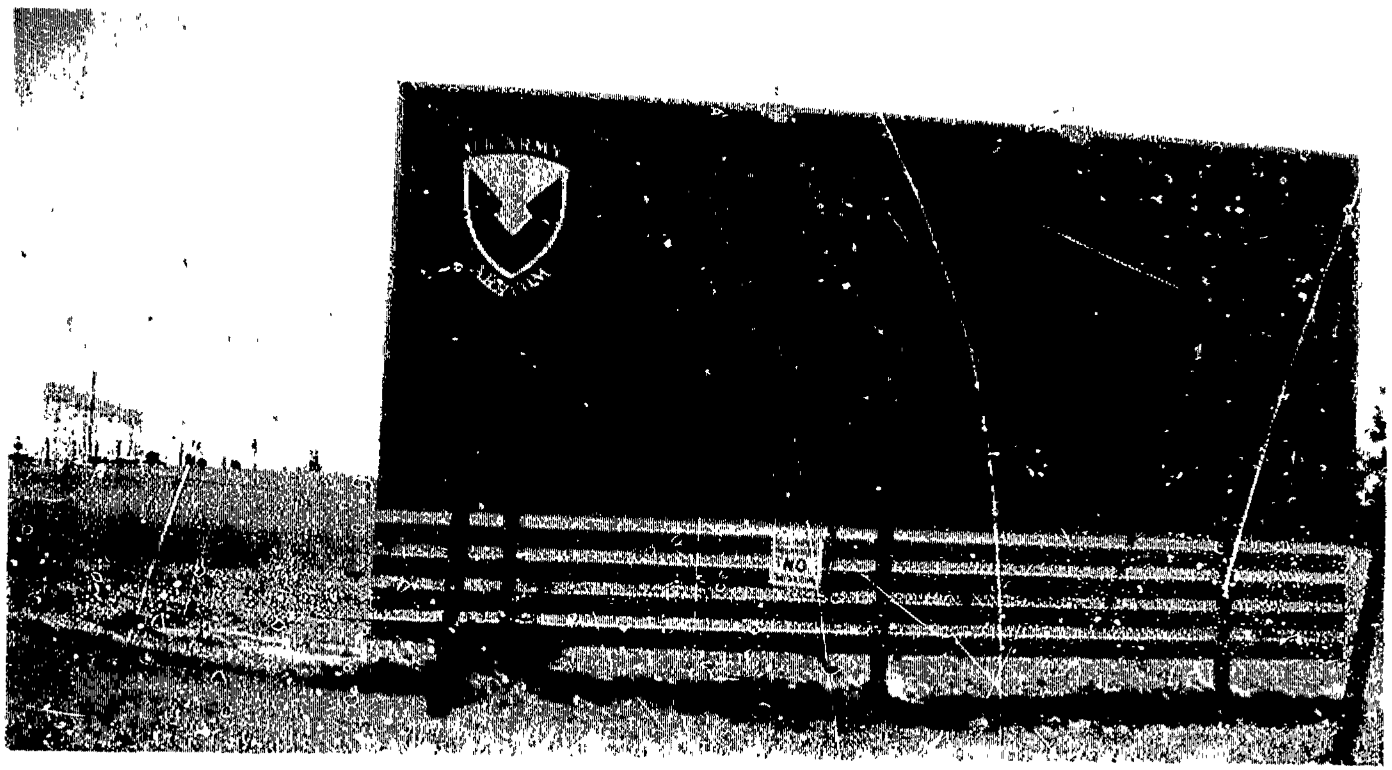

Sunflower Army Ammunition Plant, Constructed in the Early 1940's for the Purpose of Maufacturing Tank and Rocket Propellants.

Acid Scale House, Boiling Tub House, and Nitrator, C-Line

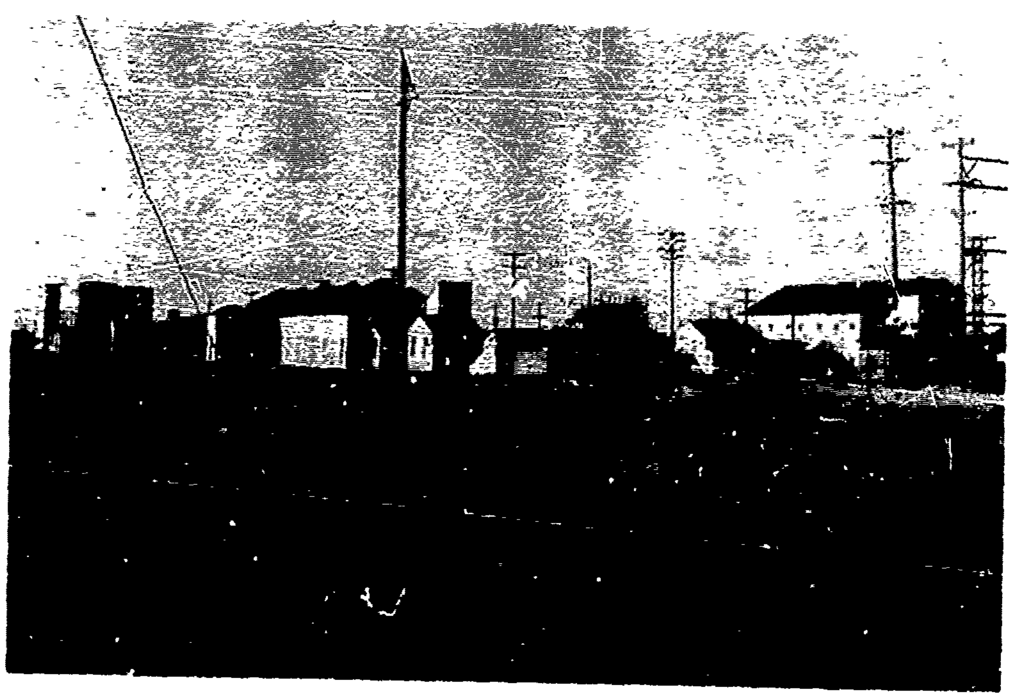

Final Wringer House, Dehydration Press House and Carbon Recovery House, B-Line

Boiling Tub House, Poach and Blend House, B-Line

Power House #2

Deterioration of "B" and "C" lines occurred over the years until it was decided in the early 1970's that the facilities should be disposed of to eliminate the unsightly and hazardous conditions they presented. Disposal was to include 143 uncontaminated and contaminated buildings and structures.

THE DISPOSAL PROJECT

Champney Wrecking Company of Topeka, Kansas started work on the 550 day disposal contract in October 1978. The contractor was later given a 240 day extension to complete the project. Prior to contract award, Champney Company had been approved by the ARRCOM safety office as qualified to perform disposal of the highly hazardous facilities. Approval was based on Champney's hiring of a retired plant operating contractor NC line supervisor to provide the expertise on the possible associated hazards.

Considerations throughout the various stages of the project included those associated to normal industrial hazards and NC hazards. The normal industrial safety concerns included: (1) proper use of protective clothing/equipment; (2) proper condition and operating of equipment; (3) proper procedures; etc. Considerations associated with NC hazards included: (1) the extreme sensitivity of dry NC to initiation by flame, impact, friction, etc; (2) delivering NC desensitizing water to possible locations of NC deposits; (3) gathering and disposing of NC; (4) decontamination of contaminated salvage materials; and (5) burning of contaminated facilities.

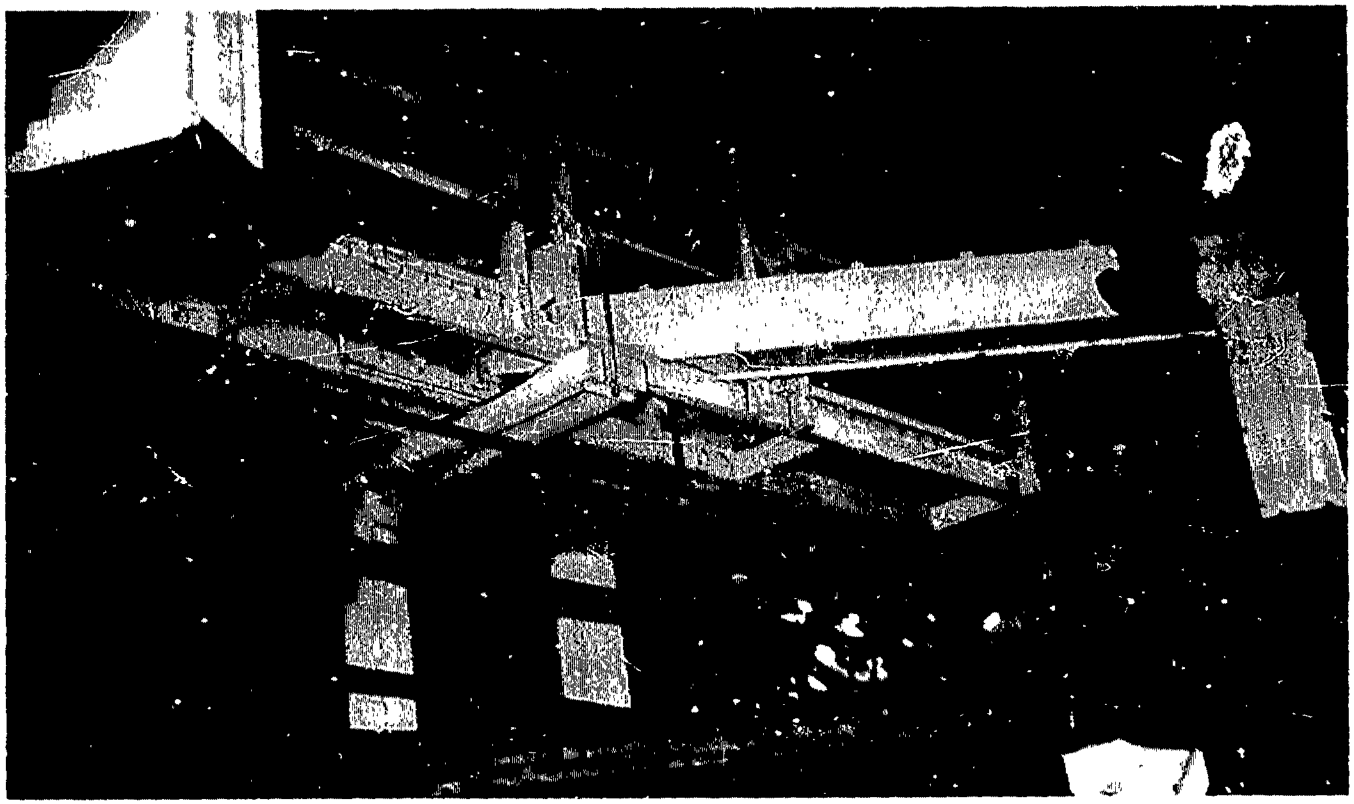

Nitrocellulose Process Fume Exhaust Ducts (Wood)

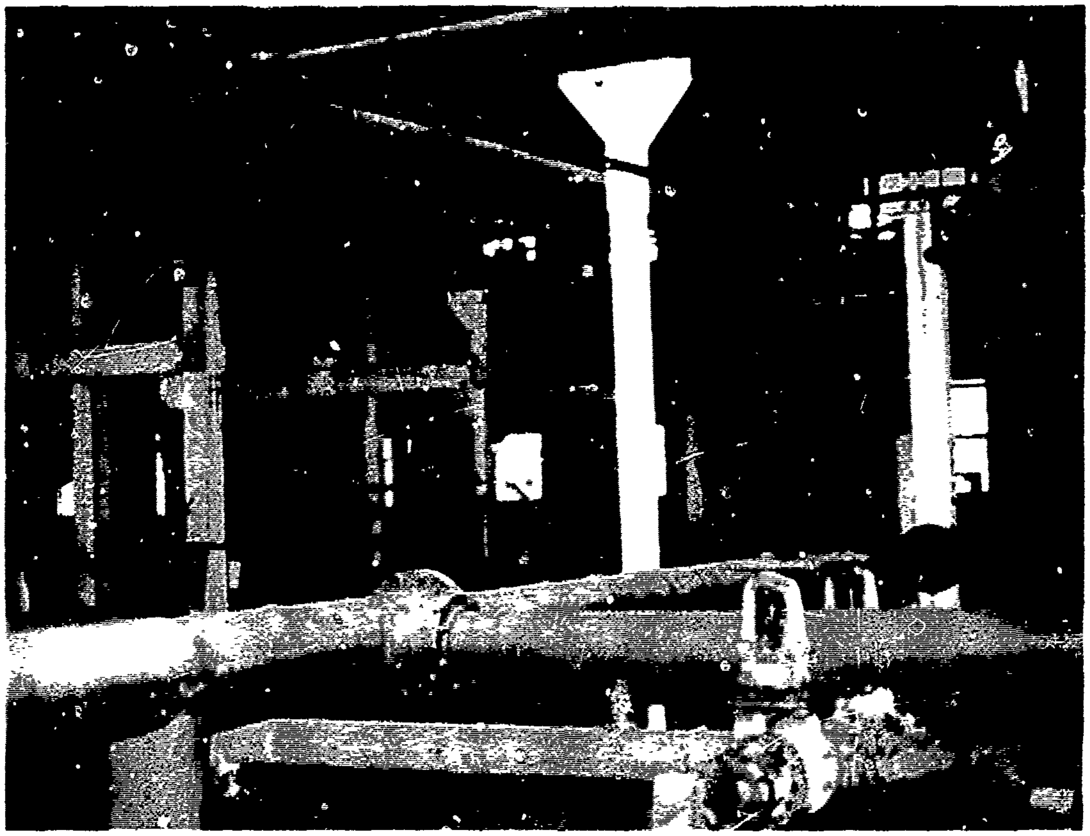

Water Lines (Top) and Nitrocellulose Process
Lines (Bottom), Poach and Blend House, B-Line

Ceiling of Poach and Blend House, C-Line

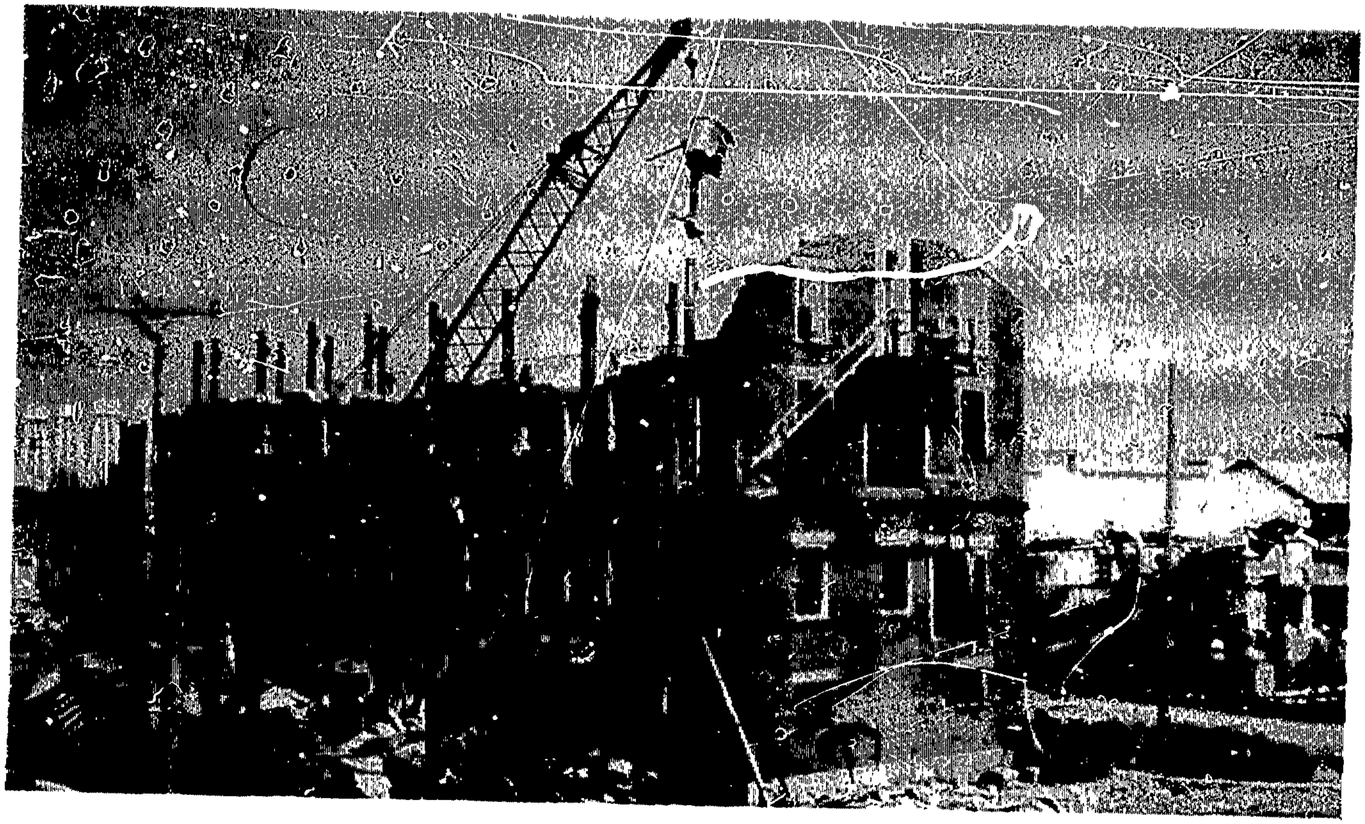

Removal of Stainless Steel Nitrating Tub from Nitrator, C-Line

There was a constant concern that the process facilities were contaminated with dry NC in unknown quantities at unknown locations. The key word in the preceeding sentence is "dry". NC is kept wet during its production in order to minimize its sensitivity; dry NC is extremely sensitive to flame, impact, friction, etc. The process lines had last been used over 30 years prior to the disposal project, so it was assumed that all remaining NC was dry, thus presenting an extreme hazard to disposal work.

Prior to starting the work in any of the contaminated structures, many hours were spent by the disposal contractor and his hired consultant inspecting the buildings. This practice provided the contractor an understanding of the process, which lines were most likely contaminated, and an overall knowledge of the extreme care required to avoid incident. One point stressed over and over was the criticality of thorough water wetting the possible locations of NC deposits, prior to heating, impacting, or moving anything at those locations. The disposal contractor also learned that the possible deposit locations included: (1) process pipes; (2) process vessels; (3) process building walls; (4) floors; or (5) sumps. Essentially anywhere in or around production buildings was suspect of holding NC.

Constant observation for deposits of NC was stressed before and during disposal work at each of several areas. On several occasions, the contractor found deposits of NC; generally, sufficient amounts of

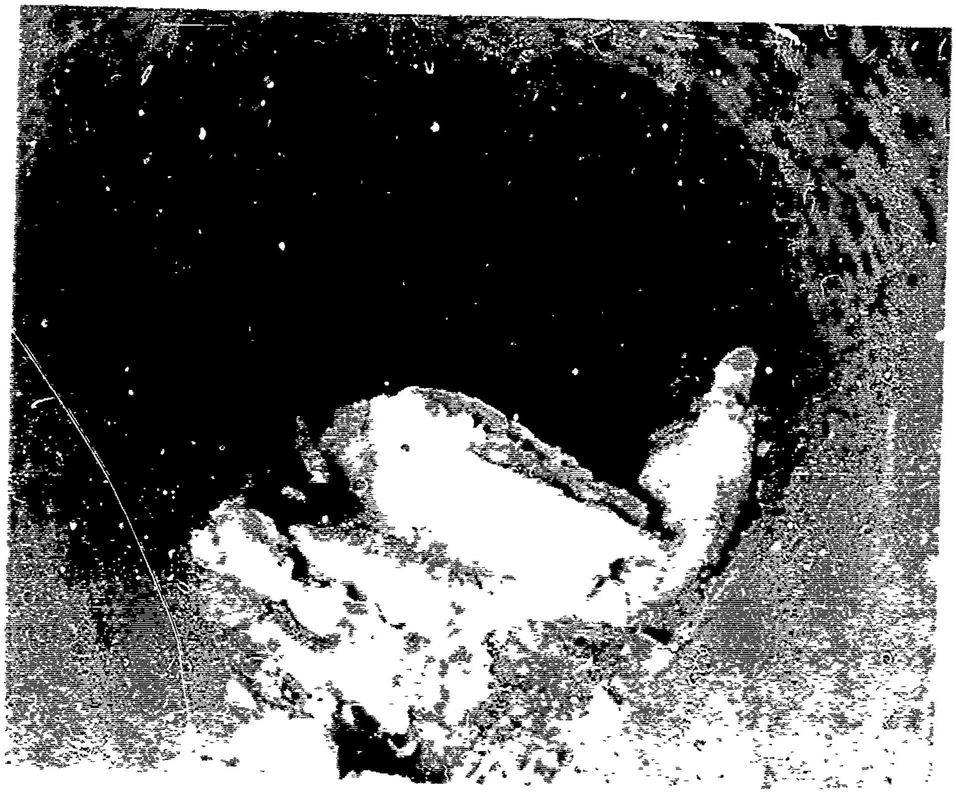

Residual Nitrocellulose Inside Process
Line, Final Wringer, B-Line

Nitrocellulose Contamination,
Column Section from Alcohol Still

water had already been delivered to the locations during preliminary wetting procedures. The plant operating contractor provided assistance by disposing of the NC found during the project.

Other considerations related to NC hazards involved scrap and salvage decontamination. The contract allowed the disposal contractor to sell 3X decontaminated materials to qualified buyers. Initially, a qualified buyer was considered anyone understanding the possible hazards associated with 3X items. Later it was determined that all contaminated salvage had to be decontaminated to a 5X level unless sold to a buyer who was in the explosives manufacturing business. Decontamination to a 5X level was attained by exposing the material to fire, such that any residual NC was burned off.

Contaminated wooden structures were burned at their locations. Considerations made for burning contaminated facilities included: (1) fire protection - fire truck placement, operable fire hydrants, placement of fire hoses, placement of water curtains; (2) utilities - turn off area electrical and gas lines; (3) security - provide road blocks to the area; (4) maintenance of fire watch stand-off at 1,000 feet; (5) clear workers from the area, or burn on weekends; (6) supervision at the burn site - coordination between plant fire chief and disposal contractor; (7) determine means to safely ignite building fires - straw and oil fuse trains worked well; (8) contact off plant fire dispatchers to inform them of the burns; and (8) contact the state air quality office prior to burns.

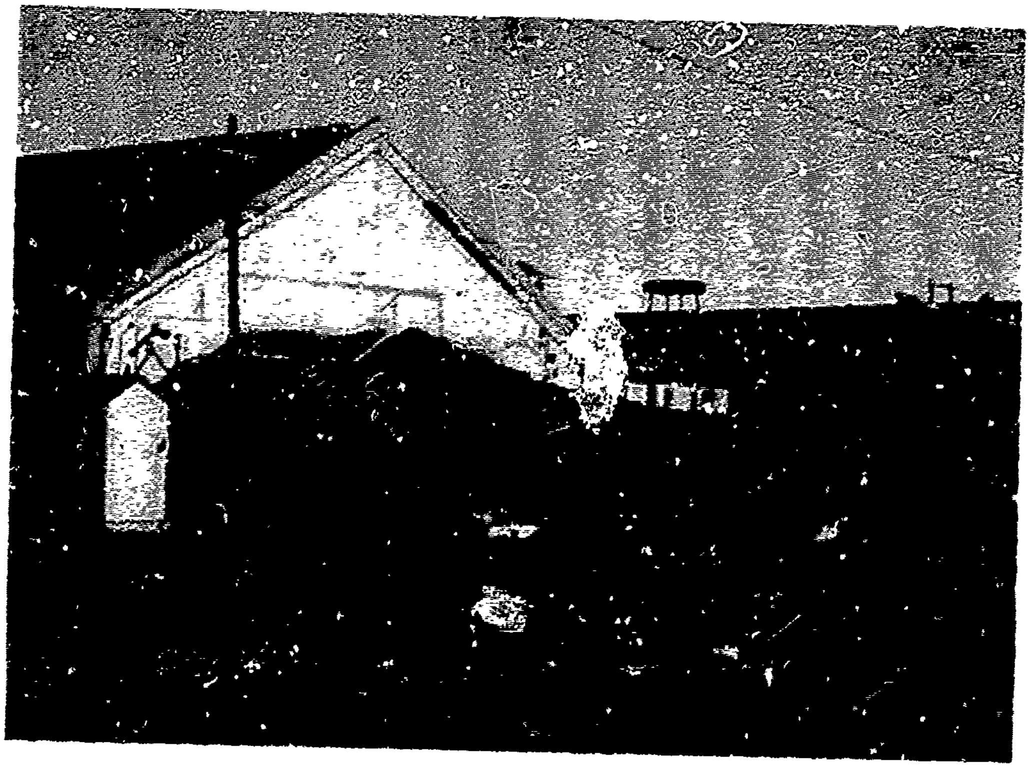

Boiling Tub House C-Line, Partially
Collapsed in Preparation for Burning

Still House Prepared for Burning

Fuel Oil and Straw Used as a Fuse Train to Ignite Building Rubble

Preparation of Fuse Train Prior to Burning Building Rubble

Burning of Poach and Blend House, Beater House, and Boiling Tub House, C-Line (Notice Water Curtain Set to Protect Steamline, right side).

Burning of Final Wringer and Dehydration Press House, C-Line. Snow cover helps Provide Fire Protection to Surrounding Buildings

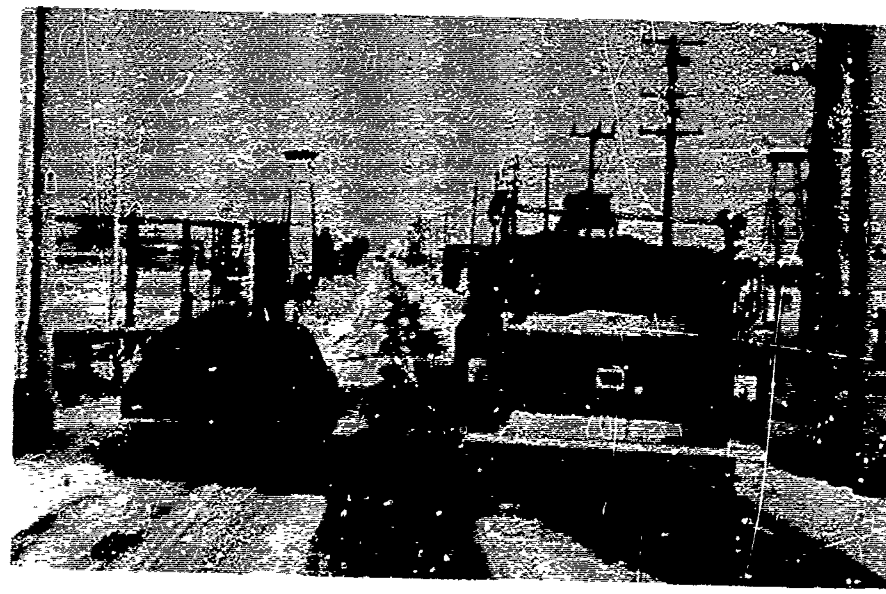

Fire Watch During Building Burn

Remains After Burn, B-Line

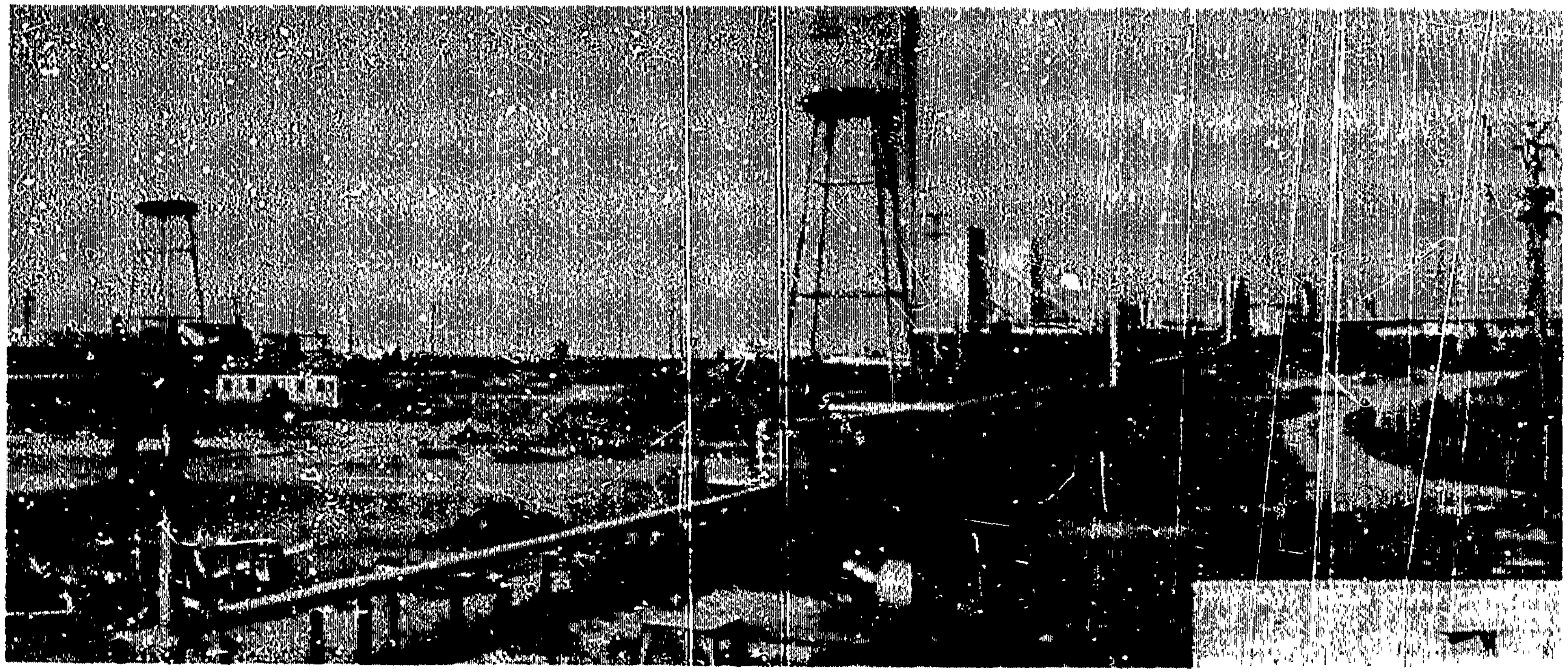

B and C Lines after Burns and Partial Cleanup

EXPLOSIVE INCIDENTS

There were occasions in which water had not been adequately delivered to depositied NC; subsequently the NC was ignited. Two minor incidents occurred in process pipes where the contractor thought adequate water had been delivered. In one case, sparks from a cutting torch operation fell into an open flange igniting NC located at a low spot in the process line. In another case, friction caused by a "T" connection breaking apart ignited NC deposited at the "T". No injury or damage resulted from these incidents.

A third incident occurred when a larger amount of NC was ignited by friction created during slight movement of a process line which ran between two process buildings. In this case, approximately 15 feet of 10 inch pipe were shattered just inside one of the buildings. No personnel were inside the building and the operator of the tractor which had moved the pipe was uninjured. An oversight by the tractor operator was due to his understanding that process lines were green or white. The pipe he moved was black between the buildings, but was green inside the buildings. Failure to verify the color inside the buildings was a serious error which fortunately caused no loss.

Another incident, very serious in nature, occurred when an alcohol storage tank exploded. It resulted in one death and one serious injury. An in-depth accident investigation was headed by LT COL Fritz Friant of Lake City Army Ammunition Plant. Authority to release the contents of the investigation report had not been received at the time of this writing.

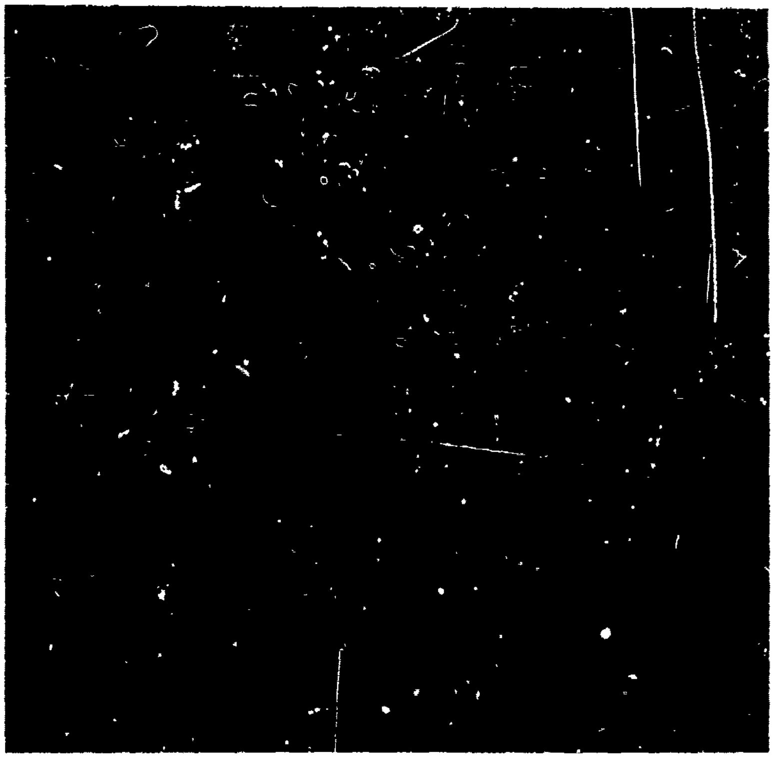

Fragments and Points of Impact, due to Pipe
Explosion, Poach and Blend House, C-Line

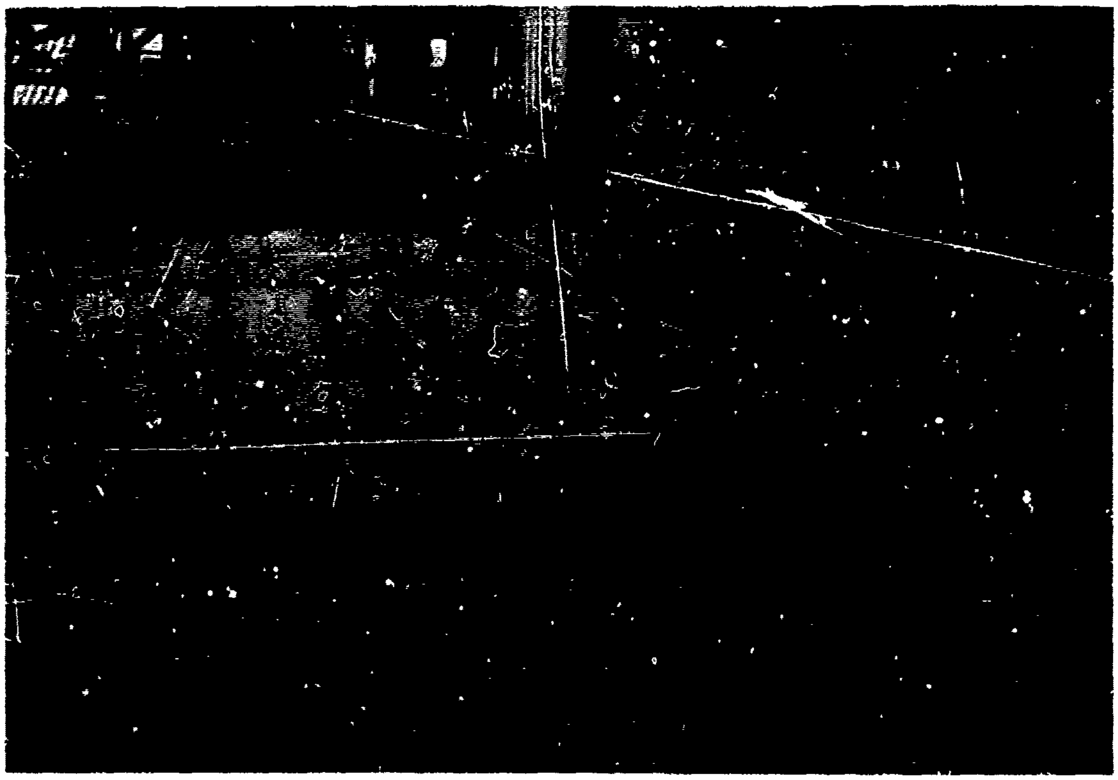

Results of Alcohol Storage Tank Explosion

CONCLUSION

The disposal of 143 contaminated and uncontaminated structures at Sunflower Army Ammunition Plant was a highly hazardous project. This was demonstrated by the fact that many pounds of nitrocellulose were found at various locations throughout the contaminated structures. Many other hazards were recognized and safely avoided or eliminated, yet accidental explosions occurred. Hopefully, through the considerations made and the lessons learned during this project, similar incidents will be avoided in future disposals of contaminated facilities.

FACILITIES DISPOSAL PROJECT

143 Buildings/Structures

Uncontaminated Buildings/Structures

- offices
- utilities
- water towers
- cotton/pulp storage
- cotton/pulp dryhouses
- latrines
- shops
- chemical storage
- railroad
- carbon recovery houses
- boiler house

Contaminated Buildings/Structures

Nitrators	NC rest houses
Catch tank houses	Pack houses
Boiling tub houses	Tray storage houses
Poacher & blender houses	Acid screen houses
Beater houses	Fume stacks
Settling pits	Alcohol still
Acid mix & weigh houses	Storage tanks
Final wringer houses	Acid lines
Dehydration houses	Acid sewers

SAFETY CONSIDERATIONS

(1) Normal Industrial Hazards

(2) Nitrocellulose Hazards

SAFETY CONSIDERATIONS ASSOCIATED
TO INDUSTRIAL HAZARDS

(1) Use of proper protective clothing/equipment

(2) Condition and operation of equipment

(3) Asbestos control

(4) Proper procedures

SAFETY CONSIDERATIONS ASSOCIATED TO NITROCELLULOSE HAZARDS

(1) Dry Nitrocellulose is explosive and very sensitive to initiation by impact, flame, friction, etc.

(2) Information sources - consultant, plant operating contractor, regulations, etc.

(3) Deliver water to possible locations of NC before applying possible source of ignition.

(4) Gather and dispose of NC.

(5) Decontamination of materials removed - 3X or 5X.

(6) Burn remains of contaminated facilities.

BURN OF CONTAMINATED FACILITIES
Plan & Coordinate:

(1) Fire protection -

fire trucks
water available
hoses laid
water curtains

(2) Utilities in area -

gas, electric off

(3) Security -

road blocks

(4) Stand off -

1000 feet for fire watches & fire trucks

(5) Workers in area -

Clear or burn on weekends

(6) Supervisors at burn site -

Fire chief and disposal contractor

(7) Setting fire -

Fuze train - oil & straw

(8) Contact outside offices -

Area fire dispatchers
State air quality

MOUND FACILITY EXPLOSIVES INCINERATOR

J. L. Harrison
F. D. Lonadier
G. R. Wirth

Mound Facility*
Miamisburg, Ohio 45342

Restrictions on open burning created the need for modifying Mound Facility's capabilities for disposal of explosives. To facilitate efficient control of high-volume waste material, especially low weight powders, the incinerator unit shown in Figure 1 was purchased. Each unit costs less than $1,000. Drum configuration, location of the air injection port, and velocity of the air (70 CFM) create a cyclonical flow pattern within the drum. High O_2 availability permits complete combustion, which eliminates the need for afterburners or stack scrubbers.

In-house modifications include a water cooling jacket, high-temperature air feed hose, and a modified drum bottom. The water jacket and flat bottomed drum permit partial control of the burning temperature. This, in turn, lowers the possiblity of a damaging detonation. Careful segregation of the materials being burned is also mandated to reduce detonation possibilities. As an additional safety precaution, all burns are conducted in a cubicle designed to withstand detonations of up to 40 pounds of explosives.

*Mound Facility is operated by Monsanto Research Corporation for the U.S. Department of Energy under Contract No. DE-AC04-76-DP00053.

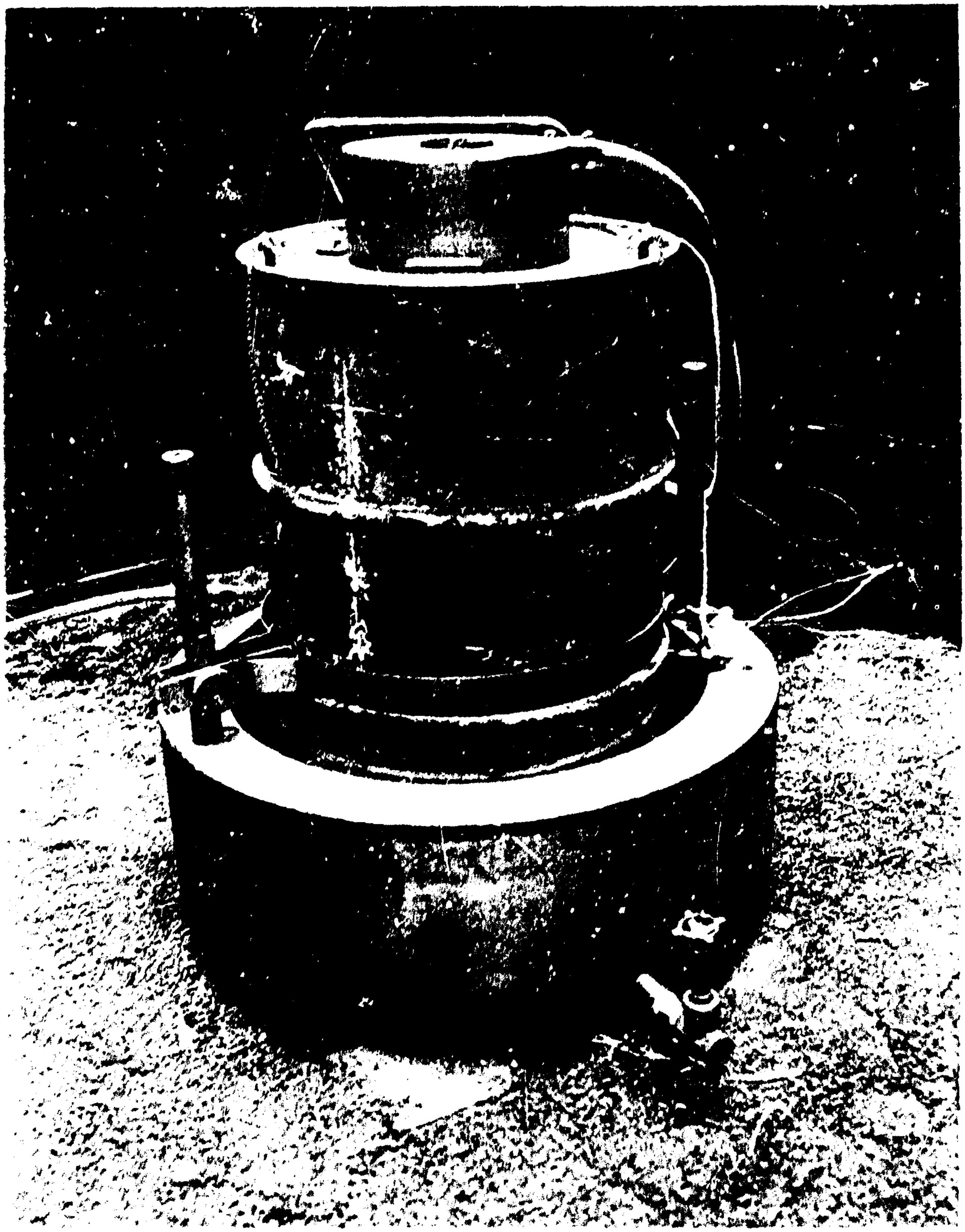

FIGURE 1 - EXPLOSIVES INCINERATOR IN PLACE

At the present time, Mound is using its third incinerator. The first two units were destroyed while completing development studies. The initial incinerator featured a small-volume drum (30 gal) as the burn chamber. This drum was placed in a water-filled pit which was dug in the sand floor of the cubicle. The pit was lined with commercial visqueen plastic and contained 30 gal of water. Three 1/2-in. steel cables anchored the incinerator to the cubicle walls. During burning operations, a hole developed in the plastic liner. The resultant loss of the heat sink effect allowed detonation to occur. Examination of a bottom piece of the incinerator barrel indicated that when the burning powder reached an area of the barrel with poor chilling characteristics, sufficient heat was generated and retained to initiate detonation. Although some debris left the cubicle, no damage occurred as a result.

The second development incinerator unit, shown in Figure 2, utilized a 55-gal drum as the burning chamber. The water jacket for this unit also contained 33 gal of water. Ethylene glycol was added for winter use. The second incinerator was utilized to develop procedures for burning trash in addition to powders. Fifty-two burns were completed in this incinerator before an improperly mixed load of explosives detonated during the burn cycle. The load consisted of 5 pounds of bulk powder on the bottom of the durm, excelsior to the top of the drum, and three broken detonators placed in the middle of the excelsior. Rapid burning at the trash-drum interface,

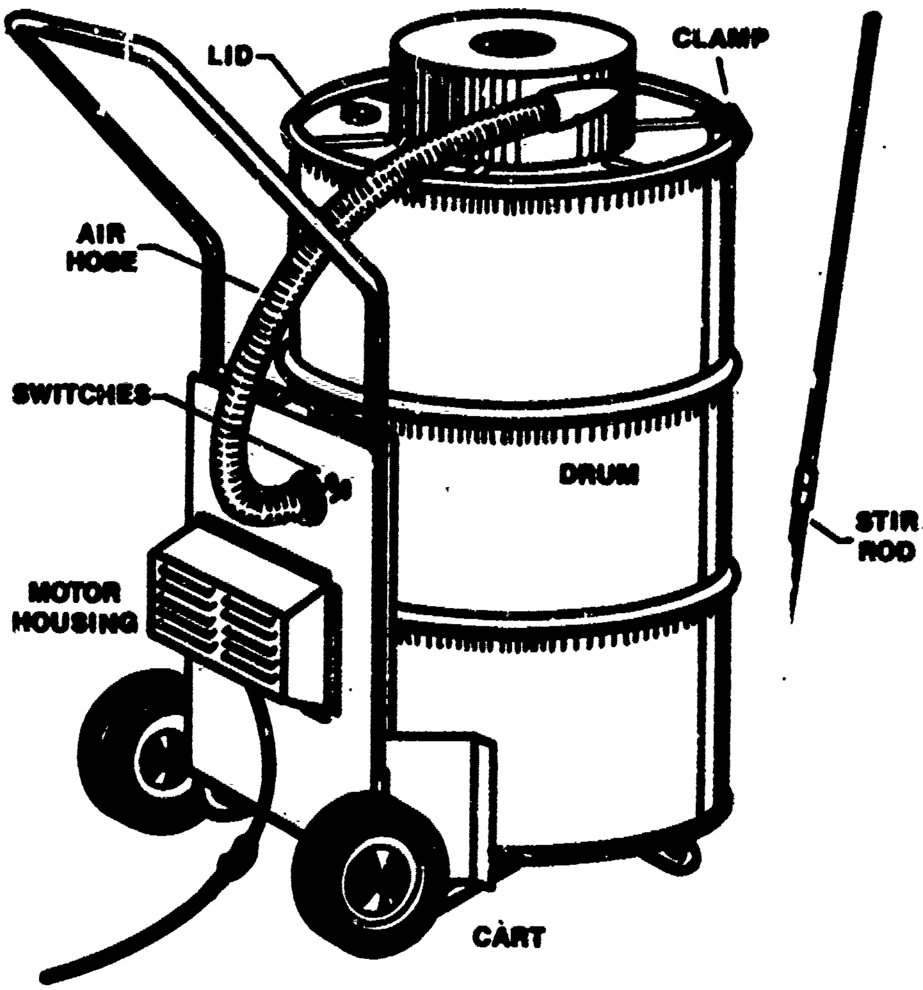

FIGURE 2 - AIR POWERED INCINERATOR

created by the air flow injected (70 CFM) in a circular pattern, reduces the trash to a cone-shaped configuration. The synergistic effect of placing the detonators in the center of the drum, of the cyclonical air flow, and of the uneven surface combustion, permitted the detonators to drop into the bulk powder where they obtained the energy needed for detonation. In this incident, the water jacket cushioned the blast, and very little debris left the cubicle. No damage related to the debris occurred outside the cubicle.

The production incinerator now in use is identical, with the exception of a modified drum bottom to the second development incinerator. The complete-combustion, low-pollution burns permit daily usage except during air alerts. These burns ($\sim$six burns/day) permit control of large-volume trash and low-weight scrap powder. Only one low-level detonation has occurred during the several production burns made with this unit. In this incident, the top was blown off the barrel but completely retained inside the cubicle. The incident occurred during the flashing of some inert units, and while it damaged the incinerator top, which is attached with three small spring clamps, no debris left the cubicle. The bent drum top was discarded.

Careful segregation and weight/volume restrictions placed on each burn provide a degree of safety against detonations. The low cost, clean burning characteristics of this incinerator have provided Mound Facility with a flexible, efficient explosives disposal unit.

STRUCTURAL RELIABILITY OF NAVFAC P-397 DESIGNS

By

J. E. Tancreto
Civil Engineering Laboratory
Naval Construction Battalion Center
Port Hueneme, CA

INTRODUCTION

A new approach to explosive safety, using risk analysis, is beginning to gain acceptance within the DOD community. For this type of analysis a determination of the structural reliability of protective structures is required. Deterministic design and analysis procedures, now in use, do not provide quantitative measures of the structural reliability nor do they result in consistent safety for each structure. Probabilistic methods allow for consideration of the uncertainties in the analysis procedures, material properties, and failure criteria to arrive at an estimate of the structural reliability (probability of a given damage level). These methods can also be used to establish design criteria that will result in structures with consistent reliability. The most cost effective structure, providing a given level of safety, and the most beneficial use of funds can also be determined.

This paper demonstrates a method for determining the probability of failure (one measure of reliability) of one-way reinforced concrete flexural elements designed with NAVFAC P-397 (Reference 1) criteria. A monte carlo simulation was used to consider the uncertainties in material properties, structural resistance, blast loads, structural response and failure deflection. Although realistic values were chosen for the analysis, the paper is only intended to demonstrate the uses of probabilistic methods for analysis and design applications.

BACKGROUND

The Naval Facilities Engineering Command (NAVFAC) has established the Navy Explosives Safety Facilities (NESF) project to develop a method for choosing the optimum procedure for mitigating safety problems. This program includes the development of a risk decision model (NOHARM) to quantify and predict hazards and risks and to evaluate risk mitigation procedures. The monte carlo simulation, described in this report, is being developed for use in NOHARM to predict damage and to evaluate risk mitigation procedures.

OBJECTIVES

The objectives of this study are:

1. To establish a procedure for quantifying the reliability of structural elements to respond within a given performance level under blast loadings.

2. To demonstrate the procedure by calculating the probability of failure (P(F)) of selected one-way structural elements designed with NAVFAC P-397 criteria.

3. To determine the probability of failure as a function of key design parameters.

4. To demonstrate the use of the P(F) function for establishing design criteria that will provide consistent levels of safety in design.

ANALYSIS PROCEDURE

Representative one-way beams, with design parameters covering a wide range of typical values, were chosen and deterministic P-397 criteria were used to establish allowable design loads. Average values and corresponding uncertainties in material properties, loads, and structural response were established and used in monte carlo simulations to determine actual response probability density functions. The response function was compared to a failure deflection function, determined from test data, to establish the P(F) of each beam.

Beam Design Parameters. Beam parameters that were varied were the length (10' to 30'), the thickness (15" to 25") and the steel percentage ($p = p'$ = 0.25% to 2.0%). Concrete cover was assumed to be 2" top and bottom (surface to steel rebar centerline). Laced and unlaced beams, having different failure criteria, were analyzed. The failure support rotation for a laced beam, using P-397 criteria, is 12^{o} whereas it is 2^{o} for an unlaced beam. In order to use available test data on failure criteria, the laced beam was also assumed to be laterally (but not rotationally) restrained at the supports. Figure 1 summarizes the range of structural parameters varied in this study.

Deterministic Design. Deterministic criteria from NAVFAC P-397 were used to obtain the allowable design triangular load function. The elasto-plastic resistance deflection function was first determined for each beam from standard ultimate moment capacity and stiffness relationships. Material properties for the deterministic designs are shown in Table 1. The allowable ductility ratio (maximum deflection/elastic deflection limit = X_m/X_E) was established using the P-397 failure criteria (Equation 1) for the applicable support rotation (either 2^{o} or 12^{o} in the sample problems).

$$X_m = \frac{L}{2} \tan \theta \qquad \text{Equation 1}$$

A single-degree-of-freedom design chart for a spring-mass system responding elasto-plastically was then used to obtain the peak design triangular pressure load at duration to natural period ratios (T/T_N) of 0.1, 1.0, and 10.0. A family of beams and associated allowable design loads were thus generated using the deterministic procedures in NAVFAC P-397. Figure 2 illustrates the load and resistance functions and shows the range of response parameters that resulted.

Probabilistic Analysis. A probabilistic analysis requires data on the distribution of values for material properties, response relationships, and loads. Data on material properties in references 2, 3 and 4 were used to obtain the estimated mean strength and corresponding coefficient of variations listed in Table 2.

Resistance values, r_u, are underestimated using standard yield moment relationships. Data in reference 5 were used to determine values for C_r in Equation 2 to obtain a mean estimate of resistance.

$$\bar{r}_u = C_r r_u \qquad \text{Equation 2}$$

with

$$\bar{C}_r = 1.15, \ \Omega_c = 0.15$$

Loading functions, determined in the P-397 design, reflect a 1.2 safety factor on the charge weight. The mean loading values for the probabilistic design must be based on the actual charge weight. The change in pressure and impulse from changes in charge weight (dP/dW and di/dW) were determined from relationships plotted in Reference 1. Equation 3 was used to relate changes in impulse to changes in duration.

$$T = 2i/B \qquad \text{Equation 3}$$

Equations 4 and 5, and Table 3 show the corrections required to obtain the actual mean loading function.

$$\overline{B} = C_p B \qquad \text{Equation 4}$$

$$\overline{T} \approx C_T T \qquad \text{Equation 5}$$

A coefficient of variation of 0.20, commonly used in blast load probability studies, was used with the mean estimate of peak pressure, $\overline{B}$, to account for uncertainties in the loading function.

Response of the structures was determined with a Newmark Beta iterative procedure (Reference 6) with $\beta = 0.25$. $\overline{X}_m$ and ΩX_m were calculated from the results of a monte carlo simulation assuming normal distributions for all of the variables. The failure deflection for a one way laterally restrained beam was taken from Reference 7 and is shown in Equation 6.

$$\overline{X}_{ur} = 0.14L \ (\Omega = 0.20) \qquad \text{Equation 6}$$

The failure deflection of a simply supported beam, without lacing or lateral restraint and with $p \approx p'$, was determined from data in reference 8. The relationship is shown in equation 7.

$$\overline{X}_{us} = 0.035L \ (\Omega = 0.20) \qquad \text{Equation 7}$$

Figure 3 shows the relationships for P(F) in terms of the probability density functions for X_m and X_u. If the distributions are log-normal equation 8 may be used for determining the P(F).

$$P(F) = 1 - \phi \left[\beta\right] \qquad \text{Equation 8}$$

where,

ϕ = Cumulative Normal Probability

$$\beta = \text{Safety Index} = \frac{\ln (\tilde{X}_u/\tilde{X}_m)}{(\Omega^2_{X_u} + \Omega^2_{X_m})^{1/2}}$$

Median deflection values ($\tilde{X}_u$ and $\tilde{X}_m$) are required for calculation of P(F) from log-normal distributions.

A monte carlo simulation does not require assumptions on the deflection distributions; however, large numbers of simulations are required to determine small P(F)'s. In a monte carlo calculation for P(F), each X_m is compared to an X_u value randomly selected from the prescribed distribution of failure deflections. The P(F) is calculated from the ratio of number of failures to number of simulations. If the P(F) is 0.001, more than 1000 simulations would be required to obtain that value. However, if the distributions are approximately log-normal, 100 simulations would adequately provide median values and corresponding coefficients of variation (C.O.V.) for use in equation 8.

RESULTS

Design $\theta = 12^{o}$. A laced one-way simply-supported flexural structure may be designed for 12^{o} rotation at the supports using criteria in NAVFAC P-397. Since failure deflection test data was available for a laterally restrained one-way beam, this restraint was also used in the demonstration problem. (A laterally restrained beam would not necessarily require lacing steel. See reference 7.) Figure 1 shows the beam support condition and range of geometry and steel parameters investigated. These design variations and the variation of duration to natural period (T/T_N), resulted in ductility ratios (X_m/X_E) and load ratios (B/r_u) within the ranges shown in Figure 2.

One hundred simulations were run in each monte carlo analysis of 31 beams. Best estimates of the actual mean values and coefficients of variation were used to describe normal distribution functions for the loads, material properties, and resistance function. Each simulation randomly chose values of each variable from its distribution function and calculated a response deflection X_m. Sample histograms for X_m are shown in Figures 4 and 5 for T/T_N of 0.1 and 10.0. Each response value, X_m, was compared to a randomly chosen failure deflection from the normal distribution described by Equation 6 and the corresponding Ω. The resulting distribution of X_u and X_u/X_m are also shown for a typical beam in Figures 4 and 5. The results shown are similar for each of the 31 beams investigated. The P(F) decreased from 7% to an average of 4% as T/T_N was increased from 0.1 (impulse load) to 10.0 (long duration load). The distribution of maximum deflections changed from being almost normally distributed at $T/T_N = 0.1$ to being highly skewed at $T/T_N = 10.0$. Comparison of the central values ($\bar{X}_m$ and $\tilde{X}_m$) show that the factors of safety inherent in the design result in a much greater mean deflection factor of safety $(\overline{X_u/X_m})$ for long duration loads than impulsive loads (15 vs. 2). The high uncertainty in response, for long duration loads, makes this a necessity for obtaining reasonbly consistent P(F)'s. NAVFAC P-397 criteria accomplish this with the 1.2 factor of safety on design charge weight. The P(F), however, still varies by a factor of 2 for this type of structural element. Table 4 shows the P(F) as a function of T/T_N as calculated in the monte carlo simulation and as calculated from an assumed log-normal distribution. T/T_N was the only parameter, of those listed in Figures 1 and 2, that had a significant effect on P(F), given the design requirements of NAVFAC P-397.

Design $\theta = 2^{o}$. An unlaced one-way simply supported structure may be designed for 2^{o} rotation at the supports using criteria in NAVFAC P-397. Failure deflection data from reference 8 (for p = p') were used to obtain equation 7 for the mean ultimate deflection. The monte-carlo simulation was run for each beam as described above for Design $\theta = 12^{o}$. Figures 1 and 2 show the support condition and range of parameters for the 2^{o} design.

Deflection values for the 2^{o} rotation (X_m and X_u) were, of course, smaller than in the 12^{o} design shown in Figures 4 and 5. Distributions, however, were similar with a normal shape at $T/T_N = 0.1$ and highly skewed results at $T/T_N = 10.0$. Since the ratio of X_u to $\tilde{X}_m$ was significantly greater for this design, the P(F) was much less than in the 12^{o} design. Because of the low P(F), values were calculated assuming a log-normal distribution using Equation 8. A monte carlo solution for P(F) would have required an unwarranted number of simulations. Results are shown in Table 5. This design criteria results in low P(F)'s which are greatly dependent on T/T_N. The P(F) under impulse loads is shown to be 350 times less than the P(F) under long duration loads. Consistent design criteria would result in essentially equal P(F)'s under all loading conditions.

These results also show that the P(F) for a 2^o failure criteria design is orders of magnitude lower than that for the 12^o failure criteria design. This can be a desirable result if one criterion is used for personnel shelters and the other is used for protecting equipment or explosives from damage.

DESIGN APPLICATION

Only recently have attempts been made to quantify structural reliability and to develop design criteria that result in structures of equal and acceptable reliability. (In this study reliability was measured by the P(F) since protection and not reusability is the first consideration in blast resistant design). Results of this study on elements designed by NAVFAC P-397 criteria indicate that the P(F) of one-way elements varies with the duration to natural period ratio (T/T_N). The P(F) of a laced one-way element is shown as a function of T/T_N and design deflection criterion in Figure 6. It can be seen that a constant P(F) could be obtained if the design deflection criterion was a function of T/T_N. For example, if a P(F) of 0.05 was the acceptable risk level, the design deflection criterion at T/T_N = 0.10 would be $\theta_D = 11^o$ (interpolating between curves on Figure 6); at T/T_N = 1.0, $\theta_D = 12^o$; at T/T_N = 10.0, $\theta_D = 14^o$.

Actually, the current design deflection criterion ($\theta_D = 12^o$) for the above example results in a relatively constant P(F) of between 4 and 7% and changes to obtain more consistency may not be warranted. However, the P(F) for the unlaced one-way element designed for 2^o rotation are highly inconsistent (see Table 5) and therefore should be equalized with a revision to the design criterion, such as varying the design deflection criteria as a function of T/T_N.

CONCLUSION

A probabilistic analysis procedure, using monte carlo simulation techniques, is being developed at CEL that will quantify the reliability of structures under blast loads. The results can be used to develop design criteria that will result in an acceptable and consistent level of risk. Risk quantification can also be used for determining the most beneficial use of available funds.

ACKNOWLEDGEMENTS

Mr. Joseph Holland developed the computer program, RISKQ, and Mr. Ray Gutierrez obtained the data used for this study. The author gratefully acknowledges the contributions by these members of the CEL staff.

REFERENCES

1. Army, Navy and Air Force, TM 5-1300/NAVFAC P-397/AFM 88-22: Structures to Resist the Effects of Accidental Explosions, Washington, D.C., June 1969.

2. University of Illinois, UILU-ENG-72-2008: A probabilistic Study of Safety Criteria for Design, by B. R. Ellingwood and A. H.-S. Ang, Urbana, Illinois, June 1972.

3. American Society of Civil Engineers, Journal of the Structures Division: Variability of Mechanical Properties of Reinforcing Bars, by S. Ali Mirza and G. MacGregor, May 1979.

4. Cornell University, NUREG/CR-1097: Safety Analysis of Nuclear Concrete Containment Structures, by P. Petrina, R. Sexsmith and R. N. White.

5. National Bureau of Standards, BSS-110: Reliability Basis of Load and Resistance Factors for Reinforced Concrete Design, by B. Ellingwood, Washington, D.C., Feb 1978.

6. ASCE Transactions, Paper No. 3384, Vol. 129, 1962, Part I, "A Method of Computation for Structural Dynamics", by N. M. Newmark.

7. Portland Cement Association, Construction Technology Laboratories: Design Criteria for Deflection of Conventionally Reinforced Concrete Slabs, Phase III - Summary of Design Criteria and Design and Construction Details - Design Examples, by T. Takayanagi and A. Derecho, Skokie, Ill., May 1980.

8. University of Illinois, DASA-1259: Investigation of Resistance and Deflection of Reinforced Concrete Members Subjected to Dynamic Loading. Part III by A. Feldman, W. A. Keenan, and C. P. Seiss, Urbana, IL, Feb 1962.

Table 1. Material Strength Properties for Deterministic Design.

Material* Property	Design Stresses (psi)	
	at $\Theta = 2^{o}$	at $\Theta = 12^{o}$
f_y	40000	40000
f_u	70000	70000
f_s	40000 1/	55000 2/
f_{ds} 3/	48000	66000
f'_c	3000	3000
$f_{dc'}$ 4/	3750	3750

*Reference 1 Rotation.

1/ $f_s = f_y$ at $\Theta \leq 2^{o}$

2/ $f_s = (f_y + f_u)/2$ at $\Theta > 5^{o}$

3/ f_{ds} = D.L.F. x f_s, D.L.F. = 1.2

4/ f'_{dc} = D.L.F. x f'_c, D.L.F. = 1.25

Table 2. Mean Strength Properties and Coefficients of Variation Used in Probabilistic Analysis.

Material Property	Design $\Theta = 2^\circ$		Design $\Theta = 12^\circ$	
	Strength (psi)	Coeff. of Variation	Strength (psi)	Coeff. of Variation
f_s	40,000		55,000	
$\overline{f}_s$	45,800	0.10	63,250	0.10
$\overline{f}_{dc}$	55,000	0.10	75,900	0.10
f'_c	3,000		3,000	
$\overline{f}'_c$	3,540	0.10	3,540	0.10
$\overline{f}'_{dc}$	4,425	0.10	4,425	0.10

Table 3. Factors for Determining Average Actual Loads from Design Loads.

Design Pressure P (psi)	C_p 1/	C_T 1/
P≤1	1.09	1.04
P=100	1.15	0.92
P≥1000	1.12	0.95

1/ Interpolate for C values when 1<P<1000 using power relationship ($C=aP^n$).

Table 4. P(F) for P-397 One-Way Simply Supported Laterally Restrained Structures. (Design $\theta = 12^o$)

T/T_N	P(F) 1/ 2/	
	Monte Carlo	Log-Normal
0.10	0.070 (0)	0.071 (0.18)
1.0	0.055 (0.09)	0.056 (0.14)
10.0	0.043 (0.11)	0.030 (0.17)

1/ Conditional P(F) given an explosion (i.e., P(F|E)).

2/ Mean value and Ω calculated from 31 values.

Table 5. P(F) for P-397 One-Way Simply-Supported Unlaced Structures. (Design $\theta = 2^o$)

T/T_N	P(F) 1/ 2/ Log-Normal
0.10	3.2×10^{-5} (0.47)
1.0	1.3×10^{-4} (0.57)
10.0	1.1×10^{-2} (0.56)

1/ Conditional P(F) given an explosion.

2/ Mean vlaue and Ω from 31 values.

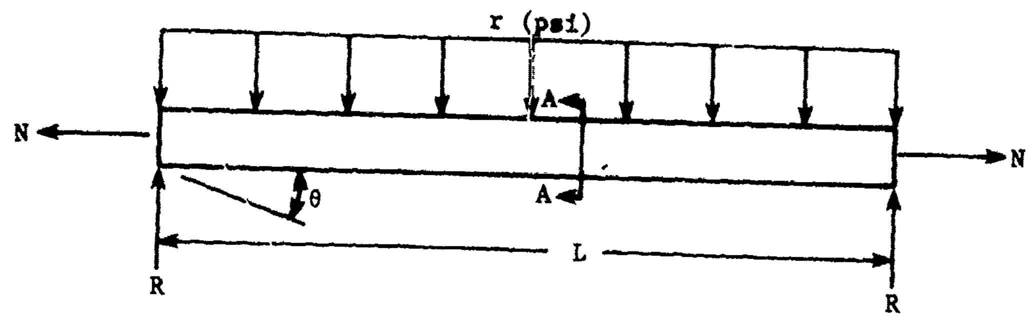

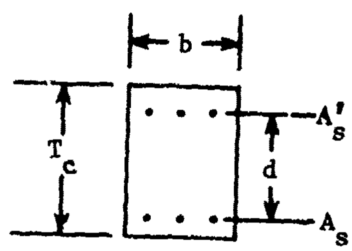

Section A-A

$$p = p' = \frac{A_s}{bd}$$

Range of Parameters

$10' \leq L \leq 30'$

$15'' \leq T_c \leq 25''$

$11'' \leq d \leq 21''$

$0.0025 \leq p \leq 0.02$

$\theta = 2^{\circ}$ $(N = 0)$

$\theta = 12^{\circ}$ $(N \neq 0)$

Figure 1. Beam geometry, support conditions, and range of parameters.

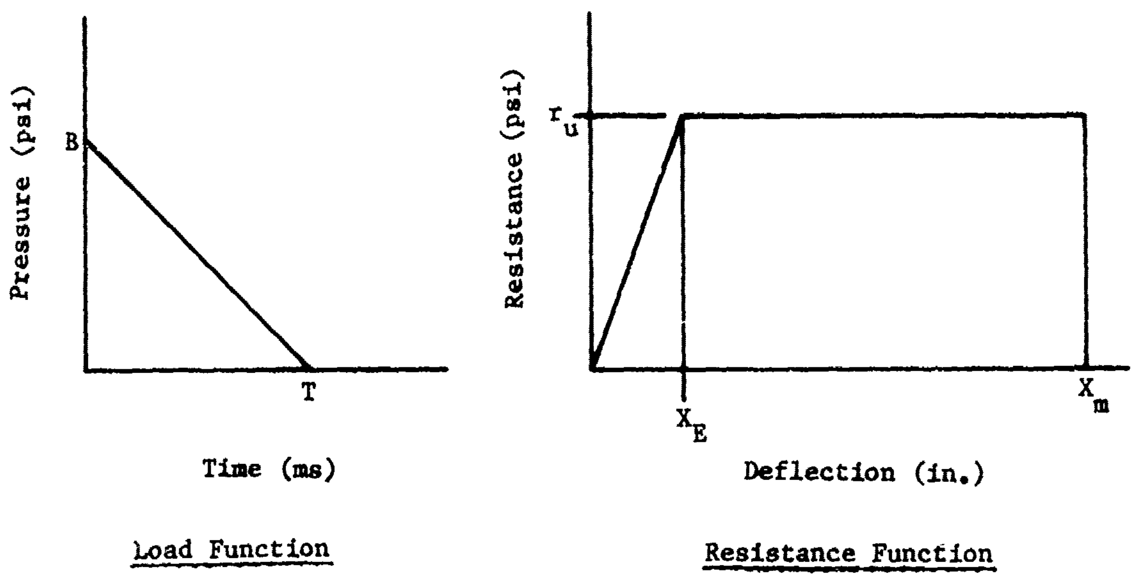

Range of Parameters

	$\theta_{DES} = 2^{o}$	$\theta_{DES} = 12^{o}$
T/T_N	0.1 - 10.0	0.1 - 10.0
X_m/X_E	2.9 - 60	13 - 130
B/r_u	0.85 - 35	1 - 50

Figure 2. Load and resistance functions and range of significant response parameters.

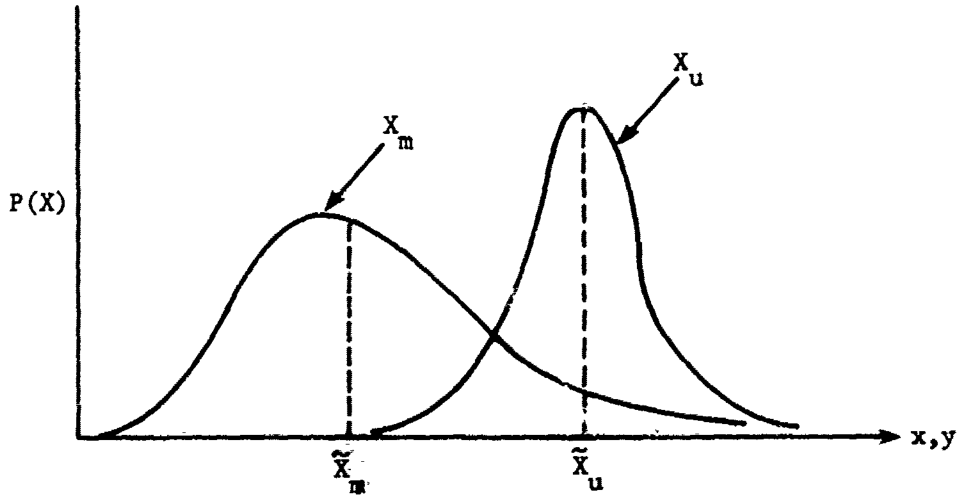

$P(X)$ = Probability of Deflection X

X_m = Maximum Response Deflection

X_u = Ultimate (Failure) Deflection

- Probability of Failure:

  $P(F) = P(X_m \geq X_u)$

- For Log-Normal Distribution:

  $P(F) = 1 - \Phi\,[\beta]$

  where β = Safety Index

$$\beta = \frac{\ln(\tilde{X}_u/\tilde{X}_m)}{(\Omega^2_{X_u} + \Omega^2_{X_m})^{1/2}}$$

- For any Distribution:

$$P(F) = \int_{-\infty}^{\infty}\int_{-\infty}^{x} X_u(y) \cdot X_m(x)\, dy dx$$

Figure 3. Probability of failure.

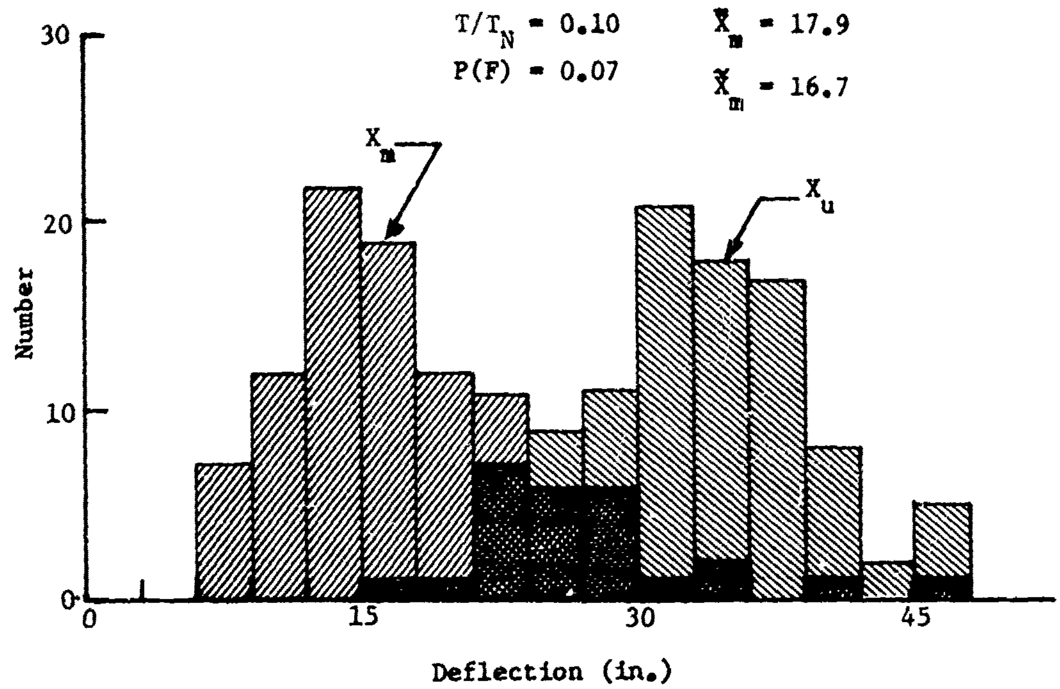

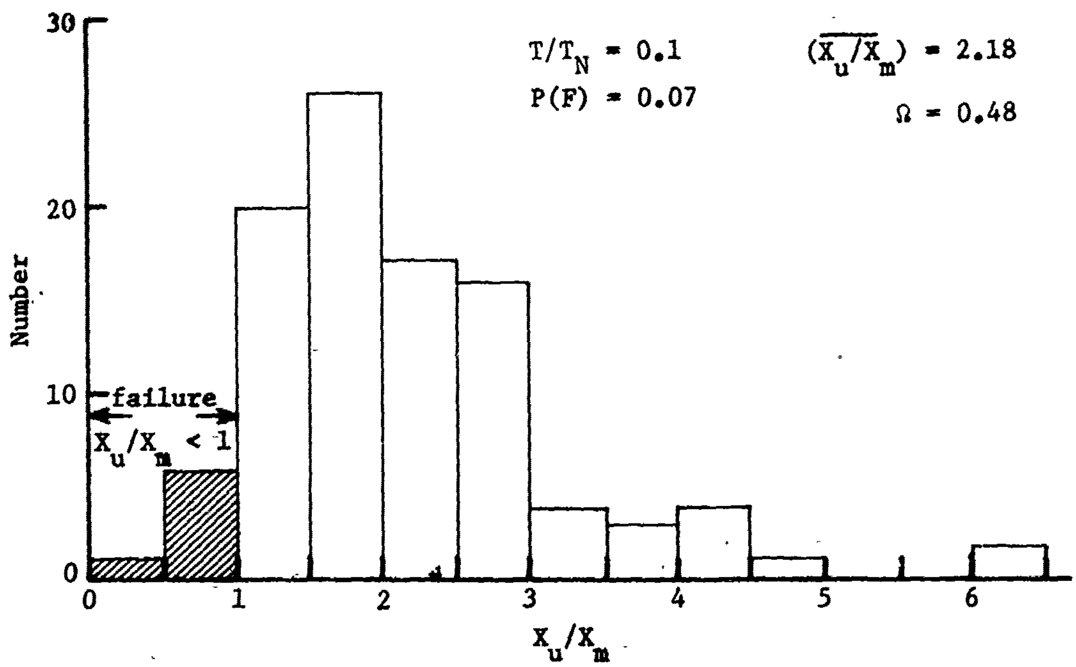

Figure 4. Response and ultimate deflection histograms and X_u/X_m histogram for T/Tn = 0.1 (design θ = 12°, L = 20', p = p' = 0.01, d = 11").

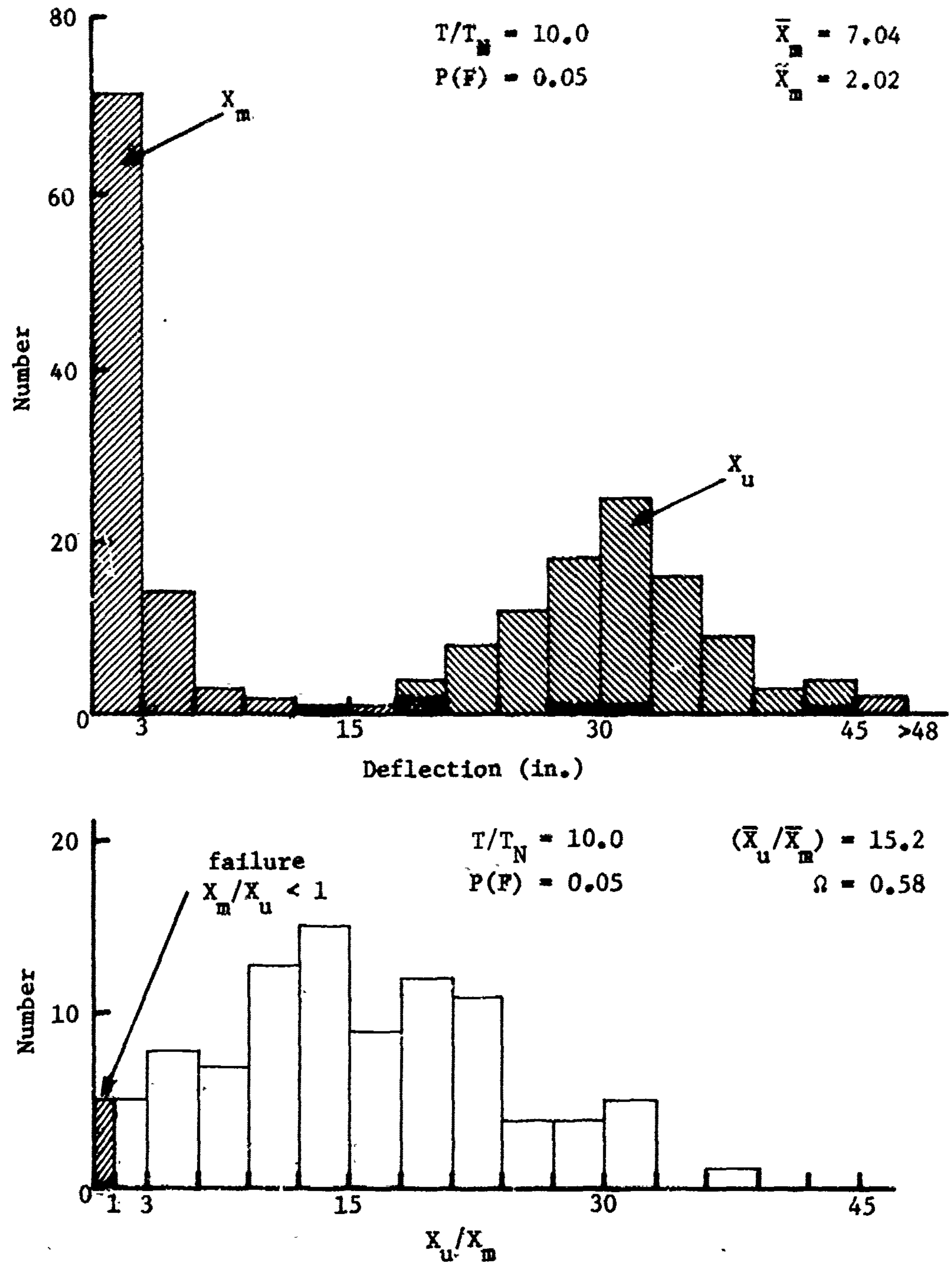

Figure 5. Response and ultimate deflection histograms and X_u/X_m histogram for $T/Tn = 10.0$ (design $\theta = 12^{\circ}$, $L = 20'$; $p = p' = 0.01$, and $d = 11''$).

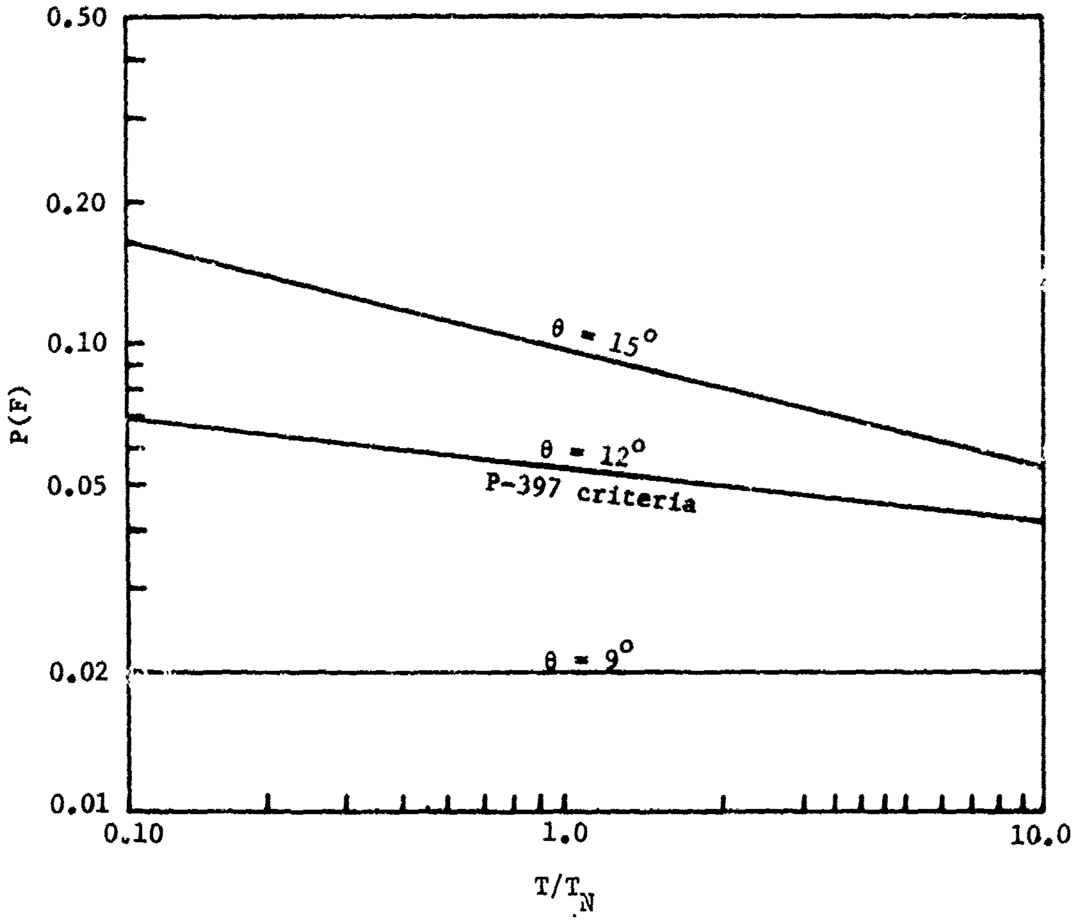

Figure 6. P(F) vs Design Deflection Criteria ($X_u' = (L/2) \tan\theta$).

FUNCTIONAL REQUIREMENT

AND

NEW AMMUNITION STORAGE CONCEPTS

Paul A. Howdyshell

Construction Engineering Research Laboratory

Champaign, Illinois

September 1980

I. INTRODUCTION

A. Background

Since the initial military utilization of explosives and ammunitions, their storage has been a major concern of the military. The Department of Defense Explosive Safety Board (DDESB) was established to develop safety standards for the storage of ammunition and explosives and to assure user compliance through design review and on-site surveillance. The Corps of Engineers and the Naval Facilities Engineering Command, in conjunction with the DDESB, have developed and tested a series of earth-covered arch magazines to empirically determine safe storage capacities, inter-magazine spacing, and distance criteria for occupied structures and public highways. The reinforced concrete and steel oval arch magazines that are currently specified and built are improved modifications of the World War II circular arch magazine. The oval arch magazines are not significantly different from the World War II circular arch magazines, other than the straight or bulging side walls and more slender concrete arches.

The Army's ammunition storage requirements have significantly expanded, particularly in Europe due to the Prepositioned Overseas Material Configured to Units Sets (POMCUS) program. Thus the construction and rehabilitation of ammunition storage facilities is a significant item in the Corps of Engineers construction budget. The 5-year (FY82-86) MCA construction plan, as of February 1980, calls for $200 million to be spent on ammunition facilities over the duration of the plan. Of this total, 1600 to 1700 new magazines are scheduled for construction at a cost of 20 to 30 million dollars.

Not only are ammunition storage facilities relatively cost intensive, they are also real estate intensive. This problem is particularly severe in Europe where most of the Army's expanded storage requirement exits. The lack of available real estate may soon impact construction schedules and significantly delay the completion of the POMCUS storage facilities.

B. Purpose and Scope

The objective of this work is to develop new and innovative ammunition storage facilities that are functional, life-cycle-cost effective, and have minimum real estate requirements. To accomplish the functional and real estate requirements, standard magazine design and cost are analyzed. Based on these findings, several alternative concepts are proposed and conceptual feasibility discussed. The study includes both the design of individual magazines and magazine layout alternatives that may provide a more effective trade between construction and real estate cost. Detailed designs and cost estimates are not made.

C. Technology Transfer

The information contained in this report on functional and real estate requirements has direct application to an OCE proposed Design Guide for Ammunition Storage Facilities. In addition, if any of the alternative concepts proposed herein prove feasible, they will impact AR 385-64, "Safety, Ammunition and Explosive Safety Standards;" DOD 5154.4S, "DOD Ammunition and Explosives Safety Standards;" and TM 9-1300-206, "Ammunition and Explosive Standards."

II. FUNCTIONAL REQUIREMENTS

The evaluation of ammunition storage functional requirements consisted of an analysis of existing procedures and documentation. In addition, further evaluation evolved from a meeting among representatives from DDESB, Army Ammunition Center and School, Office Chief of Engineers, and the Construction Engineering Research Laboratory (CERL). A follow-up letter summarizing the results of the meeting was prepared and distributed to each participating organization for review and comments. These results and findings have been divided into four major categories — safety, security, shelter, and operations — and are discussed as follows.

A. Safety Requirements

Ammunition storage facilities should provide for the protection of property, equipment, and personnel not immediately involved in ammunition handling. The protection is against blast, fragments, and fire due to an accidental ammunition detonation at a storage facility. It is specifically required that:

(1) an accidental detonation within one magazine not propagate detonations to adjacent storage magazines;

(2) protection is provided against injury from accidental explosions and related toxicity, to operations and maintenance personnel not directly handling the ammunition and to the public;

(3) protection which is provided prevents significant damage to occupied structures and public traffic routes due to blast, fragments, and fire associated with an accidental detonation at a storage facility.

In addition, safety requirements are intended to comply with the following standards:

(1) AR 385-64, "Safety, Ammunition and Explosive Safety Standards," March 1972.

(2) DOD 5154.4S, "DOD Ammunition and Explosives Safety Standards," January 1978.

(3) Manual AC/258 - D/258, "Manual on NATO Safety Principles in the Storage of Ammunition and Explosives," 1976.

(4) TM 9-1300-206, "Ammunition and Explosive Standards"

(5) DARCOMR 385-100, "Safety Manual"

Of the above standards, the best information on blast load design parameters for earth-covered magazines in found in Part II, Chapter 3, Section II of AC/258 - D/258. Technical Manual TM 5-1300, "Structures to Resist the Effects of Accidental Explosions," contains analysis information and procedures applicable to the design of blast-resistant structures. The scope of TM 5-1300 is restricted to blast loads less than 20,000 pounds net explosive weight (NEW).

B. Security Requirements

Ammunition storage facilities should provide for the prevention of loss of material and/or information to enemies, subversives, vandals, or indigenous animals. Security requirements should include the following.

(1) Stored material should be protected against damage from direct hits with small arms, and near misses with large arms.

(2) Stored material should be completely protected against damage from indigenous animals.

(3) The site should inhibit access to the stored material by intruders.

(4) There should be consistency in design to support the security requirement (no weak links); e.g., security systems will be integrated into the design.

(5) Storage facilities should have multiple access.

In addition, security requirements should comply with DOD 5100.76-M, "Security Requirements for Weapons, Ammunition and Explosives," 1979.

C. Shelter Requirements

Shelter requirements for ammunition storage are that long-term (20 years or more) and short-term preservation of the stored material is provided so that the material is usable when needed. Shelter requirements should include the following.

(1) The shelter should protect the material (and its packaging) from moisture-induced degradation.

(2) The shelter should protect the stored material from extreme temperatures and large time-temperature gradients.

(3) The shelter should protect its contents from natural catastrophies such as external fire, lightning, and high winds.

D. Operational Requirements

The operational requirements for ammunition storage facilities are the ability to move the material in and out of storage and the ability to perform required operation and maintenance on the material while in storage. Other specific operational requirements are as follows.

(1) The structure should be able to accommodate all types of explosives and ammunition.

(2) The structure should be designed to maximize storage efficiency. This should include (a) no interior beams or columns to interfere with storage operations and (b) ceiling heights over the entire floor area sufficient for a 16-foot stacking height.

(3) Doors should be large enough to accommodate the largest item stored and the equipment required to transport the item. They should be located to

minimize loss of storage space to fork lift operating areas and should be protected from foul weather interfering with their use.

(4) The interior of the structure should be of a light color, and lighting should be available and recessed. Ventilation should be sufficient to remove noxious fumes.

(5) Access roads should be all-weather and able to withstand the heaviest axle loads.

(6) Each structure should be provided with a hard surface area which will permit material-handling equipment to operate in and out of the structure and to and from the transport equipment with no obstructions/impediments.

III. ANALYSIS OF STANDARD MAGAZINES

A. Standard Magazines versus Functional Requirements

The Corps of Engineers currently has an inventory of four approved standard magazine designs. All four designs are earth-covered arches with a minimum of two feet of earth cover at the crown and massive reinforced concrete head walls. The older designs are circular arches and the newer are oval. Both reinforced concrete and corrugated steel arch barrels are approved. Nominal magazine dimensions are 25 feet wide with depths up to 100 feet. Depending on arch type, mid-span ceiling heights vary from approximately 12 to 15 feet.. Approved capacities for these standard magazines have been set at 500,000 pounds NEW.

The earth-covered arch magazines have been extensively tested under full-scale and model conditions to determine their safety characteristics and to establish a complex set of quantity-distance criteria for inter-magazine spacing, distance to occupied building, and public trafficway. The inter-magazine spacing is selected to prevent donor-receiver propagation of a full capacity detonation in the donor. The quanity-distance criteria for occupied buildings and public trafficways are based on the prevention of significant damage to the structure or vehicle (minor damage such as breakage of window glass is accepted and anticipated).

The four standard magazines are an integral part of the prescribed security requirements listed in DOD 5100.76-M. But the actual level of security provided by the structures is unknown and dependent upon the intrusion techniques employed. Thus, it is recognized that storage structures are only delay devices and are not intended to constitute complete security, unless supported by means to detect and assess intrusion and to nullify its effect. In addition to the standard magazines, security regulations normally require various combinations of barrier fences, intrusion detection systems, security lighting, and surveillance.

The existing family of standard magazines is most frequently criticized for failing to meet shelter requirements. Both the reinforced concrete and corrugated steel magazines have a long history of moisture migration and condensation problems. Many of the existing magazines leak either through bolt holes and lap joints in the corrugated steel arches or cracks in the concrete arches. Normal repair procedures for leaky magazines are to remove the earth cover and apply a one- or two-ply built-up roof membrane. Such repair procedures are effective but very expensive. Recent efforts have indicated interior patching may be a cost effective alternative if a high level of workmanship can be maintained.[1]

The condensation problems that occur in earth-covered magazines are much more difficult to control and can occur any time that the dew point of the circulating air is above the inside surface temperature of the structure. Under certain conditions the use of sprayed-on insulation may lessen the severity of the condensation by making the surface temperature of the structure more compatible with the circulating air temperature.

In addition to leakage and condensation problems, reports have been received about clogged and/or improperly designed french drains. As with any earth-covered structure, faulty or incorrectly designed drainage systems can be a major problem.

The earth-covered magazines also have several operational shortcomings. One, the basic arch shape is not an efficient storage shape. Ideally, storage structures should have straight, vertical side walls. Significant storage space is lost in the old circular arch magazines. In addition to the basic shape problem, many of the older magazines have doors that are too small for effective use of fork lifts or other loading equipment, and do not have hard surface areas immediately outside the door that are sufficient for effective loading and unloading of stored material.

Beyond these specific magazine deficiencies, many of the existing storage sites have inadequate access roads and other operational and security short-falls. But it should be remembered that the primary magazine design consideration has historically been safety, with the other functional requirements receiving only secondary consideration.

B. Economics of Conventional Magazine Construction

Construction and maintenance cost estimates on various standard magazines were developed as a baseline for comparing the cost effectiveness of new concepts. Table 1 contains the 1978-79 United States construction cost for the four standard Corps magazines. In addition to the U. S. construction cost estimates, Table 1 also contains cost estimates for a European version of the concrete oval arch. The European estimates are significantly less than the equivalent U. S. estimates but are based on quotes for 30 or more structures per construction site. A major proportion of the cost difference is associated with the effective and efficient utilization of reusable concrete forms.

Table 1 indicates that per square foot construction cost for ammunition storage is high, but adversely, Table 2 indicates that real property maintenance for ammunition storage facilities is significantly less than that for military buildings in general.

Besides the total cost of the various magazines, Table 1 indicates that the cost of the magazine barrel for a standard 80-foot magazine is about one-third of the cost of the entire structure. Thus, efforts directed at reducing the cost of the arch barrel per se have only a minor impact on the cost of the entire magazine.

IV. NEW CONCEPTS FOR AMMUNITION STORAGE

Ammunition storage design involves both the design of the magazine, and the inter-magazine and site lay-out. Thus, in evaluating new concepts, both innovative lay-outs and structural-material concepts are considered.

A. Site Lay-out Considerations

Site lay-out criteria are contained in the various Army, DOD, and NATO safety criteria listed in chapter II on functional requirements. For earth-covered magazines, two levels of criteria are involved: one is the inter-magazine spacing, and the other is the distance to occupied structures. Both the inter-magazine and distance to occupied structure criteria are based on the net explosive weight (NEW) quantity-distance criteria.

Current DDESB criteria for inter-magazine spacing vary between $1.25W^{1/3}$ to $11W^{1/3}$, depending on magazine to magazine orientation and the use of barricades. (Inter-magazine spacing is in feet and W equals net explosive weight in pounds.) The quantity-distance criteria for magazine to occupied structure varies from 40 to $50W^{1/3}$. Thus, a major factor in evaluating total storage capacity versus real estate requirement for a given depot, or site, is the maximum allowable quantity of explosives to be stored in each magazine.

To illustrate the type of real estate savings that can be achieved, figure 1 depicts the relationship between real estate requirements based on distance to occupied structure criteria as a function of facility NEW storage capacity for standard 500,000 lb., 250,000 lb., 125,000 lb. NEW magazines. The figure indicates that the real estate savings is simply a function of magazine NEW capacity and is not related to total depot or site capacity. Approximately 400 acres can be saved by reducing the allowed NEW capacity from 500,000 lbs. to 250,000 lbs., and an additional 250 to 300 acres can be saved by further reducing the magazine NEW capacity to 125,000 lbs.

The reduction of the magazine NEW capacity is a viable design consideration in areas where total site storage NEW requirements are reasonably small (less than 10 million lbs. NEW), or where real estate cost or real estate availability are significant factors. This is true even if magazine cost is constant regardless of NEW capacity. But if smaller NEW capacity magazines can be constructed at some cost savings per magazine or can approach a constant cost per square foot of storage area, the reduced capacity NEW concepts would be viable even for larger capacity storage sites or depots.

Another alternative for large depot layouts is to surround the full-capacity magazines with magazines of reduced NEW capacity, thus making more effective utilization of the real estate required to satisfy the occupied building quantity-distance criteria.

B. Structure Design Variations

The dominant magazine design since WW II has been some form of earth-covered arch structure with a massive reinforced concrete head wall where earth cover is not provided. However, the Navy has in their inventory a reasonable number of rectangular earth-covered, flat-roofed structures. As part of the ESKIMO test series, large-scale explosive model tests have recently been conducted on these structures and preliminary results indicate that the flat roof design performed satisfactorily.

One new concept that is very promising involves a flat-roof, rectangular earth-covered structure. The unique aspect of this system is that all side, rear, and wing walls would be built from reinforced earth® concrete panels with soil friction metallic tie-back strips (figure 2). The roof deck could be hollow core pre-cast, pre-stressed concrete panels and the portal (or front) wall could either be conventional cast-in-place or pre-cast concrete depending on its relative size. The advantage of the reinforced earth pre-cast roof deck system is that with the exception of the portal wall, foundation and floor slab, the system would be built from pre-cast concrete units, which would virtually eliminate the need for expensive and time consuming form work. The economic feasibility of this concept has not yet been determined, but based on its relative merits as an economic alternative for bridge abutments and retaining walls, the potential for the system's economic feasibility is good. Reinforced earth also has previously been accepted as a viable alternative for earthen barricades used for blast protection.

In addition to the reinforced earth pre-cast roof deck system, Marwais International of Luxembourg has proposed a steel arch magazine similar to the current magazines but with significantly deeper corrugations. Included in their design also is a steel-concrete-steel sandwich panel for the portal head-wall. Recent discussion with representatives of Marwais would indicate some potential for this system, particularly if certain NATO design criteria are revised.

C. New Materials and Composites

Conventional earth-covered ammunition storage magazines are constructed from reinforced concrete and/or reinforced concrete and corrugated steel (arch barrel). All concrete currently specified is conventional cast-in-place construction. One construction system that has been previously demonstrated at CERL is an inflation formed foam-shotcrete system.[2] The relative simplicity and rapidity of erecting form work are the major advantages of this system. Its major disadvantages are shotcrete quality control, the slowness of placing concrete with shotcrete equipment, and the amount of concrete waste due to rebound. Economic analysis has indicated that an earth-covered foam-shotcrete arch magazine, equivalent structurally to the conventional cast-in-place concrete magazines, is cost competitive to single-unit conventional magazine construction. But the successful construction of a large (25 foot wide) foam shotcrete arch has never been demonstrated due to construction process loads impacting the shape and structural integrity of the resulting structure. It is assumed that a detailed structural analysis of the various construction process loads and appropriate design changes could overcome the previous construction process problems.

Two other materials concepts should also be considered. They are random fibrous concrete and the previously mentioned steel-concrete-steel sandwich panel. Both systems may provide additional hardening for the critical portal wall. Both techniques significantly improve the spall characteristics of concrete and should be considered as alternatives for portal wall design.

V. CONCLUSIONS AND RECOMMENDATIONS

From the information contained in this report, the following conclusions can be made.

1. The development of functional requirements for ammunition storage proved to be difficult because existing guidance is oriented predominantly toward a solution, and requirements are only implied. Thus, the functional requirements contained in this report are non-specific and general in nature.

2. The analysis of standard magazines relative to functional requirements indicated that safety has been the dominant design consideration. The performance of these magazines relative to shelter and operational requirements is often less than completely satisfactory.

3. The use of smaller NEW capacity magazines is an effective way of reducing real estate requirements for ammunition storage facilities. This is particularly true for small (less than 10 million lbs. NEW) facilities.

4. Based on its flexibility and its economic feasibility for other applications, the reinforced earth-hollow core pre-stressed concrete roof deck is a promising new concept for earth-covered ammunition storage.

In addition to the above conclusions, these recommendations are made.

1. Ammunition facility designers should analyze the merits of reducing the NEW capacity of magazines as a technique to reduce the real estate intensity of the facility. This is even effective on perimeter magazines of large facilities.

2. The economic feasibility of the reinforced earth-hollow core pre-stressed concrete roof deck magazines should be determined.

TABLE 1

AMMO IGLOOS - COMPARATIVE ANALYSIS

Identification	Estimator	Year	Total Cost $K	Cost of Barrel $K	Total Volume ft^3	Total Cost/ Volume $	Barrel Cost/ Volume	Total Cost Floor Arch
Concrete Circular Arch	OCE	78-79	147	--	21,397	6.87	--	73.5
Steel Circular Arch	OCE	78-79	161	--	23,165	6.95	--	80.5
Concrete Oval Arch(Freelock)	OCE	78-79	171	57.093	25,446	6.72	2.24	85.5
Concrete Oval Arch(Freelock)	EUD *	May 78	71.8	23.984	25,446	2.82	0.94	35.9
Concrete Oval Arch(Freelock)	EUD *	Nov 78	92.8	30.978	25,446	3.65	1.22	46.4
Steel Oval Arch	OCE/Block Veatch	75	116.693	38.633	20,711	5.63	1.86	76.5
Steel Oval Arch	OCE	78-79	179	60.799	27,162	6.59	2.24	89.5

*Cost estimates are based on quotes for 30 or more magazines per construction site.

TABLE 2

REAL PROPERTY MAINTENANCE COST
FOR BUILDINGS ARMY WIDE (FY78)

BUILDINGS	UNIT OF MEASURE	BASE UNIT QUANTITY	TOTAL COST $	UNIT COST $
(All)	K Sq Ft	1,012,794	505,242,487	498.86
Ammo Storage	K Sq Ft	47,868	5,281,242	110.33

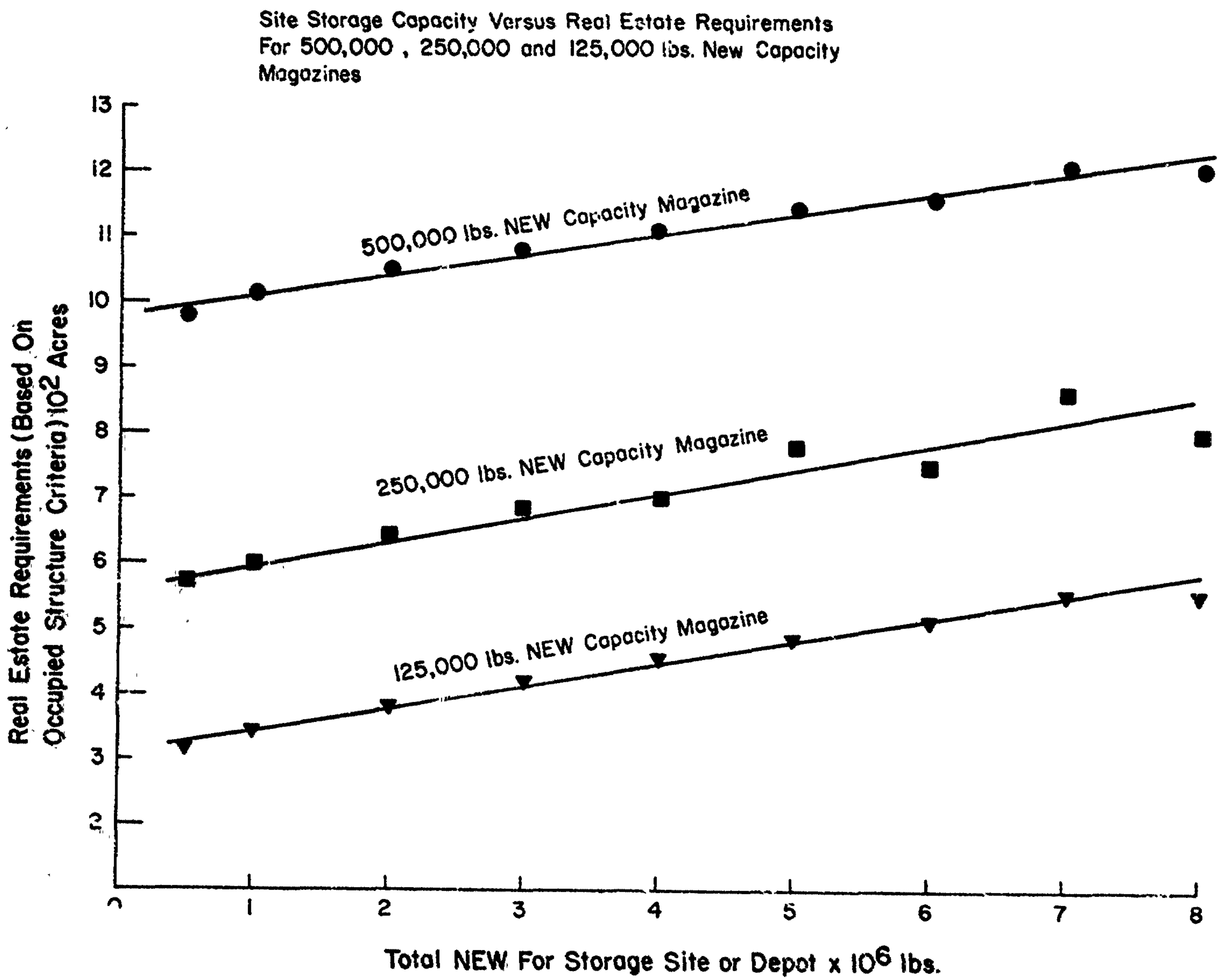
Site Storage Capacity Versus Real Estate Requirements
For 500,000 , 250,000 and 125,000 lbs. New Capacity
Magazines
Real Estate Requirements (Based On
Occupied Structure Criteria) 10^2 Acres
500,000 lbs. NEW Capacity Magazine
250,000 lbs. NEW Capacity Magazine
125,000 lbs. NEW Capacity Magazine
Total NEW For Storage Site or Depot x 10^6 lbs.

FIGURE 1

FIGURE 2

REINFORCED EARTH AMMO STORAGE CONCEPT

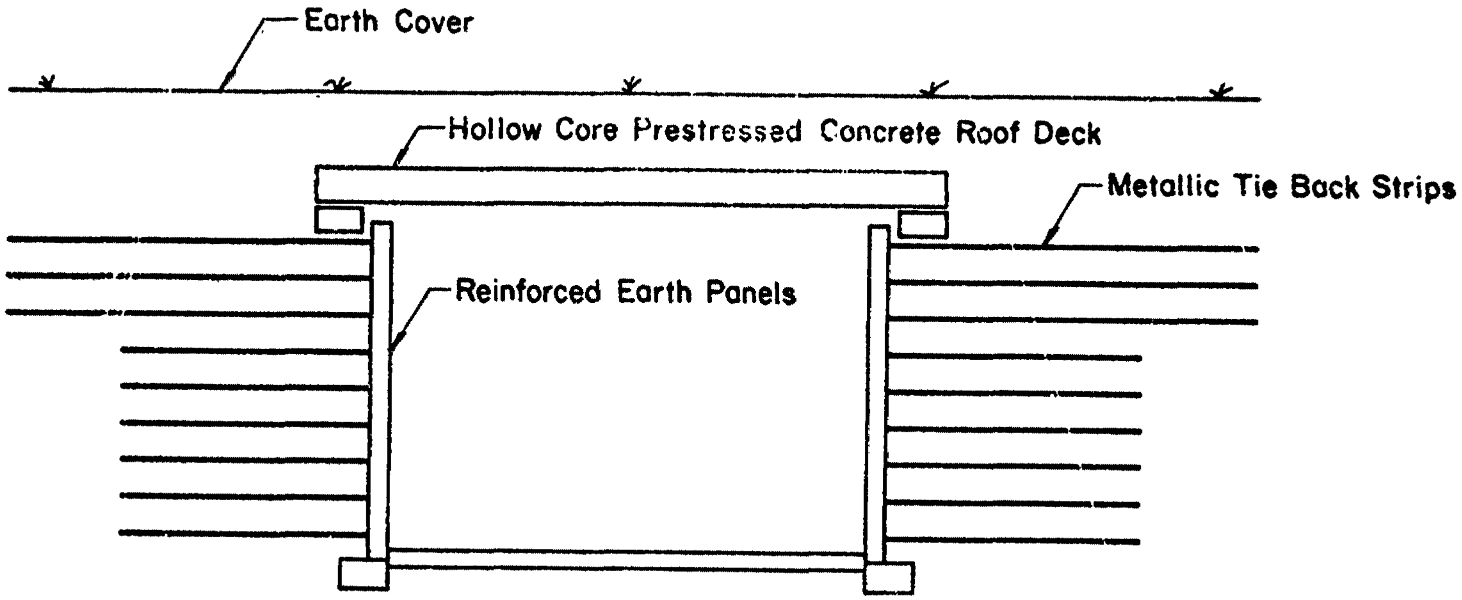

References

1. Kanarowski, Stanley M. "Investigation of Materials for Waterproofing Leaky Concrete Ammunition-Storage Bunkers from the Inside," CERL Special Report M-256, January 1979.

2. Woratzeck, M., "Inflation/Foam /Shotcrete System for Rapid Construction of Circular Arches,"CERL Special Report M-262, May 1979.

E X P L O S I V E S

S A F E T Y

C O N C E P T S

USA DARCOM FIELD SAFETY ACTIVITY

CHARLESTOWN, INDIANA 47111

EXPLOSIVE SAFETY CONCEPTS

ERIC T. OLSON
USA DARCOM Field Safety Activity
Charlestown, IN 47111

ABSTRACT

This presentation is an overview of several fundamental explosives safety requirements and concepts from the viewpoint of the hazard classification and construction plan review functions performed at the US Army Materiel Development and Readiness Command Field Safety Activity.

INTRODUCTION

1. It is appropriate to begin a series of presentations on end item and in-process hazard classification with a basic overview of several fundamental requirements and concepts that illustrate the application of more specialized work which is advancing the art and science of explosive safety. This presentation will be from the perspective of construction plan review and hazard classification functions performed at the US Army Materiel Development and Readiness Command (DARCOM) Field Safety Activity.

2. The Activity is under the administrative supervision of the Chief, Safety Office, HQ DARCOM. It is a descendent of the Ordnance Field Safety Office which was first established in 1951 to meet the urgent safety training and safety inspection requirements stemming from the Korean conflict. DOD policy at that time precluded expansion of the Office, Chief of Ordnance safety staff to meet these requirements. Indiana Army Ammunition Plant was selected as the location of the Ordnance Field Safety Office because it could provide the facilities and administrative support required and because of its central location (12 miles north of Louisville, KY). The successor AMC Field Safety Activity was established by DA General Orders 46 on 25 July 1962 and was last reorganized by DARCOM Permanent Orders 27-3, 6 October 1976. That reorganization was to improve management of the HQ DARCOM safety program and to distribute "commodity" oriented expertise out of the DARCOM Headquarters and into the "field".

3. The mission of the Activity, as outlined in DARCOM Regulation 10-18, is to "promote safety education, perform safety engineering services and conduct safety program evaluations in support of the overall DARCOM Safety Program." This is the Activity's 3E Concept which encompasses all aspects of the safety mission. The Activity is frequently called upon to provide quick response to unique safety problems, to fulfill urgent safety training needs, and to

conduct special investigations and studies involving such matters as serious accidents, chemical munitions hazards and equipment, facilities and process safety problems. The organization is divided into 4 major divisions besides the Office of the Director.

4. A major division of the Activity is the Engineering Services Division, staffed with five safety engineers, four safety specialists, two industrial hygienists and two clerical workers. The division performs DARCOM safety program evaluations, reviews site plans and safety submissions for explosives and ammunition facilities, determines hazard classifications for new development items, and exercises a safety approval authority for new ammunition peculiar equipment. During FY 80, the Site Plans Section of the Division has processed 161 construction plan reviews and has hazard classified 137 items.

DOD HAZARD CLASSIFICATION

1. Every explosive formulation, ammunition item, and explosive composition which is separately packaged for storage or transportation is hazard classified according to the scheme depicted in Figure 1. This system is based on recommendations of the United Nations Organization which establish nine classes of dangerous goods. All explosives and ammunition items containing explosives fall into Class 1. Within Class 1 there are five divisions as follows:

a. Division 1 includes mass detonating items and materials. All items in a stack of such materials would be expected to detonate almost simultaneously upon the detonation of a single item within the stack. Blast overpressure is a predominant damage mechanism associated with the detonation of these items. The primary fragment and debris hazards may also be severe.

b. Items which detonate progressively over a period of time when involved in a fire fall into division 2. Since only a relatively small amount of explosive would be involved in a single detonation, the blast hazard extends only to short distances from the stack. The hazard from primary fragments is significant, and during a fire, hazardous fragment densities (more than 1 fragment possessing 58 ft-lb kinetic energy or more per 600 ft^2) may be experienced at considerable distances from the site of the fire.

c. Division 3 material presents a mass fire hazard. There is little or no chance that a fire involving such materials could be extinguished prior to the consumption of all the items in division 3. Container pressure ruptures may occur, and firebrands may be projected causing secondary fires or injuries.

d. Division 4 materials may present a moderate fire hazard in storage, and a prudent separation between buildings containing such materials is required to limit the spread of fire.

e. Division 5 materials are very insensitive explosives. Several candidate materials are under study by DOD, and relaxed siting criteria may be accepted in the future. Currently these materials are considered the same as class 1, division 1, compatibility group D.

2. In addition to a division designation, items in divisions 1 and 3 may be assigned hazardous fragment distances, when test data warrant, indicating minimum allowable separations in hundreds of feet, independent of quantity, to certain exposures where personnel may be congregated without the benefit of protective construction. Such exposures include installation boundaries, administrative areas, and other areas as listed in paragraph 5-2F2, DOD 5154.4S. Hazardous fragment distances are indicated for all items in division 2.

3. Each explosive and ammunition item is also assigned to one of 12 storage compatibility groups, indicated by an alphabetic character.

4. The US Department of Transportation (DOT) has not adopted the UNO recommendations. In addition to the division, compatibility group, and fragment distance determinations, a DOT class, shipping name, and label must be assigned. Items in UN divisions 1 and 2 are normally DOT Class A. Items in UN division 3 are normally DOT Class B. DOT also uses a Class C which includes certain small items containing limited quantities of Class A or B materials.

DETERMINATION OF CLASSIFICATIONS

1. The final classification for explosives and ammunition are normally determined by testing the items as packaged for storage or transportation. The testing scheme is described in TB 700-2 and is graphically portrayed in Figure 2.

2. Single package tests may be performed if the package contains more than one article, or if no significant effects are expected outside the shipping container of a single article. A central item in the package is caused to function using its internal source of initiation. If there are no significant effects external to the shipping container, stack detonation testing is not necessary. "ETC" refers to explosion of essentially the total contents of the package. "NETC" means the opposite. This test is normally performed three times, or until ETC occurs.

3. The stack detonation propagation test is performed with a stack of five shipping containers under confinement. A central item in the stack is initiated. This test is also performed three times, or until ETC occurs.

4. The external fire test is normally performed with a stack of five packages, without confinement, and is instrumented for fragment collection. Assignment of an item to division 2, 3, or 4 depends on a qualitative assessment of the effects as well as additional testing, as necessary, for thermal effects and firebrand projection.

5. Items are considered compatible if the probability and potential severity of an accident involving a quantity of these items in mixed storage is not significantly greater than the probability and potential severity of an accident involving a similar quantity of any one of the items. Assignment of

an explosive composition or article to a storage compatibility group is based on a comparison of the item's configuration, function, and test results to qualitative definitions summarized in Figure 3. Limited mixed storage of items in different compatibility groups is permitted as shown in Figure 4. Two points regarding compatibility group definitions deserve emphasis:

a. The designation "without its own means of initiation" does not mean that an initiating device must not be packaged with the explosive article. If fuzes or initiating devices have multiple safety features (usually consisting of an out-of-line explosive train and safety and arming features requiring launch or firing stimuli to arm) may be packaged with or assembled to high explosive items that still qualify for assignment to group D or E.

b. Testing is a prerequisite for assignment of an item to division 4, compatibility group S. Normally this will consist of a single package test and external fire test. Only if function testing of a single item shows no explosive effects external to the item itself (as with certain explosive cable cutters, thermal batteries, etc.) can assignment to group S be made without package tests.

6. The classifications obtained through application of the criteria discussed to this point apply only to items and materials in approved packaging for storage and transportation. The siting of an operation involving unpackaged items must be based on an appropriate in-process classification which reflects the hazards of that specific operation. Hence, two operations involving the same explosive material may be classified differently depending on the explosive effects possible. For example, one operation involving a small quantity of unconfined propellant may be sited based upon division 3 criteria, whereas another operation involving a larger quantity of the material in a confined state may be sited based on division 1 criteria because of a potential transition from burning to detonation.

7. Within DARCOM, organizations sponsoring the development of or first adopting a new explosive item are responsible for planning and conducting hazard classification testing. Technical reviews of test plans and test results are accomplished at the DARCOM Field Safety Activity. Proposed final classifications are formulated and coordinated with the other services prior to forwarding the final classification to DDESB through the DARCOM Headquarters Safety Office. When conflicts can not be resolved among the services, the matter may be referred directly to DDESB for resolution. Upon DDESB approval of a final classification, the Field Safety Activity will notify the originator and will code a computer input for the new tri-service Joint Hazard Classification System. This computer data base will serve as a single authoritative source of classification data for all end and resupply items. The review process is depicted graphically in Figure 6.

SITE SELECTION AND NEW FACILITY CONSTRUCTION

1. In addition to its role in hazard classification, the DARCOM Field Safety Activity exercises final Army safety approval authority for new construction and major modification of explosives facilities, and for inert facilities or activities which might be exposed to explosives hazards if not properly located. Approval of a facility is normally obtained by DARCOM elements via two submissions, these being a preliminary site plan submission and a final safety review submission, as depicted in Figures 7 through 9.

2. Several basic explosive safety concepts and two criteria recently promulgated by DDESB are of fundamental interest in the siting of new explosives operations. These concepts can best be understood in terms of the accidental explosion environment depicted in Figure 10. Protection from explosive effects can be accomplished by physical separation, protective construction, or a combination of the two. The exact nature of the protection depends on the hazard characteristics of the explosives which may accidentally react (as reflected by the hazard classification), additional testing or analysis, and the degree of protection desired (as reflected by the type of acceptor exposure under consideration).

3. Interim Change 2 to DOD 5154.4S, 23 June 1980, prescribes allowable blast overpressure exposures for various types of acceptor facilities and operations, and lists the damage levels and types of injuries expected. Since the distance from a detonation of division 1 material at which a given blast overpressure would be experienced varies nearly proportionally with the cube root of the net explosive weight (NEW), the distance at which a predictable blast effect is expected can be expressed, without reference to quantity, as a value of K in the relationship shown in Figure 11. Where division 1 materials are processed, specific facility siting requirements are determined by selecting the greater of:

a. The hazardous fragment distance, if the exposure is of the type listed in paragraph 5-2F2, DOD 5154.4S (installation boundaries, administrative and housing areas, etc.).

b. The applicable distance based on the blast overpressure hazard.

4. It is necessary to qualify Figure 11 in that the nomenclature traditionally associated with the distances defined by the various values of K may be misleading. Specifically, the siting of successive operations in a production line is permitted at K=9, and barricading against low angle, high velocity fragments is required. Siting these exposures at K=18, or "unbarricaded intraline distance", without intervening barricades, has been a common practice. It should be noted, however, that barricades or suitable protective construction may be necessary at K=18, depending on personnel concentration, the value of equipment exposed, and the potential effects of damage to process control equipment.

5. In addition to earth barricades for fragment protection, common types of protective construction include substantial dividing walls and operational shields. These structures are intended to afford, respectively, category 3 and category 1 protection as shown in Figure 12.

a. Substantial Dividing Walls. For many years following World War II, a concept prevailed to the effect that 12 inch thick, conventionally reinforced concrete dividing walls would prevent the "simultaneous" detonation of two quantities of high explosives if the donor quantity did not exceed 5000 pounds. The thinking was that the delay in propagation through the wall would produce multiple blast waves of moderate magnitude at acceptor locations. Therefore, multi-bay facilities with 1 foot concrete walls between bays were sited based on the largest bay limit if no bay contained more than 5000 pounds. More recent testing and experience has shown that if detonation propagation from one bay to the next occurs, the blast waves will coalesce within a short distance from the explosion site. The resulting blast overpressure will be the same as that produced by a "simultaneous" detonation of both quantities. Therefore, new operations in existing buildings constructed with 1 foot concrete walls must be designed to prevent propagation, if siting is based on bay limits. Data available to date suggest that the probability of propagation will be very low if the largest bay limit does not exceed 425 pounds, as depicted in Figure 13. This presumes that the materials are properly placed within the bays, and that they are relatively insensitive (unfuzed heavy cased projectiles and the like). If the explosives are more sensitive, the quantities may have to be limited to amounts on the order of 250 pounds. New substantial dividing walls are designed to prevent propagation in accordance with TM 5-1300.

b. Operational Shields. The probability of accidental initiation of energetic material in certain operations is such that operator protection (remote operation) is required. Again, this may be accomplished with distance or protective construction. The distances required may be impractical, necessitating the use of shields which limit operator exposure to blast to 2.3 psi, which provide complete operator protection from fragments, and which limit thermal exposure in accordance with MIL STD 398.

6. Since division 2 materials do not mass detonate, the distance at which a given effect is produced is not proportional to the cube root of the NEW. Single distances, independent of quantity, based on the fragment hazard, have been used for siting with respect to inhabited buildings, installation boundaries, and similar exposures. Prior to the publication of Interim Change 1 to DOD 5154.4S, 27 August 1979, intraline distances for division 2 items were the same as for division 1 items based on the NEW, (up to half of the applicable fragment distance). These distances are shown by the bold lines on Figure 14. Interim Change 1 established single distances for intraline siting, regardless of quantity, as shown by the fine lines to the left of the K=18 curve. These recent criteria are considerably more restrictive than the old standards. DARCOM is in the process of assessing the impact of the new standards on site selection and new construction plans.

APPLICATION OF DOD HAZARD CLASSIFICATION SYSTEM

MINIMUM DISTANCE (TYP.)	HAZARD CLASS	DIVISION	COMPATIBILITY GP (TYP.)	SUPERSEDED CL
(18)	1 .	1	D	7
(08)	1 .	2	E	3, 4, 5, 6
(06)	1 .	3	C	2
	1 .	4	S	1
	1 .	5*	D	

*INSENSITIVE ITEMS - REGARDED AS 1.1

Figure 1.

DETERMINATION OF HAZARD DIVISION

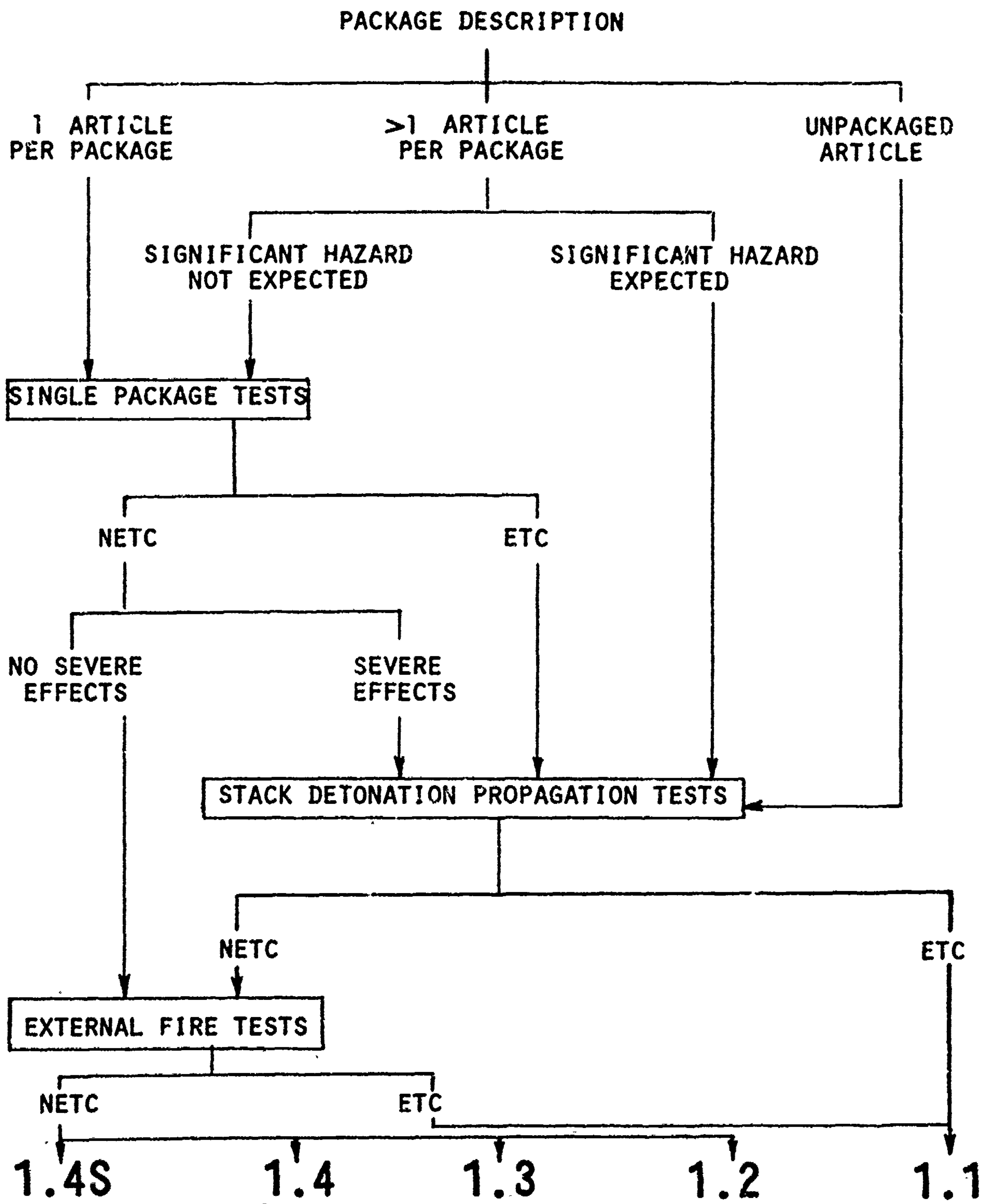

Figure 2.

COMPATIBILITY GROUPS

A	-	INITIATING EXPLOSIVES.
B	-	DETONATORS AND SIMILAR INITIATING DEVICES.
C	-	BULK PROPELLANTS AND ITEMS CONTAINING PROPELLANTS (W/ OR W/O IGNITER).
D	-	HE & HE ITEMS (W/O PROP CHARGE & W/O MEANS OF INITIATION).
E	-	HE ITEMS (W/PROP CHARGE & W/O MEANS OF INITIATION).
F	-	HE ITEMS (W/OR W/O PROP & W/MEANS OF INITIATION).
G	-	FIREWORKS, ILLUMINATING INCENDIARY, SMOKE, TEAR (NOT WATER ACTIVATED & NO WP OR FLAM LIQUID OR GEL).
H	-	AMMO W/EXPLOSIVES & WP OR OTHER PYROPHORIC MATERIAL.
J	-	AMMO W/EXPLOSIVES & FLAM LIQUID OR GEL.
K	-	AMMO W/EXPLOSIVES & TOXIC CHAMICAL AGENT (LETHAL OR INCAP).
L	-	ITEMS NOT INCLUDED IN ABOVE GROUPS -- STORE ONLY WITH ITEMS OF SIMILAR HAZARD.
S	-	AMMO PRESENTING NO SIGNIFICANT HAZARD.

Figure 3.

MIXING COMPATIBILITY GROUPS

	A	B	C	D	E	F	G	H	J	K	L	S
A	X	Z										Z
B	Z	X										X
C			X	Z	Z		Z					X
D			Z	X								X
E			Z		X							X
F						X						X
G			Z				X					X
H								X				X
J									X			X
K										Z		
L												
S	Z	X	X	X	X	X	X	X	X			X

X - MAY BE COMBINED IN STORAGE

Z - UNDER CERTAIN CIRCUMSTANCES, MAY BE COMBINED, WITH DARCOM APPROVAL.

Figure 4.

"IN-PROCESS" CLASSIFICATION

1. CLASSIFICATION OF ITEM IN SHIPPING/STORAGE CONTAINER DOES NOT APPLY TO UNPACKAGED ITEM.

2. CLASSIFICATION IS SPECIFIC TO OPERATION.

Figure 5

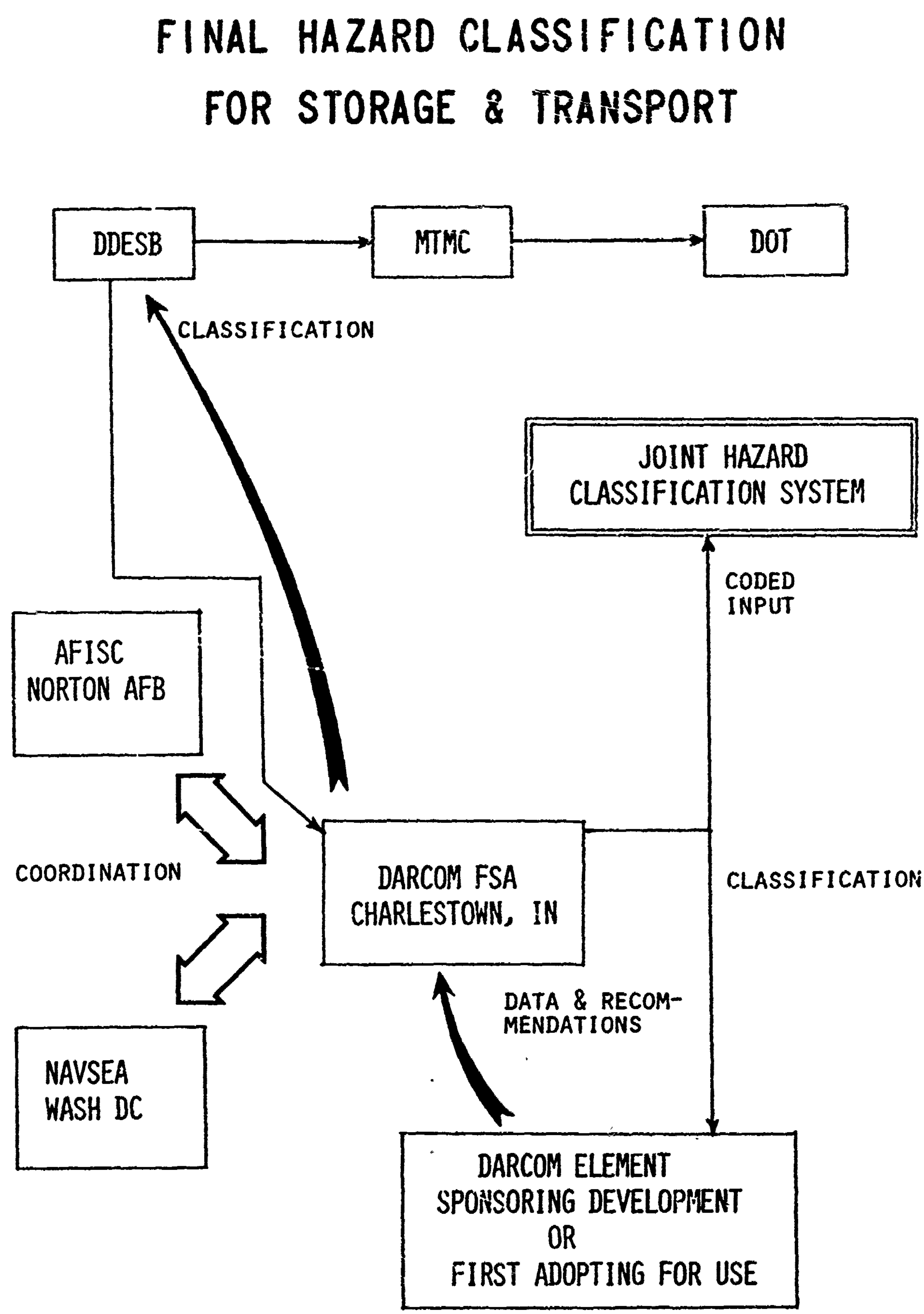
FINAL HAZARD CLASSIFICATION
FOR STORAGE & TRANSPORT
DDESB
MTMC
DOT
CLASSIFICATION
JOINT HAZARD CLASSIFICATION SYSTEM
CODED INPUT
AFISC NORTON AFB
COORDINATION
DARCOM FSA CHARLESTOWN, IN
CLASSIFICATION
NAVSEA WASH DC
DATA & RECOM- MENDATIONS
DARCOM ELEMENT SPONSORING DEVELOPMENT OR FIRST ADOPTING FOR USE

Figure 6.

PLANS REQUIRED FOR:

1. NEW CONSTRUCTION OF AMMO OR EXPLOSIVES FACILITIES.

2. MAJOR MODIFICATION OF SUCH FACILITIES OR ANY MODIFICATION WHICH MIGHT INCREASE.

   A. PERSONNEL EXPOSURE.

   B. EXPLOSIVES QUANTITY LIMITS.

   C. OTHER HAZARDS FOR WHICH FACILITY WAS DESIGNED OR SITED.

3. INERT FACILITIES OR ACTIVITIES WHICH MIGHT BE EXPOSED TO HAZARDS IF NOT PROPERLY LOCATED.

SEE:

- PARAGRAPH 3-6, DOD 5154.4S.
- PARAGRAPH 5-27, AMCR 385-100.

Figure 7.

SAFETY SITE PLAN SUBMISSION

REQUIRED PRIOR TO FINAL DESIGN.

FINAL SAFETY REVIEW SUBMISSION

REQUIRED PRIOR TO CONSTRUCTION CONTRACT AWARD OR INITIATION OF ARMY CONSTRUCTION WORK.

Figure 8.

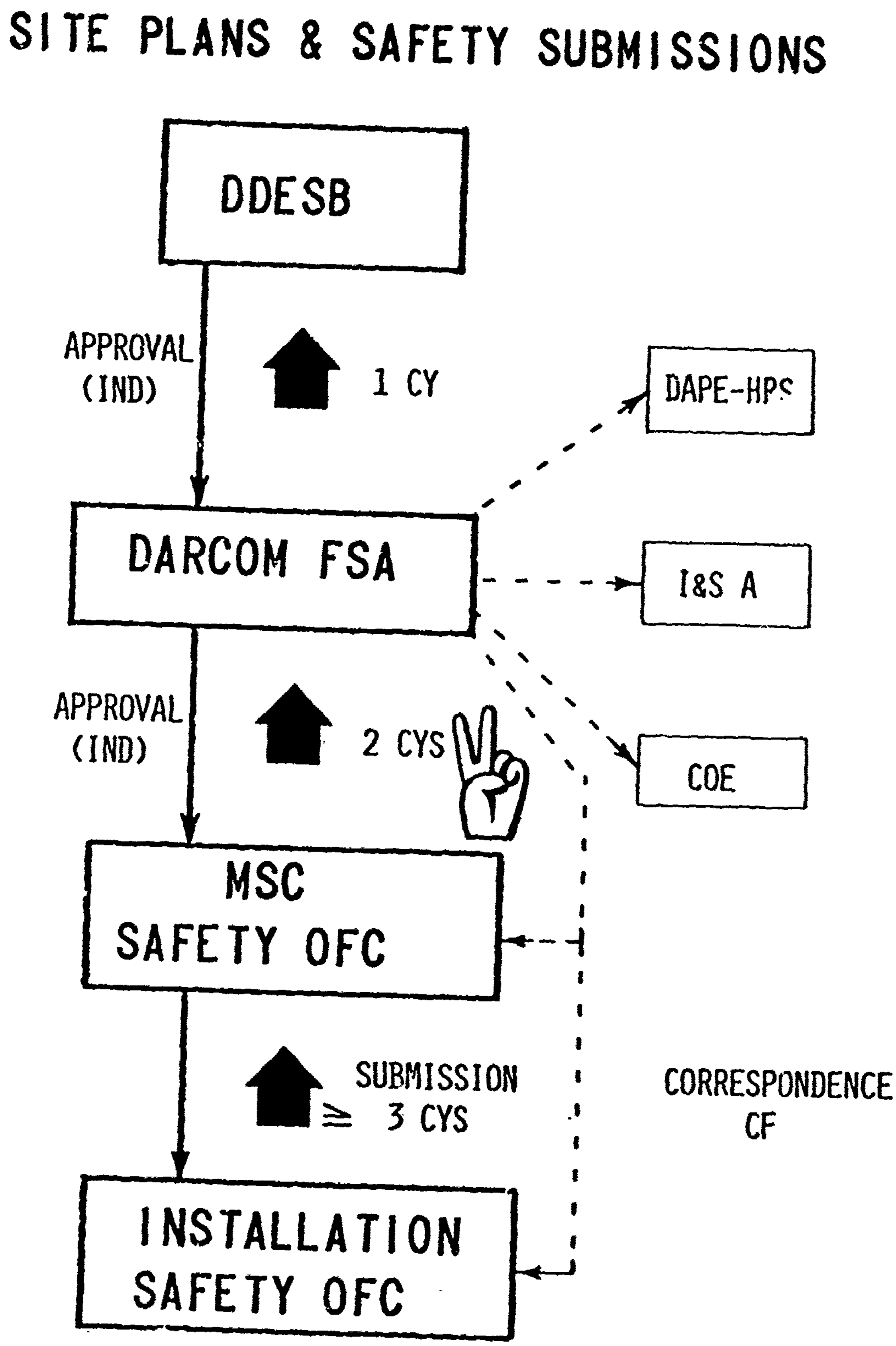
SITE PLANS & SAFETY SUBMISSIONS
DDESB
APPROVAL (IND)
1 CY
DAPE-HPS
DARCOM FSA
I&S A
APPROVAL (IND)
2 CYS
COE
MSC SAFETY OFC
SUBMISSION
≥ 3 CYS
CORRESPONDENCE CF
INSTALLATION SAFETY OFC

Figure 9.

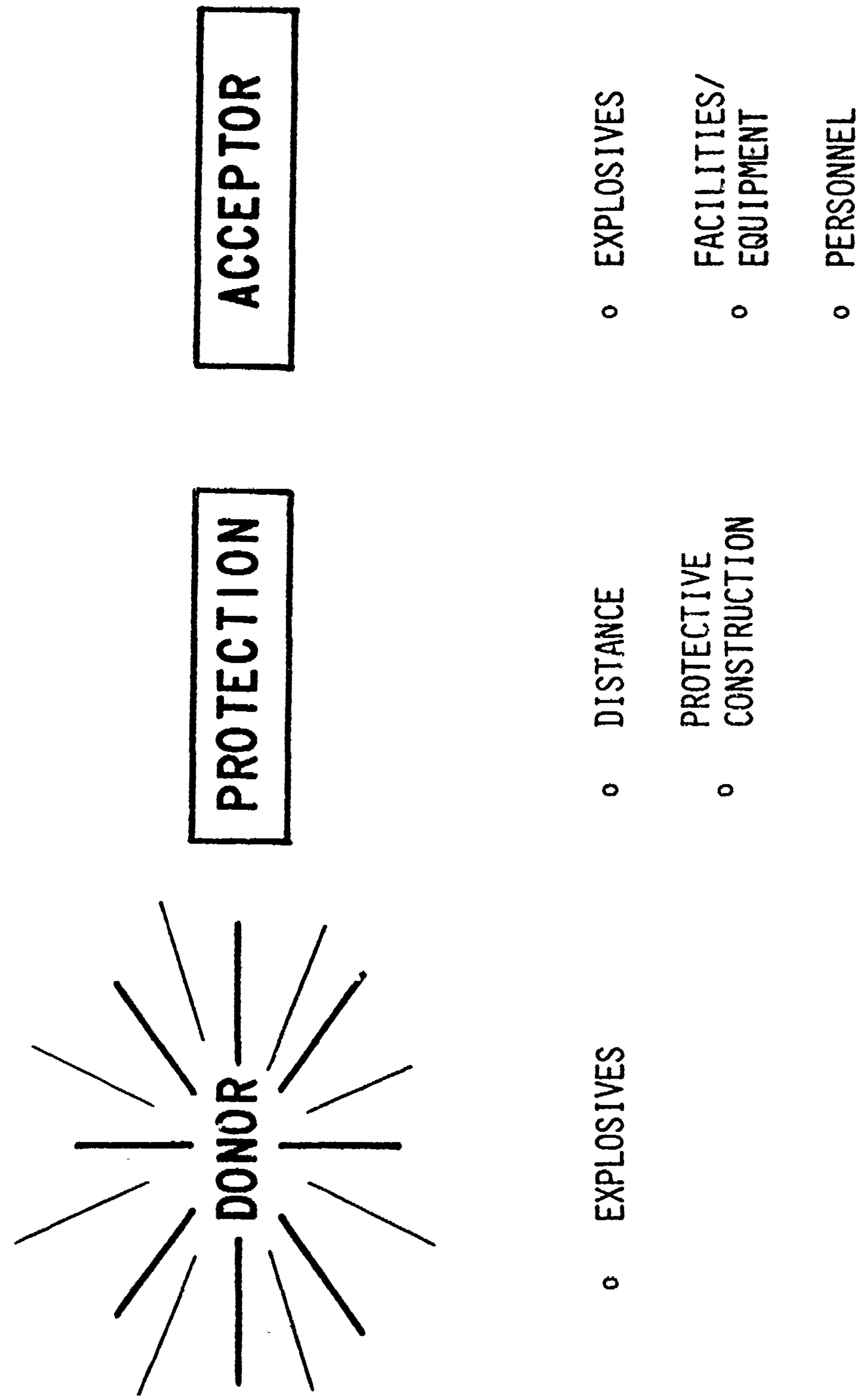
DONOR
PROTECTION
ACCEPTOR
o EXPLOSIVES
o DISTANCE
o PROTECTIVE CONSTRUCTION
o EXPLOSIVES
o FACILITIES/ EQUIPMENT
o PERSONNEL

Figure 10.

DISTANCE CATEGORIES

$$D = KW^{1/3}$$

INHABITED BUILDING DISTANCE

K = 40 (50 FOR LARGE QUANTITIES)

$P_{so} \cong 1.2$ psi

PUBLIC TRAFFIC ROUTE DISTANCE

K = 24 (30 FOR LARGE QUANTITIES)

$P_{so} \cong 2.3$ psi

INTRALINE DISTANCE

K = 18

$P_{so} \cong 3.5$ psi

BARRICADED INTRALINE DISTANCE

K = 9

$P_{so} \cong 11$ psi

MAGAZINE DISTANCE

K VARIES BETWEEN 1.1 AND 11.

Figure 11.

PROTECTIVE CONSTRUCTION CATEGORIES

1 PERSONNEL PROTECTION

2 EQUIPMENT PROTECTION

3 PREVENTION OF PROPAGATION

Figure 12.

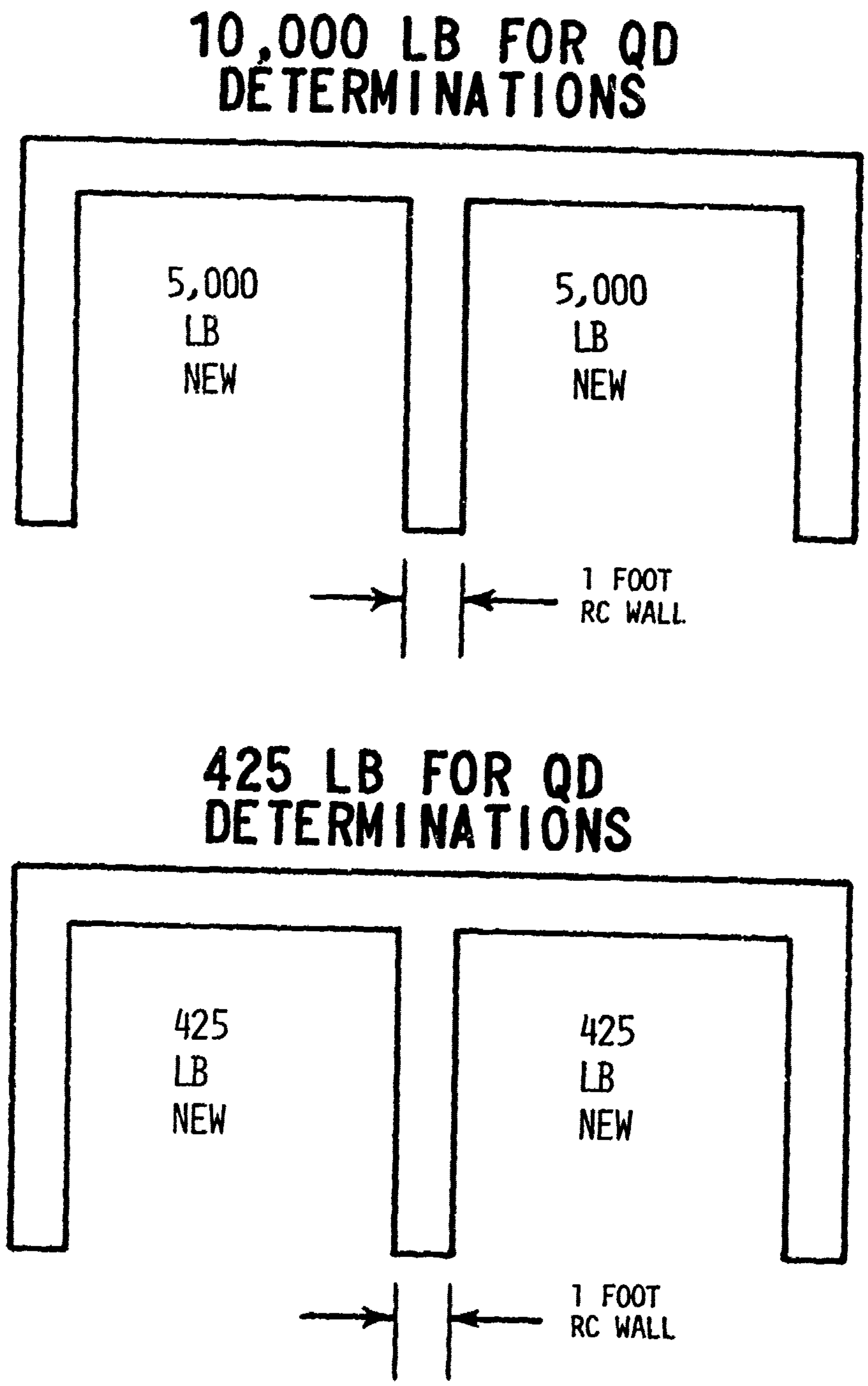
10,000 LB FOR QD DETERMINATIONS
5,000 LB NEW
5,000 LB NEW
1 FOOT RC WALL
425 LB FOR QD DETERMINATIONS
425 LB NEW
425 LB NEW
1 FOOT RC WALL

Figure 13.

INTRALINE DISTANCES FOR CLASS 1, DIVISION 2

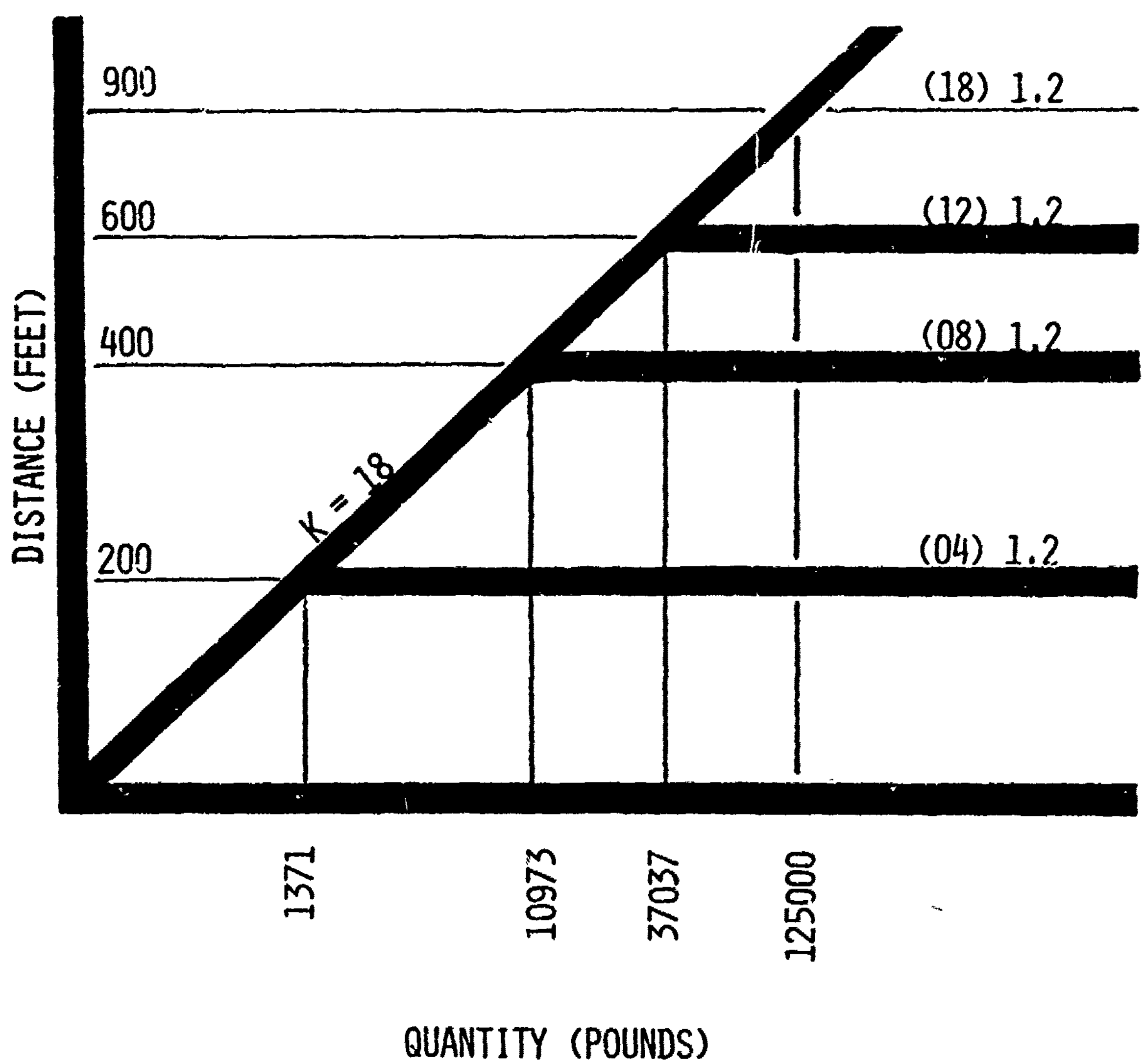

Figure 14.

REFERENCES

- DOD 5154.4S, DOD AMMUNITION AND EXPLOSIVES SAFETY STANDARDS.
- TB 700-2, DOD EXPLOSIVES HAZARD CLASSIFICATION PROCEDURES.
- UNITED NATIONS PUBLICATION, ST/SG/AC.10/1/REV. 1, TRANSPORT OF DANGEROUS GOODS.
- TITLE 49, CODE OF FEDERAL REGULATIONS, TRANSPORTATION.
- AMCR 385-21, DETERMINATION OF AMMUNITION AND EXPLOSIVES HAZARD CHARACTERISTICS AND ASSOCIATED HAZARD CLASSIFICATIONS.
- AMCR 385-100, AMC SAFETY MANUAL.

Figure 15.

Small Scale Tests for Classification of Propellant for Small Calibre Weapons Into Hazard Divisions

R. WILD

Bundesinstitut für chem. techn. Untersuchungen (BICT)
5357 Swisttal-Heimerzheim, Germany

1. Introduction

In Germany corresponding to law, all explosives must be stored according to their hazard division. The procedure of hazard division classification for storage purposes is prescribed by federal regulations which are in accordance with UN and NATO recommendations. Following tests have to be performed:

A. Single package test
B. Stack test with at least 5 packages
C. External fire test with 1 package
D. External fire test with at least 5 packages

The tests A through C must be repeated 3 times; test D must be performed once.

As these tests have to be made with the original packages for storage, a lot of test material is needed. The price for the material, e.g., for one propellant may reach $13,000. Because of these economical constraints, full scale tests are not possible in all cases.

The above mentioned federal regulation allows other experiments than full scale tests too, if an unambiguous classification is possible by these experiments. Therefore we tried to develop laboratory tests, by means of which a classification of propellant, especially for small calibre weapons should be possible.

2. Description of the Laboratory Tests

2.1 General Aspects

The main idea is to perform such laboratory tests by means of which the burning behavior of the propellant can be characterized. Following small scale tests have been selected to evaluate the burning properties.

2.2 Burning Behavior in a 2" Steel Tube

In this experiment a steel tube, open on one side, with an inner diameter of 2" is filled with propellant and is placed on the closed end. The height of the tube is 350 mm, the thickness of the wall is 3 mm. The density of the propellant is its normal bulk density. A picture of the steel tube is shown in figure 1.

50 mm above the bottom of the tube, the propellant is ignited by approximately 3 g of a gasless pyrotechnic mixture consisting of 70% Pb_3O_4 and 30% Si.
Three types of reaction are possible:

A. Burning of the propellant without destroying the steel tube

B. Mild explosion of the propellant tearing the steel tube into a maximum of three large fragments (s. fig. 2)

C. Detonation of the propellant with a complete destruction of the tube into a lot of little fragments (s. fig. 3)

2.3 Dynamic Vivacity in a Closed Vessel

In order to get an idea how the propellant reacts in a confinement, the dynamic vivacity in a closed vessel is determined. The volume of the vessel is 200 cm^3, the loading density is 0.1 g/cm^3, i.e., a sample of 20 g propellant is used. The propellant is ignited by 1 g of black powder. The dependence of pressure on time in the vessel is measured by a quartz gauge. The experimental arrangement is shown in figure 4. Figure 5 shows a sketch of the pressure time history.

The dynamic vivacity is computed from following formula:

$$V_D = \left(\frac{dp}{dt}\right)_{p = 0.5 p_{max}} \cdot \frac{1}{0.5\, p_{max}^2}$$

where p_{max} means the maximum pressure and the time derivative is taken at $p = 0.5\, p_{max}$.

The data v_d is nearly independent of the loading density and of the maximum pressure.

2.4 Burning Rate in a Groove

In this experiment the burning velocity in a groove is measured. The groove is made of an angle iron, 1 m long. In order to avoid heating of the metal, the groove is cooled by water. The experimental set up is shown in figure 6. As probes for determining the velocity thermocouples are used.

3. Results

3.1 General Remarks

From the results of the above described experiments groups of propellants with similar burning characteristics were formed. With one representative propellant of such a group a full scale test was performed in order to get some sort of calibration of the laboratory tests. Together and in comparison with the results of the full scale tests, all results of the small scale experiments lead to following rules:

> Propellants should be classified to hazard division 1.1 if
> the steel tube is fragmented into little pieces (fig. 3)
> or
> in the case of double base propellant, the dynamic vivacity exceeds 1.0 (bar s)$^{-1}$ and in the case of single base propellant the dynamic vivacity exceeds 1.3 (bar s)$^{-1}$.
> Propellant could be classified to hazard division 1.3 if
> the steel tube is torn into a maximum of 3 large fragments (fig. 2)
> and
> the dynamic vivacity in the case of double base propellant is less than 1.0 (bar s)$^{-1}$ and in the case of single base propellant is less than 1.3 (bar s)$^{-1}$.

The burning velocity in the groove did not yield unambiguous results. However it could be stated that a high burning velocity (70 - 100 mm/s) is a hint for a classification to division 1.1.

If the above mentioned rules do not apply, no final decision concerning the classification can be made by these small scale tests. However, we did this procedure with more than 50 types of propellant and only in the case of a few flake propellants (about 10% of the total amount) difficulties arose. In all other cases the small scale tests yield results which are in agreement with experience from large scale tests.

4. Summary

Small scale tests are described by means of which a classification of propellants especially for small calibre weapons into hazard divisions is possible.

Following measurements proved to yield useful results:

> burning behaviour in an open 2" steel tube
> dynamic vivacity in a closed vessel

and in some case the burning velocity in a groove.

fig. 1 2" Steel tube

fig. 2 Steel tube after mild explosion

fig. 3 Steel .ube after detonation

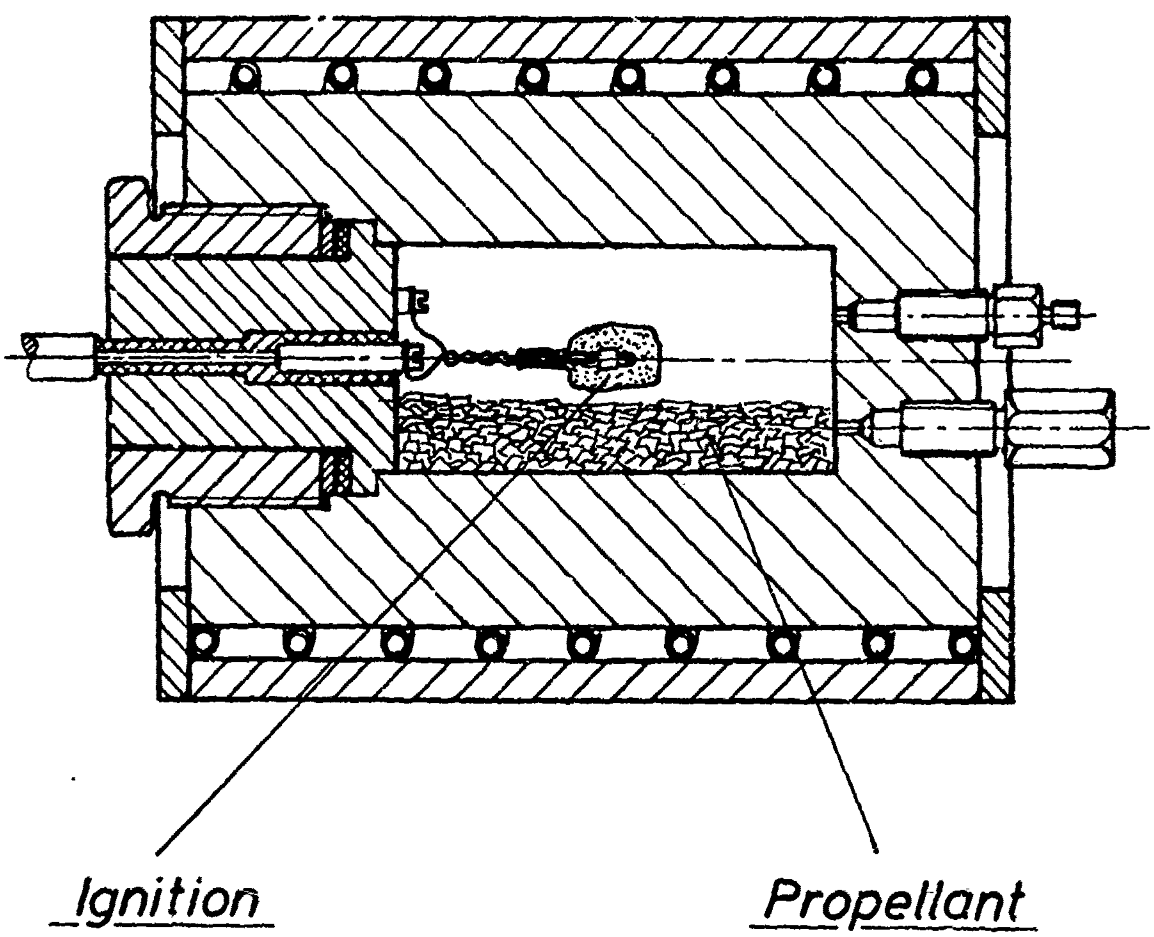

fig. 4 Closed vessel

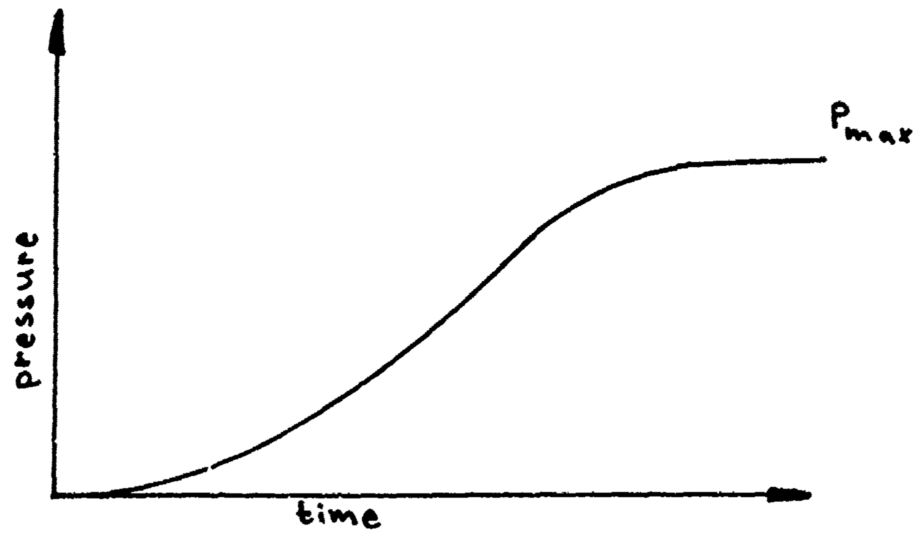

fig. 5 Sketch of pressure time history in the vessel

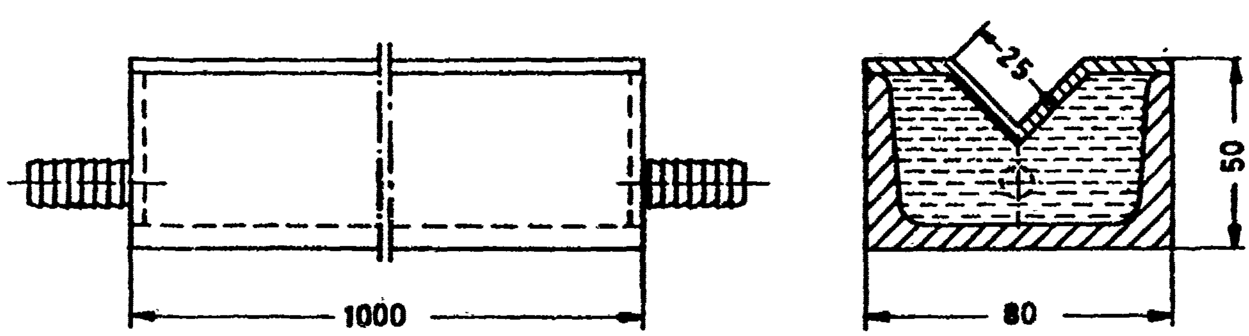

fig. 6 Experimental set up for measuring the burning velocity

HAZARD CLASSIFICATION PROCEDURE FOR INPROCESS MATERIALS

by

Ronald Pape

and

Hyla Napadensky

IIT Research Institute
Chicago, Illinois 60616

and

Richard Rindner

U. S. Army Armament Research
and Development Command
Large Caliber Weapons System
Laboratory
Dover, New Jersey 07801

ABSTRACT

A hazard classification procedure has been developed for in-process propellant and explosive materials. Accident reports in the DOD Explosive Safety Board files, hazards analyses, and existing test methods were reviewed and used as the basis for developing the preliminary structure of the procedure. The most promising tests for incorporation into the procedure were evaluated experimentally. Evaluations were completed for local impact, rubbing friction, local thermal, regional thermal, electrostatic discharge, critical diameter, critical layer thickness, tube transition, layer transition, mass explosion, mass fire, and fire spread tests. Based on the test results the procedure was finalized. Before the procedure should be used, a more comprehensive validation using sample materials with known accident histories, and extensive scrutiny by potential users and regulatory personnel should be accomplished.

OVERVIEW

Department of the Army Technical Bulletin TB700-2 (Ref 1) is the existing regulatory guide for hazard classification of explosive materials. This existing procedure is for final product explosives in transport and storage, and specifically does not address hazards which exist "during various stages of manufacture and assembly". Inprocess materials (those not covered by TB700-2) exist in a wide variety of material forms (solids, powders, flakes, grains/cylinders, strands, slurries, liquids, emulsions, vapor-air or dust-air mixtures, etc). These materials are acted on by a wide variety of normal and abnormal operation stimuli in a wide variety of process operations. If an ignition occurs, the result may be anything from a minor reaction which does not propagate, to a massive explosion. Other hazards such as toxic gas production also exist, but were not addressed in the work reported here. The objective of the work presented in this paper was to develop a procedure for inprocess propellant and explosive materials to supplement the existing procedure for final products in transport and storage. An effective hazard classification procedure for inprocess materials should be relatively simple to accomplish but must also address each of the factors discussed above in a realistic manner.

A procedure has been developed for hazard classification of inprocess materials. The procedure consists of two major parts. A <u>sensitivity evaluation</u> is conducted to indicate how likely an ignition is to occur and what the probable ignition stimuli are. Then an <u>effects evaluation</u> is accomplished to identify the expected consequence and severity. The primary classification (NATO-UN type classification) is related to the consequence and severity of an ignition and is therefore derived from the effects evaluation. The sensitivity evaluation then serves primarily to highlight the urgency (or lack of urgency) for system modifications for safety reasons. The sensitivity tests use the material in its inprocess form and attempt to realistically simulate the inprocess stimuli that could lead to an ignition. Some of the selected sensitivity tests achieve this goal reasonable well, while others still require improvement before this procedure could be adopted as a regulatory guide. Before the procedure can be adopted, a more comprehensive experimental validation should be accomplished using sample materials with known accident histories. In addition, extensive scrutiny by potential users and regulatory personnel is needed.

APPROACH

Seven major program tasks were completed leading to the development and preliminary validation of a hazard classification procedure for inprocess propellant and explosive materials. These were the following:

1. Survey historical accident reports
2. Survey hazard analysis engineering analyses
3. Survey existing test methods
4. Define classification procedure structure
5. Select candidate classification tests and evaluate
6. "Validate" the procedure
7. Finalize the procedure.

In the historical accident survey, relevant process plant accident reports in the Department of Defense Explosive Safety Board (DDESB) files were collected, reviewed, and summarized. This was accomplished early in 1978. There were 389 incident reports with identifiable causal stimuli. These are summarized in table 1 showing the causes indicated in the reports. It should be noted that in many cases more than one possible cause was cited. All of the possible causes were tallied in table 1, although obviously only one was the actual stimulus leading to the ignition.

In instances where a causal stimulus could be identified (for example impact, friction, ESD, etc) the minimum stimulus energy level could be determined from available sensitivity test data for the chemical present. Figure 1 summarizes the stimulus energy level ranges that were derived in this way for the total sample (i.e., all process operations). Similar information was also derived for many of the individual process operations. These energy levels represent the minimum stimulus energy level that had to be present in order to result in an ignition, and this information is useful in interpreting the significance of sensitivity test results.

Table 1

Summary of incident reports with the probable initiation stimuli specified

Process operation or component	Incident reports with identifiable causal stimuli[a]	Impact	Friction[b]	ESD	Thermal	Thermochemical exothermic reaction	Impingement	Adiabatic compression	Compression pinch	Electrical
Pressing	53	20	40	1	1			10	1	
Extrusion	7	2	6		1			3		
Mixing	41	12	36	5	1	3				1
Filling	75	32	43	27	1		1			
Drying	39	9	7	2	24					1
Melt-pour; casting	16	5	4	2	9					
Nitration; reactor	25	1	3			23				
Machining	20	2	20	1						
Mills	19	3	15	1	1			1		
Screening	10	5	8	4			1			
Glazing	3		1							2
Belt conveyors	3	1	2							
Screw conveyors	1	1	1							
Pneumatic conveyors	1		1							
Pumping	5	2	3		2					
Hoppers	15	5	14	5						
Tote-bin	1	1								
Washing	3	1	2		1	1				
Separators	3	1	1			2				
Distillations	2				2					
Solvent recovery	2		1	1						1
Recrystallization	3	2	2		1					
Neutralizing	2	1	[illegible]	2						1
Filter	2		2	2		1				
Maintenance	33	9	19	4	3	2				
Storage	5		2		3					
Totals	389	115	235	57	50	32	2	14	1	6

[a] Generally several stimuli were specified in each report as the probable causes.

[b] Note the incident reports giving friction as a cause do not necessarily correspond to exposure of the process material directly to friction. The exposure in many cases is indirect, such as a drive belt and stuck pulley heating up by friction. In those cases, the direct stimulus is actually thermal.

Note: Numbers shown are the mean, and the plus minus one standard deviation values

Impact

$\mu = 3.81$	7.26		$\boxed{7.26 \times 10^4 \frac{J}{m^2}}$
$\sigma = 3.45$	3.81	$\times 10^4 \frac{J}{m^2}$	
	0.36		

Friction

$\mu = 2.48$	4.23		$\boxed{4.23 \times 10^8 \frac{w}{m^2}}$
$\sigma = 1.75$	2.48	$\times 10^8 \frac{w}{m^2}$	
	.73		

ESD

$\mu = 1.06$	4.37		$\boxed{4.37 \text{ joules}}$
$\sigma = 3.32$	1.06	joules	
	-2.26		

Thermal (not runaway reactions)

$\mu = 328$	432		$\boxed{432^{o}C}$
$\sigma = 105$	328	^{o}C	
	223		

Impingement

$\mu = 152$	152	$\frac{m}{s}$	$\boxed{152 \frac{m}{s}}$
$\sigma = 0$			

Fig 1 Total sample categorized by stimulus only

Engineering analyses (generally simple calculations' estimating inprocess stimulus potential energies) that were conducted in support of hazards analyses were also reviewed as a check and supplement to the historical information. The combined historical and hazard analysis data provided the following information to varying extents for each process operation: (1) possible stimulus types, (2) corresponding stimulus energy levels, (3) possible consequences, and (4) possible severities of the consequences.

To determine what test methods already existed and were possibly useful in classifying inprocess materials, a survey of past and current tests was conducted, A tremendous variety of test methods exists. Each laboratory uses its own special purpose tests and versions of the more standard tests. The survey of tests was certainly not all inclusive, but it is felt that the survey was representative of tests with potential application to hazard classification. The entire listing of tests surveyed will not be presented here, but the tests covered can be categorized under (1) small scale impact, (2) impingement, (3) container penetration, (4) regional impact (eg container drop, SUSAN, and Flyer plate tests), (5) shock wave sensitivity, (6) small fragment impacts, (7) rubbing friction, (8) electrostatic discharge, (9) localized thermal, (10) regional thermal, (11) critical size for developing or sustaining a detonation, (12) mass explosion tests, (13) fragment evaluations, and (14) fire effects. From the extensive list of candidate test methods, twelve tests were selected as being most promising for application to hazard classification of inprocess materials, and these were evaluated experimentally using four sample materials:

M26 paste (0.829 gm/cm^3-mixing operation)
M1 strands (0.45 gm/cm^3-extrusion process)
M30 pellets (0.838 gm/cm^3-drying operation)
RDX slurry* (1.114 gm/cm^3-conveying operation)

* The RDX was used as received, rather than mixed with water to obtain the true inprocess composition.

For local impact, a modified Bureau of Mines drop weight apparatus was used to provide the impact energy. The sample holder was modified as shown in figure 2 in order to accomodate the sample in its inprocess form (unaltered for the test). In addition the sample holder provided sample material beyond the impact location so that a positive reaction could be indicated by the propogation of reaction away from the impact point.

For rubbing friction, a strip friction apparatus was evaluated at first. Although this was simple to use, it was difficult to quantify the stimulus, for example in terms of power per unit area. Therefore, the design shown in figure 2 was adopted from a Thiokol apparatus (Ref 2). This type of rotary friction apparatus provides a measure of the frictional power per unit contact area by means of rotational speed and torque data. The friction test evaluated during this program gave promising results but exhibited a construction material deterioration problem. Thus some additional work would be required before using the method as a requirement for hazard classification.

For impingement ignition, the technique described in the existing TB700-2 procedure was considered to be sound, and no additional experimental evaluation was necessary. This test is illustrated in figure 2.

For thermal ignition, two types of tests were evaluated. For ignition due to increasing the temperature of a large volume of material, differential scanning calorimetry was selected. The temperature at which the onset of an exotherm occurs is taken as the critical temperature for ignition. For localized thermal stimuli, a small metal ball was heated in an electric furnace to a predetermined temperature and then dropped onto the sample material (see figure 2 for an illustration of the apparatus).

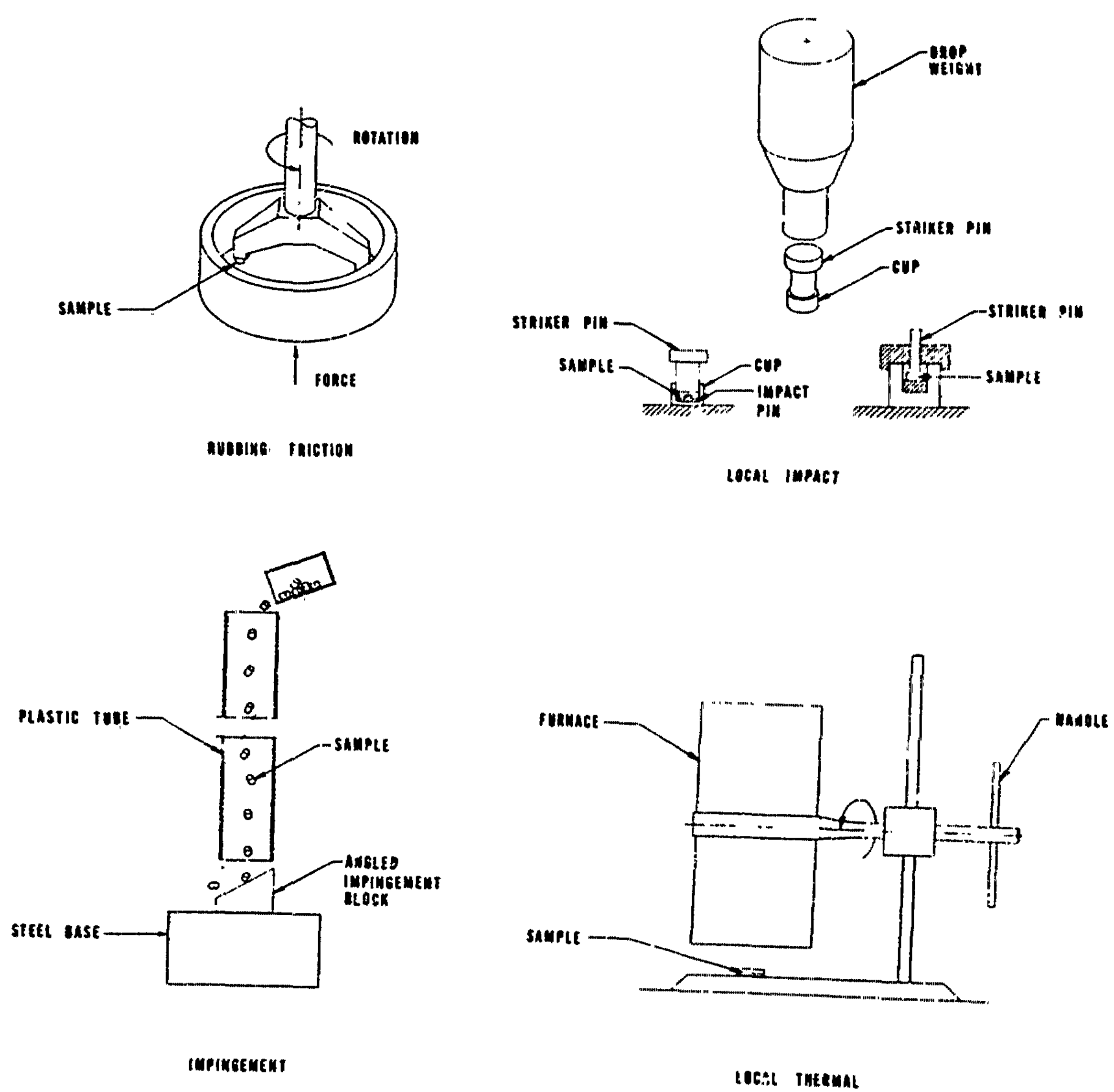

Figure 2. SELECTED SENSITIVITY TESTS

For electrostatic discharge (ESD), the tests that were evaluated consist of two types. First, tests must be conducted to estimate the charge relaxation time. This is an indicator of the material's susceptability to charging within itself. To determine the charge relaxation time, the material's permittivity ε and conductivity σ were measured as functions of applied alternating voltage frequency. The test data were extrapolated to the zero frequency (steady state) values and the ratio of ε to σ was taken as the relaxation time.

The second part of the ESD evaluation was the determination of the minimum discharge energy for ignition. This test was accomplished by discharging a capacitor across electrodes positioned within or on the surface of the sample material. To compute the discharge energy, records of current and voltage directly across the electrodes were used so that losses elsewhere in the system would not distort interpretation of the results.

The tests described above were all related to the likelihood of an ignition occurring. Therefore, they comprise what formed the sensitivity evaluation in the hazard classification procedure. Two additional issues must be resolved in classifying a material with respect to hazards. These are "what is the consequence of an ignition?" (type of event) and "how severe will the consequence be?". To help identify the type of event, a number of screening tests were considered. These were basically of two types. The first type evaluated whether a detonation can propogate in a container of the size and confinement that the actual process vessel provides. For materials in bulk configurations, the "critical diameter" test was considered, whereas for materials in layer configurations, the "critical layer thickness" test was evaluated (see figure 3).

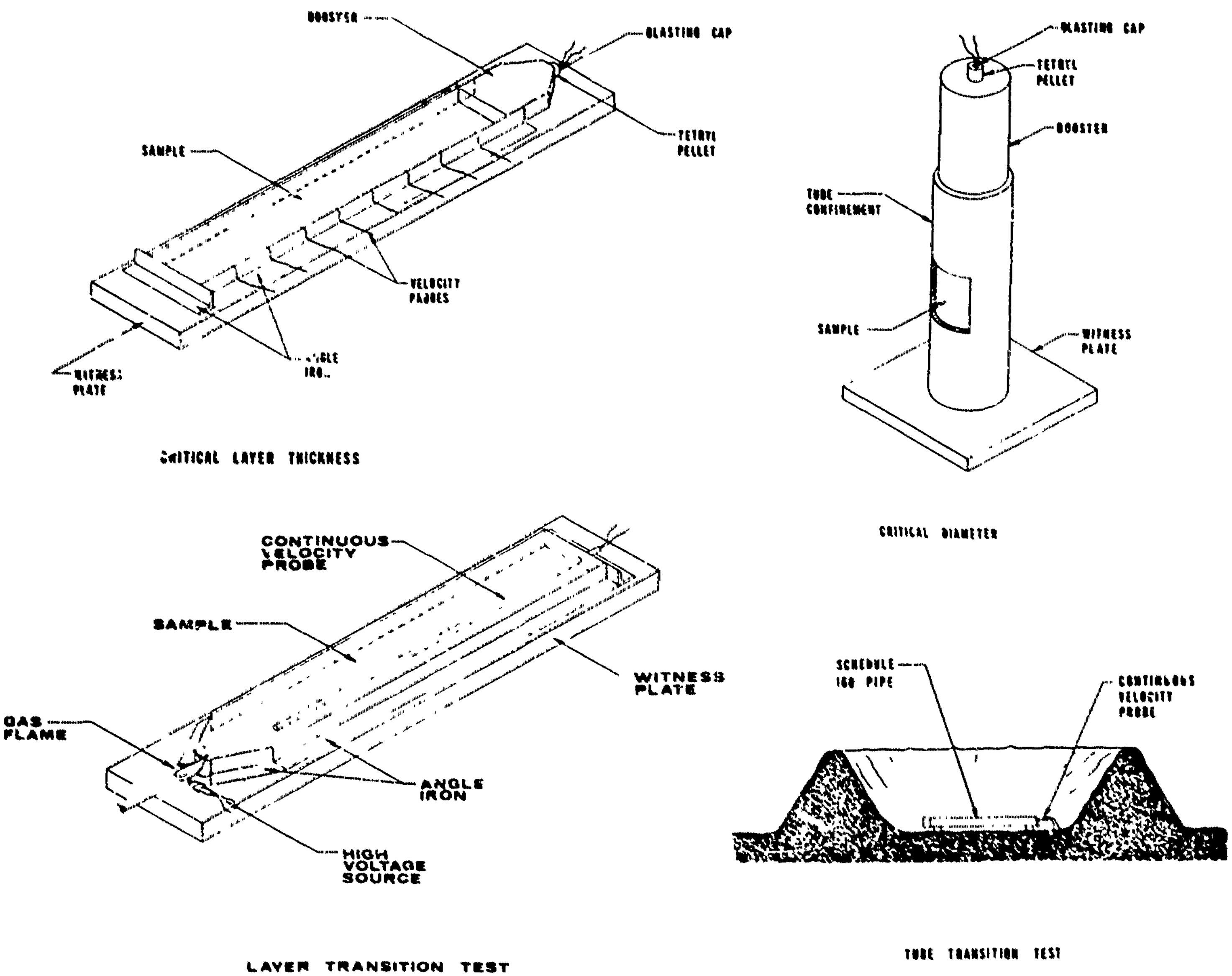

Figure 3. **SCREENING TESTS**

The second type of screening test evaluated whether a detonation could develop given that an ignition results in a burn (i.e., transition from deflagration to detonation). The two tests used for this case (see figure 3) were the "tube transition" and "layer transition" tests. The onset of detonation was sensed using steel cased continuous velocity probes.

Finally, in order to determine the severity of an event, four effects tests were evaluated experimentally. These are illustrated in figure 4. For mass explosions, the material was loaded into a hemispherical steel shell and detonated. Air blast overpressure versus time was measured at several radial distances to determine TNT equivalency. Naturally, geometric scaling of actual process vessel configurations would yield more accurate near field results and would be preferred over the idealized hemispherical geometry, if such data were available.

If the material is likely to burn in an open topped container, the mass fire test is relevant. Here the sample is weighed as it burns using a lever arm arrangement. The flame envelope (height and width) are documented by movie or video coverage. Radiant heat flux emitted at 10 meters is also measured.

For materials in layers, the flame propogation speed is of concern with respect to the adequacy of the detection-deluge system. In the fire spread test, the flame speed versus distance is measured in addition to the flame height, flame width, and the radiant heat emitted.

For materials that are actually dust suspensions inside of closed containers, the Hartmann apparatus (Ref 3) is suggested. The Bartneckt apparatus (Ref 4) would be preferable to the Hartmann due to its larger volume and more accurate results, but the Hartmann is more widely available at the present time.

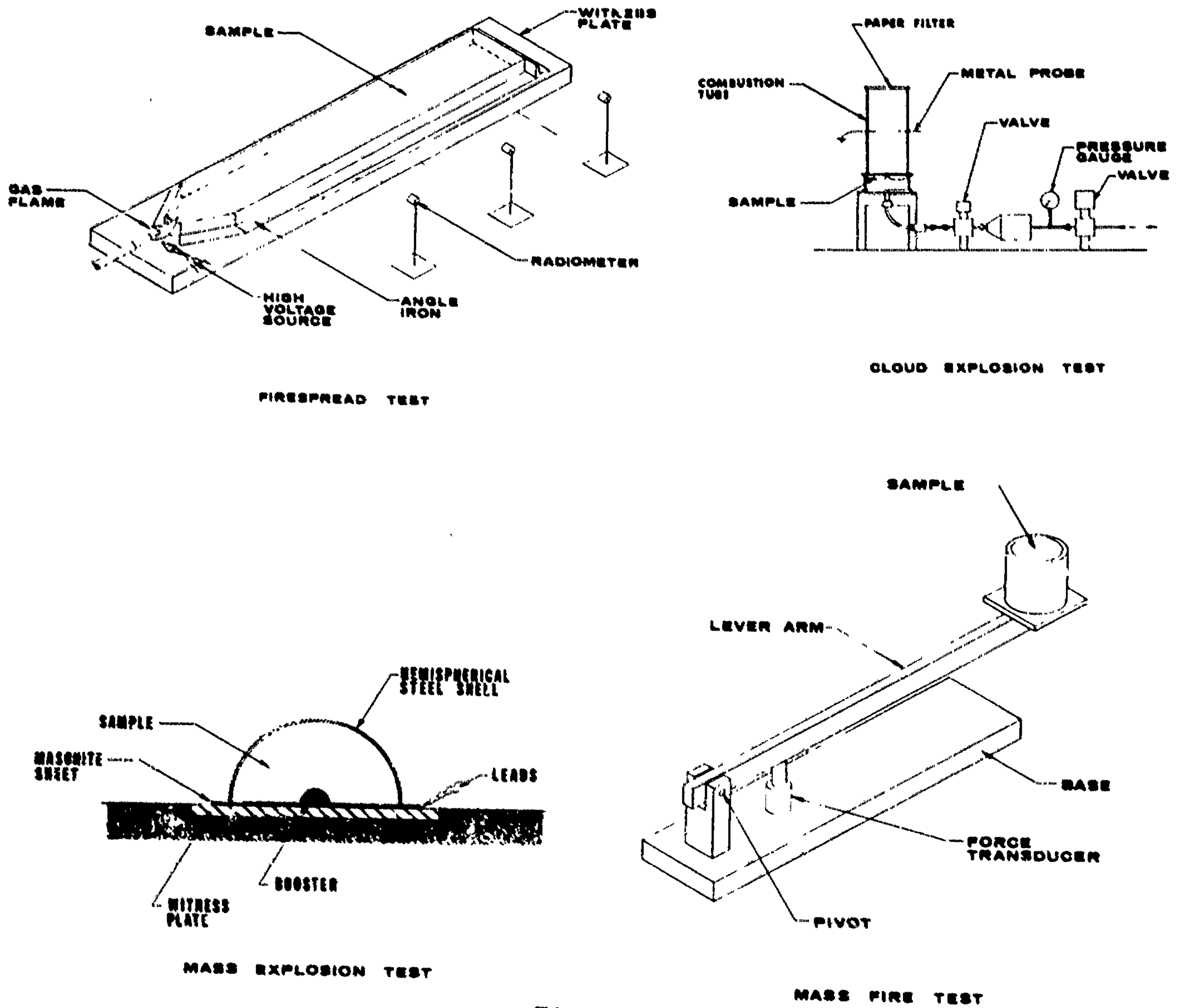

Figure 4

EFFECTS TESTS

SUMMARY OF THE PROCEDURE

The resultant hazard classification procedure is summarized in figure 5. First the sensitivity evaluation is conducted. This consists of conducting those sensitivity tests that simulate stimuli that could be present, either under normal or abnormal conditions, in the specific operation being evaluated. For example, if the milling operation is being evaluated, tests for local impact, impingement, rubbing friction, regional thermal and local thermal stimuli would be required. A melt pour operation would require a different set of sensitivity tests. Each sensitivity test determines the amount of stimulus energy (or energy related quantity) that will result in an ignition of the material 50% of the time. This ignition energy is then compared to the inprocess energy as determined for the specific process operation from the historical data and hazards analyses. The ratio of these energies is denoted the safety factor, SF.

$$SF = \frac{\text{ignition energy}}{\text{inprocess energy}}$$

The lowest of the derived safety factors from all of the required sensitivity tests is the material's overall safety factor. In the sensitivity evaluation, if the safety factor is greater than 3, the material is classified as "insensitive". If it is less than 3, the material is "sensitive".

Insensitive materials are exposed to an open flame for a specified period of time. If no reaction is observed, these materials are immediately put into Class 1.5 "very insensitive", and the classification process is completed. In all other cases, the screening tests for the effects evaluation are required.

The screening tests consist of "critical diameter" and "tube transition" tests for materials in bulk configurations and "critical layer thickness" and "layer transition" tests for materials in layer configurations. Materials in the form of a suspension do not require screening tests. For these materials, the cloud explosion test is required.

SAFETY FACTOR

$$S.F. = \frac{\text{IGNITION ENERGY}}{\text{INPROCESS POTENTIAL}}$$

Hazards classes 1.1 to 1.5 follow the general structure of the NATO-UN classification system

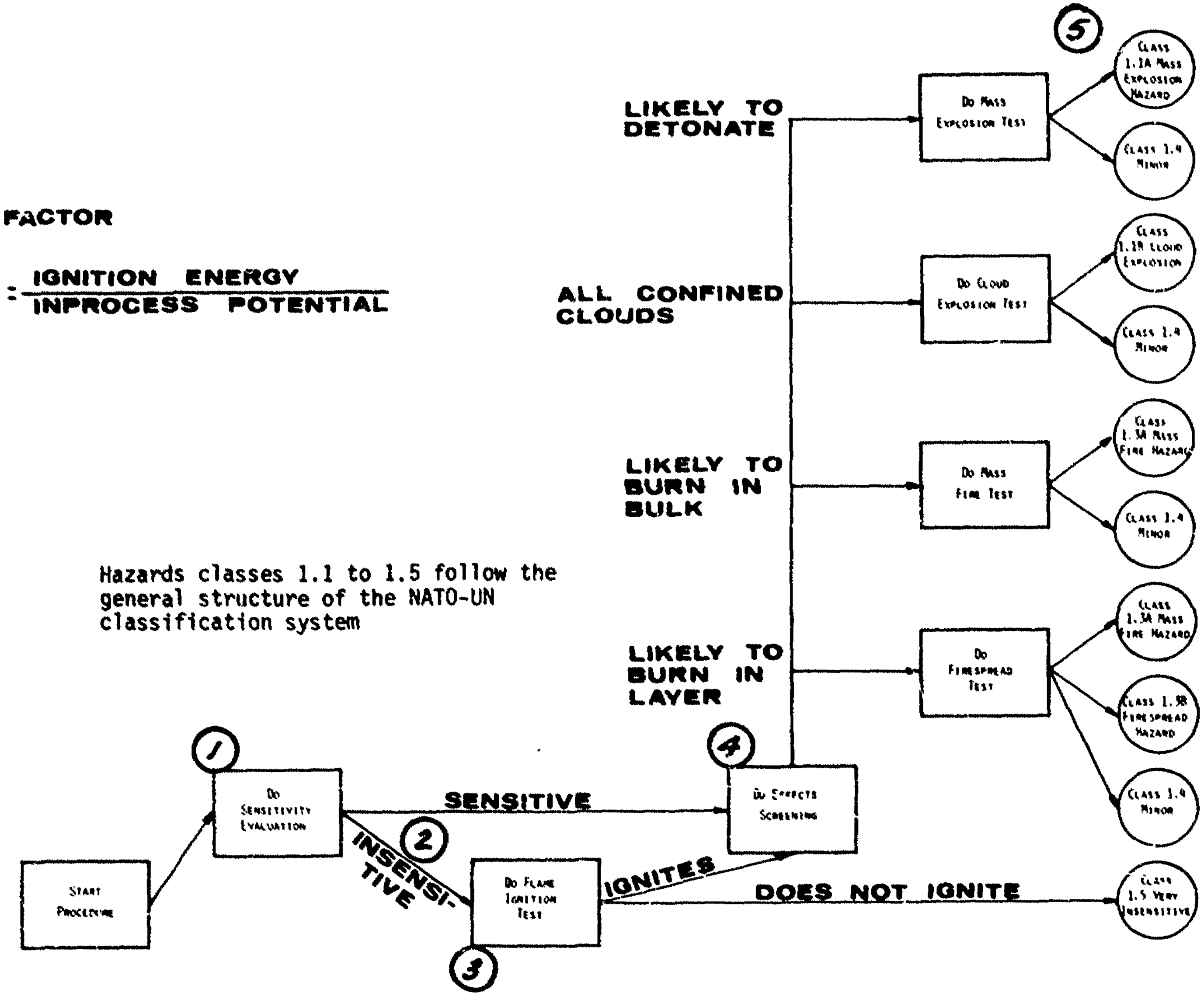

Figure 5

Overall Hazards Classification Procedure

Based on the results of the screening tests and the process vessel configuration, the most probable type of consequence is inferred using conservative logic. The logic for making this determination is presented in figure 6. The results of the required effects tests are then used to classify the material in a classification quite similar to the NATO-UN scheme for final products in transport and storage. The meaning of the different classifications is not exactly the same as the NATO-UN System because we are concerned with inprocess materials during manufacture, rather than end items during transport and storage situations. Table 2 compares the NATO-UN System with the classes derived for inprocess materials.

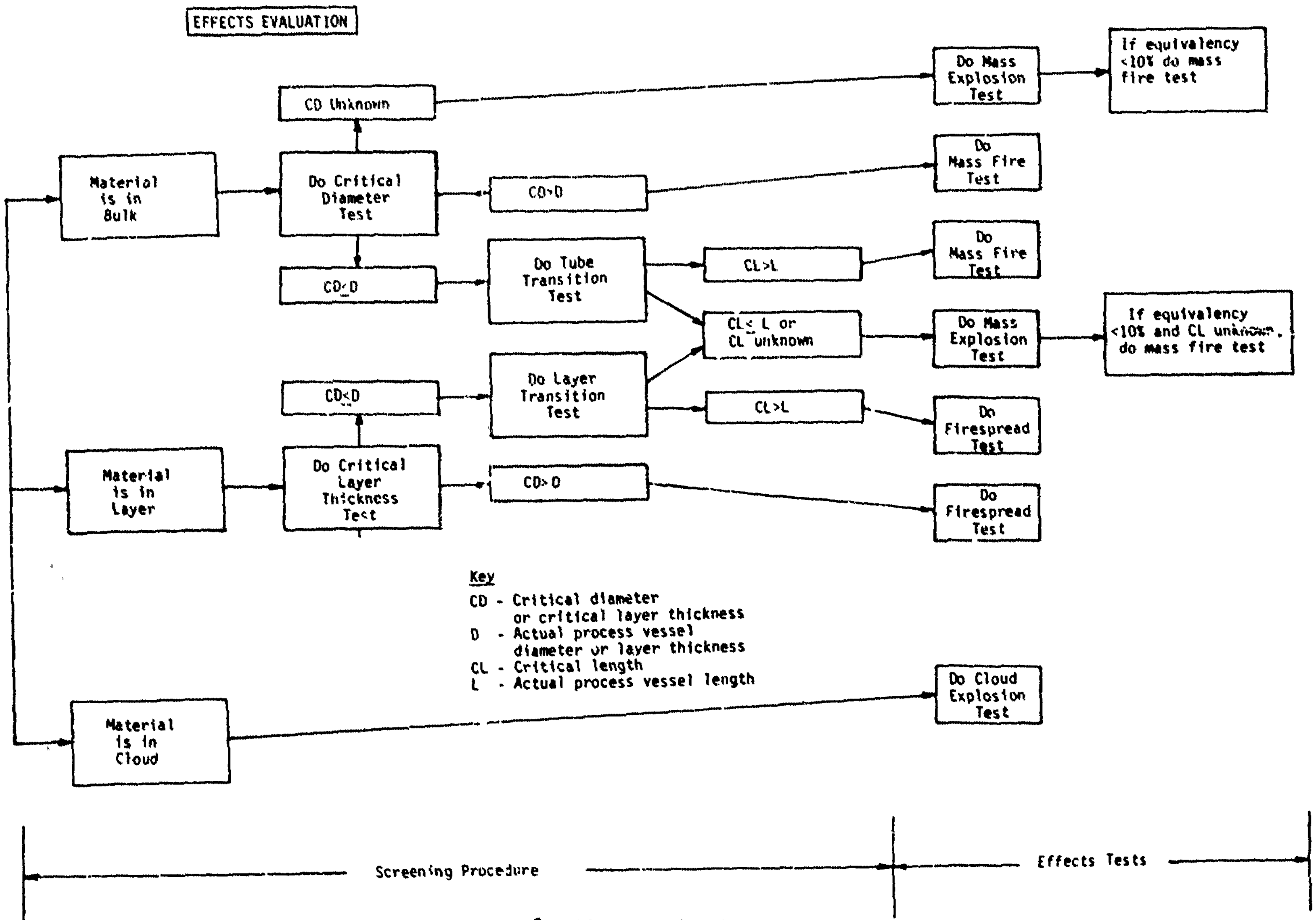

Fig 6 Effects evaluation

TABLE 2

HAZARDS CLASSIFICATIONS

NATO-UN HAZARDS CLASSES		IN-PROCESS HAZARDS CLASSES		
1.1	MASS EXPLOSION HAZARD	1.1	1.1A	MASS EXPLOSION HAZARD
			1.1B	CLOUD EXPLOSION HAZARD
1.2	PROJECTION HAZARD		1.2	PROJECTION HAZARD
1.3	FIRE HAZARD	1.3	1.3A	MASS FIRE HAZARD
			1.3B	FIRESPREAD HAZARD
1.4	NO SIGNIFICANT HAZARD		1.4	NO SIGNIFICANT HAZARD
1.5	VERY INSENSITIVE		1.5	VERY INSENSITIVE

WHATS NEXT?

As mentioned earlier, the procedure described in this paper still requires several refinements before it can be applied as a regulatory guide. First, the procedure must be reviewed in detail by the DDESB personnel and potential users. In addition, a more comprehensive validation of the procedure should be accomplished using sample materials with known accident histories. Based on these actions, the procedure should be refined and incorporated as a supplement to TB700-2. In order to best utilize the procedure, a guide should be developed that describes requirements for safe handling of materials that are in each class. The guide should also describe techniques for determining safe separation distances between buildings, if not also between containers within a building, for materials in each class. Naturally, periodic updating of the procedure is imperative in order to incorporate new developments and better understanding of the hazards in process plants.

ACKNOWLEDGEMENTS

The work described in this paper was conducted for the U. S. Army Armament R&D Command (ARRADCOM), Dover, New Jersey under contracts DAAA21-76-C-0211 and DAAK10-78-C-0029. Mr. R. Rindner was the ARRADCOM project leader, and Mr. D. Satriana was the ARRADCOM project engineer.

REFERENCES

1. "Technical Bulletin TB700-2, Explosives Hazard Classification Procedure", Department of the Army, May 1967.

2. Dinsdale, V. T., "Hazard Evaluation of Solid Propellant Systems from Research to Missile Flight," Thiokol Chemical Corporation, Sept. 1964.

3. Dorsett, H. G., "Laboratory Equipment and Test Procedures for Evaluating Explosibility of Dusts," Bureau of Mines, RI 5624, 1960.

4. Hokanson, J. C., and Seals, W. O., "M-1 Propellant Dust Explosibility," for Conference on Mechanisms of Explosions in Dispersal Energetic Materials, Nov. 1978.